PHOTOREDOX-MEDIATED METAL-FREE C–H ALKYLATION AND DUAL CATALYSIS

Jennifer K. Matsui

A DISSERTATION

in

Chemistry

Presented to the Faculties of the University of Pennsylvania

in

Partial Fulfillment of the Requirements for the

Degree of Doctor of Philosophy

2018

Supervisor of Dissertation

_____

Dr. Gary A. Molander

Hirshmann-Makineni Professor of Chemistry

Graduate Group Chairperson

_____

Dr. David W. Christianson

Roy and Diana Vagelos Professor of Chemistry

Dissertation Committee

Dr. Marisa C. Kozlowski, Professor of Chemistry

Dr. E. James Petersson, Associate Professor of Chemistry

Dr. Patrick J. Walsh, Professor of Chemistry

TABLE OF CONTENTS

ACKNOWLEDGEMENTS

Above all, I am grateful for the support and guidance from my Ph.D. advisor, Professor Gary Molander throughout my graduate career. As a young graduate student, I was immediately drawn to his enthusiasm for chemistry and, looking back, joining his group was the best decision I made in graduate school. Over the past four years, he has been a mentor, constructive critic, strong support system, and role model. I have admired Professor Molander's keen awareness of challenges in industry and the ways he has inspired the group to creatively tackle these challenges. On a personal note, I will always appreciate how Professor Molander has relentlessly supported my project ideas and future endeavors.

Furthermore, I would like to thank my committee members, Professors Marisa Kozlowski, E. James Petersson, and Patrick Walsh, for their encouragement throughout the years. Specifically, I would like to thank Professor Kozlowski for providing the career-shaping advice to explore research areas outside of synthetic organic chemistry. Also, as part of the ACDC committee, I am extraordinarily grateful for her support of the organization during its infancy. I am also extremely grateful for the numerous conversations I have had with Professor Petersson, who has provided insight into the *applications* of organic chemistry from the perspective of chemical biology. Notably, Professor Petersson has been incredibly supportive of my non-traditional career aspirations and I deeply appreciate the time he has taken to listen and understand where my motivations stem from. Finally, I am so thankful for Professor Walsh's role within the department during my graduate career. From teaching organometallics to being the Philadelphia Organic Chemists' Club Chair to becoming an integral part of my committee, Professor Walsh has consistently been a source of encouragement and advice. Resulting from numerous thought-provoking questions and comments during my committee meetings, I have embarked on subsequent mechanistic studies that have led to a deeper understanding during the reaction development process.

Next, I must thank all the past and present Molander group members. In particular, John, Dave, and DaWeon were the three graduate students that strongly encouraged me to join the Molander group. Once I officially became a member of the group, they were extraordinarily supportive during my formative months in the lab. I will cherish the fond memories during our time in lab and have enjoyed keeping in touch. During the latter half of graduate school, Alvaro has been a phenomenal coworker, organometallic whiz, and voice of reason. Shuai, Niki, and Becky were not only outstanding lab mates, but, more importantly, outstanding friends.

In addition to relationships built during my time at Penn, mentors established during my undergraduate years inspired my interest in the field of organic chemistry. Professor Patrick Harran took the time and effort to guide my foray into academic research. I am also extremely grateful for Dr. James Frederich's guidance during my undergraduate research, where he worked with me daily to establish a solid foundation to become a thorough organic chemist. At MD Anderson, I appreciate all the support that was given during my internship by my fellow coworkers and in particular, I am extremely grateful for my friendship formed with Dr. Barbara Czako.

Finally, I am so grateful for the support of my family (Mom, Dad, and Kevin). Although they were across the country, they have only been a phone call away to lend words of encouragement and understanding. Most importantly, I am eternally grateful for my husband, Drew Heitz, who has shared an appreciation for organic chemistry and has unconditionally supported me throughout my graduate journey.

ABSTRACT

PHOTOREDOX-MEDIATED METAL-FREE C–H ALKYLATION AND DUAL CATALYSIS

Jennifer K. Matsui

Gary A. Molander

Over the past decade, a resurgence of interest in photo-induced electron transfer has resulted in a new class of organic transformations. The ability to harness over 60 kcal/mol of visible light energy to activate redox-labile substrates—*via* the intermediacy of a photoredox catalyst—has enabled reactions under extraordinarily mild conditions compared to alternative two-electron modes of activation.

Recent research efforts have broadened the scope of trifluoroborate coupling partners, employed 1,4-dihydropyridines (DHPs) in mono- and dual-catalytic manifolds, and accessed new chemical space *via* C–H functionalization pathways. First, the development of alkyltrifluoroborates as latent radicals for C–H alkylation of heteroarenes under photocatalytic conditions is described. Notably, the catalytic generation of carbon-centered radicals and the BF_3 byproduct accomplishes a *regioselective* and atom-economical approach to the classical Minisci reaction. Subsequent reports disclose DHPs as unique radical precursors that do not require the use of a photocatalyst to effect a single-electron oxidation. Instead, DHPs are oxidized in the presence persulfate, facilitated by their low oxidation potentials.

Furthermore, photoredox/Ni dual catalysis protocols have been developed to overcome several inherent limitations of palladium-catalyzed cross-couplings [i.e., forcing reaction conditions, limited scope for $C(sp^3)$–$C(sp^2)$ bond formation] by invoking a *single-electron* transmetalation pathway. Within the area of photoredox/Ni catalysis, a library of natural and unnatural aryl chromanones are accessed from the corresponding trifluoroboratochromanones and

aryl bromides. In an effort to expand the radical toolbox by utilizing feedstock chemicals (e.g., aldehydes) to access radicals inspired the exploration of DHPs as radical partners in the dual catalytic paradigm. Exploiting the one-step procedure to access highly functionalized DHPs, a library of monosaccharide DHPs were synthesized and employed in the dual catalytic cross-coupling procedure with aryl bromides.

In summary, the mild, photoredox-mediated C–H alkylation of heteroarenes represents a late-stage functionalization strategy to rapidly access highly functionalized motifs. Additionally, photoredox/Ni dual catalysis has enabled the modular synthesis of functionalized aryl chromanones and monosaccharides. Throughout these reported studies, it is clear the controlled and catalytic nature of photoredox catalysis enables previously challenging transformations and is primed for significant advancements in the near future.

Chapter 1. Photoredox Catalysis: A Rapidly Growing Field in Synthetic Organic Chemistry

1.1 Introduction

Over the past decade, a resurgence of interest in photo-induced electron transfer has resulted in a new class of organic transformations.[1] The ability to harness over 60 kcal/mol of visible light energy to activate redox-labile substrates—via the intermediacy of a photoredox catalyst—has enabled reactions under extraordinarily mild conditions compared to alternative two-electron modes of activation.[†] Since the 1970s, the properties of transition metal photocatalysts (PC) have been studied, revealing that photoexcited transition metal catalysts can either undergo a single-electron oxidation or reduction (Figure 1.1).

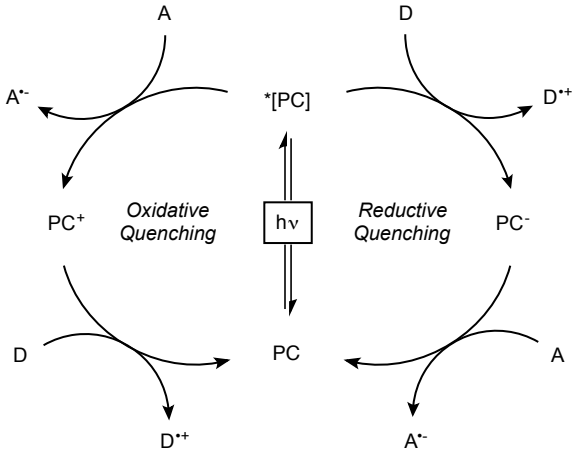

Figure 1.1. Oxidative and reductive quenching pathways.

One of the first synthetic applications of a photoredox catalyst was reported by Deronzier, wherein a ruthenium photocatalyst was used in a Pschorr-type transformation via a single-electron

---

[†] Reproduced in part from Matsui, J. K.; Lang, S. B.; Heitz, D. R.; Molander, G. A. *ACS Catal.* **2017**, *7*, 2563.

reduction of an aryl diazonium moiety (Figure 1.2).[2] Through the reported experiments, Deronzier successfully demonstrated how a photocatalyst excited by visible light can catalytically orchestrate single-electron transfer events to perform synthetically useful transformations.

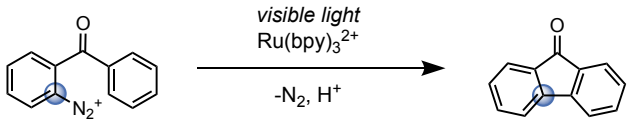

Figure 1.2. Photoredox mediated Pschorr cyclization.

In subsequent reports, Deronzier and coworkers conducted Stern-Volmer plots to confirm the presence of a single-electron transfer event between the photocatalyst and diazonium salt. As expected, a linear trend was observed during the quenching studies, strongly suggesting the diazonium decomposes to the aryl radical in the presence of irradiated ruthenium photocatalyst. Once the aryl radical forms, intramolecular cyclization occurs, albeit in a significantly slower rate (given the rigid biaryl backbone). After the cyclization, the reduction of $Ru(bpy)_3^{3+}$ is accomplished during the formation of aryl cation with rapid rearomatization, affording the tricyclic scaffold (Figure 1.3).

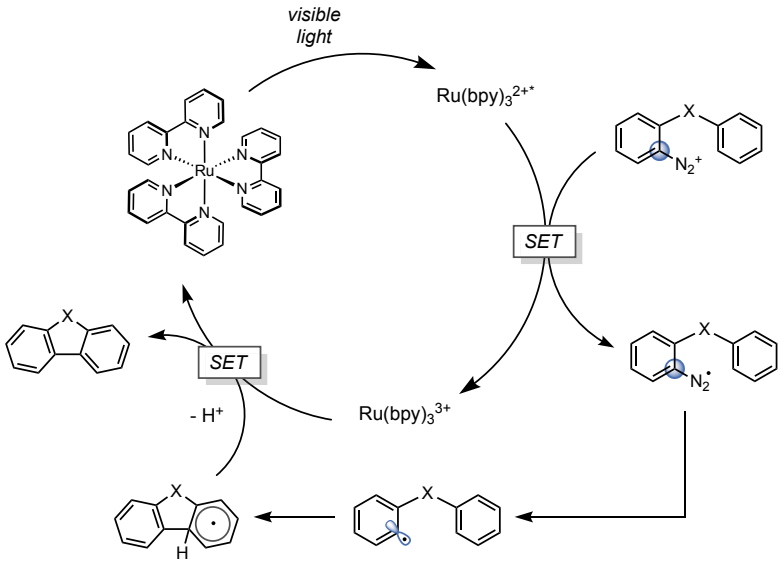

Figure 1.3. Proposed mechanism.

More recently, Yoon,[3] MacMillan,[4] and Stephenson[5] employed $Ru(bpy)_3$ to perform cycloadditions, α-alkylation of aldehydes, and dehalogenation, respectively, through both oxidative and reductive quenching pathways. Following these seminal reports, numerous groups have developed creative applications with a variety of photocatalysts to effect a myriad of mono-catalytic and dual catalytic reactions.[6]

1.2 Merging Photoredox and Nickel Catalysis

Our group became interested in photoredox catalysis as a tool to generate alkyl radicals for use in cross-coupling reactions. In 2014, we disclosed the first example of photoredox/Ni dual catalysis to forge $C(sp^2)$–$C(sp^3)$ bonds under unusually mild reaction conditions.[7] In this transformation, photoredox/Ni dual catalysis proceeds via the single-electron oxidative fragmentation of radical precursors and alkyl radical addition to a nickel catalyst, a process we refer to as single-electron transmetalation (Figure 1.4). The addition of the radical to the nickel complex using this protocol is the synthetic equivalent of the more traditional two-electron transmetalation, and the activation energy for this process is extraordinarily low.[8] This paradigm is in stark contrast to typical Pd- or Ni-catalyzed processes, where transmetalation from an organometallic nucleophile to a metal center is often the rate-determining step with a high energy of activation.[9]

This Chapter details the efforts of our laboratory to expand the scope of photocatalytic routes to radicals by targeting three major components of the dual catalytic cycle for improvement (Scheme 2): the radical precursor (A), the electrophilic coupling partner (B), and the photocatalyst (C). Beyond trifluoroborate and hypervalent silicate reagents previously exploited,[1a] we sought complementary radical precursors derived from feedstock chemicals (e.g., aldehydes), to engage in single-electron transmetalation processes. Furthermore, the development of protocols for the inclusion of electrophiles other than hetero(aryl)bromides is discussed. Additionally, our efforts in the arylation of alkyl $C(sp^3)$–H bonds using photoredox/Ni dual catalysis are detailed.

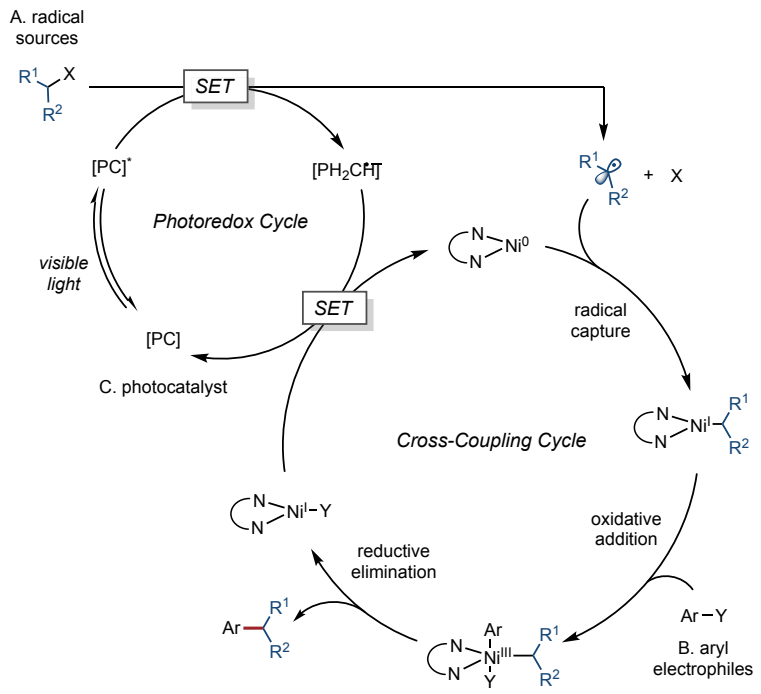

Figure 1.4. Photoredox/Ni dual catalytic cross-coupling cycle.

Another important accomplishment was the inclusion of competent, inexpensive, and sustainable organic photoredox catalysts (Figure 1.5) in many of the developed protocols.[10] Building upon Zhang's report that 4CzIPN (4) can serve as a surrogate of transition metal-based photocatalysts within the photoredox/Ni manifold, we began to incorporate it into newly developed cross-couplings.[11] We have also exploited the favorable properties of the mesityl acridinium dye (5)[12] and Eosin Y (6) to effect metal-free couplings.

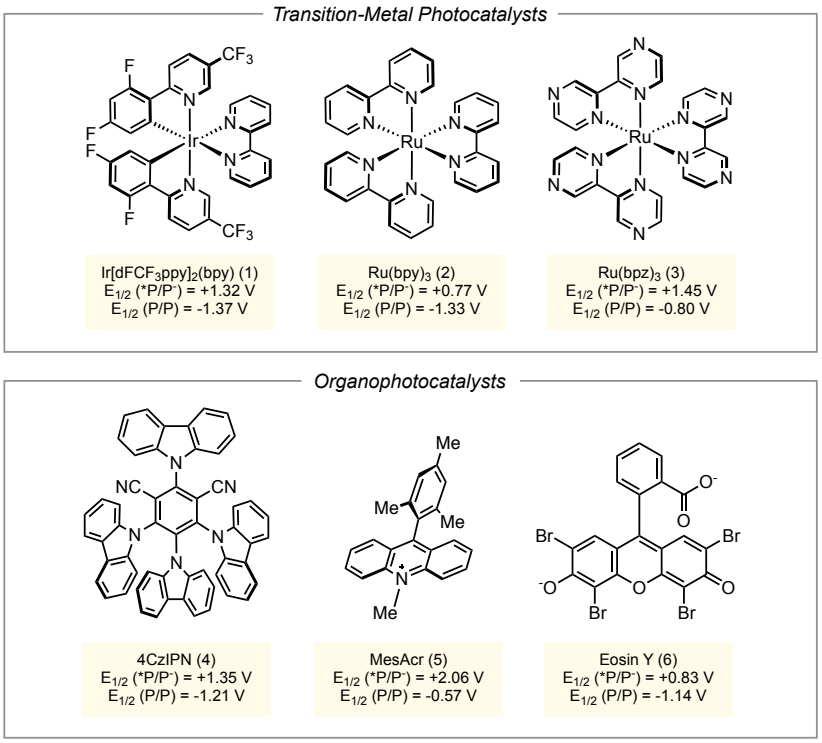

Figure 1.5. Metal-based photocatalysts and organophotocatalysts.

An overarching theme that has evolved is the catalytic generation of radicals via photoredox processes that enables transformations that would be challenging, if not impossible, to carry out under conditions in which stoichiometric reagents were utilized to generate these same radicals.

The many challenges of transition metal-catalyzed cross-coupling of sp^3-hybridized nucleophilic species with sp^2-hybridized electrophiles led our group[6] and others to develop cross-coupling protocols based upon single-electron transformations (Figure 1.4). The major advantage of using radical intermediates in such catalytic cycles derived from the extraordinarily rapid capture of these open-shell species by the transition metal cross-coupling catalysts in an event we termed "single-electron transmetalation." The success of these processes derived ultimately from the fact that these radicals were generated catalytically in a process that was tightly regulated and innately controlled by the intertwinement of the photoredox cycle and the cross-coupling cycle. Thus,

adjustment of the electronic nature and concentration of the individual catalysts are used to regulate the concentration of the radicals generated. The tuning is critical to the success of the overall process because such highly reactive intermediates, left to themselves, are subject to a variety of deleterious side-reactions, including dimerization and disproportionation. Catalytic generation of the key reactive intermediates was thus critical for the success of these intricately fused cycles, and provided the crucial, enabling transformations that could not be accomplished using stoichiometric methods based, for example, in tin hydride or electrochemical processes.

The many challenges of transition metal-catalyzed cross-coupling of sp^3-hybridized nucleophilic species with sp^2-hybridized electrophiles led our group[6] and others[4i] to develop cross-coupling protocols based upon single-electron transformations. The major advantage of using radical intermediates in such catalytic cycles derived from the extraordinarily rapid capture of these open-shell species by the transition metal cross-coupling catalysts in an event we termed "single-electron transmetalation". The success of these processes derived ultimately from the fact that these radicals were generated catalytically in a process that was tightly regulated and innately controlled by the intertwinement of the photoredox cycle and the cross-coupling cycle. Thus, adjustment of the electronic nature and concentration of the individual catalysts are used to regulate the concentration of the radicals generated. This is critical to the success of the overall process because such highly reactive intermediates, left to themselves, are subject to a variety of deleterious side-reactions, including dimerization and disproportionation. Catalytic generation of the key reactive intermediates was thus critical for the success of these intricately fused cycles, and provided the crucial, enabling transformations that could not be accomplished using stoichiometric methods based, for example, in tin hydride or electrochemical processes.

1.2 Photoredox/Ni Dual Catalysis

Alkyltrifluoroborates are exceptional reagents for photoredox processes, primarily because of their low oxidation potentials, benchtop stability, and commercial availability.[13] Additionally, complex alkyltrifluoroborates can be accessed via a variety of complementary pathways, including β-borylation of conjugated carbonyl substrates,[14] substitution of halomethyltrifluoroborates, and so on.[15] From the seminal cross-coupling of benzyltrifluoroborates, the exploration of different classes of trifluoroborates has led to the fruitful incorporation of secondary alkyl,[16] α-alkoxy,[17] α-amino,[18] and α-trifluoromethyl[19] subunits into similar manifolds. To expand the scope of radical precursors with complementary reactivity, the compatibility of bis(catecholato)-alkylsilicates was evaluated in photoredox-/Ni-catalyzed crosscouplings. Hypervalent silicon compounds have been shown to be readily oxidized, affording the corresponding alkyl radicals as initially demonstrated by Nishigaichi and co-workers.[20] The groups of Goddard, Ollivier, and Fensterbank also demonstrated that radicals derived from photooxidation of pentavalent bis(catecholato)silicates readily participated in allylation, vinylation/alkynylation, conjugate addition, and nickel-catalyzed cross-coupling reactions.[21] With an improved synthetic route to access alkyl ammonium bis(catecholato)silicates, our group built a library of silicate radical precursors containing epoxide, amine, and chloride functional groups from the corresponding trimethoxysilanes (Figure 1.6).[22]

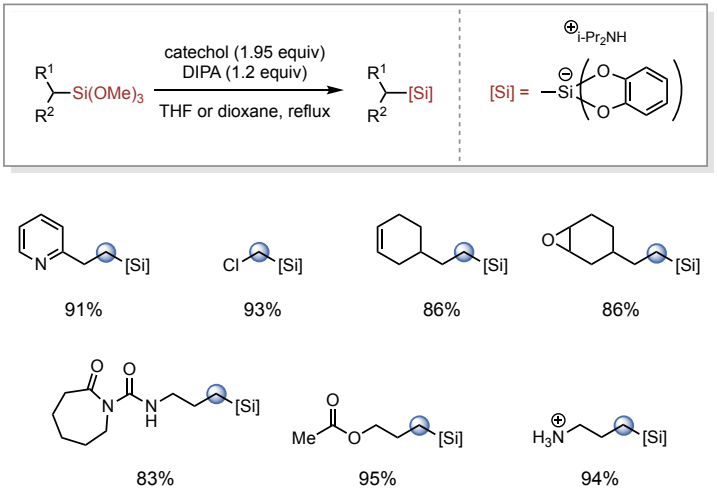

Figure 1.6. Conversion of trimethoxysilanes to alkylsilicates.

As with alkyltrifluoroborates, alkylsilicates are crystalline solids or free-flowing powders that are indefinitely bench-stable. Alkylsilicates have the added advantage of avoiding formation of the deleterious byproduct BF_3, which requires the use of basic sequestering agents in cross-coupling protocols. Furthermore, the lower oxidation potentials (E_{red} = +0.75 V vs SCE) allowed the transition from iridium photocatalysts to the significantly less expensive $Ru(bpy)_3(2PF_6)$[1b] and even organic photocatalysts. Additionally, alkylsilicates tend to be more soluble than trifluoroborate salts, which can be an important consideration in their adaptation to photoflow conditions. These advantages enabled photoredox/Ni dual cross-coupling with exquisite functional group tolerance (e.g., substrates containing amines and protic functional groups).

In 2011, our group reported the β-borylation of α,β-unsaturated amide and carbonyl compounds using a readily available copper catalyst with bisboronic acid.[14] Subsequently, we successfully engaged secondary alkyltrifluoroboratoamides in palladium-catalyzed cross-couplings.[23] Unfortunately, efforts to couple alkyl β-trifluoroborato ketones or -esters under similar conditions primarily resulted in β-hydride elimination. Other routes to similar synthons include the generation of organozinc and –lithium reagents, which also result in unproductive side reactions, specifically an intramolecular attack on the carbonyl to afford the corresponding

cyclopropanolates.[24] Therefore, we hypothesized that coupling the secondary alkyl β-trifluoroboratoketones and -esters via single-electron transmetalation using photoredox/Ni dual catalysis could address this unsolved challenge.[25]

Optimization of reaction conditions revealed that the $Ir[dFCF_3ppy]_2(bpy)PF_6$ photocatalyst (2.5 mol %), $NiCl_2$ (2.5 mol %), dtbbpy (2.5 mol %) cross-coupling catalyst, Cs_2CO_3 (0.5 equiv), and 2,6-lutidine (0.5 equiv) in dioxane afforded the highest conversion to product. Impressively, this coupling tolerated a wide range of potentially sensitive functional groups (e.g., aldehydes, ketones, esters, nitriles) and heteroaryl partners (e.g., pyridine, pyrimidine, azaindole) as shown in Scheme 5.

Tackling another challenging substrate class in palladium-catalyzed Suzuki cross-couplings, we sought to utilize α-alkoxyalkyltrifluoroborates in the dual catalytic manifold. Previous palladium-catalyzed approaches toward the coupling of α-alkoxyalkyltrifluoroborates via two-electron transmetalation pathways were limited by the need for excess base (>5 equiv Cs_2CO_3) and elevated temperatures (>100 °C), which resulted in extremely narrow functional group tolerance.[26] In fact, only a benzylic ether was compatible with the reaction conditions.[20] We postulated that single-electron transmetalation would facilitate a more general synthesis of protected secondary alcohol derivatives.[27] The mild, optimized reaction conditions associated with the dual catalytic cross-coupling manifold readily lent themselves toward a protecting group-independent and functional group-tolerant strategy to access a broad range of protected benzylic alcohol derivatives (Figure 1.7). Notably, a fully unprotected carbohydrate was readily coupled in a synthetically useful 68% yield.

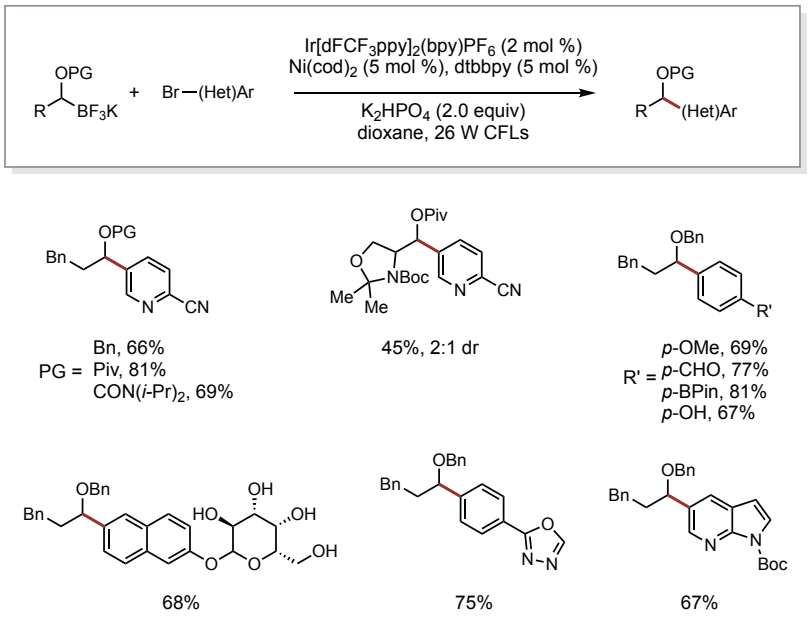

Figure 1.7. Protected secondary α–alkyoxytrifluoroborate coupling with aryl bromides.

In an effort to merge the β-trifluoroborato ketones and secondary α-alkoxyalkyltrifluoroborates, we next targeted the biologically significant chromanone core, found in myriad plant metabolites.[28] Although there have been a multitude of synthetic routes to access functionalized chromanones,[29] most disconnections involve a chalcone intermediate, making derivatization of the C2-aryl ring difficult. Conjugate addition of various arylmetallics to chromones constitutes another logical approach, but from a diversity point of view this tactic is less than ideal because it requires the synthesis of organometallic reagents, many of which are air- and moisture sensitive. We envisioned an alternate route where a trifluoroboratochromanone serves as a radical precursor to access a wide array of 2-(hetero)aryl chromanones rapidly using the corresponding aryl or heteroaryl halide directly as coupling partners.[30] This strategy would take advantage of having access to thousands of commercially available, structurally diverse aryl- and heteroaryl halides to elaborate the chromanone core. The requisite 2-trifluoroboratochromanones were prepared via the β-borylation of commercially available chromone using an inexpensive copper catalyst and bisboronic acid on gram-scale (Figure 1.8).[14]

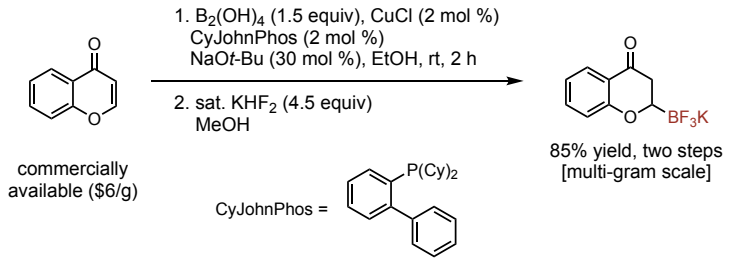

Figure 1.8. β–borylation of chromone.

A variety of 2-(hetero)aryl-substituted flavanones were synthesized in one step under the operationally simple and mild reaction conditions (Figure 1.9). Aryl bromides bearing electron-withdrawing substituents in the meta- and para- positions that may also subsequently serve as building blocks were well-tolerated. Additionally, a variety of heteroaryl bromides provided the desired flavanones in good yields. Lastly, chromones substituted on the aryl subunit were also readily borylated and then subsequently arylated, providing additional opportunities for diversification of the flavanone core.

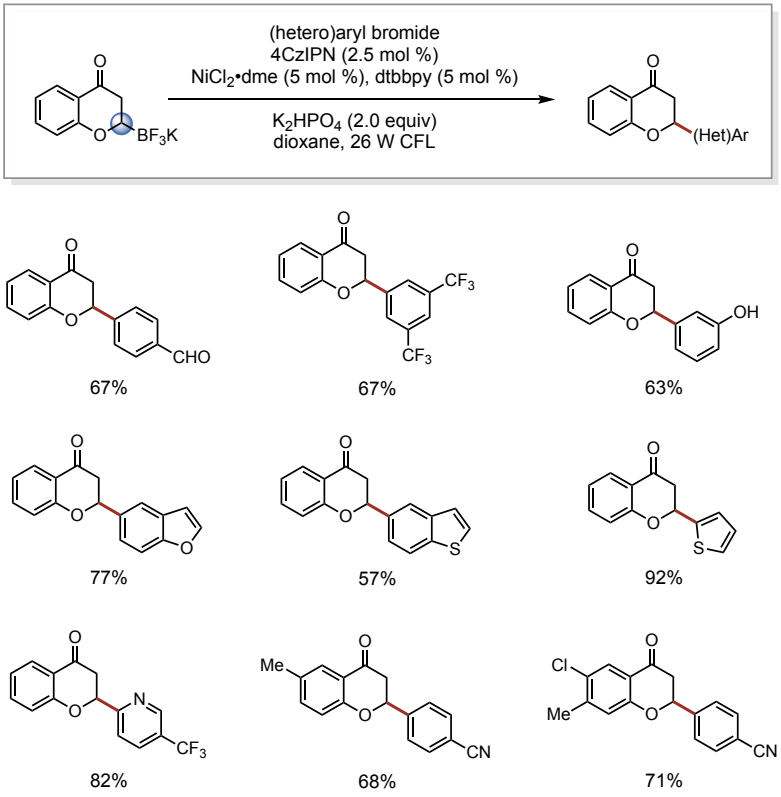

Figure 1.9. Coupling of trifluoroboratochromanones with aryl bromide.

Although we demonstrated that several reactive functional groups were untouched in the photoredox dual cross-couplings (e.g., aldehydes, chlorides), our laboratory sought to determine if boronate groups would also remain intact for iterative cross-couplings.[31] The combination of photoredox/Ni dual catalysis at room temperature indeed allowed the differentiation of reactivity sites based on the preferential tendencies for tetracoordinate, C(sp^3)-hybridized organoboron reagents to engage in single-electron transmetalation, in contrast to their tricoordinate, C(sp^2)-hybridized counterparts. Thus, reactive, tricoordinate, C(sp^2)-hybridized organoboron reagents that succumb to decomposition pathways such as oxidation and protodeboronation during traditional Pd-mediated coupling conditions remained intact using the orthogonal photoredox/Ni cross-coupling protocols (Figure 1.10).[32]

Initially, benzyltrifluoroborate was coupled with aryl bromides bearing the C(sp^2)-hybridized organoboron *N*-methyliminodiacetic acid (BMIDA) and 1,8-diaminonaphthalene (BDAN) subunits to afford the desired products in 59% and 73% yields, respectively. Tricoordinate boronate reagents were also successfully coupled and then immediately oxidized to the corresponding alcohol, because the intermediates were found to be unstable when subjected to column chromatography.

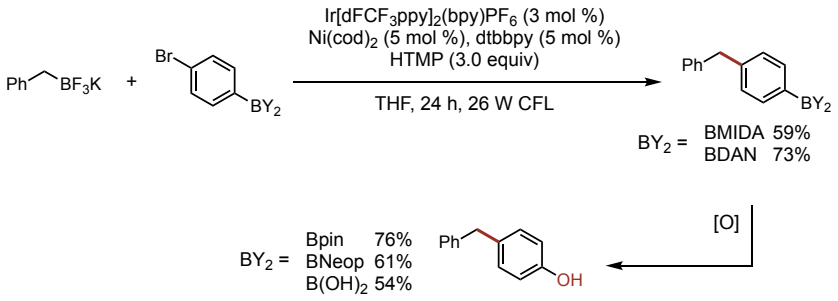

Figure 1.10. Cross-coupling with boronate aryl bromides for further derivatization.

To demonstrate the utility of this orthogonal cross-coupling strategy, 2-(4-bromo-3-chlorophenyl)-4,4,5,5-tetramethyl-1,3,2-dioxaborolane was subjected to a series of modular functionalizations, beginning with photoredox/Ni dual-catalytic cross-coupling, to provide the C(sp^3)–C(sp^2) coupled product. The crude product was then directly diverted into either Suzuki or 1,4-addition manifolds that chemoselectively activated the sp^2-hybridized organoboron lynchpin. Additional elaboration of the aryl chloride by Buchwald-Hartwig or Suzuki cross-couplings provided expedient access to diversified products without the need for protecting group manipulations (Figure 1.11).

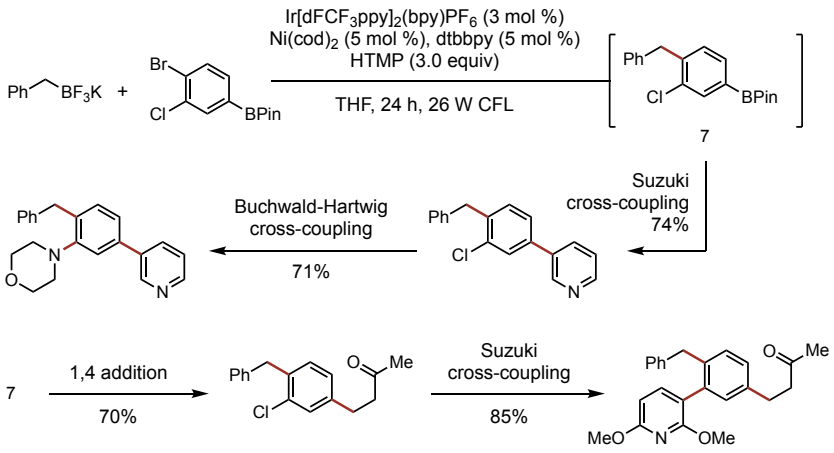

Figure 1.11. Iterative cross-coupling with aryl boronate.

A similar, iterative strategy was pursued with ammonium silicates to provide alkylated aryl- and heteroaryl boronates, providing a complementary approach (Figure 1.12).[33] $[Ru(bpy)_2](PF_6)_2$, a significantly less expensive photocatalyst ($138/g) than the commonly used $Ir[dFCF_3ppy]_2(bpy)PF_6$ (>$1,000/g), was chosen because alkyl ammonium silicates possess lower oxidation potentials (Ered = +0.75 V vs SCE). Comparable yields were also obtained when the organophotocatalyst 4CzIPN ($6/gram) was utilized, which further improved the sustainability of the reaction. An additional advantage to employing ammonium silicate radical precursors with lower oxidation potentials is the incorporation of primary, non-benzylic radicals into the dual cross-coupling manifold. Examination of the scope of the electrophilic, iterative cross-coupling partners revealed that a variety of $C(sp^2)$-hybridized boronate esters were tolerated under the optimized reaction conditions, providing the target products in moderate to excellent yields.

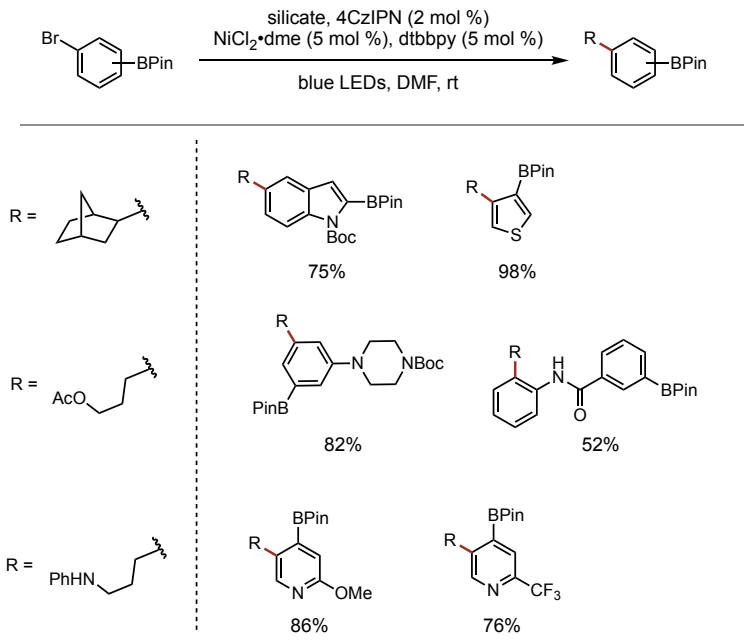

Figure 1.12. Alkylsilicate coupling with aryl boronates.

The standard conditions for silicate coupling also proved to be fruitful for iterative C(sp^3)–C(sp^2) Suzuki cross-couplings. The crude, alkylated material could be carried directly on to the next step to provide multi-functionalized molecules in good yields (Figure 1.13). When a bromo-substituted arylboronic acid was used, the catechol boronate ester that formed during the alkylation step could also be carried directly into a subsequent Suzuki reaction without purification.

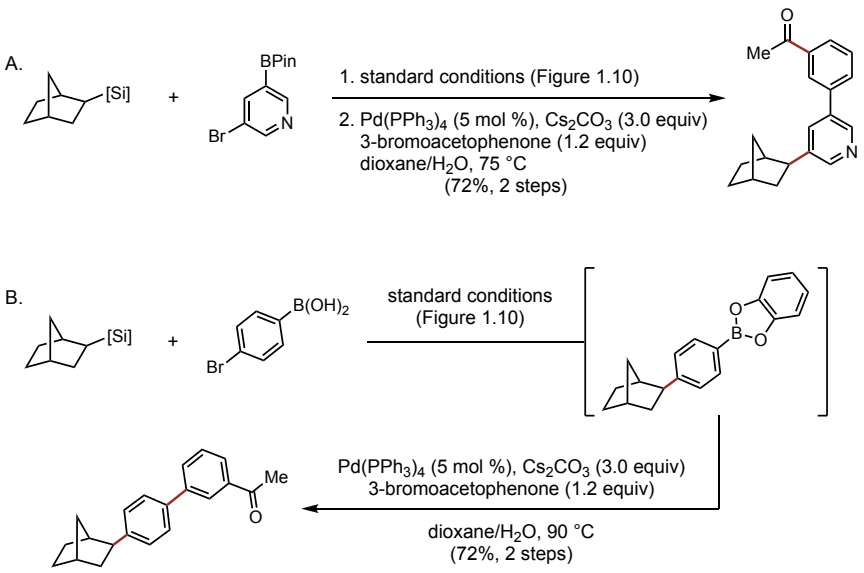

Figure 1.13. One-pot iterative cross-coupling.

Alternatives to aryl halide electrophiles were also pursued for incorporation into dual catalytic cross-coupling.[34] Aryl sulfonates, which are derived from different chemical feedstocks (phenols) than the corresponding halides, were examined because of their ability to undergo low-temperature oxidative addition toward ligated nickel species.[35] Preliminary screening revealed that 4-acetylphenyltrifluoromethanesulfonate readily participated in $C(sp^2)$–$C(sp^3)$ cross-coupling with a variety of primary and secondary alkylbis(catecholato)silicates under conditions similar to those previously reported.[14] Exploration of the aryl triflate scope revealed that although electron-neutral and electron–poor triflates provided product in acceptable yields, the use of electron-rich triflates resulted in lower reactivity (Figure 1.14).

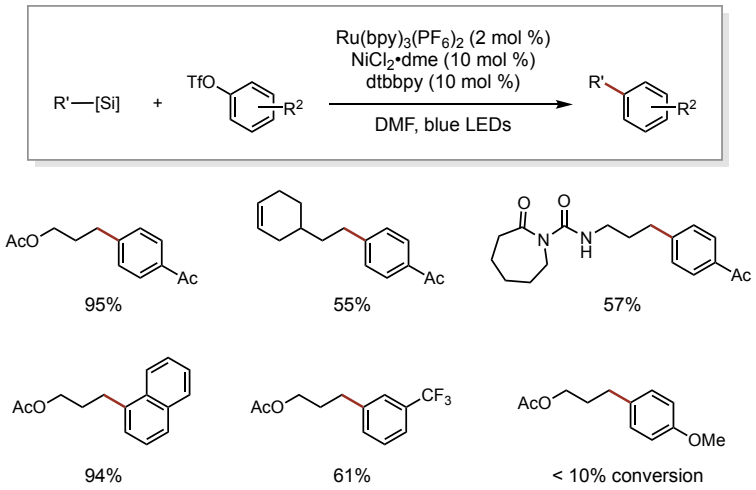

Figure 1.14. Alkysilicate coupling with aryl triflates.

Aryl tosylates and -mesylates, which display improved bench stability compared to aryl triflates, were also successfully coupled, although lower yields were observed. Additionally, the relative rates of oxidative addition of aryl bromides and aryl triflates onto Ni(I) was also investigated using 8 (Figure 1.15). In difunctionalized substrates, alkylation occurred exclusively at the position bearing the bromide, indicating that oxidative addition of aryl bromides is more rapid. This enables chemoselective transformations of poly-functionalized starting materials using dual catalysis.

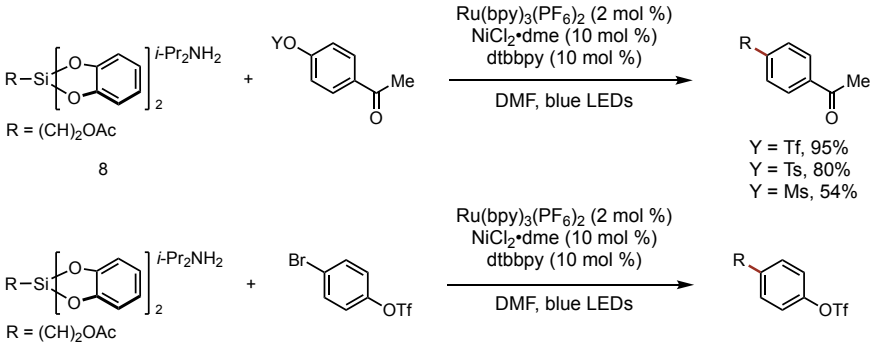

Figure 1.15. Chemoselective cross-coupling of alkysilicates with aryl bromides.

Further efforts to expand the scope of halide electrophiles in the dual catalytic manifold beyond aryl/heteroaryl moieties led to the examination of acyl chlorides. Although acyl halides are known to react with organoboron "ate" complexes in an intermolecular fashion, either air-sensitive trialkylboranes or pyrophoric/toxic additives under forcing conditions were required.[36] In contrast, we recognized that the extremely mild conditions required to activate alkyltrifluoroborates for incorporation into Ni-catalyzed cross-coupling would allow the direct synthesis of alkyl ketones containing sensitive functional groups from bench stable starting materials.[37]

A variety of α-alkoxymethyltrifluoroborates containing versatile synthetic lynchpins (i.e., alkenes, alkynes, amines) and heterocycles were readily coupled under the optimized reaction conditions to provide aliphatic α-alkoxy ketones and amides (Figure 1.16).[39a] Secondary alkyltrifluoroborates were also readily transformed into the corresponding ketones under similar reaction conditions.[39b] For both sets of trifluoroborate coupling partners, the acyl chloride was also varied to afford access to various dialkyl ketones. Lastly, it was demonstrated that the use of (4R)-4-benzyl-2-oxazoline for the cross-coupling led to the formation of an enantioenriched ketone in modest er (81:19).

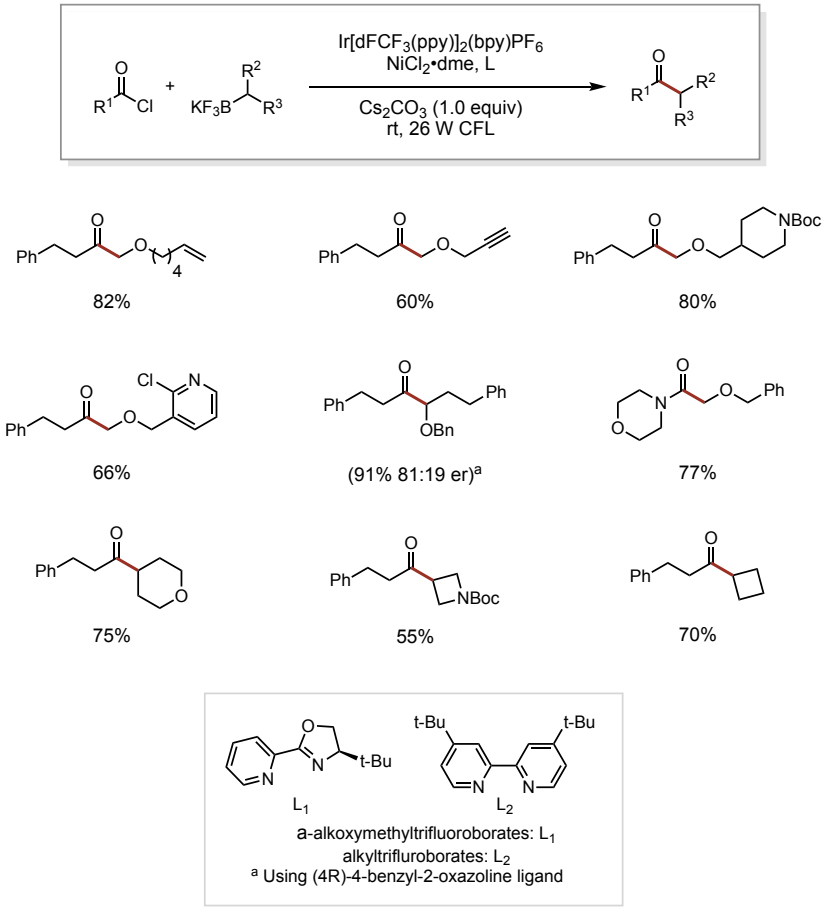

Figure 1.16. Alkylation of acyl chlorides.

Our group hoped to access additional chemical space via the development and implementation of novel radical precursors. Recognizing several potential drawbacks of alkyltrifluoroborates (e.g., formation of BF_3) and silicates (poor atom economy, limited commercial availability of silanes), we initially focused our attention on the incorporation of readily available feedstock chemicals bearing desirable functional groups (Figure 1.17).

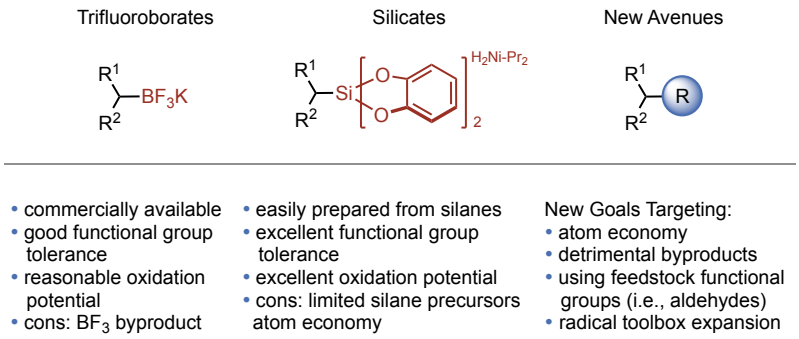

Figure 1.17. Exploring new radical precursors.

Currently, there are 12,000+ commercially available aldehydes, underlining their potential as an important chemical feedstock for the generation of radical precursors.[38] Nishibayashi and co-workers reported the synthesis of 4-alkyl-1,4-dihydropyridines for use as latent radicals from various aldehydes.[39] As shown in Figure 1.18, the Hantzsch ester presumably undergoes a single-electron oxidation to the radical cation followed by homolysis of the C–C bond to form an alkyl radical. The resulting benzylic radicals were then captured by a variety of 1,4-dicyanobenzenes. Additionally, the Nishibayashi group moved beyond benzylic radicals to heteroatom-stabilized, carbon-centered radicals (i.e., α-alkoxy, α-amino subunits).

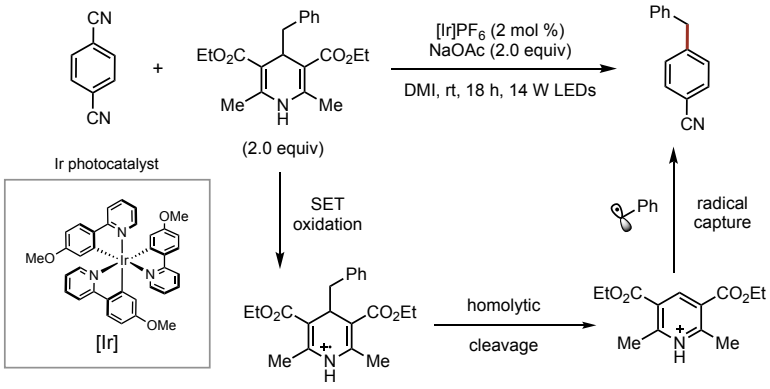

Figure 1.18. Alkylating dicyanobenzene with 1,4-dihydropyridines.

We surmised that the alkyl 1,4-dihydropyridines (DHPs) could also serve as an alternative radical source in a Ni/photoredox dual catalytic manifold.[40] A plausible mechanism is outlined in

Figure 1.19. To initiate the cycle, the DHP undergoes a single-electron oxidation followed by concomitant C–C bond cleavage, forming a radical intermediate. As described above, the radical is captured by ligated Ni(0), which then undergoes oxidative addition toward the aryl bromide to provide a Ni(III) intermediate. Reductive elimination to provide the product and Ni(I) is followed by reduction of Ni(I) to Ni(0), closing both catalytic cycles.

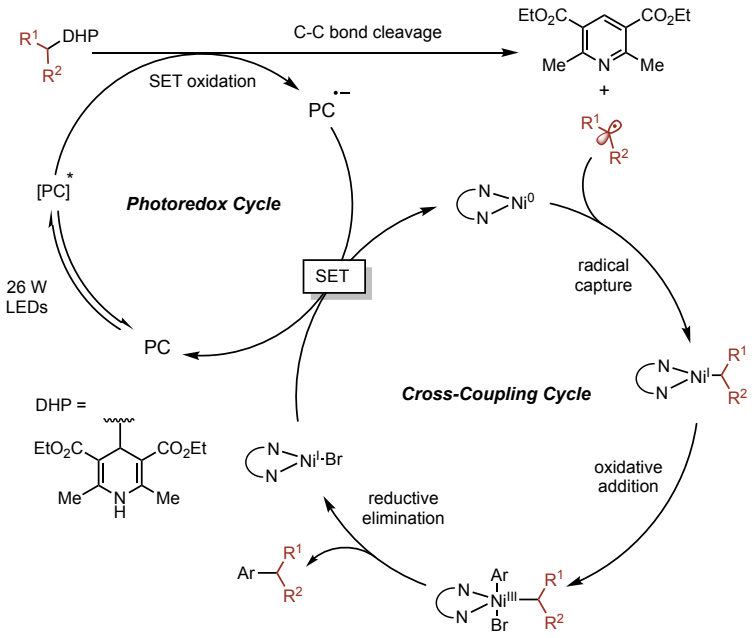

Figure 1.19. Proposed mechanism with 1,4-dihydropyridines as latent radicals.

During the optimization process, we discovered that acetone was a suitable solvent for the reaction, and additives were not required because the DHP pyridine byproduct is unreactive under the dual catalytic conditions. Additionally, the iridium photocatalyst was replaced with the inexpensive organophotocatalyst 4CzIPN. To simplify the reaction conditions even further, NiCl2 dme was pre-complexed with dtbbpy to form the bench- and air-stable nickel pre-catalyst Ni(dtbbpy)Cl_2 $4H_2O$ on multi-gram scale.

With dioxolane DHP in hand, a wide variety of aryl and heteroaryl bromides was examined. A few notable examples are showcased in Figure 1.20. A variety of DHPs and

(hetero)aryl bromides were also explored. Benzothiophenes proved to be robust partners with unstabilized secondary radicals. Electron-poor furans were also successfully coupled in decent yield with cyclohexyl DHP. Surprisingly, alkene-containing DHPs afforded excellent yields with acyclic and cyclic systems. 3-Bromo-5-chloropyridine was coupled with benzyl DHP in 42% yield, affording the chloride functional group for further derivatization.

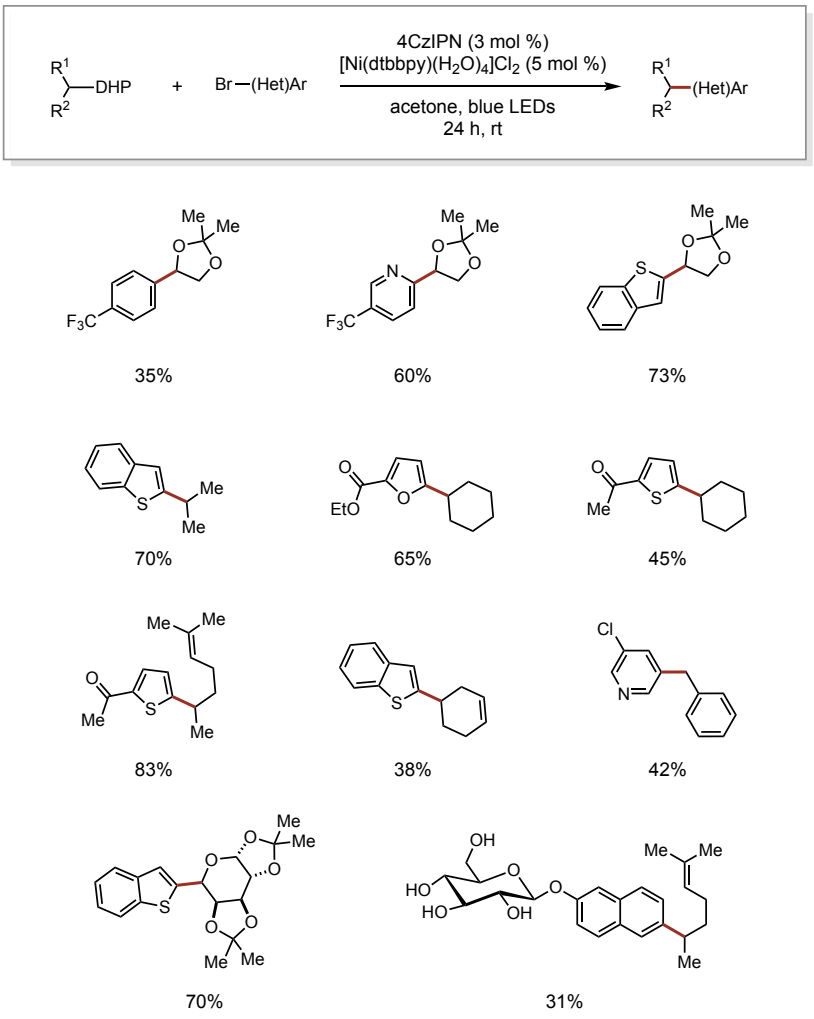

Figure 1.20. Photoredox/Ni cross-coupling with 1,4-dihydropyridines.

The robust nature of the transformation was demonstrated by using a protected carbohydrate derivative. This particular example, in which the product was isolated in 70% yield, demonstrates the complementarity between the single electron protocol and processes based on

traditional organometallic species. In the latter, any metalation on the carbohydrate core would lead to rapid β-elimination of the neighboring alkoxide. Photoredox/Ni dual catalysis thus provides rapid entry to novel chemical space. Finally, unprotected glycoside moieties were tolerated, albeit in modest yield. Previous methods based on organometallic nucleophiles would typically require protection of the free hydroxyl groups before coupling, followed by a global deprotection.

Alkyltrifluoroborates, -silicates, and -DHPs exhibit many desirable traits as partners in photoredox/Ni dual catalysis, but the coupling of pre-functionalized, redox-active substrates is inherently limited by atom, step, and redox economy. For example, one must adjust the redox profile of unreactive species (e.g., boronic acids, silanes, or aldehydes) into their active forms, adding mass and molecular complexity that is ultimately lost upon coupling. In principle, direct functionalization of a C(sp3)–H bond would provide optimal atom economy while reducing step and redox inefficiency en route to $C(sp^3)$–$C(sp^2)$ coupling products.[41] Efforts toward general approaches to Ni-catalyzed $C(sp^3)$–H arylation in the literature are limited by extreme conditions (greater than 100 °C), peroxide reagents/oxidants that often lead to unwanted byproducts, and the need for directing groups.[42] Given that photoredox catalysis is a powerful tool for accessing reactive intermediates demonstrated by numerous synthetic groups,[43] we sought to apply photoredox/Ni dual catalysis to the difficult challenge of effecting $C(sp^3)$–H arylation at room temperature.[44]

In the context of photoredox catalysis, $C(sp^3)$–H functionalization has been achieved through oxidation of N,N-dialkylanilines,[4i,45] because the formation of a nitrogen-centered radical cation significantly weakens the adjacent $C(sp^3)$–H bond. Our group envisioned targeting redox-inactive $C(sp^3)$–H bonds, from which we hoped to form alkyl radicals that could participate in dual catalytic systems. For a C–H bond to replace a stoichiometric, redox-active radical precursor within the established mechanism, an additive would need to serve two roles: (1) act as a single-electron reductant of the excited-state photocatalyst and (2) generate an alkyl radical. To accomplish this,

we sought a mediator that could serve as an electron donor as well as facilitate radical generation via H-atom transfer from C(sp^3)–H bonds. Although our group focused on diaryl ketones to facilitate direct arylation of C(sp^3)–H bonds, the MacMillan group identified quinuclidine derivatives as highly efficient additives for a related transformation.[46]

Based on the well-established reactivity of excited state diaryl ketone diradicals, which form ketyl radicals upon hydrogen atom abstraction (HAT) from both activated and unactivated C(sp^3)–H bonds,[47] we envisioned a tricatalytic mechanism for net C-H arylation (Figure 1.21). Early studies employing THF as H-atom donor and solvent with one equivalent of benzophenone under standard coupling conditions afforded the desired product, albeit in moderate conversion. Addition of Brønsted bases significantly improved conversion, presumably by quenching the HBr byproduct. Additional optimization provided adequate conditions and represented an unprecedented example of directing group-free, Ni-catalyzed C(sp^3)–H arylation at room temperature. Control studies confirmed the necessity for nickel catalyst, photocatalyst, and light, but we were surprised to discover significant conversion to the desired product without the diaryl ketone HAT mediator. The ability of iridium and nickel to co-catalyze C(sp^3)–H arylation was concurrently discovered by Doyle, who developed conditions to couple aryl chlorides using higher loadings of a Ni(0) source and a stronger phosphate base.[48]

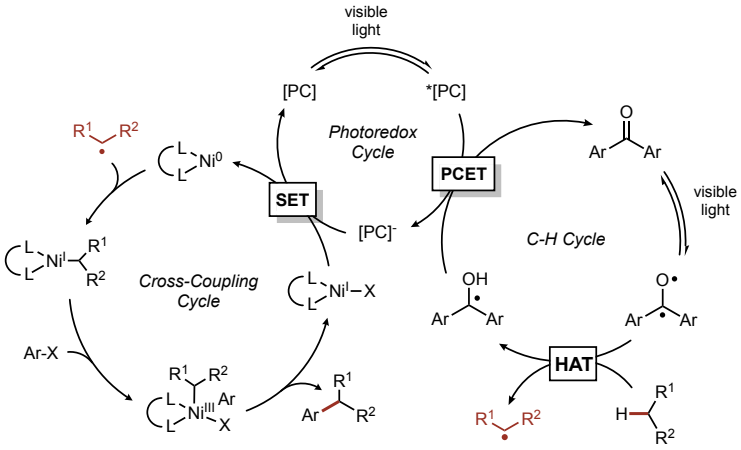

Figure 1.21. Initial mechanistic proposal.

Although control studies demonstrated our initial mechanistic hypothesis was not responsible for the observed reactivity, we opted to examine the reaction scope, hoping that the limitations therein would provide insight into the nature of the bond-activating species. Unfortunately, the alkylation scope with respect to C(sp^3)–H substrates was narrow, requiring activated partners to be used as solvent. Ethereal solvents, such as THF, 1,4-dioxane, DME, and Et_2O, were effective (Figure 1.22). Arylation of C(sp^3)–H bonds adjacent to nitrogen- and sulfur-based heterocycles was also observed, with *N*-methylpyrrolidinone and tetrahydrothiophene undergoing α-arylation. Furthermore, toluene was effectively coupled at the benzylic position. Although the scope of the reaction with respect to the C(sp^3)–H is unquestionably specific, it is also surprisingly effective given the stringent requirements for the substrate-solvent to: (1) donate an activated C(sp^3)–H, (2) effectively solvate the reaction mixture, and (3) be sufficiently volatile for removal upon completion. Similar limitations were observed by Doyle, though they reported three examples of direct C(sp^3)–H coupling with 10 equiv of H-atom donor in benzene, including an appreciable reactivity of the unactivated C(sp^3)–H bonds of cyclohexane.

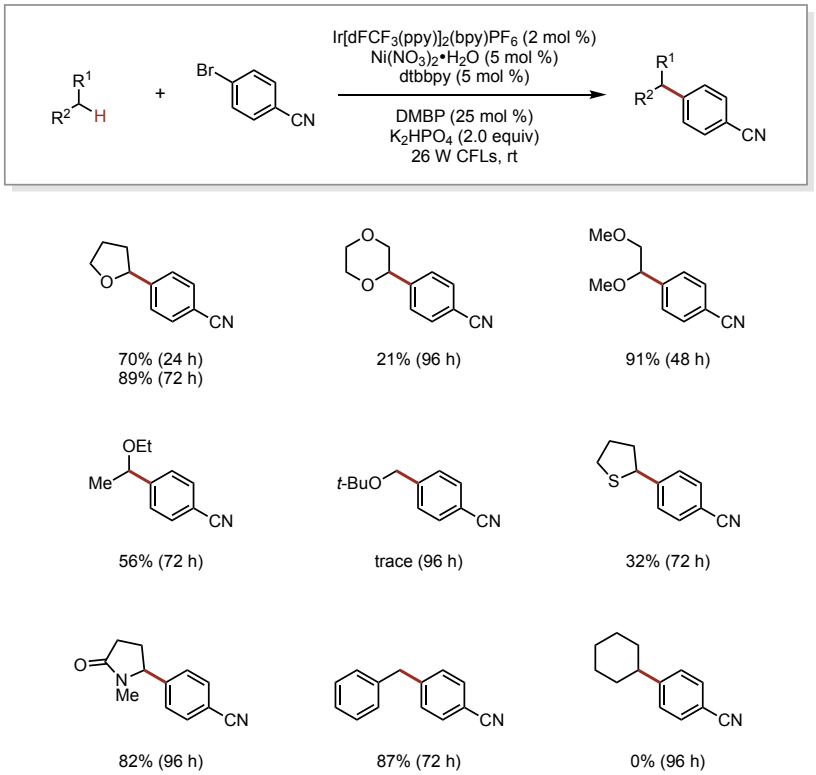

Figure 1.22. C–H functionalization via photoredox/Ni coupling.

Approaching reaction development with an incomplete or inaccurate mechanistic understanding greatly limits the steps that can be taken to improve upon underlying limitations. Thus, mechanistic studies were necessary to develop a better understanding of the unexpected reactivity in the absence of a diaryl ketone. A representative transformation was thus carried out in a 1:1 mixture of THF:d_8-THF, and this reaction displayed a kinetic isotope effect of 6:1, which is indicative of a thermodynamically-neutral H-atom transfer[49] rather than formal C–H activation by a metal center. As a result of the observed KIE and the need for activated C(sp^3)–H bonds, we suspected a bromide radical, which is capable of activating weak C(sp^3)–H bonds, was generated under the photocatalytic conditions (Figure 1.23).

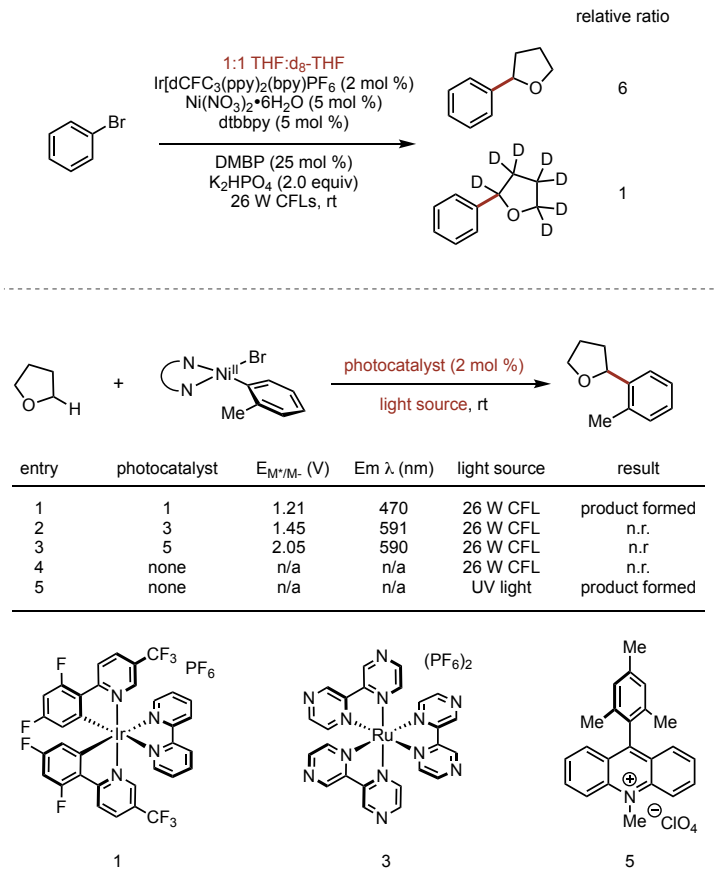

Figure 1.23. Kinetic isotope effect studies (top) and energy transfer experiments (bottom).

We first speculated that the Ni(II) oxidative addition intermediate could be oxidized to a Ni(III) state by the iridium photocatalyst. The C(sp^3)–H activation steps would occur via (1) homolysis of the Ni(III)–Br bond to generate a bromine radical, (2) H-atom transfer by the resulting bromine radical, and (3) alkyl radical addition to Ni(II). To provide support for this hypothesis, a series of photocatalysts were compared with higher oxidation potentials than the iridium photocatalyst. We first confirmed that **1** led to product and that no product formed under visible light excitation in the absence of photocatalyst. Next, to our surprise, no product was observed using the highly oxidizing ruthenium and acridinium photocatalyst 3 and 5, respectively. This suggests that simple oxidation of the Ni(II) complex by a photocatalyst may not be sufficient to explain the observed C(sp^3)–H arylation.

An alternative explanation is a triplet-triplet energy transfer facilitated by photocatalyst 1, which has a higher triplet energy than **3** and **5** based on a comparison of their emission wavelengths (Figure 1.24). To test this new hypothesis, the Ni(II) complex was subjected to UV-B irradiation with emission wavelengths between 290–315 nm. Indeed, as shown in entry 5, product was observed. These results suggest that a Ni(II) excited state, which forms in the absence of an oxidant, is sufficient to facilitate the observed C(sp^3)–H arylation. As a result, a mechanism based upon energy transfer was favored.

We proposed that irradiation with UV light could promote Ni to a high-energy state that relaxes and undergoes intersystem crossing to a Ni(II) triplet that eliminates a halide radical.[50] Alternatively, the same Ni(II) excited state could be reached through a photocatalytic process: (1) photocatalyst excitation by visible light, (2) efficient intersystem crossing by the photocatalyst, and (3) triplet-triplet energy sensitization of the Ni(II) oxidative addition intermediate by a sufficiently high energy photocatalyst triplet state (Figure 1.24). Importantly, in the energy transfer scenario, the operative Ni excited state would be inaccessible in the presence of photocatalysts with insufficiently energetic triplet states (such as those exhibited by photocatalysts 3 and 5) or by irradiation with inadequately energetic wavelengths of light (i.e., visible light). Preliminary computational work shows that the formation of a formal Ni(II) triplet state would elongate the Ni-Br bond and also result in transfer of electron density from the Ni center to the ligand, resulting in an excited-state species that may exhibit some similarities to the formal Ni(III) intermediates that are commonly invoked in photoredox/Ni cross-coupling.

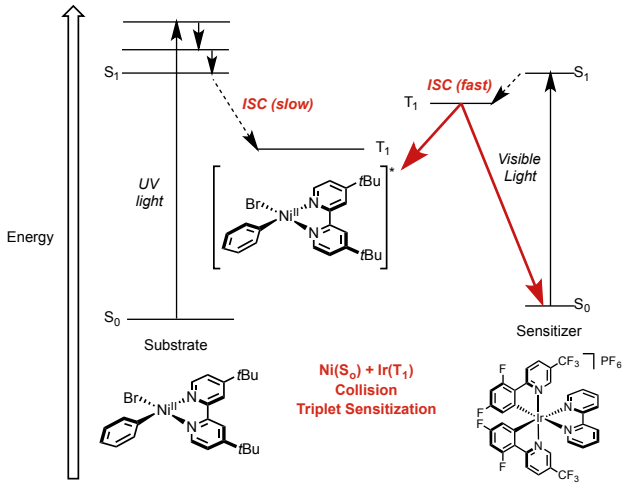

Figure 1.24. Jablonski diagram with proposed energy transfer.

Although we favor a mechanism based on energy transfer, we are admittedly unable to rule out the electron transfer-based mechanism favored in concurrently published work by Doyle et al.[51] It should be noted that the Doyle group has shown that Ni(II) oxidative addition complexes have redox potentials within the oxidation window and also display Stern-Volmer quenching of the iridium photocatalyst. However, Stern-Volmer quenching is insufficient to distinguish between energy and electron transfer processes. Transient absorption spectroscopic studies may be able to address this question[51] and provide a stronger basis for further development. Importantly, the mechanistic difference may strongly bias efforts in catalyst development to improve the efficiency of these reactions. The prevailing focus of photocatalyst development on redox potentials (SET) reflects the more typical mode of activation in organic synthesis, but optimizing for less commonly invoked energy transfer processes is largely underdeveloped.[43] Recently, Weaver et al. studied the important relationship between catalyst structure and cis/trans isomerization of alkenes via energy transfer, but energy transfer[52] between metals is particularly challenging given the lack of systems thought to operate by this mechanism and the difficulty in studying catalytic intermediates that may be transient in nature.[53]

The proposed mechanism is thus depicted in Figure 1.25. Ni(0) **9** undergoes oxidative addition with the aryl bromide followed by energy transfer (EnT) to form an excited Ni(II) complex **10**. We surmise that complex **10** can facilitate C–H abstraction from THF to form intermediate **11**, which can then undergo reductive elimination to form the corresponding product. It should be noted that the transformation from **10** to **11** is currently under investigation using computational methods. Currently, the KIE studies suggest the formation of bromine radical followed by a HAT process to form the alkyl radical. Alternatively, there is the possibility of a concerted step involving a four-membered transition state structure that is also consistent with experimental data.

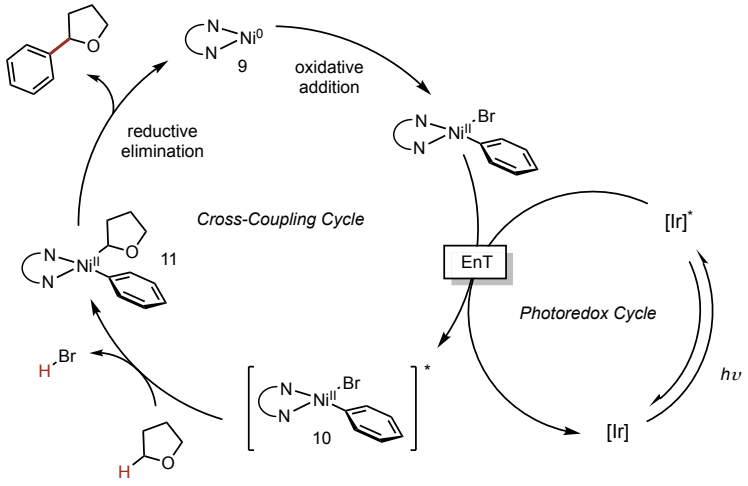

Figure 1.25. Proposed energy transfer mechanism.

Although functionalizing C(sp^3)–H bonds has historically been a challenging transformation, these preliminary results may provide a platform for further studies involving less reactive C–H bonds. Toward this end, the ability to channel visible light energy selectively into synthetically useful C(sp^3)–H activation reactions through elementary radical H-atom transfer steps has already enabled a recent, rapid growth in methods for functionalization of unactivated C–H bonds at room temperature.[54] Seeing the value of catalytic radical generation in various cross-coupling reactions, we next sought to apply the same principle to other transformations wherein the stoichiometric generation of radicals provided sub-optimal outcomes. Protocols developed

within these previous paradigms typically resulted in the use of huge excesses of radical precursors and radical-generating reagents, which we were able to avoid using photoredox-generated radicals.

The expansion of the chemical toolbox to include mild, bench-stable radical precursors as alkylating reagents under photoredox conditions was considered an attractive alternative to organometallics utilized in other C–C bond-forming reactions. The reaction of Grignard and organolithium reagents with C=O and C=N electrophiles has extensive value, but the instability and functional group intolerance of these highly reactive organometallics has always framed their use.[55] To address this issue, we imagined that nucleophilic alkyl radicals generated via photoredox catalysis could serve as mild alkylating agents to facilitate Grignard-type additions to electrophilic imines.[56] Previously reported radical-based approaches in which the radicals were generated stoichiometrically relied on conditions that were far from ideal [e.g., large excesses of flammable Et_3B/O_2 initiators, radical precursors (typically alkyl iodides), and reductants such as tin reagents or Zn], owing to the byproducts formed upon generation of the radicals.

Further, although the addition of α-heteroatom-stabilized radicals to imines has been reported, we recognized that silicate radical precursors would provide access to a broader range of alkyl radicals. A variety of nitrogen-substituted imines were transformed into the corresponding α-aryl-α-alkyl secondary amines utilizing alkyl radicals generated from bis-(catecholato)silicates. The transformation occurred readily under mild, redox neutral conditions without additives. The relatively low oxidation potentials of the silicate radical precursors facilitated the use of the organic photocatalyst 4CzIPN instead of Ru or Ir species, rendering the entire process metal-free. A variety of primary and secondary alkyl radicals bearing synthetically useful functional groups were readily intercepted by electronically varied α-(hetero)aryl imines under the optimized reaction conditions (Figure 1.26).

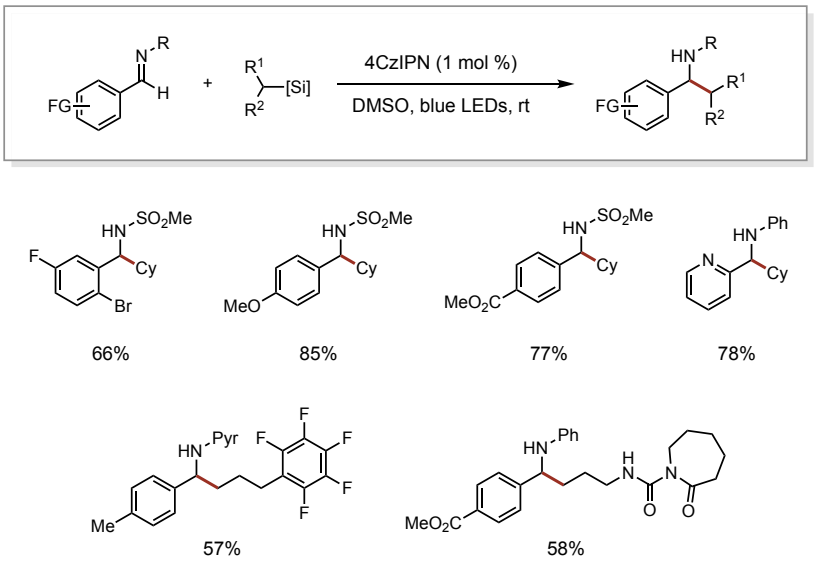

Figure 1.26. Alkylation of imines with alkylsilicates.

We also explored the incorporation of readily available organophotocatalysts in allylation and alkenylation reactions.[57] Alkenyl sulfones were employed as electrophilic reagents to effect the transition metal-free alkenylation and allylation of Boc-protected potassium α-aminomethyltrifluoroborates. The inexpensive sodium salt of the organic photocatalyst Eosin Y (E_{red} = +0.83 V vs SCE) was found to be a suitable oxidant for potassium α-pyrrolidinyltrifluoroborate (E_{red} = +0.78 V vs SCE) under the reaction conditions developed. Conversely, the related cesium carboxylate (E_{red} = +0.95 V vs SCE) required the use of an iridium photocatalyst. Exploring the scope of the alkenyl sulfones revealed that stabilization of the radical intermediates following radical addition was required. Various electron-neutral, electron-withdrawing, and electron-donating substituents on the aryl ring were well tolerated under the reaction conditions (Figure 1.27). Protected homoallylic amines bearing styrene and acrylate groups were also generated from the corresponding allylic sulfones, although lower yields were observed.

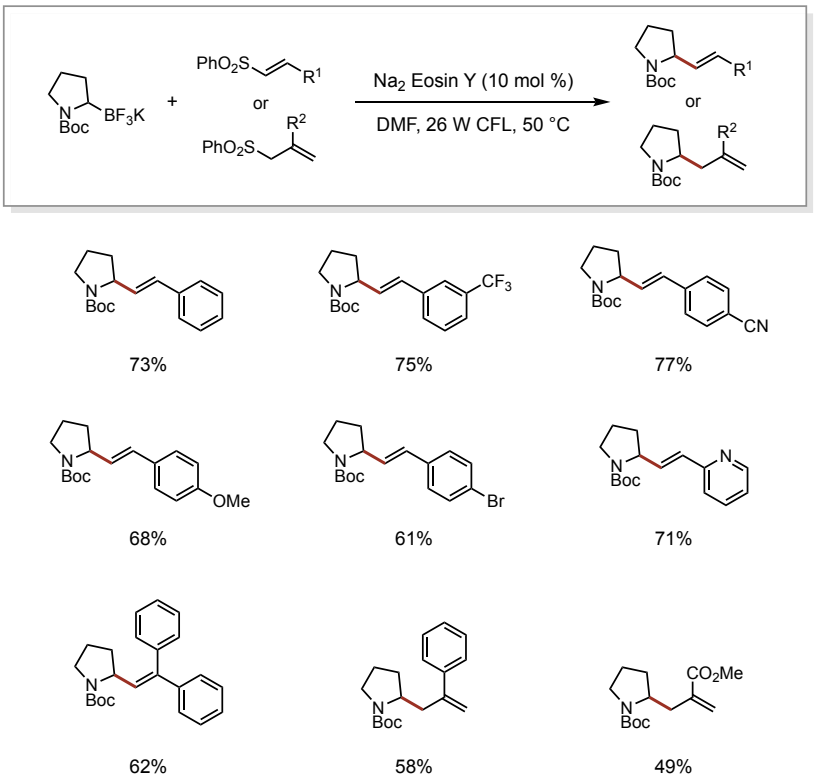

Figure 1.27. Alkylation of allylic sulfones with α-aminomethyltrifluoroborates.

A wide range of primary and secondary alkyltrifluoroborates was also incorporated into an organic photocatalyst-mediated deboronative cyanation reaction using the highly oxidizing MesAcr+ photocatalyst and tosyl cyanide (TsCN) as a radical trap (Figure 1.28). Classically, alkyl nitriles are synthesized via S_N2 displacement of halides with nucleophilic cyanide sources.[58] As a result, the formation of primary nitriles is favored over secondary and tertiary analogs. Based on the coupling of alkyltrifluoroborates with alkenyl and allylic sulfones, we sought to capture alkyl radicals (generated from photoinduced oxidation of alkyltrifluoroborates) with TsCN. By proceeding through radical intermediates, we anticipated that regiospecific cyanation should occur with mechanistic preference for less electrophilic carbon centers. The optimized reaction conditions provided access to primary and secondary as well as α-alkoxy-, γ-, β-, and α-amino alkyl nitriles under extremely mild reaction conditions. Notably, cyanation of an α-alkoxy alkyltrifluoroborate afforded a protected cyanohydrin, which can be difficult to synthesize by other methods given the

reversibility of cyanohydrin formation.[59] A plausible mechanism is presented in Scheme 28. A visible light-excited organic catalyst oxidizes the potassium alkyltrifluoroborate via a single-electron oxidation to provide an alkyl radical. The resulting radical then forms a new C–C bond in the presence of a suitable sulfonyl coupling partner while expelling a sulfonyl radical. The resultant sulfonyl radical is then reduced by one electron to close the catalytic cycle.[60]

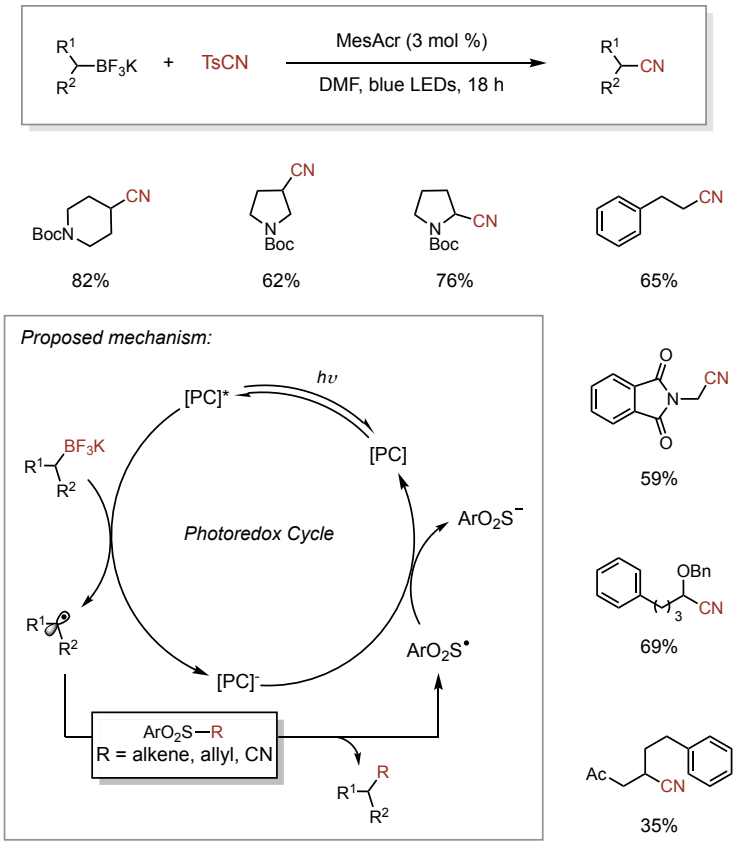

Figure 1.28. Direct cyanation of alkyltrifluoroborates.

1.3 Conclusion and Future Outlook

Since establishing photoredox/Ni dual catalysis in 2014, our group has successfully modified both radical precursors and electrophiles in further efforts to expand access to underexplored chemical space. Beyond aryl bromides, our group has demonstrated triflates, tosyl cyanide, imines, acid chlorides, and sulfones as feasible "electrophilic" partners in both dual

catalytic and metal-free manifolds. Additionally, since the initial demonstration of silicates as complementary radical precursors, a wider range of functionally rich alkyl radicals have been successfully cross-coupled. Although alkyltrifluoroborates and -silicates are fantastic reagents, step and atom economy is poor. Furthermore, the photoredox/Ni dual catalytic mechanism has led to a redefinition of alkyl coupling partners from traditional organometallic nucleophiles to redox-active radical precursors. Therefore, our group has searched for routes to access radical precursors from readily available functional groups. As demonstrated with DHPs (derived from aldehydes), feedstock functional groups hold great potential as latent radicals with wide commercial availability. Although DHPs are often more easily accessed than alkyltrifluoroborates and -silicates, there is room for improvement in atom economy. In related work, we uncovered an energy-transfer pathway targeting activated C(sp^3)–H bonds, which may inspire further related reaction design.

Finally, these studies bear witness to the value of generating highly reactive radical intermediates catalytically, in a tightly orchestrated, controlled manner to avoid deleterious side-reactions and lead to processes that are more efficacious and sustainable than those in which the radicals are created en mass by stoichiometric protocols. Herein, personal efforts in the field of photoredox catalysis are described. In addition to work accomplished in the area of dual catalysis, methods development in the area of C–H alkylation are described in addition to the development of late-stage functionalization protocols.

1.4. References

[1] (a) Tellis, J. C.; Kelly, C. B.; Primer, D. N.; Jouffroy, M.; Patel, N.; Molander, G. A. *Acc. Chem. Res.* **2016**, *49*, 1429. (b) Prier, C. K.; Rankic, D. A.; MacMillan, D. W. C. *Chem. Rev.* **2013**, *113*, 5322. (c) Tucker, J. W.; Stephenson, C. R. J. *J. Org. Chem.* **2012**, *77*, 1617. (d) Skubi, K. L.; Blum, T. R.; Yoon, T. P. *Chem. Rev.* **2016**, *116*, 10035.

[2] Cano-Yelo, H.; Deronzier, A. *Tetrahedron Lett.* **1984**, *25*, 5517.

[3] (a) Ischay, M. A.; Anzovino, M. E.; Du, J.; Yoon, T. P. *J. Am. Chem. Soc.* **2008**, *130*, 12886. (b) Du, J.; Yoon, T. P. *J. Am. Chem. Soc.* **2009**, *131*, 14604. (c) Ischay, M. A.; Lu, Z.; Yoon, T. P. *J. Am. Chem. Soc.* **2010**, *132*, 8572. (d) Yoon, T. P.; Ischay, M. A.; Du, J. *Nat. Chem.* **2010**, *2*, 527. (e) Hurtley, A. E.; Cismesia, M. A.; Ischay, M. A.; Yoon, T. P. *Tetrahedron* **2011**, *67*, 4442. (f) Lin, S.; Ischay, M. A.; Fry, C. G.; Yoon, T. P. *J. Am. Chem. Soc.* **2011**, *133*, 19350. (g) Du, J.; Ruiz Espelt, L.; Guzei, I. A.; Yoon, T. P. *Chem. Sci.* **2011**, *2*, 2115. (h) Lu, Z.; Shen, M.; Yoon, T. P. *J. Am. Chem. Soc.* **2011**, *133*, 1162.

[4] (a) Nagib, D. A.; Scott, M. E.; MacMillan, D. W. C. *J. Am. Chem. Soc.* **2009**, *131*, 10875. (b) Shih, H. − W.; Vander Wal, N.; Grange, R. L.; MacMillan, D. W. C. *J. Am. Chem. Soc.* **2010**, *132*, 13600. (c) Pham, P. V.; Nagib, D. A.; MacMillan, D. W. C. *Angew. Chem., Int. Ed.* **2011**, *50*, 6119. (d) McNally, A.; Prier, C. K.; MacMillan, D. W. C. *Science* **2011**, *334*, 1114. (e) Nagib, D. A.; MacMillan, D. W. C. *Nature* **2011**, *480*, 224.

[5] (a) Narayanam, J. M. R.; Tucker, J. W.; Stephenson, C. R. J. *J. Am. Chem. Soc.* **2009**, *131*, 8756. (b) Tucker, J. W.; Narayanam, J. M. R.; Krabbe, S. W.; Stephenson, C. R. J. *Org. Lett.* **2010**, 12, 368. (c) Condie, A. G.; Gonzalez-Gomez, J. − C.; Stephenson, C. R. J. *J. Am. Chem. Soc.* **2010**, *132*, 1464. (d) Tucker, J. W.; Nguyen, J. D.; Narayanam, J. M. R.; Krabbe, S. W.; Stephenson, C. R. J. *Chem. Commun.* **2010**, *46*, 4985. (e) Furst, L.; Matsuura, B. S.; Narayanam, J. M. R.; Tucker, J. W.; Stephenson, C. R. J. *Org. Lett.* **2010**, *12*, 3104. (f) Narayanam, J. M. R.; Stephenson, C. R. J. *Chem. Soc. Rev.* **2011**, *40*, 102. (g) Dai, C.; Narayanam, J. M. R.;

Stephenson, C. R. J. *Nat. Chem.* **2011**, *3*, 140. (h) Nguyen, J. D.; Tucker, J. W.; Konieczynska, M. D.; Stephenson, C. R. J. *J. Am. Chem. Soc.* **2011**, *133*, 4160. (i) Tucker, J. W.; Narayanam, J. M. R.; Shah, P. S.; Stephenson, C. R. J. *Chem. Commun.* **2011**, *47*, 5040. (j) Furst, L.; Narayanam, J. M. R.; Stephenson, C. R. J. *Angew. Chem., Int. Ed.* **2011**, *50*, 9655. (k) Tucker, J. W.; Stephenson, C. R. J. *Org. Lett.* **2011**, *13*, 5468.

[6] (a) Yoon, T. P. *Acc. Chem. Res.* **2016**, *49*, 2307. (b) Hopkinson, M. N.; Tlahuext-Aca, A.; Glorius, F. *Acc. Chem. Res.* **2016**, *49*, 2261. (c) Arora, A.; Weaver, J. D. *Acc. Chem. Res.* **2016**, *49*, 2273. (d) Chatterjee, T.; Iqbal, N.; You, Y.; Cho, E. J. *Acc. Chem. Res.* **2016**, *49*, 2284. (e) Staveness, D.; Bosque, I.; Stephenson, C. R. J. *Acc. Chem. Res.* **2016**, *49*, 2295. (f) Majek, M.; von Wangelin, A. J. *Acc. Chem. Res.* **2016**, *49*, 2316. (g) Koike, T.; Akita, M. *Acc. Chem. Res.* **2016**, *49*, 1937. (h) Goddard, J. − P.; Ollivier, C.; Fensterbank, L. *Acc. Chem. Res.* **2016**, *49*, 1924. (i) Dumur, F.; Gigmes, D.; Fouassier, J. − P.; Lalevee, J. *Acc. Chem. Res.* **2016**, *49*, 1980. (j) Margrey, K. A.; Nicewicz, D. A. *Acc. Chem. Res.* **2016**, *49*, 1997. (k) Nakajima, K.; Miyake, Y.; Nishibayashi, Y. *Acc. Chem. Res.* **2016**, *49*, 1946. (l) Reiser, O. *Acc. Chem. Res.* **2016**, *49*, 1990. (m) Fabry, D. C.; Rueping, M. *Acc. Chem. Res.* **2016**, *49*, 1969. (n) Chen, J.-R.; Hu, X.-Q.; Lu, L.-Q.; Xiao, W.-J. *Acc. Chem. Res.* **2016**, *49*, 1911. (o) Morris, S. A.; Wang, J.; Zheng, N. *Acc. Chem. Res.* **2016**, *49*, 1957. (p) Jamison, C. R.; Overman, L. E. *Acc. Chem. Res.* **2016**, *49*, 1578. (q) Ghosh, I.; Marzo, L.; Das, A.; Shaikh, R.; König, B. *Acc. Chem. Res.* **2016**, *49*, 1566. (r) Gentry, E. C.; Knowles, R. R. *Acc. Chem. Res.* **2016**, *49*, 1546. (s) Hernandez-Perez, A. C.; Collins, S. K. *Acc. Chem. Res.* **2016**, *49*, 1557. (t) Pitre, S. P.; McTiernan, C. D.; Scaiano, J. C. *Acc. Chem. Res.* **2016**, *49*, 1320.

[7] Tellis, J. C.; Primer, D. N.; Molander, G. A. *Science* **2014**, *345*, 433.

[8] (a) Gutierrez, O.; Tellis, J. C.; Primer, D. N.; Molander, G. A.; Kozlowski, M. C. *J. Am. Chem. Soc.* **2015**, *137*, 4896. (b) Kalyani, D.; McMurtrey, K. B.; Neufeldt, S. R.; Sanford, M. S. *J. Am. Chem. Soc.* **2011**, *133*, 18566. (c) Sahoo, B.; Hopkinson, M. N.; Glorius, F. *J. Am. Chem. Soc.* **2013**, *135*, 5505.

[9] (a) Metal-Catalyzed Cross-Coupling Reactions, 2nd Ed.; de Meijere, A.; Diederich, F., Eds.; Wiley-VCH: Weinheim, Germany, 2004. (b) Hartwig, J. F. Organotransition Metal Chemistry: From Bonding to Catalysis; University Science: Sausalito, CA, 2010.

[10] For a thorough review of organophotocatalysts see: Romero, N. A.; Nicewicz, D. A. *Chem. Rev.* **2016**, *116*, 10075.

[11] Luo, J.; Zhang, J. *ACS Catal.* **2016**, *6*, 873.

[12] Fukuzumi, S.; Kotani, H.; Ohkubo, K.; Ogo, S.; Tkachenko, N. V.; Lemmetyinen, H. *J. Am. Chem. Soc.* **2004**, *126*, 1600.

[13] Molander, G. A.; Ellis, N. *Acc. Chem. Res.* **2007**, *40*, 275.

[14] Molander, G. A.; McKee, S. A. *Org. Lett.* **2011**, *13*, 4684.

[15] Darses, S.; Genet, J. − P. *Chem. Rev.* **2008**, *108*, 288.

[16] Primer, D. N.; Karakaya, I.; Tellis, J. C.; Molander, G. A. *J. Am. Chem. Soc.* **2015**, *137*, 2195.

[17] (a) Karakaya, I.; Primer, D. N.; Molander, G. A. *Org. Lett.* **2015**, *17*, 3294. (b) Amani, J.; Sodagar, E.; Molander, G. A. *Org. Lett.* **2016**, *18*, 732.

[18] El Khatib, M.; Serafim, R.; Molander, G. A. *Angew. Chem., Int. Ed.* **2016**, *55*, 254.

[19] Ryu, D.; Primer, D. N.; Tellis, J. C.; Molander, G. A. *Chem. - Eur. J.* **2016**, *22*, 120.

[20] (a) Nishigaichi, Y.; Suzuki, A.; Takuwa, A. *Tetrahedron Lett.* **2007**, *48*, 211. (b) Matsuoka, D.; Nishigaichi, Y. *Chem. Lett.* **2014**, *43*, 559.

[21] (a) Lévêque, C.; Chenneberg, L.; Corcé, V.; Ollivier, C.; Fensterbank, L. *Chem. Commun.* **2016**, *52*, 9877. (b) Corcé, V.; Chamoreau, L.-M.; Derat, E.; Goddard, J.-P.; Ollivier, C.; Fensterbank, L. *Angew. Chem., Int. Ed.* **2015**, *54*, 11414. (c) Lévêque, C.; Chenneberg, L.; Corcé, V.; Goddard, J.-P.; Ollivier, C.; Fensterbank, L. *Org. Chem. Front.* **2016**, *3*, 462. (d) Chenneberg, L.; Lévêque, C.; Corcé, V.; Baralle, A.; Goddard, J.-P.; Ollivier, C.; Fensterbank, L. *Synlett* **2016**, *27*, 731.

[22] Jouffroy, M.; Primer, D. N.; Molander, G. A. *J. Am. Chem. Soc.* **2016**, *138*, 475.

[23] (a) Sandrock, D. L.; Jean-Gerard, L.; Chen, C. C.; Dreher, S. D.; Molander, G. A. *J. Am. Chem. Soc.* **2010**, *132*, 17108. (b) Molander, G. A.; Wisniewski, S. R.; Hosseini-Sarvari, M. *Adv. Synth. Catal.* **2013**, *355*, 3037.

[24] Cheng, K.; Carroll, P. J.; Walsh, P. J. *Org. Lett.* **2011**, *13*, 2346.

[25] Tellis, J. C.; Amani, J.; Molander, G. A. *Org. Lett.* **2016**, *18*, 2994.

[26] Molander, G. A.; Wisniewski, S. R. *J. Am. Chem. Soc.* **2012**, *134*, 16856.

[27] Karimi-Nami, R.; Tellis, J. C.; Molander, G. A. *Org. Lett.* **2016**, *18*, 2572.

[28] Gaspar, A.; Matos, M. J.; Garrido, J.; Uriarte, E.; Borges, F. *Chem. Rev*. **2014**, *114*, 4960.

[29] (a) Miao, J.; Cui, H.; Jin, J.; Lai, F.; Wen, H.; Zhang, X.; Ruda, G. F.; Chen, X.; Yin, D. *Chem. Commun.* **2015**, *51*, 881. (b) Wang, L.; Liu, X.; Dong, Z.; Fu, X.; Feng, X. *Angew. Chem., Int. Ed.* **2008**, *47*, 8670. (c) Shockley, S. E.; Holder, J. C.; Stoltz, B. M. *Org. Process Res. Dev.* **2015**, *19*, 974. (d) Kavala, V.; Lin, C.; Kuo, C. − W.; Fang, H.; Yao, C. − F. *Tetrahedron* **2012**, *68*, 1321. (e) Qin, T.; Iwata, T.; Ransom, T. T.; Beutler, J. A.; Porco, J. A. *J. Am. Chem. Soc.* **2015**, *137*, 15225.

[30] Matsui, J. K.; Molander, G. A. *Org. Lett.* **2017**, *19*, 436.

[31] Yamashita, Y.; Tellis, J. C.; Molander, G. A. *Proc. Natl. Acad. Sci. U. S. A.* **2015**, *112*, 12026.

[32] (a) Sun, C.; Potter, B.; Morken, J. P. *J. Am. Chem. Soc.* **2014**, *136*, 6534. (b) Miller, S. P.; Morgan, J. B.; Nepveux, J. B.; Morken, J. P. *Org. Lett.* **2004**, *6*, 131.

[33] Vara, B. A.; Jouffroy, M.; Molander, G. A. *Chem. Sci.* **2017**, *8*, 530.

[34] Patel, N. R.; Molander, G. A. *J. Org. Chem.* **2016**, *81*, 7271.

[35] (a) Rosen, B. M.; Quasdorf, K. W.; Wilson, D. A.; Zhang, N.; Resmerita, A.; Garg, N. K.; Percec, V. *Chem. Rev.* **2011**, *111*, 1346. (b) Mesganaw, T.; Garg, N. K. *Org. Process Res. Dev.* **2013**, *17*, 29. (c) Tasker, S. Z.; Standley, E. A.; Jamison, T. F. *Nature* **2014**, *509*, 299.

[36] Langer, F.; Waas, J.; Knochel, P. *Tetrahedron Lett.* **1993**, *34*, 5261.

[37] (a) Amani, J.; Sodagar, E.; Molander, G. A. *Org. Lett.* **2016**, *18*, 732. (b) Amani, J.; Molander, G. A. *J. Org. Chem.* **2017**, *82*, 1856.

[38] Commerically available substrates using Scifinder.

[39] Nakajima, K.; Nojima, S.; Sakata, K.; Nishibayashi, Y. *ChemCatChem* **2016**, *8*, 1028.

[40] Gutierrez-Bonet, A.; Tellis, J. C.; Matsui, J. K.; Vara, B. A.; Molander, G. A. *ACS Catal.* **2016**, *6*, 8004.

[41] Wender, P. A.; Verma, V. A.; Paxton, T. J.; Pillow, T. H. *Acc. Chem. Res.* **2008**, *41*, 40.

[42] (a) Muto, K.; Yamaguchi, J.; Itami, K. *J. Am. Chem. Soc.* **2012**, *134*, 169. (b) Amaike, K.; Muto, K.; Yamaguchi, J.; Itami, K. *J. Am. Chem. Soc.* **2012**, *134*, 13573. (c) Shiota, H.; Ano, Y.; Aihara, Y.; Fukumoto, Y.; Chatani, N. *J. Am. Chem. Soc.* **2011**, *133*, 14952. (d) Aihara, Y.; Chatani, N. *J. Am. Chem. Soc.* **2013**, *135*, 5308. (e) Aihara, Y.; Chatani, N. *J. Am. Chem. Soc.* **2014**, *136*, 898. (f) Liu, D.; Liu, C.; Li, H.; Lei, A. *Angew. Chem., Int. Ed.* **2013**, *52*, 4453. (g) Liu, D.; Li, Y.; Qi, X.; Liu, C.; Lan, Y.; Lei, A. *Org. Lett.* **2015**, *17*, 998.

[43] For a comprehensive review of photoredox C−H functionalization, see the following: Qin, Q.; Jiang, H.; Hu, Z.; Ren, D.; Yu, S. *Chem. Rev.* **2017**, *17*, 1. Additional relevant articles: (a) Hari, D. P.; König, B. *Angew. Chem., Int. Ed.* **2013**, *52*, 4734. (b) Tlahuext-Aca, A.; Hopkinson, M. N.; Sahoo, B.; Glorius, F. *Chem. Sci.* **2016**, *7*, 89. (c) Kalyani, D.; McMurtrey, K. B.; Neufeldt, S. R.; Sanford, M. S. *J. Am. Chem. Soc.* **2011**, *133*, 18566. (d) Hari, D. P.; Schroll, P.; König, B. *J. Am. Chem. Soc.* **2012**, *134*, 2958.

[44] Heitz, D. R.; Tellis, J. C.; Molander, G. A. *J. Am. Chem. Soc.* **2016**, *138*, 12715.

[45] Ahneman, D. T.; Doyle, A. G. *Chem. Sci.* **2016**, *7*, 7002.

[46] Shaw, M. H.; Shurtleff, V. W.; Terrett, J. A.; Cuthbertson, J. D.; MacMillan, D. W. C. *Science* **2016**, *352*, 1304.

[47] (a) Kamijo, S.; Hoshikawa, T.; Inoue, M. *Org. Lett.* **2011**, *13*, 5928. (b) Breslow, R.; Winnik, M. A. *J. Am. Chem. Soc.* **1969**, *91*, 3083. (c) Kamijo, S.; Hoshikawa, T.; Inoue, M. *Org. Lett.* **2011**, *13*, 5928. (d) Chen, C. *Org. Biomol. Chem.* **2016**, *14*, 8641.

[48] Shields, B. J.; Doyle, A. G. *J. Am. Chem. Soc.* **2016**, *138*, 12719.

[49] Denés, F.; Pichowicz, M.; Povie, G.; Renaud, P. *Chem. Rev.* **2014**, *114*, 2587. (b) Simmons, E. M.; Hartwig, J. F. *Angew. Chem., Int. Ed.* **2012**, *51*, 3066.

[50] Chow, Y. L.; Buono-Core, G. E.; Lee, C. W. B.; Scaiano, J. C. *J. Am. Chem. Soc.* **1986**, *108*, 7620.

[51] Arias-Rotondo, D. M.; McCusker, J. K. *Chem. Soc. Rev.* **2016**, *45*, 5803.

[52] Singh, A.; Fennell, C. J.; Weaver, J. D. *Chem. Sci.* **2016**, *7*, 6796.

[53] To the best of our knowledge, the lone example of photocatalytic energy transfer to transition metal in the context of a synthetic method is the following: Yoo, W.-J.; Tsukamoto, T.; Kobayashi, S. *Org. Lett.* **2015**, *17*, 3640.

[54] (a) Chu, J. C. K.; Rovis, T. *Nature* **2016**, *539*, 272. (b) Choi, G. J.; Zhu, Q.; Miller, D. C.; Gu, C. J.; Knowles, R. R. *Nature* **2016**, *539*, 268. (c) Mukherjee, S.; Maji, B.; Tlahuext-Aca, A.; Glorius, F. *J. Am. Chem. Soc.* **2016**, *138*, 16200.

[55] Li, C. − J.; Wei, C. *Chem. Commun.* **2002**, 268.

[56] Patel, N. R.; Kelly, C. B.; Siegenfeld, A. P.; Molander, G. A. *ACS Catal* **2017**, *7*, 1766.

[57] Heitz, D. R.; Rizwan, K.; Molander, G. A. *J. Org. Chem.* **2016**, *81*, 7308.

[58] Shaw, J. E.; Hsia, D. Y.; Parries, G. S.; Sawyer, T. K. *J. Org. Chem.* **1987**, *43*, 1017.

[59] Kraus, G. A.; Dneprovskaia, E. *Tetrahedron Lett.* **2000**, *41*, 2.

[60] Noble, A.; MacMillan, D. W. C. *J. Am. Chem. Soc.* **2014**, *136*, 11602.

Chapter 2. C–H Alkylation of Heteroarenes *via* Photoredox Catalysis

2.1 Introduction

During the process of drug development, medicinal chemists frequently employ nitrogen-containing heteroarene scaffolds.[1†] Based on a survey of the "Top 200 Drugs" in 2014, a noteworthy 59% of pharmaceuticals contained a nitrogen heterocycle.[2] Although these small molecules are considered "privileged structures" in drug discovery, pharmacokinetic studies oftentimes determine modifications are necessary to improve ADME properties. Therefore, medicinal chemists have historically sought effective ways to alkylate heteroarenes in a step- and cost-economical way.[3]

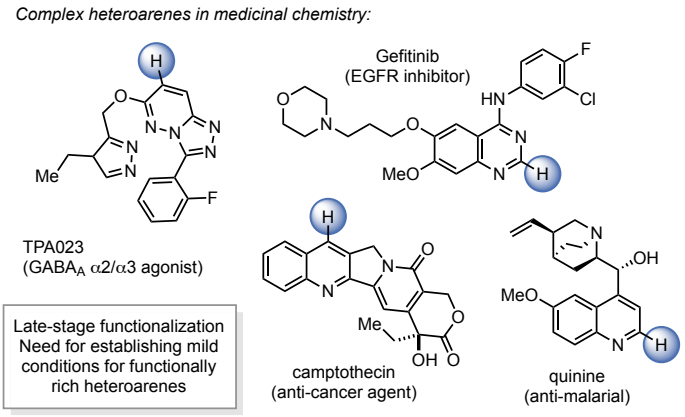

Figure 2.1. Functionally dense heterocycles and the innate positions of radical reactivity.

To overcome this challenge, two predominant (two-electron) strategies have emerged for diversifying common heteroaryl motifs: fluorination to enable facile S_NAr-based chemistry[4] and halogenation (bromination,[5] chlorination[6]) followed by cross-coupling.[7] These methods are highly effective for many systems, but in numerous cases installation of the halide at the desired site is

† Reproduced in part from Matsui, J. K.; Primer, D. N.; Molander, G. A. *Chem. Sci.* **2017**, *8*, 3512.

unselective or impossible, requiring re-evaluation of the synthetic strategy. Furthermore, when successful incorporation of halides has occurred, heteroarenes are often obstinate partners in cross-coupling chemistry,[8] requiring careful screening to achieve fruitful union. Most importantly, from an efficiency standpoint, these strategies are sub-optimal as they first require a functional handle to be installed, only to be immediately replaced in a subsequent displacement reaction.

Radical alkylations of heteroarenes (Minisci reactions)[9] represent a more direct functionalization of specific C–H bonds. For this reason, radical alkylation strategies have recently risen to prominence for the late-stage functionalization of heteroaryl systems. In this single-electron transformation, a wide range of *N*-heteroarene and radical precursors have been utilized since the 1970s (Figure 2.2).[10]

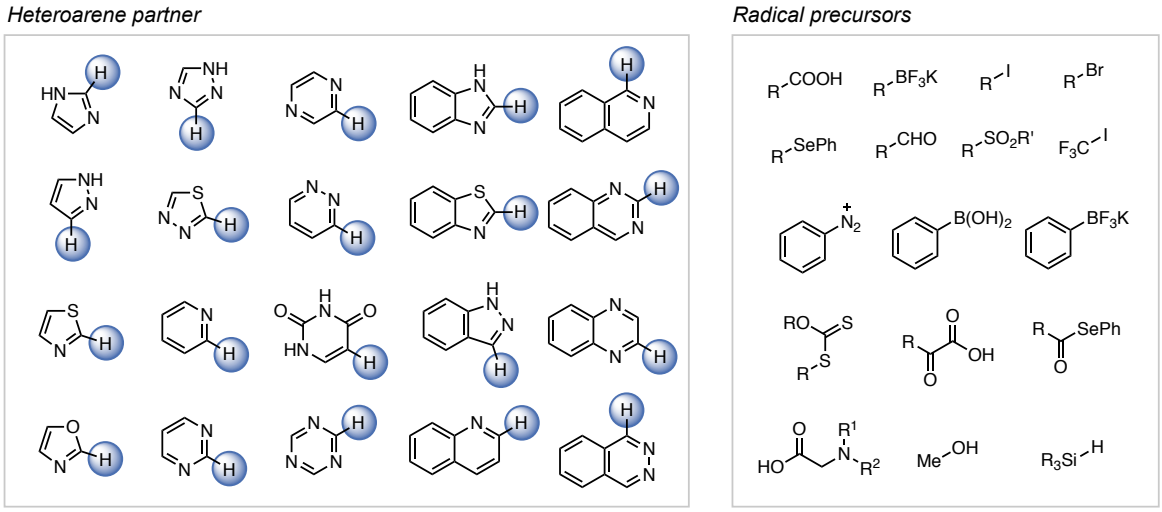

Figure 2.2. Representative heteroarenes (left) and radical precursors (right) used for Minisci chemistry. Highlighted hydrogens represent sites of native reactivity.

Although Minisci and coworkers initially used silver oxidants at elevated temperatures to generate alkyl radicals from the corresponding carboxylic acids,[9] advances in alkyl radical generation have enabled much milder methods to be developed. These have included methods using boronic acids,[11] peresters,[12] and other precursors[13] under much less forcing conditions. Most

notably, the Baran laboratory has pioneered the use of sulfinate salts[14] that have enabled the extremely facile introduction of functionalized alkyl radicals into an impressive array of heteroarenes. These methods allow the formal C-H alkylation of heterocycles in a mild, metal-free manner – drawing rapid adoption by medicinal chemists for the late stage diversification of pharmaceutically relevant compounds.

Advances in the field of Minisci-based reactions have enabled synthetic chemists to tackle markedly more complicated heterocyclic scaffolds. Notably, camptothecin (an anti-cancer agent) demonstrated inhibition of cancer cell growth *in vitro*, but structure activity relationship studies demonstrated that alkylation at the C7 position not only increased solubility, but also increased efficacy in cells.[15]

Unfortunately, even with these advances, current methods are not without their limitations, particularly with regard to the continued requirement for high loadings of both the radical partner and oxidant. Even the milder methods employing sulfinate salts often require a significant excess of an expensive and synthetically demanding precursor (3–6 equiv) and oxidant (5–10 equiv) to achieve good yields. To date, methods grounded in stoichiometric radical generation have been continually limited by parasitic reactivity (e.g., homocoupling, H-atom abstraction, and chain processes) that appear to outcompete the desired Minisci alkylation. As such, often the only solution has been to push reactions to completion with increased reagent loadings or successive dosing (Figure 2.3).

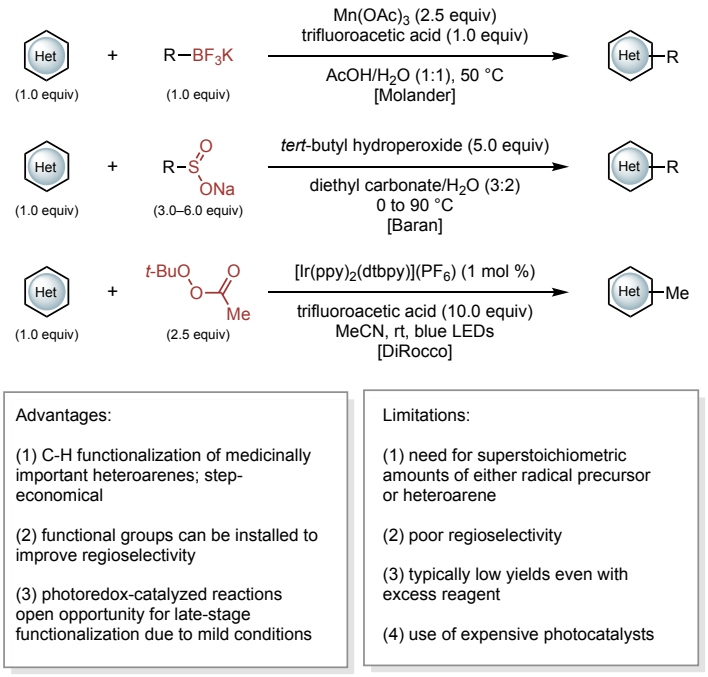

Figure 2.3. Previous Minisci methods for alkylation of heteroarenes.

To combat the disproportionate stoichiometry and typically harsh conditions, other groups have turned to photoredox catalysis for the efficient generation of radicals.[16] Contributions by the MacMillan,[17] DiRocco,[18] Chen,[19] and Barriault[20] groups have all highlighted the advantages afforded under this paradigm. Although a variety of alkyl radicals precursors were presented in these photoredox contributions, each method exhibits some inherent limitations. For example, the MacMillan group targeted weak C-H bonds and were largely limited to α-heteroatom bonds.[17] Barriault and coworkers demonstrated that alkyl bromides could be reduced to generate the corresponding alkyl radicals, but 3 equivalents of these precursors and a UVA LED light source were required.[20] Additionally, MacMillan and Barriault used expensive iridium or gold photocatalysts, respectively. The recent report by Chen addressed many of these issues with the use of sustainable boronic acid partners and inexpensive $Ru(bpy)_3$, but their method employs the use of a stoichiometric iodine oxidant that seems uniquely required for activation.[19]

In light of these advances, we recognized the potential to marry photoredox Minisci chemistry with our laboratory's interest in alkyltrifluoroborate reagents, especially given reports by our laboratory and others[21] on the favorable single electron oxidation potentials of these salts to form alkyl radicals (E_{red} = +1.10 V vs SCE for 1° benzylic[20a] and +1.50 V vs SCE for a secondary alkyltrifluoroborates). Here, with appropriate organic photocatalyst selection (for **1**: $^*E_{red}$ = +2.06 V vs SCE[22]), all representative radical classes could be activated under identical reaction conditions (Figure 2.4). In this scenario, one can envision photocatalyst excitation serving as a chaperone for steady, synchronized, catalytic radical generation. Such a protocol insures that an excess of radicals is not generated, minimizing at least some of the byproducts formed through stoichiometric processes. The photoredox catalyst-coordinated generation of radicals in this manner leads to improvement in reagent and oxidant loading, thus enhancing the efficiency and sustainability of these methods. Serendipitiously, these aforementioned concepts, in conjunction with the generation of Lewis acidic BF_3 byproduct, also led to enhanced reactivity and selectivity in these transformations.

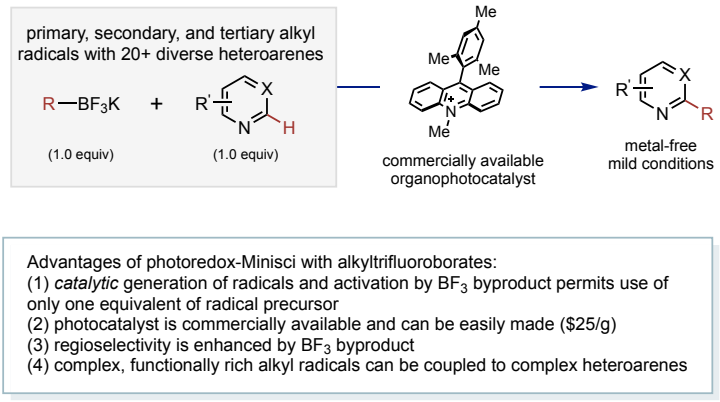

Figure 2.4. Envisioned transformation.

2.2 Reaction Design and Results

Mechanistically, we anticipated that visible light irradiation of organic photocatalyst **1** would generate the excited complex **1***, which is capable of oxidizing an alkyltrifluoroborate to release the desired alkyl radical **3** and BF_3 (Figure 2.5). The generated radical **3** can then intercept the protonated heteroarene to form the radical cation **5**. Reduction of persulfate (E_{red} = > +0.35 V vs SCE) by the reduced form of the photocatalyst **4** (E_{red} = +0.49 V vs SCE) generates the sulfate dianion and sulfate radical anion, regenerating photocatalyst **1**.[21] Finally, H-atom abstraction of **5** by the sulfate radical anion leads to rearomatization, affording the desired alkylated heteroarene **6**.[16]. Quantum yield studies indicate this is not a radical chain process as evidenced by a quantum yield of 0.31 (See Experimental Section for more details). Furthermore, addition of excess allyl acetate (a known sulfate radical anion trap[23]) did not interfere with reaction efficiency or conversion.

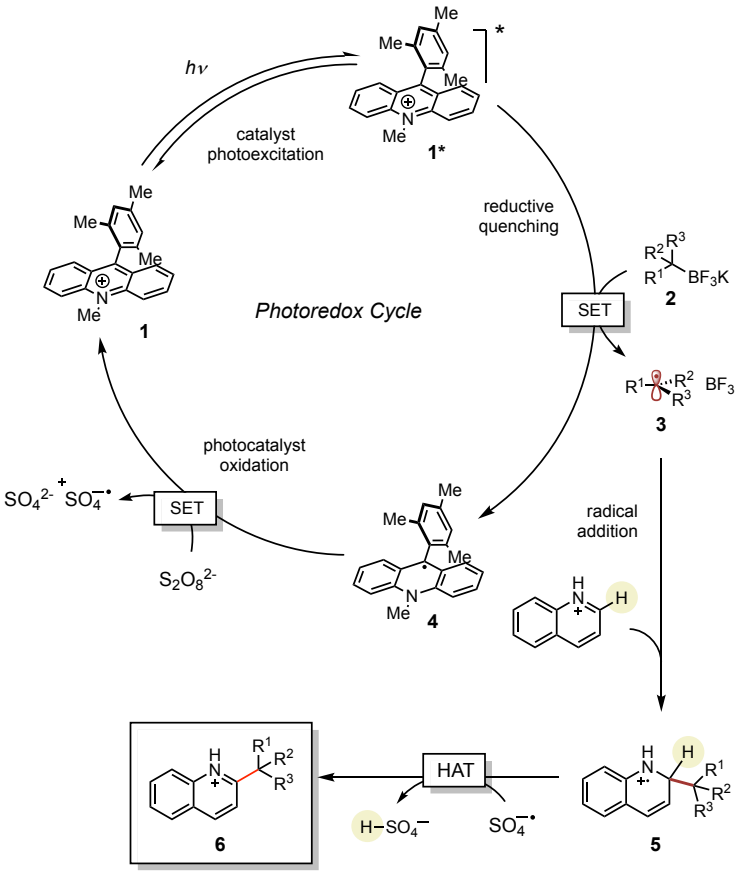

Figure 2.5. Proposed mechanism.

It was apparent from the outset of our studies that tertiary couplings were sparse in Minisci reactions.[8] Therefore, to find suitable conditions for such a coupling we selected *tert*-butyltrifluoroborate as the appropriate radical precursor and isoquinoline carboxylate as the heteroaryl partner. Before screening various photocatalysts, controls probing the need for oxidant (Table 2.1, entry 2), light (entry 3), and photocatalyst (entry 4) were completed. Additionally, the absence of acid (entry 5) afforded 30% conversion to product, although as alkyl radical **3** is generated, BF_3 (an electron-deficient Lewis acid) is concomitantly being formed. Performing the reaction in air provided a comparable yield (entry 6) to a reaction carried out under inert conditions (entry 1).

The mesityl acridinium photocatalyst was then compared to other photocatalysts (entries 7–10). Noting the need for a relatively high oxidizing potential of the photocatalyst, it was expected that ruthenium photocatalysts (with significantly lower oxidation potentials than the acridinium dyes) would experience diminished yields, which proved to be the case (entries 7, 8). During the period that photoredox catalysis has gained traction in the organic chemistry community, one major criticism has been the high cost of the key metal-based photocatalysts (i.e., those based on iridium and ruthenium). Nicewicz[24] and Zhang[25] have explored alternative organophotocatalysts that have been shown to exhibit similar reactivity to their metal-based counterparts. Surprisingly, 4CzIPN (entry 10) significantly outperformed MesAcr over a 12 h period. Neither excess alkyltrifluoroborate (entry 11) nor excess oxidant (entry 12) provided any perceived advantages.

Table 2.1. Control experiments and optimization.

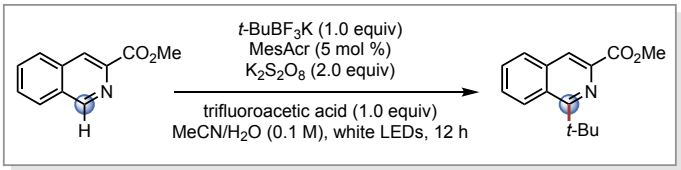

Entry	Deviation from Standard Conditions	% Yield [b]
1	none	57
2	no persulfate	<5
3	no light	<5
4	no photocatalyst	0
5	no acid	30
6	open to air (needle puncture)	53
7	$Ru(bpy)_3Cl_2$ (photocatalyst)	8
8	$Ru(bpz)_3$ (photocatalyst)	16
9	$Ir[dFCF_3ppy]_2(bpy)PF_6$ (photocatalyst)	86
10	4CzIPN (photocatalyst)	96
11	2.0 equiv trifluoroborate	45
12	4.0 equiv persulfate	84

Photocatalysts

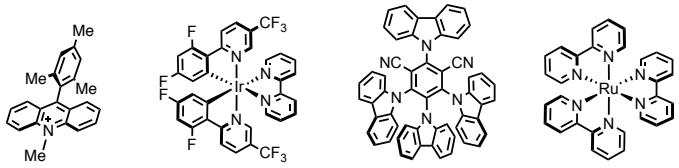

MesAcr	$Ir[dFCF_3ppy]_2(bpy)$	4CzIPN	$Ru(bpy)_3$
E_{red} = +2.06 V	E_{red} = +1.32 V	E_{red} = +1.35 V	E_{red} = +0.77 V

In view of their low cost and ease of access, going forward we focused on the two organophotocatalysts, MesAcr and 4CzIPN. To determine the most suitable organic photocatalyst

for our purposes, we scaled up the reactions described in entries 1 and 10, and discovered that running the reaction for 16 h afforded similar yields, consistent with the small scale reactions. It was important for this protocol to be general for primary, secondary, and tertiary alkyltrifluoroborates. Because primary alkyltrifluoroborates have a markedly higher oxidation potential (E_{red} = +1.80 V vs SCE) than secondary or tertiary alkyltrifluoroborates, MesAcr and 4CzIPN were compared with a primary alkyltrifluoroborate (Figure 2.6). In this assay, MesAcr outperformed CzIPN, providing 76% versus <10% isolated yields, respectively.

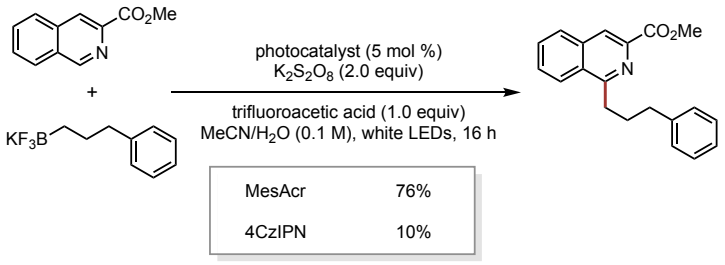

Figure 2.6. Comparing photocatalysts with a primary alkyltrifluoroborate.

Tricoordinate organoboron compounds are isoelectronic with carbocations, and thus would not be expected to be easily oxidized by single electron transfer (SET) processes. To confirm that this chemistry was unique to alkyltrifluoroborates, a variety of organoboron reagents were synthesized and analyzed by cyclic voltammetry to determine their relative oxidation potentials (Table 2.2). As expected, the trivalent organoboron variants exhibit very high oxidation potentials as compared to their tetravalent, "ate" complex analogues. Consequently, under the reaction conditions, no radical formation from the boronic acids and/or esters was observed. For the tetravalent species, triolborates exhibit exceptionally low reduction potentials. Unfortunately, the swift hydrolysis of triolborates under the acidic, aqueous reaction conditions forms the redox inactive boronic acid.[26] By contrast, alkyltrifluoroborates are both stable to the reaction conditions and redox amenable, resulting in an excellent 72% yield with methyl isoquinoline carboxylate after 16 h.

Table 2.2. Exploring various boronate compounds.

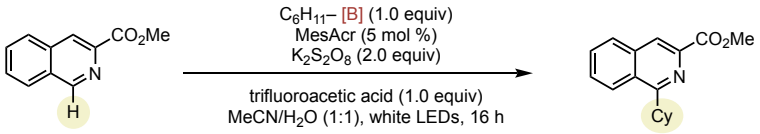

Alkylboron	Reduction Potential	Result	Drawbacks
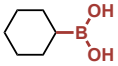	>2.5 V vs SCE	no conversion	✘ air sensitive ✘ poor redox properties
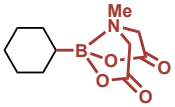	>2.5 V vs SCE	no conversion	✘ limited commerical availability ✘ poor atom economy ✘ poor redox properties
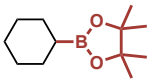	>2.5 V vs SCE	<5% conversion	✘ air sensitive ✘ poor atom economy ✘ poor redox properties
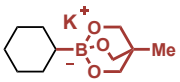	+1.1 V vs SCE	no conversion	✘ limited commercial availability ✘ hydrolytically unstable ✘ poor atom economy
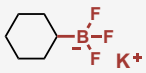	E_{red} = +1.5 V vs SCE 72% isolated yield		✔ commerically available ✔ bench-stable ✔ excellent redox properties

As mentioned previously, the use of tertiary radicals in Minisci chemistry has been very limited to date. Thus, before exploring the scope of the radical precursor, *tert*-butyltrifluoroborate was selected to examine the amenability of various heteroarene partners (Figure 2.7). Regioselectivity was probed using quinoline itself, leaving both the C2 and C4 positions available for alkylation. Currently there are two methods for installing tertiary radicals regioselectively into the quinoline core structure. Namgoong and coworkers reported the use of excess TMP-zincate to deprotonate selectively at the C2 position, followed by incorporation of the *tert*-butyl substituent.[27] This was a singular transformation, with no demonstrated scope. Additionally, Minisci and coworkers have reported selective C2 C-H substitution on quinolines using a 3-fold excess of alkyl iodide radical precursors.[8b] Although efficient, drawbacks of this approach included using peroxide as the oxidant, thereby limiting functional group tolerance, and the limited number of commercially available, complex alkyl iodides. Therefore, we were pleased to observe regiospecific addition of

the *t*-Bu group to the C2 position of the heteroarene in 72% yield (**2.7.1**). With substitution at the C4 position of quinoline, the reaction reached full conversion to product within 16 h as determined by GC-MS analysis (**2.7.2**). When isolated, a 95% yield of the desired product was achieved. Beyond alkyl substituents, halides and trifluoromethyl groups incorporated within the heteroaromatics allowed excellent conversion to product (**2.7.3, 2.7.4**).

In addition to quinoline cores (**2.7.1–2.7.4**), indazole (**2.7.5**), isoquinoline (**2.7.7**), and quinoxaline (**2.7.8**, **2.7.9**) moieties were successful partners under standard conditions. Indazole **2.7.5** is particularly notable because of its prevalence in medicinal chemistry[1] and, to the best of our knowledge, the absence of corresponding Minisci examples in the literature. As expected, the use of the benzimidazole core resulted in no conversion (**2.7.6**) because of the electron-rich nature of the C2 site. Additionally, *N*-methyl benzimidazole was similarly unreactive. Pyridines also exhibited selective mono-addition (**2.7.10–2.7.12, 2.7.14**). There has appeared only one report of nicotinamide alkylation via Minisci chemistry, wherein a statistical mixture of mono- and di-alkylated product was formed.[28] Therefore, it is remarkable that under the conditions developed herein, substitution occurred at the C6-position exclusively (**2.7.14**). A medicinally relevant core, quinazolinone **2.7.9**, afforded product in 90% yield. Purine **2.7.18** contains two sites of potential radical addition, but substitution was only observed on the pyrimidine subunit. Impressively, the method was tolerant of a wide range of functional groups as demonstrated with quinine **2.7.19** (possessing alkene, alcohol, tertiary amine groups).

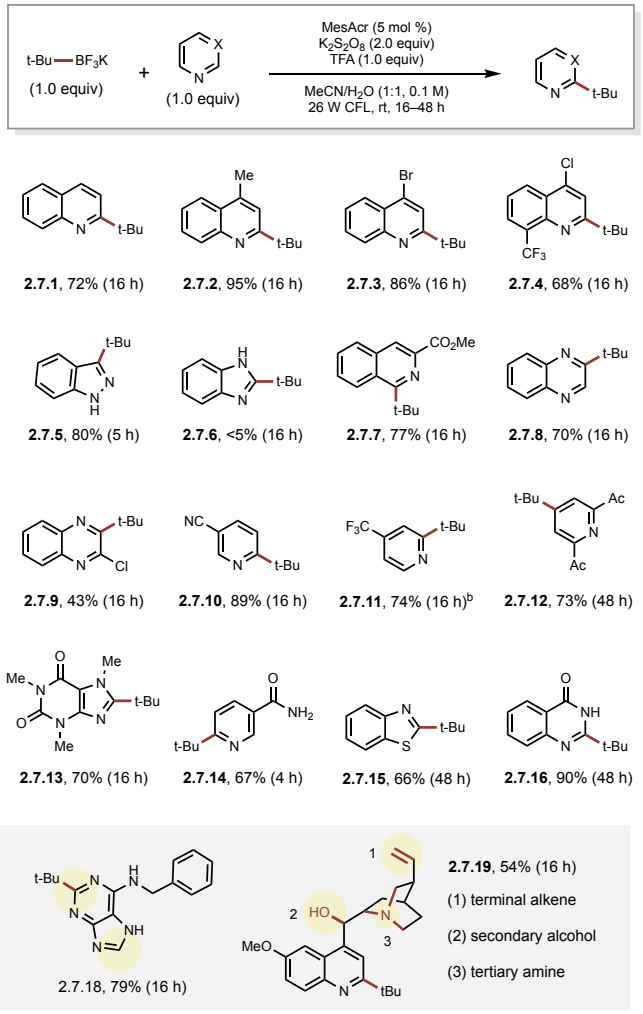

Figure 2.7. Coupling *tert*-butyltrifluoroborate with various heteroarenes.

Currently, there are a limited number of tertiary alkylboranes commercially available and no alkyltrifluoroborates. Presumably, this is a result of narrow synthetic utility compared to their primary and secondary counterparts. Although we demonstrated that *tert*-butyltrifluoroborate was viable, more highly elaborated systems could also be incorporated. Cook and coworkers recently reported a manganese-catalyzed borylation of alkyl bromides. Using Cook's procedure,[29] >1 g of pinacolborane intermediate **2.8.2** was synthesized from the corresponding alkyl bromide **2.8.1**. This borylation was followed by treatment with saturated KHF_2 to afford the corresponding alkyltrifluoroborate **2.8.3** (Figure 2.8).

With tertiary alkyltrifluoroborate **2.8.3** in hand, radical addition to caffeine **2.8.4** and benzothiophene **2.8.5** was carried out. The development of the Cook approach to 3° alkyltrifluoroborates thus allows access to an even greater array of coupling partners.

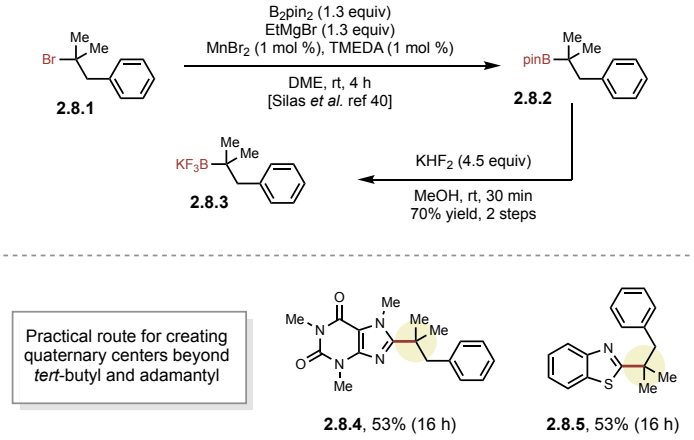

Figure 2.8. Synthesizing and utilizing a tertiary alkyltrifluoroborate.

In further studies, a wide range of alkyltrifluoroborates were found to be suitable partners in the developed photoredox Minisci conditions (Figure 2.9). First, a benzyl protected α-alkoxyalkyltrifluoroborate afforded **2.9.1** in 58% yield. Additional examples of unactivated, secondary alkyl radical precursors could be appended as in **2.9.2–2.9.10**. For **2.9.2**, the successful addition of fluorinated isosteres is encouraging, given the well-documented propensity these subunits have for modulating solubility and binding affinity in medicinal chemistry.[30] For **2.9.3–2.9.5**, the tetrahydropyranyl and piperidinyl moieties are commonly introduced ring structures that serve as useful probes for H-bond donors/acceptors in SAR efforts.[31]

To the best of our knowledge, primary alcohols appended to the radical coupling partner have not been reported in Minisci-type reactions, perhaps owing to their propensity to undergo H-atom abstraction alpha to the hydroxyl group. Therefore, we were pleased to obtain **2.9.6**, albeit in low yield. A further exploration of 5- and 4-membered heterocycles (**2.9.7–2.9.9**) was conducted with promising results, where tetrahydrofuran **2.9.7** was afforded in 34% yield, but access to

pyrrolidine **2.9.8** was not successful. For azetidine **2.9.**9, standard solvent conditions provided only trace amounts of product, but switching to DCE/H_2O (1:1) proved to be beneficial. Cyclopropyltrifluoroborate, although unproductive in previously reported photoredox/Ni dual cross-coupling methods,[20b] afforded **2.9.10**, albeit in 20% yield. 1-Adamantyltrifluoroborate has never been used in Minisci-type alkylations. Using the standard conditions, **2.9.11** was isolated in 45% yield. Lastly, exquisite chemoselectivity was observed for **2.9.12**; no radical addition to the pyridine moiety was observed, and the tertiary amine did not interfere with the photocatalytic cycle.

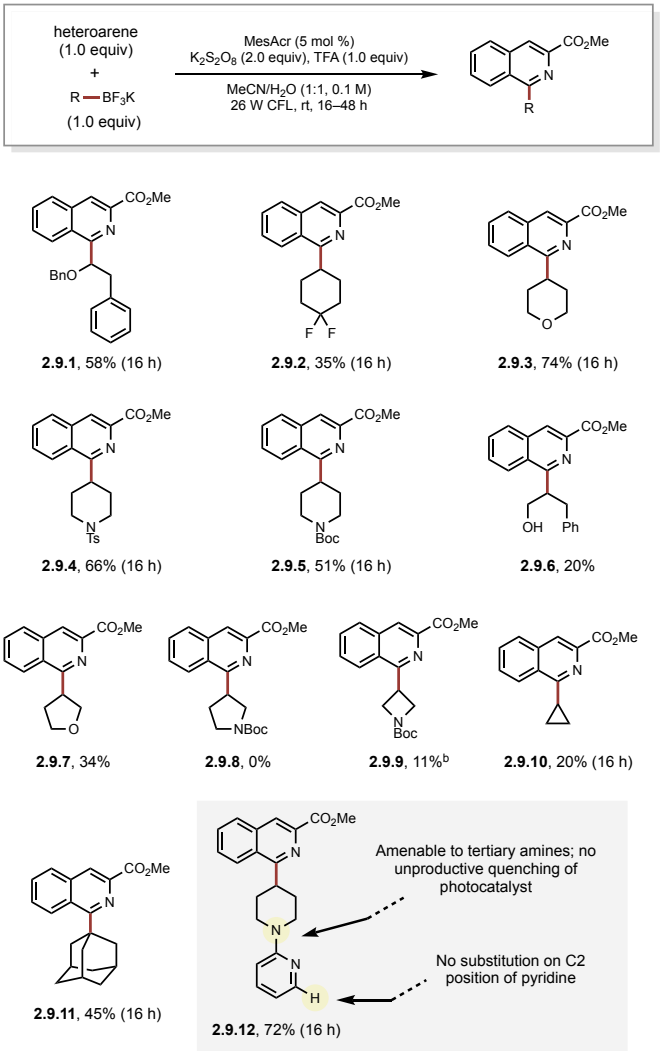

2.9.1, 58% (16 h) **2.9.2**, 35% (16 h) **2.9.3**, 74% (16 h)

2.9.4, 66% (16 h) **2.9.5**, 51% (16 h) **2.9.6**, 20%

2.9.7, 34% **2.9.8**, 0% **2.9.9**, 11%[b] **2.9.10**, 20% (16 h)

2.9.11, 45% (16 h) **2.9.12**, 72% (16 h)

Figure 2.9. Coupling secondary and tertiary alkyltrifluoroborates.

Moving forward, this Minisci process was anticipated to be broadly applicable even to primary alkyltrifluoroborates, which possess relatively high oxidation potentials (Figure 2.10). As an initial foray, we first investigated whether stabilized primary α-alkoxymethyltrifluoroborates could be competent partners in this process (**2.10.1–2.10.4**). Unstabilized alkyl radicals were also demonstrated in examples **2.10.5–2.9.12**. Notably, **2.10.10** contains an *ortho* bromide functional handle for further elaboration. More remarkably, electron deficient 3,3,3-trifluoropropyltrifluoroborate afforded **2.10.12**, albeit in lower yield.

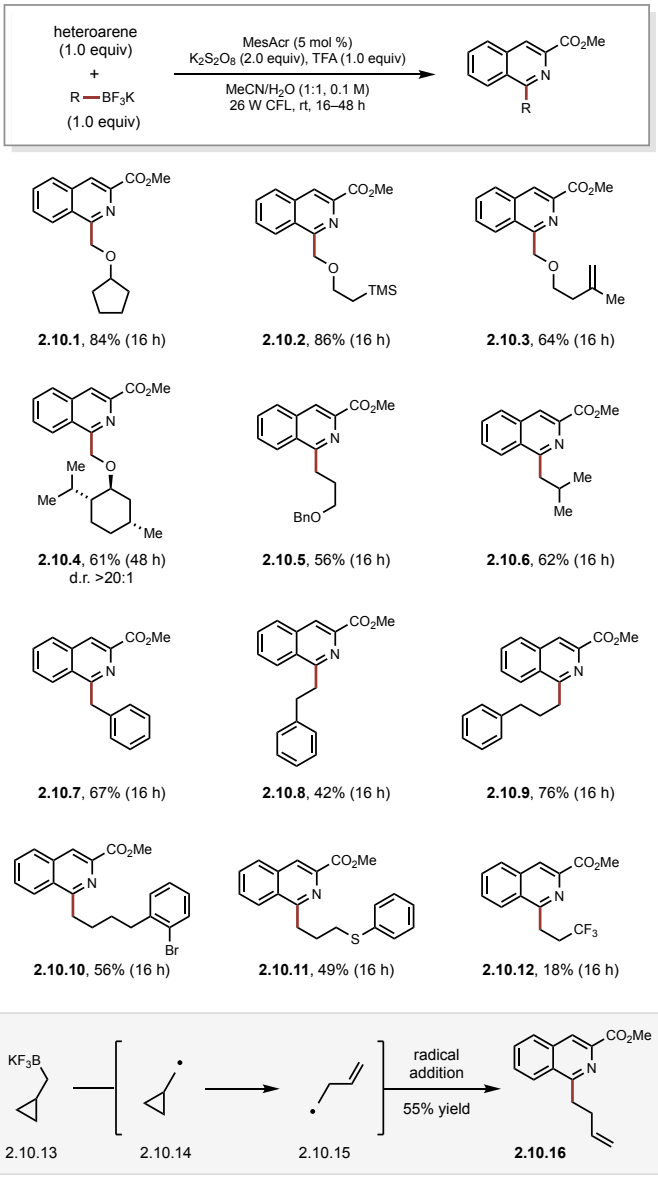

Figure 2.10. Demonstrating structural diversity for primary alkyltrifluoroborates.

As would be anticipated for the radical-based mechanism of the transformation, cyclopropylcarbinyltrifluoroborate **2.10.13** formed the corresponding radical **2.10.14** after SET oxidation and subsequent rearrangement. Following radical addition to the activated heteroaromatic, **2.10.16** was isolated in 55% yield.

The diversity of the process was expanded to underline the potential for widespread utility (Figure 2.11). Quinoline moieties were coupled with a variety of stabilized α-alkoxy (**2.11.1–2.11.3**) and unstabilized (**2.11.4–2.11.6**) radicals. With quinoline, C2 regiospecificity was again observed (**2.11.4, 2.11.5**), albeit in diminished yields. This is particularly noteworthy given the challenges associated with avoiding complex mixtures of isomers in prior Minisci-type reaction reports.[32] With heteroarene cores such as pyridine (**2.11.6**), benzothiazole (**2.11.7**), indazole (**2.11.8**), and quinazolinone (**2.11.9, 2.11.10**), exceptional yields were observed. When exploring reactivity with caffeine, methylcyclopentyltrifluoroborate afforded **2.11.11** in 37% yield. Additionally, a secondary alkyl radical was successfully appended to a functionally rich quinine as demonstrated in **2.11.12**.

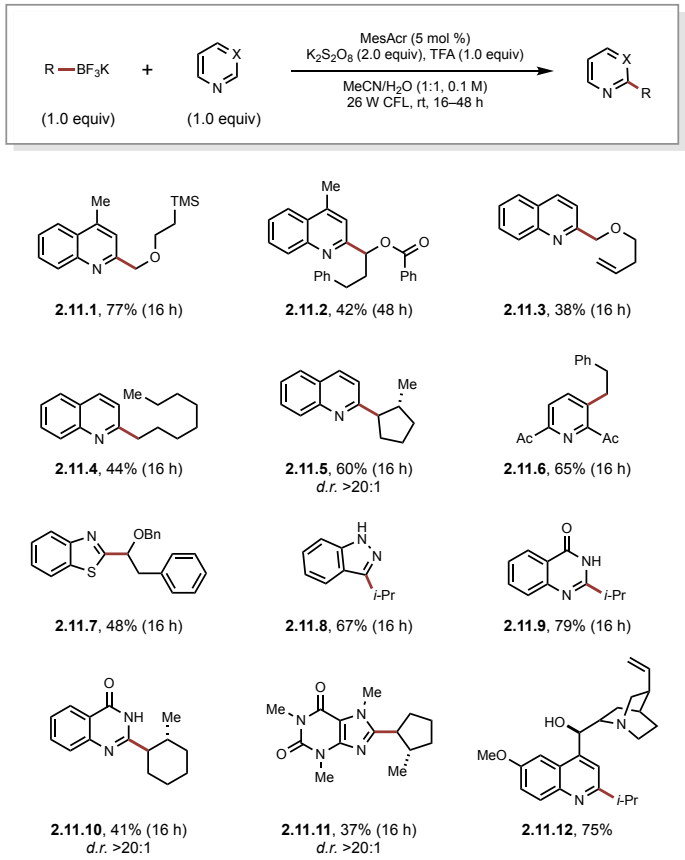

Figure 2.11. Mixed table using various alkyltrifluoroborates and heteroarenes.

Given the success of this method, the use of this technology for selective ligand modifications was envisioned (Figure 2.12). As a case study, difunctionalization of a bipyridine-based ligand was selected for further investigation. Commonly, these ligands are synthesized through the S_NAr reaction of strong nucleophiles (e.g., *tert*-butyllithium) to a fluorinated bipyridine precursor, which is unfortunate given the popularity of these ligands in Cu and Ni catalysis.[33] In contrast to the use of such pyrophoric alkylating agents, bench-stable alkyltrifluoroborates represent an attractive alternative. Gratifyingly, unfunctionalized substructures **2.12.1** and **2.12.3** were converted to the desired products in 84% and 68% yields, respectively. Pyridine ligands are also valuable for the synthesis of iridium photocatalysts. Under the same reaction conditions, heteroarene **2.12.5** afforded mono-alkylated product **2.12.6** in 82% yield. When tridentate ligand terpyridine **2.12.7** was subjected to the standard conditions with two equivalents of *tert*-butyltrifluoroborate, mono-alkylated **2.12.8** was formed exclusively.[34]

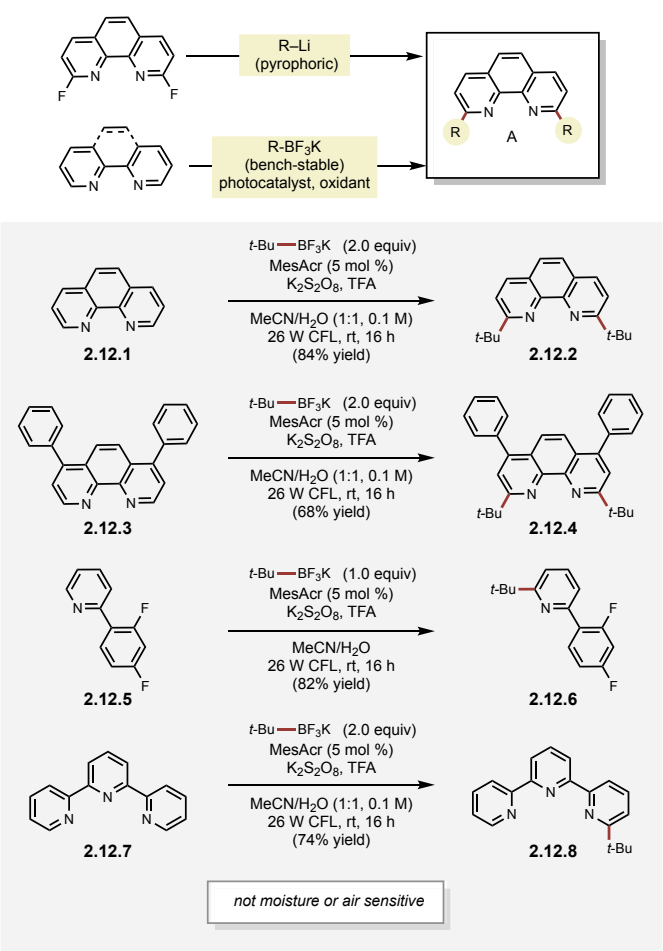

Figure 2.12. Applications within ligand design.

Although medicinal chemists have principally capitalized on late-stage Minisci heteroarene alkylation,[9] it can be advantageous to introduce alkyl substitution earlier in a synthetic sequence.[35] Using the present protocol, the installation of alkyl subunits on brominated heteroarenes provides an excellent opportunity to highlight divergency in molecular synthesis. Furthermore, the halides installed within a variety of heteroarenes can serve a dual purpose: they may serve as an electronic bias for regioselective alkylations ortho to the halide,[13d] and they provide a functional handle for cross-coupling reactions, etc.[5c] To initiate studies to explore these concepts, a number of brominated heteroarenes were selected (Figure 2.13). First, pyrimidine **2.13.1** was

paired with an α-alkoxyalkyltrifluoroborate to yield exclusively the C4-substituted product. When moving to pyridines, a mixture of C2 and C6 alkylation occurred with tosyl-protected piperidinyltrifluoroborate **2.13.2**. Conversely, with primary alkyltrifluoroborates, only the C2-substituted products were observed in examples **2.13.3** and **2.13.4**. Chloride substitution was also well tolerated as demonstrated in **2.13.4**. When 4-bromoisoquinoline was utilized as a substrate, a mixture of regioisomers **2.13.5** and **2.13.6** was generated.

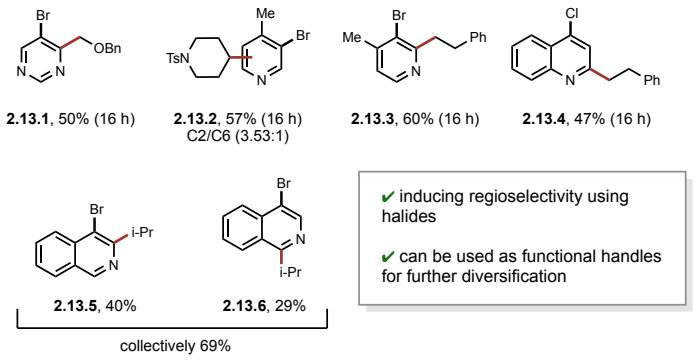

Figure 2.13. Halogenated heteroarenes primed for further derivatization.

2.3 Mechanistic Investigations

From our previous reports on Minisci chemistry[12] and the results provided herein, it became clear that the use of alkyltrifluoroborates provided clear advantages in terms of both reactivity (permitting a single equivalent of radical precursor to be employed) and regioselectivity in heteroarene alkylation. Given these observations, it seemed that there was some inherent advantage to the generation of BF_3 byproduct during the course of the reaction. Two distinct possibilities were considered: (1) the BF_3 produced was intimately involved with the generated radical, providing a shepherding effect in delivering the radical with enhanced selectivity, or (2) the BF_3 was coordinating to the heteroarene prior to the radical addition, activating the heteroaryl substrate and enhancing preference for one site beyond the activation provided by the added protic acid.

To assess the first hypothesis, DFT calculations were performed to determine the effective "bond order" for radical association with BF_3 in solution. This potential interaction was of particular interest as this escorting effect has little precedent in the chemical literature; currently, there are only examples of nitrogen- and oxygen-centered radicals interacting with BF_3 in solution.[36] Indeed, preliminary calculations suggest that a strong preference exists for the free radical over a BF_3-bound complex in solution. Noting this lack of association, we were quick to investigate an alternative hypothesis.

To probe each of the possible heteroarene complexes, we prepared stoichiometric solutions of one of our successful, selective substrates, quinoline, with no additive, trifluoroacetic acid (TFA) alone, BF_3 alone, and finally TFA with added BF_3, hoping to probe the effect of coordination on the proton and carbon shifts of heteroarene and provide some rationale for the differences between our chemistry and previously established protocols.

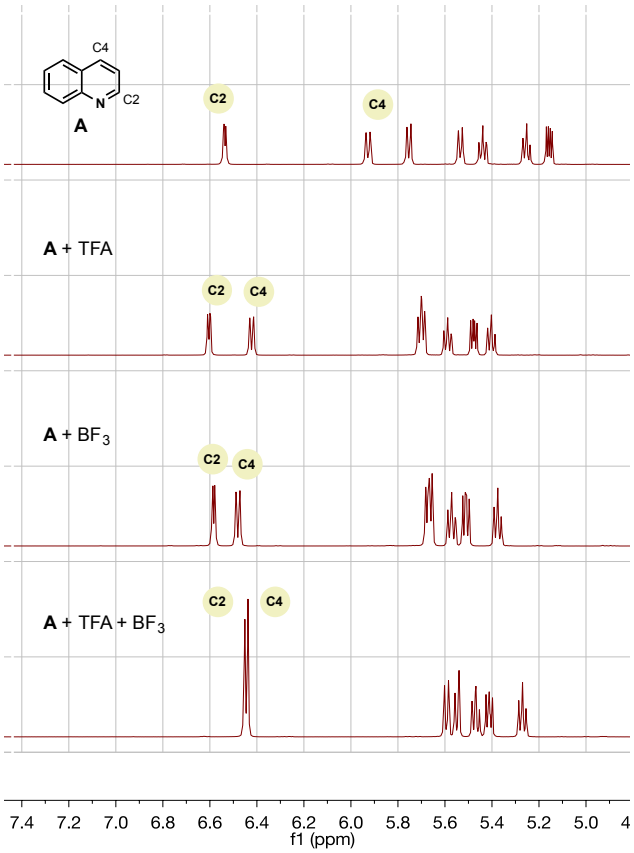

Figure 2.14. Observed proton shifts with additives.

For trifluoroacetic acid, a clear downfield shift was observed in the C2 and C4 protons of quinoline (Figure 2.14). Likewise, for the addition of BF_3, a slightly less pronounced, but clear, downfield shift was also observed for the same protons. However, the combination of both additives together produced a wholly different shift in resonances to a unique heteroarene species. Perhaps more importantly, the carbon shifts of C2 relative to C4 possess enhanced differentiation in relative downfield shift (~3 ppm) in comparison to the BF_3 and trifluoroacetic acid complexes alone (~1 ppm) (Figure 2.15). Based on these chemical shifts, it is reasonable to suggest the C2 position is preferentially activated over the C4 position[37] under the reaction conditions, resulting in the enhanced regioselective mono-alkylation observed for the quinoline system and, by analogy, many of the other systems in which alkyltrifluoroborates appear uniquely reactive and selective (vida infra).

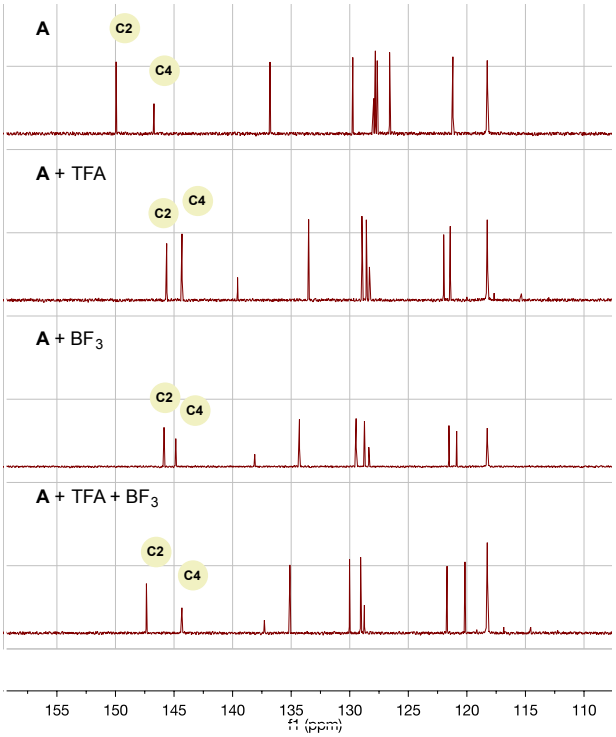

Figure 2.15. Observed carbon shifts with additives.

To probe these findings further, we hoped that the use of alternative radical precursors (e.g., sulfinate salts or carboxylic acids) could be used in the presence and/or absence of BF_3 to achieve the same desired regioselectivity. Unfortunately, under our standard conditions, sulfinate salts were universally ineffective, and carboxylic acids gave the same regio-mixture, even with added BF_3. Given this current ambiguity, this enhanced reactivity and regioselectivity appears to remain unique to the trifluoroborate precursors.

At this time, it is impossible to propose a structure for this distinct, activated species, but whatever complex is formed is likely a result of BF_3 activation of either the heteroarene π-cloud[38] or polarization of the trifluoroacetic acid[39] to increase its effective pKa. This type of dual activation could perhaps be more broadly operative in the selective alkylation of other heteroaryl cores.

2.4 Conclusion

In summary, a mild, room temperature method for the introduction of a diverse palette of alkyl groups has been developed. Under a set of unified reaction conditions, primary, secondary, and tertiary alkyltrifluoroborates can be employed in photoredox Minisci chemistry for the first time. This chemistry makes use of an inexpensive, mild oxidant, organic photocatalyst, and requires only one equivalent of alkyl radical partner, providing one of the most cost efficient and sustainable approaches to date. Additionally, enhanced regioselectivity was observed compared to current "state of the art" Minisci-type alkylations. Both of these phenomena may be related to the synchronized, catalytic generation of radicals in conjunction with the *in situ* generation of BF_3 during the course of the reaction. The resultant method has been demonstrated broadly with respect to the heteroarene and alkyltrifluoroborate partners. Furthermore, access to bipyridine-type ligands as well as the late stage diversification of medicinally relevant substructures has been showcased. Finally, NMR studies provided support for a unique, highly activated species caused by the formation of BF_3 upon the single-electron oxidation of alkyltrifluoroborates.

Given the wide array of commercially available alkyltrifluoroborates, those synthesized by our laboratory and emerging from other groups, this approach provides a valuable contribution to the Minisci-type alkylation literature and is both highly competitive and complementary to existing protocols. As alkyltrifluoroborates are well behaved, bench stable salts, these reagents will continue to serve as useful "radicals in a bottle" for synthetic chemists.

2.5 References

[1] Welsch, M. E.; Synder, S. A.; Stockwell, B. R. *Curr. Opin. Chem. Biol.* **2010**, *14*, 347.

[2] McGrath, N. A.; Brichacek, M.; Njardarson, J. T. *J. Chem. Educ.* **2010**, *87*, 1348.

[3] Ducton, M. A. *Med. Chem. Commun.* **2011**, *2*, 1135.

[4] Bunnett, J. F.; Zahler, R. E. *Chem. Rev.* **1951**, *49*, 273.

[5] Joshi, G.; Adimurthy, S. *Ind. Eng. Chem. Res.* **2011**, *50*,

[6] Rodriguez, R. A.; Pan, C. -M.; Yabe, Y.; Kawamata, Y.; Eastgate, M. D.; Baran, P. S. *J. Am. Chem. Soc.* **2014**, *136*, 6908.

[7] Billingsley, K. L.; Anderson, K. W.; Buchwald, S. L. *Angew. Chem. Int. Ed.* **2006**, *45*, 3484.

[8] Ge, S.; Hartwig, J. F. *Angew. Chem. Int. Ed.* **2012**, *51*, 12837.

[9] Minisci, F. *Acc. Chem. Res.* **1975**, *8*, 165.

[10] Minisci, F.; Bernardi, R.; Bertini, F.; Galli, R.; Perchinunmmo, M. *Tetrahedron* **1971**, *27*, 3575.

[11] Seiple, I. B.; Su, S.; Rodriguez, R. A.; Gianatassio, R.; Fujiwara, Y.; Sobel, A. L.; Baran, P. S. *J. Am. Chem. Soc.* **2010**, *132*, 13194.

[12] Foo, K.; Sella, E.; Thome, I.; Eastgate, M. D.; Baran, P. S. *J. Am. Chem. Soc.* **2014**, *136*, 5379.

[13] Molander, G. A.; Colombel, V.; Braz, V. A. *Org. Lett.* **2011**, *13*, 1852.

[14] Gianatassio, R.; Kawamura, S.; Eprile, C. L.; Foo, K.; Ge, J.; Burns, A. C.; Collins, M. R.; Baran, P. S. *Angew. Chem. Int. Ed.* **2014**, *53*, 9851.

[15] Liu, Y. –Q.; Dai, W.; Wang, C. –Y.; Morris-Natschke, S. L.; Zhou, X. –W.; Yang, L.; Yang, X. –M.; Li, W. –Q.; Lee, K. –H. *Bioorg. Med. Chem.* **2012**, *22*, 7659.

[16] Goddard, J. -P.; Ollivier, C.; Fensterbank, L. *Acc. Chem. Res.* **2016**, *49*, 1565.

[17] (a) Jin, J.; MacMillan, D. W. C. *Nature* **2015**, *525*, 87. (b) Nagib, D. A.; MacMillan, D. W. C. *Nature* **2011**, *480*, 224. (c) Jin, J.; MacMillan, D. W. C. *Angew. Chem. Int. Ed.* **2015**, *54*, 1565.

[18] DiRocco, D. A.; Dykstra, K.; Krska, S.; Vachal, P.; Conway, D. V.; Tudge, M. *Angew. Chem. Int. Ed.* **2014**, *53*, 4802.

[19] Li, G. -X.; Morales-Rivera, C. A.; Wang, Y.; Gao, F.; He, G.; Liu, P.; Chen, G. *Chem. Sci.* **2016**, *7*, 6407.

[20] McCallum, T.; Barriault, L. *Chem. Sci.* **2016**, *7*, 4754.

[21] (a) Tellis, J. C.; Primer, D. N.; Molander, G. A. *Science* **2014**, *345*, 433. (b) Primer, D. N.; Karakaya, I.; Tellis, J. C.; Molander, G. A. *J. Am. Chem. Soc.* **2015**, *137*, 2195. (c) Karakaya, I.; Primer, D. N.; Molander, G. A. *Org. Lett.* **2015**, *17*, 3294. (d) Yamashita, Y.; Tellis, J. C.; Molander, G. A. *Proc. Natl. Acad. Sci. U.S.A.* **2015**, *112*, 12026. (e) El Khatib, M.; Serafim, R. A.; Molander, G. A. *Angew. Chem. Int. Ed.* **2016**, *55*, 254. (f) Ryu, D.; Primer, D. N.; Tellis, J. C.; Molander, G. A. *Chem. Eur. J.* **2016**, *22*, 120. (g) Amani, J.; Sodagar, E.; Molander, G. A. *Org. Lett.* **2016**, *18*, 732. (h) Karimi-Nami, R.; Tellis, J. C.; Molander, G. A. *Org. Lett.* **2016**, *18*, 2572. (i) Tellis, J. C.; Amani, J.; Molander, G. A. *Org. Lett.* **2016**, *18*, 2572. (j) Yasu, Y.; Koike, T.; Akita, M. *Adv. Synth. Catal.* **2012**, *354*, 3414.

[22] Fukuzumi, S.; Kotani, H.; Ohkubo, K.; Ogo, S.; Tkachenko, N. V.; Lemmetyinen, H. *J. Am. Chem. Soc.* **2004**, *126*, 1600.

[23] Huie, R. E.; Clifton, C. L.; Neta, P. *Radiat. Physc. Chem.* **1991**, *38*, 477.

[24] (a) Hamilton, D. S.; Nicewicz, D. A. *J. Am. Chem. Soc.* **2012**, *134*, 18577. (b) Morse, P. D.; Nicewicz, D. A. *Chem. Sci.* **2015**, *6*, 270. (c) Nicewicz, D. A.; Nguyen, T. M. *ACS Catal.* **2014**, *4*, 355. (d) Grandjean, J.; Nicewicz, D. A. *Angew. Chem. Int. Ed.* **2013**, *52*, 3967. (e) Riener, M. Nicewicz, D. A. *Chem. Sci.* **2013**, *4*, 2625. (f) Wilger, D. J.; Gesmundo, N. J.; Nicewicz, D. A. *Chem. Sci.* **2013**, *4*, 3160. (g) Nguyen, T. M.; Nicewicz, D. A. *J. Am. Chem. Soc.* **2013**, *135*, 9588. (h) Perkowski, A. J.; Nicewicz, D. A. *J. Am. Chem. Soc.* **2013**, *135*, 10334. (i) Nicewicz, D. A.; Hamilton, D. S. *Synthesis* **2014**, *25*, 1191. (j) Nguyen, T. M.; Manohar, N.; Nicewicz, D. A. *Angew. Chem. Int. Ed.* **2014**, *53*, 6198. (k) Romero, N.; Nicewicz, D. A. *J. Am. Chem. Soc.* **2014**, *136*, 17024. (k) Zeller, M. A.; Riener, M.; Nicewicz, D. A. *Org. Lett.* **2014**, *16*, 4810. (l) Gesmundo, N. J.; Grandjean, J. -M. M.; Nicewicz, D. A. *Org. Lett.* **2015**, *17*, 1316.

[25] Luo, J.; Zhang, J. *ACS Catal.* **2016**, *6*, 873.

[26] Butters, M.; Harvey, J. N.; Jover, J.; Lennox, A. J. J.; Lloyd-Jones, G. C., Murray, P. M. *Angew. Chem. Int. Ed.* **2010**, *49*, 5156.

[27] Seo, H. J.; Yoon, S. J.; Jang, S. H.; Namgoong, S. K. *Tetrahedron Lett.* **2011**, *52*, 3747.

[28] Tada, M.; Yokoi, Y. *J. Heterocyclic Chem.* **1989**, *26*, 45.

[29] Atack, T. C.; Cook, S. P. *J. Am. Chem. Soc.* **2016**, *138*, 6139.

[30] a) Gillis, E. P.; Eastman, K. J.; Hill, M. D.; Donnelly, D. J.; Meanwell, N. A. *J. Med. Chem.* **2015**, *58*, 8315. (b) Purser, S.; Moore, P. R.; Swallow, S.; Gouverneur, V. *Chem. Soc. Rev.* **2008**, *37*, 320.

[31] Murphy-Benenato, K. E.; Olivier, N.; Choy, A.; Ross, P. L.; Miller, M. D.; Thresher, J.; Gao, N.; Hale, M. R. *ACS Med. Chem. Lett.* **2014**, *5*, 1213.

[32] a) Li, G. -X.; Morales-Rivera, C. A.; Wang, Y.; Gao, F.; He, G.; Liu, P.; Chen, G. *Chem. Sci.* **2016**, *7*, 6407. (b) Siddaraju, Y.; Lamani, M.; Prabhu, K. R. *J. Org. Chem.* **2014**, *79*, 3856.

[33] (a) Sammes, P. G.; Yahioglu, G. *Chem. Soc. Rev.* **1994**, *23*, 327. (b) Sammes, P. G.; Yahioglu, G. *Chem. Soc. Rev.* **1994**, *23*, 327.

[34] Gianatassio, R.; Kawamura, S.; Eprile, C. L.; Foo, K.; Ge, J.; Burns, A. C.; Collins, M. R.; Baran, P. S. *Angew. Chem. Int. Ed.* **2014**, *53*, 9851.

[35] Venditto, V. J.; Simanek, E. E. *Mol. Pharm.* **2010**, *7*, 307.

[36] (a) Mansaray, H. B.; Rowe, A. D. L.; Phillips, N.; Niemeyer, J.; Kelly, M.; Addy, D. A.; Bates, J. I.; Aldridge, S. *Chem. Comm.* **2011**, *47*, 12295. (b) Tarakeshwar, P.; Lee, S. J.; Lee, J. Y.; Kim, K. S. *J. Phys. Chem. B.* **1999**, *103*, 184.

[37] (a) Ren, J.; Cramer, C. J.; Squires, R. R. *J. Am. Chem. Soc.* **1999**, *121*, 2633. (b) Yamamoto, H.; Futatsugi, K. *Angew. Chem. Int. Ed.* **2005**, *44*, 1924.

[38] Mansaray, H. B.; Rowe, A. D. L.; Phillips, N.; Niemeyer, J.; Kelly, M.; Addy, D. A.; Bates, J. I.; Aldridge, S. *Chem. Commun.* **2011**, *47*, 12295.

[39] Ren, J.; Cramer, C. J.; Squires, R. R. *J. Am. Chem. Soc.* **1999**, *121*, 2633.

GENERAL CONSIDERATIONS:

NMR Spectra (^{1}H, ^{13}C, ^{19}F) were performed at 298 K. ^{1}H NMR spectra were referenced to residual non-deuterated chloroform (δ 7.26) in $CDCl_3$, residual DMSO-d_5 (δ 2.50) in DMSO-d_6, acetone-d_5 (δ 2.09) in acetone-d_6, and residual MeCN-d_2 (δ 1.94) in MeCN-d_3. ^{13}C NMR spectra were referenced to $CDCl_3$ (δ 77.2) and DMSO-d_6 (δ 39.5). Reactions were monitored by HPLC, GC/MS, ^{1}H NMR, and/or by TLC on silica gel plates (60 Å porosity, 250 μm thickness). TLC analysis was performed using hexanes/EtOAc as the eluant and visualized using UV light. Silica plugs utilized flash silica gel (60 Å porosity, 32–63 μm). Flash chromatography was accomplished using an automated system (visualizing at 254 nm, monitoring at 280 nm) with silica cartridges (60 Å porosity, 20–40 μm). Solvents were purified by use of drying cartridges through a solvent delivery system. Melting points (°C) are uncorrected.

Deuterated NMR solvents were either used as purchased (DMSO-d_6) or were stored over 4Å molecular sieves and/or K_2CO_3 ($CDCl_3$). Na_2SO_4, $MgSO_4$, MeOH, CH_2Cl_2, MeCN, pentane, Et_2O, trifluoroacetic acid, and $K_2S_2O_8$ were used as purchased. Heteroarenes were purchased from commercial suppliers and used without further purification. MeCN/H_2O was degassed thoroughly with N_2 and stored under N_2. The photocatalyst *N*-Me-9-mesityl acridinium tetrafluoroborate was donated by Pfizer and used without further purification.

General Procedure

To a 4.0 mL vial, alkyltrifluoroborate (0.30 mmol, 1.0 equiv), heteroarene (0.30 mmol, 1.0 equiv), photocatalyst (6.2 mg, 0.015 mmol, 0.05 equiv), and $K_2S_2O_8$ (162.2 mg, 0.60 mmol, 2.0 equiv) were added. Open to air, a mixture of 3.0 mL MeCN/H_2O (1:1) was added, followed by trifluoroacetic acid (34.2 mg, 0.30 mmol, 1.0 equiv). The mixture was stirred under 26 W CFLs (GE FLE26HT3/2/D) for 5–48 h under a fan. The reaction mixture was quenched with saturated $NaHCO_3$ and extracted with CH_2Cl_2 (3 x 20 mL). The organic extracts were combined and concentrated on Celite. The crude mixture was purified by silica gel column chromatography.

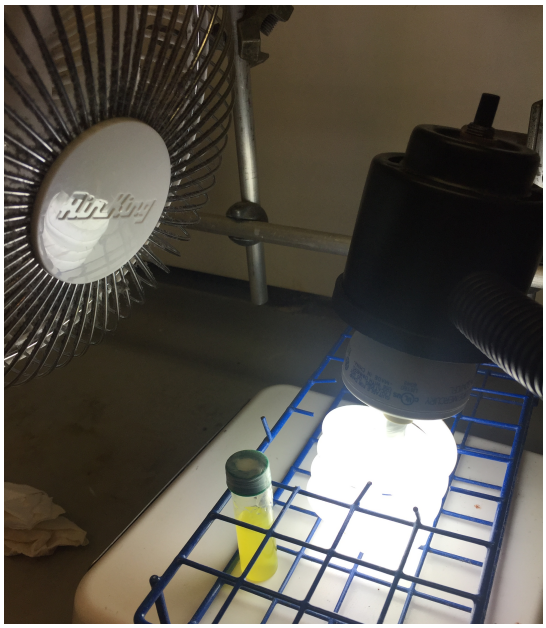

Compound Characterization

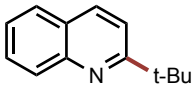

2-(*tert*-Butyl)quinoline (**2.7.1**)

Physical state: 40 mg, 72% yield, clear oil.

^{1}H NMR (500 MHz, $CDCl_3$) δ 8.07 (d, *J* = 8.6 Hz, 2H), 7.77 – 7.75 (m, 1H), 7.68 – 7.64 (m, 1H), 7.54 – 7.52 (m, 1H), 7.49 – 7.46 (m, 1H), 1.48 (s, 9H).

^{13}C NMR (126 MHz, $CDCl_3$) δ 169.4, 147.6, 136.0, 129.6, 129.1, 127.4, 126.6, 125.7, 118.3, 38.3, 30.3.

HRMS (ES+) m/z calc. for $C_{13}H_{16}N$ [M+H] 186.1283, found 186.1280.

FT-IR (cm^{-1}, neat, ATR) 2961, 1619, 1601, 1565, 1504, 1364, 1138, 1103, 829, 756, 478.

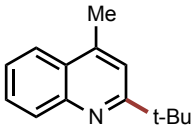

2-(*tert*-Butyl)-4-methylquinoline (**2.7.2**)

Reference: Gabriele, B.; Mancuso, R; Salerno, G.; Ruffolo, G.; Plastina, P. *J. Org. Chem.* **2007**, *72*, 6873.

Physical state: 57 mg, 95% yield, clear oil.

^{1}H NMR (500 MHz, $CDCl_3$) δ 8.05 (d, *J* = 8.4 Hz, 1H), 7.93-7.90 (m, 1H), 7.66-7.64 (m, 1H), 7.49-7.27 (m, 1H), 7.34 (s, 1H), 2.67 (s, 3H), 1.47 (s, 9H).

^{13}C NMR (126 MHz, $CDCl_3$) δ 169.1, 147.5, 143.7, 130.1, 128.8, 126.7, 125.5 123.5, 119.0, 38.1, 30.3, 19.1.

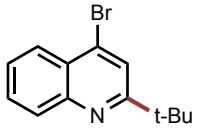

4-Bromo-2-(*tert*-butyl)quinoline (**2.7.3**)

Physical state: 68 mg, 86% yield, clear oil.

^{1}H NMR (500 MHz, $CDCl_3$) δ 8.10 (d, *J* = 8.4 Hz, 1H), 8.06-8.02 (m, 1H), 7.79 (s, 1H), 7.69 (dd *J* = 7.7, 7.6 Hz, 1H), 7.54 (dd, *J* = 7.7, 7.6 Hz, 1H), 1.45 (s, 9H).

^{13}C NMR (126 MHz, $CDCl_3$) δ 169.5, 148.3, 134.0, 130.1, 130.0, 127.0, 126.5, 126.2, 122.5, 38.3, 30.2.

HRMS (ES+) m/z calc. for $C_{13}H_{15}BrN$ [M+H] 264.0388, found 264.0397.

FT-IR (cm^{-1}, neat, ATR) 2957, 1585, 1488, 820, 756.

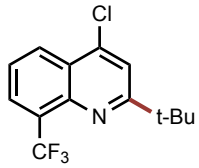

2-(*tert*-Butyl)-4-chloro-8-(trifluoromethyl)quinoline (**2.7.4**)

Physical state: 78 mg, 70% yield, clear oil.

^{1}H NMR (500 MHz, $CDCl_3$) δ 8.38 (d, *J* = 8.4 Hz, 1H), 8.08 (d, *J* = 7.2 Hz, 1H), 7.68 (s, 1H), 7.61-7.59 (m, 1H), 1.47 (s, 9H).

^{13}C NMR (126 MHz, $CDCl_3$) δ 170.5, 144.9, 142.6, 128.5 (q, *J* = 5.5 Hz), 128.3 (q, *J* = 29.1 Hz), 128.2, 125.3, 125.2, 123.1, 119.3, 38.9, 29.9.

HRMS (ES+) m/z calc. for $C_{14}H_{14}ClF_3N$ [M+H] 288.0767, found 288.0762.

FT-IR (cm^{-1}, neat, ATR) 2965, 1592, 1489, 1463, 1293, 1145, 1118, 766.

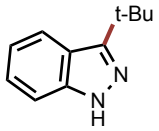

3-(*tert*-Butyl)-1*H*-indazole (**2.7.5**)

Reference: Li, P.; Wu, C.; Zhao, J.; Rogness, D. C.; Shi, F. *J. Org. Chem.* **2012**, *77*, 3149

Physical state: 41 mg, 80% yield, clear oil.

^{1}H NMR (500 MHz, $CDCl_3$) δ 10.07 (bs, 1H), 7.91 (d, *J* = 8.2 Hz, 1H), 7.44 (d, *J* = 8.2 Hz, 1H), 7.36-7.33 (m, 1H), 7.14-7.11 (m, 1H), 1.55 (s, 9H).

^{13}C NMR (126 MHz, $CDCl_3$) δ 154.8, 142.1, 126.3, 122.3, 120.7, 120.0, 110.1, 34.0, 30.2.

HRMS (ES+) m/z calc. for $C_{11}H_{15}N_2$ [M+H] 175.1235, found 175.1229.

FT-IR (cm^{-1}, neat, ATR) 3146, 3112, 3073, 2963, 2928, 2900, 1342, 739.

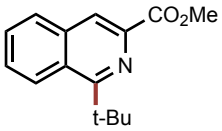

Methyl 1-(*tert*-Butyl)isoquinoline-3-carboxylate (**2.7.7**)

Physical state: 55 mg isolated, 77% yield, white solid (mp = 55 °C).

^{1}H NMR (500 MHz, $CDCl_3$) δ 11.64 (s, 1H), 8.50 – 8.45 (m, 2H), 7.72 – 7.70 (m, 2H), 4.06 (s, 3H), 1.64 (s, 9H).

^{13}C NMR (126 MHz, $CDCl_3$) δ 171.8, 158.0, 155.4, 129.6, 129.3, 129.0, 128.8, 127.3, 124.3, 118.4, 52.9, 39.7, 31.2.

HRMS: submitted.

FT-IR (cm^{-1}, neat, ATR) 2953, 1661, 1450, 1337, 1242, 1164.

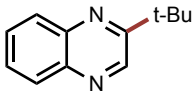

2-(*tert*-Butyl)quinoxaline (**2.7.8**)

Physical state: 39 mg, 70% yield, clear oil.

^{1}H NMR (500 MHz, $CDCl_3$) δ 8.99 (s, 1H), 8.06 (dd, *J* = 8.0, 3.8 Hz, 2H), 7.71 (m, 2H), 1.52 (s, 9H).

^{13}C NMR (126 MHz, $CDCl_3$) δ 163.8, 143.6, 141.8, 141.0, 129.8, 129.5, 129.1, 129.0, 37.4, 29.9.

HRMS (ES+) m/z calc. for $C_{12}H_{15}N_2$ [M+H] 186.1157, found 186.1158.

FT-IR (cm^{-1}, neat, ATR) 2963, 1558, 1492, 1464, 1365, 1237, 1155, 1128, 1097, 1014, 968, 761, 607.

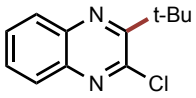

2-(*tert*-Butyl)-3-chloroquinoxaline (**2.7.9**)

Physical state: 28 mg isolated, 43% yield, clear oil.

^{1}H NMR (500 MHz, $CDCl_3$) δ 8.99 (s, 1H), 8.07 – 8.05 (m, 2H), 7.74 – 7.68 (m, 2H), 1.52 (s, 9H).

^{13}C NMR (126 MHz, $CDCl_3$) δ 163.8, 143.6, 141.8, 141.0, 129.8, 129.5, 129.1, 129.0, 37.4, 29.9.

HRMS (ES+) m/z calc. for $C_{12}H_{15}ClN_2$ [M+H] 221.0846, found 221.0844.

FT-IR (cm^{-1}, neat, ATR) 2977, 1167, 1104, 1008, 761.

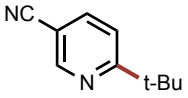

6-(*tert*-Butyl)nicotinonitrile (**2.7.10**)

Physical state: 42 mg, 89% yield, yellow oil.

^{1}H NMR (500 MHz, $CDCl_3$) δ 8.82 (s, 1H), 7.87 (d, *J* = 8.2 Hz, 1H), 7.46 (d, *J* = 8.2 Hz, 1H), 1.38 (s, 9H).

^{13}C NMR (126 MHz, $CDCl_3$) δ 174.1, 151.7, 139.5, 119.3, 117.3, 106.9, 38.4, 30.0.

HRMS (ES+) m/z calc. for $C_{10}H_{13}N_2$ [M+H] 161.1079, found 161.1078.

FT-IR (cm^{-1}, neat, ATR) 2960, 2050, 1721, 1596.

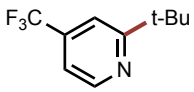

2-(*tert*-Butyl)-4-(trifluoromethyl)pyridine (**2.7.11**)

Reference: Stowers, K. J.; Fortner, K. C.; Sanford, M. S. *J. Am. Chem. Soc.* **2011**, *133*, 6541.

Physical state: 58 mg, 95% yield, light yellow oil.

^{1}H NMR (500 MHz, $CDCl_3$) δ 8.74 (d, *J* = 4.9 Hz, 1H), 7.53 (s, 1H), 7.31 (d, *J* = 5.0 Hz, 1H), 1.40 (d, *J* = 1.9 Hz, 9H).

^{13}C NMR (126 MHz, $CDCl_3$) δ 171.2, 149.7, 138.7 (q, *J* = 34.0 Hz), 123.4 (q, *J* = 271.0), 116.4 (q, *J* = 4.0 Hz), 114.8, 114.81, 38.0, 30.2.

^{19}F NMR (477 MHz) δ -64.70.

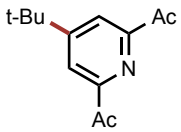

1,1'-(4-(*tert*-Butyl)pyridine-2,6-diyl)bis(ethan-1-one) (**2.7.12**)

Physical state: 48 mg, 73% yield, clear oil.

^{1}H NMR (500 MHz, $CDCl_3$) δ 8.22 (s, 2H), 2.78 (s, 6H), 1.36 (s, 9H).

^{13}C NMR (126 MHz, $CDCl_3$) δ 200.1, 162.9, 153.0, 122.0, 35.6, 30.6, 25.9.

HRMS (ES+) m/z calc. for $C_{13}H_{18}NO_2$ [M+H] 220.1338, found 220.1334.

FT-IR (cm^{-1}, neat, ATR) 2968, 2975, 1700, 1362, 1244, 1131, 610.

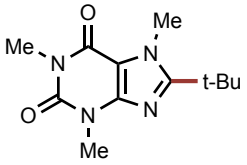

8-(*tert*-Butyl)-1,3,7-trimethyl-3,7-dihydro-1*H*-purine-2,6-dione (**2.7.13**)

Physical state: 52 mg, 70% yield, white solid (173 °C).

^{1}H NMR (500 MHz, $CDCl_3$) δ 4.11 (s, 3H), 3.56 (s, 3H), 3.39 (s, 3H), 1.47 (s, 9H).

^{13}C NMR (126 MHz, $CDCl_3$) δ 160.1, 155.8, 151.9, 147.1, 108.4, 34.3, 34.2, 29.7, 29.1, 28.0.

HRMS (ES+) m/z calc. for $C_{12}H_{19}N_4O_2$ [M+H] 251.1508, found 251.1505.

FT-IR (cm^{-1}, neat, ATR) 2974, 1699, 1656, 1543, 1492, 1428, 1364, 1240, 740.

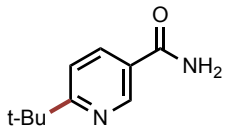

2-(*tert*-Butyl)nicotinamide **(2.7.14)**

Reference: Tada, M.; Yokoi, Y. *J. Heterocyclic Chem.* **1989**, *26*, 45.

Physical state: 36 mg, 67% yield, light yellow solid (mp = 94 °C).

^{1}H NMR (500 MHz, DMSO-d_6) δ 8.95 (d, J = 2.3 Hz, 1H), 8.17 – 7.99 (m, 2H), 7.51 (d, J = 8.2 Hz, 2H), 1.31 (s, 9H).

^{13}C NMR (126 MHz, DMSO) δ 171.2, 166.5, 147.6, 135.6, 127.0, 118.5, 20.8, 14.1.

HRMS (ES+) m/z calc. for $C_{10}H_{15}N_2O$ [M+H] 179.1184, found 179.1190.

FT-IR (cm^{-1}, neat, ATR) 3433, 2253, 2127, 1667, 1394, 1051, 1023, 820, 760.

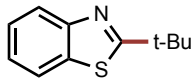

2-(*tert*-Butyl)benzo[*d*]thiazole (**2.7.15**)

Physical state: 38 mg, 66% yield, yellow oil.

^{1}H NMR (500 MHz, $CDCl_3$) δ 8.00 (d, *J* = 8.2 Hz, 1H), 7.85 (d, *J* = 7.9 Hz, 1H), 7.46 – 7.43 (m, 1H), 7.35 – 7.32 (m, 1H), 1.53 (s, 9H).

^{13}C NMR (126 MHz, $CDCl_3$) δ 182.0, 153.4, 135.1, 125.9, 124.6, 122.8, 121.6, 38.5, 30.9.

HRMS (ES+) m/z calc. for $C_{11}H_{14}NS$ [M+H] 192.0847, found 192.0847.

FT-IR (cm^{-1}, neat, ATR) 2965, 1513, 1438, 1044, 1008, 758.

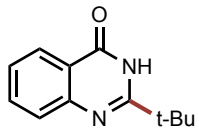

2-(*tert*-Butyl)quinazolin-4(3*H*)-one (**2.7.16**)

Reference: Li, Z.; Dong, J.; Chen, X.; Li, Q.; Zhou, Y.; Yin, S. -F. *J. Org, Chem.* **2015**, *80*, 9392.

Physical state: 54 mg, 90% yield, white solid (mp = 110–113 °C).

^{1}H NMR (500 MHz, $CDCl_3$) δ 11.40 (s, 1H), 8.29 (d, *J* = 7.6 Hz, 1H), 7.74 (d, *J* = 9.8 Hz, 2H), 7.45 (t, *J* = 7.6 Hz, 1H), 1.50 (s, 9H).

^{13}C NMR (126 MHz, $CDCl_3$) δ 164.1, 162.3, 149.4, 134.6, 127.8, 126.4, 126.3, 120.7, 100.1, 37.6, 28.4.

HRMS (ES+) m/z calc. for $C_{12}H_{15}N_2O$ [M+H] 203.1184, found 203.1183.

FT-IR (cm^{-1}, neat, ATR) 3189, 3079, 2968, 1667, 1611, 772.

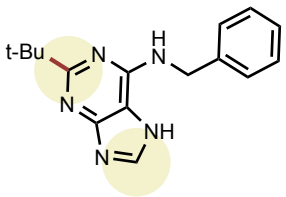

N-Benzyl-2-(*tert*-butyl)-7*H*-purin-6-amine (**2.7.18**)

Physical state: 67 mg, 79% yield, yellow solid (mp = 125–127 °C).

^{1}H NMR (500 MHz, $CDCl_3$) δ 8.45 (s, 1H), 7.44 – 7.41 (m, 2H), (dd, *J* = 7.5, 7.5 Hz, 2H), 7.29 (d, *J* = 7.5 Hz, 1H), 6.12 (bs, 1H), 4.89 (s, 2H), 1.53 (s, 9H) (highlighted proton not observed).

^{13}C NMR (126 MHz, $CDCl_3$) δ 160.7, 154.2, 151.6, 138.7, 128.8, 128.7, 128.2, 127.6, 100.1, 33.9, 29.6, 27.8.

HRMS (ES+) m/z calc. for $C_{16}H_{20}N_5$ [M+H] 282.1719, found 282.1718.

FT-IR (cm^{-1}, neat, ATR) 2972, 1619, 1598, 1351, 1299.

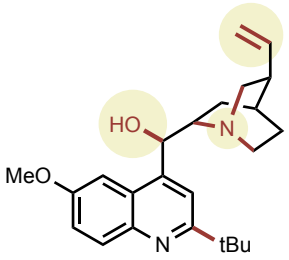

(1*R*)-(2-(*tert*-Butyl)-6-methoxyquinolin-4-yl)(5-vinylquinuclidin-2-yl)methanol (**2.7.19**)

Reference: Yardley, J. P.; Bright, R. E.; Rane, L.; Rees, R. W.; Russell, P. B.; Smith, H. *J. Med. Chem.* **1971**, *14*, 62.

Physical state: 62 mg, 54% yield, light yellow oil.

^{1}H NMR (500 MHz, $CDCl_3$) δ 7.98 (d, *J* = 9.2 Hz, 1H), 7.67 (s, 1H), 7.30 (d, *J* = 9.2 Hz, 1H), 7.20 (s, 1H), 5.73 (dt, *J* = 17.6, 9.0 Hz, 1H), 5.58 (s, 1H), 4.97 – 4.90 (m, 2H), 3.89 (s, 3H), 3.50 – 3.45 (m, 1H), 3.20 – 3.08 (m, 2H), 2.71 – 2.65 (m, 2H), 2.29 – 2.25 (m, 1H), 1.81 (s, 1H), 1.79 – 1.65 (m, 2H), 1.52 – 1.43 (m, 11H).

^{13}C NMR (126 MHz, $CDCl_3$) δ 166.6, 157.4, 146.9, 143.8, 142.0, 131.9, 124.7, 120.9, 115.5, 114.6, 101.3, 72.6, 60.1, 57.3, 55.8, 43.5, 40.1, 38.1, 30.3, 28.1, 27.8, 21.6.

HRMS (ES+) m/z calc. for $C_{24}H_{32}N_2O_2$ [M+H] 381.2536, found 381.2543.

FT-IR (cm^{-1}, neat, ATR)2954, 1621, 1601, 1561, 1505, 1471, 1363, 1343, 1263, 1231, 1106, 1034, 911, 832, 734, 645.

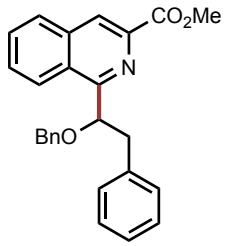

Methyl 1-(1-(Benzyloxy)-3-phenylpropyl)isoquinoline-3-carboxylate (**2.9.1**)

Physical state: 71 mg, 58% yield, clear oil.

^{1}H NMR (500 MHz, $CDCl_3$) δ 8.88 (d, *J* = 8.5 Hz, 1H), 8.52 (s, 1H), 7.98 (d, *J* = 8.0 Hz, 1H), 7.78 – 7.76 (m, 1H), 7.70 – 7.66 (m, 1H), 7.41 – 7.35 (m, 1H), 7.31 – 7.22 (m, 7H), 7.19 – 7.12 (m, 2H), 5.26 – 5.22 (m, 1H), 4.52 – 4.43 (m, 2H), 4.08 (s, 3H), 3.12 – 2.96 (m, 1H), 2.78 – 2.72 (m, 1H), 2.61 – 2.53 (m, 1H), 2.33 – 2.25 (m, 1H).

^{13}C NMR (126 MHz, $CDCl_3$) δ 166.4, 161.5, 141.7, 140.2, 138.1, 136.5, 130.6, 129.1, 128.8, 128.4, 128.2, 128.1(9), 127.8, 127.7, 127.5, 126.2, 125.7, 124.2, 85.1, 71.5, 52.8, 37.8, 32.5.

HRMS (ES+) m/z calc. for $C_{27}H_{25}NO_3Na$ [M+Na] 434.1732, found 434.1734.

FT-IR (cm^{-1}, neat, ATR) 3052, 2950, 1736, 1717, 1373, 1147, 1027, 908, 782, 490.

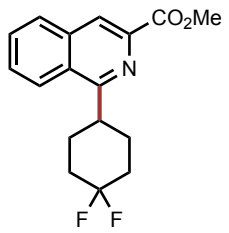

Methyl 1-(4,4-Difluorocyclohexyl)isoquinoline-3-carboxylate (**2.9.2**)

Physical state: 32 mg, 35% yield, yellow oil.

^{1}H NMR (500 MHz, $CDCl_3$) δ 8.43 (s, 1H), 8.22 (d, *J* = 7.8 Hz, 1H), 7.98 – 7.95 (m, 1H), 7.77 – 7.72 (m, 2H), 4.02 (s, 3H), 3.72 – 3.58 (m, 1H), 2.40 – 2.27 (m, 4H), 2.16 – 1.90 (m, 4H).

^{13}C NMR (126 MHz, $CDCl_3$) δ 166.7, 163.5, 163.5, 140.6, 136.1, 130.4, 129.4, 129.4, 129.3, 127.6, 125.2, 124.5, 123.3, 122.9, 121.4, 52.7, 39.7, 33.9, 33.7, 33.7, 33.5, 28.3, 28.2.

^{19}F NMR (471 MHz, C_6D6) δ 2.26 (d, *J* = 235.5 Hz), 6.03 (d, *J* = 235.5 Hz).

HRMS (ES+) m/z calc. for $C_{17}H_{17}F_2NO_3$ [M+Na] 328.1125, found 328.1124.

FT-IR (cm^{-1}, neat, ATR) 2951, 1736, 1450, 1374, 1236, 1205, 1101, 956, 784.

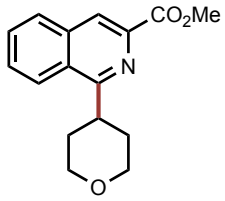

Methyl 1-(Tetrahydro-2H-pyran-4-yl)isoquinoline-3-carboxylate (**2.9.3**)

Physical state: 60 mg, 74% yield, white semi-solid.

^{1}H NMR (300 MHz, $CDCl_3$) δ 8.45 (s, 1H), 8.35 – 8.22 (m, 1H), 8.07 – 7.90 (m, 1H), 7.76 (dt, *J* = 5.4, 3.2 Hz, 2H), 4.20 (dd, *J* = 11.4, 2.6 Hz, 2H), 4.05 (s, 3H), 3.93 – 3.56 (m, 3H), 2.51 – 2.23 (m, 2H), 1.91 (dd, *J* = 13.4, 1.5 Hz, 2H).

^{13}C NMR (126 MHz, $CDCl_3$) δ 166.9, 163.9, 141.0, 140.9, 136.3, 130.4, 129.4, 127.7, 124.6, 122.9, 68.3, 52.8, 39.4, 32.0.

HRMS (ES+) m/z calc. for $C_{16}H_{17}NO_3Na$ [M+Na] 294.1106, found 294.1111.

FT-IR (cm^{-1}, neat, ATR) 2962, 1589, 1489, 1387, 850.

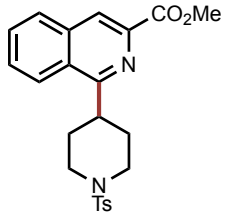

Methyl 1-(1-Tosylpiperidin-4-yl)isoquinoline-3-carboxylate (**2.9.4**)

Physical state: 84 mg, 66% yield, pale yellow solid (mp = dec ~195 ^{o}C).

^{1}H NMR (500 MHz, $CDCl_3$) δ 8.42 (s, 1H), 8.11 (d, *J* = 8.5 Hz, 1H), 7.97 (d, *J* = 8.0 Hz, 1H), 7.74-7.66 (m, 4H), 7.37 (d, *J* = 8.0 Hz, 2H), 4.03 (s, 3H), 3.98 (d, *J* = 11.5 Hz, 2H), 3.53-3.48 (m, 1H), 2.62-2.52 (m, 2H), 2.48 (s, 3H), 2.45-2.32 (m, 2H), 2.05-2.03 (m, 2H).

^{13}C NMR (126 MHz, $CDCl_3$) δ 166.5, 162.9, 143.3, 140.6, 133.3, 130.2, 129.5, 129.2, 129.1(9), 128.8, 127.8, 127.4, 124.1, 122.8, 52.6, 46.3, 39.1, 30.4, 21.5.

HRMS (ES+) m/z calc. for $C_{23}H_{25}N_2O_4S$ [M+H] 425.1535, found 425.1531.

FT-IR (cm^{-1}, neat, ATR) 2962, 1589, 1489, 1387, 850.

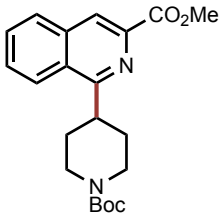

Methyl 1-(1-(*tert*-Butoxycarbonyl)piperidin-4-yl)isoquinoline-3-carboxylate (**2.9.5**)

Physical state: 41 mg, 51% yield, white semi-solid.

^{1}H NMR (500 MHz, $CDCl_3$) δ 8.42 (s, 1H), 8.25 (d, *J* = 7.3 Hz, 1H), 8.06 – 7.89 (m, 1H), 7.84 – 7.64 (m, 2H), 4.32 (m, 2H), 4.02 (s, 3H), 3.72 (t, *J* = 11.4 Hz, 1H), 2.99 (m, 2H), 2.03 (m, 4H), 1.49 (s, 9H).

^{13}C NMR (126 MHz, $CDCl_3$) δ 166.8, 164.1, 154.9, 140.8, 136.3, 130.5, 129.4, 127.8, 124.6, 122.9, 79.6, 58.5, 52.8, 40.2, 31.2, 28.7.

HRMS (ES+) m/z calc. for $C_{21}H_{27}N_2O_4$ [M+H] 371.1971, found 371.1984.

FT-IR (cm^{-1}, neat, ATR) 2962, 1589, 1489, 1387, 850.

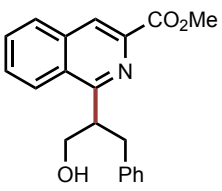

Methyl 1-(1-Hydroxy-3-phenylpropan-2-yl)isoquinoline-3-carboxylate (**2.9.6**)

Physical state: 20 mg, 20% yield, clear oil.

^{1}H NMR (500 MHz, $CDCl_3$) δ 8.48 (s, 1H), 8.13 (d, *J* = 8.4 Hz, 1H), 7.98 (d, *J* = 8.1 Hz, 1H), 7.78 – 7.75 (m, 1H), 7.72 – 7.68 (m, 1H), 7.34 – 7.18 (m, 5H), 5.65 (d, *J* = 10.1 Hz, 1H), 4.19 (d, *J* = 11.3 Hz, 1H), 4.05 (s, 3H), 3.98 – 3.93 (m, 1H), 3.88 – 3.84 (m, 1H), 3.39 – 3.34 (m, 1H), 3.12 – 3.07 (m, 1H).

^{13}C NMR (126 MHz, $CDCl_3$) δ 166.2, 165.4, 140.1, 139.6, 136.3, 131.1, 129.9, 129.5, 129.4, 128.7, 128.0, 126.5, 125.0, 123.2, 63.1, 53.0, 44.4, 38.1.

HRMS (ES+) m/z calc. for $C_{20}H_{20}NO_2$ [M+H] 322.1443, found 322.1452.

FT-IR (cm^{-1}, neat, ATR) 1734, 1451, 1244, 1207, 749, 702.

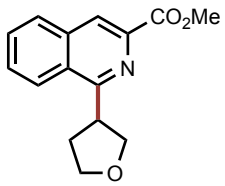

Methyl 1-(Tetrahydrofuran-3-yl)isoquinoline-3-carboxylate (**2.9.7**)

Physical state: 43.7 mg, 34% yield, colorless oil.

^{1}H NMR (500 MHz, $CDCl_3$) δ 8.45 (s, 1H), 8.27 (d, *J* = 7.2 Hz, 1H), 8.00 – 7.93 (m, 1H), 7.80 – 7.70 (m, 2H), 4.42 – 4.32 (m, 2H), 4.25 – 4.15 (m, 2H), 4.08 – 3.96 (m, 4H), 2.79 – 2.57 (m, 1H), 2.53 – 2.31 (m, 1H).

^{13}C NMR (126 MHz, $CDCl_3$) δ 166.5, 161.2, 136.0, 134.0, 130.4, 129.4, 129.0, 128.4, 124.8, 123.0, 112.7, 77.2, 68.8, 52.6, 43.4, 32.1.

HRMS (ES+) m/z calc. for $C_{15}H_{16}NO_3$ [M+H] 258.1130, found 258.1140.

FT-IR (cm^{-1}, neat, ATR) 2987, 2870, 1208, 1063, 861, 837.

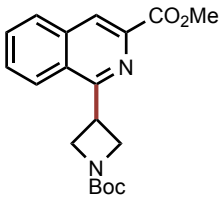

Methyl 1-(1-(*tert*-Butoxycarbonyl)azetidin-3-yl)isoquinoline-3-carboxylate (**2.9.9**)

^{1}H NMR (500 MHz, $CDCl_3$) δ 8.50 (s, 1H), 8.01 (d, *J* = 8.1 Hz, 1H), 7.89 (d, *J* = 8.2 Hz, 1H), 7.82 – 7.71 (m, 2H), 4.64 – 4.45 (m, 5H), 4.05 (s, 3H), 1.47 (s, 9H).

^{13}C NMR (126 MHz, $CDCl_3$) δ 166.3, 159.7, 156.3, 140.3, 135.9, 130.7, 129.7, 129.2, 127.7, 124.3, 123.4, 79.4, 52.6, 33.0, 28.3.

HRMS (ES+) m/z calc. for $C_{19}H_{23}N_2O_4$ [M+H] 343.1658, found 343.1666.

FT-IR (cm^{-1}, neat, ATR) 2987, 2870, 1208, 1063, 861, 837.

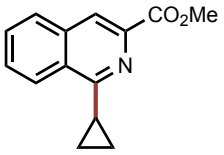

Methyl 1-Cyclopropylisoquinoline-3-carboxylate (**2.9.10**)

Physical state: 21 mg, 31% yield, clear oil.

^{1}H NMR (500 MHz, $CDCl_3$) δ 8.54 – 8.44 (m, 1H), 8.36 (s, 1H), 8.01 – 7.89 (m, 1H), 7.76 – 7.73 (m, 2H), 4.01 (s, 3H), 2.75 (tt, *J* = 8.5, 4.9 Hz, 1H), 1.37 – 1.34 (m, 2H), 1.17 – 1.13 (m, 2H).

^{13}C NMR (126 MHz, $CDCl_3$) δ 166.9, 162.5, 140.7, 135.8, 130.6, 129.5, 129.4, 129.0, 125.6, 122.3, 52.9, 14.4, 9.3.

HRMS (ES+) m/z calc. for $C_{14}H_{13}NO_2$ [M+H] 228.1025, found 228.1019.

FT-IR (cm^{-1}, neat, ATR) 2951, 1737, 1321, 1269, 1244, 988.

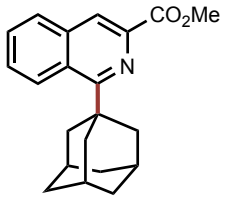

Methyl 1-((3*r*,5*r*,7*r*)-Adamantan-1-yl)isoquinoline-3-carboxylate (**2.9.11**)

Physical state: 43.4 mg, 45% yield, off-white solid (mp = 210–212 °C)

^{1}H NMR (500 MHz, $CDCl_3$) δ 11.63 (s, 1H), 8.73 – 8.71 (m, 1H), 8.58 – 8.38 (m, 1H), 7.71 – 7.70 (m, 2H), 4.08 (s, 3H), 2.38 (s, 6H), 2.21 (s, 3H), 1.89 (m, 6H).

^{13}C NMR (126 MHz, $CDCl_3$) δ 171.6, 157.4, 155.1, 129.5, 129.1, 128.6, 128.4, 126.8, 124.2, 118.5, 52.7, 42.2, 41.9, 37.0, 29.1.

HRMS (ES+) m/z calc. for $C_{21}H_{24}NO_2$ [M+H] 322.1807, found 322.1797.

FT-IR (cm^{-1}, neat, ATR) 2951, 1737, 1321, 1269, 1244, 988.

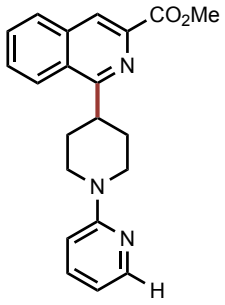

Methyl 1-(1-(Pyridin-2-yl)piperidin-4-yl)isoquinoline-3-carboxylate (**2.9.12**)

Physical state: 75 mg, 72% yield, yellow solid (mp = 154–157 °C).

^{1}H NMR (500 MHz, $CDCl_3$) δ 8.42 (s, 1H), 8.31 (s, 1H), 8.20 (s, 1H) 7.98 (d, *J* = 3.5 Hz, 1H), 7.76 – 7.74 (m, 2H), 7.49 – 7.45 (m, 1H), 6.74 (d, *J* = 8.5 Hz, 1H), 6.60-6.59 (m, 1H), 4.52 (d, *J* = 12.5 Hz, 2H), 4.00 (s, 3H), 3.82-3.80 (m, 1H), 3.12 (t, *J* = 12.5 Hz, 2H), 2.34-2.26 (m, 2H), 2.10-2.04 (m, 2H).

^{13}C NMR (126 MHz, $CDCl_3$) δ 166.9, 164.3, 159.6, 148.1, 140.9, 137.5, 136.3, 130.4, 129.4, 129.4, 127.8, 124.8, 122.9, 112.8, 107.4, 52.8, 45.8, 40.7, 31.2.

HRMS (ES+) m/z calc. for $C_{21}H_{22}N_3O_2$ [M+H] 348.1712, found 348.1714.

FT-IR (cm^{-1}, neat, ATR) 2962, 1589, 1489, 1387, 850.

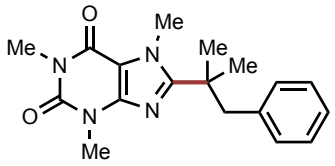

1,3,9-Trimethyl-8-(2-methyl-1-phenylpropan-2-yl)-3,9-dihydro-1H-purine-2,6-dione (**2.8.4**)

Physical state: 52 mg, 53% yield, pale yellow solid (mp = 101–103 ^oC).

^{1}H NMR (500 MHz, $CDCl_3$) δ 7.23-7.21 (m, 3H), 6.88-6.85 (m, 2H), 3.80 (s, 3H), 3.56 (s, 3H), 3.41 (s, 3H), 3.03 (s, 2H), 1.51 (s, 6H).

^{13}C NMR (126 MHz, $CDCl_3$) δ 158.7, 155.5, 146.9(4), 146.9(1), 137.4, 129.8, 128.1, 126.7, 107.7, 48.2, 39.4, 33.8, 29.5, 27.8, 27.2.

HRMS (ES+) m/z calc. for $C_{17}H_{23}N_4O_2$ [M+H] 327.1821, found 327.1820.

FT-IR (cm^{-1}, neat, ATR) 3055, 2987, 1758, 1699, 1656, 1422, 1040, 896, 733, 703.

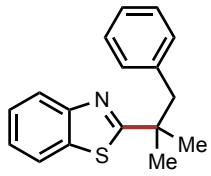

2-(2-Methyl-1-phenylpropan-2-yl)benzo[d]thiazole (**2.8.5**)

Physical state: 52 mg, 53% yield, pale yellow oil.

^{1}H NMR (500 MHz, $CDCl_3$) δ 8.05 (d, J = 8.2 Hz, 1H), 7.86 (dd, J = 8.0, 0.5 Hz, 1H), 7.53 – 7.44 (m, 1H), 7.41 – 7.32 (m, 1H), 7.27 – 7.12 (m, 3H), 7.09 – 6.98 (m, 2H), 3.18 (s, 2H), 1.52 (s, 6H).

^{13}C NMR (126 MHz, $CDCl_3$) δ 180.7, 153.2, 137.6, 134.8, 130.4, 127.8, 126.3, 125.7, 124.5, 122.7, 121.4, 49.5, 42.2, 28.0.

HRMS (ES+) m/z calc. for $C_{17}H_{18}NS$ [M+H] 268.1160, found 268.1168.

FT-IR (cm^{-1}, neat, ATR) 3028, 2927, 1505, 1495, 1385, 1280, 1005, 743, 687.

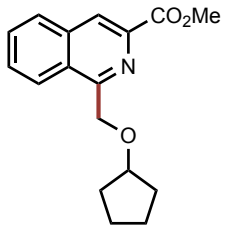

Methyl 1-((Cyclopentyloxy)methyl)isoquinoline-3-carboxylate (**2.10.1**)

Physical state: 72 mg, 84% yield, clear viscous oil.

^{1}H NMR (500 MHz, $CDCl_3$) δ 8.52 (s, 1H), 8.45 (d, *J* = 7.7 Hz, 1H), 7.94 (d, *J* = 7.4 Hz, 1H), 7.74 (s, 2H), 5.10 (s, 2H), 4.13 (s, 1H), 4.04 (s, 3H), 1.52 (m, 8H).

^{13}C NMR (126 MHz, $CDCl_3$) δ 166.5, 158.6, 140.3, 136.3, 130.9, 129.6, 129.1, 128.6, 126.7, 124.7, 82.3, 77.4, 77.2, 76.9, 72.5, 53.0, 32.4, 23.6.

HRMS (ES+) m/z calc. for $C_{17}H_{20}NO_3$ [M+H] 286.1443, found 286.1454.

FT-IR (cm^{-1}, neat, ATR) 2952, 1737, 1334, 1246, 1110, 1096, 791.

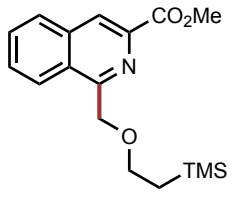

Methyl 1-((2-(Trimethylsilyl)ethoxy)methyl)isoquinoline-3-carboxylate (**2.10.2**)

Physical state: 61 mg, 86% yield, clear oil.

^{1}H NMR (500 MHz, $CDCl_3$) δ 8.53 (s, 1H), 8.47 (d, *J* = 7.9 Hz, 1H), 7.96 (d, *J* = 7.9 Hz, 1H), 7.78 – 7.71 (m, 2H), 5.13 (s, 2H), 4.04 (s, 3H), 3.76 – 3.55 (m, 2H), 1.11 – 0.90 (m, 2H), -0.03 (s, 9H).

^{13}C NMR (126 MHz, $CDCl_3$) δ 166.5, 158.4, 140.4, 136.3, 130.9, 129.6, 129.0, 128.6, 126.6, 124.7, 73.5, 68.5, 52.9, 18.5, -1.3.

HRMS (ES+) m/z calc. for $C_{17}H_{23}NO_3Si$ [M+Na] 340.1345, found 340.1347.

FT-IR (cm^{-1}, neat, ATR) 2951, 1740, 1719, 1247, 1208, 860.

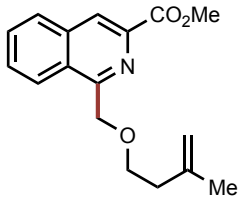

Methyl 1-(((3-Methylbut-3-en-1-yl)oxy)methyl)isoquinoline-3-carboxylate (**2.10.3**)

Physical state: 55 mg, 64% yield, clear oil.

^{1}H NMR (500 MHz, $CDCl_3$) δ 8.54 (s, 1H), 8.49 (d, *J* = 8.2 Hz, 1H), 7.96 (d, *J* = 7.9 Hz, 1H), 7.78 – 7.70 (m, 2H), 5.16 (s, 2H), 4.74 (s, 1H), 4.70 (s, 1H), 4.04 (s, 3H), 3.68 (t, *J* = 6.9 Hz, 2H), 2.32 (t, *J* = 6.9 Hz, 2H), 1.68 (s, 3H).

^{13}C NMR (126 MHz, $CDCl_3$) δ 166.4, 158.2, 142.8, 140.3, 136.3, 131.0, 129.6, 129.0, 128.6, 126.6, 124.8, 111.7, 74.2, 69.4, 53.0, 37.9, 22.7.

HRMS (ES+) m/z calc. for $C_{17}H_{19}NO_3Na$ [M+Na] 308.1263, found 308.1263.

FT-IR (cm^{-1}, neat, ATR) 2950, 1738, 1450, 1295, 1209, 1109.

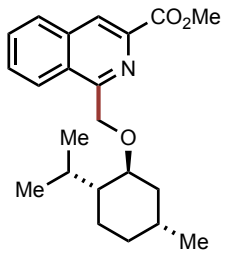

Methyl 1-((((1*R*,2*S*,5*R*)-2-Isopropyl-5-methylcyclohexyl)oxy)methyl)isoquinoline-3-carboxylate (**2.10.4**)

Physical state: 65 mg, 61% yield, clear oil.

^{1}H NMR (500 MHz, $CDCl_3$) δ 8.53 (s, 1H), 8.46 (d, *J* = 7.7 Hz, 1H), 7.95 (d, *J* = 8.2 Hz, 1H), 7.79 – 7.70 (m, 2H), 5.30 (d, *J* = 11.3 Hz, 1H), 5.04 (d, *J* = 11.3 Hz, 1H), 4.04 (s, 3H), 3.28 (td, *J* = 10.5, 4.1 Hz, 1H), 2.07 – 2.03 (m, 1H), 1.67 – 1.54 (m, 2H), 1.43 – 1.17 (m, 3H), 0.97 – 0.75 (m, 9H), 0.43 (d, *J* = 6.9 Hz, 3H).

^{13}C NMR (126 MHz, $CDCl_3$) δ 166.6, 158.9, 140.3, 136.3, 130.9, 129.4, 129.2, 128.6, 127.0, 124.8, 79.3, 71.3, 52.9, 48.5, 40.4, 34.6, 31.6, 25.3, 23.1, 22.5, 21.1, 15.7.

HRMS (ES+) m/z calc. for $C_{22}H_{29}NO_3Na$ [M+Na] 378.2047, found 378.2045.

FT-IR (cm^{-1}, neat, ATR) 2954, 2869, 1722, 1244, 1108, 984, 907, 688, 646.

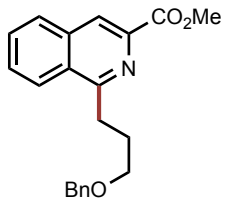

Methyl 1-(3-(Benzyloxy)propyl)isoquinoline-3-carboxylate (**2.10.5**)

Physical state: 52 mg, 56% yield, clear oil.

^{1}H NMR (500 MHz, $CDCl_3$) δ 8.45 (s, 1H), 8.21 (d, *J* = 8.3 Hz, 1H), 8.03 (d, *J* = 7.4 Hz, 2H), 7.96 (d, *J* = 8.1 Hz, 1H), 7.74 (t, *J* = 7.5 Hz, 1H), 7.68 (t, *J* = 7.6 Hz, 1H), 7.54 (t, *J* = 7.0 Hz, 1H), 7.42 (t, *J* = 7.6 Hz, 2H), 4.41 (t, *J* = 6.4 Hz, 2H), 4.04 (s, 3H), 3.46 (t, *J* = 7.9 Hz, 2H).

^{13}C NMR (126 MHz, $CDCl_3$) δ 166.8, 166.8, 162.5, 140.8, 136.1, 133.0, 133.0, 130.7, 130.6, 129.7, 129.7, 129.52, 129.1, 128.5, 125.6, 123.1, 100.1, 77.4, 77.2, 76.9, 64.9, 64.8, 62.6, 53.0, 35.3, 29.4, 29.0, 26.4, 25.4.

HRMS (ES+) m/z calc. for $C_{19}H_{17}NO_3$ [M+Na] 308.1287, found 308.1283.

FT-IR (cm^{-1}, neat, ATR) 2951, 1716, 1315, 1275, 1246, 712.

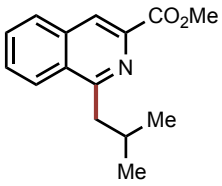

Methyl 1-Isobutylisoquinoline-3-carboxylate (**2.10.6**)

Physical state: 45 mg, 62% yield, clear oil.

^{1}H NMR (500 MHz, $CDCl_3$) δ 8.43 (s, 1H), 8.21 (d, *J* = 8.0 Hz, 1H), 7.94 (d, *J* = 7.8 Hz, 1H), 7.71 (m, 2H), 4.03 (s, 3H), 3.25 (d, *J* = 7.3 Hz, 2H), 2.32 (m, 1H), 0.98 (d, *J* = 6.7 Hz, 6H).

^{13}C NMR (126 MHz, $CDCl_3$) δ 166.9, 162.5, 140.8, 136.1, 130.5, 129.2, 129.0, 129.0, 125.9, 122.8, 52.9, 44.1, 29.8, 22.9.

HRMS (ES+) m/z calc. for $C_{15}H_{17}NO_2Na$ [M+Na] 266.1157, found 266.1161.

FT-IR (cm^{-1}, neat, ATR) 2955, 1737, 1718, 1294, 1242, 1205.

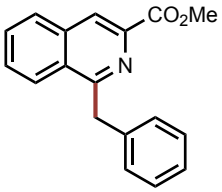

Methyl 1-Benzylisoquinoline-3-carboxylate (**2.10.7**)

Physical state: 56 mg, 67% yield, clear oil.

^{1}H NMR (500 MHz, $CDCl_3$) δ 8.51 (s, 1H), 8.16 (d, *J* = 8.4 Hz, 1H), 7.95 (d, *J* = 8.1 Hz, 1H), 7.73 – 7.68 (m, 1H), 7.64 – 7.60 (m, 1H), 7.27 – 7.20 (m, 4H), 7.19 – 7.13 (t, *J* = 7.0 Hz, 1H), 4.78 (s, 2H), 4.07 (s, 3H).

^{13}C NMR (126 MHz, $CDCl_3$) δ 166.7, 160.9, 140.8, 139.2, 136.4, 130.7, 129.6, 129.0, 128.8, 128.7 128.7, 126.5, 126.4, 123.7, 53.0, 42.6.

HRMS (ES+) m/z calc. for $C_{18}H_{16}NO_2$ [M+H] 278.1181, found 278.1171.

FT-IR (cm^{-1}, neat, ATR) 2949, 1736, 1568, 1438, 1242, 1208, 1150, 1106, 742, 692.

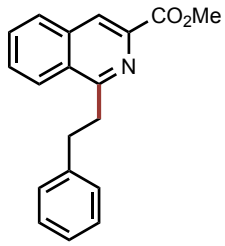

Methyl 1-Phenethylisoquinoline-3-carboxylate (**2.10.8**)

Physical state: 28 mg, 32% yield, clear oil.

^{1}H NMR (500 MHz, $CDCl_3$) δ 8.47 (s, 1H), 8.19 (d, *J* = 8.2 Hz, 1H), 7.96 (d, *J* = 7.9 Hz, 1H), 7.78 – 7.66 (m, 2H), 7.32 – 7.15 (m, 5H), 4.06 (s, 3H), 3.76 – 3.62 (m, 2H), 3.28 – 3.15 (m, 2H).

^{13}C NMR (126 MHz, $CDCl_3$) δ 166.8, 166.8, 162.0, 141.8, 140.8, 136.1, 130.7, 129.5, 129.1, 128.6, 128.6, 126.2, 125.5, 123.2, 53.0, 37.4, 35.6 (one aryl carbon peak overlaps).

HRMS (ES+) m/z calc. for $C_{19}H_{18}NO_2$ [M+H] 314.1157, found 314.1157.

FT-IR (cm^{-1}, neat, ATR) 2949, 1737, 1716, 1240, 1208, 749.

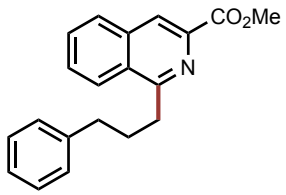

Methyl 1-(3-Phenylpropyl)isoquinoline-3-carboxylate (**2.10.9**)

Physical state: 76% yield, clear oil.

^{1}H NMR (500 MHz, $CDCl_3$) δ 8.44 (s, 1H), 8.06 (d, *J* = 8.3 Hz, 1H), 7.94 (d, *J* = 8.0 Hz, 1H), 7.76 – 7.68 (m, 2H), 7.35 – 7.26 (m, 2H), 7.25 – 7.16 (m, 3H), 4.05 (s, 3H), 3.48 – 3.27 (m, 2H), 2.81 (t, *J* = 7.7 Hz, 2H), 2.26 – 2.19 (m, 2H).

^{13}C NMR (126 MHz, $CDCl_3$) δ 166.8, 162.8, 142.1, 140.8, 136.1, 130.6 129.4, 129.0, 128.7, 128.5, 128.5, 126.0, 125.6, 123.1, 53.0, 36.1, 35.2, 31.6.

HRMS (ES+) m/z calc. for $C_{20}H_{20}NO_2$ [M+H] 306.1494, found 306.1492.

FT-IR (cm^{-1}, neat, ATR) 2949, 1736, 1716, 1242, 1209, 747.

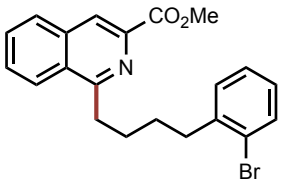

Methyl 1-(4-(2-Bromophenyl)butyl)isoquinoline-3-carboxylate (**2.10.10**)

Physical state: 67 mg, 56% yield, clear oil.

^{1}H NMR (500 MHz, $CDCl_3$) δ 8.44 (s, 1H), 8.20 (d, *J* = 8.0 Hz, 1H), 7.95 (d, *J* = 7.8 Hz, 1H), 7.75 – 7.70 (m, 2H), 7.51 (d, *J* = 8.0 Hz, 1H), 7.24 – 7.19 (m, 2H), 7.03 (s, 1H), 4.04 (s, 3H), 3.42 (t, *J* = 8.1 Hz, 2H), 2.85 – 2.76 (m, 2H), 2.01 – 1.90 (m, 2H), 1.85 – 1.76 (m, 2H).

^{13}C NMR (126 MHz, $CDCl_3$) δ 166.8, 162.9, 141.7, 140.8, 136.1, 132.9, 130.6, 130.5, 129.4, 129.0, 128.5, 127.6, 125.7, 124.6, 123.0, 53.0, 36.2, 35.7, 30.2, 29.8.

HRMS (ES+) m/z calc. for $C_{21}H_{20}BrNO_2$ [M+Na] 420.0575, found 420.0576.

FT-IR (cm^{-1}, neat, ATR) 2946, 1735, 1438, 1239, 1207, 1020, 748.

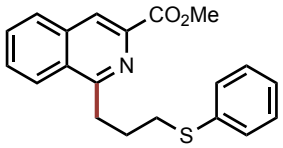

Methyl 1-(3-(Phenylthio)propyl)isoquinoline-3-carboxylate (**2.10.11**)

Physical state: 50 mg, 49% yield, clear oil.

^{1}H NMR (500 MHz, $CDCl_3$) δ 8.44 (s, 1H), 8.15 (d, *J* = 8.4 Hz, 1H), 7.95 (d, *J* = 8.1 Hz, 1H), 7.76 – 7.70 (m, 1H), 7.70 – 7.64 (m, 1H), 7.36 (d, *J* = 7.7 Hz, 2H), 7.31 – 7.21 (m, 2H), 7.19 – 7.14 (m, 1H), 4.04 (s, 3H), 3.58 – 3.46 (m, 2H), 3.11 (t, *J* = 7.0 Hz, 2H), 2.30 – 2.21 (m, 2H).

^{13}C NMR (126 MHz, $CDCl_3$) δ 166.7, 161.9, 140.7, 136.5, 136.1, 130.7, 129.6, 129.4, 129.0, 128.5, 126.1 125.6, 123.2, 53.0, 34.4, 33.6, 29.0 (one aryl peak overlaps).

HRMS (ES+) m/z calc. for $C_{20}H_{20}NO_2S$ [M+H] 338.1215, found 338.1198.

FT-IR (cm^{-1}, neat, ATR) 2950, 1737, 1716, 1449, 1325, 1294, 1243, 1210.

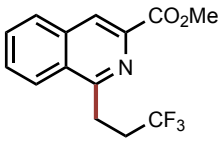

Methyl 1-(3,3,3-Trifluoropropyl)isoquinoline-3-carboxylate (**2.10.12**)

Physical state: 15 mg, 18% yield, viscous oil.

^{1}H NMR (500 MHz, $CDCl_3$) δ 8.48 (s, 1H), 8.20 (d, *J* = 8.6 Hz, 1H), 8.06 – 7.93 (m, 1H), 7.86 – 7.74 (m, 2H), 4.05 (s, 3H), 3.68 – 3.57 (m, 2H), 2.96 – 2.77 (m, 2H).

^{13}C NMR (126 MHz, $CDCl_3$) δ 166.5, 158.7, 140.6, 136.0, 131.1, 130.1, 129.3, 128.4, 124.8, 123.7, 53.1, 32.5 (q, *J* = 29.0 Hz), 29.0, 27.4.

^{19}F NMR (471 MHz, $CDCl_3$) δ -66.42.

HRMS (ES+) m/z calc. for $C_{14}H_{12}F_3NO_2Na$ [M+Na] 306.0718, found 306.0721.

FT-IR (cm^{-1}, neat, ATR) 3071, 1715, 1240, 1126.

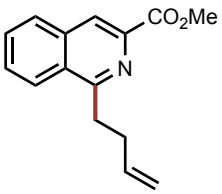

Methyl 1-(But-3-en-1-yl)isoquinoline-3-carboxylate (**2.10.16**)

Physical state: 40 mg, 55% yield, crystalline powder (mp = 54–57 °C).

^{1}H NMR (500 MHz, $CDCl_3$) δ 8.44 (s, 1H), 8.21 (d, *J* = 7.9 Hz, 1H), 7.95 (d, *J* = 7.9 Hz, 1H), 7.76 – 7.68 (m, 2H), 6.05 – 5.90 (m, 1H), 5.12 (d, *J* = 17.0 Hz, 1H), 5.01 (d, *J* = 10.2 Hz, 1H), 4.04 (s, 3H), 3.47 (t, *J* = 8.2 Hz, 2H), 2.70 – 2.60 (m, 2H).

^{13}C NMR (126 MHz, $CDCl_3$) δ 166.7, 162.3, 140.8, 137.8, 136.1, 130.6, 129.5, 129.1, 128.5, 125.6, 123.1, 115.3, 53.0, 35.0, 33.8.

HRMS (ES+) m/z calc. for $C_{15}H_{15}NO_2$ [M+Na] 264.1000, found 264.0998.

FT-IR (cm^{-1}, neat, ATR) 1748, 1656, 1596, 1157.

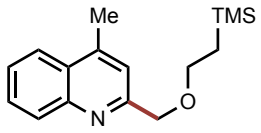

4-Methyl-2-((2-(Trimethylsilyl)ethoxy)methyl)quinoline (**2.11.1**)

Reference: Molander, G. A.; Colombel, V.; Braz, V. *Org. Lett.* **2011**, *13*, 1852.

Physical state: 62 mg, 77% yield, clear oil.

^{1}H NMR (500 MHz, $CDCl_3$) δ 8.05 (d, *J* = 8.4 Hz, 1H), 7.98 (d, *J* = 8.3 Hz, 1H), 7.71 – 7.66 (m, 1H), 7.55 – 7.51 (m, 1H), 7.46 (s, 1H), 4.74 (s, 2H), 3.72 – 3.63 (m, 2H), 2.71 (s, 3H), 1.11 – 1.03 (m, 2H), -0.03 (s, 9H).

^{13}C NMR (126 MHz, $CDCl_3$) δ 159.3, 147.5, 145.0, 129.7, 129.3, 127.7, 126.1, 123.8, 120.2, 74.1, 68.6, 19.0, 18.5, -1.2.

FT-IR (cm^{-1}, neat, ATR) 2953, 1603, 1249, 1101, 850, 836, 757.

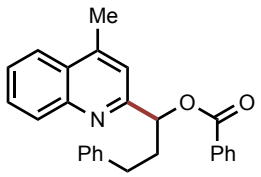

1-(4-Methylquinolin-2-yl)-3-phenylpropyl benzoate (**2.11.2**)

Physical state: 48 mg, 42% yield, clear oil.

^{1}H NMR (500 MHz, $CDCl_3$) δ 8.15 (d, *J* = 7.7 Hz, 2H), 8.10 (d, *J* = 8.4 Hz, 1H), 7.97 (d, *J* = 8.3 Hz, 1H), 7.72 – 7.69 (m, 1H), 7.62 – 7.59 (m, 1H), 7.56 – 7.52 (m, 1H), 7.51 – 7.47 (m, 2H), 7.34 (s, 1H), 7.30 – 7.12 (m, 5H), 6.20 (dd, *J* = 8.3, 5.1 Hz, 1H), 2.90 – 2.78 (m, 2H), 2.69 (s, 3H), 2.60 – 2.45 (m, 2H).

^{13}C NMR (126 MHz, $CDCl_3$) δ 166.1, 159.7, 147.6, 145.3, 141.5 133.3, 130.3, 130.0, 129.4, 128.8, 128.6, 128.4, 127.8, 126.5, 126.4, 126.1, 123.8, 119.1, 36.9, 32.1, 19.1.

HRMS (ES+) m/z calc. for $C_{26}H_{23}NO_2$ [M+Na] 404.1626, found 404.1630.

FT-IR (cm^{-1}, neat, ATR) 1719, 1602, 1451, 1270, 1111, 1070, 1027, 713.

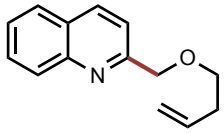

2-((But-3-en-1-yloxy)methyl)quinoline (**2.11.3**)

Physical state: 24 mg, 38% yield, clear oil.

^{1}H NMR (500 MHz, $CDCl_3$) δ 8.18 (d, *J* = 8.4 Hz, 1H), 8.05 (d, *J* = 8.7 Hz, 1H), 7.82 (d, *J* = 8.4 Hz, 1H), 7.72 – 7.68 (m, 1H), 7.64 – 7.61 (m, 1H), 7.54 – 7.51 (m, 1H), 5.92 – 5.84 (m, 1H), 5.15 – 5.06 (m, 2H), 4.82 (s, 2H), 3.65 (t, *J* = 6.6 Hz, 2H), 2.45 (m, 2H).

^{13}C NMR (126 MHz, $CDCl_3$) δ 159.6, 147.7, 136.9, 135.3, 129.7, 129.1, 127.8, 127.7, 126.4, 119.5, 116.7, 74.6, 70.5, 34.4.

HRMS (ES+) m/z calc. for $C_{14}H_{16}NO$ [M+H] 214.1232, found 214.1234.

FT-IR (cm^{-1}, neat, ATR) 2858, 1601, 1506, 1428, 1359, 1106, 996, 916, 829, 784, 755, 618.

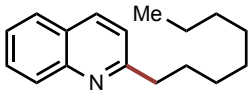

2-Octylquinoline (**2.11.4**)

Physical state: 32 mg, 44% yield, yellow oil.

^{1}H NMR (500 MHz, $CDCl_3$) δ 8.80 (d, *J* = 4.4 Hz, 1H), 8.11 (d, *J* = 8.4 Hz, 1H), 8.04 (d, *J* = 8.4 Hz, 1H), 7.71 – 7.68 (m, 1H), 7.57 – 7.54 (m, 1H), 7.23 (d, *J* = 4.3 Hz, 1H), 3.09 – 3.04 (m, 2H), 1.80 – 1.73 (m, 2H), 1.47 – 1.41 (m, 2H), 1.40 – 1.17 (m, 8H), 0.88 (t, *J* = 6.6 Hz, 3H).

^{13}C NMR (126 MHz, $CDCl_3$) δ 150.4, 148.9, 148.5, 130.4, 129.1, 127.8, 126.3, 123.8, 120.9, 32.3, 32.0, 30.3, 29.9, 29.6, 29.4, 22.8, 14.2.

HRMS (ES+) m/z calc. for $C_{17}H_{24}N$ [M+H] 242.1909, found 242.1904.

FT-IR (cm^{-1}, neat, ATR) 2924, 2855, 1592, 1508, 1463, 760.

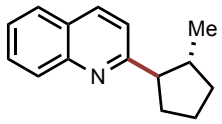

2-((2*R*)-2-Methylcyclopentyl)quinoline (**2.11.5**)

Physical state: 38 mg, 60% yield, clear oil.

^{1}H NMR (500 MHz, $CDCl_3$) δ 8.08 – 8.04 (m, 2H), 7.77 (d, *J* = 8.1 Hz, 1H), 7.69 – 7.65 (m, 1H), 7.49 – 7.45 (m, 1H), 7.31 (d, *J* = 8.6 Hz, 1H), 2.90 – 2.84 (m, 1H), 2.33 – 2.17 (m, 2H), 2.09 – 1.93 (m, 2H), 1.92 – 1.77 (m, 2H), 1.45 – 1.37 (m, 1H), 1.01 (d, *J* = 6.5 Hz, 3H).

^{13}C NMR (126 MHz, $CDCl_3$) δ 165.6, 148.1, 136.2, 129.3, 129.2, 127.6, 127.1, 125.7, 120.4, 57.3, 42.5, 35.2, 34.3, 24.5, 19.0.

HRMS (ES+) m/z calc. for $C_{15}H_{18}N$ [M+H] 212.1439, found 212.1444.

FT-IR (cm^{-1}, neat, ATR) 3050, 2946, 1601, 1255.

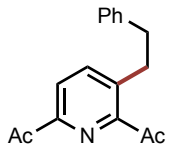

1,1'-(3-Phenethylpyridine-2,6-diyl)bis(ethan-1-one) (**2.11.6**)

Physical state: 52 mg, 65% yield, clear oil.

^{1}H NMR (500 MHz, $CDCl_3$) δ 8.04 (d, *J* = 8.0 Hz, 1H), 7.62 (d, *J* = 8.0 Hz, 1H), 7.30 – 7.25 (m, 2H), 7.22 – 7.18 (m, 3H), 3.33 – 3.30 (m, 2H), 2.93 – 2.90 (m, 2H), 2.75 (s, 3H), 2.73 (s, 3H).

^{13}C NMR (126 MHz, $CDCl_3$) δ 201.8, 199.4, 151.1, 150.6, 142.0, 141.0, 140.9, 128.8, 128.6, 126.4, 123.7, 37.4, 35.4, 28.4, 25.7.

HRMS (ES+) m/z calc. for $C_{17}H_{18}NO_2$ [M+H] 268.1338, found 268.1339.

FT-IR (cm^{-1}, neat, ATR) 1699, 1358, 1296, 700.

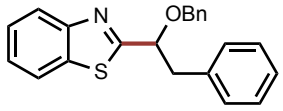

2-(1-(Benzyloxy)-2-phenylethyl)benzo[*d*]thiazole (**2.11.7**)

Physical state: 52 mg, 53% yield, colorless oil.

^{1}H NMR (500 MHz, $CDCl_3$) δ 8.07 – 8.00 (m, 1H), 7.92 (d, *J* = 8.0 Hz, 1H), 7.52 – 7.47 (m, 1H), 7.43 – 7.36 (m, 5H), 7.35 – 7.31 (m, 1H), 7.28 – 7.24 (m, 2H), 7.17 (d, *J* = 7.8 Hz, 3H), 4.85 (dd, *J* = 8.3, 4.8 Hz, 1H), 4.70 (d, *J* = 11.4 Hz, 1H), 4.52 (d, *J* = 11.4 Hz, 1H), 2.93 – 2.82 (m, 1H), 2.82 – 2.71 (m, 1H), 2.41 – 2.29 (m, 1H), 2.29 – 2.19 (m, 2H).

^{13}C NMR (126 MHz, $CDCl_3$) δ 175.4, 153.3, 141.3, 137.6, 135.1, 128.7, 128.6(5), 128.5(7), 128.3, 128.1, 126.1(5), 126.1(3), 125.3, 123.2, 122.1, 79.0, 72.3, 38.9, 31.7.

HRMS (ES+) m/z calc. for $C_{23}H_{23}NOS$ [M+H] 360.1422, found 360.1420.

FT-IR (cm^{-1}, neat, ATR) 3027, 2922, 2861, 1516, 1495, 1093, 1027, 1014, 758, 697.

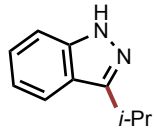

3-Isopropyl-1*H*-indazole (**2.11.8**)

Physical state: 33 mg, 69% yield, clear oil.

^{1}H NMR (500 MHz, $CDCl_3$) δ 9.84 (bs, 1H), 7.78 (d, *J* = 8.1 Hz, 1H), 7.45 – 7.42 (m, 1H), 7.38 – 7.35 (m, 1H), 7.15 – 7.12 (m, 1H), 3.44 (sept, *J* = 7.0 Hz, 1H), 1.48 (d, *J* = 7.0 Hz, 6H).

^{13}C NMR (126 MHz, $CDCl_3$) δ 152.8, 141.6, 126.7, 121.4, 120.8, 120.2, 109.9, 27.9, 22.3.

HRMS (ES+) m/z calc. for $C_{10}H_{12}N_2$ [M+] 160.1000, found 160.1001.

FT-IR (cm^{-1}, neat, ATR) 3189, 2968, 1623, 1501, 1349, 742.

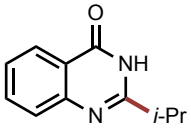

2-Isopropylquinazolin-4(3*H*)-one (**2.11.9**)

Reference: Shen, G.; Zhou, H.; Sui, Y.; Liu, Q.; Zou, K. *Tetrahedron Lett.* **2016**, *57*, 587

Physical state: 45 mg, 79% yield, white solid (mp = 123 °C).

^{1}H NMR (500 MHz, $CDCl_3$) δ 11.64 (s, 1H), 8.30 (d, *J* = 7.9 Hz, 1H), 7.79 – 7.72 (m, 2H), 7.47 – 7.45 (m, 1H), 3.06 (sept, *J* = 7.0 Hz, 1H), 1.45 (d, *J* = 7.0 Hz, 6H).

^{13}C NMR (126 MHz, $CDCl_3$) δ 164.4, 161.0, 149.6, 134.8, 127.5, 126.4, 126.4, 120.9, 35.1, 20.6.

HRMS (ES+) m/z calc. for $C_{11}H_{12}N_2ONa$ [M+Na] 211.0847, found 211.0851.

FT-IR (cm^{-1}, neat, ATR) 2970, 2932, 1622, 1609, 1472, 1384, 1252, 772.

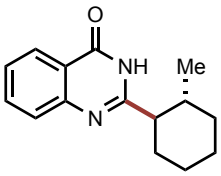

2-((1*R*,2*R*)-2-Methylcyclohexyl)quinazolin-4(3*H*)-one (**2.11.10**)

Physical state: 30 mg, 41% yield, white powder (mp = 89–93 °C).

^{1}H NMR (500 MHz, $CDCl_3$) δ 11.48 (s, 1H), 8.29 (d, *J* = 7.9 Hz, 1H), 7.80 – 7.71 (m, 2H), 7.48 – 7.46 (m, 1H), 2.39 – 2.33 (m, 1H), 2.05 – 1.96 (m, 2H), 1.92 – 1.73 (m, 4H), 1.57 – 1.49 (m, 1H), 1.43 – 1.35 (m, 1H), 1.26 – 1.12 (m, 1H), 0.88 (d, *J* = 6.5 Hz, 3H).

^{13}C NMR (126 MHz, $CDCl_3$) δ 164.1, 159.9, 149.6, 134.8, 127.5, 126.4, 120.9, 100.1, 52.9, 35.2, 35.2, 31.5, 26.2, 26.1, 20.6.

HRMS (ES+) m/z calc. for $C_{15}H_{19}N_2O$ [M+H] 243.1497, found 243.1500.

FT-IR (cm^{-1}, neat, ATR) 2926, 1668, 1471, 773.

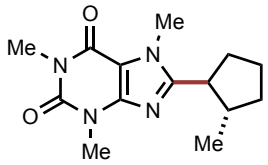

1,3,7-Trimethyl-8-((2*S*)-2-methylcyclopentyl)-3,7-dihydro-1*H*-purine-2,6-dione (**2.11.11**)

Physical state: 31 mg, 37%, light yellow oil.

^{1}H NMR (500 MHz, $CDCl_3$) δ 3.93 (s, 3H), 3.56 (s, 3H), 3.40 (s, 3H), 2.67 – 2.63 (m, 1H), 2.50 - 2.40 (m, 1H), 2.14 – 2.01 (m, 2H), 1.96 – 1.76 (m, 4H), 1.02 (d, *J* = 6.5 Hz, 3H).

^{13}C NMR (126 MHz, $CDCl_3$) δ 157.6, 155.5, 152.0, 148.4, 107.4, 44.8, 41.3, 34.6, 32.4, 31.7, 29.9, 28.0, 24.2, 19.2.

HRMS (ES+) m/z calc. for $C_{14}H_{21}N_4O_2$ [M+H] 277.1658, found 277.1661.

FT-IR (cm^{-1}, neat, ATR) 2954, 1703, 1661, 1543, 1436, 1221, 1041, 981, 747.

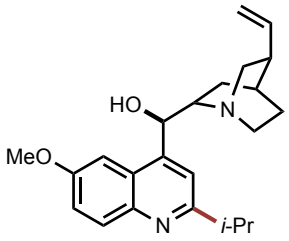

(1*R*)-(2-Isopropyl-6-methoxyquinolin-4-yl)(5-vinylquinuclidin-2-yl)methanol (**2.11.12**)

Physical state: 82 mg, 75% yield, light yellow solid (mp = 145 °C).

^{1}H NMR (500 MHz, $CDCl_3$) δ 7.89 (d, *J* = 9.1 Hz, 1H), 7.52 (s, 1H), 7.22 (d, *J* = 9.1 Hz, 1H), 7.07 (s, 1H), 5.80 (s, 1H), 5.73 – 5.60 (m, 1H), 5.00 – 4.92 (m, 2H), 3.81 – 3.73 (m, 4H), 3.26 – 3.08 (m, 3H), 2.85 – 2.75 (m, 3H), 2.42 – 2.35 (m, 1H), 1.90 – 1.80 (m, 2H), 1.65 – 1.60 (m, 1H), 1.49 – 1.39 (m, 1H), 1.34 (d, *J* = 6.9 Hz, 6H)

^{13}C NMR (126 MHz, $CDCl_3$) δ 164.7, 157.6, 146.3, 143.8, 140.1, 131.3, 124.7, 121.5, 116.5, 115.8, 100.6, 60.2, 60.1, 56.2, 55.9, 43.7, 39.0, 37.2, 27.7, 26.4, 22.7, 20.2.

HRMS (ES+) m/z calc. for $C_{23}H_{30}N_2O_2$ [M+H] 367.2361, found 367.2394.

FT-IR (cm^{-1}, neat, ATR) 2962, 1674, 1620, 1236.

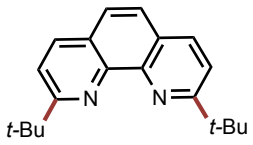

2,9-Di-*tert*-butyl-1,10-phenanthroline (**2.12.2**)

Reference: Xu, C.; Zhang, L.; Dong, C.; Xu, J.; Pan, Y.; Li, Y.; Zhang, H.; Li, H.; Yu, Z.; Xu, L. *Adv. Synth. Catal.* **2016**, *358*, 567.

Physical state: 38 mg, 42% yield, white semi-solid.

^{1}H NMR (500 MHz, $CDCl_3$) δ 8.13 (d, J = 8.4 Hz, 2H), 7.84 – 7.48 (m, 4H), 1.60 (s, 18H).

^{13}C NMR (126 MHz, $CDCl_3$) δ 169.4, 145.0, 136.0, 127.0, 125.5, 119.7, 38.8, 30.4.

HRMS (ES+) m/z calc. for $C_{20}H_{25}N$ [M+H] 293.2018, found 293.2020.

FT-IR (cm^{-1}, neat, ATR) 2962, 1589, 1489, 1387, 850.

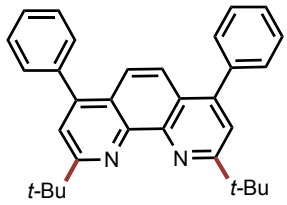

2,9-Di-*tert*-butyl-4,7-diphenyl-1,10-phenanthroline (**2.12.4**)

Reference: Sugihara, S.; Okada, T.; Hiratani, K. *Anal. Sci.* **1993**, *9*, 593.

Physical state: 152 mg, 68% yield, yellow oil.

^{1}H NMR (500 MHz, $CDCl_3$) δ 7.72 (s, 2H), 7.63 (s, 2H), 7.56 – 7.43 (m, 10H), 1.64 (s, 18H).

^{13}C NMR (126 MHz, $CDCl_3$) δ 168.8, 148.4, 145.7, 139.2, 129.9, 128.6, 128.2, 124.9, 123.1, 120.1, 38.9, 30.5.

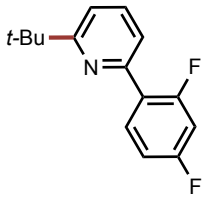

2-(*tert*-Butyl)-6-(2,4-difluorophenyl)pyridine (**2.12.6**)

Physical state: 61 mg, 82% yield, light yellow oil.

^{1}H NMR (500 MHz, $CDCl_3$) δ 8.61 (d, *J* = 5.1 Hz, 1H), 7.96 (m, 1H), 7.72 (s, 1H), 7.28 – 7.22 (m, 1H), 6.99 (t, *J* = 8.4 Hz, 1H), 6.91 (m, 1H), 1.36 (s, 9H).

^{13}C NMR (126 MHz, $CDCl_3$) δ 163.2 (dd, *J* = 250.5, 12.1 Hz), 160.6 (dd, *J* = 252.0, 11.9 Hz), 160.6, 149.8, 132.4 (dd, *J* = 9.7, 4.6 Hz), 124.5 (dd, *J* = 12.0, 3.9 Hz), 122.6, 121.5 (d, *J* = 8.9 Hz), 119.7, 111.9 (dd, *J* = 21.0, 3.8 Hz), 104.4 (m), 35.0, 30.7.

HRMS (ES+) m/z calc. for $C_{15}H_{16}F_2N$ [M+H] 248.1251, found 248.1241.

FT-IR (cm^{-1}, neat, ATR) 2949, 1736, 1716, 1242, 1209, 747, 700.

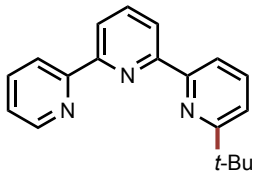

6-(*tert*-Butyl)-2,2':6',2''-terpyridine (**2.12.8**)

Physical state: 64 mg, 74% yield, yellow oil.

^{1}H NMR (500 MHz, $CDCl_3$) δ 8.75 (s, 1H), 8.71 – 8.60 (m, 3H), 8.45 (m, 2H), 7.94 (m, 1H), 7.86 (m, 1H), 7.33 (dt, *J* = 6.7, 3.5 Hz, 2H), 1.43 (s, 9H).

^{13}C NMR (126 MHz, $CDCl_3$) δ 160.9, 156.3, 155.6, 149.3, 149.3, 138.1, 137.0, 137.0, 123.9, 121.3, 121.1, 121.1, 121.0, 120.9, 118.2, 35.1, 30.7.

HRMS (ES+) m/z calc. for: submitted.

FT-IR (cm^{-1}, neat, ATR) 2963, 1602, 1579, 1548, 1456, 1391, 820, 770.

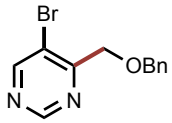

4-((Benzyloxy)methyl)-5-bromopyrimidine (**2.13.1**)

Physical state: 42 mg, 50% yield, clear oil.

^{1}H NMR (500 MHz, $CDCl_3$) δ 9.13 (s, 1H), 8.77 (s, 1H), 7.43 – 7.30 (m, 5H), 4.73 (s, 2H), 4.71 (s, 2H).

^{13}C NMR (126 MHz, $CDCl_3$) δ 164.1, 158.9, 157.1, 137.4, 128.7, 128.2, 128.2, 120.3, 73.7, 71.1.

HRMS (ES+) m/z calc. for $C_{12}H_{12}BrN_3O$ [M+H] 279.0133, found 279.0135.

FT-IR (cm^{-1}, neat, ATR) 2860, 1560, 1454, 1388, 1360, 1216, 1097, 1036, 738, 698.

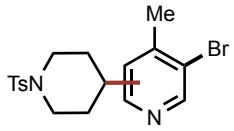

3-Bromo-4-methyl-2-(1-tosylpiperidin-4-yl)pyridine and 5-bromo-4-methyl-2-(1-tosylpiperidin-4-yl)pyridine (**2.13.2**)

Physical state: 69 mg, 57% yield, white amorphous solid (mp = 120–122 °C).

^{1}H NMR (500 MHz, $CDCl_3$) δ 8.52 (s, 1H – minor isomer), 8.31 (d, J = 4.8 Hz, 1H – major isomer), 7.72 – 7.67 (m, 3H – both isomers), 7.38 – 7.33 (m, 2H - both isomers), 7.01 (d, J = 4.8 Hz, 1H –

major isomer), 6.99 (s, 2H – minor isomer), 3.94 (m, 2H – both isomers), 3.16 (m, 1H – both isomers), 2.61 – 2.34 (m, 8H – both isomers), 2.12 – 1.79 (m, 4H – both isomers).

^{13}C NMR (126 MHz, $CDCl_3$) δ 161.0, 147.6, 147.1, 129.5, 127.7, 127.6, 123.94, 122.91, 121.68, 46.37, 41.60, 29.77, 23.46, 21.44. (major peaks)

HRMS (ES+) m/z calc. for $C_{18}H_{22}BrN_2O_2S$ [M+H] 408.0585, found 409.0586.

FT-IR (cm^{-1}, neat, ATR) 3052, 2915, 2801, 1351, 1331, 1160, 927, 726, 648, 548.

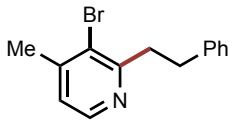

3-Bromo-4-methyl-2-phenethylpyridine (**2.13.3**)

Physical state: 50 mg, 60% yield, clear oil.

^{1}H NMR (500 MHz, $CDCl_3$) δ 8.33 (d, *J* = 4.8 Hz, 1H), 7.30 (d, *J* = 4.4 Hz, 4H), 7.21 (p, *J* = 4.1 Hz, 1H), 7.03 (d, *J* = 4.8 Hz, 1H), 3.37 – 3.22 (m, 2H), 3.05 (dd, *J* = 10.2, 6.7 Hz, 2H), 2.43 (s, 3H).

^{13}C NMR (126 MHz, $CDCl_3$) δ 159.9, 147.9, 147.2, 141.9, 128.6, 128.5, 126.1, 124.3, 123.9, 40.4, 34.8, 23.6.

HRMS (ES+) m/z calc. for $C_{14}H_{14}BrN$ [M+H] 276.0388, found 276.0388.

FT-IR (cm^{-1}, neat, ATR) 1727, 1591, 1435, 1281, 1258, 1084, 738, 698.

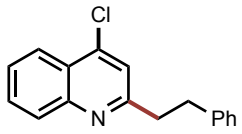

4-Chloro-2-phenethylquinoline (**2.13.4**)

Physical state: 38 mg, 47% yield, clear oil.

^{1}H NMR (500 MHz, $CDCl_3$) δ 8.20 (d, *J* = 8.3 Hz, 1H), 8.08 (d, *J* = 8.4 Hz, 1H), 7.76 (t, *J* = 7.7 Hz, 1H), 7.60 (t, *J* = 7.6 Hz, 1H), 7.35 (s, 1H), 7.30 (t, *J* = 7.5 Hz, 2H), 7.22 (dd, *J* = 15.9, 8.7 Hz, 2H), 3.29 – 3.23 (m, 2H), 3.16 (dd, *J* = 9.7, 6.3 Hz, 2H).

^{13}C NMR (126 MHz, $CDCl_3$) δ 161.9, 149.0, 142.7, 141.3, 130.5, 129.4, 128.6, 126.9, 126.3, 125.2, 124.1, 121.7, 40.9, 35.8.

HRMS (ES+) m/z calc. for $C_{17}H_{15}ClN$ [M+H] 268.0893, found 268.0896.

FT-IR (cm^{-1}, neat, ATR) 3062, 3027, 1589, 1493, 1149, 866, 759, 698.

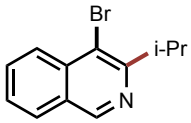

4-Bromo-3-isopropylisoquinoline (**2.13.5**)

Physical state: 30 mg, 40% yield, clear oil.

^{1}H NMR (500 MHz, $CDCl_3$) δ 8.67 (s, 1H), 8.24 – 8.18 (m, 2H), 7.79 – 7.76 (m, 1H), 7.67 – 7.64 (m, 1H), 3.91 (sept, *J* = 6.8 Hz, 1H), 1.43 (d, *J* = 6.8 Hz, 6H).

^{13}C NMR (126 MHz, $CDCl_3$) δ 166.1, 143.8, 135.0, 130.9, 127.9, 127.7, 127.0, 125.2, 117.7, 31.2, 22.3.

HRMS (ES+) m/z calc. for $C_{12}H_{13}BrN$ [M+H] 250.0231, found 250.0224.

FT-IR (cm^{-1}, neat, ATR) 2965, 2929, 1565, 1387, 1240, 1009, 928.

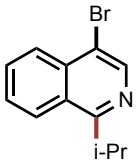

4-Bromo-1-isopropylisoquinoline (**2.13.6**)

Physical state: 22 mg, 29% yield, clear oil.

^{1}H NMR (500 MHz, $CDCl_3$) δ 8.51 (s, 1H), 8.35 (d, *J* = 8.5 Hz, 1H), 7.62 – 7.59 (m, 1H), 7.52 – 7.49 (m, 1H), 7.43 (d, *J* = 8.5 Hz, 1H), 4.08 (sept, *J* = 6.8 Hz, 1H), 1.55 (d, *J* = 6.8 Hz, 6H).

^{13}C NMR (126 MHz, $CDCl_3$) δ 166.8, 143.2, 136.3, 129.9, 127.1, 126.9, 126.3, 125.9, 125.1, 31.3, 22.4.

HRMS (ES+) m/z calc. for $C_{12}H_{14}BrN$ [M+H] 250.0231, found 250.0224.

FT-IR (cm^{-1}, neat, ATR) 2965, 1556, 1502, 1388, 1246, 765.

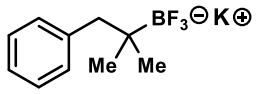

Potassium Trifluoro(2-methyl-1-phenylpropan-2-yl)borate (**1u**)

Synthesized using Silas' procedure from (2-bromo-2-methylpropyl)benzene (*J. Am. Chem. Soc.* **2016**, *138*, 6139) in 70% yield (~85% purity by mass), 840 mg white crystalline solid (mp = 170 – 172 °C).

^{1}H NMR (500 MHz, acetone-d_6) δ 7.16 – 7.13 (m, 2H), 7.08 – 7.05 (m, 3H), 2.52 (s, 2H), 0.63 (s, 6H). Peaks at 0.75 and 0.13 correspond to $EtBF_3K$ generated during borylation procedure.

^{13}C NMR (126 MHz, acetone-d_6) δ 142.1, 130.5, 126.6, 124.2, 44.5, 22.5 (carbon α to boron not observed due to quadrupolar relaxation).

^{19}F NMR (470.7 MHz, acetone-d_6) δ -153.1 (product), -142.7 ($EtBF_3K$).

^{11}B NMR (128.4 MHz, acetone-d_6) δ -6.43.

HRMS (ES+) m/z calc. for $C_{10}H_{13}BF_3^-$ [M-] calc. 201.0198, found: submitted.

FT-IR (cm^{-1}, neat, ATR) 2970, 2928, 2861, 1467, 1225, 1019, 945, 749, 702.

CYCLIC VOLTAMMETRY OF TERT-BUTYL TRIFLUOROBORATE

Electrochemical measurements were recorded on a CH Instruments: Model 600E Series Electrochemical Analyzer (observed in 0.002 M MeCN; $[N(Bu)_4](PF_6)$ = 0.1 M; Ag/AgCl = electrode; reported in SCE based on a ferrocene internal standard).

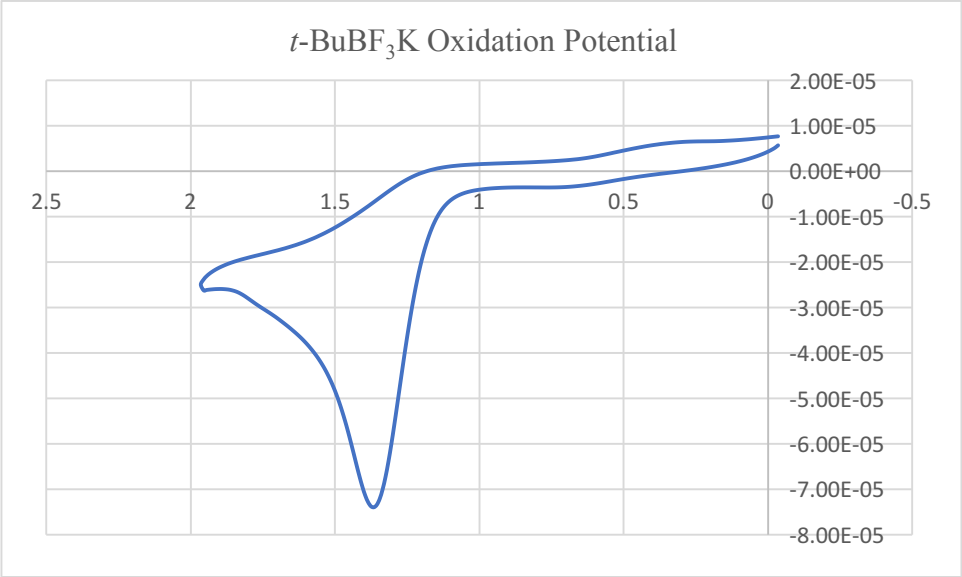

Of the organoboron reagents examined, only the potassium cyclohexyltriolborate XX (~1.1 V *vs SCE*) and potassium cyclohexyltrifluoroborate (~1.5 V *vs SCE*) exhibited oxidations within the solvent window of MeCN. These potentials have been reported previously by Akita and coworkers (*Adv. Synth. Cat*. **2012**, *354 (18)*, 3414). No features were observed for oxidation of the cyclohexyl boronic acid, MIDA, and pincaol boronates.

^{1}H ($CDCl_3$, 500 MHz) spectra of 2-(*tert*-butyl)quinoline (**2.7.1**)

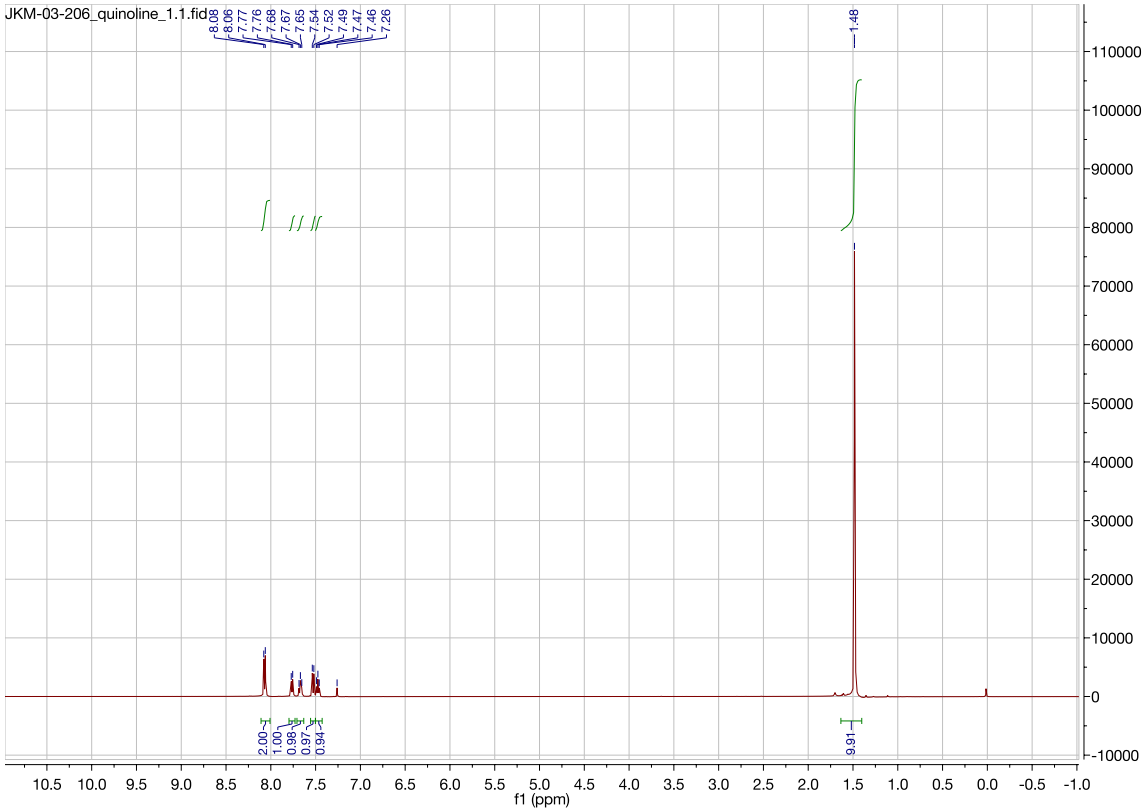

^{13}C NMR ($CDCl_3$, 125.8 MHz) spectrum of 2-(*tert*-butyl)quinoline (**2.7.1**)

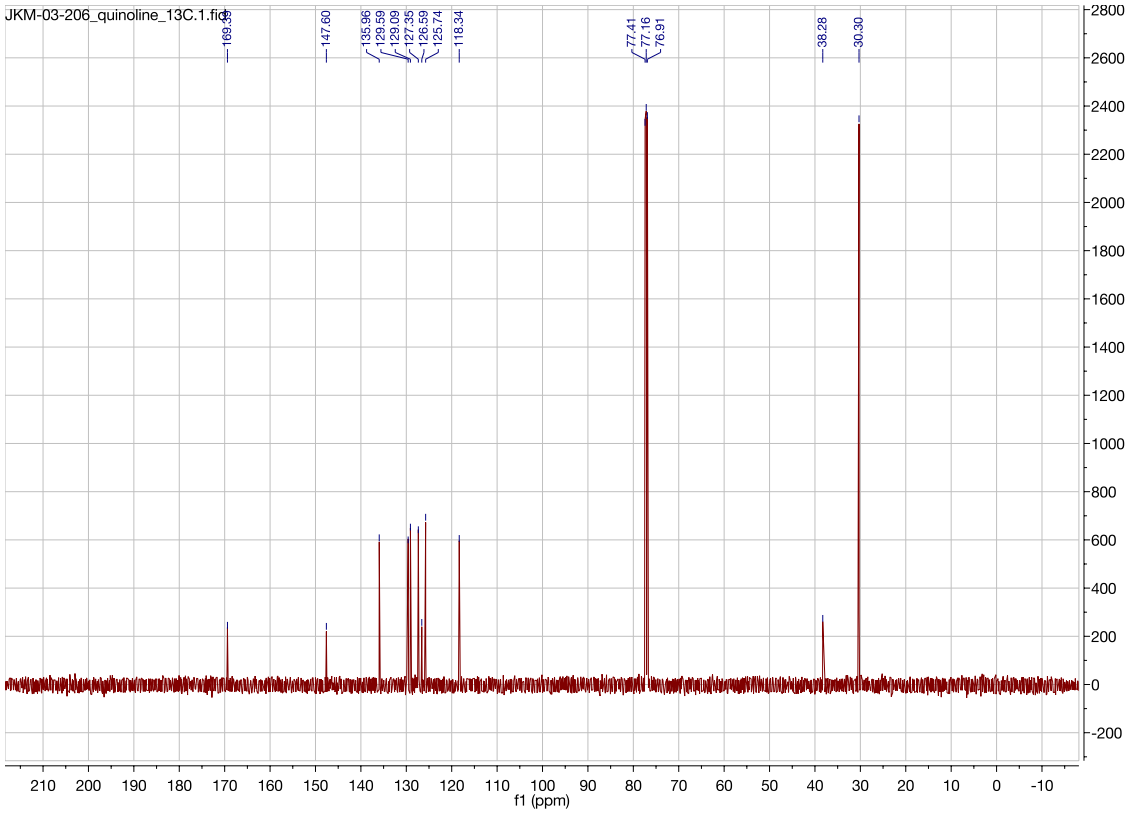

^{1}H ($CDCl_3$, 500 MHz) spectra of 2-(*tert*-butyl)-4-methylquinoline (**2.7.2**)

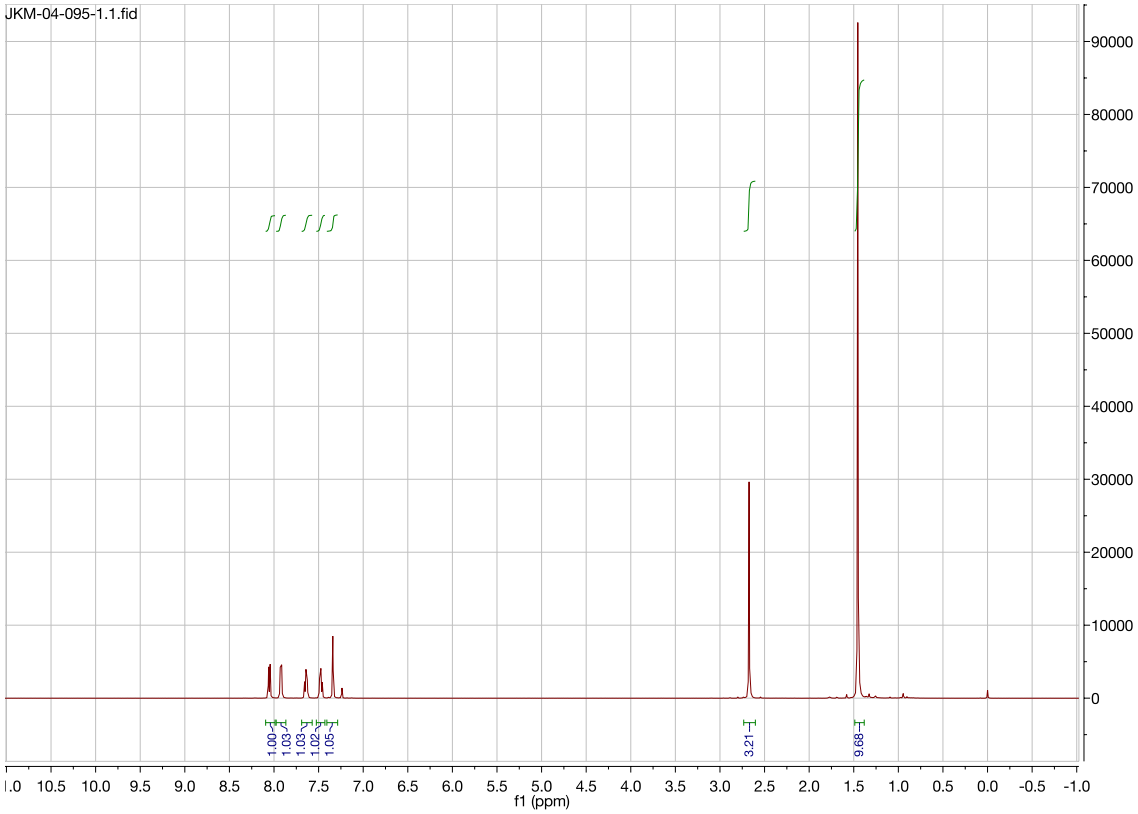

^{13}C NMR ($CDCl_3$, 125.8 MHz) spectrum of 2-(*tert*-butyl)-4-methylquinoline (**2.7.2**)

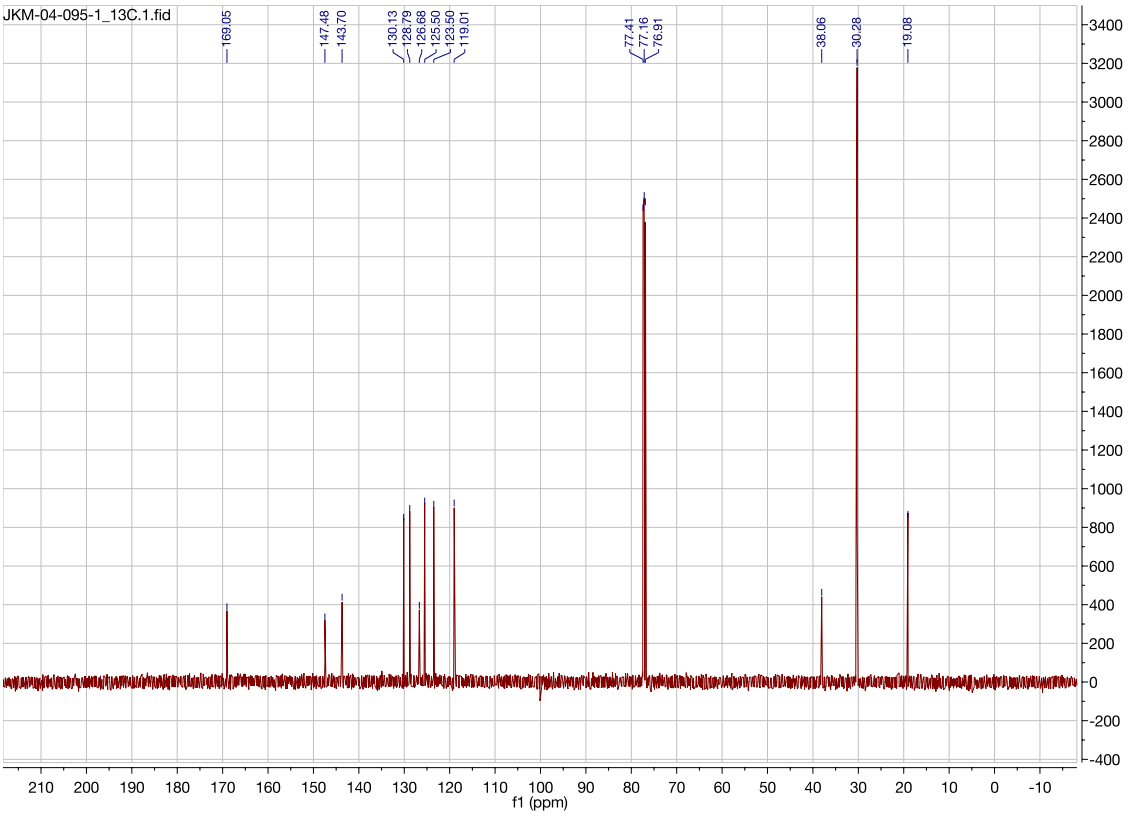

^{1}H ($CDCl_3$, 500 MHz) spectra of 4-bromo-2-(*tert*-butyl)quinoline (**2.7.3**)

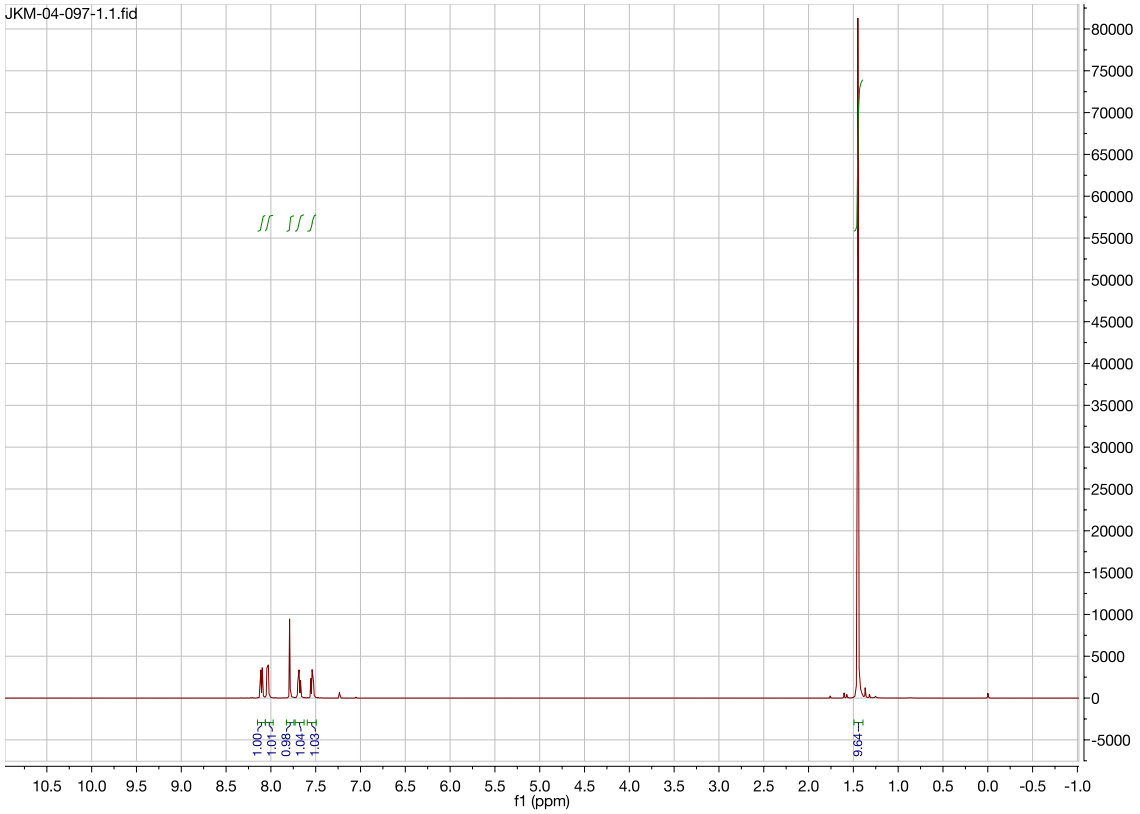

^{13}C NMR ($CDCl_3$, 125.8 MHz) spectrum of 4-bromo-2-(*tert*-butyl)quinoline (**2.7.3**)

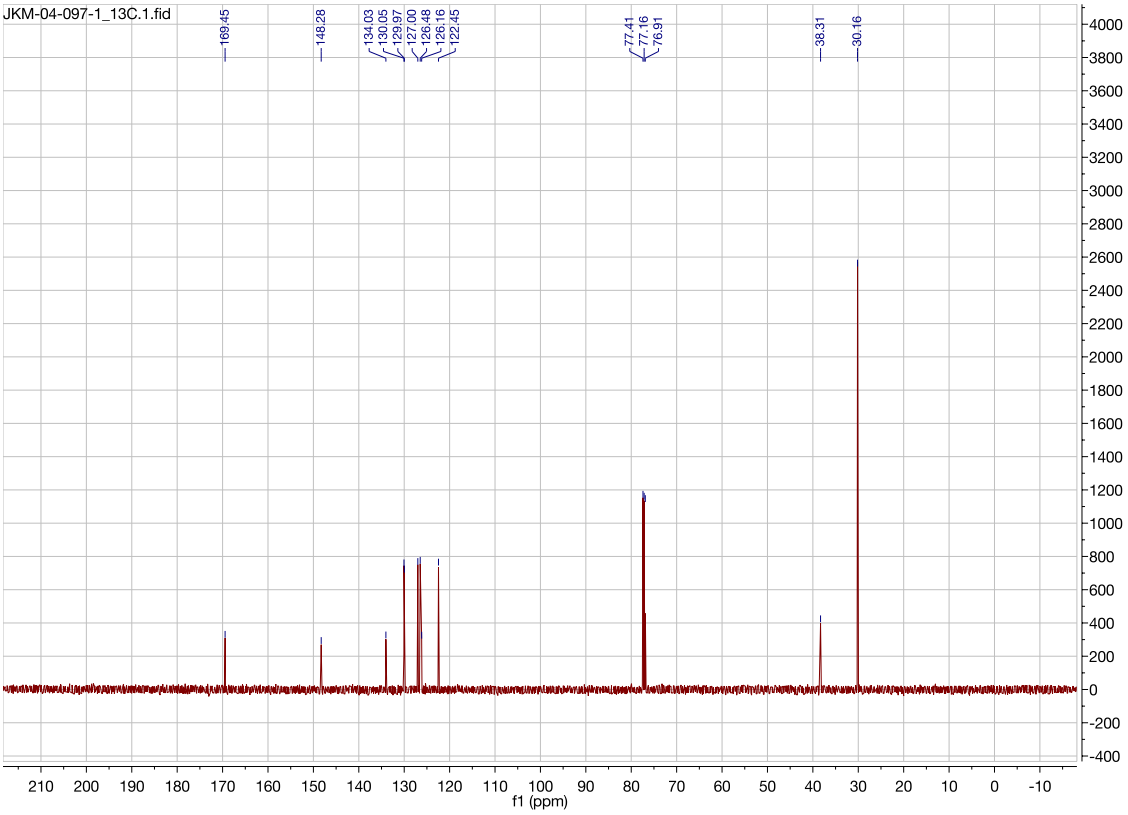

^{1}H ($CDCl_3$, 500 MHz) spectra of 2-(*tert*-butyl)-4-chloro-8-(trifluoromethyl)quinoline (**2.7.4**)

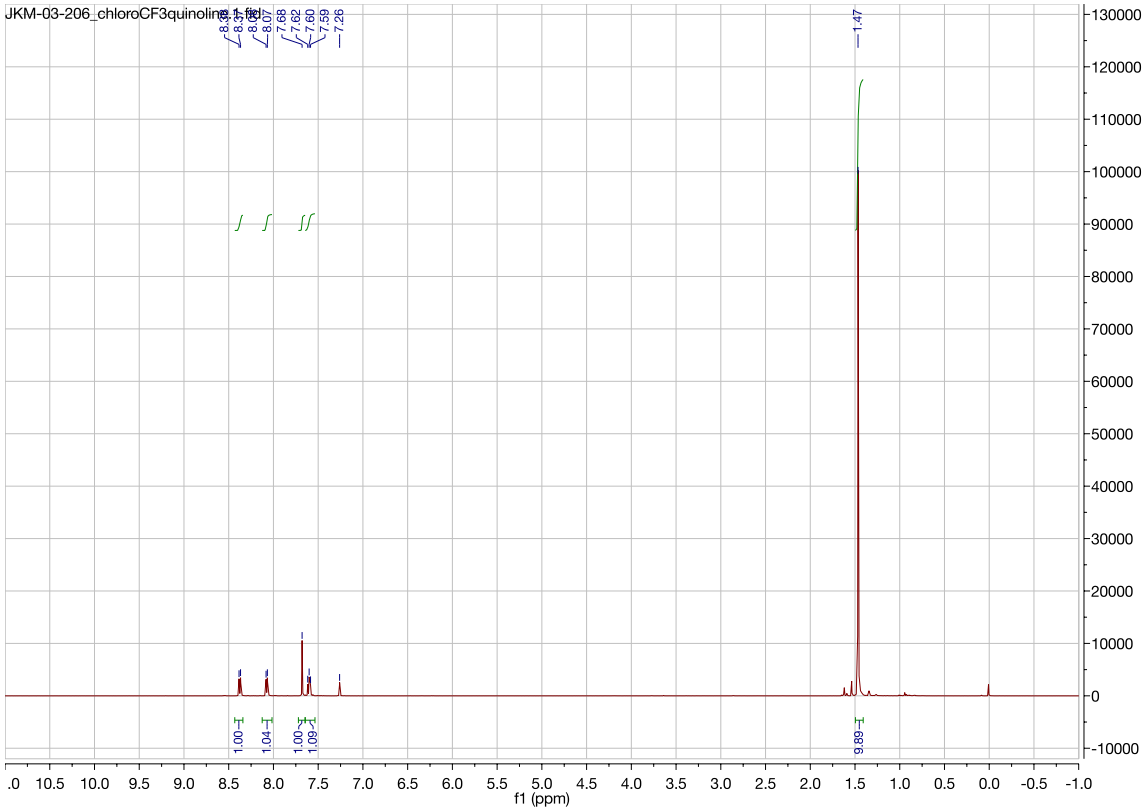

^{13}C NMR ($CDCl_3$, 125.8 MHz) spectrum of 2-(*tert*-butyl)-4-chloro-8-(trifluoromethyl)quinoline (**2.7.4**)

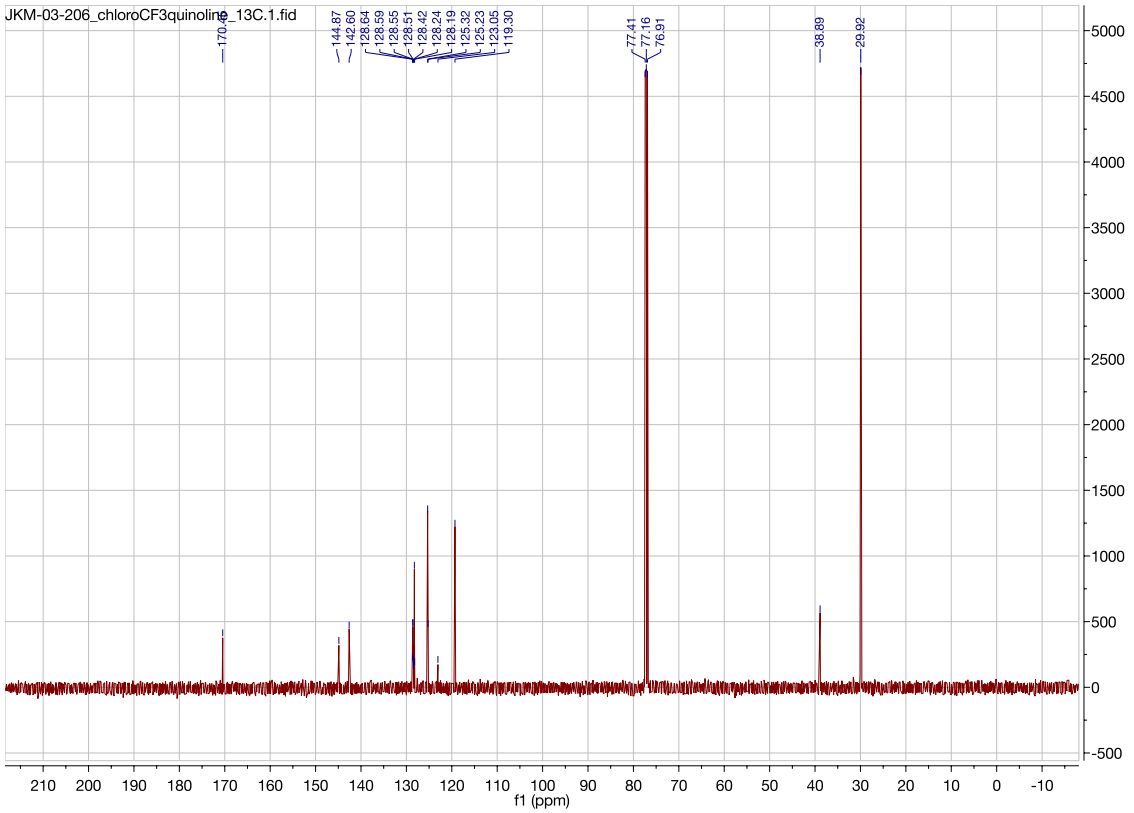

^{1}H ($CDCl_3$, 500 MHz) spectra of 3-(*tert*-butyl)-1*H*-indazole (**2.7.5**)

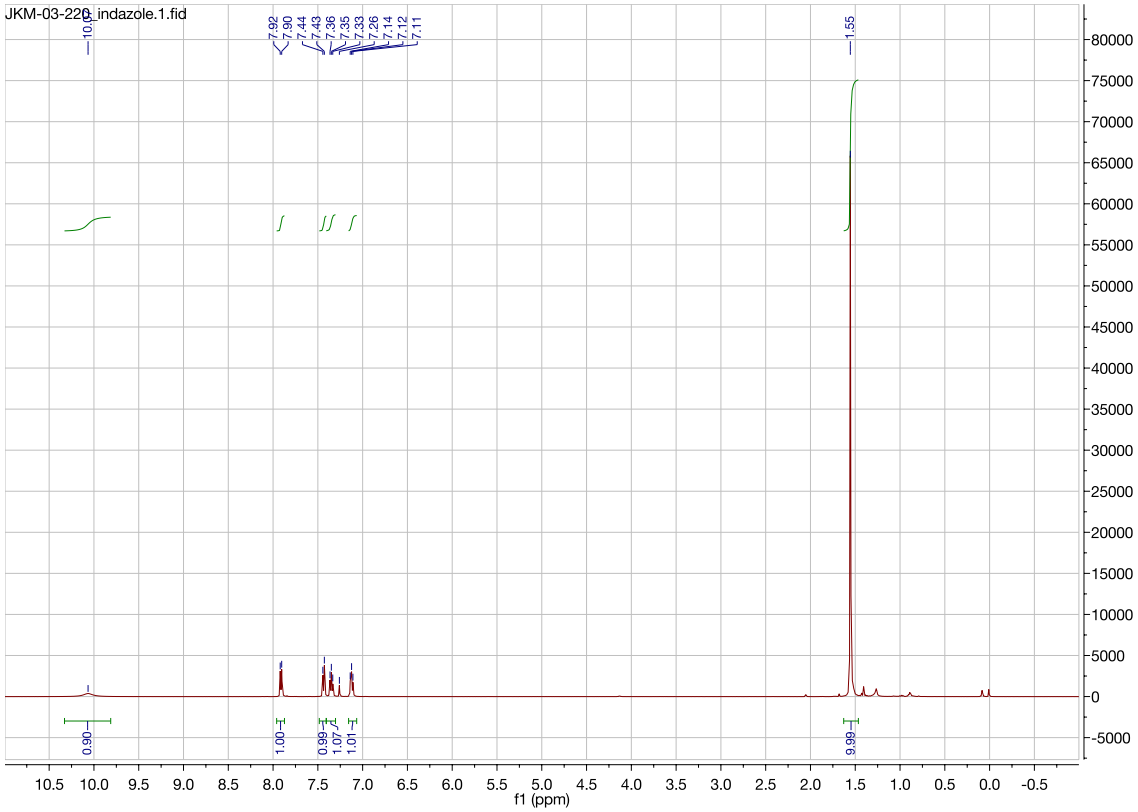

^{13}C NMR ($CDCl_3$, 125.8 MHz) spectrum of 3-(*tert*-butyl)-1*H*-indazole (**2.7.5**)

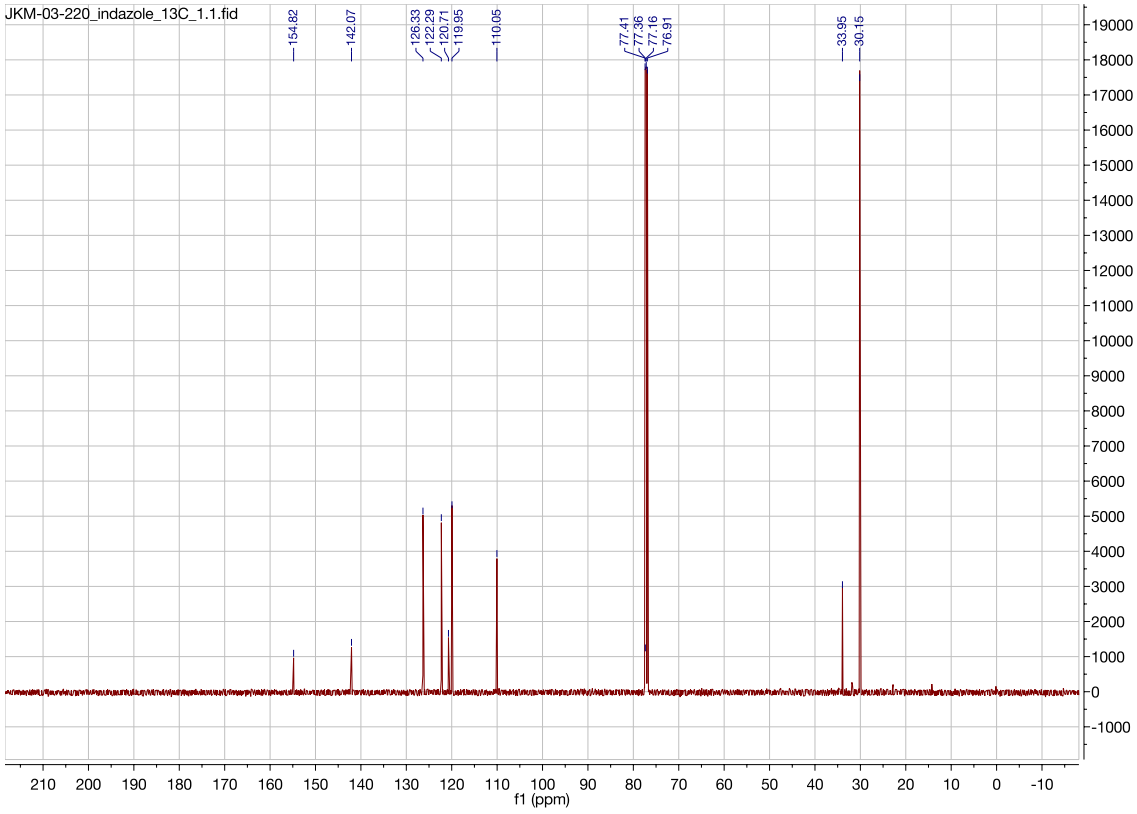

^{1}H ($CDCl_3$, 500 MHz) spectra of methyl 1-(*tert*-butyl)isoquinoline-3-carboxylate (**2.7.6**)

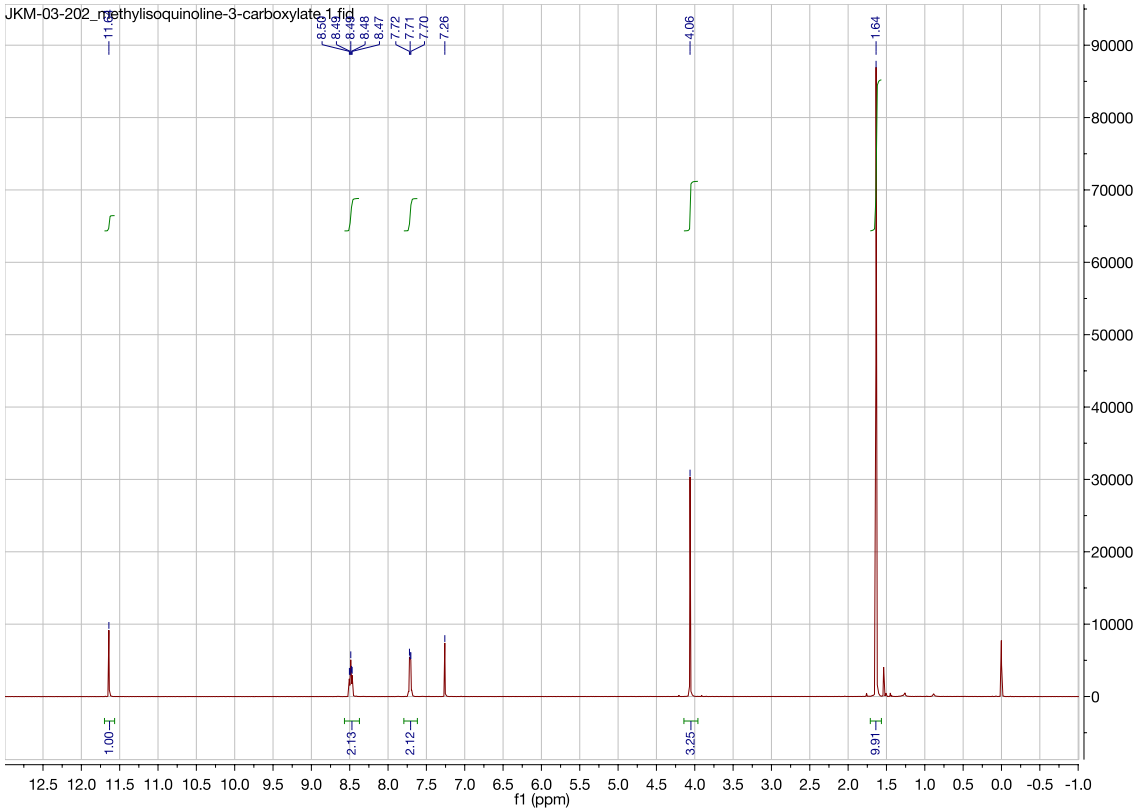

^{13}C NMR ($CDCl_3$, 125.8 MHz) spectrum of methyl 1-(*tert*-butyl)isoquinoline-3-carboxylate (**2.7.6**)

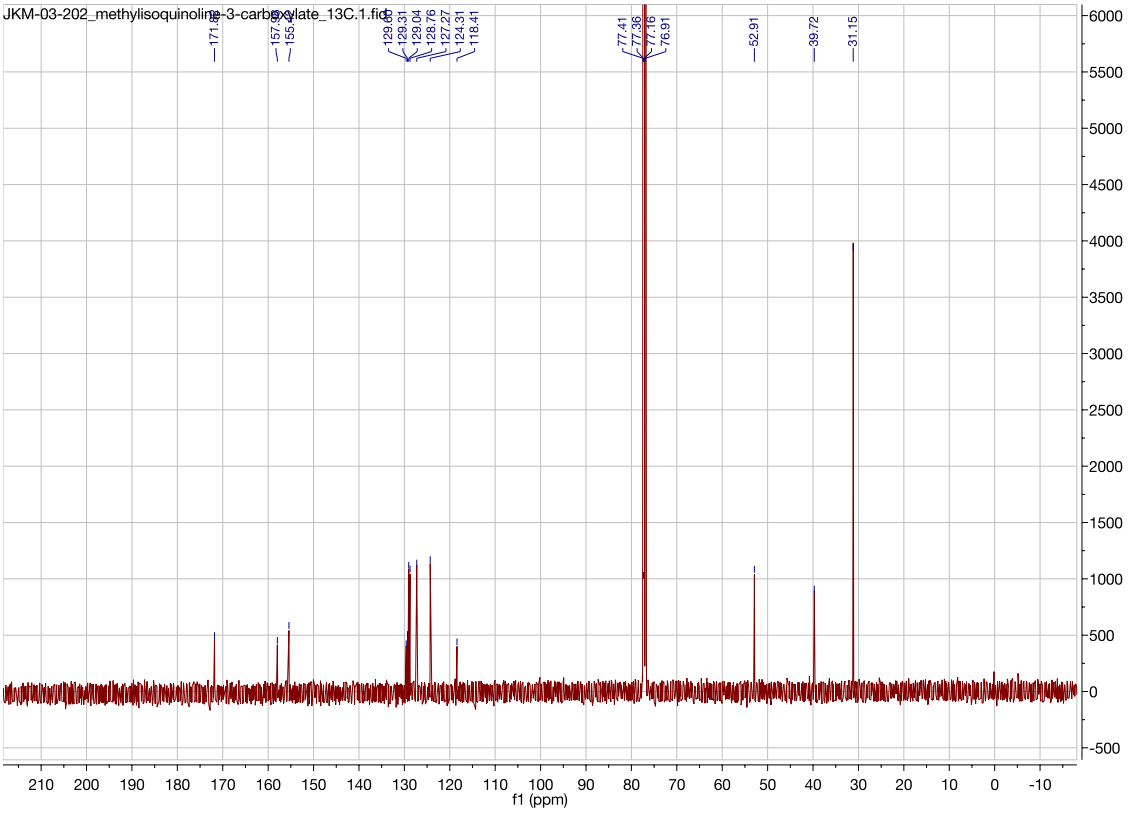

^{1}H ($CDCl_3$, 500 MHz) spectra of 2-(*tert*-butyl)quinoxaline (**2.7.8**)

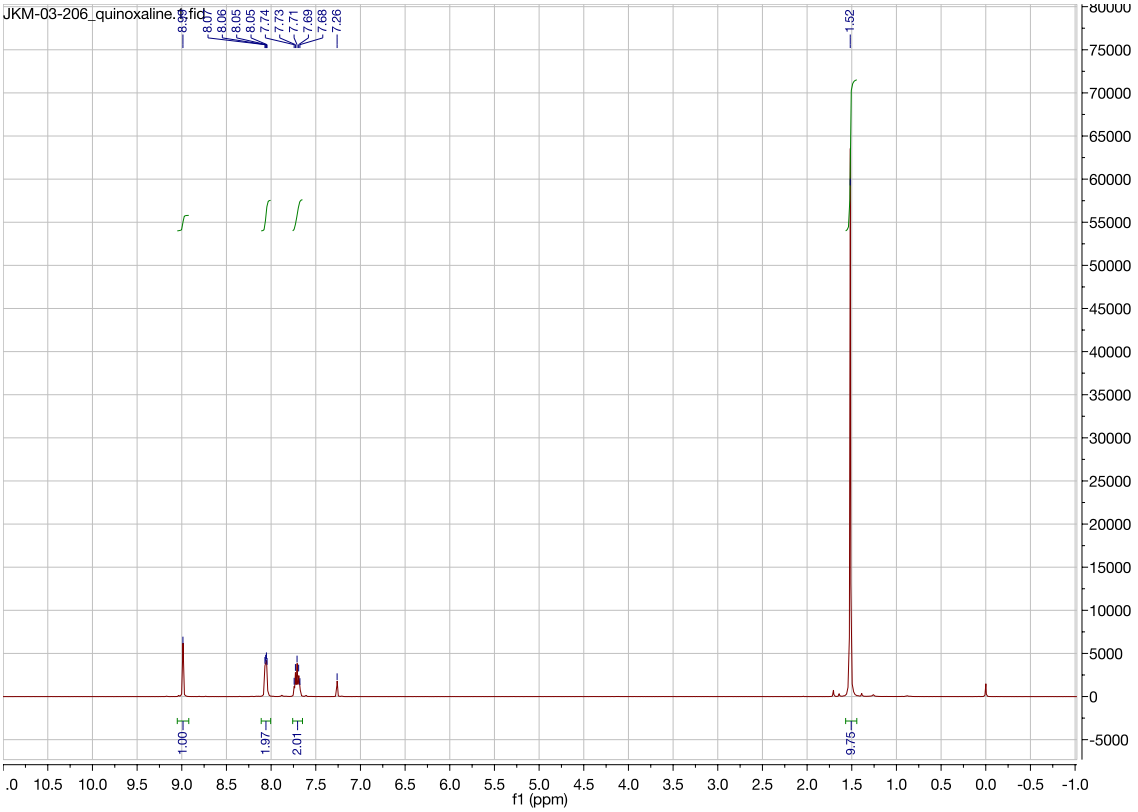

^{13}C NMR ($CDCl_3$, 125.8 MHz) spectrum of 2-(*tert*-butyl)quinoxaline (**2.7.8**)

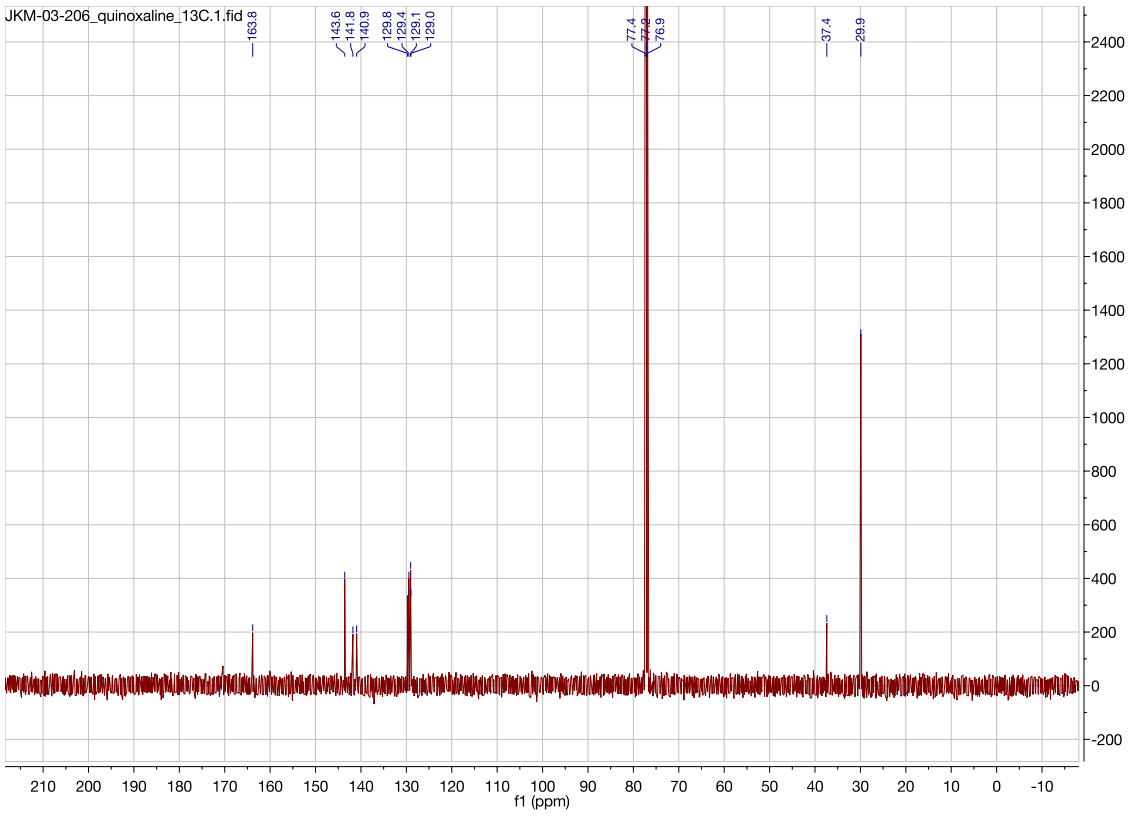

^{1}H ($CDCl_3$, 500 MHz) spectra of 2-(*tert*-butyl)-3-chloroquinoxaline (**2.7.9**)

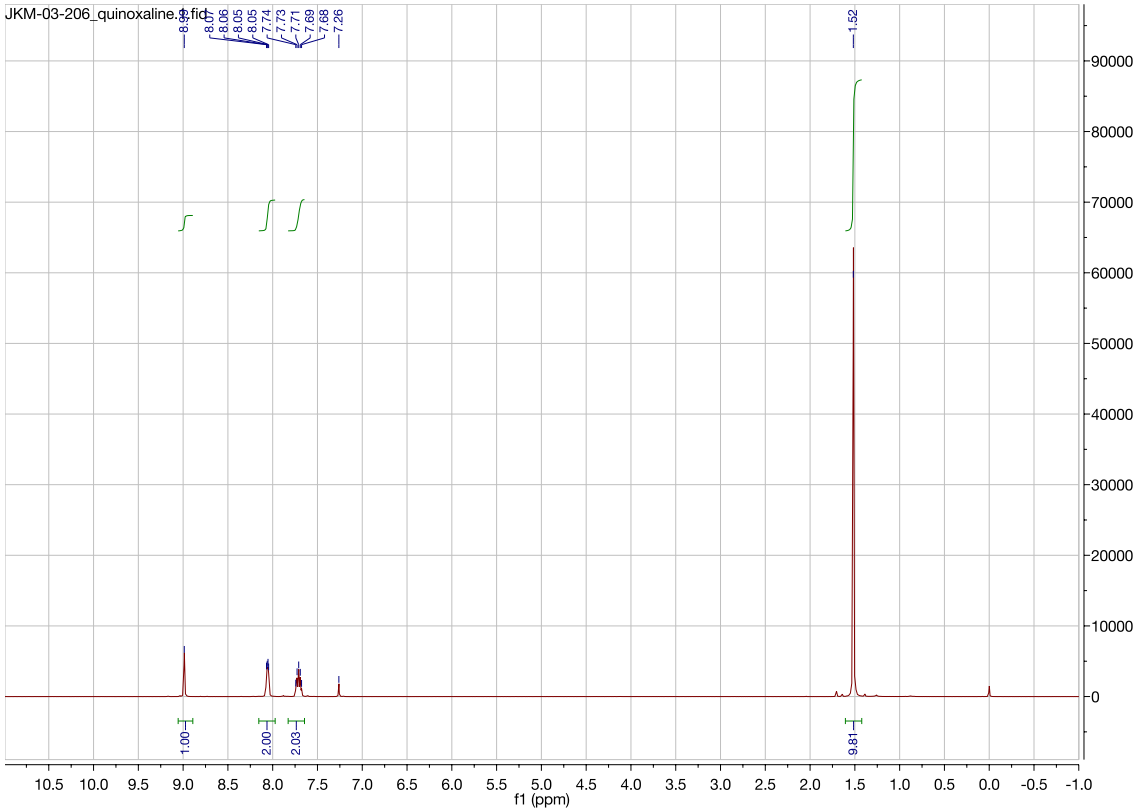

^{13}C NMR ($CDCl_3$, 125.8 MHz) spectrum of 2-(*tert*-butyl)-3-chloroquinoxaline (**2.7.9**)

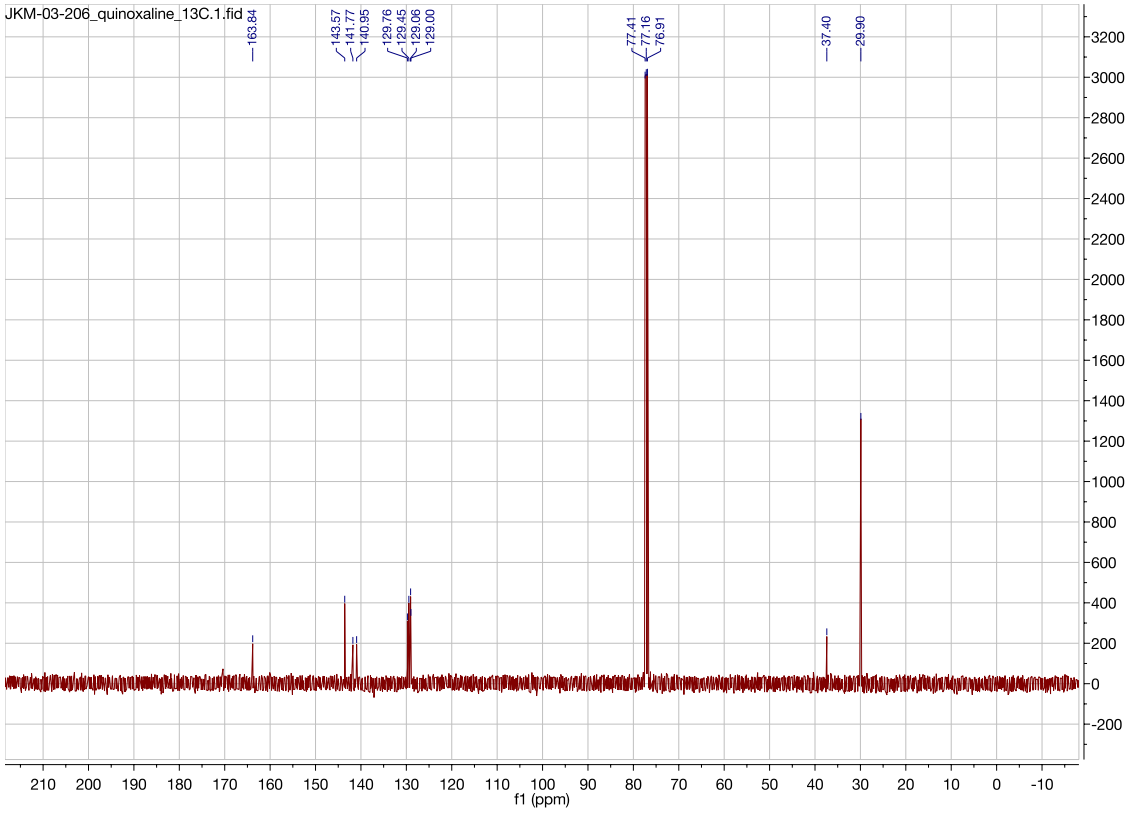

^{1}H ($CDCl_3$, 500 MHz) spectra of 6-(*tert*-butyl)nicotinonitrile (**2.7.10**)

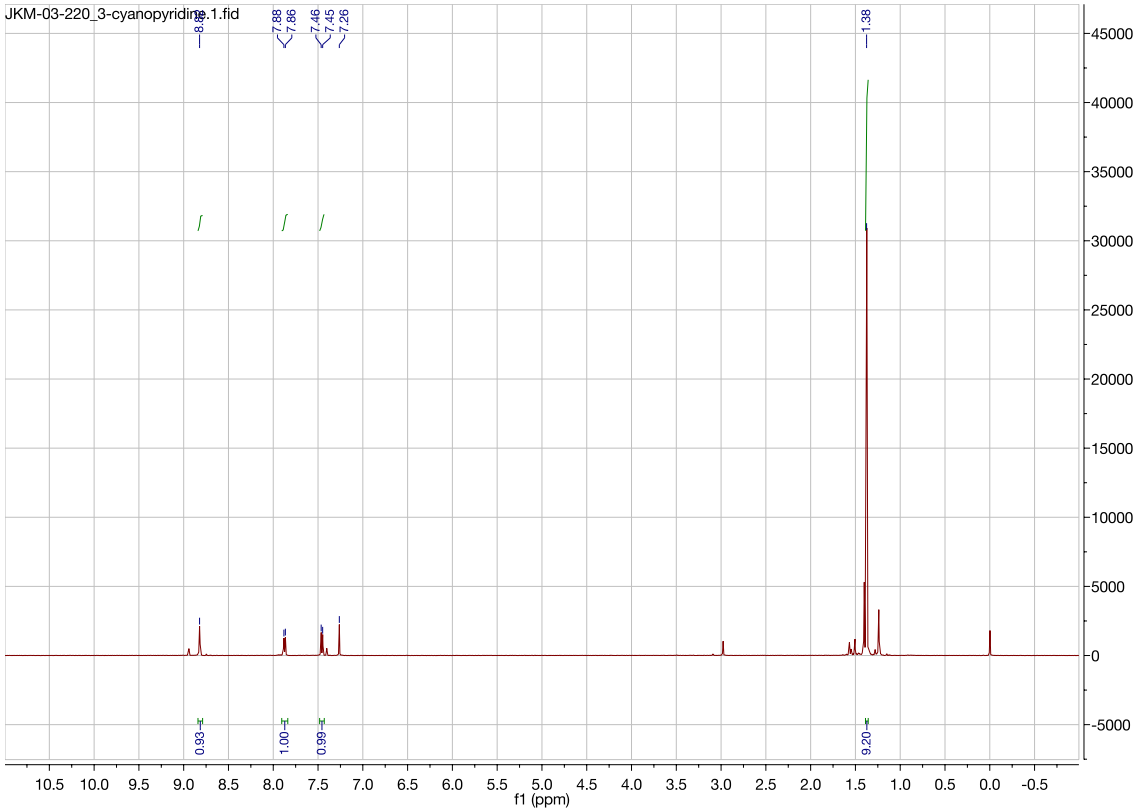

^{13}C NMR ($CDCl_3$, 125.8 MHz) spectrum of 6-(*tert*-butyl)nicotinonitrile (**2.7.10**)

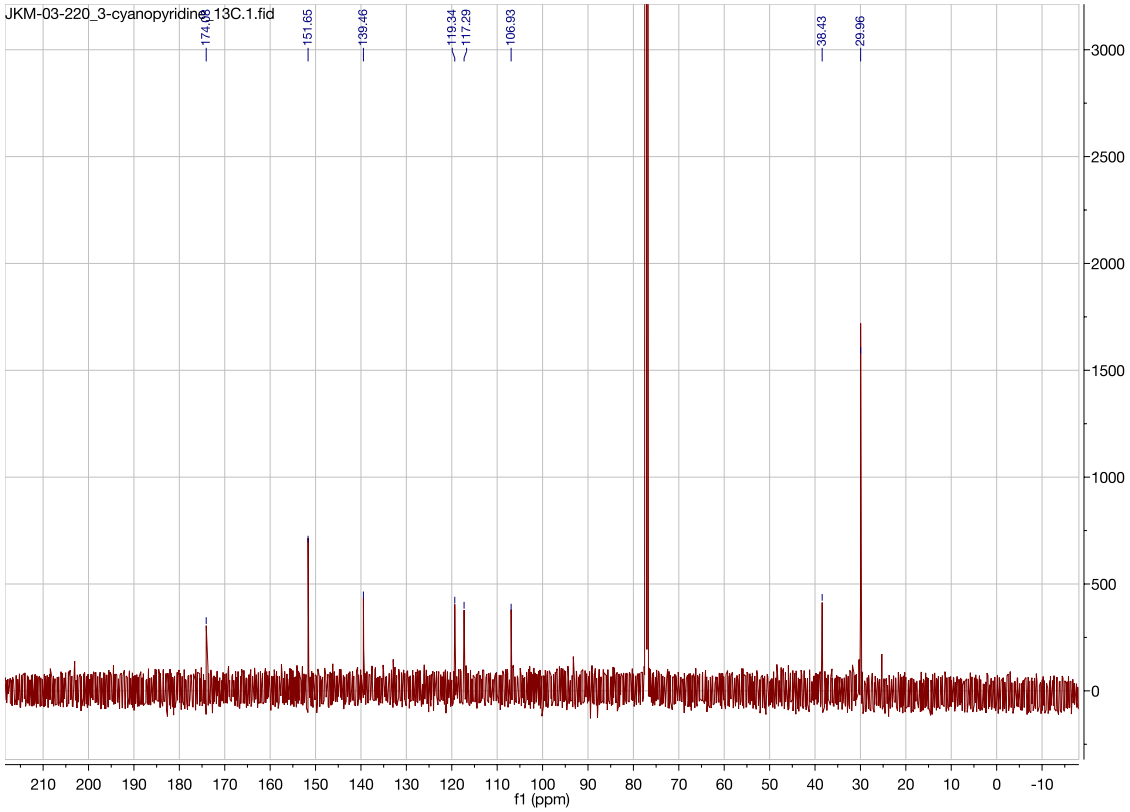

^{19}F ($CDCl_3$, 477 MHz) spectra of 2-(*tert*-Butyl)-4-(trifluoromethyl)pyridine (**2.7.11**) with fluorobenzene

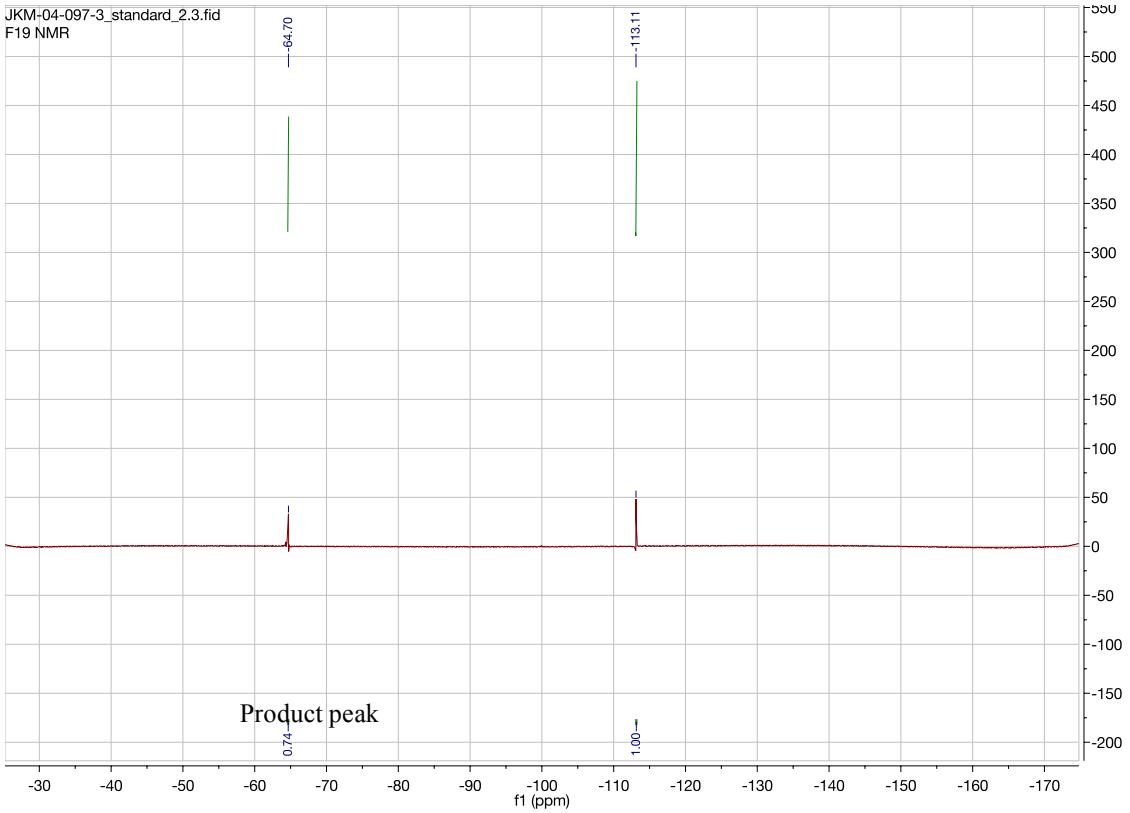

^{1}H ($CDCl_3$, 500 MHz) spectra of 1,1'-(4-(*tert*-butyl)pyridine-2,6-diyl)bis(ethan-1-one) (**2.7.12**)

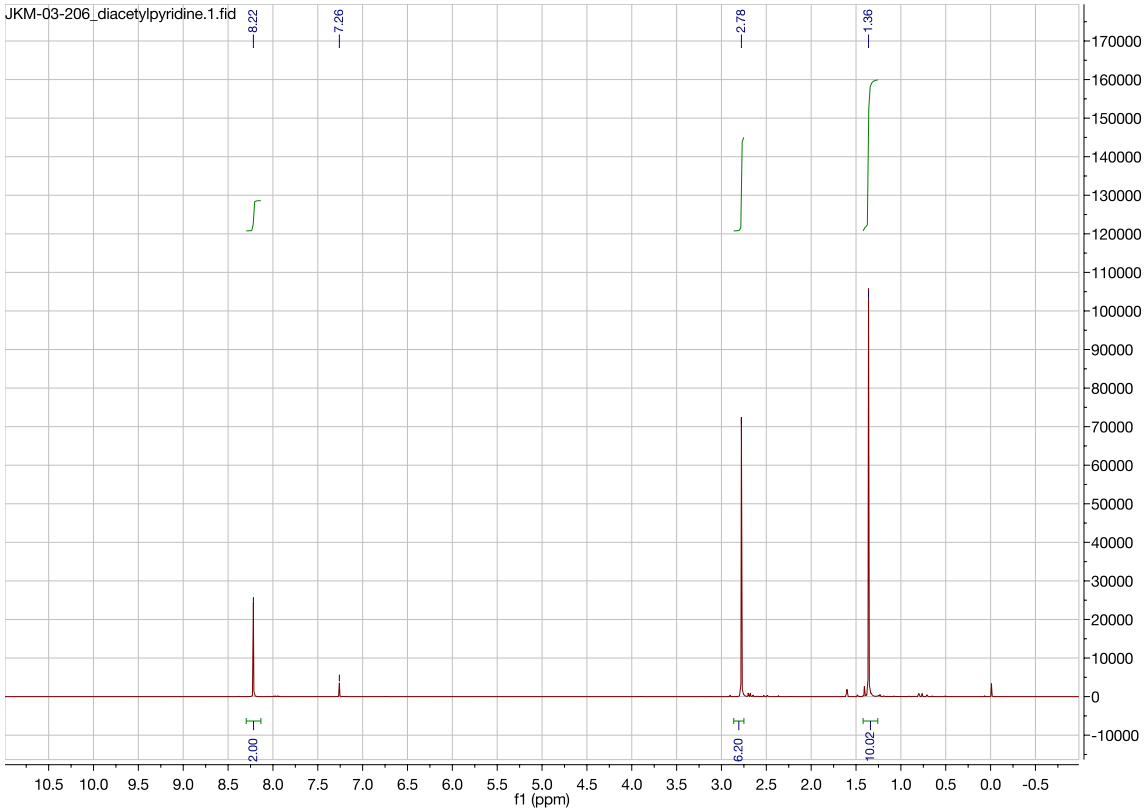

^{13}C NMR ($CDCl_3$, 125.8 MHz) spectrum of 1,1'-(4-(*tert*-butyl)pyridine-2,6-diyl)bis(ethan-1-one) (**2.7.12**)

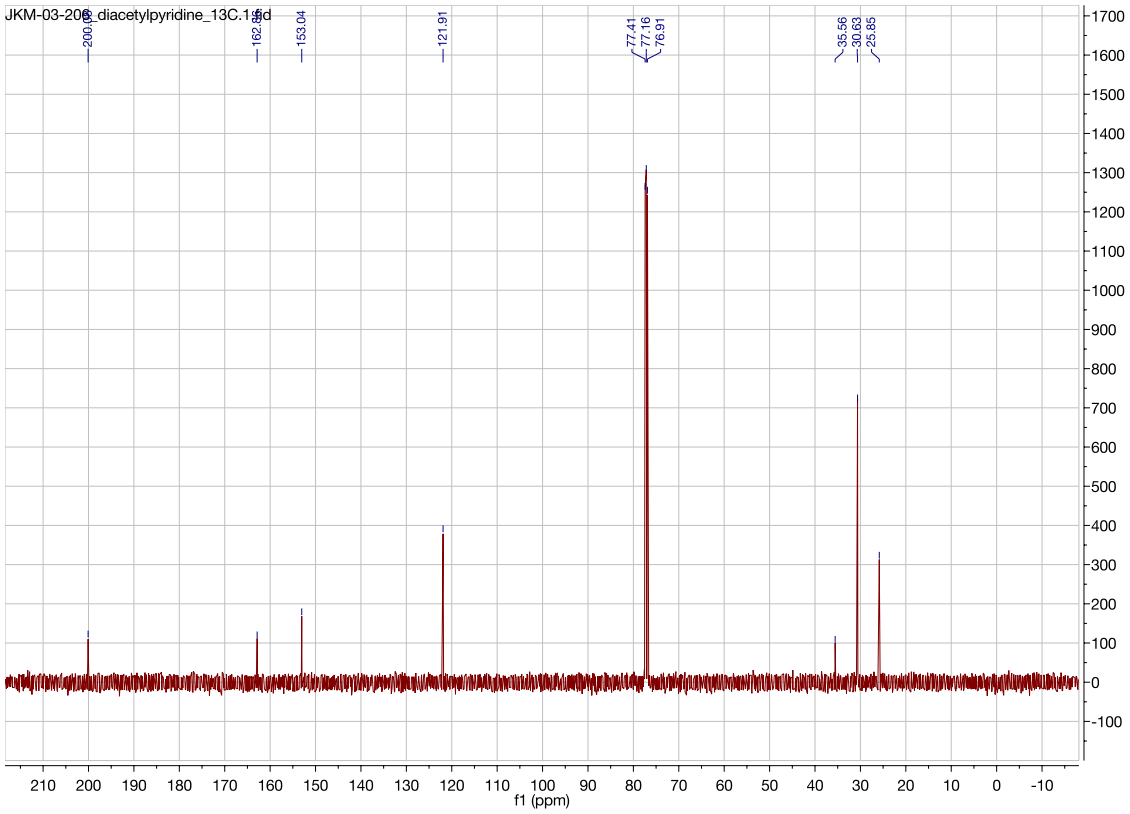

^{1}H ($CDCl_3$, 500 MHz) spectra of 8-(*tert*-butyl)-1,3,7-trimethyl-3,7-dihydro-1*H*-purine-2,6-dione (**2.7.13**)

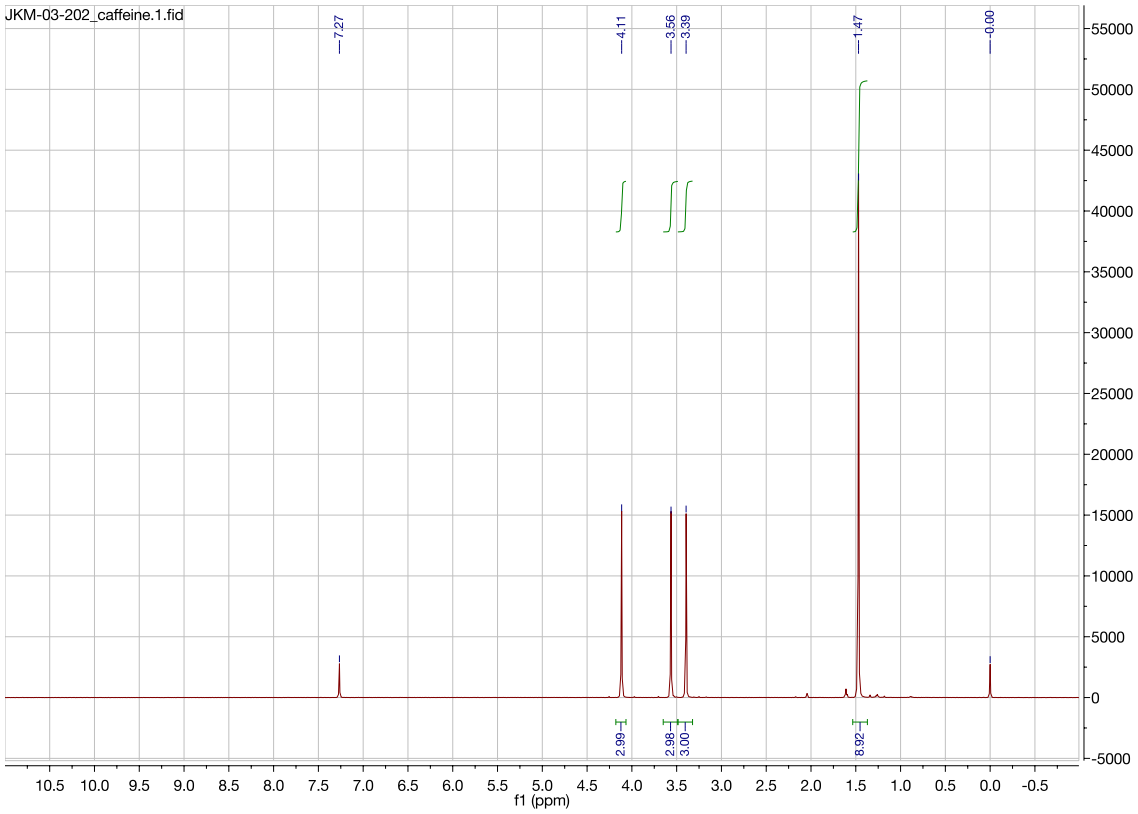

^{13}C NMR ($CDCl_3$, 125.8 MHz) spectrum of 8-(*tert*-butyl)-1,3,7-trimethyl-3,7-dihydro-1*H*-purine-2,6-dione (**2.7.13**)

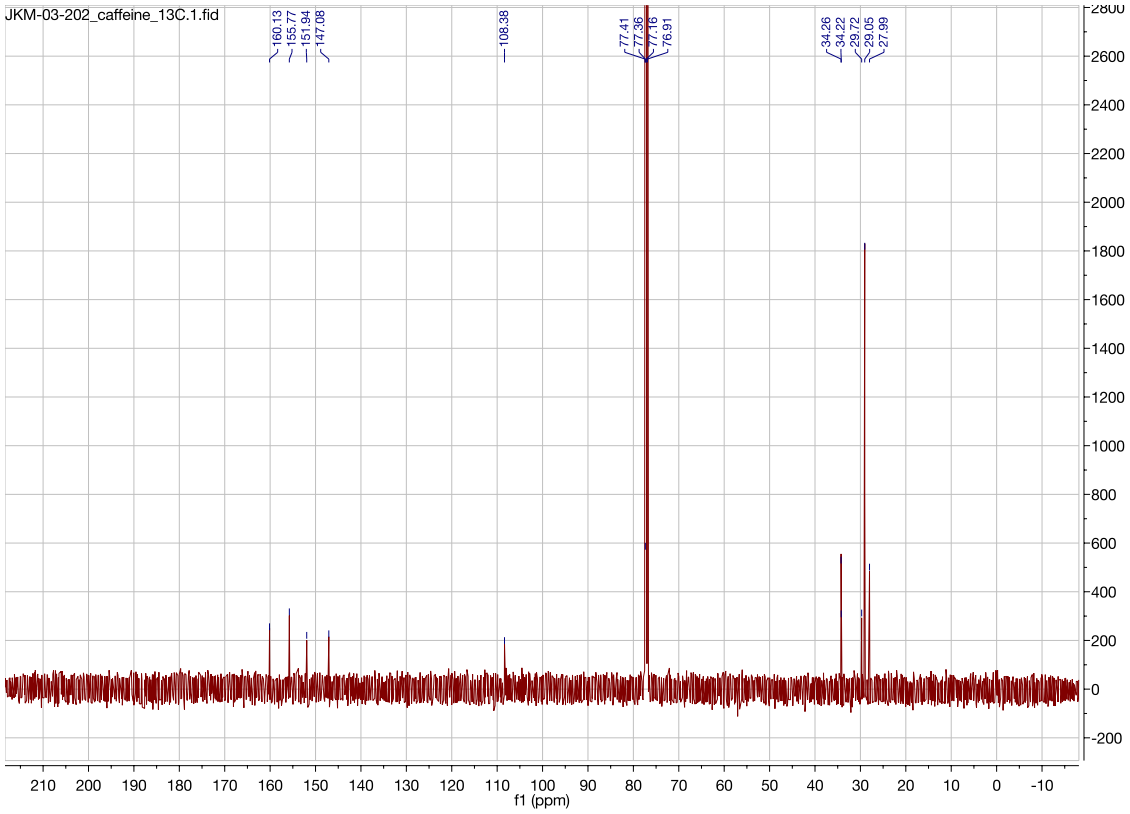

^{1}H ($CDCl_3$, 500 MHz) spectra of 2-(*tert*-butyl)nicotinamide **(2.7.14)**

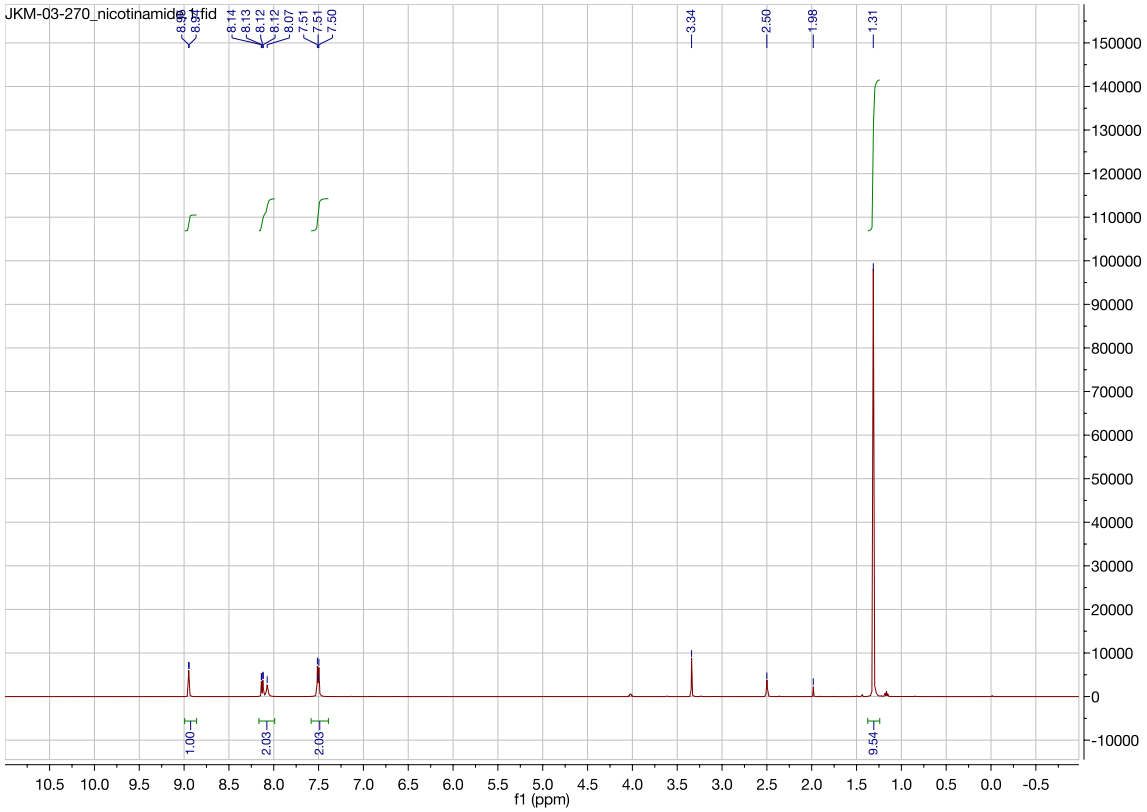

^{13}C NMR ($CDCl_3$, 125.8 MHz) spectrum of 2-(*tert*-butyl)nicotinamide **(2.7.14)**

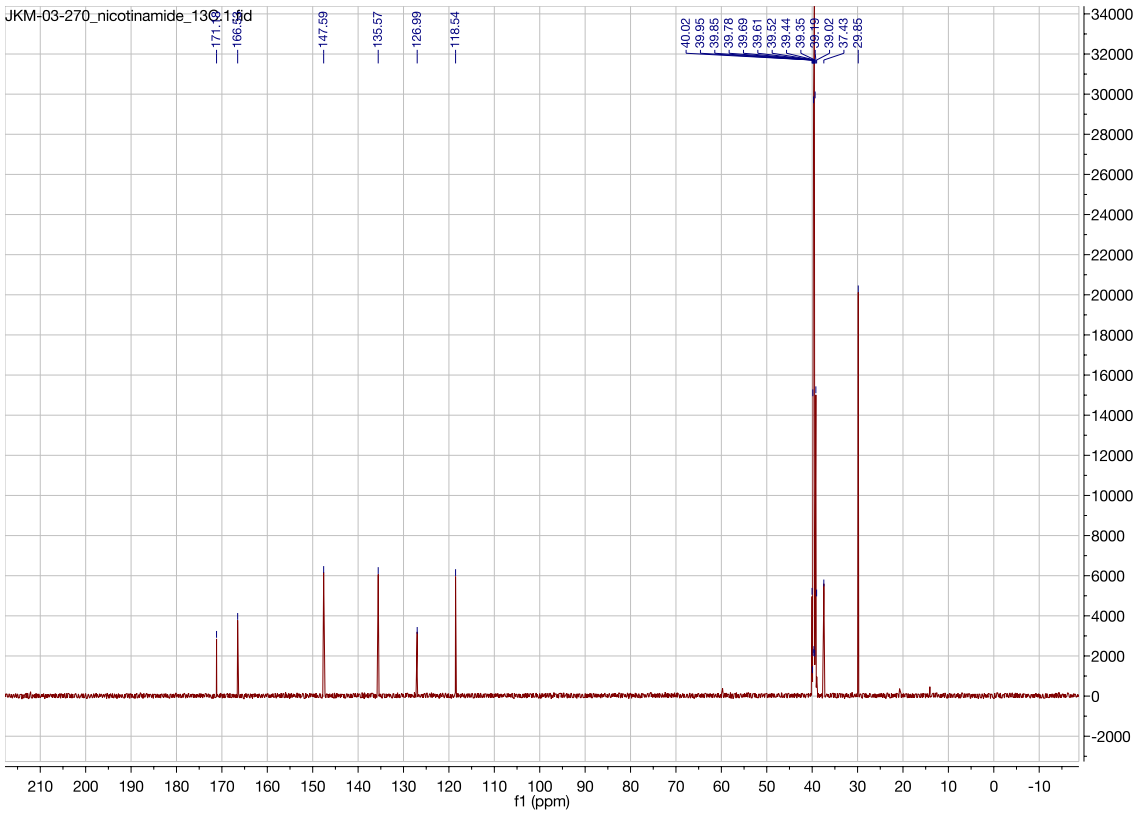

^{1}H ($CDCl_3$, 500 MHz) spectra of 2-(*tert*-butyl)benzo[*d*]thiazole (**2.7.15**)

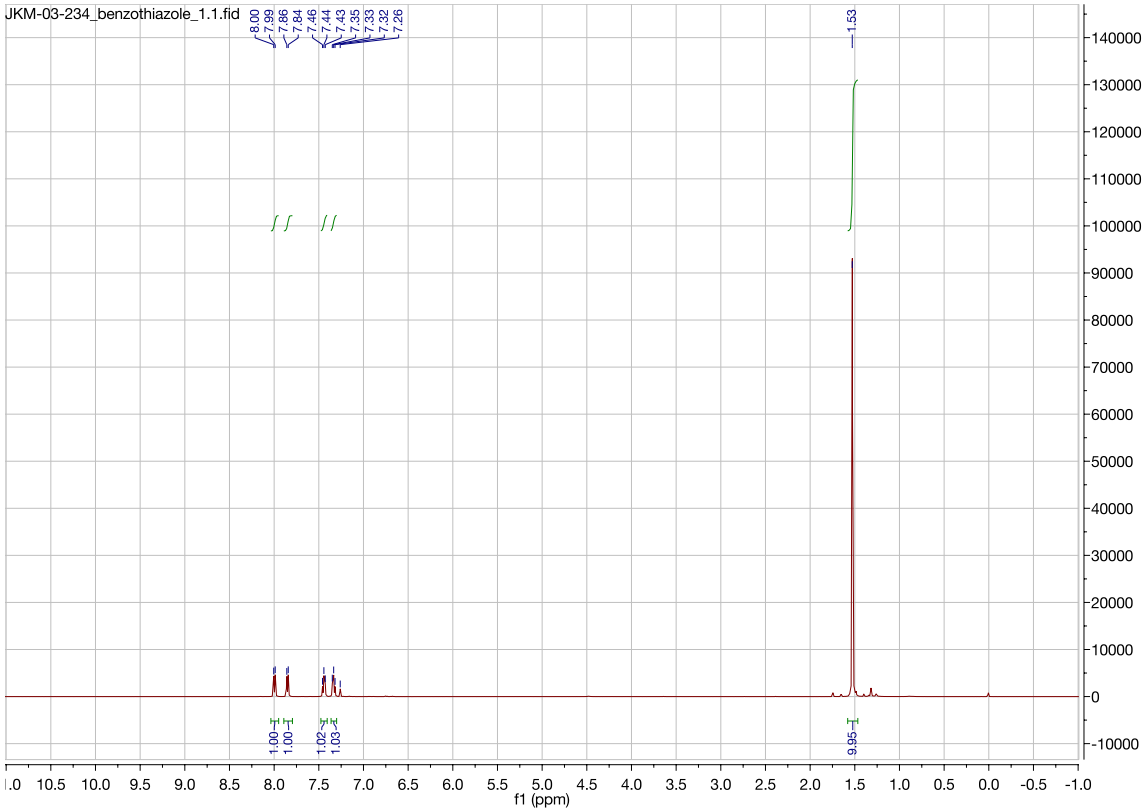

^{13}C NMR ($CDCl_3$, 125.8 MHz) spectrum of 2-(*tert*-butyl)benzo[*d*]thiazole (**2.7.15**)

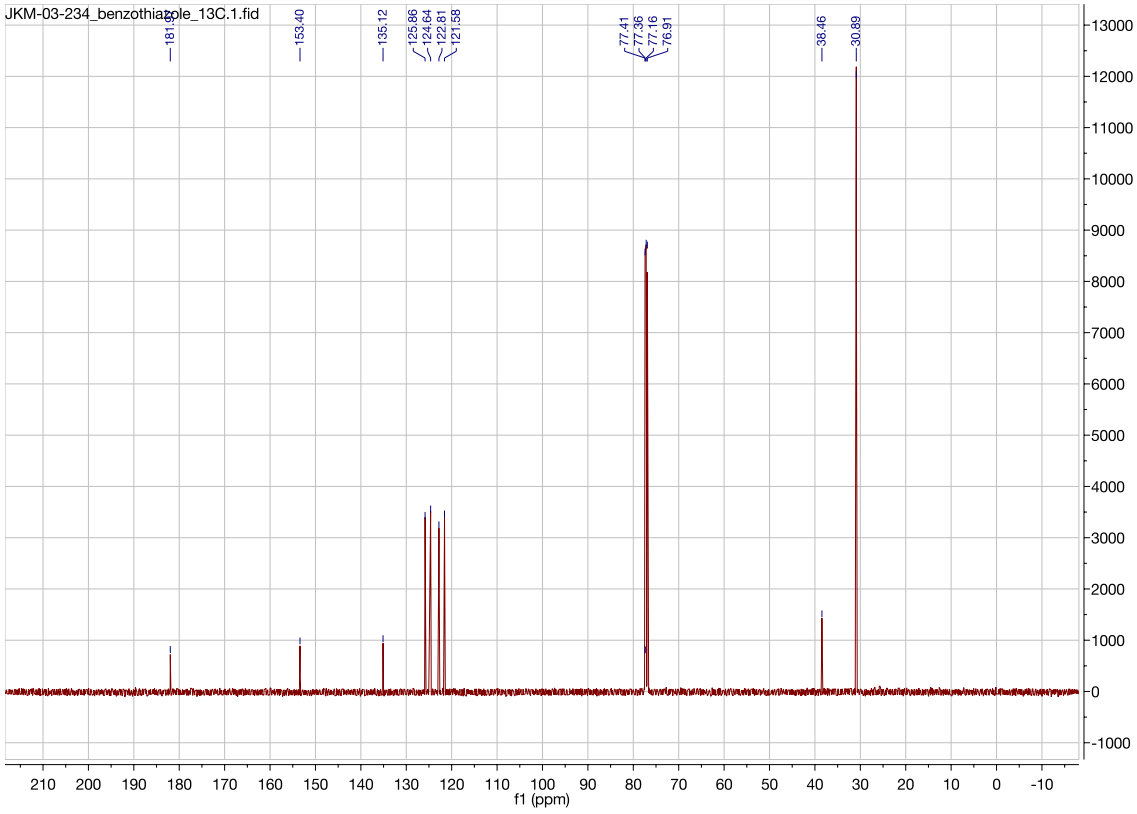

^{1}H ($CDCl_3$, 500 MHz) spectra of 2-(*tert*-butyl)quinazolin-4(3*H*)-one (**2.7.16**)

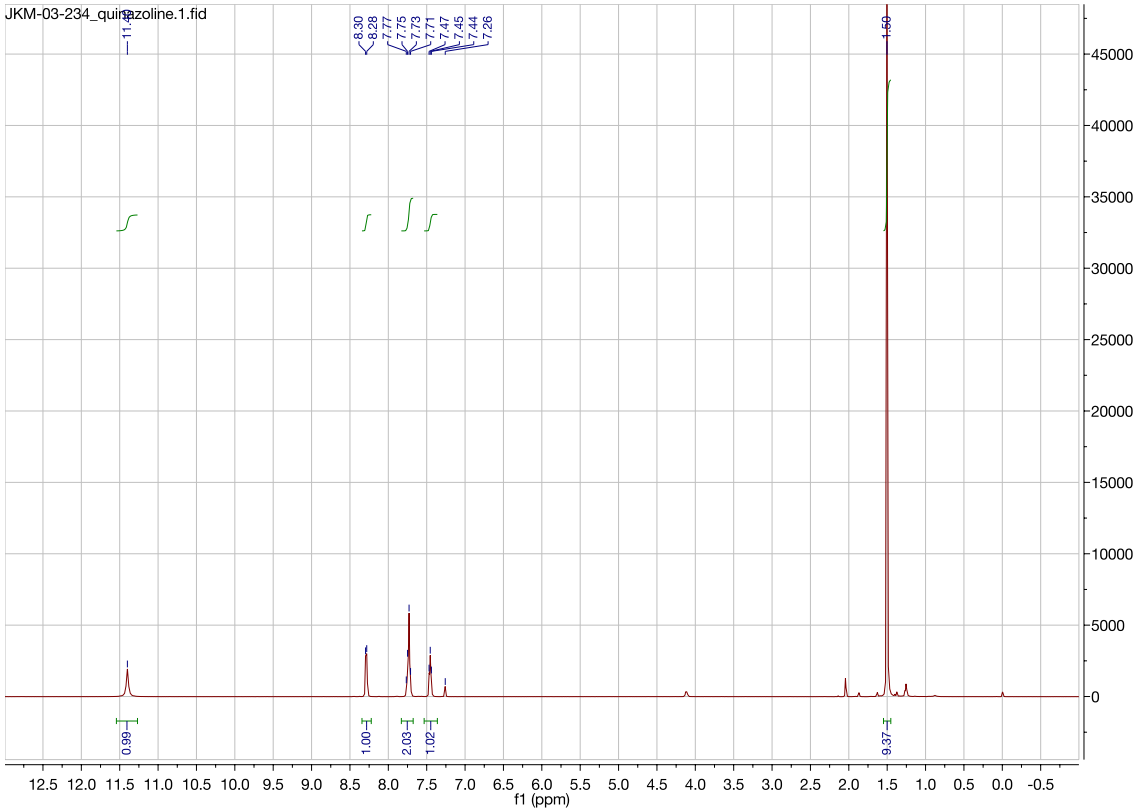

^{13}C NMR ($CDCl_3$, 125.8 MHz) spectrum of 2-(*tert*-butyl)quinazolin-4(3*H*)-one (**2.7.16**)

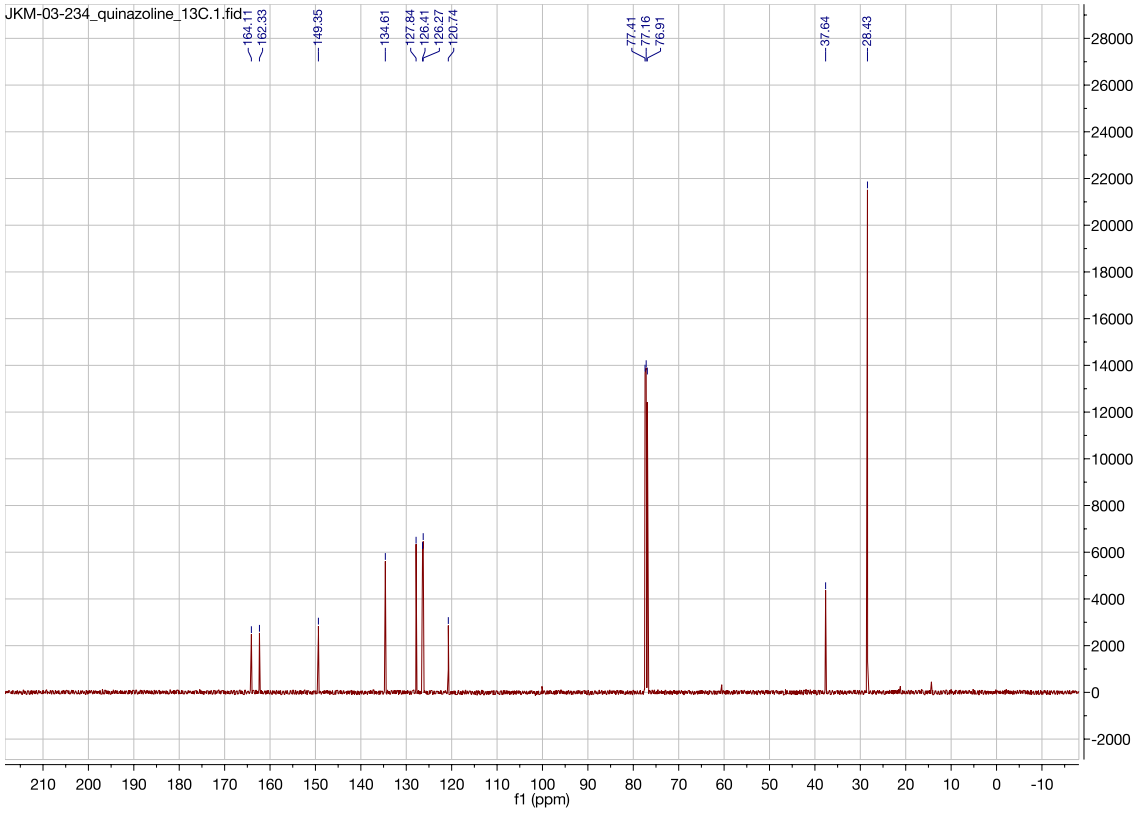

^{1}H ($CDCl_3$, 500 MHz) spectra of *N*-benzyl-2-(*tert*-butyl)-7*H*-purin-6-amine (**2.7.18**)

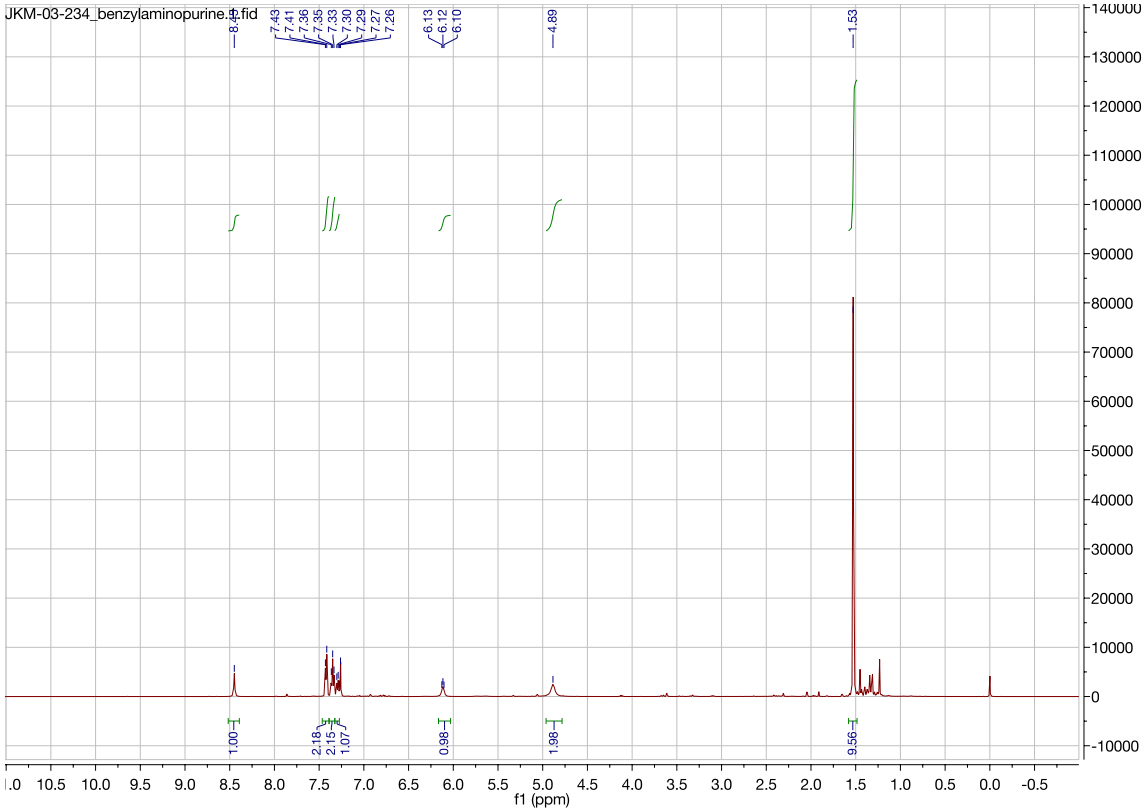

^{13}C NMR ($CDCl_3$, 125.8 MHz) spectrum of *N*-benzyl-2-(*tert*-butyl)-7*H*-purin-6-amine (**2.7.18**)

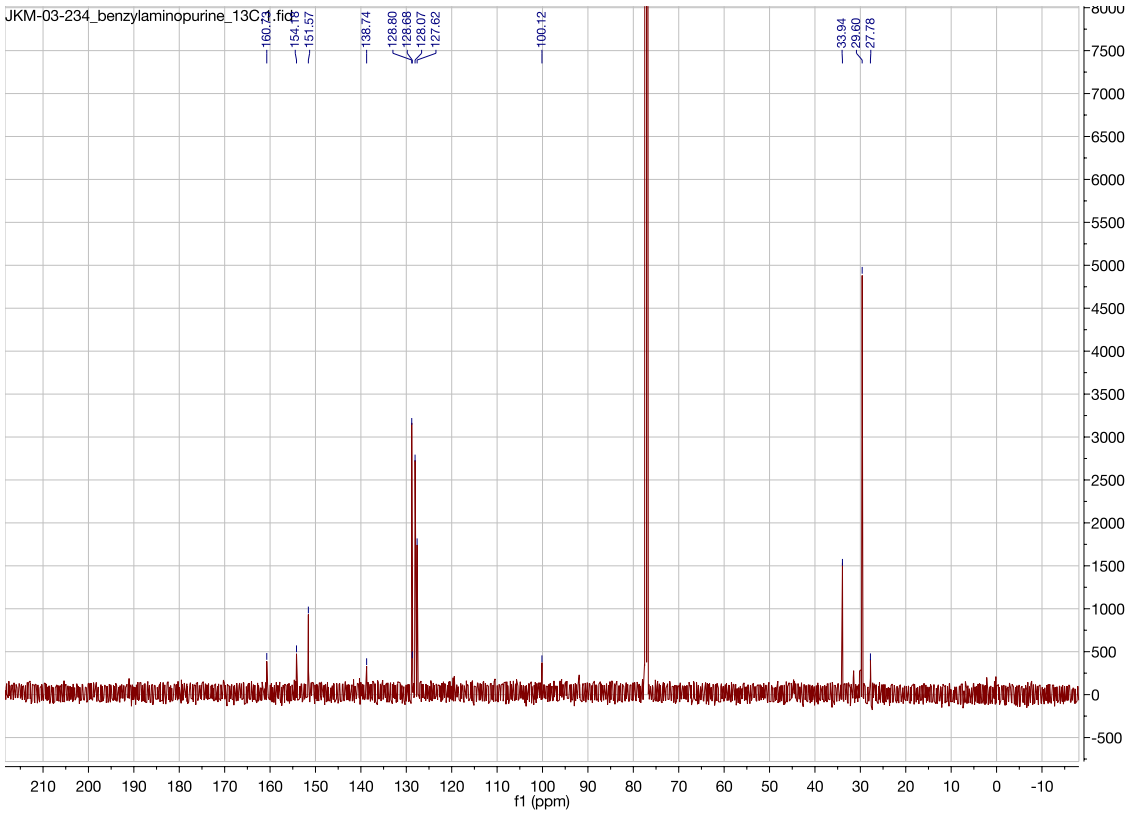

^{1}H ($CDCl_3$, 500 MHz) spectra of (1*R*)-(2-(*tert*-butyl)-6-methoxyquinolin-4-yl)(5-vinylquinuclidin-2-yl)methanol (**2.7.19**)

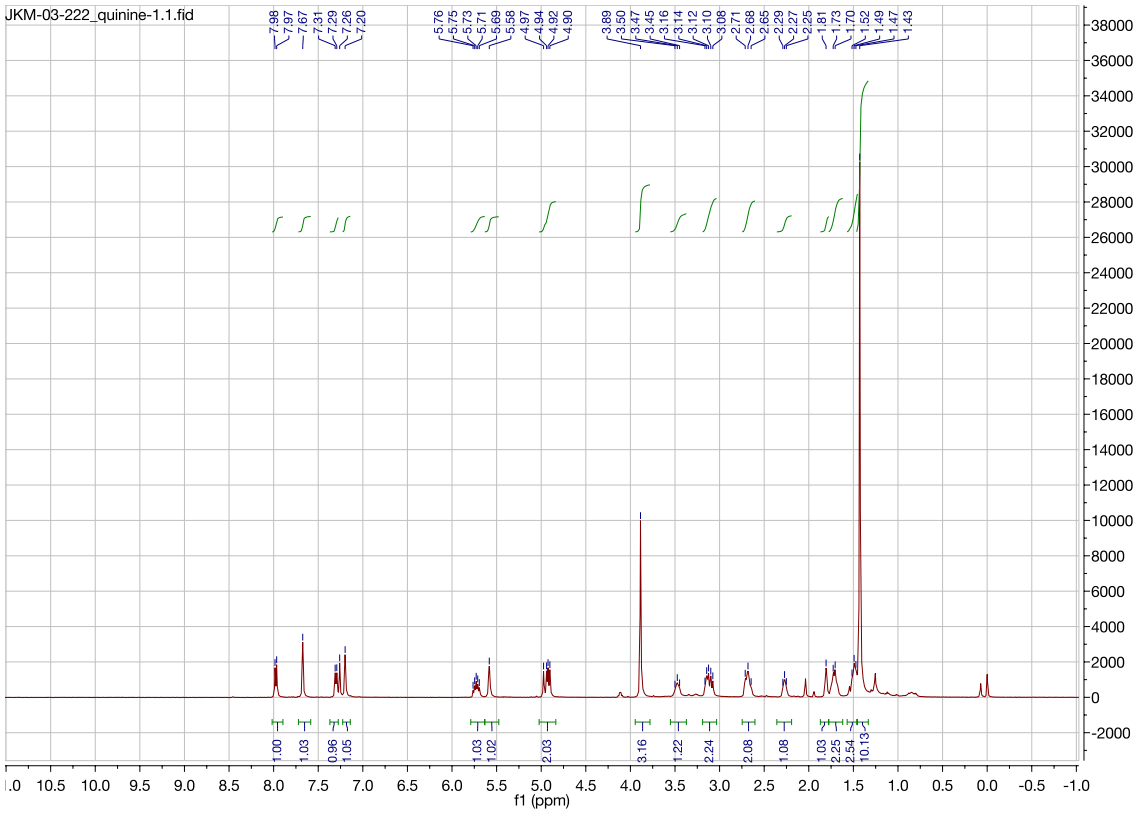

^{13}C NMR ($CDCl_3$, 125.8 MHz) spectrum of (1*R*)-(2-(*tert*-butyl)-6-methoxyquinolin-4-yl)(5-vinylquinuclidin-2-yl)methanol (**2.7.19**)

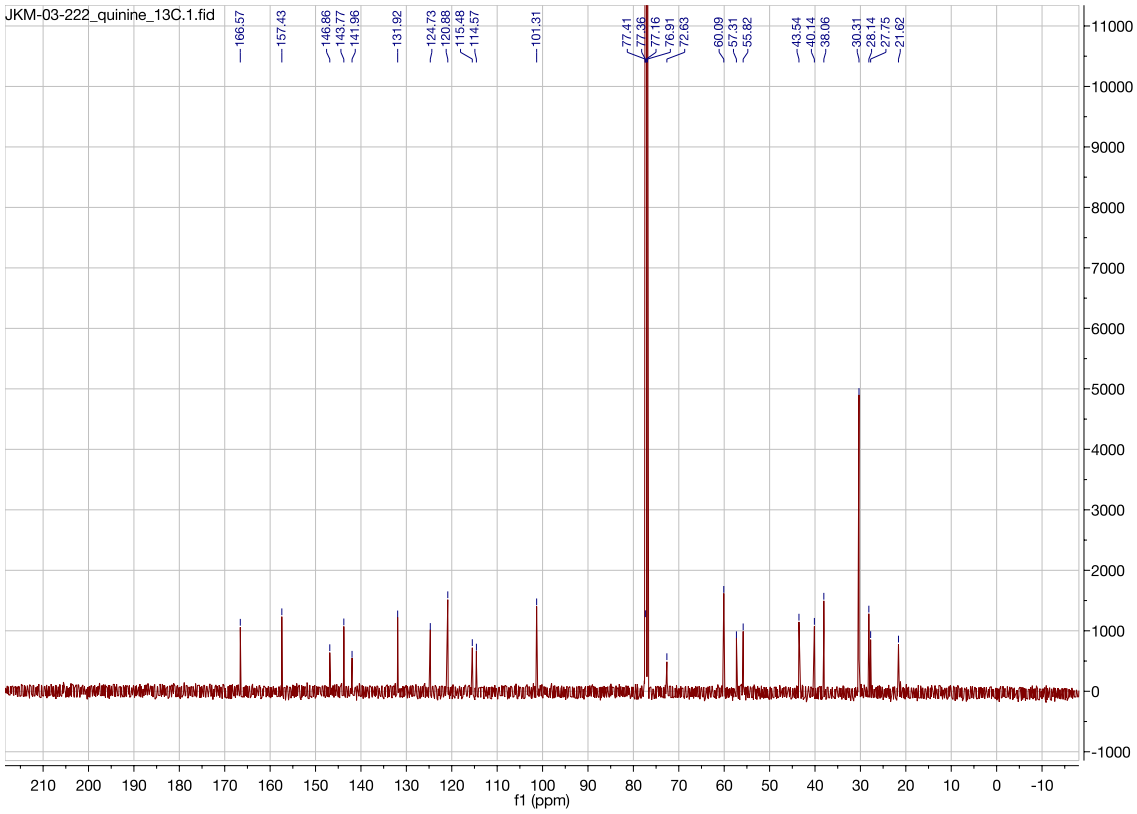

^{1}H ($CDCl_3$, 500 MHz) spectra of 1,3,9-trimethyl-8-(2-methyl-1-phenylpropan-2-yl)-3,9-dihydro-1H-purine-2,6-dione (**2.8.4**)

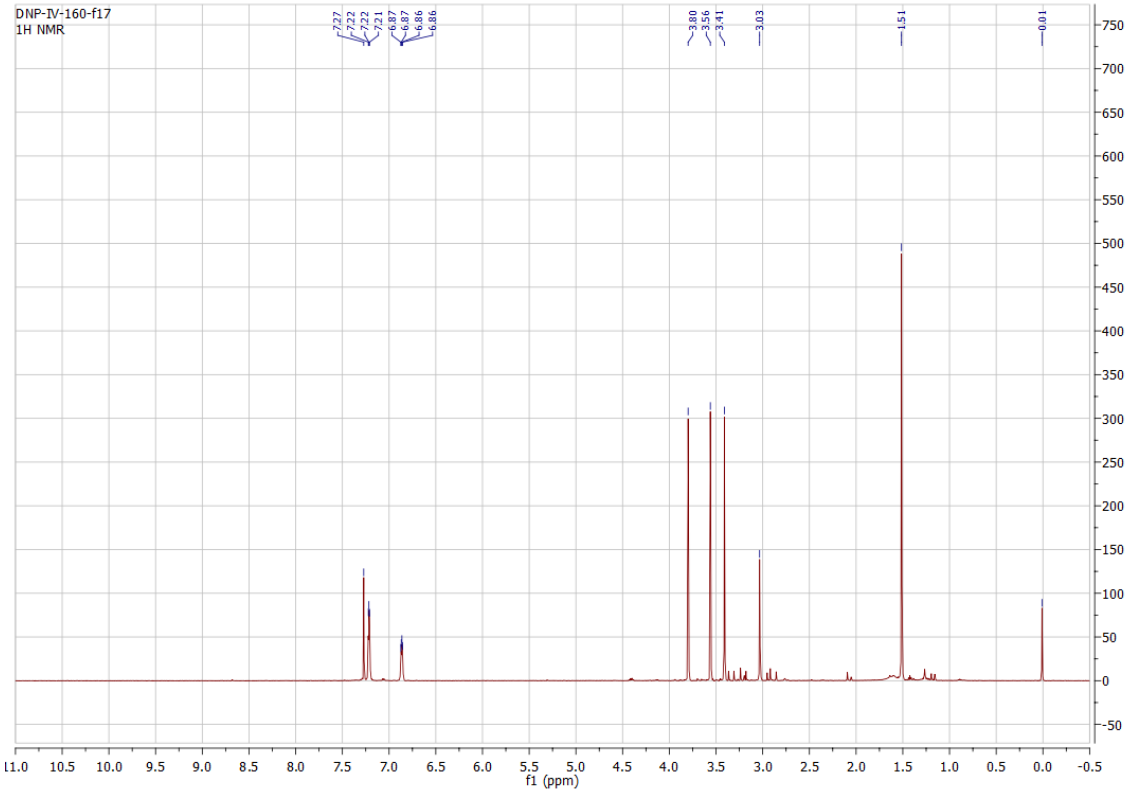

^{13}C NMR ($CDCl_3$, 125.8 MHz) spectrum of 1,3,9-trimethyl-8-(2-methyl-1-phenylpropan-2-yl)-3,9-dihydro-1H-purine-2,6-dione (**2.8.4**)

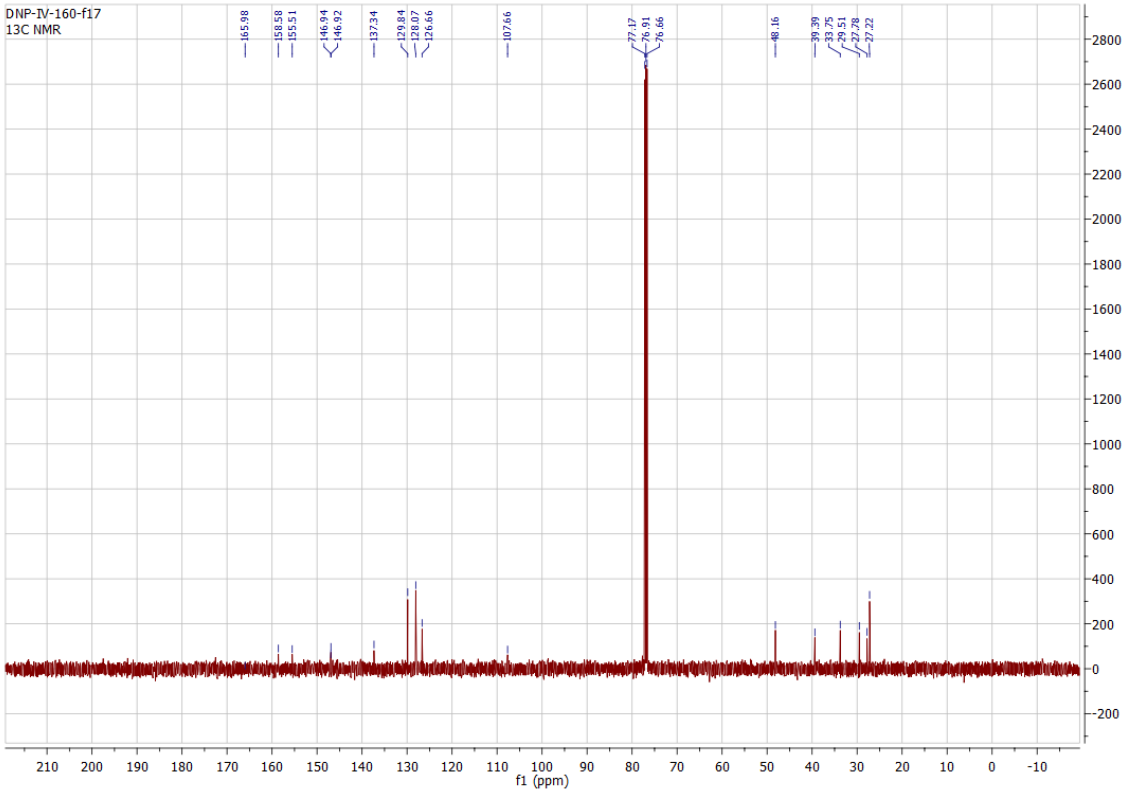

^{1}H ($CDCl_3$, 500 MHz) spectra of 2-(2-methyl-1-phenylpropan-2-yl)benzo[d]thiazole (**2.8.5**)

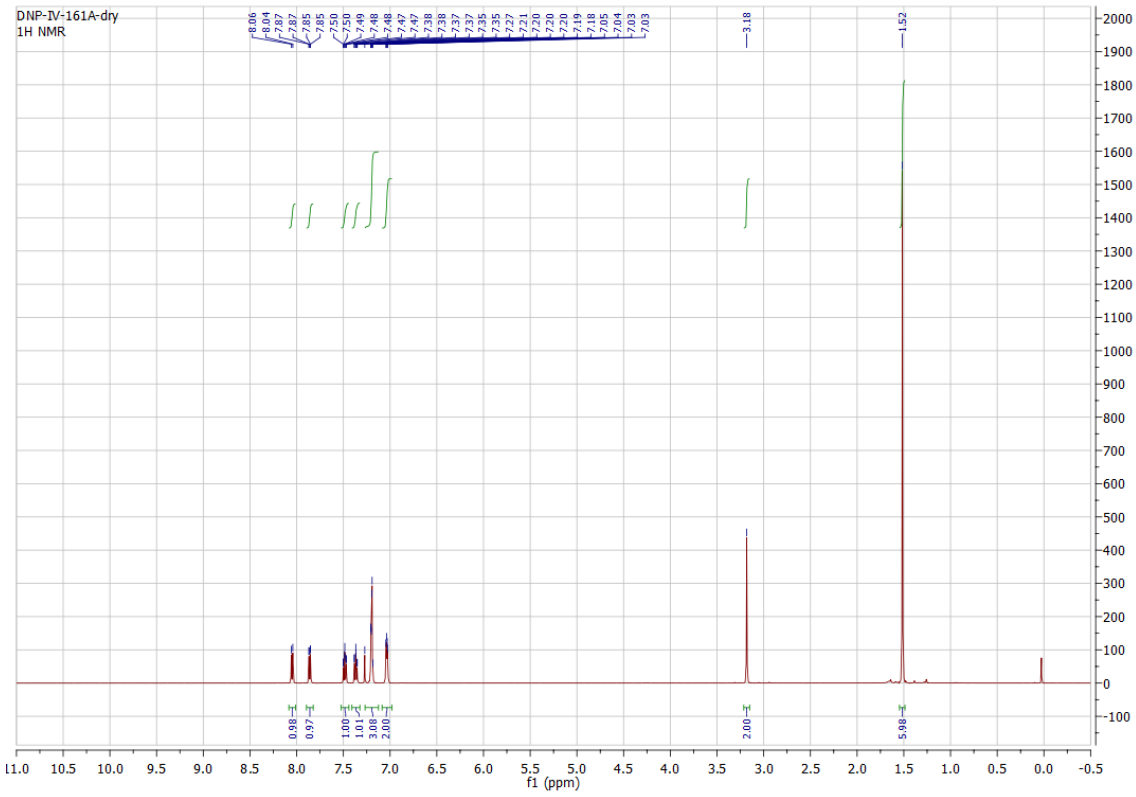

^{13}C NMR ($CDCl_3$, 125.8 MHz) spectrum of 2-(2-methyl-1-phenylpropan-2-yl)benzo[d]thiazole (**2.8.5**)

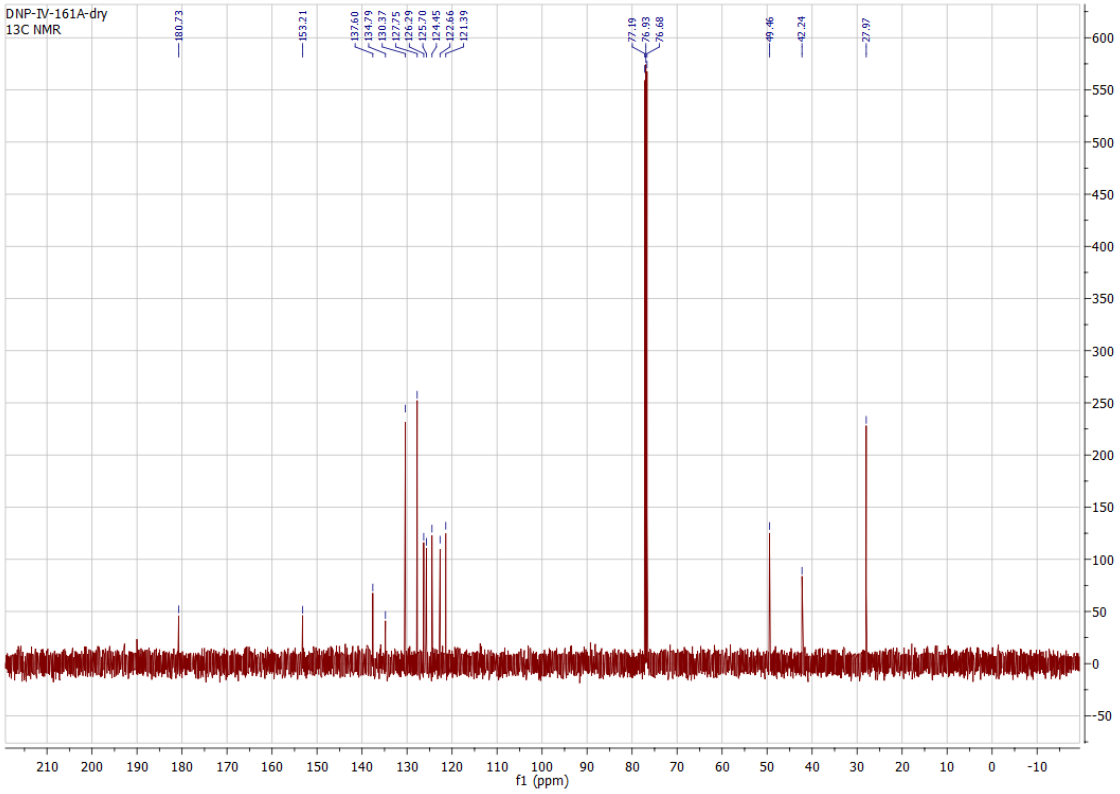

^{1}H ($CDCl_3$, 500 MHz) spectra of methyl 1-(1-(benzyloxy)-3-phenylpropyl)isoquinoline-3-carboxylate (**2.9.1**)

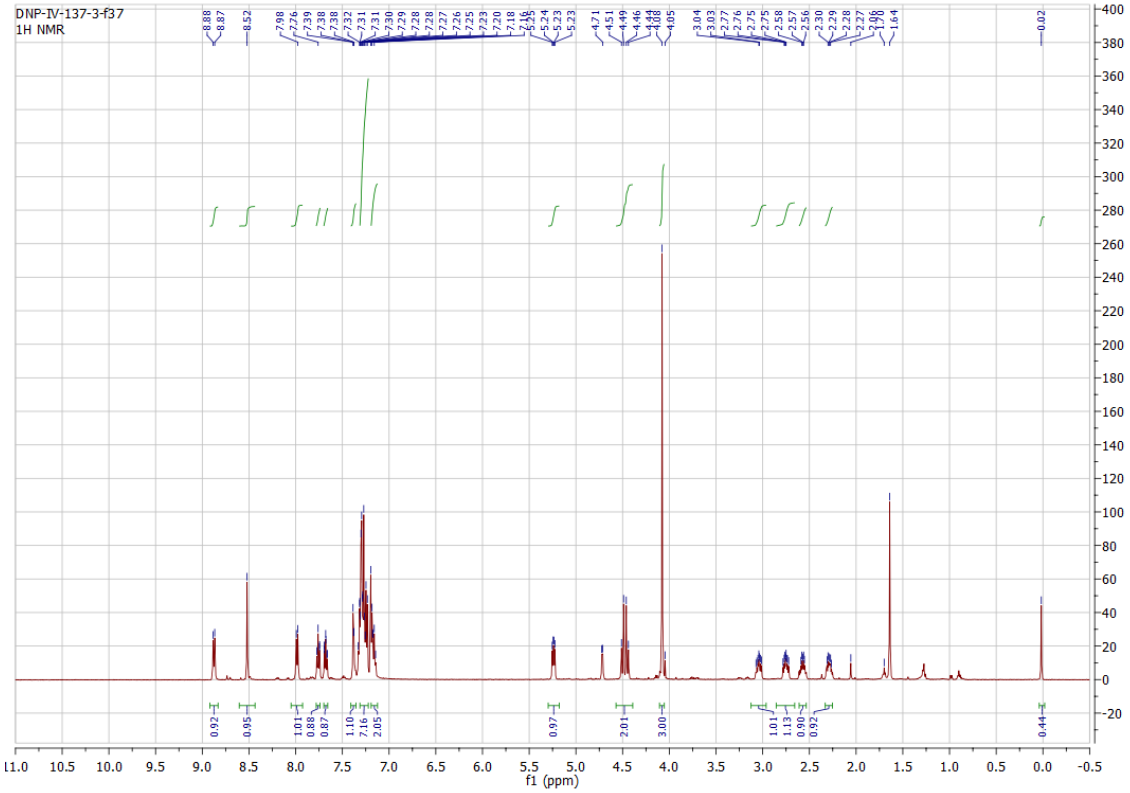

^{13}C NMR ($CDCl_3$, 125.8 MHz) spectrum of methyl 1-(1-(benzyloxy)-3-phenylpropyl)isoquinoline-3-carboxylate (**2.9.1**)

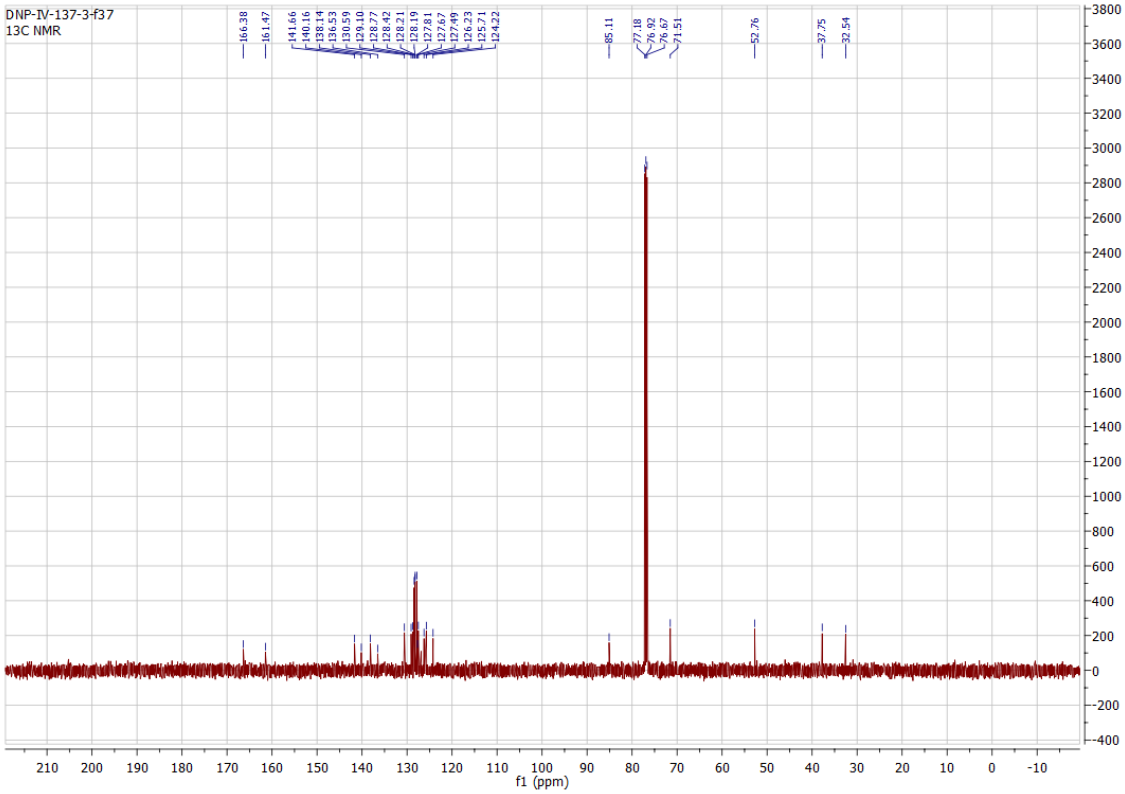

^{1}H ($CDCl_3$, 500 MHz) spectra of methyl 1-(4,4-difluorocyclohexyl)isoquinoline-3-carboxylate (**2.9.2**)

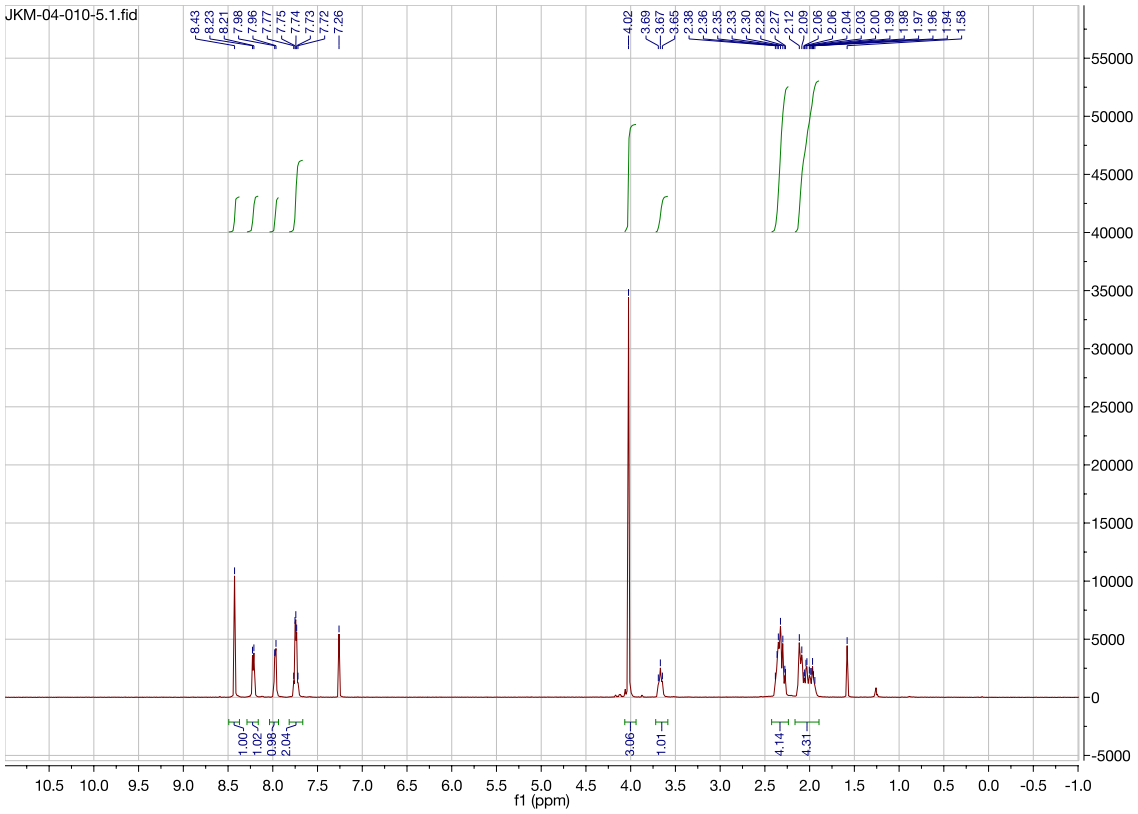

^{13}C NMR ($CDCl_3$, 125.8 MHz) spectrum of methyl 1-(4,4-difluorocyclohexyl)isoquinoline-3-carboxylate (**2.9.2**)

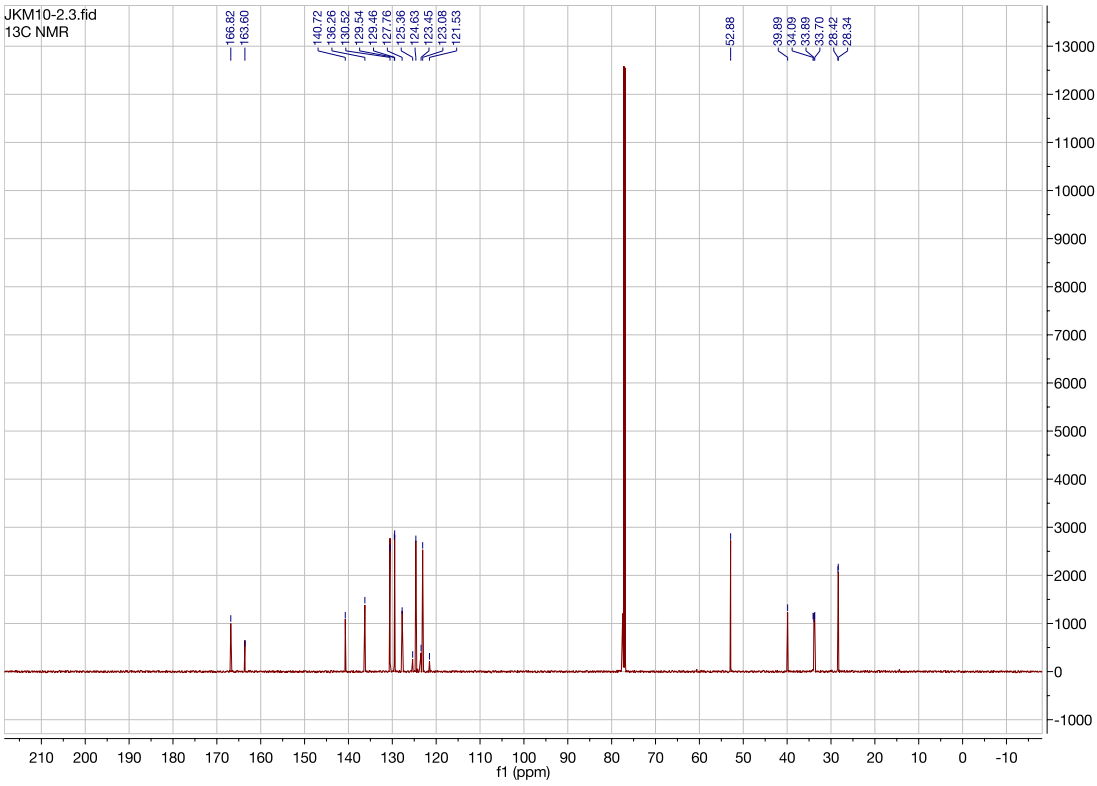

^{1}H ($CDCl_3$, 500 MHz) spectra of methyl 1-(tetrahydro-2H-pyran-4-yl)isoquinoline-3-carboxylate (**2.9.3**)

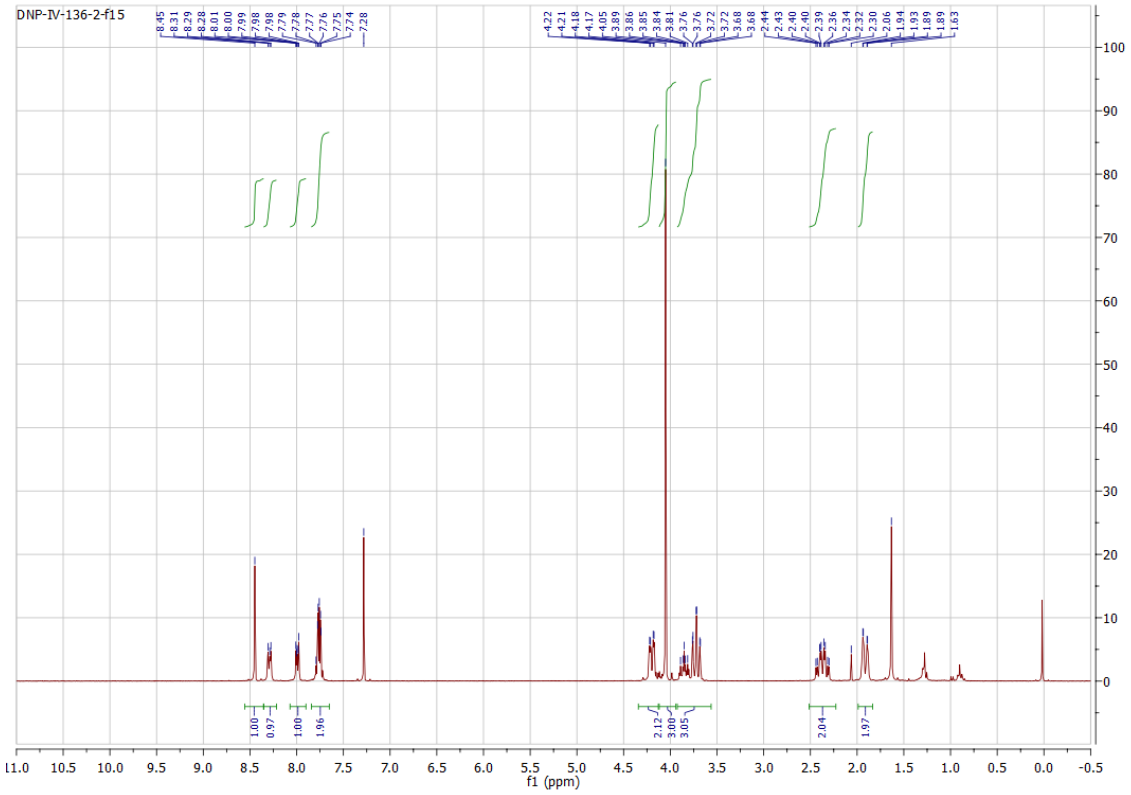

^{13}C NMR ($CDCl_3$, 125.8 MHz) spectrum of methyl 1-(tetrahydro-2H-pyran-4-yl)isoquinoline-3-carboxylate (**2.9.3**)

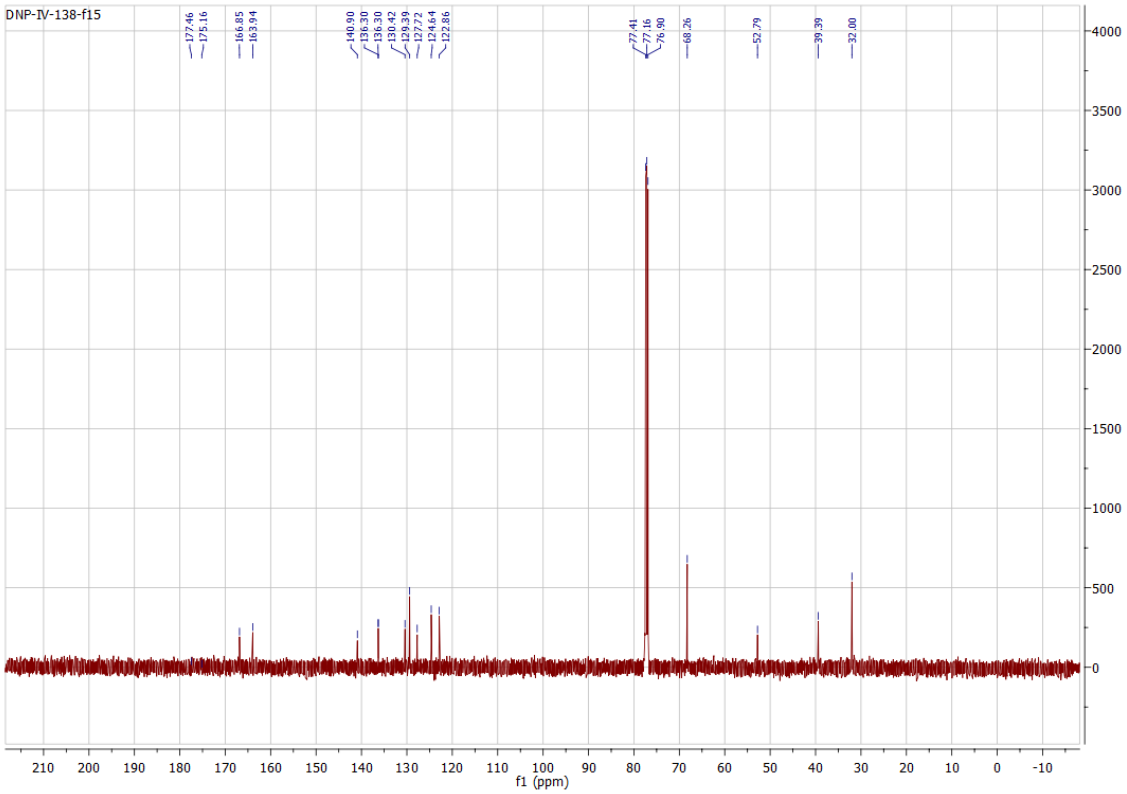

^{1}H ($CDCl_3$, 500 MHz) spectra of methyl 1-(1-tosylpiperidin-4-yl)isoquinoline-3-carboxylate (**2.9.4**)

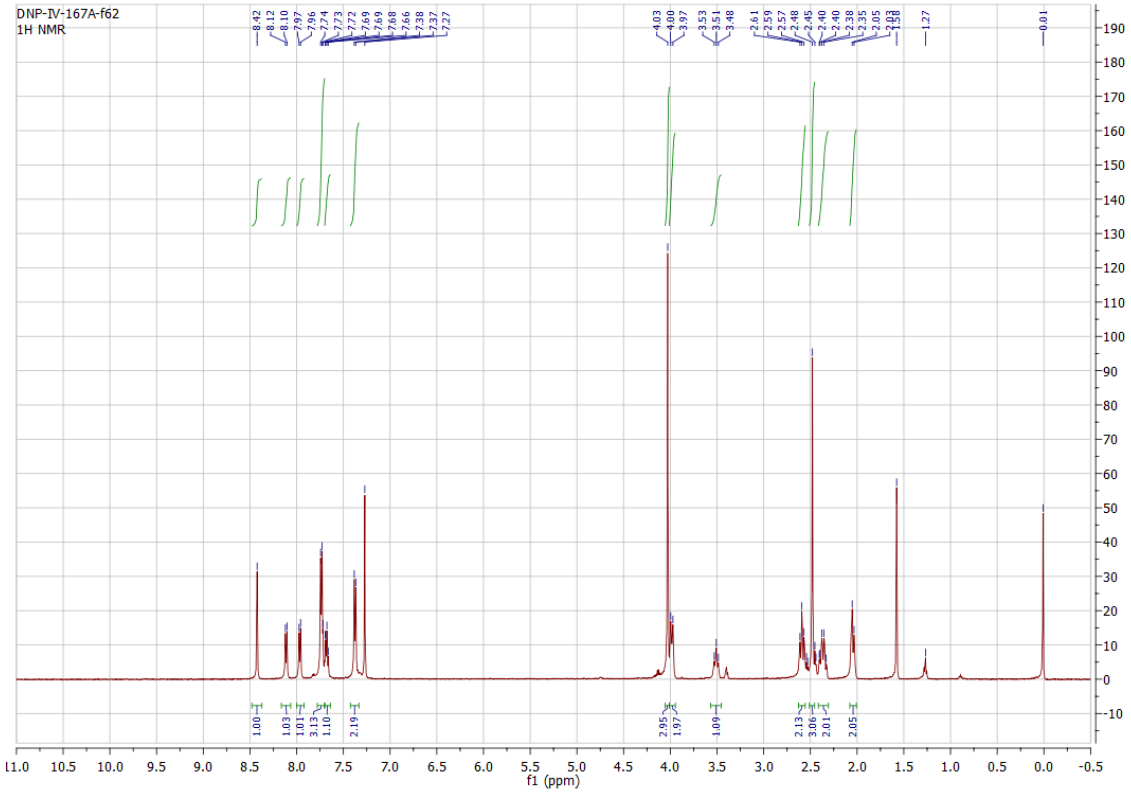

^{13}C ($CDCl_3$, 125.8 MHz) spectra of methyl 1-(1-tosylpiperidin-4-yl)isoquinoline-3-carboxylate (**2.9.4**)

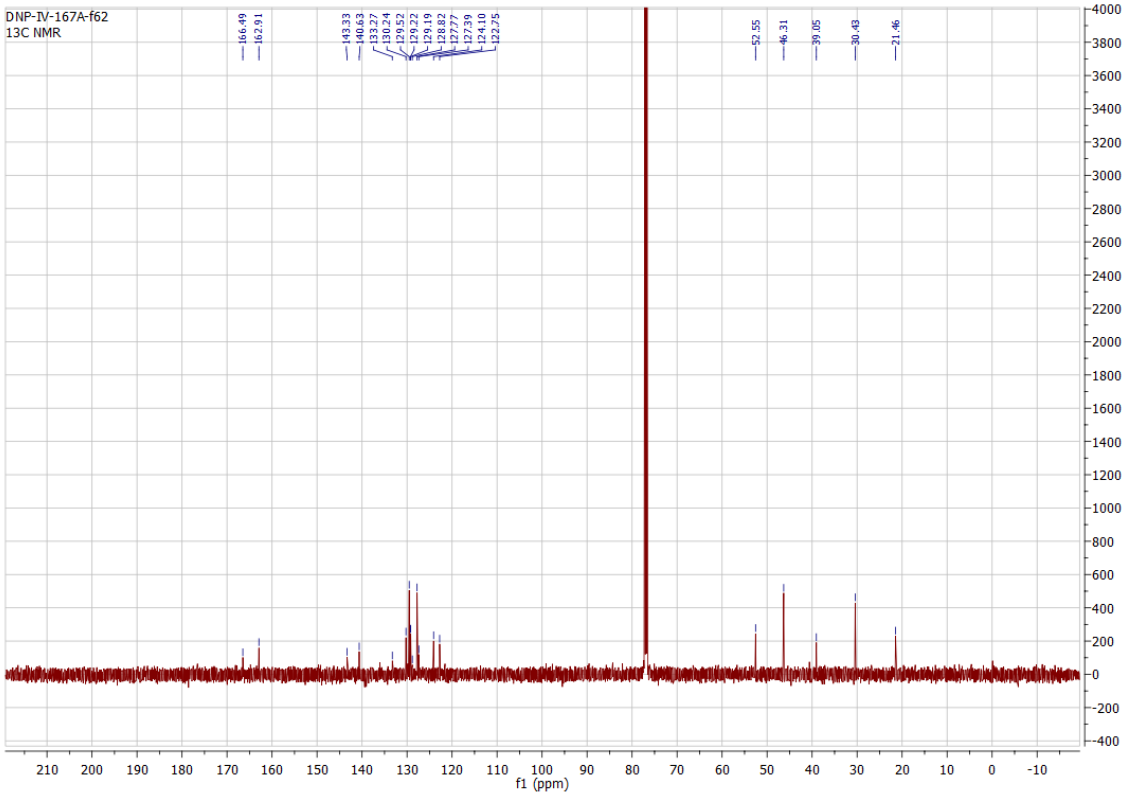

^{1}H ($CDCl_3$, 500 MHz) spectra of methyl 1-(1-(*tert*-butoxycarbonyl)piperidin-4-yl)isoquinoline-3-carboxylate (**2.9.5**)

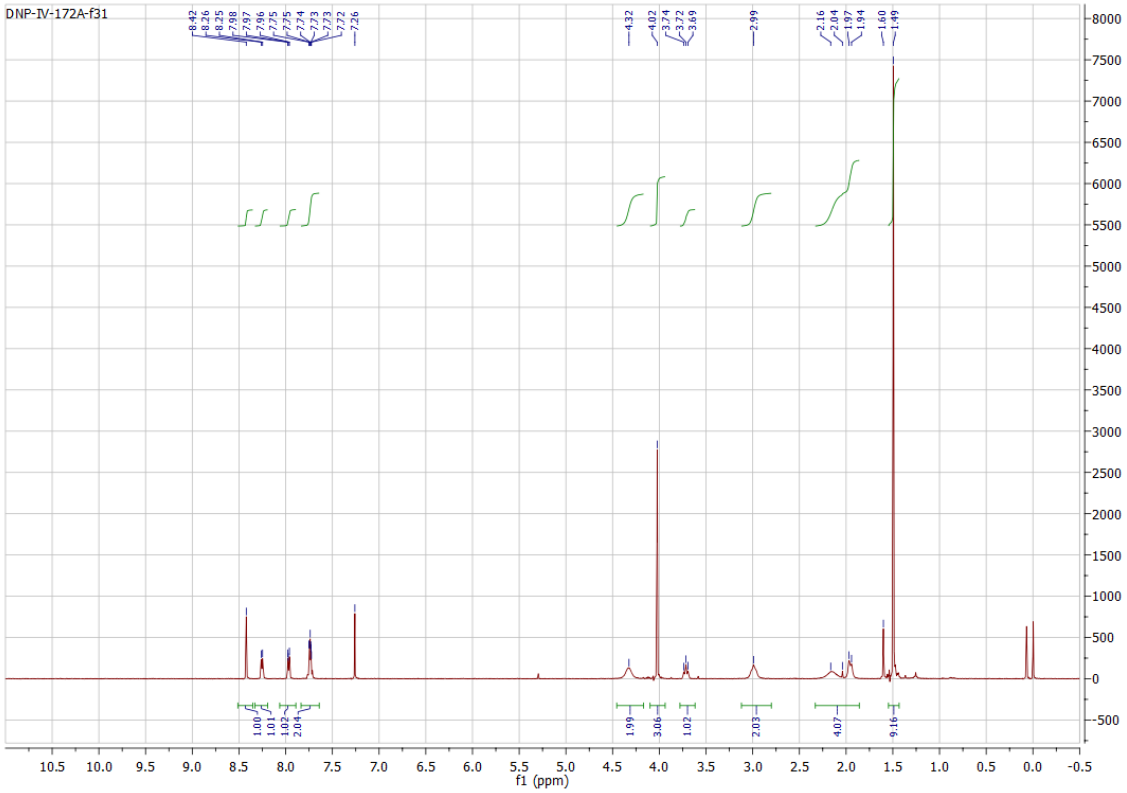

^{13}C ($CDCl_3$, 125.8 MHz) spectra of methyl 1-(1-(*tert*-butoxycarbonyl)piperidin-4-yl)isoquinoline-3-carboxylate (**2.9.5**)

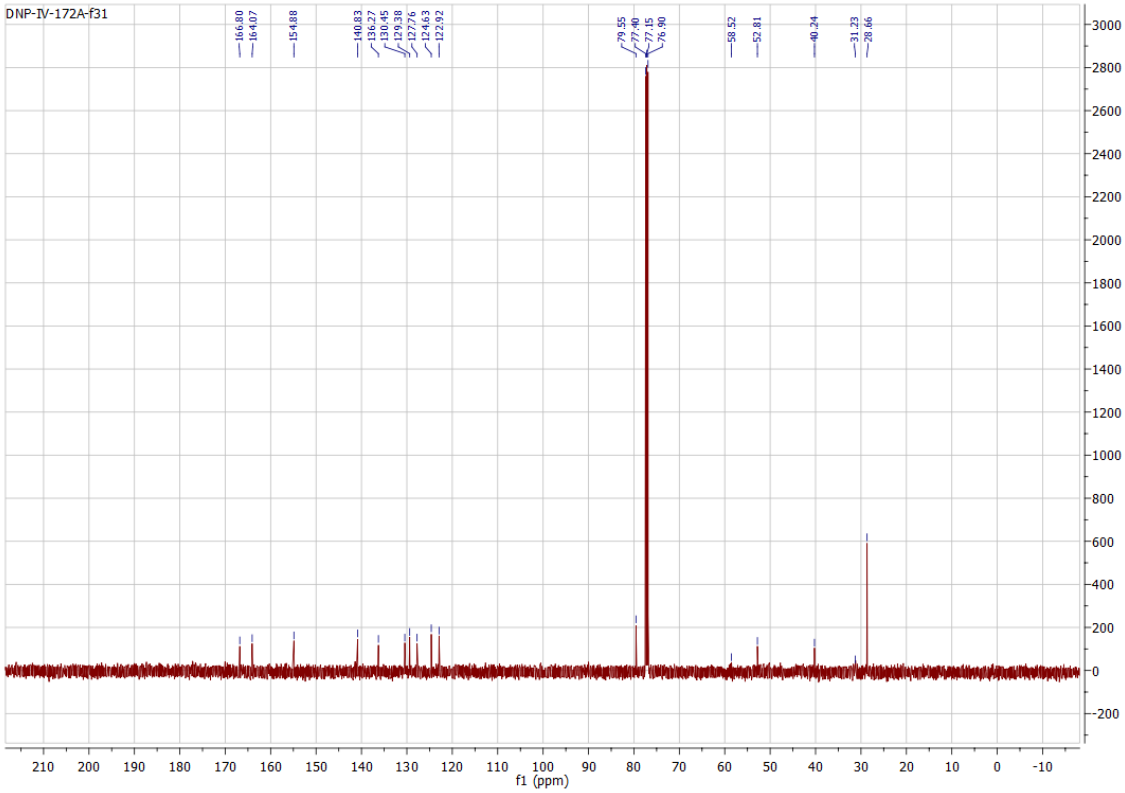

^{1}H ($CDCl_3$, 500 MHz) spectra of methyl 1-(1-hydroxy-3-phenylpropan-2-yl)isoquinoline-3-carboxylate (**2.9.6**)

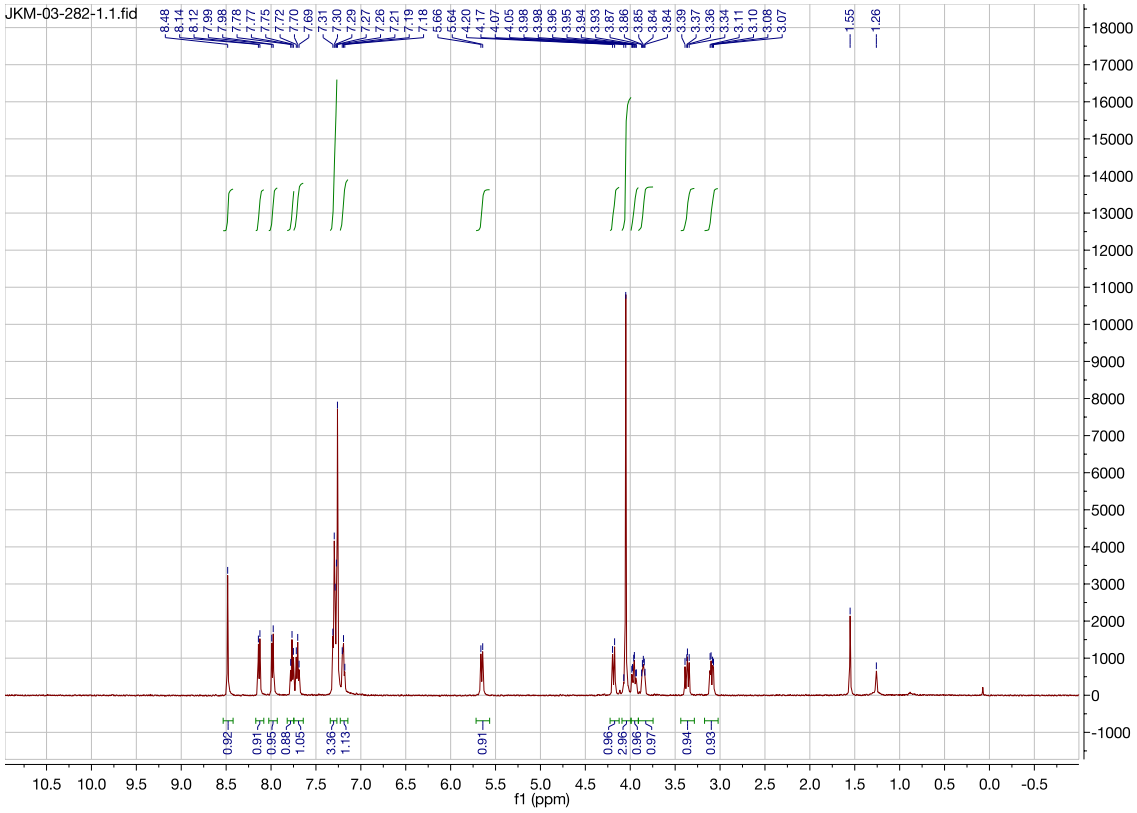

^{13}C NMR ($CDCl_3$, 125.8 MHz) spectrum of methyl 1-(1-hydroxy-3-phenylpropan-2-yl)isoquinoline-3-carboxylate (**2.9.6**)

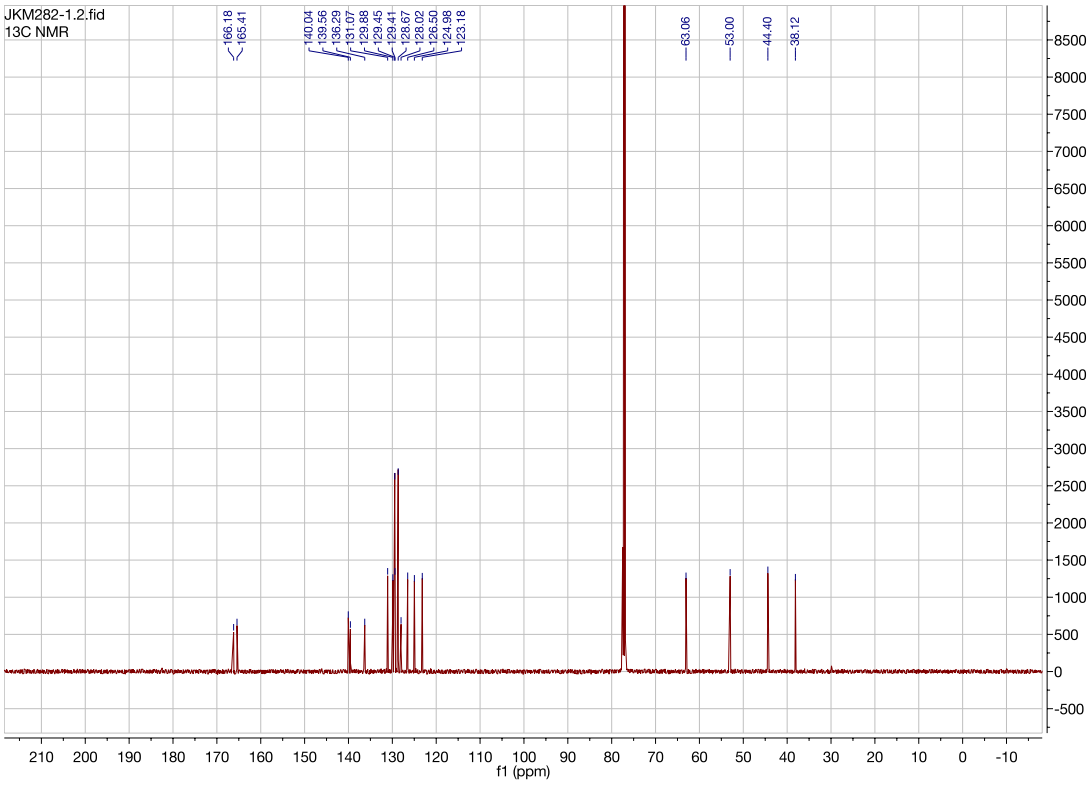

^{1}H NMR ($CDCl_3$, 500 MHz) spectrum of methyl 1-(tetrahydrofuran-3-yl)isoquinoline-3-carboxylate (**2.9.7**)

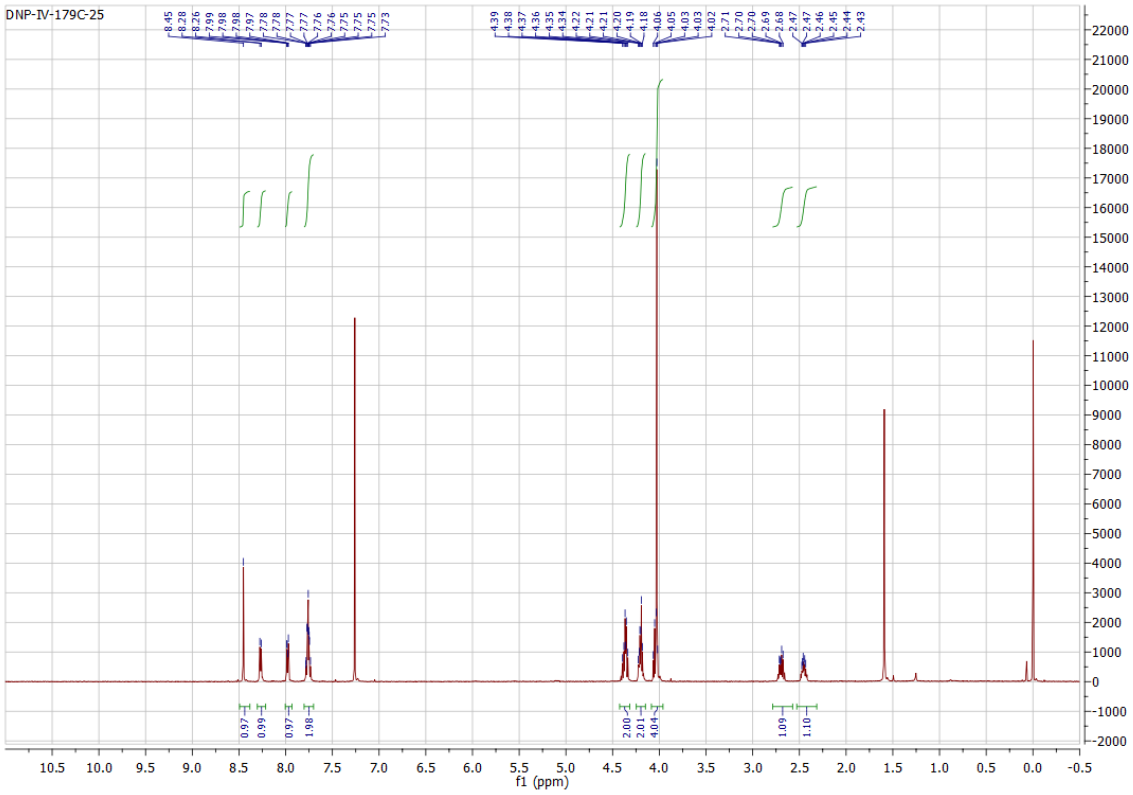

^{1}C NMR ($CDCl_3$, 125.8 MHz) spectrum of methyl 1-(tetrahydrofuran-3-yl)isoquinoline-3-carboxylate (**2.9.7**)

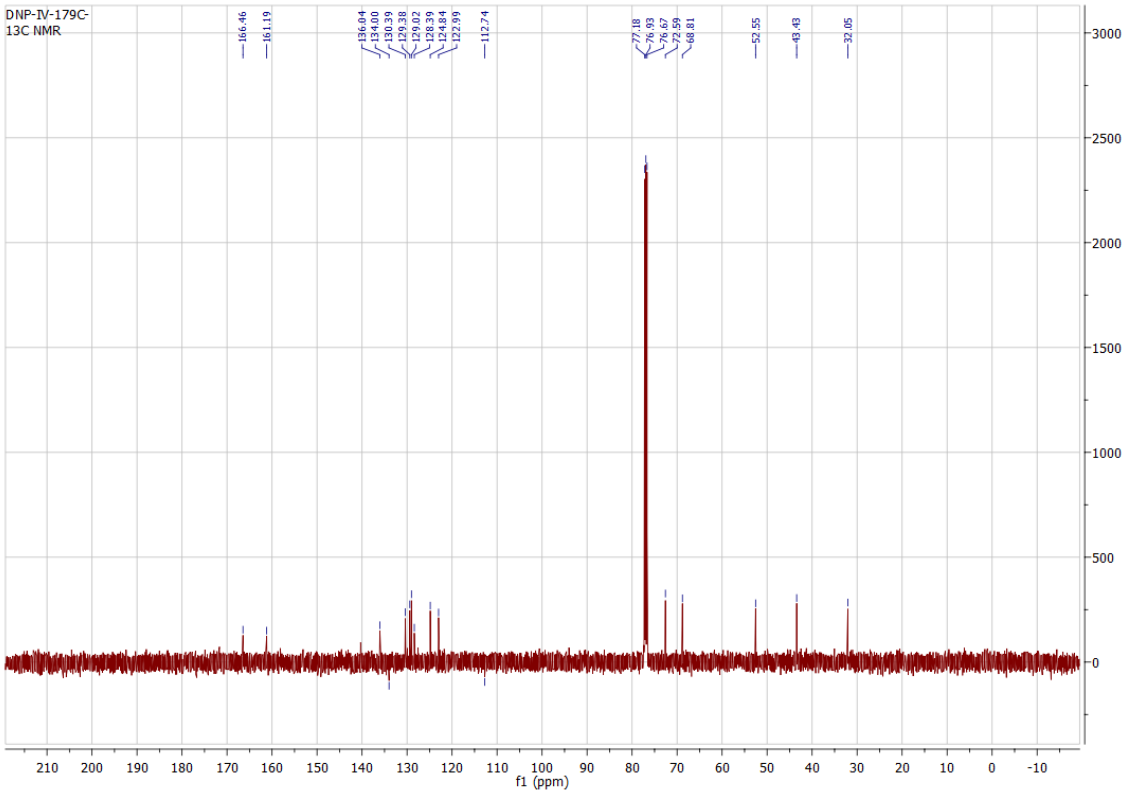

^{1}H NMR ($CDCl_3$, 500 MHz) spectrum of methyl 1-(1-(*tert*-butoxycarbonyl)azetidin-3-yl)isoquinoline-3-carboxylate (**2.9.9**)

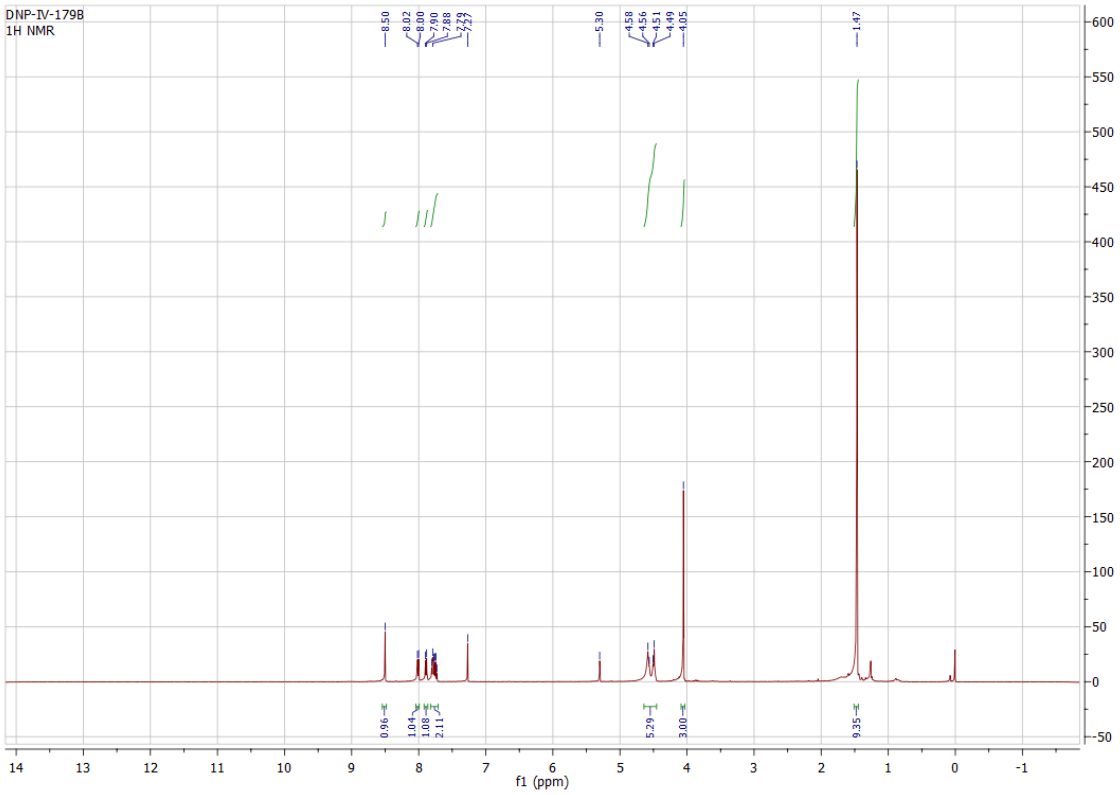

^{13}C NMR ($CDCl_3$, 125.8 MHz) spectrum of methyl 1-(1-(*tert*-butoxycarbonyl)azetidin-3-yl)isoquinoline-3-carboxylate (**2.9.9**)

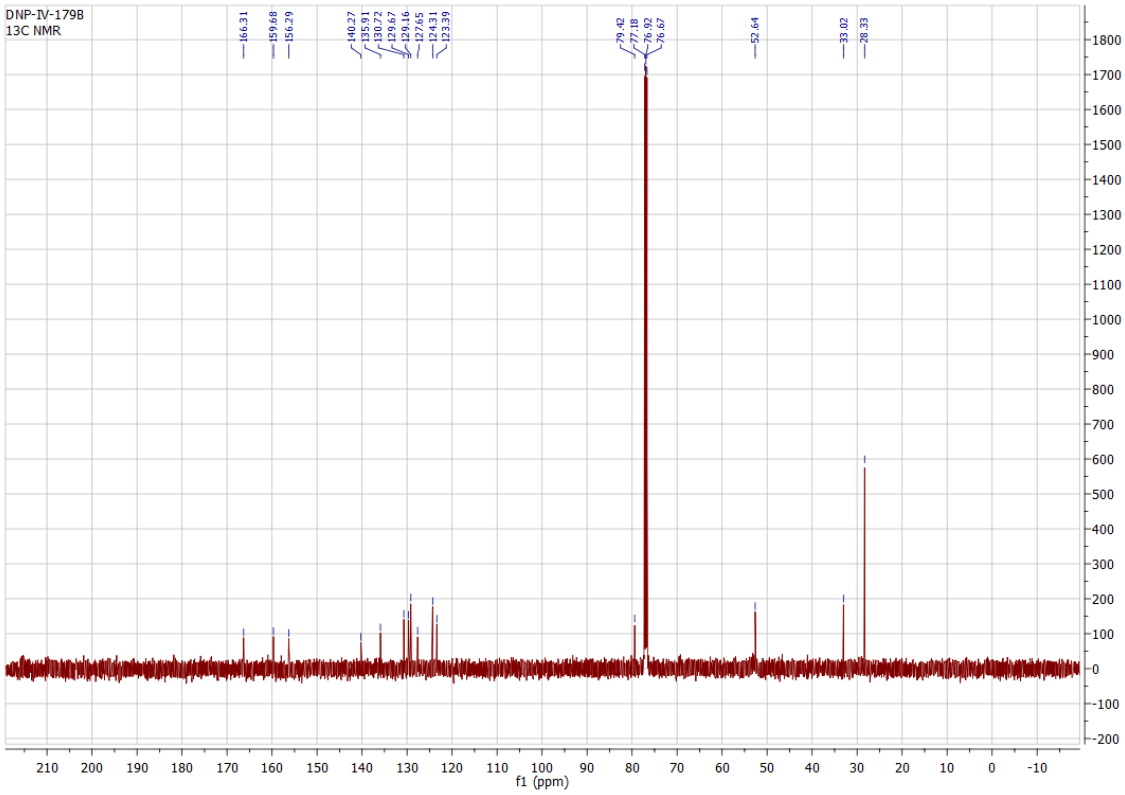

^{1}H ($CDCl_3$, 500 MHz) spectra of methyl 1-cyclopropylisoquinoline-3-carboxylate (**2.9.10**)

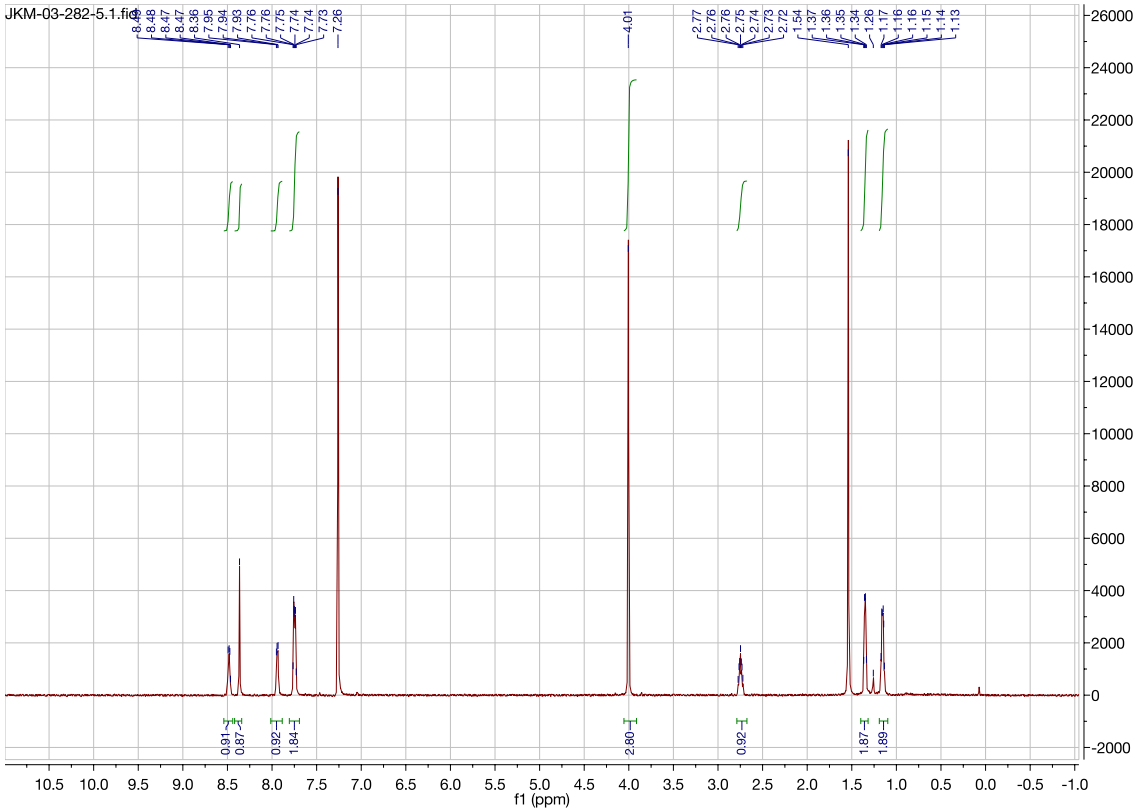

^{13}C NMR ($CDCl_3$, 125.8 MHz) spectrum of methyl 1-cyclopropylisoquinoline-3-carboxylate (**2.9.10**)

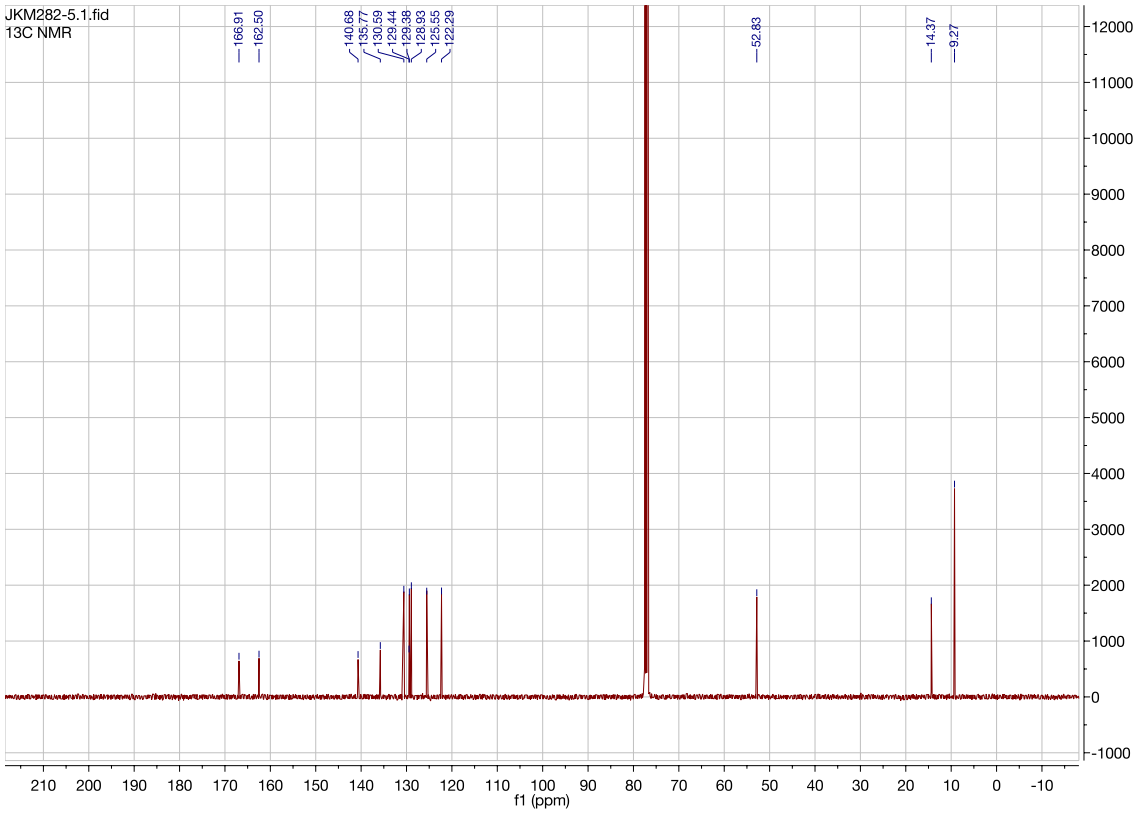

^{1}H ($CDCl_3$, 500 MHz) spectra of methyl 1-((3*r*,5*r*,7*r*)-adamantan-1-yl)isoquinoline-3-carboxylate (**2.9.11**)

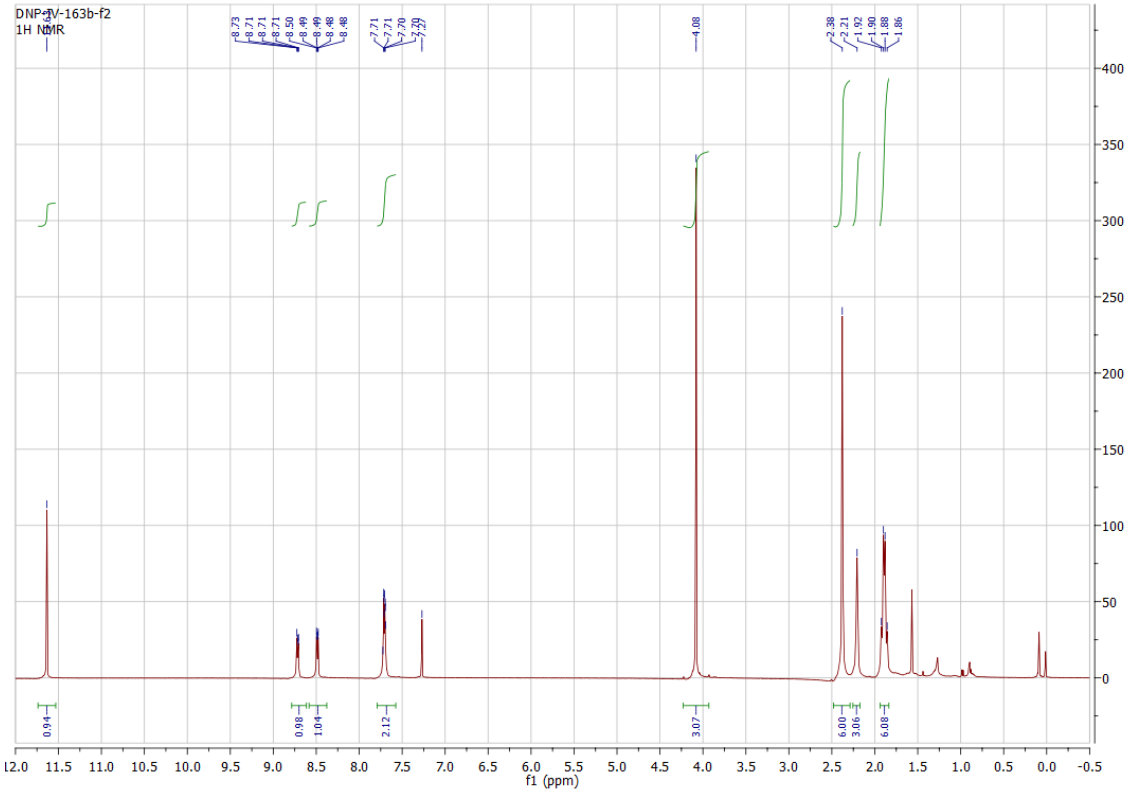

^{13}C NMR ($CDCl_3$, 125.8 MHz) spectrum of methyl 1-((3*r*,5*r*,7*r*)-adamantan-1-yl)isoquinoline-3-carboxylate (**2.9.11**)

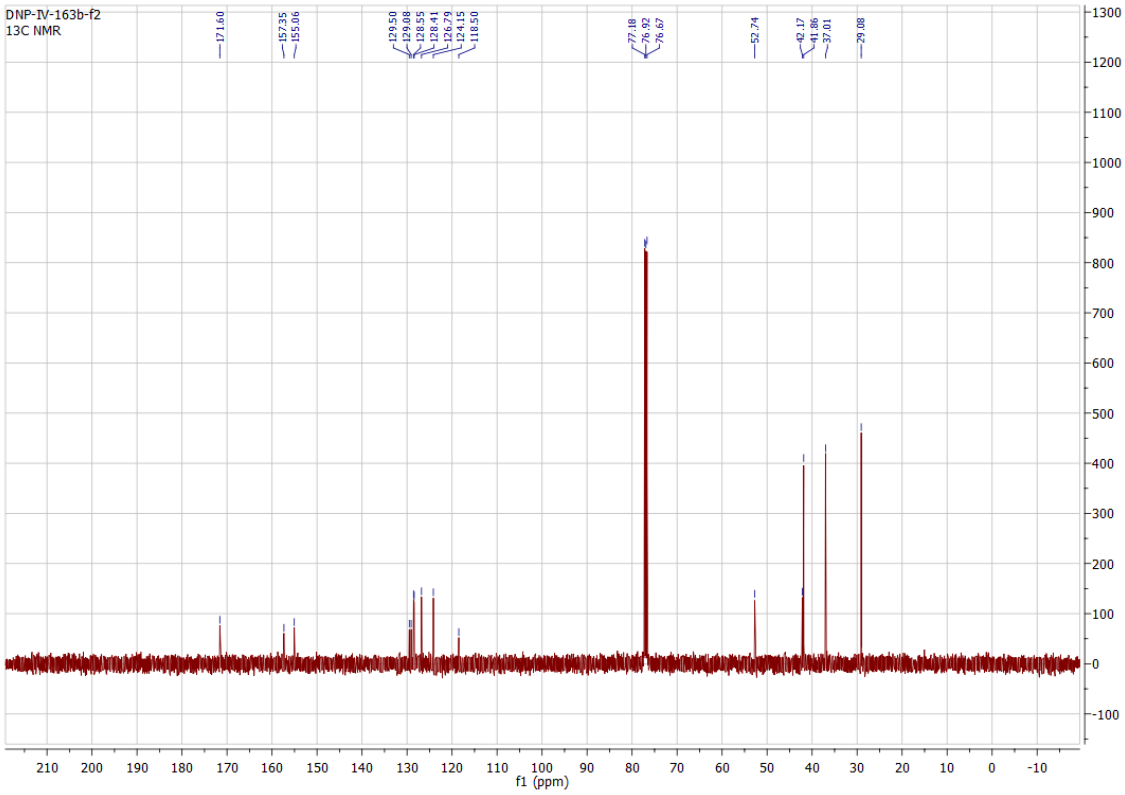

^{1}H ($CDCl_3$, 500 MHz) spectra of methyl 1-(1-(pyridin-2-yl)piperidin-4-yl)isoquinoline-3-carboxylate (**2.9.12**)

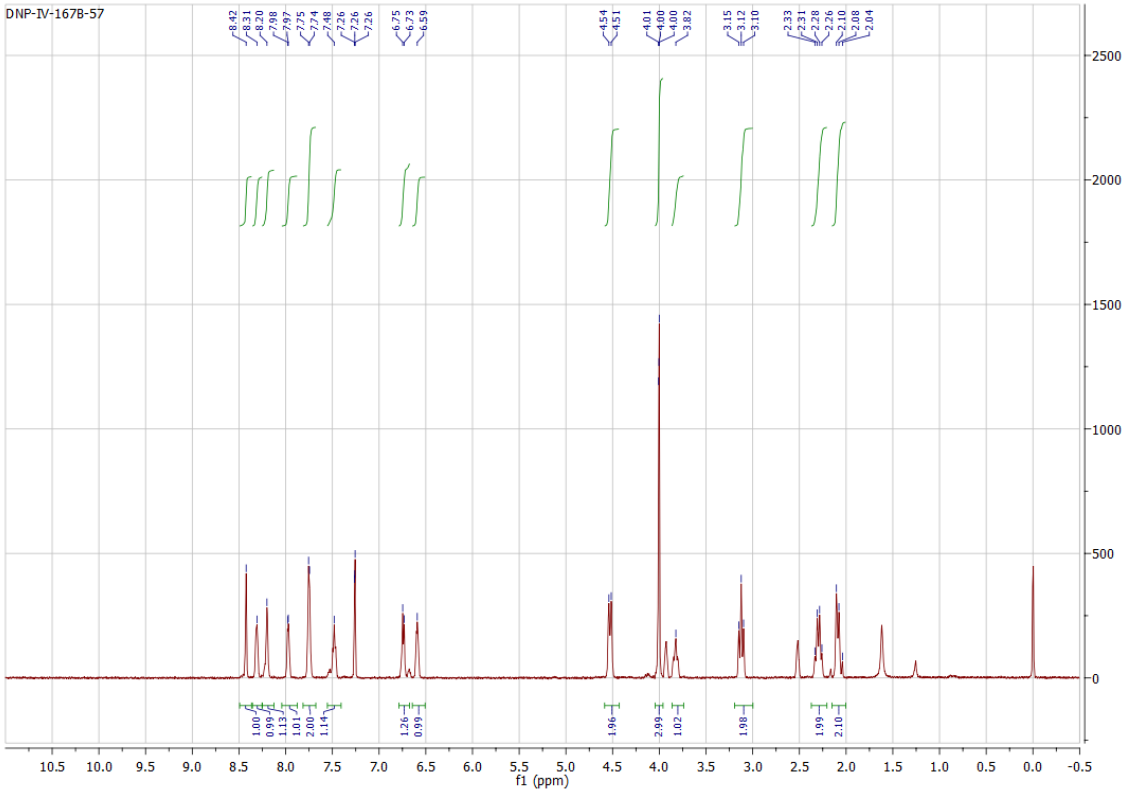

^{13}C NMR ($CDCl_3$, 125.8 MHz) spectrum of methyl 1-(1-(pyridin-2-yl)piperidin-4-yl)isoquinoline-3-carboxylate (**2.9.12**)

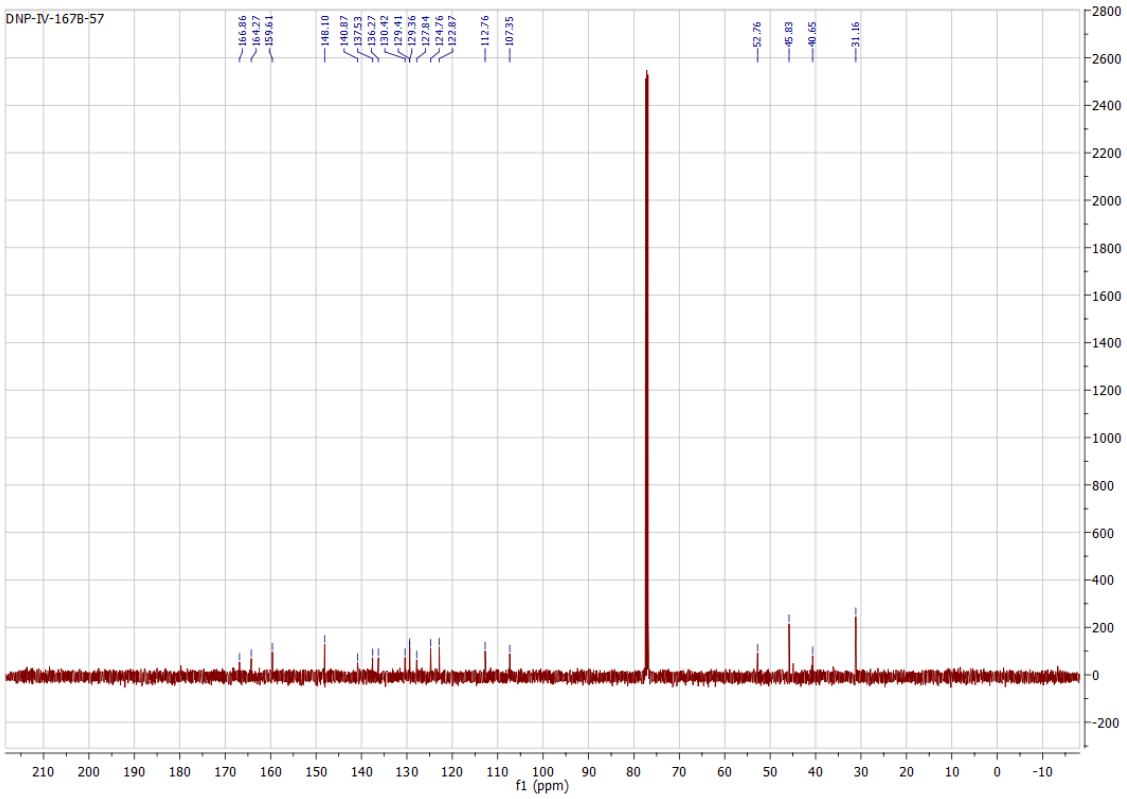

^{1}H ($CDCl_3$, 500 MHz) spectra of methyl 1-((cyclopentyloxy)methyl)isoquinoline-3-carboxylate (**2.10.1**)

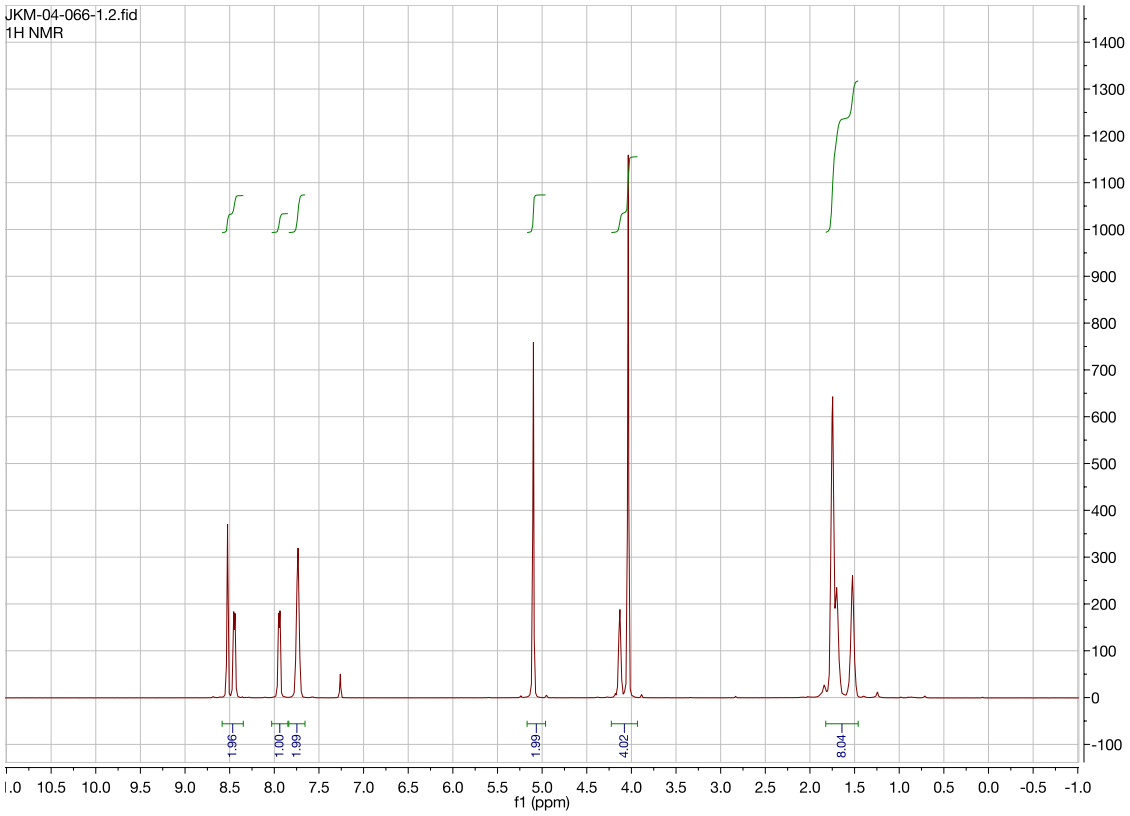

^{13}C NMR ($CDCl_3$, 125.8 MHz) spectrum of methyl 1-((cyclopentyloxy)methyl)isoquinoline-3-carboxylate (**2.10.1**)

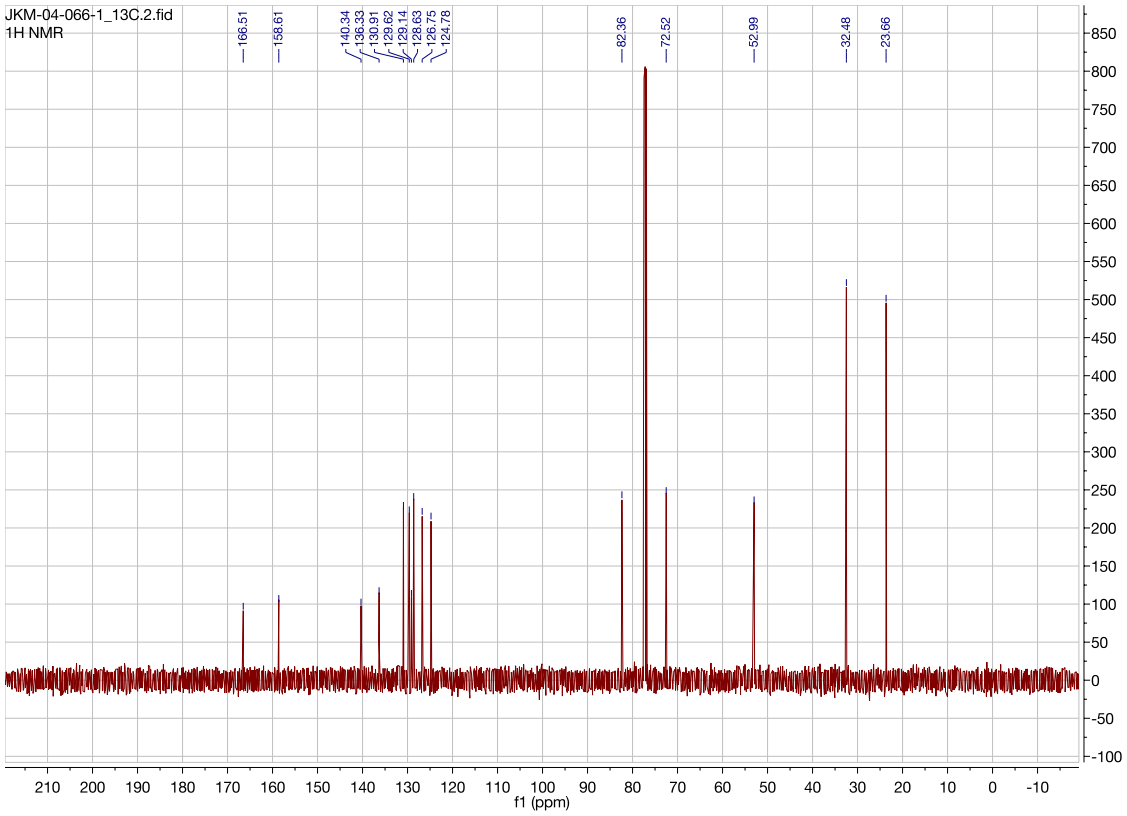

^{1}H ($CDCl_3$, 500 MHz) spectra of methyl 1-((2-(trimethylsilyl)ethoxy)methyl)isoquinoline-3-carboxylate (**2.10.2**)

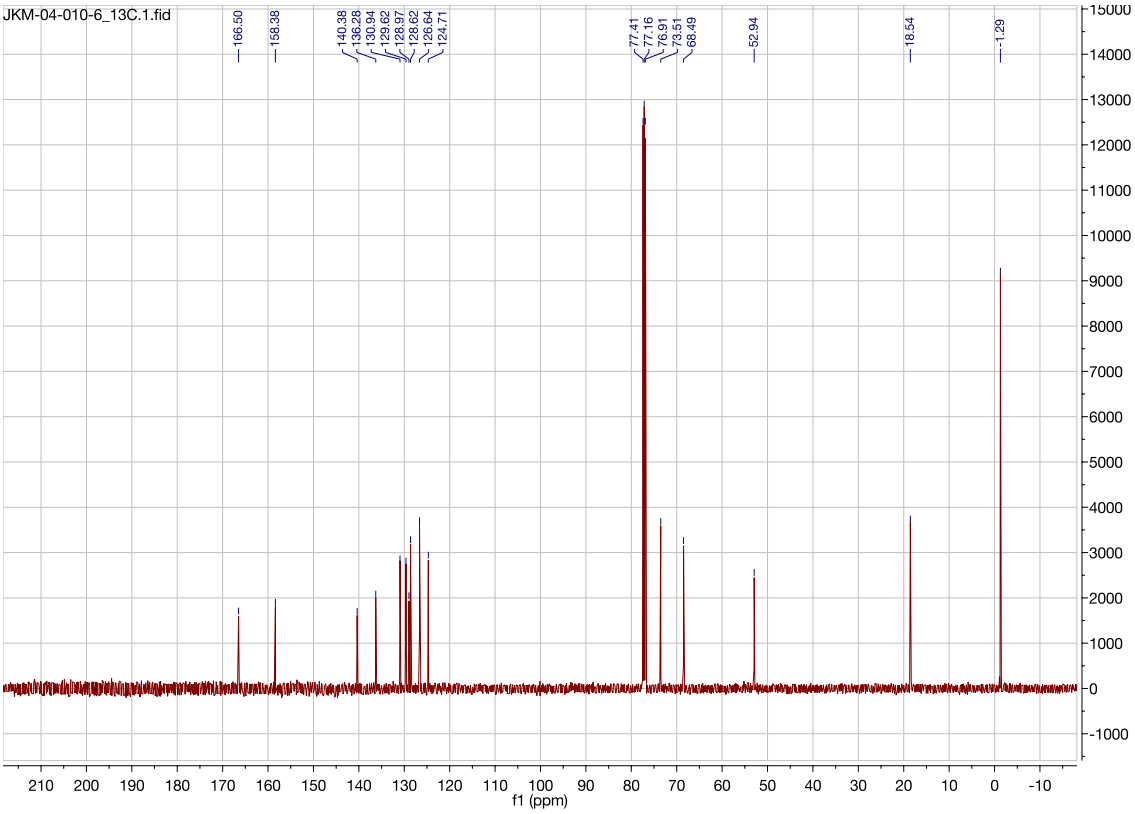

^{13}C NMR ($CDCl_3$, 125.8 MHz) spectrum of methyl 1-((2-(trimethylsilyl)ethoxy)methyl)isoquinoline-3-carboxylate (**2.10.2**)

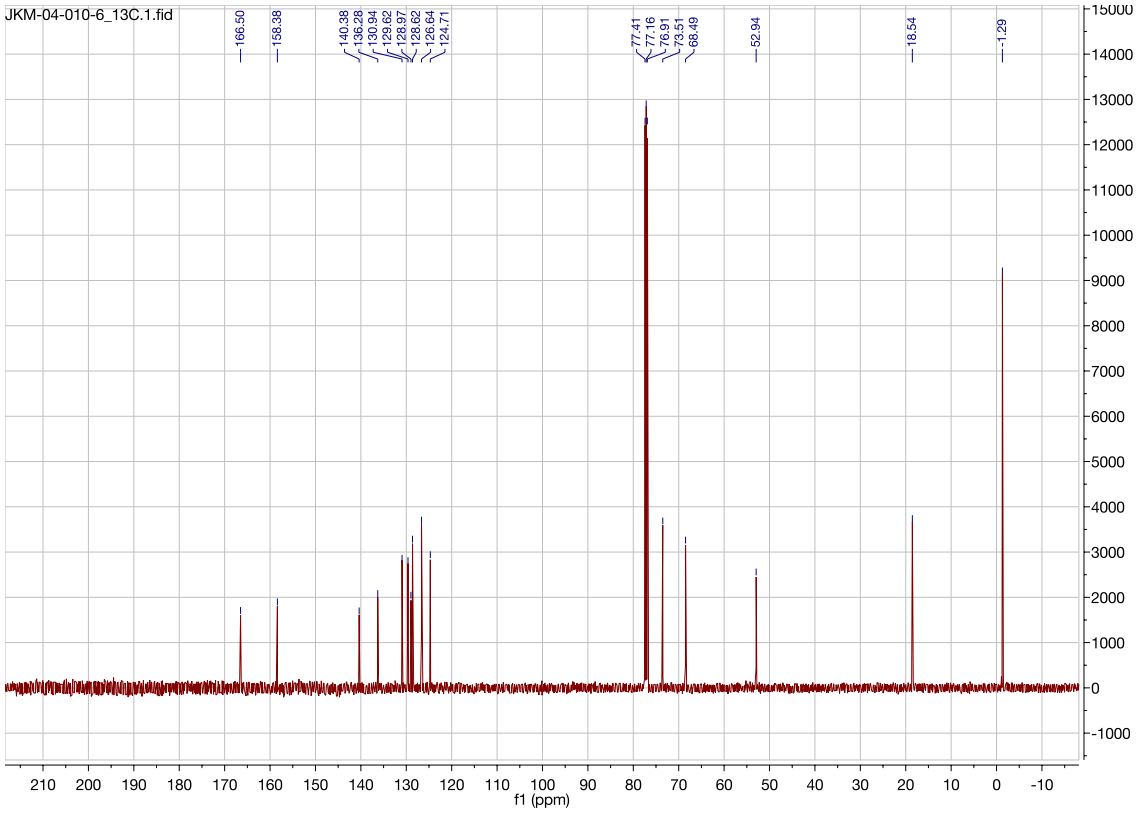

^{1}H ($CDCl_3$, 500 MHz) spectra of methyl 1-(((3-methylbut-3-en-1-yl)oxy)methyl)isoquinoline-3-carboxylate (**2.10.3**)

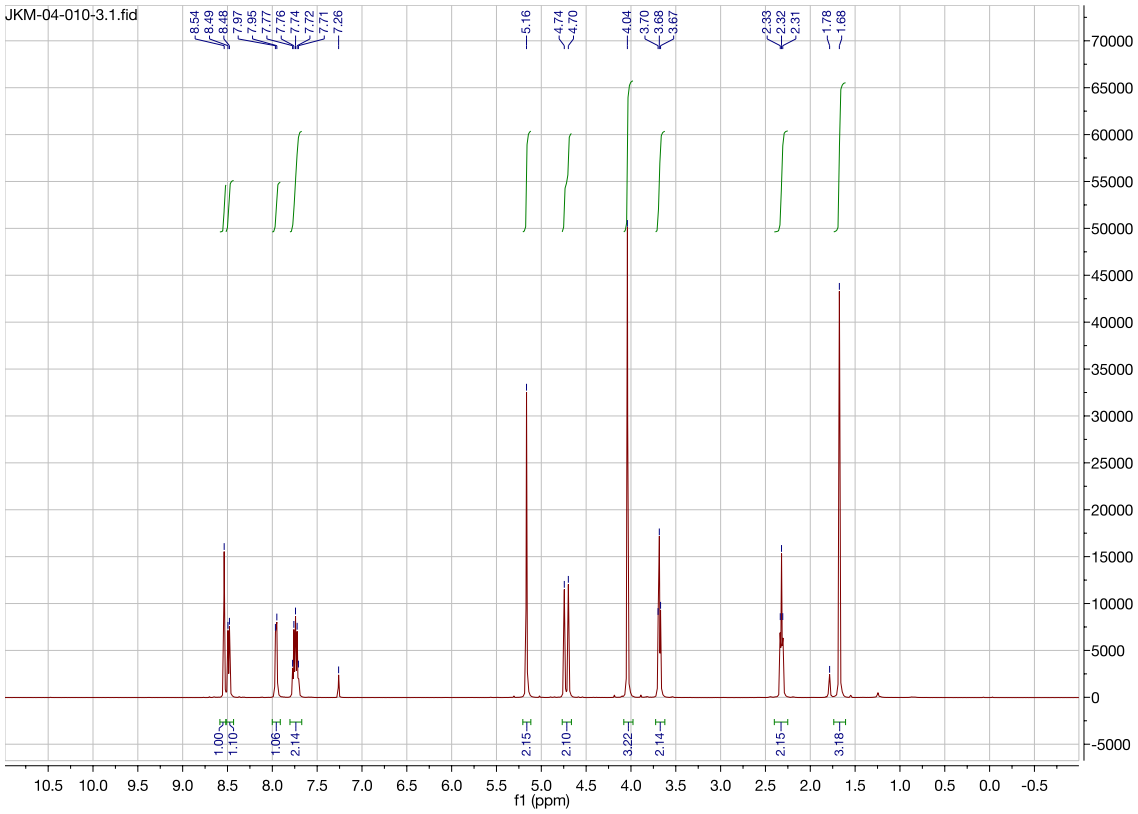

^{13}C NMR ($CDCl_3$, 125.8 MHz) spectrum of methyl 1-(((3-methylbut-3-en-1-yl)oxy)methyl)isoquinoline-3-carboxylate (**2.10.3**)

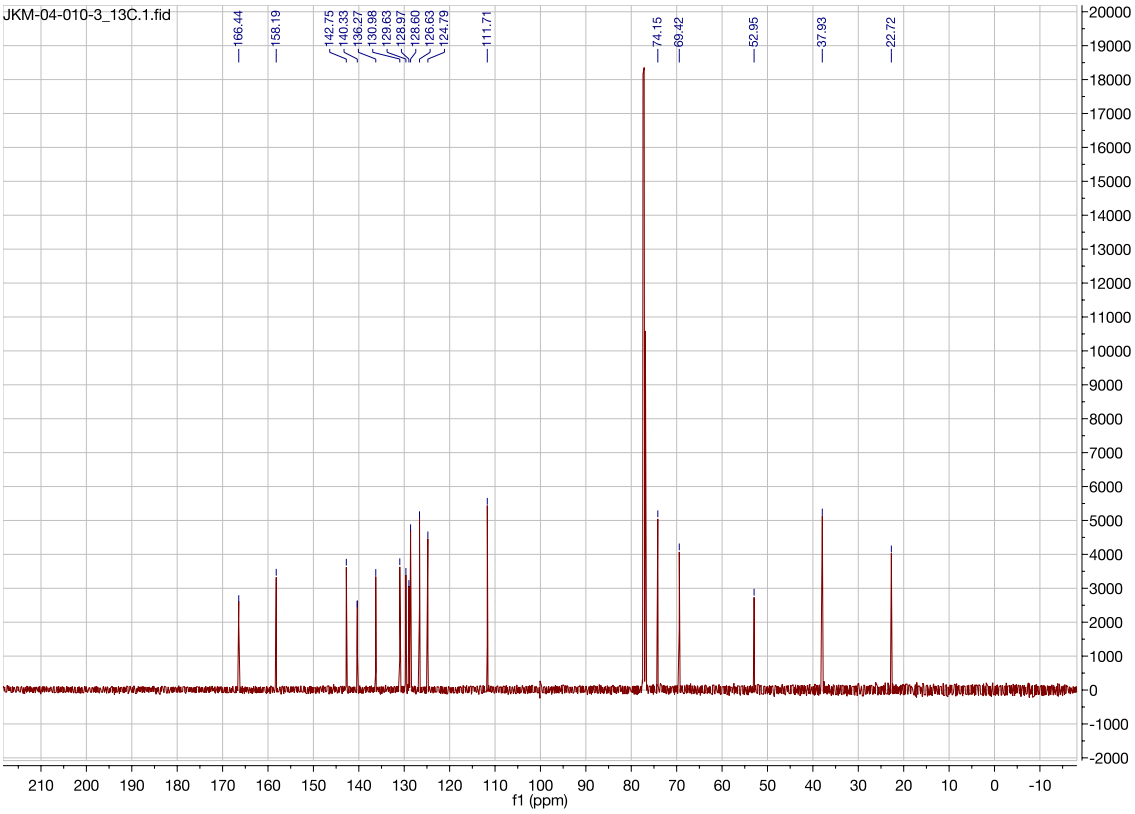

^{1}H ($CDCl_3$, 500 MHz) spectra of methyl 1-((((1*R*,2*S*,5*R*)-2-isopropyl-5-methylcyclohexyl)oxy)methyl)isoquinoline-3-carboxylate (**2.10.4**)

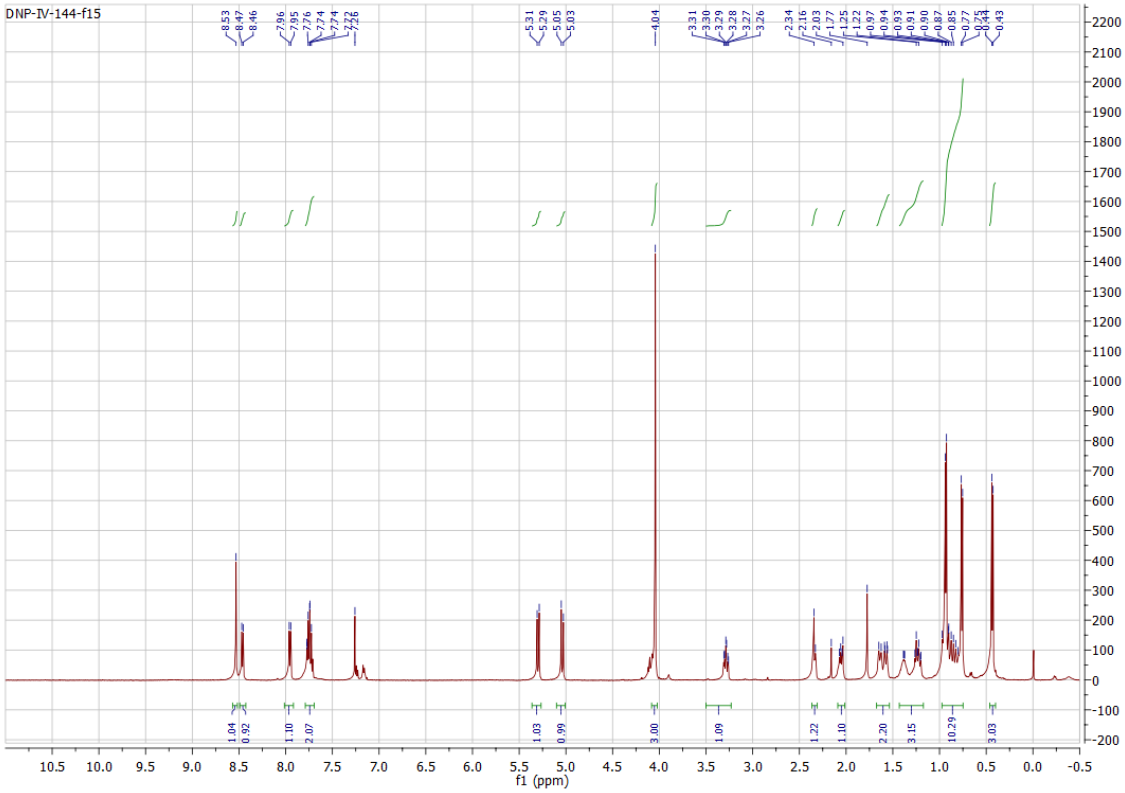

^{13}C NMR ($CDCl_3$, 125.8 MHz) spectrum of methyl 1-((((1*R*,2*S*,5*R*)-2-isopropyl-5-methylcyclohexyl)oxy)methyl)isoquinoline-3-carboxylate (**2.10.4**)

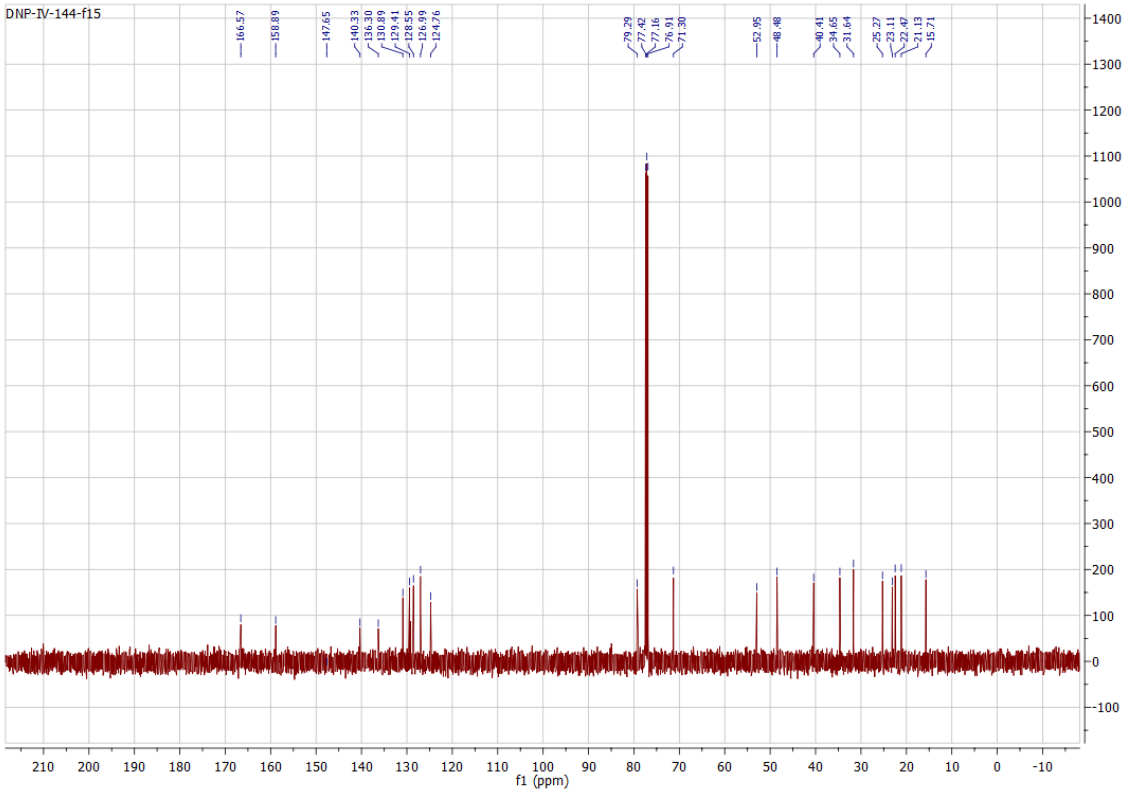

^{1}H ($CDCl_3$, 500 MHz) spectra of methyl 1-(3-(benzyloxy)propyl)isoquinoline-3-carboxylate (**2.10.5**)

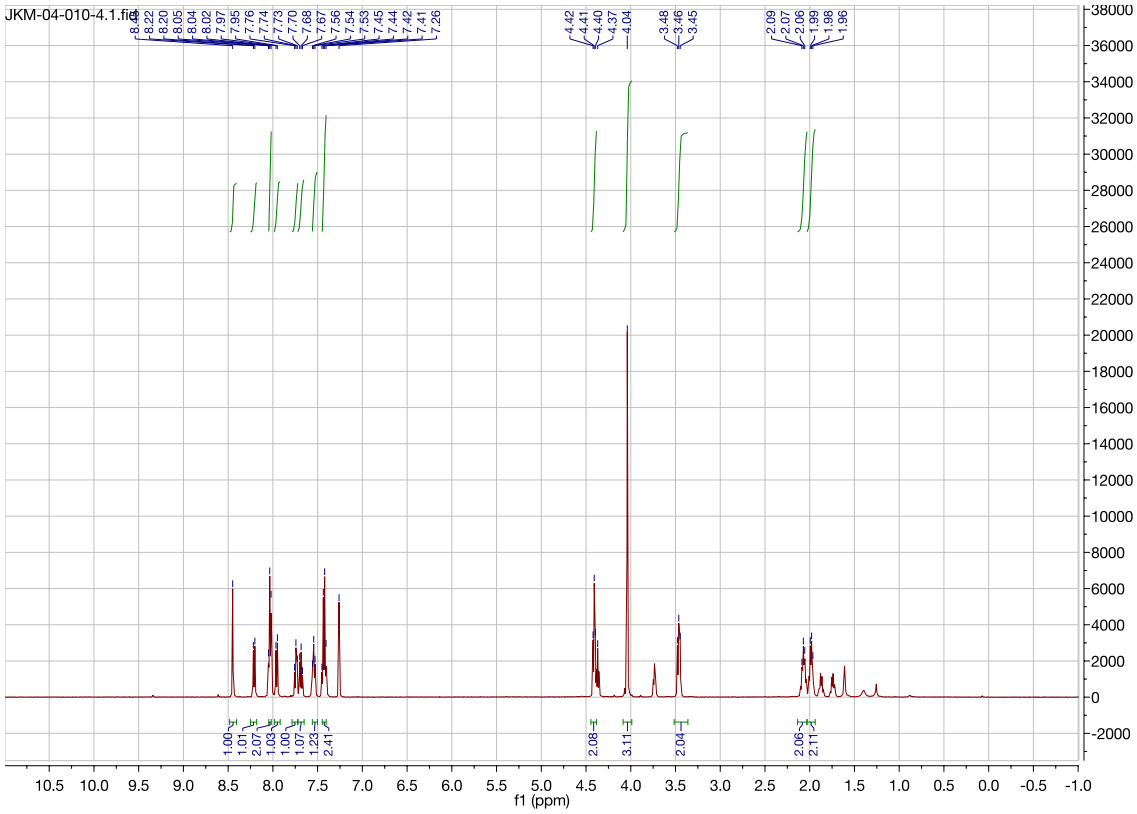

^{13}C NMR ($CDCl_3$, 125.8 MHz) spectrum of methyl 1-(3-(benzyloxy)propyl)isoquinoline-3-carboxylate (**2.10.5**)

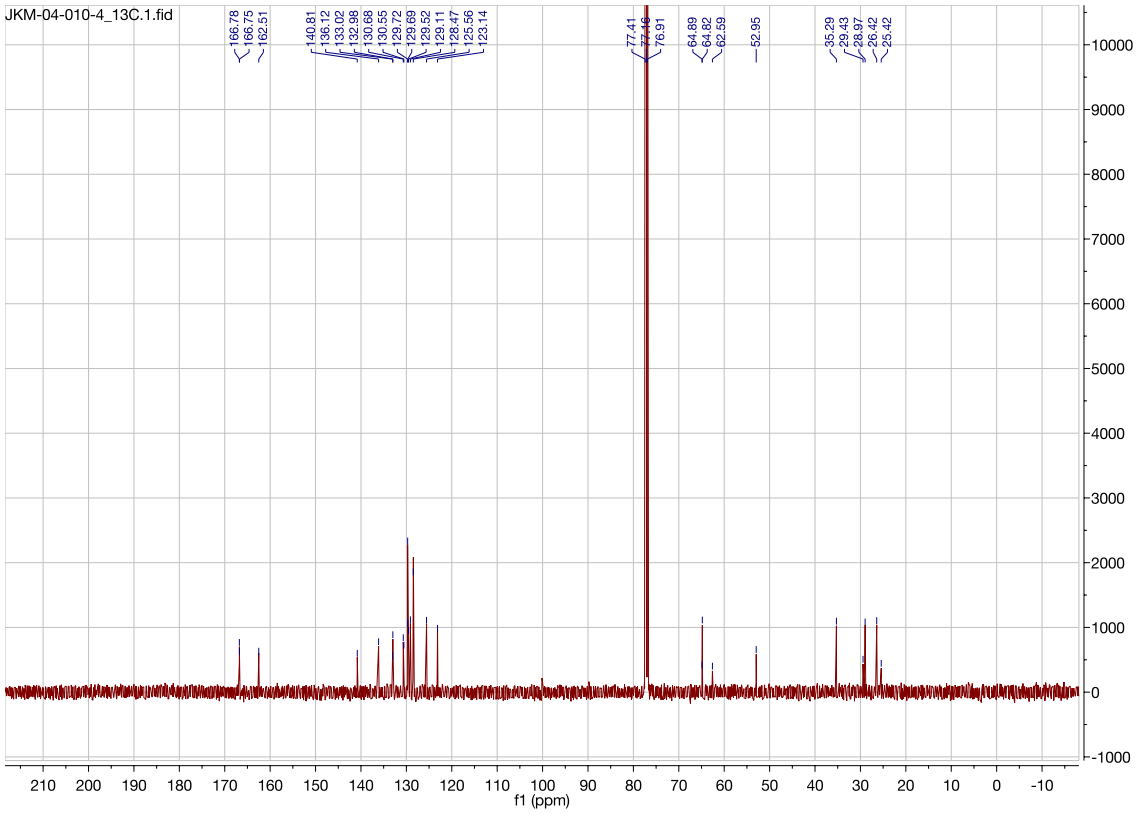

^{1}H ($CDCl_3$, 500 MHz) spectra of methyl 1-isobutylisoquinoline-3-carboxylate (**2.10.6**)

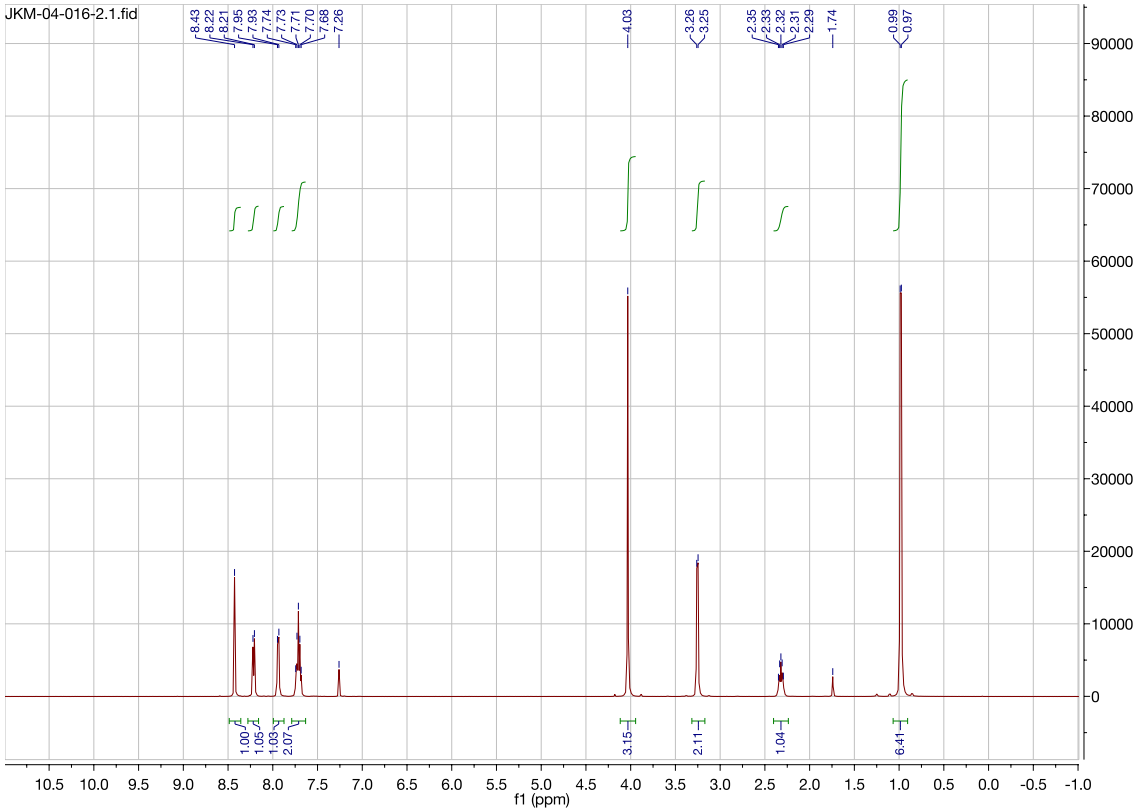

^{13}C NMR ($CDCl_3$, 125.8 MHz) spectrum of methyl 1-isobutylisoquinoline-3-carboxylate (**2.10.6**)

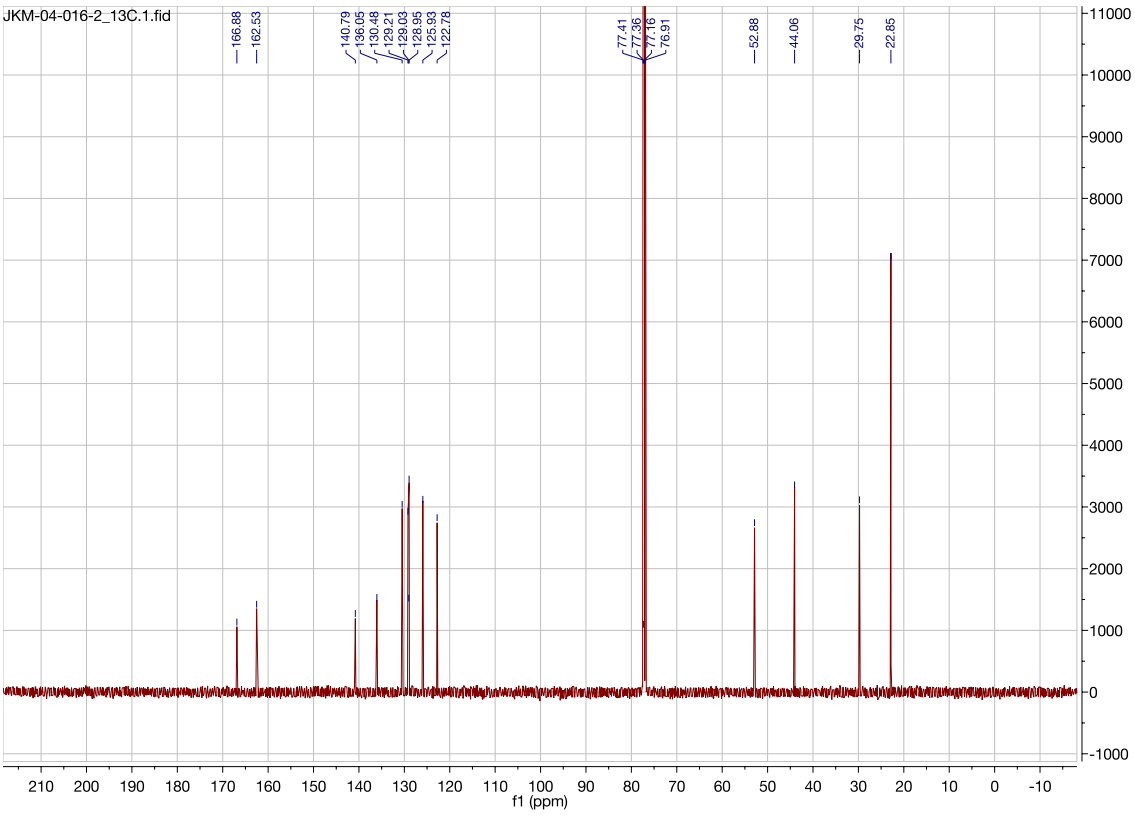

^{1}H ($CDCl_3$, 500 MHz) spectra of methyl 1-benzylisoquinoline-3-carboxylate (**2.10.7**)

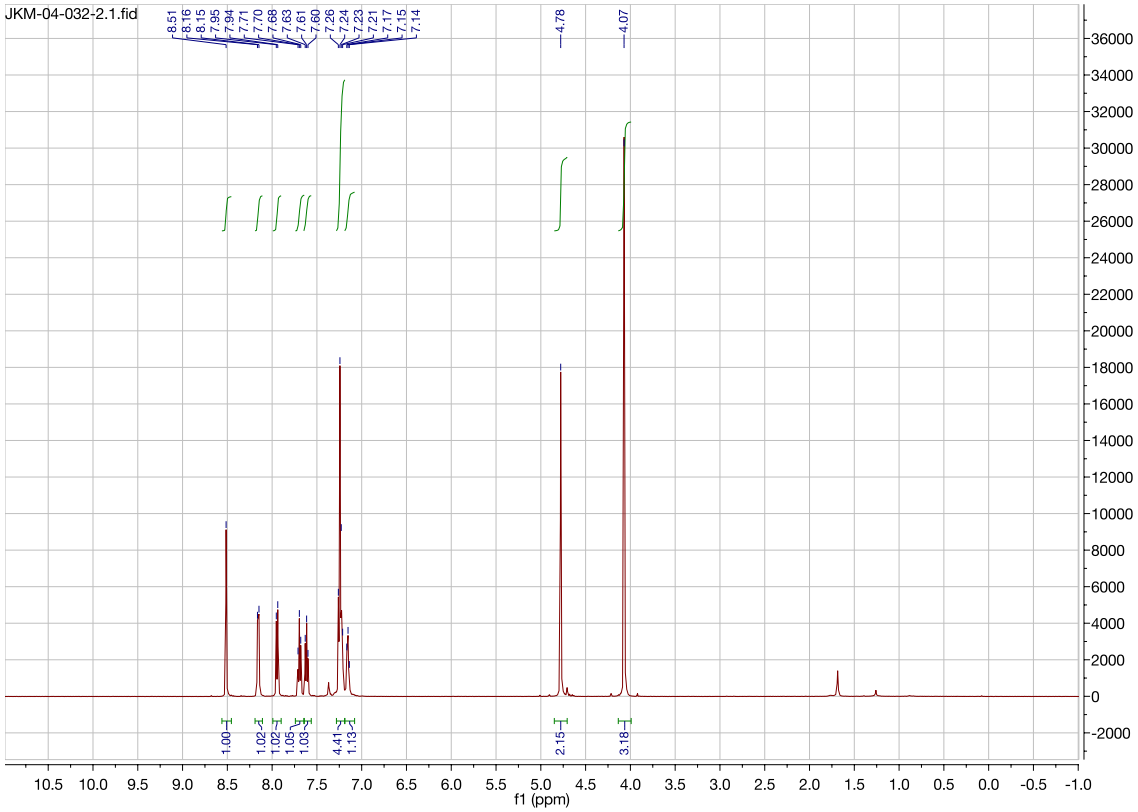

^{13}C NMR ($CDCl_3$, 125.8 MHz) spectrum of methyl 1-benzylisoquinoline-3-carboxylate (**2.10.7**)

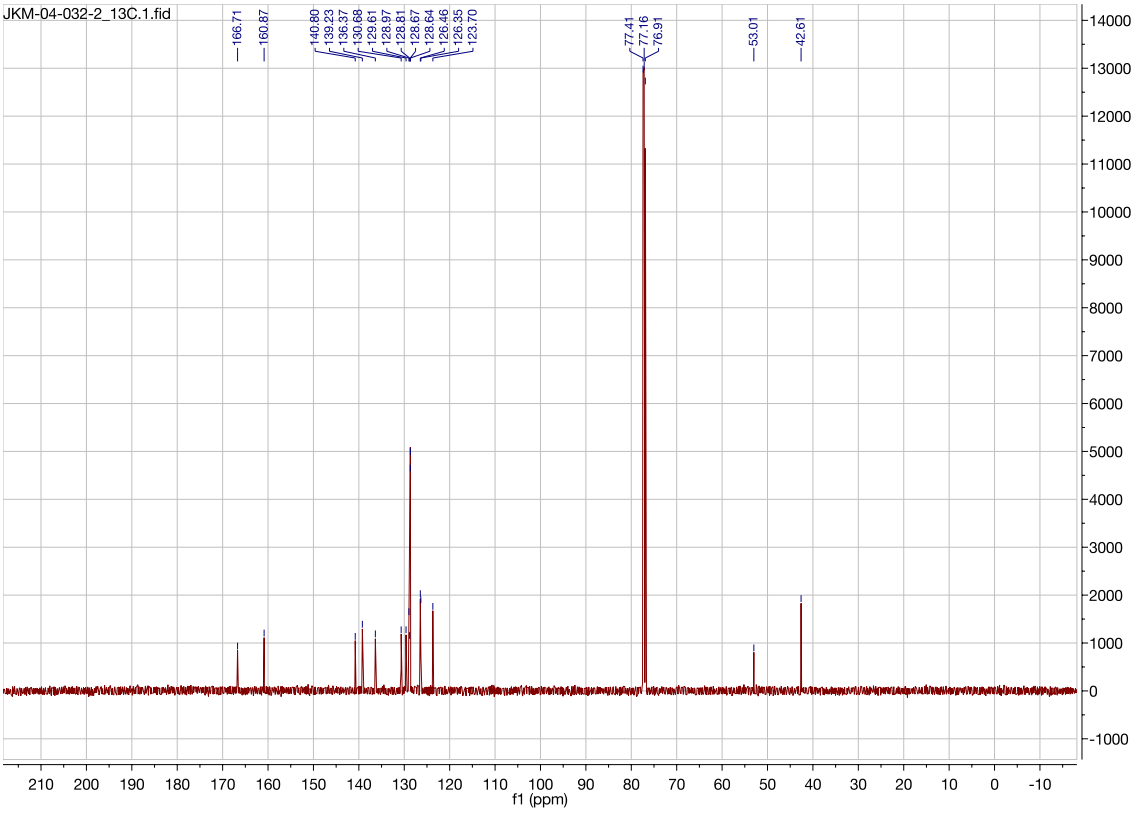

^{1}H ($CDCl_3$, 500 MHz) spectra of methyl 1-phenethylisoquinoline-3-carboxylate (**2.10.8**)

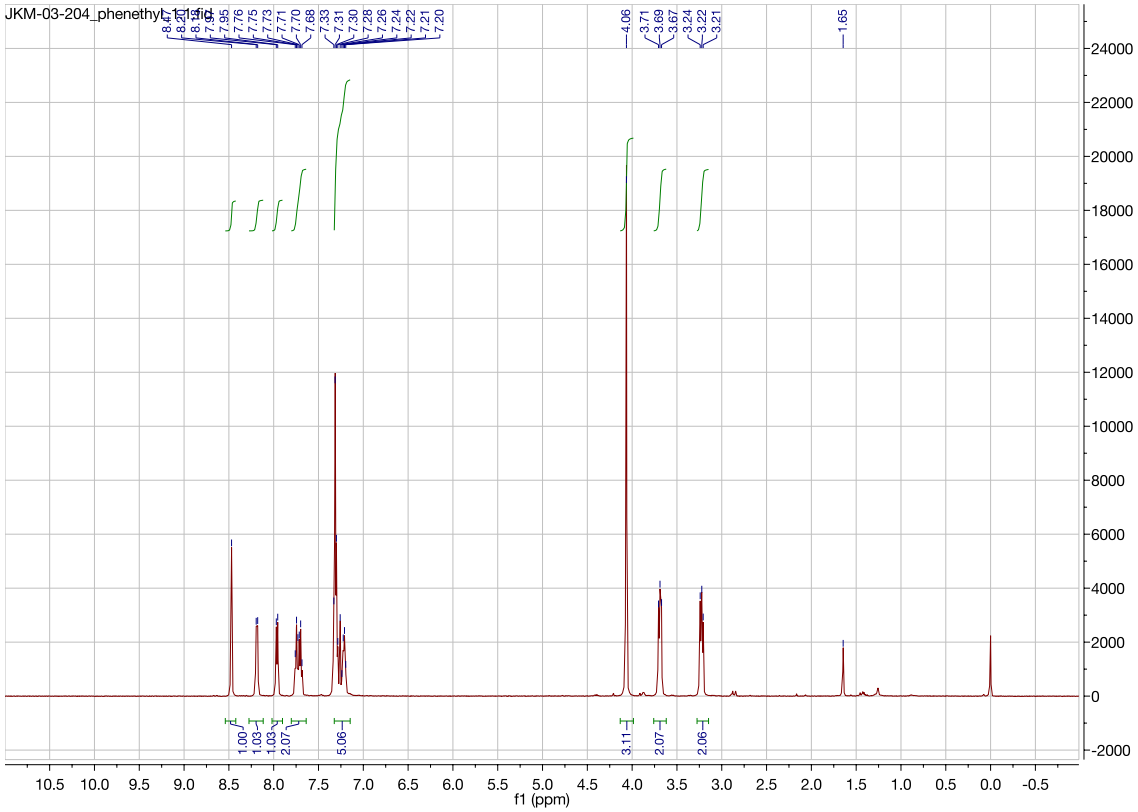

^{13}C NMR ($CDCl_3$, 125.8 MHz) spectrum of methyl 1-phenethylisoquinoline-3-carboxylate (**2.10.8**)

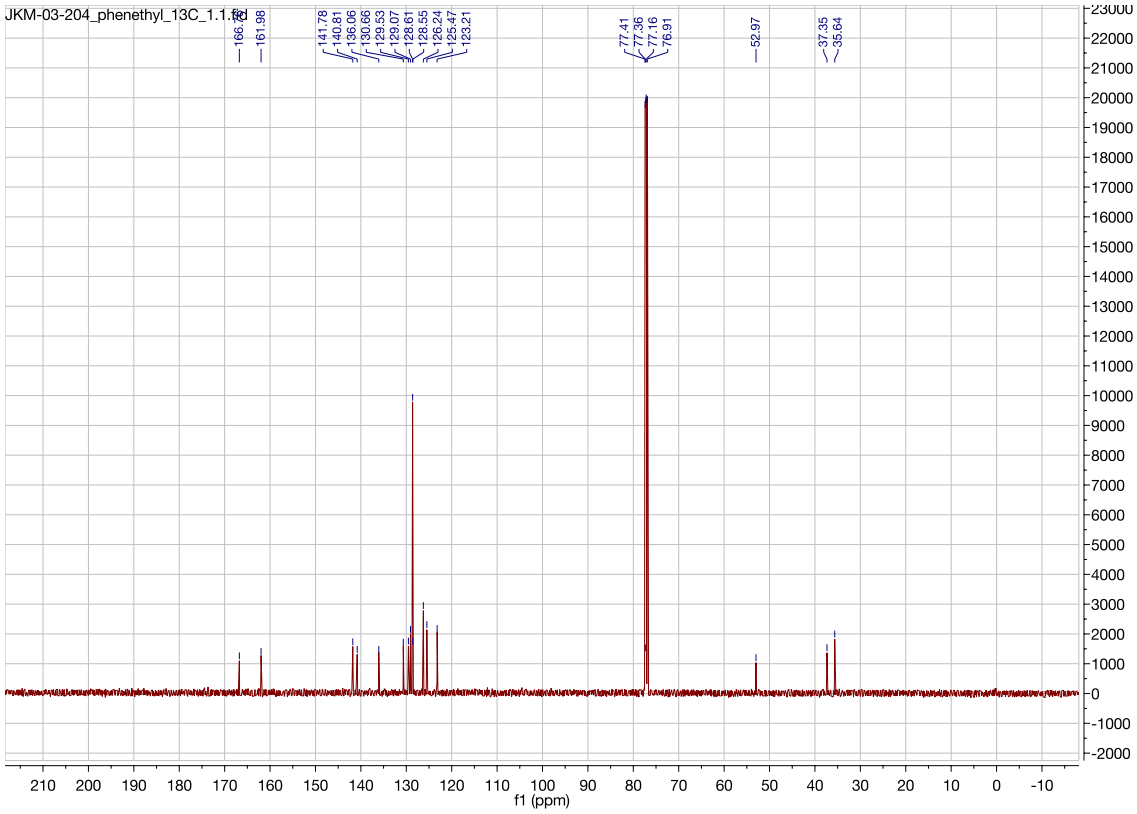

^{1}H ($CDCl_3$, 500 MHz) spectra of methyl 1-(3-phenylpropyl)isoquinoline-3-carboxylate (**2.10.9**)

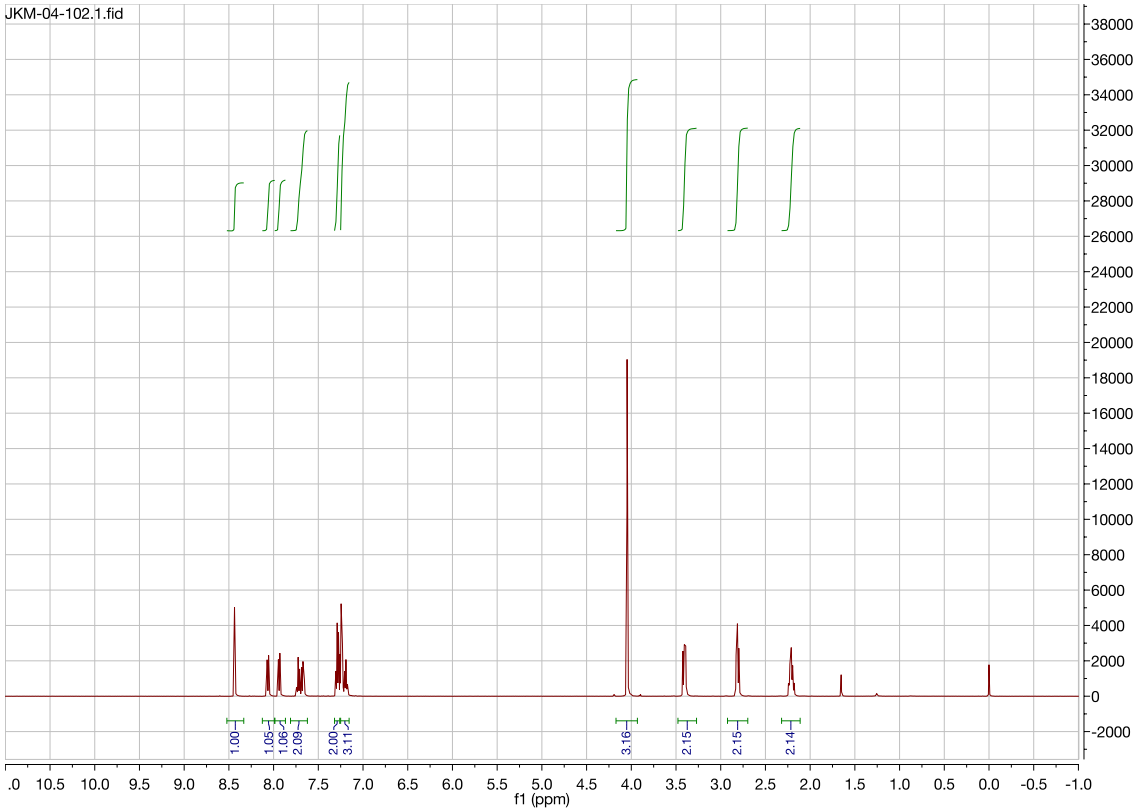

^{13}C NMR ($CDCl_3$, 125.8 MHz) spectrum of methyl 1-(3-phenylpropyl)isoquinoline-3-carboxylate (**2.10.9**)

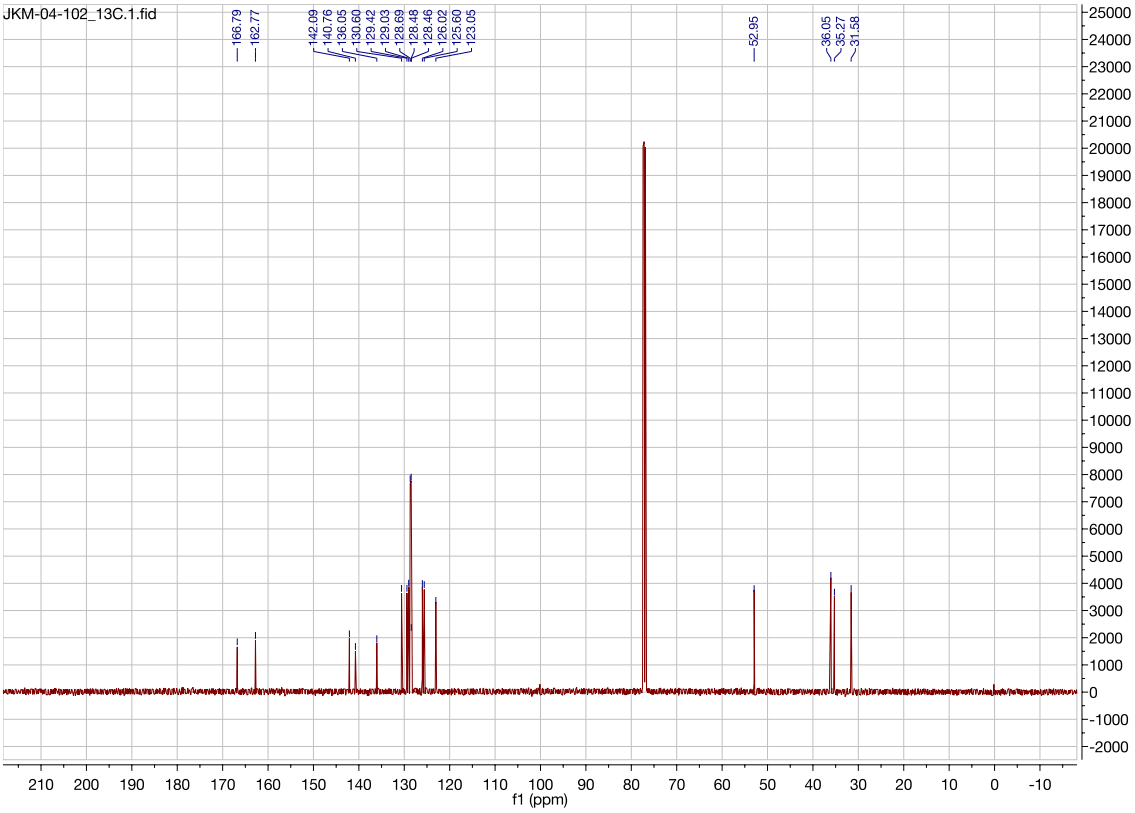

^{1}H ($CDCl_3$, 500 MHz) spectra of methyl 1-(4-(2-bromophenyl)butyl)isoquinoline-3-carboxylate (**2.10.10**)

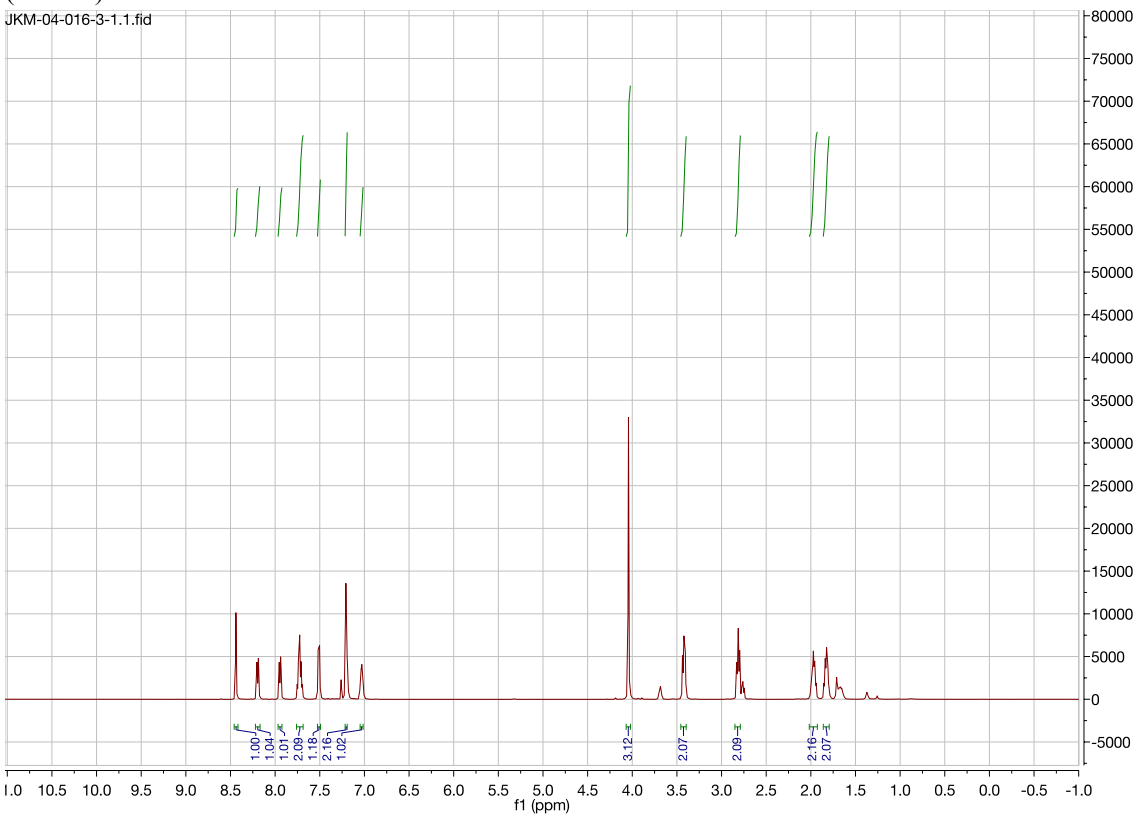

^{13}C NMR ($CDCl_3$, 125.8 MHz) spectrum of methyl 1-(4-(2-bromophenyl)butyl)isoquinoline-3-carboxylate (**2.10.10**)

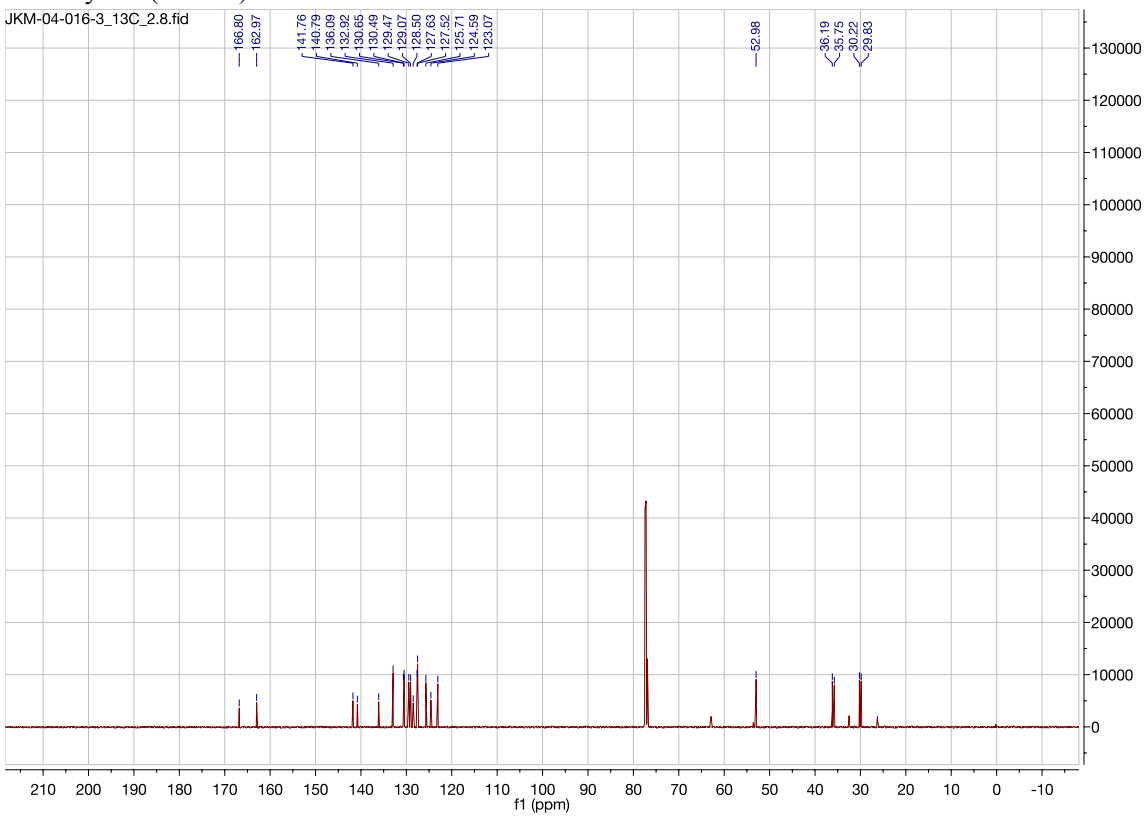

^{1}H ($CDCl_3$, 500 MHz) spectra of methyl 1-(3-(phenylthio)propyl)isoquinoline-3-carboxylate (**2.10.11**)

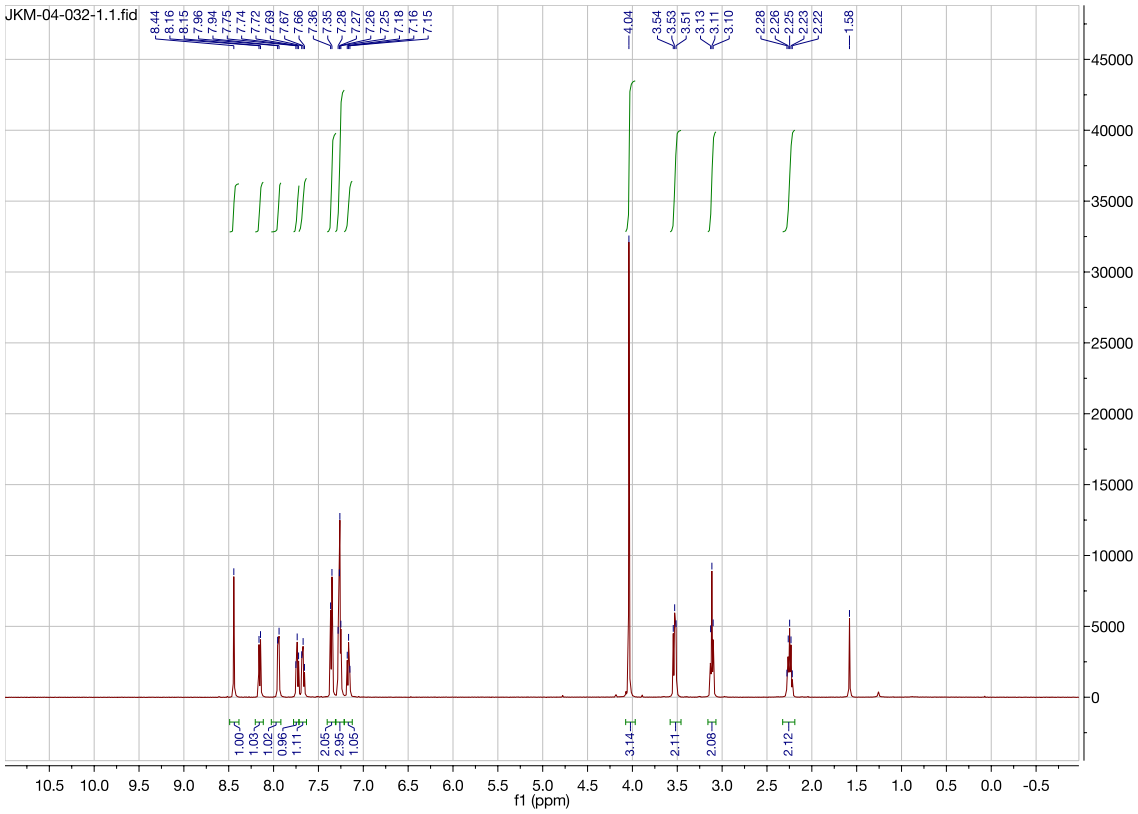

^{13}C NMR ($CDCl_3$, 125.8 MHz) spectrum of methyl 1-(3-(phenylthio)propyl)isoquinoline-3-carboxylate (**2.10.11**)

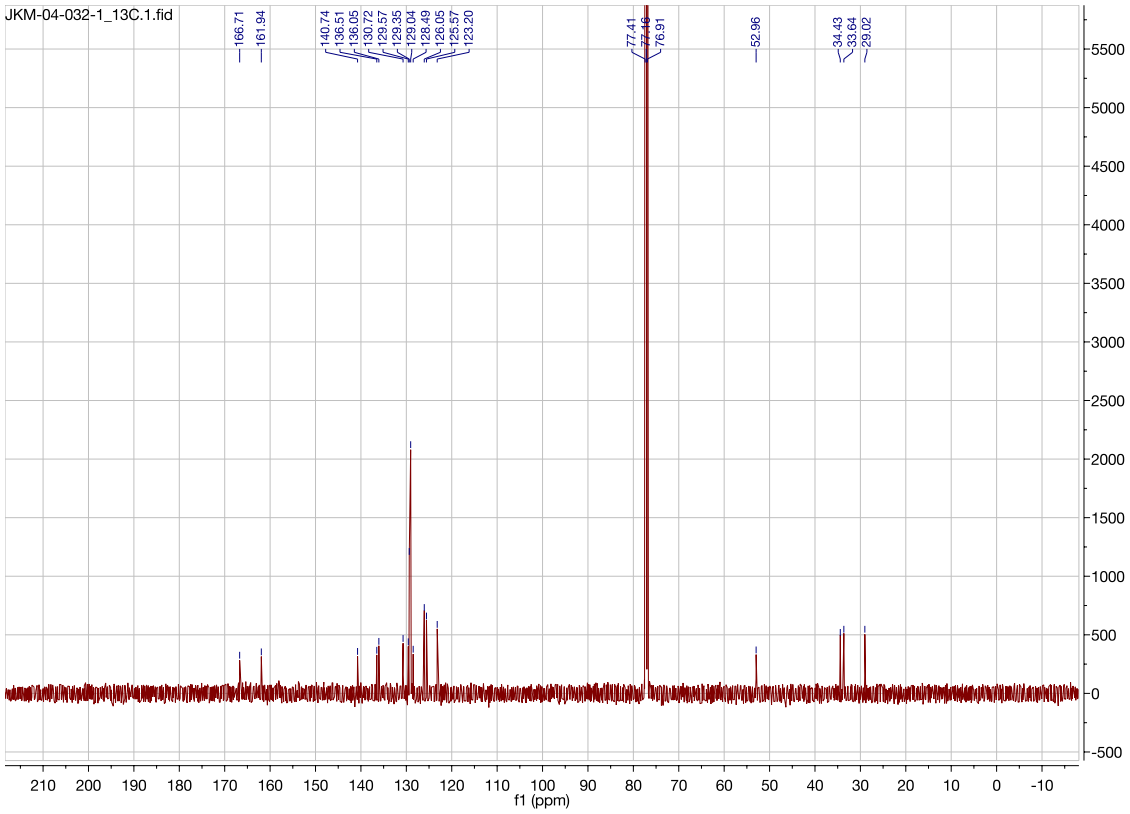

^{1}H ($CDCl_3$, 500 MHz) spectra of methyl 1-(3,3,3-trifluoropropyl)isoquinoline-3-carboxylate (**2.10.12**)

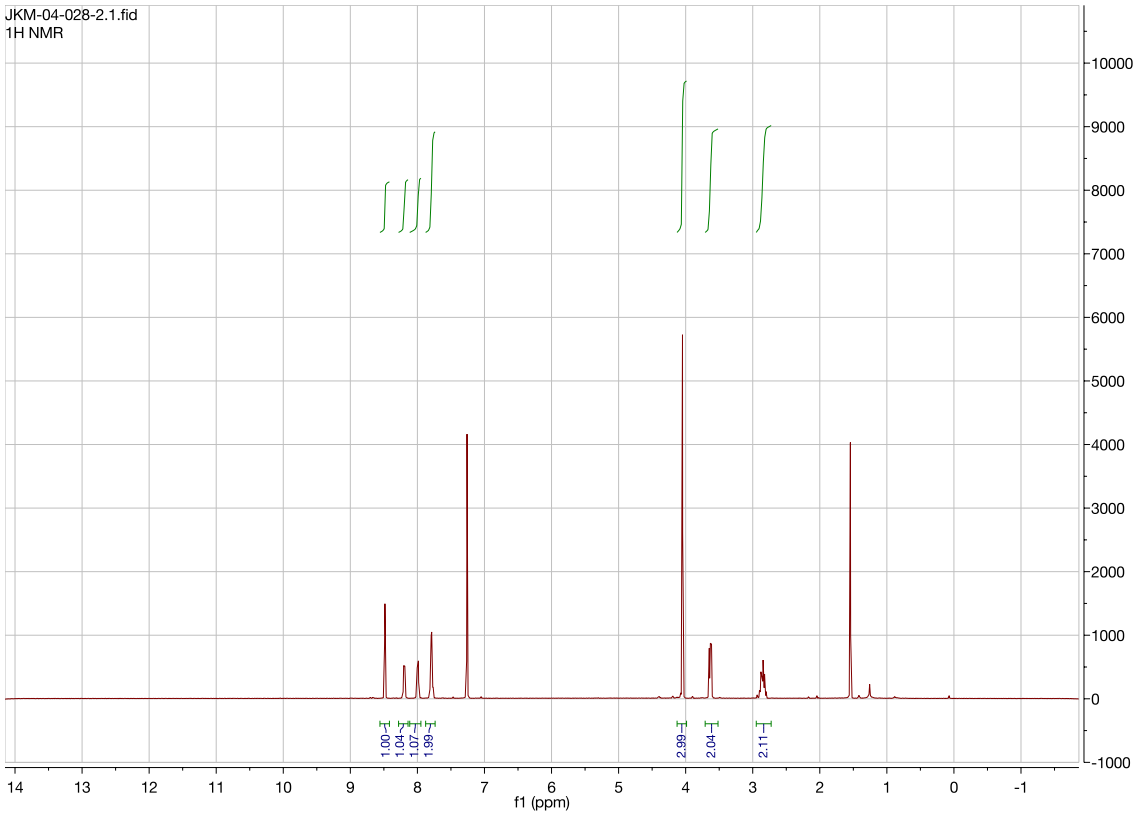

^{13}C NMR ($CDCl_3$, 125.8 MHz) spectrum of methyl 1-(3,3,3-trifluoropropyl)isoquinoline-3-carboxylate (**2.10.12**)

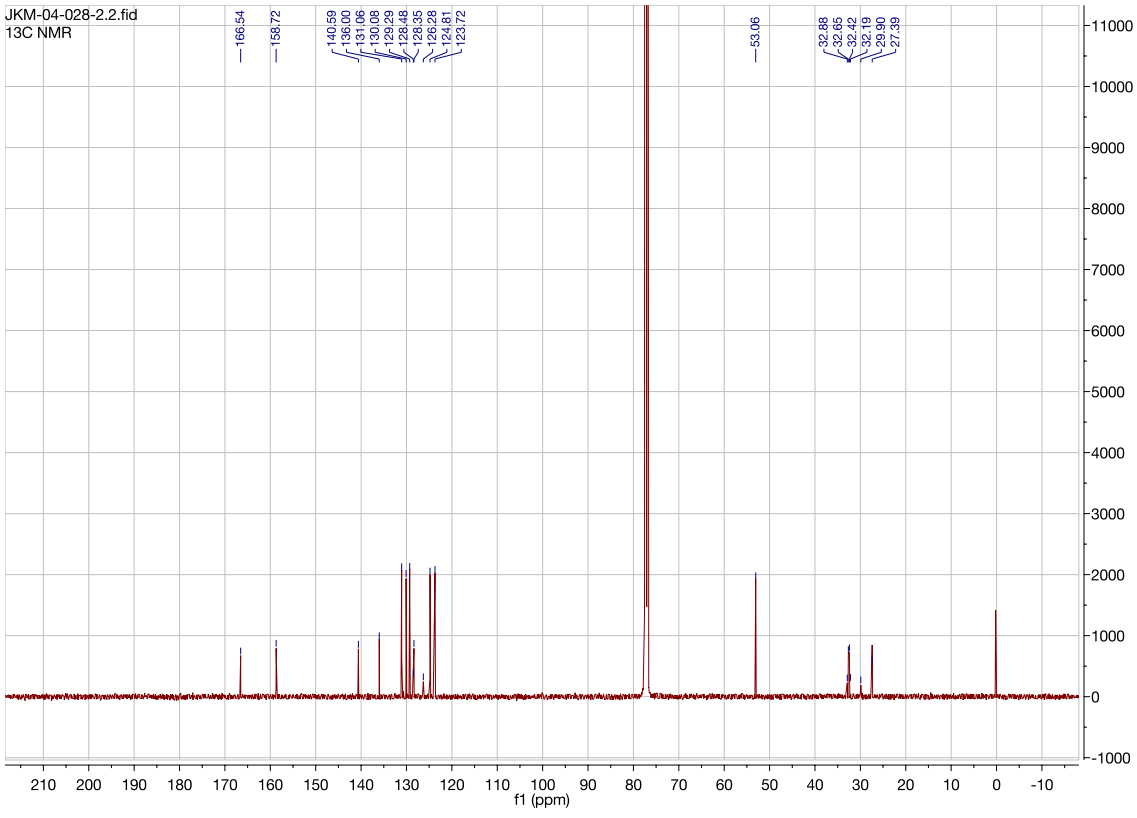

^{1}H ($CDCl_3$, 500 MHz) spectra of methyl 1-(but-3-en-1-yl)isoquinoline-3-carboxylate (**2.10.16**)

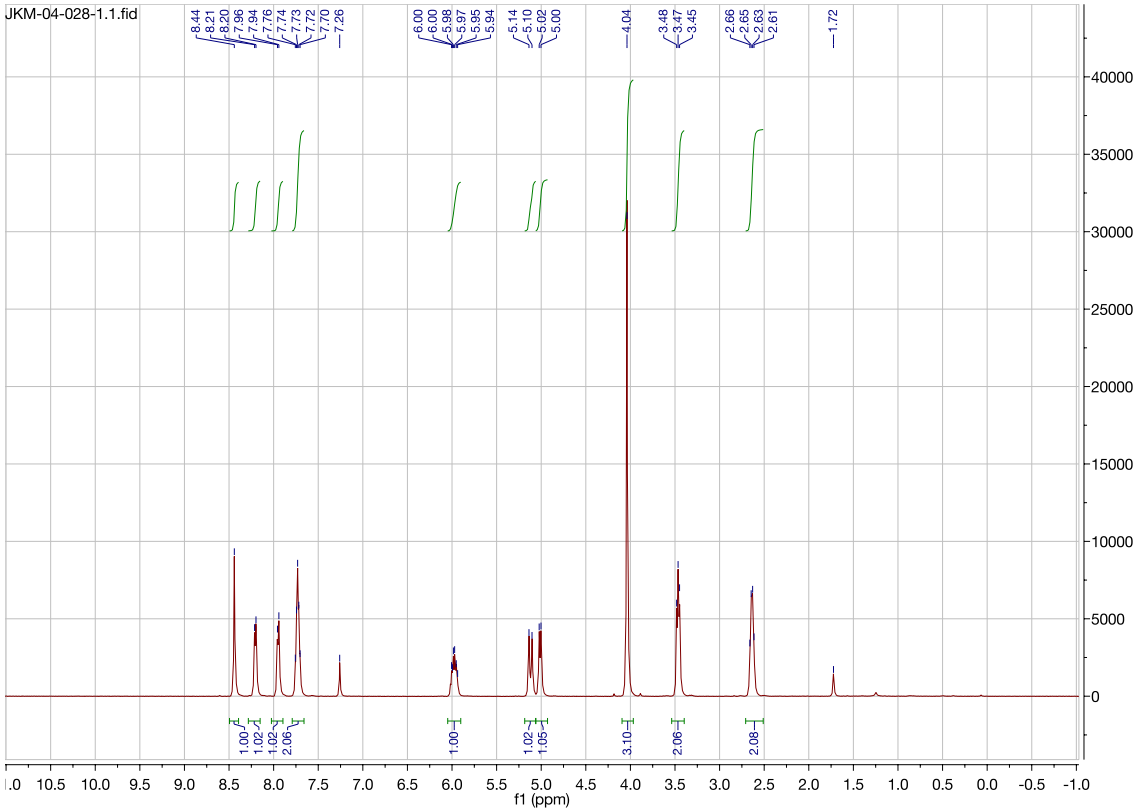

^{13}C NMR ($CDCl_3$, 125.8 MHz) spectrum of methyl 1-(but-3-en-1-yl)isoquinoline-3-carboxylate (**2.10.16**)

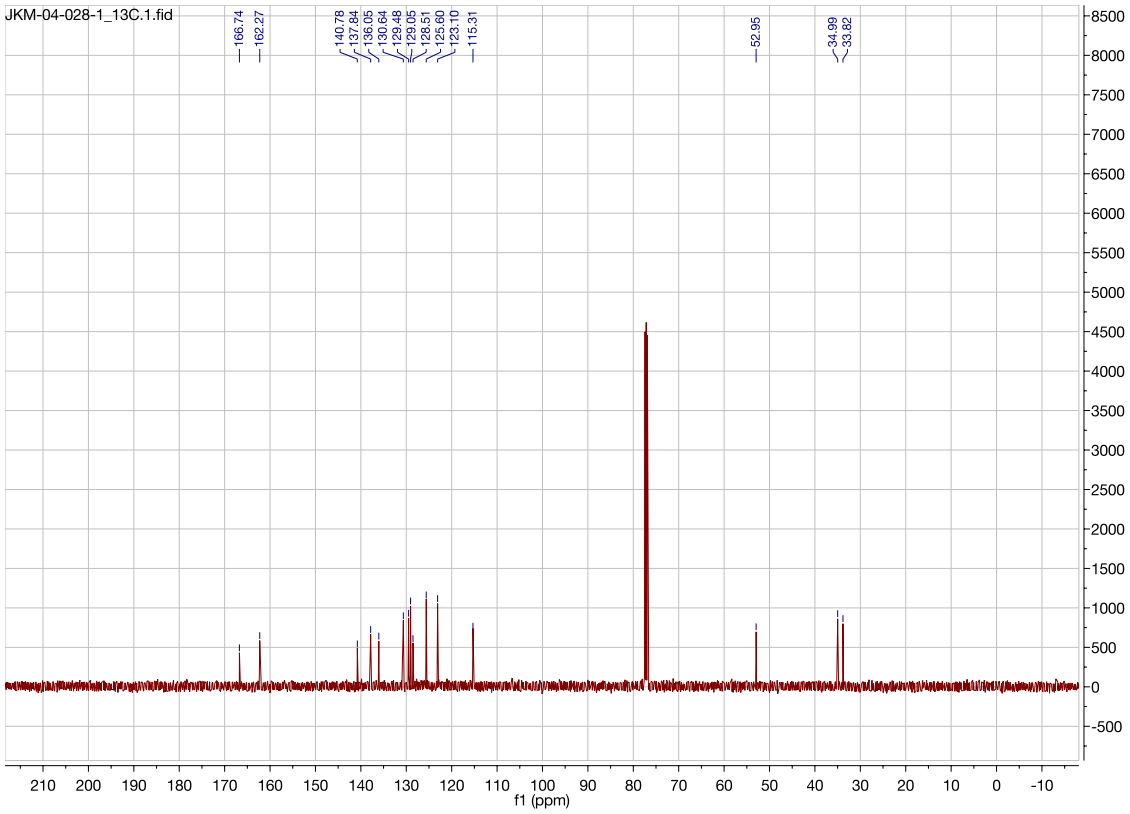

^{1}H ($CDCl_3$, 500 MHz) spectra of 4-methyl-2-((2-(trimethylsilyl)ethoxy)methyl)quinoline (**2.11.1**)

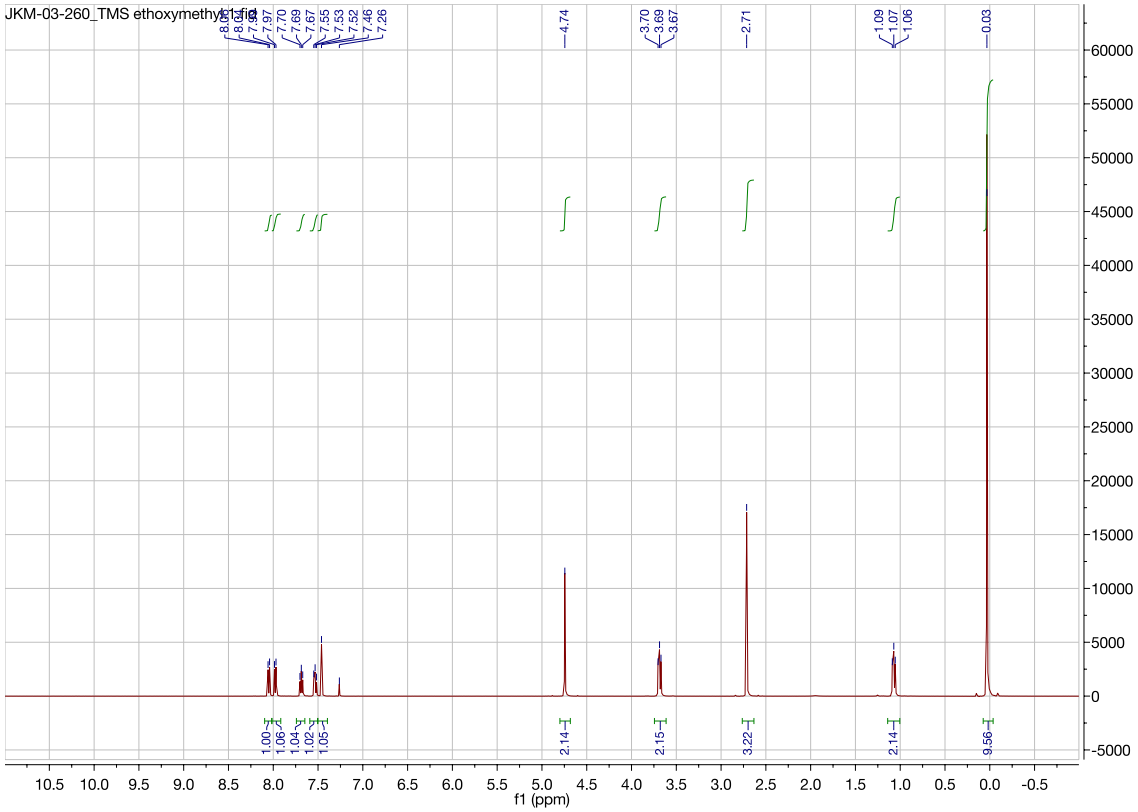

^{13}C NMR ($CDCl_3$, 125.8 MHz) spectrum of 4-methyl-2-((2-(trimethylsilyl)ethoxy)methyl)quinoline (**2.10.1**)

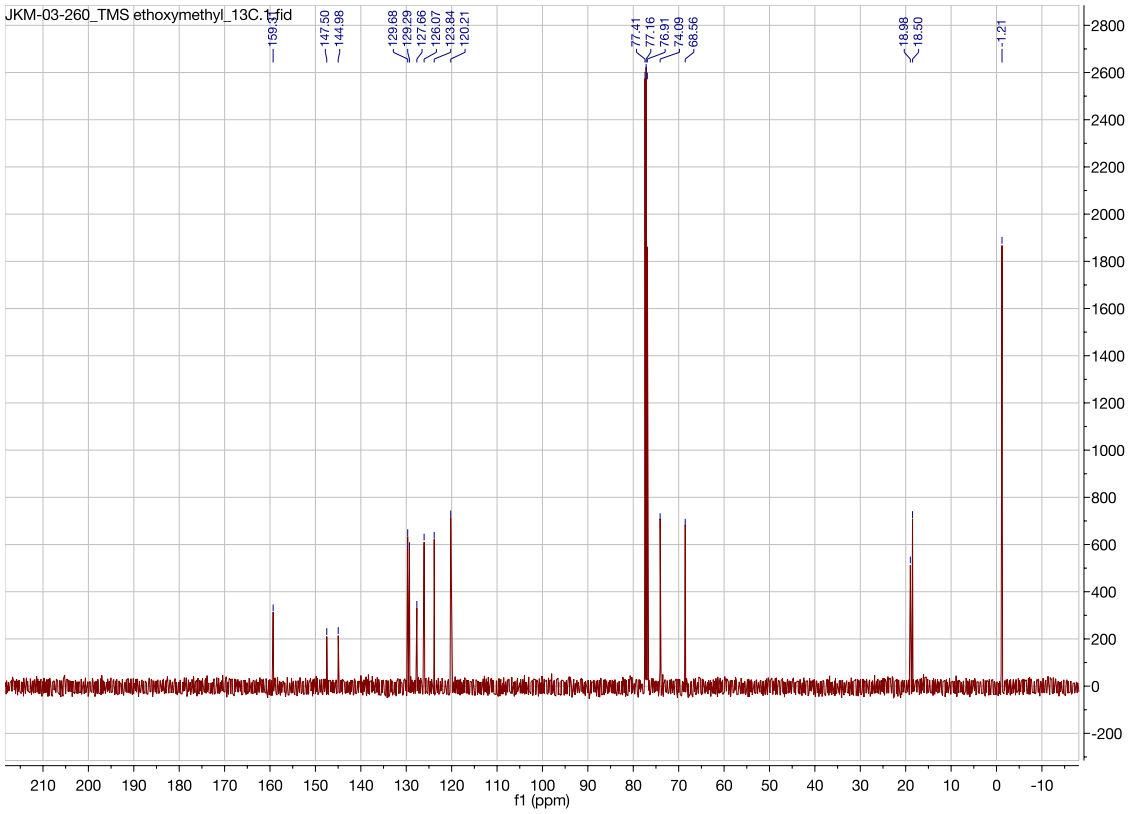

^{1}H ($CDCl_3$, 500 MHz) spectra of 1-(4-methylquinolin-2-yl)-3-phenylpropyl benzoate (**2.11.2**)

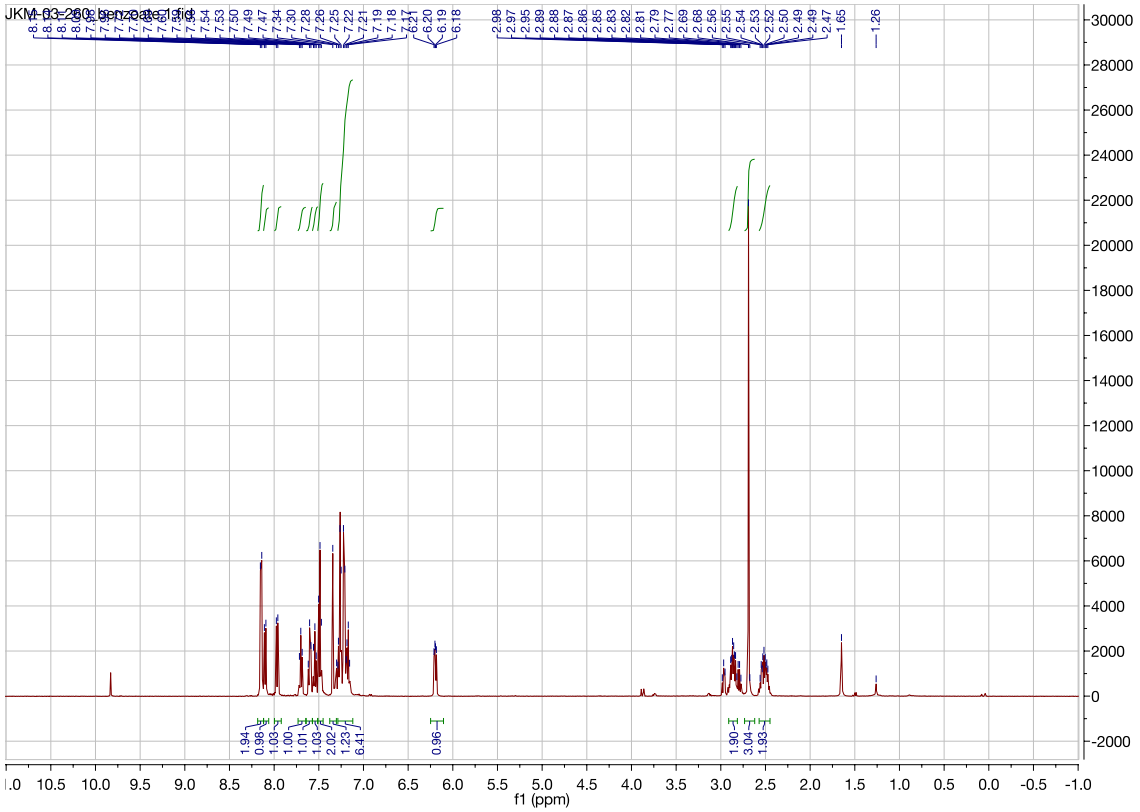

^{13}C NMR ($CDCl_3$, 125.8 MHz) spectrum of 1-(4-methylquinolin-2-yl)-3-phenylpropyl benzoate (**2.11.2**)

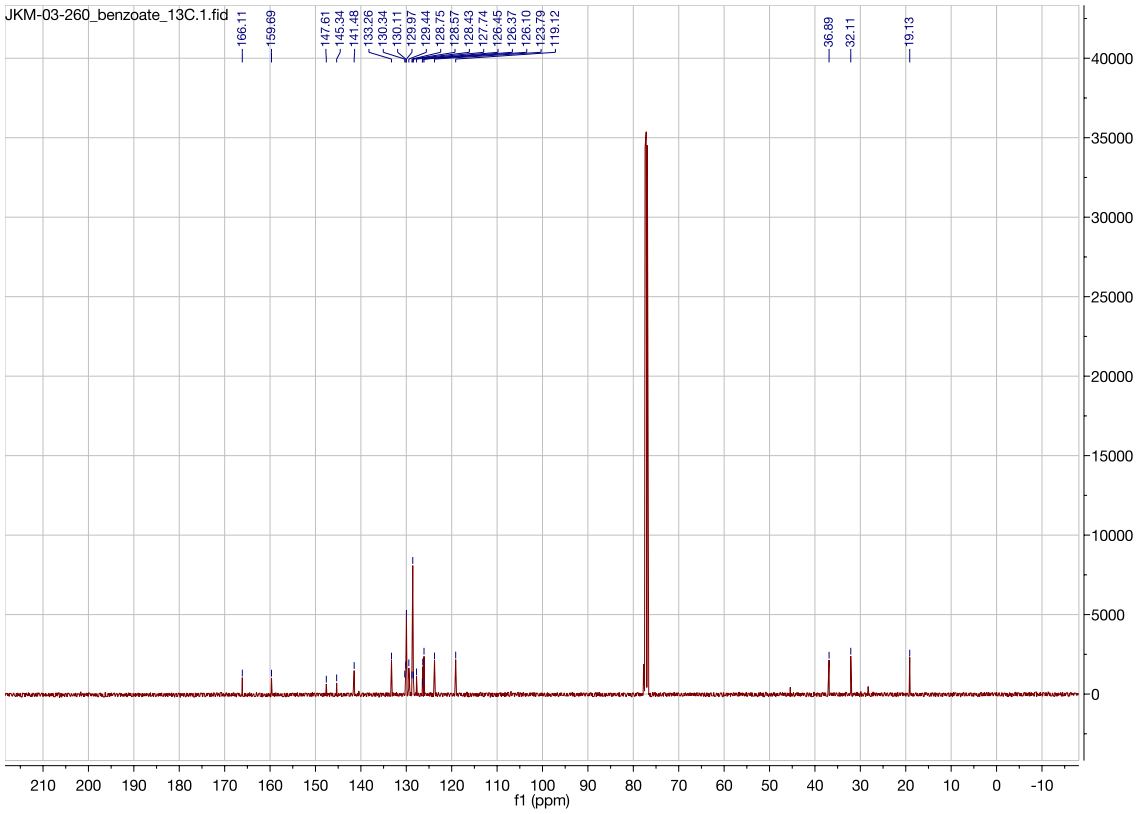

^{1}H ($CDCl_3$, 500 MHz) spectra of 2-((but-3-en-1-yloxy)methyl)quinoline (**2.11.3**)

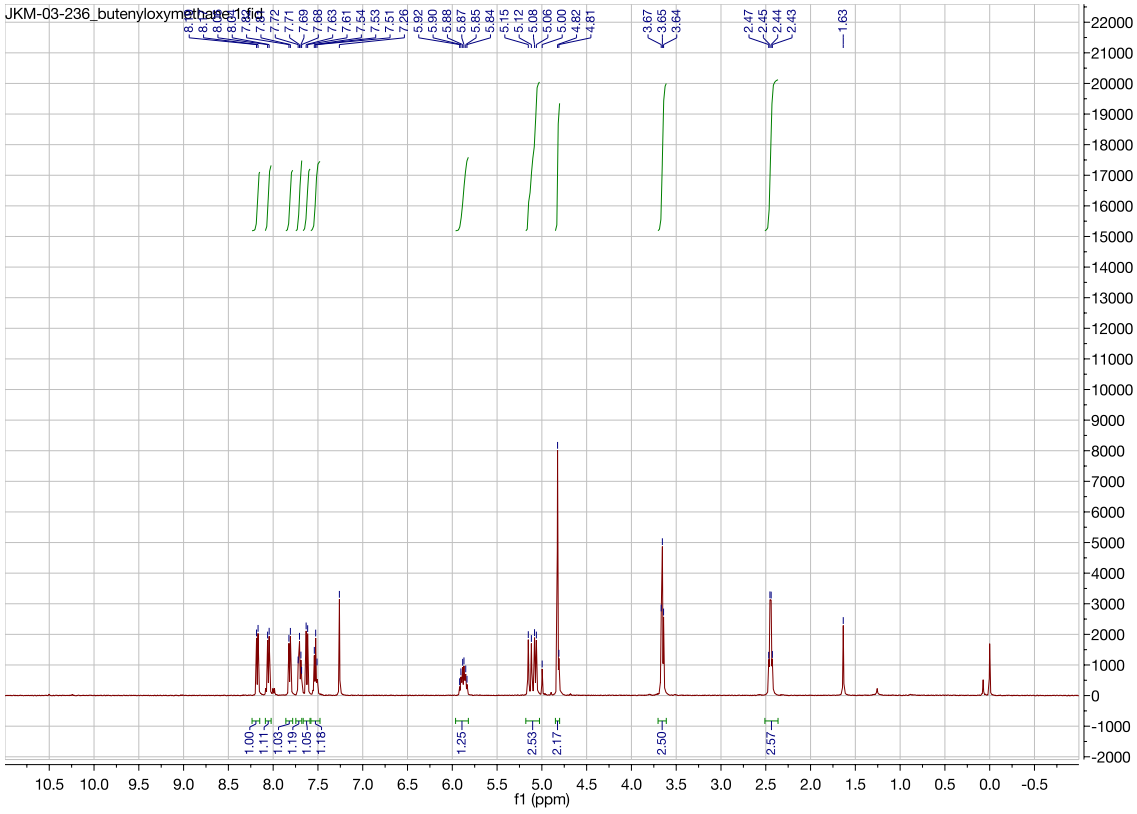

^{13}C NMR ($CDCl_3$, 125.8 MHz) spectrum of 2-((but-3-en-1-yloxy)methyl)quinoline (**2.11.**)

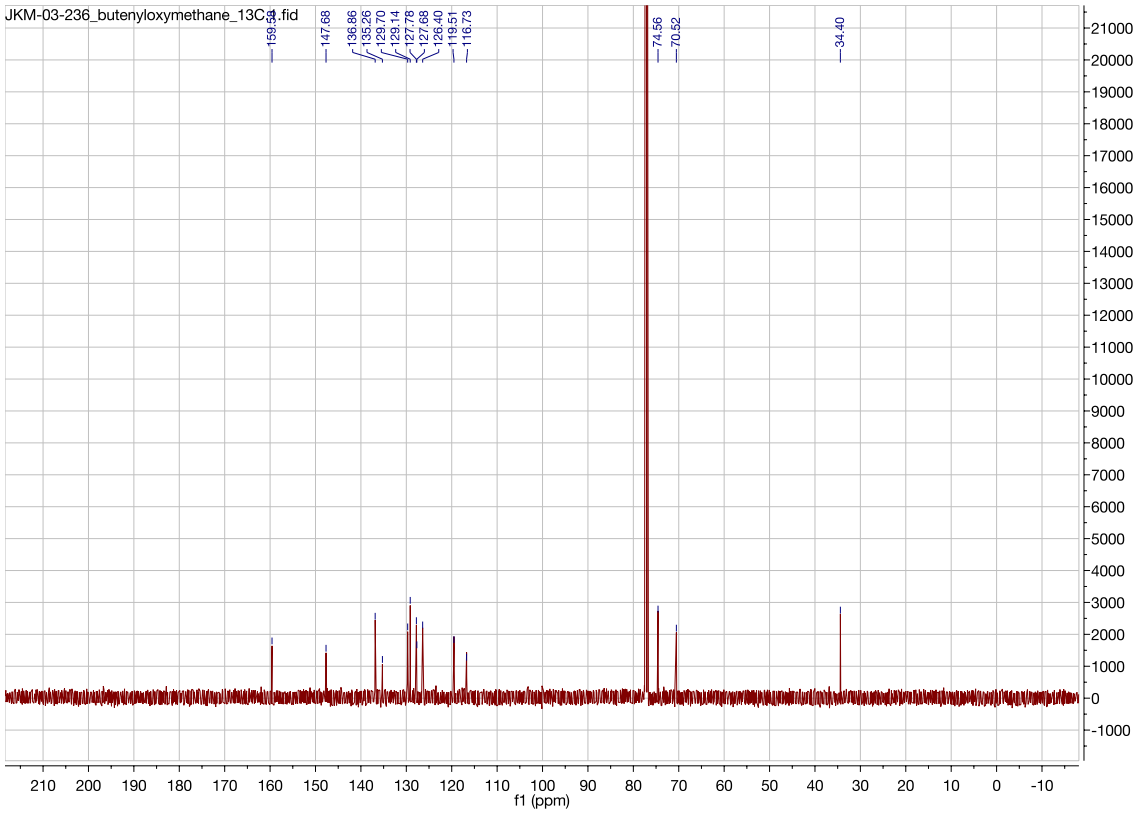

^{1}H ($CDCl_3$, 500 MHz) spectra of 2-octylquinoline (**2.11.4**)

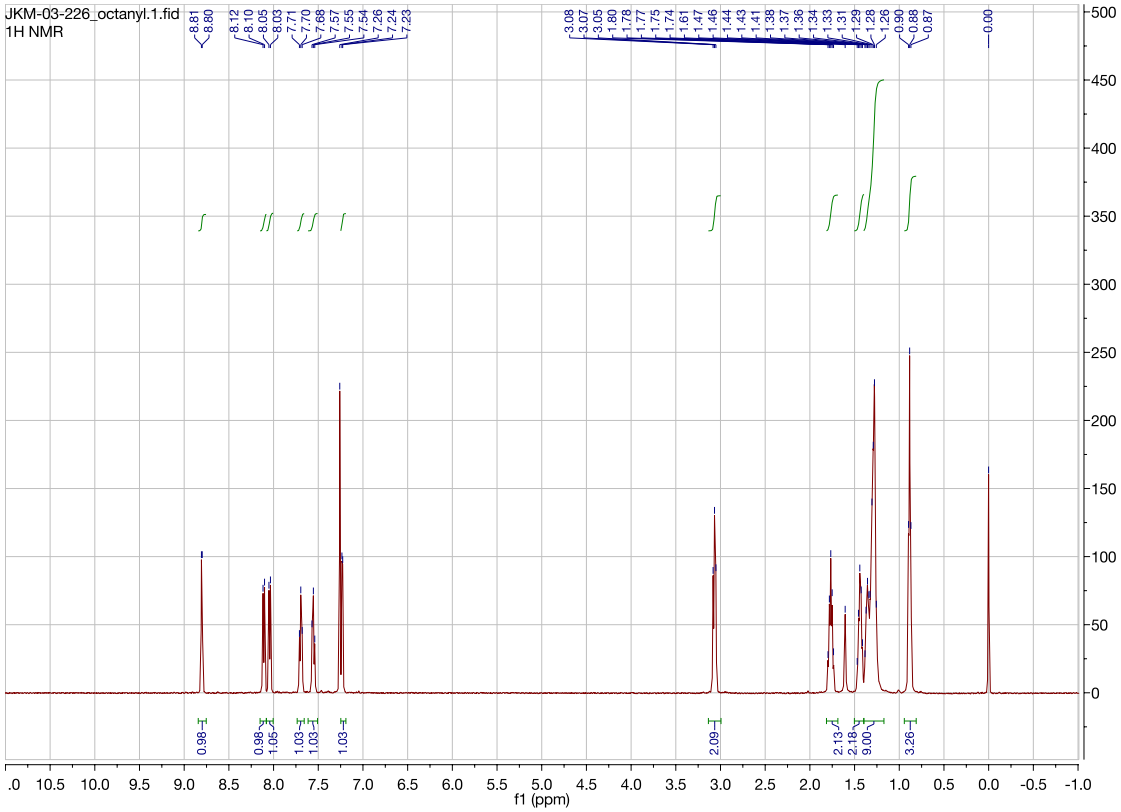

^{13}C NMR ($CDCl_3$, 125.8 MHz) spectrum of 2-octylquinoline (**2.11.4**)

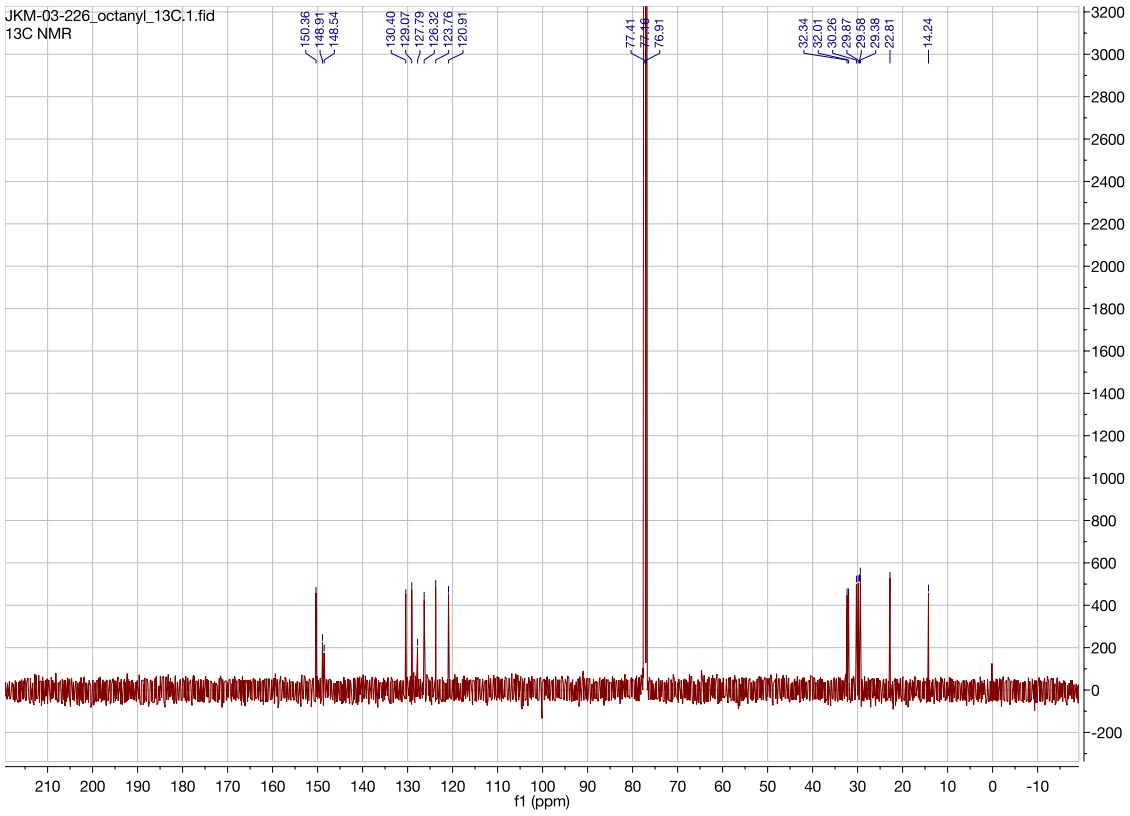

^{1}H ($CDCl_3$, 500 MHz) spectra of 2-((2*R*)-2-methylcyclopentyl)quinoline (**2.11.5**)

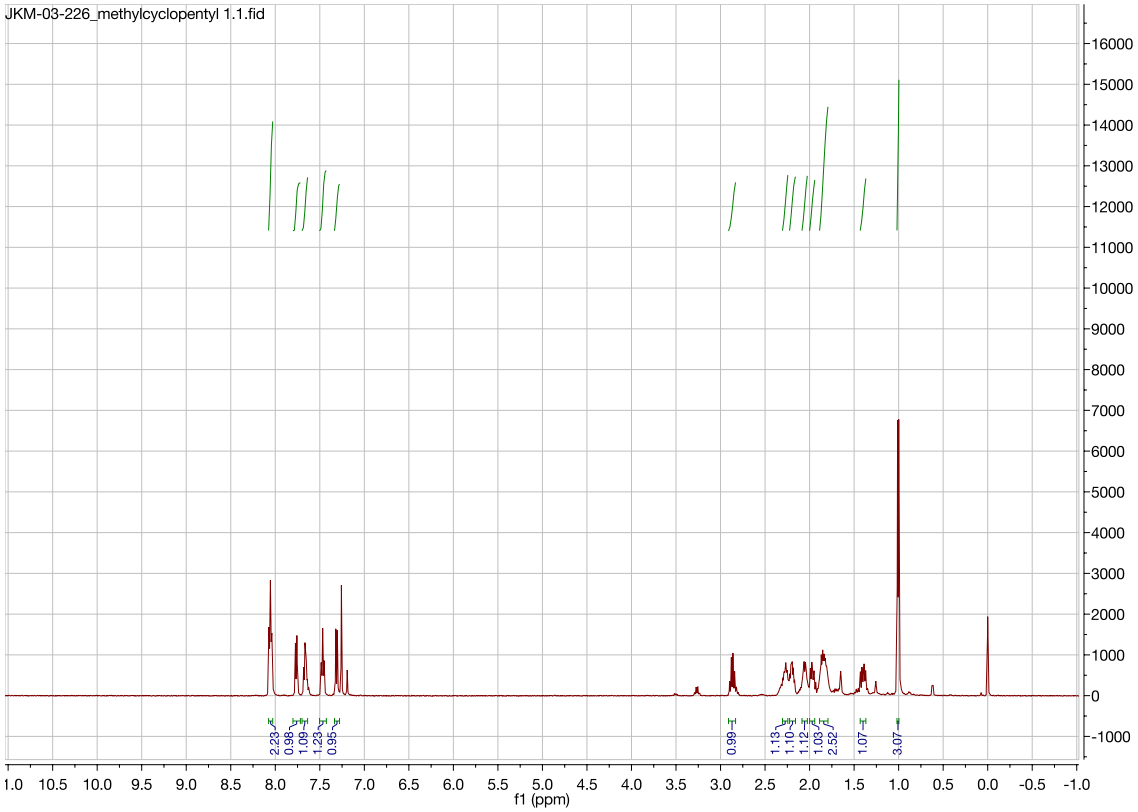

^{13}C NMR ($CDCl_3$, 125.8 MHz) spectrum of 2-((2*R*)-2-methylcyclopentyl)quinoline (**2.11.5**)

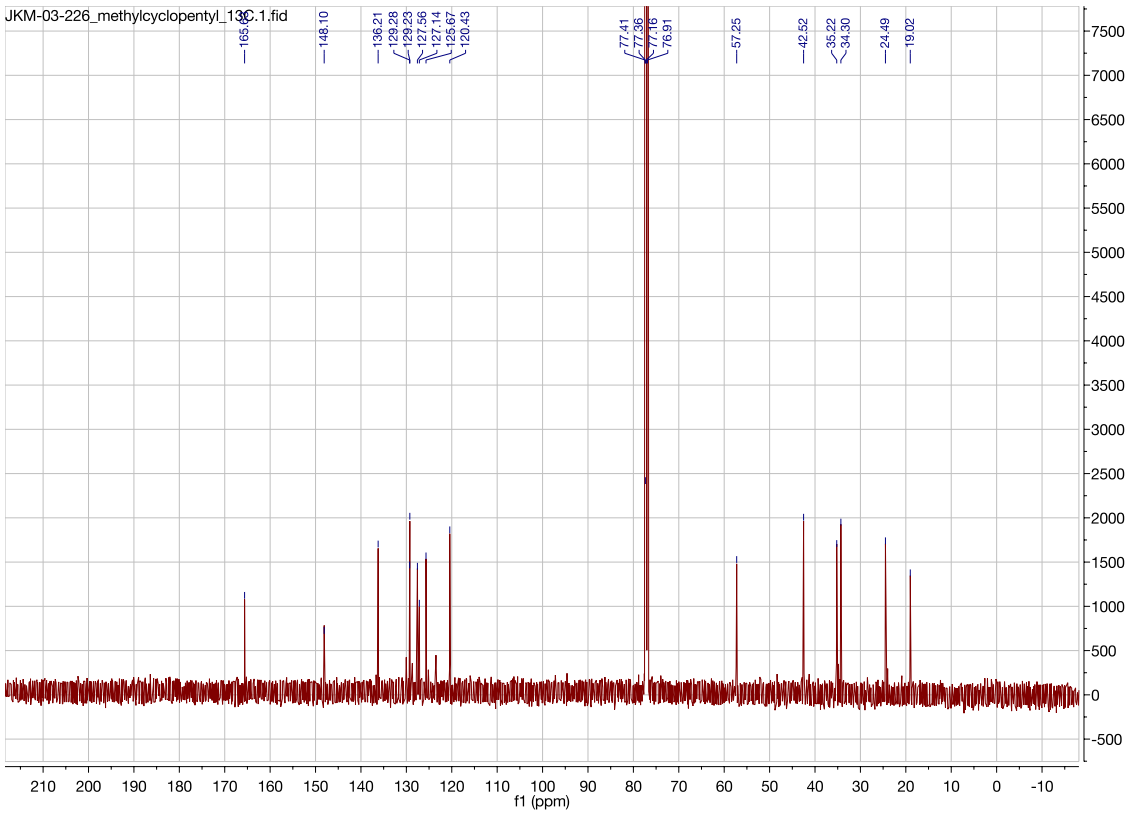

^{1}H ($CDCl_3$, 500 MHz) spectra of 1,1'-(3-phenethylpyridine-2,6-diyl)bis(ethan-1-one) (**2.11.6**)

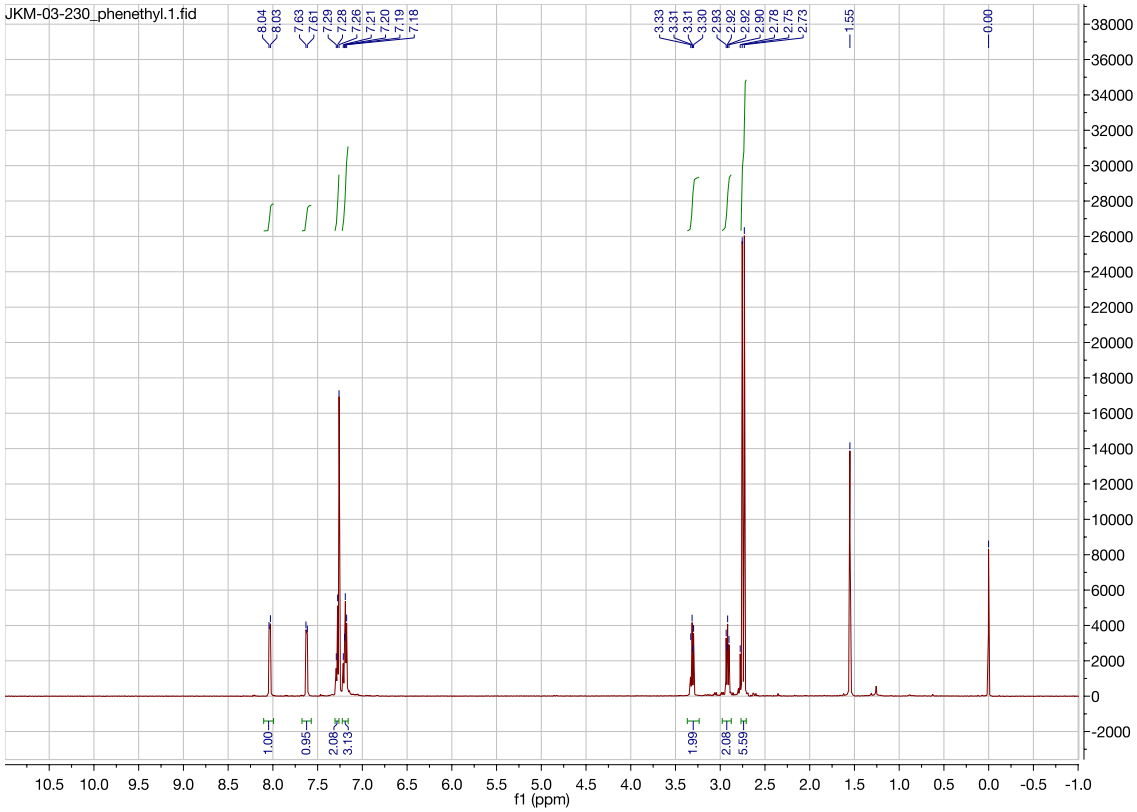

^{13}C NMR ($CDCl_3$, 125.8 MHz) spectrum of 1,1'-(3-phenethylpyridine-2,6-diyl)bis(ethan-1-one) (**2.11.6**)

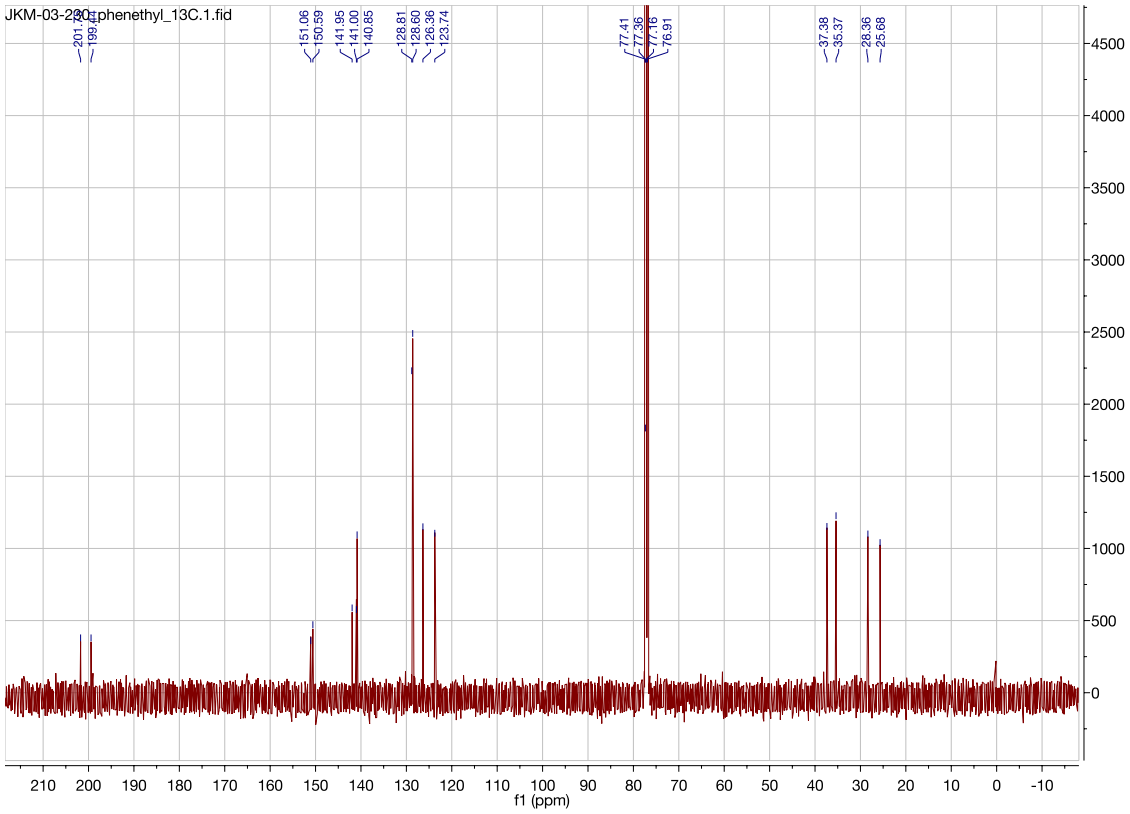

^{1}H ($CDCl_3$, 500 MHz) spectra of 2-(1-(benzyloxy)-2-phenylethyl)benzo[*d*]thiazole (**2.11.7**)

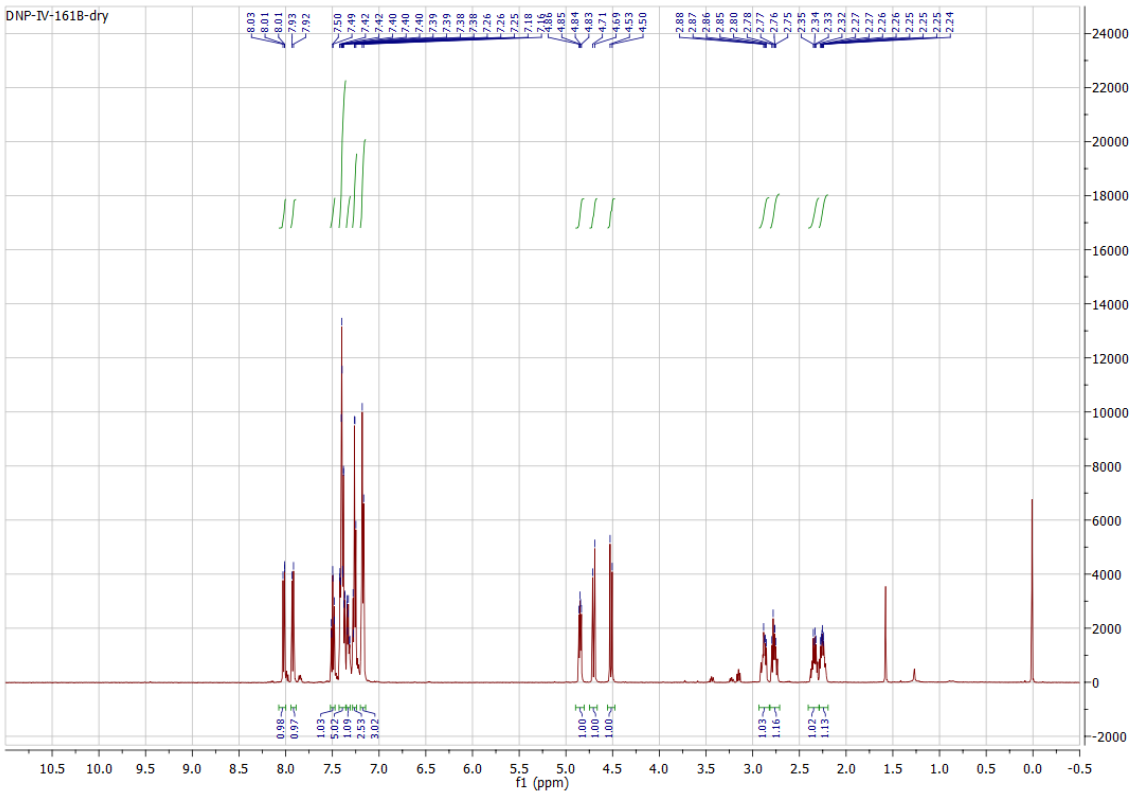

^{13}C NMR ($CDCl_3$, 125.8 MHz) spectrum of 2-(1-(benzyloxy)-2-phenylethyl)benzo[*d*]thiazole (**2.11.7**)

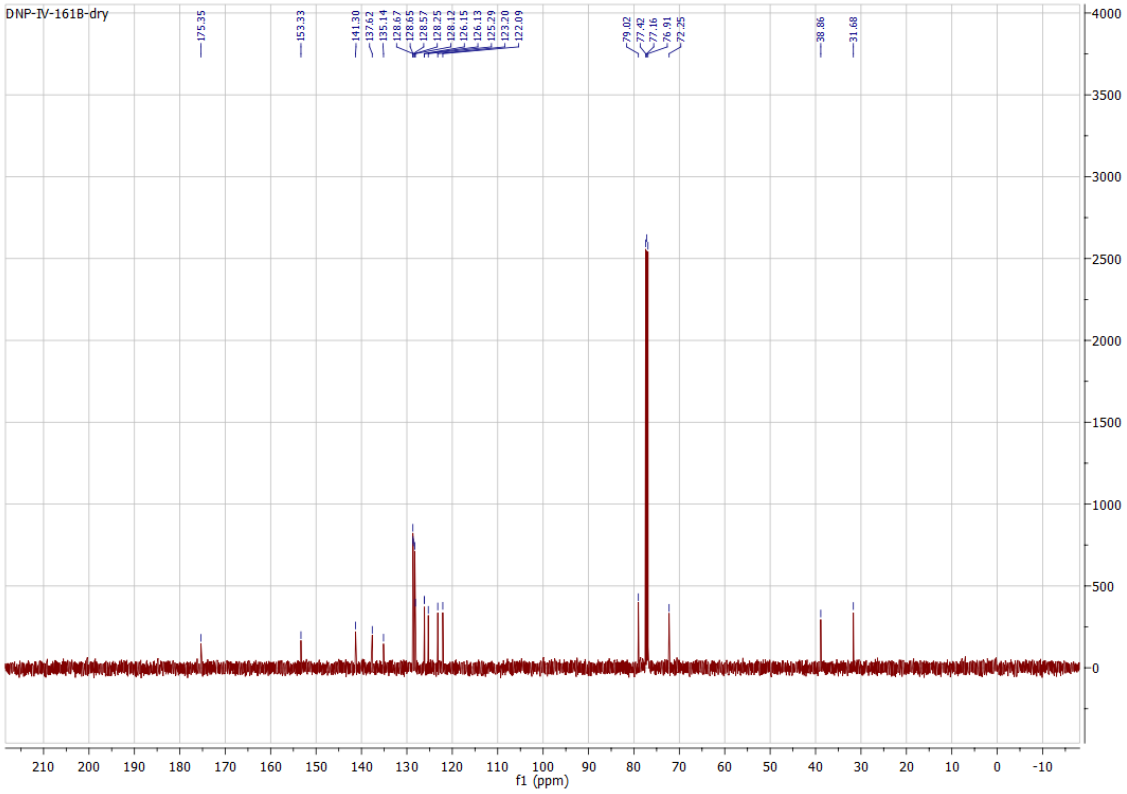

^{1}H ($CDCl_3$, 500 MHz) spectra of 3-Isopropyl-1*H*-indazole (**2.11.8**)

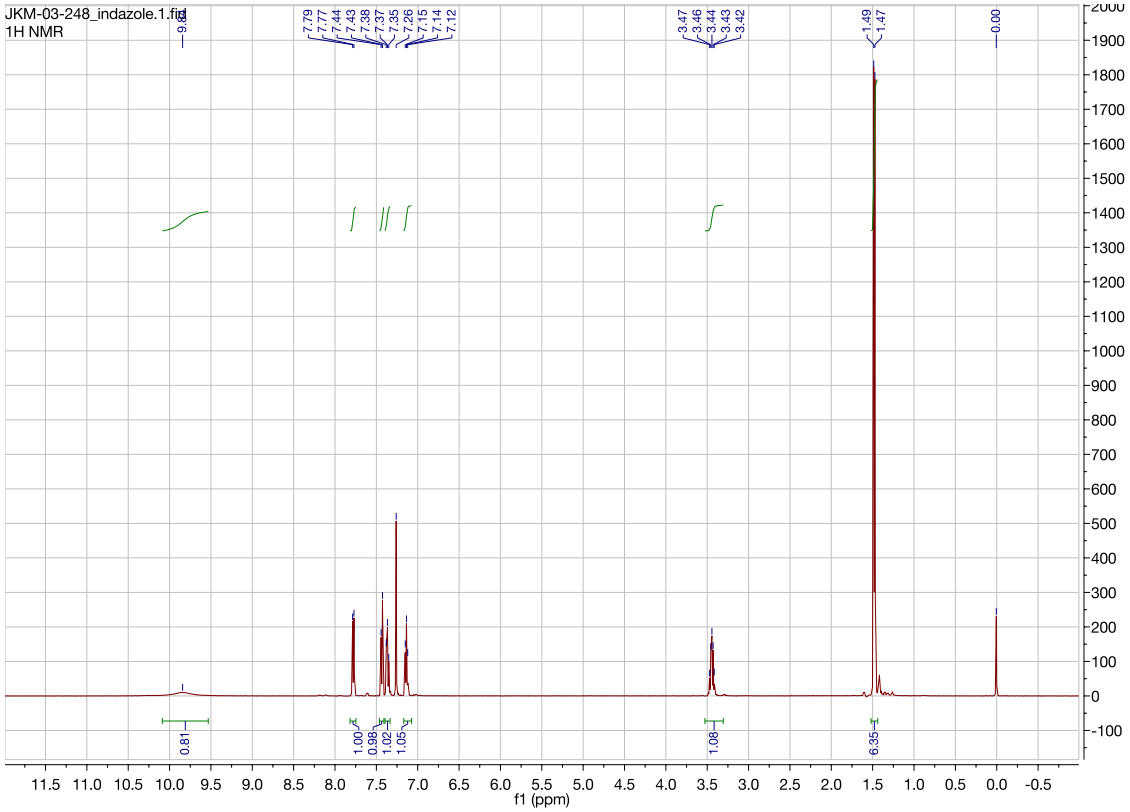

^{13}C NMR ($CDCl_3$, 125.8 MHz) spectrum of 3-isopropyl-1*H*-indazole (**2.11.8**)

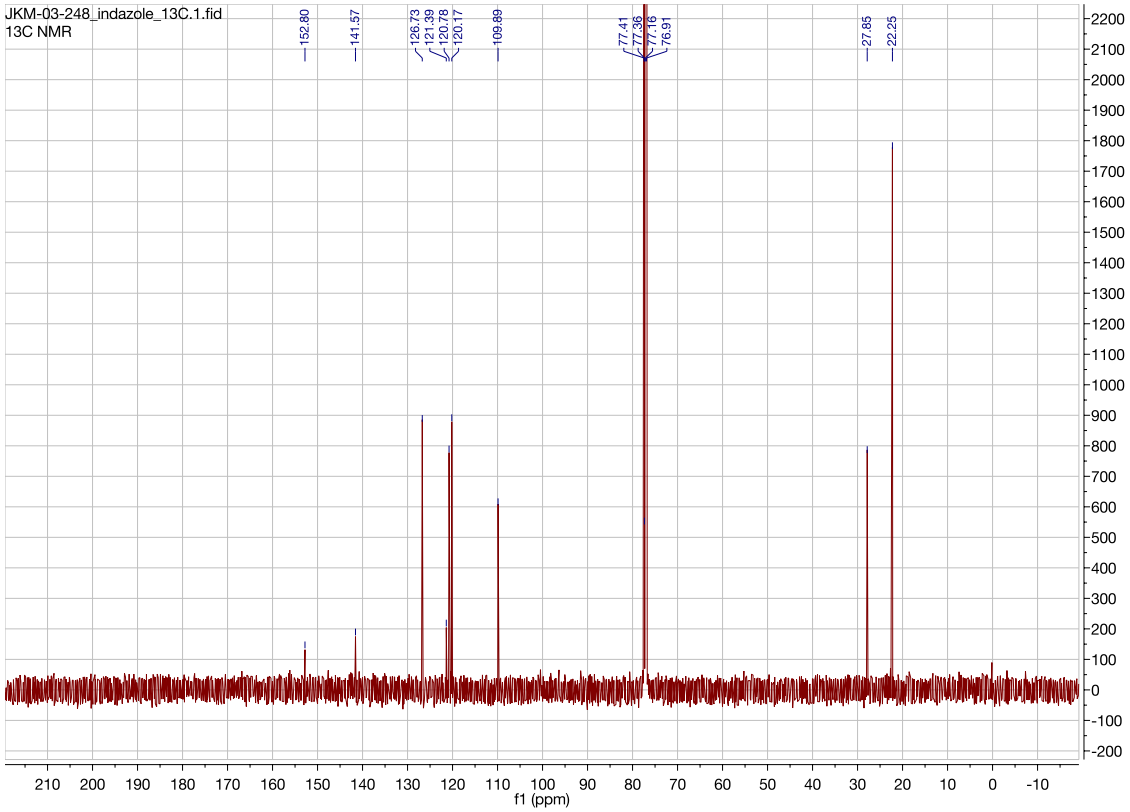

^{1}H ($CDCl_3$, 500 MHz) spectra of 2-isopropylquinazolin-4(3*H*)-one (**2.11.9**)

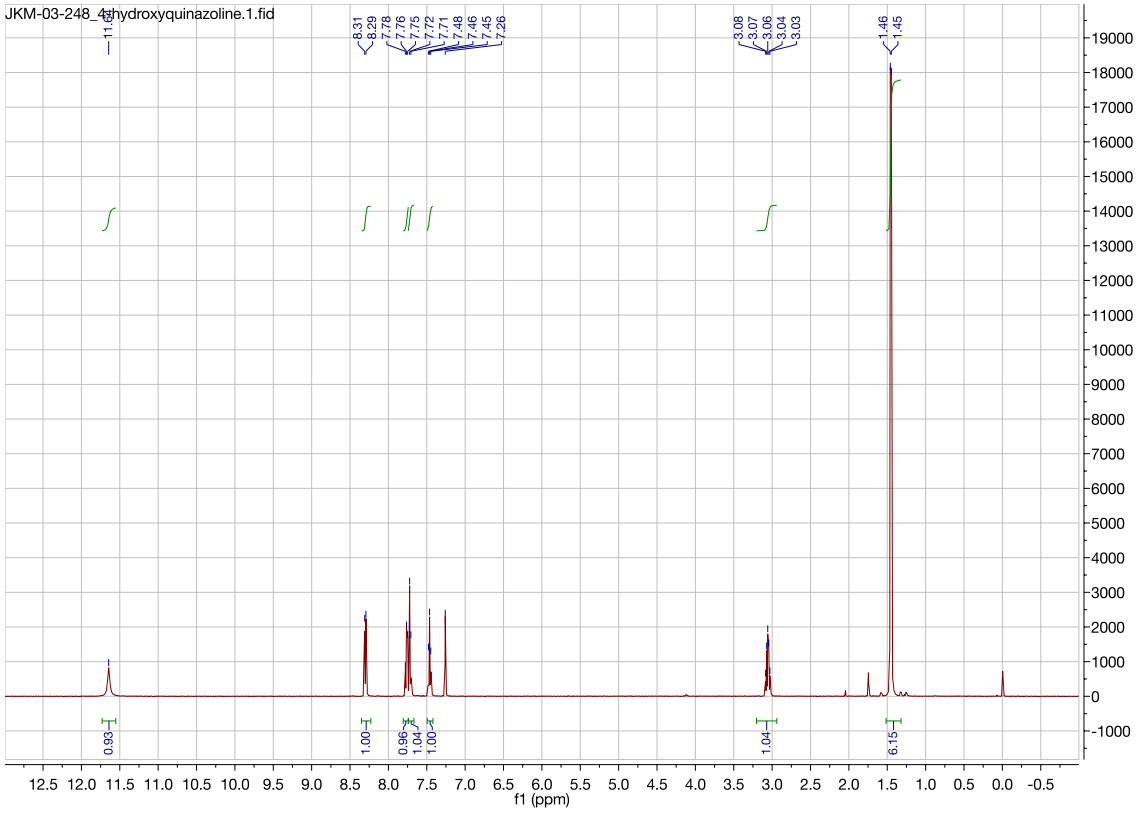

^{13}C NMR ($CDCl_3$, 125.8 MHz) spectrum of 2-isopropylquinazolin-4(3*H*)-one (**2.11.9**)

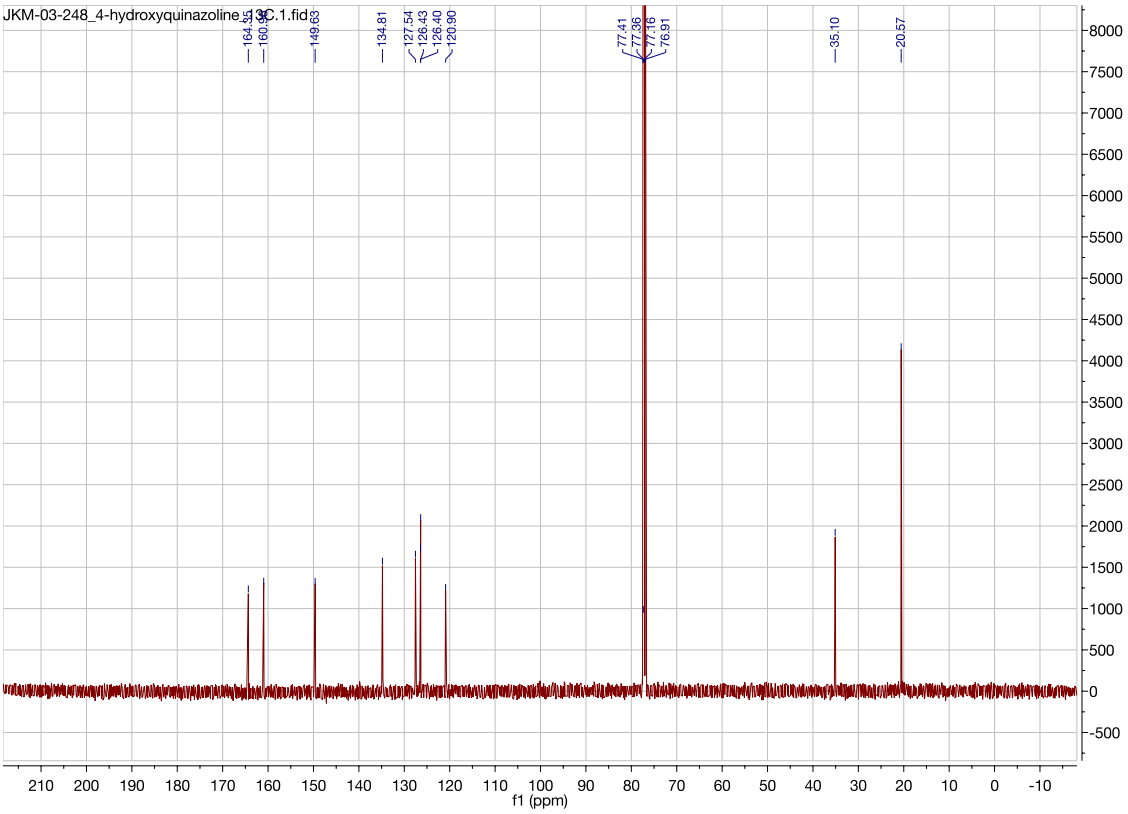

^{1}H ($CDCl_3$, 500 MHz) spectra of 2-((1*R*,2*R*)-2-methylcyclohexyl)quinazolin-4(3*H*)-one (**2.11.10**)

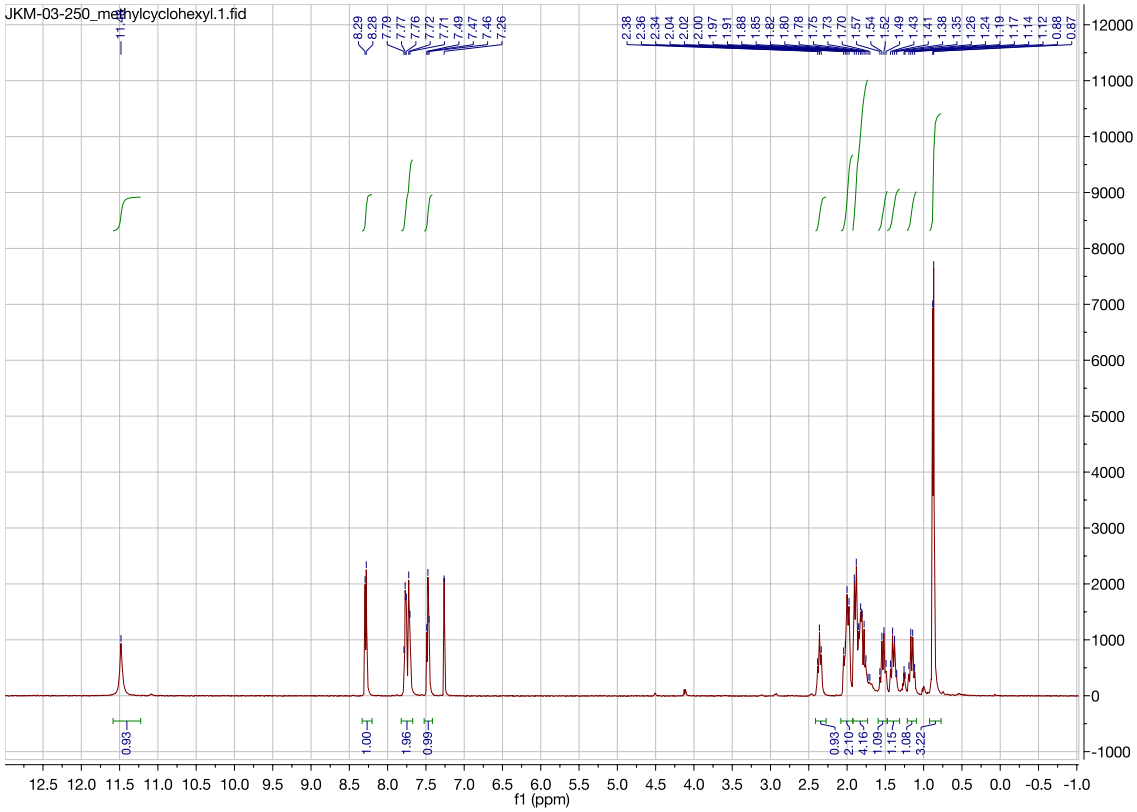

^{13}C NMR ($CDCl_3$, 125.8 MHz) spectrum of 2-((1*R*,2*R*)-2-methylcyclohexyl)quinazolin-4(3*H*)-one (**2.11.10**)

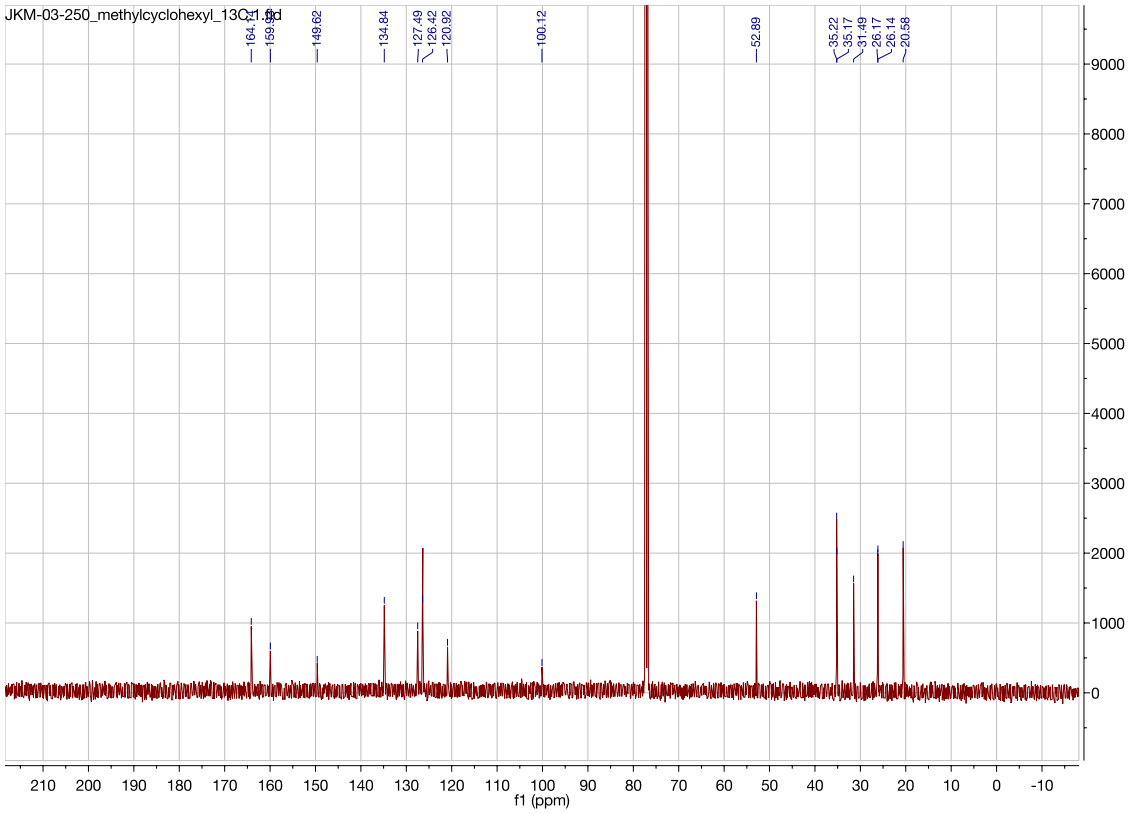

^{1}H ($CDCl_3$, 500 MHz) spectra of 1,3,7-trimethyl-8-((2*S*)-2-methylcyclopentyl)-3,7-dihydro-1*H*-purine-2,6-dione (**2.11.11**)

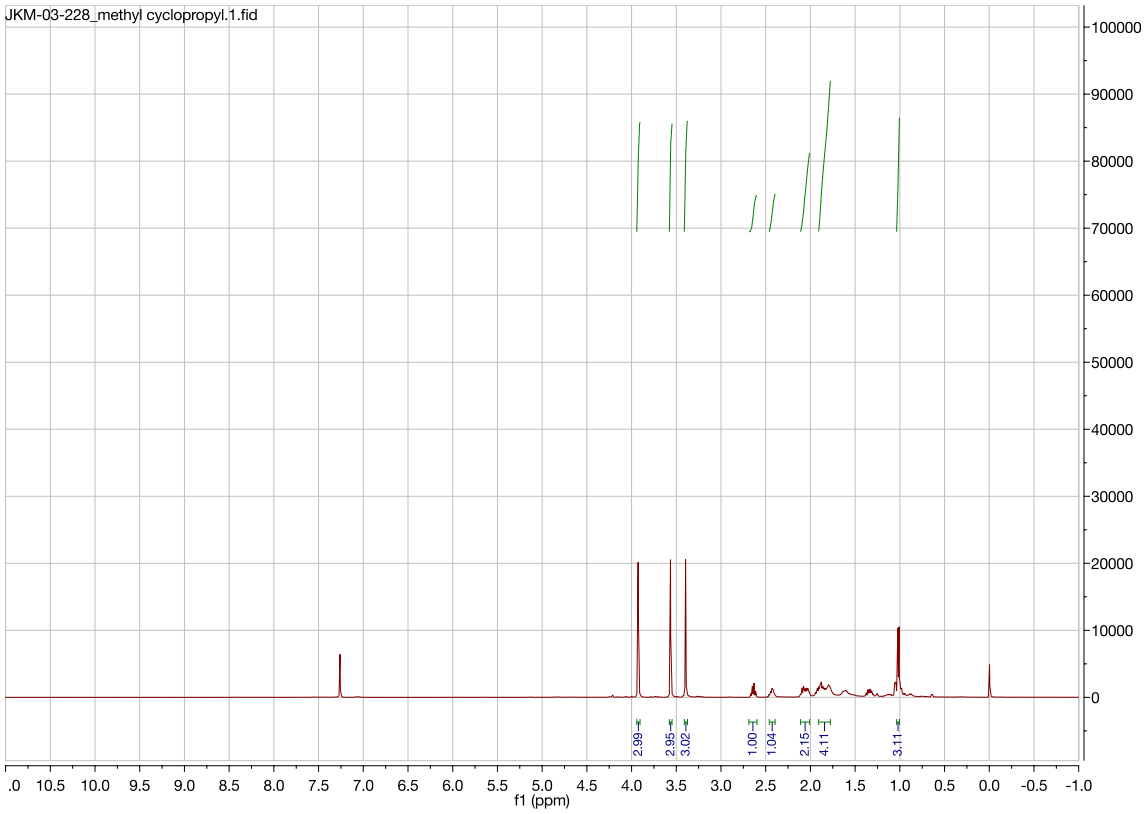

^{13}C NMR ($CDCl_3$, 125.8 MHz) spectrum of 1,3,7-trimethyl-8-((2*S*)-2-methylcyclopentyl)-3,7-dihydro-1*H*-purine-2,6-dione (**2.11.11**)

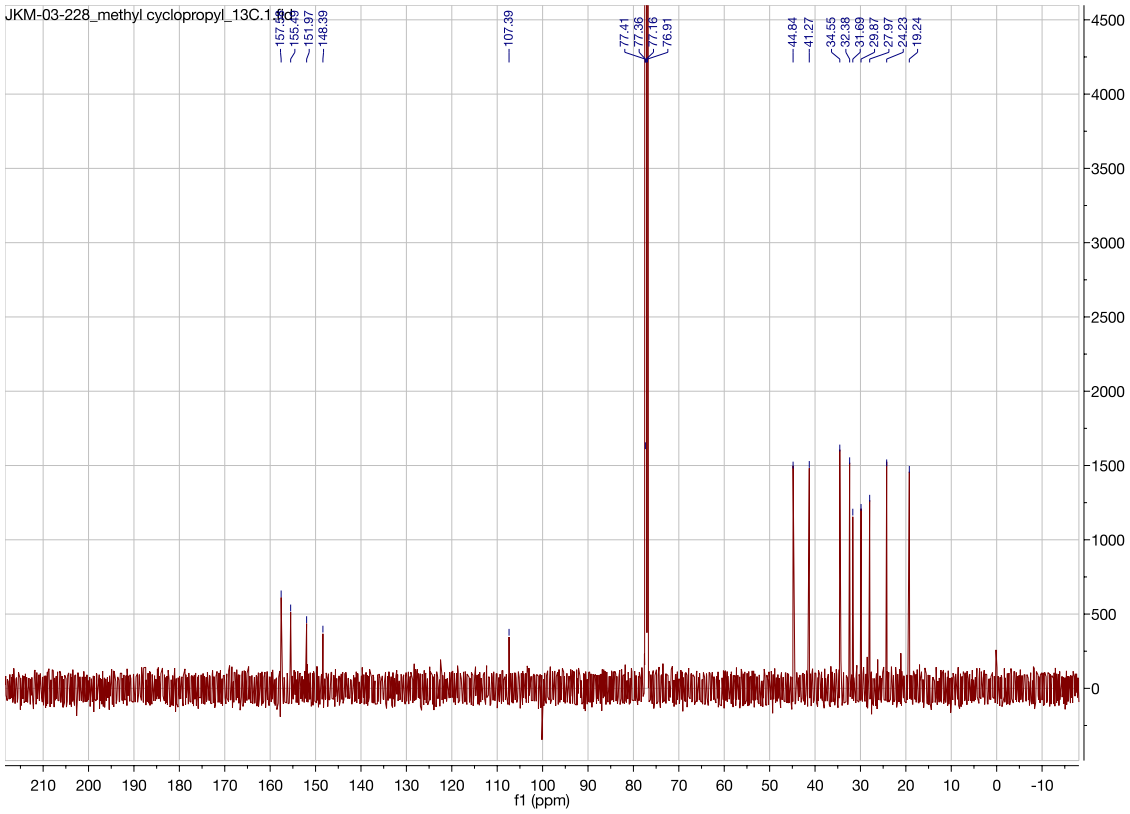

^{1}H ($CDCl_3$, 500 MHz) spectra of (1*R*)-(2-isopropyl-6-methoxyquinolin-4-yl)(5-vinylquinuclidin-2-yl)methanol (**2.11.12**)

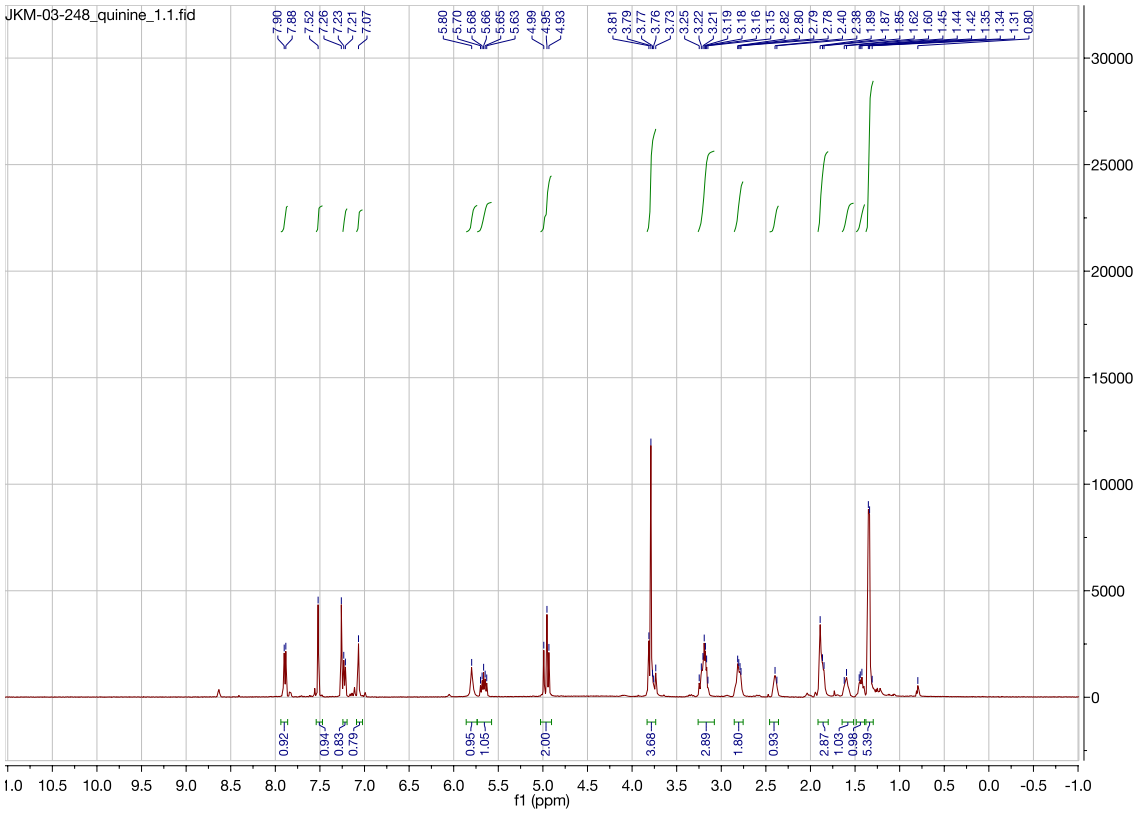

^{13}C NMR ($CDCl_3$, 125.8 MHz) spectrum of (1*R*)-(2-isopropyl-6-methoxyquinolin-4-yl)(5-vinylquinuclidin-2-yl)methanol (**2.11.12**)

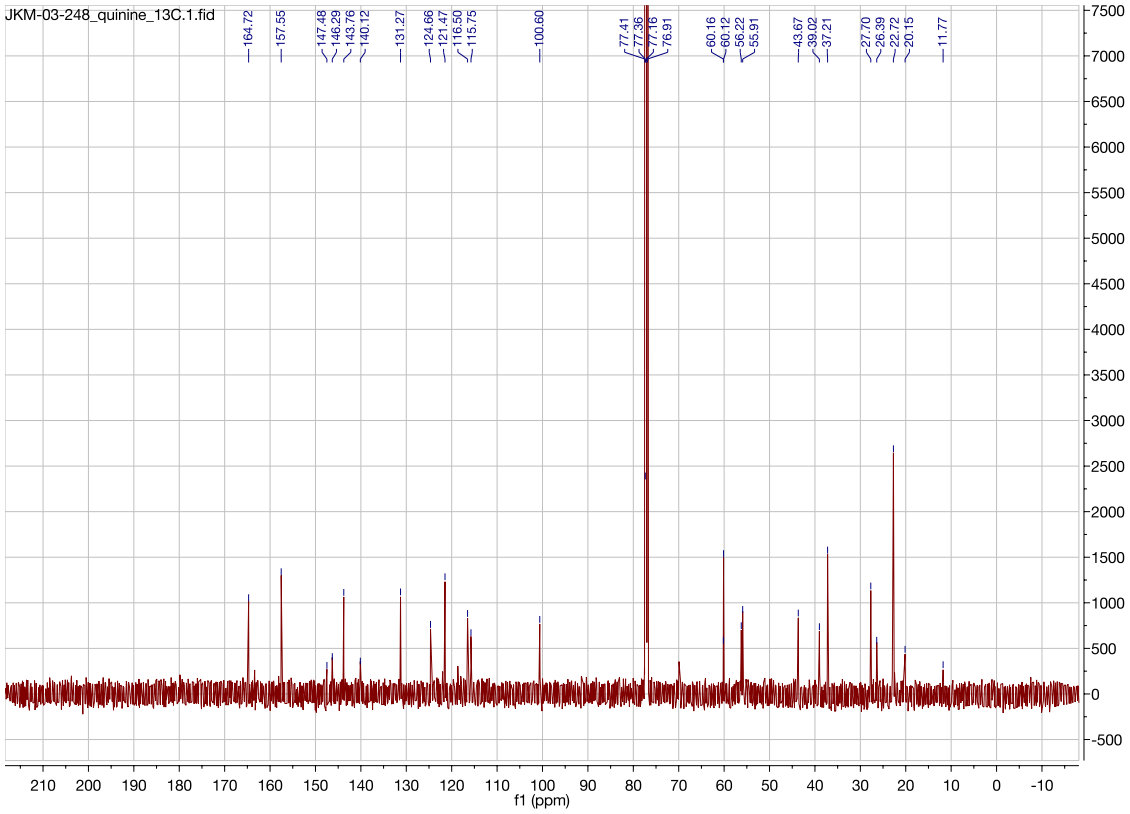

^{1}H ($CDCl_3$, 500 MHz) spectra of 2,9-di-*tert*-butyl-1,10-phenanthroline (**2.12.2**)

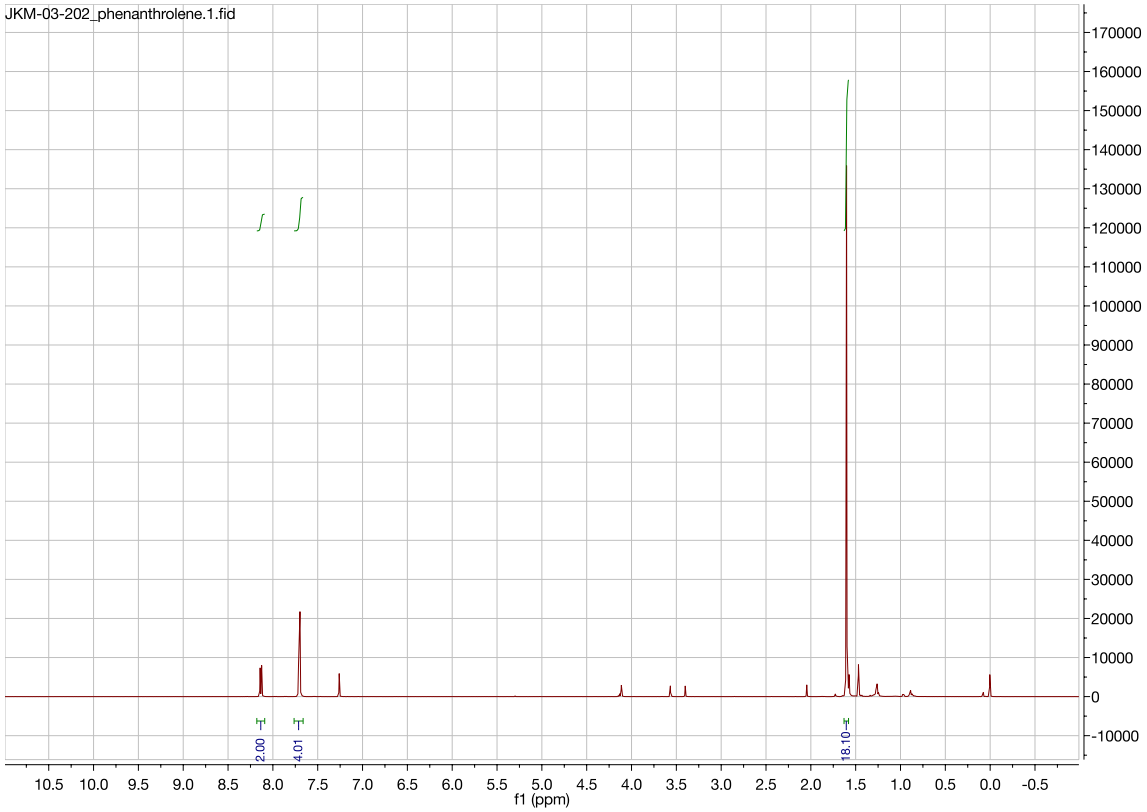

^{13}C NMR ($CDCl_3$, 125.8 MHz) spectrum of 2,9-di-*tert*-butyl-1,10-phenanthroline (**2.12.2**)

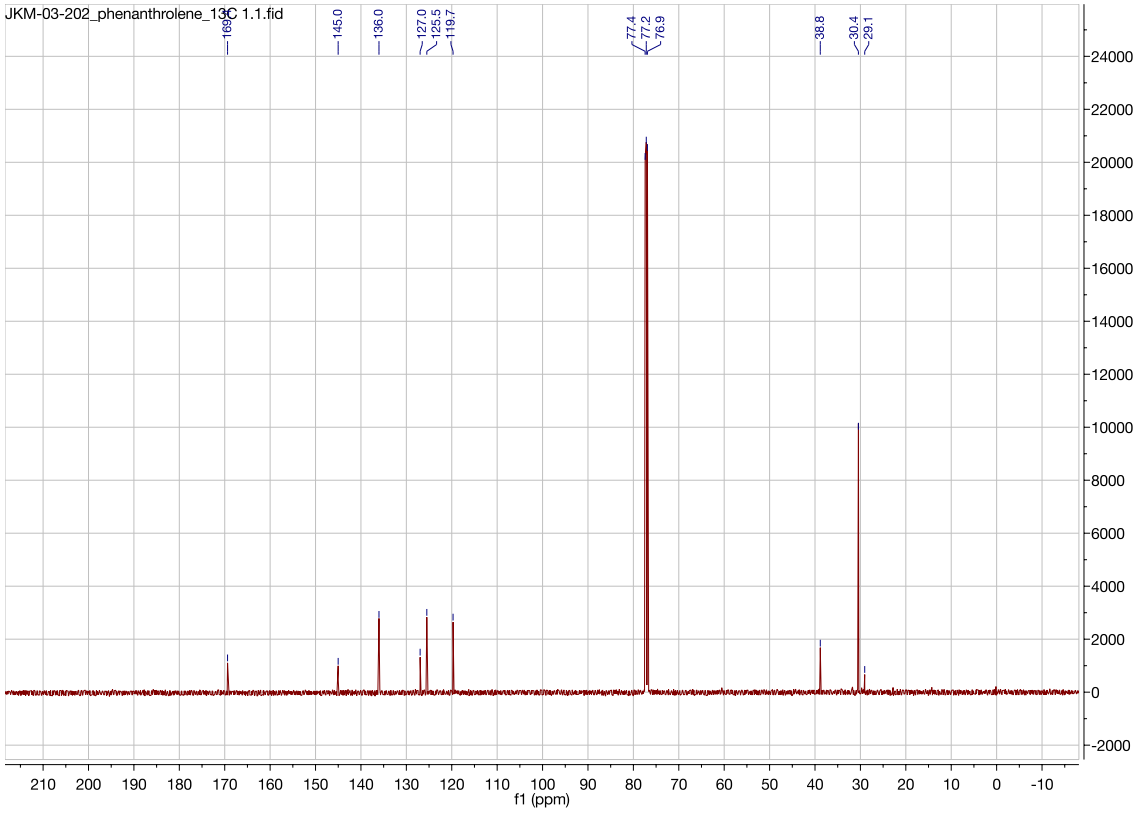

^{1}H ($CDCl_3$, 500 MHz) spectra of 2,9-di-*tert*-butyl-4,7-diphenyl-1,10-phenanthroline (**2.12.4**)

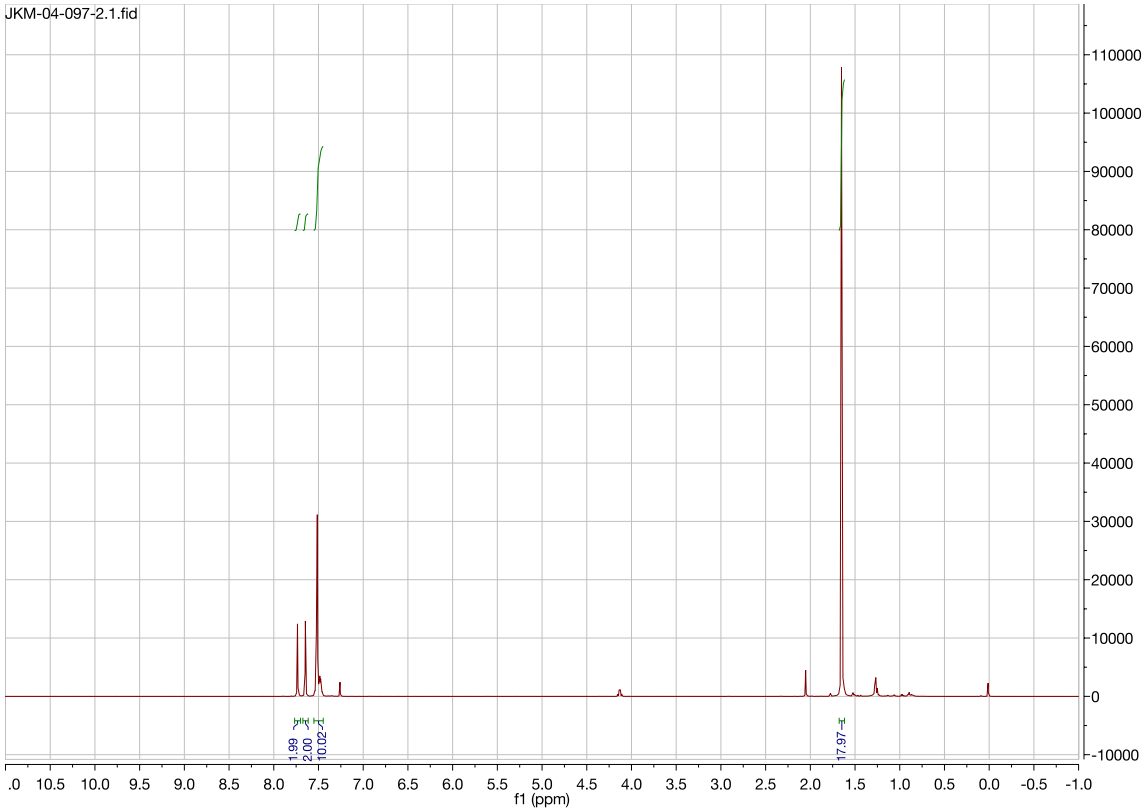

^{13}C NMR ($CDCl_3$, 125.8 MHz) spectrum of 2,9-di-*tert*-butyl-4,7-diphenyl-1,10-phenanthroline (**2.12.4**)

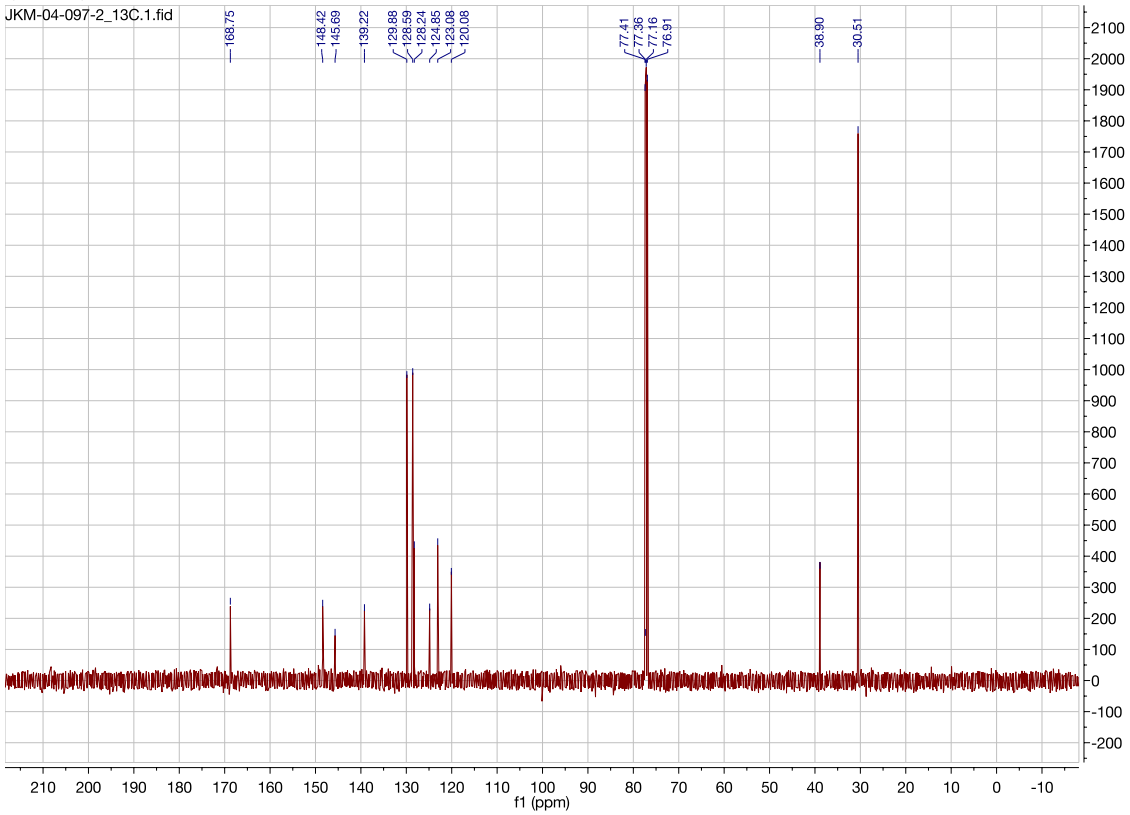

^{1}H ($CDCl_3$, 500 MHz) spectra of 2-(*tert*-butyl)-6-(2,4-difluorophenyl)pyridine (**2.12.6**)

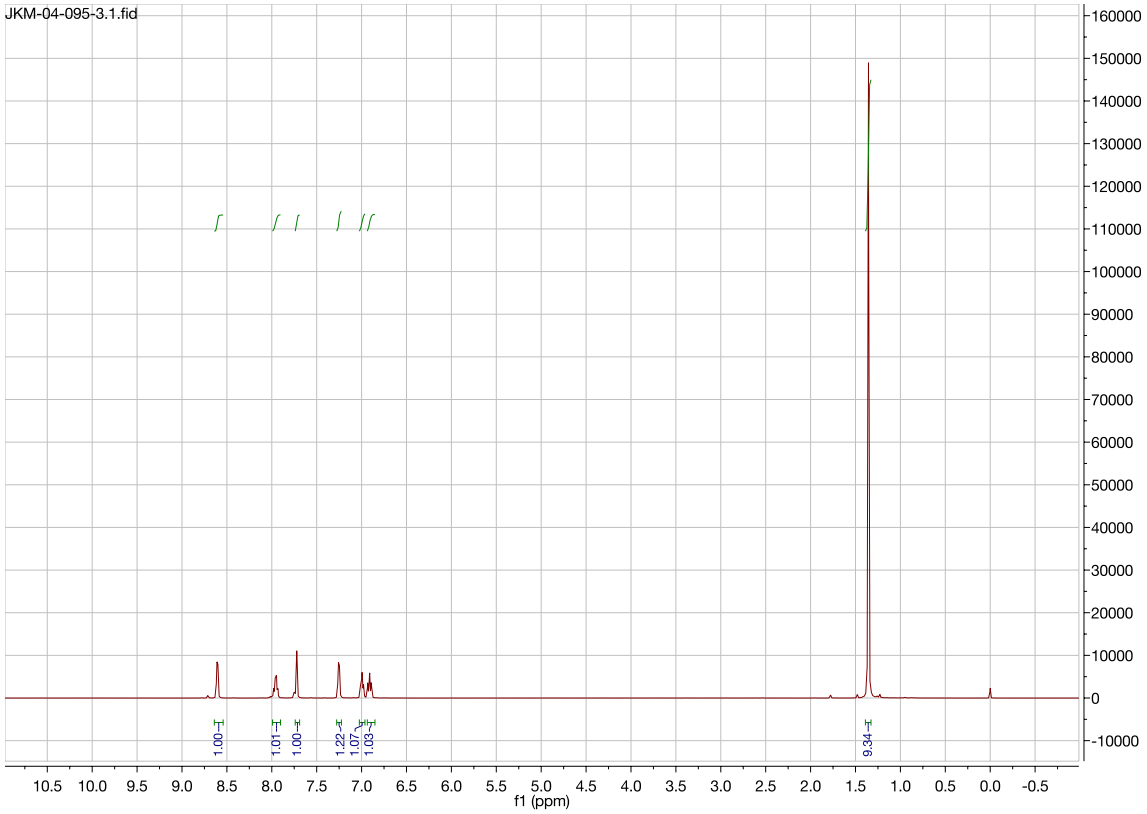

^{13}C NMR ($CDCl_3$, 125.8 MHz) spectrum of 2-(*tert*-butyl)-6-(2,4-difluorophenyl)pyridine (**2.12.6**)

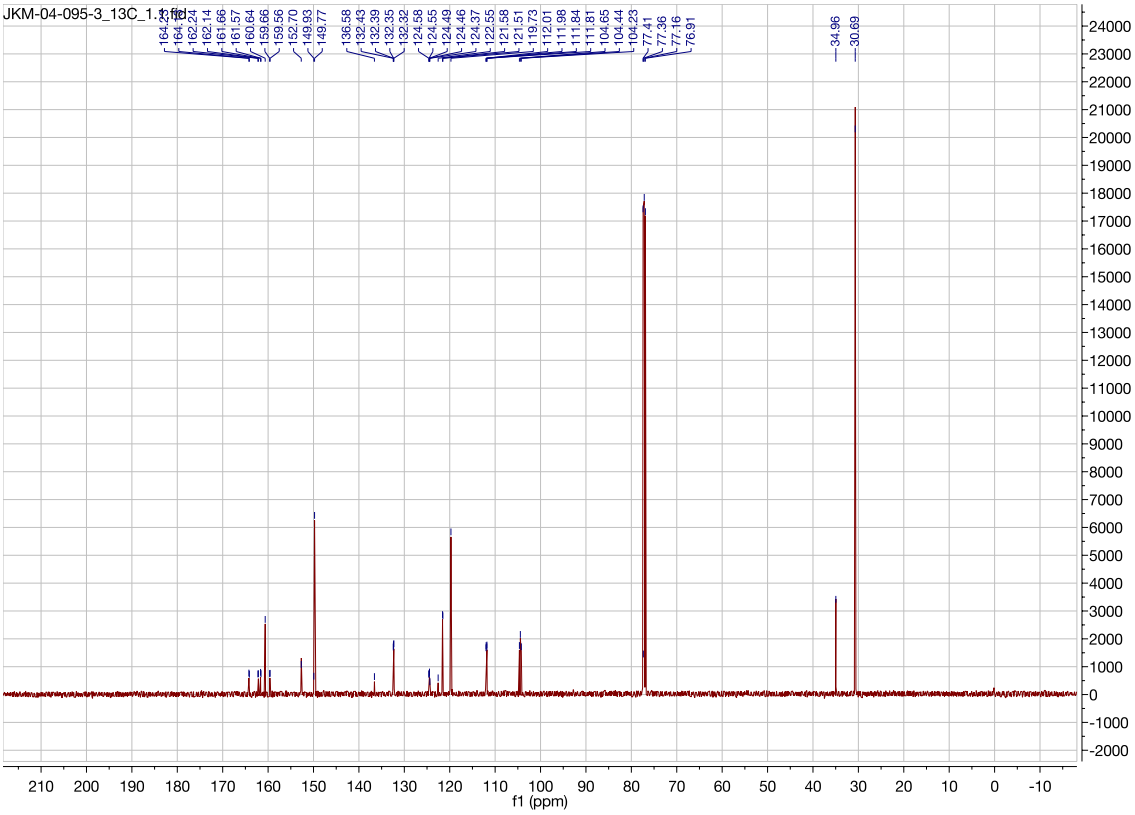

^{1}H ($CDCl_3$, 500 MHz) spectra of 6-(*tert*-butyl)-2,2':6',2''-terpyridine (**2.12.8**)

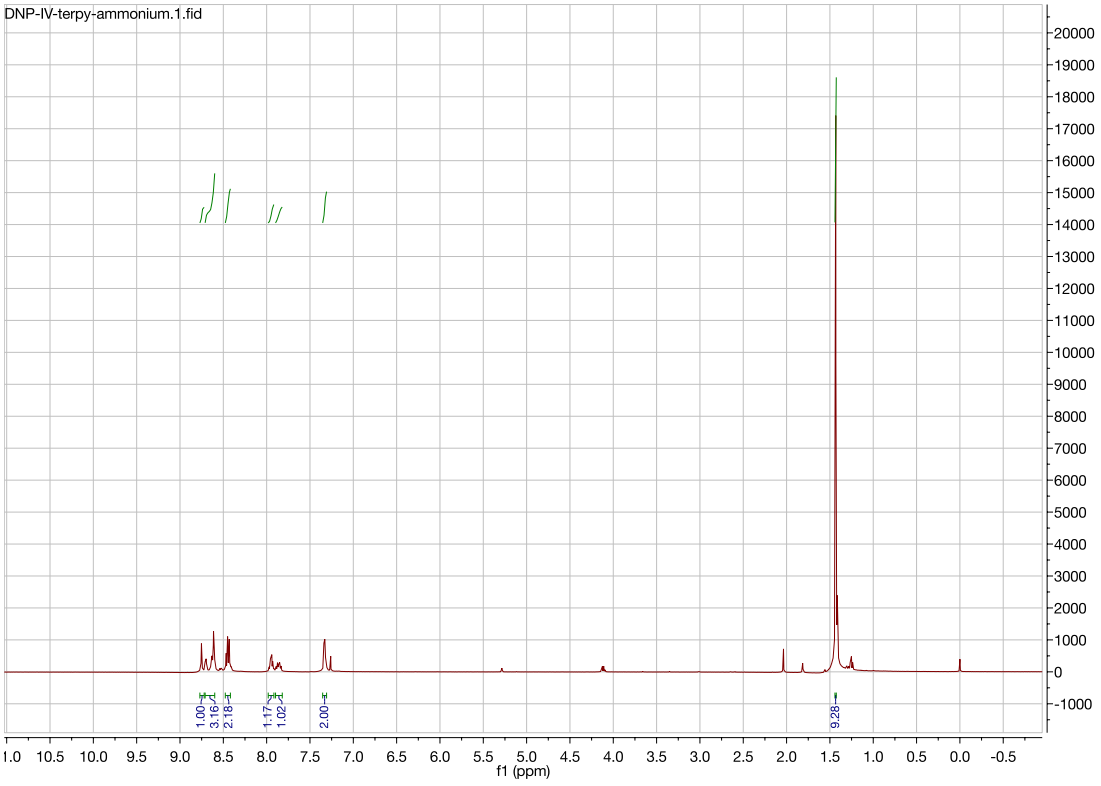

^{13}C NMR ($CDCl_3$, 125.8 MHz) spectrum of 6-(*tert*-butyl)-2,2':6',2''-terpyridine (**2.12.8**)

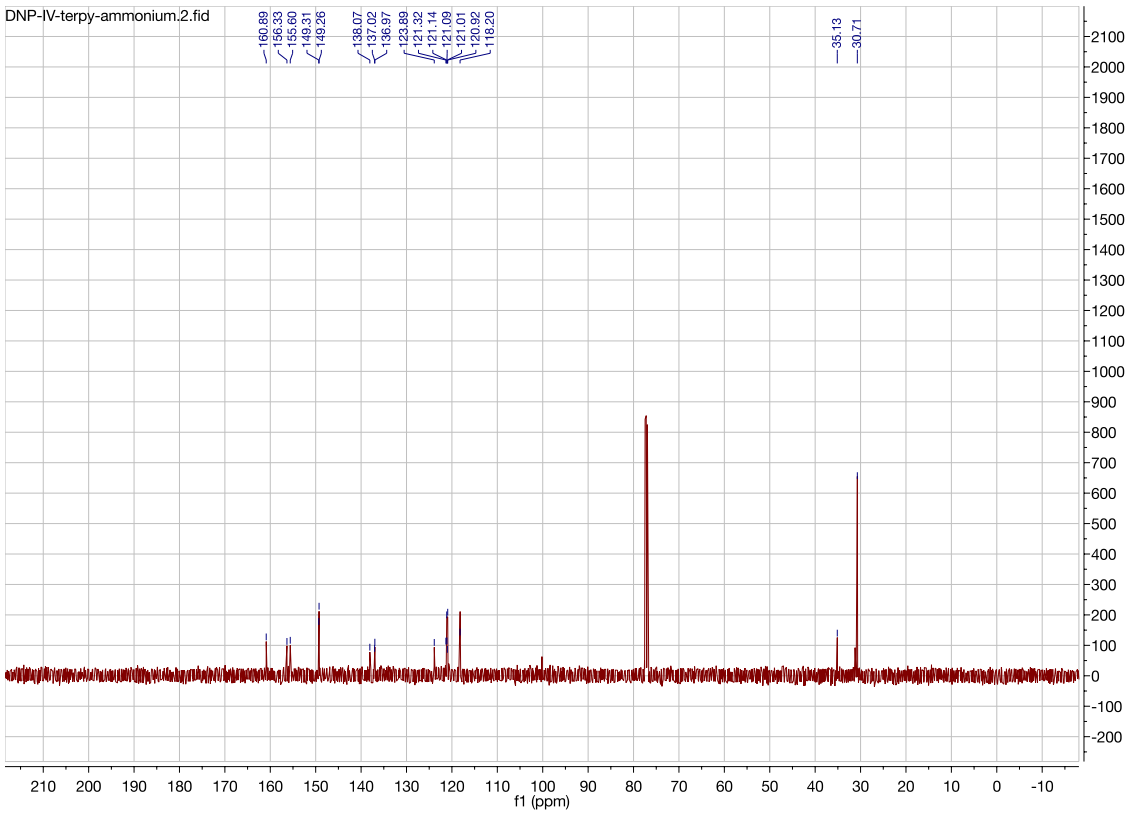

^{1}H ($CDCl_3$, 500 MHz) spectra of 4-((benzyloxy)methyl)-5-bromopyrimidine (**2.13.1**)

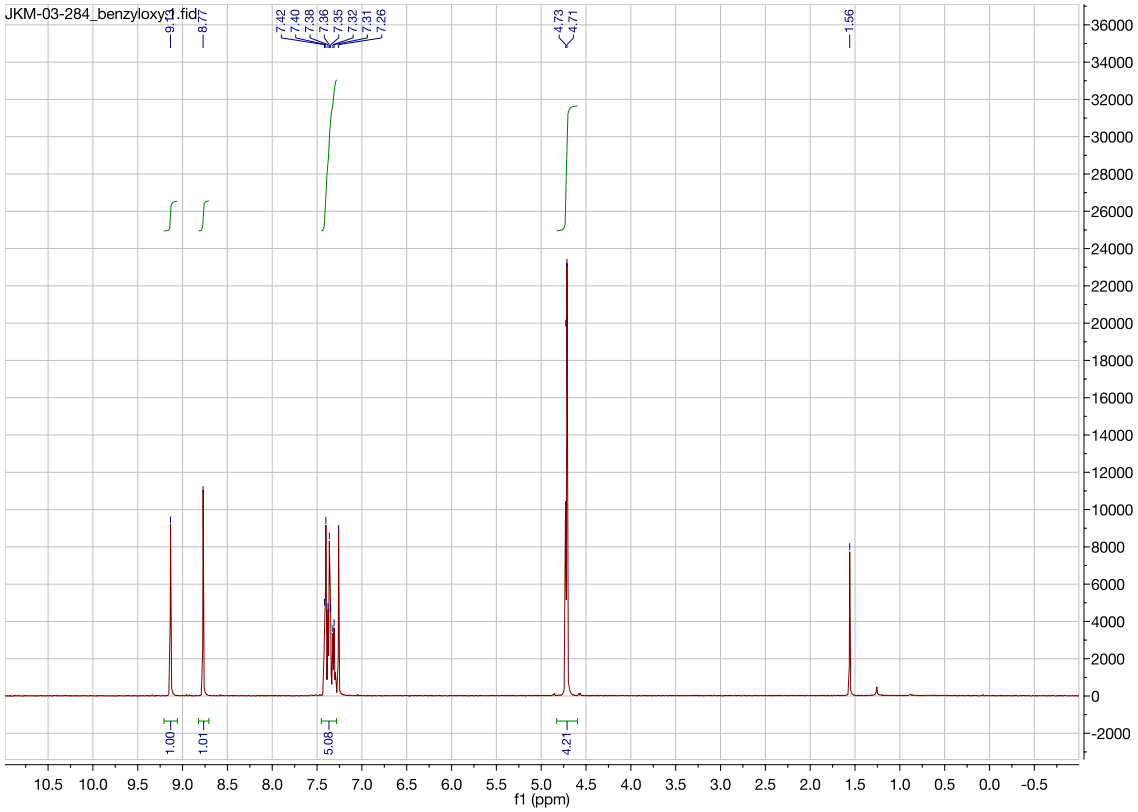

^{13}C NMR ($CDCl_3$, 125.8 MHz) spectrum of 4-((benzyloxy)methyl)-5-bromopyrimidine (**2.13.1**)

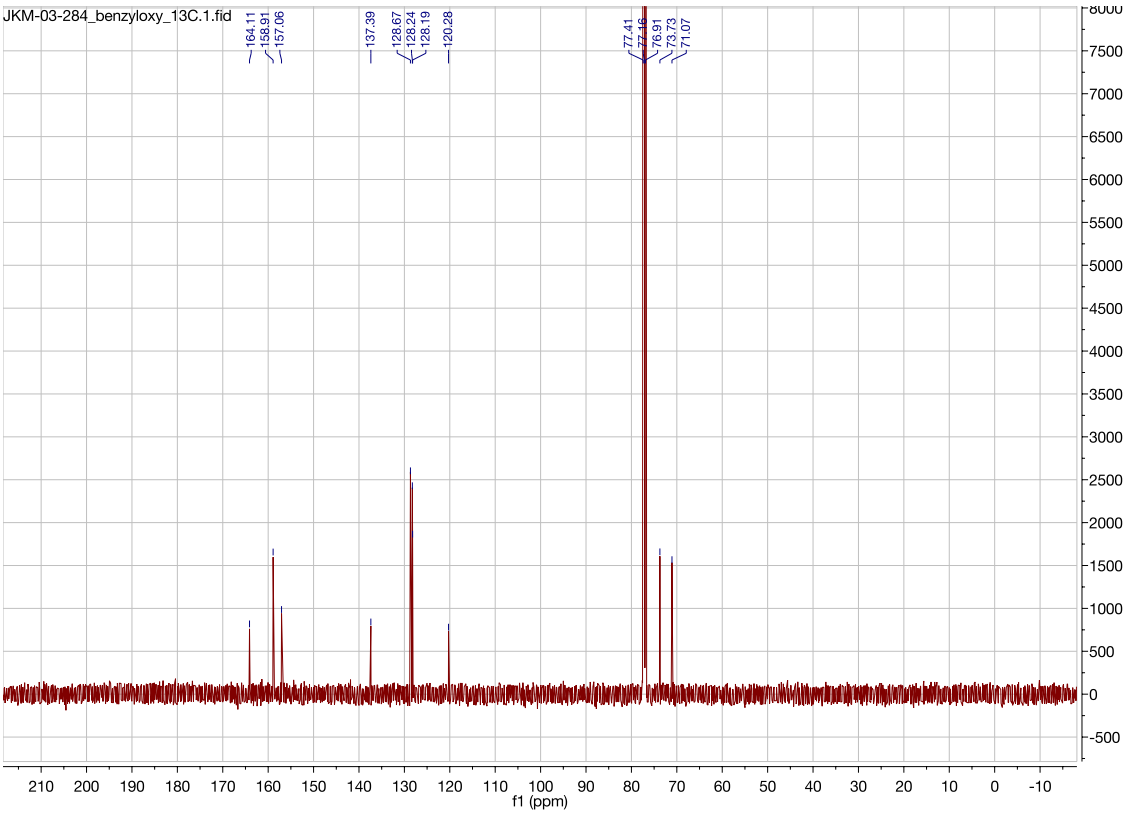

^{1}H NMR ($CDCl_3$, 500 MHz) spectrum 3-bromo-4-methyl-2-(1-tosylpiperidin-4-yl)pyridine and 5-bromo-4-methyl-2-(1-tosylpiperidin-4-yl)pyridine (**2.13.2**)

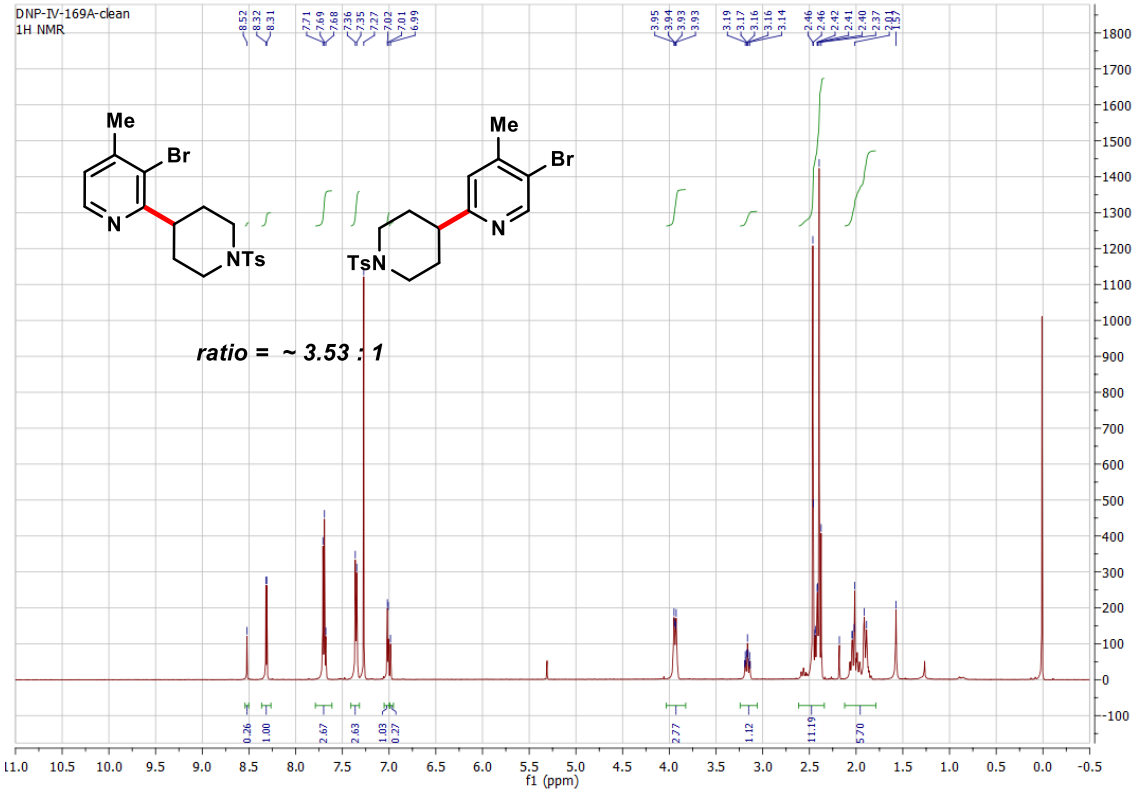

^{13}C NMR ($CDCl_3$, 125.8 MHz) spectrum of 3-bromo-4-methyl-2-(1-tosylpiperidin-4-yl)pyridine and 5-bromo-4-methyl-2-(1-tosylpiperidin-4-yl)pyridine (**2.13.2**)

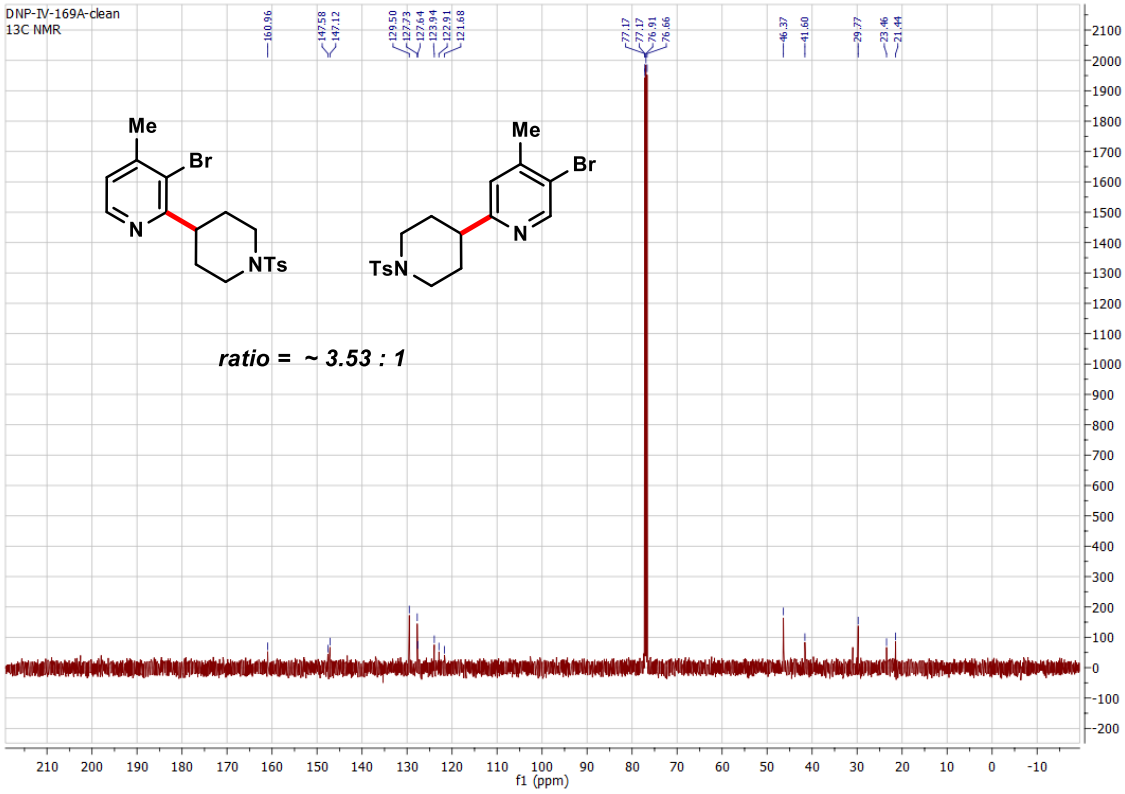

^{1}H ($CDCl_3$, 500 MHz) spectra of 3-bromo-4-methyl-2-phenethylpyridine (**2.13.3**)

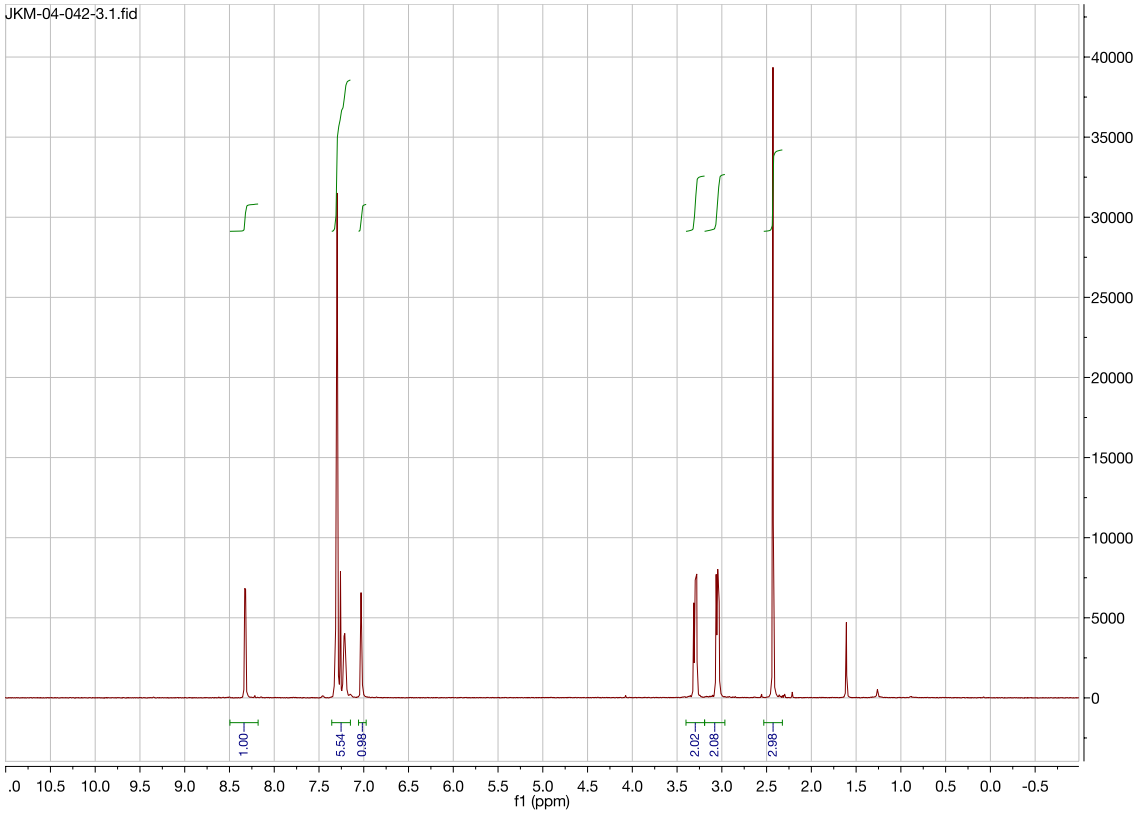

^{13}C NMR ($CDCl_3$, 125.8 MHz) spectrum of 3-bromo-4-methyl-2-phenethylpyridine (**2.13.3**)

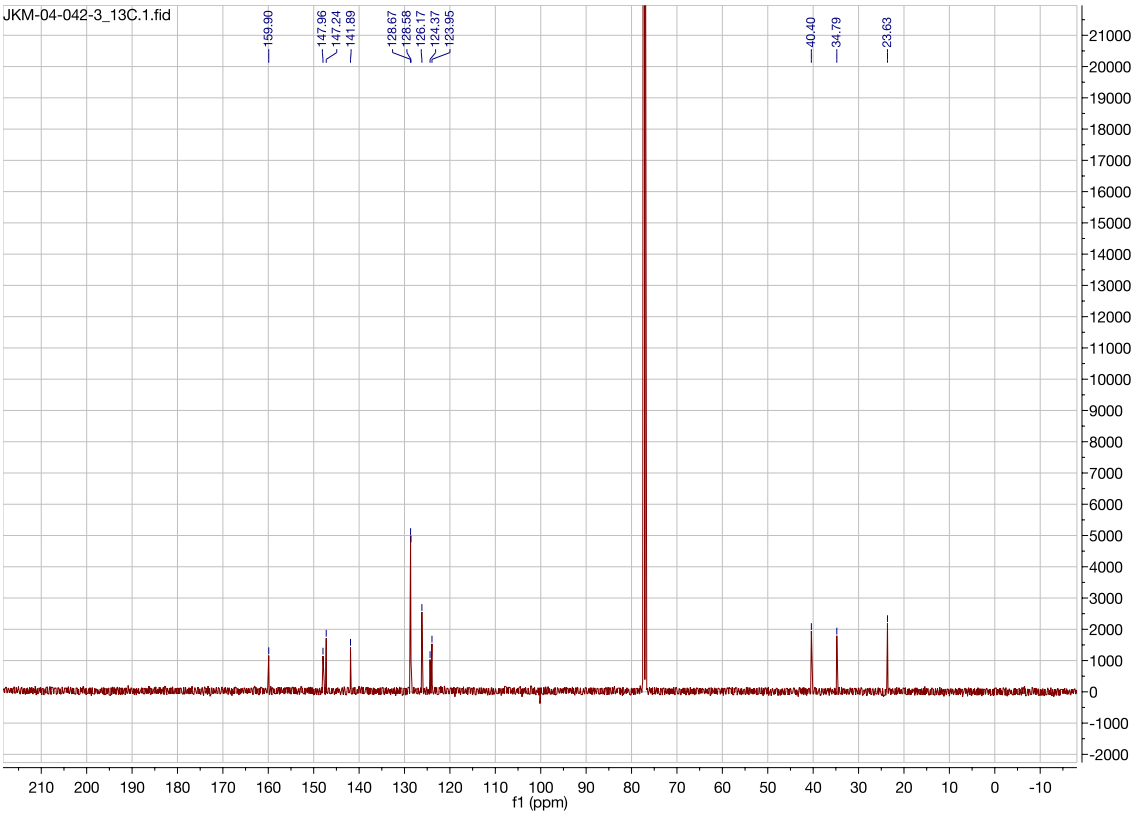

^{1}H ($CDCl_3$, 500 MHz) spectra of 4-chloro-2-phenethylquinoline (**2.13.4**)

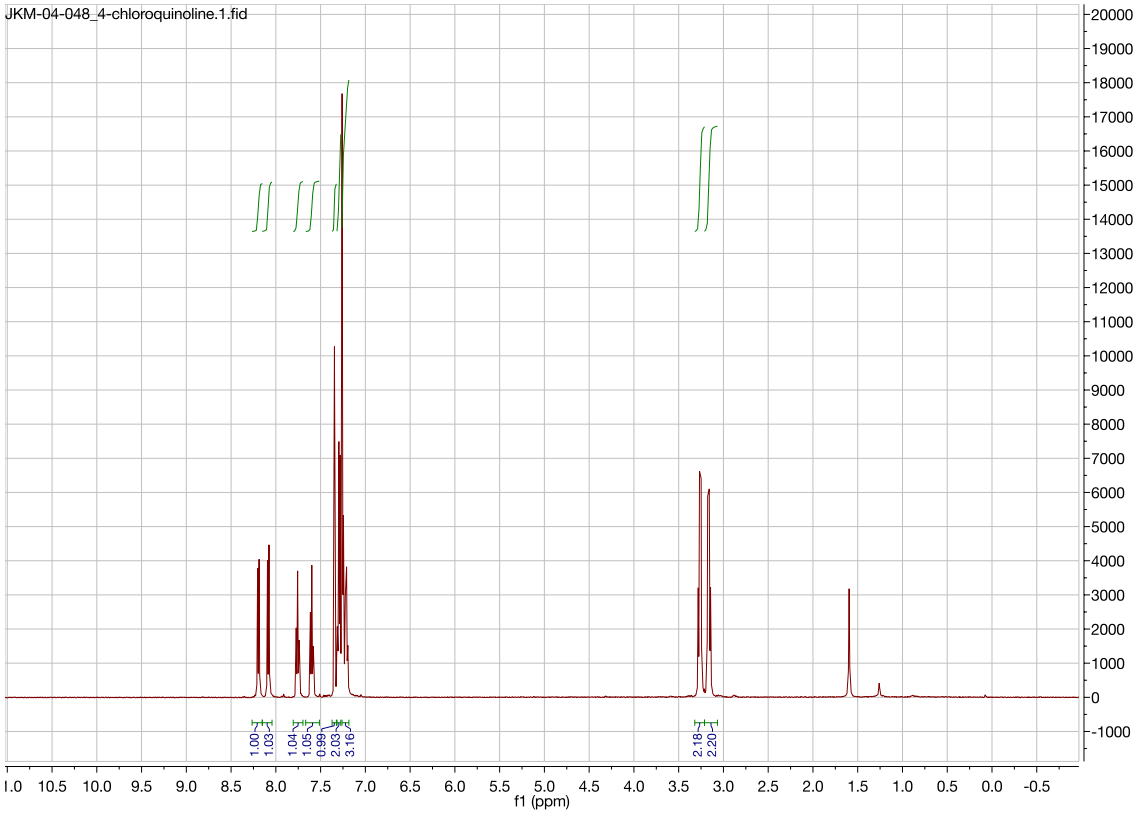

^{13}C NMR ($CDCl_3$, 125.8 MHz) spectrum of 4-chloro-2-phenethylquinoline (**2.13.4**)

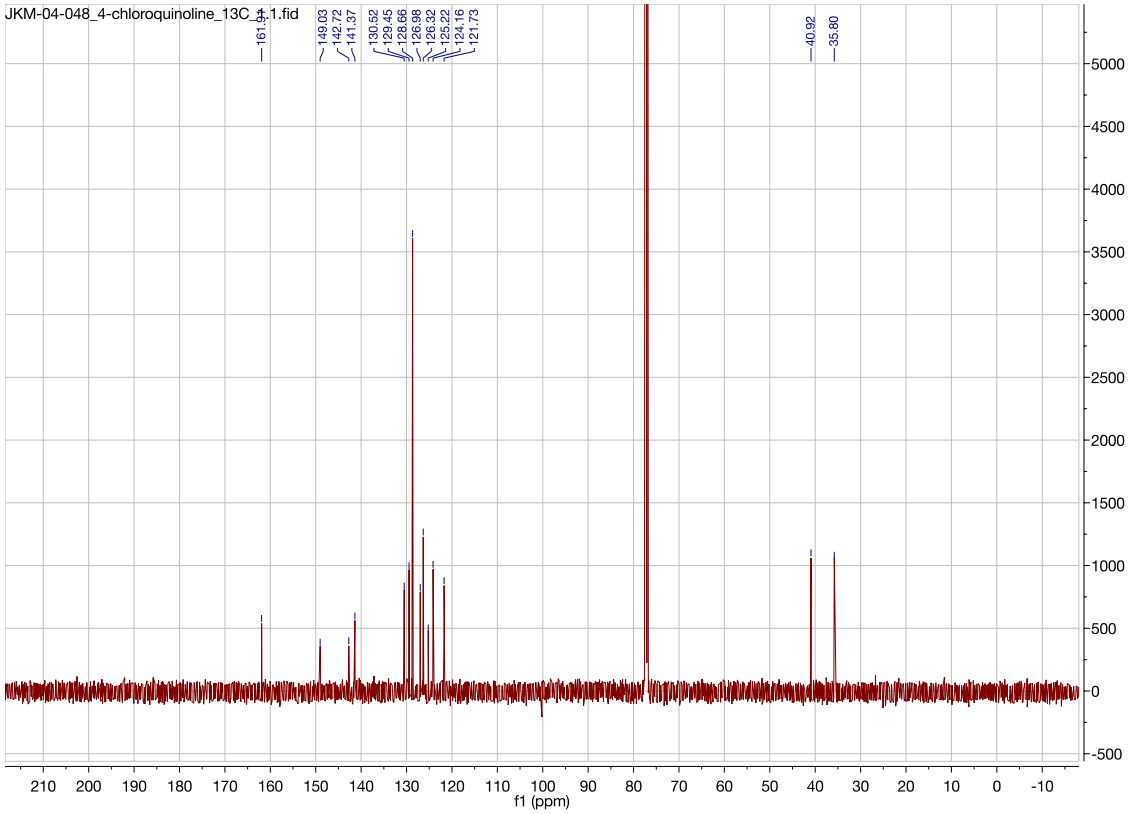

^{1}H ($CDCl_3$, 500 MHz) spectra of 4-bromo-3-isopropylisoquinoline (**2.13.5**)

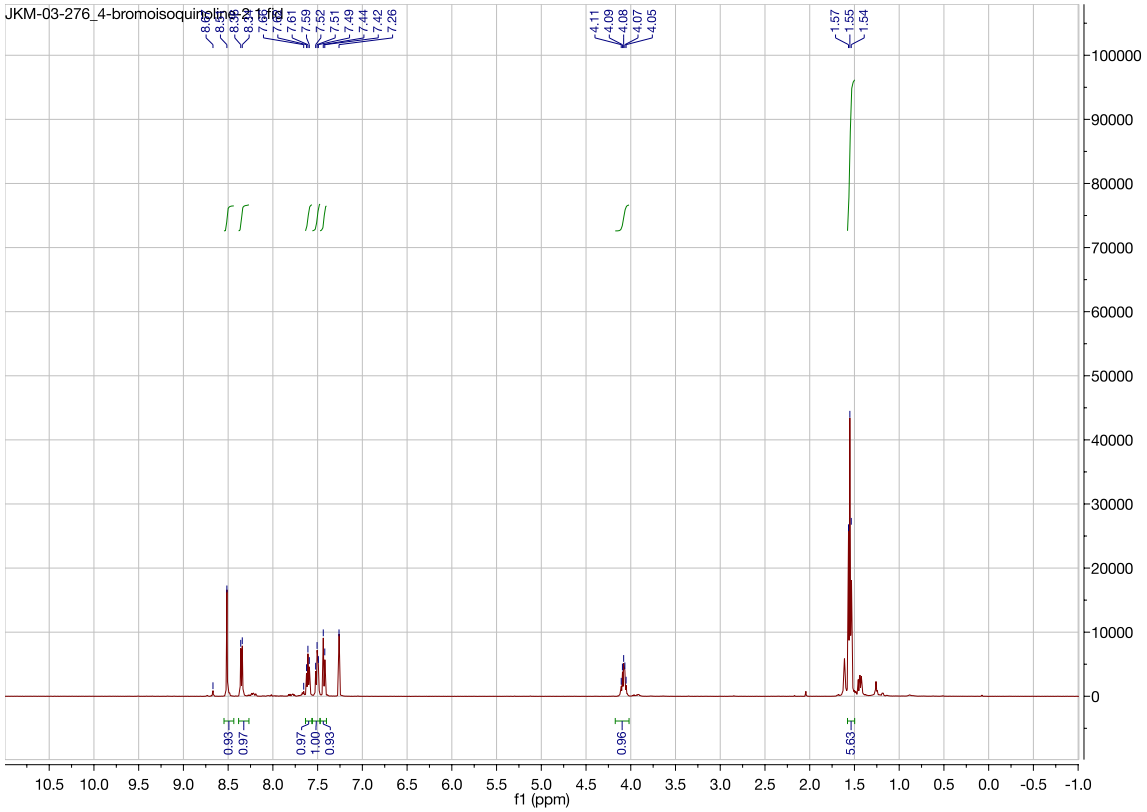

^{13}C NMR ($CDCl_3$, 125.8 MHz) spectrum of 4-bromo-3-isopropylisoquinoline (**2.13.5**)

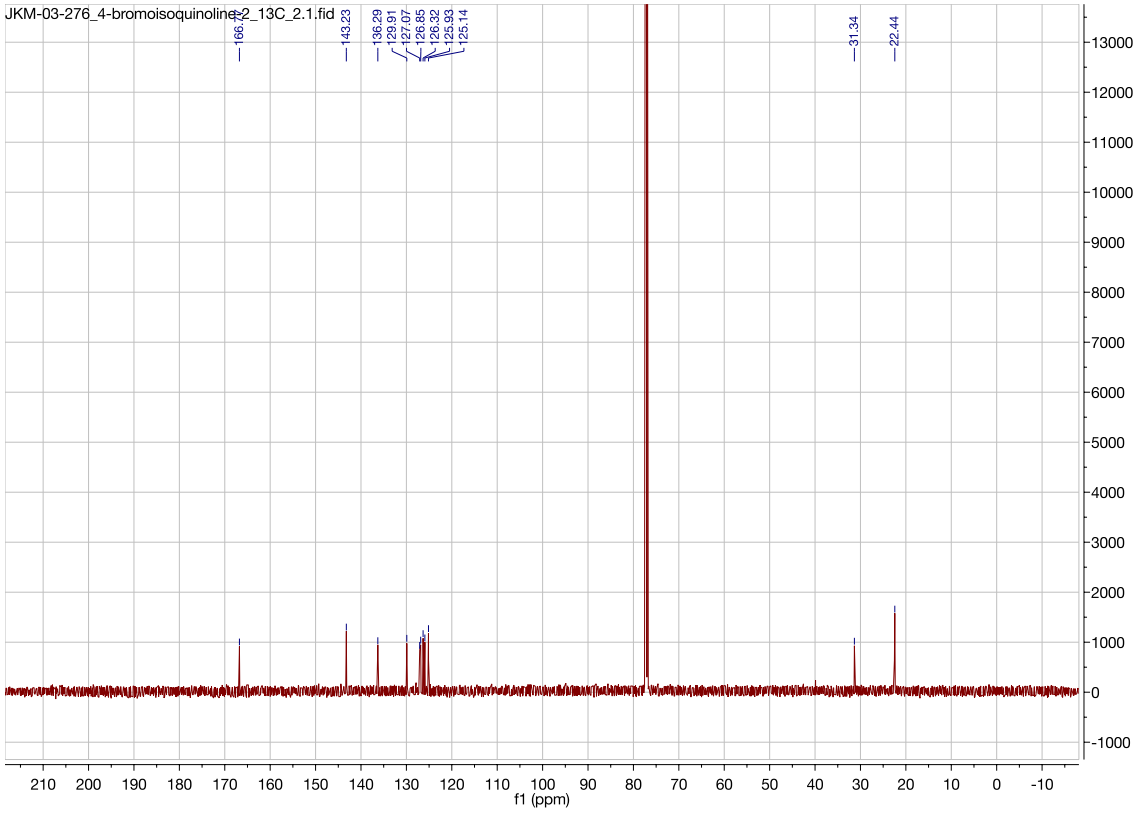

^{1}H ($CDCl_3$, 500 MHz) spectra of 4-bromo-1-isopropylisoquinoline (**2.13.6**)

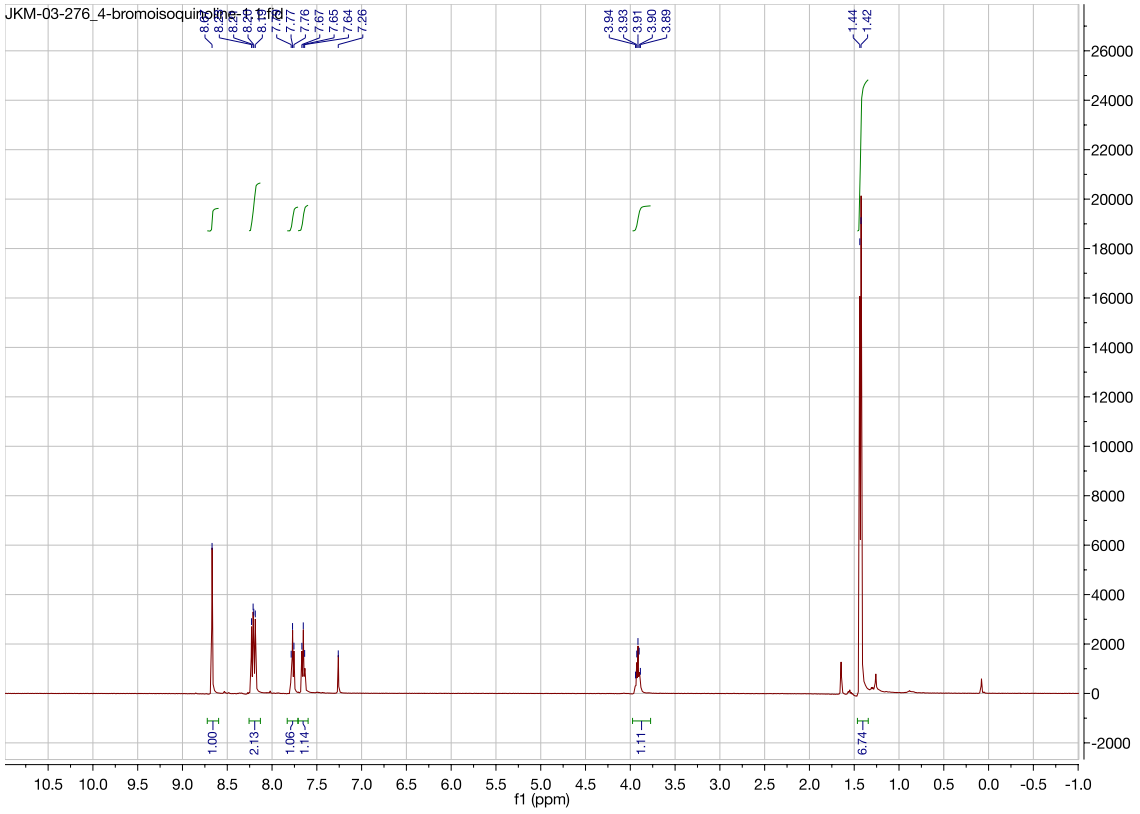

^{13}C NMR ($CDCl_3$, 125.8 MHz) spectrum of 4-bromo-1-isopropylisoquinoline (**2.13.6**)

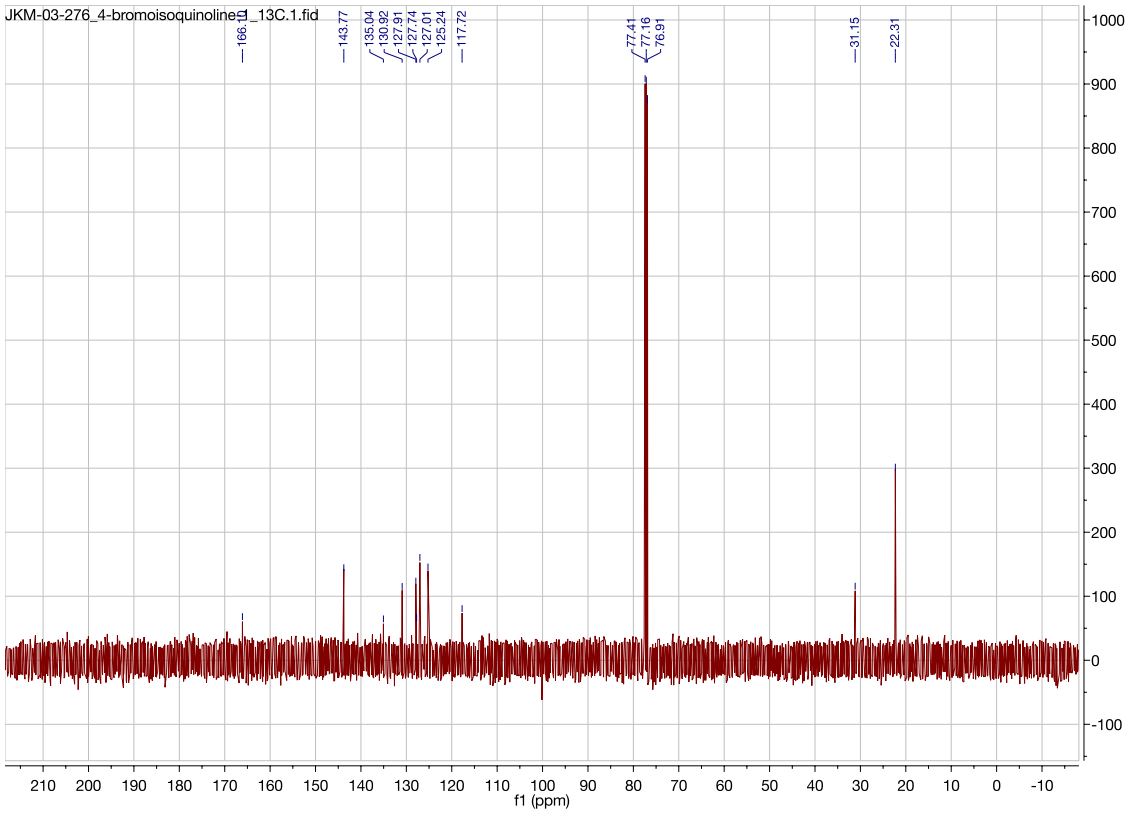

^{1}H NMR (acetone-d_6, 500 MHz) spectrum of Potassium trifluoro(2-methyl-1-phenylpropan-2-yl)borate (**1u**)

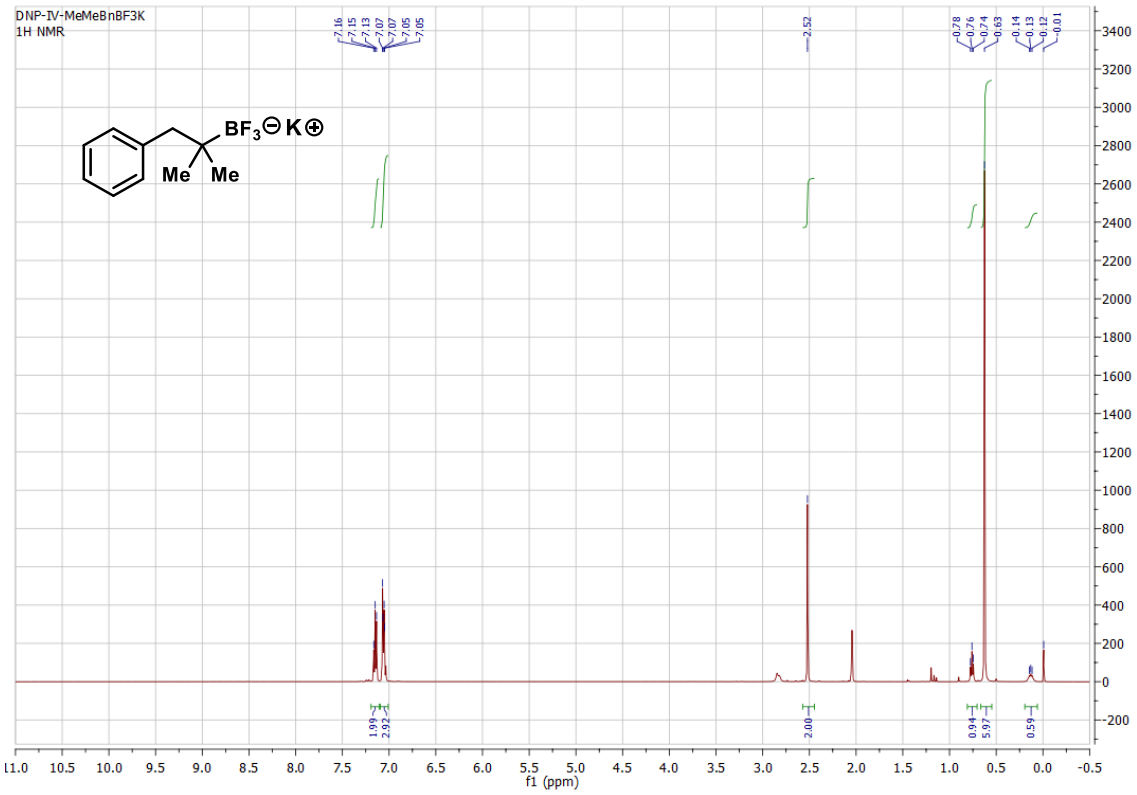

^{13}C NMR (acetone-d_6, 125.8 MHz) spectrum of Potassium trifluoro(2-methyl-1-phenylpropan-2-yl)borate (**1u**)

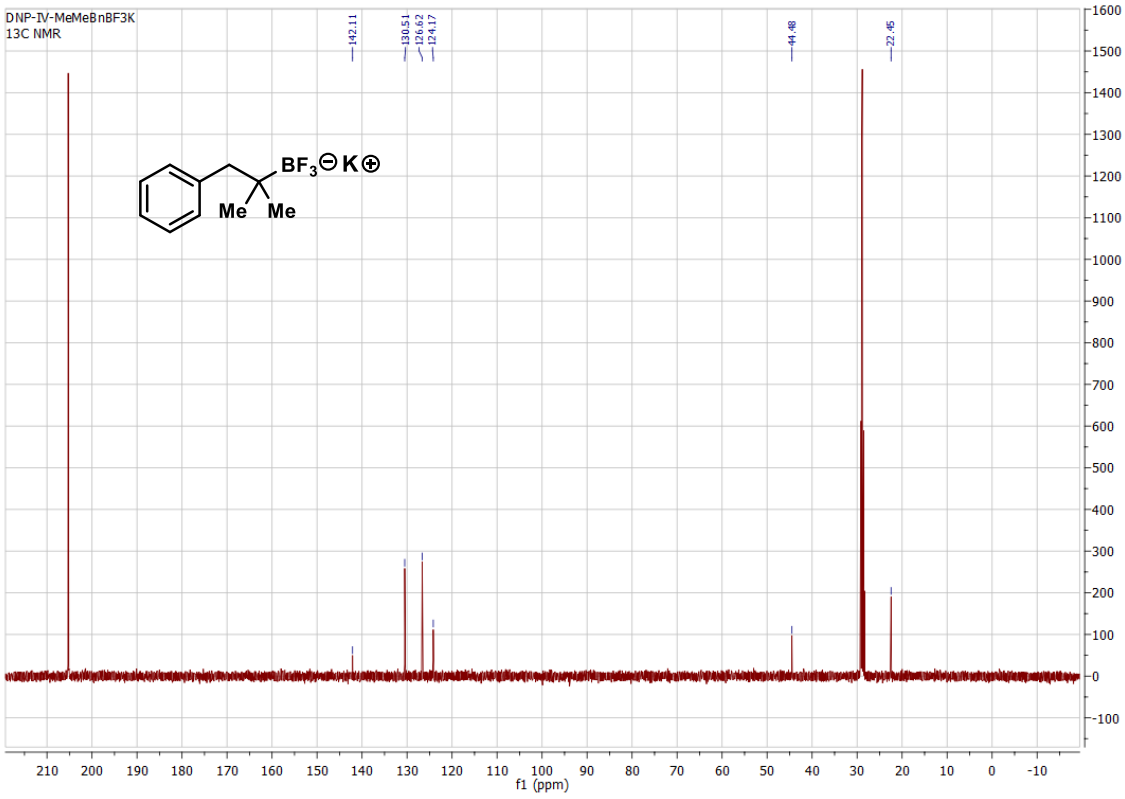

^{19}F NMR (acetone-d_6, 470.7 MHz) spectrum of Potassium trifluoro(2-methyl-1-phenylpropan-2-yl)borate (**1u**)

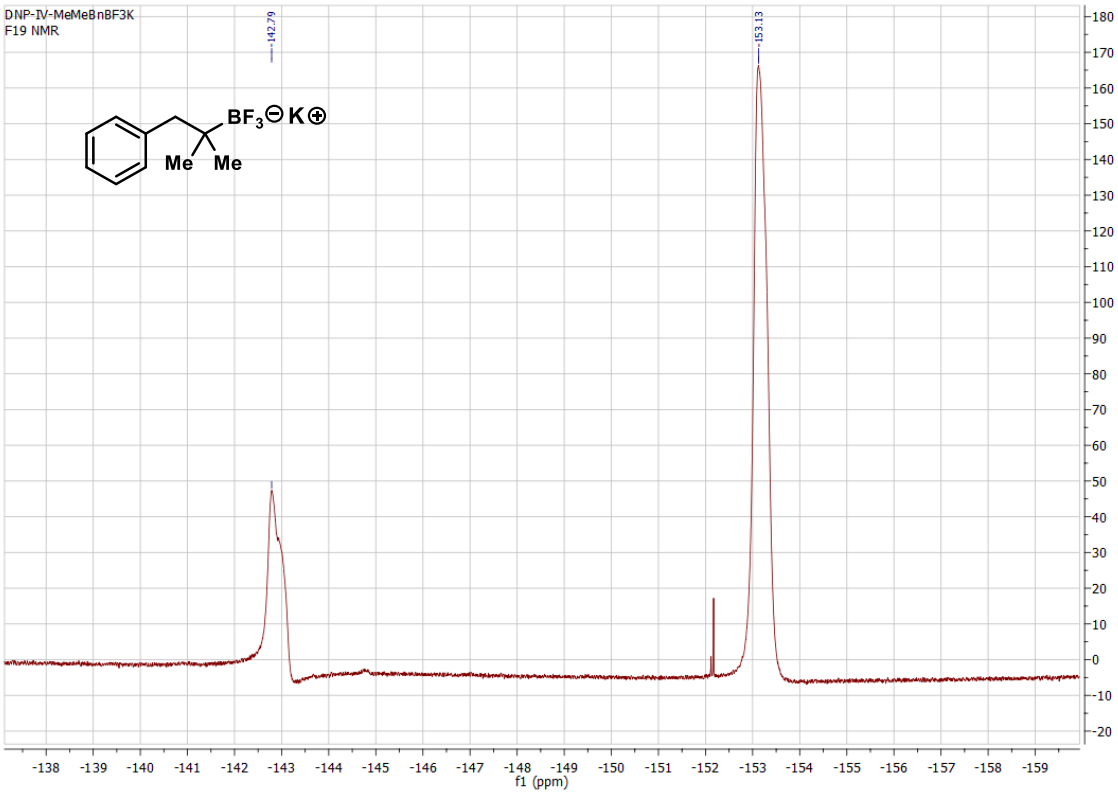

^{11}B NMR (acetone-d_6, 128.4 MHz) spectrum of Potassium trifluoro(2-methyl-1-phenylpropan-2-yl)borate (**1u**)

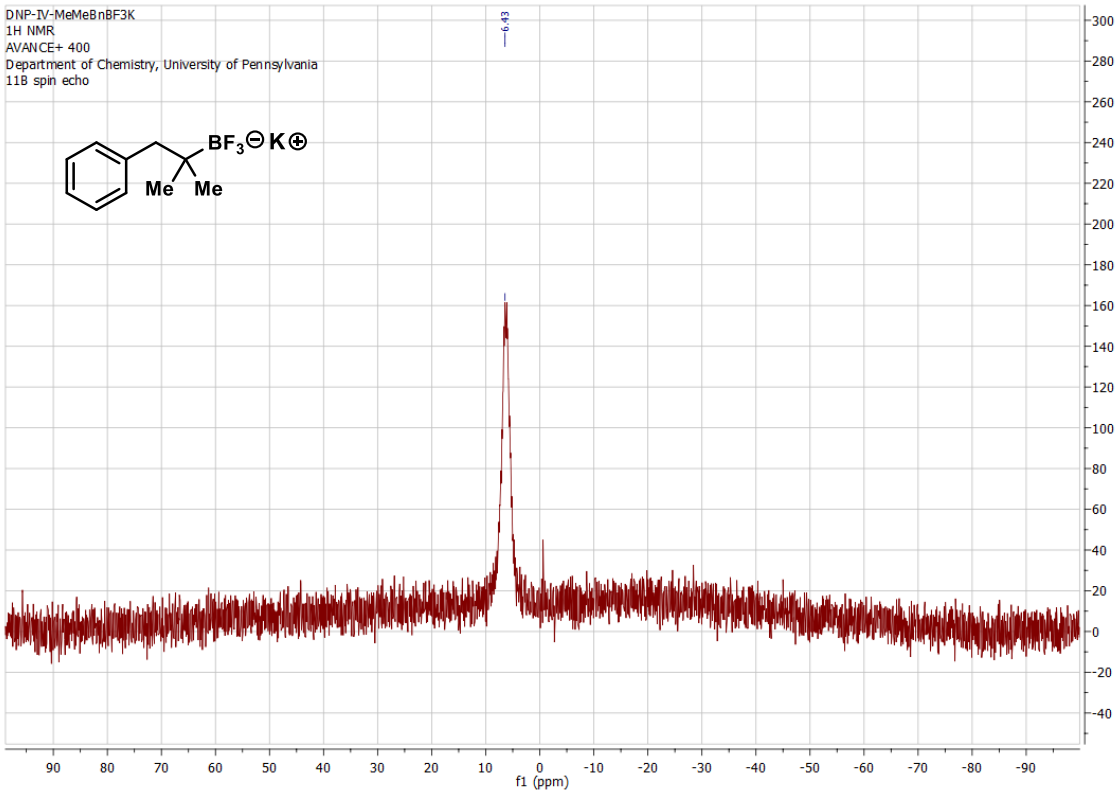

^{1}H NMR (CD_3CN, 500 MHz) spectrum of quinoline

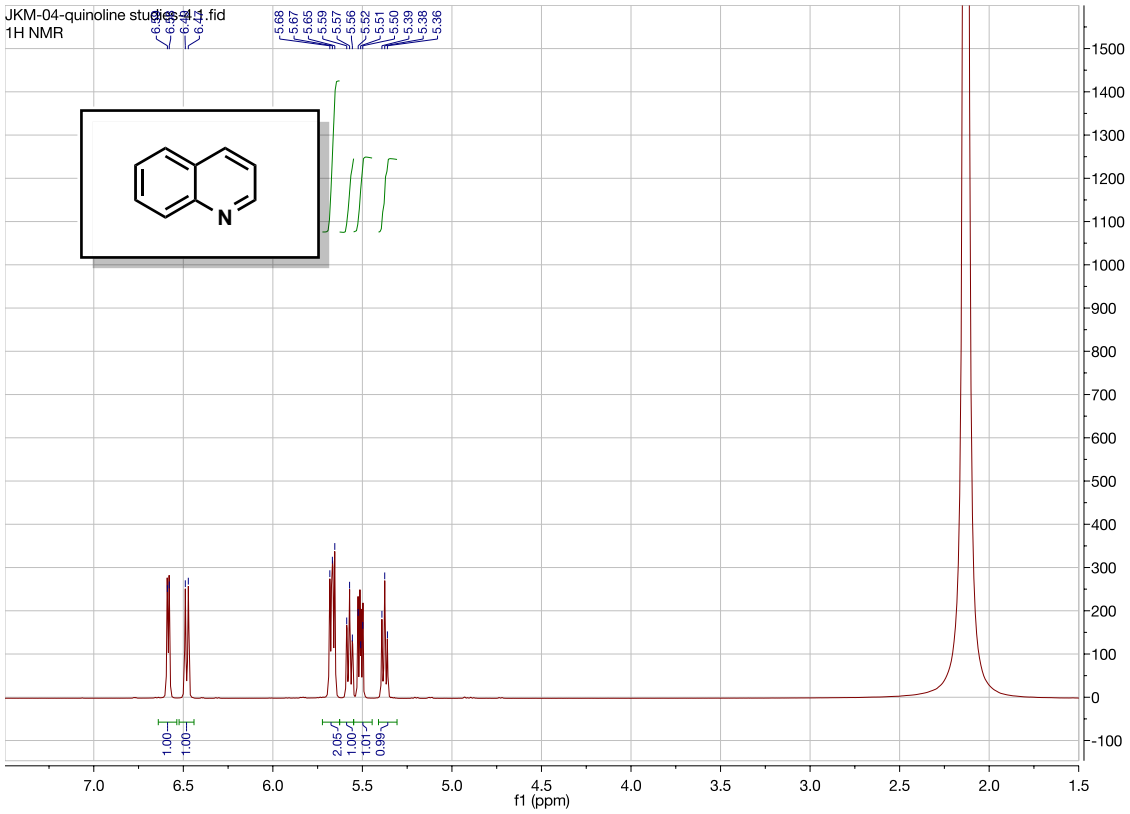

^{1}H NMR (CD_3CN, 500 MHz) spectrum of quinoline + TFA

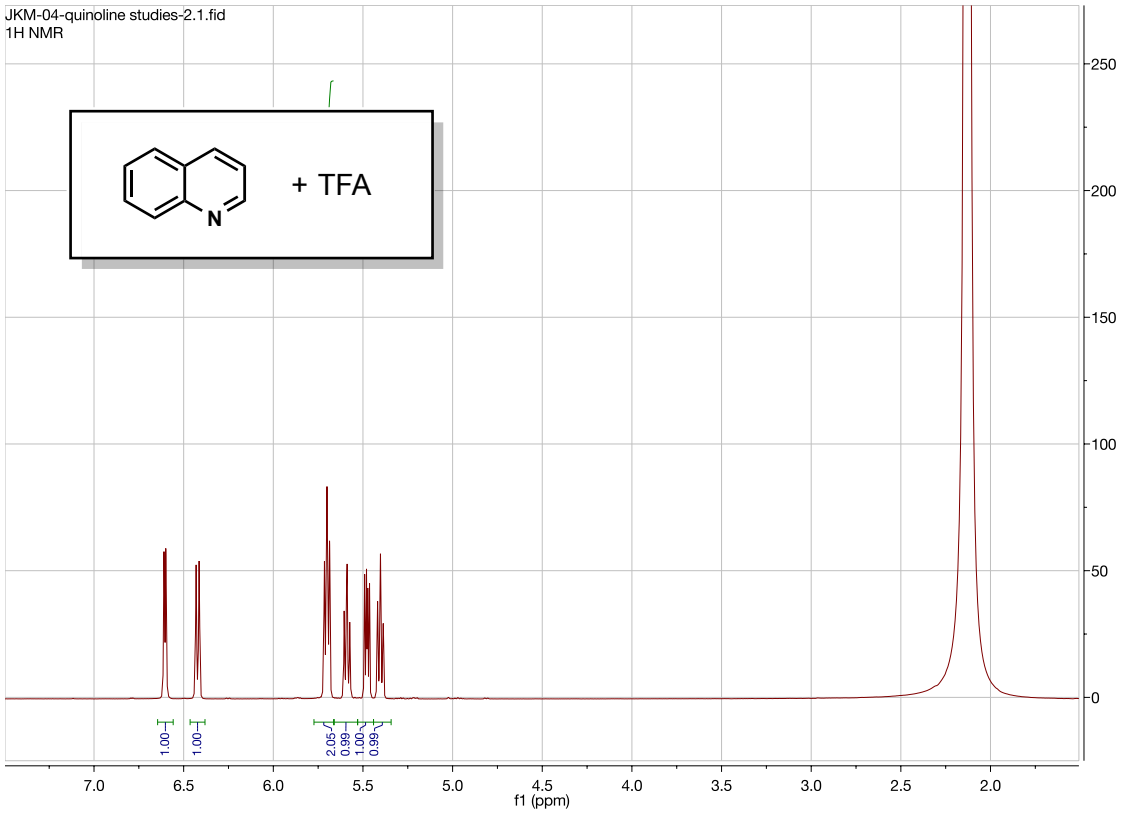

^{1}H NMR (CD_3CN, 500 MHz) spectrum of quinoline + BF_3

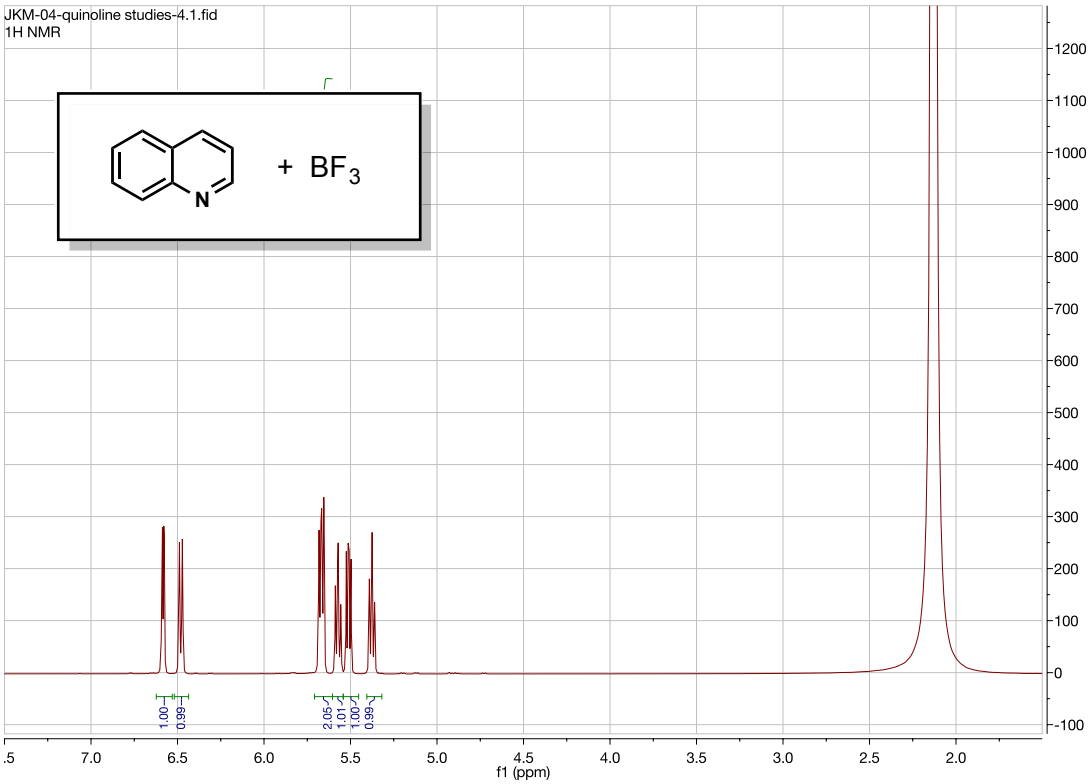

^{1}H NMR (CD_3CN, 500 MHz) spectrum of quinoline + TFA + BF_3

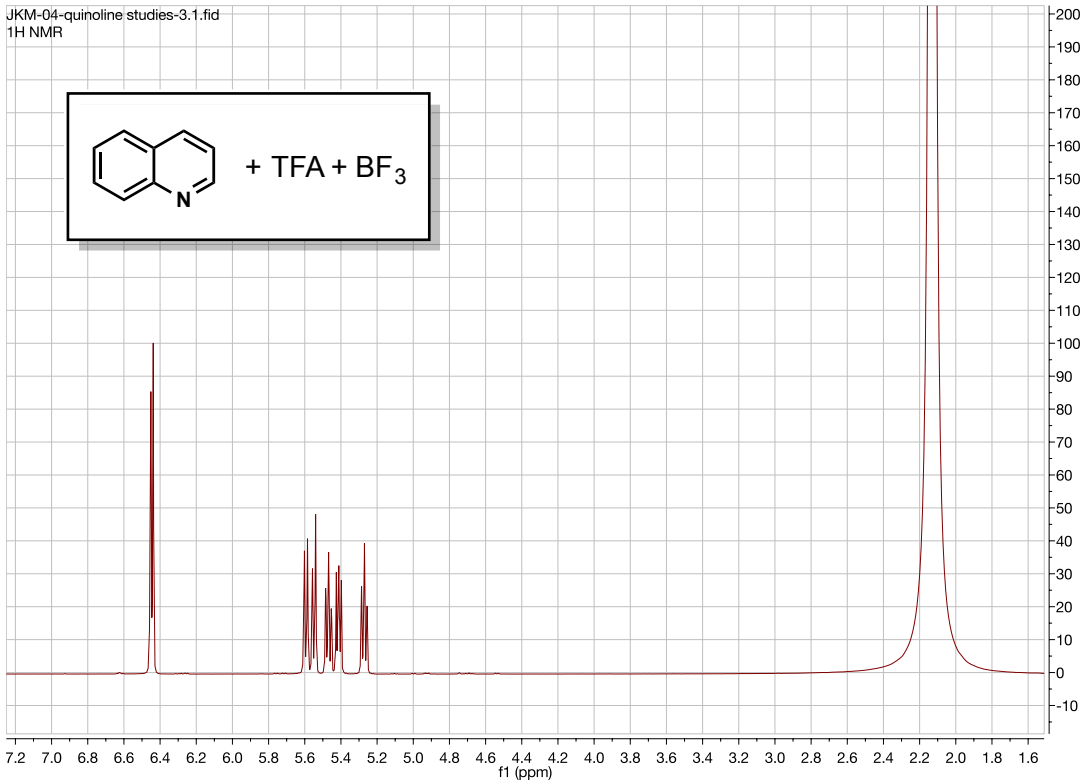

^{13}C NMR (CD_3CN, 125.8 MHz) spectrum of quinoline

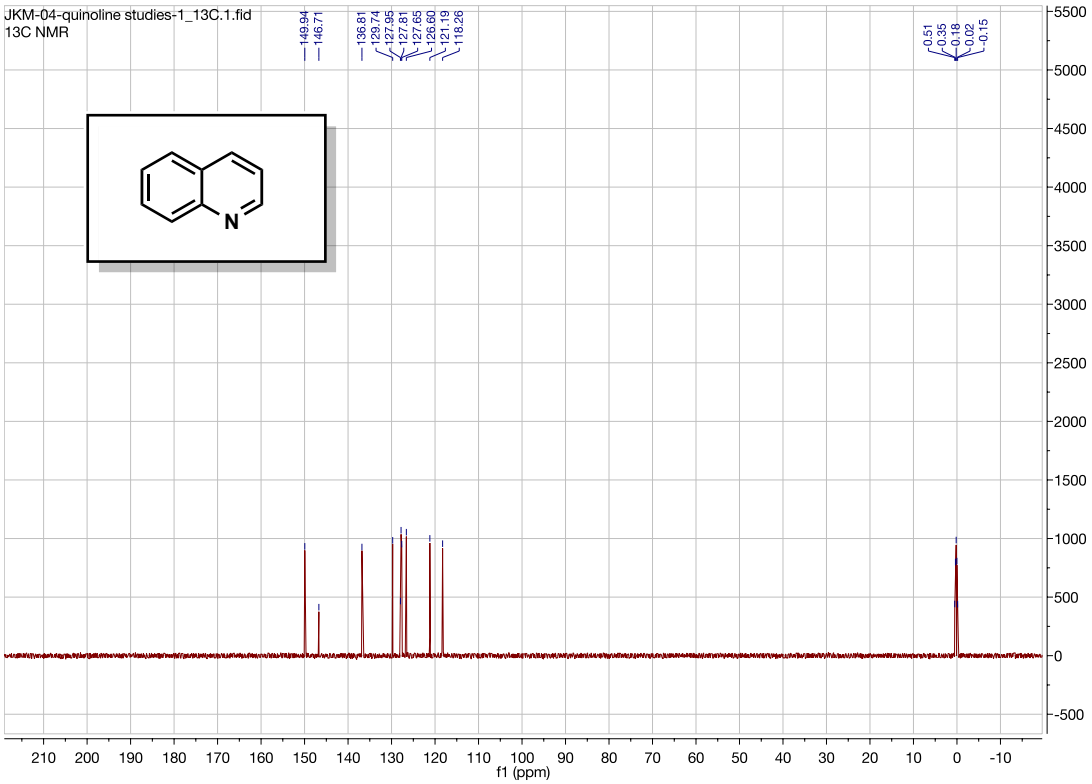

^{13}C NMR (CD_3CN, 125.8 MHz) spectrum of quinoline + TFA

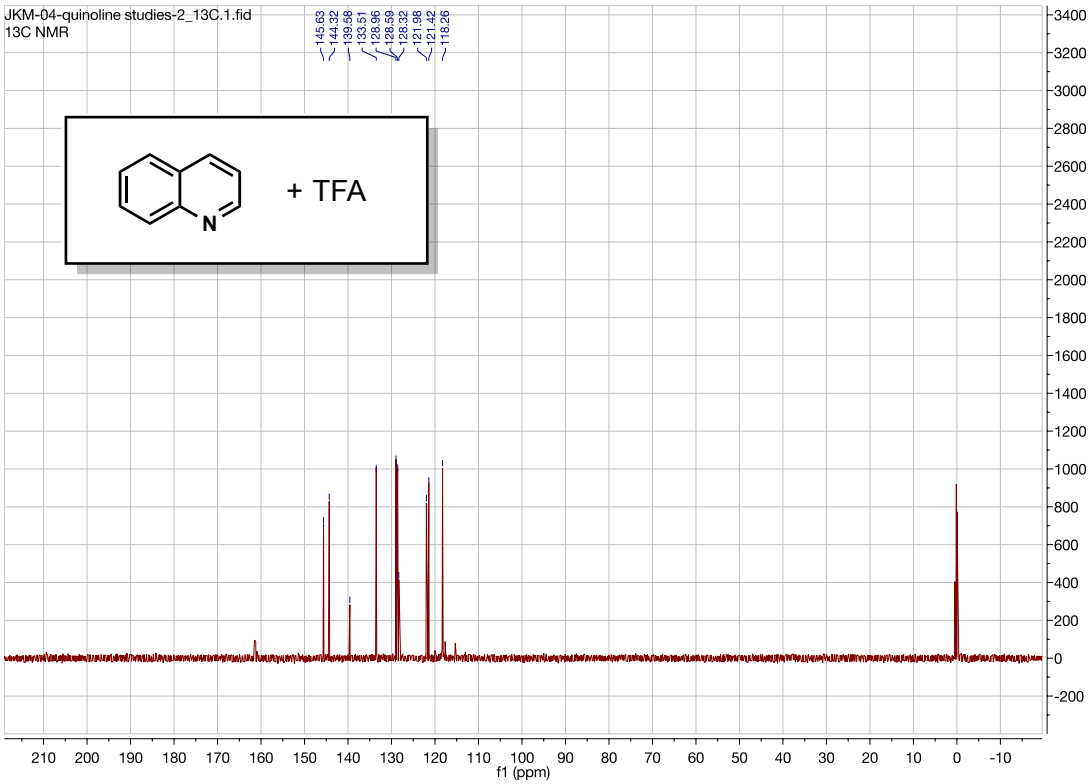

^{13}C NMR (CD_3CN, 125.8 MHz) spectrum of quinoline + BF_3

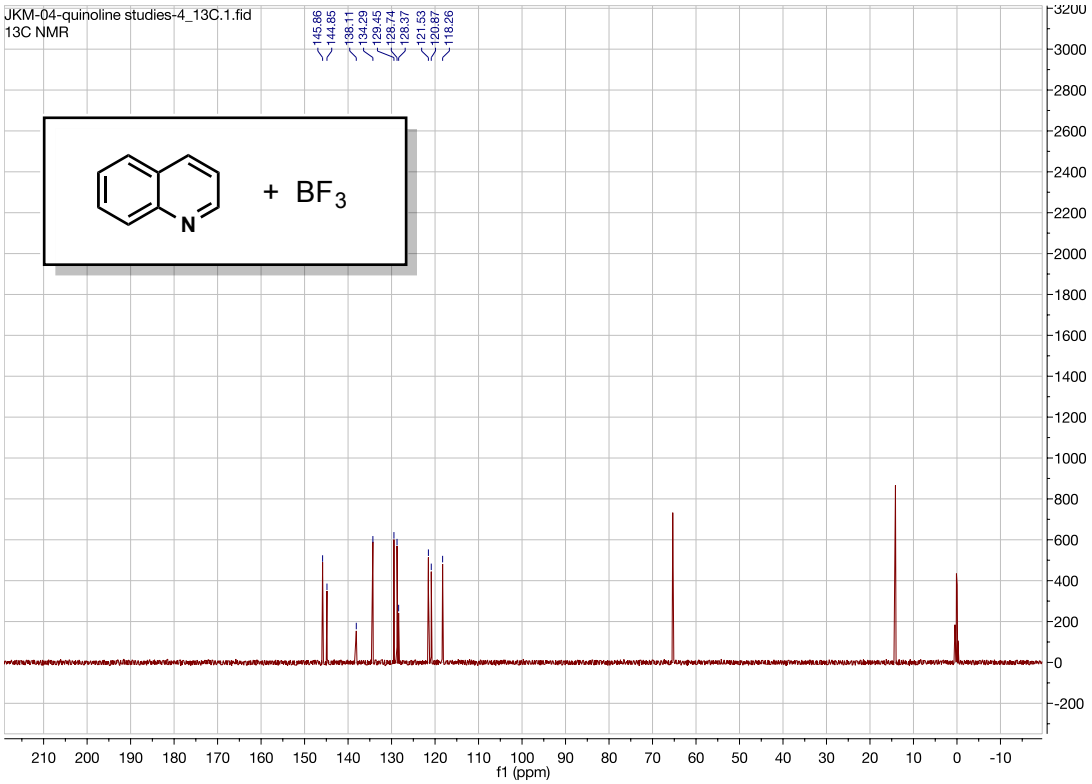

^{13}C NMR (CD_3CN, 125.8 MHz) spectrum of quinoline + TFA + BF_3

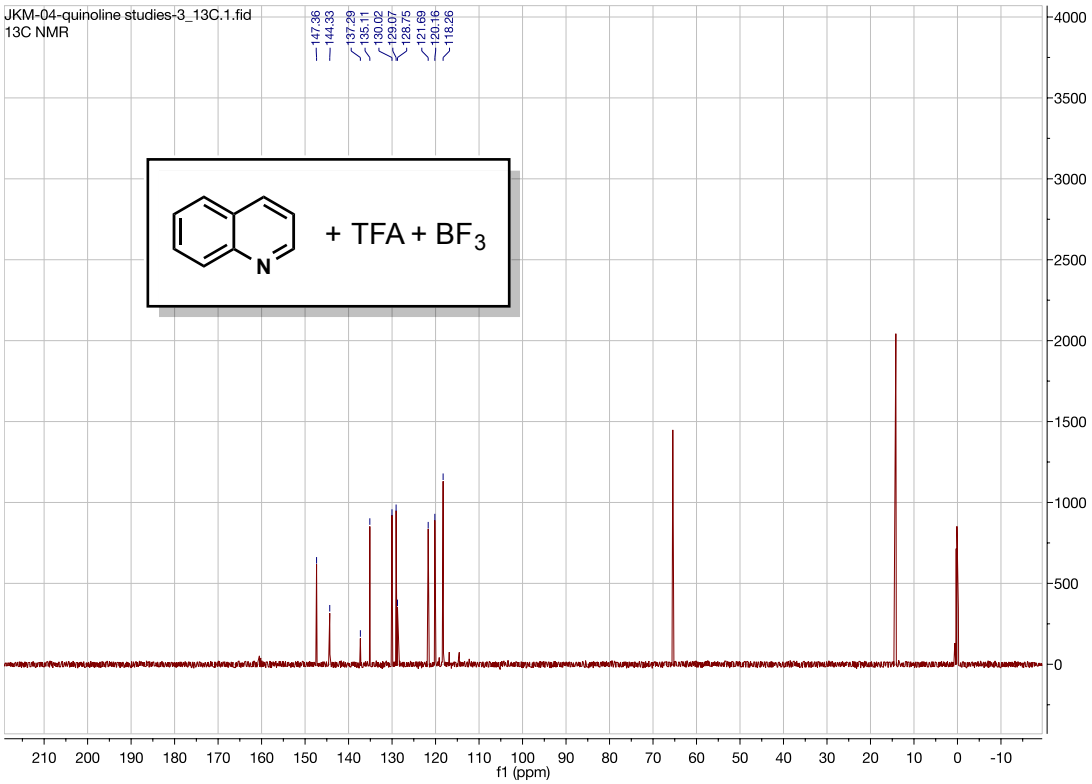

Chapter 3. Accesssing Novel Heteroaryl Chromanones *via* Photoredox-Mediated Alkylation

3.1 Introduction

For decades, chromanones have captured the attention of the synthetic community because of their prevalence in natural products and in unnatural, biologically relevant compounds.[1†] Given the immense interest in the chromanone cores as potential pharmacological cores, numerous biochemists have studied the biological pathway used to construct the flavone moieties. Based on these aforementioned studies, the proposed biological pathway starts with acetyl CoA and a chalcone scaffold.[2] After the initial coupling, the requisite chalcone can cyclize *via* an oxo-Michael addition to the enone to afford various flavanones. Subesquent *in vivo* modifications provide unsaturated bioactive intermediates.

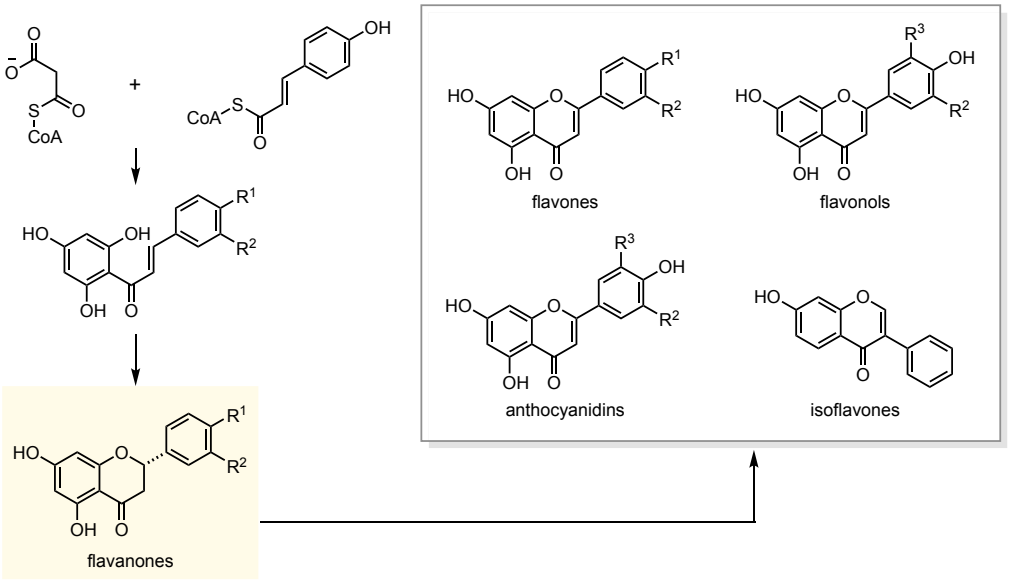

Figure 3.1. Flavone biosynthesis.

---

† Reproduced in part from Matsui, J. K.; Molander, G. A. *Org. Lett.* **2017**, *19*, 950.

Although there are a large number of 2-aryl-substituted chromanones reported in the literature, there remain significant gaps among certain subclasses of these molecules. For example, there are less than 30 reported 2-quinolinyl-substituted 4-chromanones and no examples of 2-isoquinolinyl-substituted 4-chromanones.

To date, 2-aryl-4-chromanones are primarily accessed through a chalcone precursor that is subsequently cyclized to form the pyranone ring under acidic (Figure 3.2), basic, or photochemical conditions.[3] Although these routes are effective for providing targeted substructures, accessing a diverse array of aryl- or heteroaryl-substituted chromanones is challenging using a late-stage cyclization pathway.

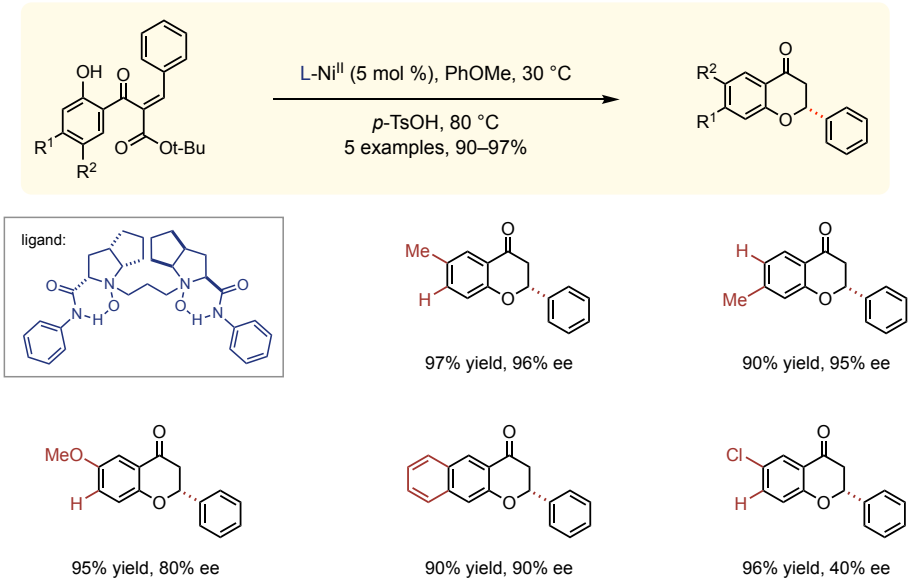

Figure 3.2. Oxa-Michael cyclization to access flavanones.

3.2 Reaction Design and Results

Inspired by these shortcomings, a photocatalyzed Minisci reaction was envisioned. Thus, we sought to deviate from the dual catalytic manifold into a singular photocatalytic cycle. Combining photoredox catalysis and C-H functionalization of heteroarenes represents a more

sustainable approach to molecule construction that is being employed with increasing frequency.[4] Until recently, Minisci reactions typically required superstoichiometric amounts of oxidant for radical generation under forcing conditions.[5] Notably, our laboratory demonstrated trifluoroborates to be viable radical sources under "classical" Minisci reaction conditions, requiring either manganese or silver oxidant.[5f,g] Radical intermediates have been accessed via photocatalysis in a significantly milder manner, but limitations remain, including the need for excess radical precursor,[4d] expensive photocatalysts,[4e] or complex radical precursors that limit substrate scope.[4e] Keeping these limitations in mind, alkyltrifluoroborates appeared to be an attractive alternative given the precedent for single-electron oxidation of trifluoroborates *via* photoredox catalysis reported by Akita and coworkers.[6] Therefore, a robust method was sought to harness the reactivity of 2-trifluoroborato-4-chromanones as radical precursors to construct a wide range of 2-heteroaryl-4-chromanones in a photo-catalytic fashion that would address the shortcomings of previously reported methods.

In this vein, we recently developed a protocol for alkylation of heteroarenes in which primary, secondary, and tertiary alkyltrifluoroborates could be used in photoredox Minisci chemistry,[7] allowing alkylation of numerous heteroarenes. The chemistry made use of an organic photocatalyst (a mesityl acridinium dye) and an inexpensive, mild oxidant, and required only one equivalent of alkyltrifluoroborate as an alkyl radical precursor (Figure 3.3).

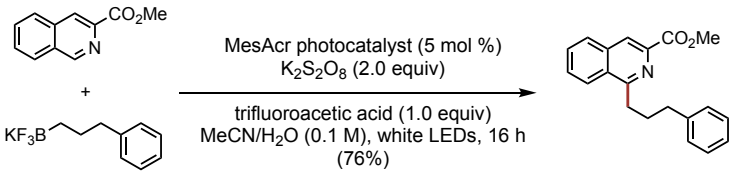

Figure 3.3. Previous demonstration of photoredox alkyltrifluoroborate C–H alkylation.

We set out to parlay this development into a method for the construction of heteroaromatic flavanones. A mechanistic scenario (Figure 3.4) was envisioned in which the excited state of a

suitable photocatalyst possessed a redox potential sufficiently high to induce a single-electron oxidation of the trifluoroboratochromanone (I) to afford the α-alkoxy radical (II). The stabilized radical (II) would add to the heteroarene, activated by a Bronsted acid. An appropriate oxidant would be required to regenerate the ground state photocatalyst as well as to rearomatize intermediate III via hydrogen atom transfer (HAT).

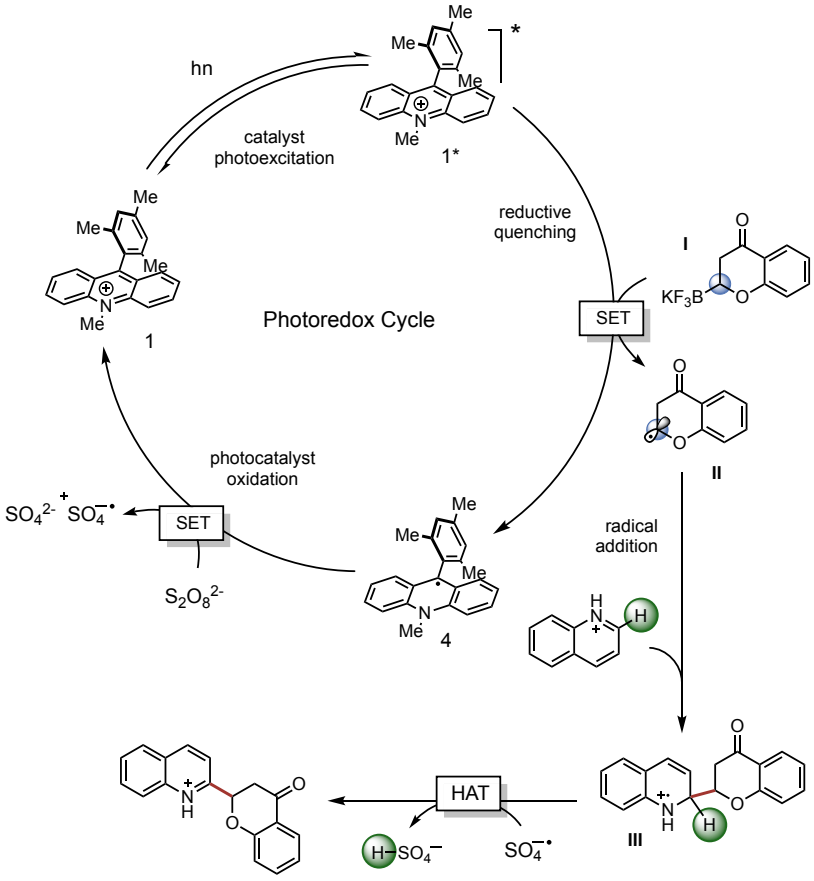

Figure 3.4. Proposed mechanism.

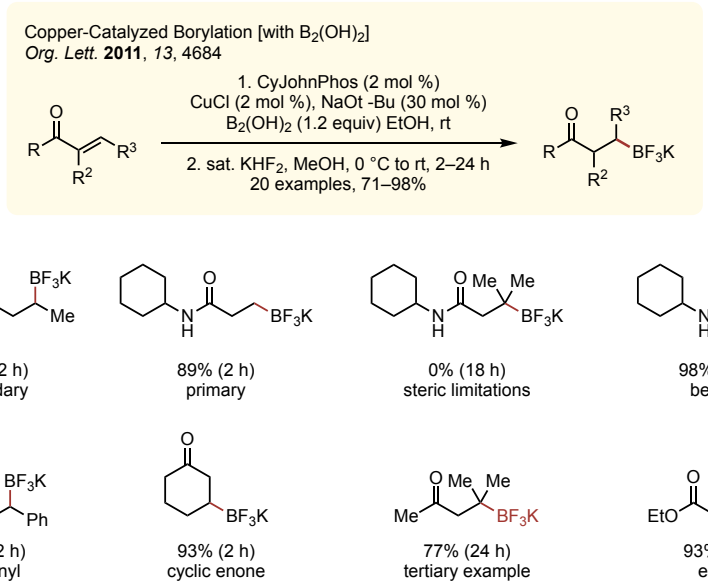

Figure 3.5. Borylation procedure for enone scaffolds.

As alluded to above, access to the requisite 2-trifluoroborato-4-chromanones was achieved through a conjugate borylation reaction previously reported by our group (Figure 3.5).[8] Although a variety of cyclic and acyclic enones were reported to engage in the β-borylation, to the best of our knowledge there were no reports of pyranone borylation (Figure 3.6). Nonetheless, with minimal optimization a variety of chromanones were acquired with excellent tolerance of functional groups and diverse substitution patterns (Figure 3.7).

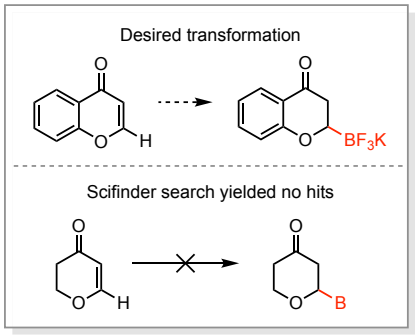

Figure 3.6. Literature search for pyranone core.

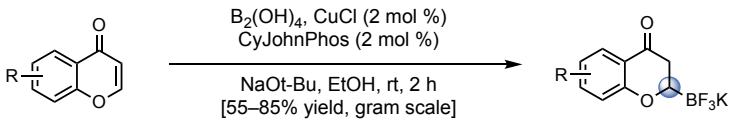

Figure 3.7. Borylation of chromanone scaffolds.

With several 2-trifluoroborato-4-chromanones in hand, the development of the Minisci coupling reaction conditions was carried out using 4-bromoquinoline as a reaction partner (Figure 3.8). A variety of photocatalysts were screened that possessed sufficiently high excited state redox potentials to oxidize the trifluoroboratochromanones ($E_{red} \approx +1.11$ V).[9] Although $Ir[dF(CF_3)ppy]_2(bpy)PF_6$ ($E^*_{1/2} = +1.21$ V)[10] and Eosin Y ($E^*_{1/2} = +0.79$ V)[10] proved to be viable catalysts, Fukuzumi's mesityl acridinium tetrafluoroborate organophotocatalyst (E*1/2 = +2.20 V), recently used by Akita and coworkers,[11] provided superior yields. Using an organic photocatalyst is particularly advantageous because of the substantially lower cost relative to transition metal counterparts.[12] Furthermore, both oxidant and protic acid loadings were lowered to one equivalent without affecting the yield. Control studies were performed to confirm the need for acid (entry 8), terminal oxidant (entry 9) and photocatalyst (entry 10).

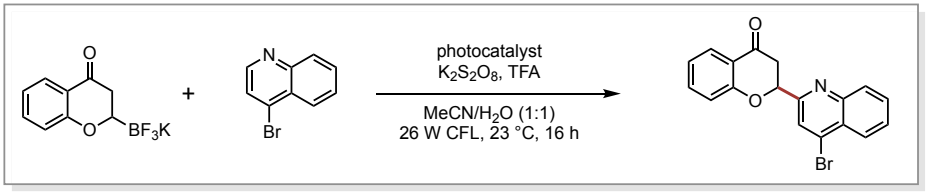

entry	photocatalyst (mol %)	oxidant equiv	acid equiv	yield (%)
1	$Ir[dFCF_3ppy]_2(bpy)PF_6$ (2)	2.0	2.0	43
2	Eosin Y (2)	2.0	2.0	40
3	MesAcr (2)	2.0	2.0	55
4	MesAcr (1)	2.0	2.0	57
5	MesAcr (0.5)	2.0	2.0	42
6	MesAcr (1)	1.0	2.0	58
7	MesAcr (1)	1.0	1.0	60
8	MesAcr (1)	1.0	none	32
9	MesAcr (1)	none	1.0	21
10	none	1.0	1.0	0
11	MesAcr (1), no light	1.0	1.0	trace

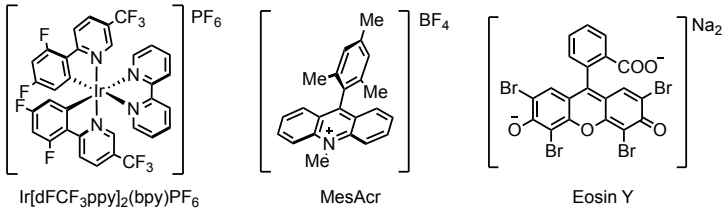

Figure 3.8. Optimization and control studies.

Stern-Volmer relationship studies are consistent with the reductive quenching of the photocatalyst by the trifluoroborate (see Supporting Information).

Interestingly, the Stern-Volmer plot exhibited an exponential fluorescence quenching (Figure 3.9) trend, suggesting a static quenching pathway (Figure 3.10).[13] Additional ^{19}F NMR experiments supported a *static quenching* pathway, where a distinct chemical shift was observed when photocatalyst was added to a solution of alkyltrifluoroborate.[14] The observed shift in fluorine signals of the trifluoroborate suggests formation of a preassociation complex between the alkyltrifluoroborate and MesAcr before the single-electron transfer occurs.

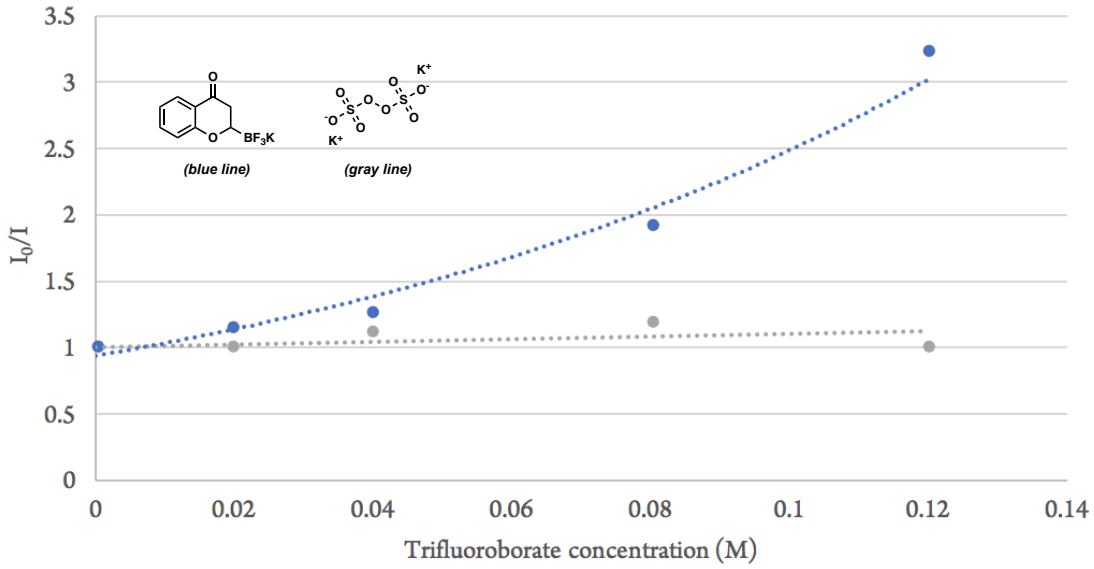

Figure 3.9. Stern-Volmer results.

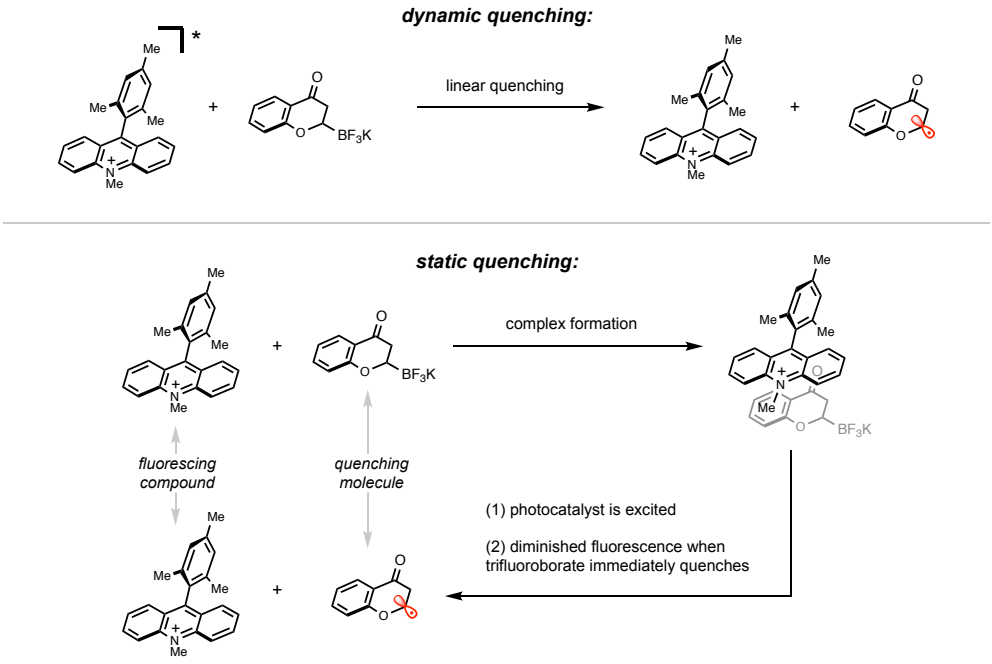

Figure 3.10. Dynamic *versus* static quenching pathways.

Quantum yield studies in a related study have indicated that this is not a radical chain process as evidenced by a quantum number of 0.31.[5] Finally, a control was run in the absence of

light to demonstrate that the catalyst is active only in its photoexcited state.[15] With the completion of control experiments and Stern-Volmer quenching studies, we proposed the mechanism outlined in Figure 3.4.

With suitable conditions in hand, the substrate scope for the heteroarene partners was explored (Figure 3.11). Lepidine, a prototypical substrate in Minisci chemistry,[3] was first used as a reacting partner. As expected, **3.11.1** was obtained regioselectively in relatively high yield (61%). Product **3.11.2** was obtained along with trace amounts of regioisomers, but was primarily selective ortho to the nitrogen.

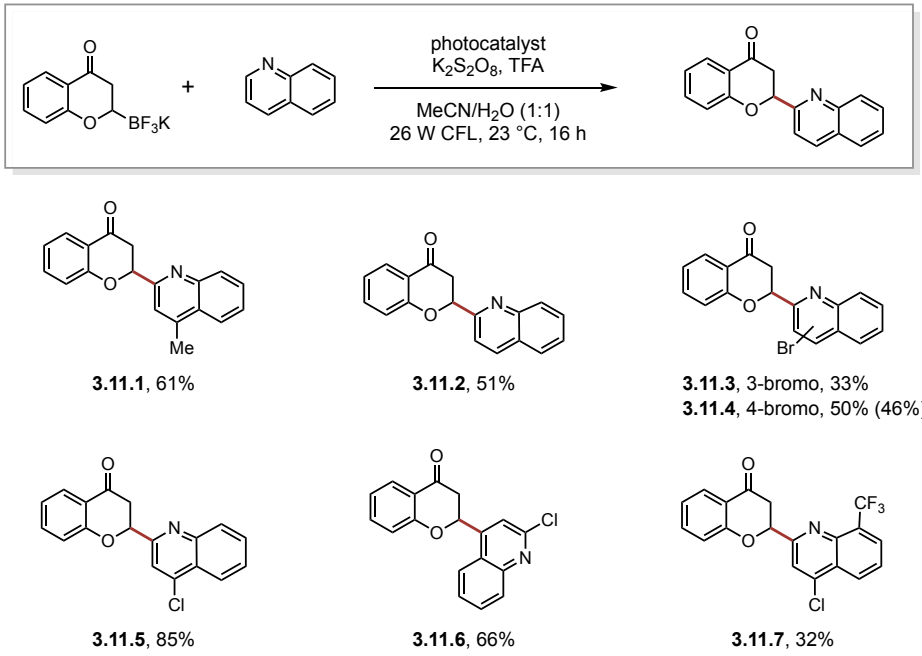

Figure 3.11. Trifluoroboratochromanone coupling with heteroarenes.

Steric sensitivity was probed with 3-bromoquinoline, affording a lower yield of **3.11.3** (33%). When 4-bromoquinoline was used, the yield of **3.11.4** improved to 50%. Notably, when the reaction was performed on gram scale, the yield was a comparable 46% yield. Conversion was significantly higher with 4-chloroquinoline, which provided an excellent yield of **3.11.5**. 2-Chloroquinoline was next explored, and selective addition to the 4-position was observed (**3.11.6**).

With a more decorated chloroquinoline, 4-chloro-8-(trifluoromethyl)quinoline, a modest 32% yield was achieved. Halogenated isoquinolines were next explored to access products possessing functional handles for further diversification (Figure 3.12). 1-Chloroisoquinoline afforded a lower 30% yield (**3.12.1**), but when the halide was appended on the adjacent ring, the yield improved to 50% (**3.12.2**). Alkyl substitution at the C4 position resulted in <5% conversion, suggesting electron-withdrawing groups enhance the electrophilicity of the isoquinoline moieties. The scope was further explored with substrates containing more heteroatoms. Quinoxaline yielded mono-substituted product **3.12.4** in 66% yield. A slightly lower yield of **3.12.5** was observed with 2-chloroquinoxaline. Caffeine, another nitrogen-rich heteroarene, also provided a modest yield of the alkylated product (**3.12.6**). Pyridine moieties, a common pharmacophore in medicinal chemistry,[16] were next probed. After screening various para-substituted pyridines, 4-trifluoromethylpyridine yielded **3.12.7** in a modest yield. Other, more electron rich, systems (e.g., substituted pyrazine **3.12.8** and benzothiazole **3.12.9**) could not be accessed. Typically, more electrophilic radicals such as CF_3 provide higher yields in reactions with such electron-rich heteroarenes.[4a]

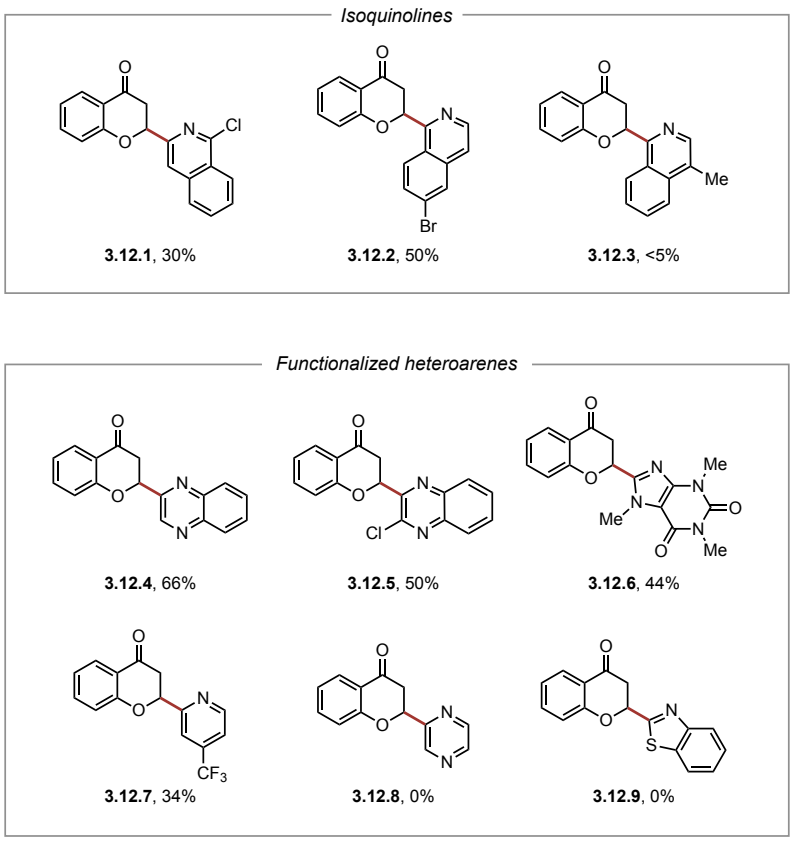

Figure 3.12. Expanding heteroarene scope.

Because 6-bromo-2-trifluoroboratochromanone (Figure 3.13) has potential for elaboration on the aryl ring, an array of substrates was explored to confirm that the reactivity was similar to that of the unfunctionalized trifluoroboratochromanone.

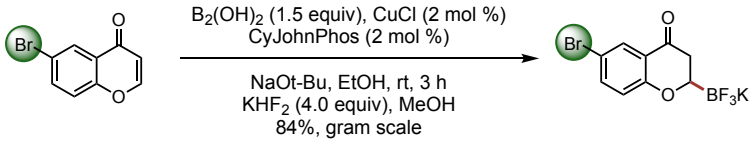

Figure 3.13. Borylation of bromo-chromanone.

Coupling the bromo-substituted trifluoroboratochromanone with 4-chloroquinoline resulted in a markedly higher yield (**3.14.1**). Other functionalized quinolines resulted in more

modest yields (**3.14.2–3.14.4**). Isoquinoline **3.14.5** could not be accessed utilizing this protocol, but quinoxaline **3.14.6** was generated in 63% yield.

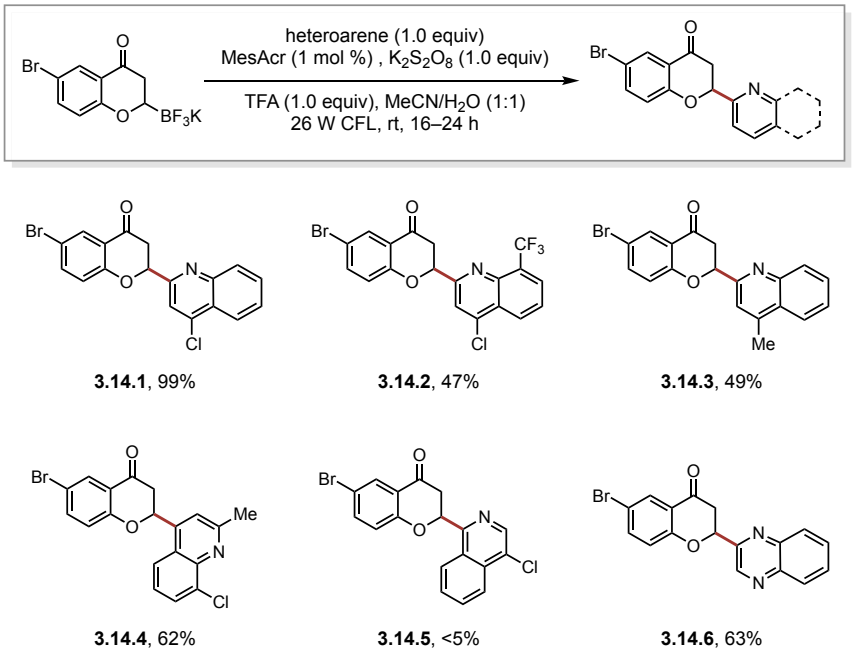

Figure 3.14. Mixed table using bromotrifluoroboratochromanone.

Finally, functionalized trifluoroboratochromanones were coupled with a variety of heteroarenes. Alkyl substitution (Figure 3.15) yielded similar results to the unfunctionalized trifluoroborate. Suprisingly, heteroaryl substitution on the aryl ring led to markedly higher yields (**3.15.1**, **3.14.3**).

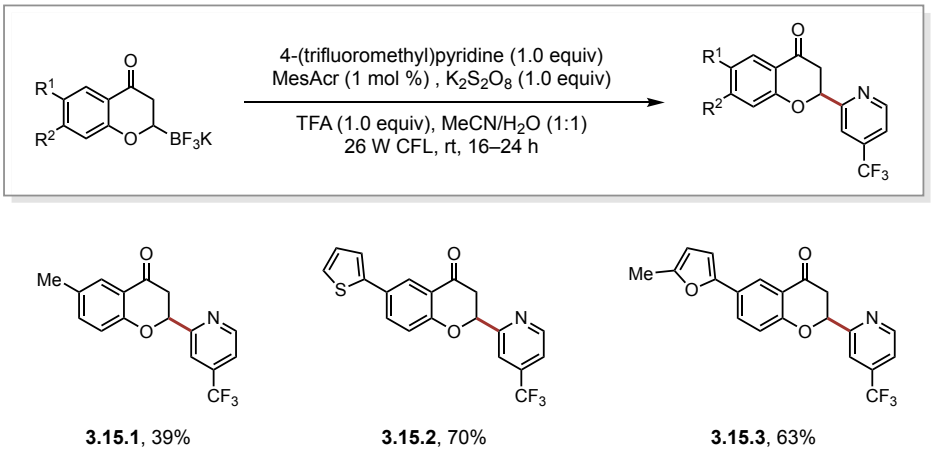

Figure 3.15. Introducing functionality on aryl ring.

3.3 Conclusion

In conclusion, a new class of 2-heteroaryl-substituted 4-chromanones has been accessed via sustainable photoredox-catalyzed coupling with a variety of heteroarene partners. An inexpensive organophotocatalyst was utilized to provide markedly higher yields relative to precious metal photocatalysts. This reaction proceeds chemo- and regioselectively, providing a viable method for radical-induced C–H functionalization of activated heteroarenes. The net result is an efficient, robust, and reasonably general route to a class of compounds that, as a class, is underrepresented in the current literature.

3.4 References

[1] Chromanones in the literature: (a) Yadav, S. K. Int. *J. Org. Chem.* **2014**, *4*, 236. (b) Holder, J. C.; Zou, L.; Marziale, A. N.; Liu, P.; Lan, Y.; Gatti, M.; Kikushima, K.; Houk, K. N.; Stoltz, B. M. *J. Am. Chem. Soc.* **2013**, *135*, 14996.

[2] (a) Yan, Y.; Kohli, A.; Koffas, A. G. *Appl. Environ. Microbiol.* **2005**,*71*, 5610. (b) Gaffield, W.; Lundin, R. E.; Gentili, B.; Horowitz, R. M. *Bioorg. Chem.* **1975**, *4*, 259. (c) Leonard, E.; Yan, Y.;

Lim, K. H.; Koffas, M. A. G. *Appl. Environ. Microbiol.* **2005**, *71*, 8241. (d) Fowler, Z. L.; Koffas, M. A. G. *Appl. Microbiol. Biotechnol.* **2009**, *83*, 799. (e) Fowler, Z. L.; Gikandi, W. W.; Koffas, M. A. G. *Appl. Environ.Microbiol.* **2009**, *75*, 5831.

[3] Synthesizing chromanones: (a) Pouget, C.; Fagnere, C.; Basly, J.; Bensson, A.; Champavier, Y.; Habrioux, G.; Chulia, A. *Bioorg. Med. Chem. Lett.* **2002**, *12*, 1059. (b) Wang, L.; Liu, X.; Dong, Z.; Fu, X.; Feng, X. *Angew. Chem., Int. Ed.* **2008**, *47*, 8670. (c) Qin, T.; Johnson, R. P.; Porco, J. A. *J. Am. Chem. Soc.* **2011**, *133*, 1714. (d) Qin, T.; Iwata, T.; Ransom, T. T.; Beutler, J. A.; Porco, J. A. *J. Am. Chem. Soc.* **2015**, *137*, 15225. (e) Holder, J. C.; Zou, L.; Marziale, A. N.; Liu, P.; Lan, Y.; Gatti, M.; Kikushima, K.; Houk, K. N.; Stoltz, B. M. *J. Am. Chem. Soc.* **2013**, *135*, 14996. (f) Wang, L.; Liu, X.; Dong, Z.; Fu, X.; Feng, X. *Angew. Chem., Int. Ed.* **2008**, *47*, 8670. (g) Vuppalapati, S. V. N.; Xia, L.; Edayadulla, N.; Lee, Y. R. *Synthesis* **2014**, *46*, 465.

[4] (a) Nagib, D. A.; MacMillan, D. W. C. *Nature* **2011**, *480*, 224. (b) Hari, D. P.; Schroll, P.; Konig, B. *J. Am. Chem. Soc.* **2012**, *134*, 2958. (c) Cheng, Y.; Yang, J.; Qu, Y.; Li, P. *Org. Lett.* **2012**, *14*, 98. (d) Jin, J.; MacMillan, D. W. C. *Angew. Chem., Int. Ed.* **2015**, *54*, 1565. (e) DiRocco, D. A.; Dykstra, K.; Krska, S.; Vachal, P.; Conway, D. V.; Tudge, M. *Angew. Chem., Int. Ed.* **2014**, *53*, 4802. (f) Li, G. -X.; Morales-Rivera, C. A.; Wang, Y.; Gao, F.; He, G.; Liu, P.; Chen, G. *Chem. Sci.* **2016**, *7*, 6407.

[5] (a) Minisci, F.; Porta, O.; Recupero, F.; Gambarotti, C.; Paganelli, R.; Pedulli, G. F.; Fontana, F. *Tetrahedron Lett.* **2004**, *45*, 1607. (b) Minisci, F. *Tetrahedron* **1971**, *27*, 3575. (c) Giordano, C.; Minisci, F.; Vismara, E.; Levi, S. J. Org. Chem. 1986, 51, 536. (d) O'Hara, F.; Blackmond, D. G.; Baran, P. S. *J. Am. Chem. Soc.* **2013**, *135*, 12122. (e) Yan, M.; Lo, J. C.; Edwards, J. T.; Baran, P. S. *J. Am. Chem. Soc.* **2016**, *138*, 12692. (f) Molander, G. A.; Colombel, V.; Braz, V. A. *Org. Lett.* **2011**, *13*, 1852. (g) Presset, M.; Fleury-Bregeot, N.; Oehlrich, D.; Rombouts, F.; Molander, G. A. *J. Org. Chem.* **2013**, *78*, 4615.

[6] Yasu, Y.; Koike, T.; Akita, M. *Adv. Synth. Catal.* **2012**, *354*, 3414.

[7] Matsui, J. K.; Primer, D. N.; Molander, G. A. *Chem. Sci* **2017**, *8*, 3512–3522.

[8] Molander, G. A.; McKee, S. A. *Org. Lett.* **2011**, *13*, 4684.

[9] Reduction potential should be similar to α-alkoxytrifluoroborates and secondary alkyl β-trifluoroboratoketones: (a) Karakaya, I.; Primer, D. N.; Molander, G. A. *Org. Lett.* **2015**, *17*, 3294. (b) Karimi-Nami, R.; Tellis, J. C.; Molander, G. A. *Org. Lett.* **2016**, *18*, 2572. (c) Tellis, J. C.; Amani, J.; Molander, G. A. *Org. Lett.* **2016**, *18*, 2994.

[10] Lowry, M.; Goldsmith, J. I.; Slinker, J. D.; Rohl, R.; Pascal, R. A.; Malliaras, G. G.; Bernhard, S. *Chem. Mater.* **2005**, *17*, 5712.

[11] Fukuzumi, S.; Kotani, H.; Ohkubo, K.; Ogo, S.; Tkachenko, N. V.; Lemmetyinen, H. *J. Am. Chem. Soc.* **2004**, *126*, 1600.

[12] Chinzei, T.; Miyazawa, K.; Yasu, Y.; Koike, T.; Akita, M. *RCS Adv.* **2015**, *5*, 21297.

[13] Fraiji, L. K.; Hayes, D. M.; Werner, T. C. *J. Chem. Educ.* **1992**, *69*, 424.

[14] Griffin, J. D.; Zeller, M. A.; Nicewicz, D. A. *J. Am. Chem. Soc.* **2015**, *137*, 11340.

[15] A reviewer suggested that the use of CFL lamps may contribute to the formation of electron donor−acceptor complexes because they are known to emit UV light, but additional experiments found blue LEDs afford comparable yields.

[16] (a) Masurier, N.; Debiton, E.; Jacquemet, A.; Bussiere, A.; Chezal, J.-M.; Ollivier, A.; Tetegan, D.; Andaloussi, M.; Galmier, M.-J.; Lacroix, J.; Canitrot, D.; Telulade, J.-C.; Gaudrealt, R. C.; Chavignon, O.; Moreau, E. *Eur. J. Med. Chem.* **2012**, *52*, 137. (b) Enyedy, I.; Sakamuri, S.; Zaman, W. A.; Johnson, K. M.; Wang, S. *Bioorg. Med. Chem. Lett.* **2003**, *13*, 513. (c) Blum, A. P.; Lester, H. A.; Dougherty, D. A. *Proc. Natl. Acad. Sci. U. S. A.* **2010**, *107*, 13206.

GENERAL PROCEDURE FOR PHOTOREDOX CATALYZED MINISCI COUPLING

An 8 mL vial equipped with a stir bar was added trifluoroborate (191 mg, 0.75 mmol, 1.5 equiv), heterocycle (0.50 mmol, 1.0 equiv), 9-mesityl-10-methylacridinium tetrafluoroborate (1.5 mg, 0.005 mmol, 0.01 equiv), and $K_2S_2O_8$ (135 mg, 0.05 mmol, 1.0 equiv). The vial was then evacuated and purged three times. Under nitrogen, degassed MeCN/H_2O (1:1, 4.0 mL) and trifluoroacetic acid (38 µL, 0.50 mmol, 1.0 equiv) were added in quick succession. The resulting solution was stirred next to two 26 W CFLs under a fan for 16–24 h. After completion, the mixture was quenched with saturated sodium bicarbonate (10 mL) and transferred to a separatory funnel with CH_2Cl_2 (15 mL) and extracted with CH_2Cl_2 (2 x 15 mL). The organic layers were combined and dried over Na_2SO_4 and dry loaded with Celite. The crude mixture was purified by column chromatography.

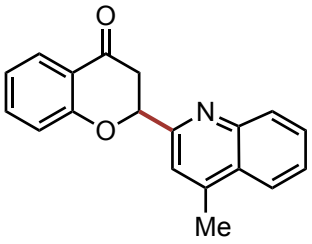

2-(4-Methylquinolin-2-yl)chroman-4-one (3.11.1)

The general procedure was followed with trifluoroborate (191 mg, 0.75 mmol, 1.5 equiv), lepidine (66 µL, 0.50 mmol, 1.0 equiv), 9-mesityl-10-methylacridinium tetrafluoroborate (1.5 mg, 0.005 mmol, 0.01 equiv), and $K_2S_2O_8$ (135 mg, 0.05 mmol, 1.0 equiv). The title compound was purified by column chromatography (silica gel, 4:1 hexanes/EtOAc), affording the coupled product (88 mg, 61% yield) as a yellow oil.

^{1}H NMR (500 MHz, $CDCl_3$) δ 8.13 (d, *J* = 8.4 Hz, 1H), 8.01 (d, *J* = 8.4 Hz, 1H), 7.84 – 7.76 (m, 2H), 7.73 (s, 1H), 7.70 – 7.64 (m, 1H), 7.64 – 7.58 (m, 1H), 7.17 (d, *J* = 8.3 Hz, 1H), 7.11 (t, *J* = 7.5 Hz, 1H), 5.93 (dd, *J* = 11.0, 3.6 Hz, 1H), 3.45 (dd, *J* = 16.9, 11.0 Hz, 1H), 3.16 – 3.05 (m, 1H), 2.75 (s, 3H).

^{13}C NMR (126 MHz, $CDCl_3$) δ 191.8, 161.2, 157.5, 147.5, 145.9, 136.2, 130.2, 129.7, 128.0, 127.3, 126.8, 123.9, 121.9, 121.5, 119.3, 118.3, 80.7, 42.8, 19.2.

FT-IR (cm^{-1}, neat, ATR) 3066, 1657, 1607, 1355, 1224, 763.

HRMS (ES+) m/z calc. for $C_{19}H_{16}NO_2$ [M+H] 290.1181, found 290.1180.

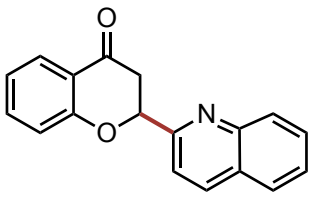

2-(Quinolin-2-yl)chroman-4-one (3.11.2)

The general procedure was followed with trifluoroborate (191 mg, 0.75 mmol, 1.5 equiv), quinoline (64.6 mg, 0.50 mmol, 1.0 equiv), 9-mesityl-10-methylacridinium tetrafluoroborate (1.5 mg, 0.005 mmol, 0.01 equiv), and $K_2S_2O_8$ (135 mg, 0.05 mmol, 1.0 equiv). The title compound was purified by column chromatography (silica gel, 4:1 hexanes/EtOAc), affording the coupled product (96 mg, 70% yield) as a light yellow oil.

^{1}H NMR (500 MHz, $CDCl_3$) δ 8.26 (d, *J* = 8.5 Hz, 1H), 8.09 (d, *J* = 8.4 Hz, 1H), 7.96 (d, *J* = 8.2 Hz, 1H), 7.85 (d, *J* = 8.0 Hz, 1H), 7.76 (dd, *J* = 18.0, 8.1 Hz, 2H), 7.55 (dt, *J* = 23.1, 7.6 Hz, 2H), 7.12 (d, *J* = 8.3 Hz, 1H), 7.07 (t, *J* = 7.5 Hz, 1H), 5.80 (dd, *J* = 11.8, 3.8 Hz, 1H), 3.33 (dd, *J* = 17.0, 11.8 Hz, 1H), 3.24 (dd, *J* = 17.0, 3.7 Hz, 1H).

^{13}C NMR (126 MHz, $CDCl_3$) δ 191.7, 161.1, 157.9, 147.6, 137.5, 136.3, 130.1, 129.6, 127.9, 127.8, 127.3, 127.1, 121.9, 121.5, 118.6, 118.3, 80.5, 42.8.

FT-IR (cm^{-1}, neat, ATR) 3075, 1691, 1607, 1464, 1305, 1223, 763.

HRMS (ES+) m/z calc. for $C_{18}H_{14}NO_2$ [M+H] 276.1025, found 276.1025.

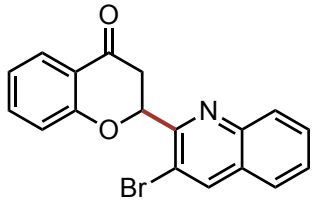

2-(3-Bromoquinolin-2-yl)chroman-4-one (3.11.3)

The general procedure was followed with trifluoroborate (191 mg, 0.75 mmol, 1.5 equiv), 3-bromoquinoline (103.5 mg, 0.50 mmol, 1.0 equiv), 9-mesityl-10-methylacridinium tetrafluoroborate (1.5 mg, 0.005 mmol, 0.01 equiv), and $K_2S_2O_8$ (135 mg, 0.05 mmol, 1.0 equiv). The title compound was purified by column chromatography (silica gel, 4:1 hexanes/EtOAc), affording the coupled product (58 mg, 33% yield) as a yellow oil.

^{1}H NMR (500 MHz, $CDCl_3$) δ 9.00 (s, 1H), 8.61 (dd, *J* = 8.4, 2.9 Hz, 1H), 8.21 – 8.15 (m, 1H), 8.04 (dt, *J* = 8.0, 2.0 Hz, 1H), 7.82 – 7.74 (m, 1H), 7.65 – 7.53 (m, 2H), 7.16 (td, *J* = 7.6, 2.4 Hz, 1H), 7.08 (dd, *J* = 8.3, 2.5 Hz, 1H), 6.45 (dd, *J* = 14.5, 3.2 Hz, 1H), 3.50 (ddd, *J* = 17.1, 14.9, 2.4 Hz, 1H), 2.90 (dd, *J* = 17.3, 3.3 Hz, 1H).

^{13}C NMR (126 MHz, $CDCl_3$) δ 190.4, 160.9, 152.2, 147.9, 140.7, 136.6, 130.8, 130.0, 127.8, 127.7, 126.9, 125.2, 122.6, 121.2, 118.4, 82.0, 80.0, 41.4.

FT-IR (cm^{-1}, neat, ATR) 3050, 2900, 1681, 1601, 1472, 1464, 1306, 1224, 731.

HRMS (ES+) m/z calc. for $C_{18}H_{13}BrNO_2$ (M+H) 354.0130, found 354.0162.

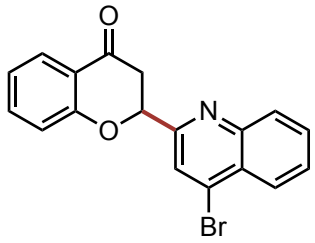

2-(4-Bromoquinolin-2-yl)chroman-4-one (3.11.4)

The general procedure was followed with trifluoroborate (191 mg, 0.75 mmol, 1.5 equiv), 4-bromoquinoline (103.5 mg, 0.50 mmol, 1.0 equiv), 9-mesityl-10-methylacridinium tetrafluoroborate (1.5 mg, 0.005 mmol, 0.01 equiv), and $K_2S_2O_8$ (135 mg, 0.05 mmol, 1.0 equiv). The title compound was purified by column chromatography (silica gel, 4:1 hexanes/EtOAc), affording the coupled product (88 mg, 50% yield) as a semi-solid.

^{1}H NMR (500 MHz, $CDCl_3$) δ 8.70 (s, 1H), 8.40 (d, *J* = 8.5 Hz, 1H), 8.25 (d, *J* = 8.5 Hz, 1H), 7.97 (dd, *J* = 7.9, 1.8 Hz, 1H), 7.85 (ddd, *J* = 8.3, 6.8, 1.2 Hz, 1H), 7.75 (ddd, *J* = 8.4, 6.9, 1.3 Hz, 1H), 7.44 (ddd, *J* = 8.7, 7.2, 1.8 Hz, 1H), 7.08 – 7.01 (m, 1H), 6.95 (d, *J* = 8.4 Hz, 1H), 6.36 (dd, *J* = 10.1, 3.7 Hz, 1H), 3.68 (dd, *J* = 17.1, 10.1 Hz, 1H), 3.14 (dd, *J* = 17.1, 3.7 Hz, 1H).

^{13}C NMR (126 MHz, $CDCl_3$) δ 191.8, 160.2, 154.2, 143.1, 135.8, 135.3, 131.4, 128.7, 127.8, 126.9, 126.9, 125.1, 121.8, 121.4, 120.9, 117.8, 40.6, 24.5.

FT-IR (cm^{-1}, neat, ATR)

HRMS (ES+) m/z calc. for $C_{18}H_{11}BrNO_2Na$ (M+Na) 375.9949, found 375.9942.

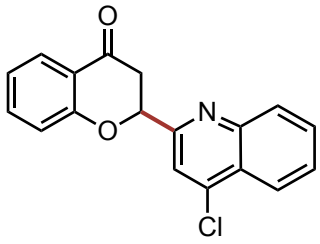

2-(4-Chloroquinolin-2-yl)chroman-4-one (3.11.5)

The general procedure was followed with trifluoroborate (191 mg, 0.75 mmol, 1.5 equiv), 4-chloroquinoline (81.5 mg, 0.50 mmol, 1.0 equiv), 9-mesityl-10-methylacridinium tetrafluoroborate (1.5 mg, 0.005 mmol, 0.01 equiv), and $K_2S_2O_8$ (135 mg, 0.05 mmol, 1.0 equiv). The title compound was purified by column chromatography (silica gel, 4:1 hexanes/EtOAc), affording the coupled product (69 mg, 85% yield) as a pale yellow solid (mp = 80–82 °C).

^{1}H NMR (500 MHz, $CDCl_3$) δ 8.25 (d, *J* = 8.4 Hz, 1H), 8.12 (d, *J* = 8.5 Hz, 1H), 7.99 – 7.89 (m, 2H), 7.81 (t, *J* = 7.7 Hz, 1H), 7.68 (t, *J* = 7.6 Hz, 1H), 7.58 – 7.51 (m, 1H), 7.14 (d, *J* = 8.4 Hz, 1H), 7.09 (t, *J* = 7.5 Hz, 1H), 5.78 (dd, *J* = 8.7, 6.8 Hz, 1H), 3.27 (d, *J* = 7.2 Hz, 2H).

^{13}C NMR (126 MHz, $CDCl_3$) δ 191.2, 165.7, 160.8, 158.0, 148.4, 143.9, 136.3, 130.9, 129.9, 128.0, 127.3, 126.0, 124.2, 122.1, 121.5, 118.8, 118.2, 42.5.

FT-IR (cm^{-1}, neat, ATR) 3055, 2900, 1694, 1606, 1496, 1473, 1412, 1362, 1303, 886, 836, 761.

HRMS (ES+) m/z calc. for $C_{18}H_{12}ClNO_2Na$ [M+Na] 332.0454, found 332.0473.

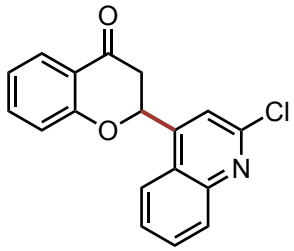

2-(2-Chloroquinolin-4-yl)chroman-4-one (3.11.6)

The general procedure was followed with trifluoroborate (191 mg, 0.75 mmol, 1.5 equiv), 2-chloroquinoline (81.5 mg, 0.50 mmol, 1.0 equiv), 9-mesityl-10-methylacridinium tetrafluoroborate

(1.5 mg, 0.005 mmol, 0.01 equiv), and $K_2S_2O_8$ (135 mg, 0.05 mmol, 1.0 equiv). The title compound was purified by column chromatography (silica gel, 4:1 hexanes/EtOAc), affording the coupled product (53.8 mg, 66% yield) as a pale yellow oil.

^{1}H NMR (500 MHz, $CDCl_3$) δ 9.19 (s, 1H), 8.84 (s, 3H), 7.51 (m, 1H), 7.48 – 7.34 (m, 1H), 7.11 (s, 1H), 7.09 – 6.89 (m, 2H), 5.86 (dd, *J* = 11.5, 3.7 Hz, 1H), 3.37 (dd, *J* = 17.0, 11.4 Hz, 1H), 3.24 (dd, *J* = 17.0, 3.7 Hz, 1H).

^{13}C NMR (126 MHz, $CDCl_3$) δ 190.8, 160.5, 152.2, 144.9, 143.3, 143.3, 142.9, 142.3, 141.5, 136.3, 130.5, 130.2, 129.4, 127.1, 122.2, 118.2, 78.5, 41.7.

FT-IR (cm^{-1}, neat, ATR) 3053, 2900, 1689, 1604, 1588, 1577, 1562, 1472, 1328, 1223, 760.

HRMS (ES+) m/z calc. for $C_{18}H_{13}ClNO_2$ (M+H) 310.0635, found 310.0623.

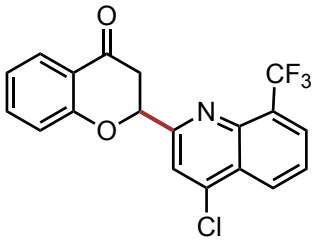

2-(4-Chloro-8-(trifluoromethyl)quinolin-2-yl)chroman-4-one (3.11.7)

The general procedure was followed with trifluoroborate (191 mg, 0.75 mmol, 1.5 equiv), 4-chloro-8-(trifluoromethyl)quinoline (115.5 mg, 0.50 mmol, 1.0 equiv), 9-mesityl-10-methylacridinium tetrafluoroborate (1.5 mg, 0.005 mmol, 0.01 equiv), and $K_2S_2O_8$ (135 mg, 0.05 mmol, 1.0 equiv). The title compound was purified by column chromatography (silica gel, 4:1 hexanes/EtOAc), affording the coupled product (60.3 mg, 32% yield) as a pale yellow oil.

^{1}H NMR (500 MHz, $CDCl_3$) δ 8.44 (d, *J* = 8.5 Hz, 1H), 8.13 (d, *J* = 7.3 Hz, 1H), 8.02 (s, 1H), 7.95 (d, *J* = 7.8 Hz, 1H), 7.69 (t, *J* = 7.9 Hz, 1H), 7.53 (t, *J* = 7.8 Hz, 1H), 7.14 (d, *J* = 8.3 Hz, 1H), 7.08 (t, *J* = 7.5 Hz, 1H), 5.78 (dd, *J* = 11.6, 3.7 Hz, 1H), 3.40 (dd, *J* = 17.1, 3.7 Hz, 1H), 3.26 (dd, *J* = 17.1, 11.5 Hz, 1H), 1.26 (s, 1H).

^{13}C NMR (126 MHz, $CDCl_3$) δ 191.2, 160.6, 158.9, 144.7, 144.1, 139.6 (q, ^{2}J = 34.3 Hz), 129.3, 128.5, 127.3, 126.6, 126.5, 124.8, 123.7 (q, ^{1}J = 218.5 Hz), 122.2, 121.7, 119.8 (q, ^{3}J = 3.2 Hz), 116.7 (q, ^{3}J = 3.5 Hz), 79.3, 41.9.

^{19}F NMR (471 MHz, $CDCl_3$) δ -60.15.

FT-IR (cm^{-1}, neat, ATR)3052, 1677, 1605, 1469, 1316, 1187.

HRMS (ES+) m/z calc. for $C_{19}H_{12}ClF_3NO_2$ (M+H) 378.0508, found 378.0492.

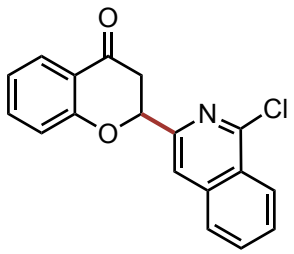

2-(1-Chloroisoquinolin-3-yl)chroman-4-one (3.12.1)

The general procedure was followed with trifluoroborate (191 mg, 0.75 mmol, 1.5 equiv), 1-chloroisoquinoline (81.5 mg, 0.50 mmol, 1.0 equiv), 9-mesityl-10-methylacridinium tetrafluoroborate (1.5 mg, 0.005 mmol, 0.01 equiv), and $K_2S_2O_8$ (135 mg, 0.05 mmol, 1.0 equiv). The title compound was purified by column chromatography (silica gel, 4:1 hexanes/EtOAc), affording the coupled product (46.4 mg, 30% yield) as a pale yellow oil.

^{1}H NMR (500 MHz, $CDCl_3$) δ 8.21 (dd, *J* = 8.0, 1.7 Hz, 1H), 7.90 (dd, *J* = 7.8, 1.8 Hz, 1H), 7.86 (d, *J* = 5.9 Hz, 1H), 7.68 (ddd, *J* = 8.7, 7.1, 1.7 Hz, 1H), 7.54 – 7.44 (m, 2H), 7.41 (ddd, *J* = 8.1,

7.2, 1.1 Hz, 1H), 7.09 – 7.02 (m, 1H), 6.99 (d, *J* = 8.2 Hz, 1H), 6.35 (d, *J* = 5.9 Hz, 1H), 3.03 (dd, *J* = 16.7, 3.5 Hz, 1H), 2.90 (dd, *J* = 16.7, 4.7 Hz, 1H).

^{13}C NMR (126 MHz, $CDCl_3$) δ 192.0, 160.4, 154.4, 143.4, 136.1, 135.5, 131.6, 128.9, 128.0, 127.1, 127.1, 125.3, 122.0, 121.6, 121.2, 118.1, 76.8, 40.9.

FT-IR (cm^{-1}, neat, ATR) 3363, 2924, 1689, 1637, 1607, 1579, 1464, 1406, 1303, 1258, 877.

HRMS

(ES+) m/z calc. for $C_{18}H_{13}ClNO_2$ (M+H) 310.0635, found 310.0633.

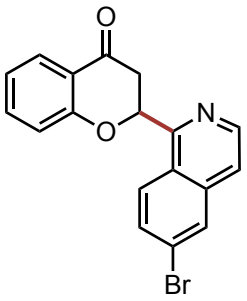

2-(5-Bromoisoquinolin-1-yl)chroman-4-one (3.12.2)

The general procedure was followed with trifluoroborate (191 mg, 0.75 mmol, 1.5 equiv), 6-bromoquinoline (103.5 mg, 0.50 mmol, 1.0 equiv), 9-mesityl-10-methylacridinium tetrafluoroborate (1.5 mg, 0.005 mmol, 0.01 equiv), and $K_2S_2O_8$ (135 mg, 0.05 mmol, 1.0 equiv). The title compound was purified by column chromatography (silica gel, 4:1 hexanes/EtOAc), affording the coupled product (88 mg, 50% yield) as a white solid (mp = 179–181 °C).

^{1}H NMR (500 MHz, $CDCl_3$) δ 7.81 (d, *J* = 8.7 Hz, 1H), 7.24 (d, *J* = 8.5 Hz, 1H), 7.13 (dd, *J* = 7.9, 1.7 Hz, 1H), 7.08 – 7.00 (m, 2H), 6.81 – 6.74 (m, 1H), 6.72 (ddd, *J* = 8.6, 7.2, 1.7 Hz, 1H), 6.31 (d, *J* = 8.3 Hz, 1H), 6.26 (s, 1H), 6.26 (dd, *J* = 15.1, 1.1 Hz, 1H), 5.00 (dd, *J* = 11.1, 4.1 Hz, 2H), 2.51 (dd, *J* = 17.0, 11.1 Hz, 2H), 2.44 (dd, *J* = 17.0, 4.1 Hz, 2H).

^{13}C NMR (126 MHz, $CDCl_3$) δ 191.4, 160.9, 158.8, 148.3, 137.0, 136.3, 130.8, 130.3, 129.5, 127.4, 127.3, 122.1, 122.0, 121.5, 119.8, 118.3, 80.0, 42.5.

FT-IR (cm^{-1}, neat, ATR) 3072, 1693, 1608, 1463, 1304, 1222, 115, 814, 764.

HRMS (ES+) m/z calc. for $C_{18}H_{13}BrNO_2$ [M+H] 354.0130, found 354.0125.

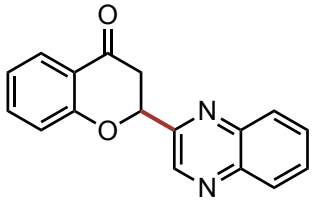

2-(Quinoxalin-2-yl)chroman-4-one (3.12.4)

The general procedure was followed with trifluoroborate (191 mg, 0.75 mmol, 1.5 equiv), quinoxaline (65.1 mg, 0.50 mmol, 1.0 equiv), 9-mesityl-10-methylacridinium tetrafluoroborate (1.5 mg, 0.005 mmol, 0.01 equiv), and $K_2S_2O_8$ (135 mg, 0.05 mmol, 1.0 equiv). The title compound was purified by column chromatography (silica gel, 3:1 hexanes/EtOAc), affording the coupled product (91 mg, 66% yield) as a yellow oil.

^{1}H NMR (500 MHz, $CDCl_3$) δ 9.22 (s, 1H), 8.18 – 8.13 (m, 1H), 8.13 – 8.07 (m, 1H), 7.96 (dd, *J* = 7.9, 1.8 Hz, 1H), 7.84 – 7.77 (m, 2H), 7.55 (ddd, *J* = 8.7, 7.2, 1.8 Hz, 1H), 7.14 (dd, *J* = 8.3, 1.0 Hz, 1H), 7.09 (ddd, *J* = 8.1, 7.1, 1.1 Hz, 1H), 5.89 (dd, *J* = 11.5, 3.7 Hz, 1H), 3.40 (dd, *J* = 17.0, 11.5 Hz, 1H), 3.27 (dd, *J* = 17.0, 3.7 Hz, 1H).

^{13}C NMR (126 MHz, $CDCl_3$) δ 191.0, 160.6, 152.3, 143.6, 142.5, 141.6, 136.5, 130.7, 130.6, 129.6, 129.5, 127.3, 122.3, 121.5, 118.3, 78.7, 41.9.

FT-IR (cm^{-1}, neat, ATR) 3072, 2898, 1691, 1607, 1578, 1493, 1472, 1462, 1367, 1304, 1226, 1206, 762.

HRMS (ES+) m/z calc. for $C_{17}H_{13}N_2O_2$ [M+H] 277.0977, found 277.0971.

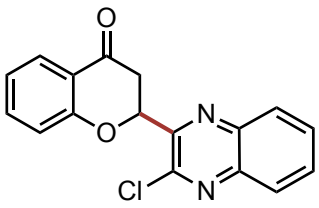

2-(3-Chloroquinoxalin-2-yl)chroman-4-one (3.12.5)

The general procedure was followed with trifluoroborate (191 mg, 0.75 mmol, 1.5 equiv), 2-chloroquinoxaline (82 mg, 0.50 mmol, 1.0 equiv), 9-mesityl-10-methylacridinium tetrafluoroborate (1.5 mg, 0.005 mmol, 0.01 equiv), and $K_2S_2O_8$ (135 mg, 0.05 mmol, 1.0 equiv). The title compound was purified by column chromatography (silica gel, 3:1 hexanes/EtOAc), affording the coupled product (77.5 mg, 50% yield) as a semi-solid.

^{1}H NMR (500 MHz, $CDCl_3$) δ 8.19 – 8.12 (m, 1H), 8.09 – 8.03 (m, 1H), 7.98 (dd, *J* = 7.9, 1.8 Hz, 1H), 7.89 – 7.78 (m, 2H), 7.51 (ddd, *J* = 8.7, 7.2, 1.8 Hz, 1H), 7.12 – 7.03 (m, 2H), 6.22 (dd, *J* = 10.7, 3.7 Hz, 1H), 3.64 (dd, *J* = 17.1, 10.7 Hz, 1H), 3.14 (dd, *J* = 17.1, 3.7 Hz, 1H).

^{13}C NMR (126 MHz, $CDCl_3$) δ 191.0, 160.3, 148.6, 146.4, 141.9, 140.1, 136.1, 131.8, 130.6, 129.4, 128.1, 126.8, 122.0, 121.2, 118.0, 75.9, 40.2.

FT-IR (cm^{-1}, neat, ATR) 3054, 2914, 1690, 1606, 1462, 1303, 1222, 1115, 1047, 934, 760.

HRMS (ES+) m/z calc. for $C_{17}H_{12}ClN_2O_2$ [M+H] 311.0587, found 311.0591.

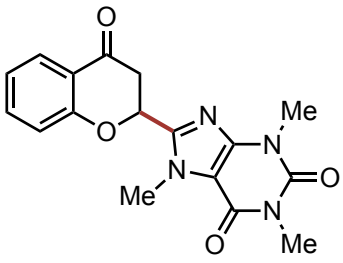

1,3,7-Trimethyl-8-(4-oxochroman-2-yl)-3,7-dihydro-1*H*-purine-2,6-dione (3.12.6)

The general procedure was followed with trifluoroborate (191 mg, 0.75 mmol, 1.5 equiv), caffeine (97.1 mg, 0.50 mmol, 1.0 equiv), 9-mesityl-10-methylacridinium tetrafluoroborate (1.5 mg, 0.005 mmol, 0.01 equiv), and $K_2S_2O_8$ (135 mg, 0.05 mmol, 1.0 equiv). The title compound was purified by column chromatography (silica gel, 3:1 hexanes/EtOAc), affording the coupled product (77.8 mg, 44% yield) as a white solid (mp = 240–242 °C).

^{1}H NMR (500 MHz, $CDCl_3$) δ 7.93 (dd, *J* = 7.9, 1.7 Hz, 1H), 7.50 (ddd, *J* = 8.6, 7.3, 1.8 Hz, 1H), 7.08 (t, *J* = 7.5 Hz, 1H), 6.99 (d, *J* = 8.3 Hz, 1H), 5.71 (dd, *J* = 9.9, 3.9 Hz, 1H), 4.12 (s, 3H), 3.56 (dd, *J* = 17.3, 9.9 Hz, 1H), 3.52 (s, 3H), 3.38 (s, 3H), 3.11 (dd, *J* = 17.2, 3.9 Hz, 1H).

^{13}C NMR (126 MHz, $CDCl_3$) δ 190.1, 159.5, 155.7, 151.7, 148.0, 147.3, 136.5, 127.3, 122.7, 121.4, 117.8, 109.1, 71.0, 40.0, 32.6, 30.0, 28.2.

FT-IR (cm^{-1}, neat, ATR) 1715, 1682, 1664, 1605, 1549, 1472, 1335, 1222, 771, 764.

HRMS (ES+) m/z calc. for $C_{17}H_{16}N_4O_4Na$ [M+Na] 363.1069, found 363.1082.

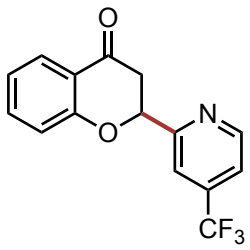

2-(4-(Trifluoromethyl)pyridin-2-yl)chroman-4-one (3.12.7)

The general procedure was followed with trifluoroborate (191 mg, 0.75 mmol, 1.5 equiv), 4-(trifluoromethyl)pyridine (58 μL, 0.50 mmol, 1.0 equiv), 9-mesityl-10-methylacridinium tetrafluoroborate (1.5 mg, 0.005 mmol, 0.01 equiv), and $K_2S_2O_8$ (135 mg, 0.05 mmol, 1.0 equiv).

The title compound was purified by column chromatography (silica gel, 3:1 hexanes/EtOAc), affording the coupled product (49.8 mg, 34% yield) as a yellow oil.

^{1}H NMR (500 MHz, $CDCl_3$) δ 8.81 (d, *J* = 5.1 Hz, 1H), 7.96 (dd, *J* = 7.8, 1.7 Hz, 1H), 7.91 (s, 1H), 7.63 – 7.45 (m, 2H), 7.19 – 7.05 (m, 2H), 5.68 (dd, *J* = 12.4, 3.5 Hz, 1H), 3.22 (dd, *J* = 17.0, 3.5 Hz, 1H), 3.11 (dd, *J* = 17.0, 12.4 Hz, 1H).

^{13}C NMR (126 MHz, $CDCl_3$) δ 191.1, 160.7, 159.7, 150.5, 140.6 (q, ^{2}J = 34.0 Hz), 136.5, 127.3, 127.2, 122.8 (q, ^{1}J = 218.4 Hz), 121.4, 119.1 (m), 118.2, 116.7 (m), 79.3, 42.8.

^{19}F NMR (471 MHz, $CDCl_3$) δ -64.75.

FT-IR (cm^{-1}, neat, ATR) 1692, 1607, 1473, 1362, 1328, 1137, 1118, 846, 703.

HRMS (ES+) m/z calc. for $C_{15}H_{11}F_3NO_2$ [M+H] 294.0742, found 294.0739.

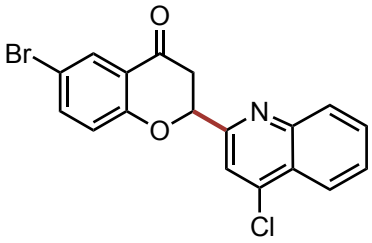

6-Bromo-2-(4-chloroquinolin-2-yl)chroman-4-one (3.14.1)

The general procedure was followed with trifluoroborate (249 mg, 0.75 mmol, 1.5 equiv), 4-chloroquinoline (81.5, 0.50 mmol, 1.0 equiv), 9-mesityl-10-methylacridinium tetrafluoroborate (1.5 mg, 0.005 mmol, 0.01 equiv), and $K_2S_2O_8$ (135 mg, 0.05 mmol, 1.0 equiv). The title compound was purified by column chromatography (silica gel, 3:1 hexanes/EtOAc), affording the coupled product (191 mg, 99% yield) as a yellow oil.

^{1}H NMR (500 MHz, $CDCl_3$) δ 8.24 (d, *J* = 8.4 Hz, 1H), 8.11 – 8.03 (m, 2H), 7.85 (s, 1H), 7.80 (t, *J* = 7.7 Hz, 1H), 7.67 (t, *J* = 7.7 Hz, 1H), 7.60 (d, *J* = 9.0 Hz, 1H), 7.03 (d, *J* = 8.7 Hz, 1H), 5.74 (dd, *J* = 9.5, 5.7 Hz, 1H), 3.33 – 3.24 (m, 2H).

^{13}C NMR (126 MHz, $CDCl_3$) δ 177.6, 155.4, 155.3, 152.9, 150.7, 129.0, 128.0, 125.2, 119.6, 118.7, 113.0, 108.1, 107.3, 77.4, 77.4, 77.2, 76.9, 13.8.

FT-IR (cm^{-1}, neat, ATR) 3060, 2975, 1685, 1596, 1459, 1414, 1272, 1212, 760.

HRMS (ES+) m/z calc. for $C_{18}H_{12}BrClNO_2$ [M+H] 387.9740, found 387.9744.

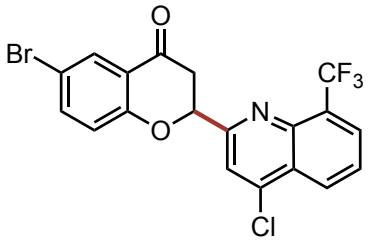

6-Bromo-2-(4-chloro-8-(trifluoromethyl)quinolin-2-yl)chroman-4-one (3.14.2)

The general procedure was followed with trifluoroborate (249 mg, 0.75 mmol, 1.5 equiv), 4-chloro-8-(trifluoromethyl)quinoline (115.5 mg, 0.50 mmol, 1.0 equiv), 9-mesityl-10-methylacridinium tetrafluoroborate (1.5 mg, 0.005 mmol, 0.01 equiv), and $K_2S_2O_8$ (135 mg, 0.05 mmol, 1.0 equiv). The title compound was purified by column chromatography (silica gel, 3:1 hexanes/EtOAc), affording the coupled product (107 mg, 47% yield) as a yellow oil.

^{1}H NMR (500 MHz, $CDCl_3$) δ 8.46 (d, *J* = 8.5 Hz, 1H), 8.15 (d, *J* = 7.3 Hz, 1H), 8.05 (d, *J* = 2.4 Hz, 1H), 7.99 (s, 1H), 7.72 (t, *J* = 7.9 Hz, 1H), 7.61 (dd, *J* = 8.8, 2.5 Hz, 1H), 7.04 (d, *J* = 8.8 Hz, 1H), 5.79 (dd, *J* = 11.0, 3.9 Hz, 1H), 3.40 (dd, *J* = 17.3, 3.9 Hz, 1H), 3.29 (dd, *J* = 17.3, 11.0 Hz, 1H).

^{13}C NMR (126 MHz, $CDCl_3$) δ 190.0, 159.4, 158.3, 144.7, 144.3, 139.0, 129.9, 129.5 (m), 128.8, 128.6 (q, ^2J = 30.0 Hz), 128.5, 127.5 (q, ^1J = 257.2 Hz), 126.6, 123.0, 120.3, 119.9, 115.1, 79.4, 41.4.

^{19}F NMR (471 MHz, $CDCl_3$) δ -60.20.

FT-IR (cm^{-1}, neat, ATR) 1690, 1606, 1578, 1564, 1462, 1318, 1279, 1222, 760.

HRMS (ES+) m/z calc. for $C_{19}H_{11}BrClF_3NO_2$ [M+H] 455.9614, found 455.9613.

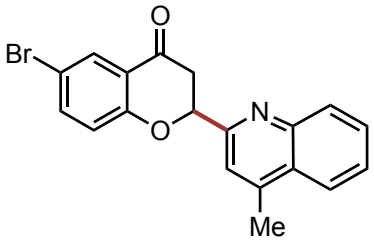

6-Bromo-2-(4-methylquinolin-2-yl)chroman-4-one (3.14.3)

The general procedure was followed with trifluoroborate (249 mg, 0.75 mmol, 1.5 equiv), lepidine (71.5 mg, 0.50 mmol, 1.0 equiv), 9-mesityl-10-methylacridinium tetrafluoroborate (1.5 mg, 0.005 mmol, 0.01 equiv), and $K_2S_2O_8$ (135 mg, 0.05 mmol, 1.0 equiv). The title compound was purified by column chromatography (silica gel, 3:1 hexanes/EtOAc), affording the coupled product (89.9 mg, 49% yield) as a yellow oil.

^{1}H NMR (500 MHz, $CDCl_3$) δ 8.12 – 8.04 (m, 2H), 8.01 (d, J = 8.4 Hz, 1H), 7.73 (t, J = 7.6 Hz, 1H), 7.63 – 7.51 (m, 3H), 7.01 (d, J = 8.7 Hz, 1H), 5.73 (dd, J = 11.8, 3.6 Hz, 1H), 3.33 (dd, J = 17.1, 11.7 Hz, 1H), 3.20 (dd, J = 17.2, 3.6 Hz, 1H), 2.77 (s, 3H).

^{13}C NMR (126 MHz, $CDCl_3$) δ 190.5, 160.0, 156.9, 147.4, 146.1, 138.8, 130.2, 129.8, 129.7, 128.0, 127.0, 123.9, 122.8, 120.3, 119.3, 114.6, 80.7, 42.2, 19.2.

FT-IR (cm^{-1}, neat, ATR) 1682, 1595, 1470, 1419, 1276, 1215, 1159, 755.

HRMS (ES+) m/z calc. for $C_{19}H_{15}BrNO_2$ [M+H] 368.0286, found 368.0285.

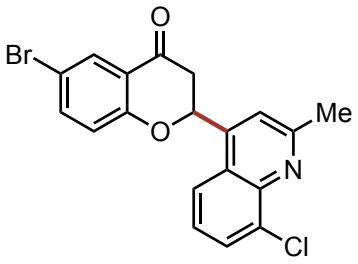

6-Bromo-2-(8-chloro-2-methylquinolin-4-yl)chroman-4-one (3.14.4)

The general procedure was followed with trifluoroborate (249 mg, 0.75 mmol, 1.5 equiv), 2-methyl-8-chloroquinoline (89 mg, 0.50 mmol, 1.0 equiv), 9-mesityl-10-methylacridinium tetrafluoroborate (1.5 mg, 0.005 mmol, 0.01 equiv), and $K_2S_2O_8$ (135 mg, 0.05 mmol, 1.0 equiv). The title compound was purified by column chromatography (silica gel, 5:1 hexanes/EtOAc), affording the coupled product (124.3 mg, 62% yield) as a semi-solid.

^{1}H NMR (500 MHz, $CDCl_3$) δ 8.09 (d, *J* = 2.5 Hz, 1H), 7.92 (d, *J* = 7.5 Hz, 1H), 7.86 (d, *J* = 8.5 Hz, 1H), 7.80 (s, 1H), 7.67 (dd, *J* = 8.8, 2.5 Hz, 1H), 7.55 (t, *J* = 8.0 Hz, 1H), 7.06 (d, *J* = 8.8 Hz, 1H), 6.20 (dd, *J* = 13.0, 3.2 Hz, 1H), 3.17 – 3.00 (m, 2H), 2.96 (s, 3H).

^{13}C NMR (126 MHz, $CDCl_3$) δ 189.3, 160.6, 159.9, 146.5, 142.6, 139.4, 132.75, 131.2, 129.9, 127.3, 124.6, 122.3, 121.4, 120.3, 120.3, 115.5, 75.9, 43.9, 25.0.

FT-IR (cm^{-1}, neat, ATR) 3076, 1694, 1639, 1599, 1505, 1466, 1417, 1381, 1330, 1272, 1219, 1181, 1133, 1091, 1056, 907, 888, 707.

HRMS (ES+) m/z calc. for $C_{19}H_{14}BrClNO_2$ [M+H] 401.9896, found 401.9890.

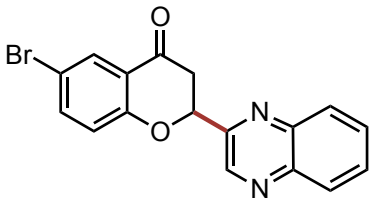

6-Bromo-2-(quinoxalin-2-yl)chroman-4-one (3.14.6)

The general procedure was followed with trifluoroborate (249 mg, 0.75 mmol, 1.5 equiv), quinoxaline (65.1 mg, 0.50 mmol, 1.0 equiv), 9-mesityl-10-methylacridinium tetrafluoroborate (1.5 mg, 0.005 mmol, 0.01 equiv), and $K_2S_2O_8$ (135 mg, 0.05 mmol, 1.0 equiv). The title compound was purified by column chromatography (silica gel, 3:1 hexanes/EtOAc), affording the coupled product (111.5 mg, 63% yield) as a clear oil.

^{1}H NMR (500 MHz, $CDCl_3$) δ 9.19 (s, 1H), 8.18 – 8.13 (m, 1H), 8.12 – 8.09 (m, 1H), 8.06 (d, *J* = 2.5 Hz, 1H), 7.83 (dt, *J* = 6.6, 3.4 Hz, 2H), 7.61 (dd, *J* = 8.8, 2.6 Hz, 1H), 7.04 (d, *J* = 8.9 Hz, 1H), 5.88 (dd, *J* = 11.1, 3.8 Hz, 1H), 3.41 (dd, *J* = 17.3, 11.4 Hz, 1H), 3.28 (dd, *J* = 17.1, 3.8 Hz, 1H).

^{13}C NMR (126 MHz, $CDCl_3$) δ 189.7, 159.4, 151.7, 143.5, 142.6, 141.6, 139.1, 130.8, 130.8, 129.8, 129.6, 129.5, 122.8, 120.4, 115.1, 78.7, 41.4.

FT-IR (cm^{-1}, neat, ATR) 3065, 2903, 1694, 1651, 1599, 1569, 1493, 1465, 1416, 1368, 1269, 1222, 1129, 1068, 1014, 1000, 933, 910, 732.

HRMS (ES+) m/z calc. for $C_{17}H_{12}BrN_2O_2$ [M+H] 355.0082, found 355.0088.

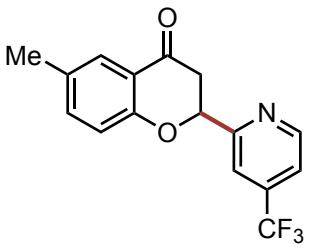

6-Methyl-2-(4-(trifluoromethyl)pyridin-2-yl)chroman-4-one (3a)

Trifluoroborate was prepared according to literature procedure and used crude (reference: Molander, G. A.; McKee, S. A. *Org. Lett.* **2011**, *13*, 4684).

The general procedure was followed with trifluoroborate (201 mg, 0.75 mmol, 1.5 equiv), 4-(trifluoromethyl)pyridine (73.5 mg, 0.50 mmol, 1.0 equiv), 9-mesityl-10-methylacridinium tetrafluoroborate (1.5 mg, 0.005 mmol, 0.01 equiv), and $K_2S_2O_8$ (135 mg, 0.05 mmol, 1.0 equiv). The title compound was purified by column chromatography (silica gel, 3:1 hexanes/EtOAc), hexanes/EtOAc), affording the coupled product (59.9 mg, 39% yield) as a yellow oil.

^{1}H NMR (500 MHz, $CDCl_3$ δ 8.81 (d, *J* = 5.0 Hz, 1H), 7.91 (s, 1H), 7.74 (d, *J* = 2.1 Hz, 1H), 7.53 (d, *J* = 5.0 Hz, 1H), 7.36 (dd, *J* = 8.4, 2.2 Hz, 1H), 7.04 (d, *J* = 8.4 Hz, 1H), 5.64 (dd, *J* = 12.4, 3.4 Hz, 1H), 3.26 – 3.14 (m, 1H), 3.08 (dd, *J* = 17.0, 12.4 Hz, 1H), 2.34 (s, 3H).

^{13}C NMR (126 MHz, $CDCl_3$) 191.2, 160.7, 160.0, 150.5, 140.8 (q, ^2J = 34.7 Hz), 136.5, 127.3, 127.2, 124.0, 122.5 (q, ^1J = 273.7 Hz), 119.1 (m), 118.2, 116.7 (m), 79.3, 42.9, 39.0.

^{19}F NMR (471 MHz, $CDCl_3$) δ -64.82.

FT-IR (cm^{-1}, neat, ATR) 2931, 1693, 1618, 1579, 1489, 1420, 1361, 1328, 1290, 1228, 1171, 1137, 1086, 1011, 906, 848, 824.

HRMS (ES+) m/z calc. for $C_{16}H_{12}F_3NO_2$ [M] 307.0820, found 307.0827.

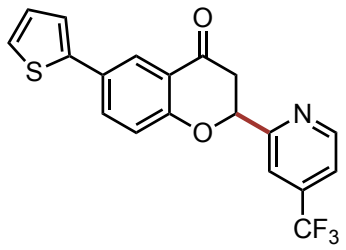

6-(Thiophen-2-yl)-2-(4-(trifluoromethyl)pyridin-2-yl)chroman-4-one (3b)

Trifluoroborate was prepared according to literature procedure and used crude (reference: Molander, G. A.; McKee, S. A. *Org. Lett.* **2011**, *13*, 4684).

The general procedure was followed with trifluoroborate (168 mg, 0.75 mmol, 1.5 equiv), 4-(trifluoromethyl)pyridine (73.5 mg, 0.50 mmol, 1.0 equiv), 9-mesityl-10-methylacridinium tetrafluoroborate (1.5 mg, 0.005 mmol, 0.01 equiv), and $K_2S_2O_8$ (135 mg, 0.05 mmol, 1.0 equiv). The title compound was purified by column chromatography (silica gel, 3:1 hexanes/EtOAc), affording the coupled product (60 mg, 32% yield) as a yellow oil.

^{1}H NMR (500 MHz, $CDCl_3$) δ 8.81 (d, *J* = 5.1 Hz, 1H), 8.17 (d, *J* = 2.4 Hz, 1H), 7.91 (s, 1H), 7.79 (dd, *J* = 8.6, 2.4 Hz, 1H), 7.53 (d, *J* = 5.0 Hz, 1H), 7.30 (d, *J* = 3.7 Hz, 1H), 7.28 (d, *J* = 5.1 Hz, 1H), 7.16 (d, *J* = 8.6 Hz, 1H), 7.10 – 7.06 (m, 1H), 5.69 (dd, *J* = 12.2, 3.5 Hz, 1H), 3.25 (dd, *J* = 17.0, 3.6 Hz, 1H), 3.14 (dd, *J* = 17.0, 12.2 Hz, 1H).

^{13}C NMR (126 MHz, $CDCl_3$) δ 191.0, 160.0, 159.6, 150.6, 142.9, 139.8, 139.6 (q, ^2J = 34.2 Hz), 134.0, 129.1, 128.3, 125.1, 124.1, 123.0 (q, ^1J = 273.3 Hz), 121.5, 119.2 (q, ^3J = 4.2 Hz), 119.0, 116.8 (q, ^3J = 4.3 Hz), 79.5, 42.8.

^{19}F NMR (471 MHz, $CDCl_3$) δ -64.73.

FT-IR (cm^{-1}, neat, ATR) 3076, 1694, 1613, 1574, 1533, 1486, 1421, 1362, 1328, 1286, 846.

HRMS (ESI) m/z calc. for $C_{19}H_{13}F_3NO_2S$ [M+H] 376.0619, found 376.0620.

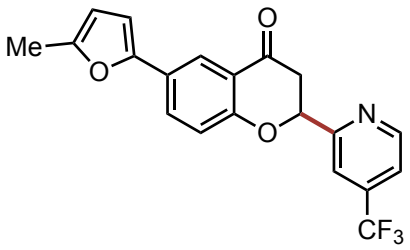

6-(5-Methylfuran-2-yl)-2-(4-(trifluoromethyl)pyridin-2-yl)chroman-4-one (3c)

Note: Trifluoroborate was prepared according to literature procedure and used crude (reference: Molander, G. A.; McKee, S. A. *Org. Lett.* **2011**, *13*, 4684).

The general procedure was followed with trifluoroborate (250.5 mg, 0.75 mmol, 1.5 equiv), 4-(trifluoromethyl)pyridine (73.5 mg, 0.50 mmol, 1.0 equiv), 9-mesityl-10-methylacridinium tetrafluoroborate (1.5 mg, 0.005 mmol, 0.01 equiv), and $K_2S_2O_8$ (135 mg, 0.05 mmol, 1.0 equiv). The title compound was purified by column chromatography (silica gel, 3:1 hexanes/EtOAc), affording the coupled product (130.6 mg, 70% yield) as a yellow oil.

^{1}H NMR (500 MHz, $CDCl_3$) δ 8.81 (d, *J* = 5.0 Hz, 1H), 8.17 (d, *J* = 2.2 Hz, 1H), 7.91 (s, 1H), 7.81 (dd, *J* = 8.7, 2.3 Hz, 1H), 7.53 (d, *J* = 5.1 Hz, 1H), 7.14 (d, *J* = 8.7 Hz, 1H), 6.52 (d, *J* = 3.2 Hz, 1H), 6.05 (d, *J* = 3.2 Hz, 1H), 5.68 (dd, *J* = 12.3, 3.6 Hz, 1H), 3.24 (dd, *J* = 17.0, 3.6 Hz, 1H), 3.13 (dd, *J* = 17.0, 12.2 Hz, 1H), 2.36 (s, 3H).

^{13}C NMR (126 MHz, $CDCl_3$) δ 191.1, 159.7, 159.4, 152.4, 151.1, 150.5, 139.9, 139.4 (q, ^2J = 34.1), 131.5, 126.1, 122.6 (q, ^1J = 273.4 Hz), 121.4, 119.1 (m), 118.6, 116.8 (m), 108.0, 106.1, 79.4, 42.9, 13.9.

^{19}F NMR (471 MHz, $CDCl_3$) δ -65.48.

FT-IR (cm^{-1}, neat, ATR) 1696, 1609, 1481, 1425, 1363, 1261, 1228, 1173, 1138.

HRMS (ESI) m/z calc. for $C_{20}H_{15}F_3NO_3$ [M+H] 374.1004, found 374.0996.

GENERAL PROCEDURE FOR BETA BORYLATION

2-(Trifluoro-λ$_4$-boranyl)chroman-4-one, potassium salt (IV)

A 50 mL round bottom flask was charged with chroman-4-one (896 mg, 4.0 mmol, 1.0 equiv) and brought into the glove box. $(HO)_2BB(OH)_2$ (538.2 mg, 6.0 mmol, 1.5 equiv), CuCl (7 mg, 0.08

mmol, 0.02 equiv), CyJohnPhos (28 mg, 0.08 mmol, 0.02 equiv), and NaO*t*-Bu (115.3 mg, 1.2 mmol, 0.3 equiv) were added to the flask, which was capped in the glovebox. Under nitrogen, freshly distilled EtOH (20 mL) was added, and the mixture was stirred for 3 h at rt. Upon completion of the reaction, the EtOH was removed *in vacuo*, and the residue was dissolved in MeOH (20 mL) and cooled to 0 °C. Saturated KHF_2 (8 mL, 4.5 M) was added dropwise to the reaction, and the resulting mixture was allowed to warm to rt. After 30 min, the solution was concentrated *in vacuo* and placed on the lyophilizer overnight. A Soxhlet extraction of the solid was performed using *i*-PrOAc for 16 h, and the extract was concentrated. The resulting red solid was dissolved in acetone (~5 mL), and Et_2O was added dropwise until precipitation was induced. Additional Et_2O (20 mL) was added, and the solid was filtered to afford a light orange powder (1.115 g, 84% yield).

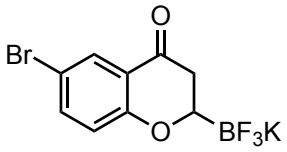

6-Bromo-2-(trifluoro-l$_4$-boranyl)chroman-4-one, potassium salt

Physical properties: light orange solid (mp = 180–184 °C).

^{1}H NMR (500 MHz, DMSO-d_6) δ 7.70 (s, 1H), 7.56 (d, J = 8.9 Hz, 1H), 6.93 (d, J = 8.9 Hz, 1H), 3.60 (d, J = 15.0 Hz, 1H), 2.68 – 2.56 (m, 1H), 2.35 (d, J = 17.1 Hz, 1H).

^{13}C NMR (126 MHz, DMSO-d_6) δ 194.1, 163.5, 137.3, 128.1, 122.4, 120.7, 110.6, 30.7, 15.2.

^{11}B NMR (128 MHz, DMSO-d_6) δ 2.6.

^{19}F NMR (471 MHz, DMSO-d_6) δ 143.39.

FT-IR (cm^{-1}, neat, ATR) 3415, 1676, 1598, 1465, 1275, 1223, 1185, 873, 820.

HRMS (ESI) m/z calc. for $C_{11}H_9O_2NBF_1$ [M-F+CH_3N] 314.9878, found 314.9879.

EMISSION QUENCHING EXPERIMENTS

A stock solution of MesAcr photocatalyst (1.5 x 10^{-5} M, 10 mL) in MeCN/H_2O (1:1) was made and degassed vigorously with N_2 for 20 min. In separate 1 dram vials, 2-(trifluoroboranyl)chroman-4-one (blue) and persulfate (green) were added. Each vial was evacuated and purged three times followed by addition of the stock solution under inert atmosphere. Data was collected using a Fluorolog-3 spectrophotometer. Samples were excited at 500 nm and the emission intensity was collected at 550 nm. Each data point is the average of five runs.

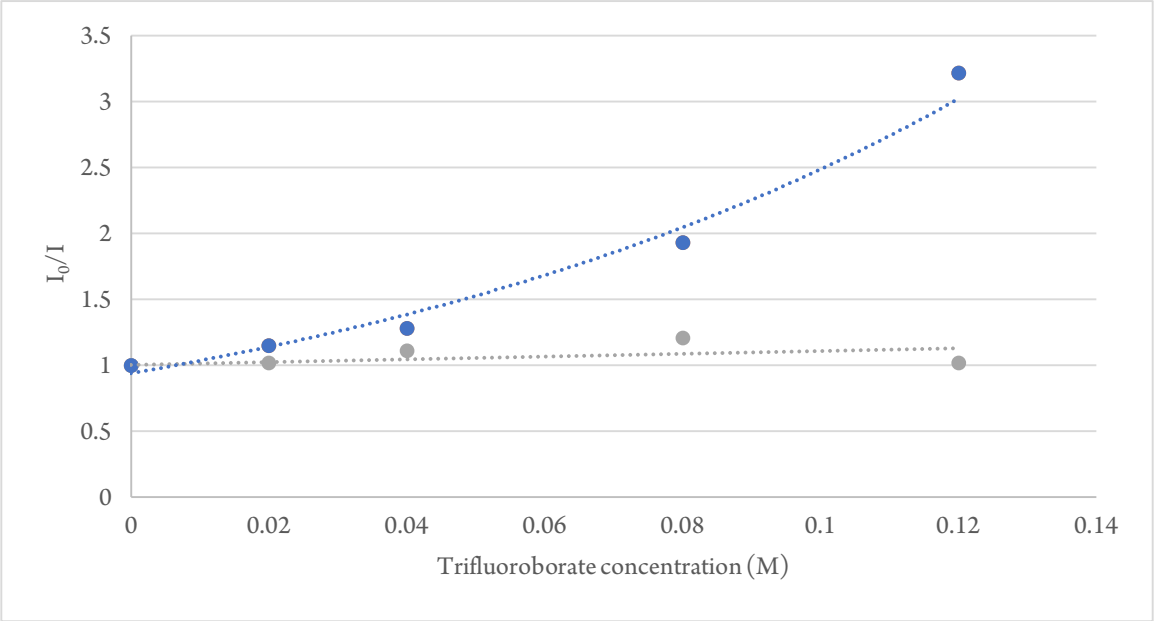

^{1}H ($CDCl_3$, 500 MHz) spectra of 2-(4-methylquinolin-2-yl)chroman-4-one (**3.11.1**)

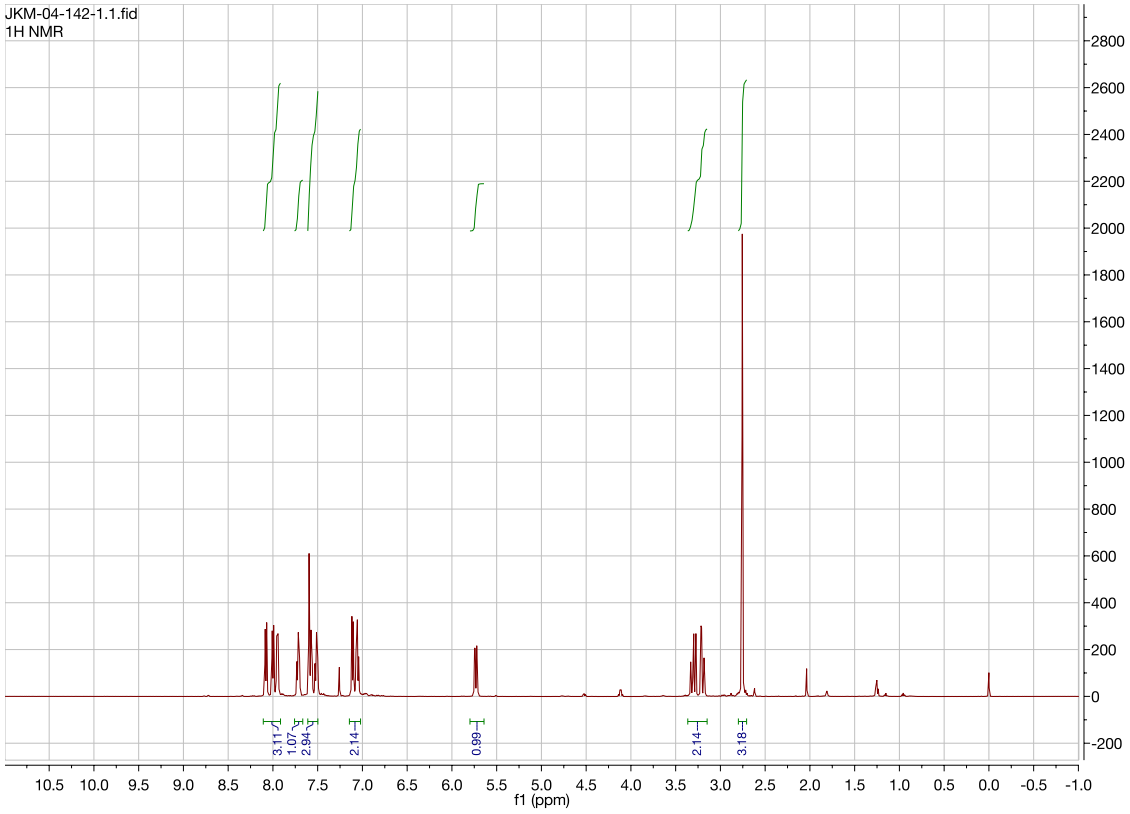

^{13}C ($CDCl_3$, 125.8 MHz) spectra of 2-(4-methylquinolin-2-yl)chroman-4-one (**3.11.1**)

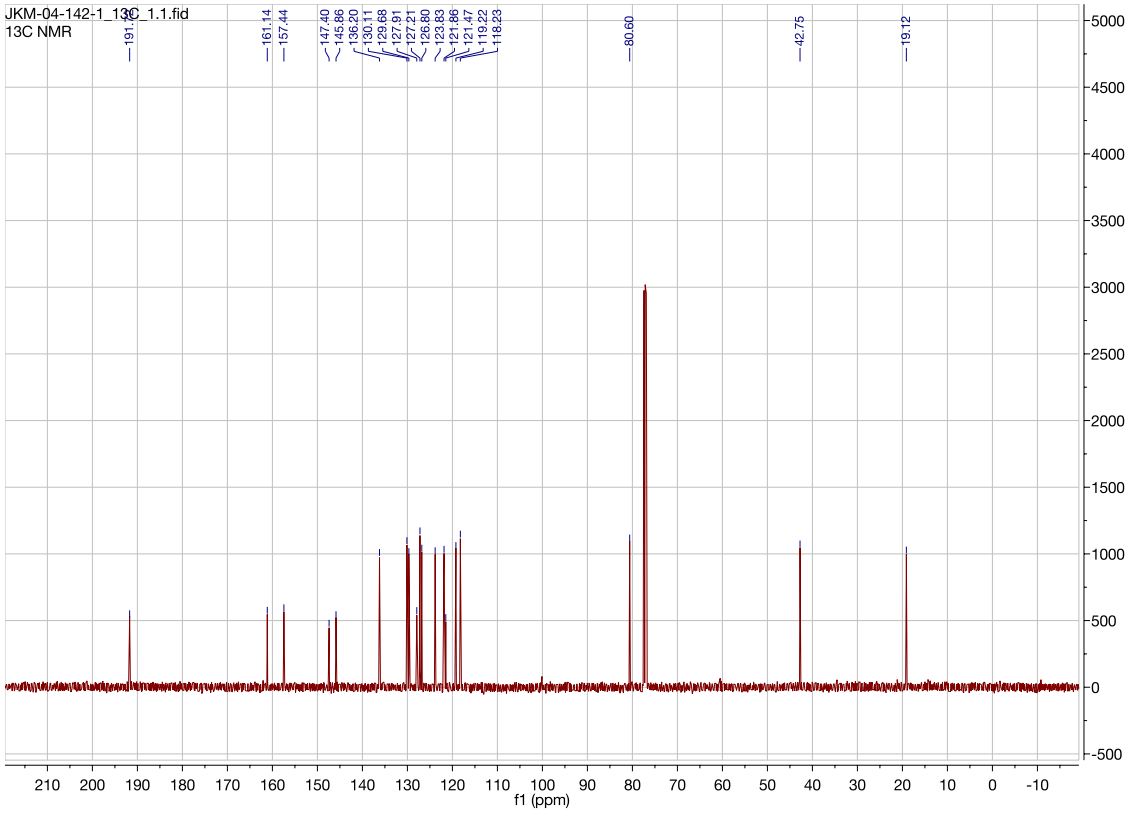

^{1}H ($CDCl_3$, 500 MHz) spectra of 2-(quinolin-2-yl)chroman-4-one (**3.11.2**)

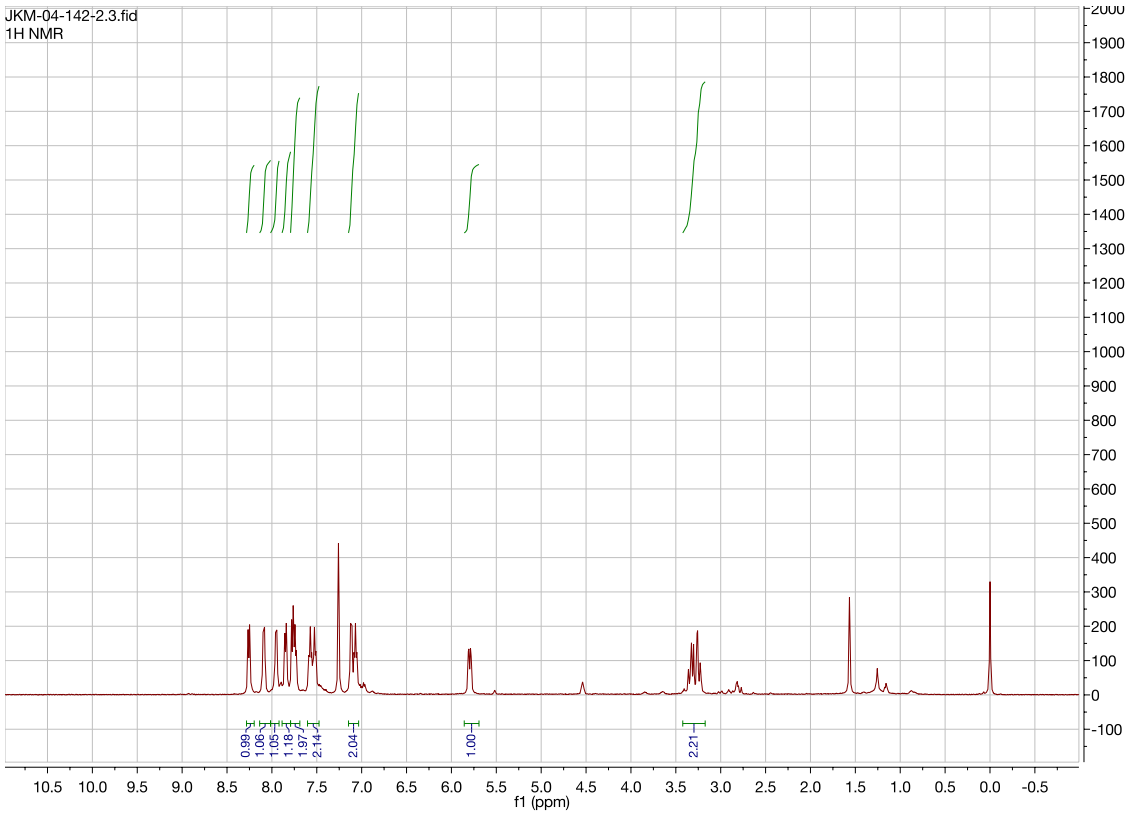

^{13}C ($CDCl_3$, 125.8 MHz) spectra of 2-(quinolin-2-yl)chroman-4-one (**3.11.2**)

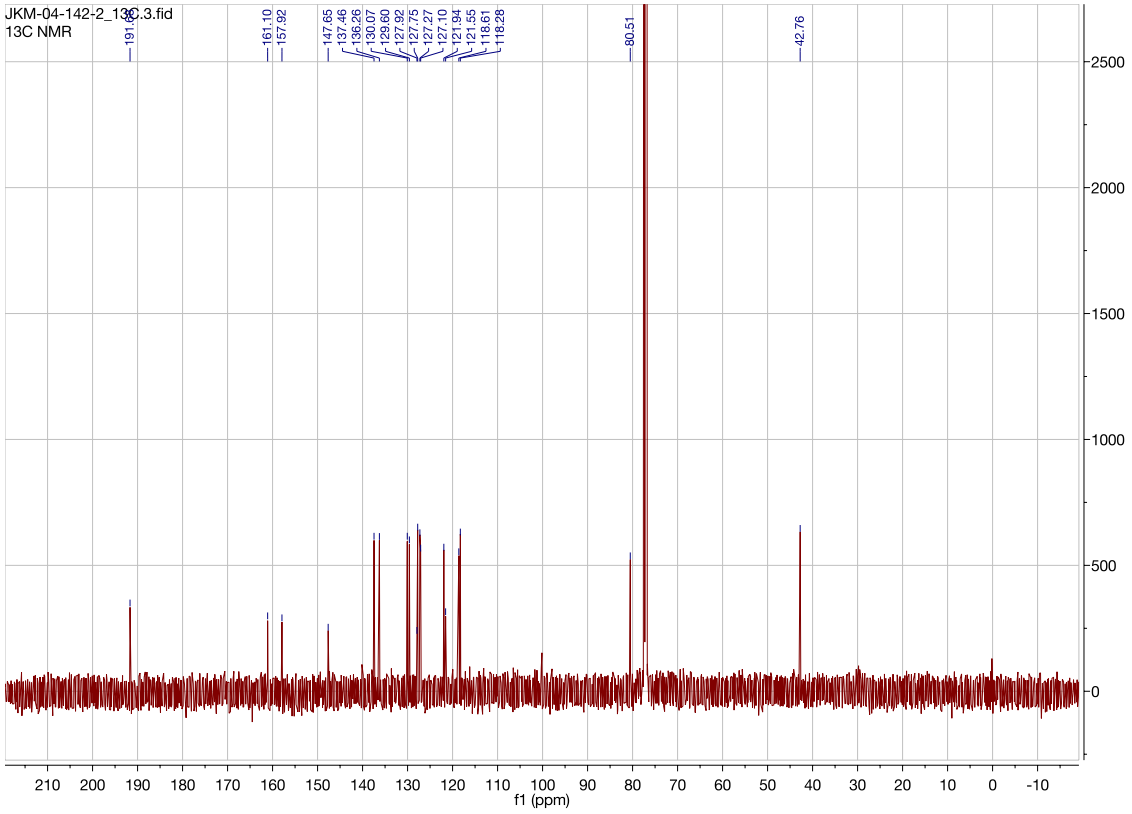

^{1}H ($CDCl_3$, 500 MHz) spectra of 2-(3-bromoquinolin-2-yl)chroman-4-one (**3.11.3**)

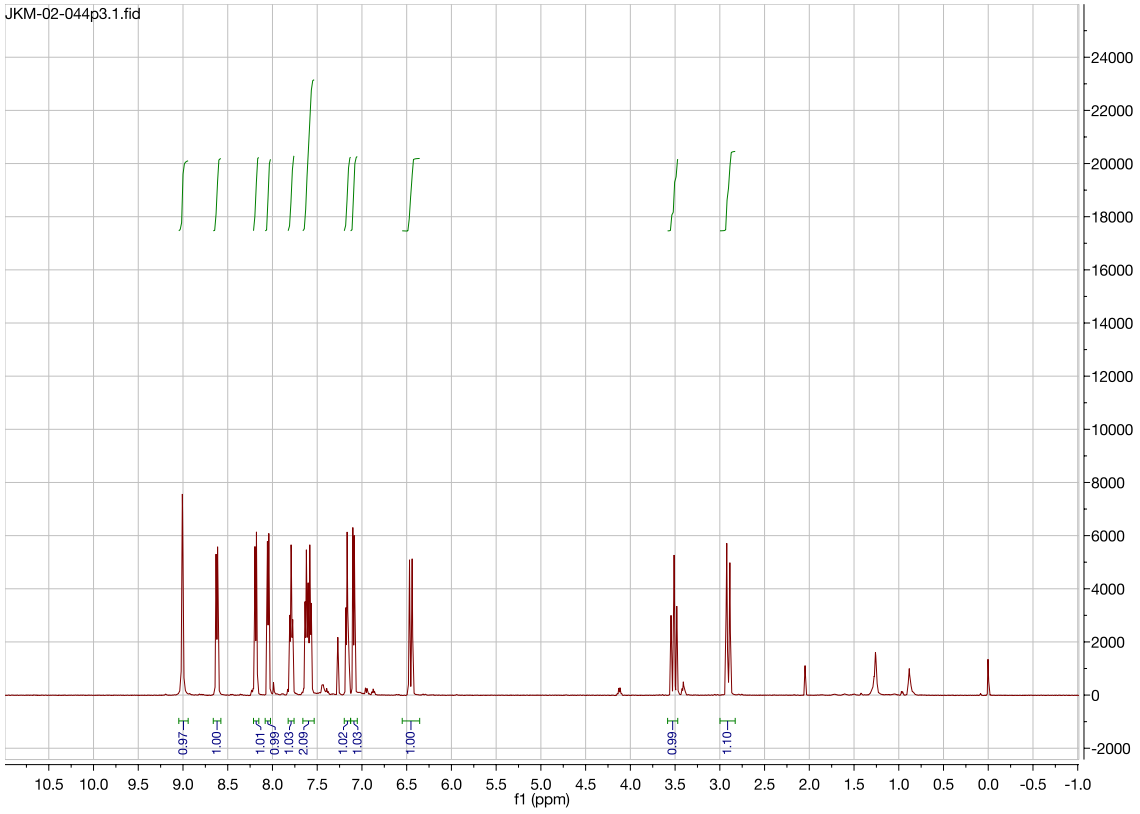

^{13}C ($CDCl_3$, 125.8 MHz) spectra of 2-(3-bromoquinolin-2-yl)chroman-4-one (**3.11.3**)

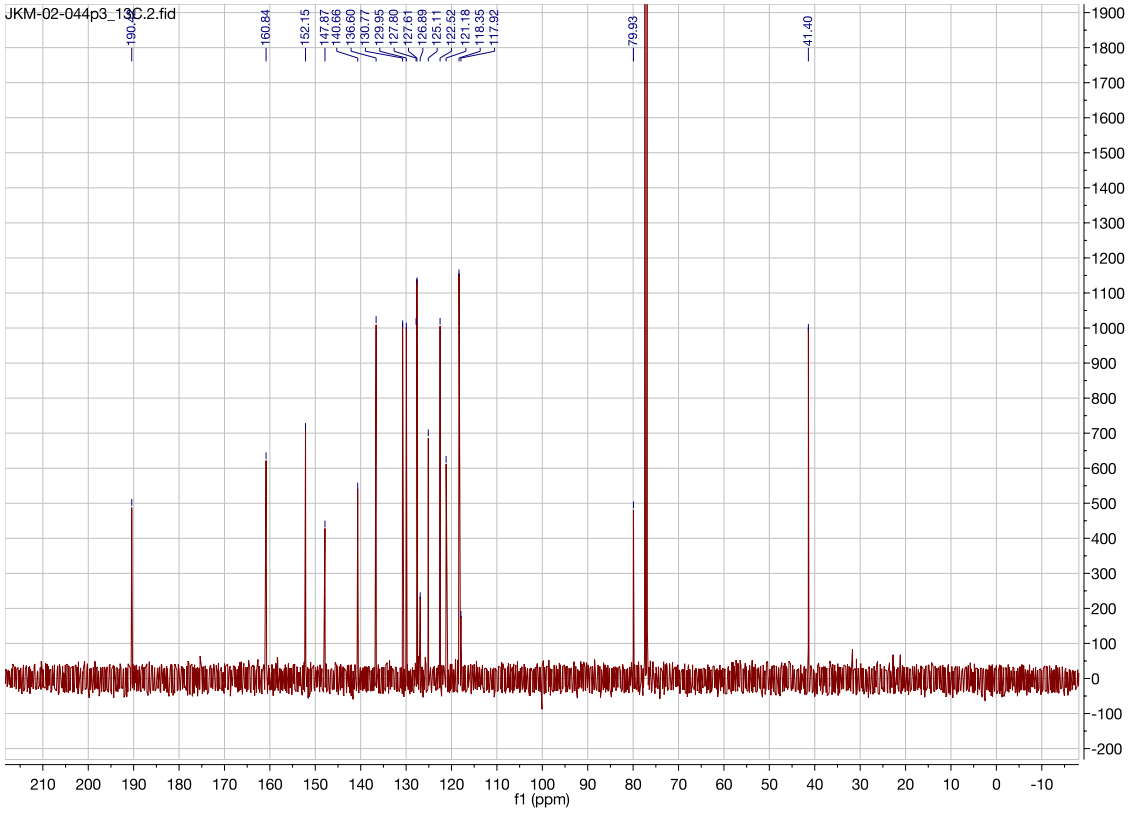

^{1}H ($CDCl_3$, 500 MHz) spectra of 2-(4-bromoquinolin-2-yl)chroman-4-one (**3.11.4**)

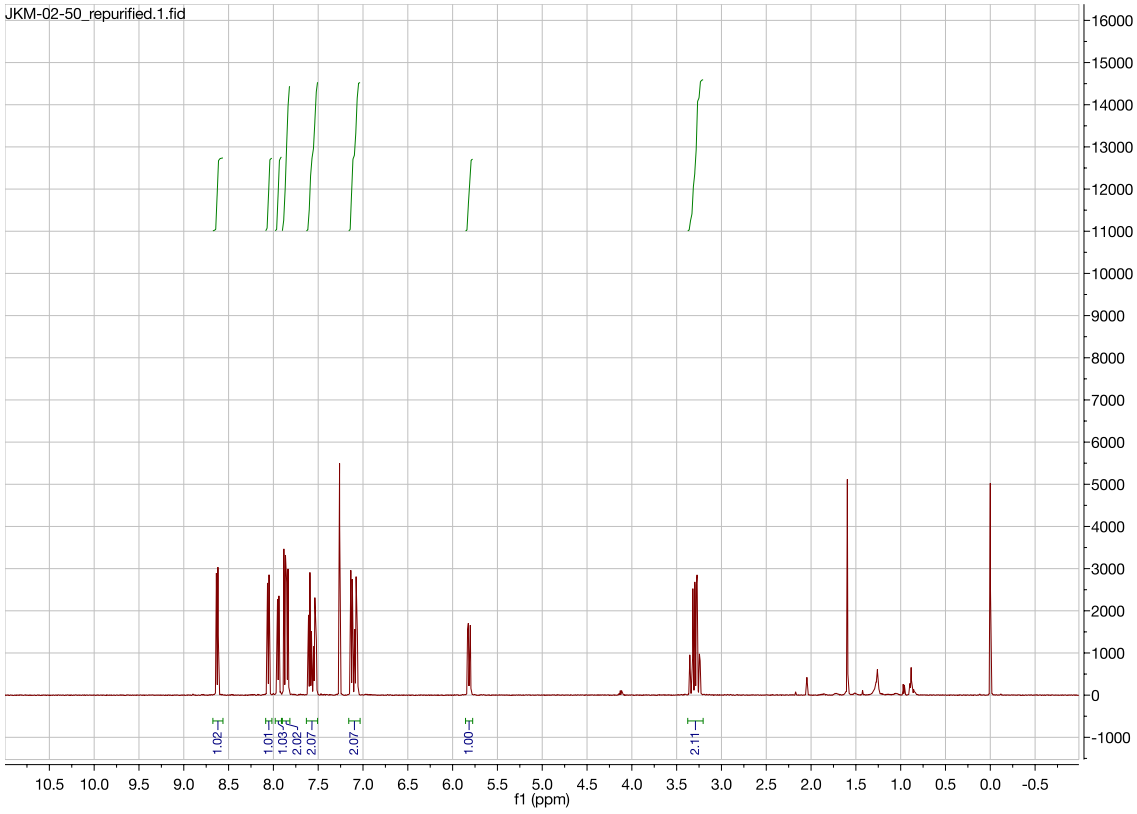

^{13}C ($CDCl_3$, 125.8 MHz) spectra of 2-(4-bromoquinolin-2-yl)chroman-4-one (**3.11.4**)

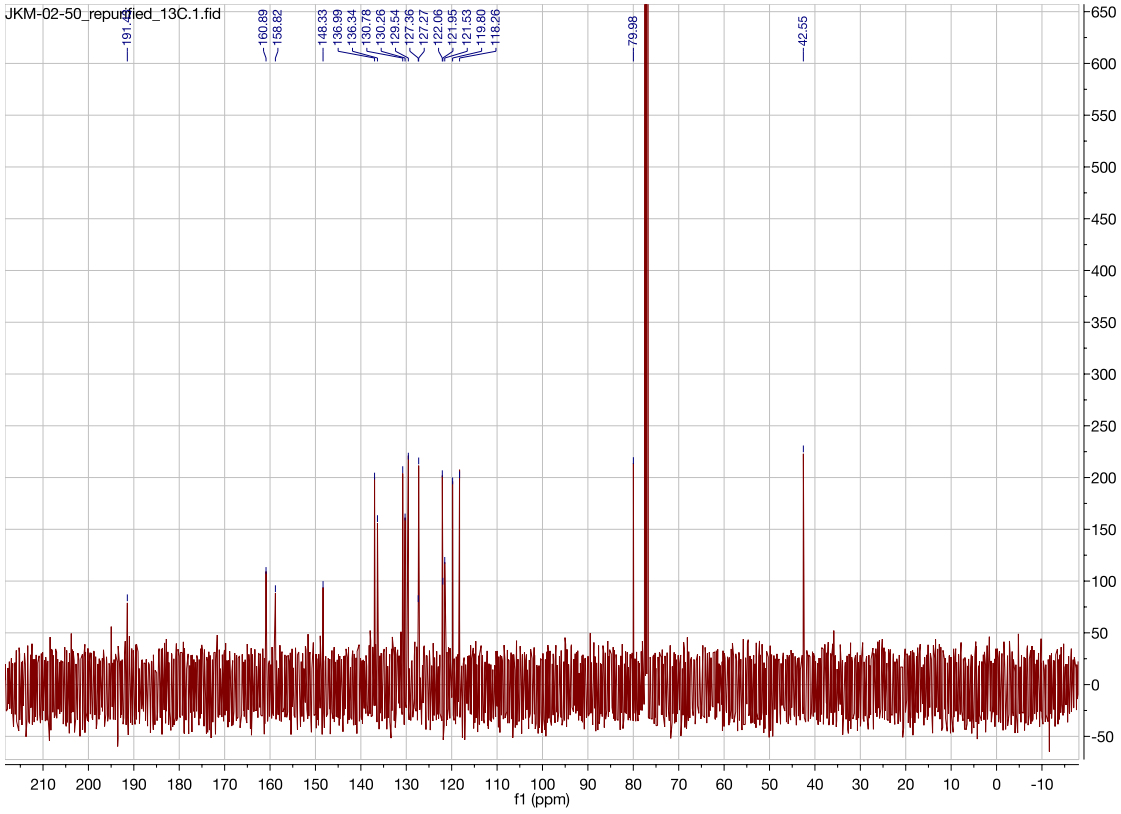

^{1}H ($CDCl_3$, 500 MHz) spectra of 2-(4-chloroquinolin-2-yl)chroman-4-one (**3.11.5**)

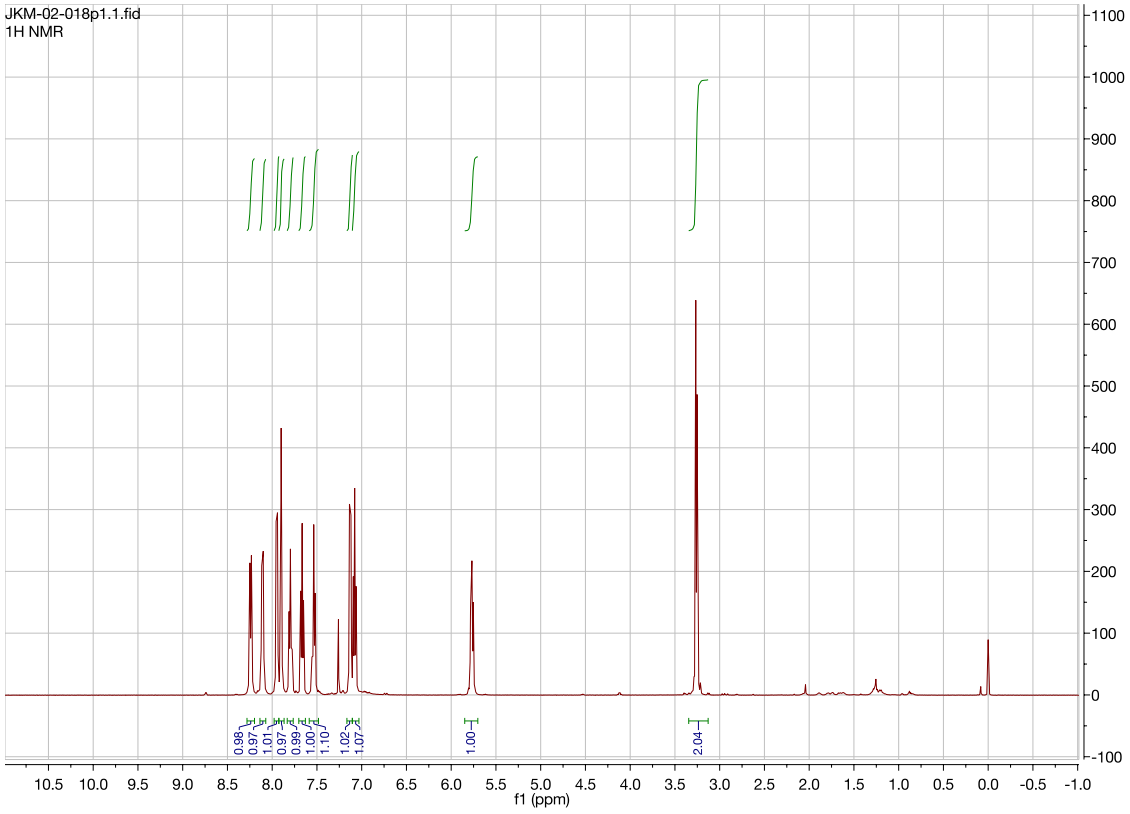

^{13}C ($CDCl_3$, 125.8 MHz) spectra of 2-(4-chloroquinolin-2-yl)chroman-4-one (**3.11.5**)

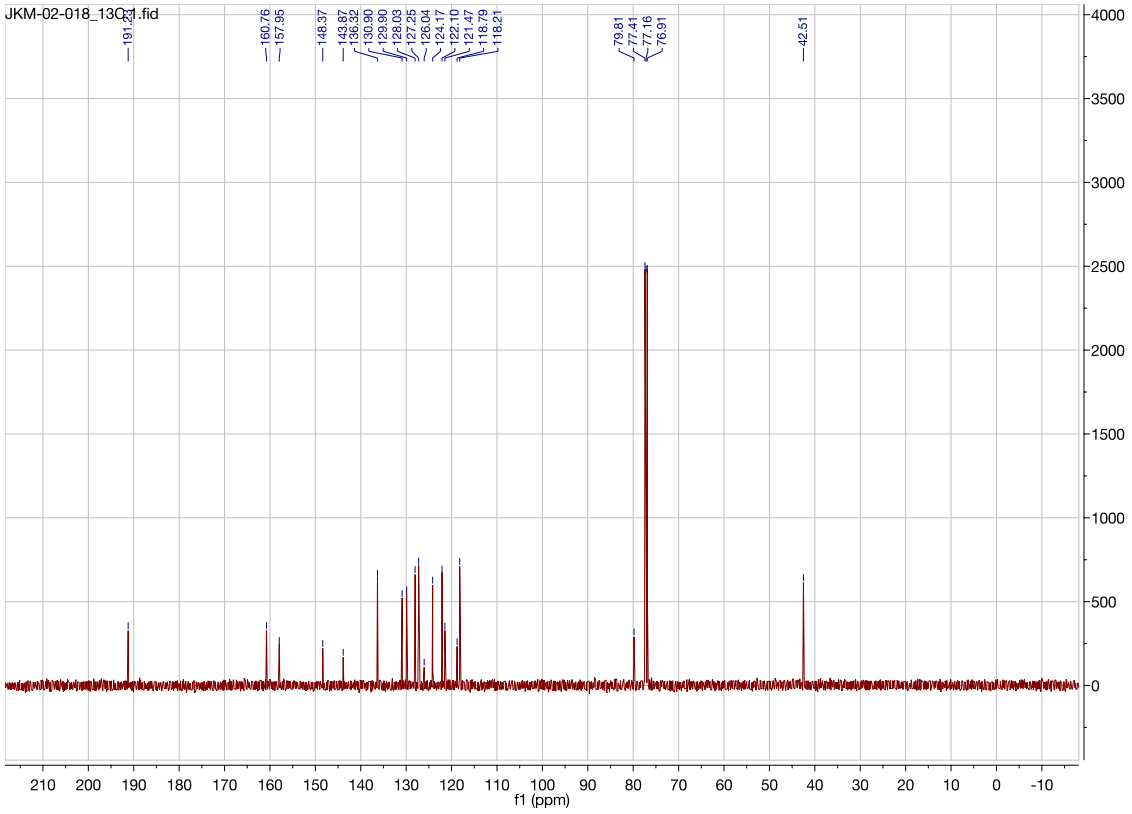

^{1}H ($CDCl_3$, 500 MHz) spectra of 2-(2-chloroquinolin-4-yl)chroman-4-one (**3.11.6**)

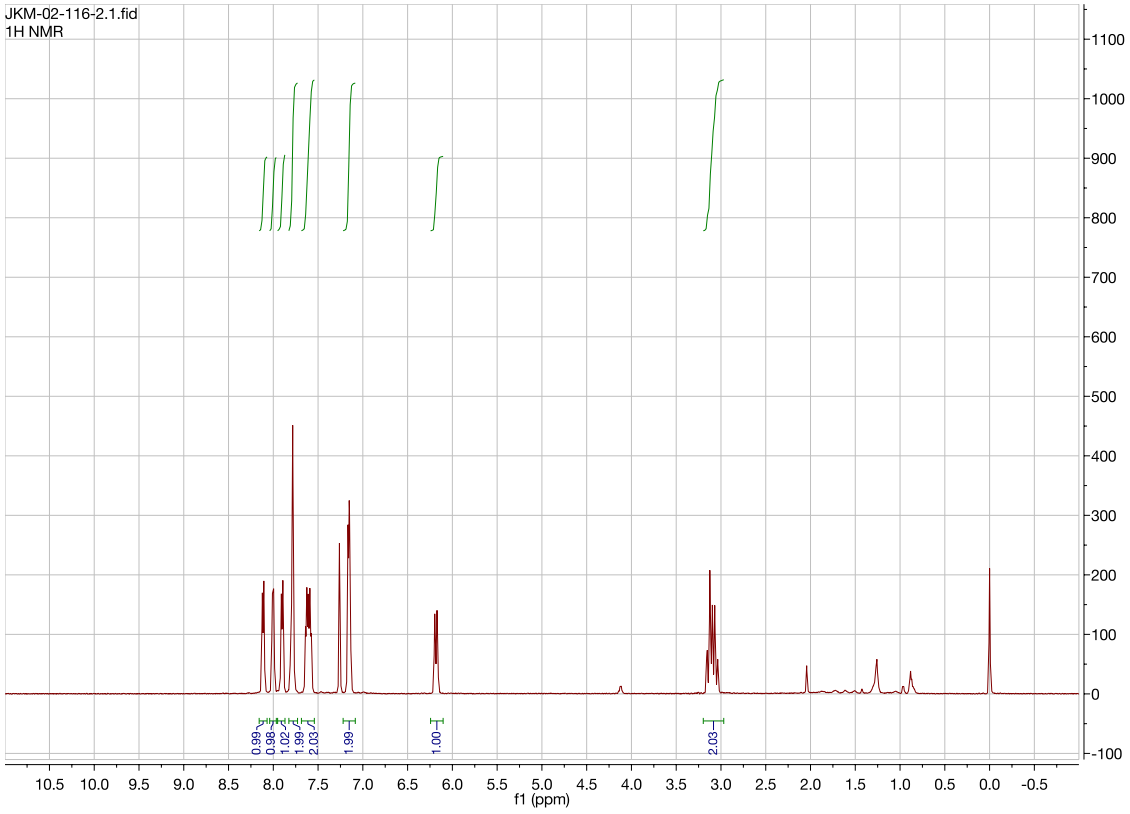

^{13}C ($CDCl_3$, 125.8 MHz) spectra of 2-(2-chloroquinolin-4-yl)chroman-4-one (**3.11.6**)

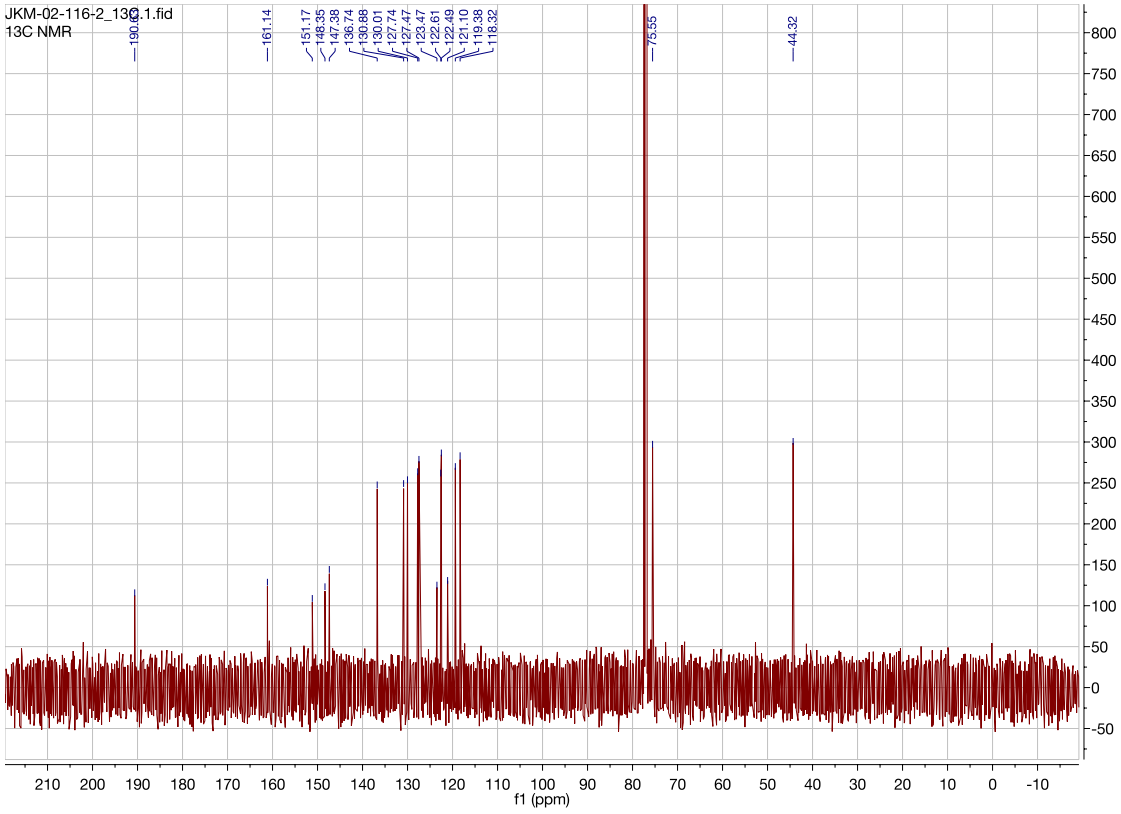

^{1}H ($CDCl_3$, 500 MHz) spectra of 2-(4-chloro-8-(trifluoromethyl)quinolin-2-yl)chroman-4-one (**3.11.7**)

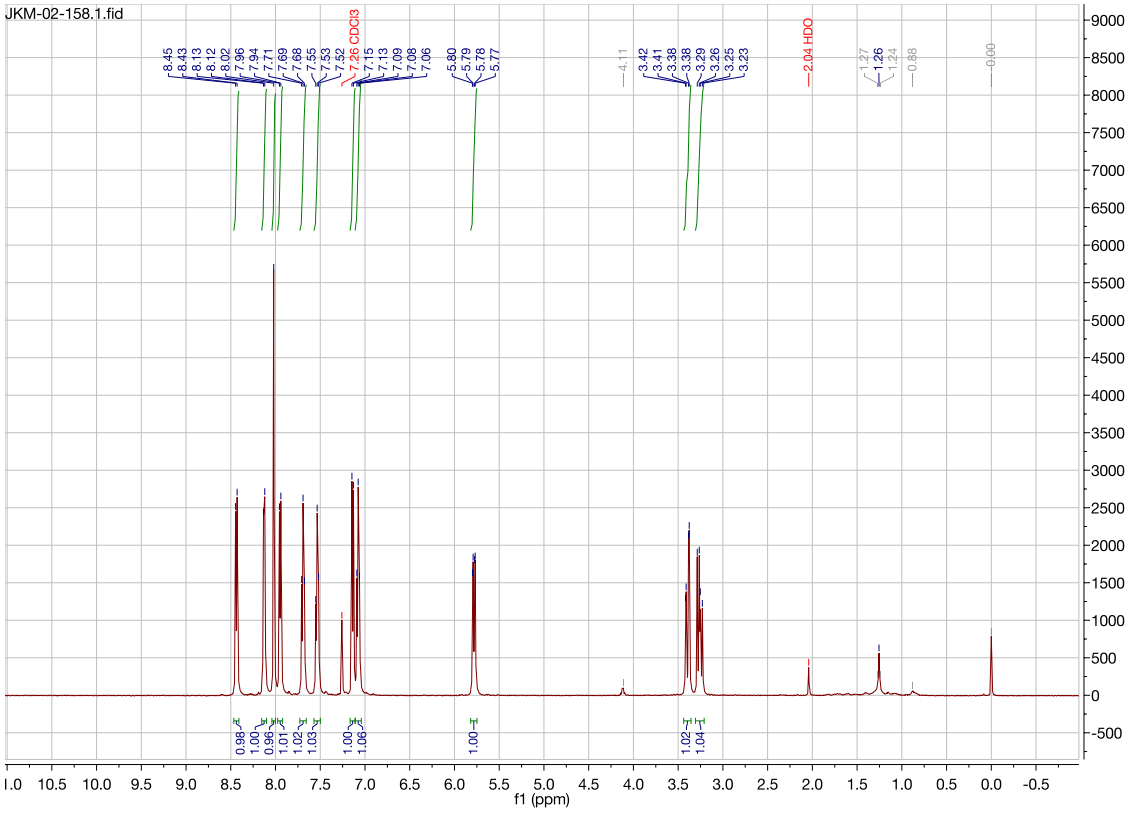

^{13}C ($CDCl_3$, 125.8 MHz) spectra of 2-(4-chloro-8-(trifluoromethyl)quinolin-2-yl)chroman-4-one (**3.11.7**)

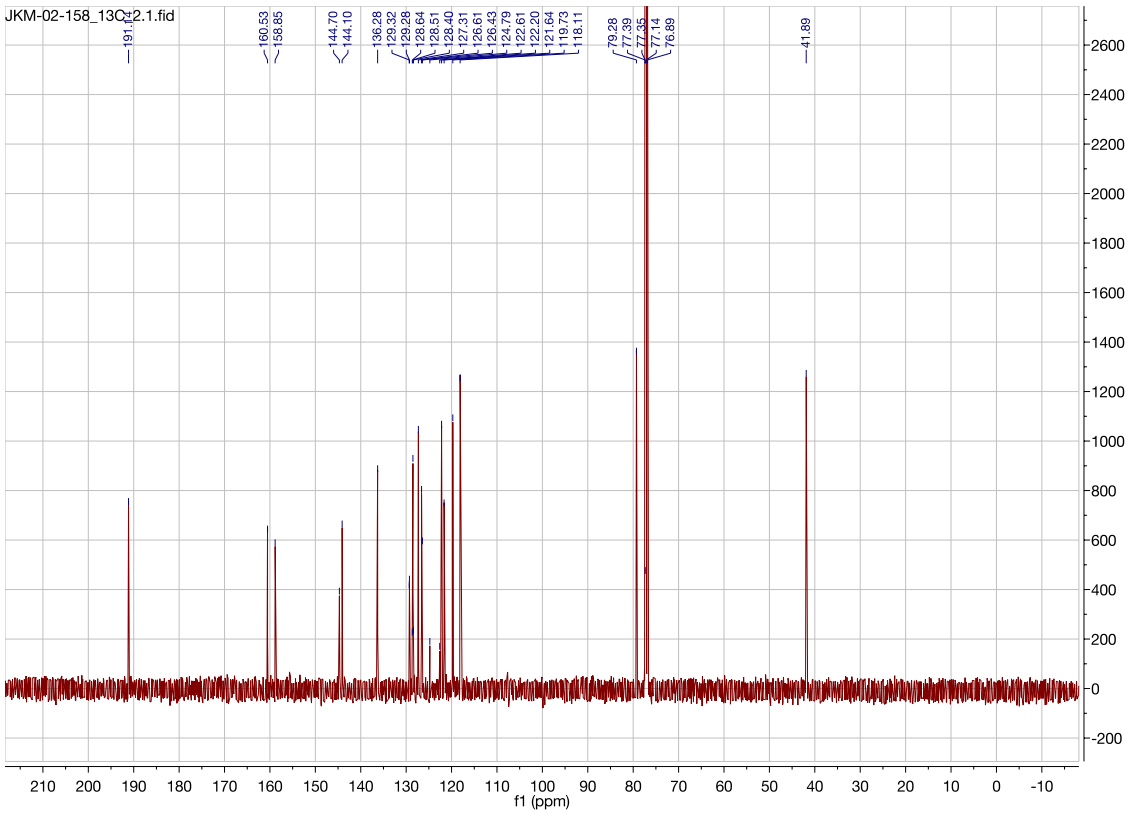

^{19}F NMR (471 MHz, $CDCl_3$) spectra of 2-(4-chloro-8-(trifluoromethyl)quinolin-2-yl)chroman-4-one (**3.11.7**)

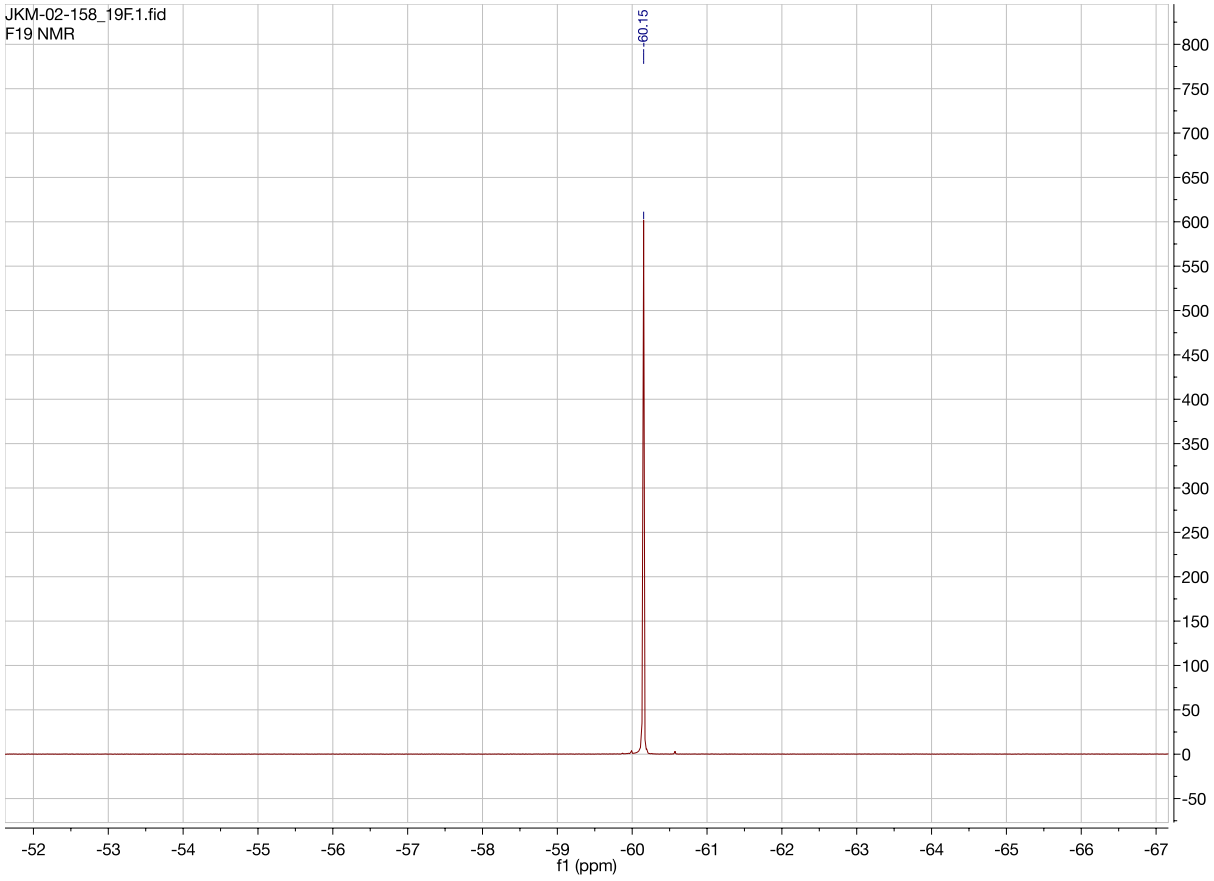

^{1}H ($CDCl_3$, 500 MHz) spectra of 2-(1-chloroisoquinolin-3-yl)chroman-4-one (**3.12.1**)

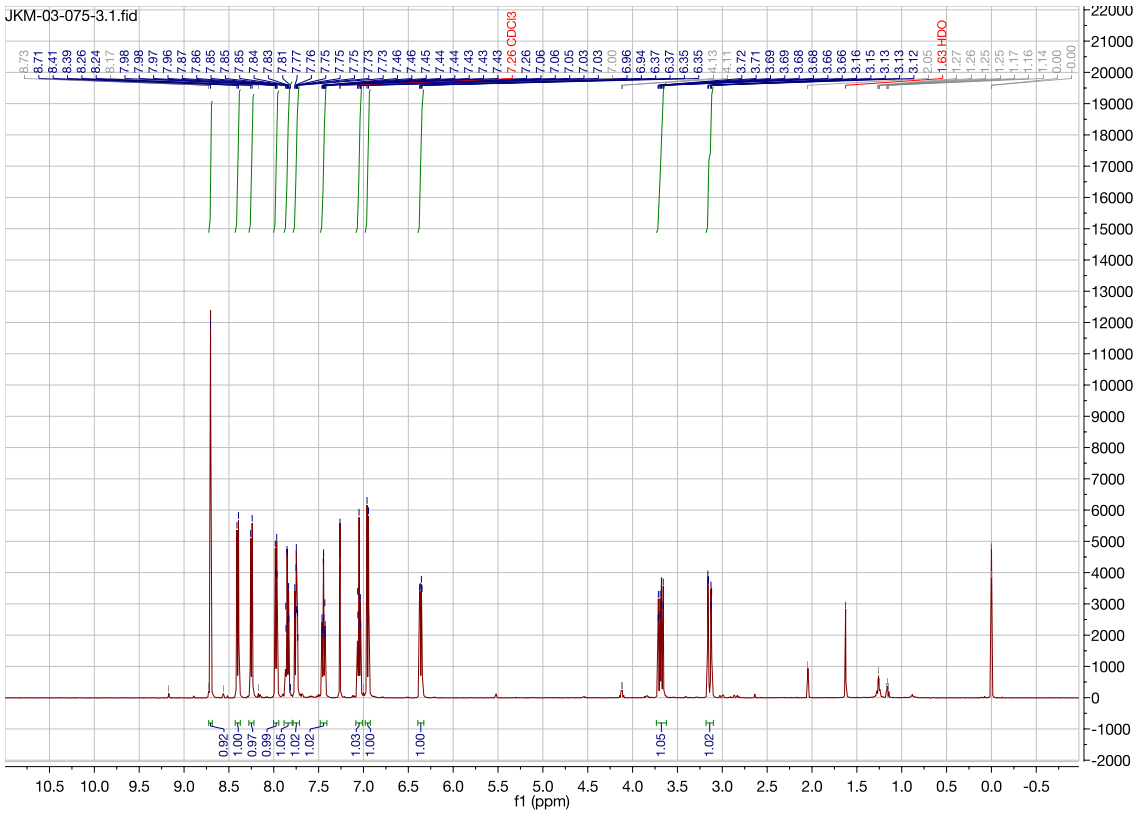

^{13}C ($CDCl_3$, 125.8 MHz) spectra of 2-(1-chloroisoquinolin-3-yl)chroman-4-one (**3.12.1**)

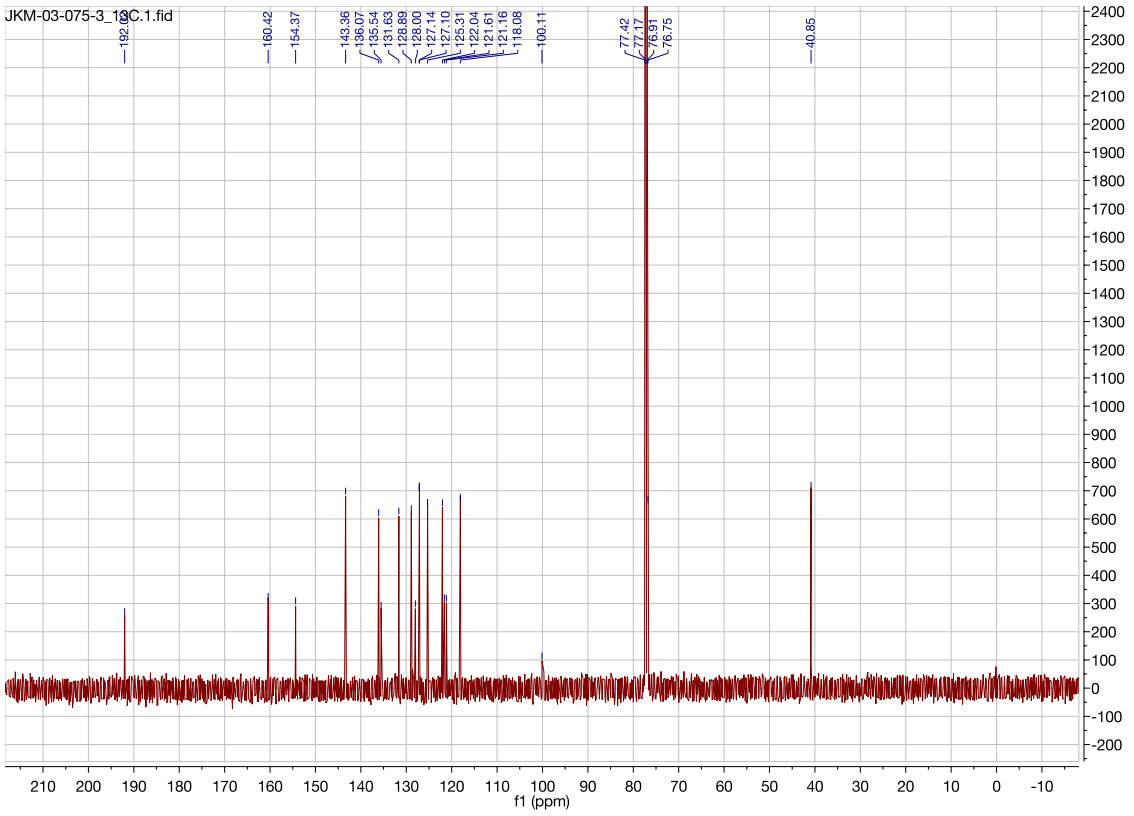

^{1}H ($CDCl_3$, 500 MHz) spectra of 2-(4-bromoisoquinolin-1-yl)chroman-4-one (**3.12.2**)

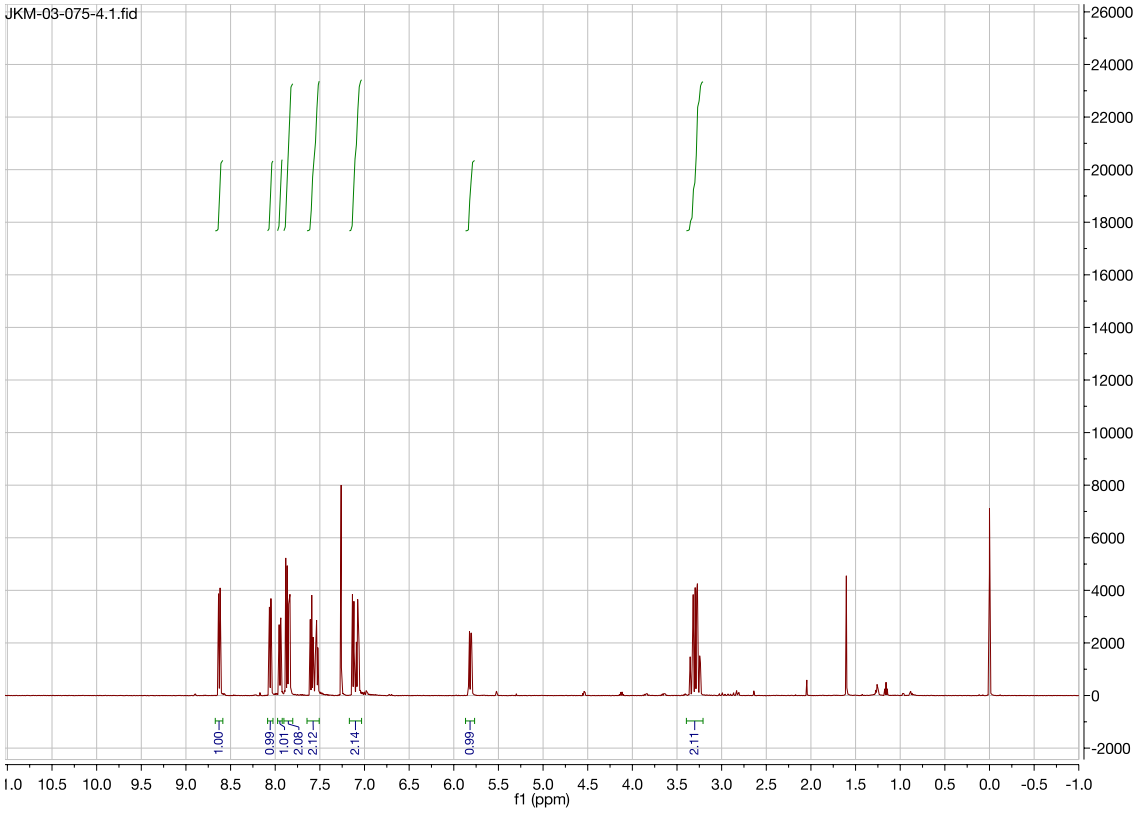

^{13}C ($CDCl_3$, 125.8 MHz) spectra of 2-(4-bromoisoquinolin-1-yl)chroman-4-one (**3.12.2**)

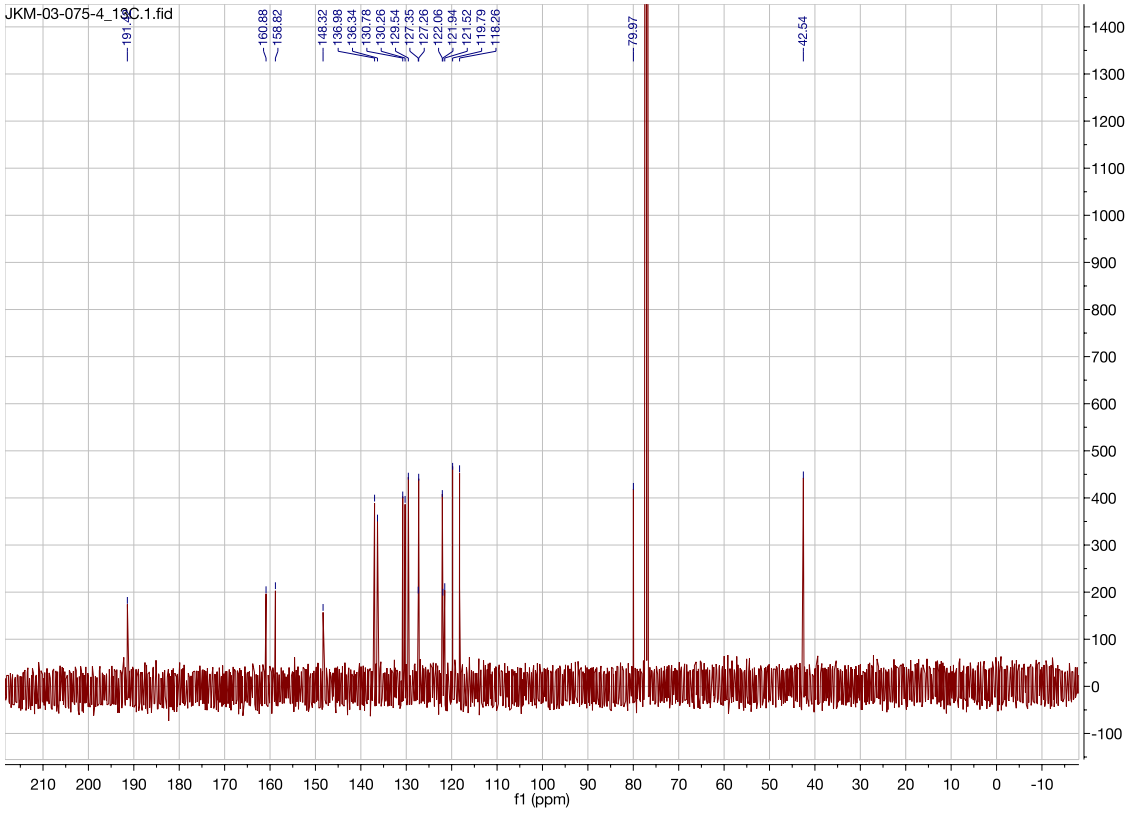

^{1}H ($CDCl_3$, 500 MHz) spectra of 2-(quinoxalin-2-yl)chroman-4-one (**3.12.4**)

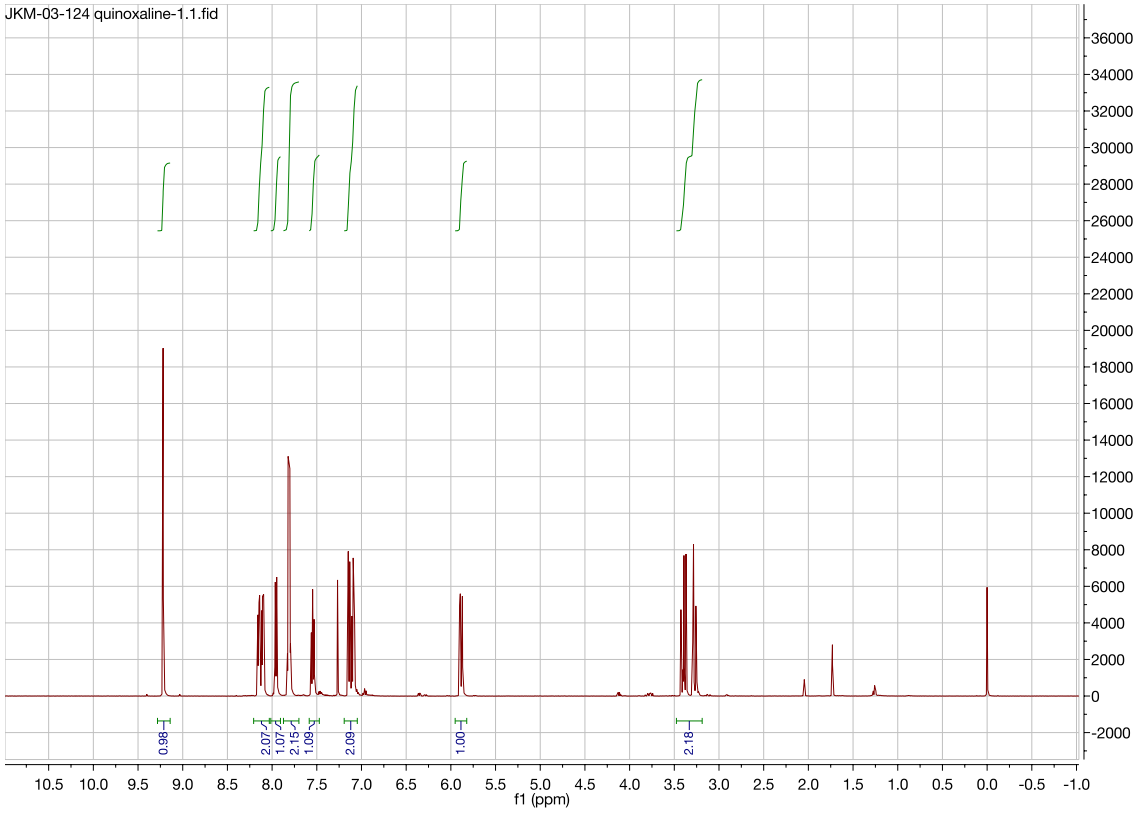

^{13}C ($CDCl_3$, 125.8 MHz) spectra of 2-(quinoxalin-2-yl)chroman-4-one (**3.12.4**)

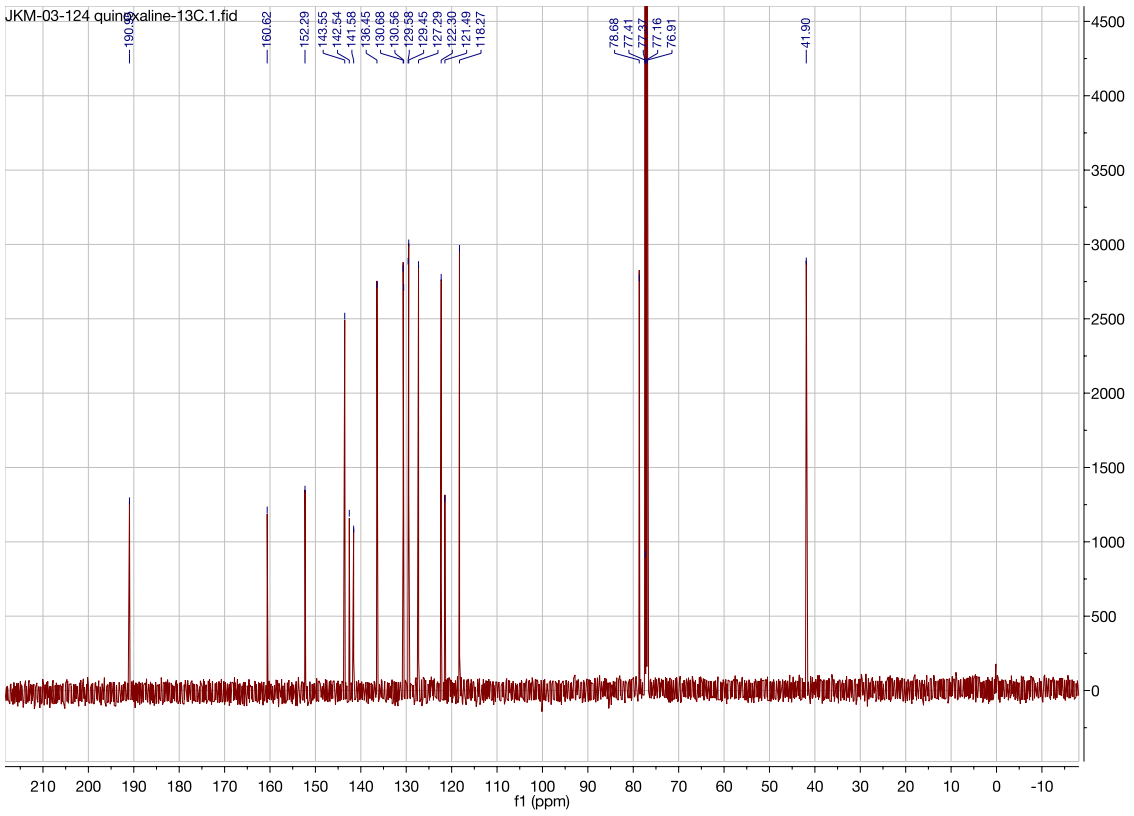

^{1}H ($CDCl_3$, 500 MHz) spectra of 2-(3-chloroquinoxalin-2-yl)chroman-4-one (**3.12.5**)

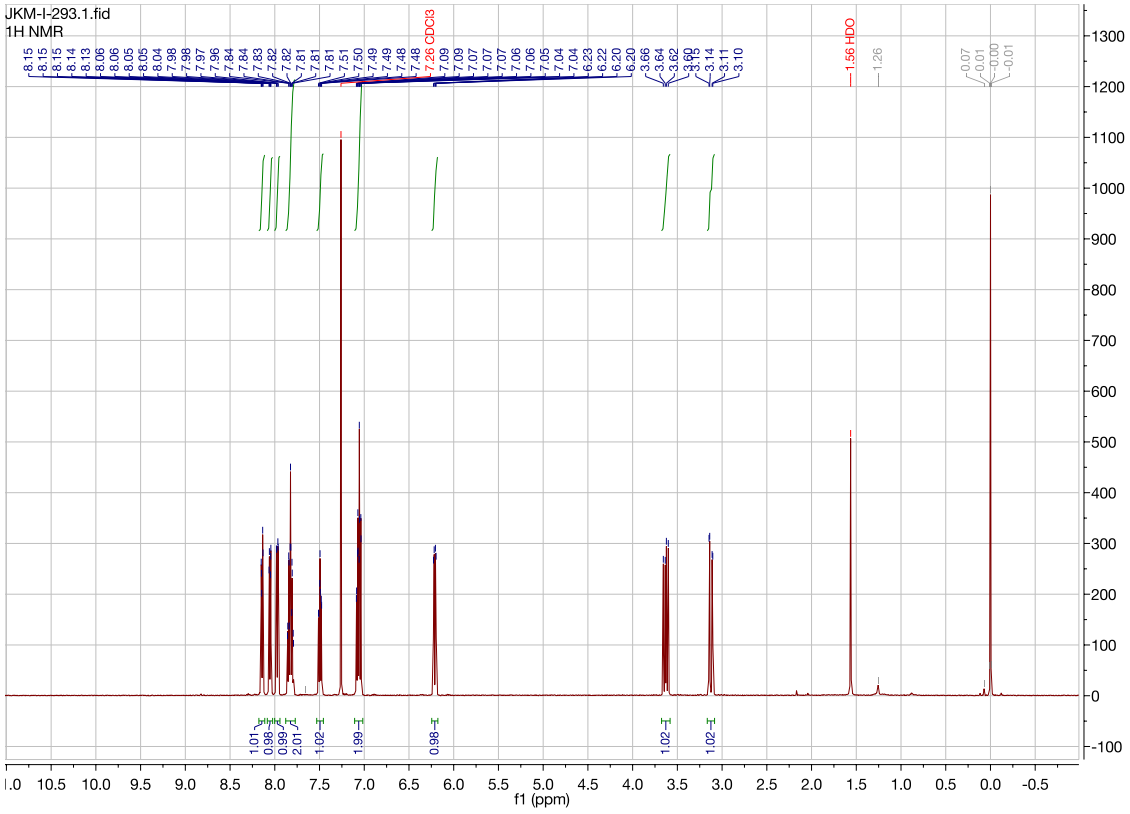

^{13}C ($CDCl_3$, 125.8 MHz) spectra of 2-(3-chloroquinoxalin-2-yl)chroman-4-one (**3.12.5**)

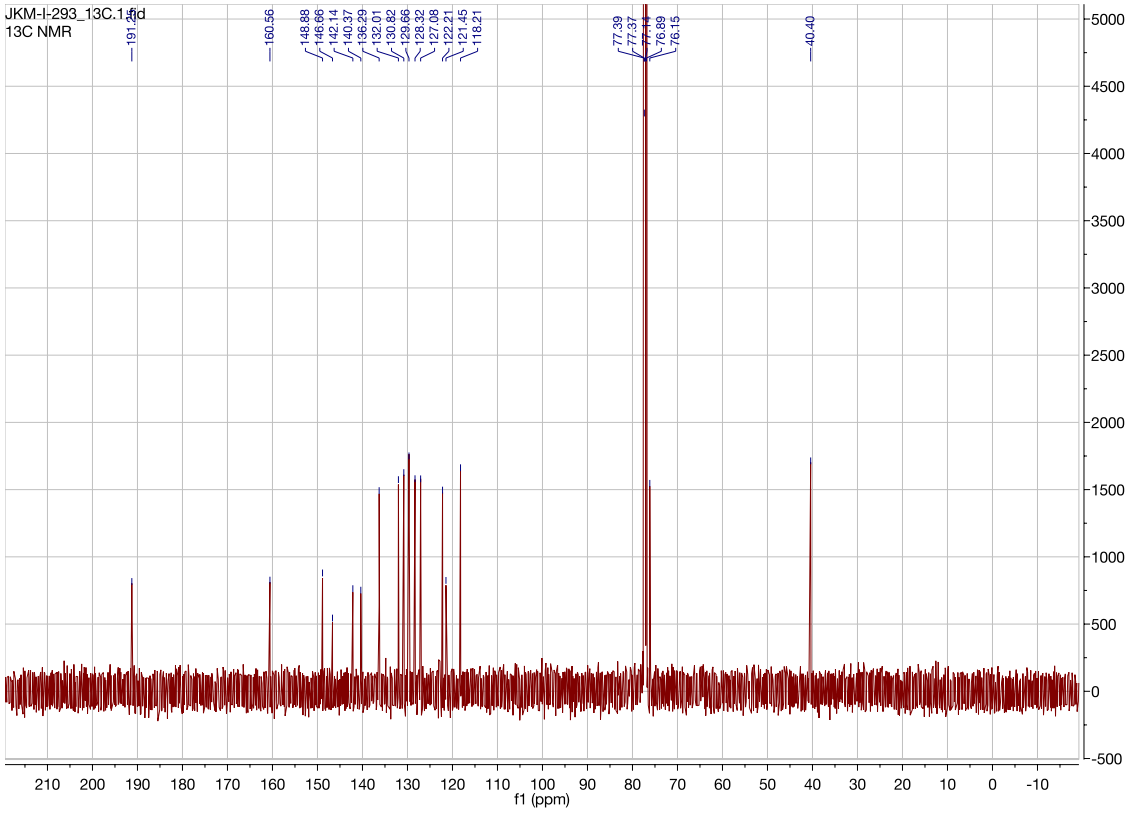

^{1}H ($CDCl_3$, 500 MHz) spectra of 1,3,7-trimethyl-8-(4-oxochroman-2-yl)-3,7-dihydro-1*H*-purine-2,6-dione (**3.12.6**)

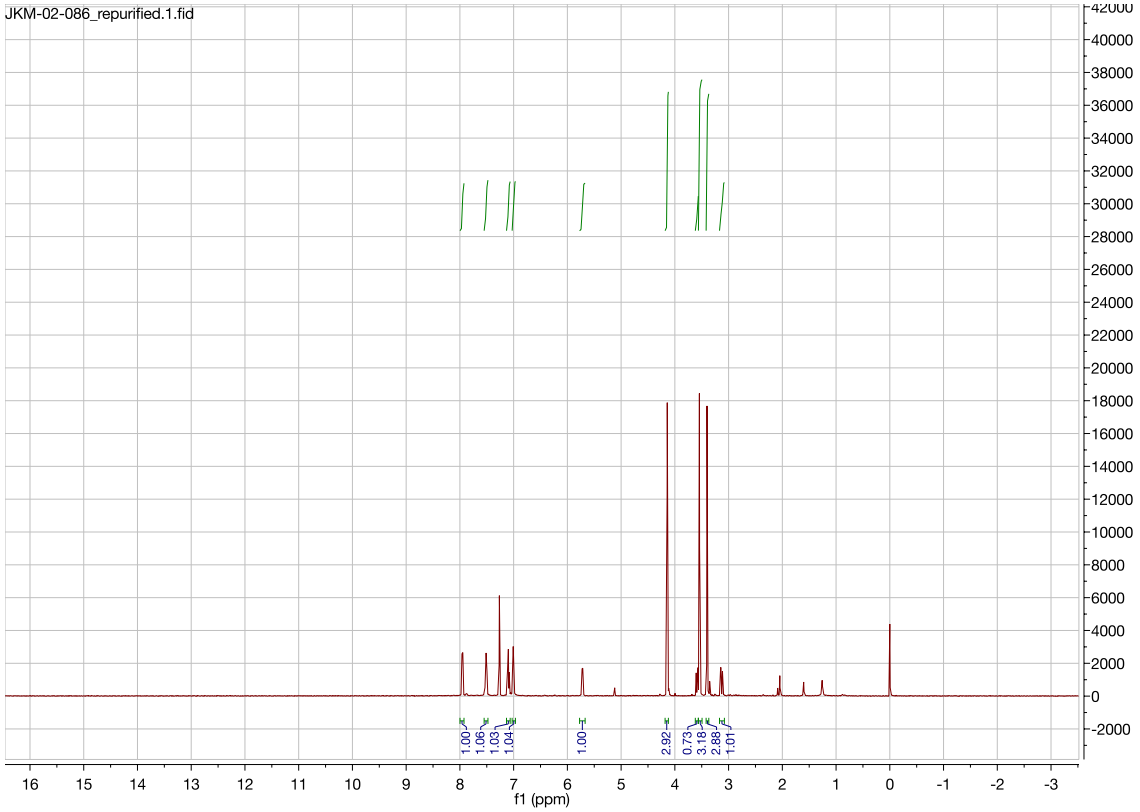

^{13}C ($CDCl_3$, 125.8 MHz) spectra of 1,3,7-trimethyl-8-(4-oxochroman-2-yl)-3,7-dihydro-1*H*-purine-2,6-dione (**3.12.6**)

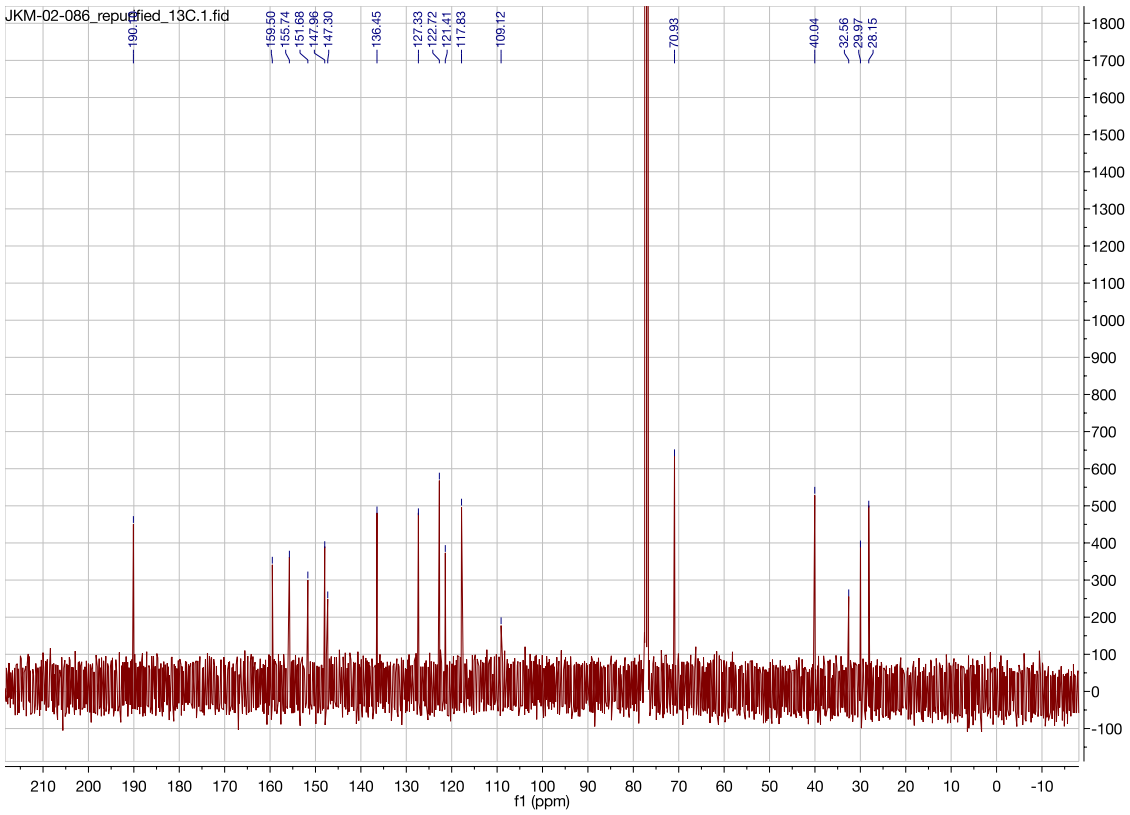

^{1}H ($CDCl_3$, 500 MHz) spectra of 2-(4-(trifluoromethyl)pyridin-2-yl)chroman-4-one **(3.12.7)**

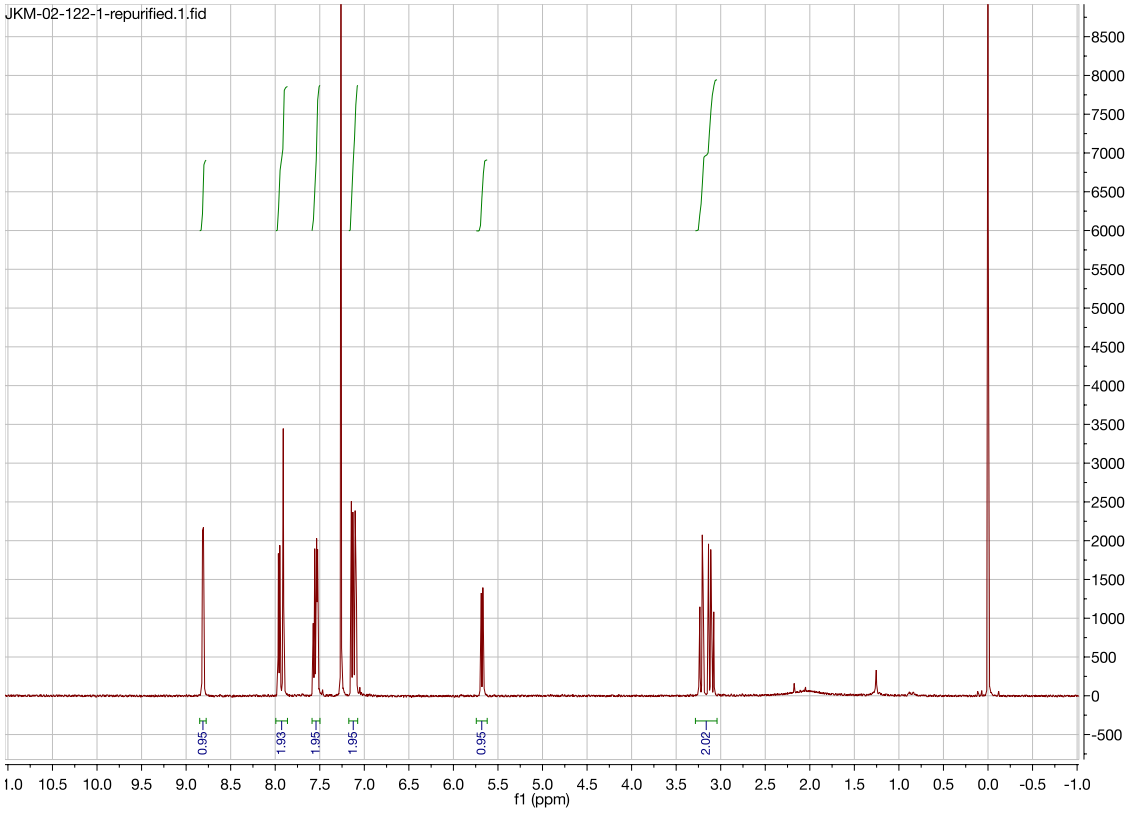

^{13}C ($CDCl_3$, 125.8 MHz) spectra of 2-(4-(trifluoromethyl)pyridin-2-yl)chroman-4-one **(3.12.7)**

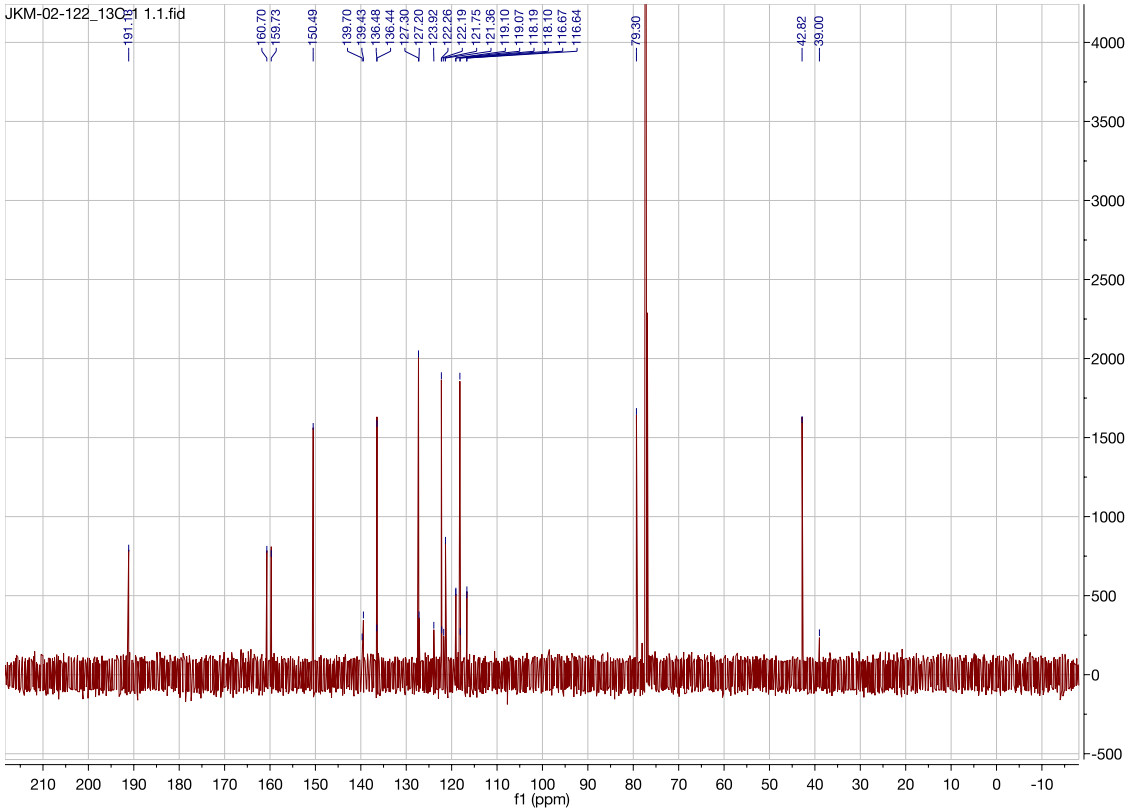

^{19}F NMR (471 MHz, $CDCl_3$) spectra of 2-(4-(trifluoromethyl)pyridin-2-yl)chroman-4-one **(3.12.7)**

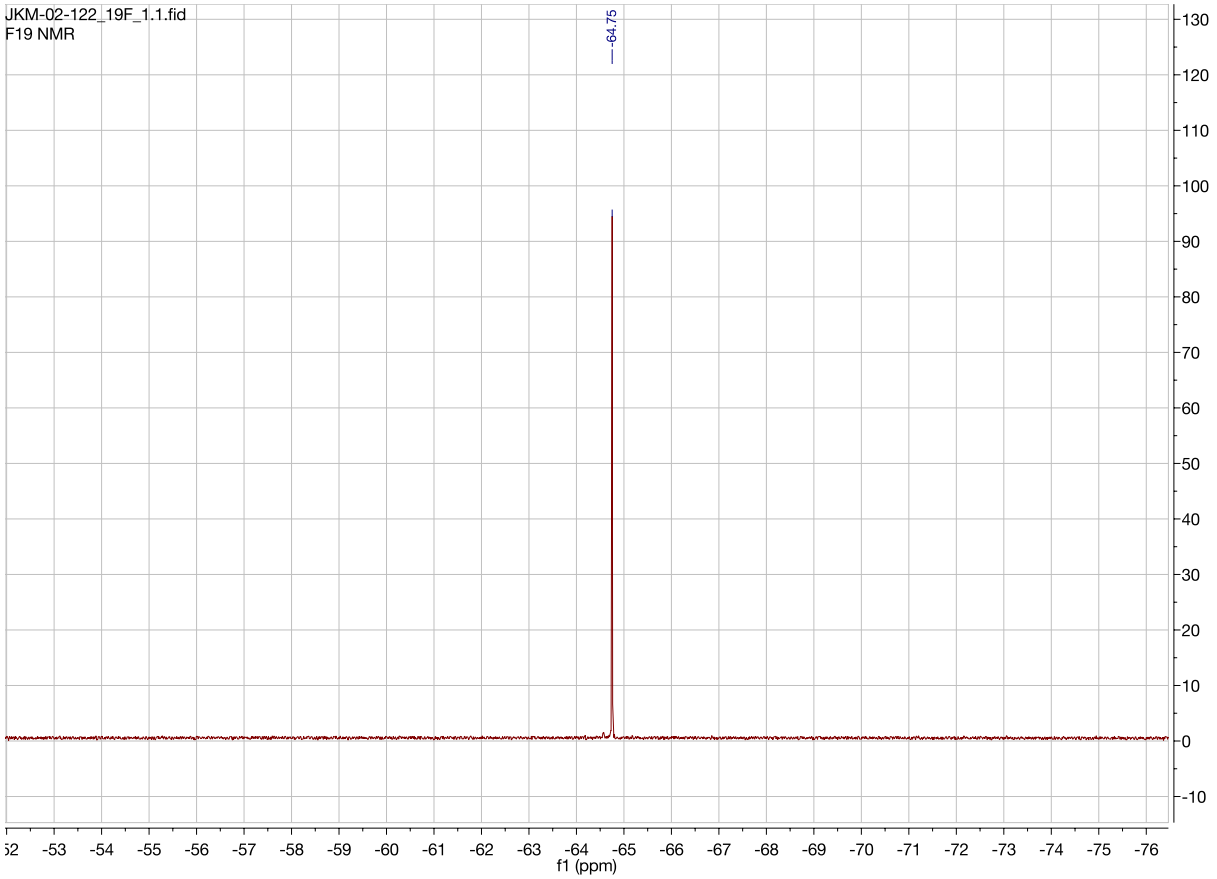

^{1}H ($CDCl_3$, 500 MHz) spectra of 6-bromo-2-(4-chloroquinolin-2-yl)chroman-4-one (**3.14.1**)

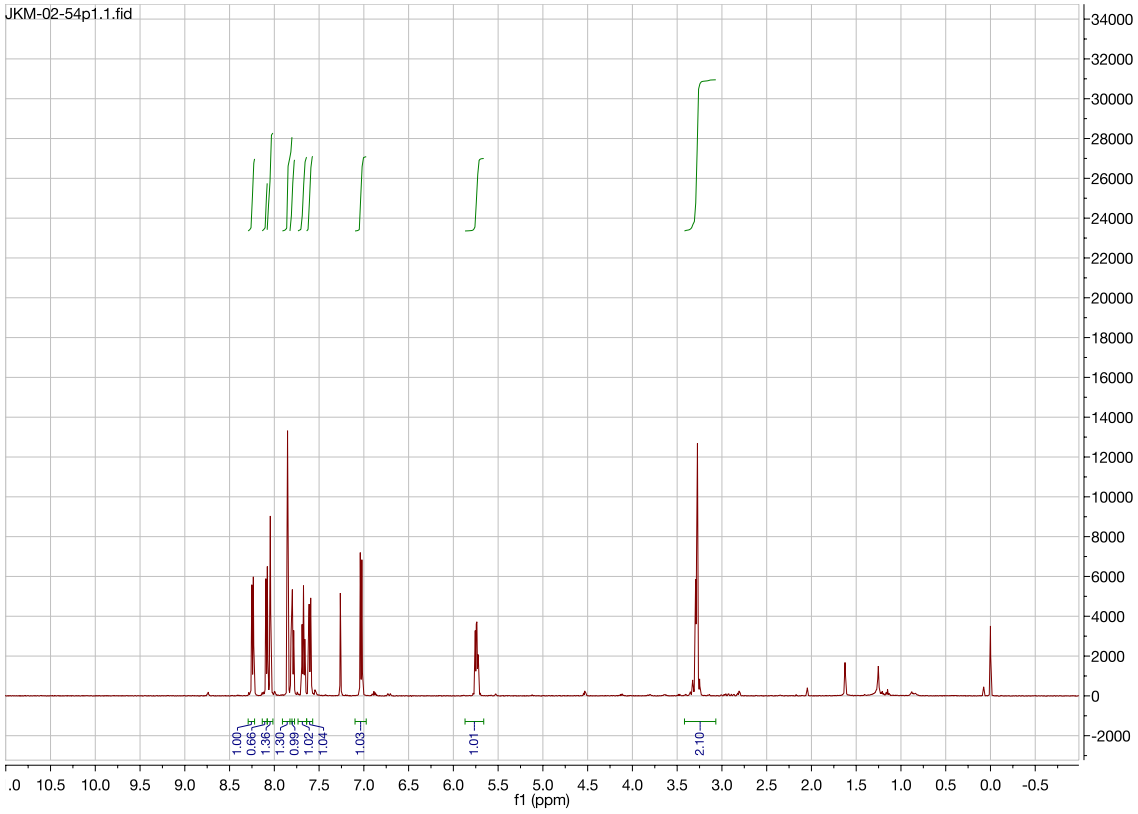

^{13}C ($CDCl_3$, 125.8 MHz) spectra of 6-bromo-2-(4-chloroquinolin-2-yl)chroman-4-one (**3.14.1**)

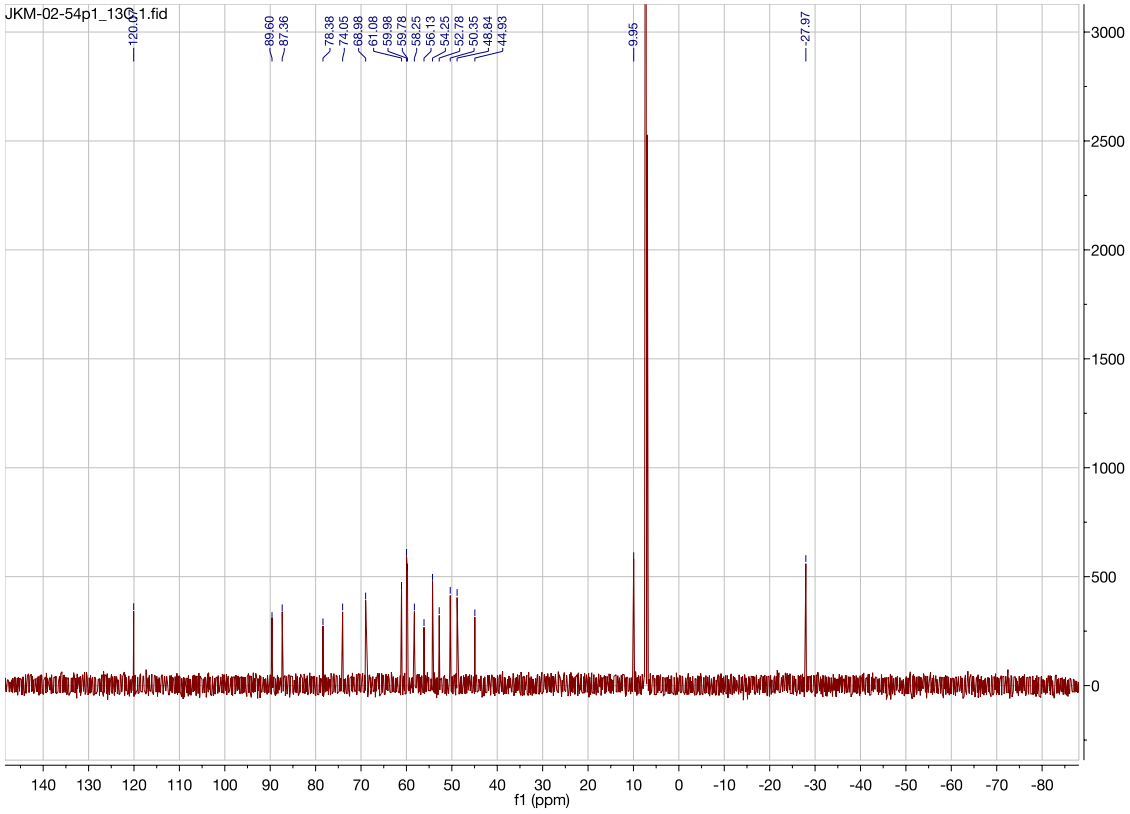

^{1}H ($CDCl_3$, 500 MHz) spectra of 6-bromo-2-(4-chloro-8-(trifluoromethyl)quinolin-2-yl)chroman-4-one (**3.14.2**)

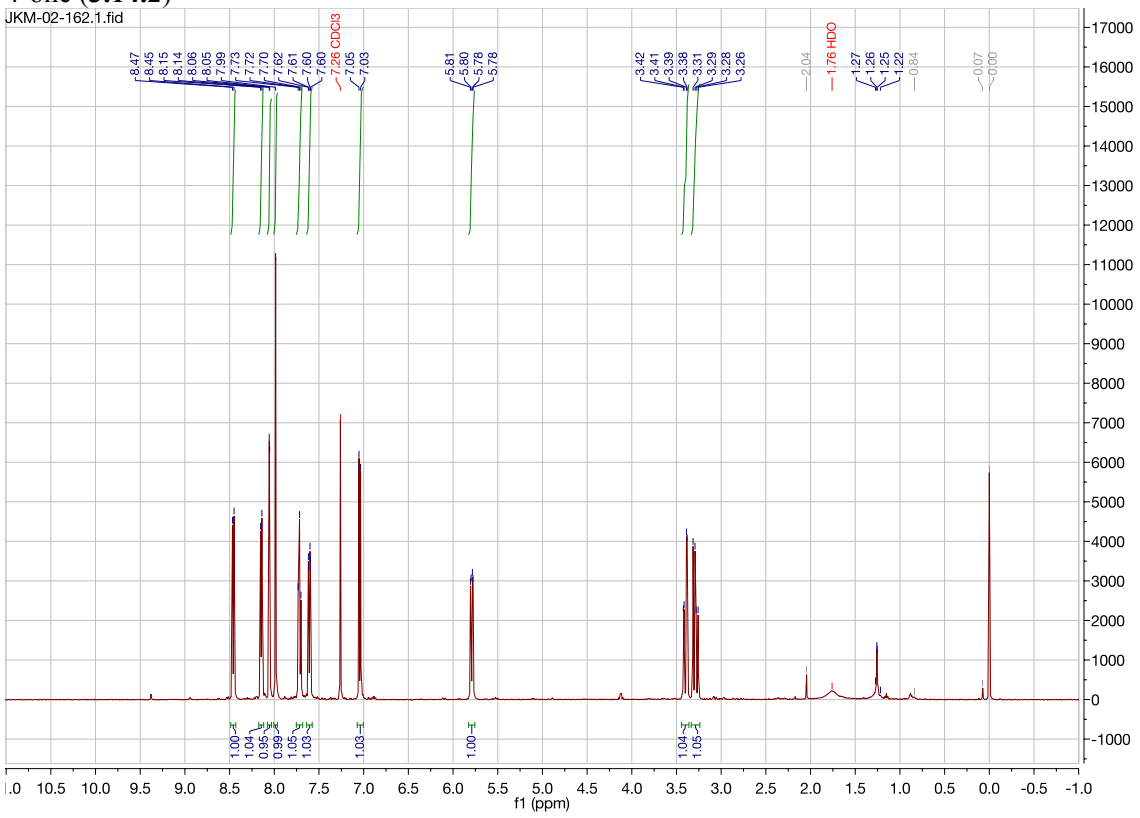

^{13}C ($CDCl_3$, 125.8 MHz) spectra of 6-bromo-2-(4-chloro-8-(trifluoromethyl)quinolin-2-yl)chroman-4-one (**3.14.2**)

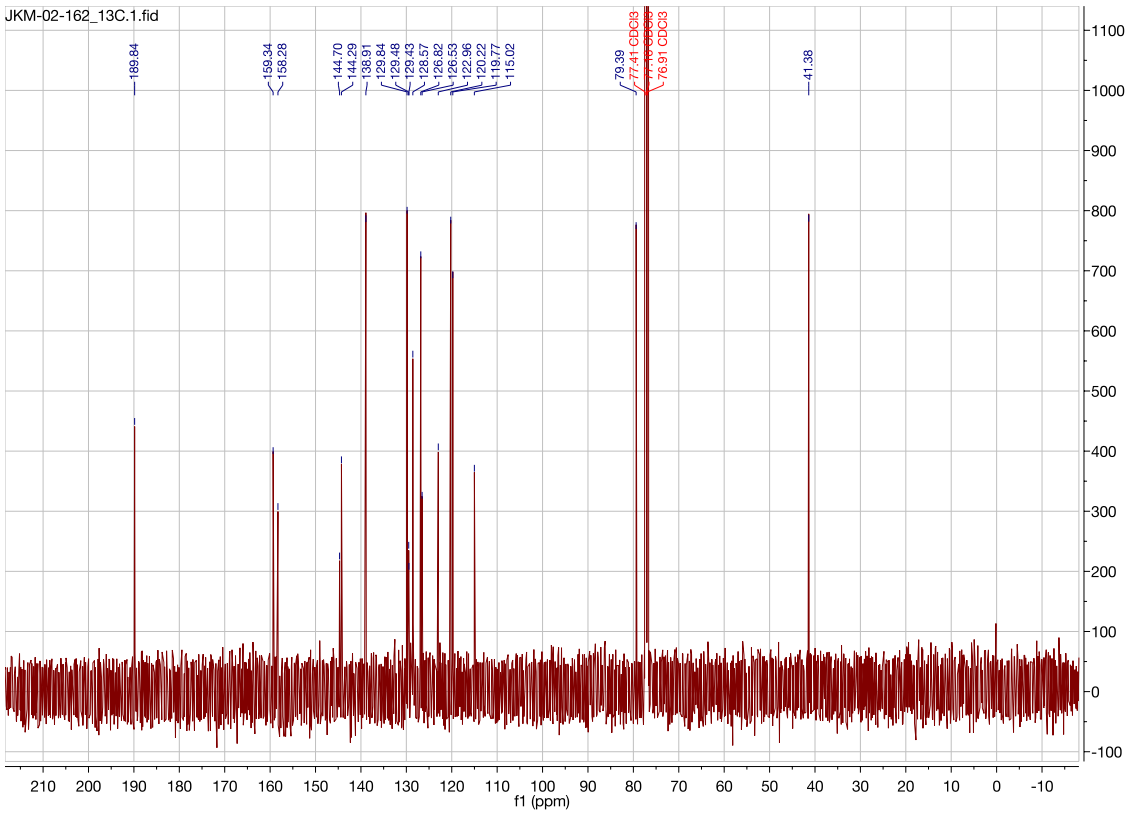

^{19}F NMR (471 MHz, $CDCl_3$) spectra of 6-bromo-2-(4-chloro-8-(trifluoromethyl)quinolin-2-yl)chroman-4-one (**3.14.2**)

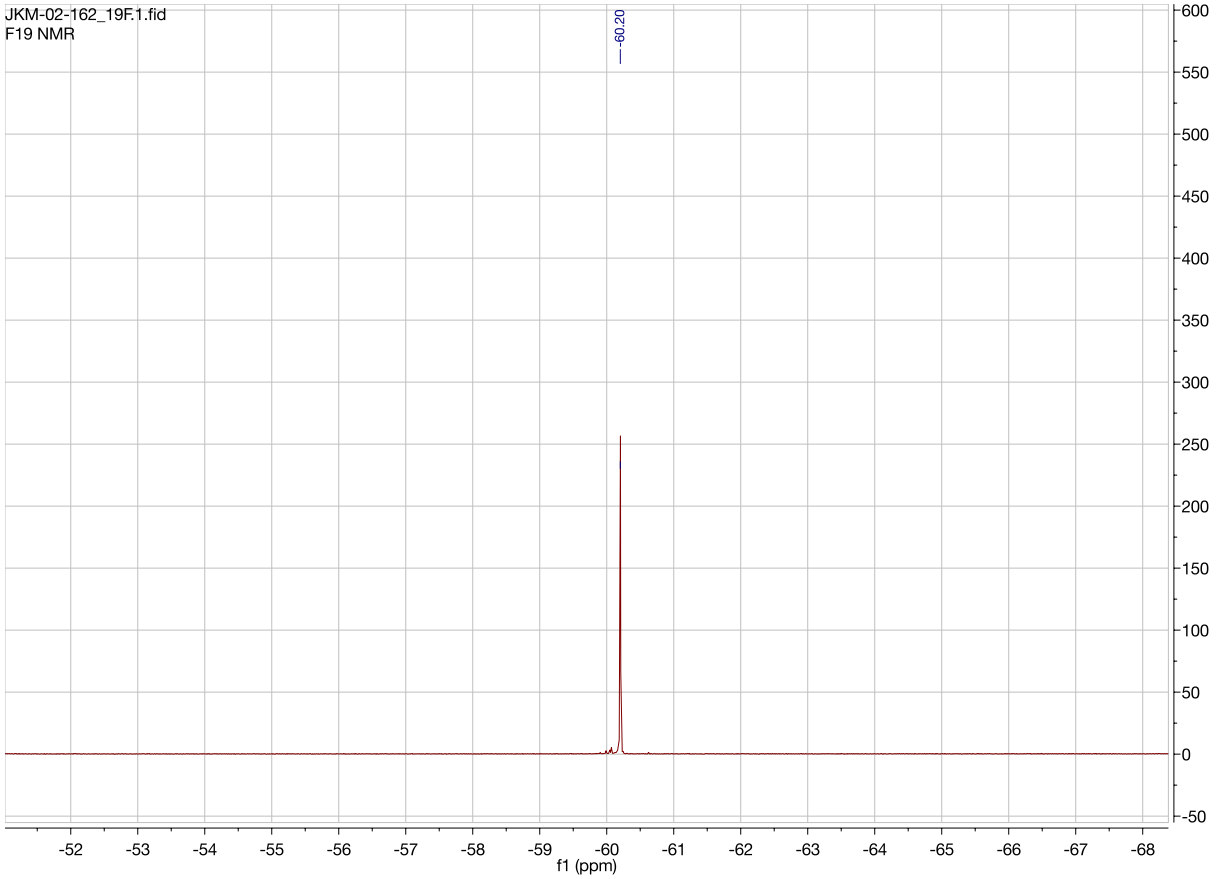

^{1}H ($CDCl_3$, 500 MHz) spectra of 6-bromo-2-(4-methylquinolin-2-yl)chroman-4-one (**3.14.3**)

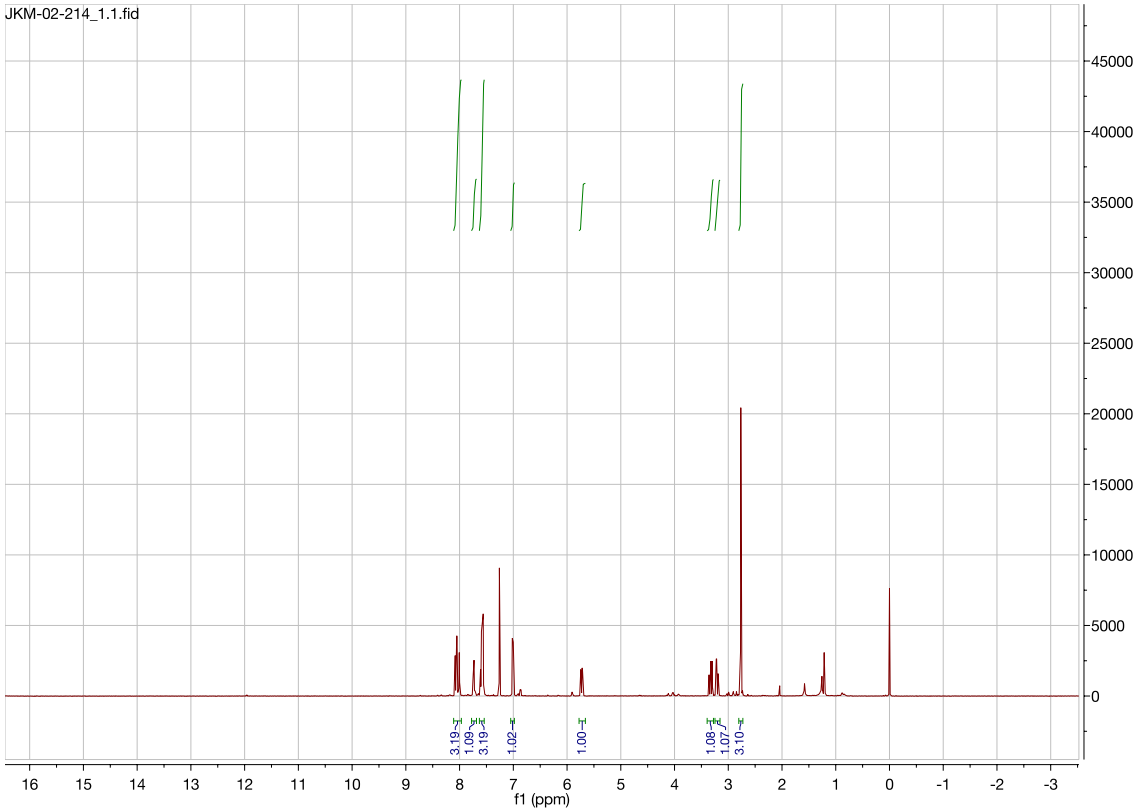

^{13}C ($CDCl_3$, 125.8 MHz) spectra of 6-bromo-2-(4-methylquinolin-2-yl)chroman-4-one (**3.14.3**)

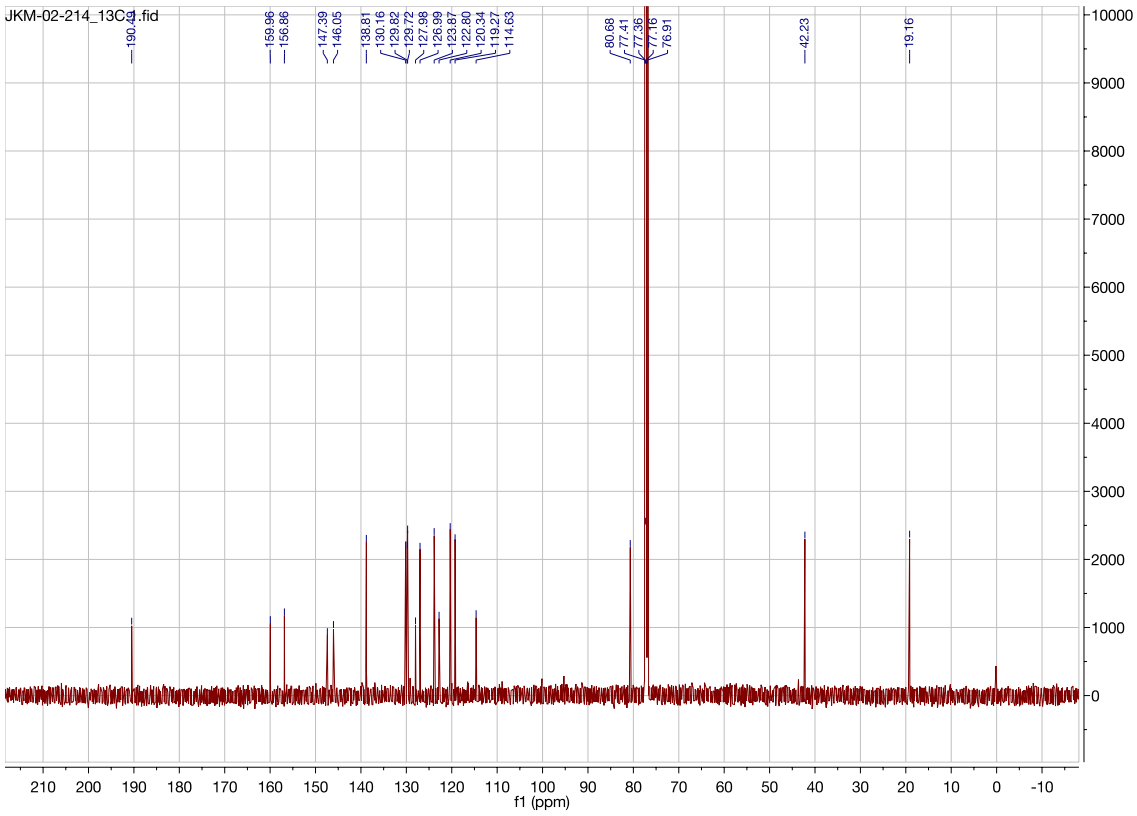

^{1}H ($CDCl_3$, 500 MHz) spectra of 2-(8-chloro-2-methylquinolin-4-yl)chroman-4-one (**3.14.4**)

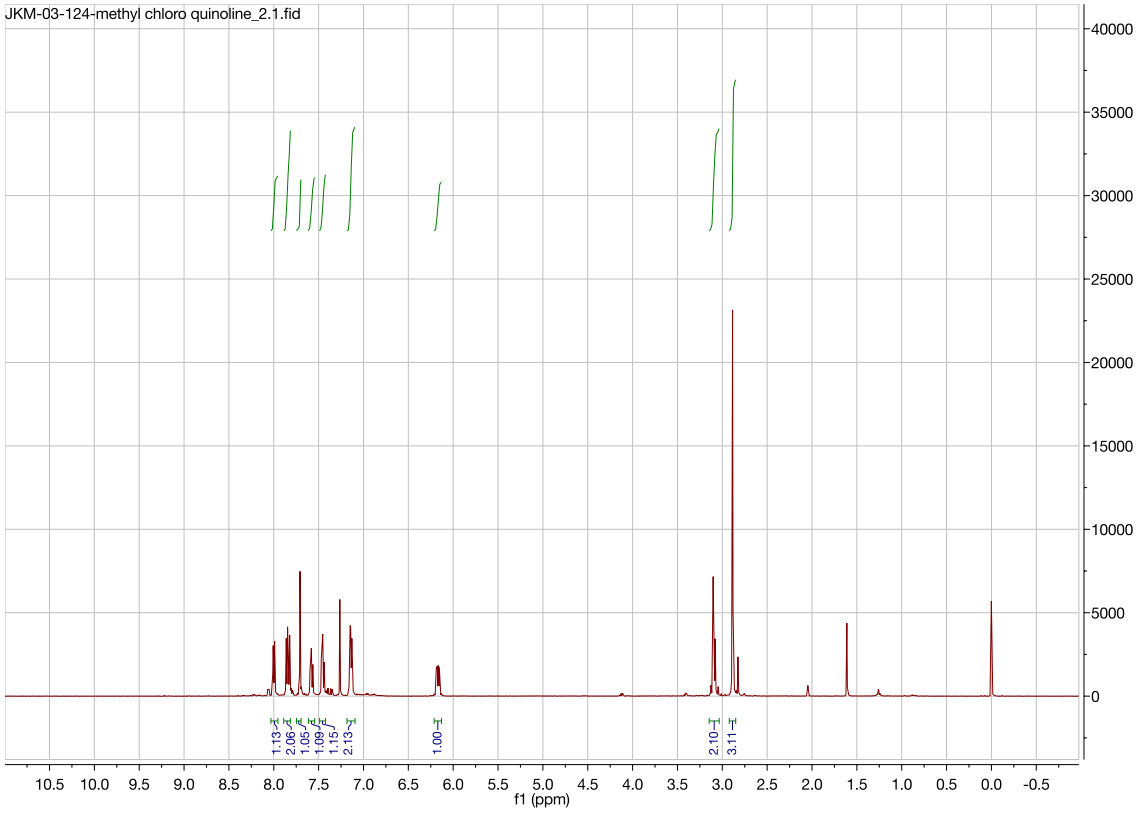

^{13}C ($CDCl_3$, 125.8 MHz) spectra of 2-(8-chloro-2-methylquinolin-4-yl)chroman-4-one (**3.14.4**)

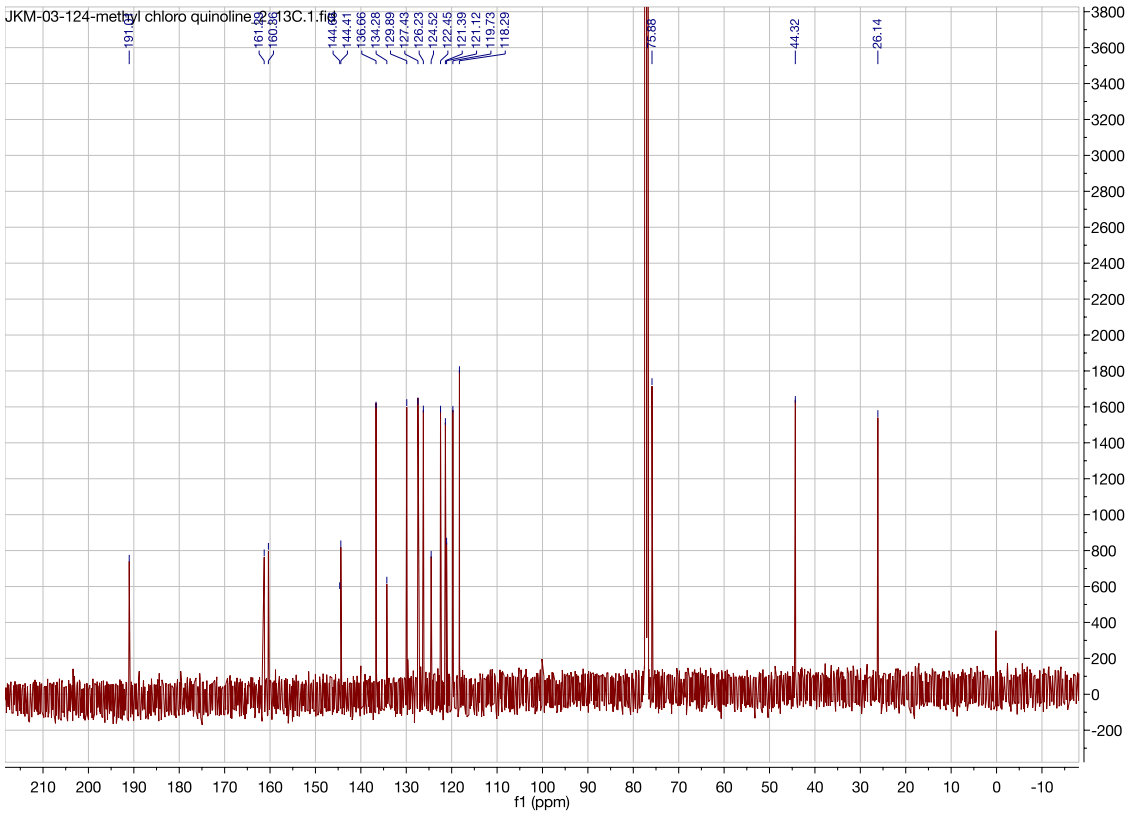

^{1}H ($CDCl_3$, 500 MHz) spectra of 6-bromo-2-(quinoxalin-2-yl)chroman-4-one (**3.14.6**)

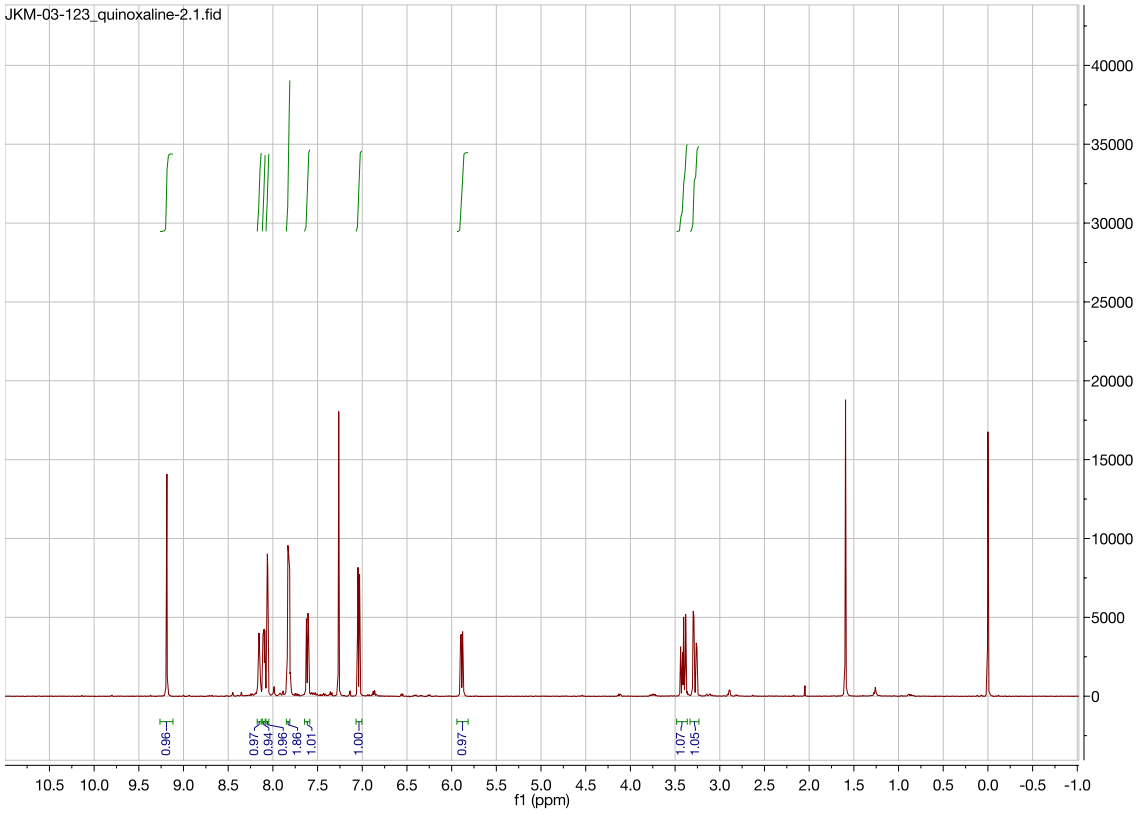

^{13}C ($CDCl_3$, 125.8 MHz) spectra of 6-bromo-2-(quinoxalin-2-yl)chroman-4-one (**3.14.6**)

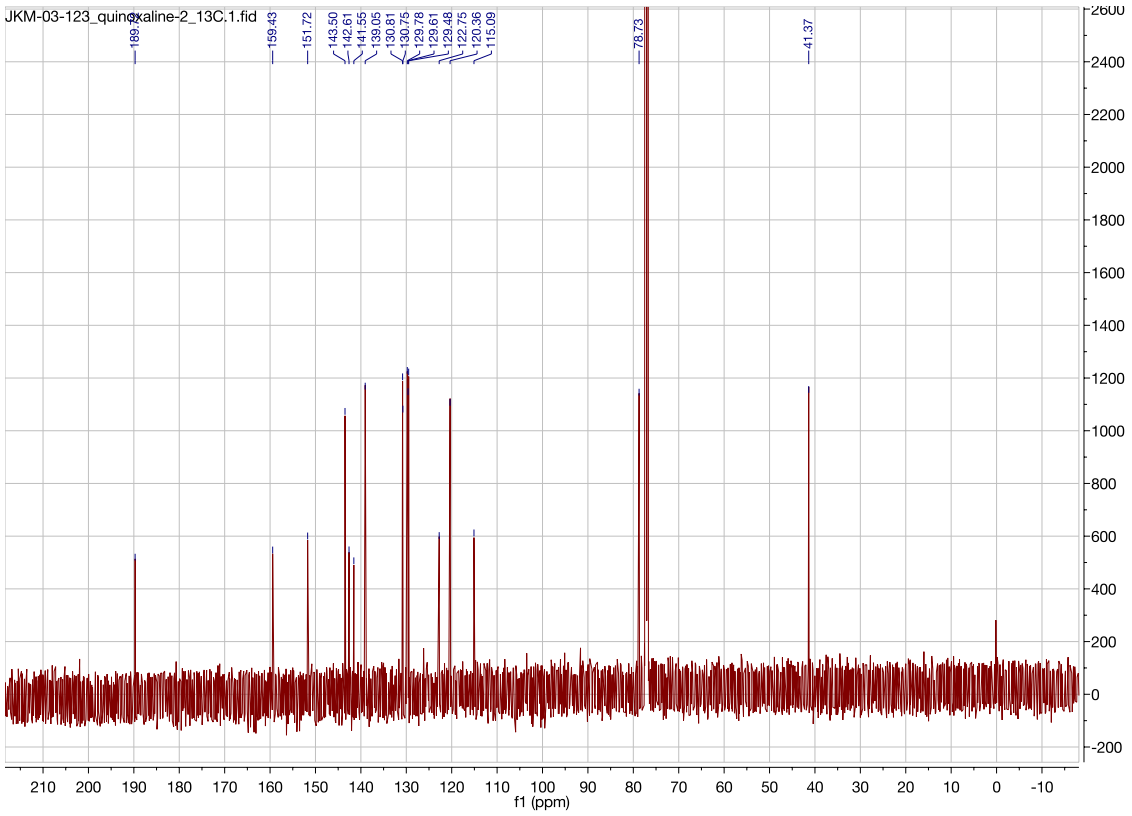
JKM-03-123_quinoxaline-2_13C.1.fid
189.23
159.43
151.72
143.50
142.61
141.55
139.05
130.81
130.75
129.78
129.61
129.48
122.75
120.36
115.09
78.73
41.37
f1 (ppm)

^{1}H ($CDCl_3$, 500 MHz) spectra of 6-methyl-2-(4-(trifluoromethyl)pyridin-2-yl)chroman-4-one (**3.15.1**)

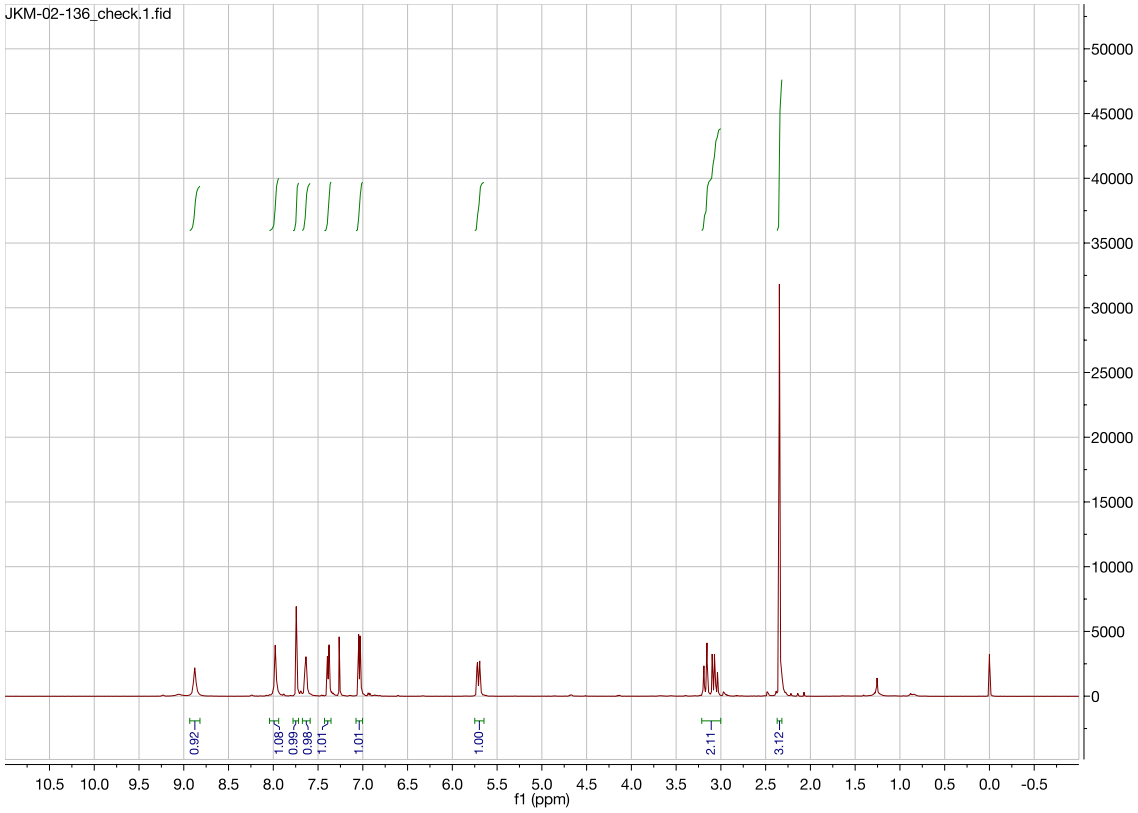

^{13}C ($CDCl_3$, 125.8 MHz) spectra of 6-methyl-2-(4-(trifluoromethyl)pyridin-2-yl)chroman-4-one (**3.15.1**)

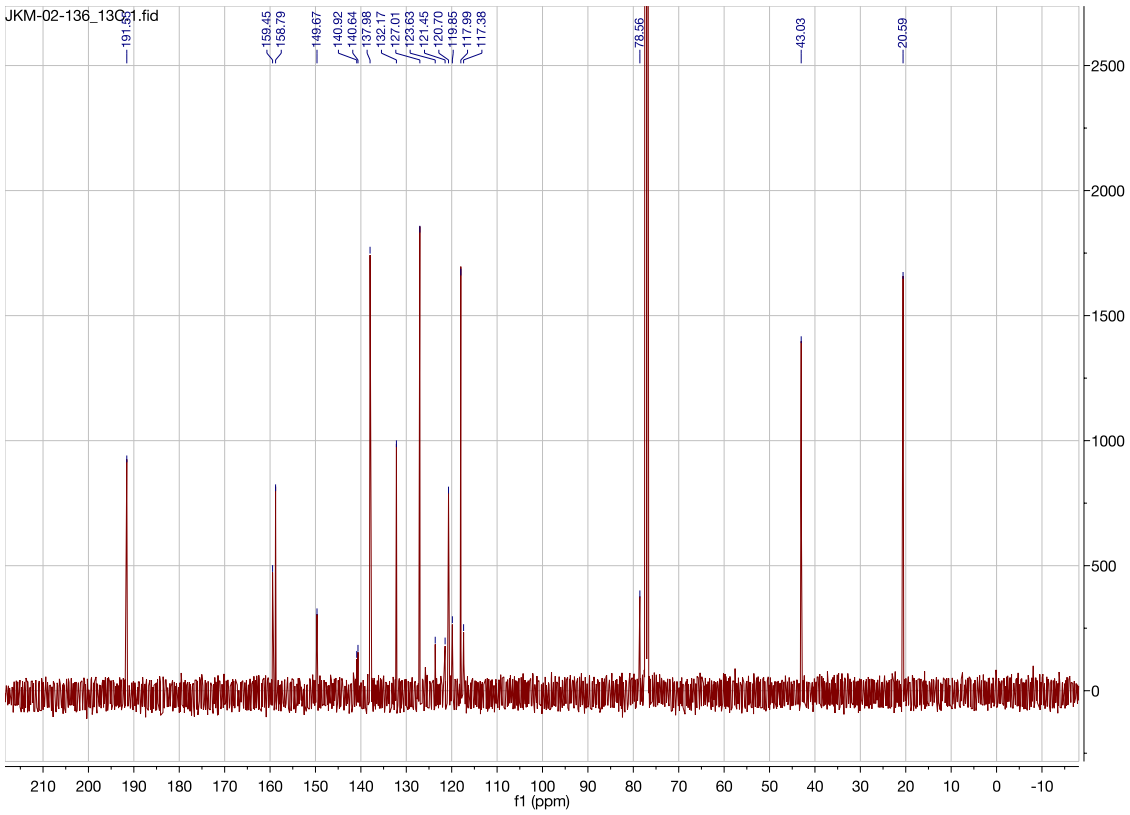

^{19}F NMR (471 MHz, $CDCl_3$) spectra of 6-methyl-2-(4-(trifluoromethyl)pyridin-2-yl)chroman-4-one (**3.15.1**)

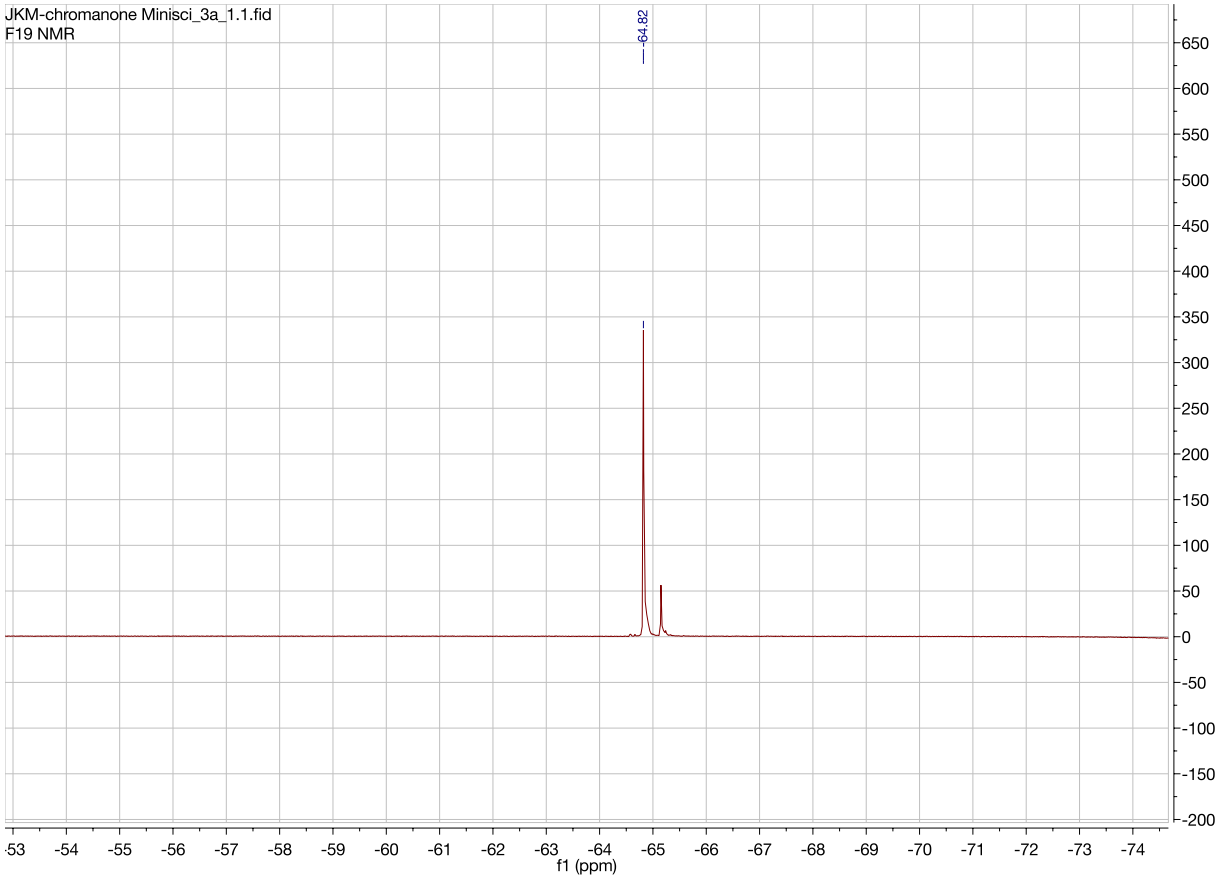

^{1}H ($CDCl_3$, 500 MHz) spectra of 6-(thiophen-2-yl)-2-(4-(trifluoromethyl)pyridin-2-yl)chroman-4-one (**3.15.2**)

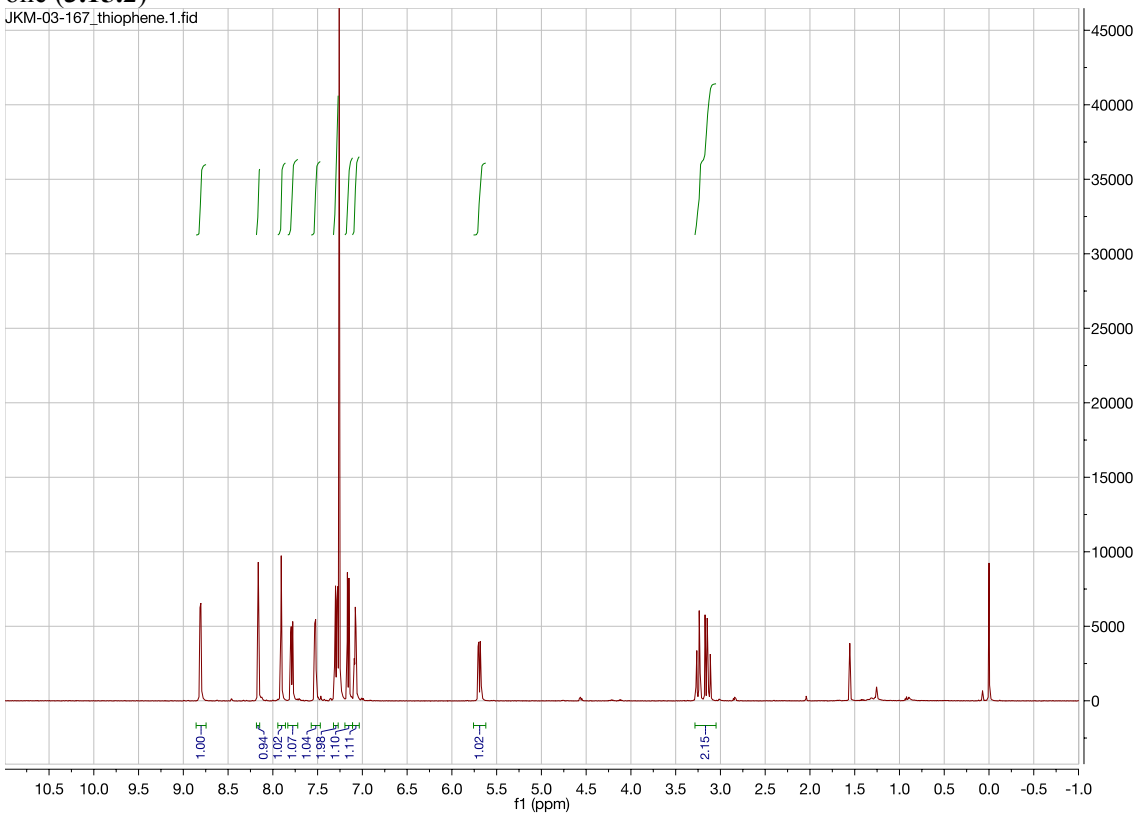

^{13}C ($CDCl_3$, 125.8 MHz) spectra of 6-(thiophen-2-yl)-2-(4-(trifluoromethyl)pyridin-2-yl)chroman-4-one (**3.15.2**)

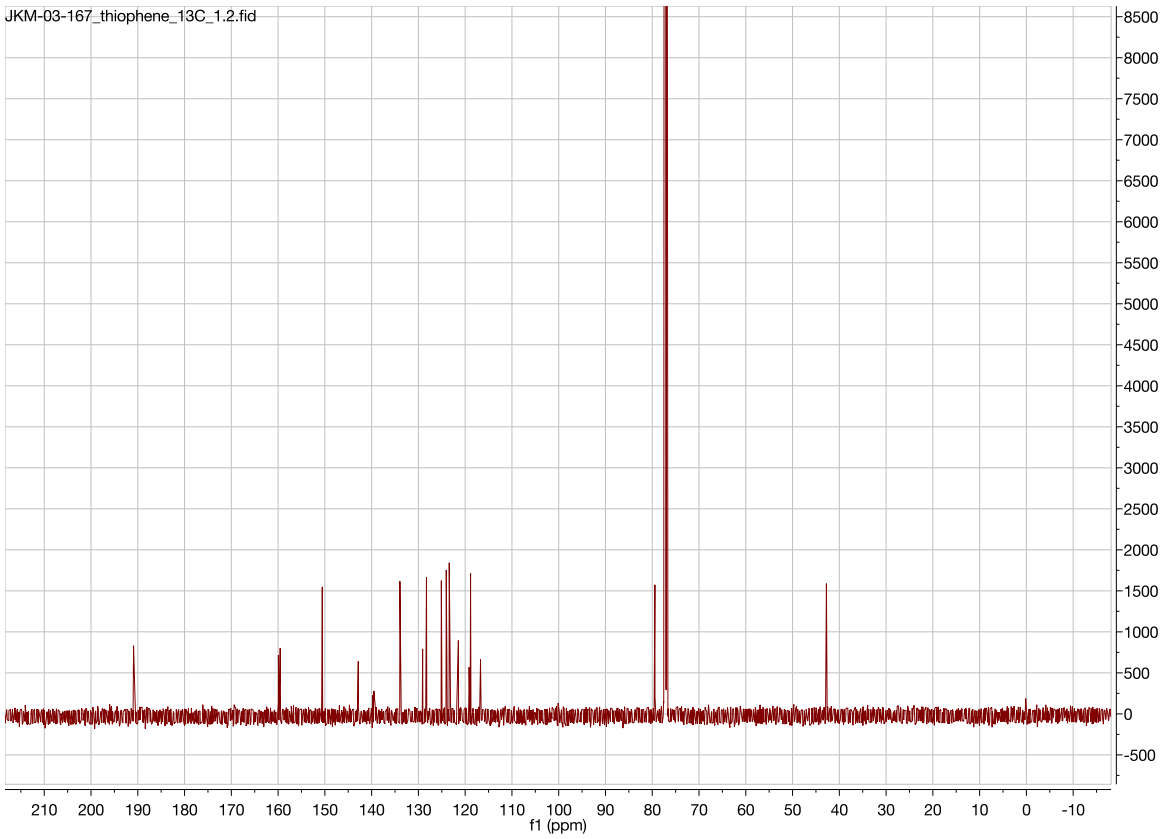

^{19}F NMR (471 MHz, $CDCl_3$) spectra of 6-(thiophen-2-yl)-2-(4-(trifluoromethyl)pyridin-2-yl)chroman-4-one (**3.15.2**)

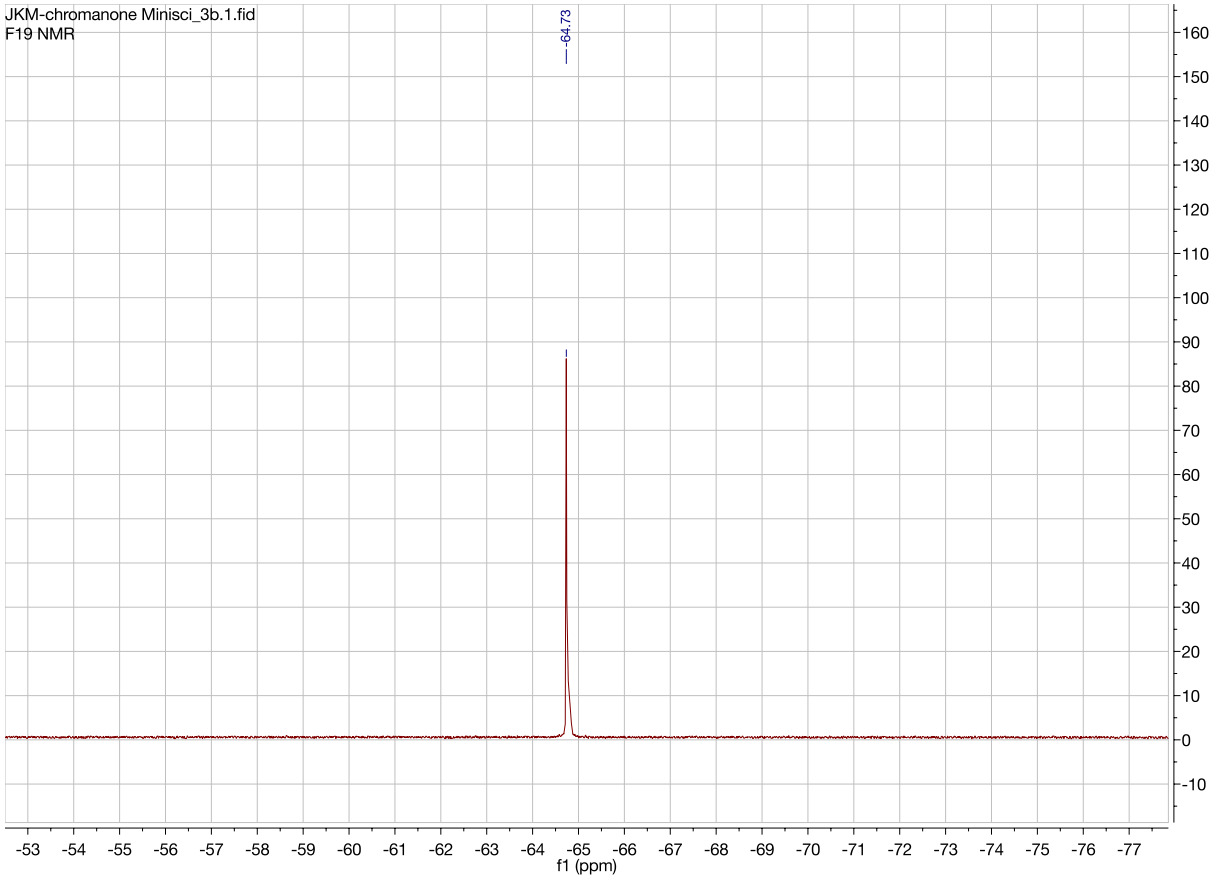

^{1}H ($CDCl_3$, 500 MHz) spectra of 6-(5-methylfuran-2-yl)-2-(4-(trifluoromethyl)pyridin-2-yl)chroman-4-one (**3.15.3**)

^{13}C ($CDCl_3$, 125.8 MHz) spectra of 6-(5-methylfuran-2-yl)-2-(4-(trifluoromethyl)pyridin-2-yl)chroman-4-one (**3.15.3**)

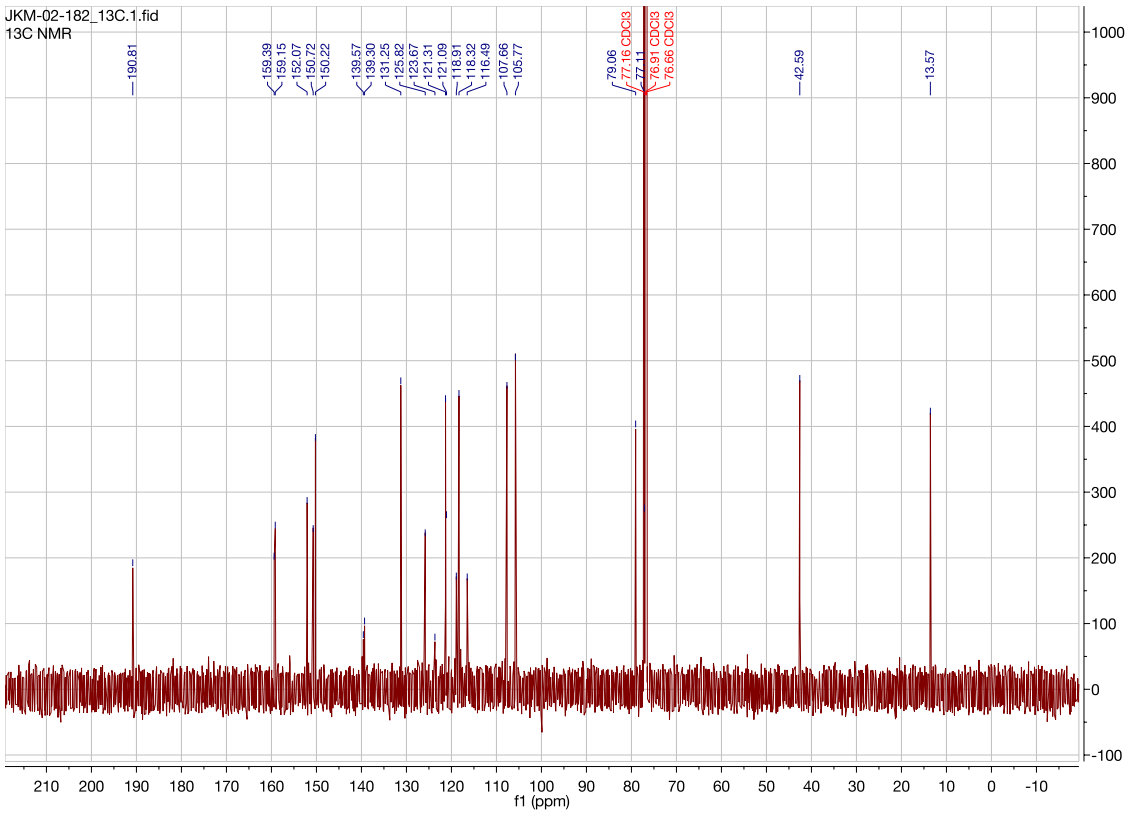

^{19}F NMR (471 MHz, $CDCl_3$) spectra of 6-(5-methylfuran-2-yl)-2-(4-(trifluoromethyl)pyridin-2-yl)chroman-4-one (**3.15.3**)

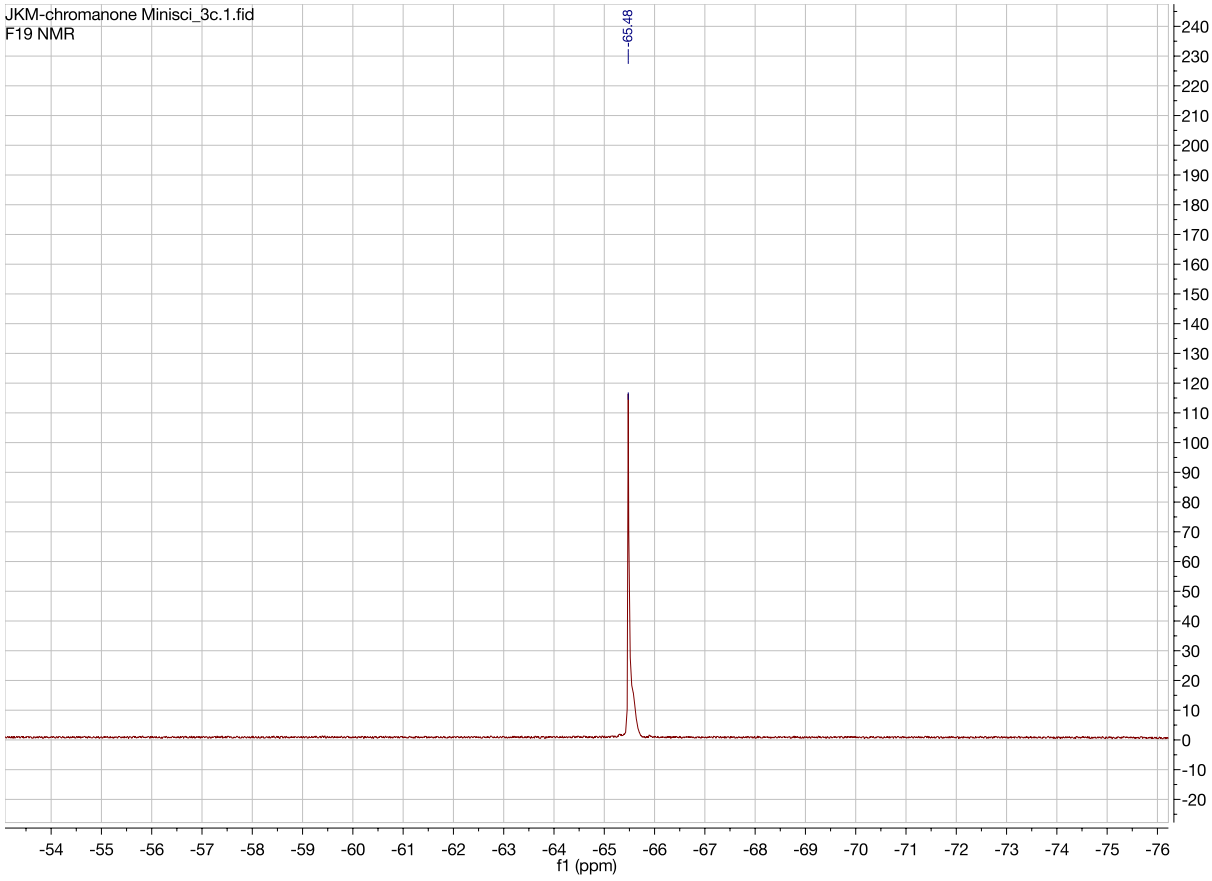

^{1}H (DMSO-d^{6}, 500 MHz) spectra of 6-bromo-2-(trifluoroboranyl)chroman-4-one, potassium salt

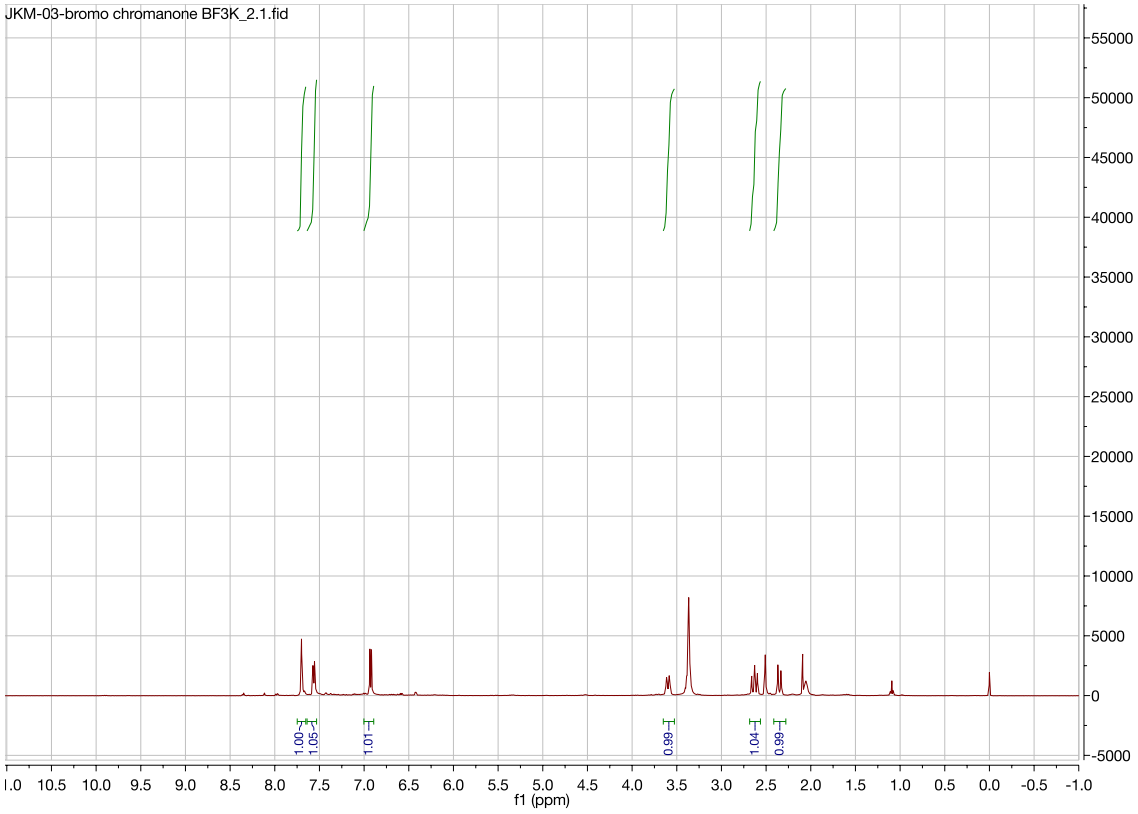

^{13}C (DMSO-d^6, 125.8 MHz) spectra of 6-bromo-2-(trifluoroboranyl)chroman-4-one, potassium salt

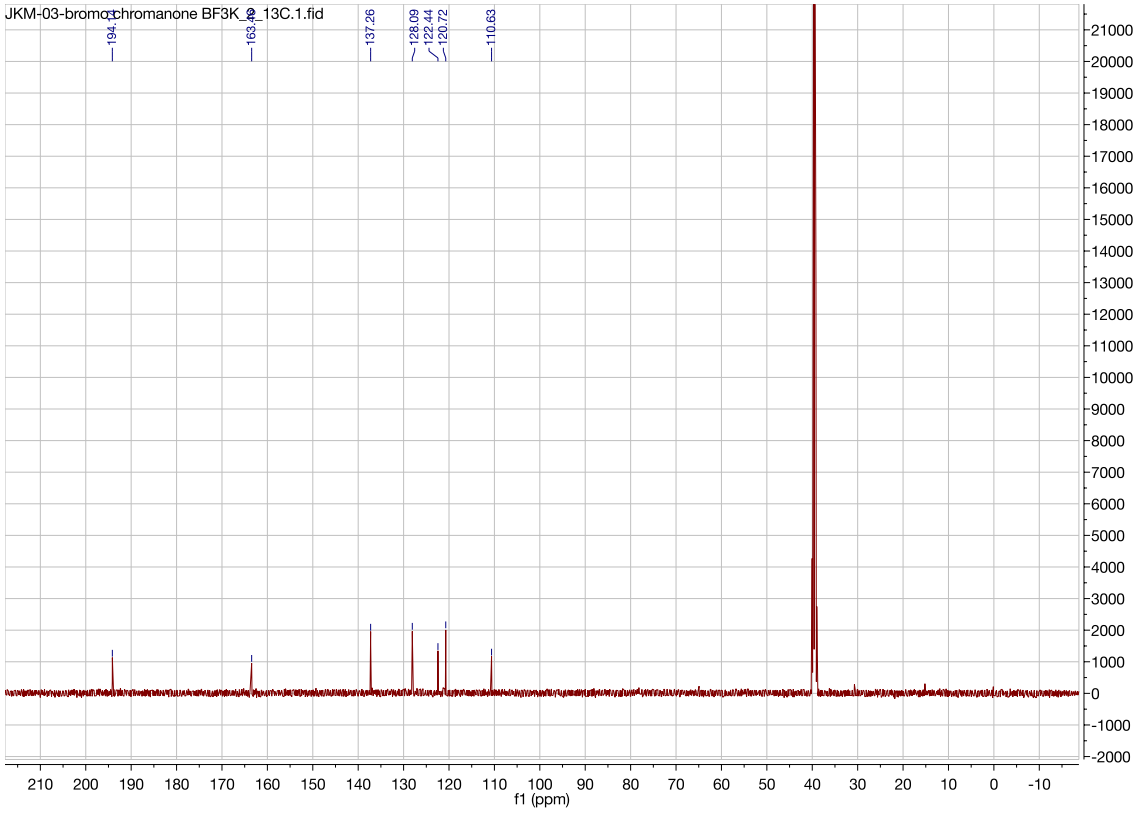

^{11}B NMR (DMSO-d^{6}, 128.4 MHz) spectra of 6-bromo-2-(trifluoroboranyl)chroman-4-one, potassium salt

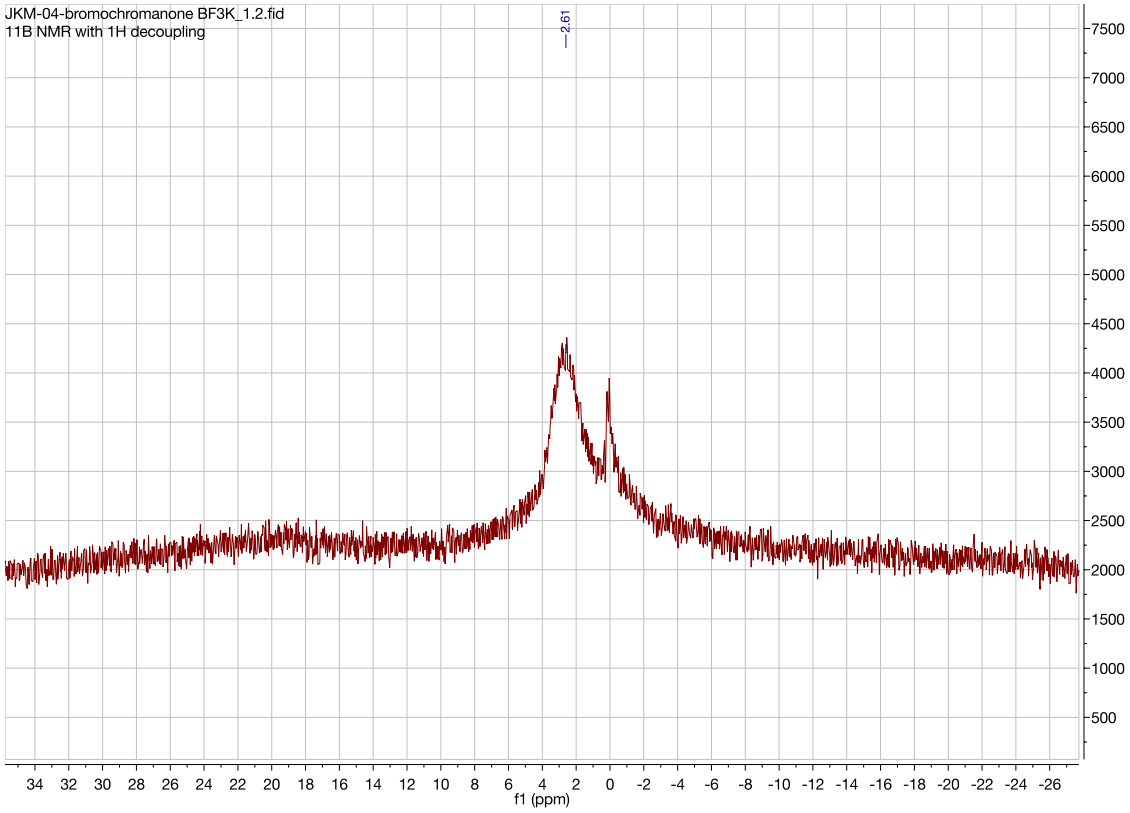

Chapter 4. Engaging 1,4-Dihydropyridines in Alkylation of Heteroarenes

4.1 Introduction

Nitrogen-containing heterocycles and quinones are ubiquitous chemical motifs present in pharmaceuticals, natural products, and ligand scaffolds among other examples, thus highlighting the importance of such structures.[1†] Late-stage modification of these entities within the context of complex molecules is not trivial, and, often, a simple modification of such compounds requires a lengthy synthetic strategy where the new substituent must be installed in early stages. In an ideal scenario, numerous derivatives should be accessible from a common and complex molecule at any stage in a synthesis. Consequently, rapid, late-stage, selective alkylation processes for complex molecules under mild reaction conditions are of great value and significance.[2] A powerful example in medicinal chemistry efforts is the derivatization of camptothecin (Figure 4.1). To date, a wide range of radical precursors have been demonstrated (e.g., aldehydes, carboxylic acids).[2]

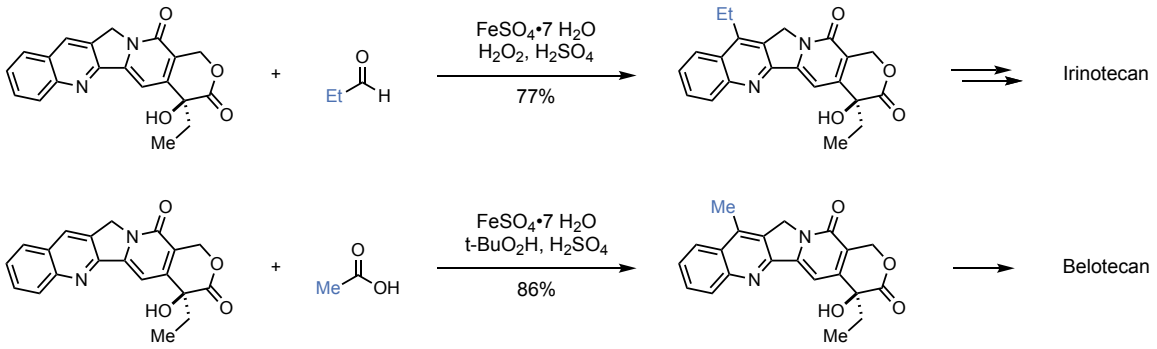

Figure 4.1. Literature examples of aldehydes and carboxylic acids as radical precursors.

† Reproduced in part from Gutierrez-Bonet, A.; Remeur, C. R., Matsui, J. K.; Molander, G. A. *J. Am. Chem. Soc.* **2017**, *139*, 12251.

Polar approaches to such transformations are limited because of their typically lower functional group tolerance. By contrast, radical processes have the advantage of tolerating a wider array of functional handles. Yet, the reaction conditions required to generate radical intermediates are themselves often harsh, thus limiting their applicability.[3] Indeed, radical alkylation of complex heterocycles has been well developed in the Minisci reaction,[4] where a radical is coupled with a heterocycle under acidic, oxidizing conditions, delivering the functionalized product. Interestingly, the regioselectivity is orthogonal to that observed for the Friedel-Crafts reaction, thus increasing the appeal of such transformations. Traditionally, carboxylic acids[5] and halides[6] have been employed as radical precursors, but more recently the toolbox has been expanded to include alcohols,[7] boronic acids,[8] sulfinate salts,[9] alkenes,[10] and alkyltrifluoroborates.[11] However, in most of the previous contributions, high temperatures, (sub)stoichiometric amounts of expensive metal salts, excess of the radical precursor, and strong oxidants or expensive photocatalysts[7,11a,12] are required to achieve good yields.

Aldehydes, which are readily available, have been employed as acyl radical precursors to access acylated products[13] and, to a lesser extent and with limited applicability, as a source of alkyl radicals as well[14] generated through decarbonylation of an acyl radical (Figure 4.2).[15] Unfortunately, this acyl radical can react with the heterocycle or undergo further oxidation, resulting in non-productive pathways. It is known that the acyl/alkyl radical equilibrium can be shifted by increasing the reaction temperature, resulting in a more efficient CO extrusion event.[16] Consequently, such transformations usually employ temperatures above 100 ˚C to improve the selectivity toward the alkylation, while an excess of the aldehyde motif is required to achieve competitive yields, thus highlighting the narrow applicability of such a strategy.[13,14]

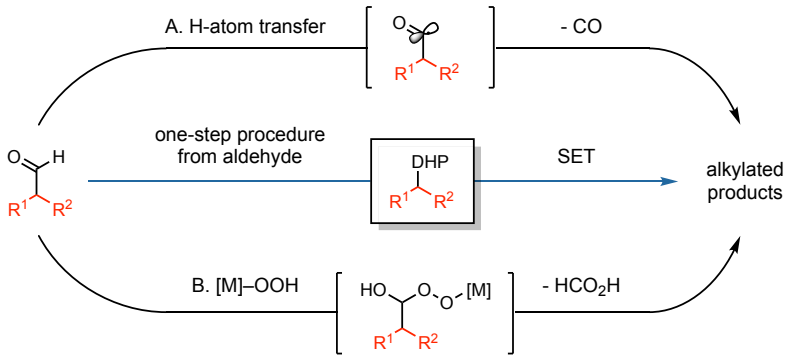

Figure 4.2. Previous strategies for fragmentation of aldehydes.

4.2 Reaction Design and Results

Recently, 1,4-dihydropyridines (DHPs), which are readily prepared from aldehydes in one step,[17] have been demonstrated to undergo homolysis under photoredox conditions to form Csp^3-centered alkyl radicals that can be engaged in different processes with prefunctionalized substrates.[18] Notably, DHPs can be regarded as masked aldehydes that exclusively deliver alkyl radicals by circumnavigating acyl radical intermediates, thus avoiding the formation of acylated byproducts or the required for high temperatures, strong oxidants, and excess of the aldehydic partner given the efficiency of oxidative fragmentation from DHPs. Based on this result, we envisioned exploration of the reactivity of DHPs in a transformation beyond prefunctionalized substrates, tar-geting, therefore, a much more appealing, yet challenging, C-H bond. In this regard, we considered the C-H alkylation of nitrogen-containing heterocycles and 1,4-quinones, so that the traditional drawbacks of Minisci chemistry with aldehydes could be overcome, thus allowing a re-introduction of this attractive feedstock into radical C-H alkylation processes.

For the optimization of the reaction conditions, we chose **4.3.3** as a model substrate in combination with *i*-Pr-DHP and found that the reaction proceeded in almost quantitative yields using a small excess of sodium persulfate as oxidant, and TFA to activate the heterocycle (Figure 4.3). Cation exchange of the persulfate oxidant had little effect on the reaction outcome (entries 4–5) whereas stronger oxidants (entry 6) typically employed for aldehydes had a deleterious effect on

the reactivity. Interestingly, the addition of TFA was not an absolute requirement for the reaction to proceed (entry 3), albeit a diminished yield was obtained without this additive. TCA showed no effect (entry 3 vs entry 7), whereas BF_3•OEt_2 (entry 9) showed activity similar to that of TFA. Not surprisingly, the solvent system played a crucial role, as in this type of process diffusion between the aqueous phase hosting the oxidant and the organic phase accommodating the organic partners is critical.[19]

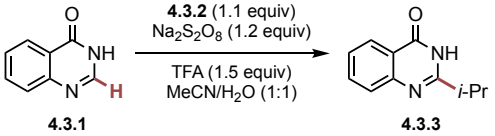

entry	deviation from standard conditions	4.3.2 (%)[b]
1	none	98 (97)[c]
2	no $Na_2S_2O_8$ added	4
3	no TFA added	71
4	$K_2S_2O_8$ instead of $Na_2S_2O_8$	91
5	$(NH_4)_2S_2O_8$ instead of $Na_2S_2O_8$	88
6	*t*-BuOOH instead of $Na_2S_2O_8$	6
7	TCA instead of TFA	72
8	CSA instead of TFA	83
9	BF_3•OEt_2 instead of TFA	95
10	CH_2Cl_2/H_2O as solvent	13
11	CH_3CN as solvent	0
12	DMSO as solvent	59
13	$Na_2S_2O_8$ (20 mol %)	47[c] (25)[c,d]

Figure 4.3. Optimization conditions.

Next, we tested this new set of reaction conditions with DHPs featuring different alkyl units at the C4-position (Figure 4.4). Both acyclic (**4.4.1–4.4.5**) and cyclic radicals (**4.4.6–4.4.8**) could be coupled with the heterocyclic backbone in moderate to good yields. Notably, alkene functional groups were well tolerated as demonstrated by the melonal-derived and cyclohexenyl DHPs (**4.4.5** and **4.4.7**, respectively). Oxygen-containing heterocyclic motifs did not hamper the reaction (**4.4.9–4.4.10**). Importantly, primary radicals could be engaged in the presence of a stabilizing α-oxygen atom (**4.4.11**). Unfortunately, non-stabilized, primary alkyl radicals did not

deliver the expected product as the corresponding DHP does not undergo homolytic C-C cleavage but rather C-H homolysis, resulting in the formation of a 4-alkylated-pyridine byproduct.[20]

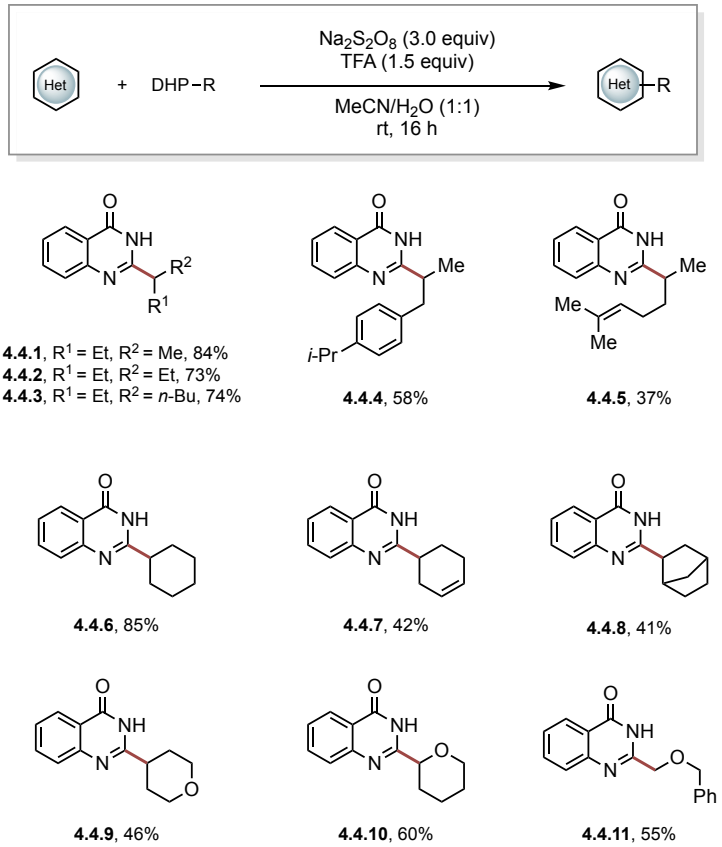

Figure 4.4. Quinazolinone scope.

Combinations of different heteroarenes with distinct DHPs were then explored in an effort to access unprecedented structural motifs (Figure 4.5). For example, C2-alkylated lepidine derivatives have shown antituberculosis activity,[21] and thus several different lepidine derivatives (**4.5.1–4.5.7**) were prepared. Whereas simple alkyl motifs gave high yields of the corresponding product (**4.5.1**), more complex motifs led to lower yields (**4.5.2–4.5.3**). Interestingly, primary α-amidomethyl radicals could be employed, although with poor yields (**4.5.3**). Substituted quinolines were explored and generated the expected products in moderate to good yields. Likewise, isoquinolines were well accommodated (**4.5.8**) as well as pyridine (**4.5.10**) pyrimidine (**4.5.11**), and benzothiazole cores (**4.5.12**). To test the regioselectivity of the protocol, heterocycles with

differentially reactive C-H bonds were tested. Unfortunately, mixtures of mono- and dialkylation were observed (**4.5.5**). However, in the presence of other leaving groups under radical conditions (e.g., $MeSO_2$-, and Cl-, **4.5.11**), exclusive addition at the C-H bond was observed.[22]

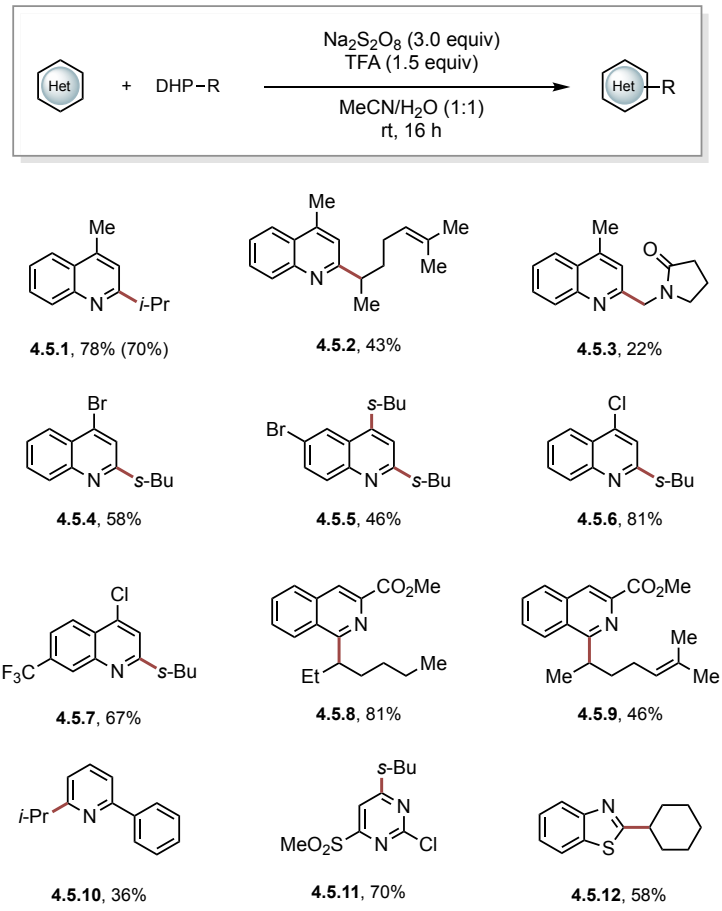

Figure 4.5. Expanding heteroarene scope.

To highlight the applicability of the protocol, we attempted the late-stage C-H alkylation of different natural products and pharmaceuticals (Figure 4.6). Notably, we observed a wide functional group tolerance (e.g., amines, alkenes, hydroxyls, sulfonamides) in alkylating natural products such as nicotine (**4.6.1**) and caffeine (**4.6.2**). Cinchonine, a common ligand scaffold for numerous organocatalytic processes,[23] could be rapidly modified (**4.6.3**), allowing the formation of a new generation of cinchonine-based ligands under mild reaction conditions. Likewise,

structurally related quinine, an antimalarial drug, could be rapidly diversified to **4.6.4**. Antivasospatic fasudil hydrochloride[24] and apoptosis inducer camptothecin were effectively elaborated under the reaction conditions, delivering the C-H alkylated product in good to high yields and excellent regioselectivity (**4.6.5**). Notably, alkylated camptothecin-derivatives have shown even higher activities than the base molecule itself.[25]

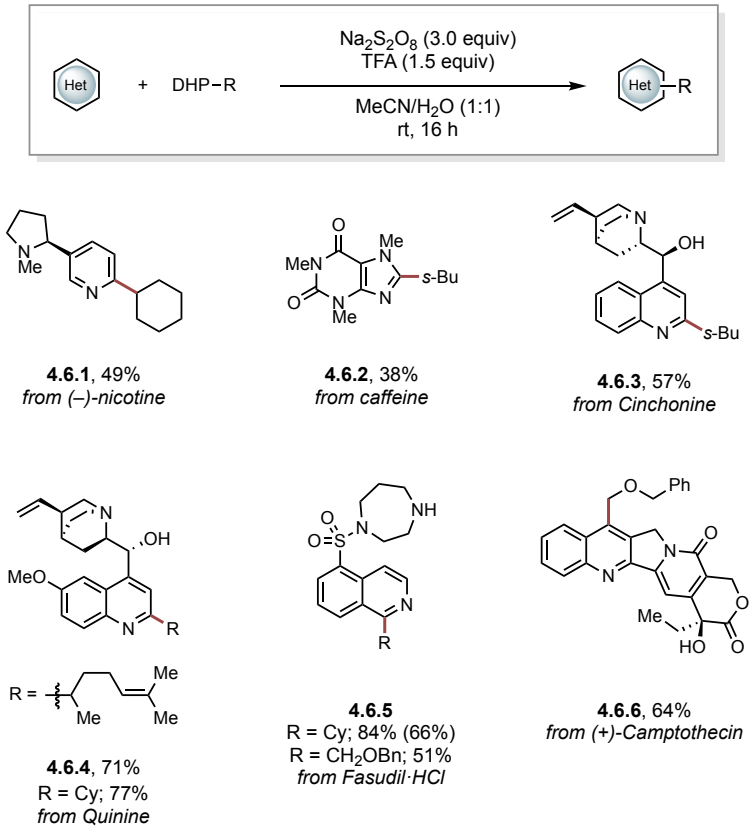

Figure 4.6. Late-stage functionalization efforts.

Spurred on by the possibility of introducing the decarbonylated aldehyde feedstock while overcoming its inherent drawbacks in radical processes, we envisioned the introduction of quinones as radical acceptors. Quinones are of extreme importance because of their ability to partake in electron transport processes in primary metabolic routes. Furthermore, they display important pharmacological activities and are very versatile intermediates for organic synthesis.[26] Because functionalization of quinones usually relies on the use of transition-metal catalysis,[27] we sought to

carry out the metal-free C-H alkylation of quinones from DHPs under mild conditions. Previously, these interesting scaffolds have been functionalized using radicals generated with metal-based catalysts to afford mostly arylated quinones from organoboron compounds[28] and carboxylic acids,[29] among others.[30] However, aldehydes have never been employed before as alkyl radical precursors with this class of substrates,[31] thus ignoring an important feedstock that could help increase the chemical space.

To demonstrate the versatility of our protocol, different 1,4-quinones were tested (Figure 4.7).[32] Interestingly, in the presence of two identical reactive sites, monoalkylation was observed in good levels (**4.7.1**). Apoptosis inducer Coenzyme Q0, with only one reactive site and two methoxy groups, was effectively coupled with different DHPs in moderate to good yields (**4.7.2–4.7.3**). Notably, π-extended naphthoquinones such as vitamin K3 (**4.7.4**) smoothly reacted, as well as 2-hydroxynaphthoquinone (Lawsone reagent) (**4.7.5–4.7.6**), which, when combined with Cy-DHP, yielded Parvaquone (marketed as Clexon®, **4.7.6**) in 54% yield. The latter is employed for the treatment of theileriosis, a cattle disease that represents an important threat to livestock production in Africa, generating losses above $200 million annually.[33] Alternatively, Atovaquone (an anti-malarial drug that acts by inhibiting the mitochondrial electron transport system and marketed as Malarone® when combined with proguanil hydrochloride),[34] could be synthesized in a 54% yield as a kinetic mixture of diastereomers that could be easily converted to the more active trans-Atovaquone under acidic conditions.[30a] Importantly, previous syntheses of Atovaquone based on a radical alkylation approach relied on the use of silver salts, significantly increasing the total cost of such a synthetic route.

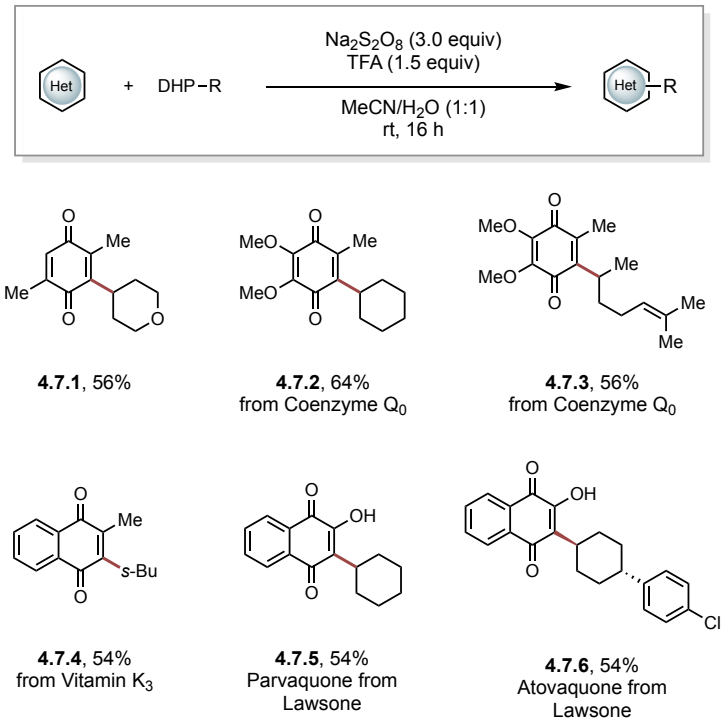

Figure 4.7. C–H alkylation of quinones.

Once the versatility of DHPs as alkylating agents was demonstrated in radical C-H alkylating processes, we moved on to study the influence of the 1,4-dihydropyridine backbone in the reaction outcome (Figure 4.8). Because of their dual role as H-atom donors and Csp^3-alkyl radical precursors, DHPs are becoming more prominent in organic synthesis.[18] Consequently, it was of interest to gain a deeper understanding of the factors controlling their reactivity. To this end, six different 1,4-dihydropyridine cores were tested under the developed reaction conditions. Interestingly, cyano-substitution at C3 and C5 on the dihydropyridine backbone led to only traces of product, whereas acridine derivative led to no conversion with 6-isopropylacridine being observed exculsively.[35] Importantly, no relationship between the oxidation potential and the reactivity was observed. However, a trend between the steric bulk of the functional groups at C3 and C5[36] and the reactivity was detected. We believe that the higher the steric hindrance at the C4-position of the pyridine byproduct formed upon oxidation is, the less prone the isopropyl radical is

to undergo competitive rebound with it, thus favoring the alkylation of lepidine and higher yields of the desired product. Notably, modification of the ester residue led to comparable yields for isopropyl substitution whereas the *tert*-butyl analog behaved poorly because of its low solubility in the solvent system.

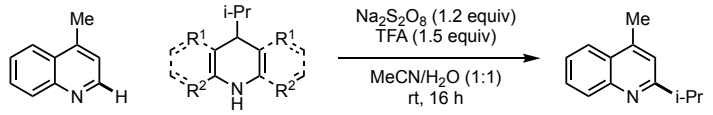

	product (%)	A-value (R)[a]	E^{ox} (V)[b]
R = CO_2Et; 2a	78	1.20	1.05
R = CO_2i-Pr; 2a-iPr	85	0.96	1.26
R = CO_2t-Bu; 2a-tBu	5	--	1.21
R = COMe; 2a-Ac	50	1.17	0.99
R = CN; 2a-CN	5	0.17	1.34
2a-Acr	n.d.	--	0.92

Figure 4.8. DHP backbone modifications.

Once the influence of the DHP backbone was studied, we then explored the subtleties of this transformation. Upon monitoring the reaction progress, an intermediate (**4.9.1**) was observed *via* HPLC that was later consumed to form product.

To confirm its role as an intermediate, a reaction with **4.9.1** under the developed reaction conditions was conducted, showing quantitative conversion to **4.9.2**, thus demonstrating its competency as intermediate (Figure 4.9). Based on the oxidation potential of **4.9.1** (E_{ox} = +1.19 V vs SCE), we believe that radical cation intermediate formed upon addition of the radical to the heterocyclic base, is reduced by the DHP [E_{ox} = +1.05 V *vs* SCE] *via* SET, thus resulting in formation of **4.9.1** and alkyl radical. Such a succession of events would be indicative of a *chain-radical mechanism*. To confirm this hypothesis, a test reaction with 20 mol % of $Na_2S_2O_8$ was performed, resulting in the isolation of product in 47% yield and intermediate **4.9.1** in 25% yield, indicating that at least 3.6 equivalents of DHP are generated per equivalent of oxidant and supporting the initial hypothesis of a radical chain propagation mechanism.[37]

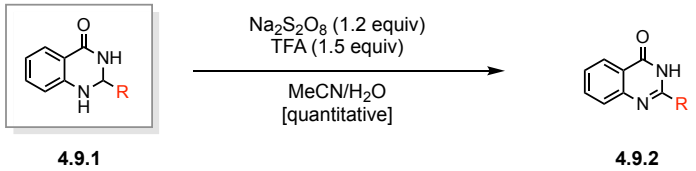

Figure 4.9. Observed intermediate oxidation.

To gain further insight into the reaction mechanism we performed two different deuterium-labelling experiments. First, an equimolar mixture of C2-deuterated and non-deuterated heterocycle 1a was treated under reaction conditions for 70 min (Figure 4.10). NMR analysis of the isolated compounds showed proton-enrichment of **4.10.1**, indicating a secondary inverse KIE of 0.79, which can be rationalized on the basis of a Csp^2–Csp^3 rehybridization upon addition of isopropyl radical to the C2-position of the heterocycle.[38] Next, two similar reactions were performed, with the only modification being the use of a deuterated solvent-system and TFA-d for one of them (Figure 4.10). Notably, a solvent KIE of 8.5 was measured[39] based on pyridine 7 formation, which probably arises from a fast scrambling of the DHP N-H proton with the deuterated protic solvent. Afterward, such a scrambling was confirmed to occur in less than 3 min by NMR analysis in 1:1 mixtures of CD_3CN/D_2O.[40]

A. KIE (Intermolecular competition)

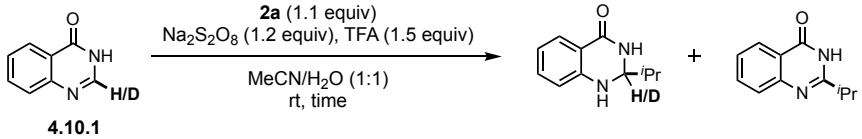

time (min)	1a	6a	3a
0	100% (50:50 *H/D*)	0%	0%
25	47% (59:41 *H/D*)	45% (60:40 *H/D*)	8%
70	18% (56:44 *H/D*)	47% (50:50 *H/D*)	21%

k_H/k_D (1a:6a) = 0.69 (25 min)
k_H/k_D (1a:6a) = 0.79 (70 min)

Figure 4.10. KIE studies with deuterated quinazolinone.

To study further the role of the N-H bond during the oxidative cleavage, a test reaction with the N-methylated DHP was conducted (Figure 4.11). No product was formed and the methylated DHP partially decomposed to several by-products as judged by GC-MS. Based on literature precedent,[41] we believe that this result might be indicative of a deprotonation of the $DHP^{+\bullet}$ prior to the homolytic cleavage.

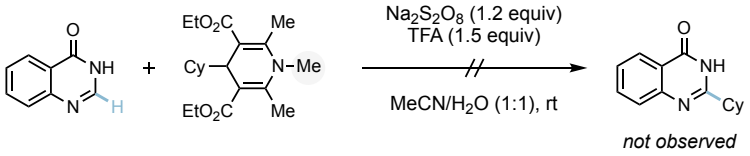

Figure 4.11. Probing role of N–H DHP bond in reaction.

On the basis of the previous observations, we envision a mechanistic scenario[40] that is initiated by SET oxidation of the DHP **4.12.1** by $Na_2S_2O_8$, resulting in the formation of pyridine **4.12.5** and alkyl radical R (Figure 4.12). The nature of such a homolysis has been discussed above. Subsequently, the Csp^3-radical adds to the protonated heterocycle, resulting in the rehybridization of the C2-carbon, which is made evident by the observed inverse KIE. Next, the resulting radical cation **4.12.2** oxidizes the DHP **4.12.1**, resulting in propagation of the radical chain while forming the observed intermediate **4.12.3**. Eventually, **4.12.3** will be oxidized by persulfate to deliver the final product **4.12.4**. Notably, the nature of this step remains unknown, with several available options such as SET oxidation to form **4.12.2** which will then undergo H-atom abstraction by $SO4^{\bullet-}$ [42] or further oxidation and deprotonation.

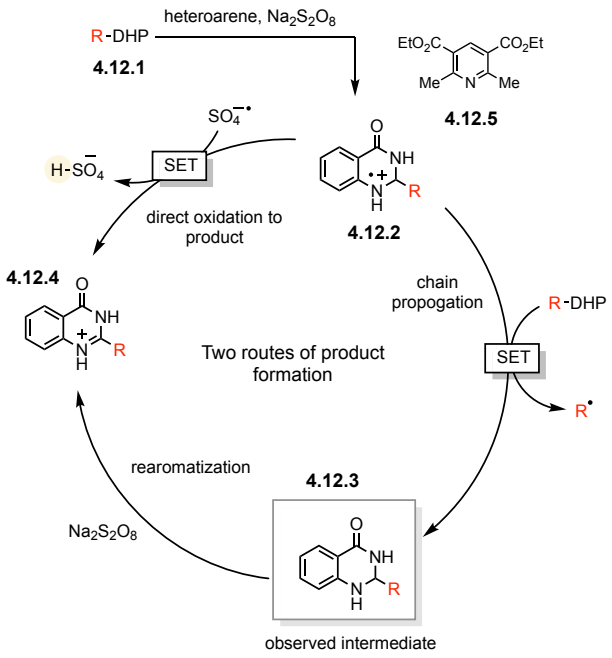

Figure 4.12. Proposed mechanism.

4.3 Conclusion

In summary, we demonstrated the ability of DHPs to deliver Csp^3-centered alkyl radicals, which can then be engaged in C-H alkylation of non-prefunctionalized heterocycles and quinones. Importantly, DHPs, which are easily accessible from aldehydes, eliminate the drawbacks associated with the latter for this kind of transformation, i.e., formation of acylated byproducts, harsh reaction conditions (strong oxidants at temperatures >100 ˚C), and use of an excess of the aldehyde motif. The mild reaction conditions developed allow late-stage C-H alkylation of natural products and drugs. More importantly, relevant marketed pharmaceuticals were prepared from readily available compounds. Finally, mechanistic studies revealed that the reaction proceeds under a radical-chain mechanism via a dearomatized intermediate. Key insights into the underlying nature of the DHP oxidation have been examined and elucidated. First, deuterium-labelling studies showed an inverse isotope effect arising from a rehybridization upon radical addition, whereas a solvent isotope effect pointed toward a slower homolytic cleavage of the DHP scaffold upon deuteration of the N-H bond.

Reactivity studies showed a relationship between the steric bulk of the DHP substituents and the reaction outcome. These studies help inform the design and synthesis of improved DHP scaffolds and provide greater understanding of fragmentation and structural reorganization in DHP-like systems.

4.4 References

[1] (a) Vitaku, E.; Smith, D. T.; Njardarson, J. T. *J. Med. Chem.* **2014**, *57*, 10257. (b) Taylor, R. D.; MacCoss, M.; Lawson, A. D. G. *J. Med. Chem.* **2014**, *57*, 5845. (c) Welsch, M. E.; Snyder, S. A.; Stockwell, B. R. *Curr. Opin. Chem. Biol.* **2010**, *14*, 347. (d) Fache, F.; Schulz, E.; Tommasino, M. L.; Lemaire, M. *Chem. Rev.* **2000**, *100*, 2159.

[2] (a) Cernak, T.; Dykstra, K. D.; Tyagarajan, S.; Vachal, P.; Krska, S. W. *Chem. Soc. Rev.* **2016**, *45*, 546. (b) Wencel-Delord, J.; Glorius, F. *Nat. Chem.* **2013**, *5*, 369.

[3] (a) Jasperse, C. P.; Curran, D. P.; Fevig, T. L. *Chem. Rev.* **1991**, *91*, 1237. (b) Yan, M.; Lo, J. C.; Edwards, T.; Baran, P. S. J. Am. Chem. Soc. 2016, 138, 12692. (c) Zhang, N.; Samanta, S. R.; Rosen, B. M.; Percec, V. *Chem. Rev*. **2014**, *114*, 5848. (d) Matsui, J. K.; Lang, S. B.; Heitz, D. R.; Molander, G. A. *ACS Catal.* **2017**, *7*, 2563.

[4] (a) Duncton, M. A. *MedChemComm* **2011**, *2*, 1135. (b) Zhang, J.-R.; Xu, L.; Liao, Y.-Y.; Deng, J.-C.; Tang, R.-Y. *Chin. J. Chem.* **2017**, *35*, 271. (c) Punta, C.; Minisci, F. *Trends Heterocycl. Chem.* **2008**, *13*, 1. (d) Minisci, F.; Bernardi, R.; Bertini, F.; Galli, R.; Perchinummo, M. *Tetrahedron* **1971**, *27*, 3575. (e) Harrowven, D. C.; Sutton, B. J. *Prog. Heterocycl. Chem.* **2005**, *16*, 27.

[5] (a) Minisci, F.; Mondelli, R.; Gardini, G. P.; Porta, O. *Tetrahedron* **1972**, *28*, 2403. (b) Kaur, N.; Lu, X.; Gershengorn, M. C.; Jain, R. *J. Med. Chem.* **2005**, *48*, 6162.

[6] (a) Minisci, F.; Vismara, E.; Fontana, F. *J. Org. Chem.* **1989**, *54*, 5224. (b) Duncton, M. A. J.; Estiarte, M. A.; Johnson, R. J.; Cox, M.; O'Mahony, D. J. R.; Edwards, W.; Kelly, M. G. *J. Org. Chem.* **2009**, *74*, 6354.

[7] Jin, J.; MacMillan, D. W. C. *Nature* **2015**, *525*, 87.

[8] Seiple, I. B.; Su, S.; Rodriguez, R. A.; Gianatassio, R.; Fujiwara, Y.; Sobel, A. L.; Baran, P. S. *J. Am. Chem. Soc.* **2010**, *132*, 13194.

[9] (a) Gianatassio, R.; Kawamura, S.; Eprile, C. L.; Foo, K.; Ge, J.; Burns, A. C.; Collins, M. R.; Baran, P. S. *Angew. Chem., Int. Ed.* **2014**, *53*, 9851. (b) Zhou, Q.; Ruffoni, A.; Gianatassio, R.; Fujiwara, Y.; Sella, E.; Shabat, D.; Baran, P. S. *Angew. Chem., Int. Ed.* **2013**, *52*, 3949. (c) Fujiwara, Y.; Dixon, J. A.; O'Hara, F.; Funder, E. D.; Dixon, D. D.; Rodriguez, R. A.; Baxter, R. D.; Herlé, B.; Sach, N.; Collins, M. R.; Ishihara, Y.; Baran, P. S. *Nature* **2012**, *492*, 95. (d) O'Hara, F.; Blackmond, D. G.; Baran, P. S. *J. Am. Chem. Soc.* **2013**, *135*, 12122−12134.

[10] (a) Ma, X.; Herzon, S. B. *J. Am. Chem. Soc.* **2016**, *138*, 8718. (b) Lo, J. C.; Kim, D.; Pan, C.-M.; Edwards, J. T.; Yabe, Y.; Gui, J.; Qin, T.; Gutiérrez, S.; Giacoboni, J.; Smith, M. W.; Holland, P. L.; Baran, P. S. *J. Am. Chem. Soc.* **2017**, *139*, 2484.

[11] (a) Matsui, J. K.; Primer, D. N.; Molander, G. A. *Chem. Sci.* **2017**, *8*, 3512. (b) Matsui, J. K.; Molander, G. A. *Org. Lett.* **2017**, *19*, 950. (c) Molander, G. A.; Colombel, V.; Braz, V. A. *Org. Lett.* **2011**, *13*, 1852.

[12] (a) DiRocco, D. A.; Dykstra, K.; Krska, S.; Vachal, P.; Conway, D. V.; Tudge, M. *Angew. Chem., Int. Ed.* **2014**, *53*, 4802. (b) Li, G.-X.; Morales-Rivera, C. A.; Wang, Y.; Gao, F.; He, G.; Liu, P.; Chen, G. *Chem. Sci.* **2016**, *7*, 6407. (c) Garza-Sanchez, R. A.; Tlahuext- Aca, A.; Tavakoli, G.; Glorius, F. *ACS Catal.* **2017**, *7*, 4057.

[13] (a) Matcha, K.; Antonchick, A. P. *Angew. Chem., Int. Ed.* **2013**, *52*, 2082. (b) Siddaraju, Y.; Lamani, M.; Prabhu, K. R. *J. Org. Chem.* **2014**, *79*, 3856. (c) Cheng, P.; Qing, Z.; Liu, S.; Liu, W.; Xie, H.; Zeng, J. *Tetrahedron Lett.* **2014**, *55*, 6647. (d) Siddaraju, Y.; Prabhu, K. R. *Tetrahedron* **2016**, *72*, 959.

[14] (a) Paul, S.; Guin, J. *Chem. - Eur. J.* **2015**, *21*, 17618. (b) Tang, R.-J.; Kang, L.; Yang, L. *Adv. Synth. Catal.* **2015**, *357*, 2055. (c) Mai, D. N.; Baxter, R. D. *Org. Lett.* **2016**, *18*, 3738. (d) Bohman, B.; Berntsson, B.; Dixon, R. C. M; Stewart, C. D.; Barrow, R. A. *Org. Lett.* **2014**, *16*, 2787.

[15] Chatgilialoglu, C.; Crich, D.; Komatsu, M.; Ryu, I. *Chem. Rev.* **1999**, *99*, 1991.

[16] Lehni, M.; Fischer, H. *Int. J. Chem. Kinet.* **1983**, *15*, 733. (b) Vollenweider, J.-K.; Paul, H. *Int. J. Chem. Kinet.* **1986**, *18*, 791.

[17] For representative examples, see: (a) Tewari, N.; Dwivedi, N.; Tripathi, R. *Tetrahedron Lett.* **2004**, *45*, 9011. (b) Adibi, H.; Samimi, H. A.; Beygzadeh, M. *Catal. Commun.* **2007**, *8*, 2119. (c) Heydari, A.; Khaksar, S.; Tajbakhsh, M.; Bijanzadeh, H. R. J. Fluorine Chem. 2009, 130, 609.

[18] (a) Gutiérrez-Bonet, Á.; Tellis, J. C.; Matsui, J. K.; Vara, B. A.; Molander, G. A. *ACS Catal.* **2016**, *6*, 8004. (b) Nakajima, K.; Nojima, S.; Nishibayashi, Y. *Angew. Chem., Int. Ed.* **2016**, *55*, 14106. (c) Nakajima, K.; Nojima, S.; Sakata, K.; Nishibayashi, Y. *ChemCatChem* **2016**, *8*, 1028. (d) Chen, W.; Liu, Z.; Tian, J.; Li, J.; Ma, J.; Cheng, X.; Li, G. *J. Am. Chem. Soc.* **2016**, *138*, 12312. For a review, see: (e) Huang, W.; Cheng, X. *Synlett* **2017**, *28*, 148.

[19] For the use of DHPs as imine alkylating agents in the presence of $BF_3 \cdot Et_2O$, see: Li, G.; Chen, R.; Wu, L.; Fu, Q.; Zhang, X.; Tang, Z. *Angew. Chem., Int. Ed.* **2013**, *52*, 8432.

[20] Baxter, R. D.; Liang, Y.; Hong, X.; Brown, T. A.; Zare, R. N.; Houk, K. N.; Baran, P. S.; Blackmond, D. G. *ACS Cent. Sci.* **2015**, *1*, 456.

[21] Zhang, D.; Wu, L.-Z.; Zhou, L.; Han, X.; Yang, Q.-Z.; Zhang, L.- P.; Tung, C.-H. *J. Am. Chem. Soc.* **2004**, *126*, 3440.

[22] (a) Jain, R.; Vaitilingam, B.; Nayyar, A.; Palde, P. B. *Bioorg. Med. Chem. Lett.* **2003**, *13*, 1051. (b) Beena; Rawat, D. S. *Med. Res. Rev.* **2013**, *33*, 693.

[23] (a) Prier, C. K.; MacMillan, D. W. C. *Chem. Sci.* **2014**, *5*, 4173. (b) Kamijo, S.; Kamijo, K.; Murafuji, T. *J. Org. Chem.* **2017**, *82*, 2664.

[24] (a) Yoon, T. P.; Jacobsen, E. N. *Science* **2003**, *299*, 1691. (b) Kacprzak, K.; Gawroński, J. *Synthesis* **2001**, 961.

[25] Shi, J.; Wei, L. J. *Cardiovasc. Pharmacol.* **2013**, *62*, 341.

[26] (a) Thomas, C. J.; Rahier, N. J.; Hecht, S. M. *Bioorg. Med. Chem.* **2004**, *12*, 1585. (b) Sriram, D.; Yogeeswari, P.; Thirumurugan, R.; Ratan Bal, T. *Nat. Prod. Res.* **2005**, *19*, 393.

[27] (a) Nawrat, C. C.; Moody, C. J. *Angew. Chem., Int. Ed.* **2014**, *53*, 2056. (b) Abraham, I.; Joshi, R.; Pardasani, P.; Pardasani, R. T. J. *Braz. Chem. Soc.* **2011**, *22*, 385. (c) Monks, T. J.; Jones, D. C. *Curr. Drug Metab.* **2002**, *3*, 425. (d) Garuti, L.; Roberti, M.; Pizzirani, D. *Mini-Rev. Med. Chem.* **2007**, *7*, 481.

[28] (a) Walker, S. E.; Jordan-Hore, J. A.; Johnson, D. G.; Macgregor, S. A.; Lee, A.-L. *Angew. Chem., Int. Ed.* **2014**, *53*, 13876. (b) Gan, X.; Jiang, W.; Wang, W.; Hu, L. *Org. Lett.* **2009**, *11*, 589. (c) Echavarren, A. M.; de Frutos, Ó.; Tamayo, N.; Noheda, P.; Calle, P. *J. Org. Chem.* **1997**, *62*, 4524. (d) Rao, M. L. N.; Giri, S. *RSC Adv.* **2012**, *2*, 12739. (e) Moon, Y.; Jeong, Y.; Kook, D.; Hong, S. *Org. Biomol. Chem.* **2015**, *13*, 3918. (f) Zhao, Y.; Zhang, Y.; Wang, J.; Li, H.; Wu, L.; Liu, Z. *Synlett* **2010**, 2352. (g) Xu, X.-L.; Li, Z. *Angew. Chem., Int. Ed.* **2017**, *56*, 8196.

[29] (a) Fujiwara, Y.; Domingo, V.; Seiple, I. B.; Gianatassio, R.; Del Bel, M.; Baran, P. S. *J. Am. Chem. Soc.* **2011**, *133*, 3292.

(b) Usui, I.; Lin, D. W.; Masuda, T.; Baran, P. S. *Org. Lett.* **2013**, *15*, 2080. (c) Dixon, D. D.; Lockner, J. W.; Zhou, Q.; Baran, P. S. *J. Am. Chem. Soc.* **2012**, *134*, 8432. (d) Wang, J.; Wang, S.; Wang, G.; Zhang, J.; Yu, X.-Q. *Chem. Commun.* **2012**, *48*, 11769. (e) Ilangovan, A.; Polu, A.; Satish, G. *Org. Chem. Front.* **2015**, *2*, 1616.

[30] (a) Dike, S. Y.; Singh, D.; Thankachen, B. N.; Sharma, B.; Mathur, P. K.; Kore, S.; Kumar, A. *Org. Process Res. Dev.* **2014**, *18*, 618. (b) Lu, X.; Altharawi, A.; Gut, J.; Rosenthal, P. J.; Long, T. E. *ACS Med. Chem. Lett.* **2012**, *3*, 1029. (c) Nasiri, H. R.; Ferner, J.; Tükek, C.; Krishnathas, R.; Schwalbe, H. *Tetrahedron Lett.* **2015**, *56*, 2231.

[31] (a) Huyser, E. A.; Amini, B. *J. Org. Chem.* **1968**, *33*, 576. (b) Wang, D.; Ge, B.; Li, L.; Shan, J.; Ding, Y. *J. Org. Chem.* **2014**, *79*, 8607. (c) Patil, P.; Nimonkar, A.; Akamanchi, K. G. *J. Org. Chem.* **2014**, *79*, 2331. (d) Ilangovan, A.; Saravanakumar, S.; Malayappasamy, S. *Org. Lett.* **2013**, *15*, 4968. (e) Baral, E. R.; Kim, S. H.; Lee, Y. R. *Asian J. Org. Chem.* **2016**, *5*, 1134. (f) Marcos, I. S.; Conde, A.; Moro, R. F.; Basabe, P.; Díez, D.; Urones, J. G. *Tetrahedron* **2010**, *66*, 8280.

[32] (a) For the use of aldehydes as acyl radical sources, see: Waske, P. A.; Mattay, J.; Oelgemöller, M. *Tetrahedron Lett.* **2006**, *47*, 1329. (b) For the arylation of phenyliodonium ylides with aryl aldehydes, see: Glinis, E.; Malamidou-Xenikaki, E.; Skouros, H.; Spyroudis, S.; Tsanakopoulou, M. *Tetrahedron* **2010**, *66*, 5786.

[33] Although not completely necessary, addition of TFA ensures higher yields as previously observed for the heterocyclic bases.

[34] (a) Gardner, M. J.; Bishop, R.; Shah, T.; De Villiers, E. P.; Carlton, J. M.; Hall, N.; Ren, Q.; Paulsen, I. T.; Pain, A.; Berriman, M.; Mann, R. J. M.; Xiong, Z.; Shallom, S. J.; Weidman, J.; Jiang, L.; Lynn, J.; Weaver, B.; Shoaibi, A.; Domingo, A. R.; Wasawo, D.; Crabtree, J.; Wortmanm, J. R.; Haas, B.; Angiuoli, S. V.; Creasy, T. H.; Lu, C.; Suh, B.; Silva, J. C.; Utterback, T. R.; Feldblyum, T. V.; Pertea, M.; Allen, J.; Nierman, W. C.; Taracha, E. L. N.; Salzberg, S. L.; White, O. R.; Fitzhugh, H. A.; Morzaria, S.; Venter, J. C.; Fraser, C. M.; Nene, V. *Science* **2005**, *309*, 134. (b) Nene, V.; Kiara, H.; Lacasta, A.; Pelle, R.; Svitek, N.; Steinaa, L. *Ticks Borne Dis.* **2016**, *7*, 549.

[35] (a) Painter, H. J.; Morrisey, J. M.; Mather, M. W.; Vaidya, A. B. *Nature* **2007**, *446*, 88. (b) Fry, M.; Pudney, M. *Biochem. Pharmacol.* **1992**, *43*, 1545. (c) Olliaro, P. *Pharmacol. Ther.* **2001**, *89*, 207 and references therein.

[36] The reviewers are acknowledged for their suggestions.

[37] Further experiments suggest a C−C homolysis delivering isopropyl radical and acridinium, which will then react, forming 9- isopropylacridine. See Experimental Section for further details.

[38] (a) Liang, C.; Bruell, C. J.; Marley, M. C.; Sperry, K. L. *Chemosphere* **2004**, *55*, 1213−1223. (b) Schweizer, S.; Tresse, C.; Bisseret, P.; Lalévee, J.; Evano, G.; Blanchard, N. *Org. Lett.* **2015**, *17*, 1794.

[39] Eliel, E. L.; Wilen, S. H.; Doyle, M. P. *Basic Organic Stereochemistry*; Wiley: Chichester, **2001**; p 443.

[40] Gómez-Gallego, M.; Sierra, M. A. *Chem. Rev.* **2011**, *111*, 4857.

[41] We observed that deuteration of the N−H bond of 2a in a 1:1 CD_3CN/D_2O occurred in less than 3 min (the time necessary to run an NMR). Furthermore, in 10% of D_2O in CD_3CN, the observed rate constant was $k_{obs} = 2$ Å$\sim 10^{-3}$ s^{-1}.

[42] Hu, Y.; Chen, L.; Li, B. *RSC Adv.* **2016**, *6*, 65196.

GENERAL CONSIDERATIONS

Reagents

All reactions were carried out under an inert atmosphere of nitrogen or argon unless otherwise noted. Standard Schlenk techniques were used for the manipulation of solvents and reagents. Reactions were monitored by GC/MS, HPLC, ^{1}H NMR, and/or by TLC on silica gel plates (60 Å porosity, 250 μm thickness). TLC analysis was performed using hexanes/EtOAc as the eluent and visualized using permanganate stain and/or UV light. Silica plugs utilized flash silica gel (60 Å porosity, 32-63 μm). Flash chromatography was accomplished using an automated system (visualizing at 254 nm and 280 nm) with silica cartridges (60 Å porosity, 20-40 μm). All chemicals were used as received unless otherwise noted. Solvents were purified by use of drying cartridges through a solvent delivery system.

Analytical Methods

Melting points (°C) are uncorrected. NMR Spectra (^{1}H, ^{13}C{1H}) were recorded on a 500 MHz spectrometer at 298 K. All ^{1}H NMR spectra are reported in parts per million (ppm) downfield of TMS and were measured relative to the signals for $CHCl_3$ (7.26 ppm). All ^{13}C NMR spectra were reported in ppm relative to residual $CHCl_3$ (77.2 ppm) and were obtained with ^{1}H decoupling. Coupling constants, *J*, are reported in Hertz (Hz). In the case of diastereomeric mixtures, crude NMR was recorded to determine the ratio. HRMS was obtained by either ESI or CI with a TOF spectrometer in MeCN or CH_2Cl_2. IR spectra were obtained on neat samples.

C-H Alkylation of *N*-Containing Heterocycles

General Procedure II: A vial was charged with the heterocyclic substrate (0.5 mmol, 1.0 equiv), 4-alkyl-1,4-dihydropyridine (0.55 mmol, 1.1 equiv) and $Na_2S_2O_8$ (142.9 mg, 0.6 mmol, 1.2 equiv). Then, the vial was capped and purged with three cycles of vacuum/argon and then, under argon atmosphere, degassed CH_3CN/H_2O (5.0 mL, 1:1 v/v, 0.1 M) and TFA (114.9 mg, 0.75 mmol, 1.5 equiv) were added. The reaction was vigorously stirred for 18 h at rt. After completion, the reaction was quenched by addition of aq $NaHCO_3$ (sat, 10.0 mL) and extracted three times with EtOAc (10.0 mL). The combined organic layers were washed with brine (20.0 mL), dried ($MgSO_4$), filtered, and concentrated. The crude product was then adsorbed on Celite® and purified on an automated system.

Characterization Data: C-H Alkylation of N-Containing Heterocycles.

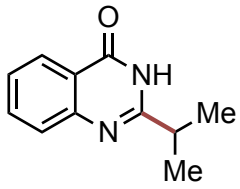

2-Isopropylquinazolin-4(3*H*)-one (4.4.1): Following General Procedure II using 4-hydroxyquinazoline (43.8 mg, 0.3 mmol, 1.0 equiv), diethyl 4-isopropyl-2,6-dimethyl-1,4-dihydropyridine-3,5-dicarboxylate (97.5 mg, 0.33 mmol, 1.1 equiv), $Na_2S_2O_8$ (85.7 mg, 0.36 mmol, 1.2 equiv) and TFA (51.3 mg, 0.45 mmol, 1.5 equiv) in CH_3CN/H_2O (3.0 mL, 1:1 v/v, 0.1 M). The product was isolated as a white fluffy solid (54.2 mg, 97% yield). mp= 218-221 ºC. ^{1}H NMR (500 MHz, $CDCl_3$) δ 10.35 (s, 1H), 8.28 (d, *J* = 7.9 Hz, 1H), 7.76 (t, *J* = 7.5 Hz, 1H), 7.71 (d, *J* = 8.2 Hz, 1H), 7.46 (t, *J* = 7.5 Hz, 1H), 2.99 (hept, *J* = 6.8 Hz, 1H), 1.43 (d, *J* = 7.0 Hz, 6H) ppm. ^{13}C NMR (126 MHz, $CDCl_3$) δ 163.9, 160.7, 149.6, 134.8, 127.6, 126.5, 126.4, 121.0, 35.1, 20.6 ppm. Spectral data is consistent with previously reported values. [10]

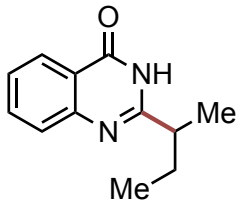

2-(*sec*-Butyl)quinazolin-4(3*H*)-one (4.4.1): Following General Procedure II using 4-hydroxyquinazoline (73.1 mg, 0.5 mmol, 1.0 equiv), diethyl 4-(*sec*-butyl)-2,6-dimethyl-1,4-dihydropyridine-3,5-dicarboxylate (170.1 mg, 0.55 mmol, 1.1 equiv), $Na_2S_2O_8$ (142.8 mg, 0.6 mmol, 1.2 equiv) and TFA (85.5 mg, 0.75 mmol, 1.5 equiv) in CH_3CN/H_2O (5.0 mL, 1:1 v/v, 0.1 M). The product was isolated as a white solid (87.0 mg, 86% yield). mp = 173-175 ºC. ^{1}H NMR (500 MHz, $CDCl_3$) δ 11.74 (s, 1H), 8.30-8.29 (m, 1H), 7.77-7.71 (m, 2H), 7.47-7.44 (m, 1H), 2.85-2.78 (m, 1H), 2.00-1.91 (m, 1H), 1.79-1.71 (m, 1H), 1.43 (d, *J* = 6.9 Hz, 3H), 0.98 (t, *J* = 7.4 Hz, 3H) ppm. ^{13}C NMR (126 MHz, $CDCl_3$) δ 164.3, 160.4, 149.6, 134.7, 127.5, 126.3 (2C), 120.9, 42.3, 28.2, 18.3, 12.0 ppm. Spectral data is consistent with previously reported values.[11]

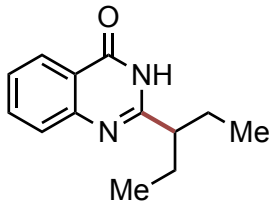

2-(Pentan-3-yl)quinazolin-4(3*H*)-one (4.4.2): Following General Procedure II using 4-hydroxyquinazoline (73.1 mg, 0.5 mmol, 1.0 equiv), diethyl 2,6-dimethyl-4-(pentan-3-yl)-1,4-dihydropyridine-3,5-dicarboxylate (177.8 mg, 0.55 mmol, 1.1 equiv), $Na_2S_2O_8$ (142.8 mg, 0.6 mmol, 1.2 equiv) and TFA (85.5 mg, 0.75 mmol, 1.5 equiv) in CH_3CN/H_2O (3.0 mL, 1:1 v/v, 0.1 M). The product was isolated as a white solid (81.0 mg, 75% yield). mp = 140-143 ºC. ^{1}H NMR (500 MHz, $CDCl_3$) δ 11.69 (s, 1H), 8.31-8.29 (m, 1H), 7.78-7.71 (m, 2H), 7.48-7.45 (m, 1H), 2.63-2.57 (m, 1H), 1.96-1.77 (m, 4H), 0.94 (t, *J* = 7.3 Hz, 6H) ppm. ^{13}C NMR (126 MHz, $CDCl_3$) δ 164.3, 159.6, 149.6, 134.7, 127.5, 126.4, 126.3, 120.8, 50.1, 26.5, 12.1 ppm. IR (neat, cm^{-1}): 2964,

2875, 1676, 1608, 1466, 889, 768. HRMS (EI+) *calcd for* $C_{13}H_{16}N_2O$ [M^+] 216.1263, *found 216.1264*.

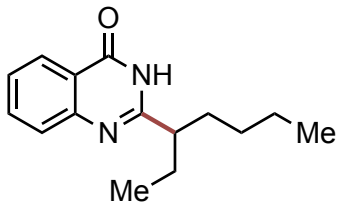

2-(Heptan-3-yl)quinazolin-4(3*H*)-one (4.4.3): Following General Procedure II using 4-hydroxyquinazoline (73.1 mg, 0.5 mmol, 1.0 equiv), diethyl 4-(heptan-3-yl)-2,6-dimethyl-1,4-dihydropyridine-3,5-dicarboxylate (193.3 mg, 0.55 mmol, 1.1 equiv), $Na_2S_2O_8$ (142.8 mg, 0.6 mmol, 1.2 equiv) and TFA (85.5 mg, 0.75 mmol, 1.5 equiv) in CH_3CN/H_2O (5.0 mL, 1:1 v/v, 0.1 M). The product was isolated as a white solid (90.0 mg, 74% yield). mp = 117-120 ºC. ^{1}H NMR (500 MHz, $CDCl_3$) δ 11.43 (s, 1H), 8.30-8.29 (m, 1H), 7.78-7.71 (m, 2H), 7.47-7.44 (m, 1H), 2.68-2.62 (m, 1H), 1.93-1.71 (m, 4H), 1.40-1.22 (m, 4H), 0.94 (t, *J* = 7.40 Hz, 3H), 0.83 (t, *J* = 7.03 Hz, 3H) ppm. ^{13}C NMR (126 MHz, $CDCl_3$) δ 164.1, 159.7, 149.6, 134.7, 127.5, 126.3, 126.3, 120.9, 48.5, 33.2, 29.8, 26.9, 22.7, 14.0, 12.1 ppm. Spectral data is consistent with previously reported values.[12]

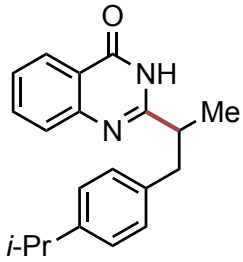

2-(1-(4-Isopropylphenyl)propan-2-yl)quinazolin-4(3*H*)-one (4.4.4): Following General Procedure II using quinazolin-4(3*H*)-one (29.2 mg, 0.20 mmol, 1.0 equiv), diethyl 4-(1-(4-isopropylphenyl)propan-2-yl)-2,6-dimethyl-1,4-dihydropyridine-3,5-dicarboxylate (90.9 mg, 0.22 mmol, 1.1 equiv), $Na_2S_2O_8$ (57.1 mg, 0.24 mmol, 1.2 equiv) and TFA (23.0 μL, 0.75 mmol, 1.5

equiv) in CH_3CN/H_2O (2.0 mL, 1:1 v/v, 0.1 M). The product was isolated as a pale oil (36.0 mg, 59% yield). ^{1}H NMR (500 MHz, $CDCl_3$) δ 11.38 (d, *J* = 8.4 Hz, 1H), 8.31 (d, *J* = 7.9 Hz, 1H), 7.77 (dt, *J* = 15.7, 8.0 Hz, 2H), 7.49 (t, *J* = 7.4 Hz, 1H), 7.19 (d, *J* = 7.8 Hz, 2H), 7.11 (d, *J* = 7.9 Hz, 2H), 3.24 (dd, *J* = 13.4, 6.4 Hz, 1H), 3.13 (q, *J* = 7.1 Hz, 1H), 2.87 (ddd, *J* = 26.4, 12.9, 7.6 Hz, 2H), 1.40 (d, *J* = 6.9 Hz, 3H), 1.20 (d, *J* = 7.0 Hz, 6H) ppm. ^{13}C NMR (126 MHz, $CDCl_3$) δ 164.0, 159.9, 149.6, 147.1, 136.6, 134.8, 129.2, 129.1, 127.6, 126.6, 126.5, 126.4, 121.0, 42.5, 41.0, 33.8, 24.1, 24.1, 18.0 ppm. IR (neat, cm^{-1}): 2961, 1678, 1610, 1469, 772, 629. HRMS (EI+) *calcd for* $C_{20}H_{22}N_2O$ [M^+] 306.1732, *found* 306.1742.

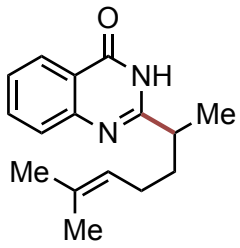

2-(6-Methylhept-5-en-2-yl)quinazolin-4(3*H*)-one (4.4.5): Following General Procedure II using 4-hydroxyquinazoline (73.1 mg, 0.5 mmol, 1.0 equiv), diethyl 2,6-dimethyl-4-(7-methyloct-6-en-3-yl)-1,4-dihydropyridine-3,5-dicarboxylate (199.9 mg, 0.55 mmol, 1.1 equiv), $Na_2S_2O_8$ (142.8 mg, 0.6 mmol, 1.2 equiv) and TFA (85.5 mg, 0.75 mmol, 1.5 equiv) in CH_3CN/H_2O (5.0 mL, 1:1 v/v, 0.1 M). The product was isolated as a white solid (47.4 mg, 37% yield). mp = 134-136 ºC. ^{1}H NMR (500 MHz, $CDCl_3$) δ 11.59 (s, 1H), 8.29 (d, *J* = 7.85 Hz, 1H), 7.76 (t, *J* = 7.78 Hz, 1H), 7.71 (d, *J* = 8.10 Hz, 1H), 7.45 (t, *J* = 7.48 Hz, 1H), 5.12-5.10 (m, 1H), 2.92-2.87 (m, 1H), 2.13-1.96 (m, 3H), 1.76-1.70 (m, 1H), 1.61 (s, 3H), 1.53 (s, 3H), 1.43 (d, *J* = 7.00 Hz, 3H) ppm. ^{13}C NMR (126 MHz, $CDCl_3$) δ 164.2, 160.4, 149.6, 134.7, 132.4, 127.5, 126.3, 126.3, 123.7, 120.9, 40.3, 35.1, 26.0, 25.7, 18.7, 17.7 ppm. IR (neat, cm^{-1}): 2970, 1675, 1618, 1468, 896, 771. HRMS (EI+) *calcd for* $C_{17}H_{20}N_2O$ $[M+H]^+$ 257.1654, *found* 257.1652.

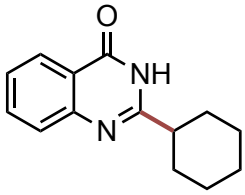

2-Cyclohexylquinazolin-4(3*H*)-one (4.4.6): Following General Procedure II using 4-hydroxyquinazoline (73.1 mg, 0.5 mmol, 1.0 equiv), diethyl 4-cyclohexyl-2,6-dimethyl-1,4-dihydropyridine-3,5-dicarboxylate (184.5 mg, 0.55 mmol, 1.1 equiv), $Na_2S_2O_8$ (142.8 mg, 0.6 mmol, 1.2 equiv) and TFA (85.5 mg, 0.75 mmol, 1.5 equiv) in CH_3CN/H_2O (5.0 mL, 1:1 v/v, 0.1 M). The product was isolated as a white solid (97.1 mg, 85% yield). mp = 213-215 ºC. ^{1}H NMR (500 MHz, $CDCl_3$) δ 11.78 (s, 1H), 8.29-8.27 (m, 1H), 7.77-7.70 (m, 2H), 7.47-7.44 (m, 1H), 2.77-2.70 (m, 1H), 2.06-2.04 (m, 2H), 1.93-1.91 (m, 2H), 1.81-1.73 (m, 3H), 1.49-1.38 (m, 3H) ppm. ^{13}C NMR (126 MHz, $CDCl_3$) δ 164.4, 160.3, 149.7, 134.8, 127.5, 126.4, 126.3, 120.9, 45.0, 30.6, 26.1, 25.8 ppm. IR (neat, cm^{-1}): 2929, 2852, 1679, 1605, 1467, 976, 776. Spectral data is consistent with previously reported values.[13]

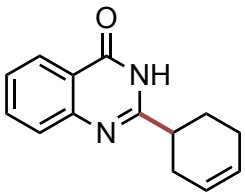

2-(Cyclohex-3-en-1-yl)quinazolin-4(3*H*)-one (4.4.7): Following General Procedure II using 4-hydroxyquinazoline (73.1 mg, 0.5 mmol, 1.0 equiv), diethyl 4-(cyclohex-3-en-1-yl)-2,6-dimethyl-1,4-dihydropyridine-3,5-dicarboxylate (183.3 mg, 0.55 mmol, 1.1 equiv), $Na_2S_2O_8$ (142.8 mg, 0.6 mmol, 1.2 equiv) and TFA (85.5 mg, 0.75 mmol, 1.5 equiv) in CH_3CN/H_2O (5.0 mL, 1:1 v/v, 0.1 M). The product was isolated as a white solid (47.5 mg, 42% yield). mp = 236-238 ºC. ^{1}H NMR (500 MHz, $CDCl_3$) δ 11.42 (s, 1H), 8.27 (d, J = 7.90 Hz, 1H), 7.76 (t, J = 7.60 Hz, 1H), 7.70 (d, J = 8.05 Hz, 1H), 7.46 (t, J = 7.43 Hz, 1H), 5.84-5.79 (m, 2H), 3.02-2.96 (m, 1H), 2.59-2.53 (m, 1H),

2.47-2.42 (m, 1H), 2.33-2.25 (m, 2H), 2.17-2.14 (m, 1H), 2.01-1.93 (m, 1H) ppm. ^{13}C NMR (126 MHz, $CDCl_3$) δ 164.1, 159.6, 149.6, 134.8, 127.5, 127.0, 126.5, 126.4, 125.5, 120.9, 40.4, 29.0, 27.0, 25.1 ppm. IR (neat, cm^{-1}): 2830, 1675, 1607, 1468, 987, 897, 769. HRMS (ES-) *calcd for* $C_{14}H_{13}N_2O$ $[M-H]^+$ 225.1028, *found* 225.1029.

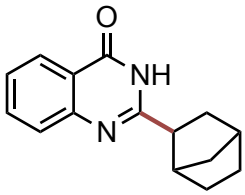

2-(Bicyclo[2.2.1]heptan-2-yl)quinazolin-4(3*H*)-one (4.4.8): Following General Procedure II using 4-hydroxyquinazoline (73.1 mg, 0.5 mmol, 1.0 equiv), diethyl 4-(bicyclo[2.2.1]heptan-2-yl)-2,6-dimethyl-1,4-dihydropyridine-3,5-dicarboxylate (191.1 mg, 0.55 mmol, 1.1 equiv), $Na_2S_2O_8$ (142.8 mg, 0.6 mmol, 1.2 equiv) and TFA (85.5 mg, 0.75 mmol, 1.5 equiv) in CH_3CN/H_2O (5.0 mL, 1:1 v/v, 0.1 M). The product was isolated as a white solid (49.0 mg, 41% yield). mp = 210-213 ºC. ^{1}H NMR of the crude reaction mixture showed a >20:1 dr. ^{1}H NMR (500 MHz, $CDCl_3$) δ 11.08 (s, 1H), 8.26 (d, *J* = 7.8 Hz, 1H), 7.83 – 7.62 (m, 2H), 7.45 (t, *J* = 7.2 Hz, 1H), 2.76 (dd, *J* = 8.6, 5.0 Hz, 1H), 2.63 (d, *J* = 4.0 Hz, 1H), 2.43 (s, 1H), 2.37 – 2.29 (m, 1H), 1.83 – 1.58 (m, 4H), 1.55 – 1.27 (m, 1H), 1.40 – 1.30 (m, 1H), 1.21 (d, *J* = 9.8 Hz, 1H) ppm. ^{13}C NMR (126 MHz, $CDCl_3$) δ 164.0, 158.9, 149.4, 134.7, 127.8, 126.4, 126.3, 120.8, 47.2, 42.6, 36.5, 36.2, 34.2, 30.1, 29.0 ppm. IR (neat, cm^{-1}): 2953, 2867, 1666, 1608, 1465, 1248, 902, 771. HRMS (EI+) *calcd for* $C_{15}H_{16}N_2O$ [M+] 240.1263, *found 240.1258*.

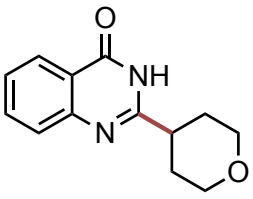

2-(Tetrahydro-2*H*-pyran-4-yl)quinazolin-4(3*H*)-one (4.4.9): Following General Procedure II using 4-hydroxyquinazoline (73.1 mg, 0.5 mmol, 1.0 equiv), diethyl 2,6-dimethyl-4-(tetrahydro-2H-pyran-4-yl)-1,4-dihydropyridine-3,5-dicarboxylate (185.5 mg, 0.55 mmol, 1.1 equiv), $Na_2S_2O_8$ (142.8 mg, 0.6 mmol, 1.2 equiv) and TFA (85.5 mg, 0.75 mmol, 1.5 equiv) in CH_3CN/H_2O (5.0 mL, 1:1 v/v, 0.1 M). The product was isolated as a white solid (52.9 mg, 46% yield). mp = 215-217 ºC. ^{1}H NMR (500 MHz, $CDCl_3$) δ 11.61 (s, 1H), 8.28 (d, *J* = 7.85 Hz, 1H), 7.78 (t, *J* = 7.48 Hz, 1H), 7.72 (d, *J* = 8.00 Hz, 1H), 7.49 (t, *J* =7.28 Hz, 1H), 4.14 (d, *J* = 10.45 Hz, 2H), 3.60 (t, *J* = 11.58 Hz, 2H), 2.98 (m, 1H), 2.14-2.07 (m, 2H), 2.00-1.98 (m, 2H) ppm. ^{13}C NMR (126 MHz, $CDCl_3$) δ 164.2, 158.0, 149.5, 134.9, 127.7, 126.7, 126.3, 120.9, 67.6, 41.5, 30.2 ppm. IR (neat, cm^{-1}): 3023, 2838, 1681, 1468, 908, 777, 625. HRMS (ES-) *calcd for* $C_{13}H_{13}N_2O_2[M-H]^+$ 229.0977, *found* 229.0973.

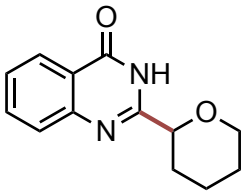

2-(Tetrahydro-2*H*-pyran-2-yl)quinazolin-4(3*H*)-one (4.4.10): Following General Procedure II using 4-hydroxyquinazoline (73.1 mg, 0.5 mmol, 1.0 equiv), diethyl 2,6-dimethyl-4-(tetrahydro-2H-pyran-2-yl)-1,4-dihydropyridine-3,5-dicarboxylate (185.5 mg, 0.55 mmol, 1.1 equiv), $Na_2S_2O_8$ (142.8 mg, 0.6 mmol, 1.2 equiv) and TFA (85.5 mg, 0.75 mmol, 1.5 equiv) in CH_3CN/H_2O (5.0 mL, 1:1 v/v, 0.1 M). The product was isolated as a white solid (69.2 mg, 60% yield). mp = 122-125 ºC. ^{1}H NMR (500 MHz, $CDCl_3$) δ 9.68 (s, 1H), 8.26 (dd, *J* = 7.95, 1.35 Hz, 1H), 7.74-7.71 (m, 1H), 7.64 (d, *J* = 7.95 Hz, 1H), 7.46-7.42 (m, 1H), 4.36 (dd, *J* = 11.20, 2.60 Hz, 1H), 4.18-4.15 (m, 1H), 3.65-3.60 (m, 1H), 2.26-2.23 (m, 1H), 1.99-1.96 (m, 1H), 1.70-1.52 (m, 4H) ppm. ^{13}C NMR (126 MHz, $CDCl_3$) δ 161.6, 155.9, 149.0, 134.6, 127.2, 126.7 (2C), 121.6, 76.2, 68.7, 30.9, 25.5,

23.0 ppm. IR (neat, cm^{-1}): 2930, 1683, 1624, 1467, 1175, 888, 775. HRMS (ES-) *calcd for* $C_{13}H_{13}N_2O_2$ $[M-H]^+$ 229.0977, *found* 229.0968.

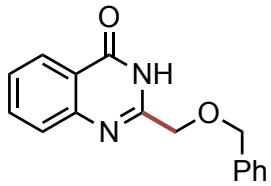

2-((Benzyloxy)methyl)quinazolin-4(3*H*)-one (4.4.11): Following General Procedure II using 4-hydroxyquinazoline (73.1 mg, 0.5 mmol, 1.0 equiv), diethyl 4-((benzyloxy)methyl)-2,6-dimethyl-1,4-dihydropyridine-3,5-dicarboxylate (205.4 mg, 0.55 mmol, 1.1 equiv), $Na_2S_2O_8$ (142.8 mg, 0.6 mmol, 1.2 equiv) and TFA (85.5 mg, 0.75 mmol, 1.5 equiv) in CH_3CN/H_2O (5.0 mL, 1:1 v/v, 0.1 M). The product was isolated as a white solid (73.3 mg, 55% yield). mp = 159-161 ºC. ^{1}H NMR (500 MHz, $CDCl_3$) δ 9.84 (s, 1H), 8.26 (d, *J* = 7.90 Hz, 1H), 7.74 (t, *J* = 7.63 Hz, 1H), 7.63 (d, *J* = 8.15 Hz, 1H), 7.46 (t, *J* = 7.53 Hz, 1H), 7.38-7.33 (m, 5H), 4.69 (s, 2H), 4.55 (s, 2H) ppm. ^{13}C NMR (126 MHz, $CDCl_3$) δ 161.7, 152.8, 148.8, 136.4, 134.9, 128.9, 128.6, 128.3, 127.2, 126.9, 126.8, 121.8, 73.9, 68.7 ppm. IR (neat, cm^{-1}): 1675, 1609, 1466, 1116, 869, 771. HRMS (ES+) *calcd for* $C_{16}H_{15}N_2O_2$ $[M+H]^+$ 267.1134, *found* 267.1135.

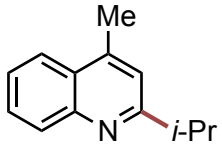

2-Isopropyl-4-methylquinoline (4.5.1): Following General Procedure II using lepidine (71.6 mg, 0.5 mmol, 1.0 equiv), diethyl 4-isopropyl-2,6-dimethyl-1,4-dihydropyridine-3,5-dicarboxylate (162.4 mg, 0.55 mmol, 1.1 equiv), $Na_2S_2O_8$ (142.8 mg, 0.6 mmol, 1.2 equiv) and TFA (85.5 mg, 0.75 mmol, 1.5 equiv) in CH_3CN/H_2O (5.0 mL, 1:1 v/v, 0.1 M). The product was isolated as a yellow oil (71.2 mg, 78% yield). ^{1}H NMR (500 MHz, $CDCl_3$) δ 8.05 (d, *J* = 8.45 Hz, 1H), 7.94 (d, *J* = 8.30 Hz, 1H), 7.66 (t, *J* = 7.60 Hz, 1H), 7.05 (t, *J* = 8.45 Hz, 1H), 7.17 (s, 1H), 3.21 (sept, *J* =

6.93 Hz, 1H), 2.68 (s, 3H), 1.39 (d, J = 6.95 Hz, 6H) ppm. ^{13}C NMR (126 MHz, $CDCl_3$) δ 167.4, 147.7, 144.3, 129.7, 129.0, 127.1, 125.5, 123.6, 119.9, 37.3, 22.6, 18.9 ppm. IR (neat, cm^{-1}): 2929, 2852, 1679, 1605, 1467, 976, 776. Spectral data is consistent with previously reported values.[14]

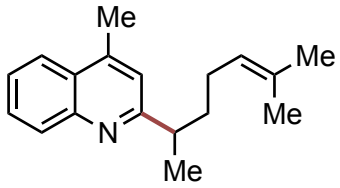

4-Methyl-2-(4-(5-methylhex-2-en-1-yl)cyclohex-3-en-1-yl)quinoline (mixture of isomers) (4.5.2): Following General Procedure II using 4-methylquinoline (66.3 mg, 0.5 mmol, 1.0 equiv), diethyl (*E*)-2,6-dimethyl-4-(4-(5-methylhex-2-en-1-yl)cyclohex-3-en-1-yl)-1,4-dihydropyridine-3,5-dicarboxylate (236.1 mg, 0.55 mmol, 1.1 equiv), $Na_2S_2O_8$ (142.8 mg, 0.60 mmol, 1.2 equiv) and TFA (85.5 mg, 0.75 mmol, 1.5 equiv) in CH_3CN/H_2O (5.0 mL, 1:1 v/v, 0.1 M). The product was isolated as a clear oil (53.0 mg, 35% yield). The compound was isolated as a mixture of different diastereomers coming from the commercially available aldehyde. ^{1}H NMR (500 MHz, $CDCl_3$) δ 8.06 (d, J = 8.5 Hz, 1H), 7.95 (d, J = 8.2 Hz, 1H), 7.67 (t, J = 7.8 Hz, 1H), 7.50 (t, J = 7.6 Hz, 1H), 7.18 (s, 1H), 5.53 (d, J = 11.7 Hz, 1H), 5.43 – 5.05 (m, 2H), 3.16 – 3.01 (m, 1H), 2.69 (d, J = 4.3 Hz, 3H), 2.40 (d, J = 8.4 Hz, 2H), 2.32 – 2.16 (m, 2H), 2.07 (m, 6H), 1.95 (ddt, J = 17.5, 11.7, 5.8 Hz, 2H), 1.71 – 1.68 (m, 3H), 1.64 – 1.59 (m, 4H) ppm. ^{13}C NMR (126 MHz, $CDCl_3$) δ 166.2, 166.2, 147.8, 144.5, 144.5, 137.8, 137.7, 137.3, 131.6, 131.5, 129.6, 129.1, 127.2, 125.6, 124.5, 124.5, 124.3, 123.7, 120.6, 120.5, 120.5, 120.3, 117.4, 43.8, 43.4, 38.0, 37.9, 37.7, 37.5, 34.9, 31.8, 29.5, 29.2, 29.0, 28.7, 26.7, 26.7, 26.6, 25.9, 25.9, 19.0, 17.9, 17.8 ppm. IR (neat, cm^{-1}): 2964, 2914, 2838, 1603, 1438, 862, 757. HRMS (EI+) *calcd for* $C_{22}H_{27}N$ [M^+] 305.2144, *found* 305.2155.

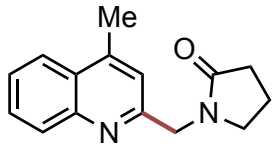

1-((4-Methylquinolin-2-yl)methyl)pyrrolidin-2-one (4.5.3): Following General Procedure II using lepidine (71.6 mg, 0.5 mmol, 1.0 equiv), diethyl 2,6-dimethyl-4-((2-oxopyrrolidin-1-yl)methyl)-1,4-dihydropyridine-3,5-dicarboxylate (192.7 mg, 0.55 mmol, 1.1 equiv), $Na_2S_2O_8$ (261.9 mg, 1.1 mmol, 2.2 equiv) and TFA (85.5 mg, 0.75 mmol, 1.5 equiv) in CH_3CN/H_2O (5.0 mL, 1:1 v/v, 0.1 M). The product was isolated as a yellow semi-solid that melts when handled (26.7 mg, 22% yield). ^{1}H NMR (500 MHz, $CDCl_3$) δ 8.05 (d, *J* = 8.4 Hz, 1H), 7.98 (d, *J* = 8.3 Hz, 1H), 7.70 (t, *J* = 7.6 Hz, 1H), 7.56 (t, *J* = 7.6 Hz, 1H), 7.22 (s, 1H), 4.73 (s, 2H), 3.41 (t, *J* = 7.1 Hz, 2H), 2.69 (s, 3H), 2.50 (t, *J* = 8.1 Hz, 2H), 2.12 – 1.95 (m, 2H) ppm. ^{13}C NMR (126 MHz, $CDCl_3$) δ 175.4, 157.0, 147.6, 145.6, 129.8, 129.5, 127.6, 126.4, 123.9, 120.7, 49.4, 47.4, 31.0, 18.9, 18.1 ppm. IR (neat, cm^{-1}): 3256, 2948, 1599, 1438, 1422, 1286, 1261, 753. HRMS (EI+) *calcd for* $C_{15}H_{16}NO_2$ [M^+] 240.1263, *found* 240.1287.

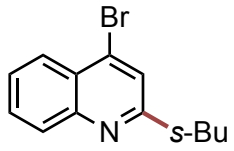

4-Bromo-1-(*sec*-butyl)isoquinoline (4.5.4): Following General Procedure II using 4-bromoisoquinoline (104.0 mg, 0.5 mmol, 1.0 equiv), diethyl 4-(*sec*-butyl)-2,6-dimethyl-1,4-dihydropyridine-3,5-dicarboxylate (170.1 mg, 0.55 mmol, 1.1 equiv), $Na_2S_2O_8$ (142.8 mg, 0.60 mmol, 1.2 equiv) and TFA (85.5 mg, 0.75 mmol, 1.5 equiv) in CH_3CN/H_2O (5.0 mL, 1:1 v/v, 0.1 M). The product was isolated as a clear oil (76.0 mg, 58% yield). ^{1}H NMR (500 MHz, $CDCl_3$) δ 8.69 (s, 1H), 8.21 (dd, *J* = 12.1, 8.5 Hz, 2H), 7.77 (t, *J* = 7.6 Hz, 1H), 7.64 (t, *J* = 7.7 Hz, 1H), 3.67 (m, 1H), 2.01 (m, 1H), 1.74 (dq, *J* = 14.0, 7.0 Hz, 1H), 1.39 (d, *J* = 6.8 Hz, 3H), 0.89 (t, *J* = 7.4 Hz, 3H) ppm. ^{13}C NMR (126 MHz, $CDCl_3$) δ 165.6, 143.8, 135.0, 130.9, 128.4, 127.9, 127.0, 125.2, 117.6, 37.9, 29.7, 20.3, 12.5 ppm. IR (neat, cm^{-1}): 2964, 2931, 1460, 1297, 919, 758. HRMS (EI+) *calcd for* $C_{13}H_{14}NBr$ [M^+] 263.0310, *found* 263.0323.

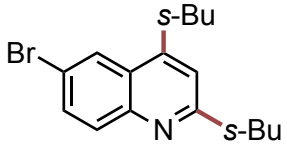

6-Bromo-2,4-di-*sec*-butylquinoline (4.5.5): Following General Procedure II using 6-bromoquinoline (104.0 mg, 0.5 mmol, 1.0 equiv), diethyl 4-(*sec*-butyl)-2,6-dimethyl-1,4-dihydropyridine-3,5-dicarboxylate (170.1 mg, 0.55 mmol, 1.1 equiv), $Na_2S_2O_8$ (142.8 mg, 0.60 mmol, 1.2 equiv) and TFA (85.5 mg, 0.75 mmol, 1.5 equiv) in CH_3CN/H_2O (5.0 mL, 1:1 v/v, 0.1 M). The product was isolated as a yellow oil (40.0 mg, 46% yield with DHP as the limiting reagent). ^{1}H NMR (500 MHz, $CDCl_3$) δ 8.17 (s, 1H), 7.92 (d, *J* = 8.7 Hz, 1H), 7.71 (d, *J* = 9.0 Hz, 1H), 7.15 (s, 1H), 3.38 (m, 1H), 2.95 (m, 1H), 1.83 (dt, *J* = 14.5, 7.2 Hz, 2H), 1.71 (dt, *J* = 12.2, 6.5 Hz, 2H), 1.35 (d, *J* = 7.0 Hz, 6H), 0.90 (dt, *J* = 20.7, 7.4 Hz, 7H) ppm. ^{13}C NMR (126 MHz, $CDCl_3$) δ 167.3, 152.7, 147.0, 132.1, 131.9, 127.6, 125.5, 119.5, 117.2, 117.0, 44.8, 35.3, 30.1, 30.0, 20.9, 20.4, 20.3, 12.3, 12.1 ppm. IR (neat, cm^{-1}): 2963, 2930, 2874, 1599, 1556, 1489, 1460, 1379, 829. HRMS (EI+) *calcd for* $C_{17}H_{22}NBr$ 319.0936 [M+], *found* 319.0936.

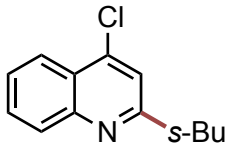

2-(*sec*-Butyl)-4-chloroquinoline (4.5.6): Following General Procedure II using 4-chloroquinoline (81.8 mg, 0.5 mmol, 1.0 equiv), diethyl 4-(*sec*-butyl)-2,6-dimethyl-1,4-dihydropyridine-3,5-dicarboxylate (170.1 mg, 0.55 mmol, 1.1 equiv), $Na_2S_2O_8$ (142.8 mg, 0.60 mmol, 1.2 equiv) and TFA (85.5 mg, 0.75 mmol, 1.5 equiv) in CH_3CN/H_2O (5.0 mL, 1:1 v/v, 0.1 M). The product was isolated as a clear oil (89.0 mg, 81% yield). ^{1}H NMR (500 MHz, $CDCl_3$) δ 8.17 (d, *J* = 8.3 Hz, 1H), 8.07 (d, *J* = 8.4 Hz, 1H), 7.71 (t, *J* = 7.7 Hz, 1H), 7.55 (t, *J* = 7.6 Hz, 1H), 7.38 (s, 1H), 2.97 (m, 1H), 1.85 (m, 1H), 1.70 (dq, *J* = 14.2, 7.1 Hz, 1H), 1.36 (d, *J* = 7.1 Hz, 3H), 0.90 (t, *J* = 7.4 Hz,

3H) ppm. ^{13}C NMR (126 MHz, $CDCl_3$) δ 167.1, 148.8, 142.7, 130.2, 129.5, 126.7, 125.2, 124.0, 119.9, 44.6, 29.9, 20.3, 12.3 ppm. IR (neat, cm^{-1}): 2962, 2930, 2874, 1589, 1493, 869. HRMS (EI+) *calcd for* $C_{13}H_{14}NCl$ [M^+] 219.0815, *found* 219.0827.

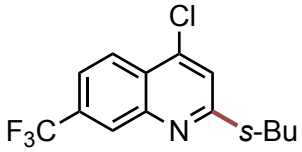

2-(*sec*-Butyl)-4-chloro-7-(trifluoromethyl)quinoline (4.5.7): Following General Procedure II using 4-chloro-7-(trifluoromethyl)quinoline (47.6 mg, 0.2 mmol, 1.0 equiv), diethyl 4-(*sec*-butyl)-2,6-dimethyl-1,4-dihydropyridine-3,5-dicarboxylate (95.9 mg, 0.31 mmol, 1.5 equiv), $Na_2S_2O_8$ (73.8 mg, 0.31 mmol, 1.5 equiv) and TFA (35.3 mg, 0.31 mmol, 1.5 equiv) in CH_3CN/H_2O (2.0 mL, 1:1 v/v, 0.1 M). The product was isolated as a yellow oil (38.7 mg, 67% yield). ^{1}H NMR (500 MHz, $CDCl_3$) δ 8.39 (s, 1H), 8.30 (d, *J* = 8.7 Hz, 1H), 7.75 (d, *J* = 8.6 Hz, 1H), 7.49 (s, 1H), 3.14 – 2.90 (m, 1H), 1.85 (dq, *J* = 14.3, 7.1 Hz, 1H), 1.73 (dq, *J* = 13.7, 6.9 Hz, 1H), 1.37 (d, *J* = 6.9 Hz, 3H), 0.90 (t, *J* = 7.4 Hz, 3H) ppm. ^{13}C NMR (126 MHz, $CDCl_3$) δ 168.8, 148.0, 142.7, 132.1 (q, *J* = 32.6 Hz), 127.5 (q, *J* = 4.0 Hz), 126.9, 125.4, 124.0 (q, *J* = 272.5 Hz), 122.4 (q, *J* = 3.2 Hz), 122.0, 44.6, 29.9, 20.2, 12.2 ppm. ^{19}F NMR (471 MHz, $CDCl_3$) δ -62.8 ppm. IR (neat, cm^{-1}): 2956, 1594, 1230, 1165, 1126, 1061, 826. HRMS (EI+) *calcd for* $C_{14}H_{13}NClF_3$ [M+] 287.0689, *found* 287.0700.

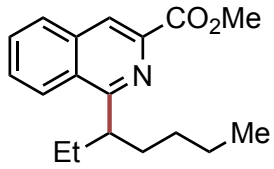

Methyl 1-(heptan-3-yl)isoquinoline-3-carboxylate (4.5.8): Following General Procedure II using methyl isoquinoline-3-carboxylate (93.6 mg, 0.5 mmol, 1.0 equiv), diethyl 4-(heptan-3-yl)-2,6-dimethyl-1,4-dihydropyridine-3,5-dicarboxylate (193.2 mg, 0.55 mmol, 1.1 equiv), $Na_2S_2O_8$ (142.8 mg, 0.60 mmol, 1.2 equiv) and TFA (85.5 mg, 0.75 mmol, 1.5 equiv) in CH_3CN/H_2O (5.0 mL, 1:1 v/v, 0.1 M). The product was isolated as a clear oil (120.0 mg, 84% yield). ^{1}H NMR (500 MHz,

$CDCl_3$) δ 8.38 (s, 1H), 8.29 (d, *J* = 7.9 Hz, 1H), 7.94 (d, *J* = 7.7 Hz, 1H), 7.70 (m, 2H), 4.02 (s, 3H), 3.59 (m, 1H), 2.05 (dt, *J* = 15.7, 7.6 Hz, 2H), 1.89 – 1.78 (m, 2H), 1.27 (dd, *J* = 13.4, 6.8 Hz, 3H), 1.09 (td, *J* = 11.3, 5.5 Hz, 1H), 0.80 (dt, *J* = 11.3, 5.1 Hz, 6H) ppm. ^{13}C NMR (126 MHz, $CDCl_3$) δ 167.1, 166.0, 141.1, 136.1, 130.2, 129.4, 129.1, 129.1, 125.1, 122.1, 52.7, 44.1, 35.0, 30.3, 28.4, 23.0, 14.1, 12.6 ppm. IR (neat, cm^{-1}): 2956, 1740, 1717, 1238, 1202, 782, 750. HRMS (EI+) *calcd for* $C_{18}H_{23}NO_2$ [M^+] 285.1729, *found* 285.1743.

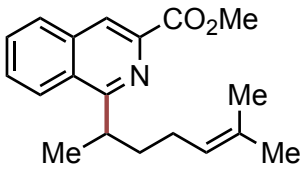

Methyl 1-(6-Methylhept-5-en-2-yl)isoquinoline-3-carboxylate (4.5.9): Following General Procedure II using methyl isoquinoline-3-carboxylate (93.6 mg, 0.5 mmol, 1.0 equiv), diethyl 4-(*sec*-butyl)-2,6-dimethyl-1,4-dihydropyridine-3,5-dicarboxylate (170.1 mg, 0.55 mmol, 1.1 equiv), $Na_2S_2O_8$ (142.8 mg, 0.60 mmol, 1.2 equiv) and TFA (85.5 mg, 0.75 mmol, 1.5 equiv) in CH_3CN/H_2O (5.0 mL, 1:1 v/v, 0.1 M). The product was isolated as a clear oil (68.0 mg, 46% yield). ^{1}H NMR (500 MHz, $CDCl_3$) δ 8.39 (s, 1H), 8.26 (d, *J* = 7.9 Hz, 1H), 7.94 (d, *J* = 7.6 Hz, 1H), 7.71 (m, 2H), 5.14 (t, *J* = 7.4 Hz, 1H), 4.02 (s, 3H), 3.81 (m, 1H), 2.15 (dq, *J* = 14.1, 7.3 Hz, 1H), 2.00 (q, *J* = 7.5 Hz, 2H), 1.80 (dq, *J* = 14.0, 7.1 Hz, 1H), 1.64 (s, 3H) 1.50 – 1.41 (m, 6H) ppm. ^{13}C NMR (126 MHz, $CDCl_3$) δ 167.0, 166.4, 140.9, 136.2, 131.9, 130.2, 129.1, 129.1, 128.3, 125.1, 124.6, 122.4, 52.7, 36.4, 36.3, 26.4, 25.8, 20.4, 17.7 ppm. IR (neat, cm^{-1}): 2927, 1740, 1716, 1322, 1239, 780, 750. HRMS (EI+) *calcd for* $C_{19}H_{23}NO_2$ [M^+] 297.1729, *found* 297.1733.

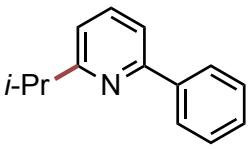

2-Isopropyl-6-phenylpyridine and 2,4-Diisopropyl-6-phenylpyridine (4.5.10): Following General Procedure II using 2-phenyl pyridine (77.5 mg, 0.5 mmol, 1.0 equiv), diethyl 4-isopropyl-2,6-dimethyl-1,4-dihydropyridine-3,5-dicarboxylate (324.7 mg, 0.55 mmol, 1.1 equiv), $Na_2S_2O_8$

(85.7 mg, 0.36 mmol, 1.2 equiv) and TFA (51.3 mg, 0.45 mmol, 1.5 equiv) in CH_3CN/H_2O (3.0 mL, 1:1 v/v, 0.1 M). A 1:1 mixture of mono- and di-substituted compound was obtained as a clear oil, 72% overall yield). ^{1}H NMR (500 MHz, $CDCl_3$) δ 8.05 (t, *J* = 8.7 Hz, 4H), 7.66 (s, 1H), 7.54 (d, *J* = 7.8 Hz, 1H), 7.46 (d, *J* = 8.4 Hz, 4H), 7.40 (s, 3H), 7.12 (d, *J* = 7.7 Hz, 1H), 6.97 (s, 1H), 3.13 (dq, *J* = 14.2, 7.2 Hz, 2H), 2.93 (q, *J* = 7.3 Hz, 1H), 1.37 (d, *J* = 6.8 Hz, 12H), 1.32 (s, 6H) ppm. ^{13}C NMR (126 MHz, $CDCl_3$) δ 167.3, 158.5, 156.6, 156.5, 140.5, 140.1, 137.1, 128.8, 128.7, 128.6, 127.2, 127.1, 119.0, 117.8, 117.4, 116.3, 36.7, 34.1, 29.9, 23.5, 22.9, 22.8. IR (neat, cm^{-1}): 2963, 1600, 1571, 1446, 1162, 762 ppm. HRMS (EI+) *calcd for* $C_{14}H_{15}N$ [M^+] 197.1204, *found* 197.1205 (mono alkylated). HRMS (EI+) *calcd for* $C_{17}H_{21}N$ [M+] 239.1674, *found* 239.1660 (double alkylated product).

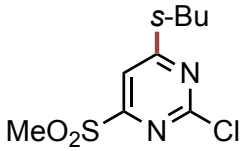

4-(*sec*-Butyl)-2-chloro-6-(methylsulfonyl)pyrimidine (4.5.11): Following General Procedure II using 2-chloro-4-(methylsulfonyl)pyrimidine (96.0 mg, 0.5 mmol, 1.0 equiv), diethyl 4-(*sec*-butyl)-2,6-dimethyl-1,4-dihydropyridine-3,5-dicarboxylate (170.1 mg, 0.55 mmol, 1.1 equiv), $Na_2S_2O_8$ (142.8 mg, 0.60 mmol, 1.2 equiv) and TFA (85.5 mg, 0.75 mmol, 1.5 equiv) in CH_3CN/H_2O (5.0 mL, 1:1 v/v, 0.1 M). The product was isolated as a clear oil (120.0 mg, 70% yield). ^{1}H NMR (500 MHz, $CDCl_3$) δ 7.74 (s, 1H), 3.27 (s, 3H), 2.91 (m, 1H), 1.80 (m, 1H), 1.66 (m, 1H), 1.31 (d, *J* = 6.9 Hz, 3H), 0.88 (t, *J* = 7.4 Hz, 3H) ppm. ^{13}C NMR (126 MHz, $CDCl_3$) δ 183.3, 167.7, 166.1, 162.3, 161.6, 141.1, 123.2, 113.0, 66.0, 61.6, 44.1, 39.3, 29.3, 25.1, 19.3, 15.4, 14.4, 12.0 ppm. IR (neat, cm^{-1}): 2969, 1719, 1522, 1320, 1232, 748, 532. HRMS (EI+) *calcd for* $C_9H_{13}N_2ClSO_2$ [M^+] 248.0386, *found* 248.0380.

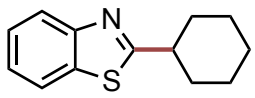

2-Cyclohexylbenzo[d]thiazole (4.5.12): Following General Procedure II using benzothiazole (68.1 mg, 0.5 mmol, 1.0 equiv), diethyl 4-cyclohexyl-2,6-dimethyl-1,4-dihydropyridine-3,5-dicarboxylate (335.4 mg, 1.0 mmol, 2.0 equiv), $Na_2S_2O_8$ (357.2 mg, 1.5 mmol, 3.0 equiv) and TFA (85.5 mg, 0.75 mmol, 1.5 equiv) in CH_3CN/H_2O (5.0 mL, 1:1 v/v, 0.1 M). The product was isolated as a colorless oil (62.5 mg, 58% yield). ^{1}H NMR (500 MHz, $CDCl_3$) δ 7.97 (d, *J* = 8.2 Hz, 1H), 7.85 (d, *J* = 8.0 Hz, 1H), 7.44 (t, *J* = 7.7 Hz, 1H), 7.34 (t, *J* = 7.6 Hz, 1H), 3.11 (tt, *J* = 11.6, 3.4 Hz, 1H), 2.21 (d, *J* = 12.6 Hz, 2H), 1.98 – 1.85 (m, 2H), 1.82 – 1.73 (m, 1H), 1.65 (qd, *J* = 12.4, 3.2 Hz, 2H), 1.53 – 1.39 (m, 2H), 1.39 – 1.21 (m, 1H) ppm. ^{13}C NMR (126 MHz, $CDCl_3$) δ 177.7, 153.3, 134.7, 125.9, 124.6, 122.7, 121.7, 43.6, 33.6, 26.2, 25.9 ppm. Spectral data is consistent with previously reported values.[15]

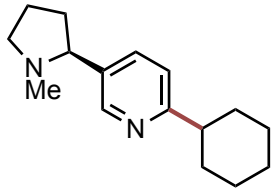

(*S*)-2-Cyclohexyl-5-(1-methylpyrrolidin-2-yl)pyridine (4.6.1): Following General Procedure II using (-)-nicotine (81.1 mg, 0.5 mmol, 1.0 equiv), diethyl 4-cyclohexyl-2,6-dimethyl-1,4-dihydropyridine-3,5-dicarboxylate (184.5 mg, 0.55 mmol, 1.1 equiv), $Na_2S_2O_8$ (142.9 mg, 0.6 mmol, 1.2 equiv) and TFA (85.5 mg, 0.75 mmol, 1.5 equiv) in CH_3CN/H_2O (5.0 mL, 1:1 v/v, 0.1 M). The product was isolated as a colorless oil (59.7 mg, 49% yield). ^{1}H NMR (500 MHz, $CDCl_3$) δ 8.41 (s, 1H), 7.61 (d, *J* = 8.0 Hz, 1H), 7.12 (d, *J* = 8.0 Hz, 1H), 3.23 (t, *J* = 8.5 Hz, 1H), 3.04 (t, *J* = 8.3 Hz, 1H), 2.69 (t, *J* = 11.7 Hz, 1H), 2.29 (q, *J* = 9.0 Hz, 1H), 2.16 (s, 3H), 1.95 (d, *J* = 11.4 Hz, 2H), 1.85 (d, *J* = 12.5 Hz, 3H), 1.78 – 1.72 (m, 2H), 1.52 (q, *J* = 12.4 Hz, 2H), 1.41 (q, *J* = 11.4, 10.2 Hz, 3H), 1.35 – 1.24 (m, 2H) ppm. ^{13}C NMR (126 MHz, $CDCl_3$) δ 165.6, 148.9, 135.8, 135.4, 121.0, 68.9, 57.2, 46.4, 40.6, 35.2, 33.2, 26.8, 26.3, 22.7 ppm. Spectral data is consistent with previously reported values.[16]

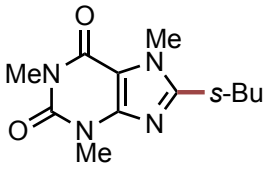

8-(*sec*-Butyl)-1,3,7-trimethyl-3,7-dihydro-1*H*-purine-2,6-dione (4.6.2): Following General Procedure II using 1,3,7-trimethyl-3,7-dihydro-1*H*-purine-2,6-dione (65.0 mg, 0.5 mmol, 1.0 equiv), diethyl 4-(*sec*-butyl)-2,6-dimethyl-1,4-dihydropyridine-3,5-dicarboxylate (170.1 mg, 0.55 mmol, 1.1 equiv), $Na_2S_2O_8$ (142.8 mg, 0.60 mmol, 1.2 equiv) and TFA (85.5 mg, 0.75 mmol, 1.5 equiv) in CH_3CN/H_2O (5.0 mL, 1:1 v/v, 0.1 M). The product was isolated as a clear oil (47.0 mg, 38% yield). ^{1}H NMR (500 MHz, $CDCl_3$) δ 3.92 (s, 3H), 3.56 (s, 3H), 3.39 (s, 3H), 2.83 (q, *J* = 7.2 Hz, 1H), 1.84 (dq, *J* = 14.5, 7.5 Hz, 1H), 1.68 (tt, *J* = 14.1, 7.2 Hz, 1H), 1.31 (d, *J* = 6.8 Hz, 3H), 0.88 (t, *J* = 7.4 Hz, 3H) ppm. ^{13}C NMR (126 MHz, $CDCl_3$) δ 158.5, 155.6, 151.9, 148.4, 107.1, 33.2, 31.6, 29.9, 28.8, 28.0, 19.0, 12.1 ppm. IR (neat, cm^{-1}): 1698, 1662, 1648, 1427, 755, 738. HRMS (EI+) *calcd for* $C_{12}H_{18}N_4O_2$ [M^+] 250.1430, *found* 250.1410.

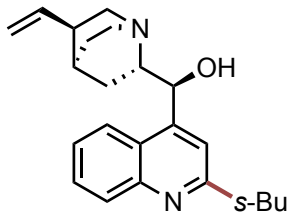

(1*S*)-(2-(*sec*-Butyl)quinolin-4-yl)((1*S*,2*S*,4*S*,5*R*)-5-vinylquinuclidin-2-yl)methanol (4.6.3): Following General Procedure II using cinchonine (147.2 mg, 0.5 mmol, 1.0 equiv), diethyl 4-(*sec*-butyl)-2,6-dimethyl-1,4-dihydropyridine-3,5-dicarboxylate (170.2 mg, 0.55 mmol, 1.1 equiv), $Na_2S_2O_8$ (142.9 mg, 0.6 mmol, 1.2 equiv) and TFA (85.5 mg, 0.75 mmol, 1.5 equiv) in CH_3CN/H_2O (5.0 mL, 1:1 v/v, 0.1 M). The product was isolated as a white solid (100.2 mg, 57% yield). mp = 154-156 ºC. ^{1}H NMR showed a 1:1 *dr.* ^{1}H NMR (500 MHz, $CDCl_3$) δ 8.07 (d, *J* = 8.4 Hz, 1H), 7.91 (d, *J* = 8.4 Hz, 1H), 7.65 (t, *J* = 7.7 Hz, 1H), 7.53 (d, *J* = 3.5 Hz, 1H), 7.44 (t, *J* = 7.6 Hz, 1H), 6.02 – 5.87 (m, 1H), 5.79 – 5.70 (m, 1H), 5.07 – 4.94 (m, 2H), 3.31 – 3.19 (m, 1H), 3.14 – 3.07 (m,

1H), 3.03 – 2.97 (m, 1H), 2.96 – 2.86 (m, 2H), 2.82 – 2.73 (m, 1H), 2.26 – 2.16 (m, 1H), 2.02 – 1.94 (m, 1H), 1.90 – 1.81 (m, 1H), 1.78 – 1.67 (m, 2H), 1.56 – 1.48 (m, 2H), 1.36 (d, *J* = 7.0 Hz, 3H), 1.21 – 1.13 (m, 1H), 0.88 (t, *J* = 7.4 Hz, 3H) ppm. ^{13}C NMR (126 MHz, $CDCl_3$) δ 166.8, 149.2, 148.0, 140.7, 130.0, 128.8, 125.8, 124.5, 122.7, 116.8, 116.6, 114.7, 71.9, 60.1, 50.3, 49.8, 49.8, 44.9, 44.9, 40.2, 30.1, 30.0, 28.5, 26.4, 20.7, 20.7, 20.5, 20.5, 12.4, 12.3 ppm. IR (neat, cm^{-1}): 3068, 2932, 1596, 1454, 1110, 993, 905, 752. HRMS (EI+) *calcd for* $C_{23}H_{30}N_2O$ [M^+] 350.2358, *found* 350.2368.

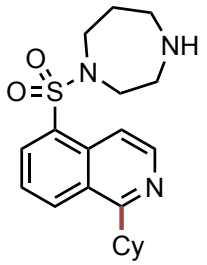

5-((1,4-Diazepan-1-yl)sulfonyl)-1-cyclohexylisoquinoline (4.6.5.1): Following General Procedure II using Fasudil hydrochloride (164.4 mg, 0.5 mmol, 1.0 equiv), diethyl 4-cyclohexyl-2,6-dimethyl-1,4-dihydropyridine-3,5-dicarboxylate (251.6 mg, 0.75 mmol, 1.5 equiv), $Na_2S_2O_8$ (178.6 mg, 0.75 mmol, 1.5 equiv) and TFA (85.5 mg, 0.75 mmol, 1.5 equiv) in CH_3CN/H_2O (5.0 mL, 1:1 v/v, 0.1 M). The product was isolated as a brown solid (156.9 mg, 84% yield). mp= 108-112 ºC. ^{1}H NMR (500 MHz, $CDCl_3$) δ 8.62 (d, *J* = 6.1 Hz, 1H), 8.47 (d, *J* = 8.6 Hz, 1H), 8.31 (d, *J* = 7.3 Hz, 1H), 8.27 (d, *J* = 6.1 Hz, 1H), 7.64 (t, *J* = 8.0 Hz, 1H), 3.62 – 3.51 (m, 1H), 3.53 – 3.43 (m, 4H), 3.04 – 2.95 (m, 4H), 2.77 – 2.57 (m, 1H), 2.00 – 1.91 (m, 4H), 1.91 – 1.78 (m, 5H), 1.59 – 1.46 (m, 2H), 1.46 – 1.32 (m, 1H) ppm. ^{13}C NMR (126 MHz, $CDCl_3$) δ 166.7, 144.0, 135.3, 132.4, 132.4, 130.4, 127.1, 125.2, 115.6, 50.9, 50.3, 47.7, 47.5, 42.2, 32.9, 31.0, 26.9, 26.3 ppm. IR (neat, cm^{-1}): 2922, 1318, 1138, 818, 596. HRMS (EI+) *calcd for* $C_{20}H_{27}N_3O_2S$ [M^+] 373.1824, *found* 373.1830.

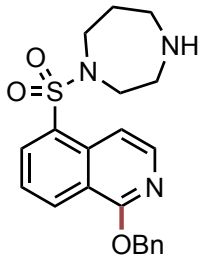

5-((1,4-Diazepan-1-yl)sulfonyl)-1-((benzyloxy)methyl)isoquinoline (4.6.5.2): Following General Procedure II using Fasudil hydrochloride (164.4 mg, 0.5 mmol, 1.0 equiv), diethyl 4-((benzyloxy)methyl)-2,6-dimethyl-1,4-dihydropyridine-3,5-dicarboxylate (280.1 mg, 0.75 mmol, 1.5 equiv), $Na_2S_2O_8$ (178.6 mg, 0.75 mmol, 1.5 equiv) and TFA (85.5 mg, 0.75 mmol, 1.5 equiv) in CH_3CN/H_2O (5.0 mL, 1:1 v/v, 0.1 M). The product was isolated as a yellow thick oil (105.3 mg, 51% yield). ^{1}H NMR (500 MHz, $CDCl_3$) δ 8.62 (t, *J* = 7.9 Hz, 2H), 8.44 (d, *J* = 6.1 Hz, 1H), 8.34 (d, *J* = 7.4 Hz, 1H), 7.67 (t, *J* = 7.9 Hz, 1H), 7.37 – 7.33 (m, 4H), 7.32 – 7.28 (m, 1H), 5.17 (s, 2H), 4.64 (s, 2H), 3.49 (t, *J* = 6.1 Hz, 2H), 3.48 – 3.41 (m, 2H), 3.09 – 2.90 (m, 4H), 2.22 – 1.98 (m, 1H), 1.90 – 1.81 (m, 2H) ppm. ^{13}C NMR (126 MHz, $CDCl_3$ δ 158.2, 143.7, 137.7, 135.2, 132.8, 132.5, 131.7, 128.6, 128.2 (2C), 128.1, 125.9, 118.1, 73.4, 73.1, 51.1, 50.4, 47.8, 47.5, 31.1 ppm. IR (neat, cm^{-1}): 2918, 2850, 1453, 1321, 1146, 1070, 697, 587. HRMS (EI+) *calcd for* $C_{22}H_{25}N_3O_3S$ [M^+] 411.1617, *found* 411.1624.

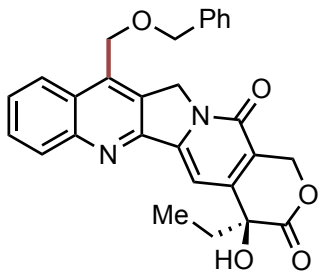

(*S*)-11-((Benzyloxy)methyl)-4-ethyl-4-hydroxy-1,12-dihydro-14*H*-pyrano[3',4':6,7]indolizino[1,2-*b*]quinoline-3,14(4*H*)-dione (4.6.6): Following General

Procedure II using (*S*)-(+)-Camptothecin (50.0 mg, 0.14 mmol, 1.0 equiv), diethyl 4-((benzyloxy)methyl)-2,6-dimethyl-1,4-dihydropyridine-3,5-dicarboxylate (104.6 mg, 0.28 mmol, 2.0 equiv), $Na_2S_2O_8$ (66.7 mg, 0.28 mmol, 2.0 equiv) and TFA (31.9 mg, 0.28 mmol, 2.0 equiv) in CH_3CN/H_2O (1.4 mL, 1:1 v/v, 0.1 M). The product was isolated as a yellow solid (42.2 mg, 64% yield). mp = 213-215 ºC. ^{1}H NMR (500 MHz, $CDCl_3$) δ 8.23 (d, *J* = 8.5 Hz, 1H), 7.98 (d, *J* = 8.2 Hz, 1H), 7.80 (t, *J* = 7.6 Hz, 1H), 7.64 (d, *J* = 10.3 Hz, 2H), 7.44 – 7.38 (m, 4H), 7.36 (d, *J* = 4.7 Hz, 1H), 5.76 (d, *J* = 16.3 Hz, 1H), 5.43 (s, 2H), 5.31 (d, *J* = 16.2 Hz, 1H), 5.18 (s, 2H), 4.79 (s, 2H), 3.73 (s, 1H), 1.99 – 1.81 (m, 2H), 1.04 (t, *J* = 7.4 Hz, 3H) ppm. ^{13}C NMR (126 MHz, $CDCl_3$) δ 174.1, 157.7, 152.7, 150.1, 149.0, 146.5, 139.4, 137.2, 130.7, 130.3, 128.9, 128.5, 128.1, 128.0, 127.1, 125.9, 123.5, 118.8, 97.9, 73.9, 72.9, 67.2, 66.6, 50.9, 31.8, 8.0 ppm. Spectral data is consistent with previously reported values.[17]

C-H Alkylation of Quinones

General Procedure III: A vial was charged with quinone starting material (0.5 mmol, 1.0 equiv), 4-alkyl-1,4-dihydropyridine (1.0 mmol, 2.0 equiv) and $Na_2S_2O_8$ (357.2 mg, 1.5 mmol, 3.0 equiv). Then, the vial was capped and purged with three cycles of vacuum/argon and then, under an argon atmosphere, degassed CH_3CN/H_2O (5.0 mL, 1:1 v/v, 0.1 M) and TFA (114.9 mg, 0.75 mmol, 1.5 equiv) were added. The reaction was vigorously stirred for 36-48 h at rt. After completion, the reaction was quenched by addition of aq $NaHCO_3$ (sat, 0.0 mL), and extracted three times with EtOAc (10.0 mL). The combined organic layers were washed with brine (20.0 mL), dried ($MgSO_4$), filtered and concentrated. The crude product was then adsorbed on Celite® and purified on an automated system.

Characterization Data: C-H Alkylation of Quinones.

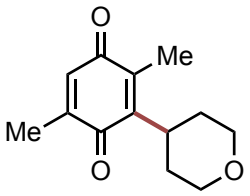

2,5-Dimethyl-3-(tetrahydro-2H-pyran-4-yl)cyclohexa-2,5-diene-1,4-dione (4.7.1): Following General Procedure III using 2,5-dimethyl-*p*-benzoquinone (68.1 mg, 0.5 mmol, 1.0 equiv) and diethyl 2,6-dimethyl-4-(tetrahydro-2H-pyran-4-yl)-1,4-dihydropyridine-3,5-dicarboxylate (337.4 mg, 1.0 mmol, 2.0 equiv). The product was isolated as an orange solid (61.3 mg, 56% yield). mp = 93-96 ºC. ^{1}H NMR (500 MHz, $CDCl_3$) δ 6.56 (d, *J* = 1.6 Hz, 1H), 4.06 (dd, *J* = 11.4, 4.4 Hz, 2H), 3.45 (td, *J* = 11.9, 2.1 Hz, 2H), 3.05 (tt, *J* = 12.4, 3.6 Hz, 1H), 2.31 (qd, *J* = 12.6, 4.4 Hz, 2H), 2.10 (s, 3H), 2.02 (d, *J* = 1.6 Hz, 3H), 1.47 – 1.36 (m, 2H) ppm. ^{13}C NMR (126 MHz, $CDCl_3$) δ 187.9, 187.8, 146.1, 145.9, 141.2, 132.8, 68.6, 37.1, 29.7, 16.1, 12.0 ppm. IR (neat, cm^{-1}): 29583, 1647, 1439, 1267, 1119, 833. HRMS (EI+) *calcd for* $C_{13}H_{16}O_3$ [M^+] 220.1099, *found* 220.1106.

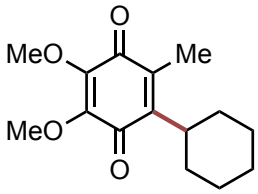

3,4-Dimethoxy-6-methyl-[1,1'-bi(cyclohexane)]-3,6-diene-2,5-dione (4.7.2): Following General Procedure III using 2,3-dimethoxy-5-methyl-*p*-benzoquinone (Coenzyme Q_0) (91.1 mg, 0.5 mmol, 1.0 equiv) and diethyl 4-cyclohexyl-2,6-dimethyl-1,4-dihydropyridine-3,5-dicarboxylate (335.4 mg, 1.0 mmol, 2.0 equiv). The product was isolated as an orange solid (84.3 mg, 64% yield). mp = 59-63 ºC. ^{1}H NMR (500 MHz, $CDCl_3$) δ 3.98 (s, 3H), 3.97 (s, 3H), 2.81 – 2.64 (m, 1H), 2.05 (s, 3H), 1.99 – 1.86 (m, 2H), 1.86 – 1.78 (m, 2H), 1.77 – 1.68 (m, 1H), 1.58 – 1.46 (m, 2H), 1.40 – 1.21 (m, 3H) ppm. ^{13}C NMR (126 MHz, $CDCl_3$) δ 185.1, 184.5, 146.1, 144.5, 143.7, 138.8, 61.2,

61.2, 40.1, 30.1, 27.1, 26.0, 12.0 ppm. IR (neat, cm^{-1}): 2934, 2913, 1659, 1647, 1635, 1599, 1193, 1074, 976. HRMS (EI+) *calcd for* $C_{15}H_{20}O_4$ [M^+] 264.1362, *found* 264.1354.

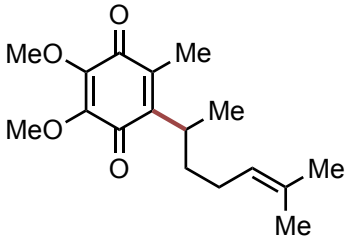

2,3-Dimethoxy-5-methyl-6-(6-methylhept-5-en-2-yl)cyclohexa-2,5-diene-1,4-dione (4.7.2): Following General Procedure III using 2,3-dimethoxy-5-methyl-*p*-benzoquinone (Coenzyme Q_0) (91.1 mg, 0.5 mmol, 1.0 equiv) and diethyl 2,6-dimethyl-4-(6-methylhept-5-en-2-yl)-1,4-dihydropyridine-3,5-dicarboxylate (363.5 mg, 1.0 mmol, 2.0 equiv). The product was isolated as a red oil (81.5 mg, 56% yield). ^{1}H NMR (500 MHz, $CDCl_3$) δ 5.03 (t, *J* = 7.0 Hz, 1H), 3.99 (s, 3H), 3.97 (s, 3H), 2.99 – 2.87 (m, 1H), 2.01 (s, 3H), 1.95 – 1.81 (m, 3H), 1.72 – 1.66 (m, 1H), 1.65 (s, 3H), 1.52 (s, 3H), 1.23 (d, *J* = 7.1 Hz, 3H) ppm. ^{13}C NMR (126 MHz, $CDCl_3$) δ 184.9, 184.3, 146.3, 144.6, 143.7, 139.2, 132.1, 124.5, 61.2 (2C), 35.1, 34.2, 26.9, 25.8, 19.1, 17.8, 11.9 ppm. IR (neat, cm^{-1}): 2930, 2857, 1646, 1604, 1115, 1066, 747. HRMS (EI+) *calcd for* $C_{17}H_{24}O_4$ [M^+] 292.1675, *found* 292.1693.

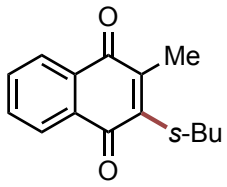

2-(*sec*-Butyl)-3-methylnaphthalene-1,4-dione (4.7.4): Following General Procedure II using 2-chloro-4-(methylsulfonyl)pyrimidine (96.0 mg, 0.5 mmol, 1.0 equiv), diethyl 4-(*sec*-butyl)-2,6-dimethyl-1,4-dihydropyridine-3,5-dicarboxylate (170.1 mg, 0.55 mmol, 1.1 equiv), $Na_2S_2O_8$ (142.8 mg, 0.60 mmol, 1.2 equiv) and TFA (85.5 mg, 0.75 mmol, 1.5 equiv) in CH_3CN/H_2O (5.0 mL, 1:1 v/v, 0.1 M). The product was isolated as a clear oil (120.0 mg, 70% yield). ^{1}H NMR (500 MHz, $CDCl_3$) δ 8.12 – 7.96 (m, 2H), 7.71 – 7.60 (m, 2H), 3.02 (m, 1H), 2.21 (s, 3H), 1.89 (dq, *J* = 15.4,

7.6 Hz, 1H), 1.75 (dq, *J* = 14.6, 7.3 Hz, 1H), 1.33 (d, *J* = 7.1 Hz, 3H), 0.87 (t, *J* = 7.5 Hz, 3H) ppm. ^{13}C NMR (126 MHz, $CDCl_3$) δ 185.7, 185.1, 150.7, 143.8, 133.5, 133.2, 132.9, 132.0, 126.3, 126.2, 37.0, 28.1, 18.8, 13.1, 12.8 ppm. IR (neat, cm^{-1}): 2963, 2932, 1657, 1289, 717. HRMS (EI+) *calcd for* $C_{15}H_{16}O_2$ [M^+] 228.1150, *found* 228.1161.

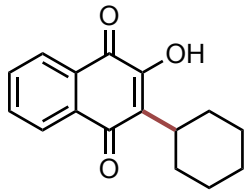

2-Cyclohexyl-3-hydroxynaphthalene-1,4-dione (Parvaquone, 4.7.5): Following General Procedure III using 2-hydroxy-1,4-naphthoquinone (Lawsone) (87.1 mg, 0.5 mmol, 1.0 equiv) and diethyl 4-cyclohexyl-2,6-dimethyl-1,4-dihydropyridine-3,5-dicarboxylate (335.4 mg, 1.0 mmol, 2.0 equiv). The product was isolated as a yellow solid (69.8 mg, 54% yield). mp = 128-130 ºC. ^{1}H NMR (500 MHz, $CDCl_3$) δ 8.11 (d, *J* = 7.7 Hz, 1H), 8.06 (d, *J* = 7.0 Hz, 1H), 7.78 – 7.71 (m, 1H), 7.70 – 7.63 (m, 1H), 7.41 (s, 1H), 3.08 (tt, *J* = 12.1, 3.3 Hz, 1H), 2.04 – 1.91 (m, 2H), 1.86 – 1.77 (m, 2H), 1.77 – 1.70 (m, 1H), 1.66 – 1.58 (m, 2H), 1.44 – 1.22 (m, 3H) ppm. ^{13}C NMR (126 MHz, $CDCl_3$) δ 184.7, 182.1, 153.0, 135.0, 133.3, 132.8, 129.4, 128.0, 127.1, 126.0, 35.3, 29.4, 26.9, 26.1 ppm. Spectral data is consistent with previously reported values.[18]

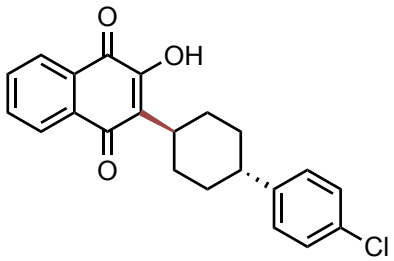

2-[4-(4-Chlorophenyl)cyclohexyl]-3-hydroxy-1,4-naphthalenedione (Atovaquone, 4.7.6): Following General Procedure III using 2-hydroxy-1,4-naphthoquinone (Lawsone) (64.4 mg, 0.37 mmol, 1.0 equiv) and diethyl 4-(*trans*-4-(4-chlorophenyl)cyclohexyl)-2,6-dimethyl-1,4-dihydropyridine-3,5-dicarboxylate (327.2 mg, 0.73 mmol, 2.0 equiv). The product was isolated as

a yellow solid (73.7 mg, 54% yield). HPLC analysis showed a 62:38 *cis/trans* ratio. Over the yellow solid (26.1 mg), conc H_2SO_4 (0.3 mL) was added and the reaction was stirred at rt until HPLC analysis showed complete isomerization to the *trans* isomer (30 min-1 h). At this point, H_2O (5.0 mL) was added over the reaction mixture, and the yellow solid was filtered off and washed several times with H_2O (5.0 mL x 3). The following spectral data are of the pure *trans* product. mp = 204-206 ºC. ^{1}H NMR (500 MHz, $CDCl_3$) δ 8.14 (d, *J* = 7.7 Hz, 1H), 8.08 (d, *J* = 7.6 Hz, 1H), 7.77 (t, *J* = 7.5 Hz, 1H), 7.69 (t, *J* = 7.6 Hz, 1H), 7.48 (s, 1H), 7.29 – 7.26 (m, 2H), 7.18 (d, *J* = 8.0 Hz, 2H), 3.20 – 3.12 (m, 1H), 2.68 – 2.55 (m, 1H), 2.27 – 2.12 (m, 2H), 2.00 – 1.94 (m, 2H), 1.81 – 1.74 (m, 2H), 1.66 – 1.52 (m, 2H) ppm. ^{13}C NMR (126 MHz, $CDCl_3$) δ 184.7, 181.9, 153.1, 146.2, 135.2, 133.3, 133.0, 131.6, 129.3, 128.6, 128.3, 127.4, 127.1, 126.2, 43.4, 34.6, 34.5, 29.3 ppm. Spectral data is consistent with previously reported values.[5]

Cyclic Voltammetry Measurements

Voltammetric measurement were recorded on a CH Instrument: Model 600E Series Electrochemical Analyzer using a standard three electrodes setup in dry, degassed MeCN (10.0 mL), with ferrocene as internal reference ($E^0_{1/2}$ = + 0.41 V vs SCE) and Bu_4NPF_6 as electrolyte (0.1 mmol). Cyclic voltammograms were recorded with a step potential of 0.002 V at a scan rate of 0.1 V/s. Voltammetric measurements were repeated at different scan rates to ensure the accuracy of the measurement.

Cyclic Voltammetry of Compound

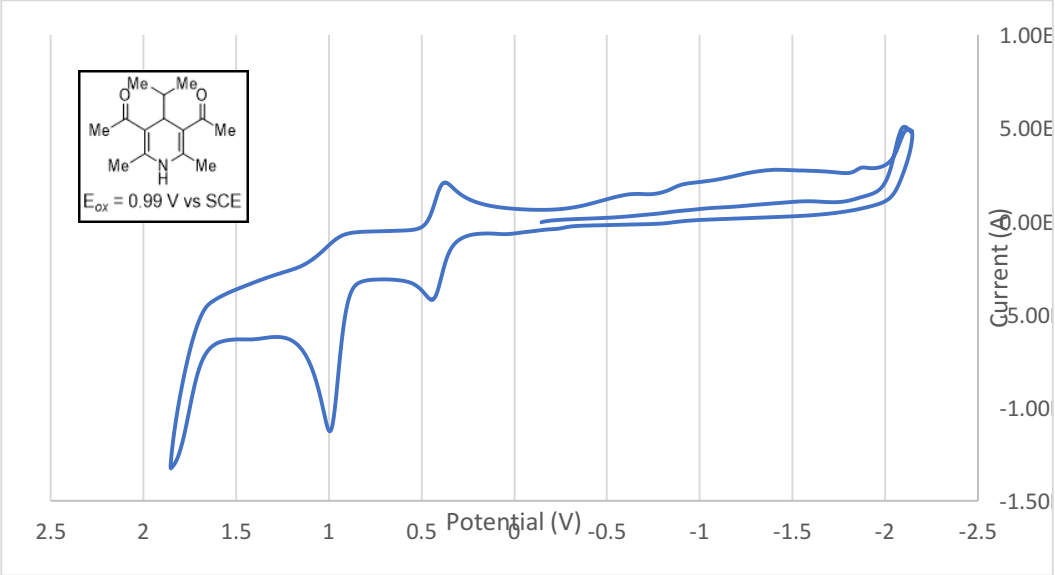

Cyclic Voltammetry of Compound

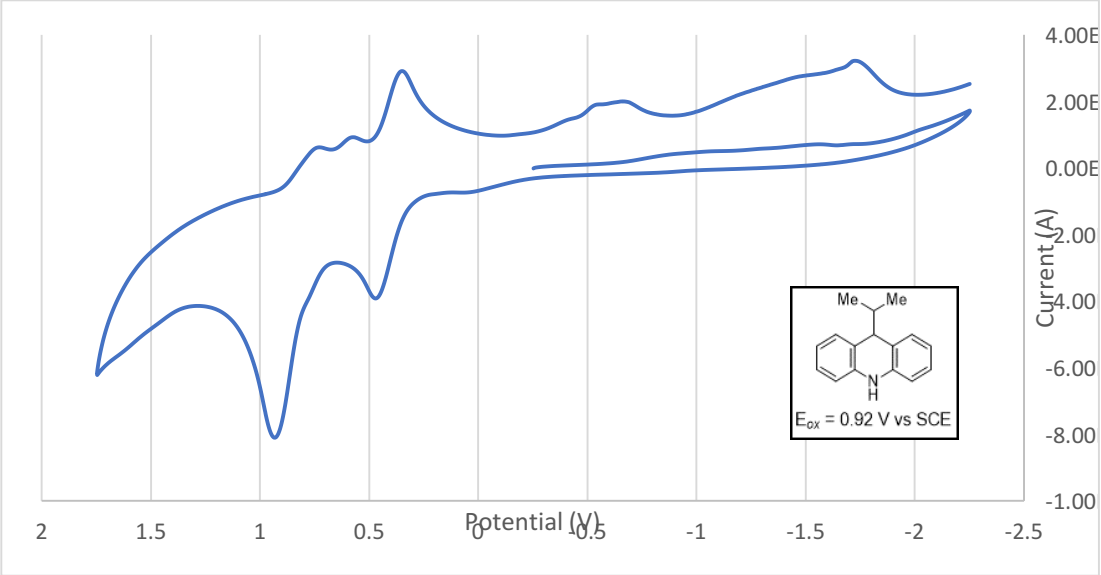

Cyclic Voltammetry of Compound

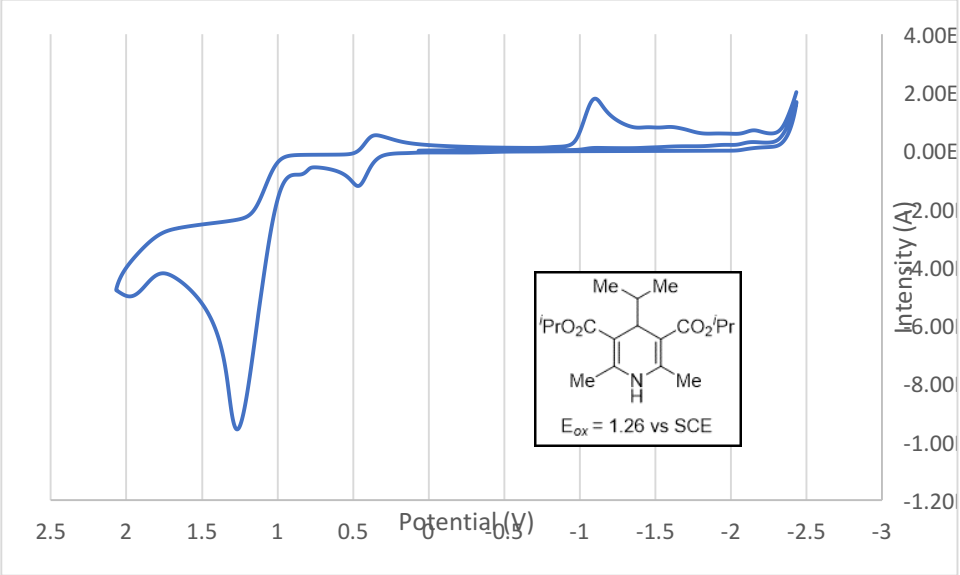

Cyclic Voltammetry of Compound

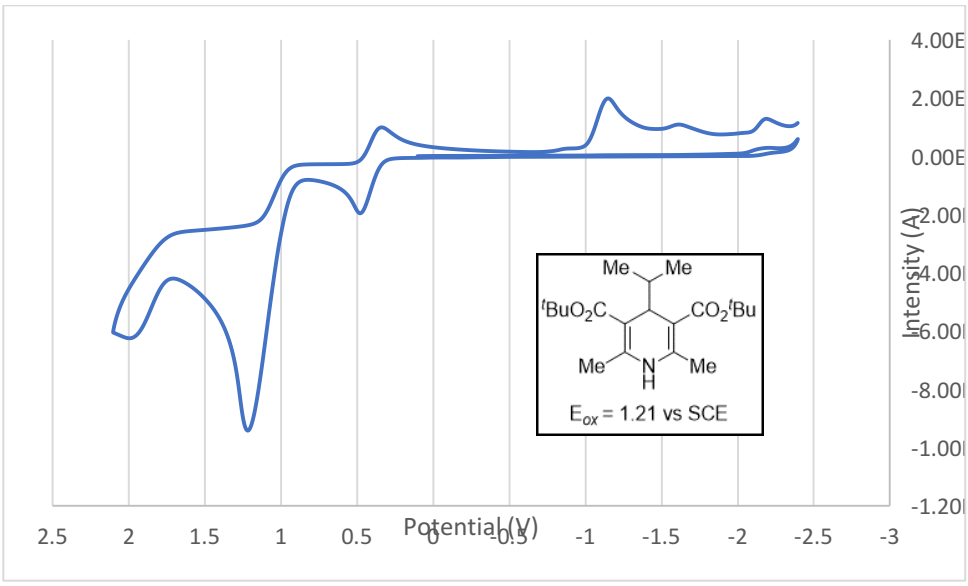

Cyclic Voltammetry of Compound

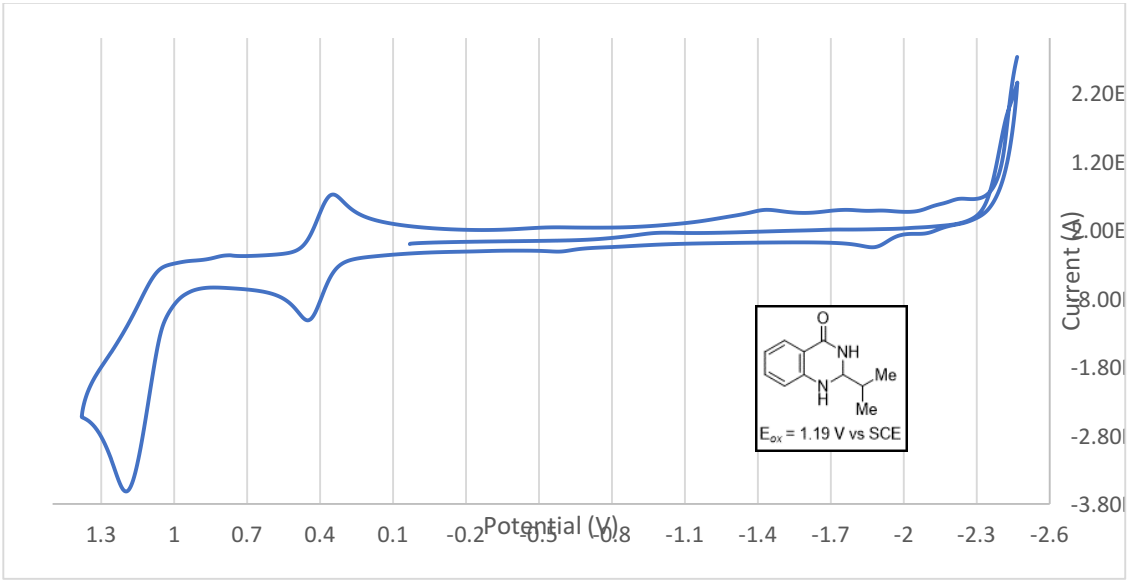

Cyclic Voltammetry of Compound

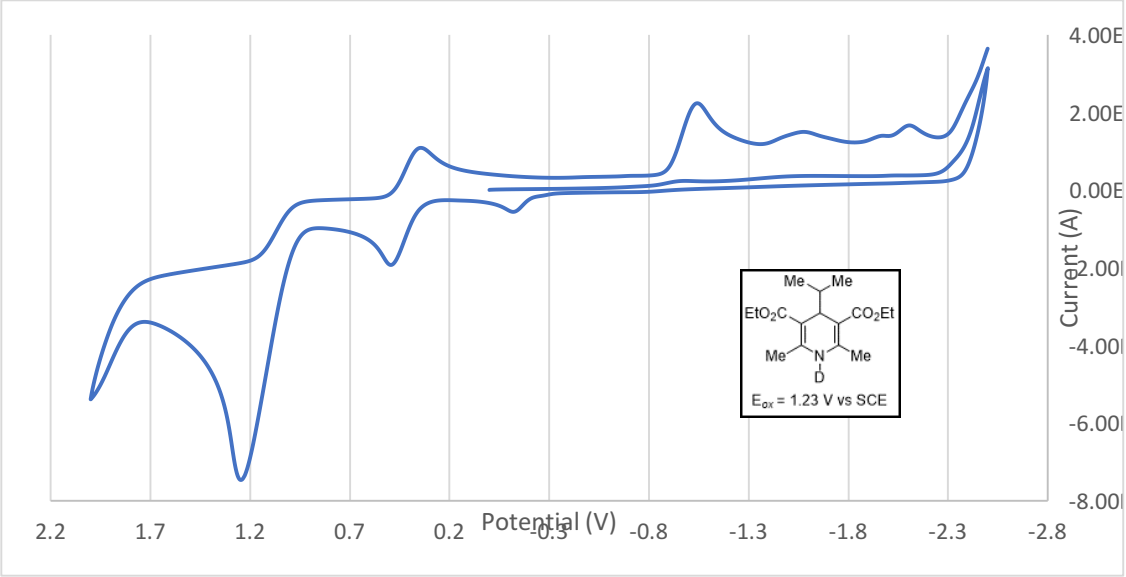
4.00E
2.00E
0.00E
-2.00
-4.00
-6.00
-8.00
Current (A)
2.2
1.7
1.2
0.7
0.2
-0.3
-0.8
-1.3
-1.8
-2.3
-2.8
Potential (V)
Me
Me
EtO2C
CO2Et
Me
N
Me
D
Eox = 1.23 V vs SCE

^{1}H and ^{13}C NMR Spectra

^{1}H NMR ($CDCl_3$, 500 MHz) of 2-isopropylquinazolin-4(3H)-one (**4.3.3**)

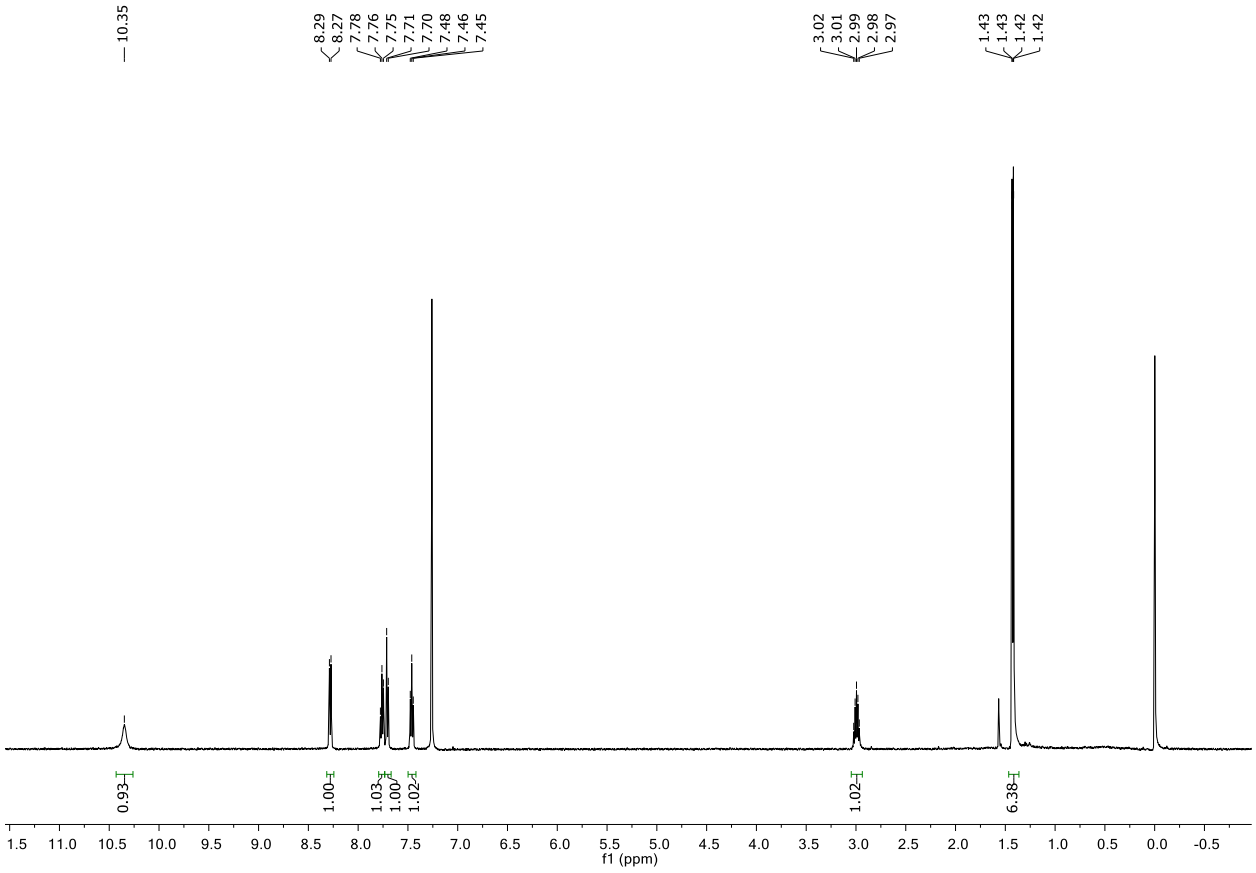

^{13}C NMR ($CDCl_3$, 126 MHz) of 2-isopropylquinazolin-4(3H)-one (**4.3.3**)

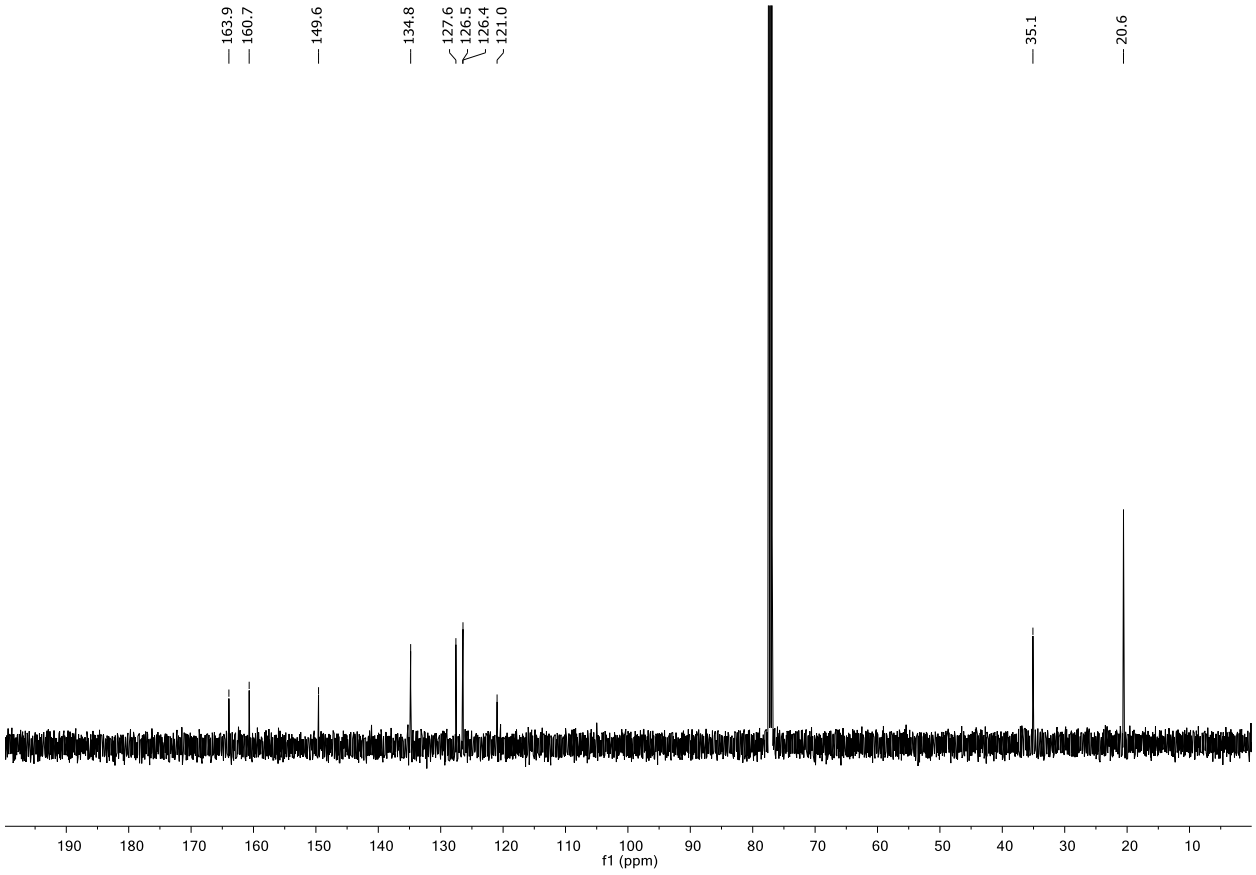

^{1}H NMR ($CDCl_3$, 500 MHz) of 2-(*sec*-butyl)quinazolin-4(3*H*)-one (**4.4.1**)

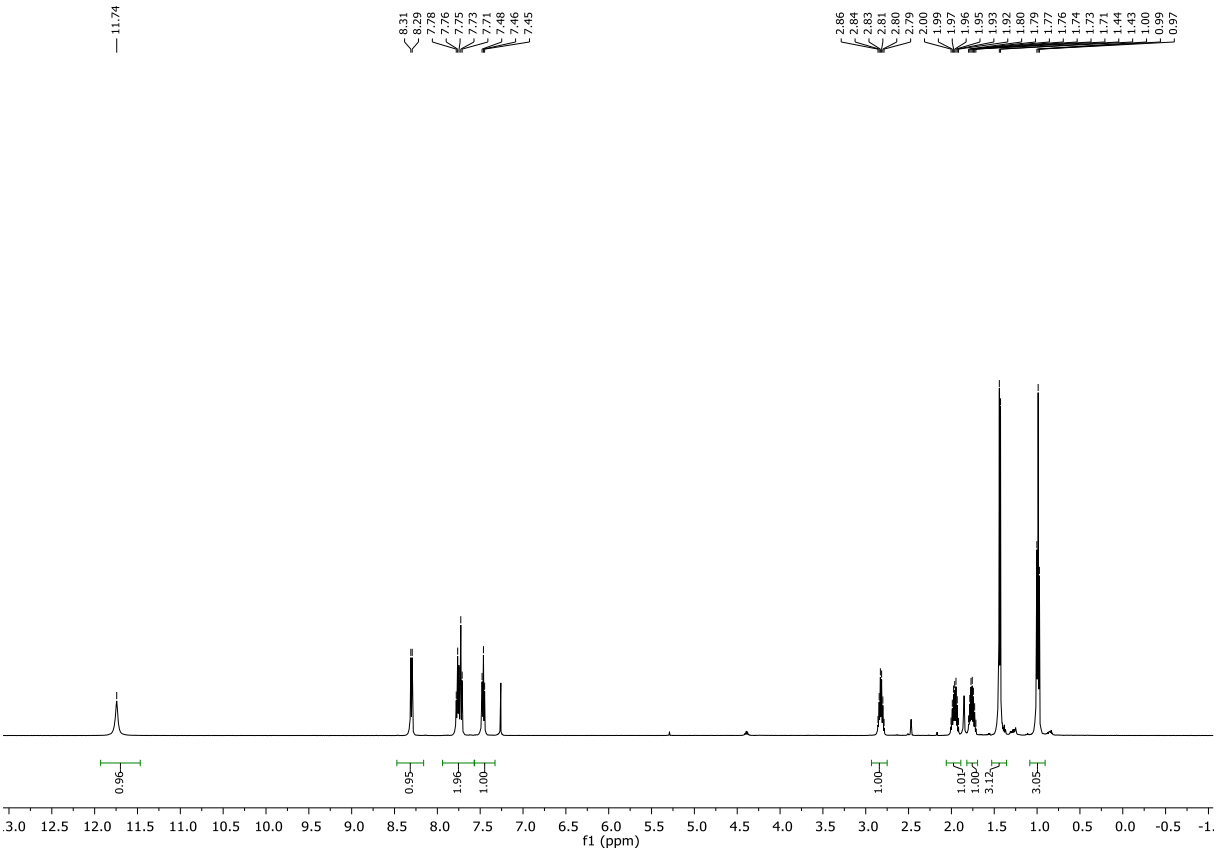

^{13}C NMR ($CDCl_3$, 126 MHz) of 2-(*sec*-butyl)quinazolin-4(3*H*)-one (**4.4.1**)

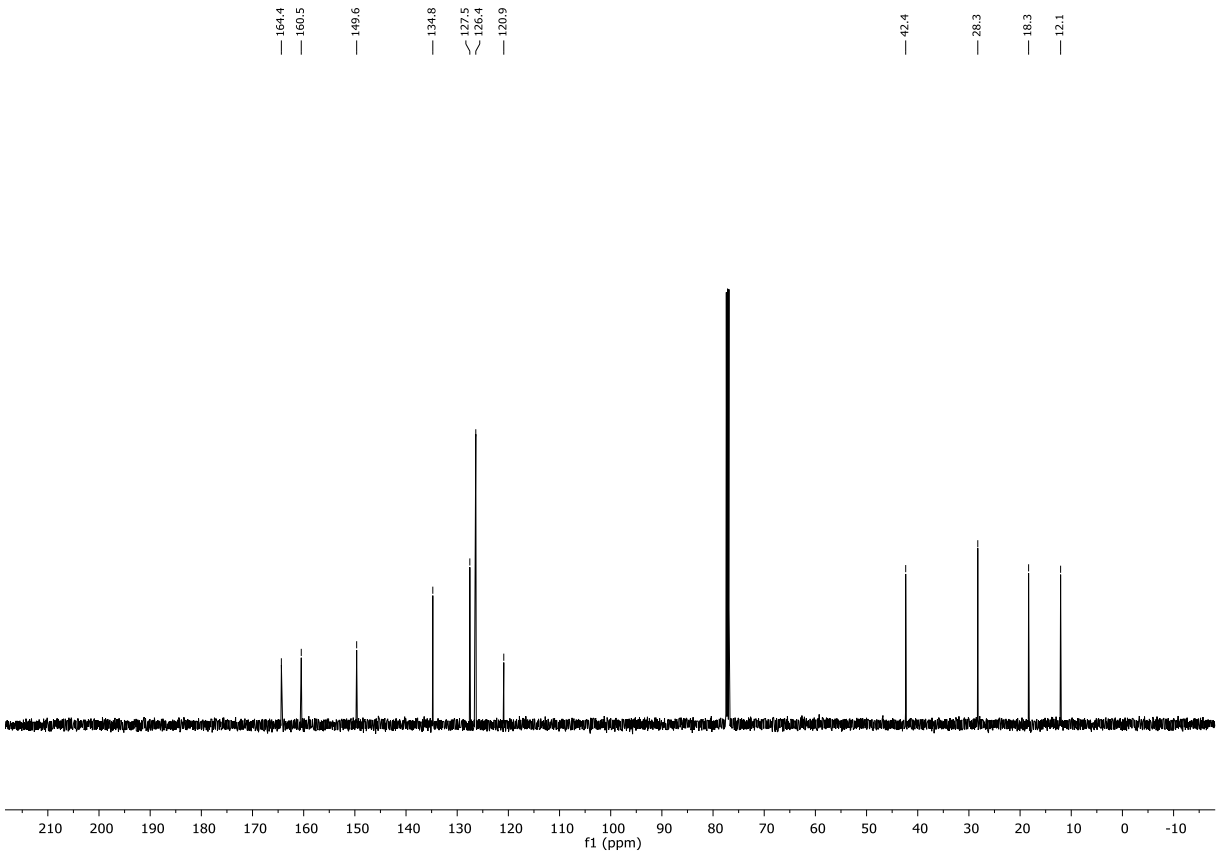

^{1}H NMR ($CDCl_3$, 500 MHz) of 2-(pentan-3-yl)quinazolin-4(3*H*)-one (**4.4.2**)

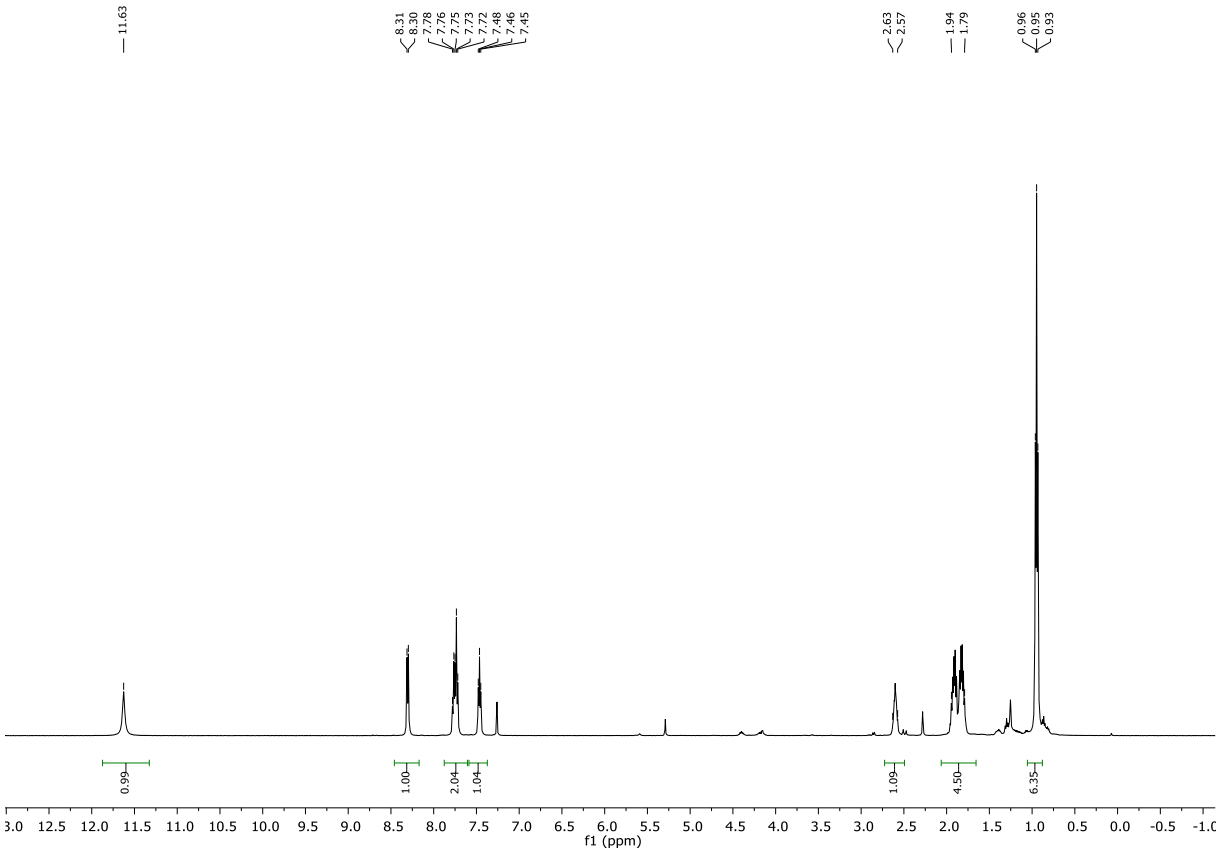

^{13}C NMR ($CDCl_3$, 126 MHz) of 2-(pentan-3-yl)quinazolin-4(3*H*)-one (**4.4.2**)

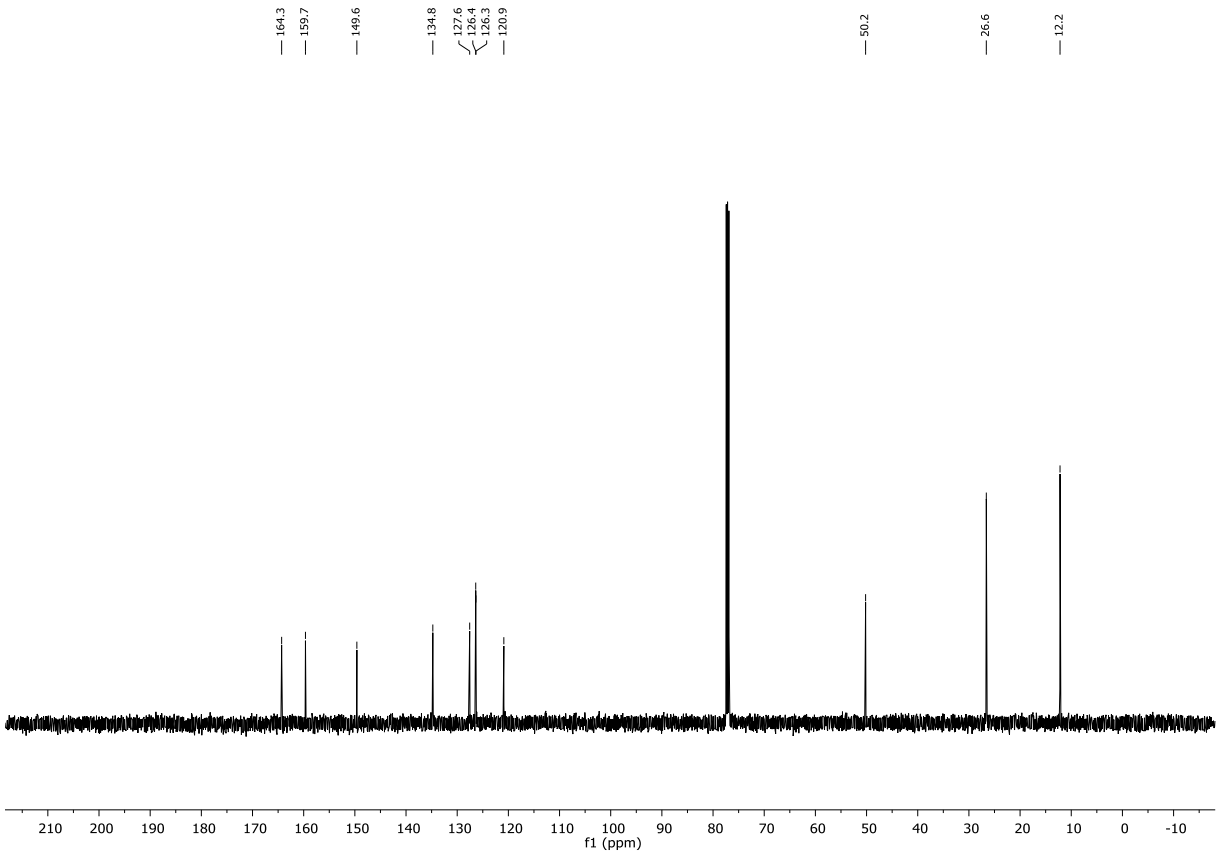

^{1}H NMR ($CDCl_3$, 500 MHz) of 2-(heptan-3-yl)quinazolin-4(3*H*)-one (**4.4.3**)

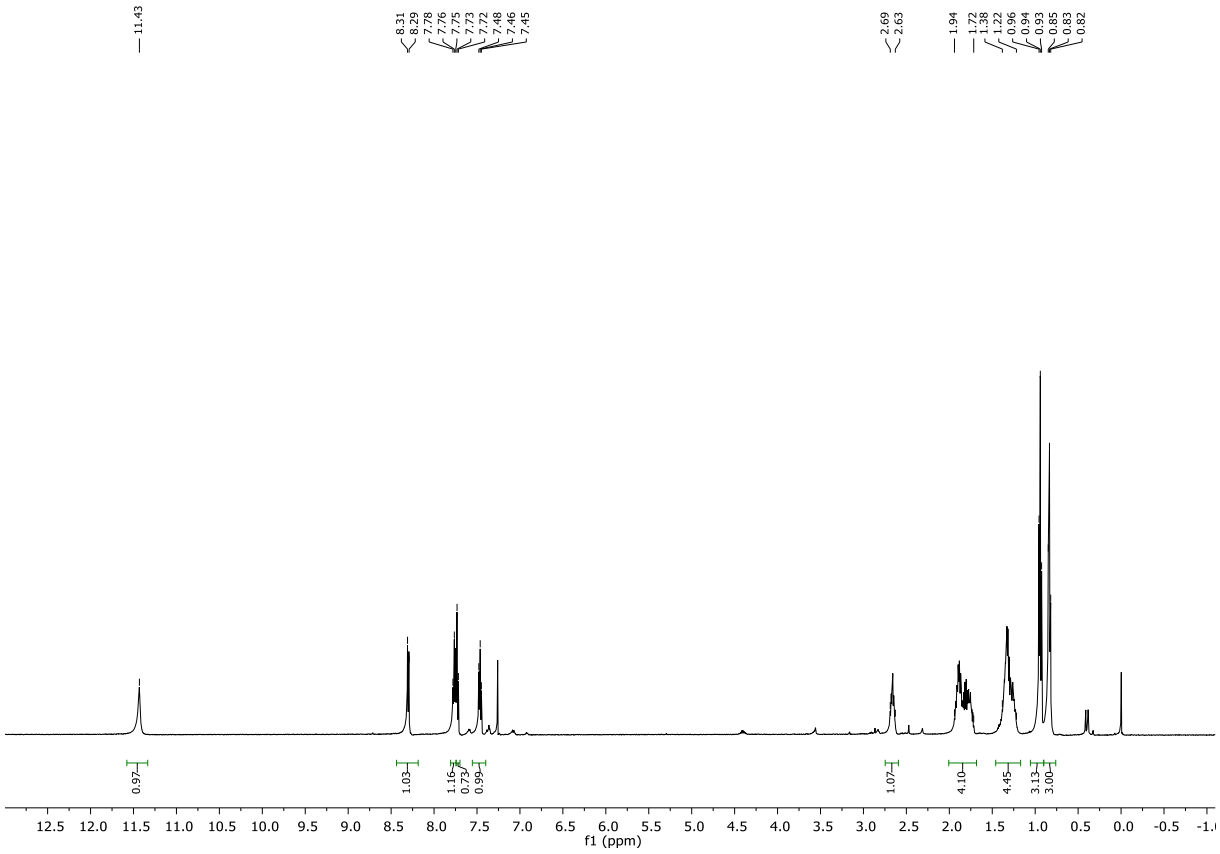

^{13}C NMR ($CDCl_3$, 126 MHz) of 2-(heptan-3-yl)quinazolin-4(3*H*)-one (**4.4.3**)

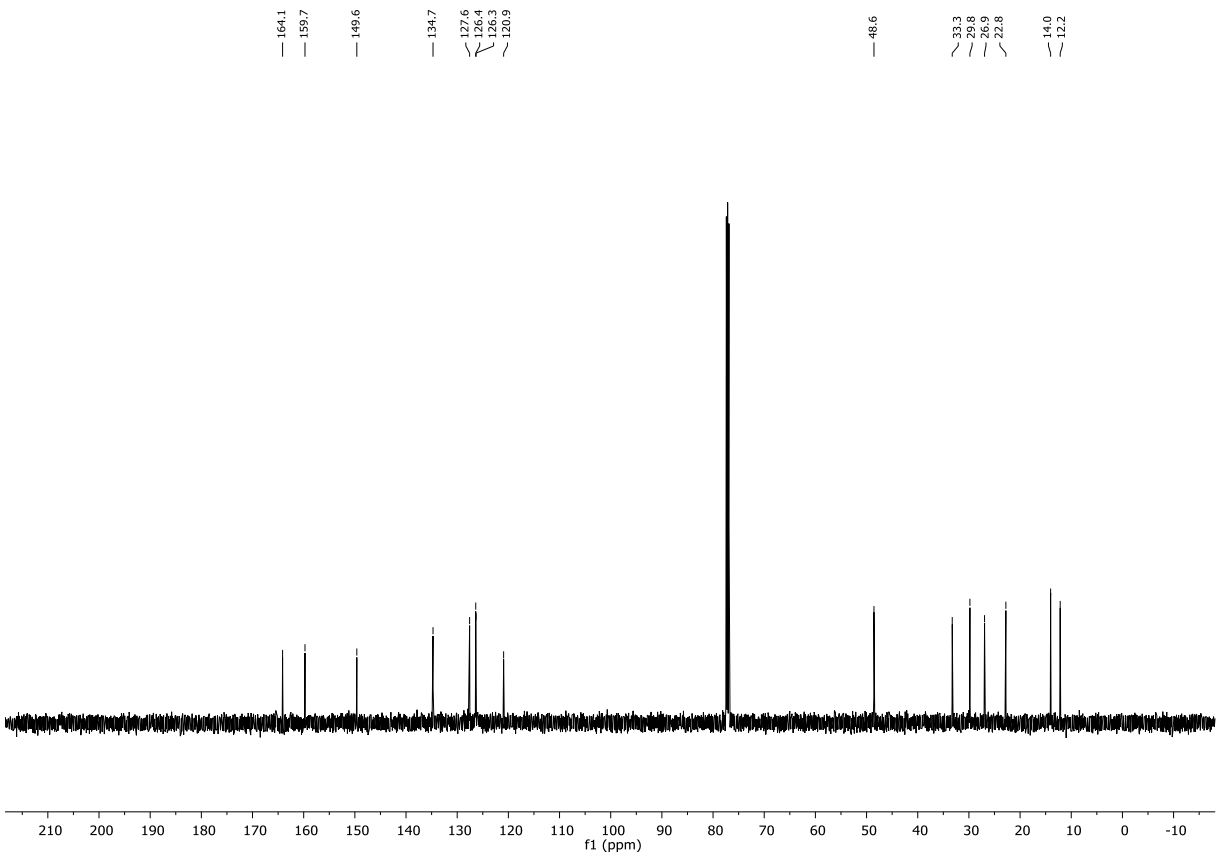

^{1}H NMR ($CDCl_3$, 500 MHz) of 2-(1-(4-isopropylphenyl)propan-2-yl)quinazolin-4(3*H*)-one (**4.4.4**)

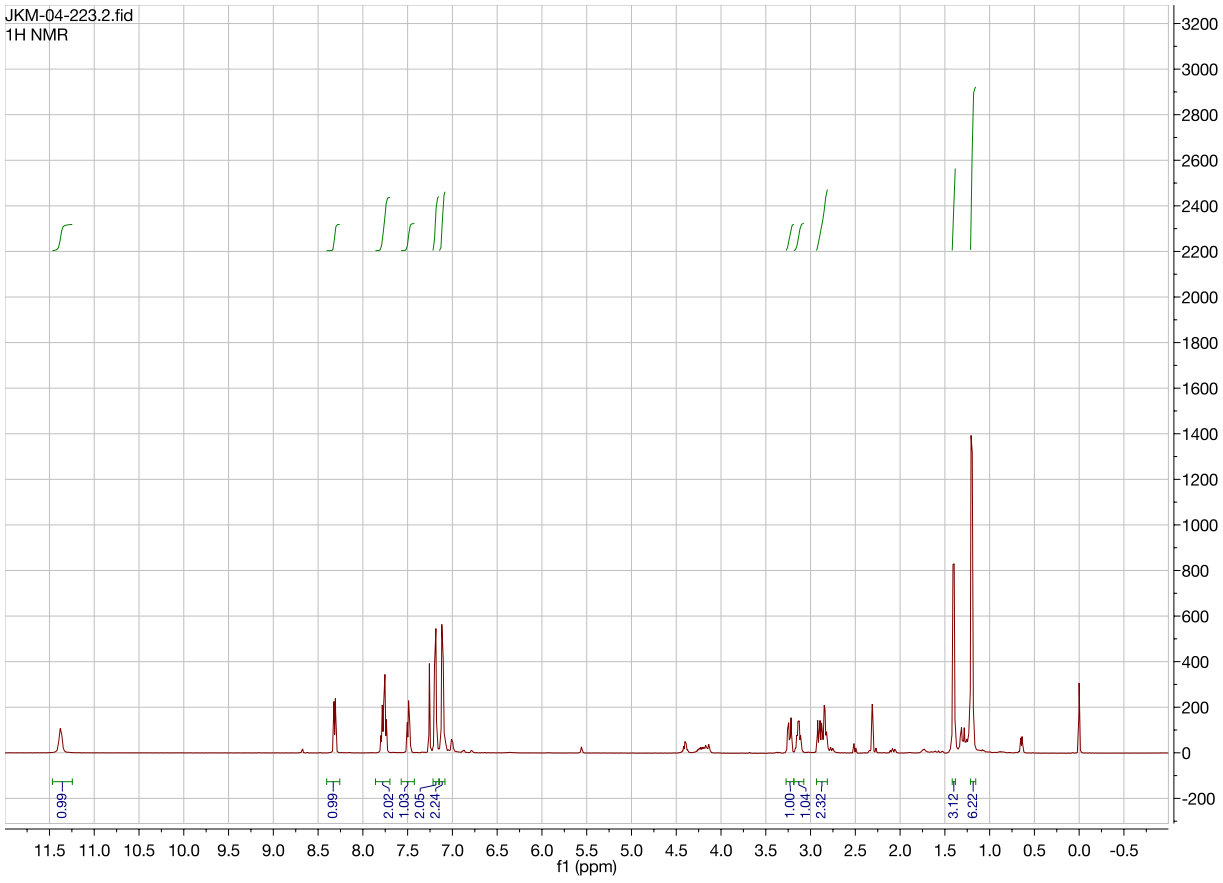

^{13}C NMR ($CDCl_3$, 126 MHz) of 2-(1-(4-isopropylphenyl)propan-2-yl)quinazolin-4(3*H*)-one (**4.4.4**)

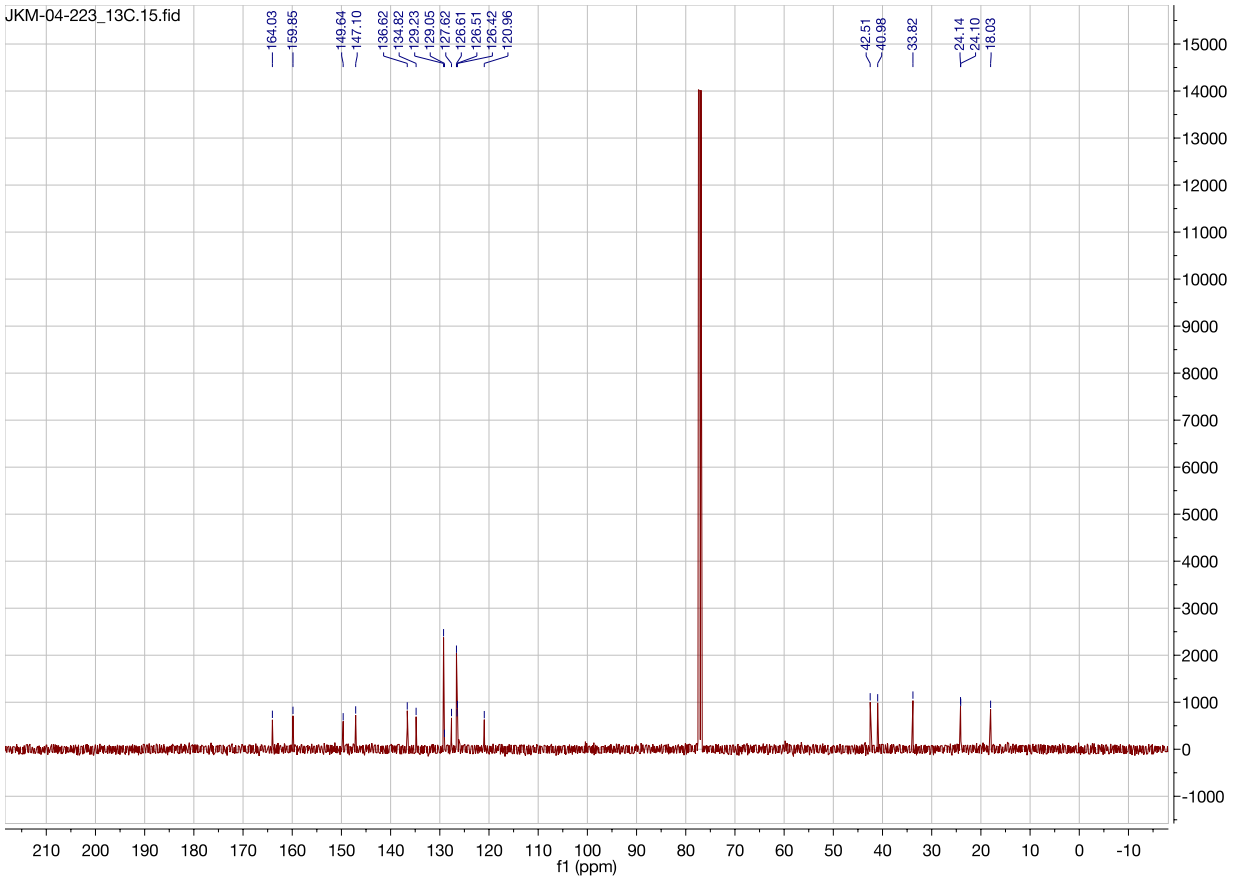

^{1}H NMR ($CDCl_3$, 500 MHz) of 2-(6-methylhept-5-en-2-yl)quinazolin-4(3*H*)-one (**4.4.5**)

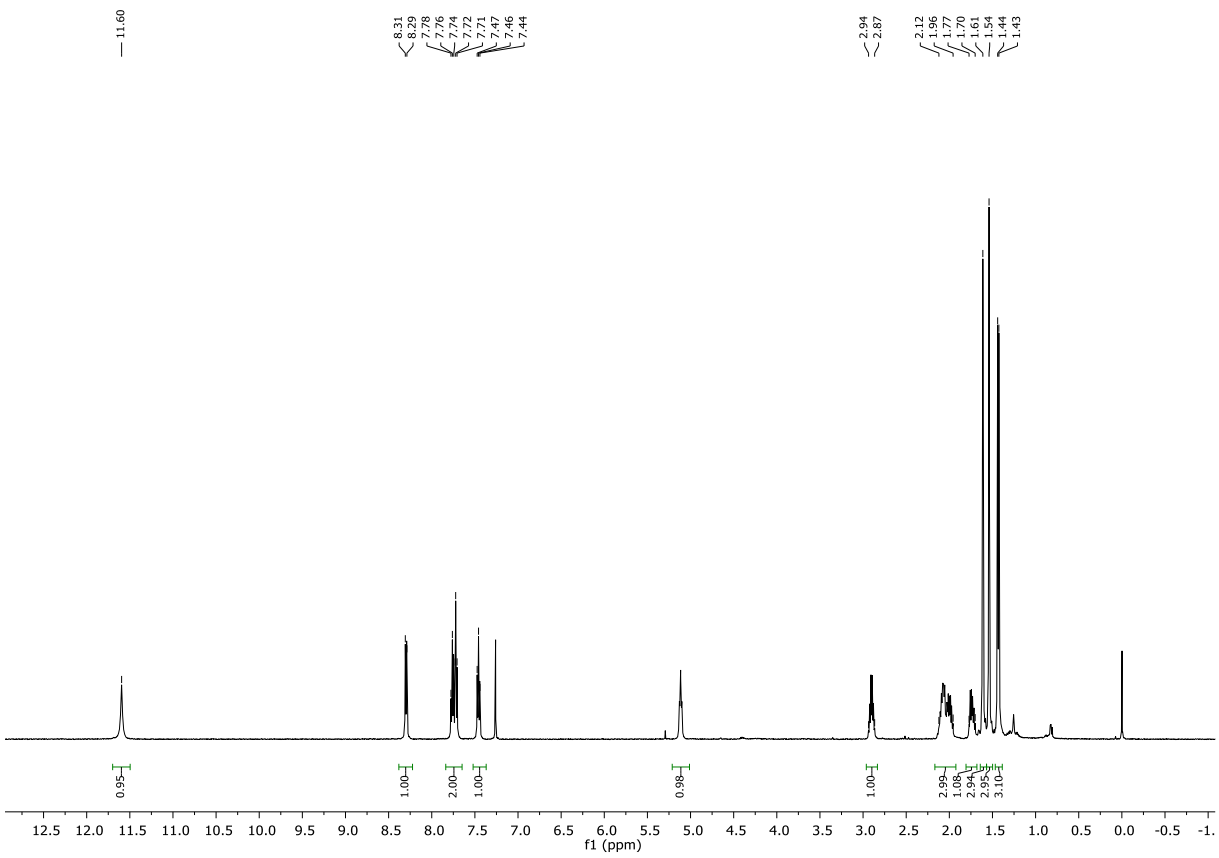

^{13}C NMR ($CDCl_3$, 126 MHz) of 2-(6-methylhept-5-en-2-yl)quinazolin-4(3*H*)-one (**4.4.5**)

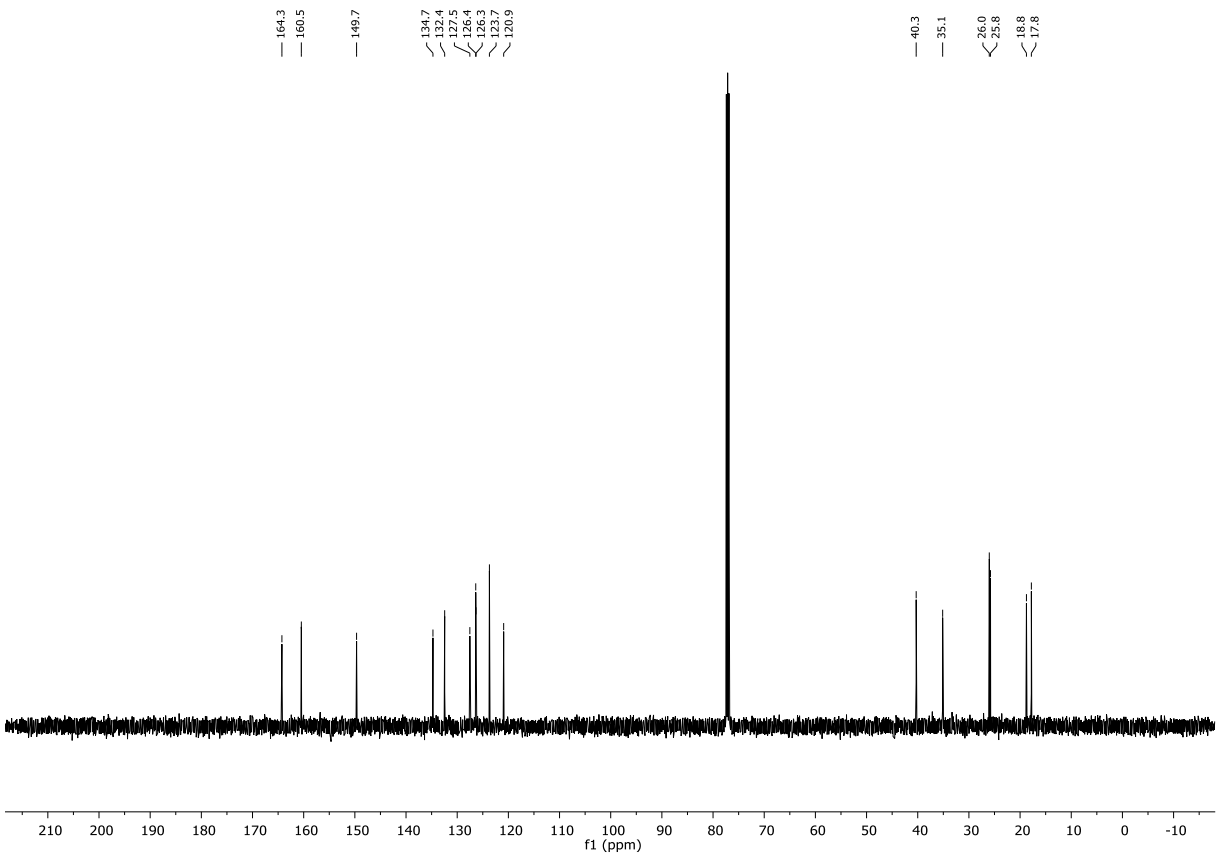

^{1}H NMR ($CDCl_3$, 500 MHz) of 2-cyclohexylquinazolin-4(3*H*)-one (**4.4.6**)

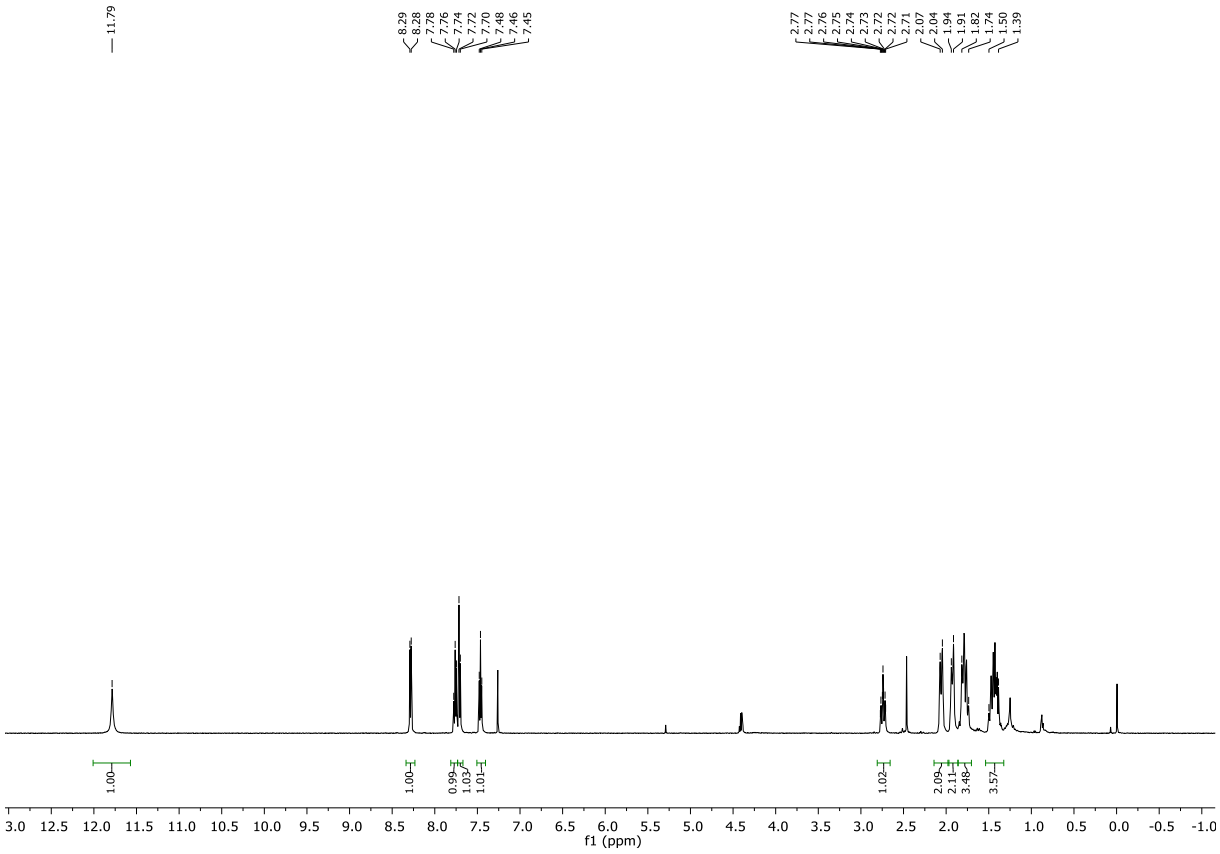

^{13}C NMR ($CDCl_3$, 126 MHz) of 2-cyclohexylquinazolin-4(3*H*)-one (**4.4.6**)

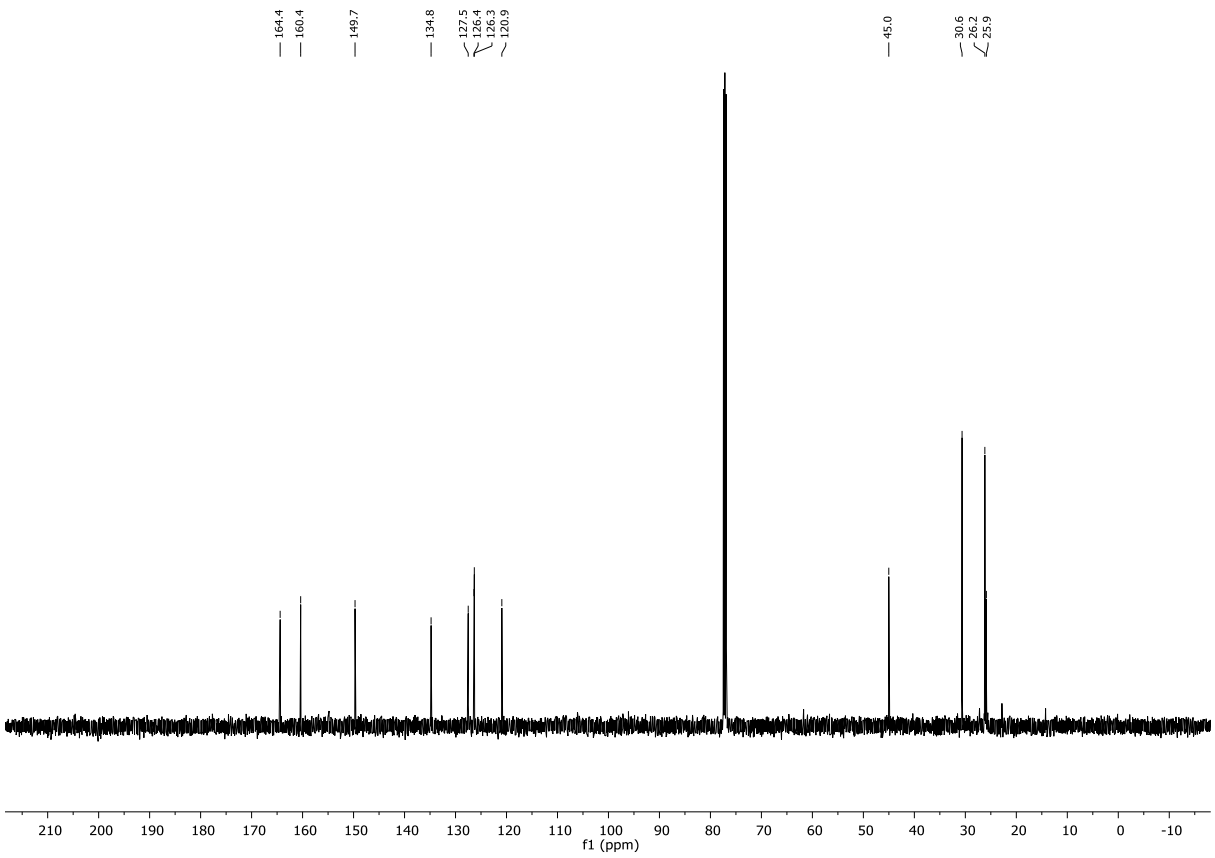

^{1}H NMR ($CDCl_3$, 500 MHz) of 2-(cyclohex-3-en-1-yl)quinazolin-4(3*H*)-one (**4.4.7**)

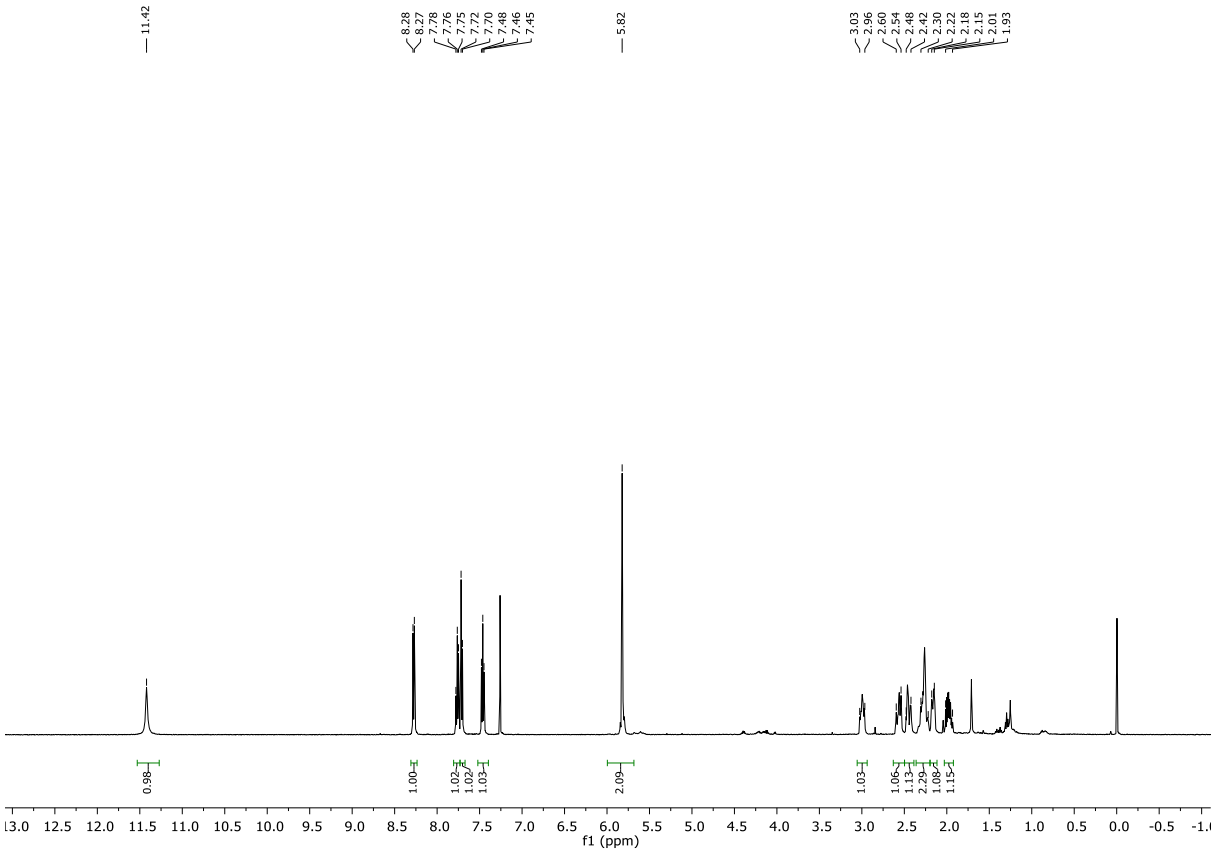

^{13}C NMR ($CDCl_3$, 126 MHz) of 2-(cyclohex-3-en-1-yl)quinazolin-4(3*H*)-one (**4.4.7**)

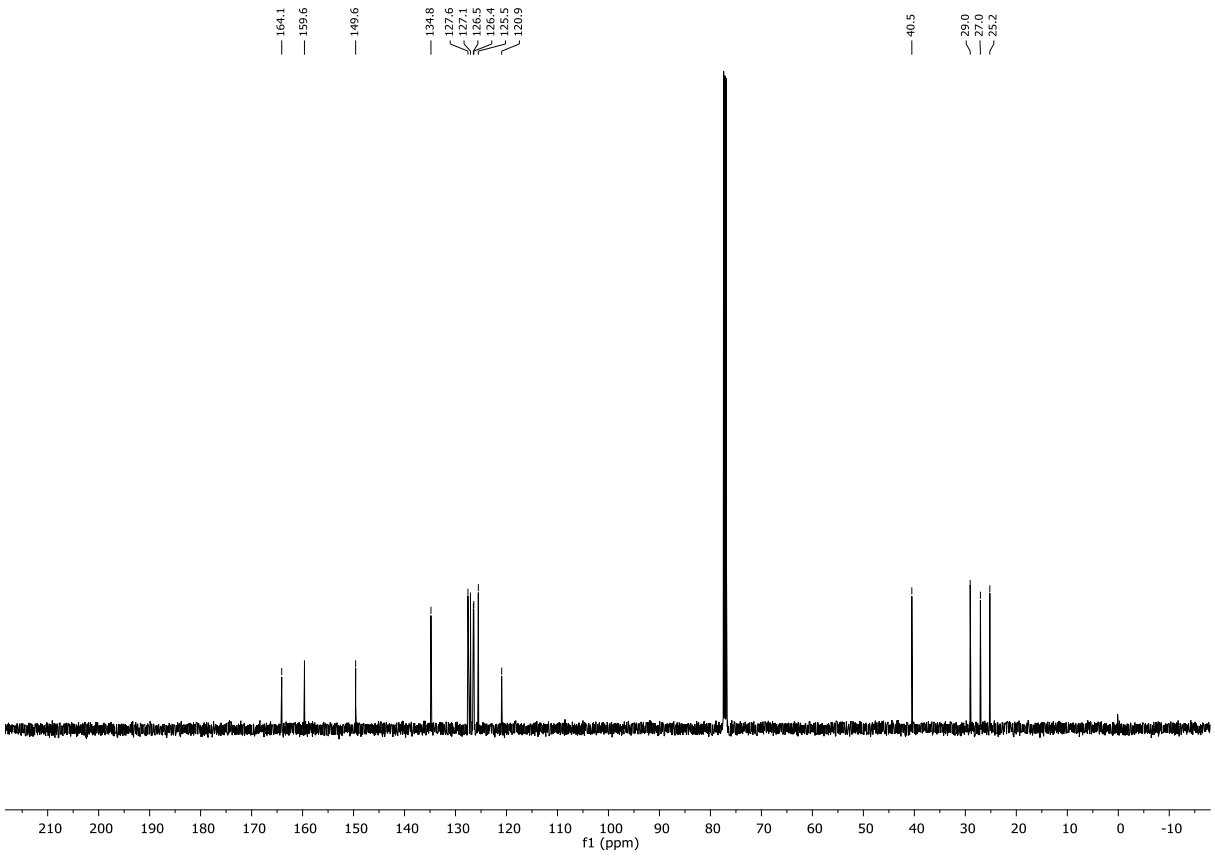

^{1}H NMR ($CDCl_3$, 500 MHz) of 2-(bicyclo[2.2.1]heptan-2-yl)quinazolin-4(3*H*)-one (**4.4.8**)

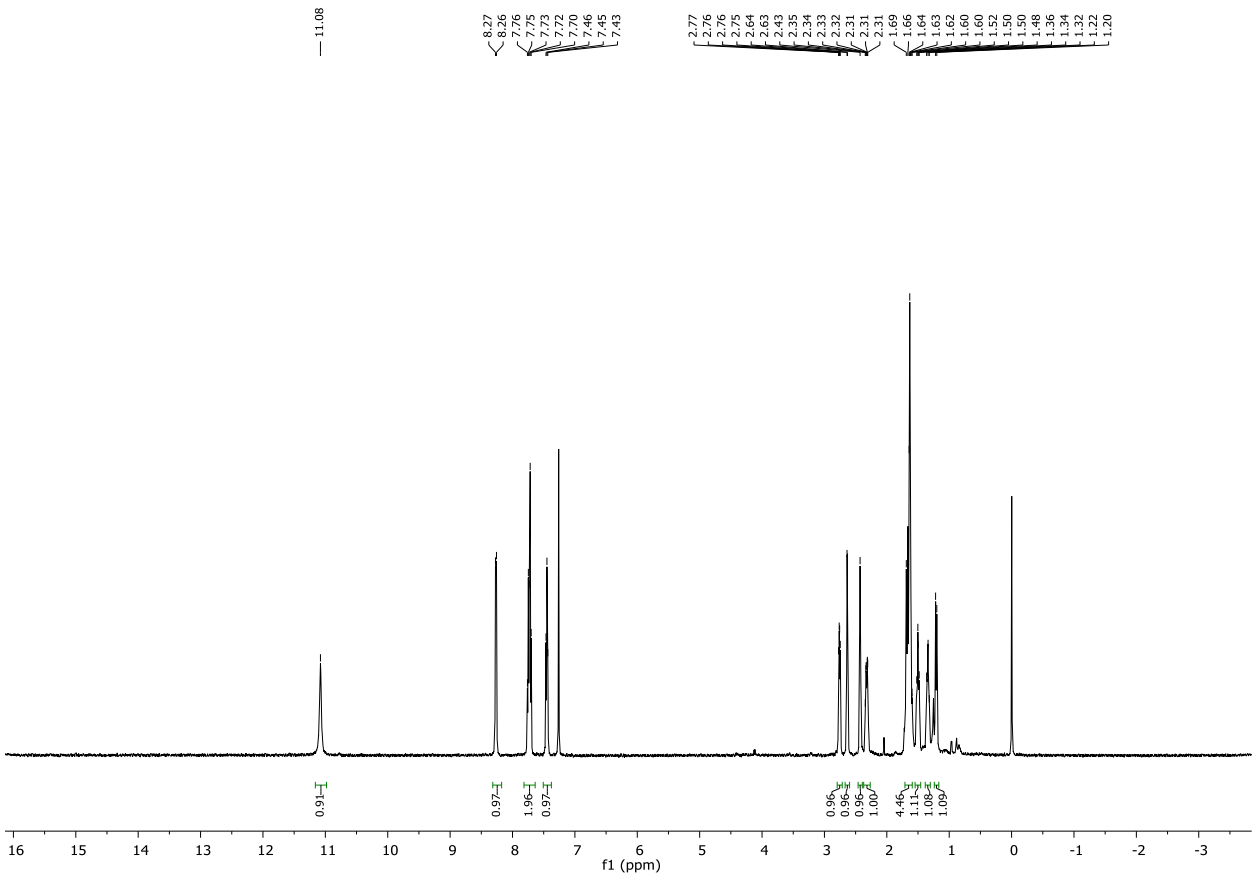

^{13}C NMR ($CDCl_3$, 126 MHz) of 2-(bicyclo[2.2.1]heptan-2-yl)quinazolin-4(3*H*)-one (**4.4.8**)

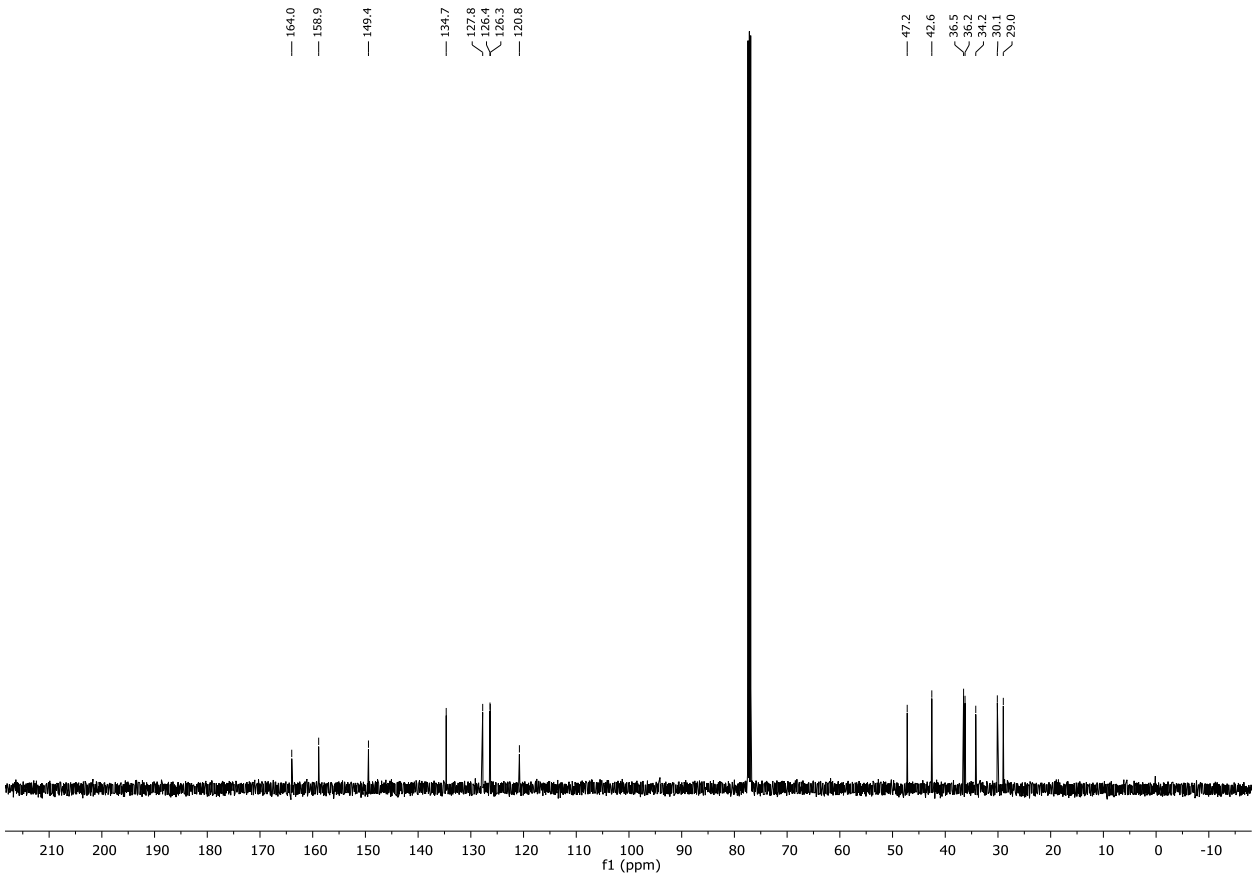

^{1}H NMR ($CDCl_3$, 500 MHz) of 2-(tetrahydro-2*H*-pyran-4-yl)quinazolin-4(3*H*)-one (**4.4.9**)

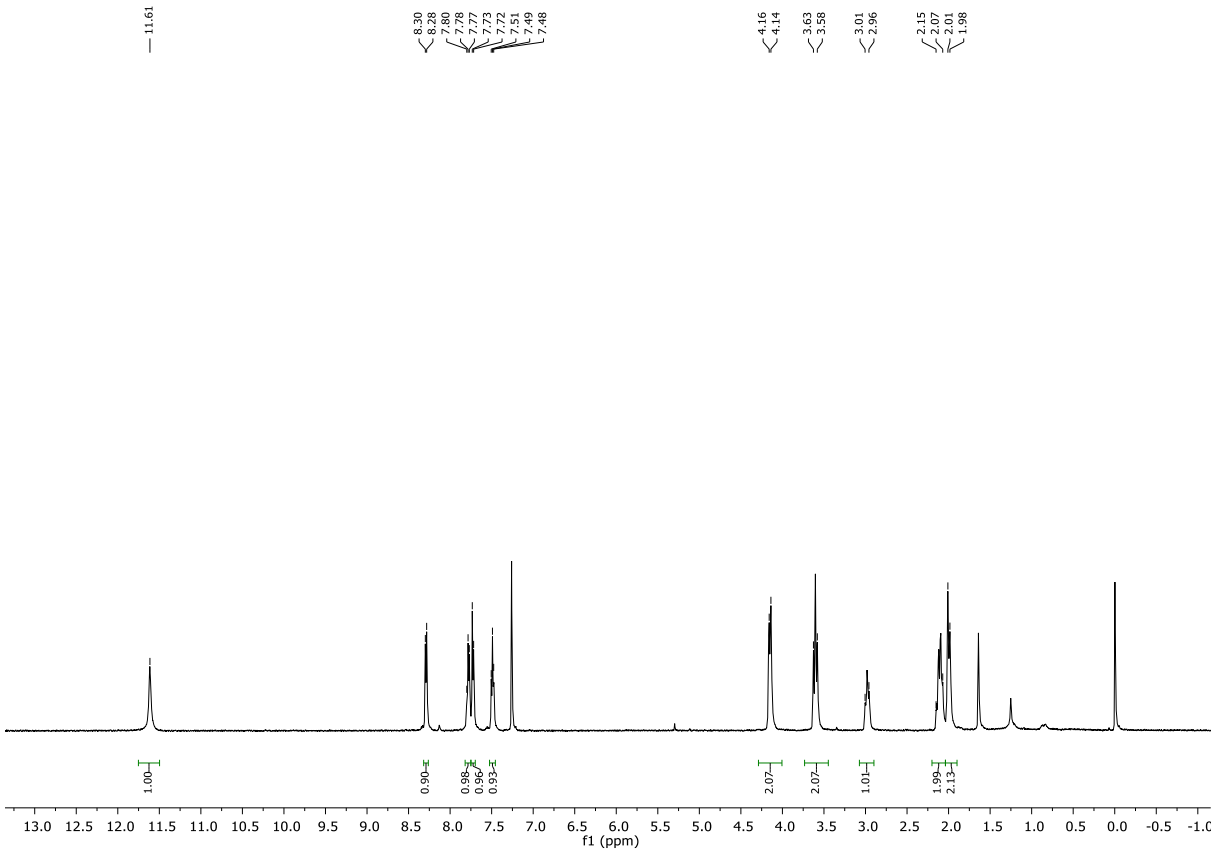

^{13}C NMR ($CDCl_3$, 126 MHz) of 2-(tetrahydro-2*H*-pyran-4-yl)quinazolin-4(3*H*)-one (**4.4.9**)

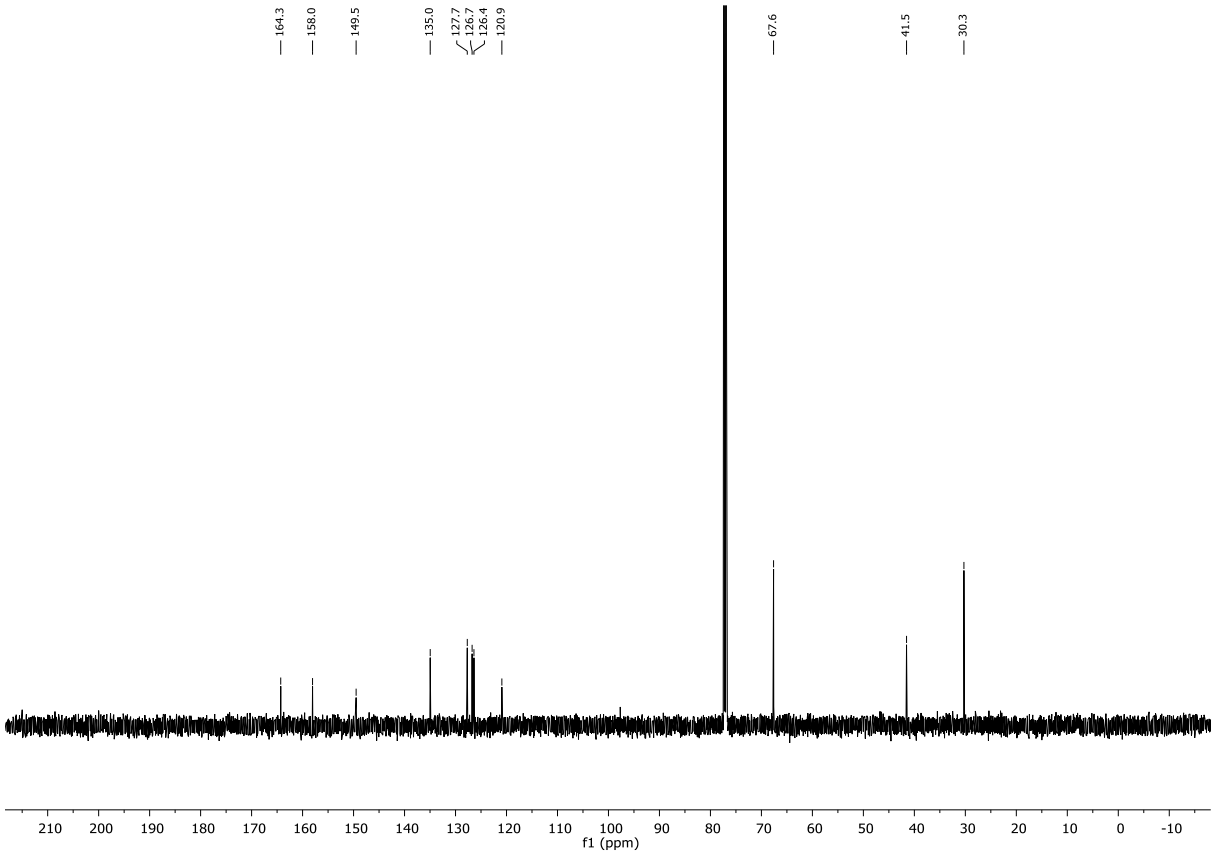

^{1}H NMR ($CDCl_3$, 500 MHz) of 2-(tetahydro-2*H*-pyran-2-yl)quinazolin-4(3*H*)-one (**4.4.10**)

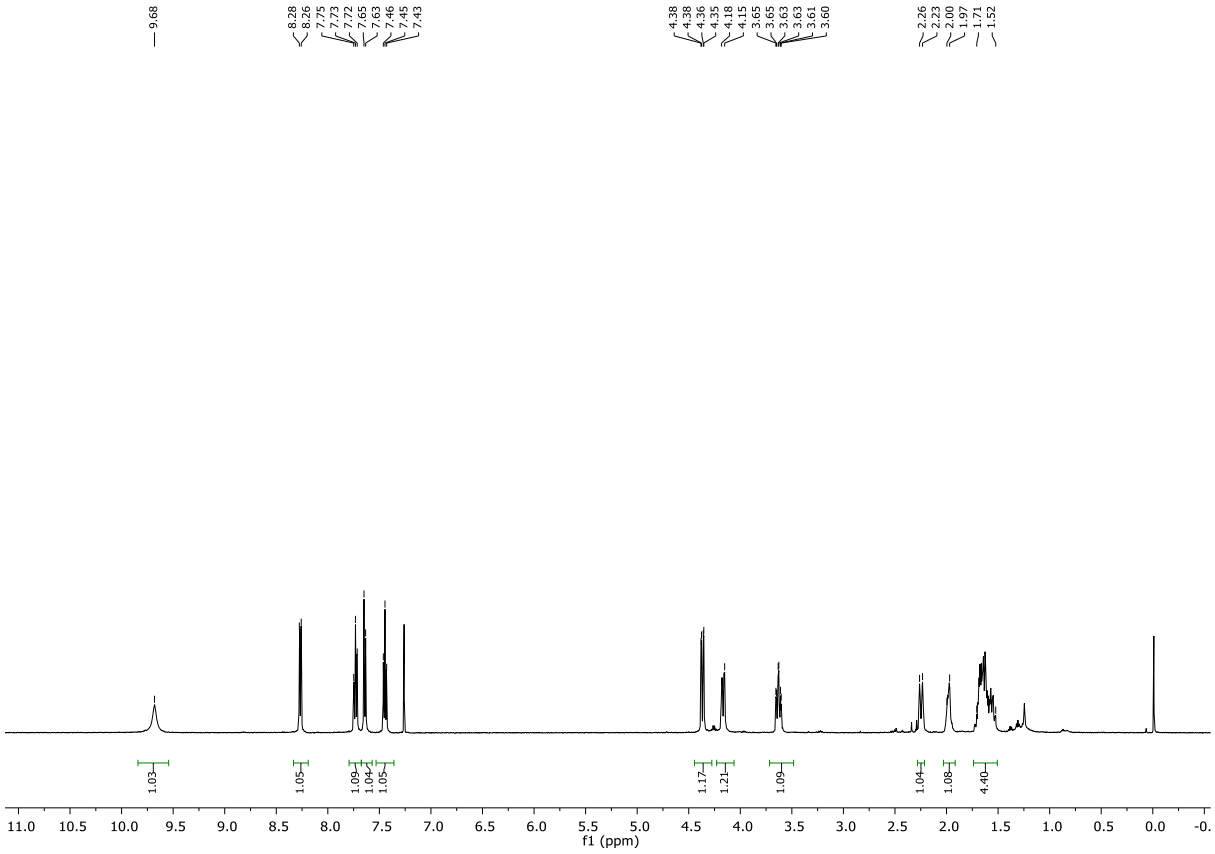

^{13}C NMR ($CDCl_3$, 126 MHz) of 2-(tetahydro-2*H*-pyran-2-yl)quinazolin-4(3*H*)-one (**4.4.10**)

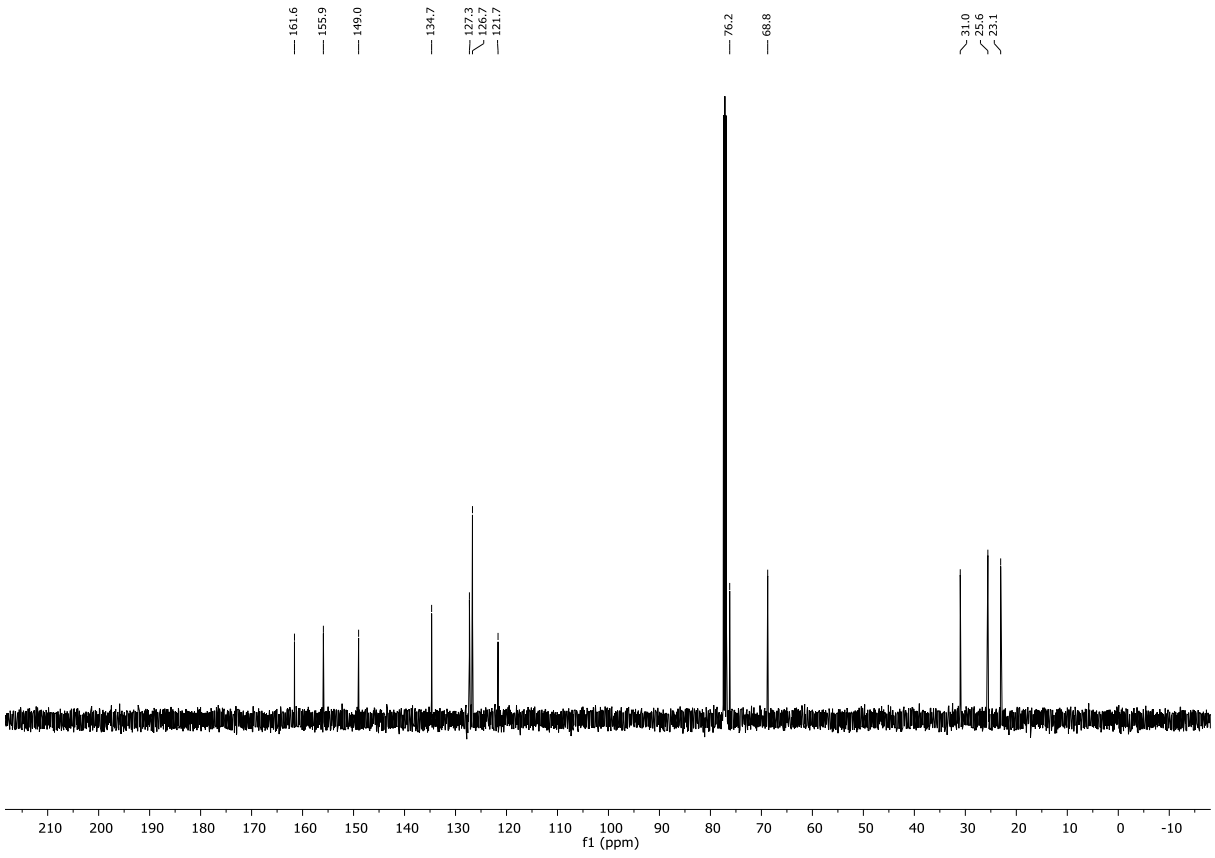

^{1}H NMR ($CDCl_3$, 500 MHz) of 2-((benzyloxy)methyl)quinazolin-4(3*H*)-one (**4.4.11**)

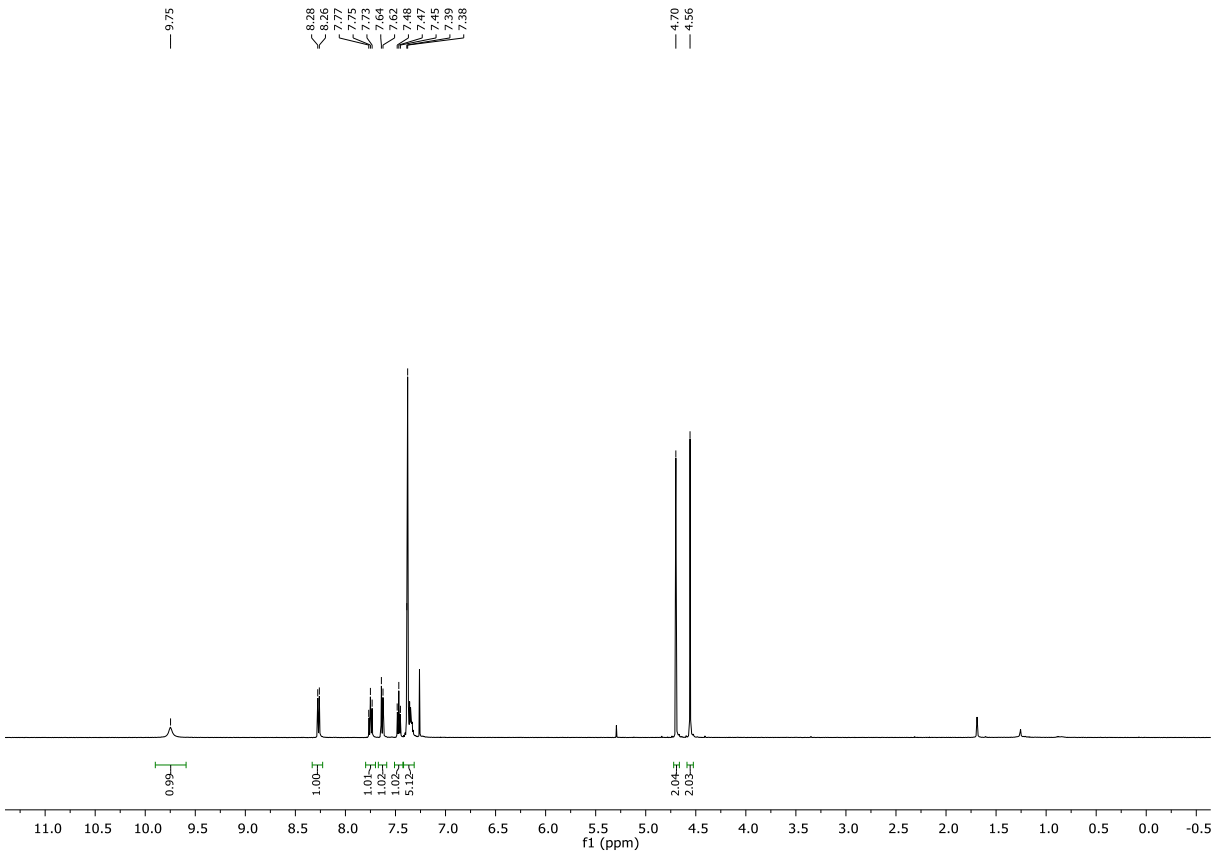

^{13}C NMR ($CDCl_3$, 126 MHz) of 2-((benzyloxy)methyl)quinazolin-4(3*H*)-one (**4.4.11**)

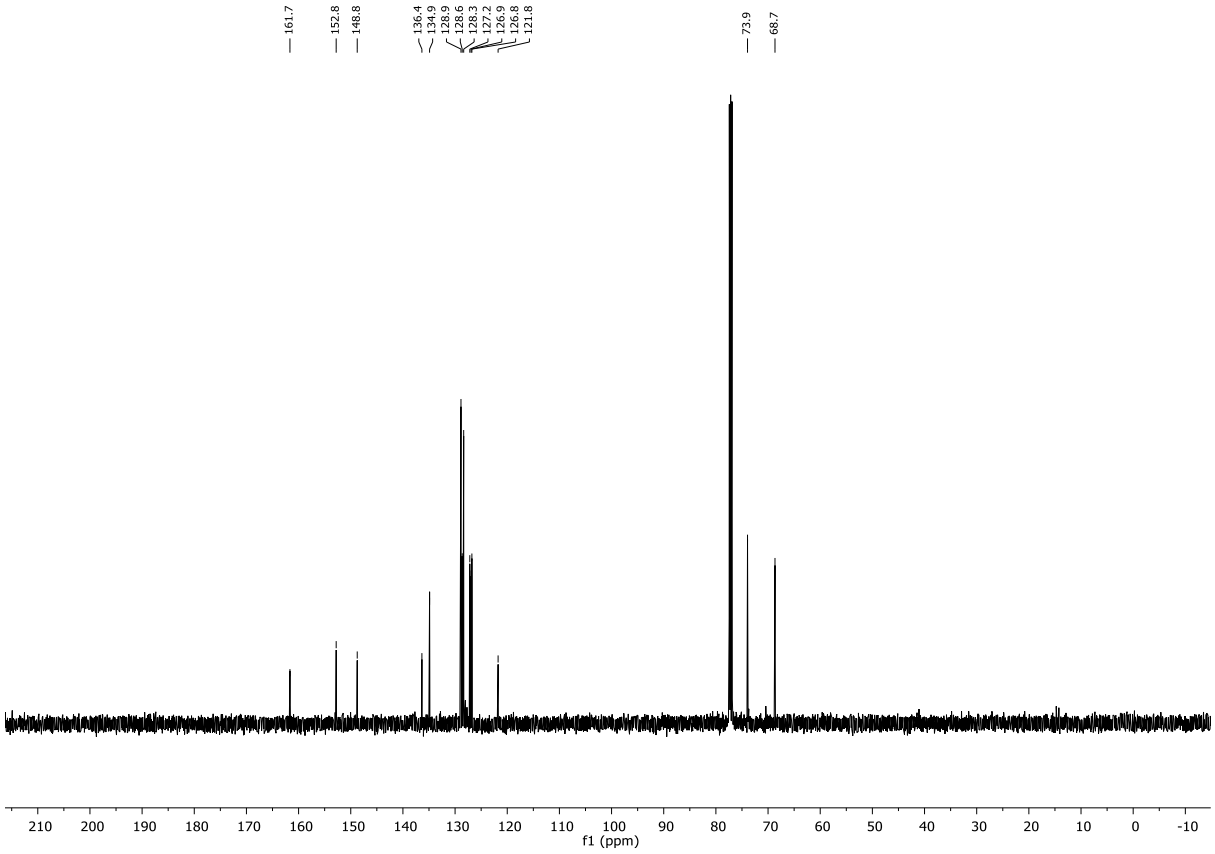

^{1}H NMR ($CDCl_3$, 500 MHz) of 2-isopropyl-4-methylquinoline (**4.5.1**)

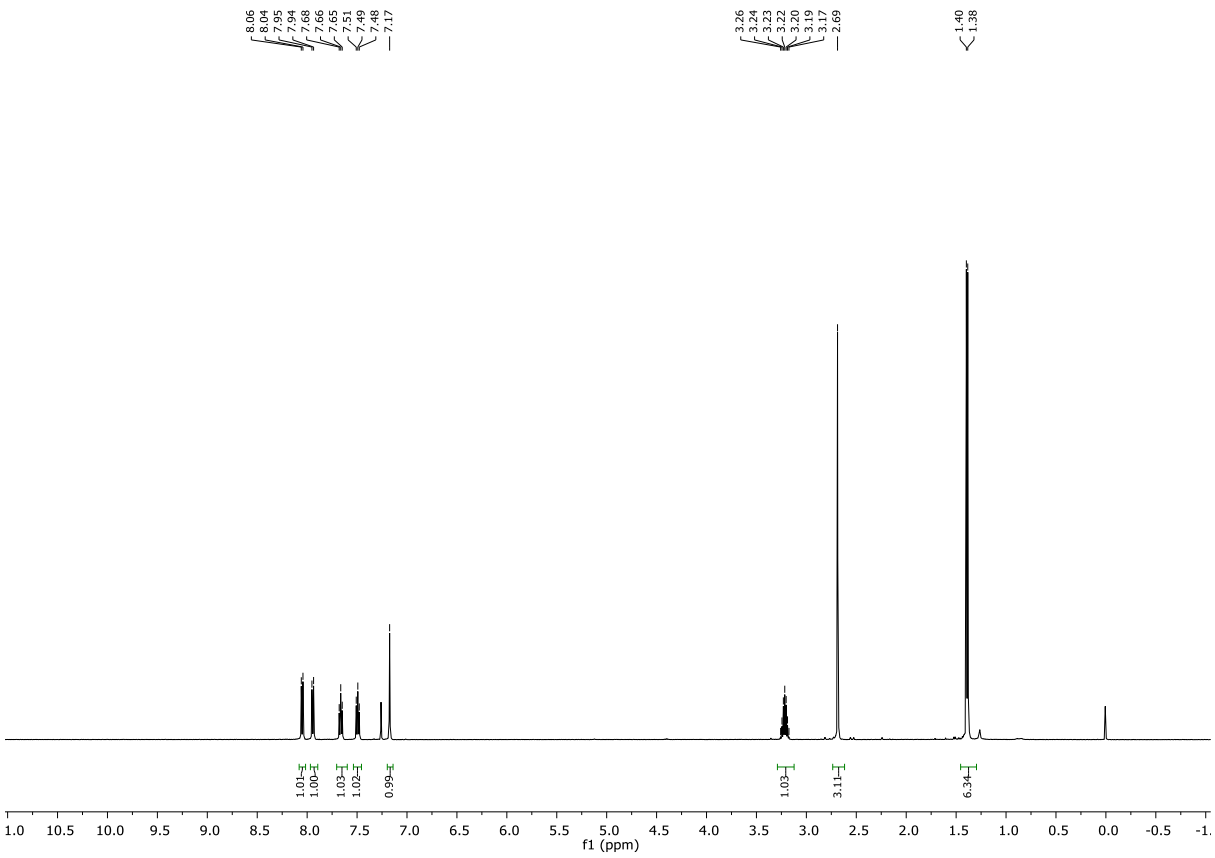

^{13}C NMR ($CDCl_3$, 126 MHz) of 2-isopropyl-4-methylquinoline (**4.5.1**)

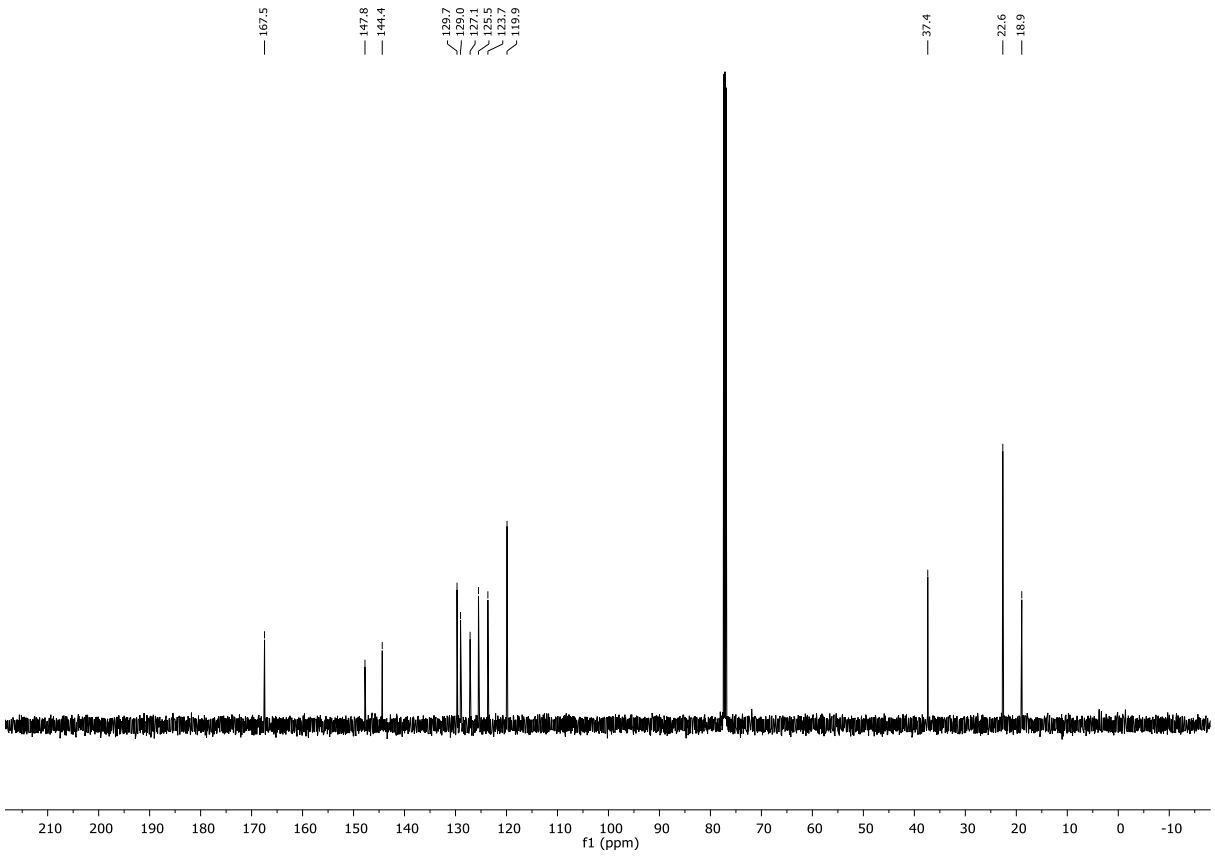

^{1}H NMR ($CDCl_3$, 500 MHz) of 4-methyl-2-(4-(5-methylhex-2-en-1-yl)cyclohex-3-en-1-yl)quinoline (mixture of isomers) (**4.5.2**)

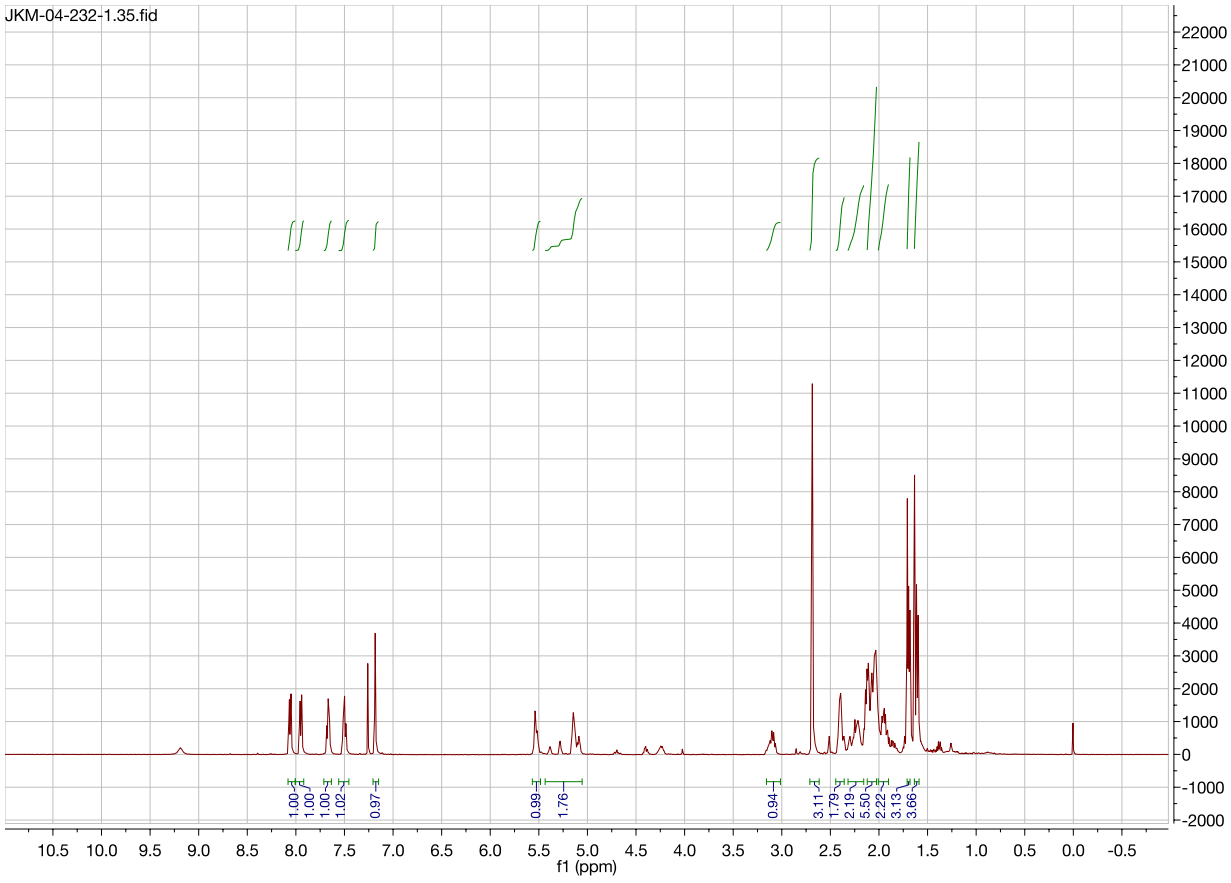

^{13}C NMR ($CDCl_3$, 126 MHz) of 4-methyl-2-(4-(5-methylhex-2-en-1-yl)cyclohex-3-en-1-yl)quinoline (mixture of isomers) (**4.5.2**)

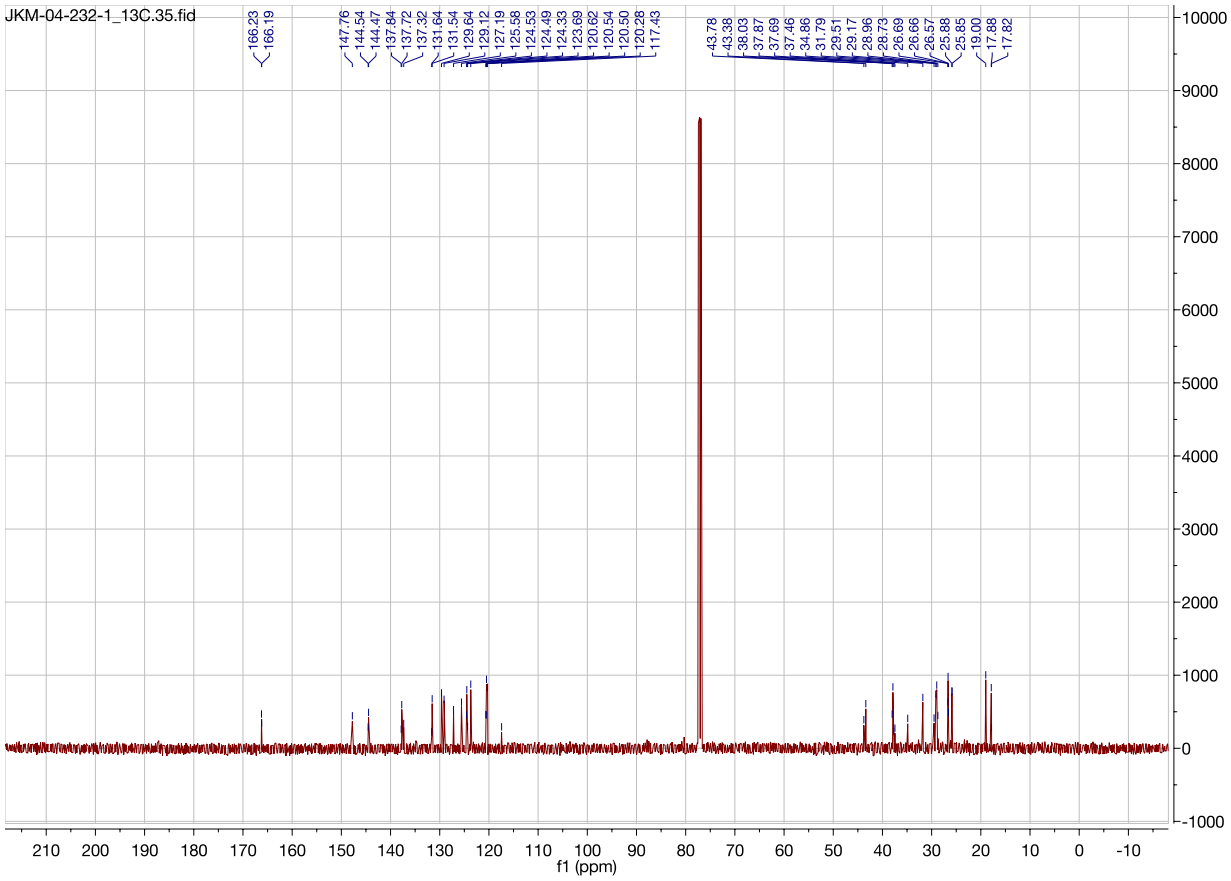

^{1}H NMR ($CDCl_3$, 500 MHz) of 1-((4-methylquinolin-2-yl)methyl)pyrrolidin-2-one (**4.5.3**)

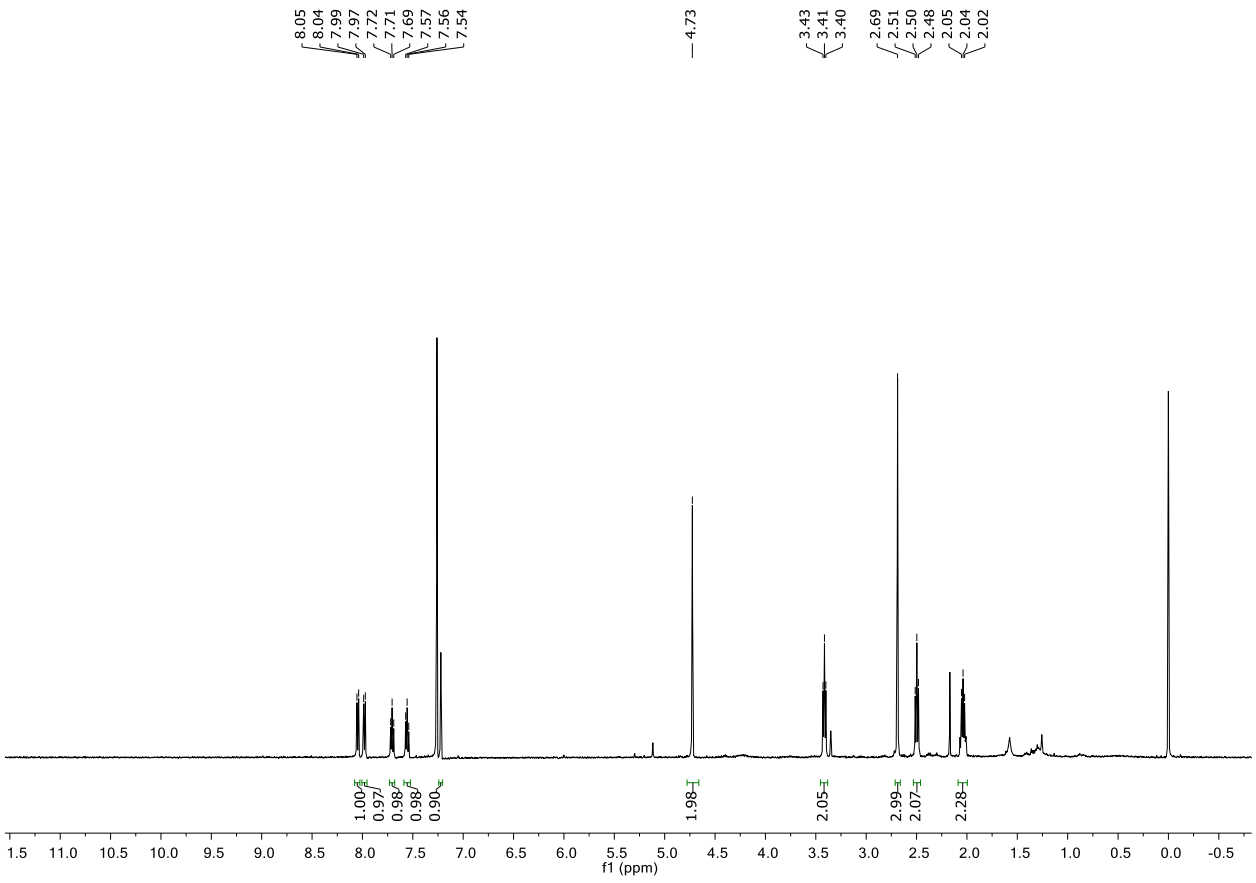

^{13}C NMR ($CDCl_3$, 126 MHz) of 1-((4-methylquinolin-2-yl)methyl)pyrrolidin-2-one (**4.5.3**)

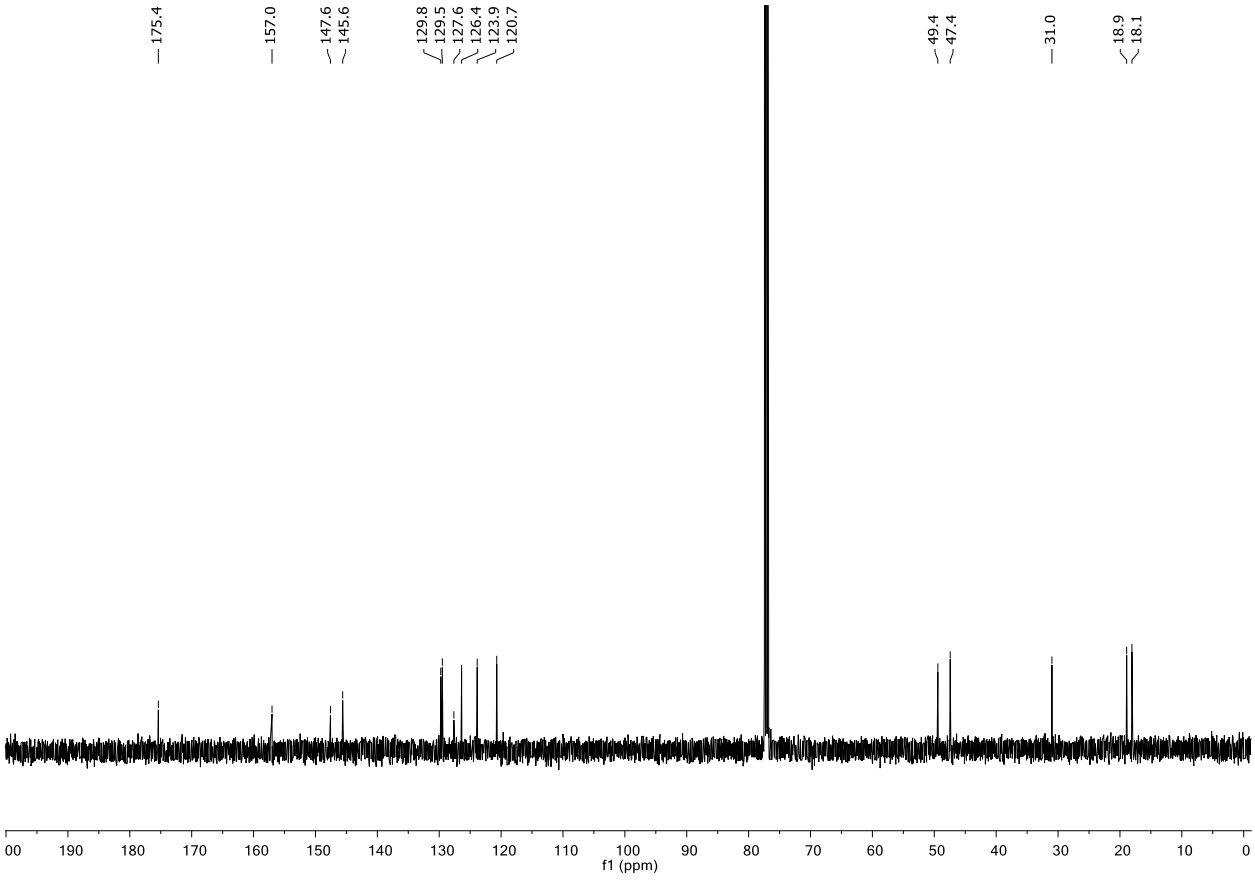

^{1}H NMR ($CDCl_3$, 500 MHz) of 4-bromo-1-(*sec*-butyl)isoquinoline (**4.5.4**)

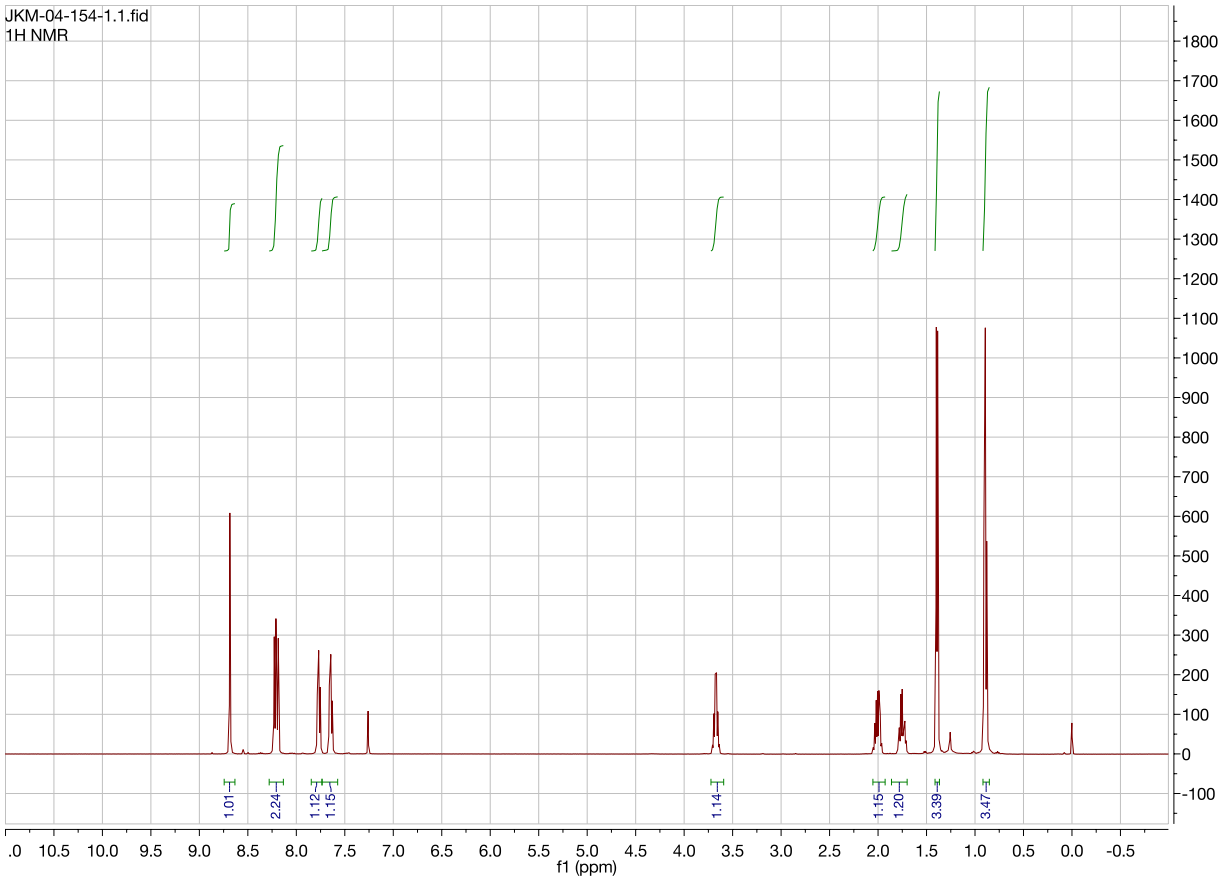

^{13}C NMR ($CDCl_3$, 126 MHz) of 4-bromo-1-(*sec*-butyl)isoquinoline (**4.5.4**)

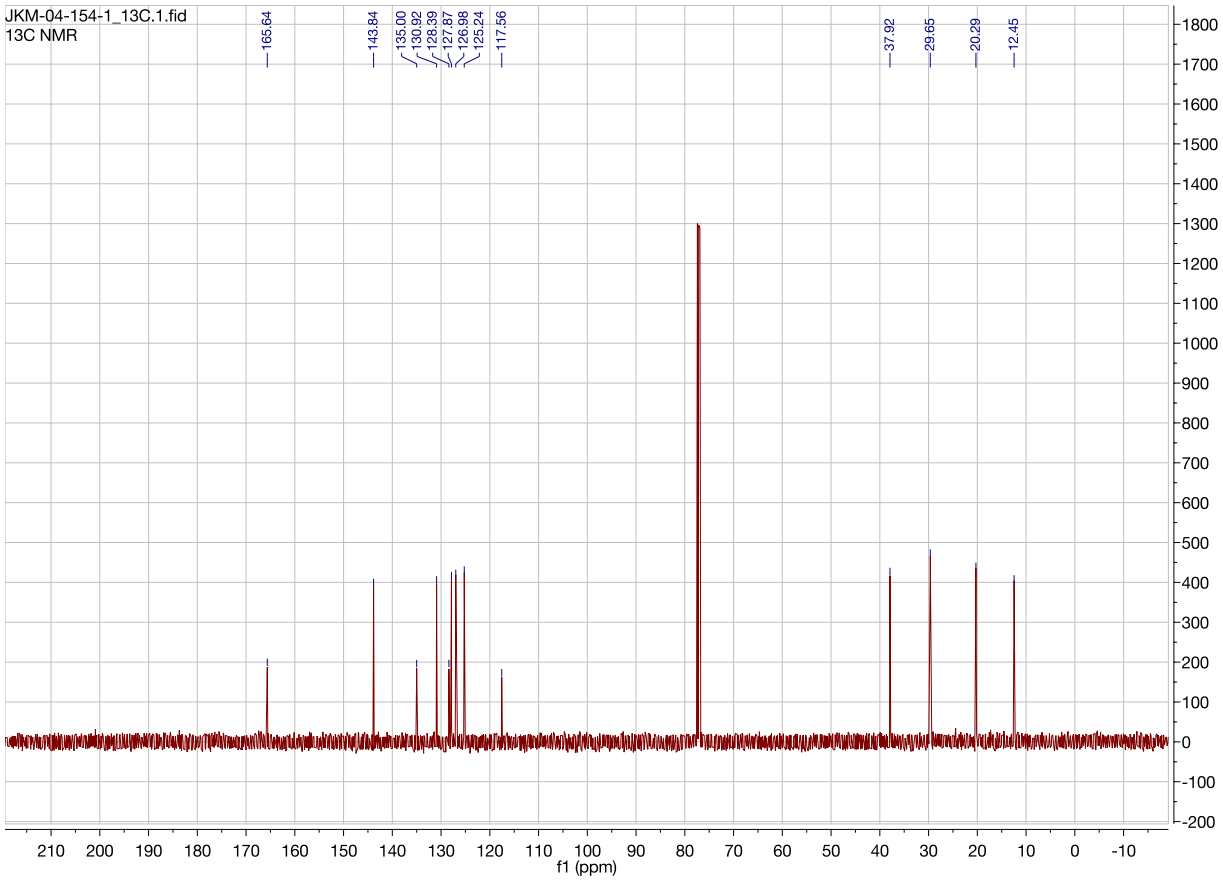

^{1}H NMR ($CDCl_3$, 500 MHz) of 6-bromo-2,4-di-*sec*-butylquinoline (**4.5.5**)

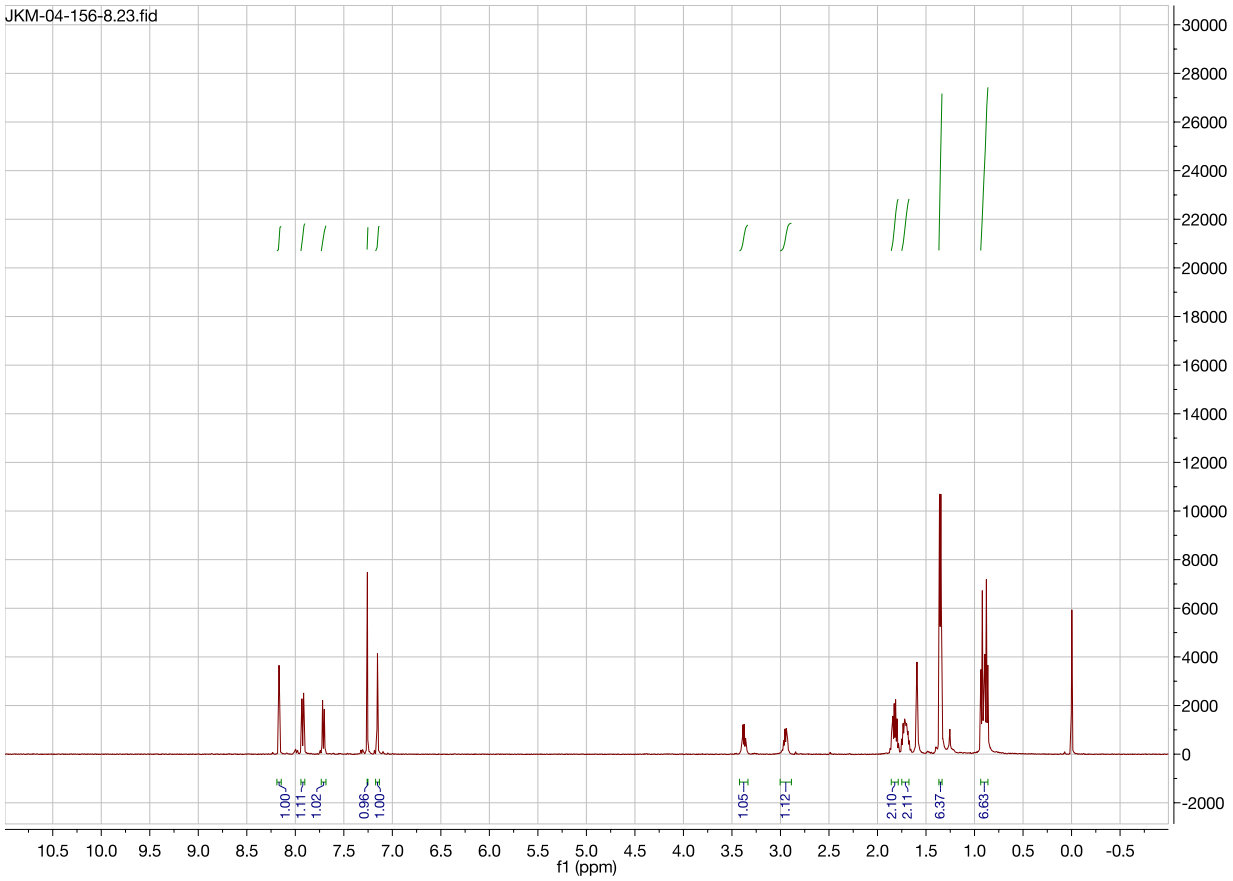

^{13}C NMR ($CDCl_3$, 126 MHz) of 6-bromo-2,4-di-*sec*-butylquinoline (**4.5.5**)

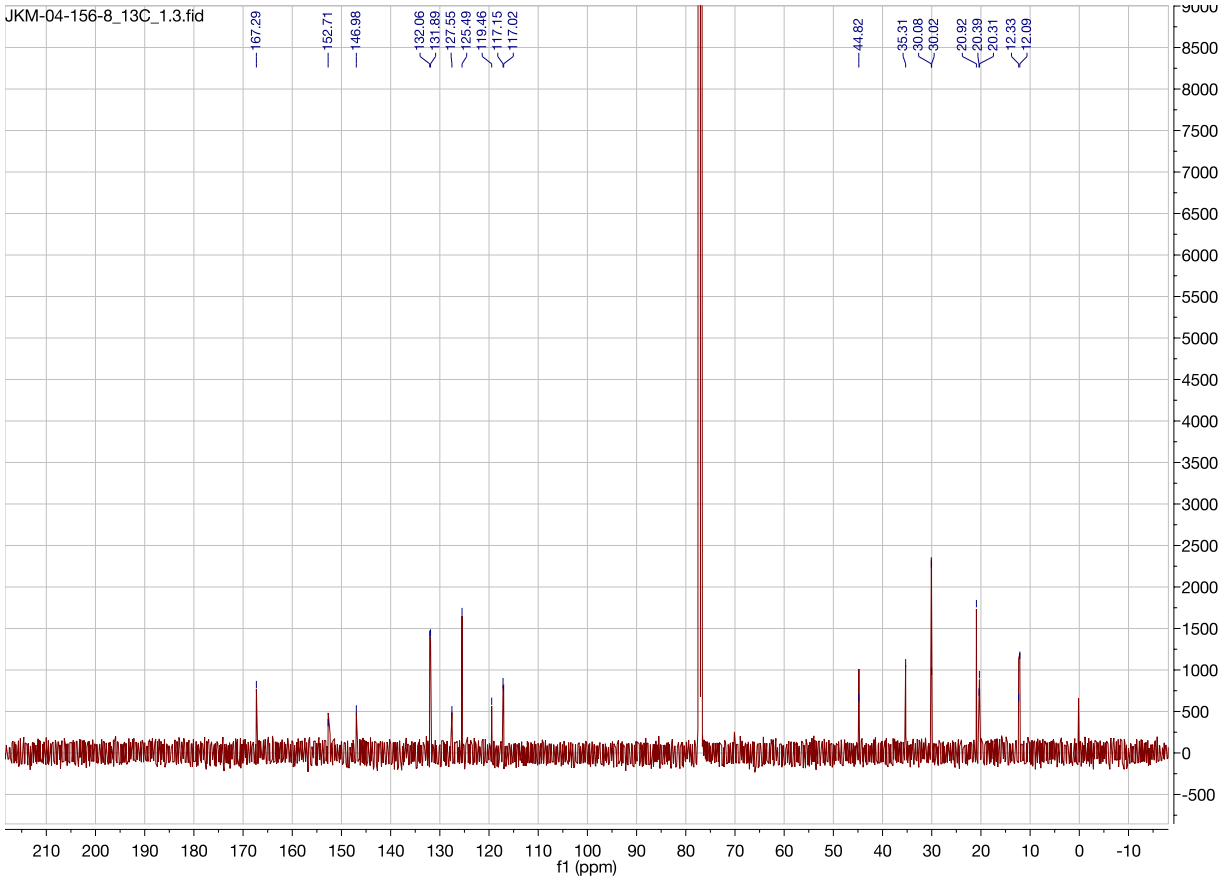

^{1}H NMR ($CDCl_3$, 500 MHz) of 2-(*sec*-butyl)-4-chloroquinoline (**4.5.6**)

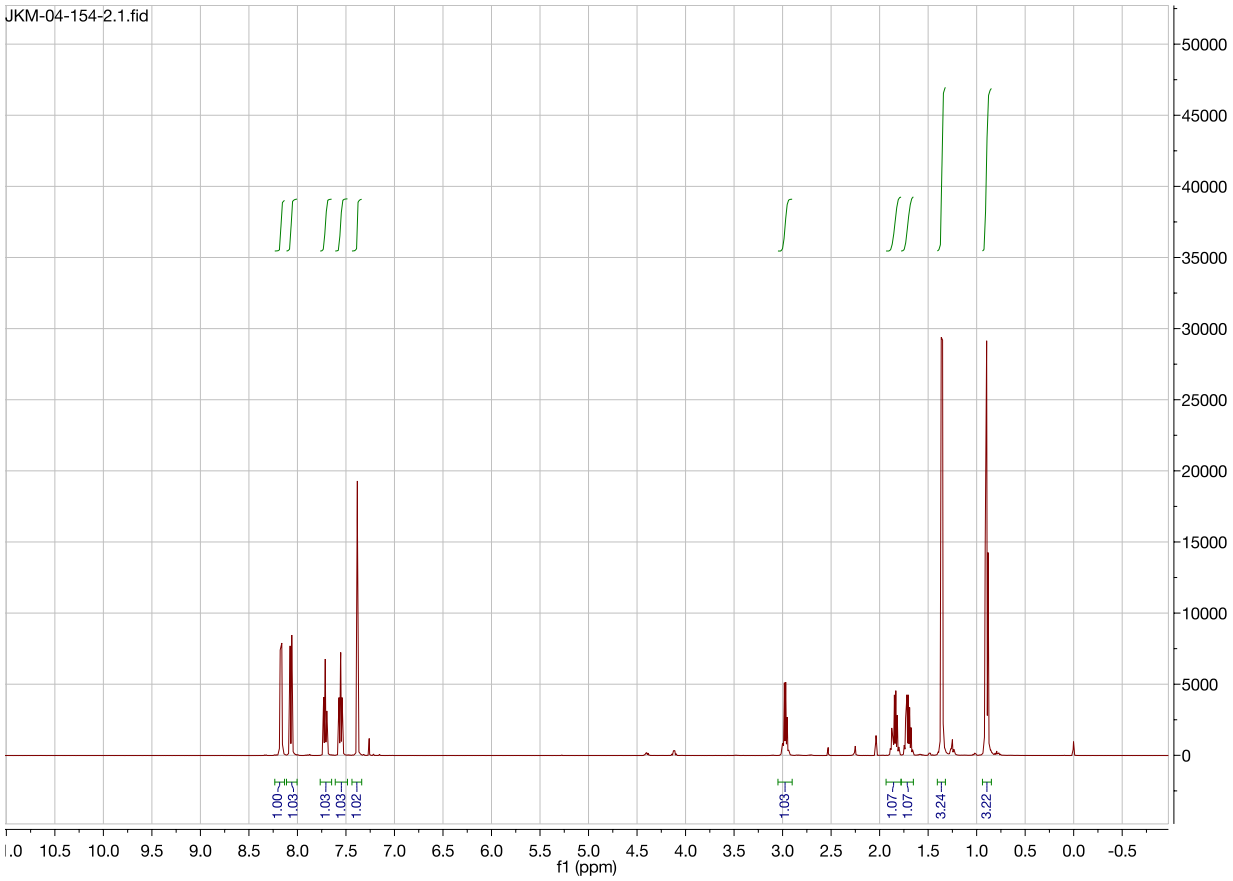

^{13}C NMR ($CDCl_3$, 126 MHz) of 2-(*sec*-butyl)-4-chloroquinoline (**4.5.6**)

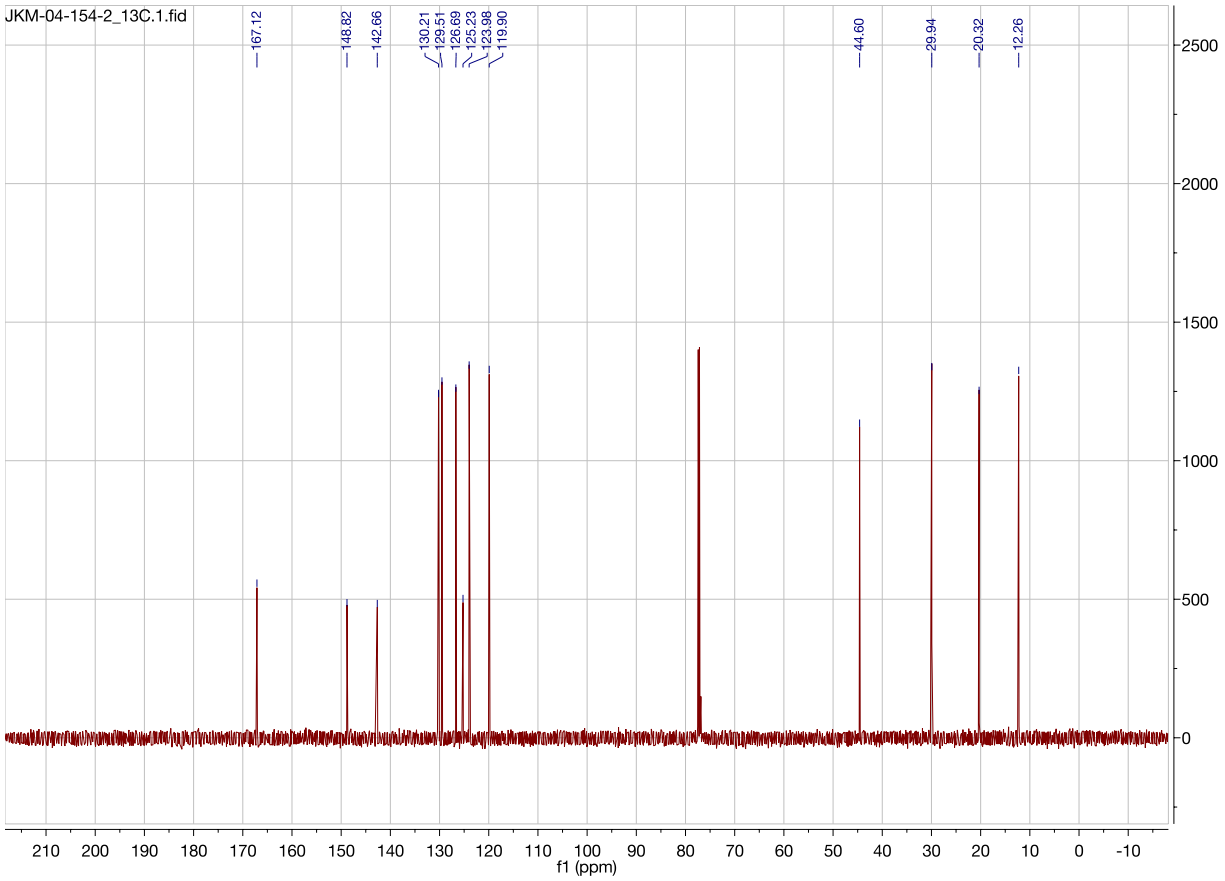

^{1}H NMR ($CDCl_3$, 500 MHz) of 2-(*sec*-butyl)-4-chloro-7-(trifluoromethyl)quinoline (**4.5.7**)

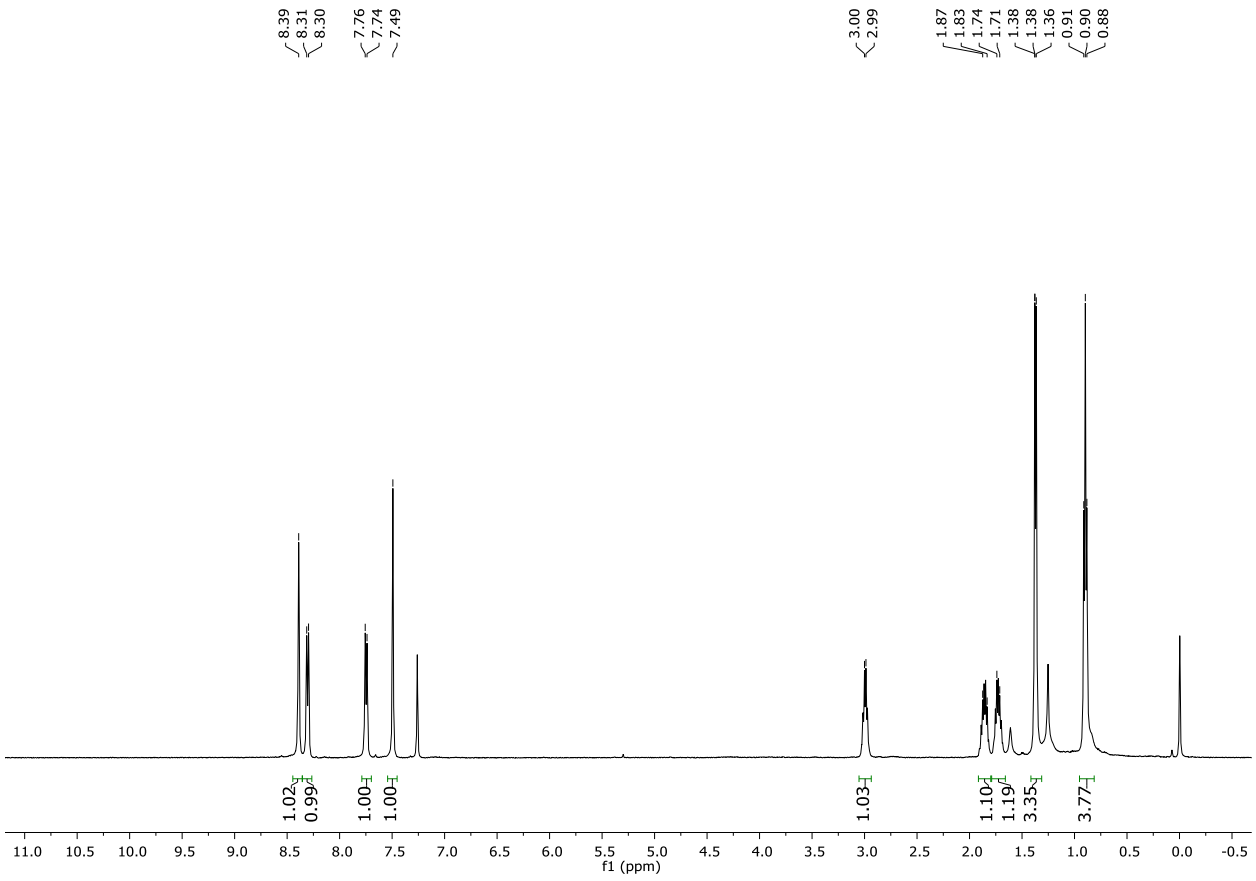

^{13}C NMR ($CDCl_3$, 126 MHz) of 2-(*sec*-butyl)-4-chloro-7-(trifluoromethyl)quinoline (**4.5.7**)

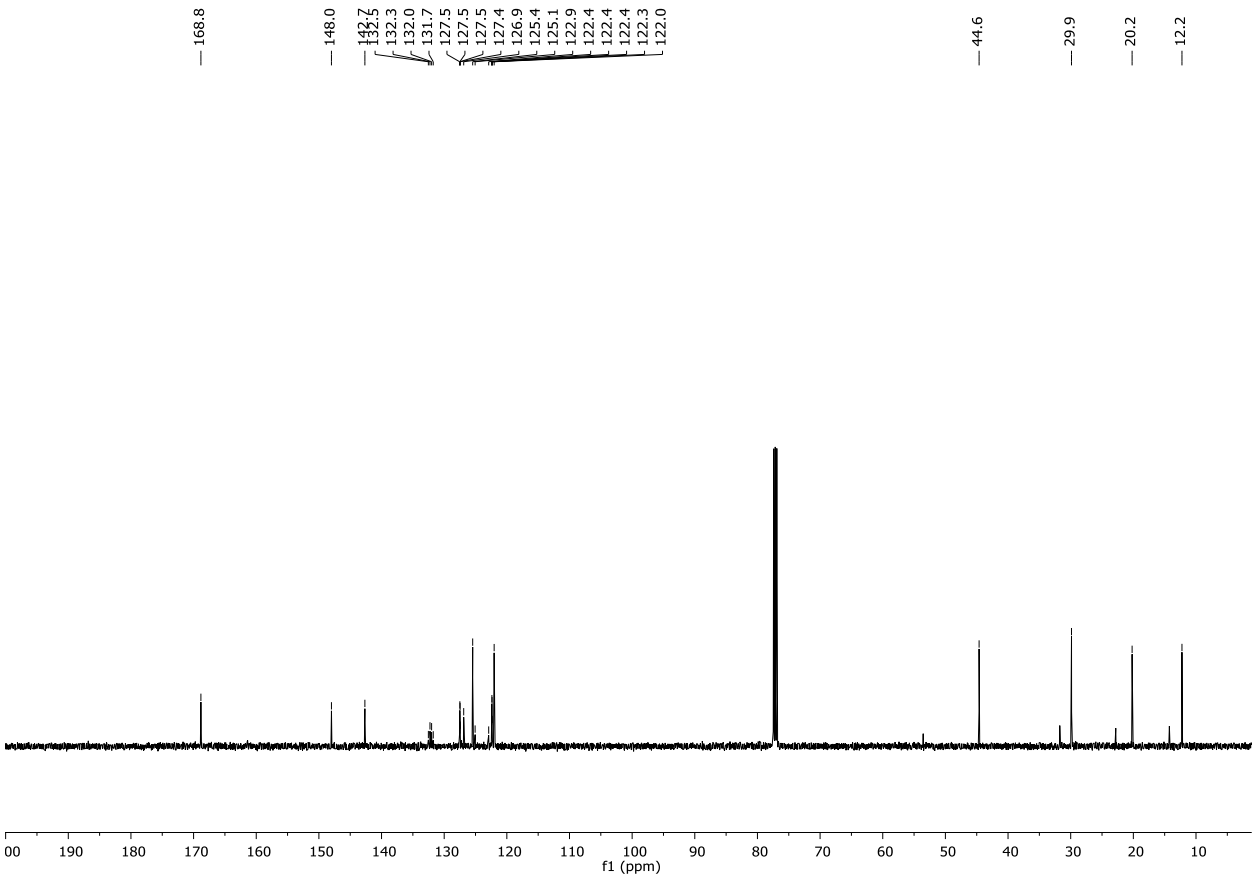

^{19}F NMR (471 MHz, $CDCl_3$) of 2-(*sec*-butyl)-4-chloro-7-(trifluoromethyl)quinoline (**4.5.7**)

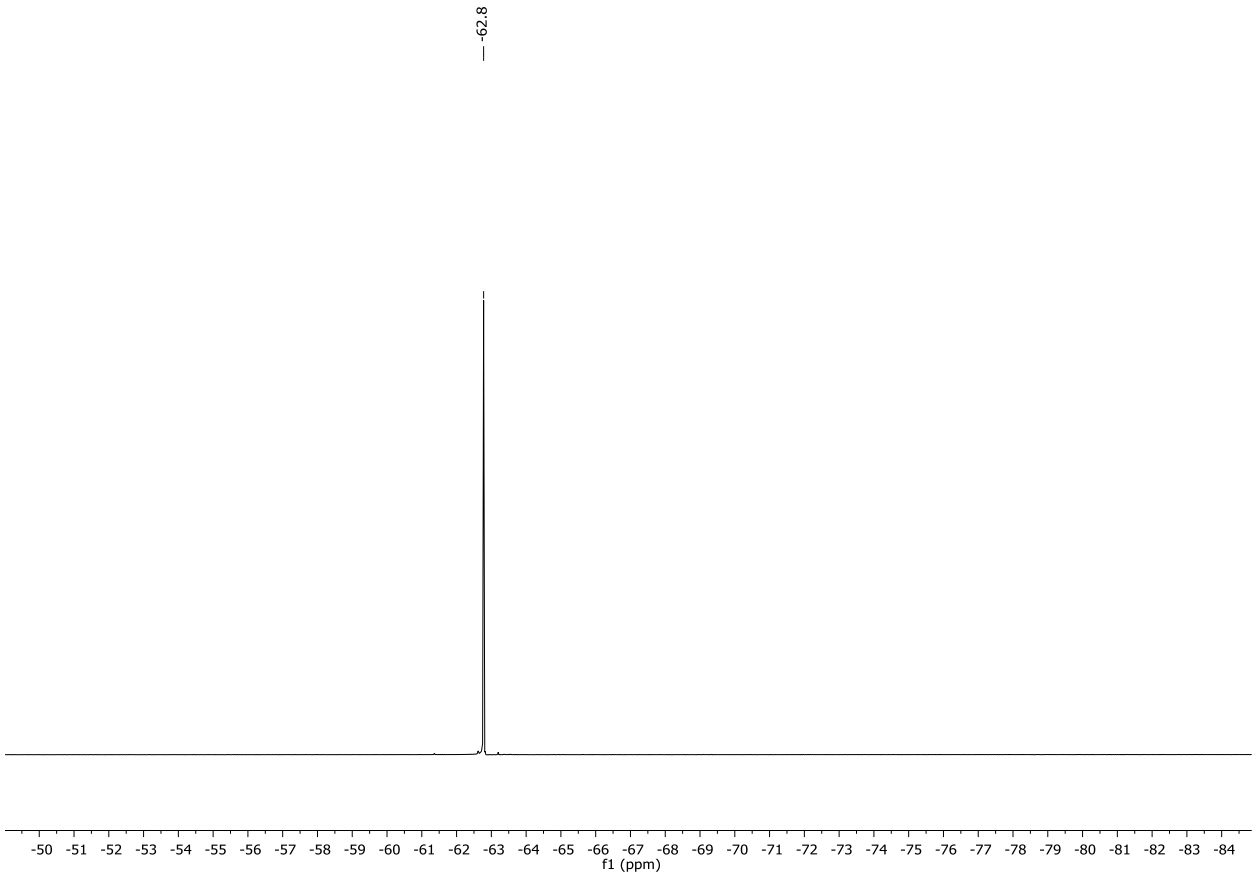

^{1}H NMR ($CDCl_3$, 500 MHz) of methyl 1-(heptan-3-yl)isoquinoline-3-carboxylate (**4.5.8**)

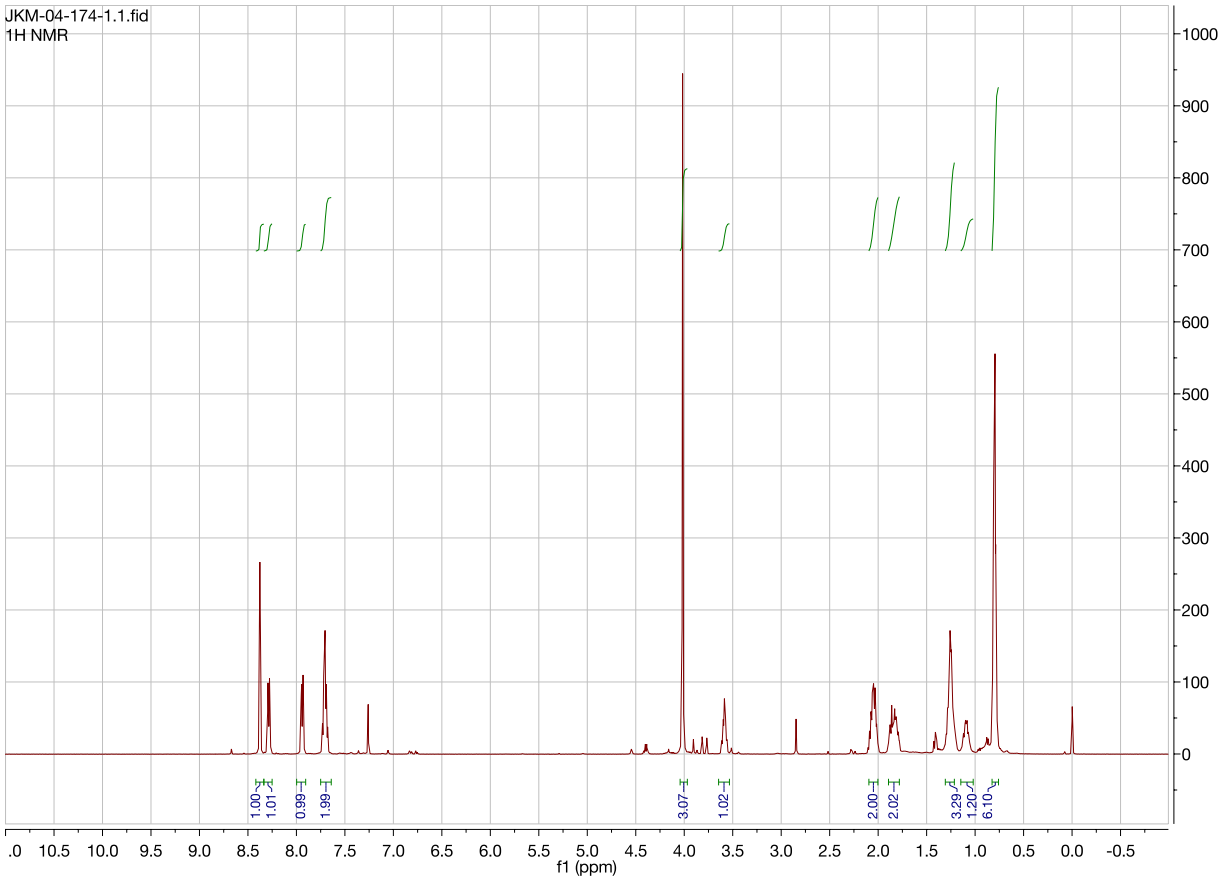

^{13}C NMR ($CDCl_3$, 126 MHz) of methyl 1-(heptan-3-yl)isoquinoline-3-carboxylate (**4.5.8**)

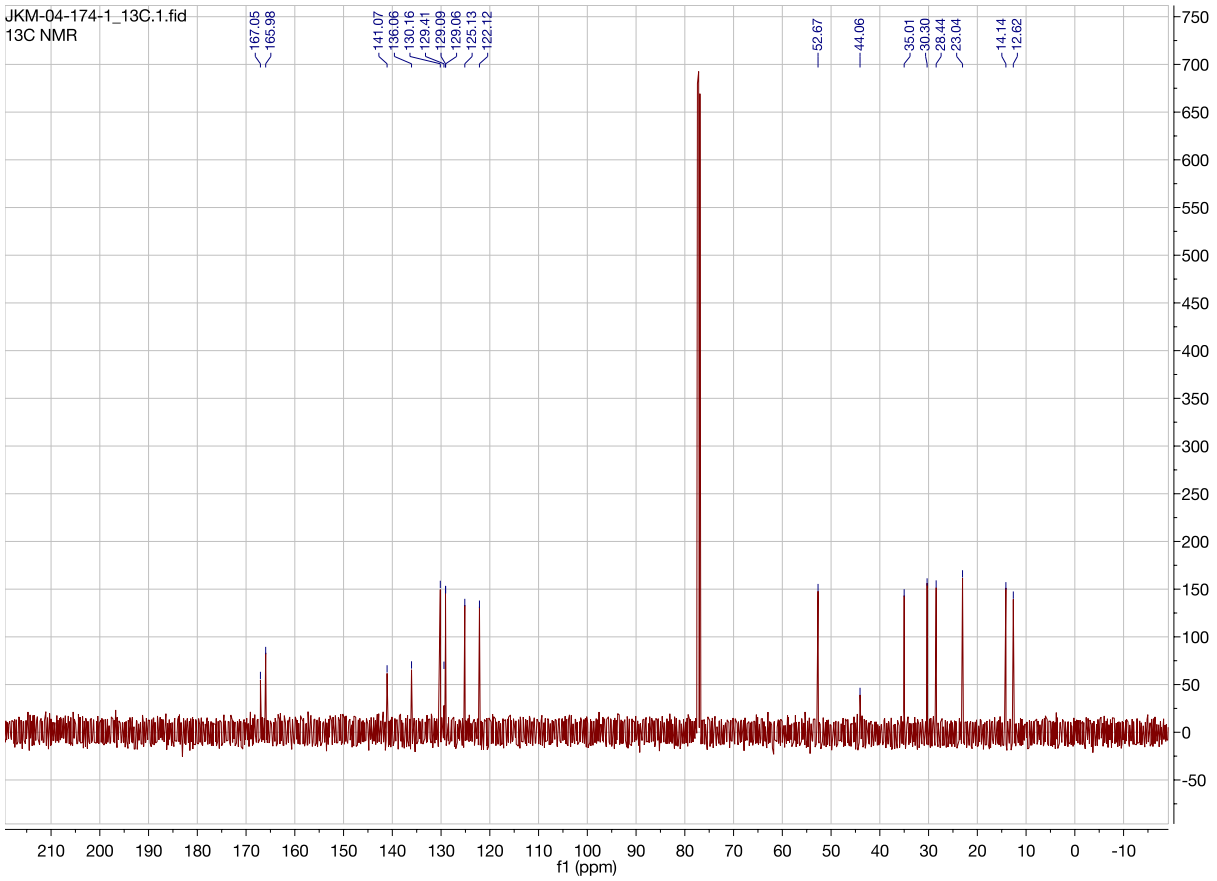

^{1}H NMR ($CDCl_3$, 500 MHz) of methyl 1-(6-methylhept-5-en-2-yl)isoquinoline-3-carboxylate (**4.5.9**)

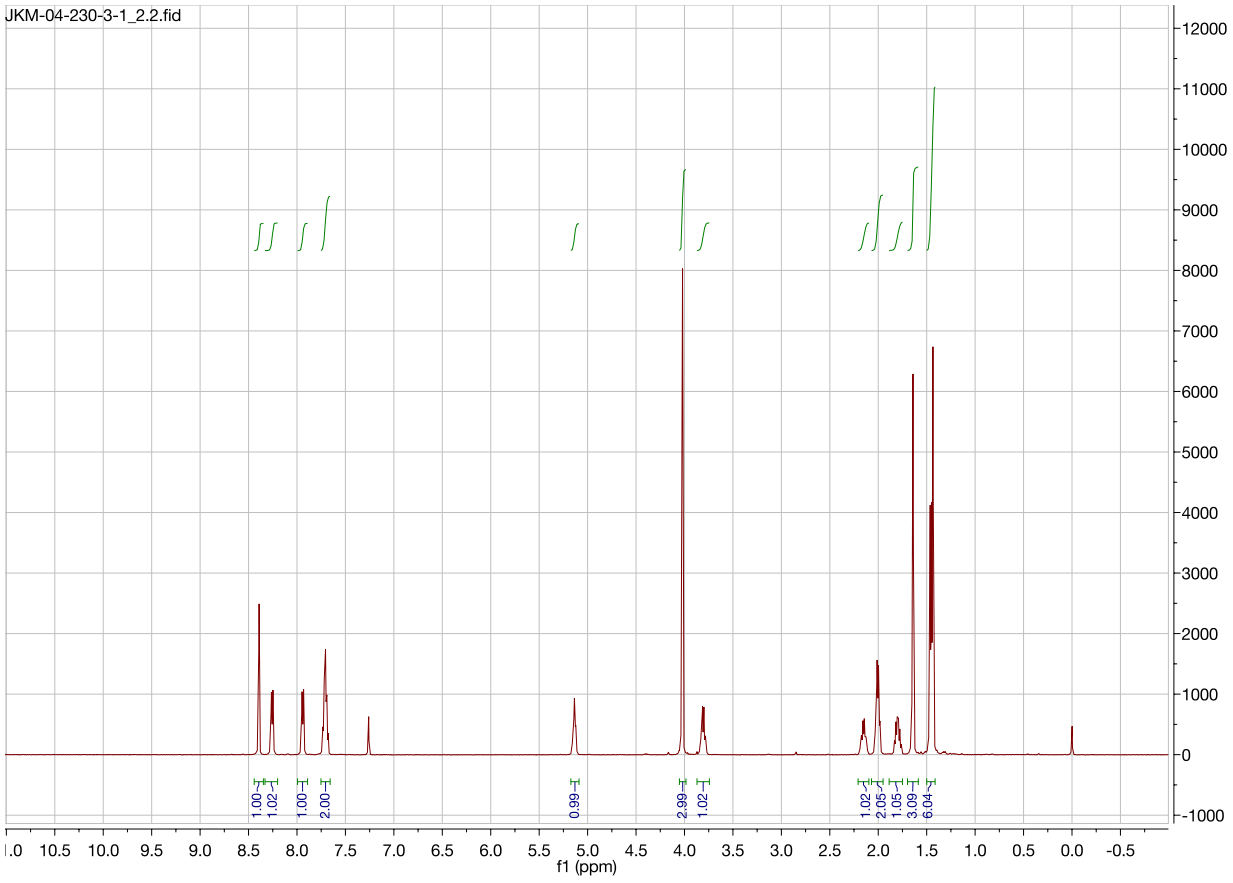

^{13}C NMR ($CDCl_3$, 126 MHz) of methyl 1-(6-methylhept-5-en-2-yl)isoquinoline-3-carboxylate (**4.5.9**)

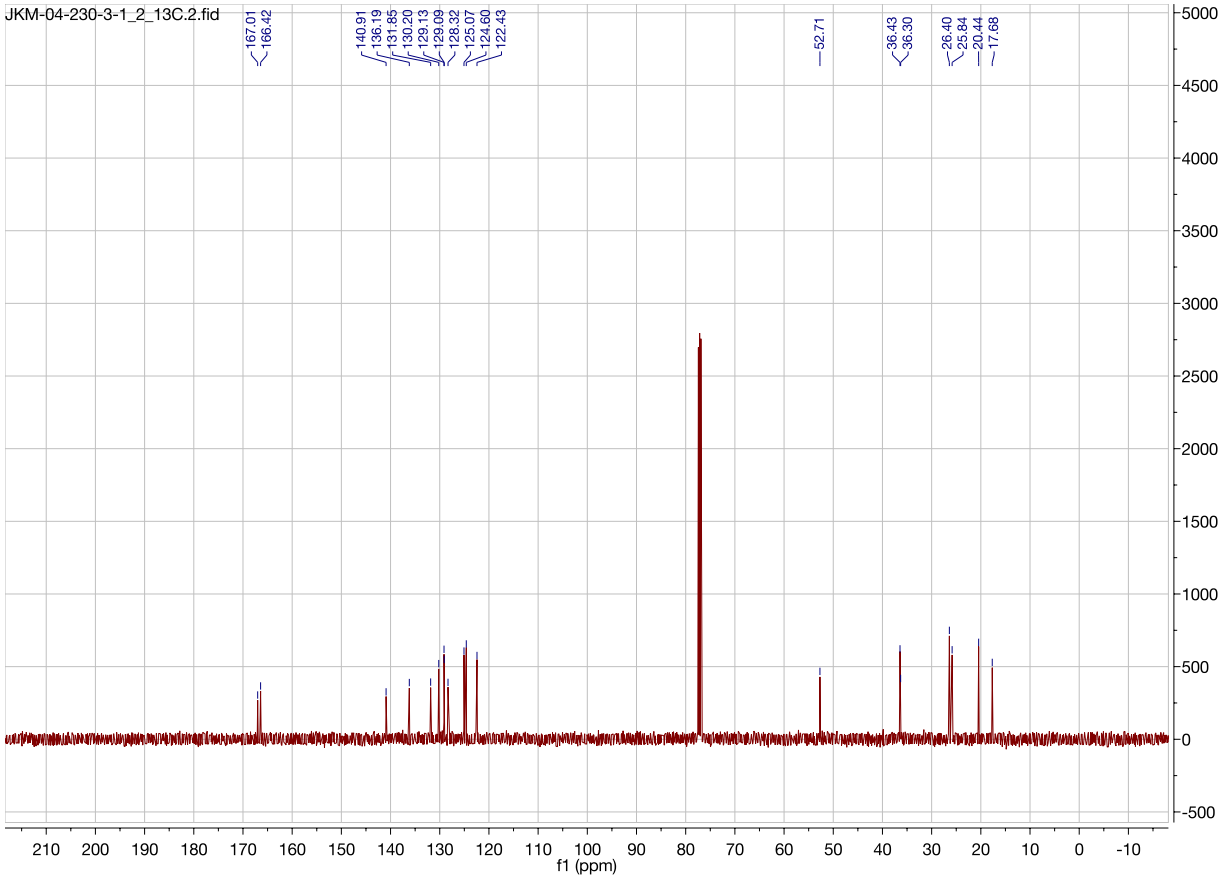

^{1}H NMR ($CDCl_3$, 500 MHz) of 2-isopropyl-6-phenylpyridine and 2,4-Diisopropyl-6-phenylpyridine (**4.5.10**)

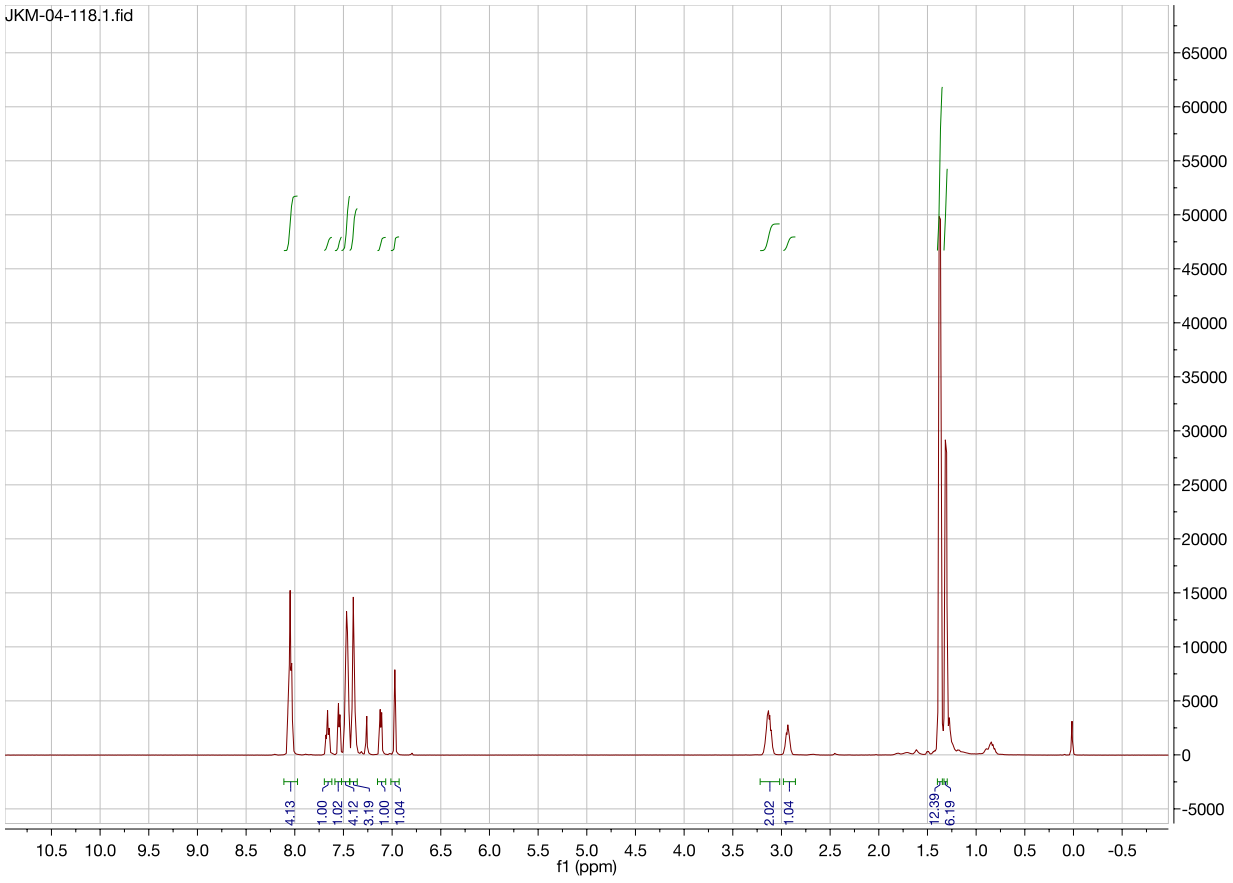

^{13}C NMR ($CDCl_3$, 126 MHz) of 2-isopropyl-6-phenylpyridine and 2,4-Diisopropyl-6-phenylpyridine (**4.5.10**)

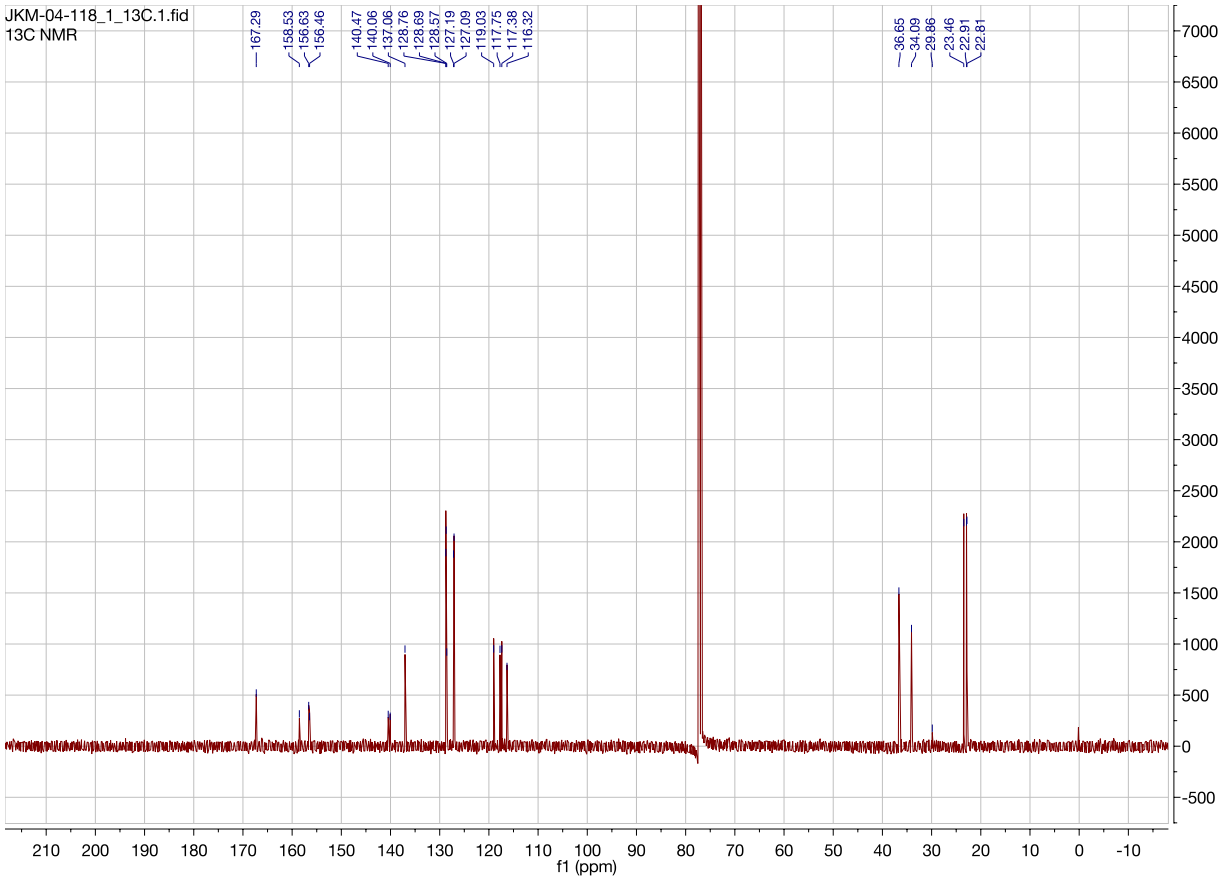

^{1}H NMR ($CDCl_3$, 500 MHz) of 4-(*sec*-butyl)-2-chloro-6-(methylsulfonyl)pyrimidine (**4.5.11**)

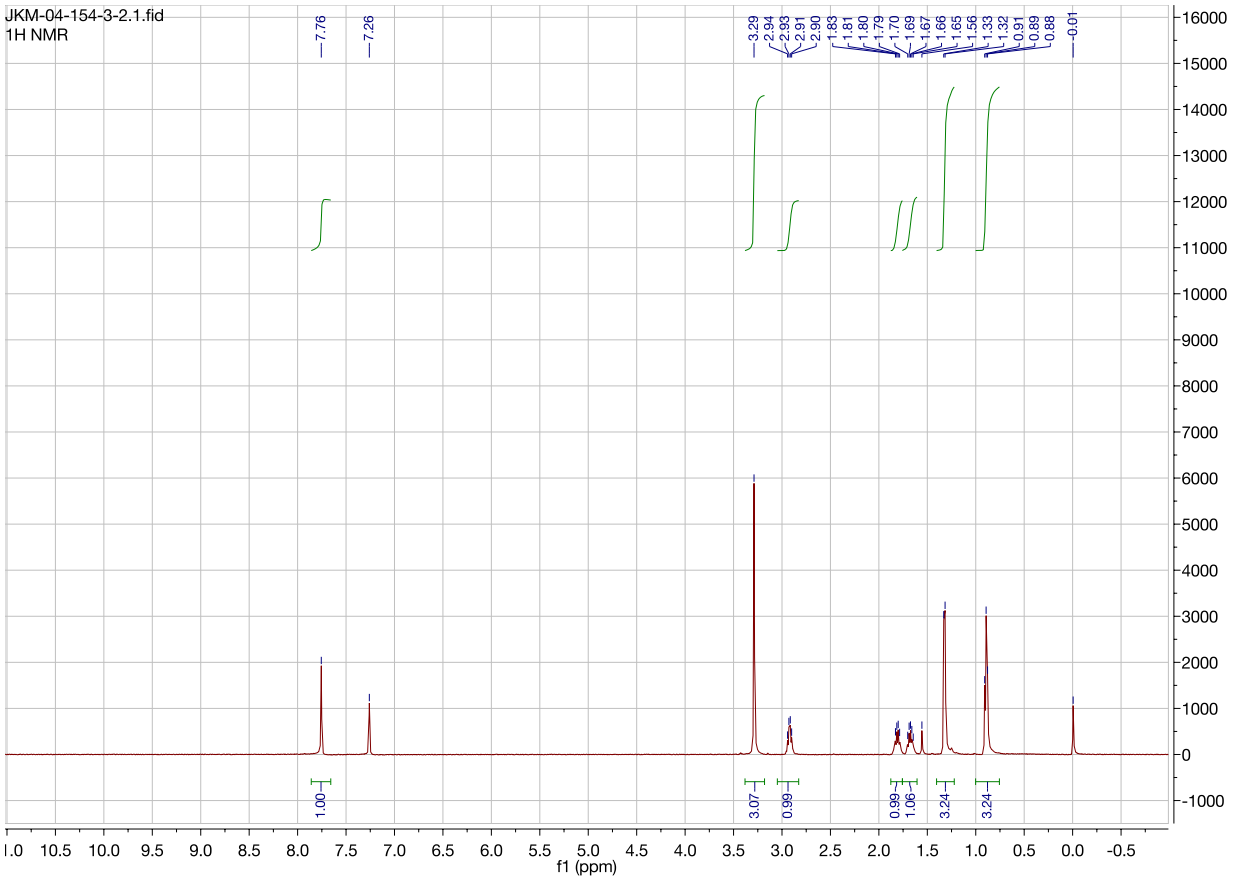

^{13}C NMR ($CDCl_3$, 126 MHz) of 4-(*sec*-butyl)-2-chloro-6-(methylsulfonyl)pyrimidine (**4.5.11**)

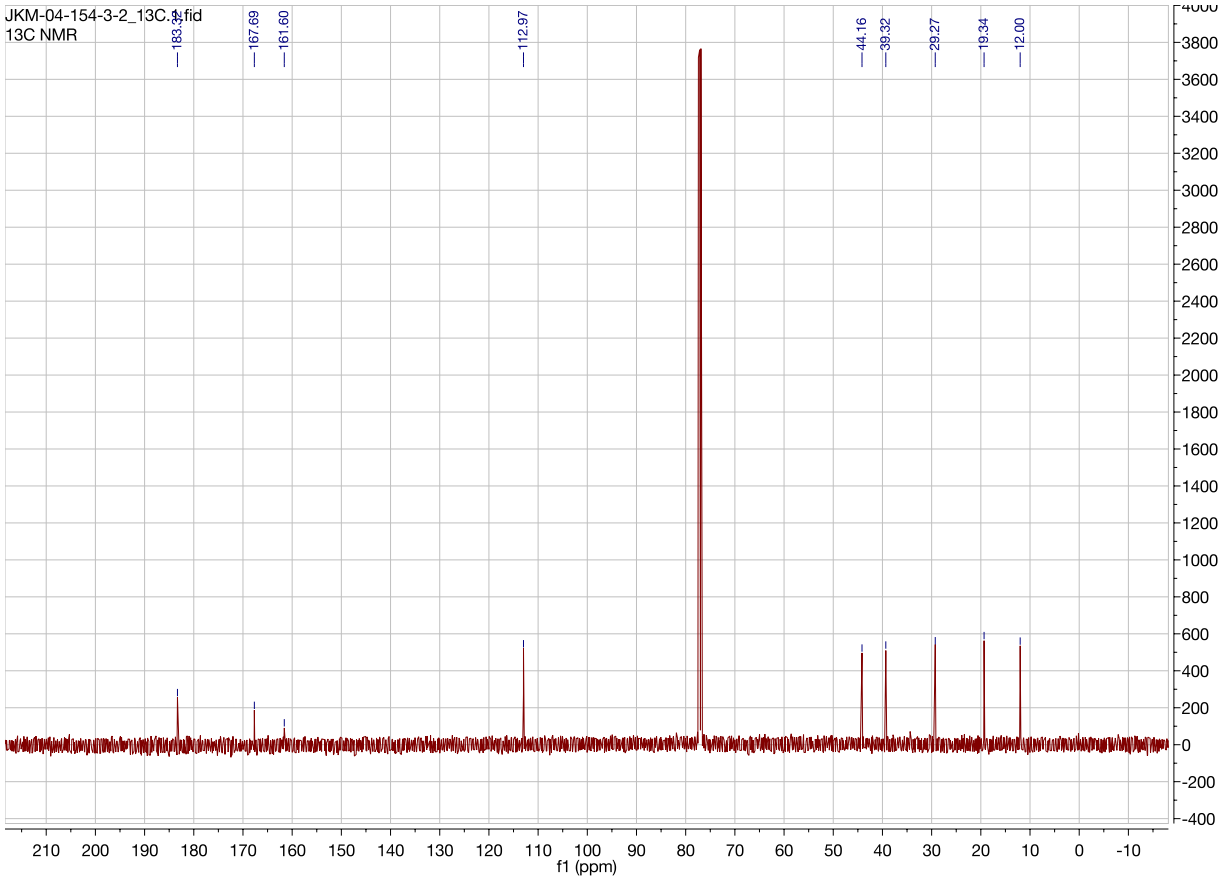

^{1}H NMR ($CDCl_3$, 500 MHz) of 2-cyclohexylbenzo[d]thiazole (**4.5.12**)

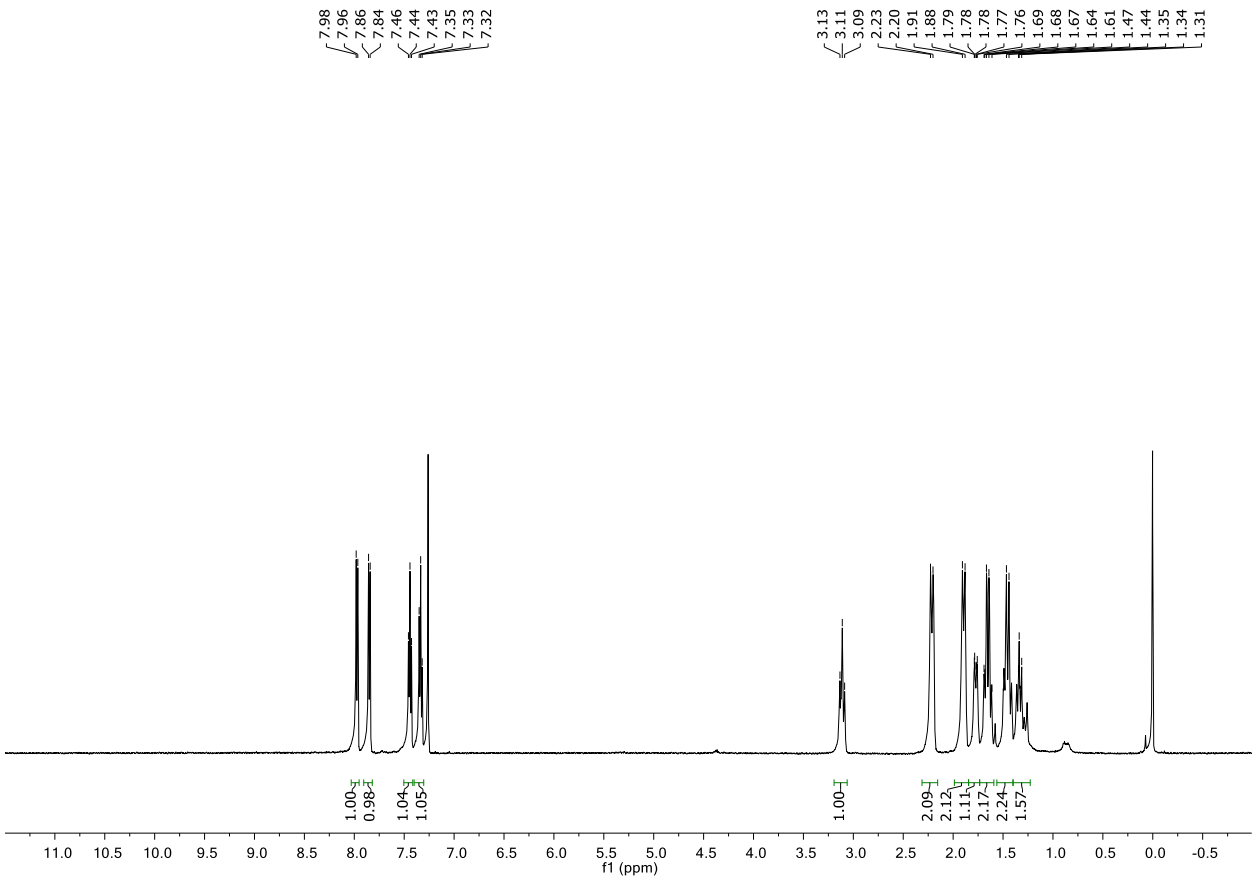

^{13}C NMR ($CDCl_3$, 126 MHz) of 2-cyclohexylbenzo[d]thiazole (**4.5.12**)

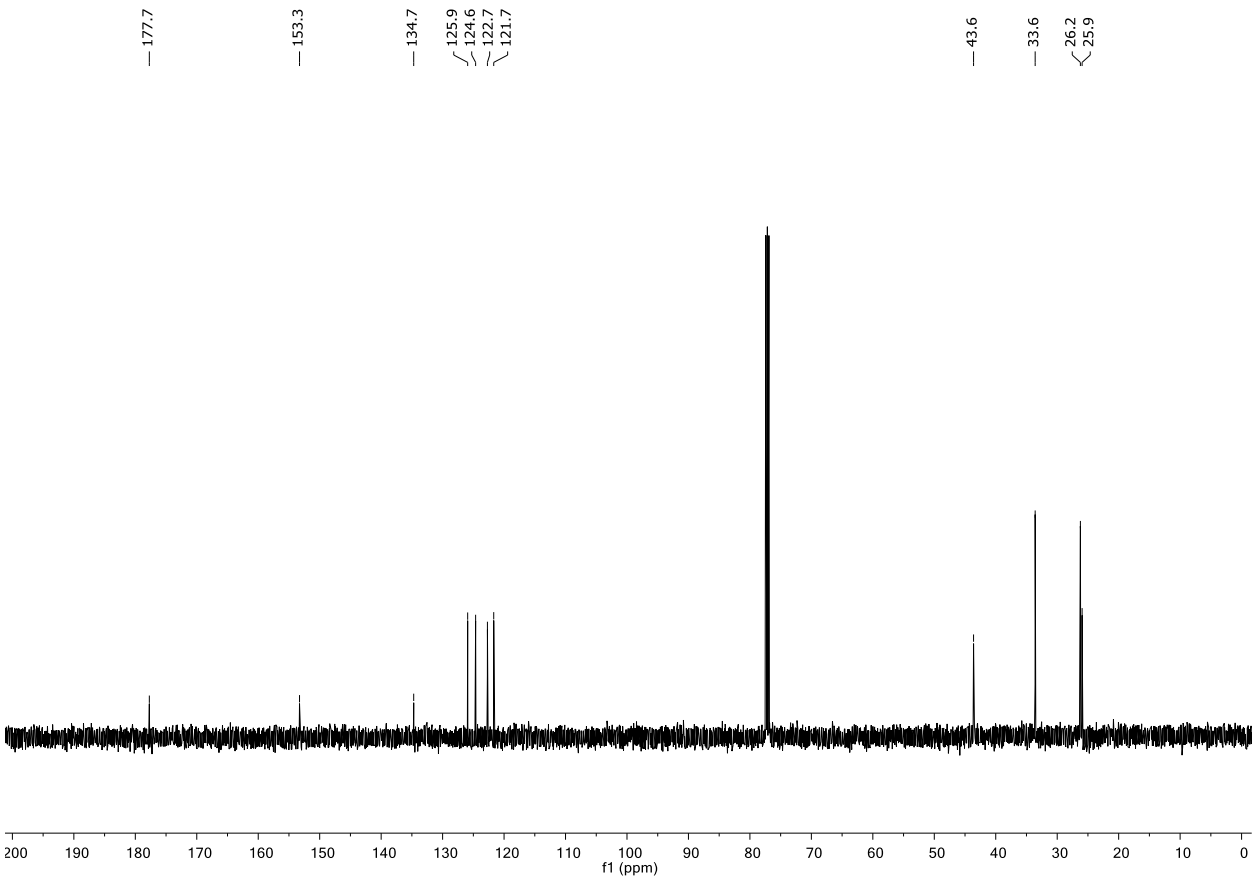

^{1}H NMR ($CDCl_3$, 500 MHz) of (*S*)-2-cyclohexyl-5-(1-methylpyrrolidin-2-yl)pyridine (**4.6.1**)

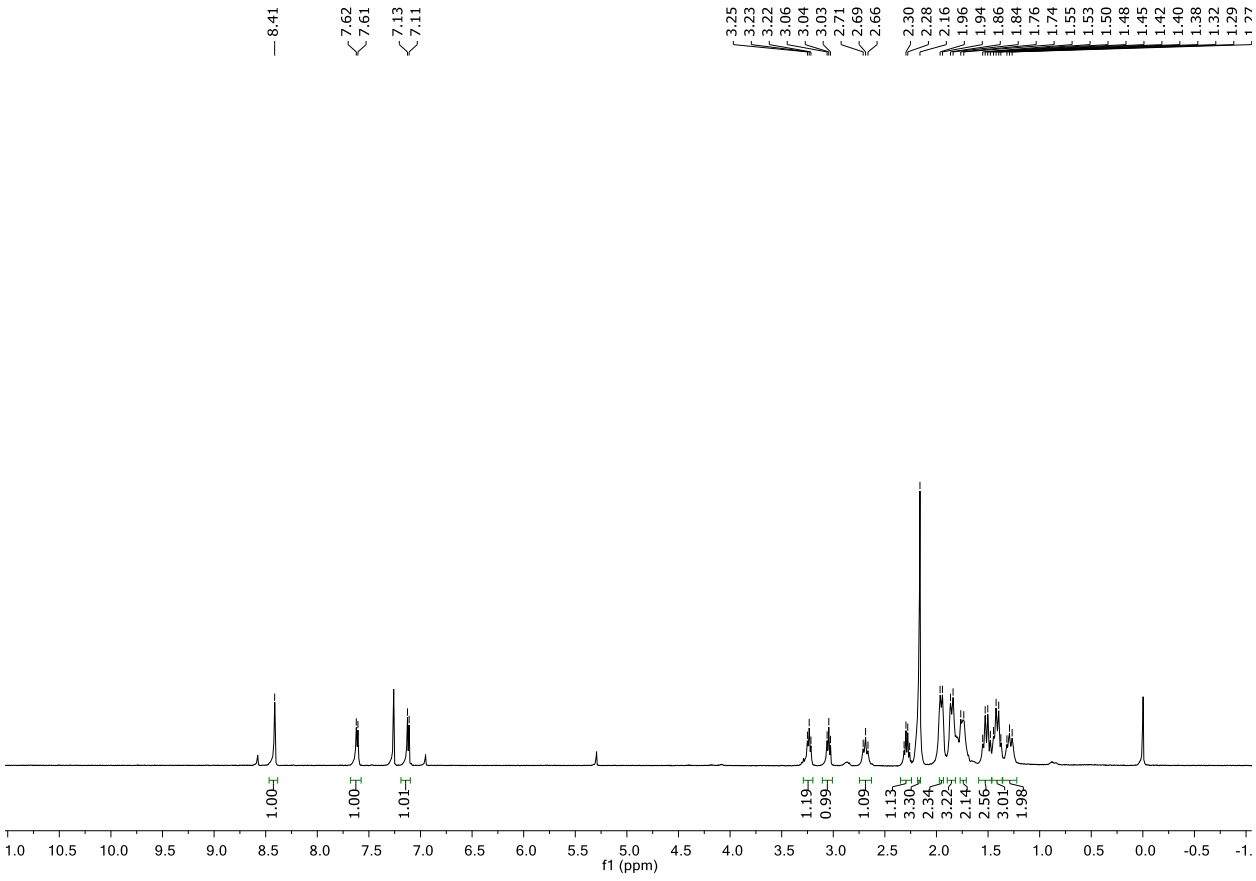

^{13}C NMR ($CDCl_3$, 126 MHz) of (*S*)-2-cyclohexyl-5-(1-methylpyrrolidin-2-yl)pyridine (**4.6.1**)

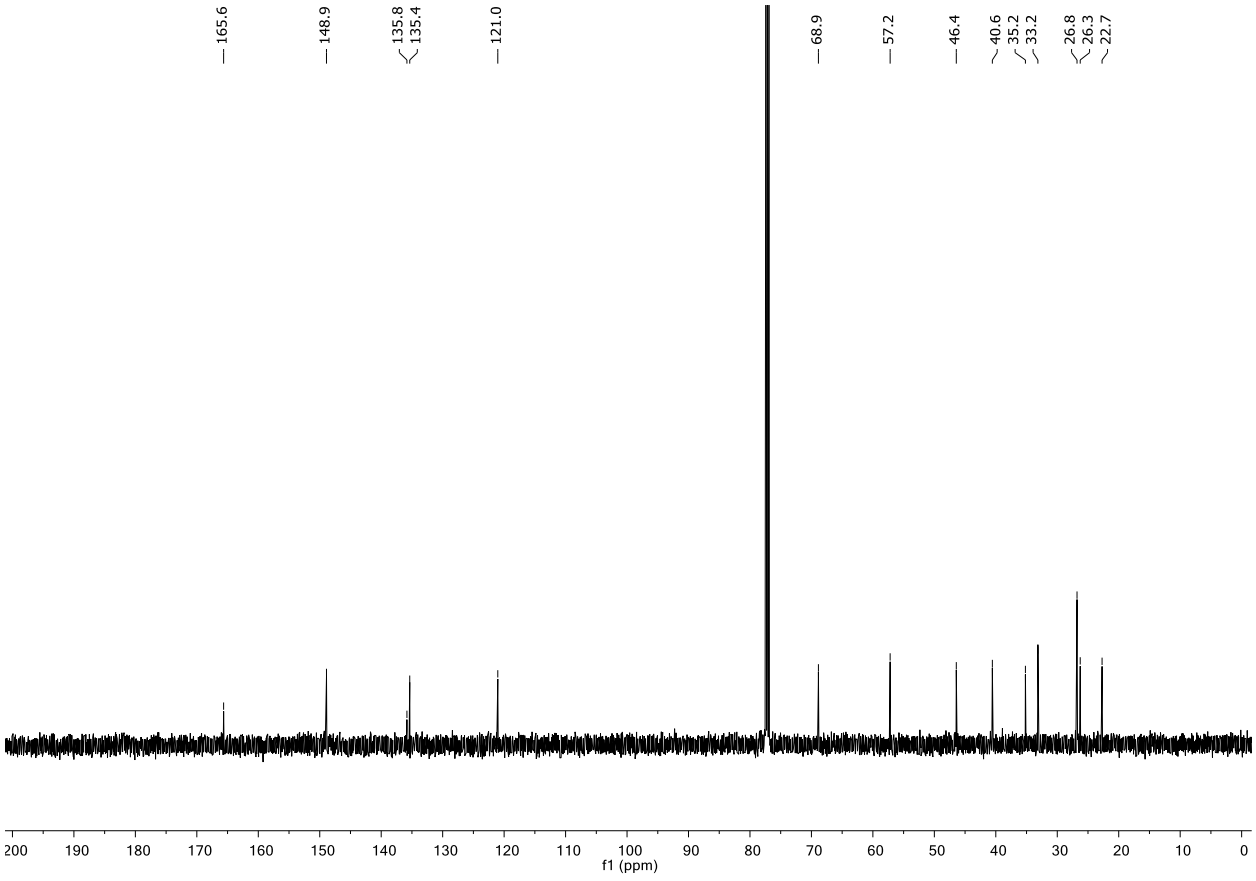

^{1}H NMR ($CDCl_3$, 500 MHz) of 8-(*sec*-butyl)-1,3,7-trimethyl-3,7-dihydro-1*H*-purine-2,6-dione (**4.6.2**)

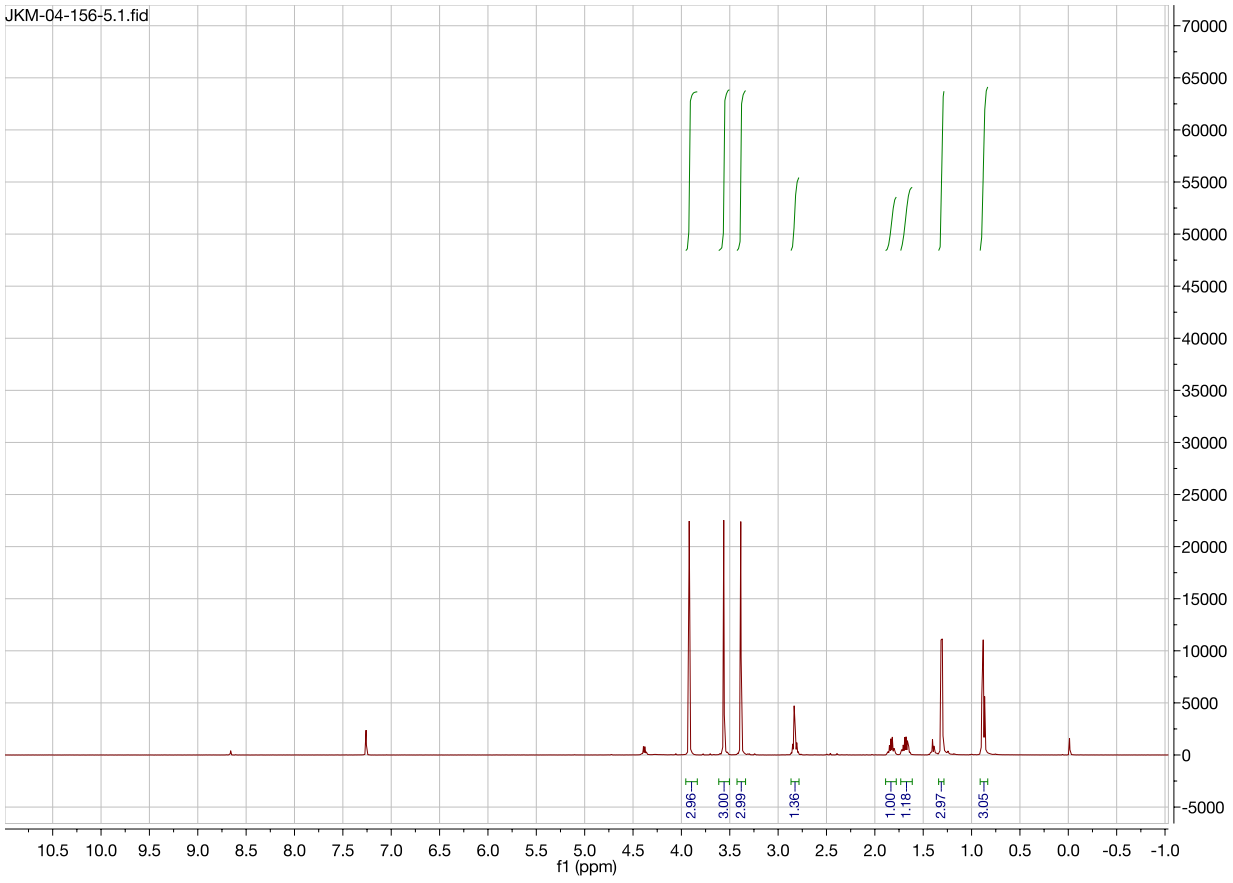

^{13}C NMR ($CDCl_3$, 126 MHz) of 8-(*sec*-butyl)-1,3,7-trimethyl-3,7-dihydro-1*H*-purine-2,6-dione (**4.6.2**)

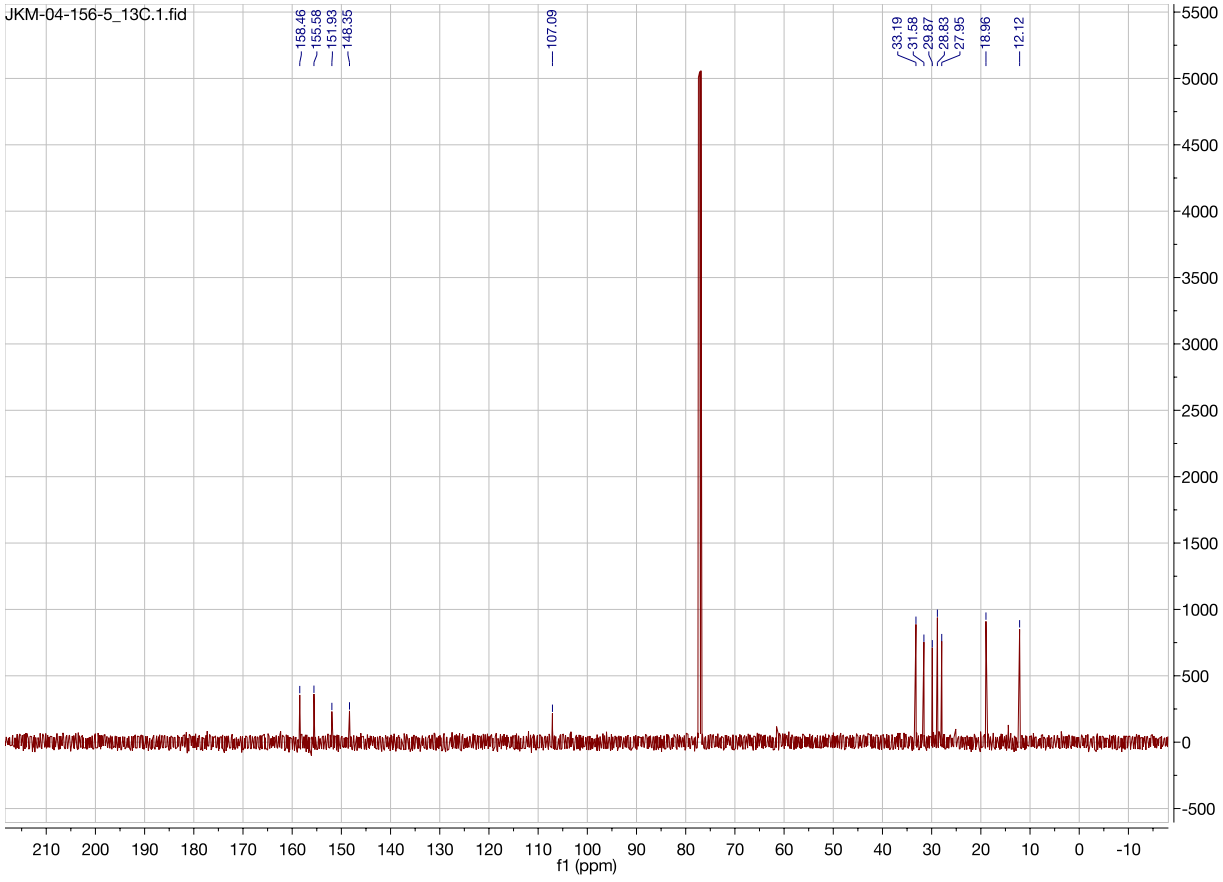

^{1}H NMR ($CDCl_3$, 500 MHz) of (1*S*)-(2-(*sec*-butyl)quinolin-4-yl)((1*S*,2*S*,4*S*,5*R*)-5-vinylquinuclidin-2-yl)methanol (**4.6.3**)

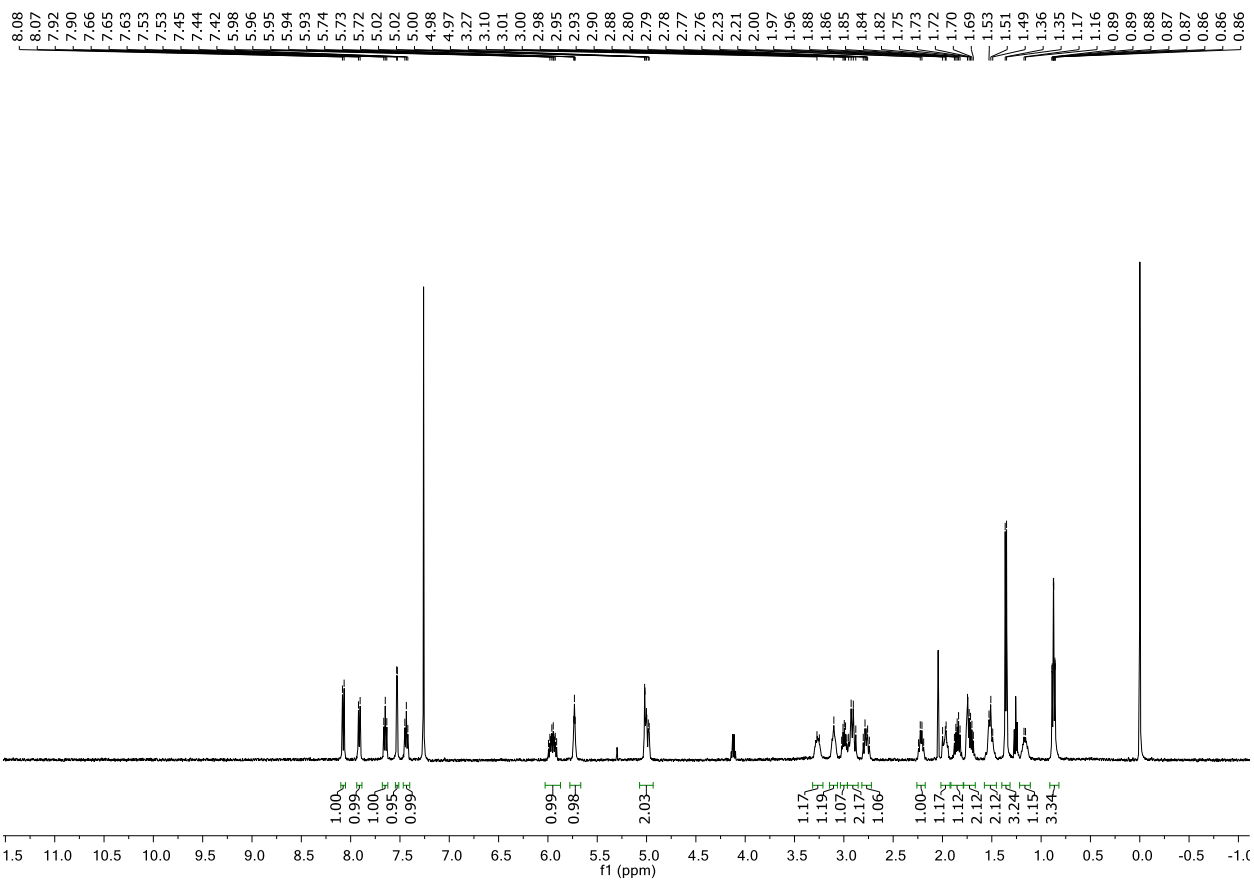

^{13}C NMR ($CDCl_3$, 126 MHz) of (1*S*)-(2-(*sec*-butyl)quinolin-4-yl)((1*S*,2*S*,4*S*,5*R*)-5-vinylquinuclidin-2-yl)methanol (**4.6.3**)

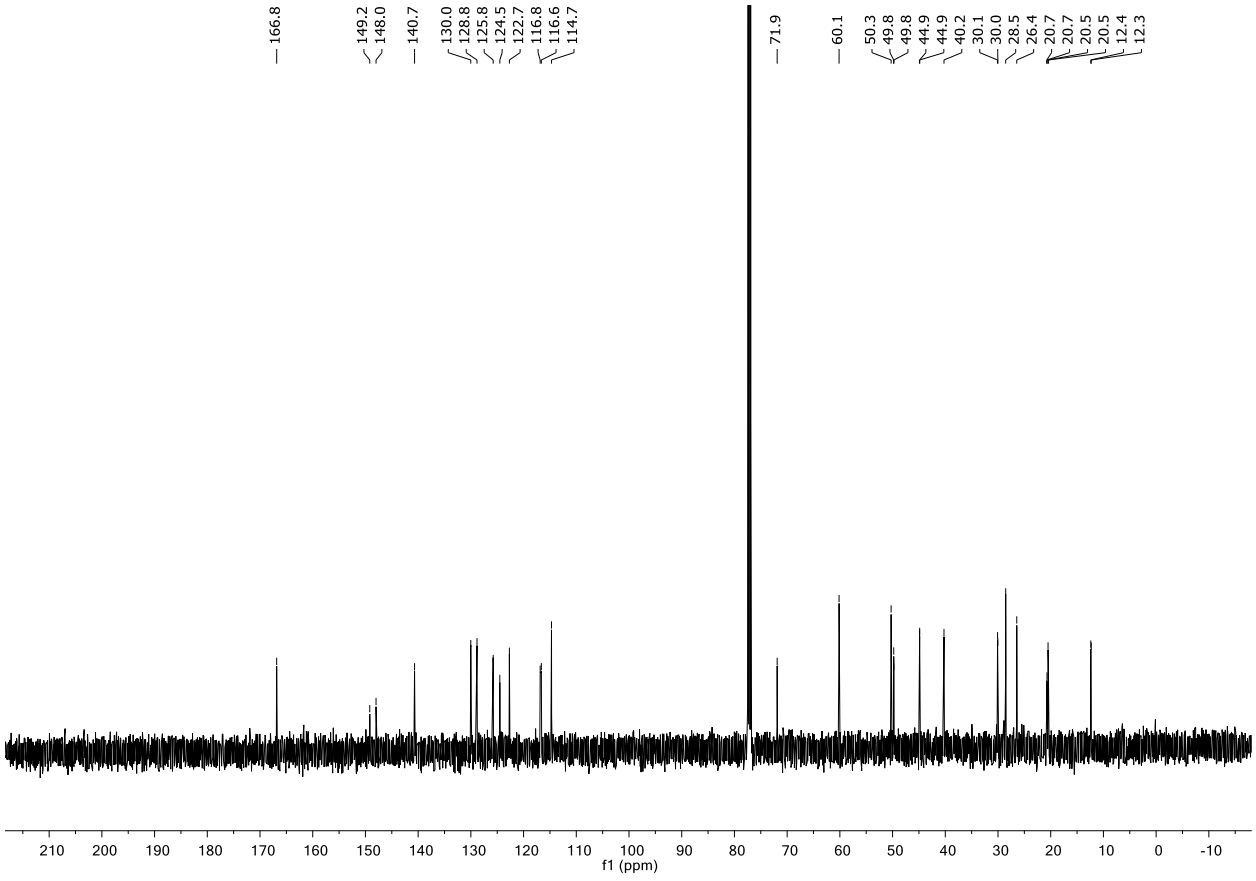

^{1}H NMR ($CDCl_3$, 500 MHz) of (1*R*)-(2-(1-(4-isopropylphenyl)propan-2-yl)-6-methoxyquinolin-4-yl)(5-vinylquinuclidin-2-yl)methanol (**4.6.4.1**)

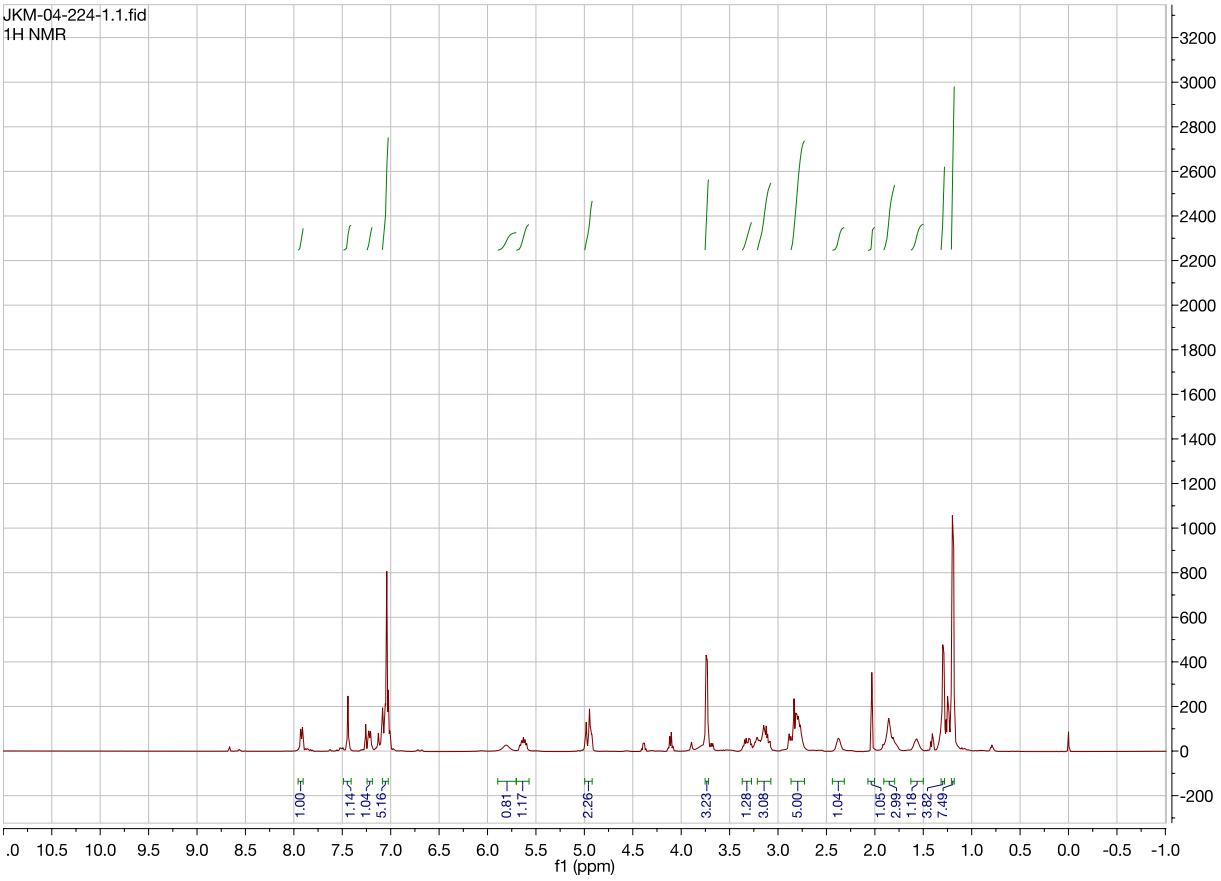

^{13}C NMR ($CDCl_3$, 126 MHz) of (1*R*)-(2-(1-(4-isopropylphenyl)propan-2-yl)-6-methoxyquinolin-4-yl)(5-vinylquinuclidin-2-yl)methanol (**4.6.4.1**)

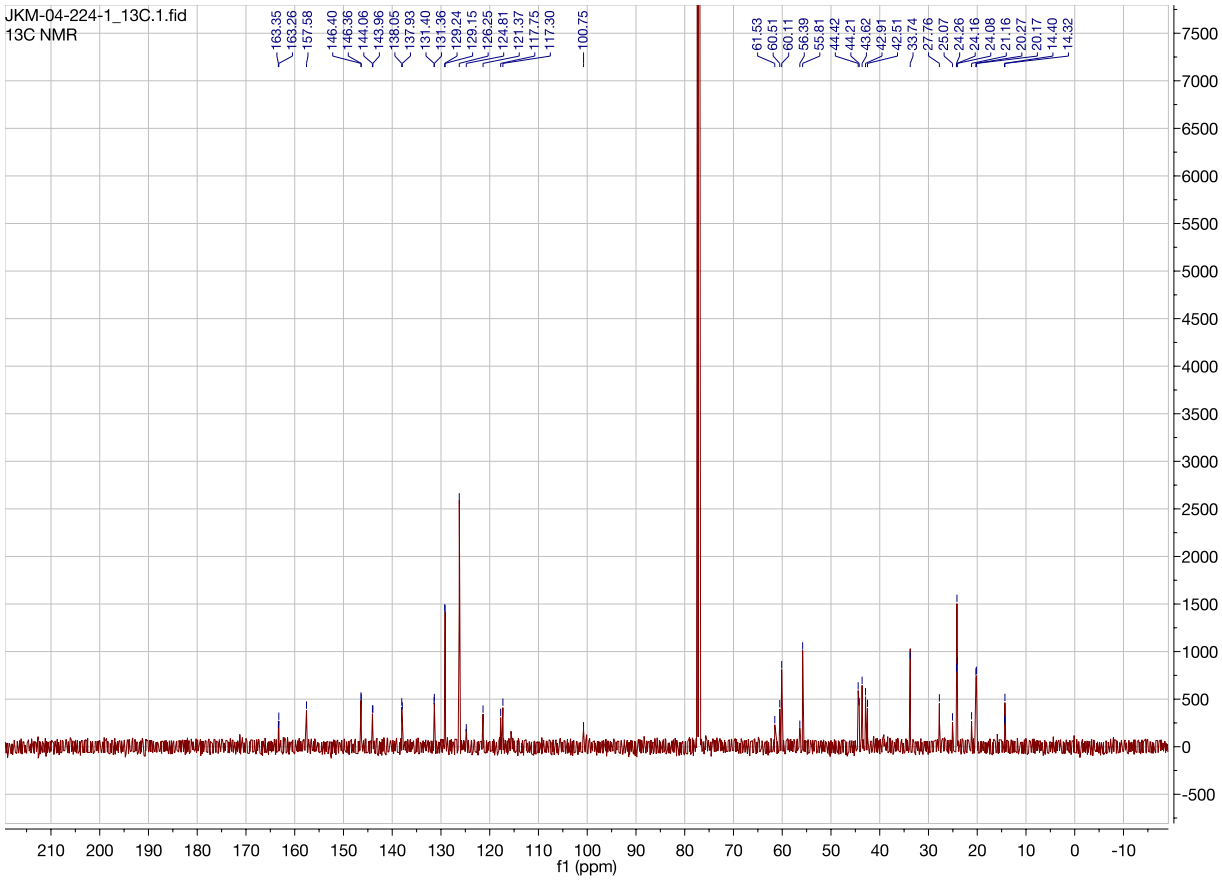

^{1}H NMR ($CDCl_3$, 500 MHz) of 5-((1,4-diazepan-1-yl)sulfonyl)-1-cyclohexylisoquinoline (**4.6.5**)

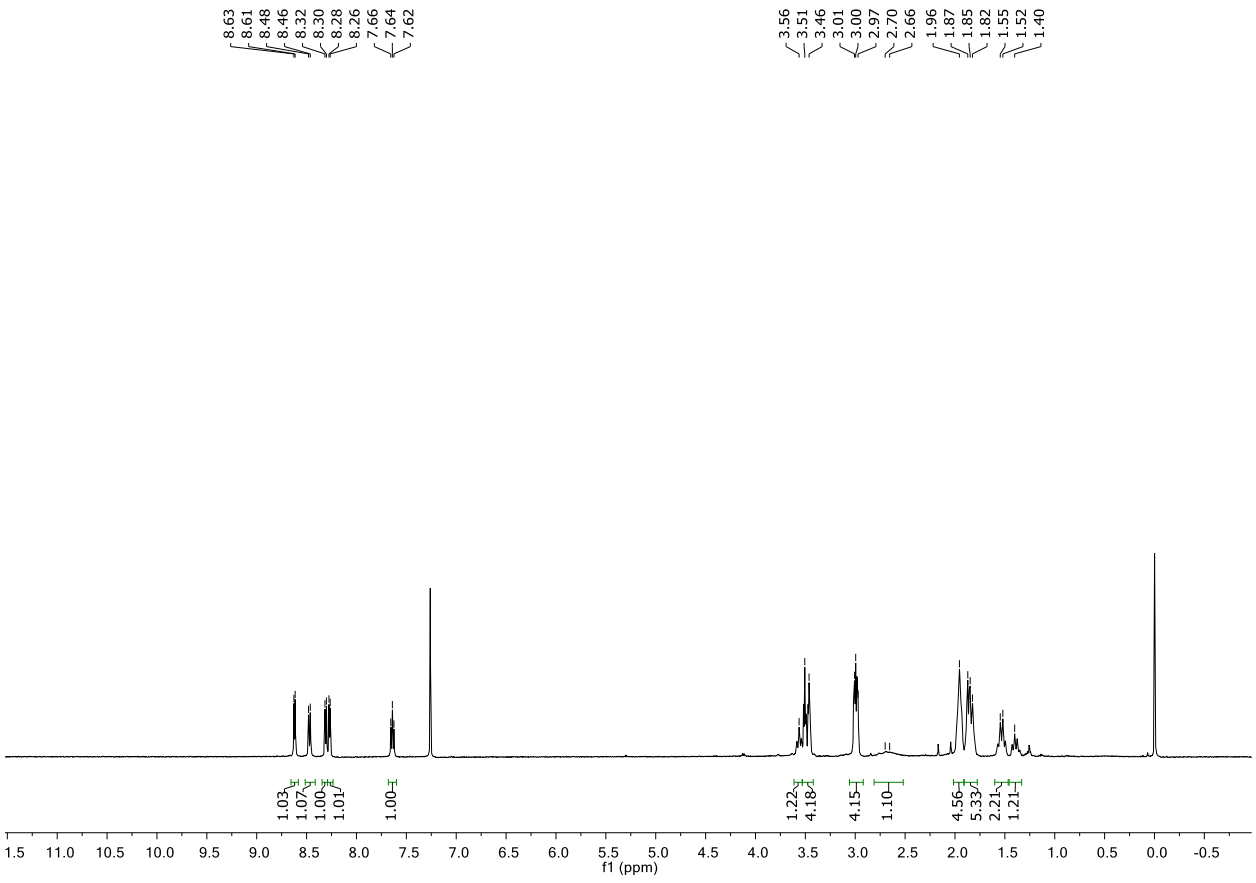

^{13}C NMR ($CDCl_3$, 126 MHz) of 5-((1,4-diazepan-1-yl)sulfonyl)-1-cyclohexylisoquinoline (**4.6.5**)

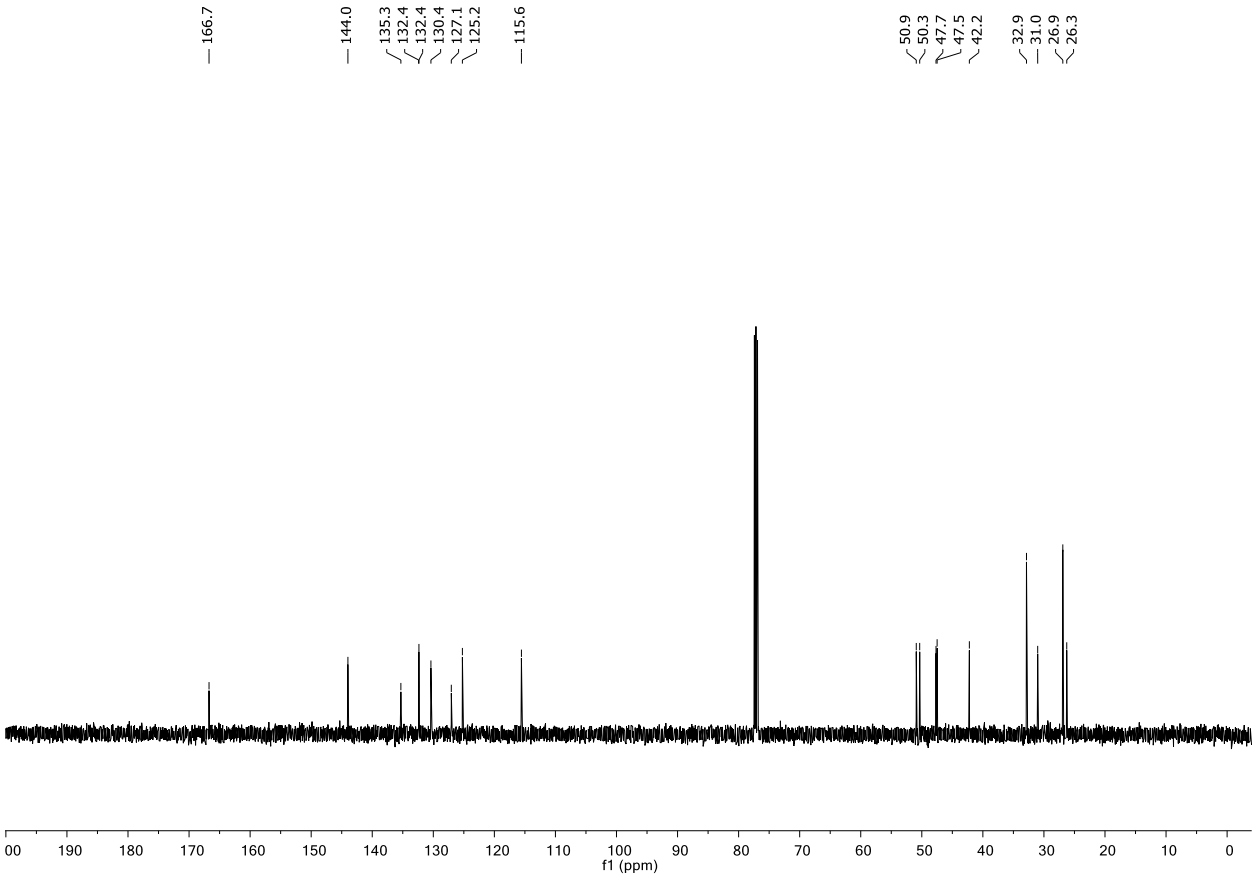

^{1}H NMR ($CDCl_3$, 500 MHz) of 5-((1,4-diazepan-1-yl)sulfonyl)-1-((benzyloxy)methyl)isoquinoline (**4.6.6**)

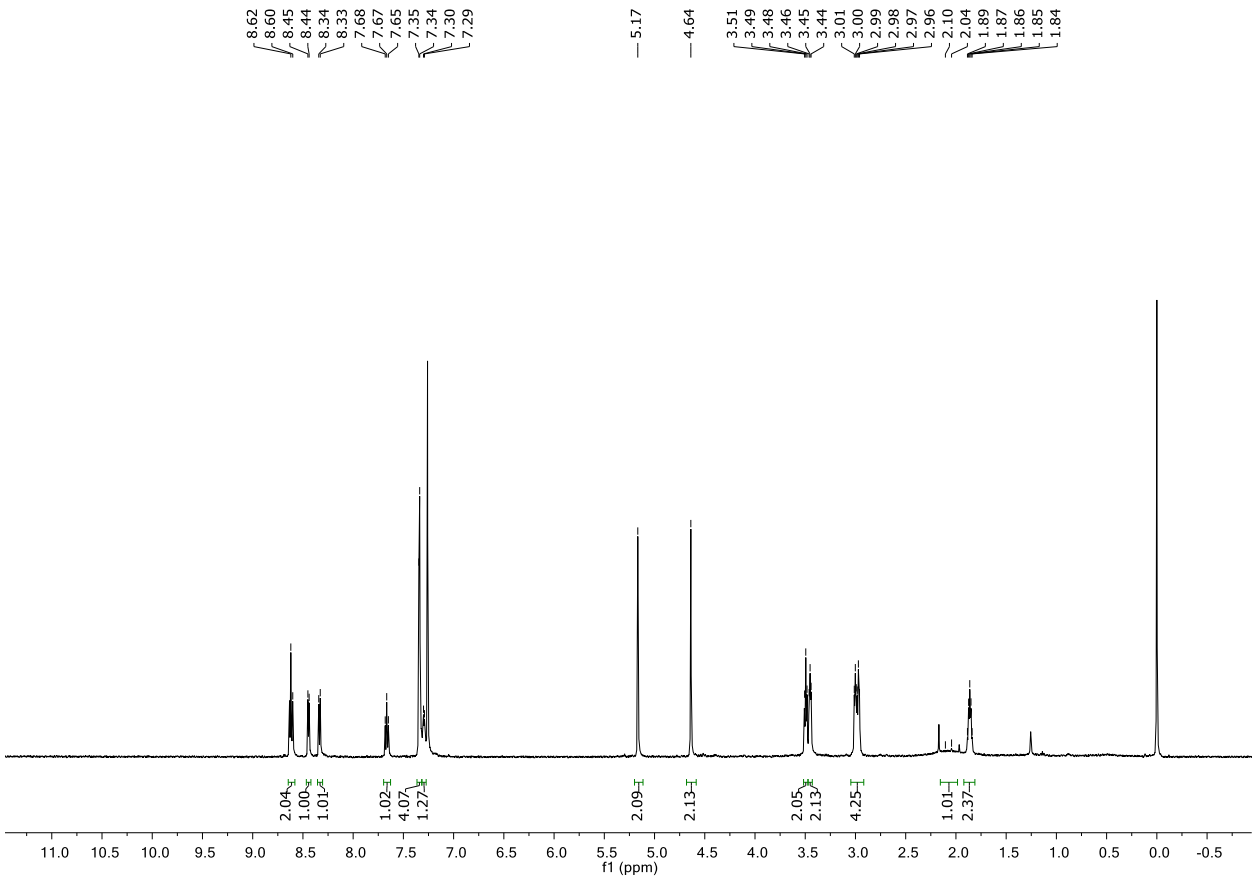

^{13}C NMR ($CDCl_3$, 126 MHz) of 5-((1,4-diazepan-1-yl)sulfonyl)-1-((benzyloxy)methyl)isoquinoline (**4.6.6**)

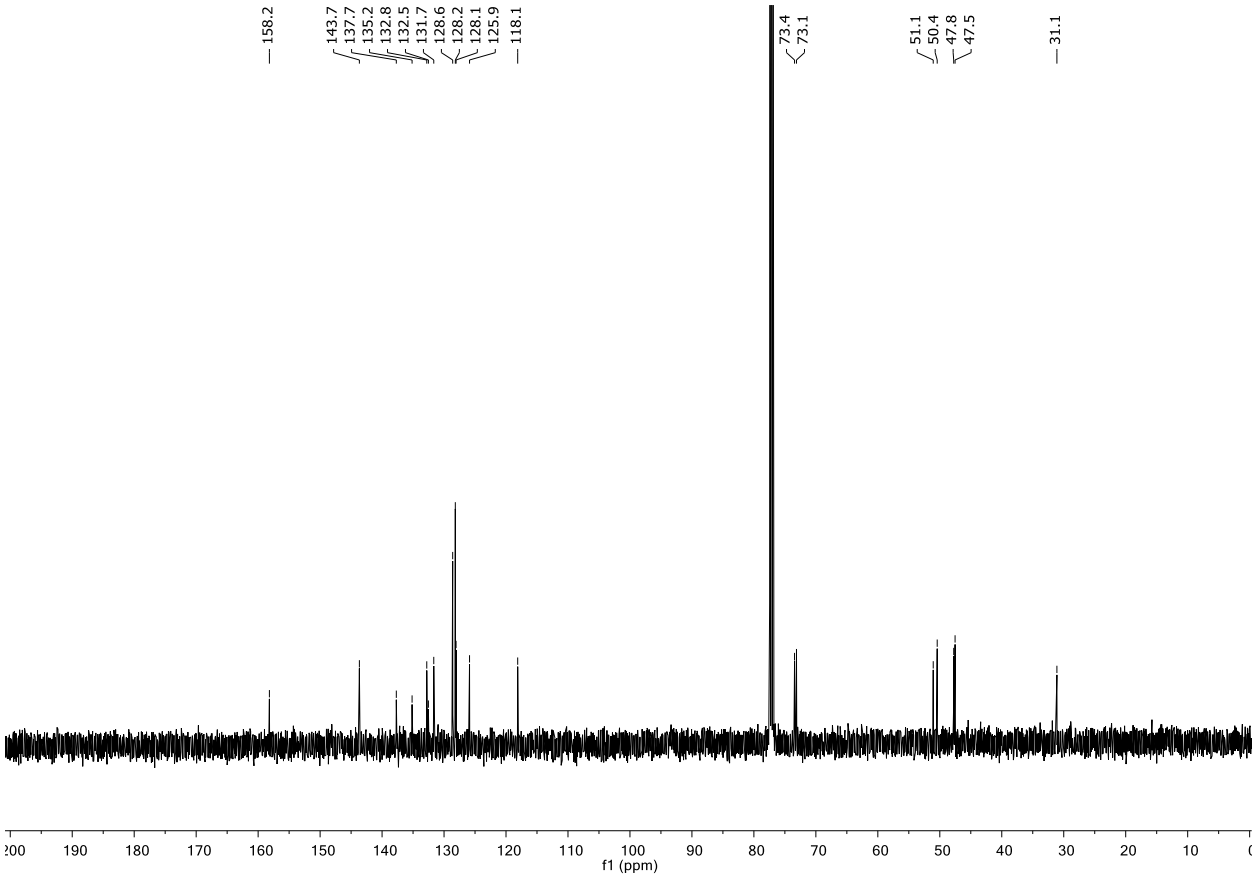

^{1}H NMR ($CDCl_3$, 500 MHz) of (*S*)-11-((benzyloxy)methyl)-4-ethyl-4-hydroxy-1,12-dihydro-14*H*-pyrano[3',4':6,7]indolizino[1,2-*b*]quinoline-3,14(4*H*)-dione (**4.7.1**)

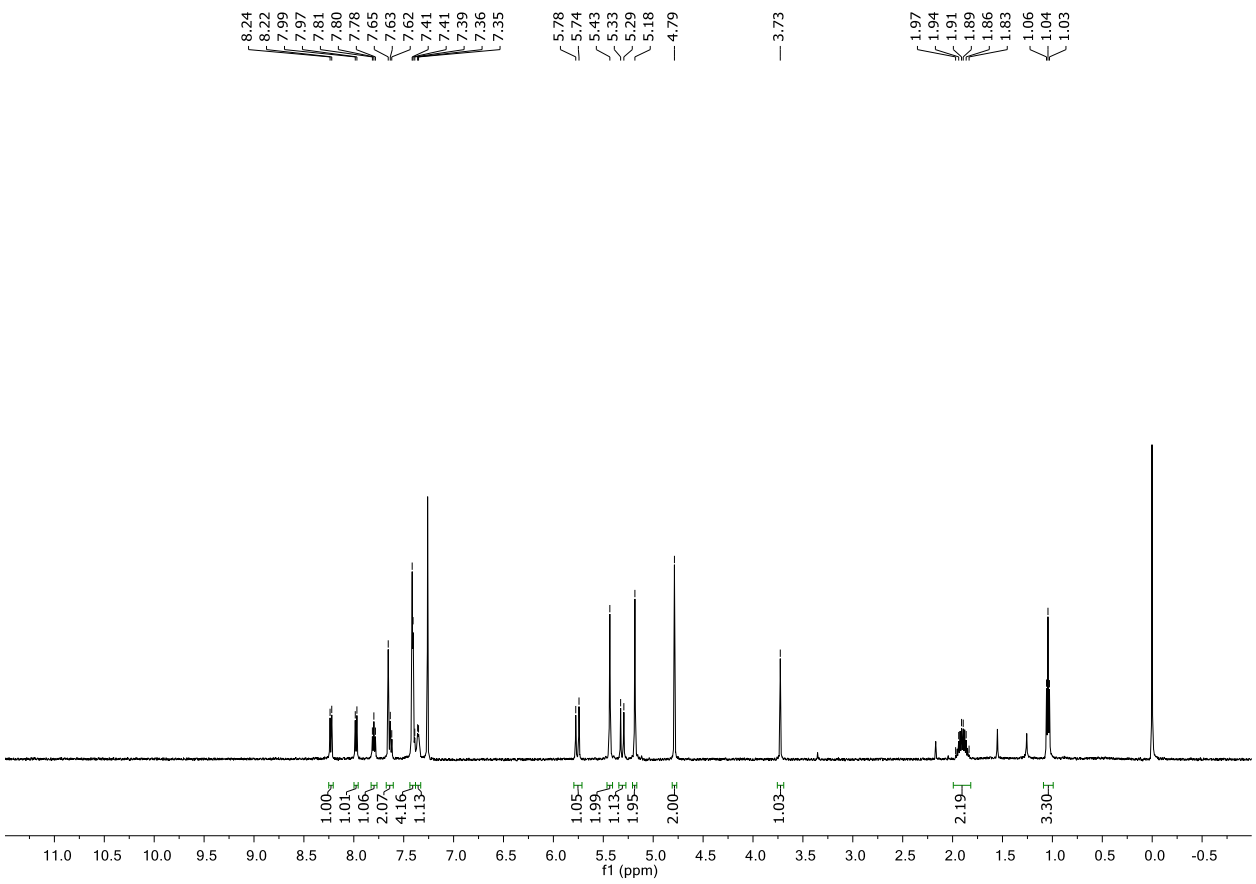

^{13}C NMR ($CDCl_3$, 126 MHz) of (*S*)-11-((benzyloxy)methyl)-4-ethyl-4-hydroxy-1,12-dihydro-14*H*-pyrano[3',4':6,7]indolizino[1,2-*b*]quinoline-3,14(4*H*)-dione (**4.7.1**)

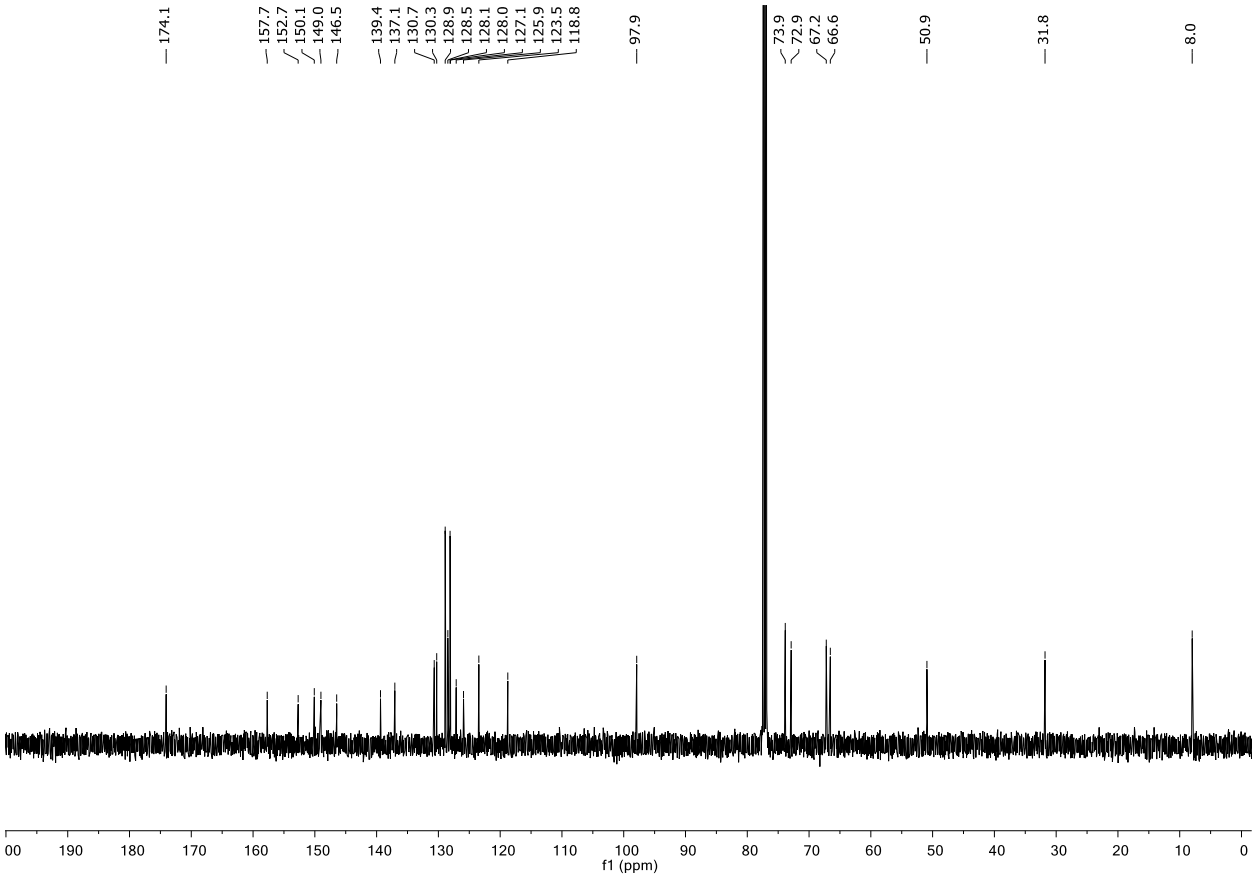

^{1}H NMR ($CDCl_3$, 500 MHz) of 2,5-dimethyl-3-(tetrahydro-2H-pyran-4-yl)cyclohexa-2,5-diene-1,4-dione (**4.7.2**)

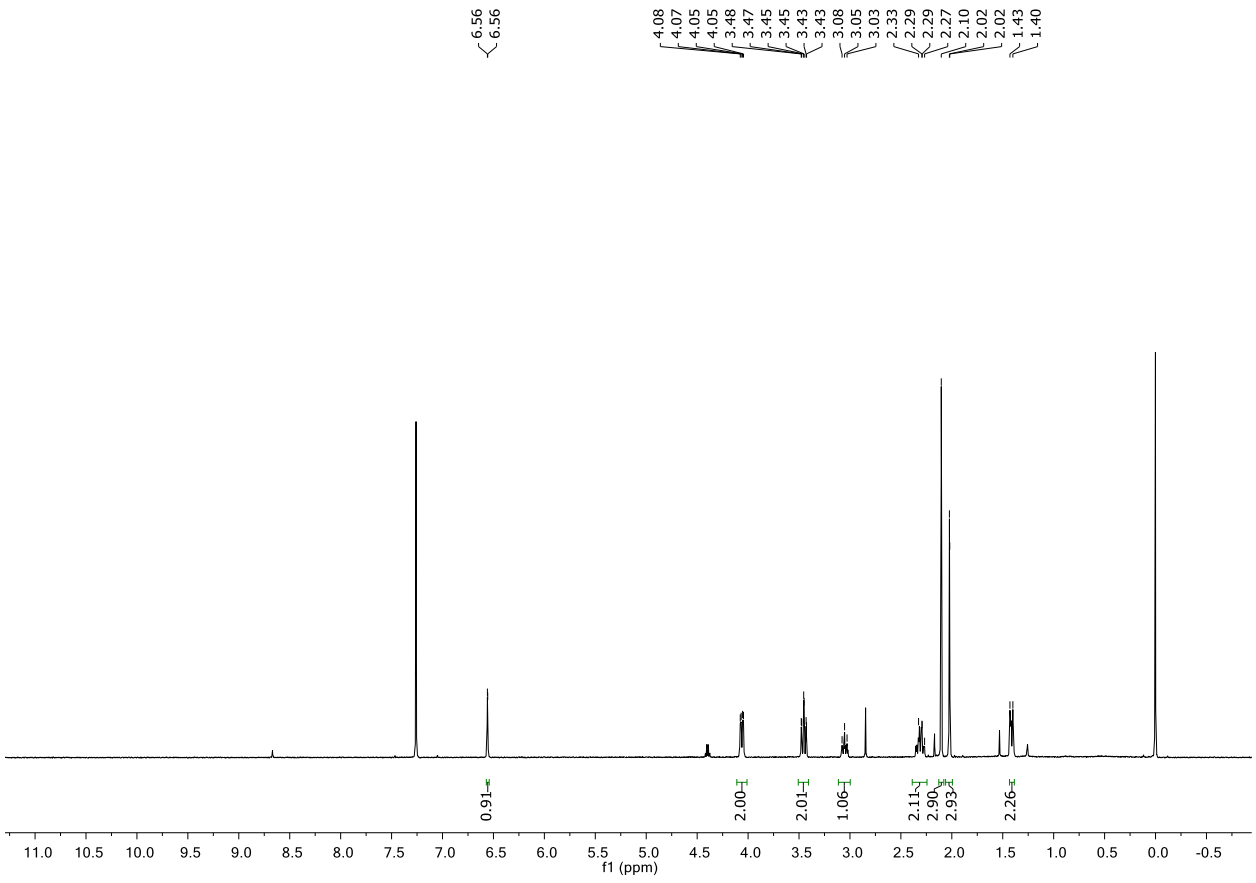

^{13}C NMR ($CDCl_3$, 126 MHz) of 2,5-dimethyl-3-(tetrahydro-2H-pyran-4-yl)cyclohexa-2,5-diene-1,4-dione (**4.7.2**)

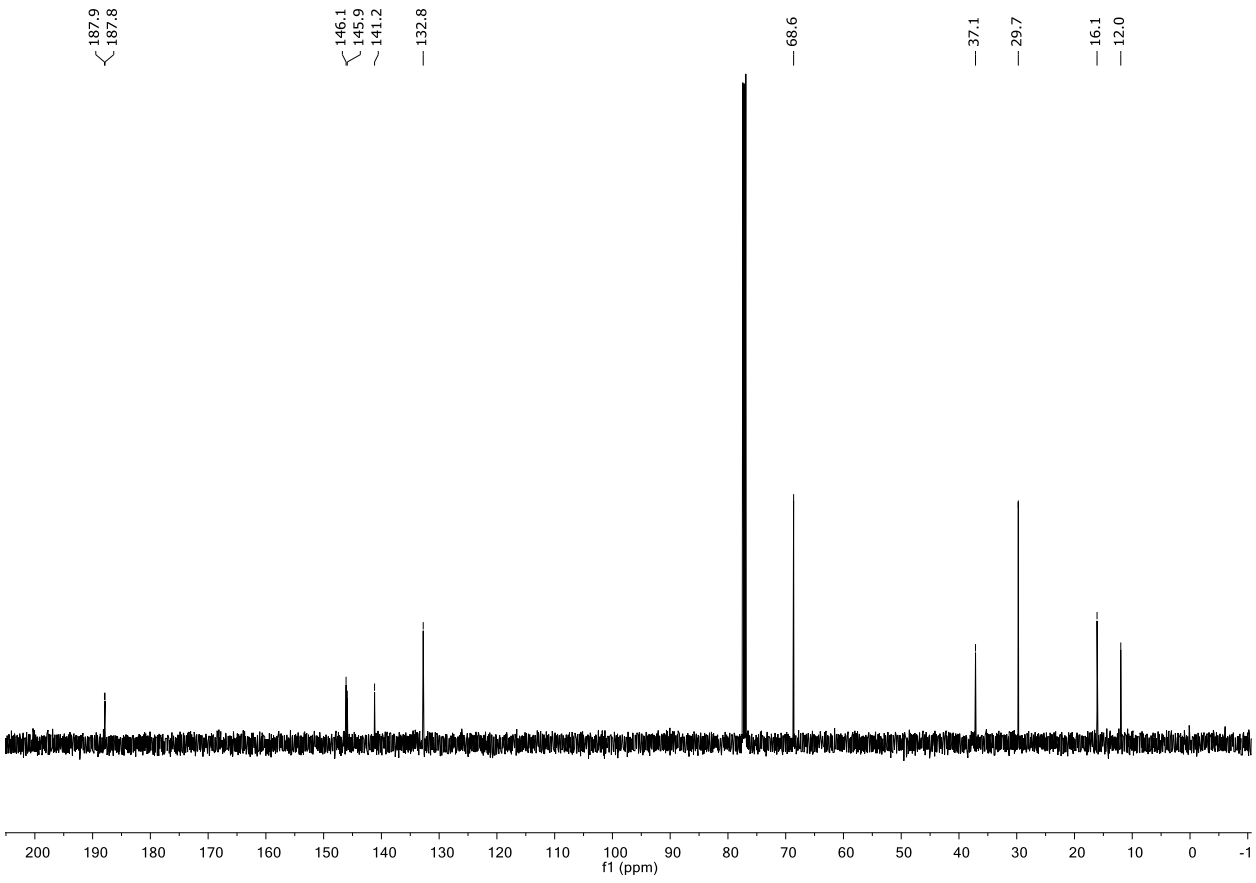

^{1}H NMR ($CDCl_3$, 500 MHz) of 3,4-dimethoxy-6-methyl-[1,1'-bi(cyclohexane)]-3,6-diene-2,5-dione (**4.7.3**)

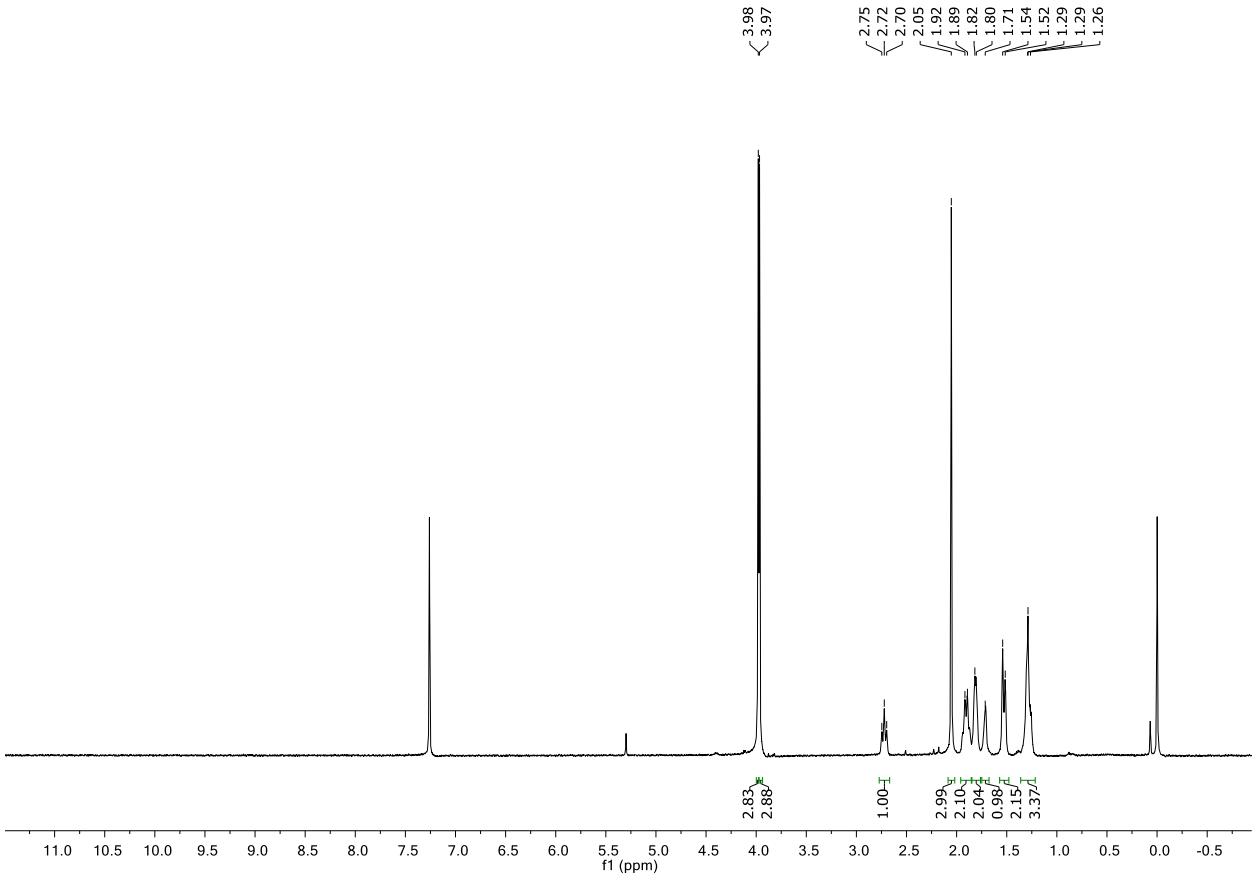

^{13}C NMR ($CDCl_3$, 126 MHz) of 3,4-dimethoxy-6-methyl-[1,1'-bi(cyclohexane)]-3,6-diene-2,5-dione (**4.7.3**)

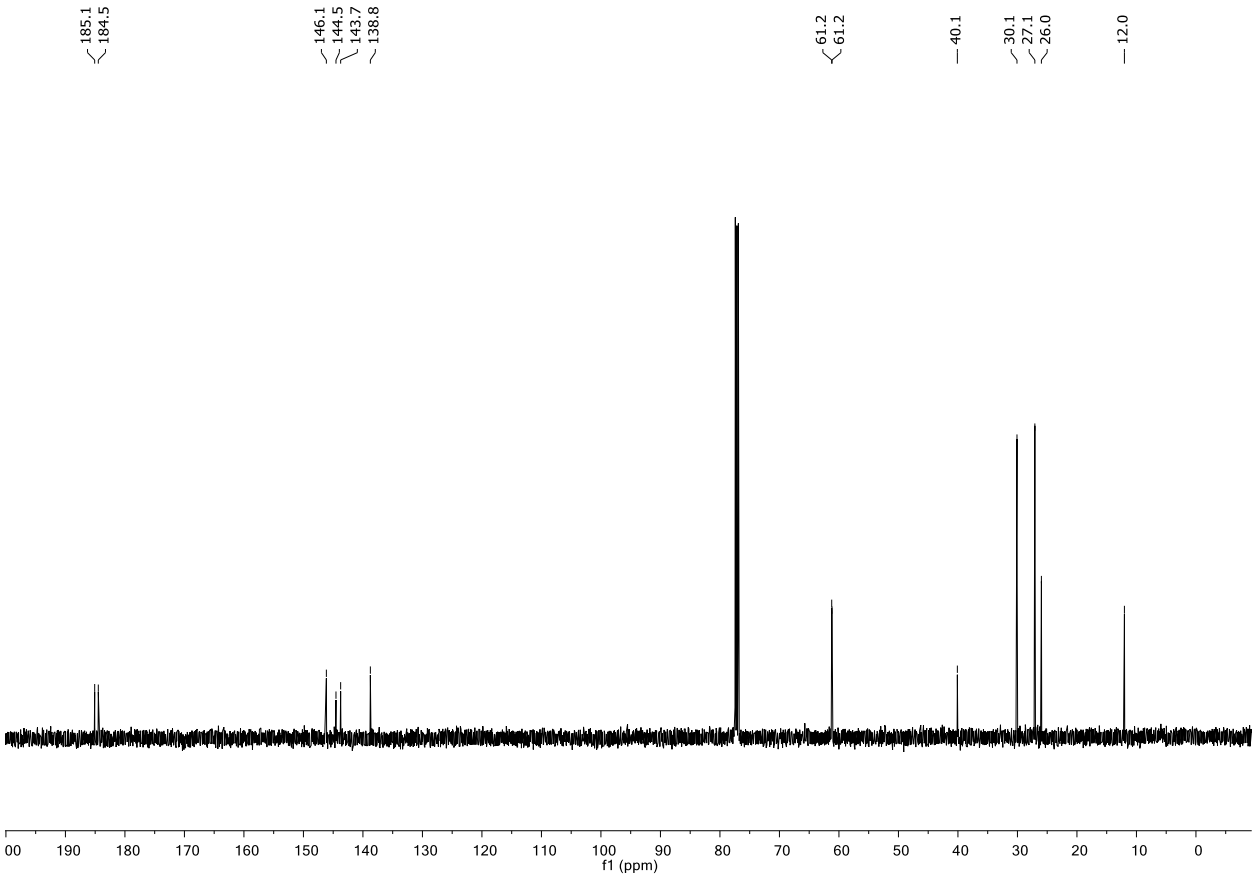

^{1}H NMR ($CDCl_3$, 500 MHz) of 2,3-dimethoxy-5-methyl-6-(6-methylhept-5-en-2-yl)cyclohexa-2,5-diene-1,4-dione (**4.7.3**)

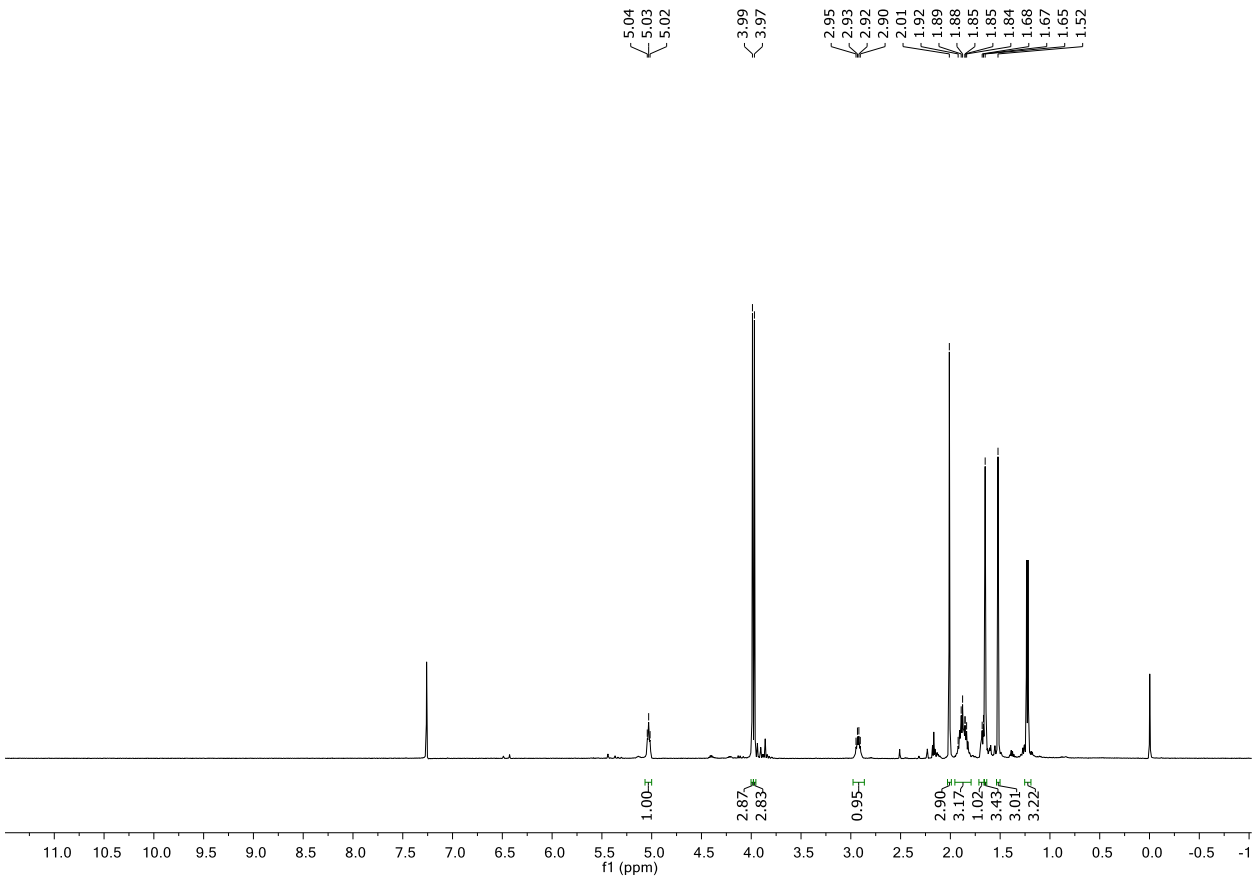

^{13}C NMR ($CDCl_3$, 126 MHz) of 2,3-dimethoxy-5-methyl-6-(6-methylhept-5-en-2-yl)cyclohexa-2,5-diene-1,4-dione (**4.7.3**)

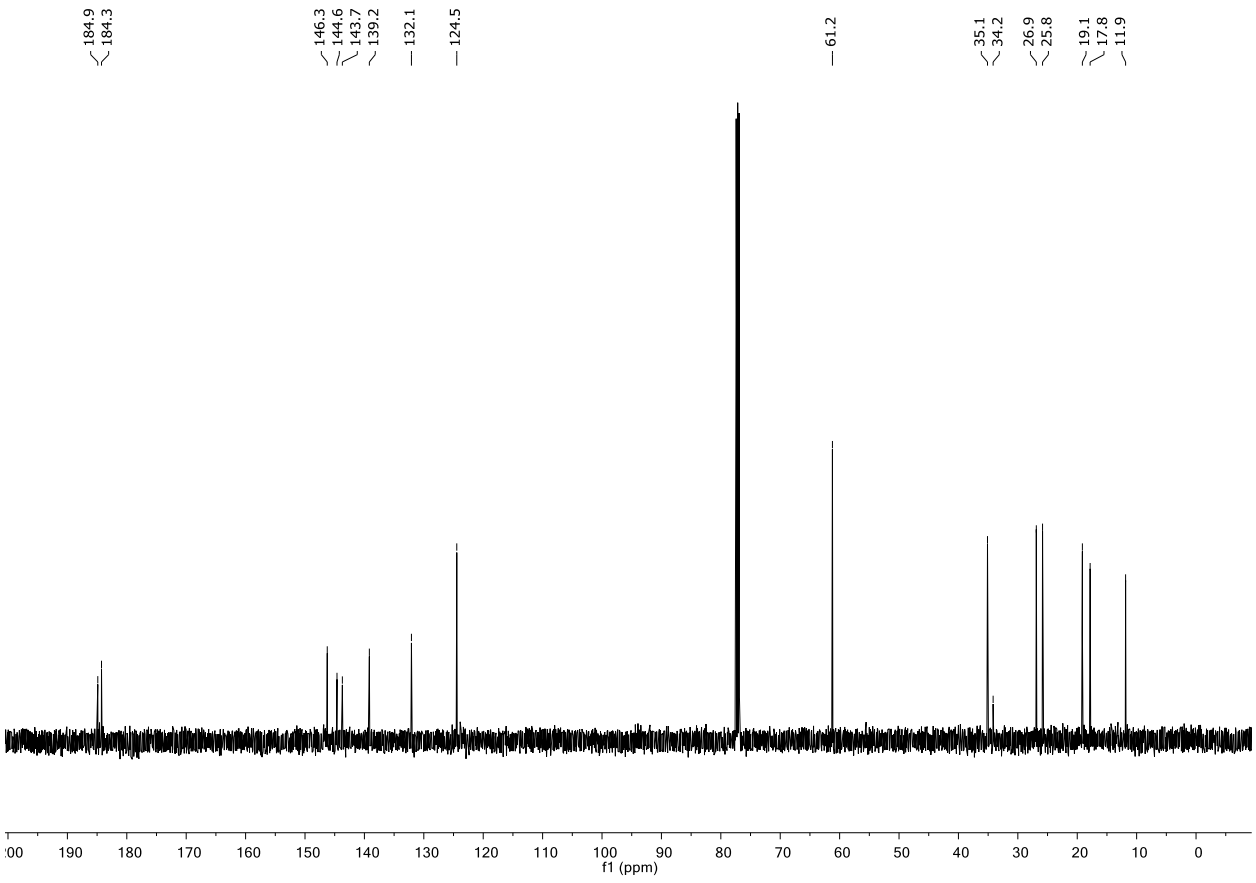

^{1}H NMR ($CDCl_3$, 500 MHz) of 2-(*sec*-butyl)-3-methylnaphthalene-1,4-dione (**4.7.4**)

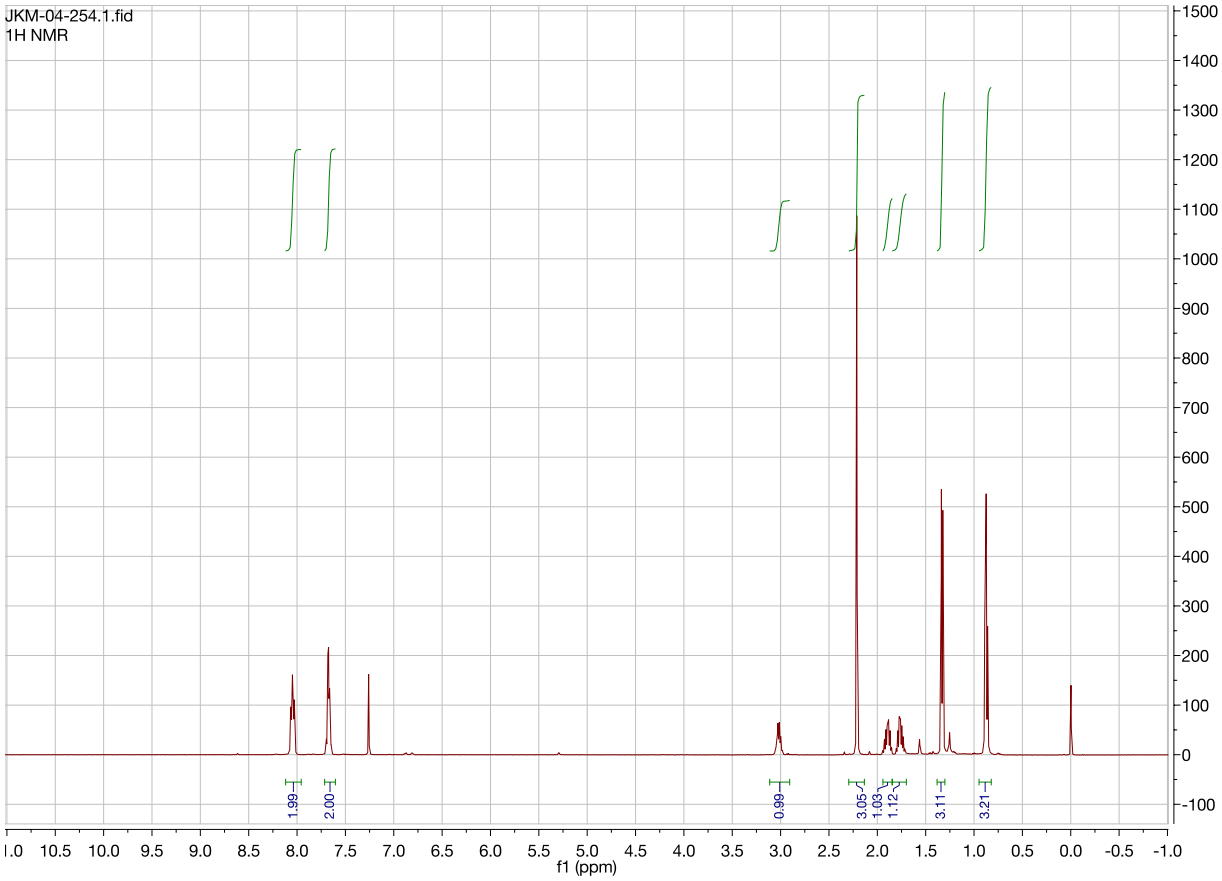

^{13}C NMR ($CDCl_3$, 126 MHz) of 2-(*sec*-butyl)-3-methylnaphthalene-1,4-dione (**4.7.4**)

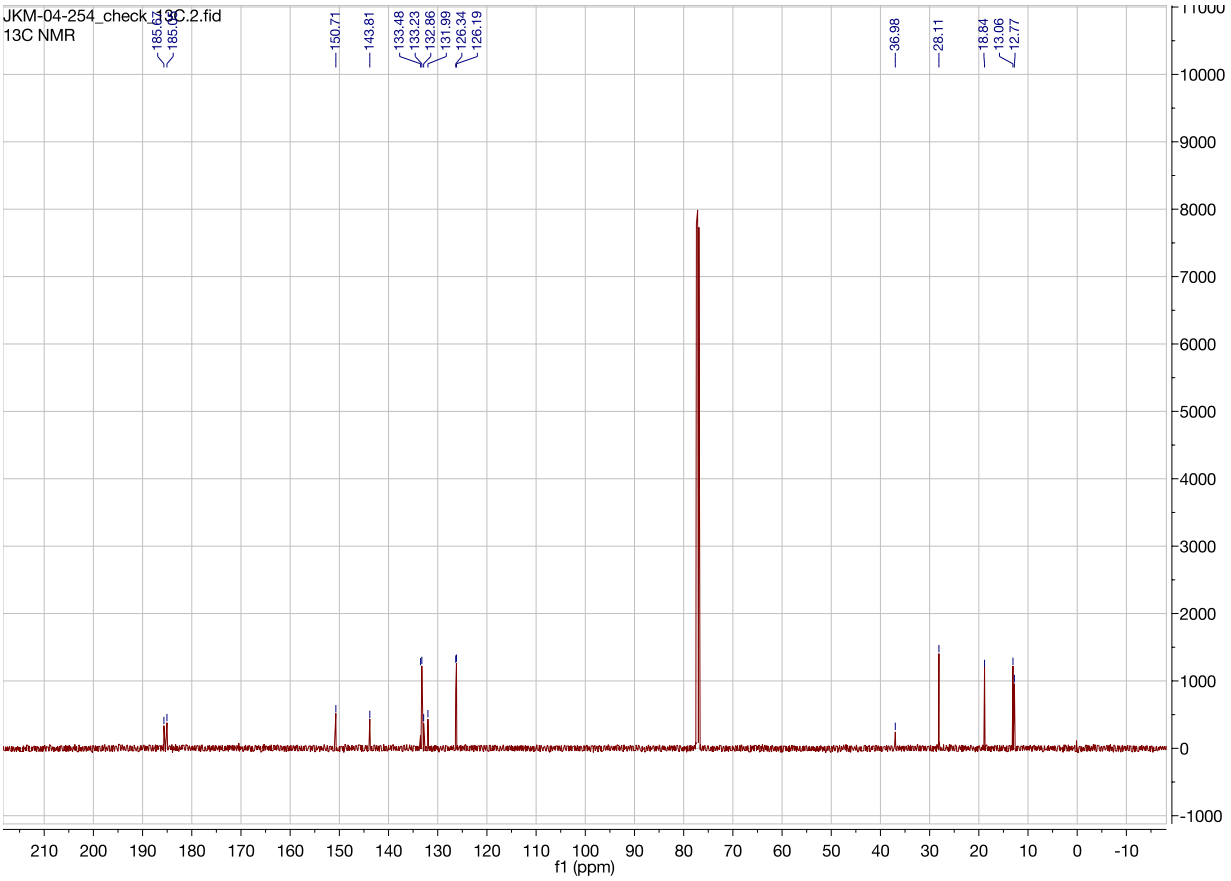

^{1}H NMR ($CDCl_3$, 500 MHz) of 2-cyclohexyl-3-hydroxynaphthalene-1,4-dione (Parvaquone, **4.7.5**)

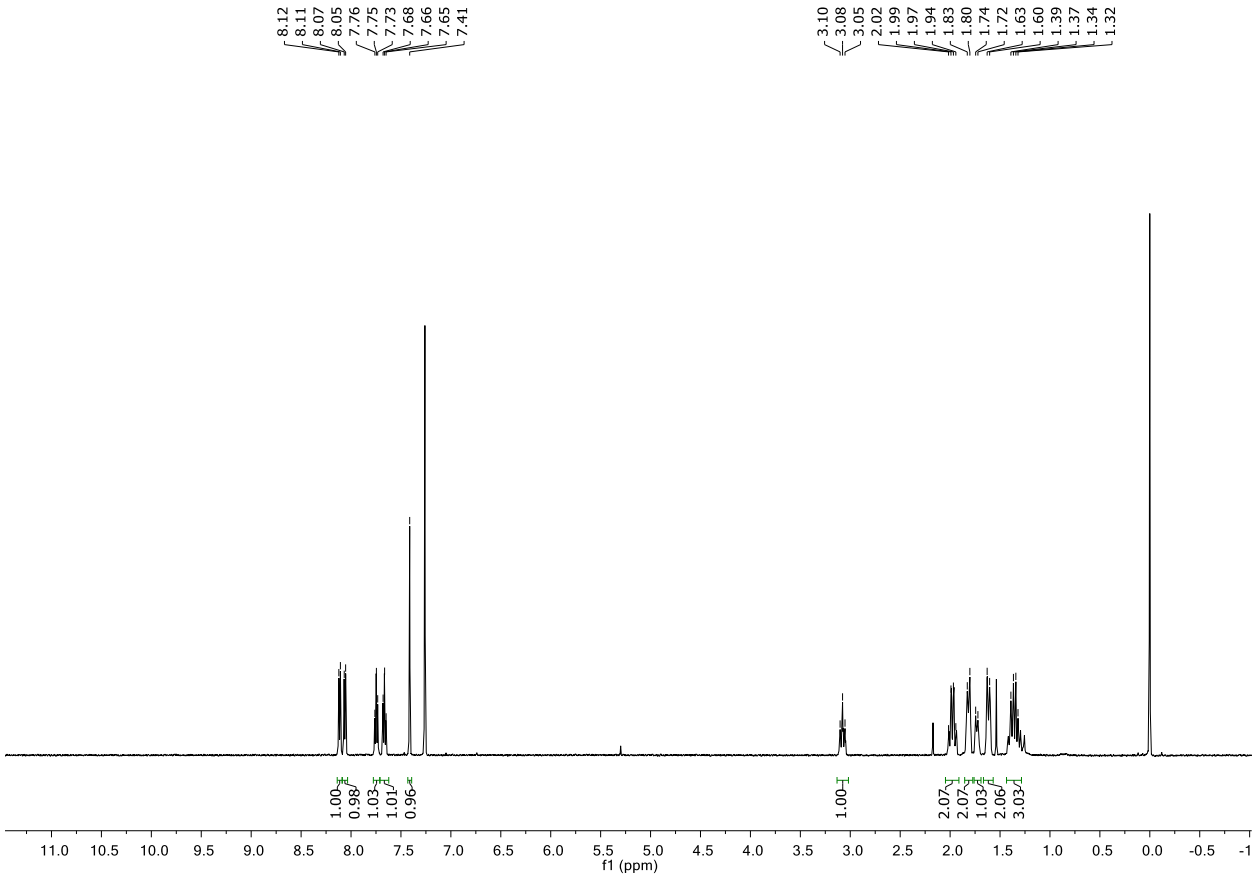

^{13}C NMR ($CDCl_3$, 126 MHz) of 2-cyclohexyl-3-hydroxynaphthalene-1,4-dione (Parvaquone, **4.7.5**)

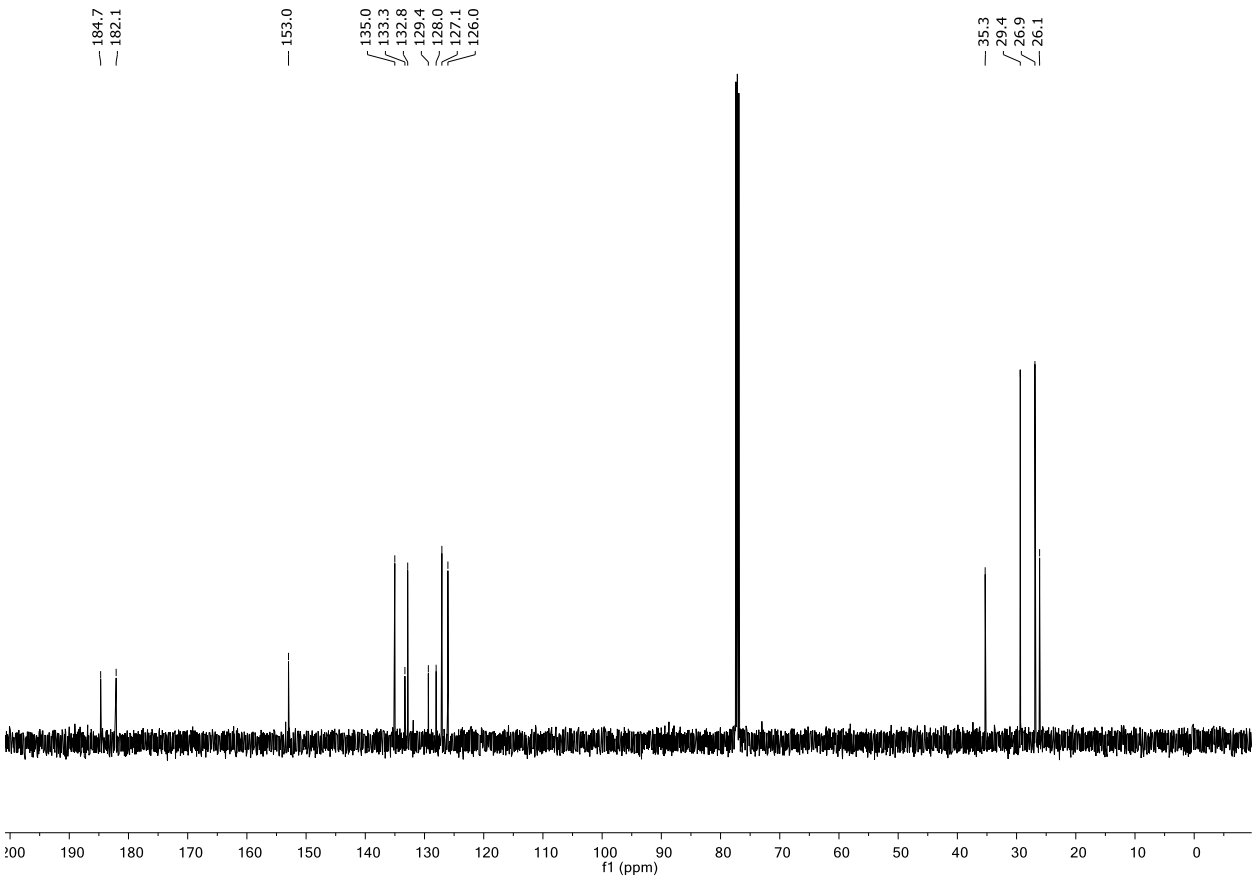

^{1}H NMR ($CDCl_3$, 500 MHz) of 2-[4-(4-chlorophenyl)cyclohexyl]-3-hydroxy-1,4-naphthalenedione (Atovaquone, **4.7.6**)

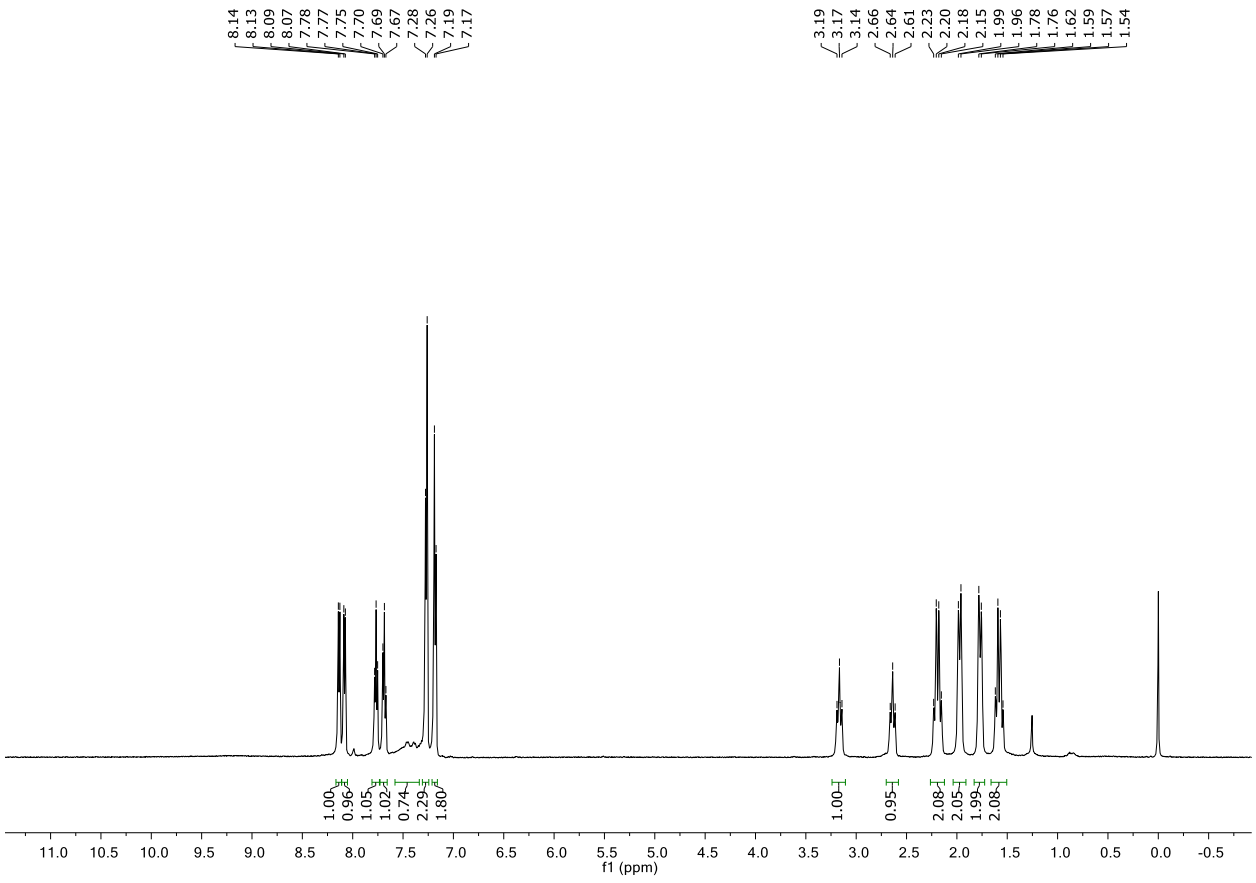

^{13}C NMR ($CDCl_3$, 126 MHz) of 2-[4-(4-chlorophenyl)cyclohexyl]-3-hydroxy-1,4-naphthalenedione (Atovaquone, **4.7.6**)

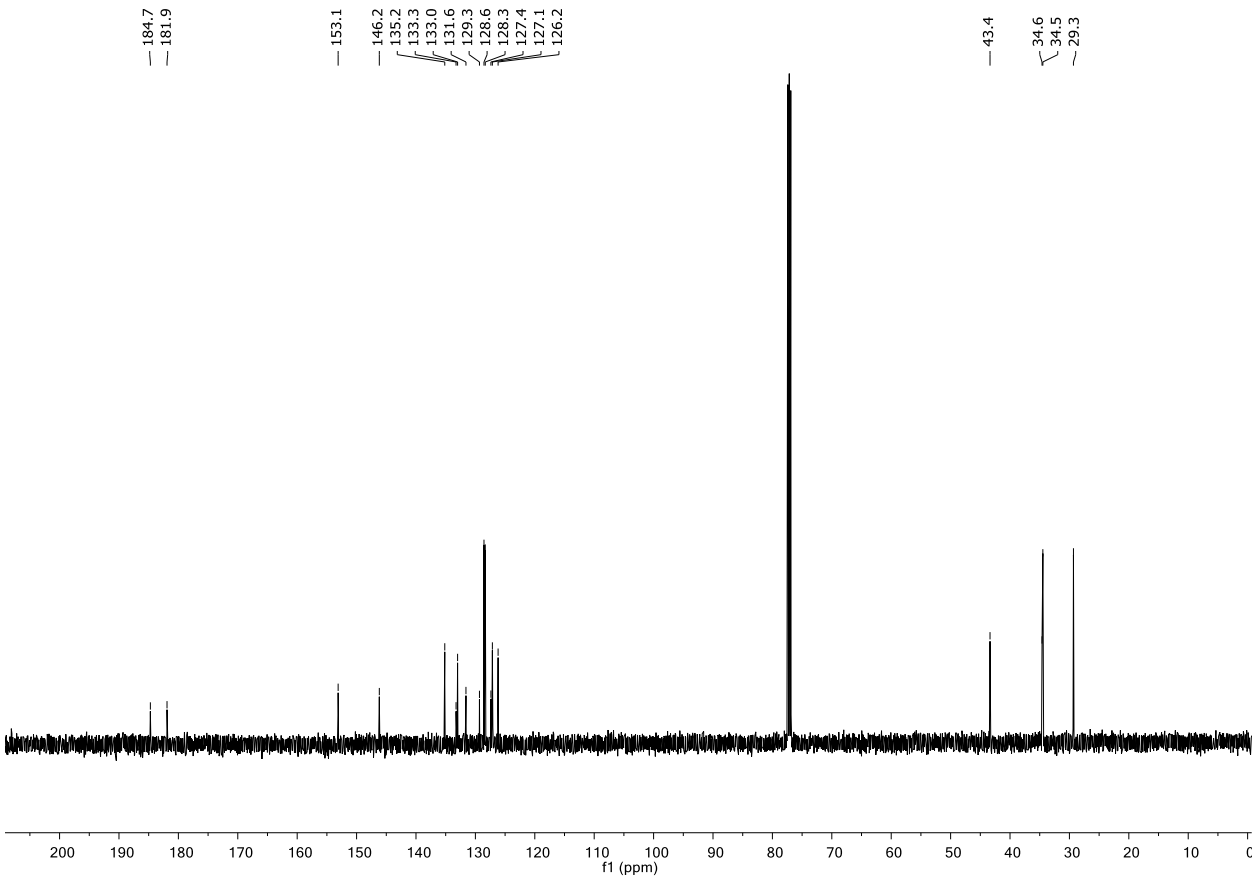

^{1}H NMR ($CDCl_3$, 500 MHz) of 4-hydroxyquinazoline-2-*d* (**1a-*d***)

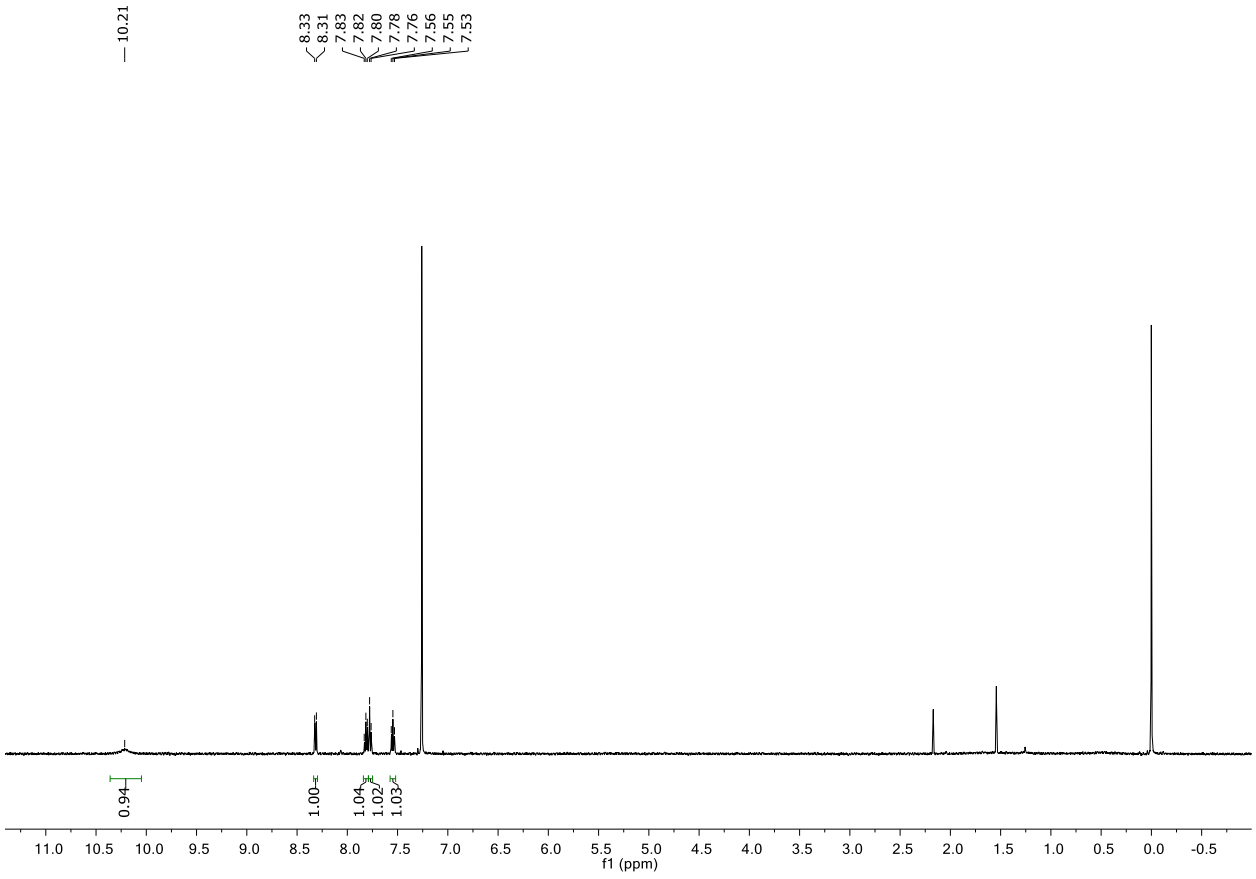

^{13}C NMR ($CDCl_3$, 126 MHz) of 4-hydroxyquinazoline-2-*d* (**1a-*d***)

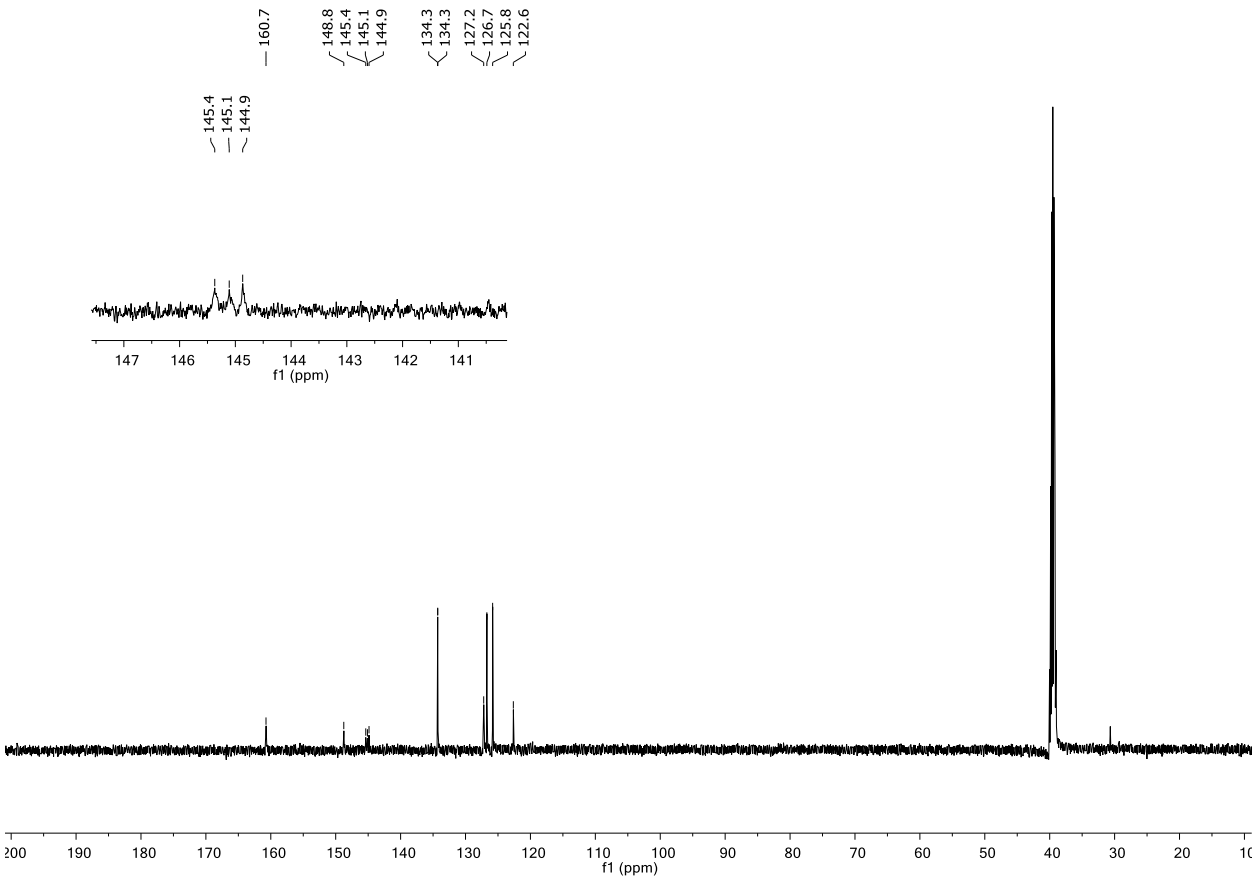

^{1}H NMR (DMSO-d_6, 500 MHz) of 2-isopropyl-2,3-dihydroquinazolin-4(1H)-one (**6a**)

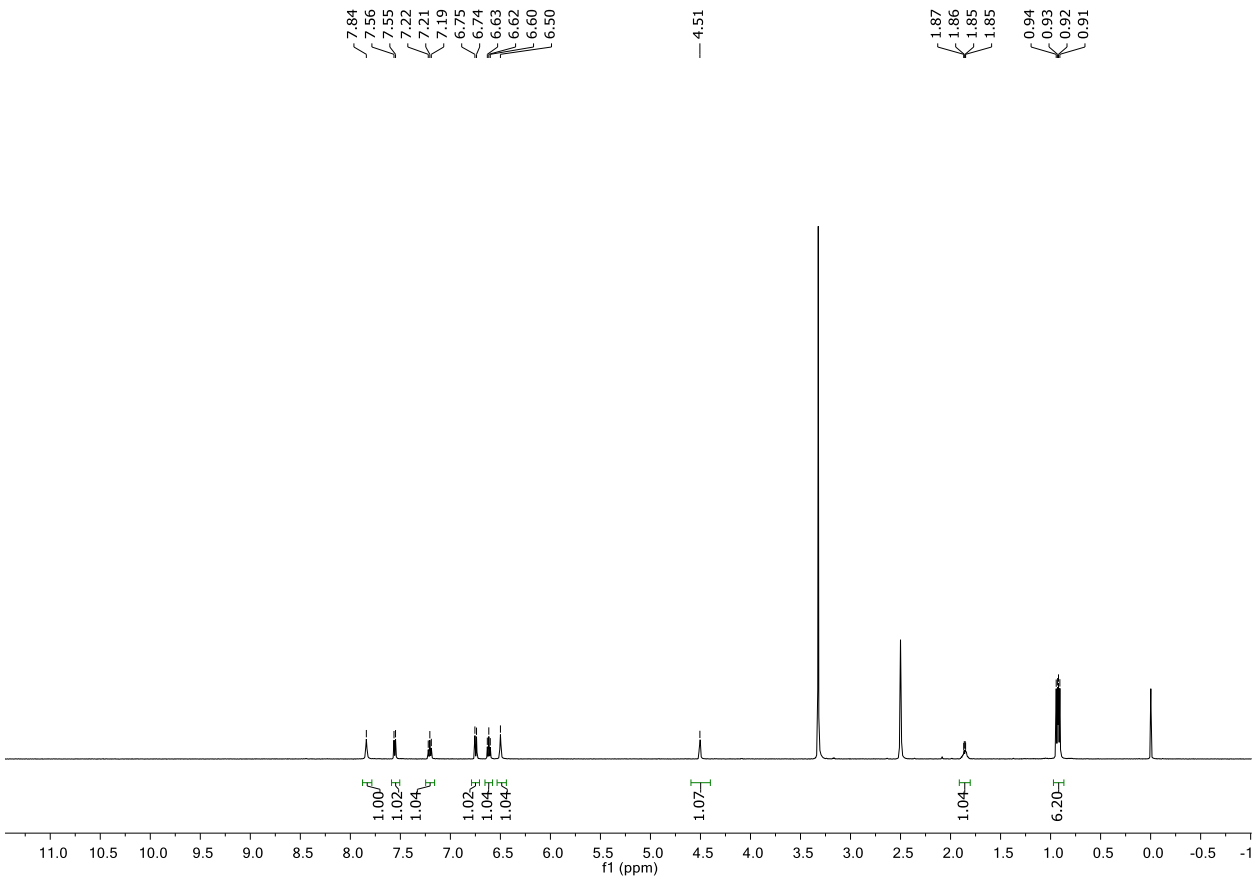

^{13}C NMR ($CDCl_3$, 126 MHz) of 2-isopropyl-2,3-dihydroquinazolin-4(1H)-one (**6a**)

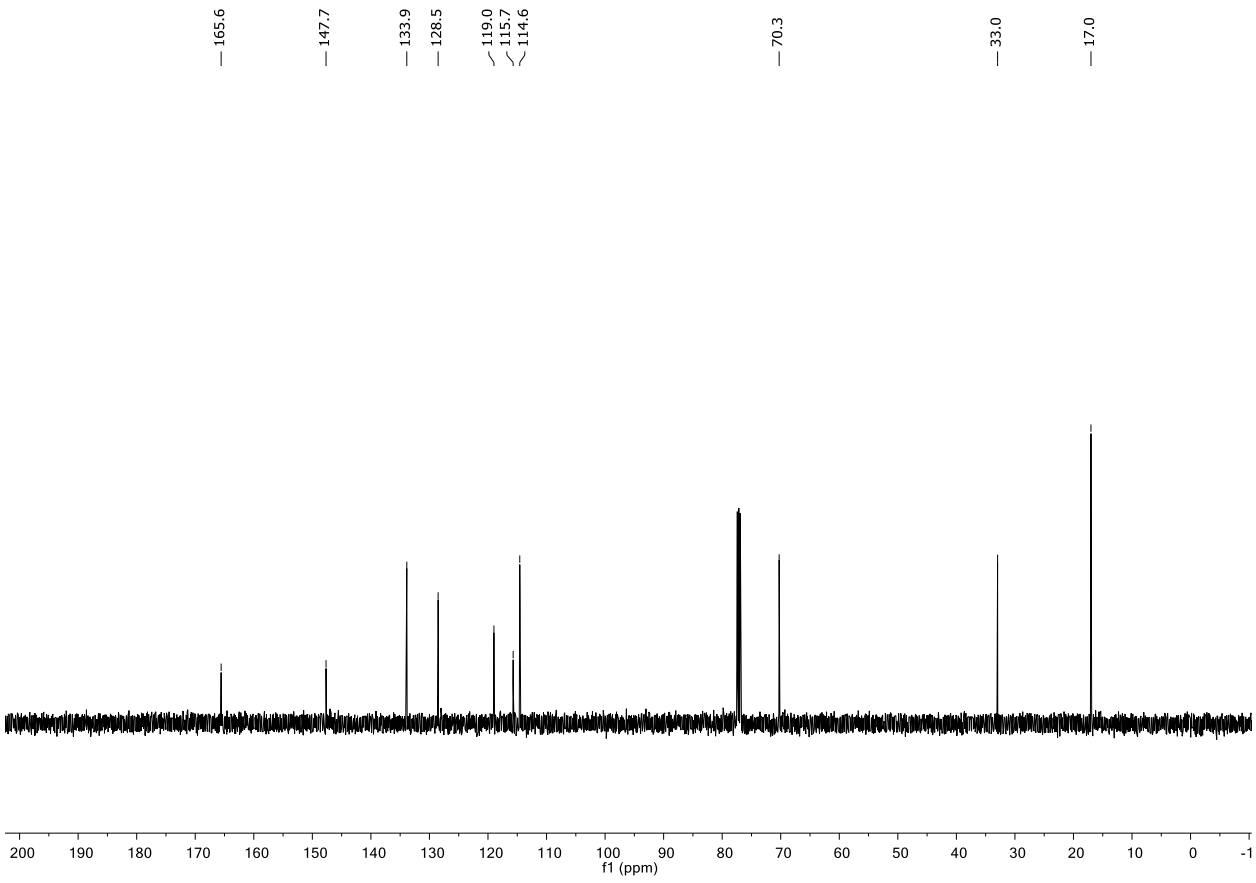

^{1}H NMR ($CDCl_3$, 500 MHz) of 4-isopropyl-2,6-dimethyl-1,4-dihydropyridine-3,5-dicarboxylate-1-*d* (**2a-*d***)

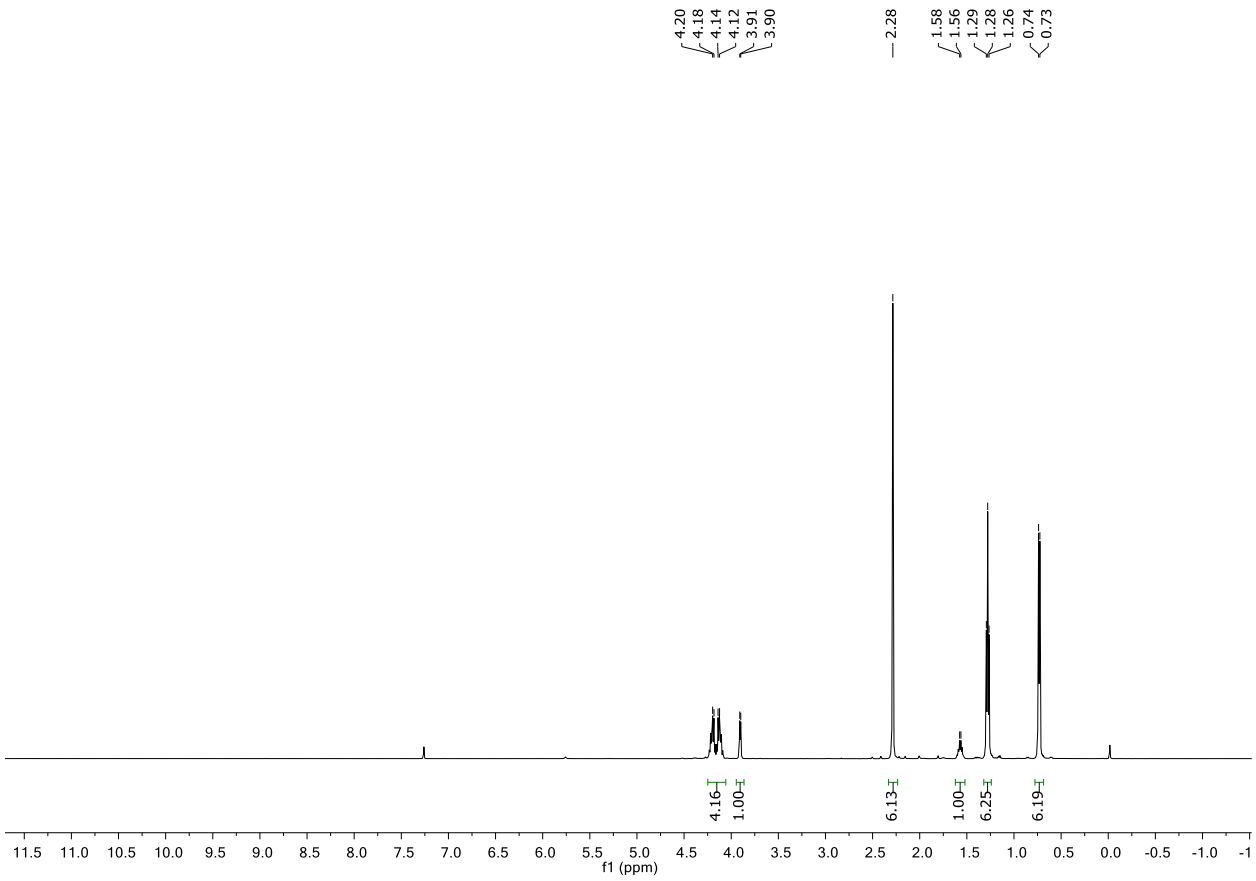

^{13}C NMR ($CDCl_3$, 126 MHz) of 4-isopropyl-2,6-dimethyl-1,4-dihydropyridine-3,5-dicarboxylate-1-*d* (**2a-*d***)

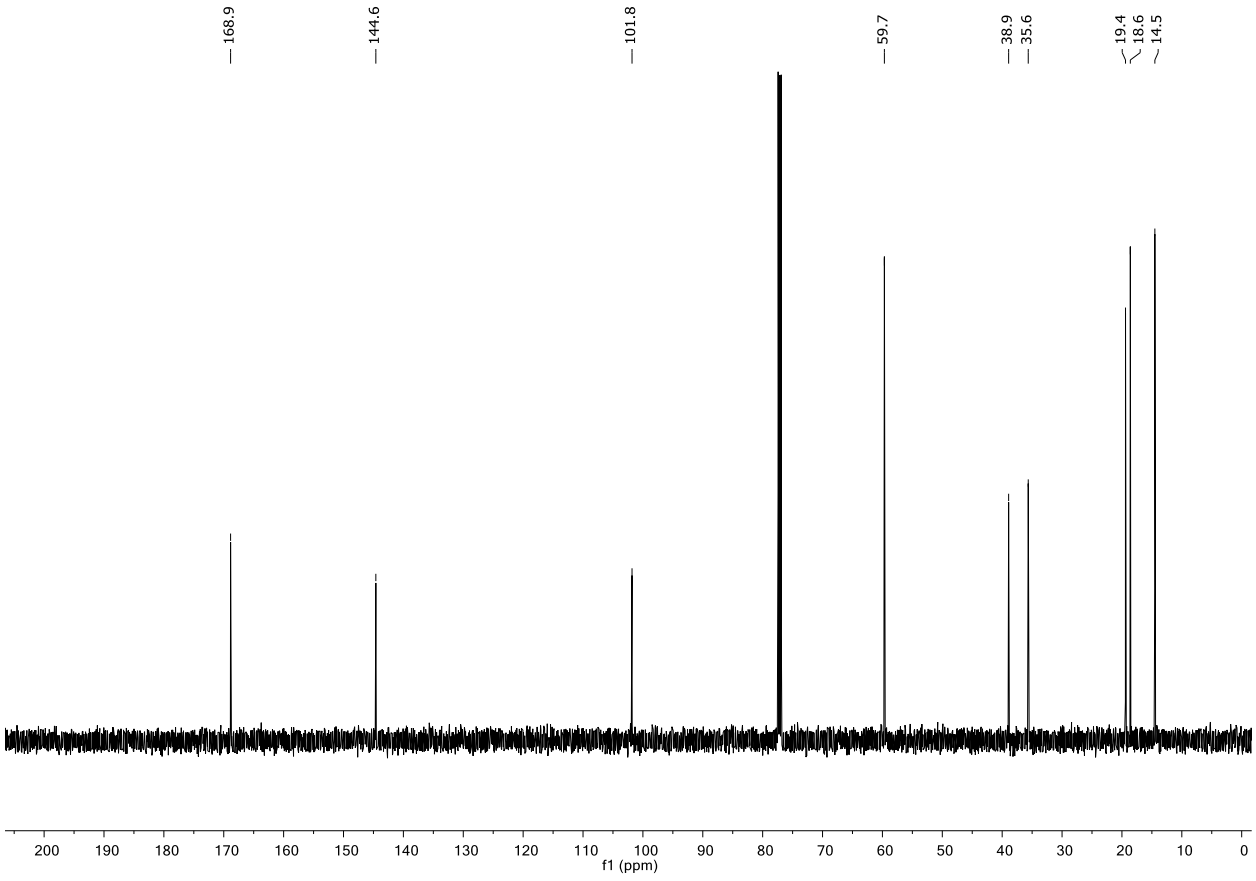

Chapter 5. C–H Alkylation of Heteroarenes *via* Photoredox Catalysis

5.1 Introduction

Over the past 15 years, the number of known flavanones has increased significantly, to the point of where they can be considered a class of their own, alongside the related flavones.[1†] Flavanones are readily found in nature (e.g., citrus fruits), and their role in flavonoid biosynthetic pathways has been extensively studied.[2] Chalcone cores are typically the biosynthetic precursors to flavanones (Figure 5.1), accessed through a cyclization of the reactive chalcone moiety. In turn, flavanone cores are intermediates in the synthesis of a wide range of flavonoids (Figure 5.1).[3] Because of the natural abundance of the flavonoids, many practical uses for these materials have been explored. For decades, flavanones and flavonoids have been used as dietary supplements and also as potent therapeutic agents (e.g., as antianxiety agents[2c] and inhibitors of HIV-1 reverse transcriptase[4]). Additionally, substituted flavones have recently been used as fluorescent scaffolds.[5]

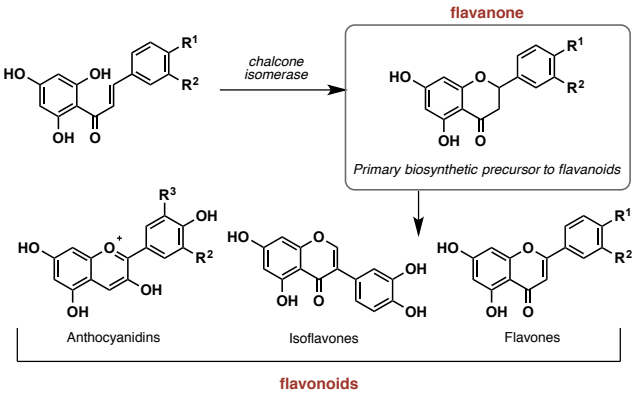

Figure 5.1. Biosynthetic pathways for flavonoid synthesis.

† Reproduced in part from Matsui, J. K.; Molander, G. A. *Org. Lett.* **2017**, *19*, 950.

Currently, the primary synthetic route to access functionalized flavanones has traversed through chalcones, in analogy to the biosynthetic pathway.[6] Although there have been robust methods developed, synthesis of the chalcone precursor is not necessarily straightforward. Limitations become even more apparent when attempting to move to more complex cores. As a result, there have been significant efforts devoted toward alternative synthetic routes. For example, the Porco group disclosed a vinylogous addition to specifically functionalized chromones, synthesizing a variety of chromanone butenolides (Figure 5.2, eq 1).[7] The Stoltz group also published a palladium-catalyzed conjugate addition of arylboronic acids to chromone cores, accessing 2-aryl flavanones (Figure 5.2, eq 2).[8] In a complementary approach, Glorius and coworkers reported a ruthenium-catalyzed asymmetric hydrogenation of flavones to the corresponding enantioenriched flavanols, which were subsequently oxidized by PCC to the optically active flavanones (Figure 5.2, eq 3).[9]

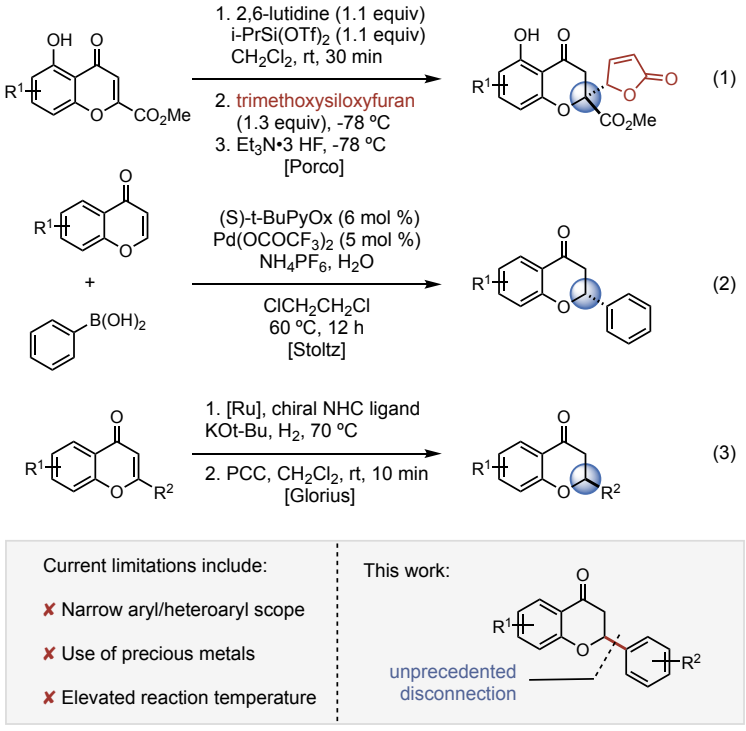

Figure 5.2. Synthetic routes toward flavanones.

We were interested in establishing a complementary route, allowing access to both 2-aryl- and 2-heteroaryl-substituted flavanones. Inspired by recent work in our group,[10] novel trifluoroboratochromanones were envisioned to serve as radical precursors in the photoredox/Ni dual catalytic cross-coupling with a variety of aryl- and heteroaryl bromides. By synthesizing such unprecedented 2-trifluoroboratochromanone building blocks, a large library of natural and unnatural flavanones could quickly be accessed.

In the past decade, photoredox catalysis has experienced renewed popularity in the organic synthesis community, largely because of the mild and robust conditions typically used.[11] Our group disclosed a dual catalytic photoredox/nickel paradigm, making previously challenging cross-couplings possible at room temperature.[10a] More recently, there have been reports of α-alkoxy couplings, creating precedent for the transformation proposed herein.[10c–d] Previous examples were composed exclusively of 1º alkoxymethyltrifluoroborates and acyclic 2º alkoxyalkyltrifluoroborates,[12] the latter of which would be anticipated to exhibit a similar or even more favorable redox profile as the 1º counterpart (E_{red} = +1.11 V vs SCE). Before exploring the feasibility of the proposed transformation, a robust route to the desired, but previously unknown, 2-trifluoroboratochromanones **5.3.1** was needed.

5.1 Reaction Design and Scope

In a first effort toward the synthesis of **5.3.1**, a copper-catalyzed method reported by our group was used.[13] Although there were numerous methods for β-borylation of β-unsaturated carbonyl substrates,[14] these conditions were ultimately chosen because they incorporated an inexpensive, readily available copper catalyst and the atom economical bisboronic acid. Gratifyingly, little optimization was required, for a 75% yield of **5.3.1** was achieved using published conditions. Slightly higher yields were achieved by increasing the CuCl and ligand loadings to 2 mol % from 1 mol % (Figure 5.3). Alkyl substituents were tolerated as demonstrated

in **5.3.2**. Chloride moieties were also preserved during the borylation (**5.5.3**), thus providing a handle for further decoration.

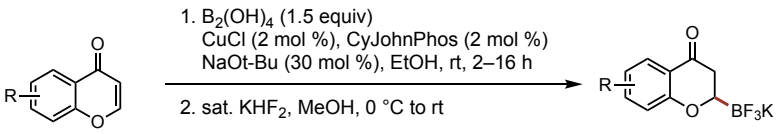

chromone	product	% yield	time, h
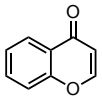	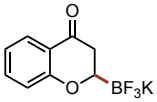 **5.3.1**	85	2
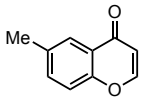	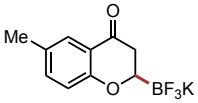 **5.3.2**	55	2
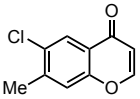	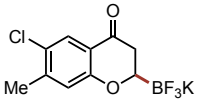 **5.3.3**	62	16

Figure 5.3. Chromone borylation scope.

With the trifluoroborate building blocks in hand, the viability of the coupling was explored. Using conditions that were appropriate for 2º alkyltrifluoroborate cross-couplings using Ir catalyst 3 (2.5 mol %), $NiCl_2$•dme (5 mol %), dtbbpy (5 mol %), Cs_2CO_3 (1.5 equiv), and dioxane,[10b] a modest 24% yield was achieved. To assess more suitable conditions quickly, high throughput experimentation[15] was utilized to screen various nickel sources, bases, and solvents. Although $Ni(COD)_2$ was found to yield slightly higher conversions, $NiCl_2$•dme was ultimately chosen because of its stability and consequent ease of handling. K_2HPO_4 was found to be the preferred additive to sequester the BF_3 generated in the oxidation of the trifluoroborate, and dioxane was a suitable solvent.

Our attention was next directed to the photocatalyst (Figure 5.4). It was noted that the ultimate practicality of the reaction was hampered by the high cost of the iridium photocatalyst

5.4.2 (~$1/mg). Other, less expensive photocatalysts were compared, including organophotocatalysts Eosin Y[15] and MesAcr (Figure 5.4, bottom). Although the oxidation potential for MesAcr is more than sufficient (E_{red} = +2.06 V vs SCE) to oxidize the trifluoroborate,[11c] the reduction potential (E_{red} = +0.49 V vs SCE)[11c] was not adequate to turn over the nickel cycle (E_{red} = +1.10 V vs SCE).[16] Conversely, Eosin Y has insufficient oxidation potential to induce a single electron oxidation (E_{red} = +0.83 V vs SCE)[22] of **5.3.1**. During the optimization process, the Zhang group disclosed the synthesis of a rationally designed organophotocatalyst amenable to photoredox/nickel dual catalytic manifolds.[17] At merely $6/g, 4CzIPN (**5.4.4**) was a highly attractive alternative. Just as Zhang and coworkers observed in their systems, 4CzIPN outperformed the iridium photocatalyst (entry 4) and was therefore used in the remainder of the study.

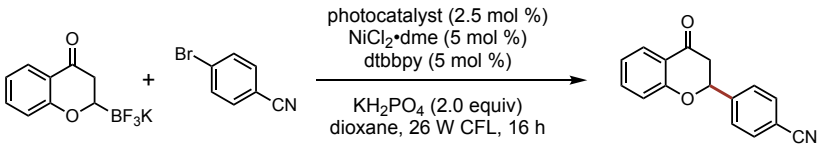

entry	photocatalyst	conditions	% yield
1	Eosin Y (2)	26 W CFL	0
2	$Ir[dFCF_3ppy]_2(bpy)PF_6$ (3)	26 W CFL	75
3	MesAcridinium (4)	26 W CFL	0
4	4CzIPN (5)	26 W CFL	80
5	4CzIPN	no light	trace

Photocatalysts Screened

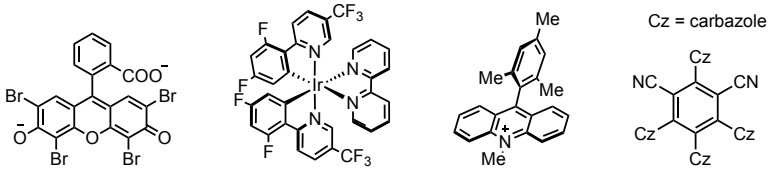

Eosin Y **5.4.1** | $Ir[dFCF_3ppy]_2(bpy)PF_6$ **5.4.2** | MesAcr **5.4.3** | 4CzIPN **5.4.4**

Figure 5.4. Optimization with various photocatalysts.

After establishing suitable conditions, the scope of the reaction in terms of aryl/heteroaryl bromide partners was explored (Figure 5.5). Initially, aryl bromides with various functional groups were investigated (**5.5.2–5.5.4**). The activated 4-bromocyanobenzene used for optimization afforded a 70% yield, but when steric pressure was applied at the ortho position (**5.5.4**), the yield was significantly reduced. An aldehyde functional group was tolerated, providing a respectable 67% yield (**5.5.2**). Chloride groups would allow further functionalization; thus, **5.5.3** is appropriately functionalized for additional cross-coupling, and **5.5.9** is primed for subsequent S_N2 reactions. Trifluoromethyl substituents, commonly used in medicinal chemistry, were well tolerated (**5.5.6**, **5.5.8**, **5.5.15**). Additionally, protic functional groups as in the halide partner leading to **5.5.10** also proved viable.

Next, the heteroaryl halide scope was probed. Suprisingly, heteroarenes such as thiophene (**5.5.13**), benzofuran (**5.5.11**), and pyridine (**5.5.15**) had markedly higher yields than their aryl counterparts. Although electron deficient pyridines were well tolerated, electron-donating groups led to diminished reactivity (**5.5.14**). Additionally, bromo-substituted indoles and pyrroles were not suitable partners, presumably because of their electron rich nature. Lastly, it is worth noting that although they are relatively simple derivatives, only 7 arylchromanones have been previously reported in the literature, highlighting the utility of this protocol for accessing a wide range of novel, functionalized flavanones.

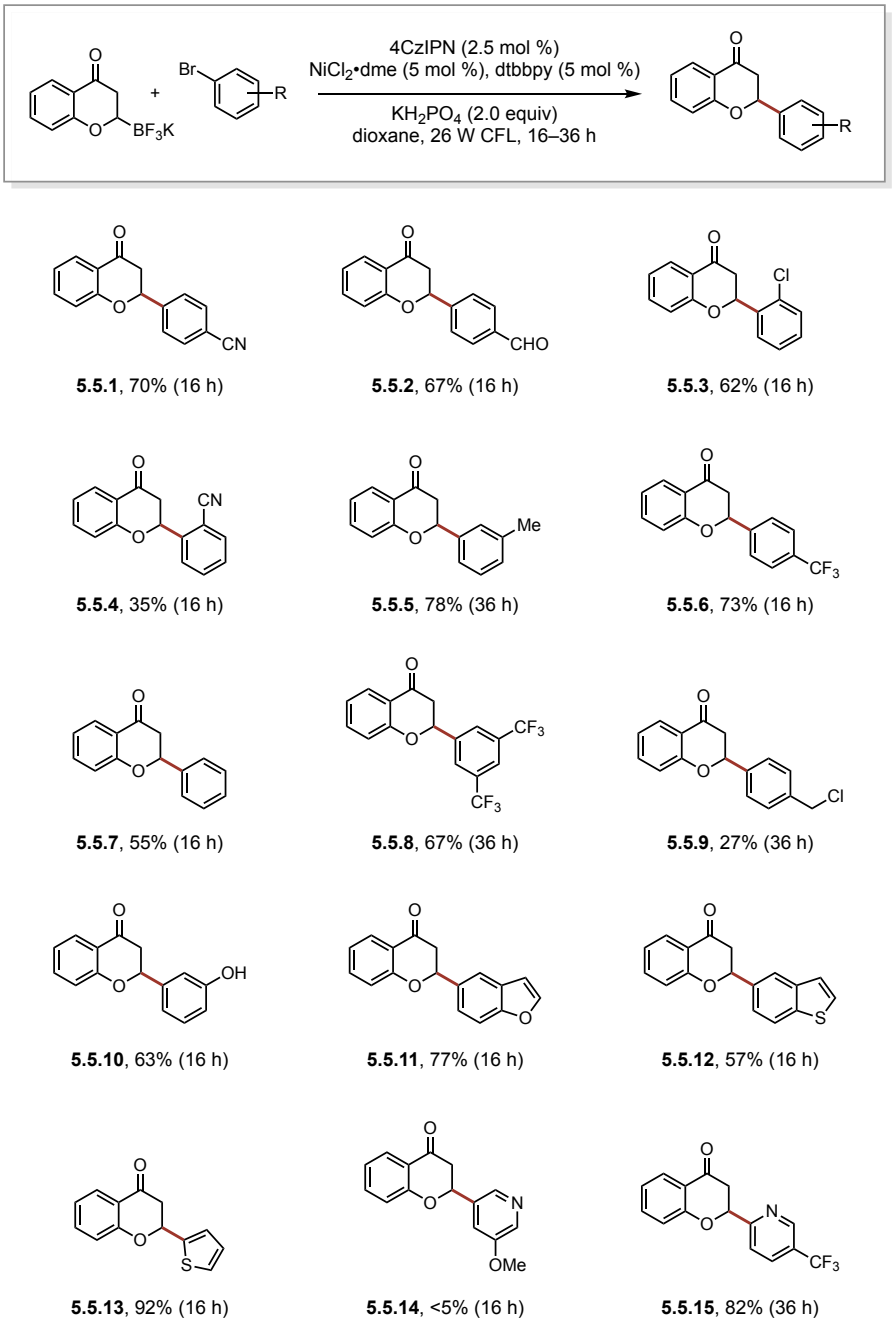

Figure 5.5. Engaging trifluoroboratochromanone in cross-coupling with aryl bromides.

Subsequently, the scope for functionalized 2-trifluoroboratochromanones was explored (Figure 5.6). The yield for an alkyl-substituted chromanone (**5.6.1**) was found to be comparable to the unsubstituted example (**5.5.1**). The chloro-chromanone **5.6.3** demonstrates the feasibility for

further diversification within the heteroaryl core. Although unexplored at this time, we predict halide substituents at different positions of the aryl ring would yield similar results. Finally, nitro substituents were not tolerated (**5.6.2**), as observed by other groups in photoredox-catalyzed processes.[18]

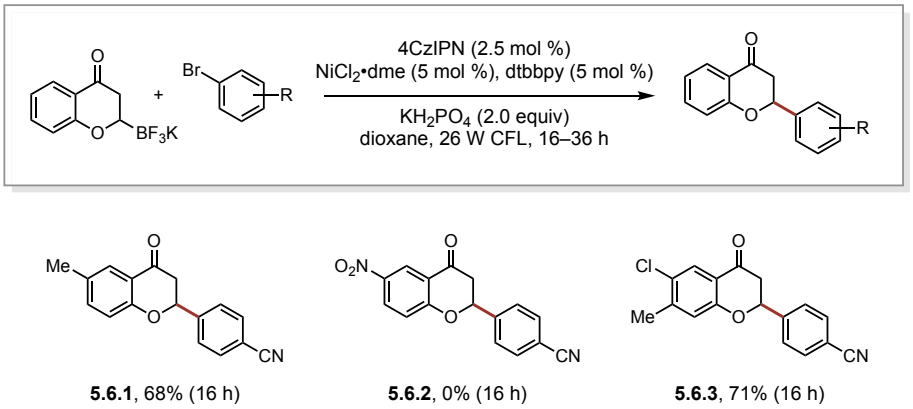

Figure 5.6. Varying aryl backbone of chromanone.

5.3 Conclusion

In conclusion, a simple and robust method has been established for accessing the increasingly important flavanone core. This study details the first synthesis of 2-boryl-substituted chromanones. With this procedure in place, practitioners are well equipped to access 2-aryl/heteroaryl flavanones quickly and efficiently, and these substructures can be decorated with a wide range of functional groups owing to the availability of literally thousands of diverse, commercially available (hetero)aryl bromide partners. The photoredox/Ni dual catalytic cross-coupling reactions proceed with a sustainable organic photocatalyst and a base-metal cross-coupling catalyst under extraordinarily mild conditions (weak base, ambient temperature, visible light). Lastly, the method highlights the applicability of photoredox/nickel dual catalysis for challenging coupling reactions that are typically prone to undesirable side reactions (e.g., β-hydride elimination), allowing access to unique structures by transformations that are complementary to more traditional approaches.

5.4 References

[1] Khan, M. K.; Huma, Z. E.; Dangles, O. J. *Food Compos. Anal.* **2014**, *33*, 85.

[2] (a) Yan, Y.; Kohli, A.; Koffas, A. G. *Appl. Environ. Microbiol.* **2005**, *71*, 5610. (b) Gaffield, W.; Lundin, R. E.; Gentili, B.; Horowitz, R. M. *Bioorg. Chem.* **1975**, *4*, 259. (c) Leonard, E.; Yan, Y.; Lim, K. H.; Koffas, M. A. G. *Appl. Environ. Microbiol.* **2005**, *71*, 8241. (d) Fowler, Z. L.; Koffas, M. A. G. *Appl. Microbiol. Biotechnol.* **2009**, *83*, 799. (e) Fowler, Z. L.; Gikandi, W. W.; Koffas, M. A. G. *Appl. Environ. Microbiol.* **2009**, *75*, 5831. (f) Chandler, I. M.; McIntyre, C. R.; Simpson, T. J. *J. Chem. Soc., Perkin Trans. 1* **1992**, 2271. (g) Martens, S.; Mithofer, A. *Phytochemistry* **2005**, *66*, 2399.

[3] Forkmann, G.; Martens, S. *Curr. Opin. Biotechnol.* **2001**, *12*, 155.

[4] Xu, Z.-Q.; Buckheit, R. W.; Stup, T. L.; Flavin, M. T.; Khilevich, A.; Rizzo, J. D.; Lin, L.; Zembower, D. E. *Bioorg. Med. Chem. Lett.* **1998**, *8*, 2179.

[5] Miao, J.; Cui, H.; Jin, J.; Lai, F.; Wen, H.; Zhang, X.; Ruda, G. F.; Chen, X.; Yin, D. *Chem. Commun.* **2015**, *51*, 881.

[6] (a) Wang, L.; Liu, X.; Dong, Z.; Fu, X.; Feng, X. *Angew. Chem., Int. Ed.* **2008**, *47*, 8670. (b) Ahmed, N.; Konduru, N. K.; Praveen; Kumar, A.; Kamaluddin. *J. Mol. Catal. A: Chem.* **2013**, *373*, 135. (c) Naik, M. M.; Tilve, S. G.; Kamat, V. P. *Tetrahedron Lett.* **2014**, *55*, 3340. (d) Kabbe, H.-J.; Widdig, A. *Angew. Chem., Int. Ed.***1982**, *21*, 247. (e) Stermitz, F. R.; Adamovics, J. A.; Geigert, J. *Tetrahedron* **1975**, *31*, 1593. (f) Patonay, T.; Varma, R. S.; Vass, A.; Levai, A.; Dudas, J. *Tetrahedron Lett.* **2001**, *42*, 1403. (g) Kavala, V.; Lin, C.; Kuo, C.-W.; Fang, H.; Yao, C.-F. *Tetrahedron* **2012**, *68*, 1321.

[7] (7) Qin, T.; Johnson, R. P.; Porco, J. A. *J. Am. Chem. Soc.* **2011**, *133*, 1714.

[8] Shockley, S. E.; Holder, J. C.; Stoltz, B. M. *Org. Process Res. Dev.* **2015**, *19*, 974.

[9] Zhao, D.; Beiring, B.; Glorius, F. *Angew. Chem., Int. Ed.* **2013**, *52*, 8454.

[10] (a) Tellis, J. C.; Primer, D. N.; Molander, G. A. *Science* **2014**, *345*, 433. (b) Primer, D. N.; Karakaya, I.; Tellis, J. C.; Molander, G. A. *J. Am. Chem. Soc.* **2015**, *137*, 2195. (c) Karakaya, I.; Primer, D. N.; Molander, G. A. *Org. Lett.* **2015**, *17*, 3294. (d) Amani, J.; Sodagar, E.; Molander, G. A. *Org. Lett.* **2016**, *18*, 732.

[11] Recent reviews on photoredox chemistry: (a) Narayanam, J. M. R.; Stephenson, C. R. *J. Chem. Soc. Rev.* ***2011***, *40*, 102. (b) Prier, C. K.; Rankic, D. A.; MacMillan, D. W. C. *Chem. Rev.* **2013**, *113*, 5322. Example with MesAcr photocatalyst: (c) Nguyen, T. M.; Manohar, N.; Nicewicz, D. A. *Angew. Chem., Int. Ed.* **2014**, *53*, 6198. (d) Tellis, J. C.; Kelly, C. B.; Primer, D. N.; Jouffroy, M.; Patel, N. R.; Molander, G. A. *Acc. Chem. Res.* **2016**, *49*, 1429.

[12] (a) Miyazawa, K.; Yasu, Y.; Koike, T.; Akita, M. *Chem. Commun.* **2013**, *49*, 7249. (b) Karimi-Nami, R.; Tellis, J. C.; Molander, G. A. *Org. Lett.* **2016**, *18*, 2572.

[13] Molander, G. A.; McKee, S. A. *Org. Lett.* **2011**, *13*, 4684.

[14] (a) Lawson, Y.; Lesly, G.; Marder, T.; Norman, N.; Rice, C. *Chem. Commun.* **1997**, *7*, 4674. (b) Thorpe, S. B.; Calderone, J. A.; Santos, W. L. *Org. Lett.* **2012**, *14*, 1918. (c) Lee, J. C. H.; Hall, D. G. *J. Am. Chem. Soc.* **2010**, *132*, 5544. (d) Schiffner, J. A.; Muther, K.; Oestreich, M. *Angew. Chem., Int. Ed.* **2010**, *49*, 1194.

[15] Hari, D. P.; Konig, B. *Chem. Commun.* **2014**, *50*, 6688.

[16] (a) Dreher, S. D.; Dormer, P.G.; Sandrock, D. L.; Molander, G. A. *J. Am. Chem. Soc.* **2008**, *130*, 9257. (b) Schmink, J. R.; Bellomo, A.; Berritt, S. *Aldrichimica Acta* **2013**, *46*, 71.

[17] Luo, J.; Zhang, J. *ACS Catal.* **2016**, *6*, 873.

[18] Paria, S.; Reiser, O. *Adv. Synth. Catal.* **2014**, *356*, 557.

GENERAL PROCEDURE FOR BETA BORYLATION

2-(Trifluoro-λ_4-boranyl)chroman-4-one, potassium salt (5.3.1)

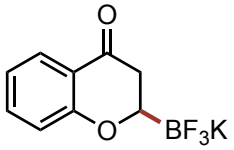

A 50 mL round bottom flask was charged with chroman-4-one (585 mg, 4.0 mmol, 1.0 equiv) and brought into the glove box. $(HO)_2BB(OH)_2$ (538.2 mg, 6.0 mmol, 1.5 equiv), Cu(I)Cl (7 mg, 0.08 mmol, 0.02 equiv), CyJohnPhos (28 mg, 0.08 mmol, 0.02 equiv), and NaO*t*-Bu (115.3 mg, 1.2 mmol, 0.3 equiv) were added to the flask, which was capped in the glovebox. Under nitrogen, freshly distilled EtOH (20 mL) was added, and the mixture was stirred for 3 h at rt. Upon completion of the reaction, the EtOH was removed *in vacuo*, and the residue was dissolved in MeOH (20 mL) and cooled to 0 °C. Saturated KHF_2 (8 mL, 4.5 M) was added dropwise to the reaction, and the resulting mixture was allowed to warm to rt. After 30 min, the solution was concentrated *in vacuo* and placed on the lyophilizer overnight. A Soxhlet extraction of the solid was performed using *i*-PrOAc for 16 h, and the extract was concentrated. The resulting red solid was dissolved in acetone (~5 mL), and Et_2O was added dropwise until precipitation was induced. Additional Et_2O (20 mL) was added, and the solid was filtered to afford a light orange powder (650 mg, 64% yield). mp = 135–140 °C.

^{1}H NMR (500 MHz, $CDCl_3$) δ 7.64 (dd, *J* = 7.8, 1.8 Hz, 1H), 7.41 (ddd, *J* = 8.6, 6.9, 1.8 Hz, 1H), 7.00 – 6.75 (m, 2H), 3.79 – 3.47 (m, 1H), 2.72 – 2.55 (m, 1H), 2.30 (dd, *J* = 16.9, 2.4 Hz, 1H).

^{13}C NMR (126 MHz, DMSO) δ 206.5, 195.4, 164.5, 134.9, 126.1, 120.9, 118.9, 117.9, 30.7.

^{19}F NMR (471 MHz, C_6D_6) δ -143.3.

^{11}B NMR (128 MHz, DMSO) δ 3.9.

FT-IR (cm^{-1}, neat, ATR) 2848, 1674, 1604, 1463, 1308, 1149, 907, 755.

HRMS (ESI) m/z calc. for $C_9H_7O_2BF_3$ (M^-) 215.0491, found 215.0483.

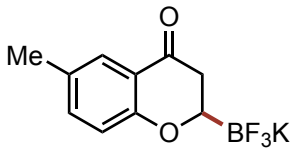

6-Methyl-2-(trifluoro-l_4-boranyl)chroman-4-one, potassium salt (5.3.2)

The general procedure was followed with chromone (320.2 mg, 2.0 mmol, 1.0 equiv). After 2 h at rt, the title compound was isolated (294 mg, 1.10 mmol, 55% yield).

Physical properties: light yellow solid (mp = 122–125 °C).

^{1}H NMR (500 MHz, DMSO-d_6) δ 7.44 (s, 1H), 7.23 (d, J = 8.6 Hz, 1H), 6.81 (d, J = 8.6 Hz, 1H), 3.52 (d, J = 15.6 Hz, 1H), 2.58 (t, J = 15.9 Hz, 1H), 2.28 (d, J = 16.9 Hz, 1H), 2.22 (s, 3H).

^{13}C NMR (126 MHz, DMSO) δ 195.4, 162.5, 135.9, 127.7, 125.7, 120.5, 117.8, 30.7, 20.0 (did not observe highlighted carbon).

^{19}F NMR (471 MHz, C_6D_6) δ -143.40.

^{11}B NMR (128 MHz, DMSO) δ 2.8.

FT-IR (cm^{-1}, neat, ATR) 2877, 1676, 1489, 1293, 996, 868.

HRMS (ESI) m/z calc. for $C_{12}H_{12}O_3NBF_2$ [M-F+CH_3N] 251.0929, found 251.0929.

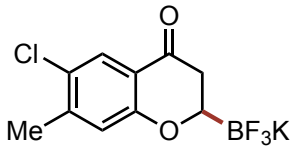

6-Chloro-7-methyl-2-(trifluoro-l_4-boranyl)chroman-4-one, potassium salt (5.3.3)

The general procedure was followed with chromone (388 mg, 2.0 mmol, 1.0 equiv). After 2 h at rt, the title compound was isolated (374 mg, 1.24 mmol, 62% yield).

Physical properties: white powdery solid (mp = 165 °C).

^{1}H NMR (500 MHz, DMSO-d_6) δ 7.54 (s, 1H), 6.92 (s, 1H), 3.57 (t, J = 16.7 Hz, 1H), 3.04 – 2.97 (m, 1H), 2.56 (d, J = 15.7 Hz, 1H), 2.29 (s, 3H).

^{13}C NMR (126 MHz, DMSO) δ 193.9, 163.0, 142.8, 125.3, 123.9, 120.3, 47.3, 20.1 (did not observe highlighted carbon.)

^{19}F NMR (471 MHz, C_6D_6) δ -155.36.

^{11}B NMR (128 MHz, DMSO) δ 2.6.

FT-IR (cm^{-1}, neat, ATR) 2952, 3592, 1665, 1611, 1452, 1091, 863.

HRMS (ESI) m/z calc. for $C_{10}H_8BClF_3O_2$ [M] 263.0258, found 263.0237.

GENERAL PROCEDURE FOR PHOTOREDOX/NICKEL ARYLATION

To an 8 mL vial equipped with a stir bar was added trifluoroborate (191 mg, 0.75 mmol, 1.5 equiv), 4CzIPN photocatalyst (7.9 mg, 0.004 mmol, 0.02 equiv), $NiCl_2$ dme (5.5 mg, 0.025 mmol, 0.05 equiv), 4,4'-di-*tert*-butyl bipyridine (6.7 mg, 0.025 mmol, 0.05 equiv), K_2HPO_4 (174.2 mg, 1.0 mmol, 2.0 equiv), and aryl halide (0.50 mmol, 1.0 equiv). The vial was then evacuated and purged three times. Under nitrogen, degassed dioxane (4.0 mL) was added under nitrogen. The resulting solution was stirred next to a 26 W CFL for varying amounts of time. After completion, the mixture was quenched with saturated $NaHCO_3$ (10 mL) and transferred to a separatory funnel with CH_2Cl_2 (15 mL) and extracted with CH_2Cl_2 (2 x 15 mL). The organic layers were combined and dry loaded with Celite. The crude mixture was purified by column chromatography.

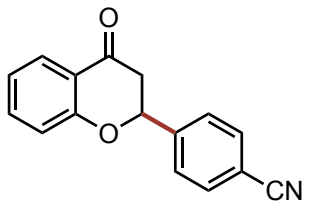

4-(4-Oxochroman-2-yl)benzonitrile (5.5.1)

Reference: Wang, L. *Angew. Chem. Int. Ed.* **2008**, *47*, 8670.

The general procedure was followed with trifluoroborate (191 mg, 0.75 mmol, 1.5 equiv), 4-bromobenzonitrile (91 mg, 0.50 mmol, 1.0 equiv), 4CzIPN photocatalyst (7.9 mg, 0.004 mmol, 0.02 equiv), $NiCl_2$ dme (5.5 mg, 0.025 mmol, 0.05 equiv), 4,4'-di-*tert*-butyl bipyridine (6.7 mg, 0.025 mmol, 0.05 equiv), and K_2HPO_4 (174.2 mg, 1.0 mmol, 2.0 equiv). Under a 26 W CFL, the reaction was allowed to run for 36 h. The title compound was purified by column chromatography (silica gel, 4:1 hexanes/EtOAc) to afford a crystalline solid (81 mg, 65% yield). mp = 75–77 °C (lit mp = 84–86 °C).

^{1}H NMR (500 MHz, $CDCl_3$) δ 8.14 (dd, *J* = 7.9, 1.8 Hz, 1H), 8.05 (dd, *J* = 8.1, 1.8 Hz, 1H), 7.97 (dd, *J* = 7.9, 1.8 Hz, 1H), 7.87 – 7.78 (m, 2H), 7.53 – 7.47 (m, 1H), 7.11 – 7.00 (m, 2H), 6.21 (dd, *J* = 10.6, 3.6 Hz, 1H), 3.63 (dd, *J* = 17.0, 10.7 Hz, 1H), 3.12 (dd, *J* = 17.1, 3.7 Hz, 1H).

^{13}C NMR (126 MHz, $CDCl_3$) δ 191.3, 160.6, 148.9, 146.7, 142.2, 140.4, 136.3, 132.0, 127.1, 122.2, 121.5, 118.2, 76.2, 40.4.

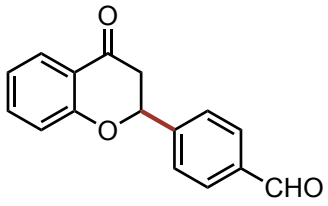

4-(4-Oxochroman-2-yl)benzaldehyde (5.5.2)

Reference: Ahmed, N.; Konduru, N. K.; Ahmad, S.; Owais, M. *Eur. J. Med. Chem.* **2014**, *75*, 233.

The general procedure was followed with trifluoroborate (191 mg, 0.75 mmol, 1.5 equiv), 4-bromo benzaldehyde (93 mg, 0.50 mmol, 1.0 equiv), 4CzIPN photocatalyst (7.9 mg, 0.004 mmol, 0.02 equiv), $NiCl_2$ dme (5.5 mg, 0.025 mmol, 0.05 equiv), 4,4'-di-*tert*-butyl bipyridine (6.7 mg, 0.025 mmol, 0.05 equiv), and K_2HPO_4 (174.2 mg, 1.0 mmol, 2.0 equiv). Under a 26 W CFL, the reaction was allowed to run for 16 h. The title compound was purified by column chromatography (silica gel, 5:1 hexanes/EtOAc) to afford a light yellow oil (85 mg, 67% yield).

^{1}H NMR (500 MHz, $CDCl_3$) δ 10.09 (s, 1H), 8.02 – 7.96 (m, 3H), 7.71 (d, *J* = 7.9 Hz, 2H), 7.58 (t, *J* = 7.8 Hz, 1H), 7.13 (dd, *J* = 8.0, 5.3 Hz, 2H), 5.62 (dd, *J* = 13.0, 3.2 Hz, 1H), 3.08 (dd, *J* = 16.8, 13.1 Hz, 1H), 3.03 – 2.95 (m, 1H).

^{13}C NMR (126 MHz, $CDCl_3$) δ 191.8, 191.2, 161.3, 145.4, 136.7, 136.6, 130.4, 127.3, 126.7, 122.2, 121.1, 118.3, 79.0, 44.8.

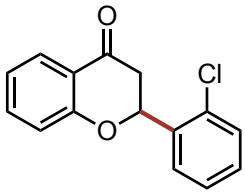

2-(2-Chlorophenyl)chroman-4-one (5.5.3)

Reference: Jiang, H.; Zheng, X.; Yin, Z.; Xie, J. *J. Chem. Res.* **2011**, *35*, 220.

The general procedure was followed with trifluoroborate (191 mg, 0.75 mmol, 1.5 equiv), 1-bromo-2-chlorobenzene (96 mg, 0.50 mmol, 1.0 equiv), 4CzIPN photocatalyst (7.9 mg, 0.004 mmol, 0.02 equiv), $NiCl_2$ dme (5.5 mg, 0.025 mmol, 0.05 equiv), 4,4'-di-*tert*-butyl bipyridine (6.7 mg, 0.025 mmol, 0.05 equiv), and K_2HPO_4 (174.2 mg, 1.0 mmol, 2.0 equiv). Under a 26 W CFL, the reaction was allowed to run for 16 h. The title compound was purified by column chromatography (silica gel, 5:1 hexanes/EtOAc) to afford a yellow oil (120 mg, 93% yield).

^{1}H NMR (500 MHz, $CDCl_3$) δ 7.96 (d, J = 7.9 Hz, 1H), 7.76 (d, J = 7.7 Hz, 1H), 7.53 (t, J = 7.8 Hz, 1H), 7.40 (q, J = 7.7 Hz, 2H), 7.32 (t, J = 7.7 Hz, 1H), 7.08 (t, J = 7.7 Hz, 2H), 5.88 (dd, J = 13.5, 2.6 Hz, 1H), 3.04 (dd, J = 16.7, 2.8 Hz, 1H), 2.89 (dd, J = 16.8, 13.3 Hz, 1H).

^{13}C NMR (126 MHz, $CDCl_3$) δ 191.6, 161.7, 136.9, 136.3, 131.8, 129.9, 129.74, 127.6, 127.4, 127.3, 122.0, 121.1, 118.2, 76.7, 43.7.

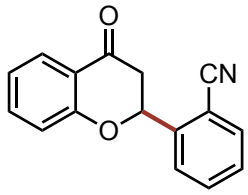

2-(4-Oxochroman-2-yl)benzonitrile (5.5.4)

The general procedure was followed with trifluoroborate (191 mg, 0.75 mmol, 1.5 equiv), 2-bromobenzonitrile (91 mg, 0.50 mmol, 1.0 equiv), 4CzIPN photocatalyst (7.9 mg, 0.004 mmol, 0.02 equiv), $NiCl_2$ dme (5.5 mg, 0.025 mmol, 0.05 equiv), 4,4'-di-*tert*-butyl bipyridine (6.7 mg, 0.025 mmol, 0.05 equiv), and K_2HPO_4 (174.2 mg, 1.0 mmol, 2.0 equiv). Under a 26 W CFL, the reaction was allowed to run for 36 h. The title compound was purified by column chromatography (silica gel, 4:1 hexanes/EtOAc) to afford a clear oil (32 mg, 35% yield).

^{1}H NMR (500 MHz, $CDCl_3$) δ 7.97 (d, *J* = 7.7 Hz, 1H), 7.79 (d, *J* = 7.9 Hz, 1H), 7.77 – 7.69 (m, 2H), 7.53 (dt, *J* = 15.4, 7.7 Hz, 2H), 7.15 – 7.05 (m, 2H), 5.85 (dd, *J* = 13.1, 3.4 Hz, 1H), 3.16 – 2.93 (m, 2H).

^{13}C NMR (126 MHz, $CDCl_3$) δ 190.6, 161.2, 142.3, 136.6, 133.6, 133.5, 129.3, 127.4, 127.1, 122.4, 121.1, 118.2, 116.9, 110.9, 77.3, 44.1.

FT-IR (cm^{-1}, neat, ATR) 3072, 2223, 1688, 1605, 1463, 1225, 730.

HRMS (ES+) m/z calc. for $C_{16}H_{11}NO_2$ [M+H] 250.0868, found 250.0874.

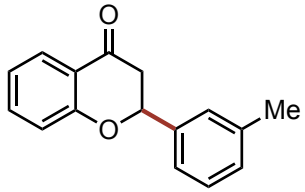

2-(3-Tolyl)chroman-4-one (5.5.5)

Reference: Zhao, D.; Beiring, B.; Glorius, F. *Angew. Chem. Int. Ed.* **2013**, *52*, 8454.

The general procedure was followed with trifluoroborate (191 mg, 0.75 mmol, 1.5 equiv), 1-bromo-3-methylbenzene (85 mg, 0.50 mmol, 1.0 equiv), 4CzIPN photocatalyst (7.9 mg, 0.004 mmol, 0.02 equiv), $NiCl_2$ dme (5.5 mg, 0.025 mmol, 0.05 equiv), 4,4'-di-*tert*-butyl bipyridine (6.7 mg, 0.025 mmol, 0.05 equiv), and K_2HPO_4 (174.2 mg, 1.0 mmol, 2.0 equiv). Under a 26 W CFL, the reaction was allowed to run for 16 h. The title compound was purified by column chromatography (silica gel, 5:1 hexanes/EtOAc) to afford a clear oil (93 mg, 78% yield).

^{1}H NMR (500 MHz, $CDCl_3$) δ 7.93 (d, *J* = 7.8 Hz, 1H), 7.51 (t, *J* = 7.9 Hz, 1H), 7.37 (d, *J* = 5.0 Hz, 1H), 7.14 (d, *J* = 3.5 Hz, 1H), 7.08 – 7.02 (m, 3H), 5.75 (dd, *J* = 11.7, 3.3 Hz, 1H), 3.26 – 3.15 (m, 1H), 3.07 (dd, *J* = 16.8, 3.3 Hz, 1H), 2.88 (d, *J* = 16.7 Hz, 1H), 2.40 (s, 3H).
^{13}C NMR (126 MHz, $CDCl_3$) δ 192.2, 161.8, 138.8, 138.8, 136.3, 129.7, 128.9, 127.2, 127.0, 123.4, 121.7, 121.1, 118.3, 79.9, 44.9, 21.6.

FT-IR (cm^{-1}, neat, ATR) 3070, 2924, 2925, 1691, 1608, 1577, 1472, 1463, 1378, 1304, 1224, 1149, 1114, 1066, 1035, 982, 891, 851, 764, 708, 530, 490.

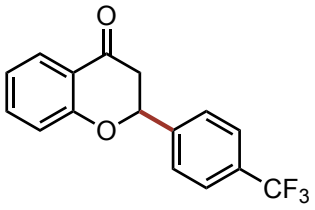

2-(4-(Trifluoromethyl)phenyl)chroman-4-one (5.5.6)

Reference: Zhao, D.; Beiring, B.; Glorius, F. *Angew. Chem. Int. Ed.* **2013**, *52*, 8454.

The general procedure was followed with trifluoroborate (191 mg, 0.75 mmol, 1.5 equiv), 1-bromo-4-(trifluoromethyl)benzene (112 mg, 0.50 mmol, 1.0 equiv), 4CzIPN photocatalyst (7.9 mg, 0.004 mmol, 0.02 equiv), $NiCl_2$ dme (5.5 mg, 0.025 mmol, 0.05 equiv), 4,4'-di-*tert*-butyl bipyridine (6.7 mg, 0.025 mmol, 0.05 equiv), and K_2HPO_4 (174.2 mg, 1.0 mmol, 2.0 equiv). Under a 26 W CFL, the reaction was allowed to run for 16 h. The title compound was purified by column chromatography (silica gel, 5:1 hexanes/EtOAc) to afford a clear oil (107 mg, 73% yield).

^{1}H NMR (500 MHz, $CDCl_3$) δ 7.93 (d, *J* = 7.8 Hz, 1H), 7.52 (t, *J* = 7.6 Hz, 1H), 7.42 (d, *J* = 2.1 Hz, 4H), 7.11 – 7.02 (m, 2H), 5.47 (dd, *J* = 13.2, 3.0 Hz, 1H), 3.04 (dd, *J* = 16.9, 13.2 Hz, 1H), 2.89 (dd, *J* = 16.8, 3.0 Hz, 1H).

^{13}C NMR (126 MHz, $CDCl_3$) δ 191.2, 161.3, 142.9, 136.5, 130.9 (q, *J* = 32.5 Hz), 127.3, 126.5, 126.0 (q, *J* = 3.7 Hz), 124.0 (q, *J* = 272.0 Hz), 121.1, 118.2, 78.9, 44.8.

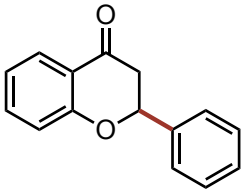

2-Phenylchroman-4-one (5.5.7)

Reference: Zhao, D.; Beiring, B.; Glorius, F. *Angew. Chem. Int. Ed.* **2013**, *52*, 8454.

The general procedure was followed with trifluoroborate (191 mg, 0.75 mmol, 1.5 equiv), bromobenzene (78.5 mg, 0.50 mmol, 1.0 equiv), 4CzIPN photocatalyst (7.9 mg, 0.004 mmol, 0.02 equiv), $NiCl_2$ dme (5.5 mg, 0.025 mmol, 0.05 equiv), 4,4'-di-*tert*-butyl bipyridine (6.7 mg, 0.025 mmol, 0.05 equiv), and K_2HPO_4 (174.2 mg, 1.0 mmol, 2.0 equiv). Under a 26 W CFL, the reaction was allowed to run for 16 h. The title compound was purified by column chromatography (silica

gel, 5:1 hexanes/EtOAc) to afford a white solid (62 mg, 55% yield). mp = 68–70 °C (lit mp = 64–66 °C).

^{1}H NMR (500 MHz, $CDCl_3$) δ 7.94 (d, *J* = 7.4 Hz, 1H), 7.55 – 7.35 (m, 6H), 7.06 (dt, *J* = 7.5, 3.2 Hz, 2H), 5.49 (dd, *J* = 13.4, 2.9 Hz, 1H), 3.10 (dd, *J* = 16.9, 13.3 Hz, 1H), 2.90 (dd, *J* = 16.9, 2.9 Hz, 1H).

^{13}C NMR (126 MHz, $CDCl_3$) δ 192.1, 161.7, 138.9, 136.4, 129.0, 128.9, 127.2, 126.3, 121.8, 121.1, 118.3, 79.8, 44.9.

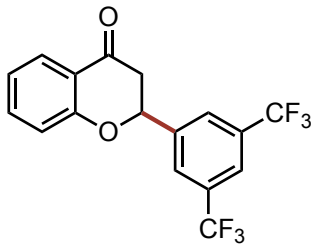

2-(3,5-Bis(trifluoromethyl)phenyl)chroman-4-one (5.5.8)

The general procedure was followed with trifluoroborate (191 mg, 0.75 mmol, 1.5 equiv), 3,5-bistrifluoromethyl bromobenzene (84 μL, 0.50 mmol, 1.0 equiv), 4CzIPN photocatalyst (7.9 mg, 0.004 mmol, 0.02 equiv), $NiCl_2$ dme (5.5 mg, 0.025 mmol, 0.05 equiv), 4,4'-di-*tert*-butyl bipyridine (6.7 mg, 0.025 mmol, 0.05 equiv), and K_2HPO_4 (174.2 mg, 1.0 mmol, 2.0 equiv). Under a 26 W CFL, the reaction was allowed to run for 16 h. The title compound was purified by column chromatography (silica gel, 4:1 hexanes/EtOAc) to afford a clear oil (120 mg, 67% yield).

^{1}H NMR (500 MHz, $CDCl_3$) δ 7.96 (d, *J* = 7.4 Hz, 3H), 7.92 (s, 1H), 7.57 (t, *J* = 7.8 Hz, 1H), 7.12 (t, *J* = 7.6 Hz, 2H), 5.61 (dd, *J* = 13.1, 3.3 Hz, 1H), 3.11 – 2.91 (m, 2H).

^{13}C NMR (126 MHz, $CDCl_3$) δ 190.5, 161.0, 141.7, 136.7, 132.7, 132.4, 132.1, 127.4, 126.3, 124.3, 122.8, 122.5, 122.2, 121.0, 118.2, 78.3, 44.9.

FT-IR (cm^{-1}, neat, ATR) 2934, 1698, 1605, 1354, 1339, 1308, 1287, 1227, 1204, 1164, 1151, 1126, 1077, 897, 882, 856, 843, 768, 705, 685.

HRMS (ES+) m/z calc. for $C_{17}H_{11}FO_2$ [M+H] 361.0623, found 361.0651.

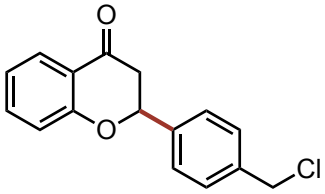

2-(4-(Chloromethyl)phenyl)chroman-4-one (5.5.9)

Reference: Wang, L. *Angew. Chem. Int. Ed.* **2008**, *47*, 8670.

The general procedure was followed with trifluoroborate (191 mg, 0.75 mmol, 1.5 equiv), 4-bromo benzyl chloride (103 mg, 0.50 mmol, 1.0 equiv), 4CzIPN photocatalyst (7.9 mg, 0.004 mmol, 0.02 equiv), $NiCl_2$ dme (5.5 mg, 0.025 mmol, 0.05 equiv), 4,4'-di-*tert*-butyl bipyridine (6.7 mg, 0.025 mmol, 0.05 equiv), and K_2HPO_4 (174.2 mg, 1.0 mmol, 2.0 equiv). Under a 26 W CFL, the reaction was allowed to run for 16 h. The title compound was purified by column chromatography (silica gel, 5:1 hexanes/EtOAc) to afford a clear oil (74 mg, 27% yield).

^{1}H NMR (500 MHz, $CDCl_3$) δ 7.86 (dd, *J* = 7.8, 1.8 Hz, 1H), 7.52 – 7.40 (m, 3H), 7.18 – 7.11 (m, 2H), 7.01 (t, *J* = 7.3 Hz, 1H), 6.96 (d, *J* = 8.3 Hz, 1H), 4.65 (dq, *J* = 9.0, 6.3 Hz, 1H), 3.14 (dd, *J* = 14.1, 6.8 Hz, 1H), 3.00 (dd, *J* = 14.1, 5.7 Hz, 1H), 2.70 – 2.65 (m, 2H).

^{13}C NMR (126 MHz, $CDCl_3$) δ 192.1, 161.4, 136.2, 135.4, 131.8, 131.5, 127.1, 121.6, 121.1, 121.1, 118.1, 78.0, 42.4, 40.7.

FT-IR (cm^{-1}, neat, ATR) 2076, 2930, 1692, 1606, 1464, 1305, 1227, 1119, 764.

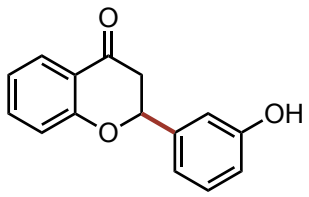

2-(3-Hydroxyphenyl)chroman-4-one (5.5.10)

Reference: Jung, H.; Shin, S. Y.; Jung, Y.; Tran, T. A.; Lee, H. O.; Jung, K. -Y. Koh, D.; Cho, S. K.; Lim, Y. *Chem. Biol. Drug, Des.* **2015**, *86*, 496.

The general procedure was followed with trifluoroborate (191 mg, 0.75 mmol, 1.5 equiv), 3-bromophenol (86 mg, 0.50 mmol, 1.0 equiv), 4CzIPN photocatalyst (7.9 mg, 0.004 mmol, 0.02 equiv), $NiCl_2$ dme (5.5 mg, 0.025 mmol, 0.05 equiv), 4,4'-di-*tert*-butyl bipyridine (6.7 mg, 0.025 mmol, 0.05 equiv), and K_2HPO_4 (174.2 mg, 1.0 mmol, 2.0 equiv). Under a 26 W CFL, the reaction was allowed to run for 16 h. The title compound was purified by column chromatography (silica gel, 5:1 hexanes/EtOAc) to afford a white semi-solid (76 mg, 63% yield).

^{1}H NMR (500 MHz, $CDCl_3$) δ 7.93 (d, J = 7.8 Hz, 1H), 7.52 (t, J = 7.6 Hz, 1H), 7.42 (d, J = 2.1 Hz, 4H), 7.11 – 7.02 (m, 2H), 5.75 (br s, 1H), 5.47 (dd, J = 13.2, 3.0 Hz, 1H), 3.04 (dd, J = 16.9, 13.2 Hz, 1H), 2.89 (dd, J = 16.8, 3.0 Hz, 1H).

^{13}C NMR (126 MHz, $CDCl_3$) δ 192.6, 161.7, 156.3, 140.6, 136.6, 130.3, 127.2, 125.9, 121.9, 121.0, 118.4, 118.31, 115.9, 113.3, 44.7.

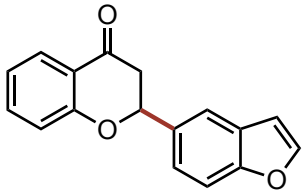

2-(Benzofuran-5-yl)chroman-4-one (5.5.11)

The general procedure was followed with trifluoroborate (191 mg, 0.75 mmol, 1.5 equiv), 5-bromo benzofuran (98 mg, 0.50 mmol, 1.0 equiv), 4CzIPN photocatalyst (7.9 mg, 0.004 mmol, 0.02 equiv), $NiCl_2$ dme (5.5 mg, 0.025 mmol, 0.05 equiv), 4,4'-di-*tert*-butyl bipyridine (6.7 mg, 0.025 mmol, 0.05 equiv), and K_2HPO_4 (174.2 mg, 1.0 mmol, 2.0 equiv). Under a 26 W CFL, the reaction was allowed to run for 16 h. The title compound was purified by column chromatography (silica gel, 4:1 hexanes/EtOAc) to afford a clear oil (102 mg, 77% yield).

^{1}H NMR (500 MHz, $CDCl_3$) δ 7.95 (d, *J* = 8.0 Hz, 1H), 7.74 (s, 1H), 7.68 (s, 1H), 7.57 (d, *J* = 8.5 Hz, 1H), 7.52 (t, *J* = 7.8 Hz, 1H), 7.43 (s, 1H), 7.07 (t, *J* = 6.9 Hz, 2H), 6.81 (s, 1H), 5.58 (dd, *J* = 13.5, 2.7 Hz, 1H), 3.17 (dd, *J* = 16.7, 13.6 Hz, 1H), 2.93 (dd, *J* = 16.9, 2.3 Hz, 1H).

^{13}C NMR (126 MHz, $CDCl_3$) δ 192.2, 161.8, 155.1, 146.1, 136.4, 133.6, 127.95, 127.2, 122.8, 121.8, 121.1, 119.4, 118.3, 111.9, 106.9, 80.1, 45.2.

FT-IR (cm^{-1}, neat, ATR) 3076, 2896, 1688, 1606, 1578, 1572, 1472, 1464, 1449, 1377, 1305, 1265, 1224, 1149, 1128, 1114, 765.

HRMS (ES+) m/z calc. for $C_{17}H_{13}O_3$ [M+H] 265.0865, found 265.0864.

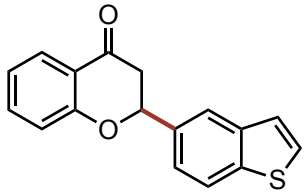

2-(Benzo[*b*]thiophen-5-yl)chroman-4-one (5.5.12)

The general procedure was followed with trifluoroborate (191 mg, 0.75 mmol, 1.5 equiv), 2-bromo benzothiophene (103 mg, 0.50 mmol, 1.0 equiv), 4CzIPN photocatalyst (7.9 mg, 0.004 mmol, 0.02 equiv), $NiCl_2$ dme (5.5 mg, 0.025 mmol, 0.05 equiv), 4,4'-di-*tert*-butyl bipyridine (6.7 mg, 0.025 mmol, 0.05 equiv), and K_2HPO_4 (174.2 mg, 1.0 mmol, 2.0 equiv). Under a 26 W CFL, the reaction was allowed to run for 36 h. The title compound was purified by column chromatography (silica gel, 4:1 hexanes/EtOAc) to afford a clear oil (80 mg, 57% yield).

^{1}H NMR (500 MHz, $CDCl_3$) δ 7.92 (d, *J* = 7.6 Hz, 1H), 7.84 – 7.80 (m, 1H), 7.77 – 7.74 (m, 1H), 7.51 (t, *J* = 7.7 Hz, 1H), 7.38 – 7.31 (m, 3H), 7.06 (dd, *J* = 14.0, 7.7 Hz, 2H), 5.84 (dd, *J* = 10.8, 3.7 Hz, 1H), 3.25 (dd, *J* = 16.9, 10.8 Hz, 1H), 3.15 (dd, *J* = 16.8, 3.7 Hz, 1H).

^{13}C NMR (126 MHz, $CDCl_3$) δ 190.9, 160.8, 142.2, 139.9, 139.1, 136.5, 136.4, 127.2, 125.1, 124.7, 124.1, 122.6, 122.1, 121.2, 118.4, 75.7, 44.1.

FT-IR (cm^{-1}, neat, ATR) 3368, 3059, 2900, 1687, 1604, 1577, 1471, 1461, 1438, 1362, 1299, 1221, 1148, 1112, 1066, 906, 891, 862, 828, 761, 747, 726, 558.

HRMS (ES+) m/z calc. for $C_{17}H_{13}O_2S$ [M+H] 281.0636, found 281.0658.

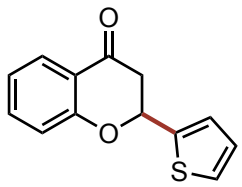

2-(Thiophen-2-yl)chroman-4-one (5.5.13)

Reference: Kavala, V.; Lin, C.; Kuo, C. -W.; Fang, H.; Yao, C. -F. *Tetrahedron* **2012**, *68*, 1321.

The general procedure was followed with trifluoroborate (191 mg, 0.75 mmol, 1.5 equiv), 2-bromothiophene (81 mg, 0.50 mmol, 1.0 equiv), 4CzIPN photocatalyst (7.9 mg, 0.004 mmol, 0.02 equiv), $NiCl_2$ dme (5.5 mg, 0.025 mmol, 0.05 equiv), 4,4'-di-*tert*-butyl bipyridine (6.7 mg, 0.025 mmol, 0.05 equiv), and K_2HPO_4 (174.2 mg, 1.0 mmol, 2.0 equiv). Under a 26 W CFL, the reaction was allowed to run for 16 h. The title compound was purified by column chromatography (silica gel, 5:1 hexanes/EtOAc) to afford a clear oil (105 mg, 91% yield).

^{1}H NMR (500 MHz, $CDCl_3$) δ 7.93 (d, *J* = 7.8 Hz, 1H), 7.51 (t, *J* = 7.9 Hz, 1H), 7.37 (d, *J* = 5.0 Hz, 1H), 7.14 (d, *J* = 3.5 Hz, 1H), 7.08 – 7.02 (m, 3H), 5.75 (dd, *J* = 11.7, 3.3 Hz, 1H), 3.26 – 3.15 (m, 1H), 3.07 (dd, *J* = 16.8, 3.3 Hz, 1H).

^{13}C NMR (126 MHz, $CDCl_3$) δ 191.3, 161.1, 141.6, 136.4, 127.2, 127.0, 126.5, 126.0, 122.0, 121.2, 118.4, 75.3, 44.5.

FT-IR (cm^{-1}, neat, ATR) 3070, 2924, 2925, 1691, 1608, 1577, 1472, 1463, 1378, 1304, 1224, 1149, 1114, 1066, 1035, 982, 891, 851, 764, 708, 530, 490.

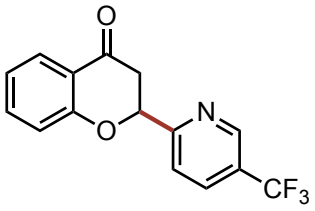

2-(5-(Trifluoromethyl)pyridin-2-yl)chroman-4-one (5.5.15)

The general procedure was followed with trifluoroborate (191 mg, 0.75 mmol, 1.5 equiv), 2-bromo-5-trifluoromethyl pyridine (113 mg, 0.50 mmol, 1.0 equiv), 4CzIPN photocatalyst (7.9 mg, 0.004 mmol, 0.02 equiv), $NiCl_2$ dme (5.5 mg, 0.025 mmol, 0.05 equiv), 4,4'-di-*tert*-butyl bipyridine (6.7 mg, 0.025 mmol, 0.05 equiv), and K_2HPO_4 (174.2 mg, 1.0 mmol, 2.0 equiv). Under a 26 W CFL, the reaction was allowed to run for 16 h. The title compound was purified by column chromatography (silica gel, 5:1 hexanes/EtOAc) to afford a yellow oil (120 mg, 82% yield).

^{1}H NMR (500 MHz, $CDCl_3$) δ 8.88 (s, 1H), 8.02 (d, *J* = 8.2 Hz, 1H), 7.95 (d, *J* = 7.8 Hz, 1H), 7.81 (d, *J* = 8.3 Hz, 1H), 7.54 (t, *J* = 7.8 Hz, 1H), 7.10 (dd, *J* = 12.7, 7.7 Hz, 2H), 5.68 (dd, *J* = 11.9, 3.7 Hz, 1H), 3.22 (dd, *J* = 16.9, 3.7 Hz, 1H), 3.12 (dd, *J* = 17.0, 11.9 Hz, 1H).

^{13}C NMR (126 MHz, $CDCl_3$) δ 191.0, 161.8, 160.7, 147.8, 146.5 (q, *J* = 4.2 Hz), 134.5 (q, *J* = 3.4 Hz), 127.8, 126.6, 126.3, 122.3, 121.4, 120.6, 118.2, 79.4, 42.7.

FT-IR (cm^{-1}, neat, ATR) 3063, 1681, 1609, 1578, 1474, 1328, 1217, 1161, 1135, 1116, 1084, 1017, 852, 769, 759.

HRMS (ES+) m/z calc. for $C_{15}H_{11}F_3NO_2$ [M+H] 294.0742, found 294.0754.

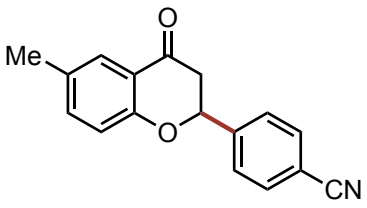

4-(6-Methyl-4-oxochroman-2-yl)benzonitrile (3b)

The general procedure was followed with trifluoroborate (201.0 mg, 0.75 mmol, 1.5 equiv), 4-bromobenzonitrile (91.0 mg, 0.50 mmol, 1.0 equiv), 4CzIPN photocatalyst (7.9 mg, 0.004 mmol, 0.02 equiv), $NiCl_2$•dme (5.5 mg, 0.025 mmol, 0.05 equiv), 4,4'-di-*tert*-butyl bipyridine (6.7 mg, 0.025 mmol, 0.05 equiv), and K_2HPO_4 (174.2 mg, 1.0 mmol, 2.0 equiv). Under a 26 W CFL, the

reaction was allowed to run for 16 h. The title compound was purified by column chromatography (silica gel, 5:1 hexanes/EtOAc) to afford a clear oil (89.5 mg, 68% yield).

^{1}H NMR (500 MHz, $CDCl_3$) δ 7.73 (d, *J* = 8.1 Hz, 3H), 7.61 (d, *J* = 7.9 Hz, 2H), 7.35 (d, *J* = 8.5 Hz,1H), 6.98 (d, *J* = 8.5 Hz, 1H), 5.52 (d, *J* = 12.4 Hz, 1H), 3.07 – 2.83 (m, 2H), 2.34 (s, 3H).

^{13}C NMR (126 MHz, $CDCl_3$) δ 191.1, 159.2, 144.2, 137.7, 132.8, 131.8, 126.9, 126.8, 120.7, 118.5, 118.0, 112.7, 78.6, 44.7, 20.6.

FT-IR (cm^{-1}, neat, ATR) 2918, 1687, 1617, 1489, 1134, 829, 596.

HRMS (ES+) m/z calc. for $C_{17}H_{14}NO_2$ [M+H] 263.0946, found 264.1016.

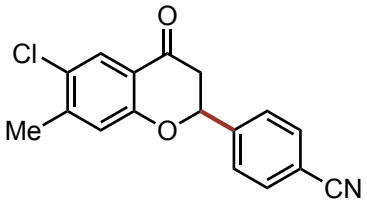

4-(6-chloro-7-methyl-4-oxochroman-2-yl)benzonitrile (2d)

The general procedure was followed with trifluoroborate (226.5 mg, 0.75 mmol, 1.5 equiv), 4-bromobenzonitrile (91.0 mg, 0.50 mmol, 1.0 equiv), 4CzIPN photocatalyst (7.9 mg, 0.004 mmol, 0.02 equiv), $NiCl_2$•dme (5.5 mg, 0.025 mmol, 0.05 equiv), 4,4'-di-*tert*-butyl bipyridine (6.7 mg, 0.025 mmol, 0.05 equiv), and K_2HPO_4 (174.2 mg, 1.0 mmol, 2.0 equiv). Under a 26 W CFL, the reaction was allowed to run for 16 h. The title compound was purified by column chromatography (silica gel, 5:1 hexanes/EtOAc) to afford a clear oil (105.4 mg, 71% yield).

^{1}H NMR (500 MHz, $CDCl_3$) δ 7.86 (s, 1H), 7.73 (d, *J* = 8.0 Hz, 2H), 7.59 (d, *J* = 7.9 Hz, 2H), 6.97 (s, 1H), 5.52 (d, *J* = 12.3 Hz, 1H), 3.02 – 2.84 (m, 2H), 2.40 (s, 3H).

^{13}C NMR (126 MHz, $CDCl_3$) δ 189.6, 159.3, 145.8, 143.7, 132.9, 128.5, 127.0, 126.7, 120.3, 120.0, 118.4, 112.82, 78.8, 44.3, 21.0.

FT-IR (cm^{-1}, neat, ATR) 3066, 1690, 1613, 1407, 1236, 1154, 893, 837, 655.

HRMS: compound unstable.

^{1}H NMR (DMSO-d^{6}, 500 MHz) spectrum of 2-(trifluoro-λ_4-boranyl)chroman-4-one, potassium salt (**5.3.1**)

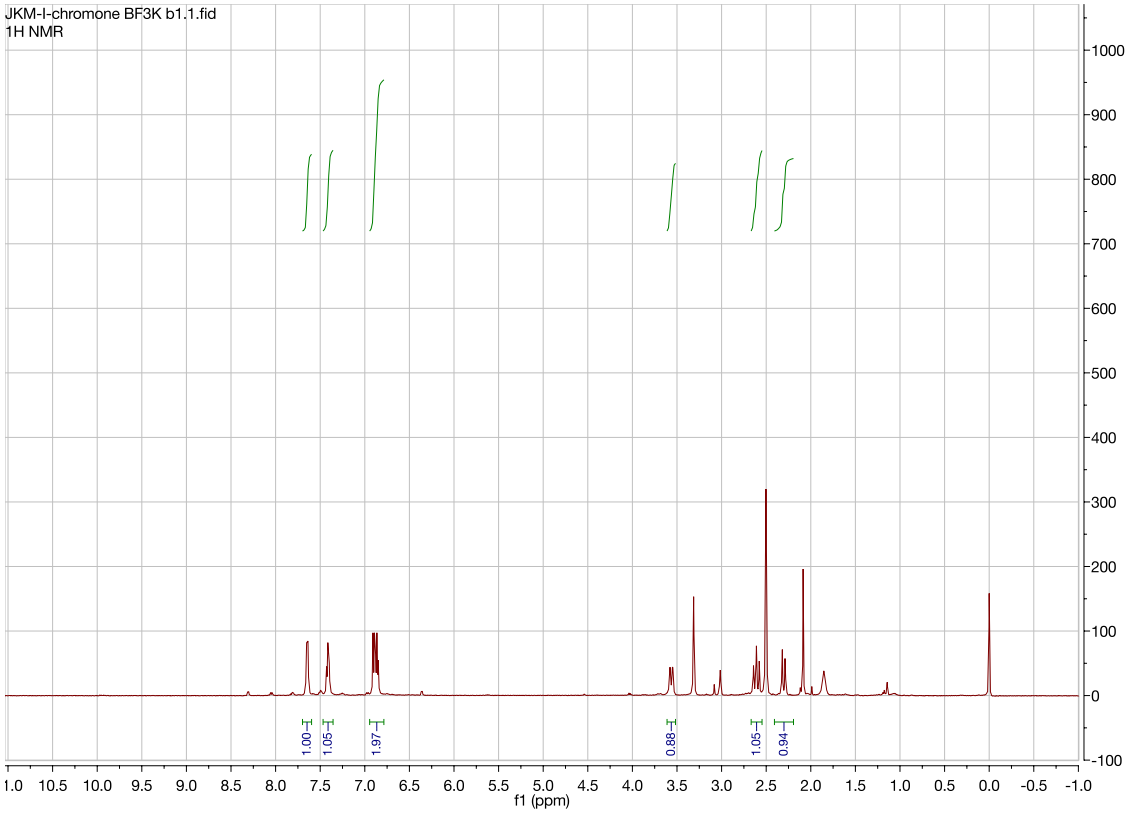

^{13}C NMR (DMSO-d^{6}, 125.8 MHz) spectrum of 2-(trifluoro-λ_4-boranyl)chroman-4-one, potassium salt (**5.3.1**)

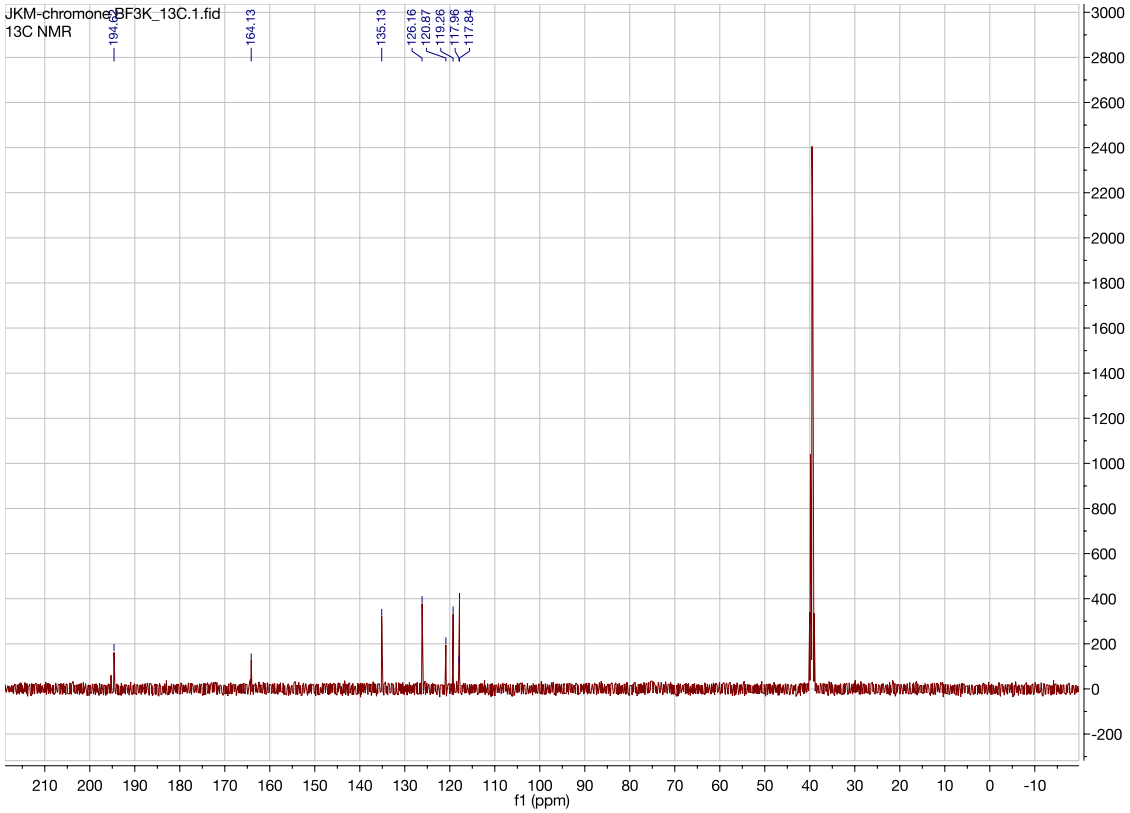

^{19}F NMR (DMSO-d^{6}, 470.8 MHz) spectrum of 2-(trifluoro-λ_4-boranyl)chroman-4-one, potassium salt (**5.3.1**)

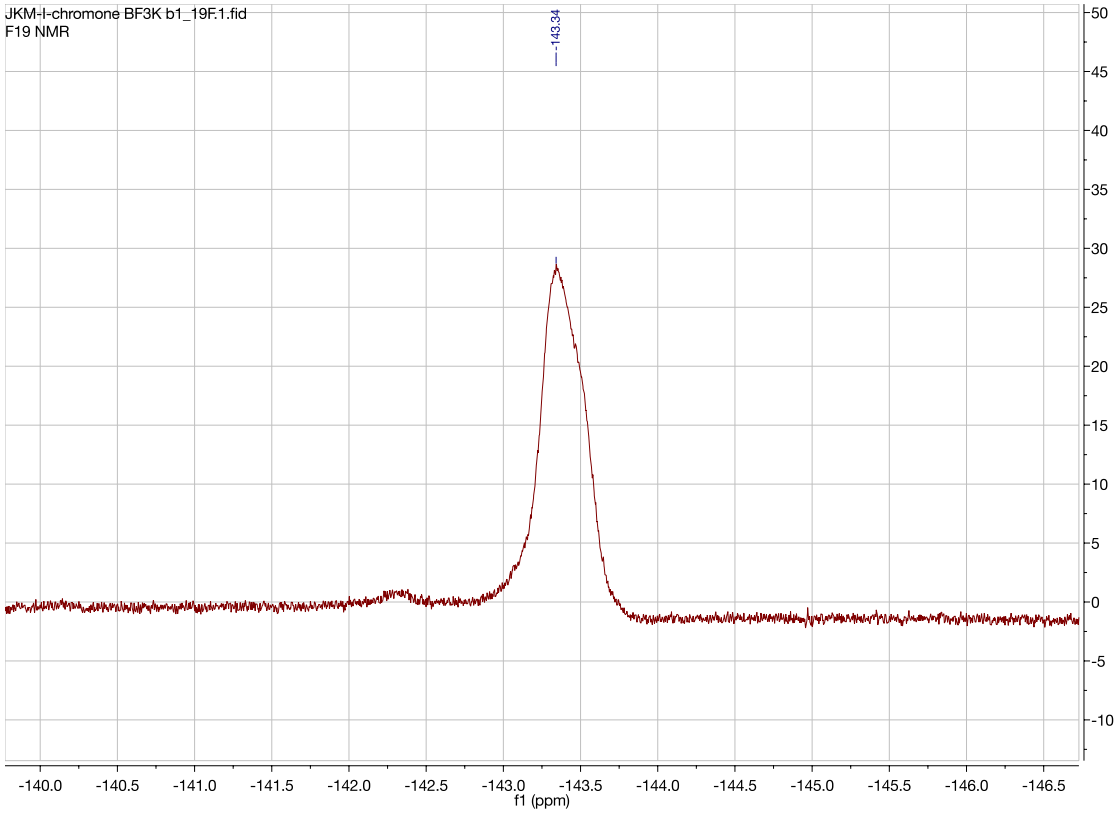

^{11}B NMR (DMSO-d^{6}, 128.4 MHz) spectrum of 2-(trifluoro-λ_4-boranyl)chroman-4-one, potassium salt (**5.3.1**)

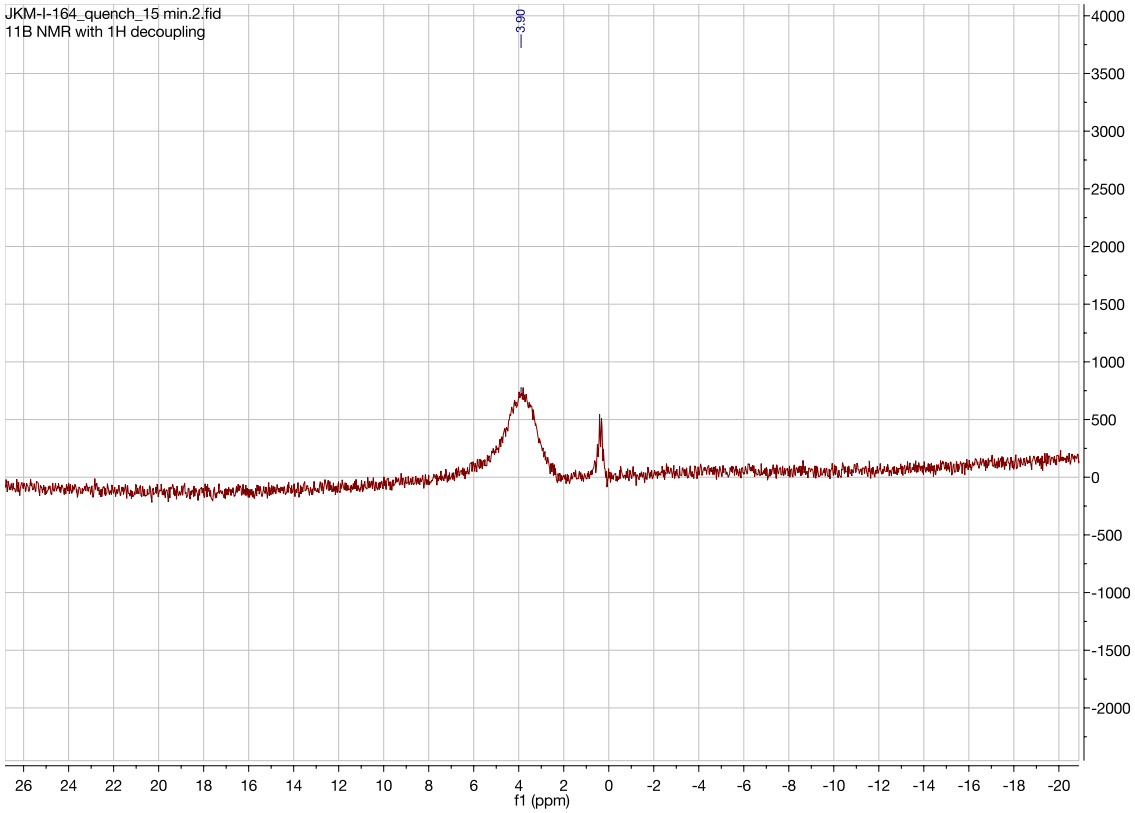

^{1}H NMR (DMSO-d^{6}, 500 MHz) spectrum of 6-methyl-2-(trifluoro-l$_{4}$-boranyl)chroman-4-one, potassium salt (**5.3.2**)

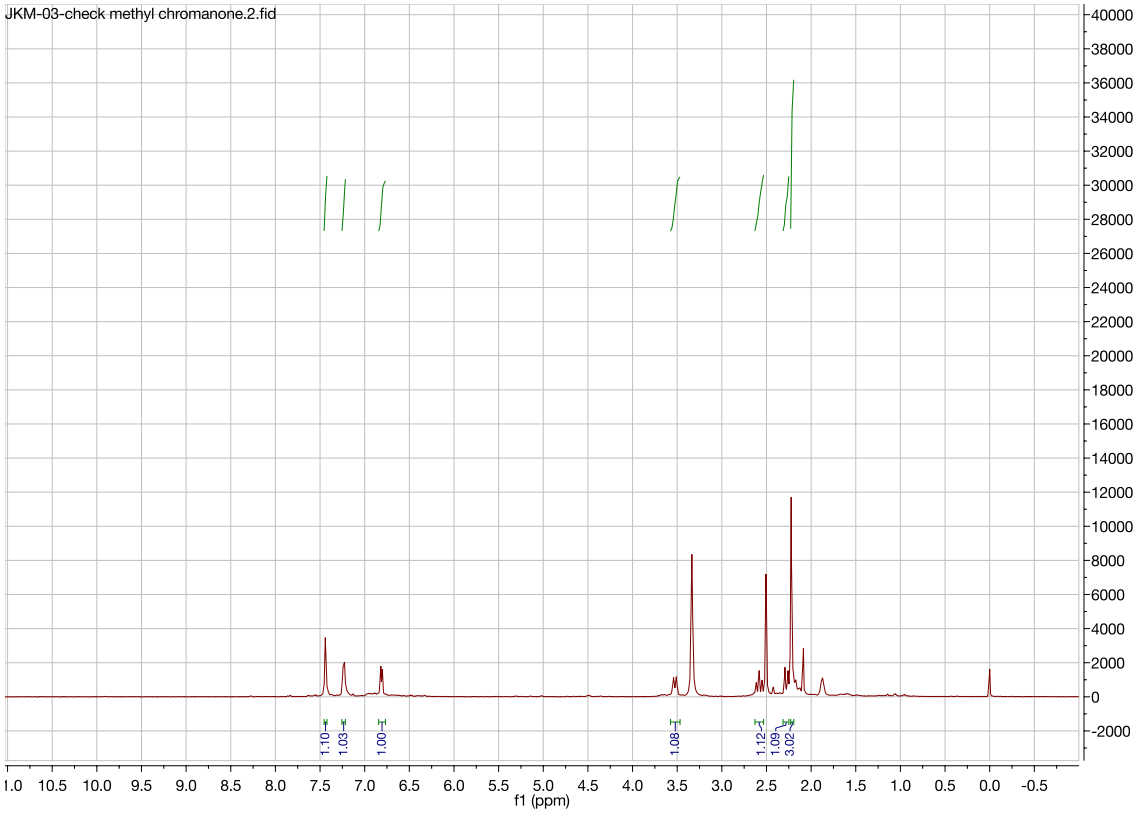

^{13}C NMR (DMSO-d^{6}, 125.8 MHz) spectrum of 6-methyl-2-(trifluoro-l$_{4}$-boranyl)chroman-4-one, potassium salt (**5.3.2**)

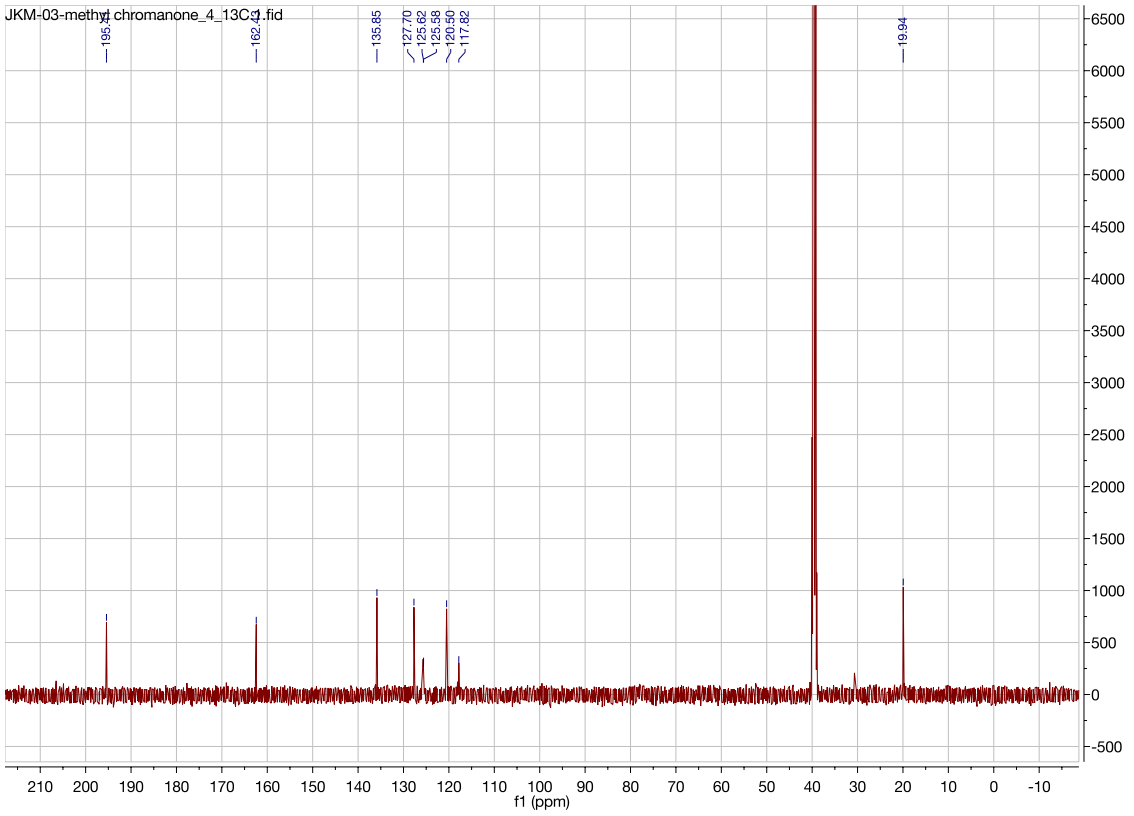

^{19}F NMR (DMSO-d^{6}, 470.8 MHz) spectrum of 6-methyl-2-(trifluoro-l$_{4}$-boranyl)chroman-4-one, potassium salt (**5.3.2**)

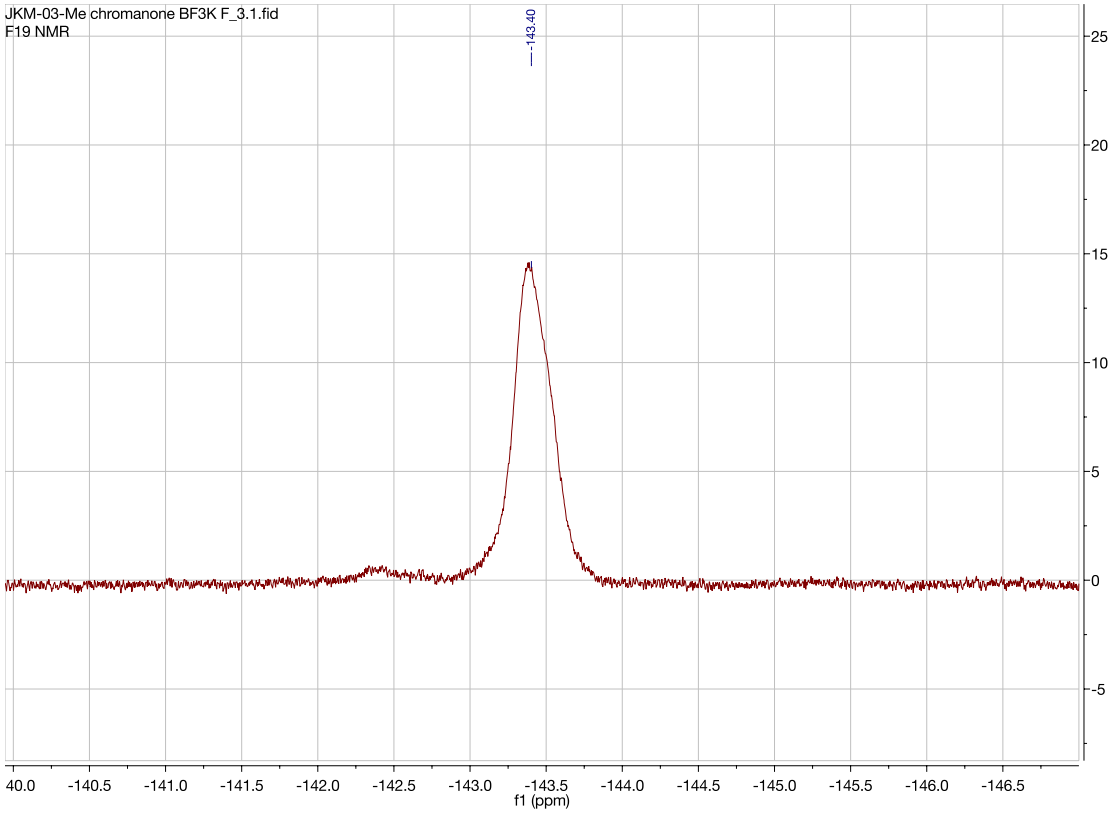

^{11}B NMR (DMSO-d^{6}, 128.4 MHz) spectrum of 6-methyl-2-(trifluoro-l$_{4}$-boranyl)chroman-4-one, potassium salt (**5.3.2**)

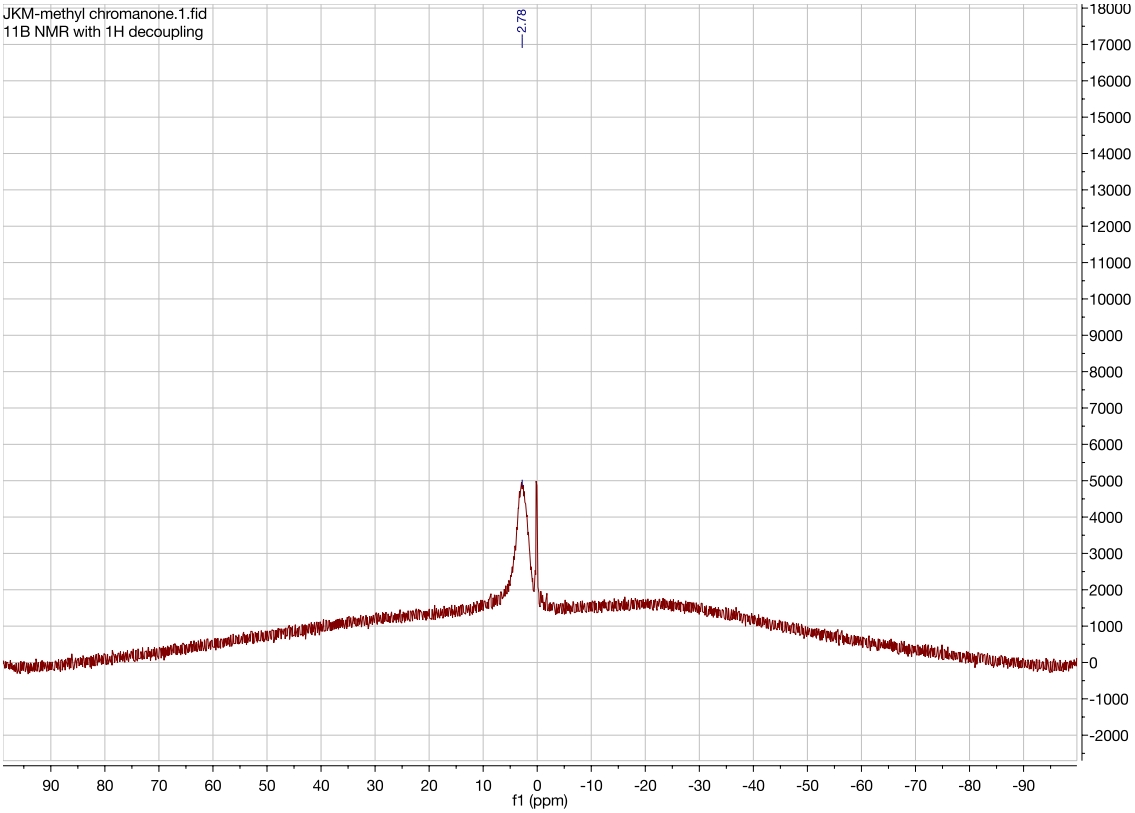

^{1}H NMR (DMSO-d^{6}, 500 MHz) spectrum of 6-chloro-7-methyl-2-(trifluoro-l$_{4}$-boranyl)chroman-4-one, potassium salt (**5.3.3**)

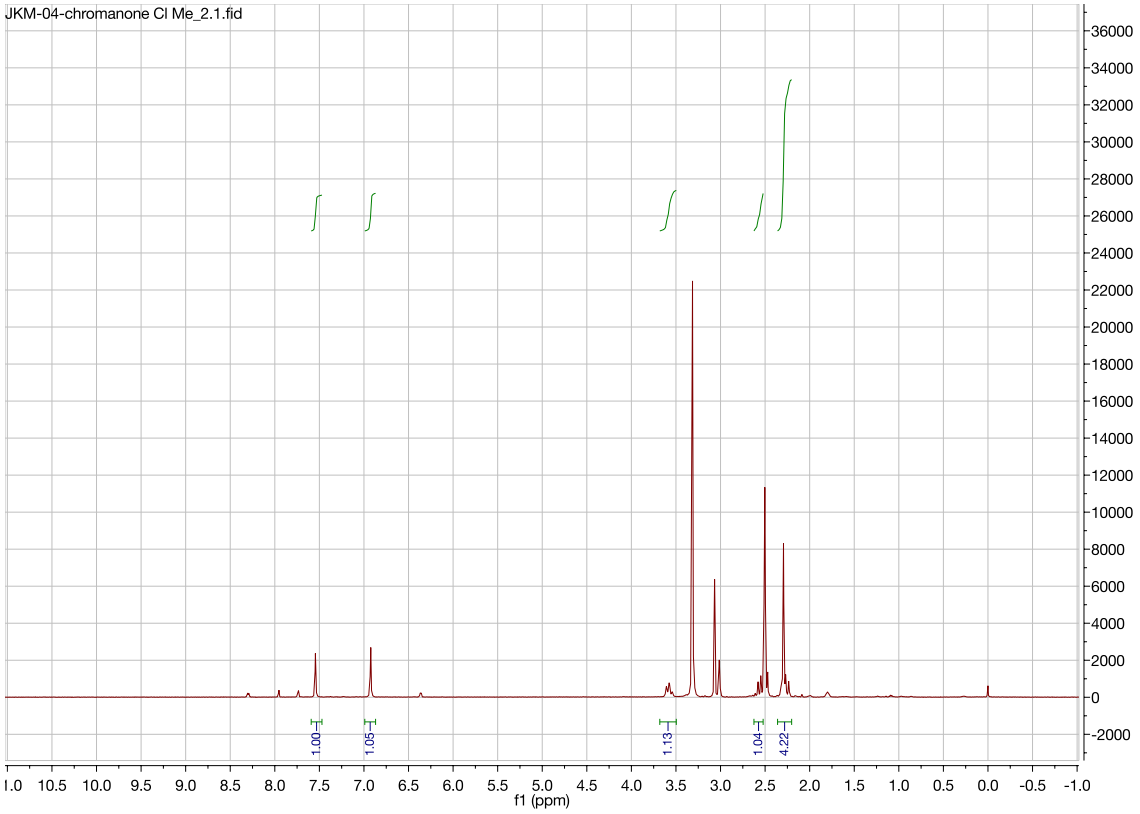

^{13}C NMR (DMSO-d^6, 125.8 MHz) spectrum of 6-chloro-7-methyl-2-(trifluoro-l_4-boranyl)chroman-4-one, potassium salt (**5.3.3**)

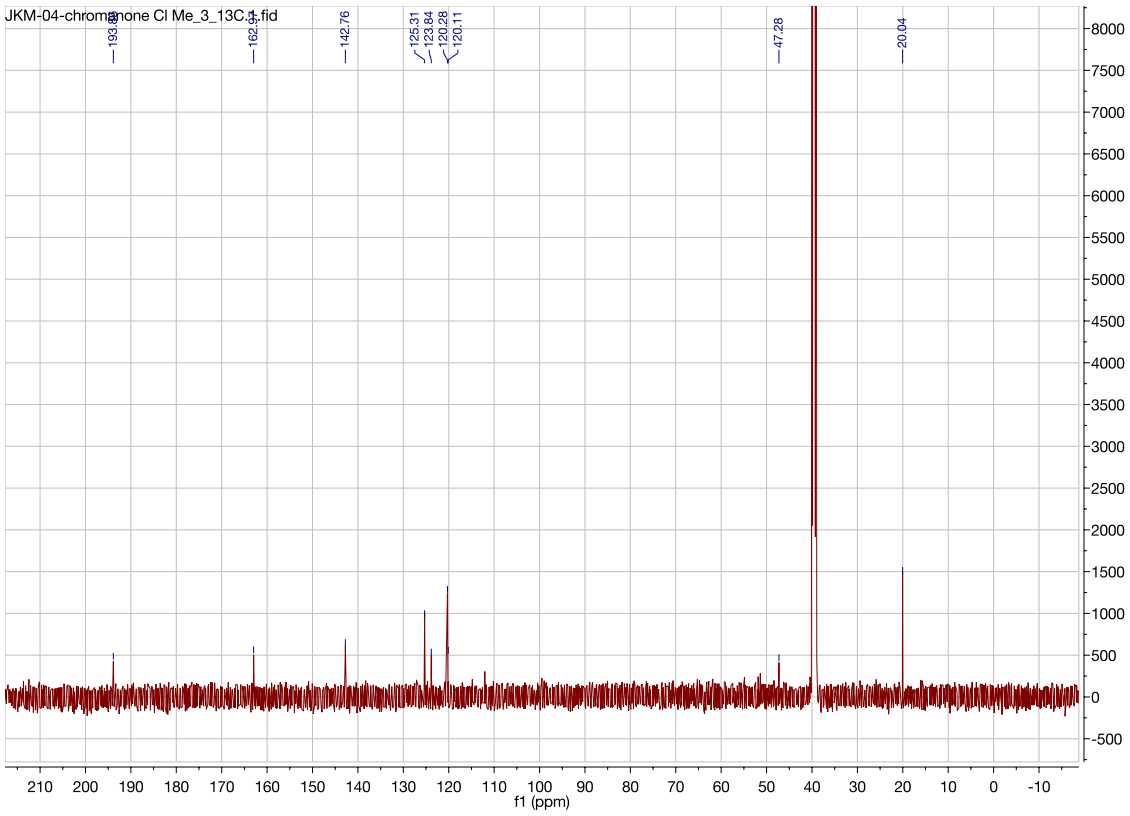

^{19}F NMR (DMSO-d^{6}, 470.8 MHz) spectrum of 6-chloro-7-methyl-2-(trifluoro-l$_{4}$-boranyl)chroman-4-one, potassium salt (**5.3.3**)

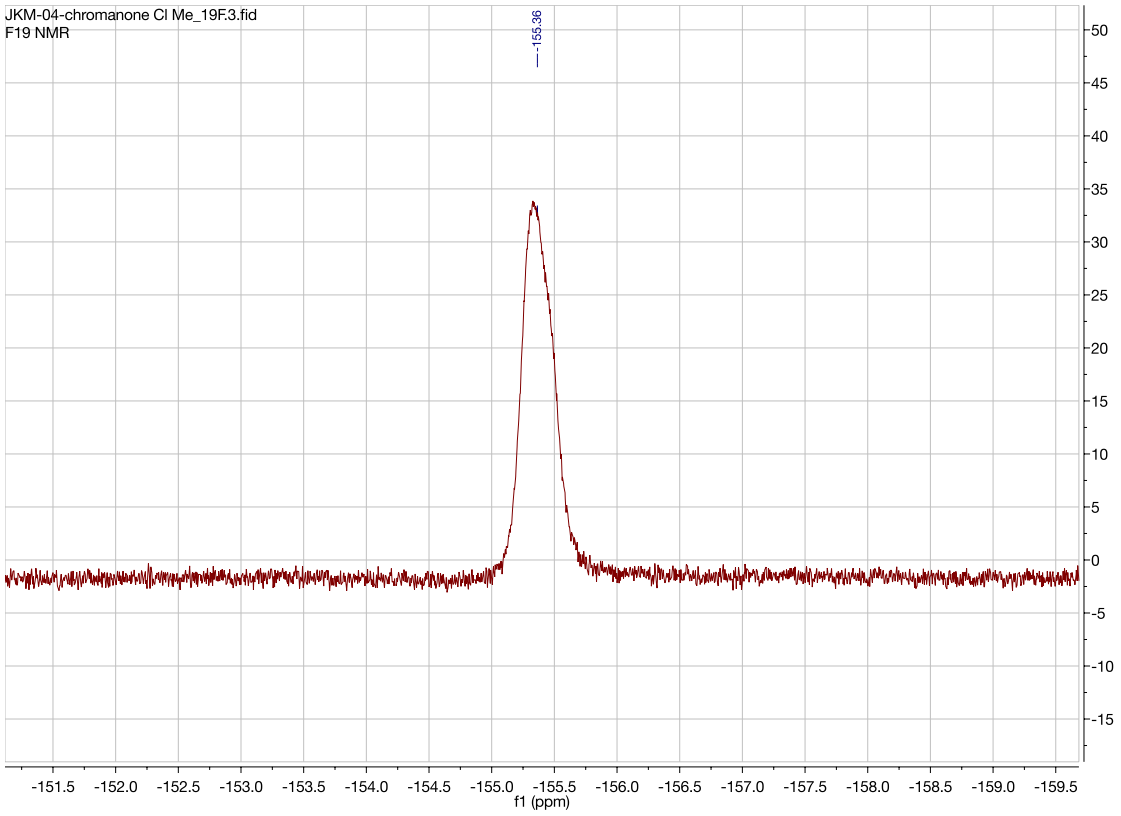

^{1}H ($CDCl_3$, 500 MHz) spectra of 2-(4-(chloromethyl)phenyl)chroman-4-one (**5.5.1**)

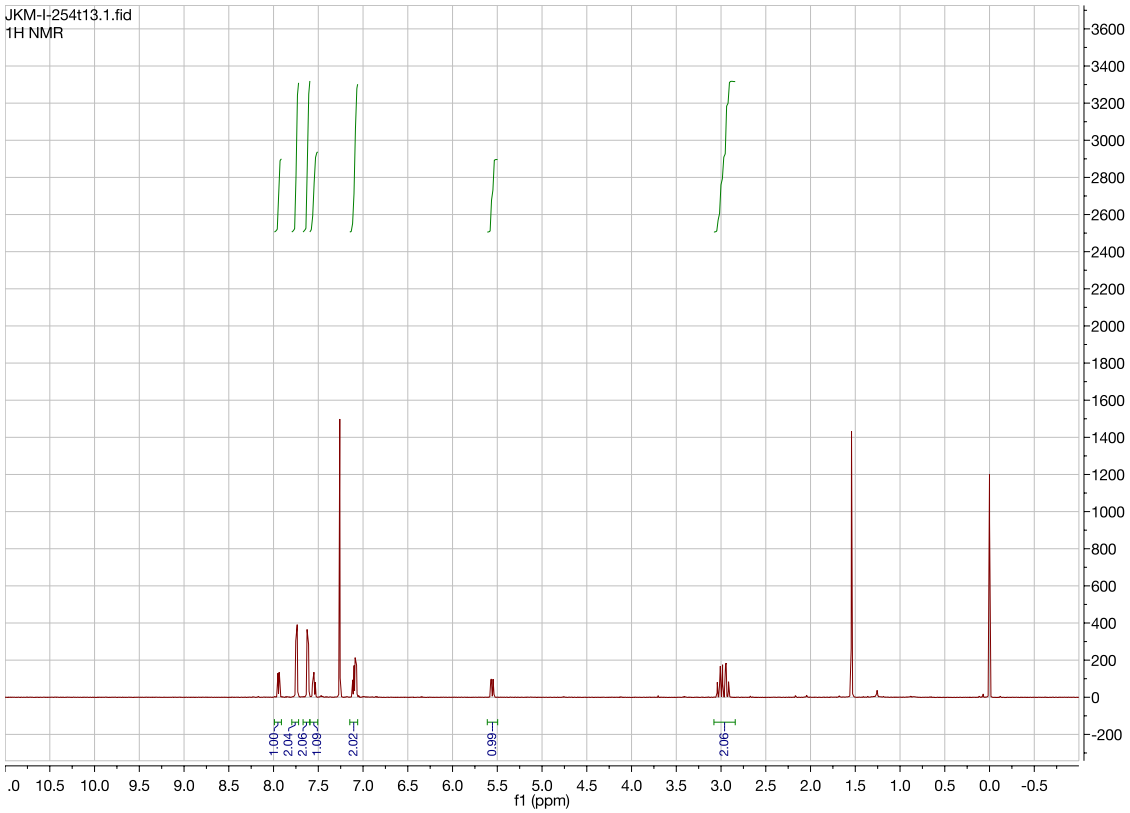

^{13}C NMR ($CDCl_3$, 125.8 MHz) spectrum of 4-(4-oxochroman-2-yl)benzaldehyde (**5.5.2**)

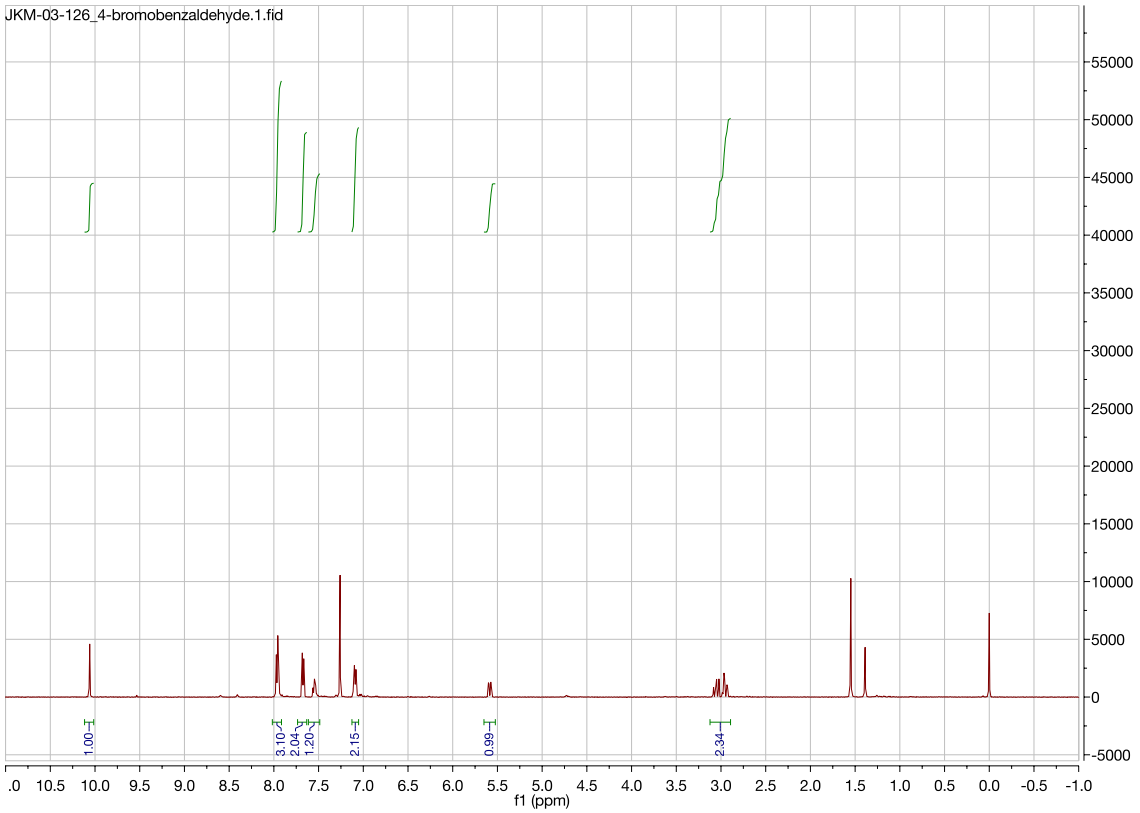

^{1}H ($CDCl_3$, 500 MHz) spectra of 2-(4-chlorophenyl)chroman-4-one (**5.5.3**)

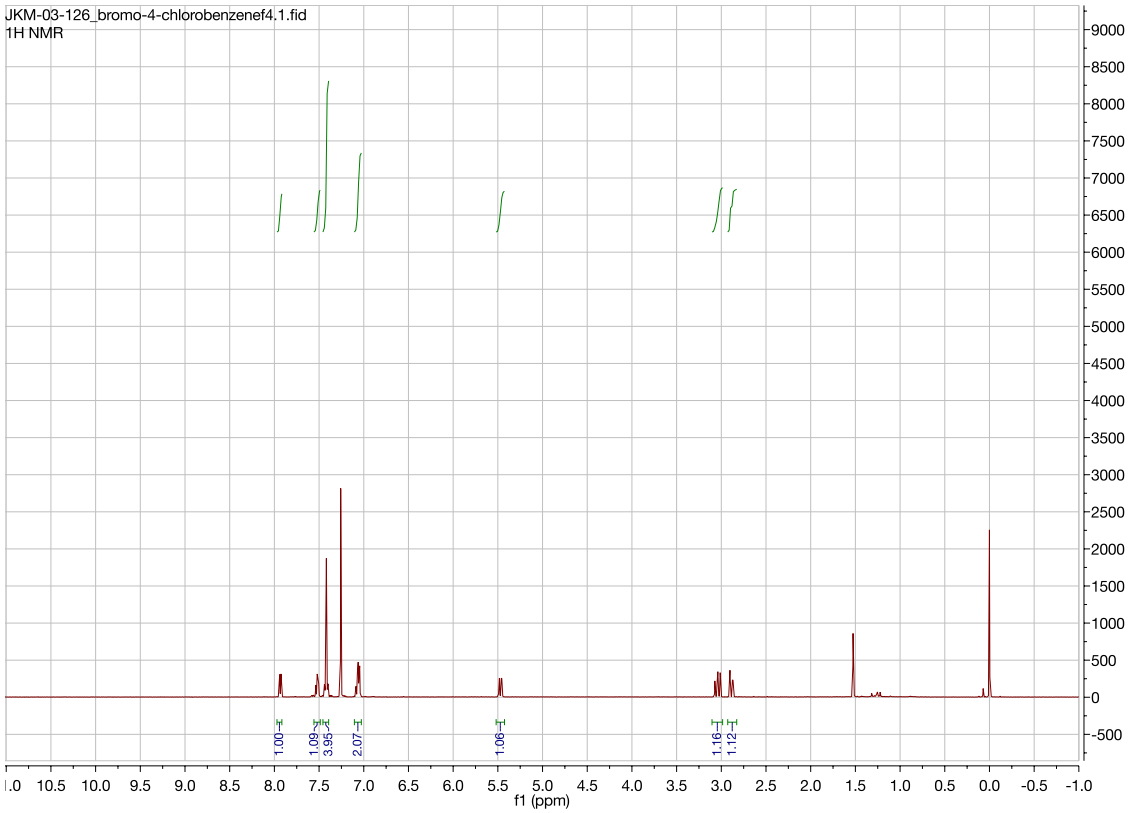

^{1}H ($CDCl_3$, 500 MHz) spectra of 2-(4-oxochroman-2-yl)benzonitrile (**5.5.4**)

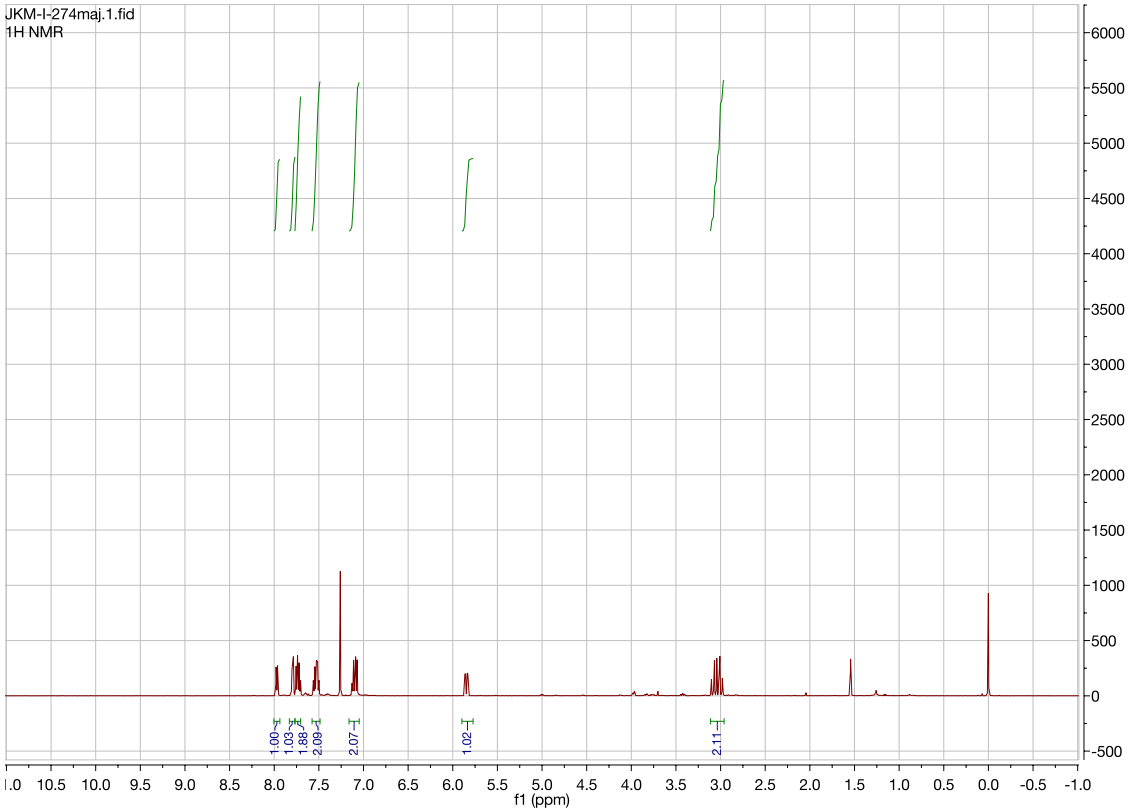

^{13}C NMR ($CDCl_3$, 125.8 MHz) spectrum of 2-(4-oxochroman-2-yl)benzonitrile (**5.5.4**)

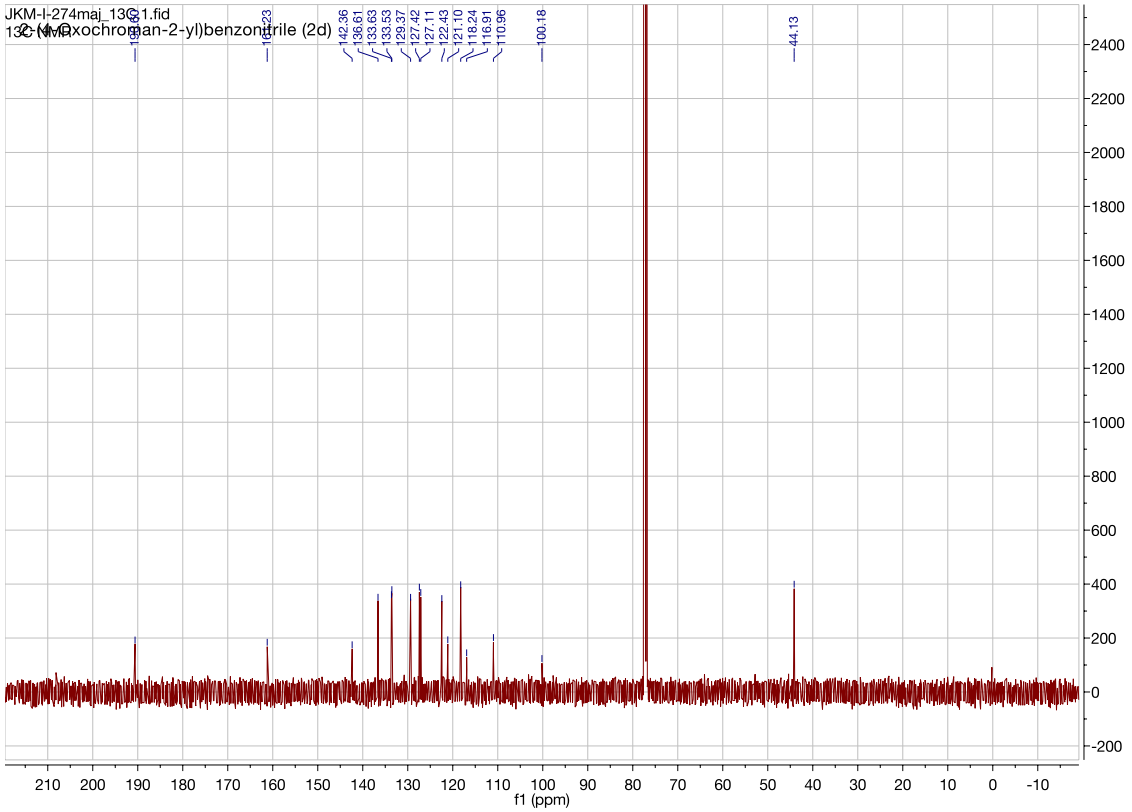

^{1}H ($CDCl_3$, 500 MHz) spectra of 2-(*m*-tolyl)chroman-4-one (**5.5.5**)

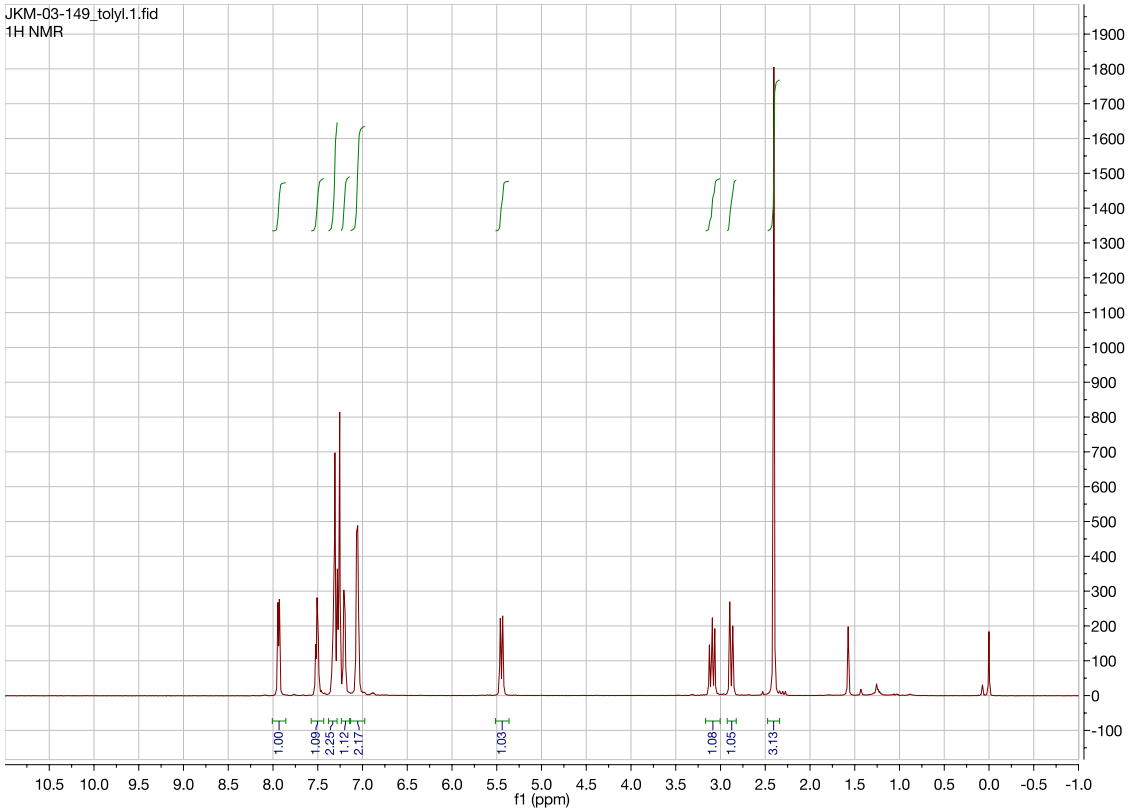

^{13}C NMR ($CDCl_3$, 125.8 MHz) spectrum of 2-(*m*-tolyl)chroman-4-one (**5.5.5**)

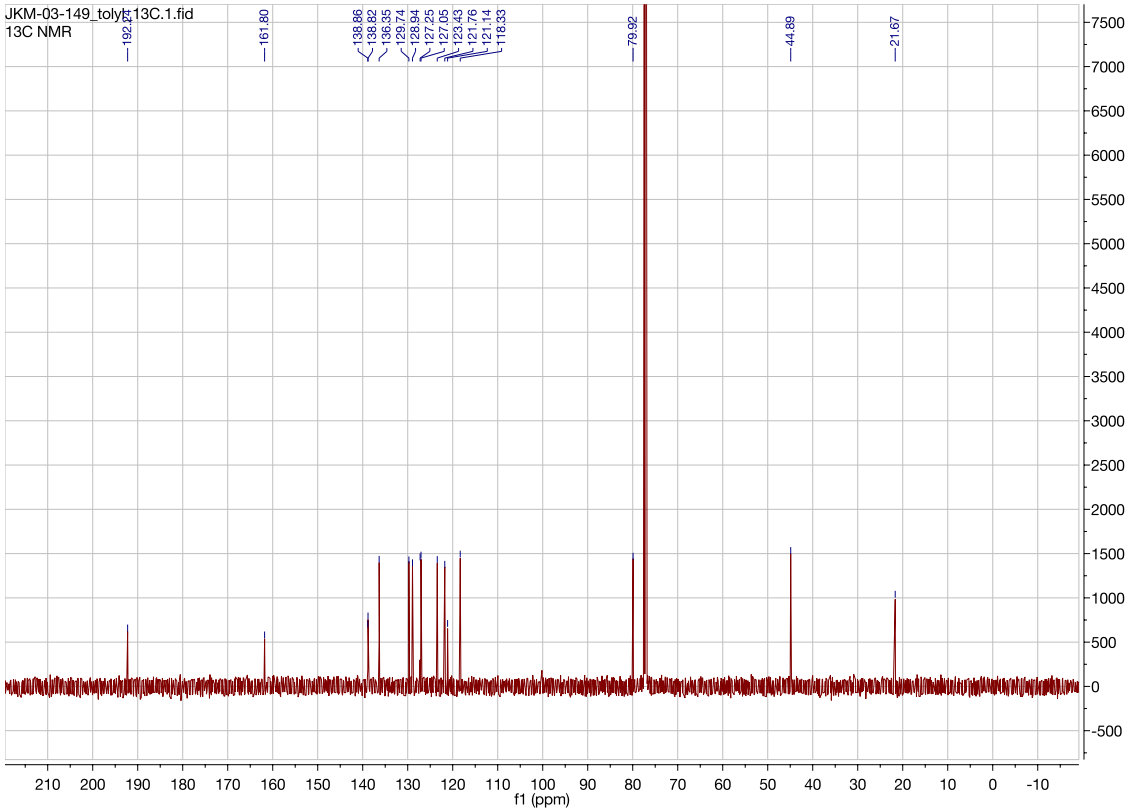

^{1}H ($CDCl_3$, 500 MHz) spectra of 2-(4-(trifluoromethyl)phenyl)chroman-4-one (**5.5.6**)

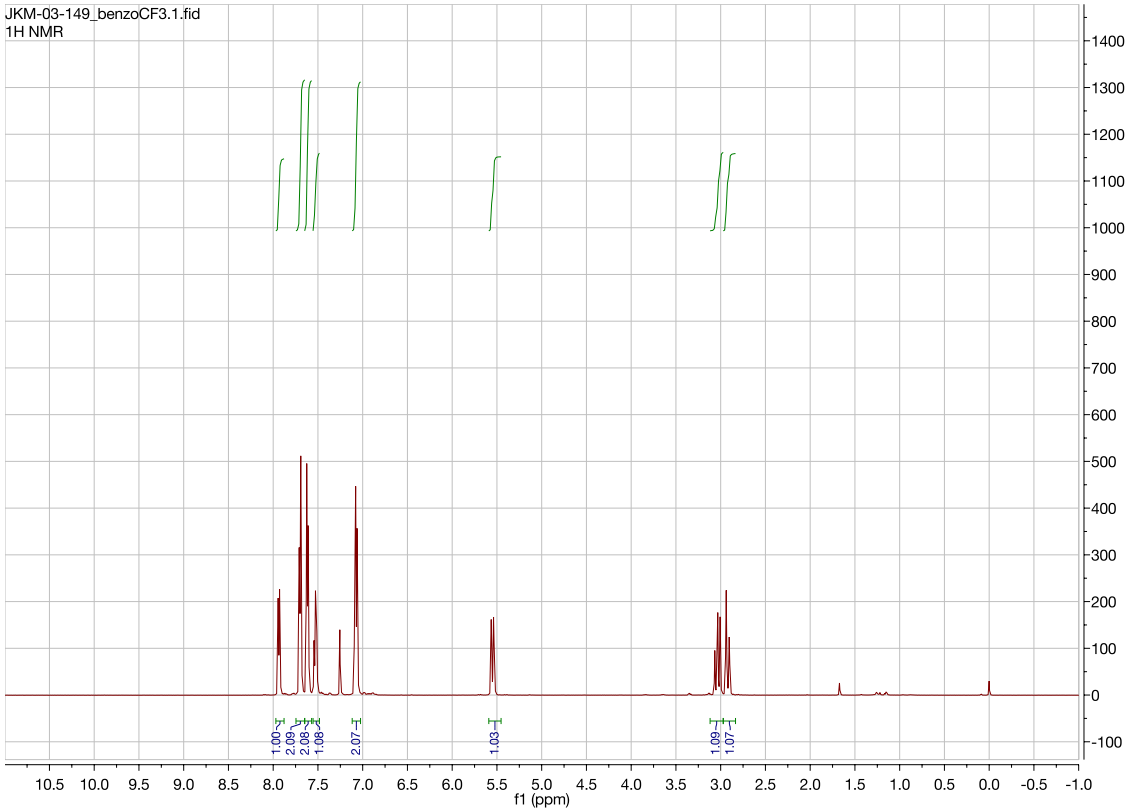

^{1}H ($CDCl_3$, 500 MHz) spectra of 2-phenylchroman-4-one (**5.5.7**)

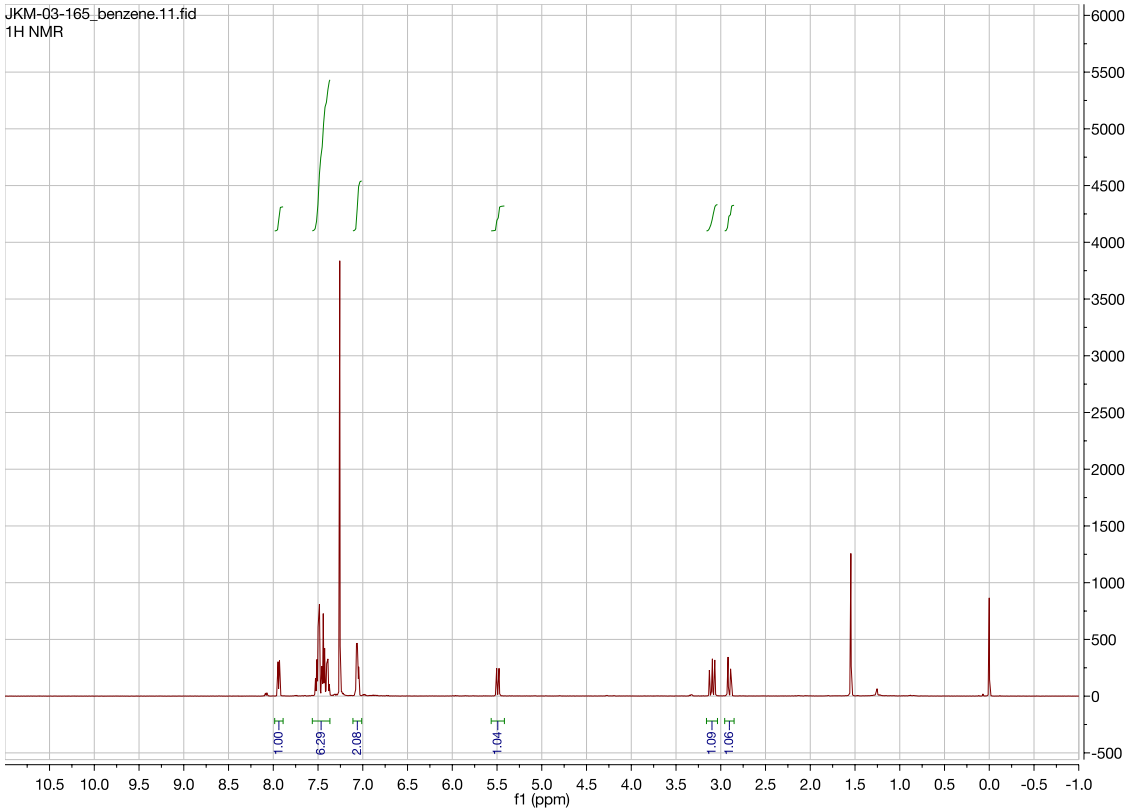

^{1}H ($CDCl_3$, 500 MHz) spectra of 2-(3,5-bis(trifluoromethyl)phenyl)chroman-4-one (**5.5.8**)

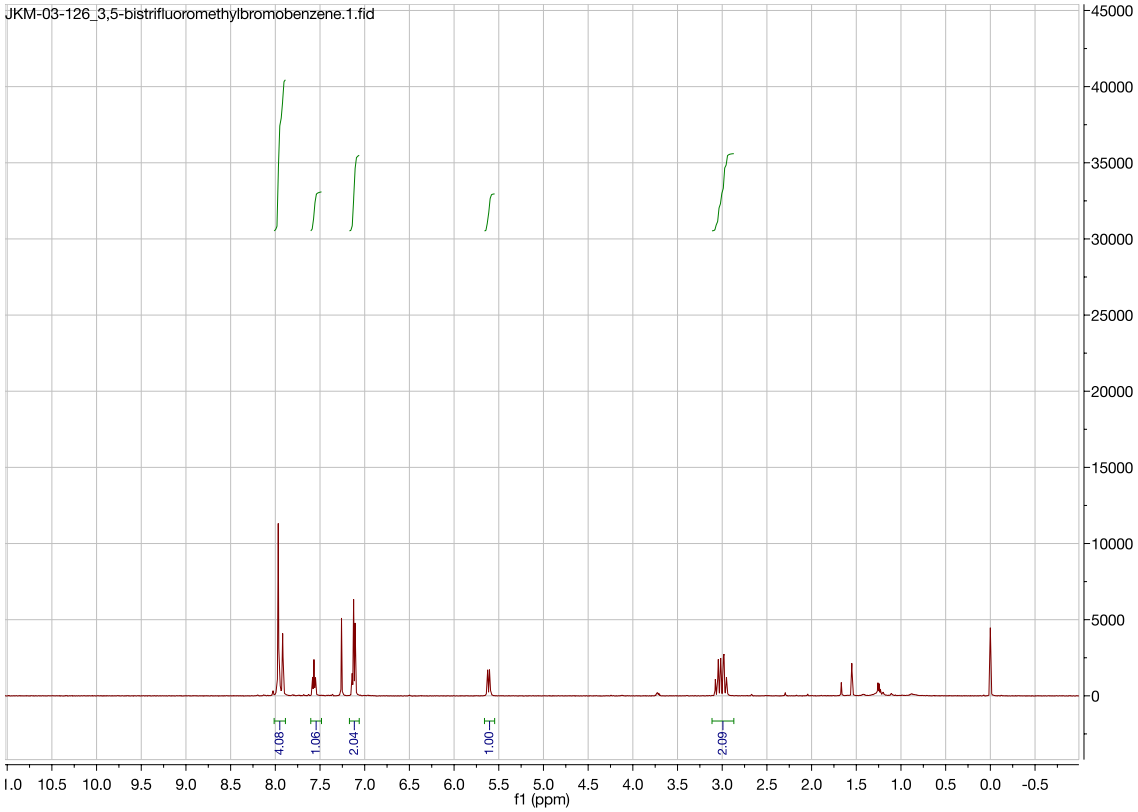

^{13}C NMR ($CDCl_3$, 125.8 MHz) spectrum of 2-(3,5-bis(trifluoromethyl)phenyl)chroman-4-one (**5.5.8**)

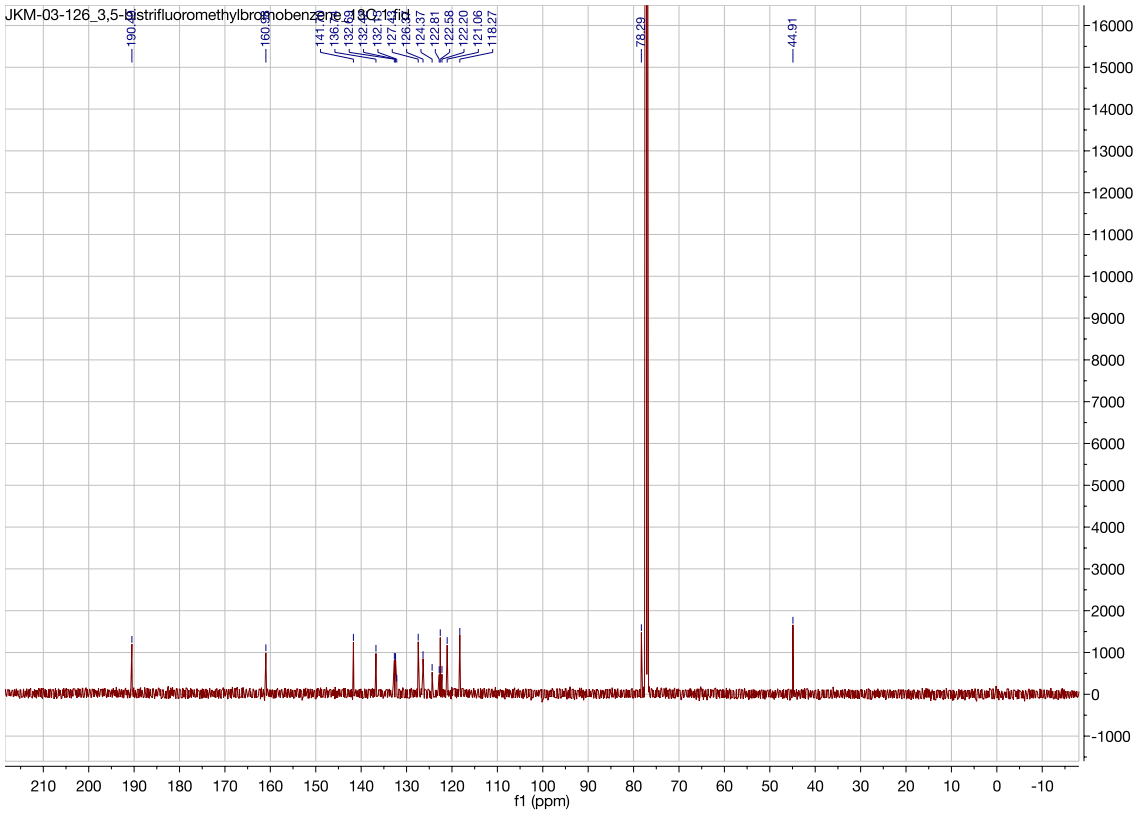

^{1}H ($CDCl_3$, 500 MHz) spectra of 2-(4-(chloromethyl)phenyl)chroman-4-one (**5.5.9**)

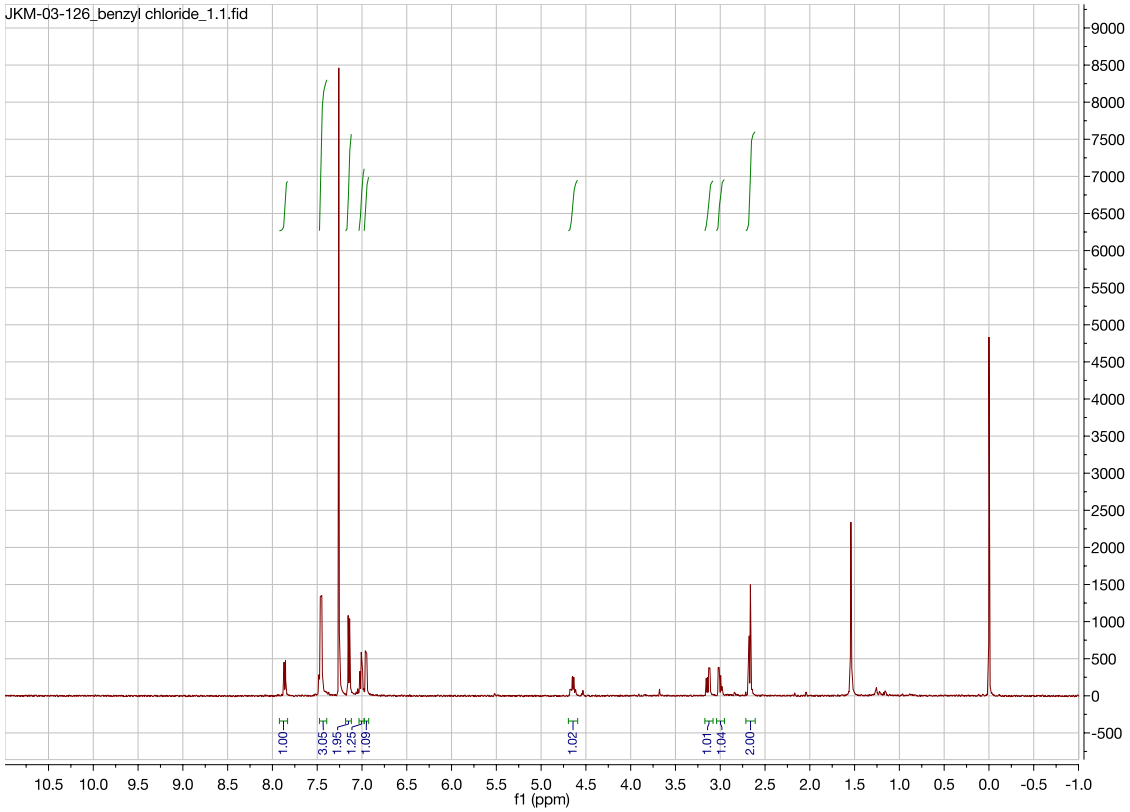

^{1}H ($CDCl_3$, 500 MHz) spectra of 2-(3-hydroxyphenyl)chroman-4-one (**5.5.10**)

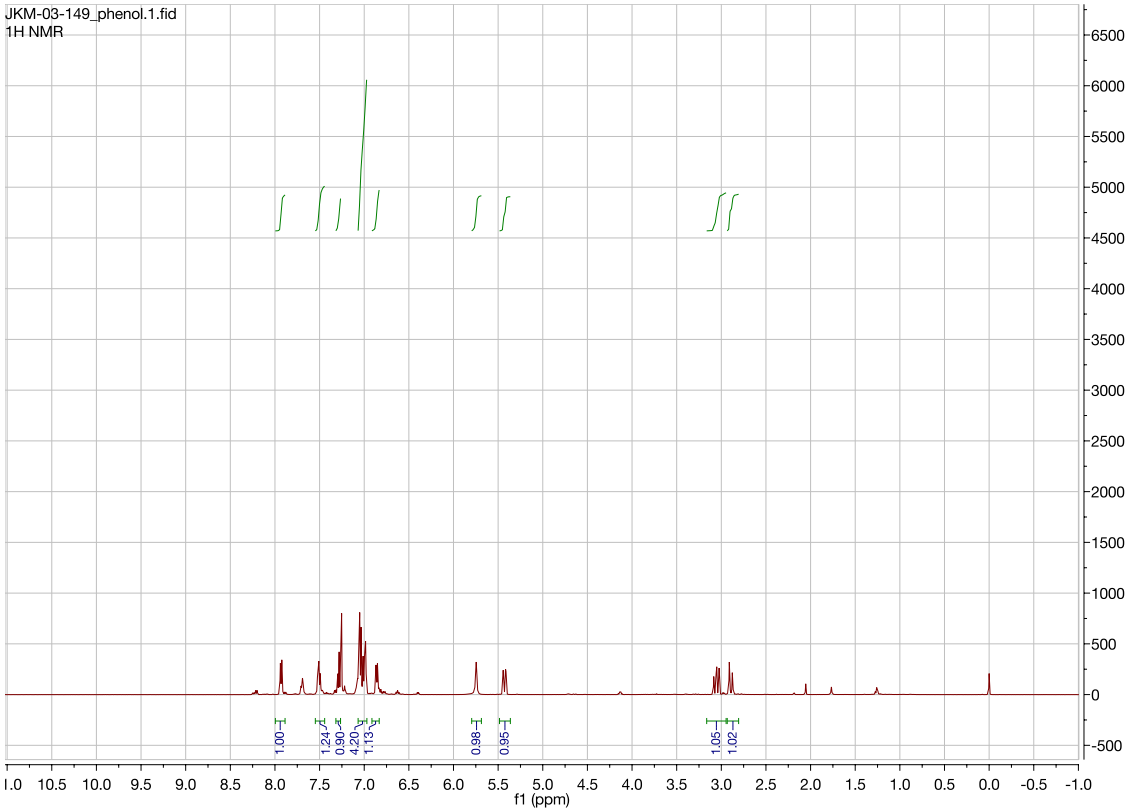

^{1}H ($CDCl_3$, 500 MHz) spectra of 2-(benzofuran-5-yl)chroman-4-one (**5.5.11**)

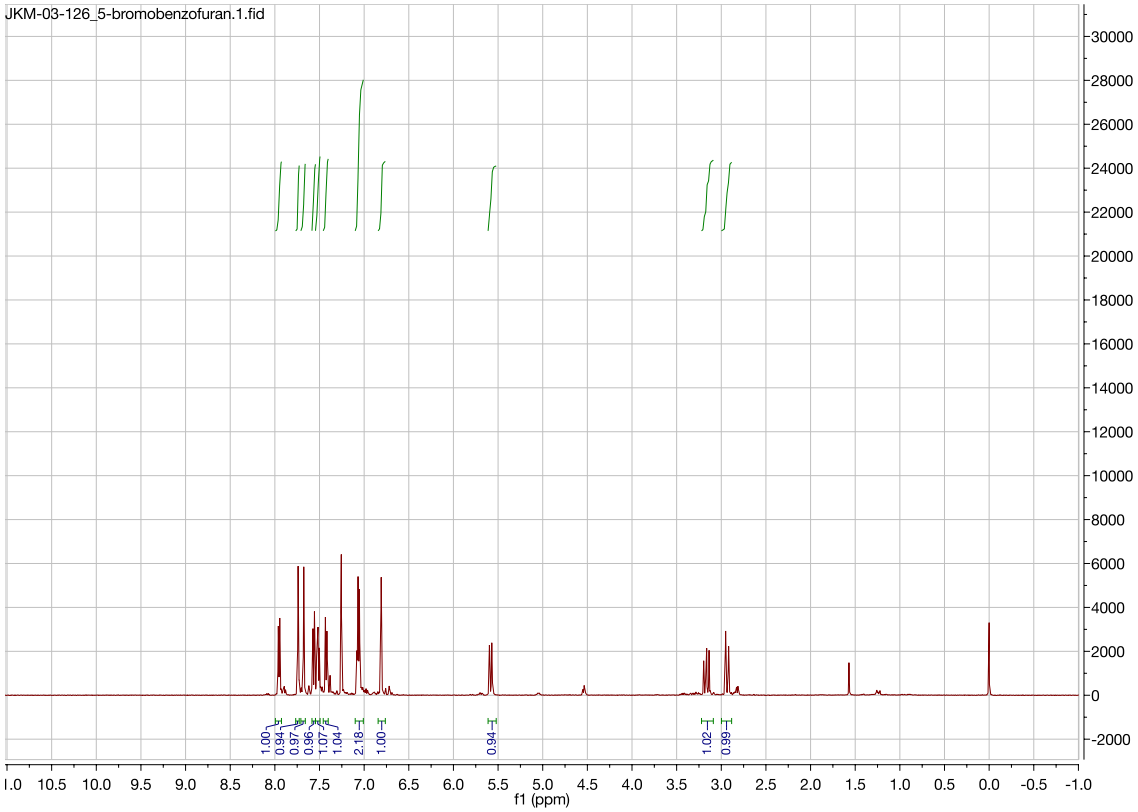

^{13}C NMR ($CDCl_3$, 125.8 MHz) spectrum of 2-(benzofuran-5-yl)chroman-4-one (**5.5.11**)

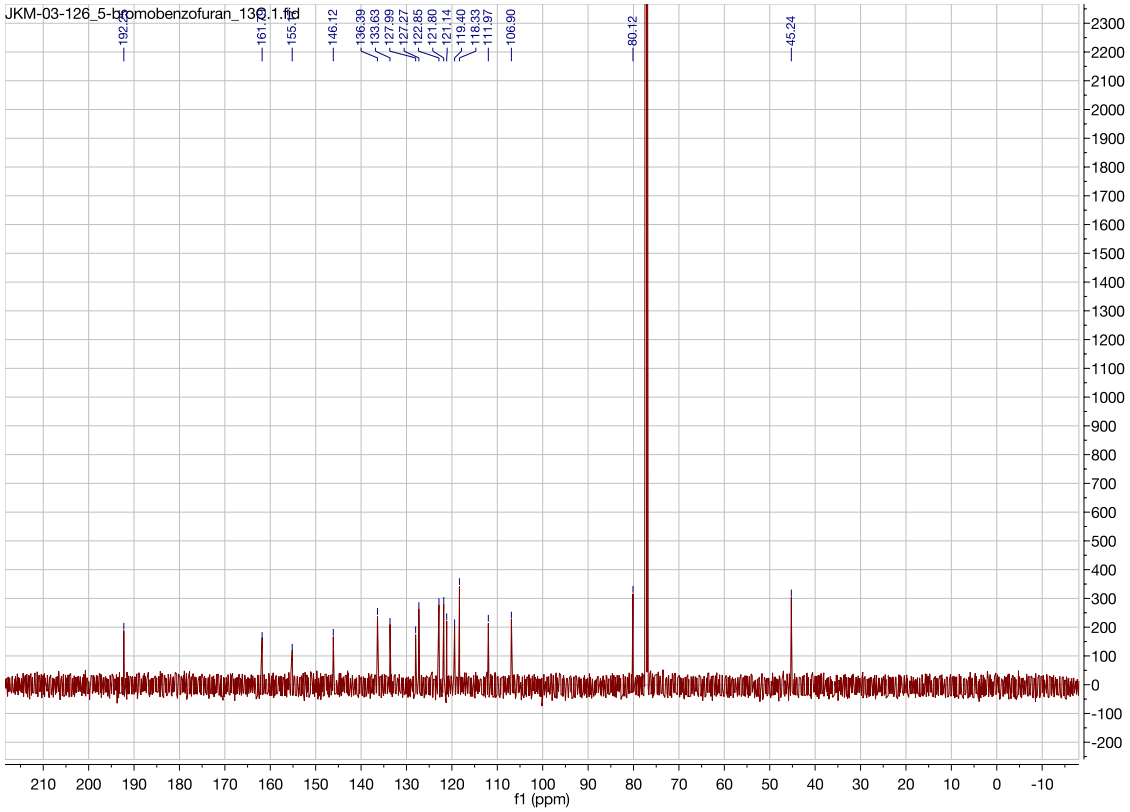

^{1}H ($CDCl_3$, 500 MHz) spectra of 2-(benzo[*b*]thiophen-5-yl)chroman-4-one (**5.5.12**)

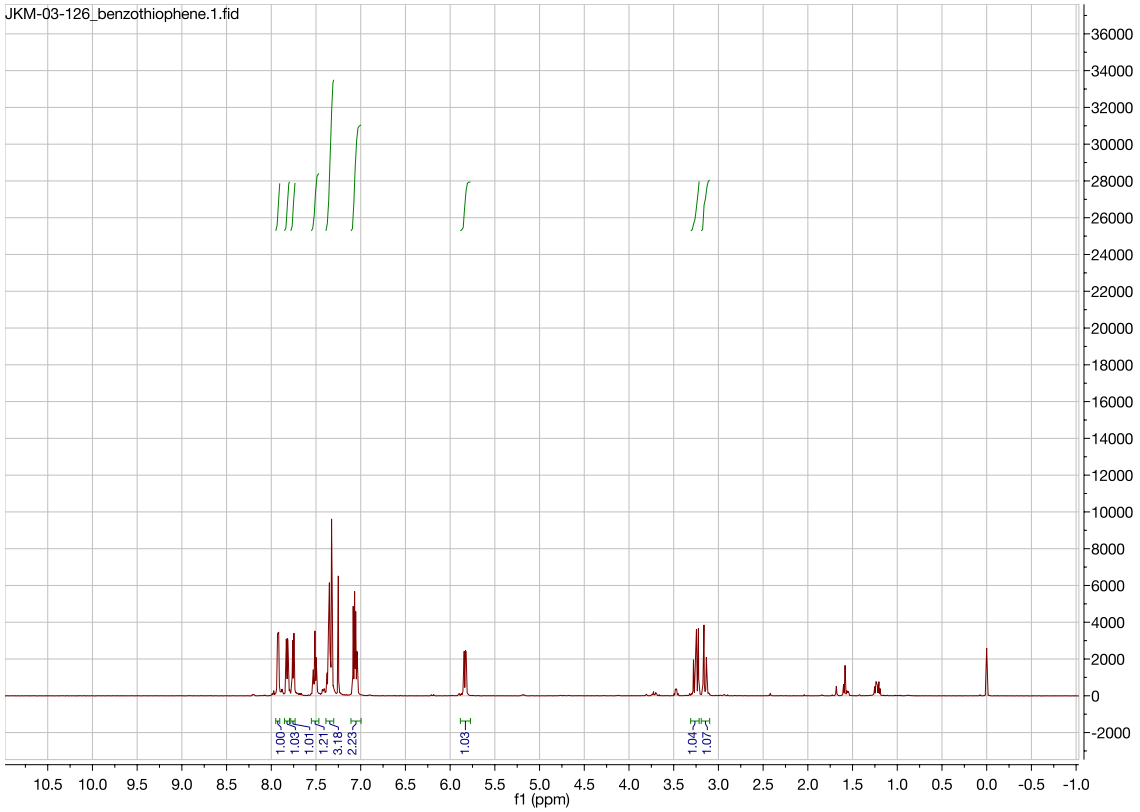

^{13}C NMR ($CDCl_3$, 125.8 MHz) spectrum of 2-(benzo[*b*]thiophen-5-yl)chroman-4-one (**5.5.12**)

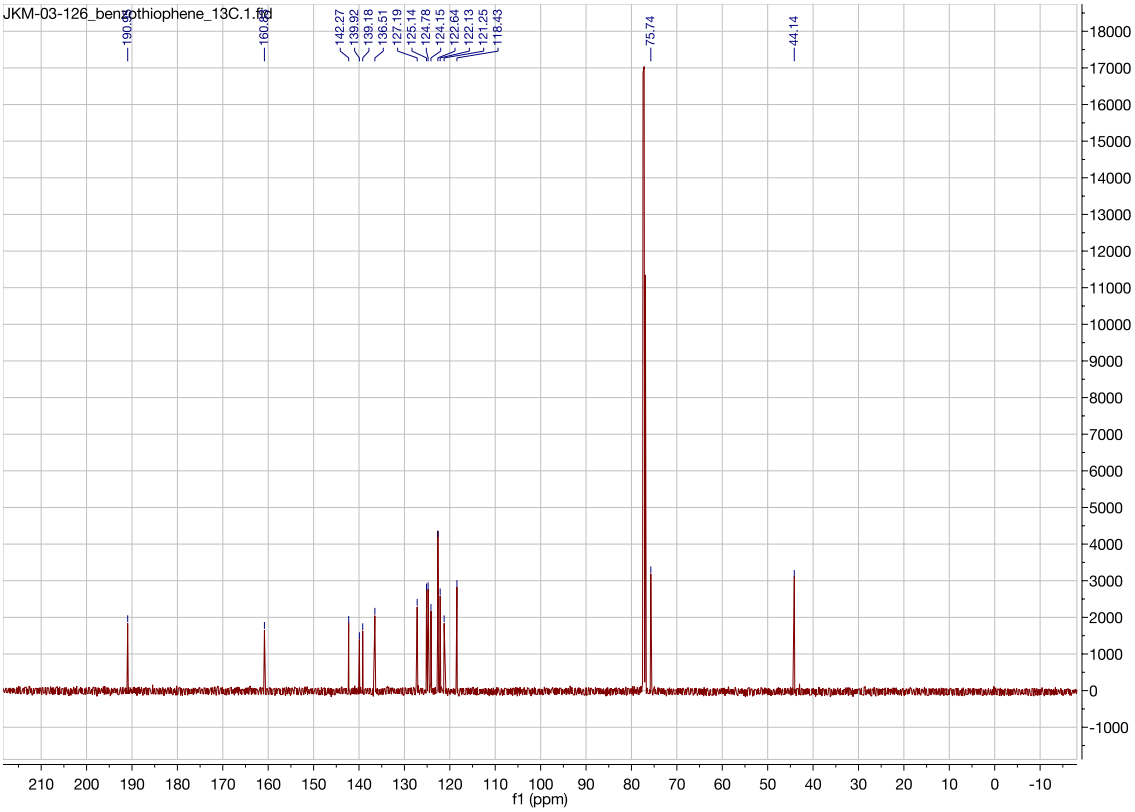

^{1}H ($CDCl_3$, 500 MHz) spectra of 2-(thiophen-2-yl)chroman-4-one (**5.5.13**)

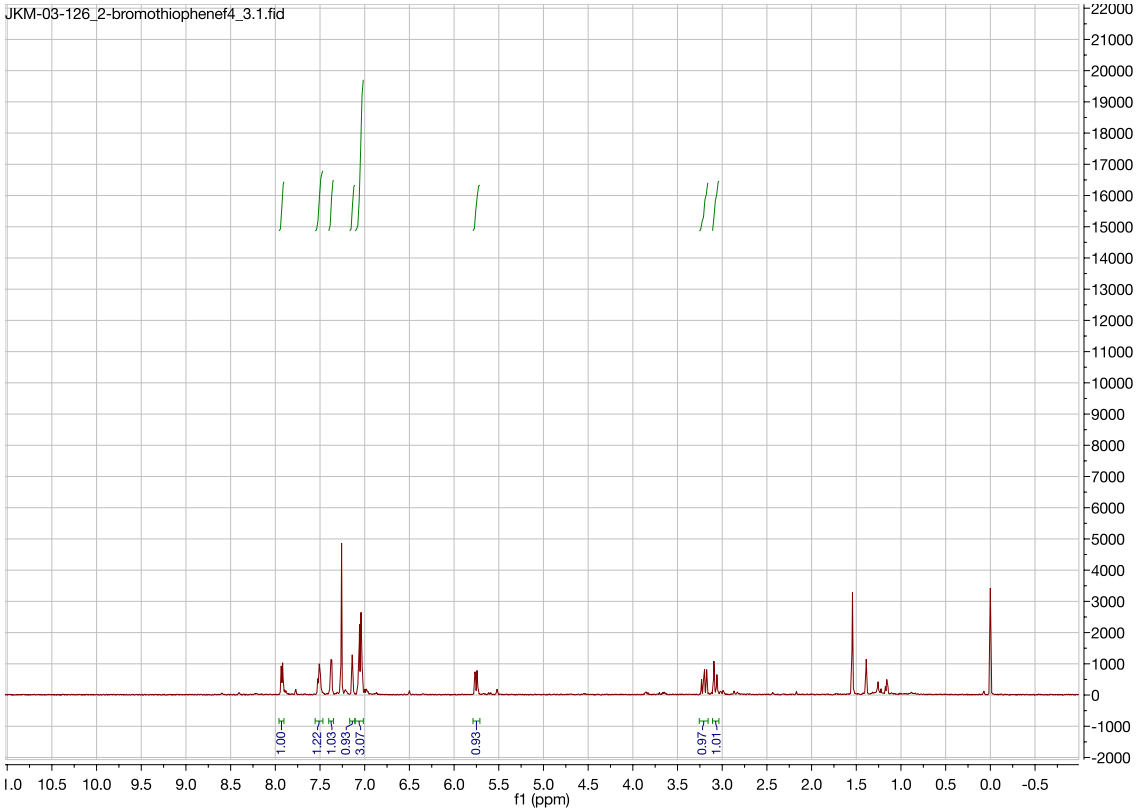

^{1}H ($CDCl_3$, 500 MHz) spectra of 2-(5-(trifluoromethyl)pyridin-2-yl)chroman-4-one (**5.5.15**)

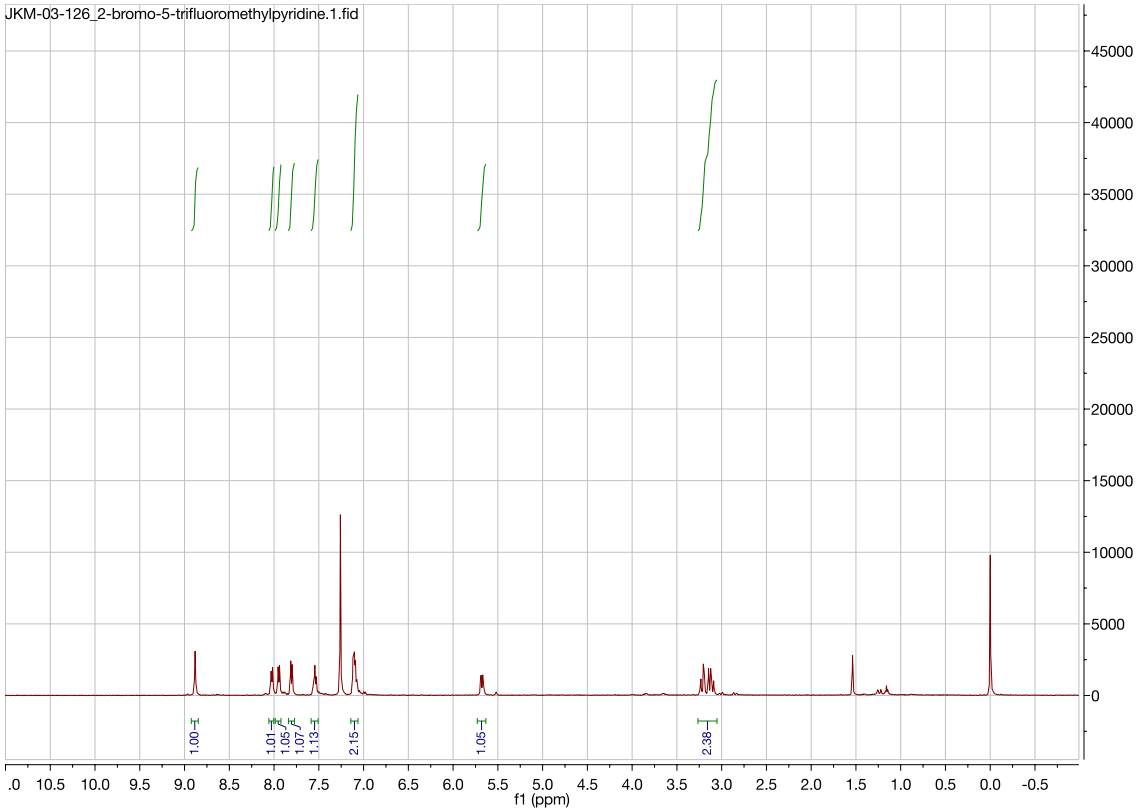

^{13}C NMR ($CDCl_3$-d^6, 125.8 MHz) spectrum of 2-(5-(trifluoromethyl)pyridin-2-yl)chroman-4-one (**5.5.15**)

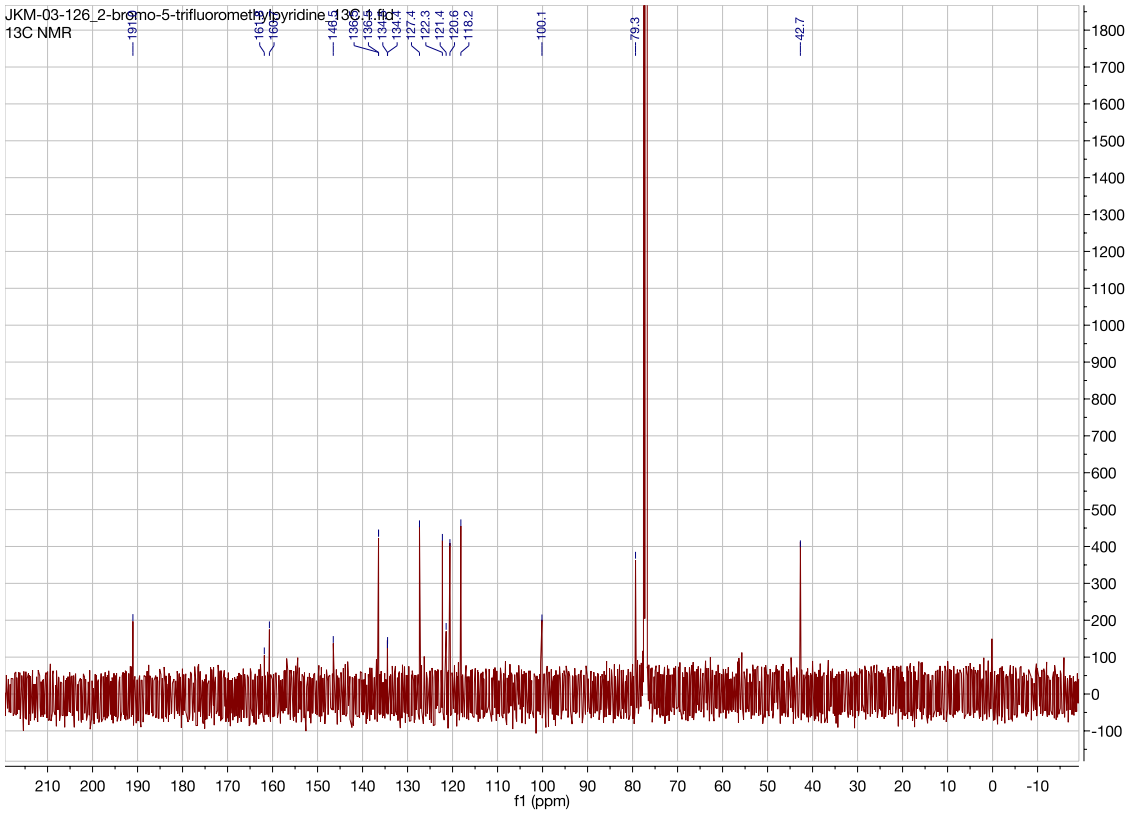

^{1}H ($CDCl_3$, 500 MHz) spectra of 4-(6-methyl-4-oxochroman-2-yl)benzonitrile (**5.6.1**)

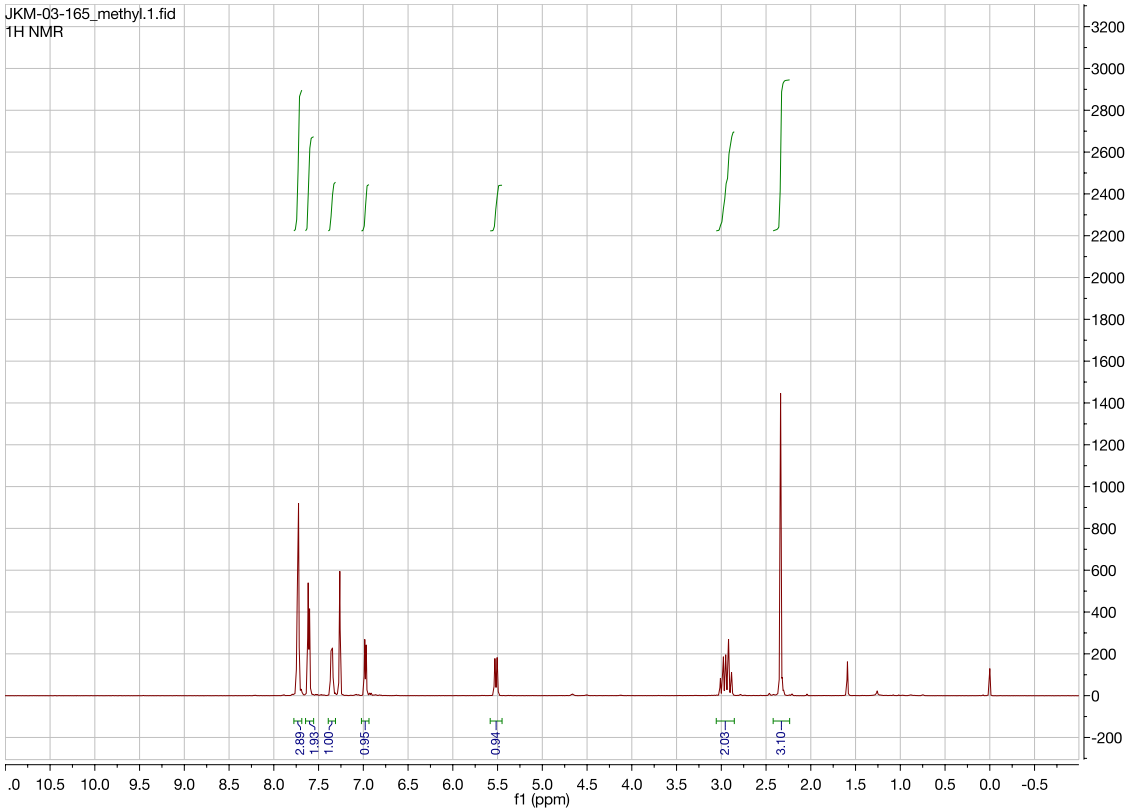

^{13}C NMR ($CDCl_3$, 125.8 MHz) spectrum of 4-(6-methyl-4-oxochroman-2-yl)benzonitrile (**5.6.1**)

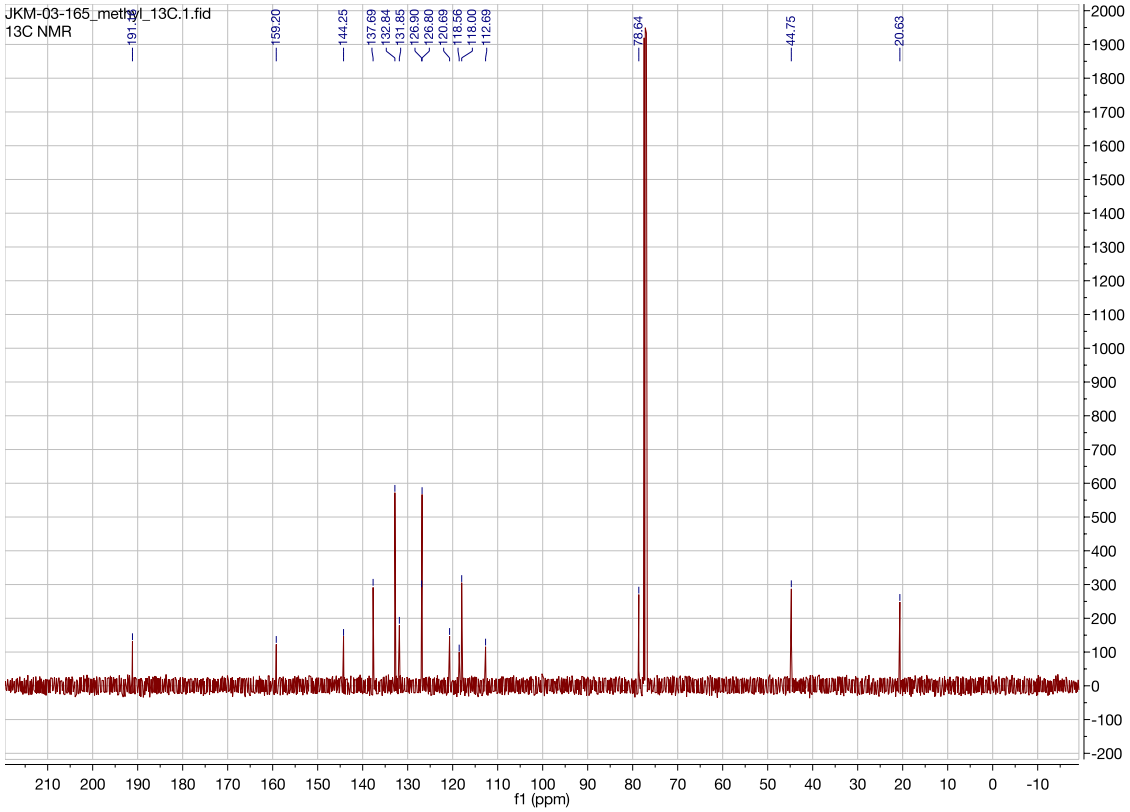

^{1}H ($CDCl_3$, 500 MHz) spectra of 4-(6-chloro-7-methyl-4-oxochroman-2-yl)benzonitrile (**5.6.3**)

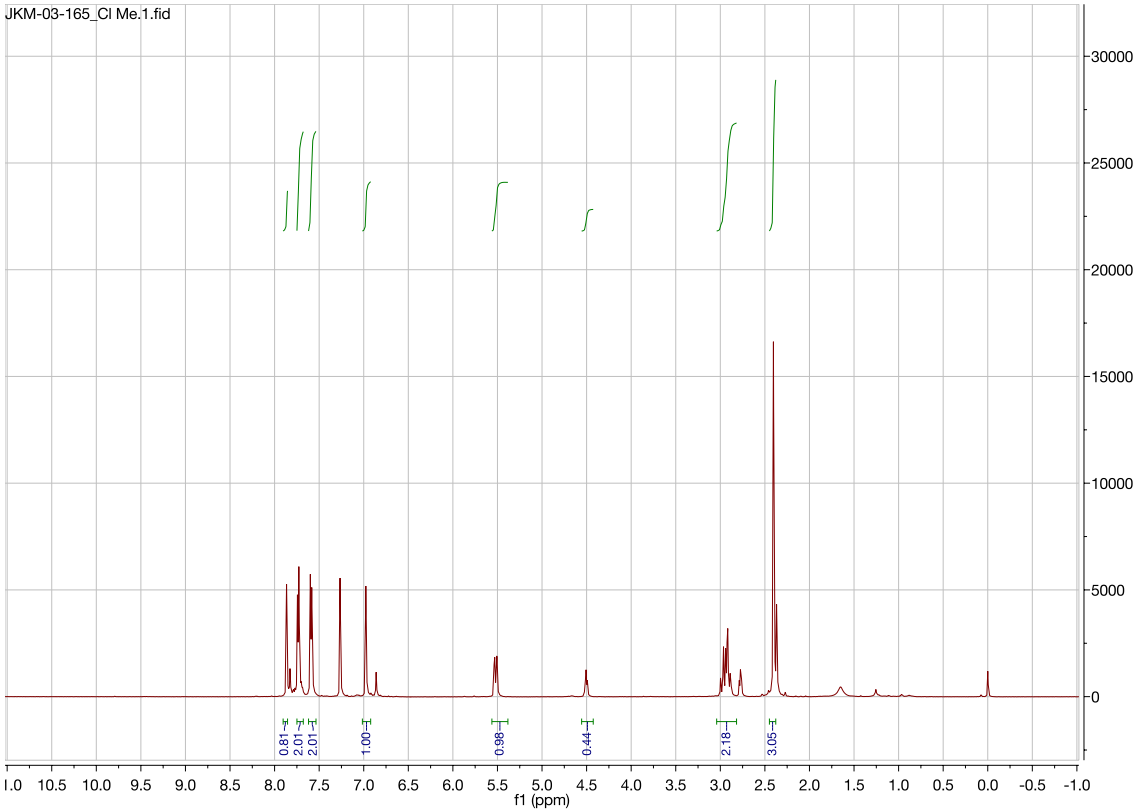

^{13}C NMR ($CDCl_3$, 125.8 MHz) spectrum of 4-(6-chloro-7-methyl-4-oxochroman-2-yl)benzonitrile (**5.6.3**)

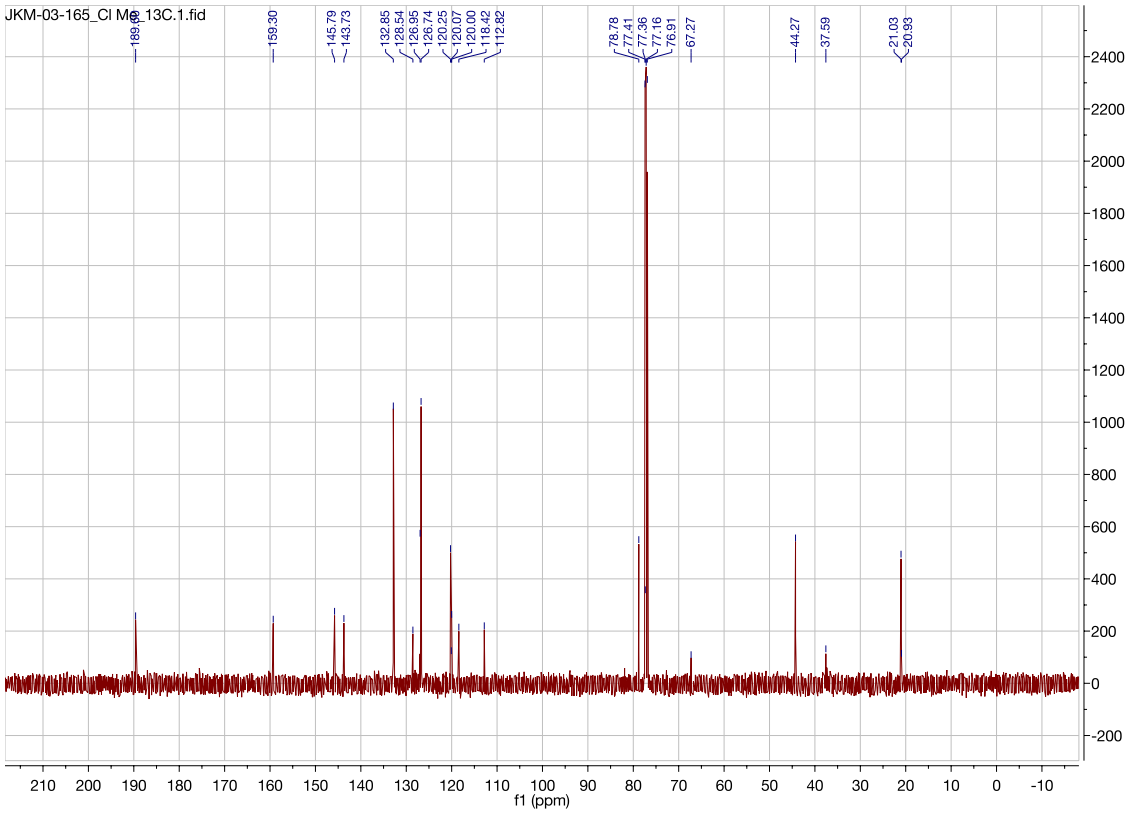

Chapter 6. Introduction 1,4-Dihydropyridines to Photoredox/Ni Dual Catalysis

6.1 Introduction

In the last decades, cross-coupling reactions have become among the most employed means to construct new C-C bonds.[1†] However, despite their numerous advantages, cross-coupling reactions, especially in the context of Csp^2–Csp^3 bond formation, suffer from some limitations that hinder their more widespread utilization. In particular, the high activation energy barrier associated with the transmetalation step in the coupling of many Csp^3 nucleophiles results in a need to use unstable and functional group-intolerant organometallic reagents, negatively impacting the generality and operational simplicity of these methods.[2] In this regard, the recently developed nickel/photoredox dual catalytic process has proved to be an excellent alternative and complementary approach to overcome such limitations[3] by triggering a facile transmetalation-like event that is initiated by single-electron oxidation of an organometallic reagent. The odd-electron nature of this reactivity paradigm proceeds most rapidly with Csp^3 coupling partners, effectively inverting the reactivity hierarchy observed in more conventional cross-coupling processes. As a result, reactive organometallic nucleophiles can be exchanged for a variety of functional group-tolerant radical precursors.

Among alkyl radical precursors, different partners have been previously reported such as trifluoroborates,[4] silicates,[5] carboxylic acids,[6] halides,[7] and activated C-H bonds.[8] However, it remains of utmost importance to introduce new feedstock functional groups amenable to oxidative fragmentation, forming suitable alkyl radicals.[9] Within this context, aldehydes represent an attractive option because aliphatic aldehydes are abundant in nature and readily available from

---

† Reproduced in part from Gutierrez-Bonet, A.; Tellis, J. C.; Matsui, J. K.; Vara, B. A.; Molander, G. A. *ACS Catal.* **2016**, *6*, 8004.

commercial sources. Although nature has long ago developed very effective means to promote oxidative deformylation reactions,[10] such transformations still pose significant challenges for the scientific community, which rely on two distinct approaches (Figure 6.1). First, an acyl radical can be formed through a hydrogen-atom transfer (HAT) process, usually involving thiyl radicals, then, decarbonylation delivers the targeted alkyl radical (route **A**).[11] This latter step is usually slow, and acylated byproducts are often observed. Alternatively, superoxometal complexes have been employed (route **B**);[12] however, strong, stoichiometric oxidants are required, thus hampering the applicability and breadth of substrates employed.

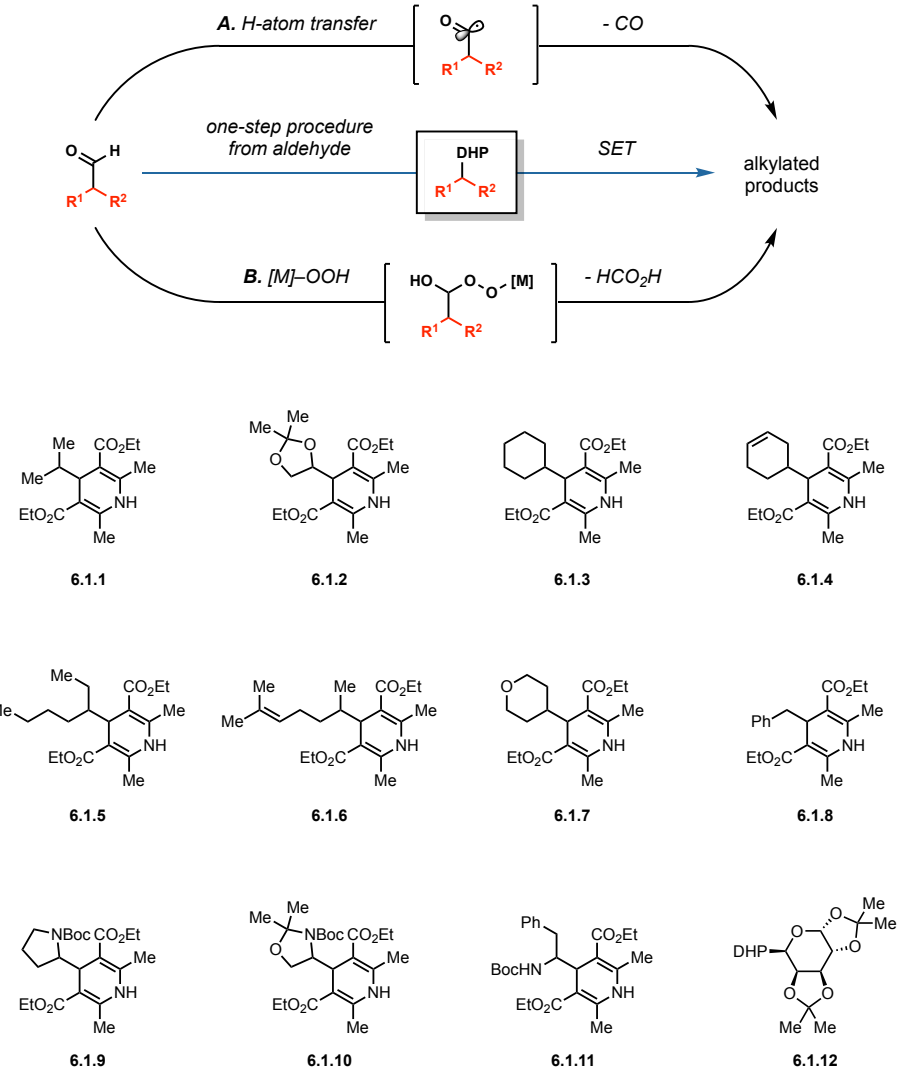

Figure 6.1. Generating carbon-centered radicals from aldehydes.

6.2 Reaction Design and Results

Aware of the inherent difficulties associated with the formation of alkyl radicals directly from aldehydes,[13] we explored different aldehyde derivatives able to undergo photochemical homolysis. 1,4-Dihydropyridines (DHPs) can be easily prepared from aldehydes in one step, even with high functionalization levels,[14] and their photochemical oxidation delivers hydrogen (H_2) with concomitant pyridine formation. However, in the presence of alkyl substituents in the 4-position, the oxidation has been shown to generate carbon-centered alkyl radicals.[15] Importantly, the Nishibayashi group[16] has successfully applied such an approach in aromatic substitution reactions. More recently, Ma and Cheng coupled a variety of DHPs with activated tertiary alkyl bromides under photocatalytic conditions.[17]

To ensure effective oxidative cleavage of the 1,4-DHP (E_{ox} = +1.05 V vs SCE),[18] the organic dye 4CzIPN (excited state E_{red} = +1.35 V vs SCE) was employed as a photocatalyst,[19] and different nickel(II) sources were tested (Figure 6.2, entries 1–5).[20] As shown, dtbbpy outperformed other ligands tested, with dMeObpy and bpy showing lower yields (entries 2–4). Interestingly, the preformed $[Ni(dtbbpy)(H_2O)_4]Cl_2$ afforded the higher yields with no deleterious effects observed from the water. Other photocatalysts were also explored (entries 6–7). Not surprisingly, $[Ru(bpy)_3](PF_6)_2$ only delivered traces of product, likely because of its low oxidation potential (E_{red} = +0.77 V vs SCE) whereas an Ir-photocatalyst (entry 6) delivered the product in moderate yields (E_{red} = +1.32 V vs. SCE). The highly oxidizing organic photocatalyst mesityl acridinium (E_{ox} = 2.06 V vs SCE)[23] was next explored but afforded no product likely because of its inability to reduce the putative Ni(I) intermediate.[4j] Consequently, 4CzIPN was chosen because of its lower cost ($6.01/g), more straightforward preparation, and higher activity. Finally, although other common solvents for photoredox cross-coupling reactions were examined (entries 8–9), acetone out-performed both CH_3CN and DMF. As anticipated, control experiments showed that all parameters were essential for the reaction to proceed. Importantly, we observed complete consumption of 1a

in the presence of the photocatalyst, delivering the pyridine byproduct. Therefore, in some cases we decided to boost the reactivity by increasing the amount of Ni-catalyst and DHP, thus obtaining higher yields. It should be noted that the disclosed reaction conditions are particularly user-friendly, allowing the construction of complex structural motifs in a "dump and stir" fashion.

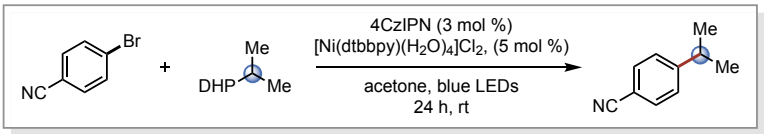

entry	deviation from standard conditions	3aa (%)[b]
1	none	78 (60)[c]
2	$NiCl_2$·dme/dtbbpy	74
3	$NiCl_2$·dme/bpy	69
4	$NiCl_2$·dme/dMeObpy	67
5	$NiBr_2$·dme/dtbbpy	59
6	$[Ir\{dF(CF_3)_2ppy\}(bpy)]PF_6$	51
7	$[Ru(bpy)_3](PF_6)_2$	3
8	$(MesAcr)ClO_4$	0
9	CH_3CN	57
10	DMF	50

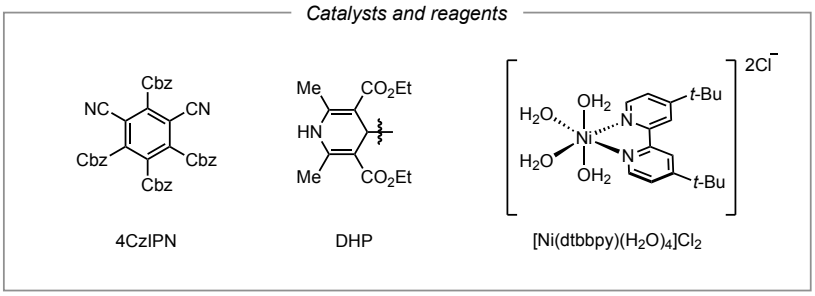

Figure 6.2. Control studies and optimization.

Encouraged by these results, we turned our attention to study the influence of several (hetero)aryl bromides in the reaction. As illustrated in Figure 6.3, different (hetero)aryl bromides were well accommodated with aromatic substrates (**6.3.1**–**6.3.2**) and heteroaromatic entities such as pyridines (**6.3.3**), thiazole (**6.3.4**), and thiophene (**6.3.6**–**6.3.7**). Notably, we observed that 2-bromoheteroarenes were more reactive than other heteroaryl bromides.[21] Likewise, bifunctional heteroaryl bromides bearing carbonyl moieties (**6.3.6**–**6.3.7**) proved to be useful coupling partners,

and the products of these reactions thus contain reactive groups that can be used for further elaboration.

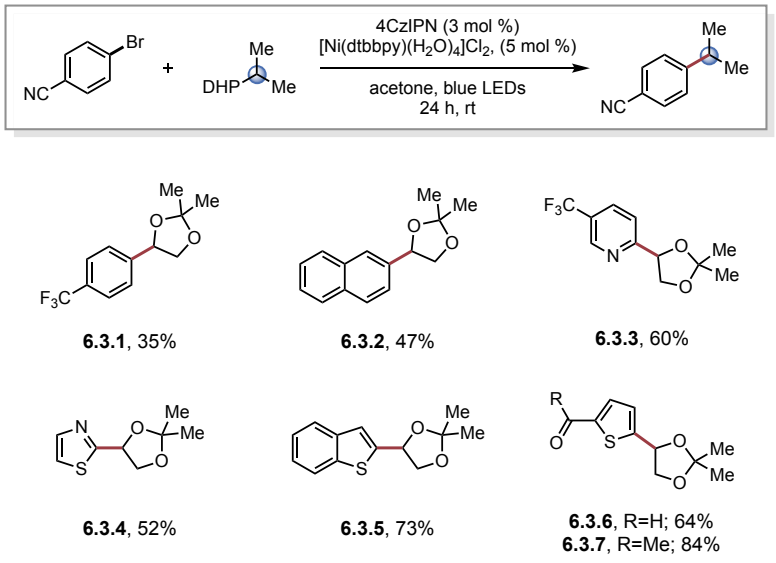

Figure 6.3. Scope of (hetero)aryl bromides.

Once the versatility of the protocol was demonstrated against different (hetero)aryl bromides, we decided to focus our attention on both the DHP radical precursors and the aryl bromide partners simultaneously in an effort to showcase the "real-world" utility of this method in cases where both the nucleophilic and electrophilic partner present structural and/or electronic challenges (Figure 6.4). The developed reaction conditions were highly general, and various substitution patterns were well accommodated. The diverse range of alkylated arenes and heteroarenes were isolated in modest to high yields. Unactivated secondary alkyl DHPs could be coupled independently of the cyclic or acyclic nature of the radical. More interestingly, alkyl radicals bearing distal alkenes (**6.4.5**–**6.4.7**) were well tolerated. No evidence of radical cyclization was observed for the melonal-derived DHP (**6.4.10**). A pyran-derived DHP was likewise tolerated, and the resulting product was isolated in good yield (**6.4.11**). Importantly, even at almost 10-fold higher scale the reaction went to 60% yield without further optimization. Similar results were achieved for a benzylic DHP when coupled with a challenging pyridine (**6.4.12**). In addition to unactivated

alkyl radicals, α-heteroalkyl substrates could be employed. Pyrrolidine (**6.4.13**) as well as protected amino alcohol (**6.4.14**) and amino acid-derived (**6.4.15**) DHPs all succeeded in delivering the cross-coupled product, although in modest yields.

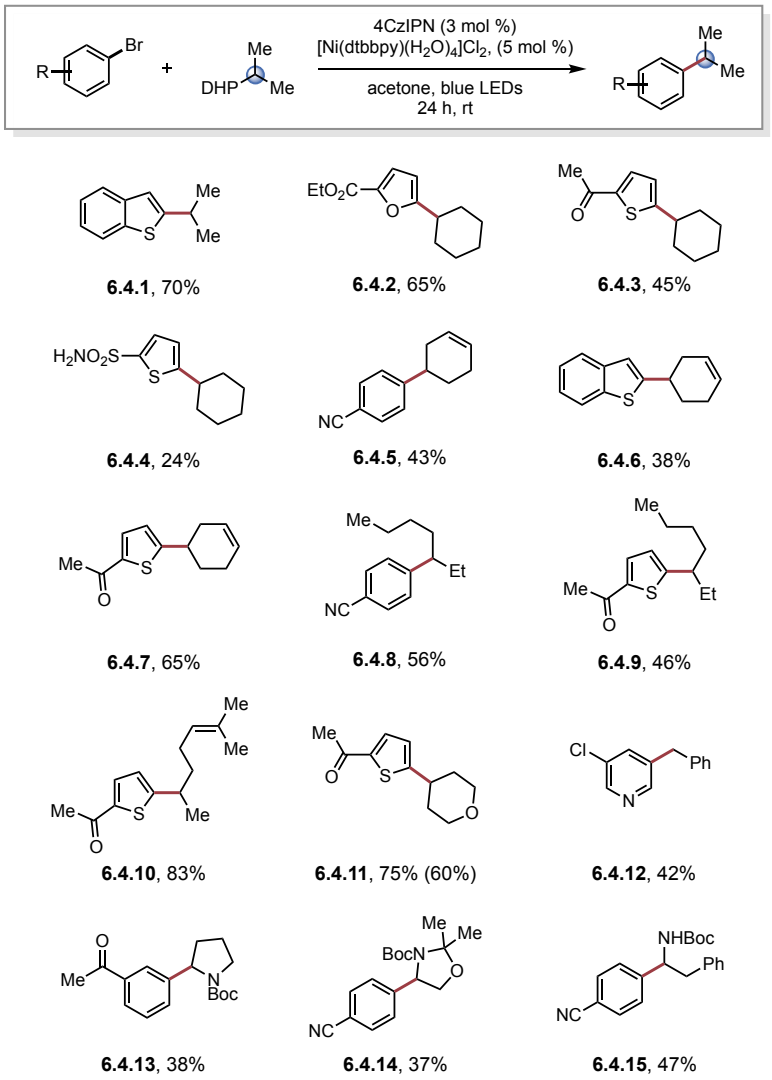

Figure 6.4. Exploring radical breadth.

To demonstrate further the applicability of the developed method, the protocol was tested for the synthesis of two saccharide derivatives. Previous literature reports for the synthesis of C -aryl glycosides *via* cross-coupling relied on the employment of alkenyl stannane[22] or alkenyl boronate[23] derivatives, presumably because the alkyllithium intermediates required for the

synthesis of the requisite alkyl glycosidic stannanes and alkyl boronates would suffer β-elimination of the adjacent alkoxy group. Thus, current approaches require a cumbersome synthesis of the dihydropyranylmetallics, followed by coupling and hydrogenation. By contrast, for the present transformation, 1,4-dihydropyridines from saccharides are readily available,[14a] and the particularly mild reaction conditions allow the formation of saccharide-containing product (**6.5.1**) in good yield and excellent diastereoselectivity. Access to **6.5.2** demonstrates that a fully deprotected carbohydrate core can be coupled, albeit in modest yield (Figure 6.5).

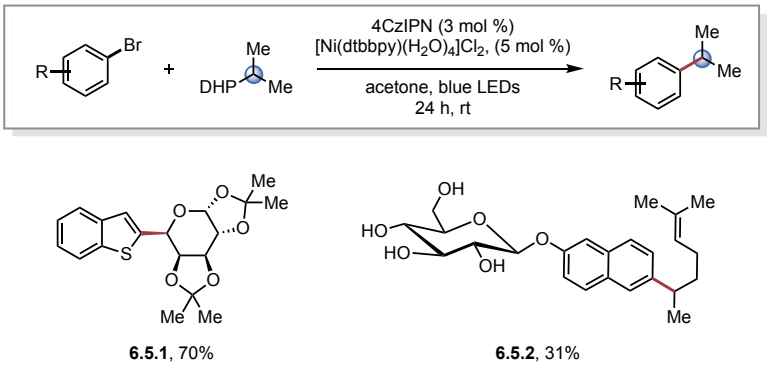

Figure 6.5. Incorporating monosaccharide moieties.

The developed method does present a few limitations[24] owing to the intrinsic stability of the radical intermediate formed. Consequently, primary alkyl or cyclopropyl DHPs did not succeed in delivering the cross-coupling product, because oxidation of the DHP delivers only the 4-alkylated pyridine byproduct.[15] Nonetheless, this is arguably a minor limitation considering complementary cross-coupling protocols available for primary or cyclopropyl motifs.[2a]

Based on our previous studies with alkyltrifluoroborates[25] as well as previous studies detailing the photochemical oxidative cleavage of DHPs,[15,16] we propose the mechanistic scenario depicted in Figure 6.6. First, photoexcitation of the organic photocatalyst to its triplet state generates a species that is a sufficient SET oxidant. At this point, the photocatalyst is oxidatively

quenched by the DHP derivative (**6.6.1**), thus forming a radical cation (not pictured), which undergoes homolysis, delivering the carbon-centered alkyl radical **6.6.2**. This radical reacts with active Ni(0) catalyst, forming the alkylnickel(I) intermediate **6.6.3**, which undergoes further oxidative addition with the aryl bromide, forming the Ni(III) complex **6.6.4**.[26,27] Subsequently, reductive elimination delivers the cross-coupled product along with Ni(I) complex **6.6.3**, which can be reduced to Ni(0) by the reduced photo-catalyst, thus regenerating both active catalysts. We believe that the homolysis of the DHP unit occurs *via* formation of a radical cation followed by a deprotonation step, forming an aminyl radical that will then undergo homolysis.[15,16] Notably, we observed that N-Me DHP failed to deliver the cross-coupling product under reaction conditions, thus supporting the deprotonation prior to the C-C cleavage event hypothesis.

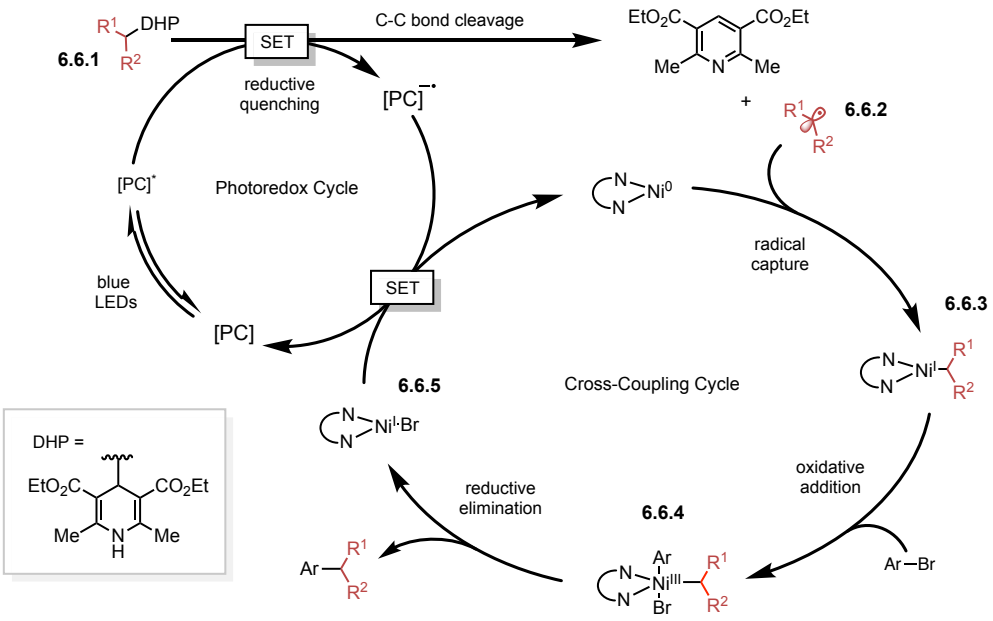

Figure 6.6. Proposed dual catalytic mechanism.

6.3 Conclusion

In summary, the use of DHPs as radical precursors has allowed the successful and general introduction of an interesting feedstock into the dual Ni/photoredox cross-coupling toolbox. Because DHPs are derived from their corresponding, commercially available aldehydes, previously

unrepresented radicals can be accessed, thereby expanding the chemical space of Csp^2-Csp^3 cross-couplings. Importantly, the reaction is characterized by its sustainability, as the only metal introduced in the entire process is the base metal cross-coupling catalyst. The transformation furthermore proceeds under extremely mild reaction conditions using visible light, allowing the inclusion of diverse and unexplored coupling partners such as carbohydrate cores.

6.4 References

[1] (a) Corbet, J.-P.; Mignani, G. *Chem. Rev.* **2006**, *106*, 2651. (b) Brown, D. G.; Boström, J. *J. Med. Chem.* **2016**, *59*, 4443. (c) Johansson Seechurn, C. C. C.; Kitching, M. O.; Colacot, T. J.; Snieckus, V. *Angew. Chem., Int. Ed.* **2012**, *51*, 5062. (d) Chemler, S. R.; Trauner, D.; Danishefsky, S. J. *Angew. Chem., Int. Ed.* **2001**, *40*, 4544.

[2] (a) Jana, R.; Pathak, T. P.; Sigman, M. S. *Chem. Rev.* **2011**, *111*, 1417. (b) Lennox, A. J. J.; Lloyd-Jones, G. C. *Angew. Chem., Int. Ed.* **2013**, *52*, 7362.

[3] (a) Tellis, J. T.; Kelly, C. B.; Primer, D. N.; Jouffroy, M.; Patel, N. R.; Molander, G. A. *Acc. Chem. Res.* **2016**, *49*, 1429. (b) Shaw, M. H.; Twilton, J.; MacMillan, D. W. C. *J. Org. Chem.* **2016**, *81*, 6898. (c) Prier, C. K.; Rankic, D. A.; MacMillan, D. W. C. *Chem. Rev.* **2013**, *113*, 5322.

[4] (a) Tellis, J. C.; Amani, J.; Molander, G. A. *Org. Lett.* **2016**, *18*, 2994. (b) Karimi-Nami, R.; Tellis, J. C.; Molander, G. A. *Org. Lett.* **2016**, *18*, 2572. (c) Amani, J.; Sodagar, E.; Molander, G. A. *Org. Lett.* **2016**, *18*, 732. (d) Ryu, D.; Primer, D. N.; Tellis, J. C.; Molander, G. A. *Chem. Eur. J.* **2016**, *22*, 120. (e) El Khatib, M.; Serafim, R. A. M.; Molander, G. A. *Angew. Chem., Int. Ed.* **2016**, *55*, 254. (f) Yamashita, Y.; Tellis, J. C.; Molander, G. A. *Proc. Natl. Acad. Sci. U. S. A.* **2015**, *112*, 12026. (g) Karakaya, I.; Primer, D. N.; Molander, G. A. *Org. Lett.* **2015**, *17*, 3294. (h)

Primer, D. N.; Karakaya, I.; Tellis, J. C.; Molander, G. A. *J. Am. Chem. Soc.* **2015**, *137*, 2195. (i) Tellis, J. C.; Primer, D. N.; Molander, G. A. *Science* **2014**, *345*, 433.

[5] (a) Corce, V.; Chamoreau, L.-M.; Derat, E.; Goddard, J.-P.; Ollivier, C.; Fensterbank, L. *Angew. Chem., Int. Ed.* **2015**, *54*, 11414. (b) Jouffroy, M.; Primer, D. N.; Molander, G. A. *J. Am. Chem. Soc.* **2016**, *138*, 475. (c) Patel, N. R.; Kelly, C. K.; Jouffroy, M.; Molander, G. A. *Org. Lett.* **2016**, *18*, 764. (d) Jouffroy, M.; Kelly, C. K.; Molander, G. A. *Org. Lett.* **2016**, *18*, 876. (e) Leveque, C.; Chenneberg, L.; Corce, V.; Goddard, J.-P.; Ollivier, C.; Fensterbank, L. *Org. Chem. Front.* **2016**, *3*, 462. (f) Patel, N. R.; Molander, G. A. *J. Org. Chem.* **2016**, *81*, 7271.

[6] (a) Zuo, Z.; Ahneman, D. T.; Chu, L.; Terrett, J. A.; Doyle, A. G.; MacMillan, D. W. C. *Science* **2014**, *345*, 437. For anhydrides as radical precursors, see: (b) Le, C.; MacMillan, D. W. C. *J. Am. Chem. Soc.* **2015**, *137*, 11938. (7) (a) Zhang, P.; Le, C.; MacMillan, D. W. C. *J. Am. Chem. Soc.* **2016**, *138*, 8084. (b) Duan, Z.; Li, W.; Lei, A. *Org. Lett.* **2016**, *18*, 4012.

[7] (a) Zhang, P.; Le, C.; MacMillan, D. W. C. *J. Am. Chem. Soc.* **2016**, 138, 8084. (b) Duan, Z.; Li, W.; Lei, A. *Org. Lett.* **2016**, *18*, 4012.

[8] (a) Shaw, M. H.; Shurtleff, V. W.; Terrett, J. A.; Cuthbertson, J. D.; MacMillan, D. W. C. *Science* **2016**, *352*, 1304.

[9] For the use of tertiary alcohol feedstock as radical precursors, see: Nawrat, C. C.; Jamison, C. R.; Slutskyy, Y.; MacMillan, D. W. C.; Overman, L. E. *J. Am. Chem. Soc.* **2015**, *137*, 11270.

[10] Marsh, E. N. G.; Waugh, M. W. *ACS Catal.* **2013**, *3*, 2515 and references therein.

[11] (a) Berman, J. D.; Stanley, J. H.; Sherman, W. V.; Cohen, S. G. *J. Am. Chem. Soc.* **1963**, *85*, 4010. (b) Winstein, S.; Seubold, F. H., Jr. *J. Am. Chem. Soc.* **1947**, *69*, 2916. (c) Harris, E. F. P.; Waters, W. A. *Nature* **1952**, *170*, 212. (d) Déne s, F.; Pichowicz, M.; Povie, G.; Renaud, P. *Chem. Rev.* **2014**, *114*, 2587. For examples not involving thiyl radical mediation, see: (e) Esposti, S.; Dondi, D.; Fagnoni, M.; Albini, A. *Angew. Chem., Int. Ed.* **2007**, *46*, 2531. (f) Tsujimoto, S.; Iwahama, T.; Sakaguchi, S.; Ishii, Y. *Chem. Commun.* **2001**, 2352.

[12] (a) Watanabe, E.; Kaiho, A.; Kusama, H.; Iwasawa, N. *J. Am. Chem. Soc.* **2013**, *135*, 11744. (b) Ellington, B. R.; Paul, B.; Das, D.; Vitek, A. K.; Zimmerman, P. M.; Marsh, N. G. *ACS Catal.* **2016**, *6*, 3293. (c) Shokri, A.; Que, L., Jr. *J. Am. Chem. Soc.* **2015**, *137*, 7686. (d) Cho, J.; Sarangi, R.; Nam, W. *Acc. Chem. Res.* **2012**, *45*, 1321.

[13] Chatgilialoglu, C.; Crich, D.; Komatsu, M.; Ryu, I. *Chem. Rev.* **1999**, *99*, 1991.

[14] For representative examples, see: (a) Tewari, N.; Dwivedi, N.; Tripathi, R. *Tetrahedron Lett.* **2004**, *45*, 9011. (b) Adibi, H.; Samimi, H. A.; Beygzadeh, M. *Catal. Commun*. **2007**, *8*, 2119. (c) Heydari, A.; Khaksar, S.; Tajbakhsh, M.; Bijanzadeh, H. R. *J. Fluorine Chem.* **2009**, *130*, 609.

[15] (a) Zhang, D.; Wu, L.-Z.; Zhou, L.; Han, X.; Yang, Q.-Z.; Zhang, L.-P.; Tung, C.-H. *J. Am. Chem. Soc.* **2004**, *126*, 3440. (b) Wei, X.; Wang, L.; Jia, W.; Du, S.; Wu, L.; Liu, Q. Chin. *J. Chem.* **2014**, *32*, 1245. (c) Fukuzumi, S.; Suenobu, T.; Patz, M.; Hirasaka, T.; Itoh, S.; Fujitsuka, M.; Ito, O. *J. Am. Chem. Soc.* **1998**, *120*, 8060. (d) Wang, D.; Liu, Q.; Chen, B.; Zhang, L.; Tung, C.; Wu, L. *Chin. Sci. Bull.* **2010**, *55*, 2855.

[16] Nakajima, K.; Nojima, S.; Sakata, K.; Nishibayashi, Y. *ChemCatChem* **2016**, *8*, 1028.

[17] Chen, W.; Liu, Z.; Tian, J.; Li, J.; Ma, J.; Cheng, X.; Li, G. *J. Am. Chem. Soc.* **2016**, *138*, 12312.

[18] See Experimental Section for further details.

(19) The value is in agreement with the previously reported: E_{ox} = +0.654 V (Fc+/Fc) for 1a. See: Cheng, J.-P.; Lu, Y.; Zhu, X.-Q.; Sun, Y.; Bi, F.; He, J. *J. Org. Chem.* **2000**, *65*, 3853.

(20) Interestingly, 1a-CN (E_{ox} = +1.34 vs SCE) did not succeed in delivering the product. After oxidative fragmentation, the carbon centered radical appears to react preferentially with the pyridine byproduct, delivering the 4-alkylated pyridine, which was observed in quantitative yield. See the Experimental Section for further details.

[19] Luo, J.; Zhang, J. *ACS Catal.* **2016**, *6*, 873.

[20] $[Ni(dtbbpy)(H_2O)_4]Cl_2$ was prepared using 1.0 equiv of $NiCl_2(H_2O)_6$ and 1.0 equiv of dtbbpy (see the Experimental Section for detailed procedure and X-ray crystal structure).

$[Ni(dtbbpy)(H_2O)_4]Cl_2$ is a bench-stable complex that simplifies the reaction setup, making it a more user-friendly process.

[21] (a) Legault, C. Y.; Garcia, Y.; Merlic, C. A.; Houk, K. N. *J. Am. Chem. Soc.* **2007**, *129*, 12664. (b) Garcia, Y.; Schoenebeck, F.; Legault, C. Y.; Merlic, C. A.; Houk, K. N. *J. Am. Chem. Soc.* **2009**, *131*, 6632.

[22] (a) Friesen, R. W.; Sturino, C. F. *J. Org. Chem.* **1990**, *55*, 2572. (b) Dubois, E.; Beau, J.-M. *Tetrahedron Lett.* **1990**, *31*, 5165. (c) Friesen, R. W.; Sturino, C. F.; Daljeet, A. K.; Kolaczewska, A. *J. Org. Chem.* **1991**, *56*, 1944.

[23] (a) Sakamaki, S.; Kawanishi, E.; Nomura, S.; Ishikawa, T. *Tetrahedron* **2012**, *68*, 5744. (b) Parkan, K.; Pohl, R.; Kotora, M. *Chem. Eur. J.* **2014**, *20*, 4414.

[24] Electron-rich aryl bromides could not be coupled because of a demanding oxidative addition step under the developed reaction conditions, resulting in recovered starting material. On the other hand, in those cases with moderate yields, the formation of aryl chloride or protodebrominated starting material was observed, thus indicating that the more demanding steps in those cases was not the oxidative addition.

[25] Gutierrez, O.; Tellis, J. C.; Primer, D. N.; Molander, G. A.; Kozlowski, M. C. *J. Am. Chem. Soc.* **2015**, *137*, 4896.

[26] For examples of Ni(I)-promoted oxidative addition into C−X bonds see: (a) Anderson, T. J.; Jones, G. D.; Vicic, D. A. *J. Am. Chem. Soc.* **2004**, *126*, 8100. (b) Jones, G. D.; McFarland, C.; Anderson, T. J.; Vicic, D. A. *Chem. Commun.* **2005**, 4211. (c) Anton, M.; Clos, N.; Muller, G. *J. Organomet. Chem.* **1984**, *267*, 213.

[27] At this point, we cannot rule out a mechanistic scenario consisting of an oxidative addition of Ni(0) complex with the aryl bromide followed by radical addition, delivering Ni(III) complex. Additionally, while this work was under revision, Nishibayashi *et al.* reported the cross-coupling of aryl iodides with DHPs under Ni/photoredox dual catalysis Nakajima, K.; Nojima, S.; Nishibayashi, Y. *Angew. Chem. Int. Ed.* **2016**, *55*, 14106.

GENERAL CONSIDERATIONS

Reagents

All reactions were carried out under an inert atmosphere of nitrogen or argon unless otherwise noted. Standard Schlenk techniques were used for the manipulation of solvents and reagents. Reactions were monitored by GC/MS, HPLC, ^{1}H NMR, and/or by TLC on silica gel plates (60 Å porosity, 250 μm thickness). TLC analysis was performed using hexanes/EtOAc as the eluant and visualized using permanganate stain and/or UV light. Silica plugs utilized flash silica gel (60 Å porosity, 32-63 μm). Flash chromatography was accomplished using an automated system (visualizing at 254 nm, monitoring at 280 nm) with silica cartridges (60 Å porosity, 20-40 μm). Solvents were purified either by distillation over sodium or CaH_2 or by use of drying cartridges through a solvent delivery system. Irradiation of reaction vessels was accomplished using blue LEDs (Light-emitting diode) at a distance of ~3 cm. A fan was employed to ensure reactions remained at or near rt when using LEDs.

Analytical Methods

Melting points (°C) are uncorrected. NMR Spectra (^{1}H, ^{13}C {^{1}H}) were recorded on a 500 or 400 MHz spectrometer at 298 K. All ^{1}H NMR spectra are reported in parts per million (ppm) downfield of TMS and were measured relative to the signals for $CHCl_3$ (7.26 ppm). All ^{13}C NMR spectra were reported in ppm relative to residual $CHCl_3$ (77.2 ppm) and were obtained with ^{1}H decoupling. Coupling constants, *J*, are reported in Hertz (*Hz*). In the case of diastereisomeric mixtures, a crude NMR was recorded to determine the ratio. HRMS was obtained by either ESI or CI with a TOF spectrometer in MeCN or CH_2Cl_2. IR spectra were obtained on neat samples. The yields reported in Table 2 and Table 3 refer to isolated yields and represent an average of at least two independent runs. The procedures described in this section are representative. Thus, the yields may differ slightly from those given in Tables 2 and 3.

Synthesis of 1,4-Dihydropyridines

General Procedure I: Synthesis of 1,4-dihydropyridnes: 1,4-Dihydropyridnes were prepared following a modified literature protocol.[1] Into a round-bottom flask charged with ethyl 3-aminocrotonate (1.0 equiv) was added ethylene glycol (2.5 M). Next, ethyl acetoacetate (1.0 equiv) was added followed by the aldehyde (1.0 equiv).[2] Finally, Bu_4NHSO_4 (12 mol %) was added in one portion. The flask was closed with a septum and heated at 80 ºC for 3-4 h. At this time, the reaction was cooled to rt and diluted with EtOAc. The solution was poured into a separatory funnel containing brine and extracted three times with EtOAc. After drying over $MgSO_4$, it was filtered and taken to dryness. The crude reaction mixture was purified using an automated system (visualizing at 254 nm, monitoring at 280 nm) with silica cartridges (60 Å porosity, 20-40 μm) using hexanes/EtOAc (0 to 40%) as eluent.

Characterization Data: 1,4-Dihydropyridines

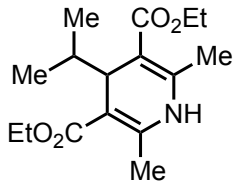

Diethyl 4-isopropyl-2,6-dimethyl-1,4-dihydropyridine-3,5-dicarboxylate (6.1.1)

Following General Procedure I using isobutyraldehyde (793.2 mg, 11.0 mmol, 1.0 equiv). The product was isolated as a white solid (2.01 g, 62% yield). Mp = 95-97 ºC.

^{1}H NMR (500 MHz, $CDCl_3$) δ 5.51 (s, 1H), 4.27 – 4.08 (m, 4H), 3.92 (d, J = 5.4 Hz, 1H), 2.30 (s, 6H), 1.63 – 1.57 (m, 1H), 1.29 (t, J = 7.1 Hz, 6H), 0.75 (d, J = 6.9 Hz, 6H) ppm.

^{13}C NMR (126 MHz, $CDCl_3$) δ 168.9, 144.7, 101.9, 59.7, 38.9, 35.7, 19.5, 18.6, 14.5 ppm.

The spectral data were in agreement with those previously reported.[3]

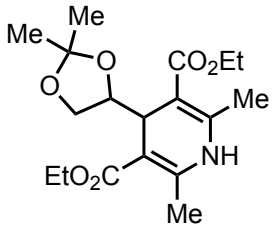

Diethyl 4-(2,2-dimethyl-1,3-dioxolan-4-yl)-2,6-dimethyl-1,4-dihydropyridine-3,5-dicarboxylate (6.1.2)

Following General Procedure I using (*R*)-2,2-dimethyl-1,3-dioxolane-4-carboxaldehyde (1.0 g, 7.7 mmol, 1.0 equiv). The product was isolated as a white solid (1.85 g, 68% yield). Mp = 106-109 ºC.

^{1}H NMR (500 MHz, $CDCl_3$) δ 5.61 (br s, 1H), 4.32 (d, *J* = 4.9 Hz, 1H), 4.26 – 4.13 (m, 4H), 4.04 – 3.96 (m, 1H), 3.83 (td, *J* = 8.1, 1.9 Hz, 1H), 3.79 – 3.69 (m, 1H), 2.31 (dd, *J* = 5.0, 2.0 Hz, 6H), 1.36 – 1.24 (m, 12H) ppm.

^{13}C NMR (126 MHz, $CDCl_3$) δ 168.2, 168.1, 146.1, 145.5, 108.7, 99.8, 99.4, 79.6, 66.3, 59.9, 36.2, 26.3, 25.8, 19.6, 19.5, 14.5 ppm. IR (neat, cm^{-1}): 3327, 2984, 1693, 1664, 1206, 1095, 1046, 775. HRMS *calcd for* ($C_{18}H_{27}NO_6$+H) 354.1917, *found* 354.1903.

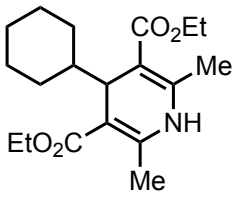

Diethyl 4-cyclohexyl-2,6-dimethyl-1,4-dihydropyridine-3,5-dicarboxylate (6.1.3)

Following General Procedure I using cyclohexanecarboxaldehyde (1.1 g, 10.0 mmol, 1.0 equiv). The product was isolated as a white solid (1.88 g, 56% yield). Mp = 111-114 ºC.

^{1}H NMR (500 MHz, $CDCl_3$) δ 5.51 (s, 1H), 4.27 – 4.09 (m, 4H), 3.92 (d, *J* = 5.6 Hz, 1H), 2.30 (s, 6H), 1.70 – 1.62 (m, 2H), 1.58 – 1.51 (m, 3H), 1.30 (t, *J* = 7.1 Hz, 6H), 1.25 – 1.17 (m, 1H), 1.13 – 1.03 (m, 3H), 0.99 – 0.86 (m, 2H) ppm.

^{13}C NMR (126 MHz, $CDCl_3$) δ 168.9, 145.0, 101.5, 59.6, 45.8, 38.4, 28.8, 26.7, 26.6, 19.2, 14.4 ppm. The spectroscopical data were in agreement with those previously reported.[4]

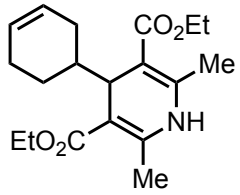

Diethyl 4-(cyclohex-3-en-1-yl)-2,6-dimethyl-1,4-dihydropyridine-3,5-dicarboxylate (6.1.4)

Following General Procedure I using 3-cyclohexene-1-carboxaldehyde (1.4 g, 12.8 mmol, 1.0 equiv) The product was isolated as a white solid (2.26 g, 53% yield). Mp = 127-130 ºC.

^{1}H NMR (500 MHz, $CDCl_3$) δ 5.64 – 5.56 (m, 2H), 5.55 (s, 1H), 4.30 – 4.08 (m, 4H), 4.02 (d, *J* = 5.9 Hz, 1H), 2.31 (s, 6H), 2.11 – 1.84 (m, 3H), 1.82 – 1.72 (m, 1H), 1.68 – 1.59 (m, 1H), 1.58 – 1.50 (m, 1H), 1.30 (t, *J* = 7.1 Hz, 6H), 1.26 – 1.13 (m, 1H) ppm.

^{13}C NMR (126 MHz, $CDCl_3$) δ 168.7, 168.6, 144.9, 144.8, 127.2, 126.8, 101.8, 59.8, 41.7, 37.9, 27.6, 26.2, 25.1, 19.7, 19.6, 14.5 ppm.

IR (neat, cm^{-1}): 3350, 1644, 1485, 1215, 1098, 1049, 661.

HRMS *calcd for* ($C_{19}H_{27}NO_4$+Na) 356.1838, *found* 358.1827.

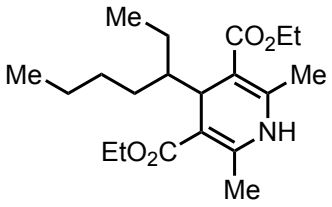

Diethyl 4-(heptan-3-yl)-2,6-dimethyl-1,4-dihydropyridine-3,5-dicarboxylate (6.1.5)

Following General Procedure I using 2-ethylhexanal (1.3 g, 10.3 mmol, 1.0 equiv). The product was isolated as a yellow solid (2.20 g, 61% yield). Mp = 63-65 ºC.

^{1}H NMR (500 MHz, $CDCl_3$) δ 5.89 – 5.45 (m, 1H), 4.22 – 4.10 (m, 5H), 2.28 (d, *J* = 2.6 Hz, 6H), 1.30 (t, *J* = 7.1 Hz, 6H), 1.27 – 1.17 (m, 5H), 1.15 – 1.07 (m, 4H), 0.86 (t, *J* = 7.0 Hz, 6H) ppm.

^{13}C NMR (126 MHz, $CDCl_3$) δ 169.0, 169.0, 144.9, 144.8, 102.1, 102.0, 59.7, 48.2, 35.0, 29.6, 28.4, 23.3, 21.8, 19.3, 19.3, 14.4, 14.2, 11.9 ppm.

IR (neat, cm^{-1}): 3361, 1618, 1486, 1268, 1200, 1110, 1096, 1017, 741.

HRMS *calcd for* ($C_{20}H_{33}NO_4$+Na) 374.2307, *found* 374.2320.

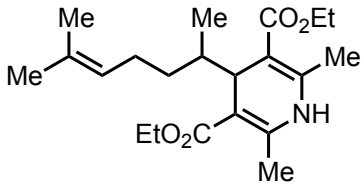

Diethyl 2,6-dimethyl-4-(7-methyloct-6-en-3-yl)-1,4-dihydropyridine-3,5-dicarboxylate (6.1.6)

Following General Procedure I using 2,6-dimethyl-5-heptenal (1.7 g, 12.1 mmol, 1.0 equiv). The product was isolated as a yellow oil (2.47 g, 54% yield).

^{1}H NMR (500 MHz, $CDCl_3$) δ 5.46 (s, 1H), 5.03 (t, *J* = 7.0 Hz, 1H), 4.25 – 4.09 (m, 4H), 4.01 (d, *J* = 4.4 Hz, 1H), 2.29 (d, *J* = 3.6 Hz, 6H), 2.03 – 1.93 (m, 1H), 1.92 – 1.82 (m, 1H), 1.66 (s, 3H), 1.58 (s, 3H), 1.48 – 1.40 (m, 1H), 1.38 – 1.32 (m, 1H), 1.29 (td, *J* = 7.1, 2.7 Hz, 6H), 1.05 – 0.94 (m, 1H), 0.73 (d, *J* = 6.8 Hz, 3H) ppm.

^{13}C NMR (126 MHz, $CDCl_3$) δ 169.0, 168.6, 144.8, 144.6, 130.9, 125.3, 102.2, 101.4, 59.7, 59.7, 41.0, 38.1, 32.8, 26.2, 25.8, 19.5, 19.4, 17.8, 15.1, 14.5, 14.5 ppm.

The spectral data were in agreement with those previously reported.[5]

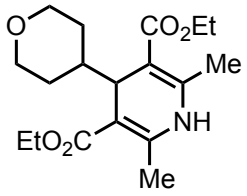

Diethyl 2,6-dimethyl-4-(tetrahydro-2H-pyran-4-yl)-1,4-dihydropyridine-3,5-dicarboxylate (6.1.7)

Following General Procedure I using 4-formyltetrahydropyran (2.0 g, 17.8 mmol, 1.0 equiv). The product was isolated as a yellowish solid (4.09 g, 68% yield). Mp = 113-117 ºC.

^{1}H NMR (500 MHz, $CDCl_3$) δ 5.60 (s, 1H), 4.25 – 4.12 (m, 4H), 3.99 (d, *J* = 5.9 Hz, 1H), 3.95 – 3.87 (m, 2H), 3.30 – 3.14 (m, 2H), 2.32 (s, 6H), 1.50 – 1.32 (m, 5H), 1.30 (t, *J* = 7.1 Hz, 6H) ppm.

^{13}C NMR (126 MHz, $CDCl_3$) δ 168.4, 145.2, 101.3, 68.5, 59.8, 42.7, 37.8, 29.0, 19.6, 14.5 ppm.

IR (neat, cm^{-1}): 3342, 1698, 1646, 1223, 1205, 1139, 1087, 772. HRMS *calcd for* ($C_{18}H_{27}NO_5$+H) 338.1967, *found* 338.1970.

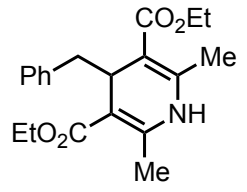

Diethyl 4-benzyl-2,6-dimethyl-1,4-dihydropyridine-3,5-dicarboxylate (6.1.8)

Following General Procedure I using phenylacetaldehyde (1.4 g, 11.5 mmol, 1.0 equiv). The product was isolated as a white solid (2.06 g, 52% yield). Mp = 102-106 ºC.

^{1}H NMR (500 MHz, $CDCl_3$) δ 7.20 – 7.11 (m, 3H), 7.02 (d, *J* = 7.8 Hz, 2H), 5.17 (s, 1H), 4.20 (t, *J* = 5.4 Hz, 1H), 4.13 – 3.98 (m, 4H), 2.58 (d, *J* = 5.5 Hz, 2H), 2.18 (s, 6H), 1.23 (t, *J* = 7.2 Hz, 6H) ppm.

^{13}C NMR (126 MHz, $CDCl_3$) δ 167.9, 145.5, 139.4, 130.2, 127.4, 125.7, 102.0, 59.7, 42.4, 35.6, 19.4, 14.5 ppm.

The spectral data were in agreement with those previously reported.[4]

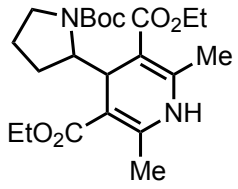

Diethyl 4-(1-(*tert*-butoxycarbonyl)pyrrolidin-2-yl)-2,6-dimethyl-1,4-dihydropyridine-3,5-dicarboxylate (6.1.9)

Following General Procedure I using Boc-L-prolinal (1.0 g, 5.0 mmol, 1.0 equiv). The product was isolated as a yellow semisolid (1.31 g, 62% yield). Mixture of rotamers, major is reported:

^{1}H NMR (400 MHz, $CDCl_3$): δ 7.85 (br s, 1H), 4.23–4.06 (m, 4H), 3.93 (d, *J* = 9.6 Hz, 1H), 3.63 (dd, *J* = 10.4, 6.4 Hz, 1H), 3.26–3.22 (m, 2H), 2.32 (s, 3H), 2.20 (s, 3H), 2.01–1.78 (m, 4H), 1.38 (s, 9H), 1.30 (t, *J* = 7.0 Hz, 6H) ppm.

^{13}C NMR (101 MHz, $CDCl_3$): δ 168.2, 154.9, 147.9, 100.2, 78.6, 59.3, 45.6, 34.9, 28.4, 27.7, 24.9, 22.6, 19.0, 14.3 ppm.

IR (neat, cm^{-1}): 2977, 2934, 1690, 1671, 1481, 1446, 1390, 1366, 1341, 1302, 1286, 1250, 1210, 1165, 1121, 1098, 1050, 1019.

HRMS *calcd for* ($C_{22}H_{34}N_2O_6$+H) 423.2495, *found* 423.2485.

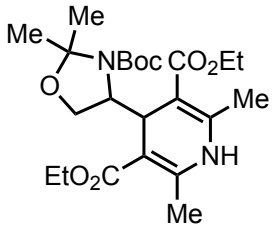

Diethyl 4-(3-(*tert*-butoxycarbonyl)-2,2-dimethyloxazolidin-4-yl)-2,6-dimethyl-1,4-dihydropyridine-3,5-dicarboxylate (6.1.10)

Following General Procedure I using (*S*)-(-)-3-Boc-2,2-dimethyloxazolidine-4-carboxaldehyde (424.1 mg, 1.85 mmol, 1.0 equiv). The product was isolated as a white semisolid (524.0 mg, 63% yield). Mixture of rotamers, major is reported:

^{1}H NMR (500 MHz, $CDCl_3$): δ 6.97 (s, 1H), 4.29 (d, *J* = 9.0 Hz, 1H), 4.23–4.16 (m, 4H), 3.90 (m, 1H), 3.76–3.73 (m, 1H), 3.67–3.65 (m, 1H), 2.32 (s, 3H), 2.24 (s, 3H), 1.48 (s, 3H), 1.43 (s, 9H), 1.39 (s, 3H), 1.27 (t, *J* = 7.0 Hz, 6H) ppm.

^{13}C NMR (126 MHz, $CDCl_3$): δ 167.8, 153.6, 146.8, 100.0, 64.0, 79.6, 65.6, 60.3, 59.6, 36.1, 28.4, 26.6 (gem dimethyl), 24.5 (gem dimethyl), 19.3, 14.4 ppm.

IR (neat, cm^{-1}): 3333, 2979, 2937, 1692, 1551, 1480, 1366, 1285, 1252, 1213, 1170, 1096, 1049, 951.

HRMS *calcd for* ($C_{23}H_{36}N_2O_7$+Na) 475.2420, *found* 475.2417.

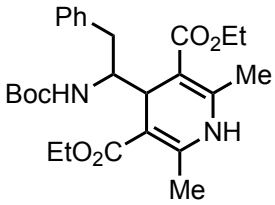

Diethyl 4-(1-((*tert*-butoxycarbonyl)amino)-2-phenylethyl)-2,6-dimethyl-1,4-dihydropyridine-3,5-dicarboxylate (6.1.11)

Following General Procedure I using *N*-Boc-L-phenylalaninal (1.0 g, 4.0 mmol, 1.0 equiv). The product was isolated as a white solid (701.2 mg, 37% yield). Mp = 146–147 °C; Mixture of rotamers, major is reported (Coalescence was observed at 330 K):

^{1}H NMR (400 MHz, DMSO-d_6): δ 8.92 (s, 1H), 7.15–7.12 (m, 2H), 7.11–7.06 (m, 3H), 5.95 (d, J = 6.0 Hz, 1H), 4.11–3.96 (m, 4H), 3.90 (d, J = 7.2 Hz, 1H), 3.37–3.35 (m, 1H), 3.59–2.54 (m, 2H), 2.23 (s, 3H), 2.18 (s, 3H), 1.04 (br s, 15H) ppm.

^{13}C NMR (101 MHz, DMSO-d_6): δ 167.4, 155.0, 146.6, 140.2, 128.7, 127.7, 125.4, 98.6, 76.7, 58.9, 55.5, 37.7, 30.6, 28.1, 18.4, 14.4 ppm.

IR (neat, cm^{-1}): 1693, 1659, 1632, 1528, 1474, 1368, 1303, 1252, 1236, 1206, 1166, 1122, 1097, 1053, 1038, 1010, 776.

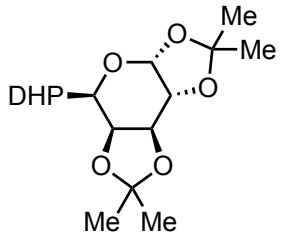

Diethyl 2,6-dimethyl-4-((3a*R*,5*R*,5a*S*,8a*S*,8b*R*)-2,2,7,7-tetramethyltetrahydro-5H-bis([1,3]dioxolo)[4,5-b:4',5'-d]pyran-5-yl)-1,4-dihydropyridine-3,5-dicarboxylate (6.1.12)

Following General Procedure using (3a*R*,5*S*,5a*R*,8a*S*,8b*R*)-2,2,7,7-tetramethyltetrahydro-5H-bis([1,3]dioxolo)[4,5-b:4',5'-d]pyran-5-carbaldehyde[6] (1.24 g, 4.94 mmol, 1.0 equiv). The product was isolated as a white solid (1.27 g, 53% yield). Mp = 154-159 ºC.

^{1}H NMR (500 MHz, $CDCl_3$) δ 5.40 (d, *J* = 4.9 Hz, 1H), 4.49 (d, *J* = 7.3 Hz, 1H), 4.46 (d, *J* = 7.9 Hz, 1H), 4.26 – 4.08 (m, 6H), 3.46 (d, *J* = 7.5 Hz, 1H), 2.31 (s, 3H), 2.29 (s, 3H), 1.42 (s, 3H), 1.37 (s, 3H), 1.33 – 1.23 (m, 12H) ppm.

^{13}C NMR (126 MHz, $CDCl_3$) δ 168.5, 168.3, 145.7, 144.0, 109.2, 108.2, 101.1, 99.4, 96.8, 71.7, 71.3, 70.1, 59.9, 59.5, 35.0, 26.1, 26.0, 25.2, 24.9, 19.2, 14.4, 14.4 ppm.

The spectroscopical data were in agreement with those previously reported.[1]

2.1 Synthesis and Characterization of compound 4-isopropyl-2,6-dimethyl-1,4-dihydropyridine-3,5-dicarbonitrile (1a-CN)

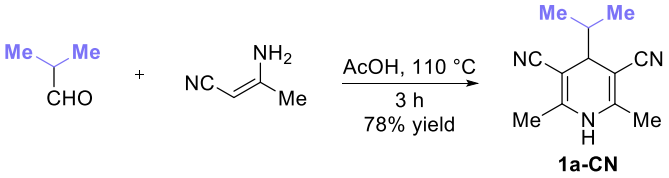

1a-CN

A round bottom flask was charged with 3-aminocrotononitrile (1.6 g, 20 mmol), butyraldehyde (721.2 mg, 10 mmol) and glacial AcOH (10 mL). The reaction was heated at 110 ºC with stirring for 3 h. Then it was allowed to cool to rt, diluted with H_2O and extracted with EtOAc three times. The combined organic layers were neutralized with a saturated solution of $NaHCO_3$ until a netural pH was reached, washed with brine, dried ($MgSO_4$), and filtered. The crude reaction mixture was purified using an automated system using hexanes/EtOAc (0 to 40%) as eluent, obtaining the product as a white solid (1.56 g, 78% yield). Mp = 118-120 ºC.

^{1}H NMR (500 MHz, $CDCl_3$) δ 5.87 (s, 1H), 3.16 (d, *J* = 3.3 Hz, 1H), 2.13 (s, 6H), 1.95 – 1.86 (m, 1H), 1.00 (d, *J* = 7.0 Hz, 6H) ppm.

^{13}C NMR (126 MHz, $CDCl_3$) δ 148.2, 120.0, 81.9, 42.2, 35.9, 18.3, 18.3 ppm.

IR (neat, cm-1): 3277, 3234, 3118, 2197, 1655, 1507, 1435, 1287, 1012, 622.

HRMS *calcd for* ($C_{12}H_{15}N_3$+H) 202.1344, *found* 202.1350.

General Procedures for Cross-Coupling

General Procedure A (GP-A): A 20.0 mL sealable screw cap vial was charged with DHP (0.6 mmol, 1.2 equiv) and aryl bromide (0.5 mmol, 1.0 equiv) if solids followed by addition of $[Ni(dtbbpy)(H_2O)_4]Cl_2$ (11.8 mg, 0.025 mmol, 5 mol %) and 4CzlPN (11.8 mg, 0.015 mmol, 3 mol %). The vial was sealed and three vacuum/argon cycles were made. Next, dry, degassed acetone[6] was added (10.0 mL, 0.05 M). If the (hetero)aryl bromide **2** or **1** were oils, they were added at this point as a solution in acetone or directly via microsyringe. The reaction was placed under blue LED irradiation and stirred for 24 h at rt. Next, the reaction was taken to dryness and purified on an automated liquid chromatographic system, obtaining the pure product.

General Procedure B (GP-B): A 20.0 mL sealable screw cap vial was charged with DHP (0.75 mmol, 1.5 equiv) and aryl bromide (0.5 mmol, 1.0 equiv) if solids followed by addition of $[Ni(dtbbpy)(H_2O)_4]Cl_2$ (23.6 mg, 0.025 mmol, 10 mol %) and 4CzlPN (11.8 mg, 0.015 mmol, 3 mol %). The vial was sealed and three vacuum/argon cycles were made. Next, dry, degassed acetone[6] was added (10.0 mL, 0.05 M). If the (hetero)aryl bromide **2** or **1** were oils, they were added at this point as a solution in acetone or directly via microsyringe. The reaction was placed under blue LED irradiation and stirred for 24 h at rt. Next, the reaction was taken to dryness and purified on an automated liquid chromatographic system, obtaining the pure product.

Characterization Data: (Hetero)aryl bromide scope

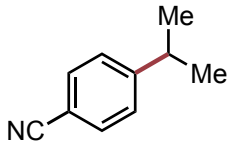

4-Isopropylbenzonitrile (6.2.1)

Prepared following GP-A. The product was purified using hexanes/EtOAc (0 to 5%) on an automated system and was obtained as a colorless oil (43.8 mg, 60% yield).

^{1}H NMR (500 MHz, $CDCl_3$) δ 7.58 (d, *J* = 7.1 Hz, 2H), 7.32 (d, *J* = 7.7 Hz, 2H), 3.00 – 2.90 (m, 1H), 1.26 (d, *J* = 6.9 Hz, 6H) ppm.

^{13}C NMR (126 MHz, $CDCl_3$) δ 154.5, 132.4, 127.4, 119.3, 109.7, 34.5, 23.7 ppm.

The spectral data were in agreement with those previously reported.[7]

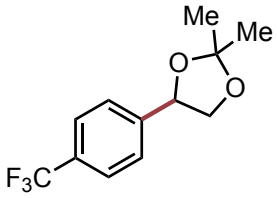

2,2-Dimethyl-4-(4-(trifluoromethyl)phenyl)-1,3-dioxolane (6.3.1)

Prepared following GP-B. The product was purified using pentane/Et_2O (0 to 15%) on an automated system and was obtained as a colorless oil (42.5 mg, 35% yield).

^{1}H NMR (500 MHz, $CDCl_3$) δ 7.62 (d, *J* = 7.9 Hz, 2H), 7.48 (d, *J* = 7.8 Hz, 2H), 5.13 (t, *J* = 7.1 Hz, 1H), 4.35 (t, *J* = 7.6 Hz, 1H), 3.69 (t, *J* = 8.2 Hz, 1H), 1.55 (s, 3H), 1.50 (s, 3H) ppm.

^{13}C NMR (126 MHz, $CDCl_3$) δ 143.7, 130.3 (q, *J* = 32.8 Hz), 126.5, 125.6 (q, *J* = 3.6 Hz), 124.2 (q, *J* = 272.0 Hz), 110.3, 77.3, 71.6, 26.6, 26.0 ppm.

IR (neat, cm^{-1}): 2989, 1621, 1323, 1160, 1122, 1112, 1063, 833.

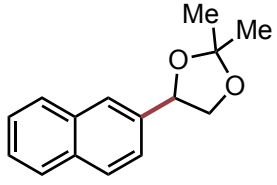

2,2-Dimethyl-4-(naphthalen-2-yl)-1,3-dioxolane (6.3.2)

Prepared following GP-B. The product was purified using hexanes/Et_2O (3:1) and obtained as a colorless oil (47.0 mg, 46% yield).

^{1}H NMR (500 MHz, $CDCl_3$) δ 7.85 (d, *J* = 6.6 Hz, 4H), 7.49 (d, *J* = 7.7 Hz, 3H), 5.26 (s, 1H), 4.39 (s, 1H), 3.81 (t, *J* = 8.4 Hz, 1H), 1.63 (s, 3H), 1.55 (s, 3H) ppm.

^{13}C NMR (126 MHz, $CDCl_3$) δ 136.7, 133.4, 133.3, 128.6, 128.1, 127.9, 126.4, 126.1, 125.4, 124.0, 110.0, 78.2, 71.7, 26.8, 26.1 ppm.

IR (neat, cm^{-1}): 2985, 1379, 1370, 1212, 1154, 1060, 855.

HRMS *calcd for* ($C_{15}H_{16}O_2$+H) 229.1229, *found* 229.1226.

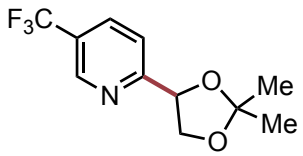

2-(2,2-Dimethyl-1,3-dioxolan-4-yl)-5-(trifluoromethyl)pyridine (6.3.3)

Prepared following GP-A. The product was purified using pentane/Et_2O (0 to 40%) on an automated system and obtained as a colorless oil (74.1 mg, 60% yield).

^{1}H NMR (500 MHz, $CDCl_3$) δ 8.80 (s, 1H), 7.94 (dd, *J* = 8.3, 2.3 Hz, 1H), 7.69 (d, *J* = 8.2 Hz, 1H), 5.25 (t, *J* = 6.7 Hz, 1H), 4.50 (dd, *J* = 8.5, 7.0 Hz, 1H), 3.98 (dd, *J* = 8.5, 6.3 Hz, 1H), 1.53 (s, 3H), 1.51 (s, 3H) ppm.

^{13}C NMR (126 MHz, $CDCl_3$) δ 164.7, 146.1 (q, *J* = 3.4 Hz), 134.0 (q, *J* = 3.4 Hz), 126.9 – 124.7 (m), 122.6, 119.9, 110.8, 77.9, 70.2, 26.6, 25.6 ppm.

IR (neat, cm^{-1}): 2990, 1607, 1373, 1325, 1213, 1159, 1124, 1077, 844.

HRMS *calcd for* ($C_{11}H_{12}F_3NO_2$+H) 248.0898, *found* 248.0891.

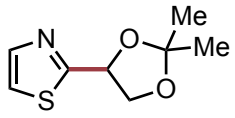

2-(2,2-Dimethyl-1,3-dioxolan-4-yl)thiazole (6.3.4)

Prepared following GP-B. The product was purified using pentane/Et_2O (0 to 40%) on an automated system and obtained as a yellow oil (48.4 mg, 52% yield).

^{1}H NMR (500 MHz, $CDCl_3$) δ 7.74 (d, *J* = 3.3 Hz, 1H), 7.30 (d, *J* = 3.3 Hz, 1H), 5.40 (t, *J* = 6.1 Hz, 1H), 4.44 (dd, *J* = 8.6, 6.6 Hz, 1H), 4.08 (dd, *J* = 8.6, 5.6 Hz, 1H), 1.57 (s, 3H), 1.47 (s, 3H) ppm.

^{13}C NMR (126 MHz, $CDCl_3$) δ 172.0, 143.1, 119.3, 111.1, 75.7, 70.5, 26.6, 25.5 ppm. IR (neat, cm^{-1}): 2987, 2936, 1721, 1210, 1142, 842, 724, 510.

HRMS *calcd for* ($C_8H_{11}NO_2S$+H) 186.0589, *found* 186.0589.

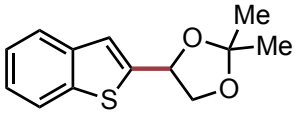

4-(Benzo[b]thiophen-2-yl)-2,2-dimethyl-1,3-dioxolane (6.3.5)

Prepared following GP-B. The product was purified using hexanes/Et_2O (5:1) and obtained as a colorless oil (34.0 mg, 73% yield).

^{1}H NMR (500 MHz, $CDCl_3$) δ 7.73 (d, *J* = 7.7 Hz, 1H), 7.64 (d, *J* = 7.6 Hz, 1H), 7.31 – 7.17 (m, 2H), 7.16 (s, 1H), 5.32 (t, *J* = 6.7 Hz, 1H), 4.34 – 4.19 (m, 1H), 3.89 (t, *J* = 7.8 Hz, 1H), 1.50 (s, 3H), 1.41 (s, 3H) ppm.

^{13}C NMR (126 MHz, $CDCl_3$) δ 144.1, 139.8, 139.6, 124.5, 124.5, 123.6, 122.6, 121.5, 110.5, 74.6, 71.4, 26.7, 26.0 ppm.

IR (neat, cm^{-1}): 3056, 2986, 2935, 1208, 1061, 837, 583.

HRMS *calcd for* ($C_{13}H_{14}O_2S$) 234.0711, *found* 234.0715.

HRMS *calcd for* ($C_{13}H_{14}O_2S$+H) 235.0793, *found* 235.0782.

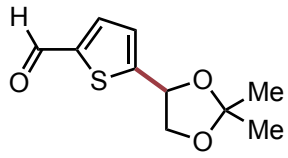

5-(2,2-Dimethyl-1,3-dioxolan-4-yl)thiophene-2-carbaldehyde (6.3.6)

Prepared following GP-A. The product was purified using hexanes/EtOAc (0 to 20%) on an automated system and was obtained as a yellow oil (71.4 mg, 67% yield).

^{1}H NMR (500 MHz, $CDCl_3$) δ 9.87 (s, 1H), 7.65 (d, *J* = 3.1 Hz, 1H), 7.09 (d, *J* = 3.3 Hz, 1H), 5.32 (t, *J* = 6.5 Hz, 1H), 4.36 (t, *J* = 7.3 Hz, 1H), 3.86 (t, *J* = 7.6 Hz, 1H), 1.55 (s, 3H), 1.46 (s, 3H) ppm.

^{13}C NMR (126 MHz, $CDCl_3$) δ 183.0, 154.8, 143.2, 136.4, 125.4, 110.9, 74.1, 71.6, 26.6, 25.8 ppm.

IR (neat, cm^{-1}): 3073, 1418, 1231, 1212, 1044, 726, 663.

HRMS *calcd for* ($C_{11}H_{14}O_3S$+H) 227.0743, *found* 227.0742.

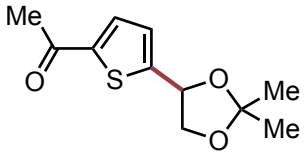

1-(5-(2,2-Dimethyl-1,3-dioxolan-4-yl)thiophen-2-yl)ethan-1-one (6.3.7)

Prepared following GP-B. The product was purified using hexanes/Et_2O (5:1) and obtained as a yellow oil (39.0 mg, 86%).

^{1}H NMR (500 MHz, $CDCl_3$) δ 7.56 (s, 1H), 7.01 (s, 1H), 5.28 (d, *J* = 6.7 Hz, 1H), 4.34 (t, *J* = 7.5 Hz, 1H), 3.85 (t, *J* = 7.8 Hz, 1H), 2.53 (s, 3H), 1.54 (s, 3H), 1.46 (s, 3H) ppm.

^{13}C NMR (126 MHz, $CDCl_3$) δ 197.2, 190.7, 152.8, 143.9, 132.4, 125.4, 110.8, 74.1, 71.6, 26.8, 26.6, 25.9 ppm.

IR (neat, cm^{-1}): 2987, 1662, 1276, 1061.

HRMS *calcd for* ($C_{11}H_{14}O_3S$+H) 227.0742, *found* 227.0743.

Characterization Data: (Hetero)aryl bromide Scope

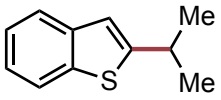

2-Isopropylbenzo[b]thiophene (6.4.1)

Prepared following GP-B. The product was purified using hexanes/Et_2O (5:1) and obtained as a clear oil (61.2, 70% yield).

^{1}H NMR (500 MHz, $CDCl_3$) δ 7.79 (d, *J* = 8.0 Hz, 1H), 7.68 (d, *J* = 7.9 Hz, 1H), 7.32 (t, *J* = 7.6 Hz, 1H), 7.27 (d, *J* = 7.7 Hz, 1H), 7.03 (s, 1H), 3.26 (hept, *J* = 7.0 Hz, 1H), 1.42 (d, *J* = 6.8 Hz, 6H) ppm.

^{13}C NMR (126 MHz, $CDCl_3$) δ 154.2, 140.2, 139.0, 124.1, 123.5, 122.9, 122.3, 118.4, 30.7, 24.5 ppm.

IR (neat, cm^{-1}): 2962, 2930, 1457, 1436, 1071, 1001, 855.

HRMS *calcd for* ($C_{11}H_{12}S$+H) 177.0738, *found* 177.0745.

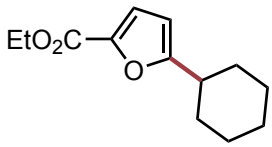

Ethyl 5-cyclohexylfuran-2-carboxylate (6.4.2)

Prepared following GP-A. The product was purified using hexanes/EtOAc (0 to 20%) on an automated system and was obtained as a colorless oil (73.5 mg, 66% yield).

^{1}H NMR (500 MHz, $CDCl_3$) δ 7.08 (d, *J* = 3.5 Hz, 1H), 6.08 (d, *J* = 3.4 Hz, 1H), 4.34 (q, *J* = 7.1 Hz, 2H), 2.73 – 2.66 (m, 1H), 2.05 (d, *J* = 10.8 Hz, 2H), 1.80 (d, *J* = 12.6 Hz, 2H), 1.71 (d, *J* = 12.8 Hz, 1H), 1.46 – 1.30 (m, 7H), 1.30 – 1.19 (m, 1H) ppm.

^{13}C NMR (126 MHz, $CDCl_3$) δ 165.8, 159.1, 142.9, 118.9, 105.5, 60.7, 37.6, 31.4, 26.0, 25.9, 14.5 ppm. IR (neat, cm^{-1}): 2929, 2855, 1517, 1294, 1213, 1174, 1138, 1120, 799.

HRMS *calcd for* ($C_{13}H_{18}O_3$+H) 223.1334, *found* 223.1344.

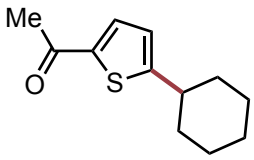

1-(5-Cyclohexylthiophen-2-yl)ethan-1-one (6.4.3)

Prepared following GP-A. The product was purified using hexanes/EtOAc (0 to 15%) on an automated system and was obtained as a white solid (47.2 mg, 45% yield). Mp = 48-52 ºC.

^{1}H NMR (500 MHz, $CDCl_3$) δ 7.54 (d, *J* = 3.6 Hz, 1H), 6.83 (d, *J* = 3.7 Hz, 1H), 2.87 – 2.77 (m, 1H), 2.51 (s, 3H), 2.04 (d, *J* = 11.3 Hz, 2H), 1.83 (d, *J* = 11.7 Hz, 2H), 1.73 (d, *J* = 11.3 Hz, 1H), 1.52 – 1.33 (m, 4H), 1.32 – 1.19 (m, 1H) ppm.

^{13}C NMR (126 MHz, $CDCl_3$) δ 190.7, 162.4, 141.4, 132.8, 123.6, 40.2, 35.2, 26.6, 26.4, 25.9 ppm.

IR (neat, cm^{-1}): 2927, 2854, 1645, 1447, 1354, 1030, 927, 807, 595.

HRMS *calcd for* ($C_{12}H_{16}O_S$+H) 209.1000, *found* 209.0991.

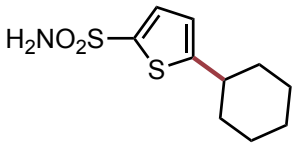

5-Cyclohexylthiophene-2-sulfonamide (6.4.4)

Prepared according to GP-B. The product was purified using hexanes/EtOAc (9:1) and obtained as a yellow oil (12.0 mg, 24% yield).

^{1}H NMR (500 MHz, $CDCl_3$) δ 7.50 (d, *J* = 3.8 Hz, 1H), 6.76 (d, *J* = 3.8 Hz, 1H), 4.87 (s, 2H), 2.82 (s, 1H), 2.05 (d, *J* = 10.0 Hz, 2H), 1.84 (d, *J* = 10.6 Hz, 2H), 1.41 (h, *J* = 12.3 Hz, 4H), 1.26 (s, 1H).

^{13}C NMR (126 MHz, $CDCl_3$) δ 160.4, 139.0, 132.1, 122.4, 40,0, 35.3, 26.4, 25.8 ppm.

IR (neat, cm^{-1}): 2931, 1447, 1334, 1157.

HRMS *calcd for* ($C_{10}H_{15}NO_2S_2$+H) 246.0622, *found* 246.0630.

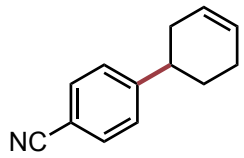

1',2',3',6'-Tetrahydro-[1,1'-biphenyl]-4-carbonitrile (6.4.5)

Prepared following GP-A. The product was purified using hexanes/EtOAc (0 to 5%) on an automated system and was obtained as a white solid (39.0 mg, 43% yield). Mp = 53-55 ºC.

^{1}H NMR (500 MHz, $CDCl_3$) δ 7.59 (d, *J* = 8.0 Hz, 2H), 7.33 (d, *J* = 7.9 Hz, 2H), 5.77 (s, 2H), 2.93 – 2.80 (m, 1H), 2.33 – 2.25 (m, 1H), 2.24 – 2.08 (m, 3H), 1.97 – 1.89 (m, 1H), 1.79 – 1.71 (m, 1H) ppm.

^{13}C NMR (126 MHz, $CDCl_3$) δ 152.9, 132.4, 127.9, 127.2, 126.2, 119.2, 109.9, 40.4, 32.9, 29.4, 25.5 ppm.

IR (neat, cm^{-1}): 3024, 2917, 2836, 226, 1607, 830, 690, 651, 561. HRMS *calcd for* ($C_{13}H_{13}N$+H) 184.1126, *found* 184.1123.

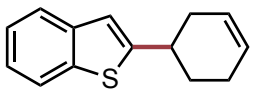

2-(Cyclohex-3-en-1-yl)benzo[b]thiophene (6.4.6)

Prepared following GP-B. The product was purified using hexanes/Et_2O (5:1) and obtained as a clear oil (40.3 mg, 38% yield).

^{1}H NMR (500 MHz, $CDCl_3$) δ 7.79 (d, *J* = 8.0 Hz, 1H), 7.69 (d, *J* = 7.9 Hz, 1H), 7.32 (t, *J* = 7.5 Hz, 1H), 7.25 (d, *J* = 7.3 Hz, 1H), 7.06 (s, 1H), 5.78 (s, 2H), 3.20 (s, 1H), 2.57 – 2.40 (m, 1H), 2.27 – 2.18 (m, 1H), 2.16 – 2.04 (m, 3H), 2.00 – 1.86 (m, 1H), 1.79 – 1.59 (m, 1H) ppm.

^{13}C NMR (126 MHz, $CDCl_3$) δ 152.2, 140.2, 139.0, 127.2, 126.0, 124.2, 123.6, 123.0, 122.3, 118.8, 36.2, 33.6, 30.7, 25.5 ppm.

IR (neat, cm^{-1}): 3023, 2916, 1436, 1068, 854, 734.

HRMS *calcd for* ($C_{14}H_{14}S$+H) 215.0894, *found* 215.0891.

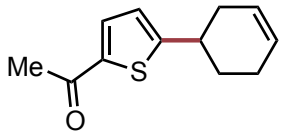

1-(5-(Cyclohex-3-en-1-yl)thiophen-2-yl)ethan-1-one (6.4.7)

Prepared following GP-B. The product was purified using hexanes/Et_2O (5:1) and was obtained as a clear oil (67.3 mg, 65% yield).

^{1}H NMR (500 MHz, $CDCl_3$) δ 7.55 (d, *J* = 3.8 Hz, 1H), 6.87 (d, *J* = 3.7 Hz, 1H), 5.75 (s, 2H), 3.14 (tt, *J* = 9.5, 4.1 Hz, 1H), 2.52 (s, 3H), 2.49 – 2.37 (m, 1H), 2.28 – 2.13 (m, 3H), 2.13 – 2.04 (m, 1H), 1.76 (m, 1H) ppm.

^{13}C NMR (126 MHz, $CDCl_3$) δ 209.7, 190.7, 161.3, 141.8, 132.8, 127.2, 125.7, 124.0, 36.2, 33.6, 30.7, 26.6, 25.3 ppm.

IR (neat, cm^{-1}): 3025, 2913, 2837, 1659, 1455, 1278, 670.

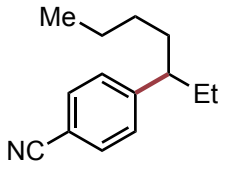

4-(Heptan-3-yl)benzonitrile (6.4.8): Prepared following GP-A. The product was purified using hexanes/EtOAc (0 to 5%) on an automated system and was obtained as a colorless oil (56.2 mg, 56% yield).

^{1}H NMR (500 MHz, $CDCl_3$) δ 7.57 (d, *J* = 6.8 Hz, 2H), 7.23 (d, *J* = 6.9 Hz, 2H), 2.52 – 2.41 (m, 1H), 1.75 – 1.61 (m, 2H), 1.59 – 1.46 (m, 2H), 1.34 – 1.16 (m, 2H), 1.20 – 1.08 (m, 1H), 1.10 – 0.98 (m, 1H), 0.82 (t, *J* = 7.3 Hz, 3H), 0.74 (t, *J* = 7.2 Hz, 3H) ppm.

^{13}C NMR (126 MHz, $CDCl_3$) δ 152.1, 132.2, 128.7, 119.3, 109.7, 48.3, 36.0, 29.8, 29.5, 22.8, 14.1, 12.2 ppm.

IR (neat, cm^{-1}): 2959, 2927, 2873, 2858, 2227, 1607, 1460, 834, 570.

HRMS *calcd for* ($C_{14}H_{19}N$+H) 202.1596, *found* 202.1595.

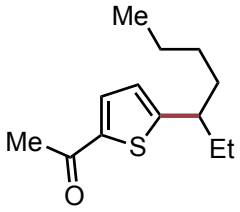

1-(5-(Heptan-3-yl)thiophen-2-yl)ethan-1-one (6.4.9)

Prepared following GP-B. The product was purified using hexanes/Et_2O (5:1) and was obtained as a clear oil (51.3 mg, 46%).

^{1}H NMR (500 MHz, $CDCl_3$) δ 7.54 (d, *J* = 3.8 Hz, 1H), 6.80 (d, *J* = 3.8 Hz, 1H), 2.74 (tt, *J* = 9.4, 5.2 Hz, 1H), 2.52 (s, 3H), 1.71 (m, 2H), 1.64 – 1.50 (m, 2H), 1.37 – 1.11 (m, 4H), 0.84 (m, 6H).

^{13}C NMR (126 MHz, $CDCl_3$) δ 190.6, 160.9, 141.9, 132.7, 125.3, 44.1, 37.2, 30.8, 29.7, 26.6, 22.7, 14.1, 12.0 ppm.

IR (neat, cm^{-1}): 2960, 2929, 1661, 1457, 1278, 809.

HRMS *calcd for* ($C_{14}H_{22}OS$+H) 239.1470, *found* 239.1470.

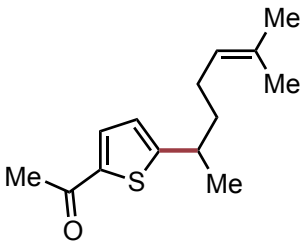

1-(5-(6-Methylhept-5-en-2-yl)thiophen-2-yl)ethan-1-one (6.4.10)

Prepared following GP-B. The product was purified using hexanes/Et_2O (5:1) and was obtained as a yellow oil (92.0 mg, 83% yield).

^{1}H NMR (500 MHz, $CDCl_3$) δ 7.53 (s, 1H), 6.81 (s, 1H), 5.06 (s, 1H), 3.05 – 3.01 (m, 1H), 2.50 (s, 3H), 1.95 (m, 2H), 1.65 (m, 5H), 1.53 (s, 3H), 1.31 (d, J = 7.0 Hz, 3H).

^{13}C NMR (126 MHz, $CDCl_3$) δ 190.6, 162.2, 141.7, 132.7, 132.2, 124.3, 123.7, 39.2, 35.8, 26.6, 25.9, 25.8, 23.0, 17.8 ppm.

IR (neat, cm^{-1}): 2965, 2918, 1600, 1447, 1276, 807.

HRMS *calcd for* ($C_{14}H_{20}OS$+H) 237.1313, *found* 237.1296.

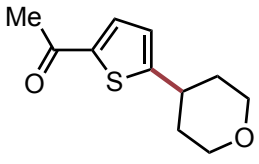

1-(5-(Tetrahydro-2H-pyran-4-yl)thiophen-2-yl)ethan-1-one (6.4.11)

Prepared following GP-A. The product was purified using hexanes/EtOAc (0 to 30%) on an automated system and was obtained as a white solid (80.1 mg, 77% yield). Mp = 58-61 ºC.

^{1}H NMR (500 MHz, $CDCl_3$) δ 7.56 (d, *J* = 3.8 Hz, 1H), 6.87 (d, *J* = 3.8 Hz, 1H), 4.26 – 3.91 (m, 2H), 3.52 (td, *J* = 11.8, 2.1 Hz, 2H), 3.11 – 3.00 (m, 1H), 2.52 (s, 3H), 2.01 – 1.89 (m, 2H), 1.82 (ddd, *J* = 24.7, 11.9, 4.0 Hz, 2H) ppm.

^{13}C NMR (126 MHz, $CDCl_3$) δ 190.5, 159.6, 141.9, 132.8, 123.8, 67.8, 37.3, 34.5, 26.6 ppm.

IR (neat, cm^{-1}): 1650, 1448, 1271, 1087, 1015, 877, 818, 600

HRMS *calcd for* ($C_{11}H_{14}O_2S$+H) 211.0793, *found* 211.0780.

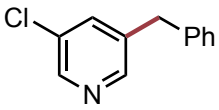

3-Benzyl-5-chloropyridine (6.4.12)

Prepared following GP-A and [Ni(dme)(dtbbpy)]Br_2 (14.0 mg, 0.025 mmol, 5 mol %). The product was purified using pentane/Et_2O (0 to 40%) on an automated system and was obtained as a colorless oil (42.9 mg, 42% yield).

^{1}H NMR (500 MHz, $CDCl_3$) δ 8.43 (s, 1H), 8.38 (s, 1H), 7.45 (s, 1H), 7.33 (t, *J* = 7.4 Hz, 2H), 7.29 – 7.21 (m, 1H), 7.17 (d, *J* = 7.4 Hz, 2H), 3.97 (s, 2H) ppm.

^{13}C NMR (126 MHz, $CDCl_3$) δ 148.0, 146.7, 138.9, 138.0, 136.1, 132.1, 129.0 (2C), 126.9, 38.7 ppm.

IR (neat, cm^{-1}): 3029, 1579, 1419, 1104, 1025, 708, 696, 682.

HRMS *calcd for* ($C_{12}H_{10}$ClN+H) 204.0580, *found* 204.0587.

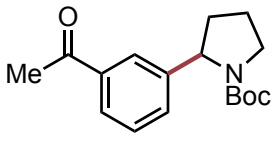

***tert*-Butyl 2-(3-acetylphenyl)pyrrolidine-1-carboxylate (6.4.13)**

Prepared following GP-B. The product was purified using hexanes/EtOAc (0 to 20%) on an automated system to afford a light yellow oil (55.0 mg, 38% yield); Mixture of rotamers, major is reported:

^{1}H NMR (500 MHz, $CDCl_3$): δ 7.77 (m, 1H), 7.75 (s, 1H), 7.40–7.35 (m, 2H), 4.79 (br s, 1H), 3.63 (br, 2H), 2.57 (s, 3H), 2.34 (br, 1H), 1.87–1.82 (m, 3H), 1.43 (s, 4H, Boc), 1.14 (s, 5H, Boc) ppm.

^{13}C NMR (126 MHz, $CDCl_3$): δ 198.0, 154.4, 145.7, 137.1, 130.1, 128.4, 126.7, 125.3, 79.3, 61.1, 47.1, 35.9, 34.8, 28.4, 26.6, 23.2 ppm.

IR (neat, cm^{-1}): 2974, 2931, 2899, 1684, 1602, 1587, 1478, 1390, 1364, 1256, 1159, 1115, 1080, 957, 905, 876.

HRMS *calcd for* ($C_{17}H_{23}NO_3$+Na) 312.1576, *found* 312.1561.

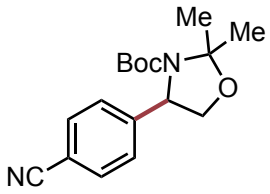

***tert*-Butyl 4-(4-cyanophenyl)-2,2-dimethyloxazolidine-3-carboxylate (6.4.14)**

Prepared following GP-B. The product was purified using hexanes/EtOAc (0 to 10%) on an automated system to afford a light yellow oil (22.0 mg, 37% yield); Mixture of rotamers, major is reported:

^{1}H NMR (500 MHz, $CDCl_3$): δ 7.64 (d, J = 8.0 Hz, 2H), 7.42 (m, 2H), 4.83 (br s, 1H), 4.30 (dd, J = 9.0, 7.0 Hz, 1H), 3.83 (m, 1H), 1.60 (s, 3H), 1.58 (s, 3H), 1.45 (s, 9H) ppm.

^{13}C NMR (126 MHz, $CDCl_3$): δ 151.6, 140.9, 132.4, 127.1, 118.7, 111.2, 95.0, 80.3, 70.2, 60.8, 28.3, 26.0 (gem dimethyl), 24.9 (gem dimethyl) ppm.

IR (neat, cm^{-1}): 2980, 2929, 2229, 1695, 1609, 1505, 1478, 1457, 1376, 1365, 1255, 1206, 1171, 1146, 1088, 1057.

HRMS *calcd for* ($C_{17}H_{22}N_2O_3$+H) 303.1709, *found* 303.1712.

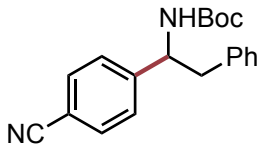

***tert*-Butyl (1-(4-cyanophenyl)-2-phenylethyl)carbamate (6.4.15)**

Prepared following GP-B. The product was purified using hexanes/EtOAc (0 to 20%) on an automated system to afford a light yellow oil (28.1 mg, 47%).

^{1}H NMR (500 MHz, $CDCl_3$): δ 7.58 (d, *J* = 8.5 Hz, 2H), 7.36–7.21 (m, 5H), 7.01 (d, *J* = 6.5 Hz, 2H), 4.97 (br s, 2H), 3.02 (br s, 2H), 1.40 (s, 9H) ppm.

^{13}C NMR (126 MHz, $CDCl_3$): δ 155.1, 136.3, 132.4, 129.4 (2C), 128.7, 127.3, 127.1, 118.9, 111.1, 80.2, 55.8, 43.1, 28.4 ppm.

IR (neat, cm^{-1}) 2978, 2229, 1695, 1608, 1495, 1455, 1391, 1366, 1289, 1247, 1163, 1108, 1045, 1018, 911.

HRMS *calcd for* ($C_{20}H_{22}N_2O_2$+H) 323.1760, *found* 323.1772.

Characterization Data: Synthesis of Aryl-containing Saccharides

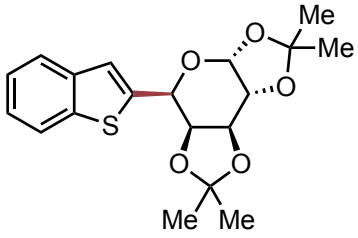

(3a*R*,5*S*,5a*R*,8a*S*,8b*R*)-5-(Benzo[b]thiophen-2-yl)-2,2,7,7-tetramethyltetrahydro-5H-bis([1,3]dioxolo)[4,5-b:4',5'-d]pyran (6.5.1)

Prepared following GP-B. The product was purified using hexanes/EtOAc (0 to 30%) on an automated system and was obtained as a white solid with a >20:1 dr (89.3 mg, 70% yield). Mp = 118-120 ºC.

^{1}H NMR (500 MHz, DMSO-d_6) δ 7.91 (d, J = 7.7 Hz, 1H), 7.80 (d, J = 7.6 Hz, 1H), 7.41 (s, 1H), 7.38 – 7.28 (m, 2H), 5.63 (d, J = 5.0 Hz, 1H), 5.15 (s, 1H), 4.74 (dd, J = 7.8, 2.3 Hz, 1H), 4.54 (dd, J = 7.8, 2.0 Hz, 1H), 4.47 (dd, J = 4.7, 1.9 Hz, 2H), 1.53 (s, 3H), 1.39 (s, 3H), 1.34 (s, 3H), 1.28 (s, 3H) ppm.

^{13}C NMR (126 MHz, DMSO-d_6) δ 141.8, 139.2, 138.7, 124.1, 124.0, 123.3, 122.1, 121.3, 108.6, 108.2, 96.2, 72.8, 70.4, 69.9, 66.7, 25.9 (2C), 24.7, 24.2 ppm. The absolute configuration was determined by NOE NMR experiments in combination with HSQC and HMBC experiments.

IR (neat, cm^{-1}): 2927, 1377, 1163, 1142, 1065, 1040, 996, 895, 746.

HRMS *calcd for* ($C_{19}H_{22}O_5S$+H) 363.1266, *found* 363.1248.

Crystals suitable for X-Ray difraction were achieved by slow evaporation of an acetonitrile solution of compound **3lf.**

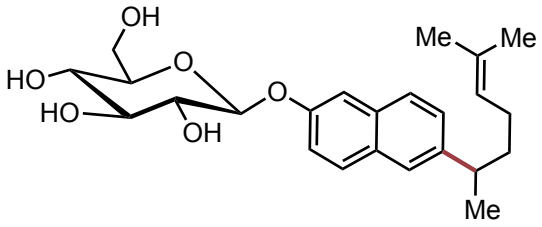

(2*R*,3*S*,4*S*,5*R*,6*S*)-2-(Hydroxymethyl)-6-((6-(6-methylhept-5-en-2-yl)naphthalen-2-yl)oxy)tetrahydro-2H-pyran-3,4,5-triol (6.5.2)

Prepared following GP-B. The product was purified using EtOAc/MeOH (9:1) and obtained as a light yellow oil (262.0 mg, 31% yield).

^{1}H NMR (500 MHz, DMSO-d_6) δ 7.78 (d, J = 8.9 Hz, 1H), 7.72 (d, J = 8.5 Hz, 1H), 7.61 (s, 1H), 7.42 (s, 1H), 7.35 (d, J = 8.5 Hz, 1H), 7.22 (d, J = 9.1 Hz, 1H), 5.33 (d, J = 4.5 Hz, 1H), 5.12 – 5.05 (m, 2H), 5.00 (dd, J = 11.8, 6.1 Hz, 2H), 4.56 (t, J = 5.8 Hz, 1H), 3.73 (dd, J = 12.1, 5.2 Hz, 1H), 3.50 (dt, J = 11.9, 6.1 Hz, 1H), 3.40 (t, J = 7.8 Hz, 1H), 3.32 – 3.27 (m,

2H), 3.21 (dt, J = 14.2, 6.8 Hz, 1H), 2.81 (h, J = 7.1 Hz, 1H), 1.83 (tt, J = 14.5, 7.3 Hz, 2H), 1.73 – 1.54 (m, 5H), 1.44 (s, 3H), 1.26 (d, J = 6.9 Hz, 3H) ppm.

^{13}C NMR (126 MHz, DMSO-d_6) δ 155.3, 143.2, 133.2, 131.4, 129.8, 129.3, 127.6, 126.7, 126.7, 125.3, 125.3, 124.9, 119.3, 111.0, 111.0, 101.3, 101.3, 77.7, 77.3, 73.9, 70.4, 61.3, 39.3, 38.4, 26.3, 26.1, 22.8, 18.1 ppm.

IR (neat, cm^{-1}): 3413, 2254, 2128, 1659, 1208, 1023, 823.

X-Ray Crystallographic data

X-Ray Crystallograpic data for [Ni(dtbbpy)(H_2O)$_4$]Cl_2:

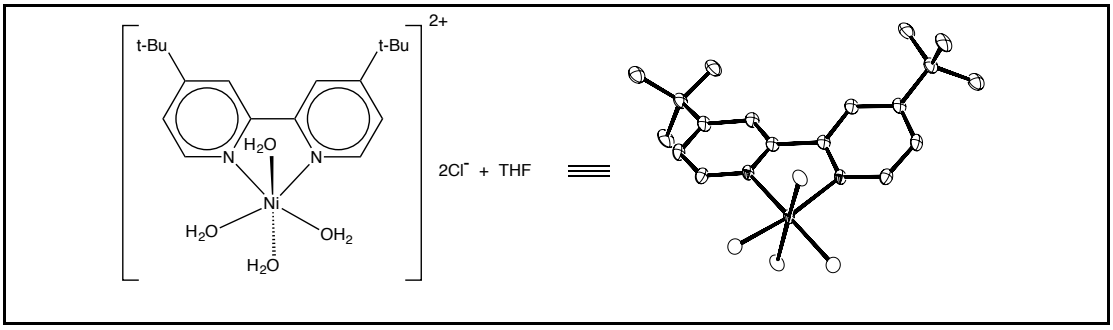

Compound [Ni(dtbbpy)(H_2O)$_4$]Cl_2, $C_{22}H_{40}Cl_2N_2NiO_5$, crystallizes in the monoclinic space group C2/c (systematic absences hkl: h+k=odd, h0l: l=odd) with a=13.0843(9)Å, b=30.400(2)Å, c=6.6223(5)Å, β=92.470(2)°, V=2631.7(3)Å^3, Z=4, and d_{calc}=1.368 g/cm$_3$. X-ray intensity data were collected on a Bruker D8QUEST [1] CMOS area detector employing graphite-monochromated Mo-Kα radiation (λ=0.71073Å) at a temperature of 100K. Preliminary indexing was performed from a series of twenty-four 0.5° rotation frames with exposures of 10 seconds. A total of 1614 frames were collected with a crystal to detector distance of 34.1 mm, rotation widths of 0.5° and exposures of 15 seconds:

scan type	2θ	ω	φ	χ	Frames
	0.00	195.50	0.00	54.72	298
	-1.00	345.19	0.00	54.72	720
	0.00	195.50	90.00	54.72	298
	0.00	195.50	180.00	54.72	298

Rotation frames were integrated using SAINT [2], producing a listing of unaveraged F^2 and $\sigma(F^2)$ values. A total of 36013 reflections were measured over the ranges $6.234 \leq 2\theta \leq 50.876°$, $-15 \leq h \leq 15$, $-36 \leq k \leq 36$, $-7 \leq l \leq 7$ yielding 2417 unique reflections (R_{int} = 0.0650).

The intensity data were corrected for Lorentz and polarization effects and for absorption using SADABS [3] (minimum and maximum transmission 0.5113, 0.7456). The structure was solved by direct methods - SHELXT [4]. Refinement was by full-matrix least squares based on F^2 using SHELXL-2014 [5]. All reflections were used during refinement. The weighting scheme used was $w=1/[\sigma^2(F_o^2)+ (0.1083P)^2 + 11.2889P]$ where $P = (F_o^2 + 2F_c^2)/3$. Non-hydrogen atoms were refined anisotropically and hydrogen atoms were refined using a riding model, except for the water hydrogens, which were located on a difference map, but were not refined. Refinement converged to R1=0.0571 and wR2=0.1568 for 2217 observed reflections for which $F > 4\sigma(F)$ and R1=0.0617 and wR2=0.1639 and GOF =1.083 for all 2417 unique, non-zero reflections and 149 variables. The maximum Δ/σ in the final cycle of least squares was 0.001 and the two most prominent peaks in the final difference Fourier were +2.33 and -1.28 e/Å^3.

Table S1. lists cell information, data collection parameters, and refinement data. Final positional and equivalent isotropic thermal parameters are given in Tables S2. and S3. Anisotropic thermal parameters are in Table S4. Tables S5. and S6. list bond distances and bond angles. Figure S2. is an ORTEP representation of the molecule with 50% probability thermal ellipsoids displayed.

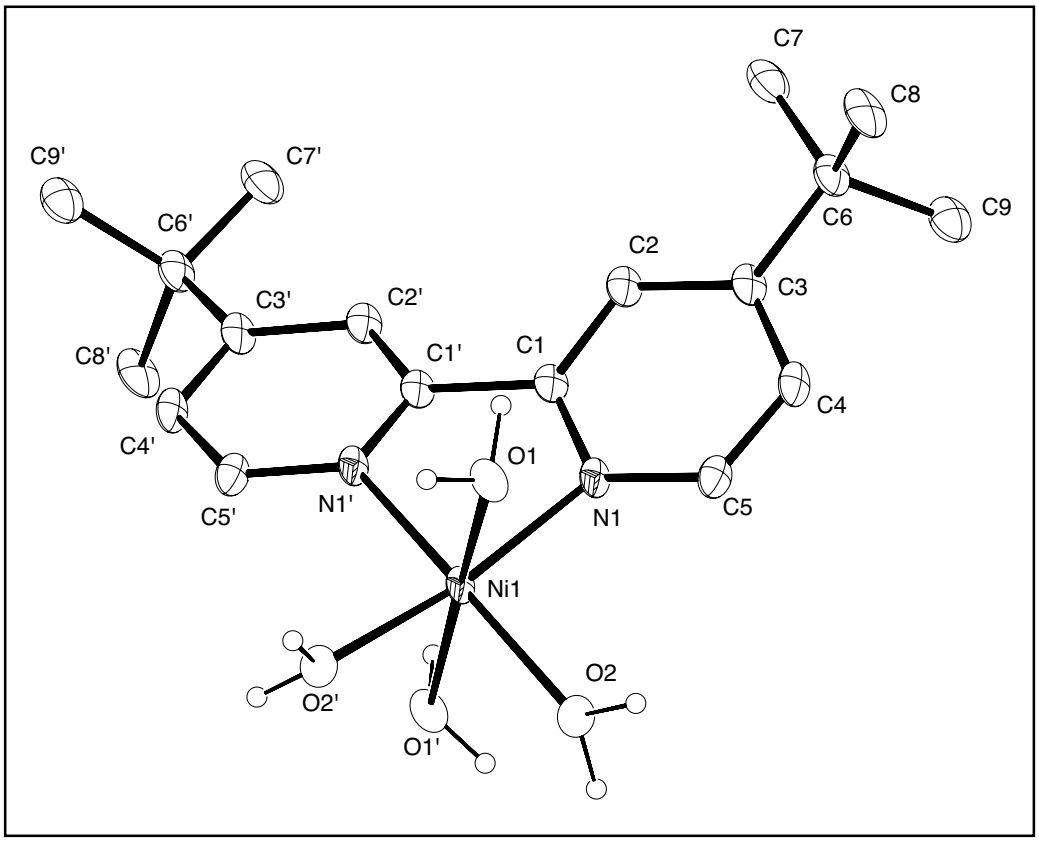

ORTEP drawing of the title compound with 50% thermal ellipsoids.

Table S1. Summary of Structure Determination of Compound $[Ni(dtbbpy)(H_2O)_4]Cl_2$

Empirical formula	$C_{22}H_{40}Cl_2N_2NiO_5$
Formula weight	542.17
Temperature/K	100
Crystal system	monoclinic
Space group	C2/c
a	13.0843(9)Å
b	30.400(2)Å
c	6.6223(5)Å
β	92.470(2)°
Volume	2631.7(3)$Å^3$
Z	4
d_{calc}	1.368 g/cm^3
μ	0.974 mm^{-1}
F(000)	1152.0
Crystal size, mm	0.28 × 0.18 × 0.03
2θ range for data collection	6.234 - 50.876°

Index ranges	$-15 \leq h \leq 15, -36 \leq k \leq 36, -7 \leq l \leq 7$
Reflections collected	36013
Independent reflections	2417[R(int) = 0.0650]
Data/restraints/parameters	2417/0/149
Goodness-of-fit on F^2	1.083
Final R indexes [I>=2σ (I)]	$R_1 = 0.0571$, $wR_2 = 0.1568$
Final R indexes [all data]	$R_1 = 0.0617$, $wR_2 = 0.1639$
Largest diff. peak/hole	2.33/-1.28 $eÅ^{-3}$

Table S2. Refined Positional Parameters for Compound $[Ni(dtbbpy)(H_2O)_4]Cl_2$

Atom	*x*	*y*	*z*	U(eq)
Ni1	0.5	0.75601(2)	0.75	0.0138(2)
O1	0.34718(18)	0.76087(8)	0.8088(4)	0.0195(5)
O2	0.47754(17)	0.80527(8)	0.5361(4)	0.0200(5)
N1	0.45760(19)	0.70343(9)	0.5649(4)	0.0152(6)
C1	0.4691(2)	0.66373(11)	0.6532(5)	0.0157(7)
C2	0.4241(2)	0.62601(11)	0.5727(5)	0.0171(7)
C3	0.3651(2)	0.62789(11)	0.3920(5)	0.0172(7)
C4	0.3560(2)	0.66888(12)	0.2989(5)	0.0180(7)
C5	0.4021(2)	0.70527(12)	0.3898(5)	0.0181(7)
C6	0.3068(2)	0.58811(11)	0.3054(5)	0.0194(7)
C7	0.3345(3)	0.54563(12)	0.4189(6)	0.0269(8)
C8	0.1919(2)	0.59735(14)	0.3260(6)	0.0256(8)
C9	0.3289(3)	0.58191(12)	0.0807(6)	0.0242(8)
Cl1	0.69206(6)	0.81637(3)	0.31042(12)	0.0181(3)
O3	0	0.50320(12)	0.75	0.0273(8)

C10	0.0828(3)	0.53080(13)	0.8217(6)	0.0265(8)
C11	0.0407(3)	0.57674(13)	0.8358(6)	0.0281(8)

Table S3. Positional Parameters for Hydrogens in Compound $[Ni(dtbbpy)(H_2O)_4]Cl_2$

Atom	*x*	*y*	*z*	U(eq)
H1a	0.3391	0.7728	0.9211	0.05
H1b	0.334	0.7305	0.8116	0.05
H2a	0.4259	0.8094	0.4652	0.05
H2b	0.5279	0.8162	0.4574	0.05
H2	0.4331	0.5993	0.6394	0.023
H4	0.3191	0.6718	0.1764	0.024
H5	0.3943	0.7324	0.3262	0.024
H7a	0.4067	0.5404	0.413	0.04
H7b	0.2976	0.5215	0.3575	0.04
H7c	0.3167	0.5484	0.5575	0.04
H8a	0.153	0.5722	0.2809	0.038
H8b	0.1723	0.6224	0.245	0.038
H8c	0.1789	0.6032	0.465	0.038
H9a	0.4002	0.5756	0.0679	0.036
H9b	0.3114	0.6083	0.0078	0.036

H9c	0.2888	0.5579	0.0263	0.036
H10a	0.138	0.53	0.7287	0.035
H10b	0.1089	0.5209	0.9533	0.035
H11a	0.093	0.5987	0.8144	0.037
H11b	0.011	0.5819	0.9654	0.037

Table S4. Refined Thermal Parameters (U's) for Compound $[Ni(dtbbpy)(H_2O)_4]Cl_2$

Atom	U_{11}	U_{22}	U_{33}	U_{23}	U_{13}	U_{12}
Ni1	0.0037(3)	0.0250(4)	0.0126(4)	0	-0.0016(2)	0
O1	0.0078(12)	0.0304(13)	0.0204(13)	-0.005(1)	0.0008(9)	-0.0016(9)
O2	0.0088(11)	0.0308(13)	0.0202(12)	0.0051(10)	-0.0029(9)	0.0005(9)
N1	0.0056(12)	0.0267(14)	0.0133(13)	-0.0002(11)	-0.0011(10)	0.0008(10)
C1	0.0049(14)	0.0271(17)	0.0152(16)	-0.0004(13)	0.0014(12)	-0.0006(12)
C2	0.0083(15)	0.0259(17)	0.0172(16)	-0.0006(13)	0.0004(12)	0.0009(12)
C3	0.0042(15)	0.0302(18)	0.0171(16)	-0.0016(13)	0.0003(12)	0.0000(12)
C4	0.0078(15)	0.0313(18)	0.0147(16)	0.0000(13)	-0.0020(12)	0.0025(13)
C5	0.0110(15)	0.0282(18)	0.0151(16)	0.0025(13)	-0.0003(12)	0.0026(13)
C6	0.0102(16)	0.0274(18)	0.0202(18)	-0.0015(13)	-0.0026(13)	-0.0014(13)
C7	0.0210(18)	0.0289(19)	0.030(2)	-0.0005(15)	-0.0080(15)	-0.0072(15)
C8	0.0074(17)	0.041(2)	0.028(2)	-0.0068(16)	-0.0015(14)	-0.0036(14)
C9	0.0151(17)	0.0320(19)	0.0254(19)	-0.0046(15)	0.0008(14)	-0.0027(14)
Cl1	0.0078(4)	0.0288(5)	0.0174(5)	0.0010(3)	-0.0018(3)	0.0004(3)
O3	0.0175(18)	0.031(2)	0.033(2)	0	-0.0010(15)	0

C10	0.0127(17)	0.037(2)	0.030(2)	0.0014(16)	-0.0021(14)	-0.0001(14)
C11	0.0157(17)	0.036(2)	0.033(2)	-0.0028(16)	-0.0012(16)	-0.0037(15)

Table S5. Bond Distances in Compound $[Ni(dtbbpy)(H_2O)_4]Cl_2$, Å

Ni1-O1	2.059(2)	Ni1-O1	2.059(2)	Ni1-O2	2.073(2)
Ni1-O2	2.073(2)	Ni1-N1	2.075(3)	Ni1-N1	2.075(3)
N1-C1	1.347(4)	N1-C5	1.343(4)	C1-C1	1.486(6)
C1-C2	1.385(5)	C2-C3	1.397(5)	C3-C4	1.393(5)
C3-C6	1.529(5)	C4-C5	1.386(5)	C6-C7	1.530(5)
C6-C8	1.540(4)	C6-C9	1.540(5)	O3-C10	1.435(4)
O3-C10	1.435(4)	C10-C11	1.505(5)	C11-C11	1.524(7)

[1]1-X,+Y,3/2-Z; [2]-X,+Y,3/2-Z

Table S6. Bond Angles in Compound $[Ni(dtbbpy)(H_2O)_4]Cl_2$, °

O1-Ni1-O1[1]	171.76(14)	O1-Ni1-O2[1]	85.93(9)	O1-Ni1-O2[1]	88.12(10)
O1-Ni1-O2	88.12(10)	O1-Ni1-O2	85.93(9)	O1-Ni1-N1[1]	100.41(10)
O1-Ni1-N1	100.41(10)	O1-Ni1-N1[1]	85.99(10)	O1-Ni1-N1	85.98(10)
O2-Ni1-O2[1]	87.53(14)	O2-Ni1-N1[1]	170.46(10)	O2-Ni1-N1	170.46(10)
O2-Ni1-N1	97.26(10)	O2-Ni1-N1[1]	97.26(10)	N1-Ni1-N1	79.24(15)

C1-N1-Ni1	114.3(2)	C5-N1-Ni1	126.8(2)	C5-N1-C1	117.3(3)
N1-C1-C1	114.91(18)	N1-C1-C2	122.5(3)	C2-C1-C1	122.6(2)
C1-C2-C3	120.4(3)	C2-C3-C6	122.5(3)	C4-C3-C2	116.7(3)
C4-C3-C6	120.6(3)	C5-C4-C3	119.6(3)	N1-C5-C4	123.5(3)
C3-C6-C7	112.3(3)	C3-C6-C8	107.2(3)	C3-C6-C9	110.3(3)
C7-C6-C8	108.8(3)	C7-C6-C9	108.7(3)	C9-C6-C8	109.4(3)
C10-O3-C10	108.4(4)	O3-C10-C11	106.9(3)	C10-C11-C11	101.5(2)

[1]1-X,+Y,3/2-Z; [2]-X,+Y,3/2-Z

Table S7. Hydrogen Bonds for [Ni(dtbbpy)(H_2O)$_4$]Cl_2.

D	H	A	d(D-H)/Å	d(H-A)/Å	d(D-A)/Å	D-H-A/°
O1	H1a	Cl1[1]	0.838(2)	2.2683(8)	3.095(2)	169.09(17)
O1	H1b	Cl1[2]	0.940(2)	2.3404(8)	3.104(2)	138.10(14)
O2	H2a	Cl1[3]	0.816(2)	2.3486(8)	3.141(2)	164.06(17)
O2	H2b	Cl1	0.920(2)	2.3960(8)	3.254(2)	155.18(15)

[1]1-X,+Y,3/2-Z; [2]-1/2+X,3/2-Y,1/2+Z; [3]1-X,+Y,1/2-Z

This report has been created with Olex2 [6], compiled on 2016.05.11 svn.r3296 for OlexSys.

X-Ray crystallographic data for compound (3a*R*,5*S*,5a*R*,8a*S*,8b*R*)-5-(Benzo[b]thiophen-2-yl)-2,2,7,7-tetramethyltetrahydro-5H-bis([1,3]dioxolo)[4,5-b:4',5'-d]pyran (3lf)

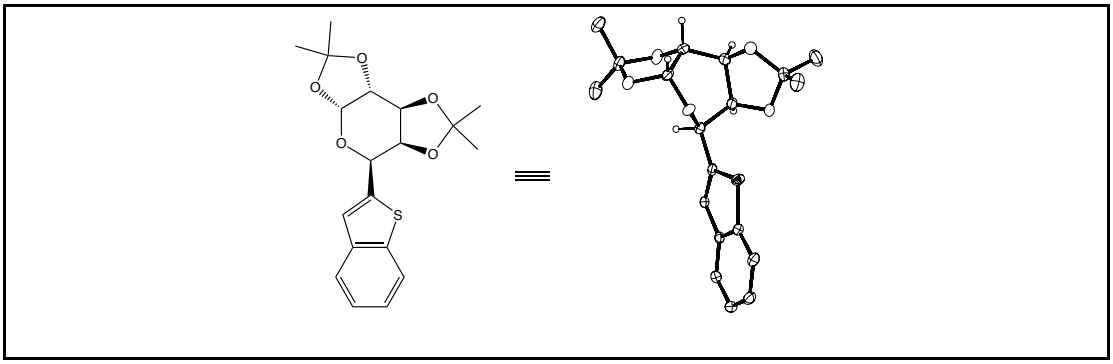

Compound **3lf**, $C_{19}H_{22}O_5S$, crystallizes in the orthorhombic space group $P2_12_12_1$ (systematic absences h00: h=odd, 0k0: k=odd and 00l: l=odd) with a=5.63430(10)Å, b=17.0439(4)Å, c=18.3976(4)Å, V=1766.73(6)Å^3, Z=4, and d_{calc}=1.363 g/cm$_3$. X-ray intensity data were collected on a Bruker APEXII [1] CCD area detector employing graphite-monochromated Mo-Kα radiation (λ=0.71073Å) at a temperature of 100K. Preliminary indexing was performed from a series of thirty-six 0.5° rotation frames with exposures of 10 seconds. A total of 4232 frames were collected with a crystal to detector distance of 37.4 mm, rotation widths of 0.5° and exposures of 10 seconds:

scan type	2θ	ω	φ	χ	Frames
	24.50	7.41	12.48	28.88	739
	-23.00	334.21	44.72	73.66	727
	-20.50	342.55	321.55	-73.06	542
	-23.00	333.49	158.99	-70.01	69

scan type	2θ	ω	φ	χ	Frames
	-25.50	330.51	47.91	-56.95	137
	27.00	276.67	5.00	57.63	227
	-23.00	315.83	12.48	28.88	739
	19.50	59.55	348.71	-26.26	739
	17.00	321.50	184.44	82.07	116
	-10.50	306.95	272.07	99.72	80
	17.00	321.08	318.36	83.36	117

Rotation frames were integrated using SAINT [2], producing a listing of unaveraged F^2 and $\sigma(F^2)$ values. A total of 76138 reflections were measured over the ranges $3.258 \leq 2\theta \leq 55.2°$, $-7 \leq h \leq 7$, $-22 \leq k \leq 22$, $-23 \leq l \leq 23$ yielding 4098 unique reflections ($R_{int} = 0.0244$). The intensity data were corrected for Lorentz and polarization effects and for absorption using SADABS [3] (minimum and maximum transmission 0.7252, 0.7456). The structure was solved by direct methods - SHELXS-97 [4]. Refinement was by full-matrix least squares based on F^2 using SHELXL-2014 [5]. All reflections were used during refinement. The weighting scheme used was $w=1/[\sigma^2(F_o^2)+ (0.0372P)^2 + 0.4474P]$ where $P = (F_o^2 + 2F_c^2)/3$. Non-hydrogen atoms were refined anisotropically and hydrogen atoms were refined using a riding model. Refinement converged to R1=0.0236 and wR2=0.0627 for 3997 observed reflections for which $F > 4\sigma(F)$ and R1=0.0244 and wR2=0.0636 and GOF =1.032 for all 4098 unique, non-zero reflections and 230 variables. The maximum Δ/σ in the final cycle of least squares was 0.001 and the two most prominent peaks in the final difference Fourier

were +0.26 and -0.20 e/Å^3. The Flack absolute structure parameter refined to a value of 0.000(8) thus corroborating the assigned stereochemistry.

Table S8 lists cell information, data collection parameters, and refinement data. Final positional and equivalent isotropic thermal parameters are given in Tables S9 and S10. Anisotropic thermal parameters are in Table S11 Tables S12 and S13 list bond distances and bond angles. Figure S3 is an ORTEP representation of the molecule with 50% probability thermal ellipsoids displayed.

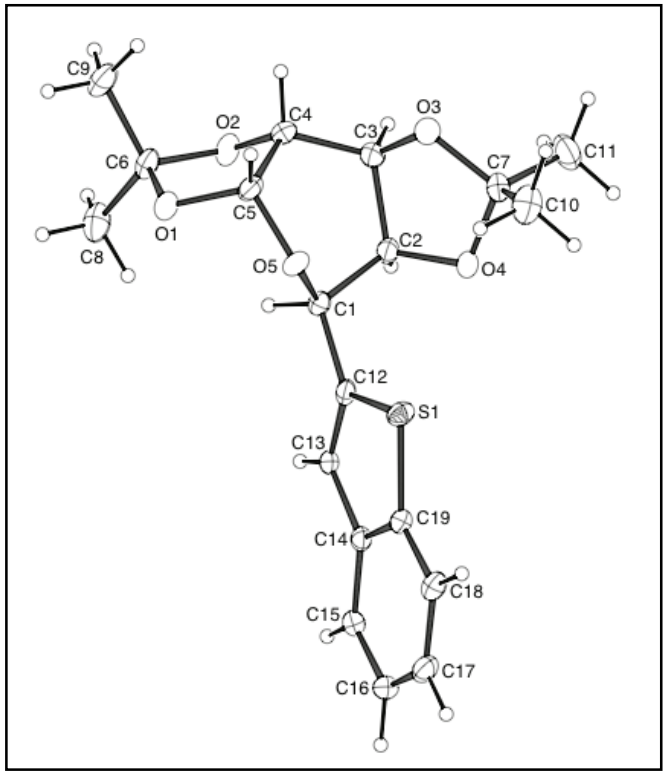

Figure S3. ORTEP drawing of the compound **3lf** with 50% thermal ellipsoids.

Table S8. Summary of Structure Determination of Compound 3lf

Empirical formula	$C_{19}H_{22}O_5S$
Formula weight	362.42
Temperature/K	100
Crystal system	orthorhombic
Space group	$P2_12_12_1$
a	5.63430(10)Å
b	17.0439(4)Å
c	18.3976(4)Å
Volume	1766.73(6)$Å^3$
Z	4
d_{calc}	1.363 g/cm^3
μ	0.210 mm^{-1}
F(000)	768.0
Crystal size, mm	0.27 × 0.22 × 0.07
2θ range for data collection	3.258 - 55.2°

Index ranges	$-7 \leq h \leq 7, -22 \leq k \leq 22, -23 \leq l \leq 23$
Reflections collected	76138
Independent reflections	4098[R(int) = 0.0244]
Data/restraints/parameters	4098/0/230
Goodness-of-fit on F^2	1.032
Final R indexes [I>=2σ (I)]	$R_1 = 0.0236$, $wR_2 = 0.0627$
Final R indexes [all data]	$R_1 = 0.0244$, $wR_2 = 0.0636$
Largest diff. peak/hole	0.26/-0.20 $eÅ^{-3}$
Flack parameter	0.000(8)

Table S9. Refined Positional Parameters for Compound 3lf

Atom	*x*	*y*	*z*	U(eq)
C1	0.6373(3)	0.50568(9)	0.51875(8)	0.0145(3)
C2	0.7001(3)	0.42985(9)	0.47838(8)	0.0172(3)
C3	0.5746(3)	0.35804(9)	0.51175(9)	0.0222(3)
C4	0.4763(3)	0.37244(9)	0.58716(8)	0.0207(3)
C5	0.3429(3)	0.45049(9)	0.59475(8)	0.0178(3)
C6	0.5803(3)	0.4253(1)	0.69607(8)	0.0195(3)
C7	0.4446(3)	0.37174(10)	0.39391(9)	0.0225(3)
C8	0.7835(3)	0.46938(13)	0.73007(10)	0.0286(4)
C9	0.4471(4)	0.37383(11)	0.74995(9)	0.0274(4)
C10	0.2302(3)	0.40696(13)	0.35715(10)	0.0306(4)
C11	0.5599(4)	0.30581(11)	0.35112(10)	0.0304(4)
C12	0.6783(3)	0.57838(9)	0.47468(8)	0.0144(3)
C13	0.8724(3)	0.62536(8)	0.47743(8)	0.0137(3)
C14	0.8484(3)	0.69286(9)	0.42958(8)	0.0144(3)
C15	1.0044(3)	0.75587(9)	0.41932(8)	0.0175(3)
C16	0.9400(3)	0.81664(9)	0.37318(9)	0.0206(3)

C17	0.7226(3)	0.81538(10)	0.33700(9)	0.0211(3)
C18	0.5653(3)	0.75346(9)	0.34553(8)	0.0191(3)
C19	0.6295(3)	0.69260(9)	0.39259(8)	0.0153(3)
O1	0.4194(2)	0.48015(7)	0.66282(6)	0.0193(2)
O2	0.6695(2)	0.37960(7)	0.63673(6)	0.0219(3)
O3	0.3764(3)	0.34537(7)	0.46493(7)	0.0282(3)
O4	0.6157(2)	0.43222(7)	0.40557(6)	0.0217(3)
O5	0.39104(19)	0.50437(6)	0.53894(6)	0.0162(2)
S1	0.46110(7)	0.61115(2)	0.41498(2)	0.01748(9)

Table S10. Positional Parameters for Hydrogens in Compound 3lf

Atom	***x***	***y***	***z***	**U(eq)**
H1	0.7355	0.5088	0.5639	0.019
H2	0.8759	0.4218	0.4788	0.023
H3	0.6822	0.3114	0.5116	0.03
H4	0.3712	0.3279	0.602	0.028
H5	0.1684	0.4401	0.5966	0.024
H8a	0.8601	0.5023	0.6932	0.043

H8b	0.8991	0.432	0.7496	0.043
H8c	0.7234	0.5026	0.7695	0.043
H9a	0.3871	0.4063	0.7899	0.041
H9b	0.5547	0.3338	0.7693	0.041
H9c	0.3137	0.3483	0.7253	0.041
H10a	0.1675	0.4498	0.387	0.046
H10b	0.108	0.3666	0.3512	0.046
H10c	0.2759	0.4274	0.3094	0.046
H11a	0.6138	0.3259	0.304	0.046
H11b	0.4443	0.2637	0.3434	0.046
H11c	0.6961	0.2854	0.3783	0.046
H13	1.0074	0.6154	0.507	0.018
H15	1.153	0.757	0.4437	0.023
H16	1.0451	0.8596	0.3662	0.027
H17	0.6814	0.8577	0.3059	0.028
H18	0.4184	0.7524	0.3202	0.025

Table S11. Refined Thermal Parameters (U's) for Compound 3lf

Atom	U_{11}	U_{22}	U_{33}	U_{23}	U_{13}	U_{12}
C1	0.0155(7)	0.0154(7)	0.0127(6)	0.0013(5)	-0.0005(6)	0.0007(6)
C2	0.0235(8)	0.0155(7)	0.0126(7)	0.0002(5)	0.0006(6)	0.0022(6)
C3	0.0363(10)	0.0141(7)	0.0163(7)	-0.0002(6)	0.0001(7)	-0.0014(7)
C4	0.0313(8)	0.0157(7)	0.0150(7)	0.0041(6)	-0.0004(7)	-0.0036(6)
C5	0.0187(7)	0.0211(7)	0.0136(7)	0.0041(6)	0.0011(6)	-0.0029(6)
C6	0.0225(8)	0.0236(8)	0.0124(7)	0.0028(6)	0.0005(6)	0.0044(7)
C7	0.0314(9)	0.0208(8)	0.0152(7)	-0.0028(6)	0.0003(7)	-0.0021(7)
C8	0.0239(8)	0.0431(11)	0.0187(8)	-0.0027(8)	-0.0016(7)	-0.0001(8)
C9	0.0338(9)	0.0306(9)	0.0176(7)	0.0084(6)	0.0027(8)	0.0037(8)
C10	0.0280(9)	0.0404(11)	0.0234(9)	-0.0018(8)	0.0012(7)	0.0029(8)
C11	0.0425(11)	0.0230(8)	0.0257(8)	-0.0083(7)	-0.0042(8)	0.0033(8)
C12	0.0179(7)	0.0155(7)	0.0097(6)	-0.0001(5)	0.0000(5)	0.0030(6)
C13	0.0169(6)	0.0136(7)	0.0106(6)	-0.0020(5)	0.0024(5)	-0.0001(5)
C14	0.0170(7)	0.0145(6)	0.0115(6)	-0.0013(5)	0.0011(5)	0.0011(6)
C15	0.0211(7)	0.0172(7)	0.0142(7)	-0.0022(5)	0.0000(6)	-0.0027(6)
C16	0.0288(8)	0.0154(7)	0.0177(7)	-0.0001(6)	0.0036(7)	-0.0041(6)

C17	0.0287(8)	0.0186(7)	0.0159(7)	0.0038(6)	0.0030(6)	0.0024(7)
C18	0.0208(7)	0.0219(7)	0.0147(7)	0.0031(6)	0.0001(6)	0.0023(6)
C19	0.0171(7)	0.0160(7)	0.0128(6)	-0.0002(5)	0.0024(5)	-0.0008(6)
O1	0.0247(6)	0.0200(5)	0.0133(5)	0.0018(4)	-0.0007(4)	0.0031(4)
O2	0.0295(6)	0.0231(6)	0.0131(5)	0.0016(4)	0.0001(5)	0.0073(5)
O3	0.0422(8)	0.0251(6)	0.0171(6)	0.0000(5)	-0.0006(5)	-0.0124(6)
O4	0.0346(6)	0.0190(5)	0.0115(5)	-0.0002(4)	-0.0007(5)	-0.0034(5)
O5	0.0150(5)	0.0184(5)	0.0153(5)	0.0052(4)	0.0011(4)	0.0005(4)
S1	0.01670(17)	0.01913(17)	0.01660(17)	0.00510(14)	-0.00268(14)	-0.00218(14)

Table S12. Bond Distances in Compound 3lf, Å

C1-C2	1.532(2)	C1-C12	1.499(2)	C1-O5	1.4363(19)
C2-C3	1.541(2)	C2-O4	1.4221(18)	C3-C4	1.514(2)
C3-O3	1.427(2)	C4-C5	1.534(2)	C4-O2	1.425(2)
C5-O1	1.4176(19)	C5-O5	1.4038(18)	C6-C8	1.505(3)
C6-C9	1.522(2)	C6-O1	1.4387(19)	C6-O2	1.4323(19)
C7-C10	1.509(3)	C7-C11	1.518(2)	C7-O3	1.434(2)

C7-O4	1.428(2)	C12-C13	1.356(2)	C12-S1	1.7368(15)
C13-C14	1.455(2)	C14-C15	1.401(2)	C14-C19	1.409(2)
C15-C16	1.388(2)	C16-C17	1.394(3)	C17-C18	1.387(2)
C18-C19	1.399(2)	C19-S1	1.7310(16)		

Table S13. Bond Angles in Compound 3lf. °

C12-C1-C2	113.55(12)	O5-C1-C2	109.61(13)	O5-C1-C12	107.57(12)
C1-C2-C3	111.77(13)	O4-C2-C1	110.82(13)	O4-C2-C3	104.15(13)
C4-C3-C2	113.83(13)	O3-C3-C2	103.82(12)	O3-C3-C4	106.93(15)
C3-C4-C5	113.78(13)	O2-C4-C3	108.70(14)	O2-C4-C5	103.99(12)
O1-C5-C4	103.93(12)	O5-C5-C4	113.96(13)	O5-C5-O1	110.74(12)
C8-C6-C9	113.09(14)	O1-C6-C8	109.36(14)	O1-C6-C9	109.92(14)
O2-C6-C8	108.75(14)	O2-C6-C9	110.86(14)	O2-C6-O1	104.50(12)
C10-C7-C11	113.86(15)	O3-C7-C10	108.58(15)	O3-C7-C11	110.80(14)
O4-C7-C10	108.71(14)	O4-C7-C11	108.86(15)	O4-C7-O3	105.70(12)
C1-C12-S1	119.95(12)	C13-C12-C1	126.34(14)	C13-C12-S1	113.69(11)
C12-C13-C14	111.69(14)	C15-C14-C13	129.01(14)	C15-C14-C19	119.14(14)
C19-C14-C13	111.78(14)	C16-C15-C14	119.38(15)	C15-C16-C17	120.69(15)
C18-C17-C16	121.27(15)	C17-C18-C19	117.99(15)	C14-C19-S1	111.56(11)
C18-C19-C14	121.53(15)	C18-C19-S1	126.90(13)	C5-O1-C6	109.60(12)
C4-O2-C6	105.44(12)	C3-O3-C7	107.02(13)	C2-O4-C7	110.29(12)
C5-O5-C1	112.69(11)	C19-S1-C12	91.27(8)		

This report has been created with Olex2 [6], compiled on 2016.08.25 svn.r3337 for OlexSys.

References

[1] APEX2 2014.11-0

[2] SAINT v8.34A

[3] SADABS v2014/5

[4] SHELXS-97

[5] SHELXL-2014/7

[6] Olex2 (Dolomanov et al., 2009)

10. References

(1) Tewari, N.; Dwivedi, N.; Tripathi, R. *Tetrahedron Lett.,* **2004**, *45*, 9011-9014.

(2) In cases where the aldehyde was too thick it could be dissolved in dichloromethane and added to the reaction mixture with any noticeable effect.

(3) Nakajima, K.; Nojima, S.; Sakata, K.; Nishibayashi, Y. *ChemCatChem.,* **2016**, *8*, 1028-1032.

(4) Heydari, A.; Khaksar, S.; Tajbakhsh, M.; Bijanzadeh, H. R. *J. Fluorine Chem.,* **2009**, *130*, 609-614.

(5) Li, G.; Chen, R.; Wu, L.; Fu, Q.; Zhang, X.; Tang, Z. *Angew. Chem. Int. Ed.* **2013**, *52*, 8432-8436.

(6) Prepared following the reported procedure: Bobbitt, J, M.; Bartelson, A. L.; Bailey, W. F.; Hamlin, T. A.; Kelly, C. B. *J. Org. Chem.* **2014**, *79*, 1055-1067.

(7) The solvent was purged with argon for 30 minutes prior to use.

(8) Han, C.; Buchwald, S. L. *J. Am. Chem. Soc.* **2009**, *131*, 7532-7533.

(9) (a) Zhang, D.; Wu, L.-Z.; Zhou, L.; Han, X.; Yang, Q.-Z.; Zhang, L.-P.; Tung, C.-H. *J. Am. Chem. Soc.* **2004**, *126*, 3440-3441. (b) Wei, X.; Wang, L.; Jia, W.; Du, S.; Wu, L.; Liu, Q. *Chin. J. Chem.* **2014**, *32*, 1245-1250. (c) Fukuzumi, S.; Suenobu, T.; Patz, M.; Hirasaka, T.; Itoh, S.; Fujitsuka, M.; Ito, O. *J. Am. Chem. Soc.* **1998**, *120*, 8060-8068. (d) Wang, D.; Liu, Q.; Chen, B.; Zhang, L.; Tung, C.; Wu, L. *Chinese Sci. Bull.* **2010**, *55*, 2855-2858.

^{1}H and ^{13}C NMR Spectra: 1,4-Dihydropyridines

^{1}H NMR ($CDCl_3$, 500 MHz) of diethyl 4-isopropyl-2,6-dimethyl-1,4-dihydropyridine-3,5-dicarboxylate (**6.1.1**)

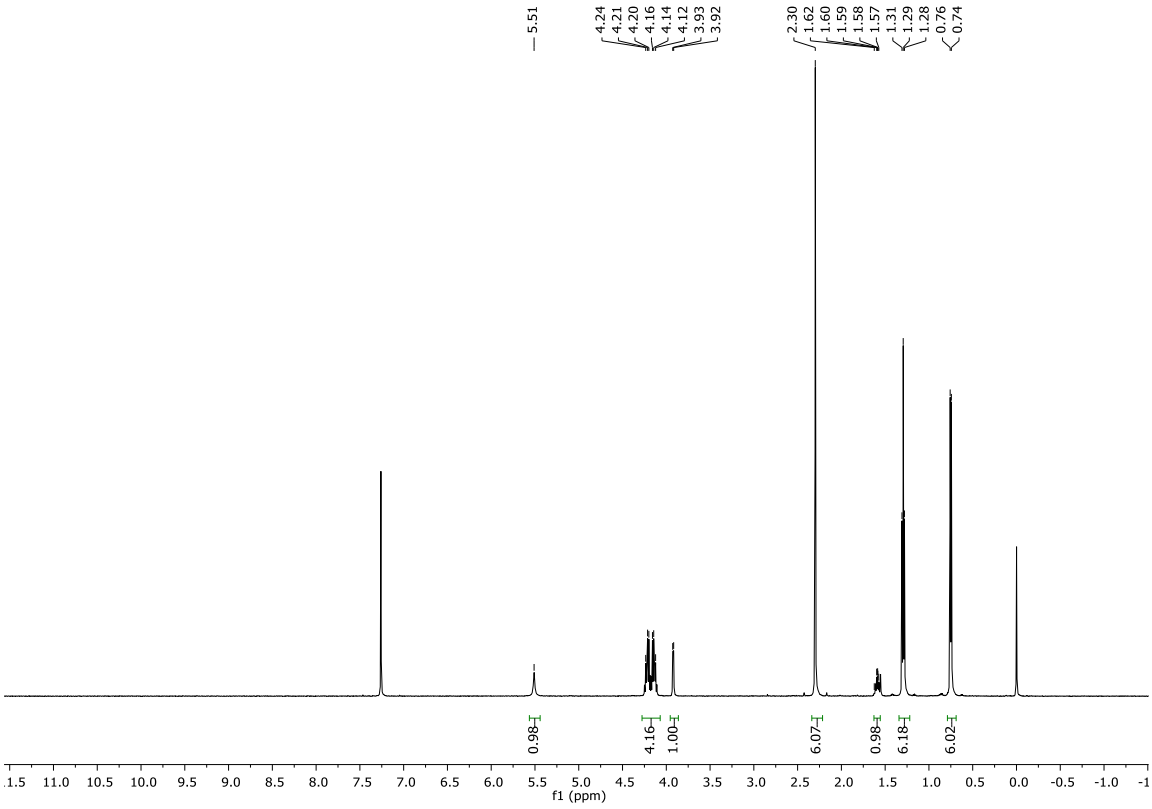

^{13}C NMR ($CDCl_3$, 126 MHz) of diethyl 4-isopropyl-2,6-dimethyl-1,4-dihydropyridine-3,5-dicarboxylate (**6.1.1**)

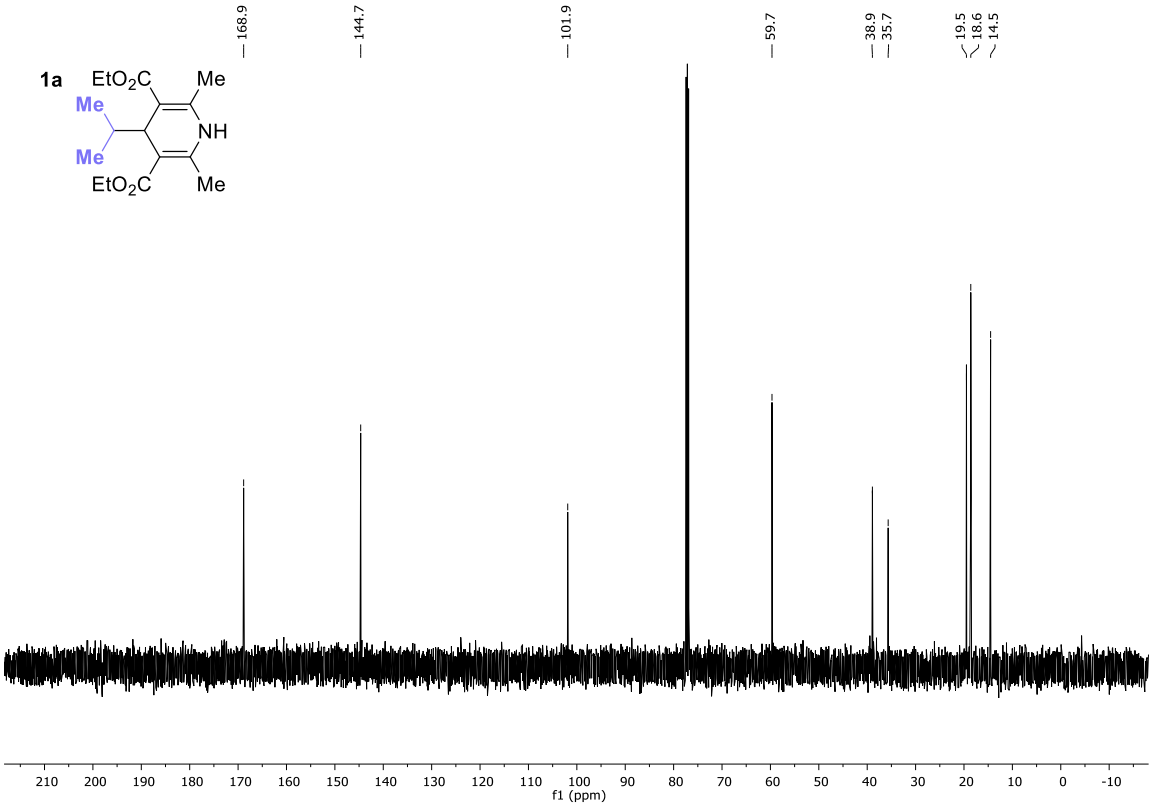

^{1}H NMR ($CDCl_3$, 500 MHz) of diethyl 4-(2,2-dimethyl-1,3-dioxolan-4-yl)-2,6-dimethyl-1,4-dihydropyridine-3,5-dicarboxylate (**6.1.2**)

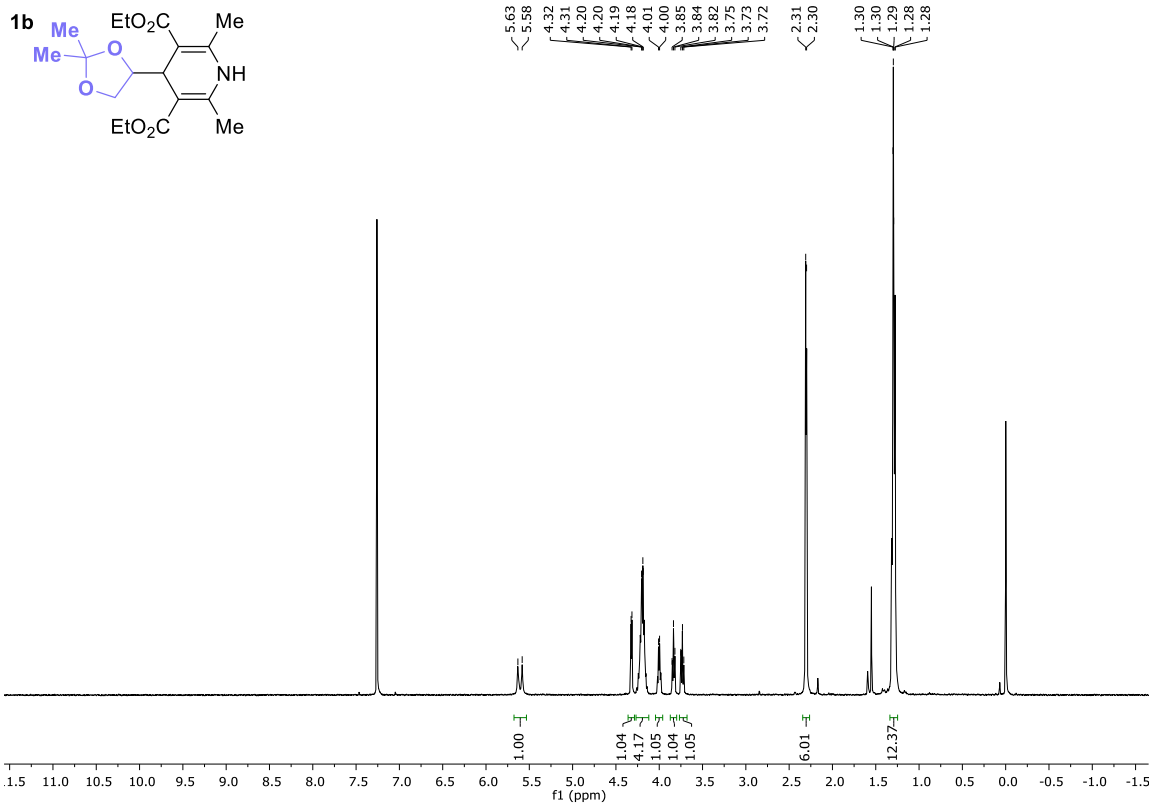

^{13}C NMR ($CDCl_3$, 126 MHz) of diethyl 4-(2,2-dimethyl-1,3-dioxolan-4-yl)-2,6-dimethyl-1,4-dihydropyridine-3,5-dicarboxylate (**6.1.2**)

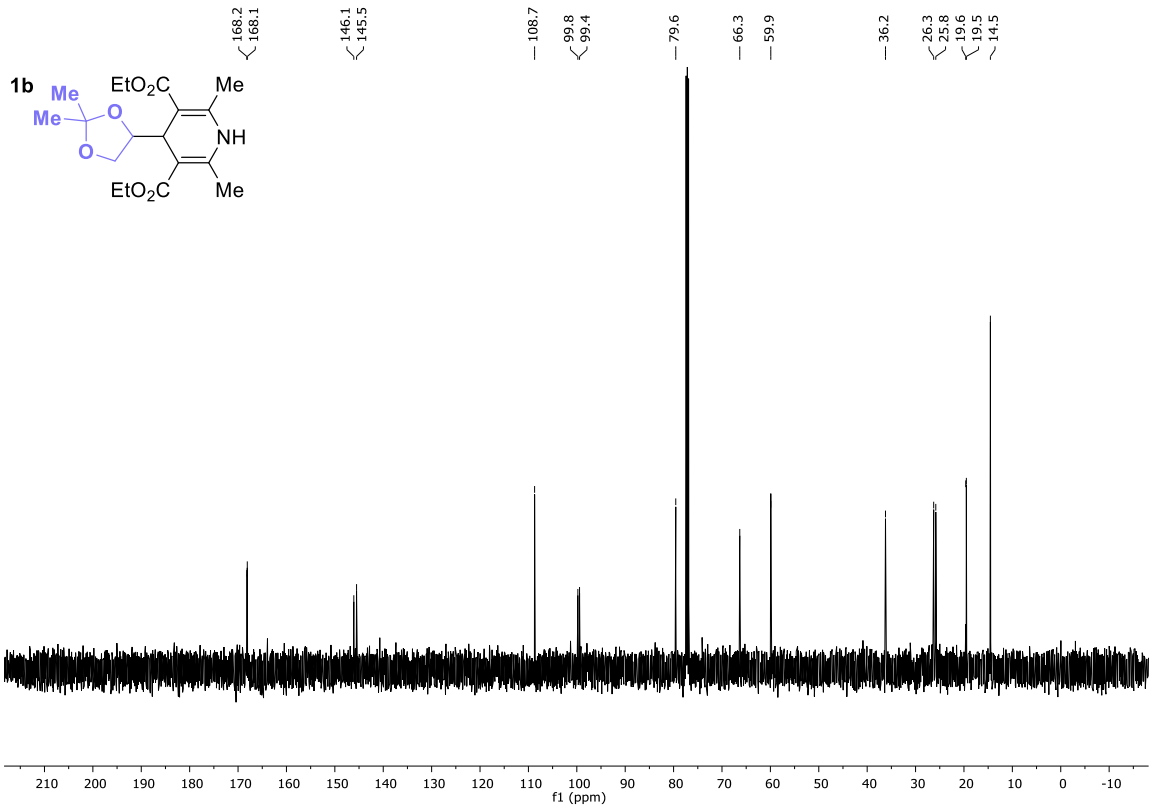

^{1}H NMR ($CDCl_3$, 500 MHz) of diethyl 4-cyclohexyl-2,6-dimethyl-1,4-dihydropyridine-3,5-dicarboxylate (**6.1.3**)

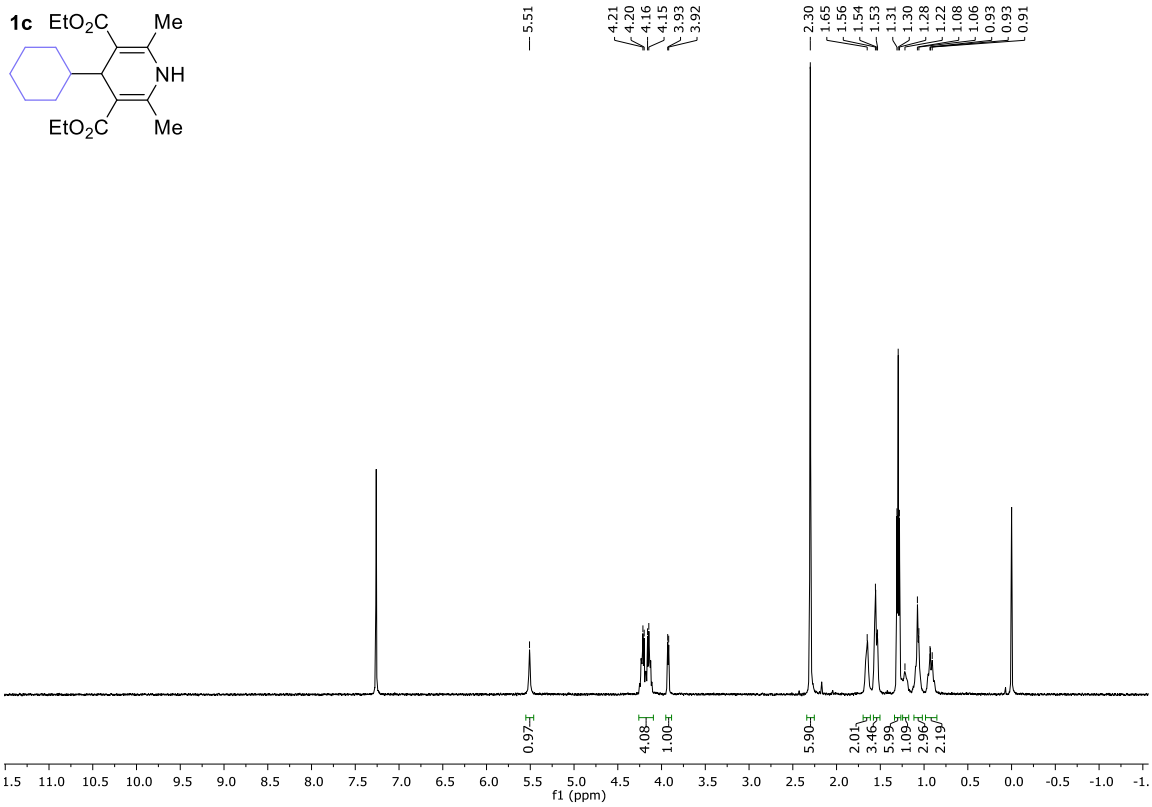

^{13}C NMR ($CDCl_3$, 126 MHz) of diethyl 4-cyclohexyl-2,6-dimethyl-1,4-dihydropyridine-3,5-dicarboxylate (**6.1.3**)

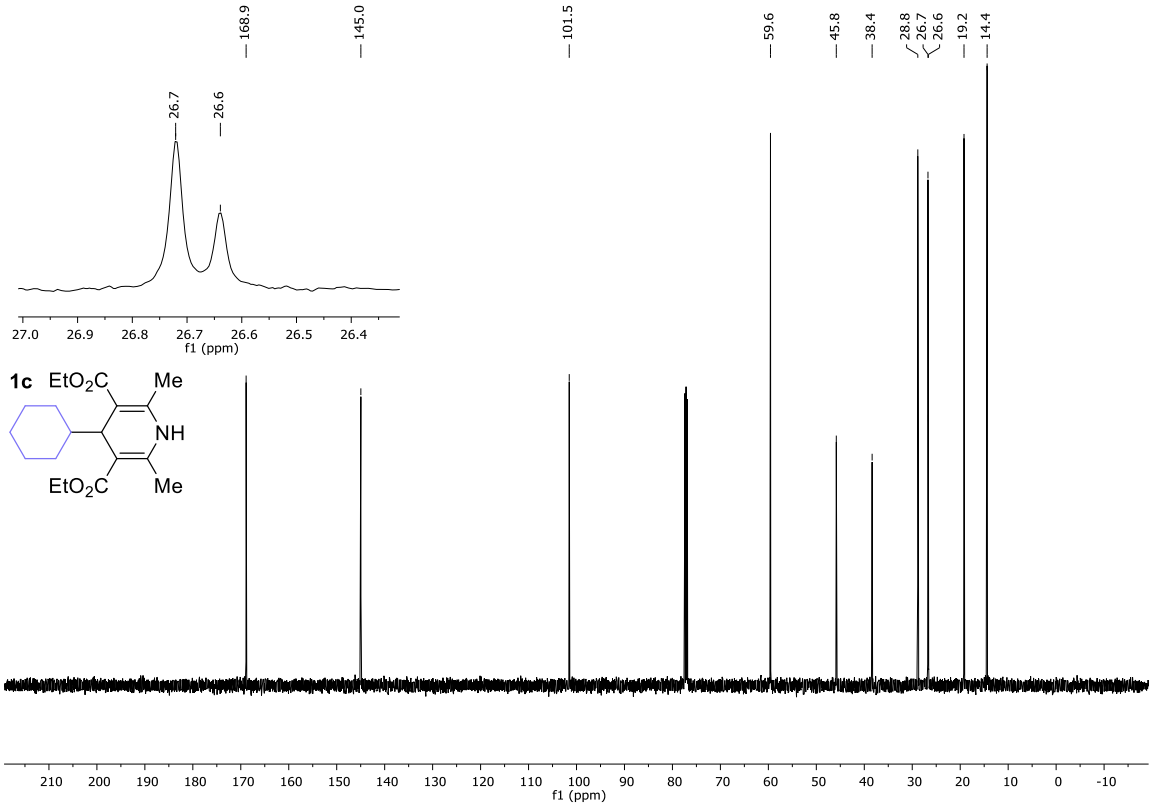

^{1}H NMR ($CDCl_3$, 500 MHz) of diethyl 4-(cyclohex-3-en-1-yl)-2,6-dimethyl-1,4-dihydropyridine-3,5-dicarboxylate (**6.1.4**)

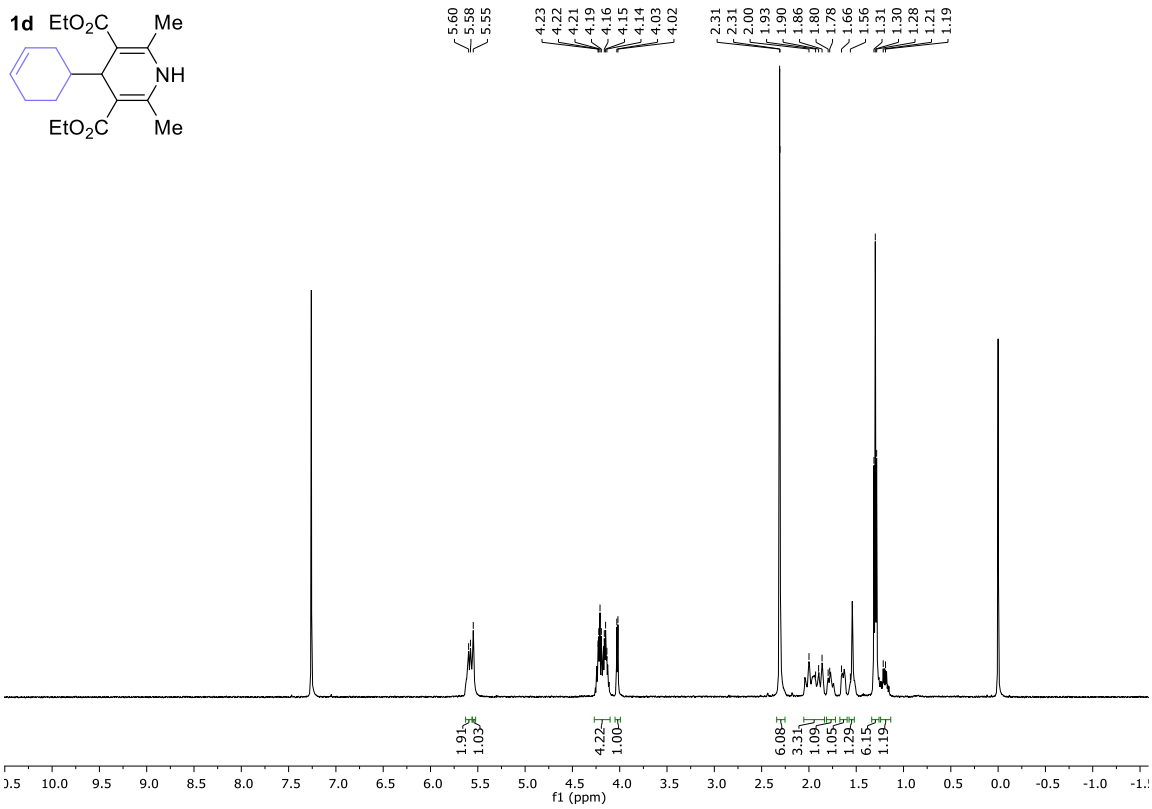

^{13}C NMR ($CDCl_3$, 126 MHz) of diethyl 4-(cyclohex-3-en-1-yl)-2,6-dimethyl-1,4-dihydropyridine-3,5-dicarboxylate (**6.1.4**)

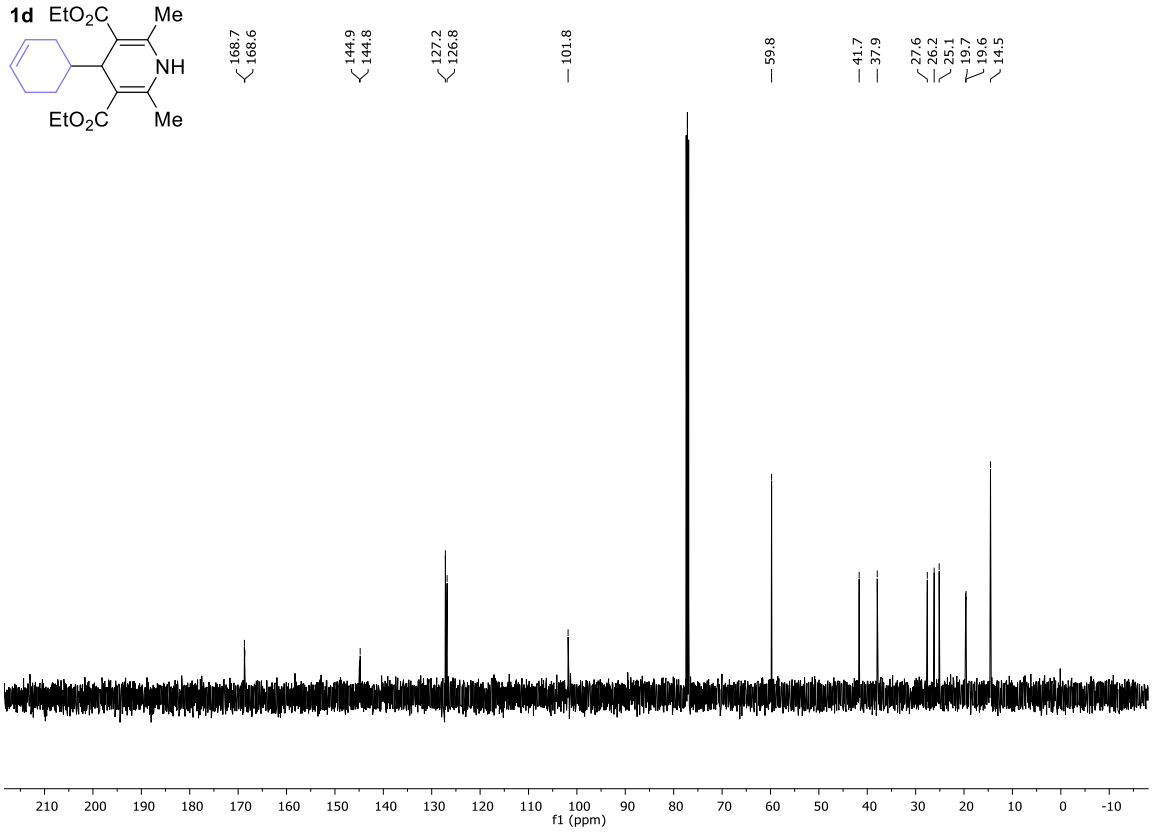

^{1}H NMR ($CDCl_3$, 500 MHz) of diethyl 4-(heptan-3-yl)-2,6-dimethyl-1,4-dihydropyridine-3,5-dicarboxylate (**6.1.5**)

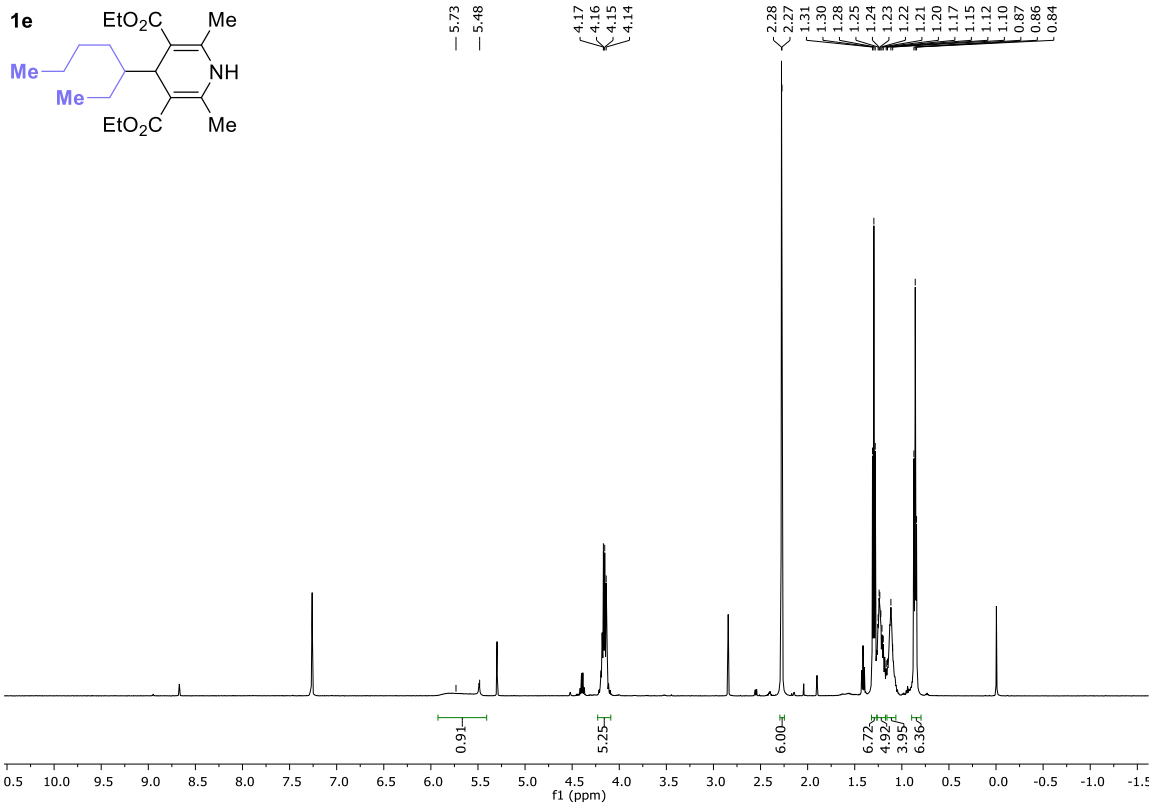

^{13}C NMR ($CDCl_3$, 126 MHz) of diethyl 4-(heptan-3-yl)-2,6-dimethyl-1,4-dihydropyridine-3,5-dicarboxylate (**6.1.5**)

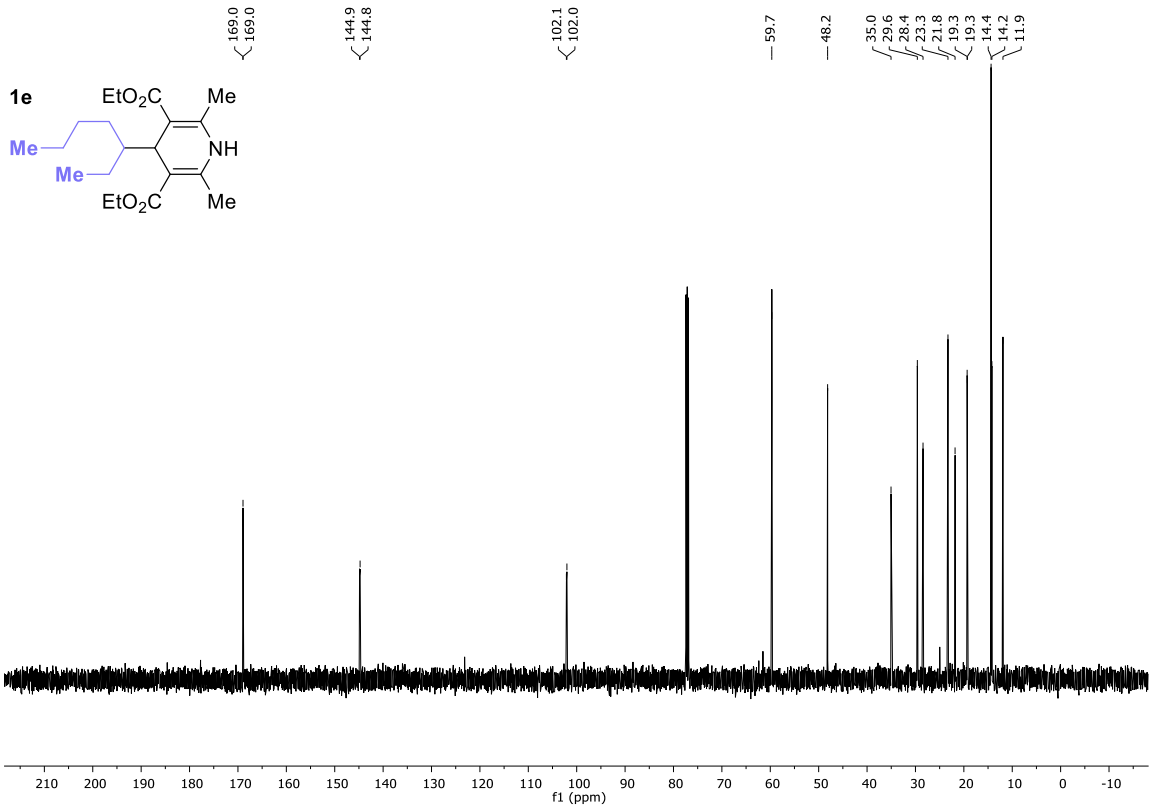

^{1}H NMR ($CDCl_3$, 500 MHz) of diethyl 2,6-dimethyl-4-(7-methyloct-6-en-3-yl)-1,4-dihydropyridine-3,5-dicarboxylate (**6.1.6**)

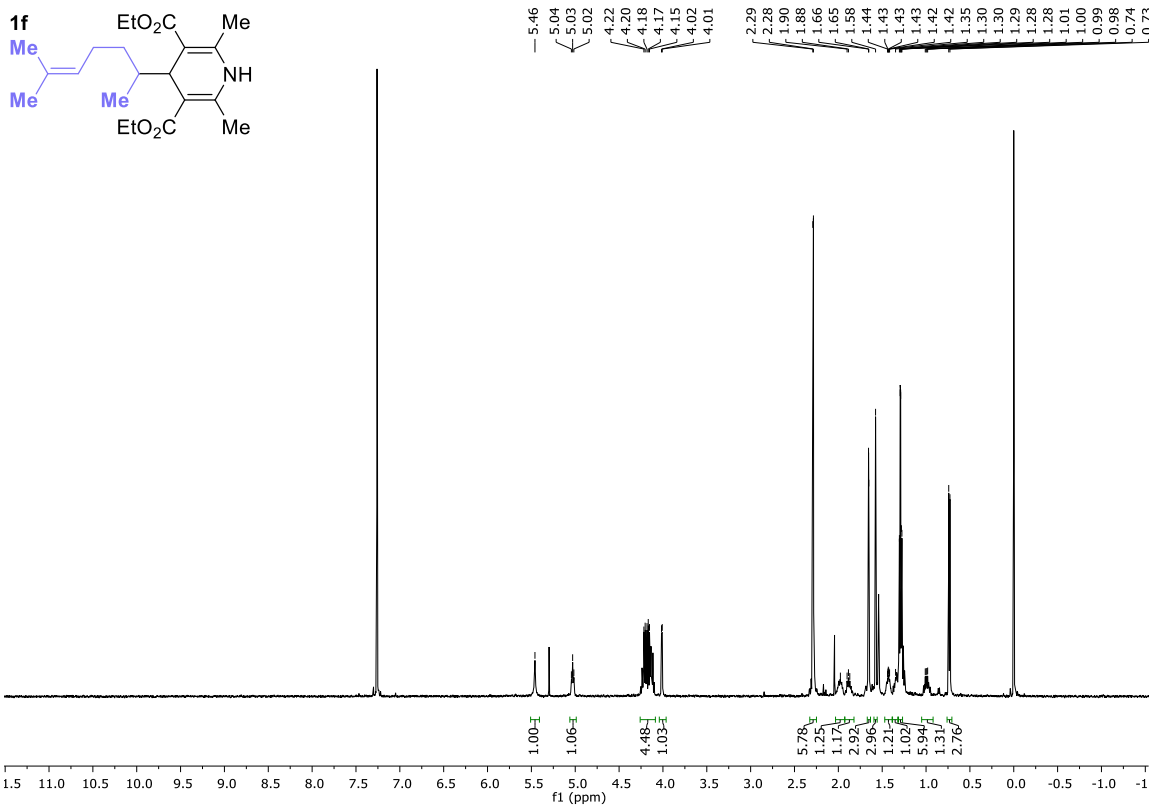

^{13}C NMR ($CDCl_3$, 126 MHz) of diethyl 2,6-dimethyl-4-(7-methyloct-6-en-3-yl)-1,4-dihydropyridine-3,5-dicarboxylate (**6.1.6**)

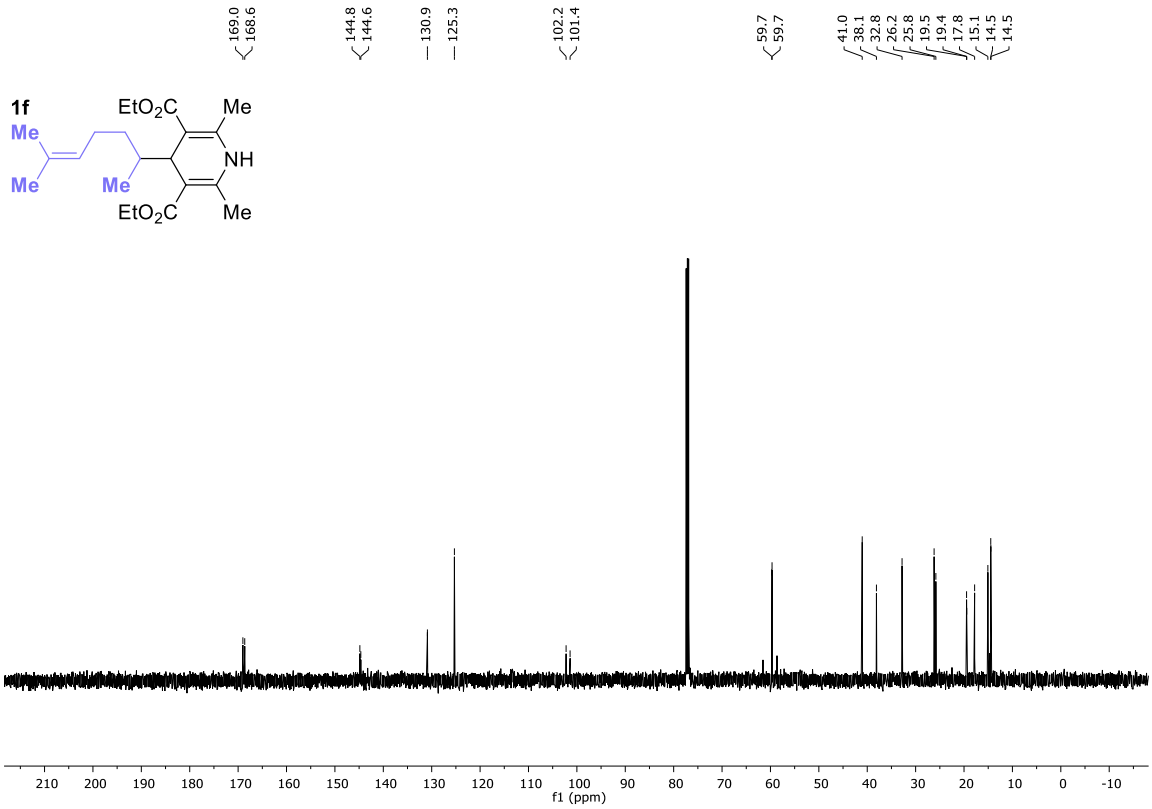

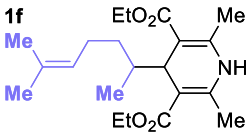

^{1}H NMR ($CDCl_3$, 500 MHz) of diethyl 2,6-dimethyl-4-(tetrahydro-2H-pyran-4-yl)-1,4-dihydropyridine-3,5-dicarboxylate (**6.1.7**)

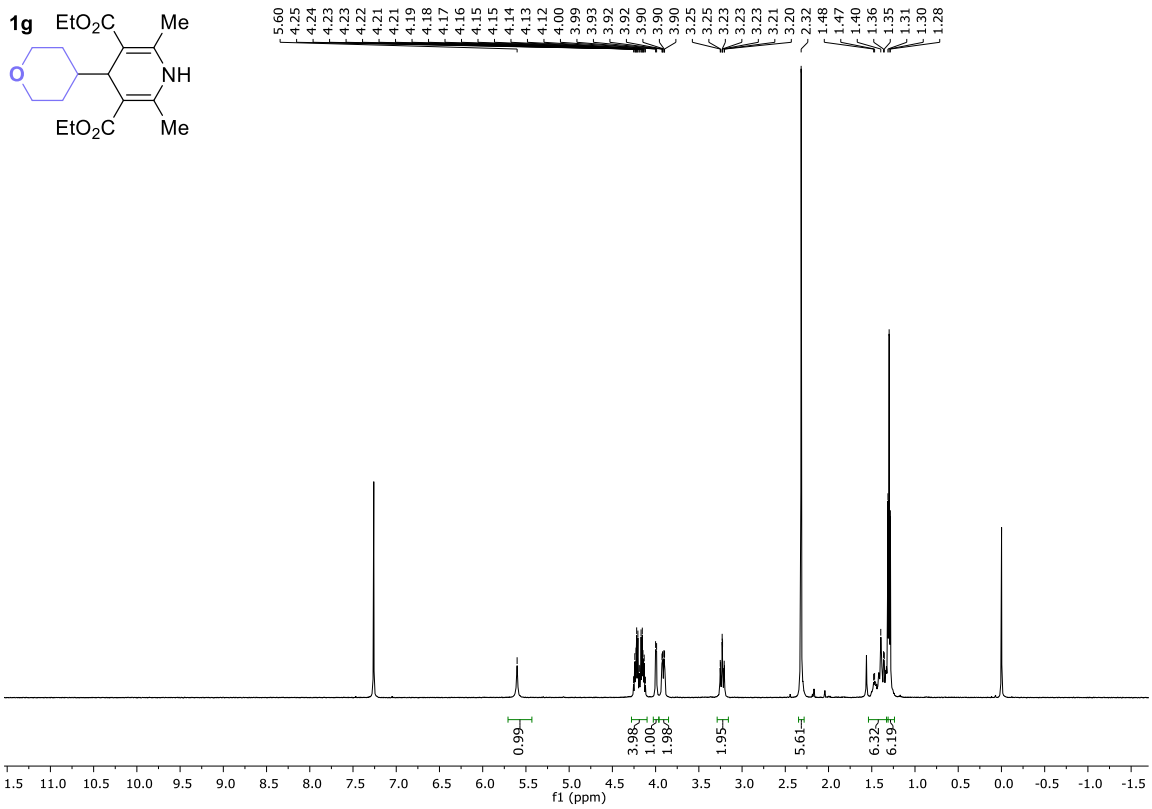

^{13}C NMR ($CDCl_3$, 126 MHz) of diethyl 2,6-dimethyl-4-(tetrahydro-2H-pyran-4-yl)-1,4-dihydropyridine-3,5-dicarboxylate (**6.1.7**)

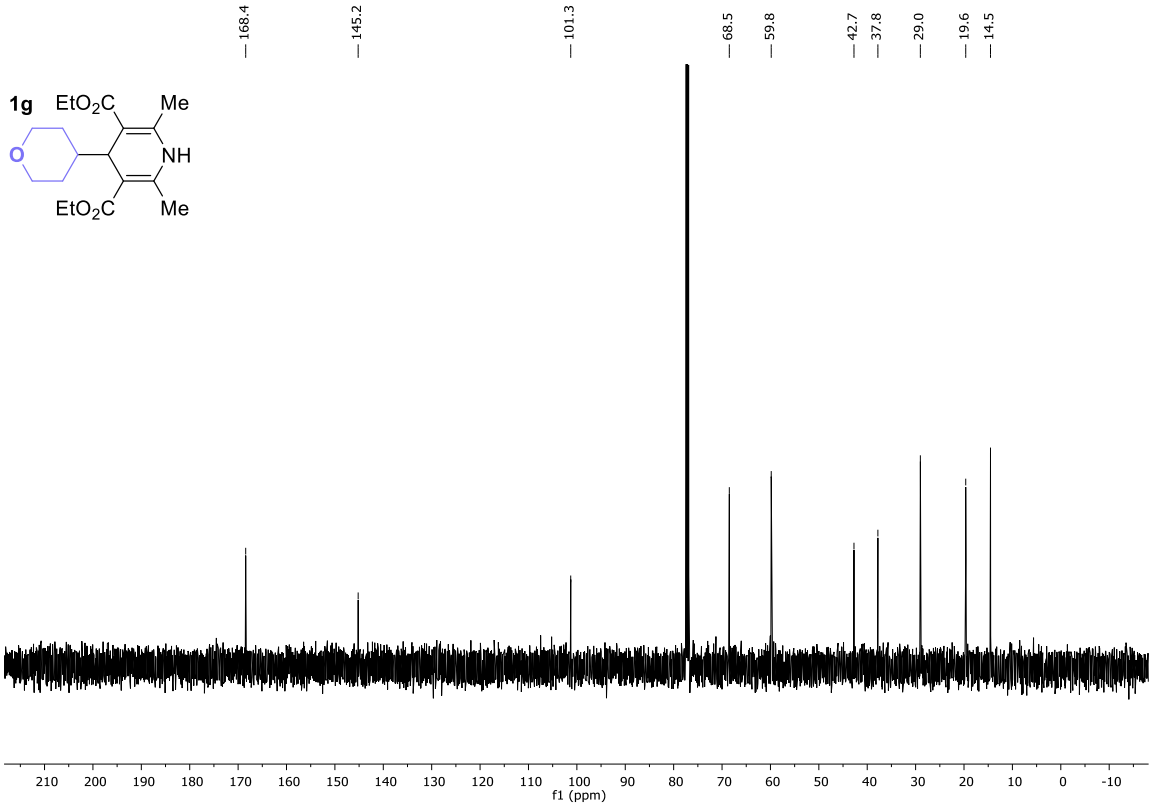

^{1}H NMR ($CDCl_3$, 500 MHz) of diethyl 4-benzyl-2,6-dimethyl-1,4-dihydropyridine-3,5-dicarboxylate (**6.1.8**)

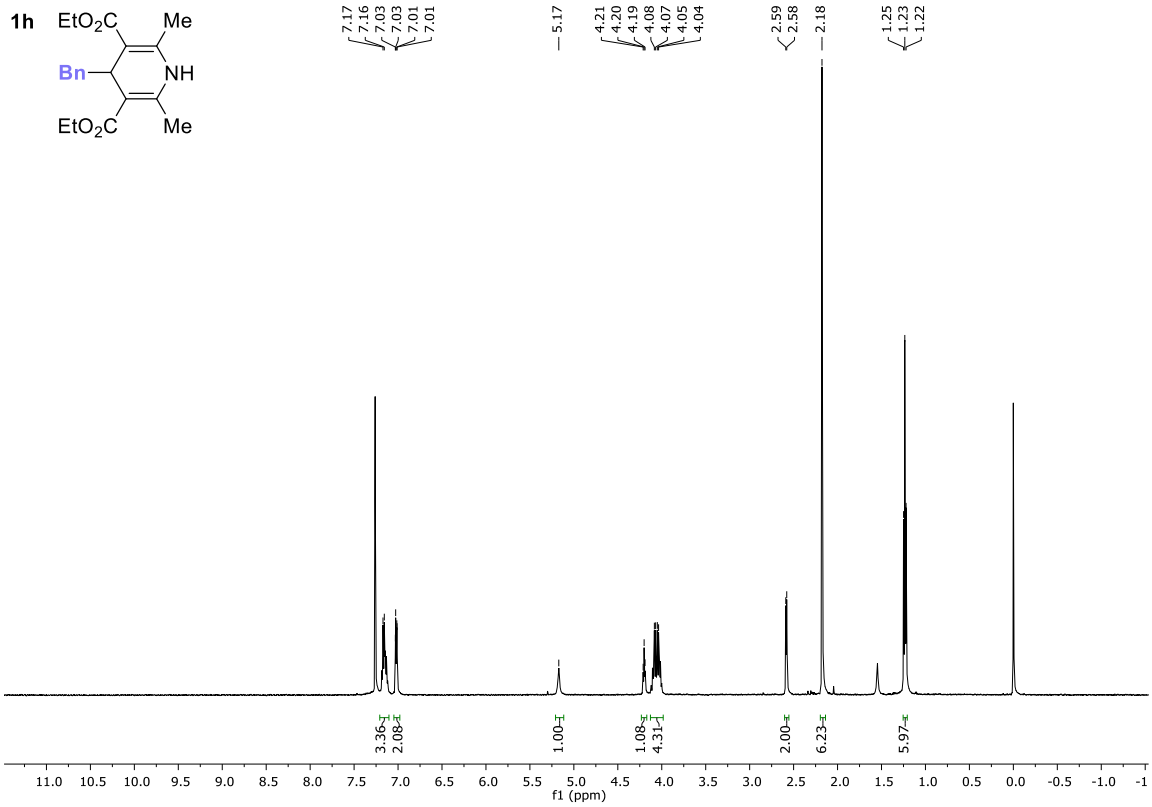

^{13}C NMR ($CDCl_3$, 126 MHz) of diethyl 4-benzyl-2,6-dimethyl-1,4-dihydropyridine-3,5-dicarboxylate (**6.1.8**)

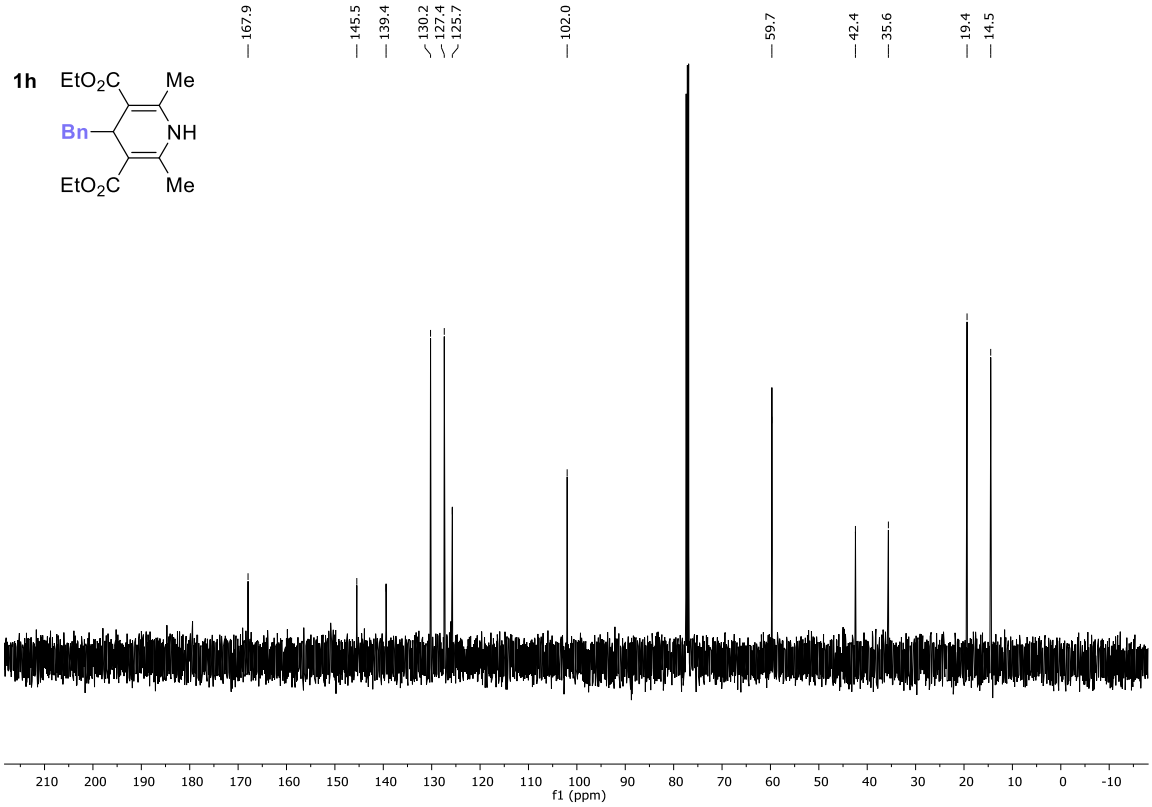

^{1}H NMR ($CDCl_3$, 400 MHz) of diethyl 4-(1-(*tert*-butoxycarbonyl)pyrrolidin-2-yl)-2,6-dimethyl-1,4-dihydropyridine-3,5-dicarboxylate (**6.1.9**)

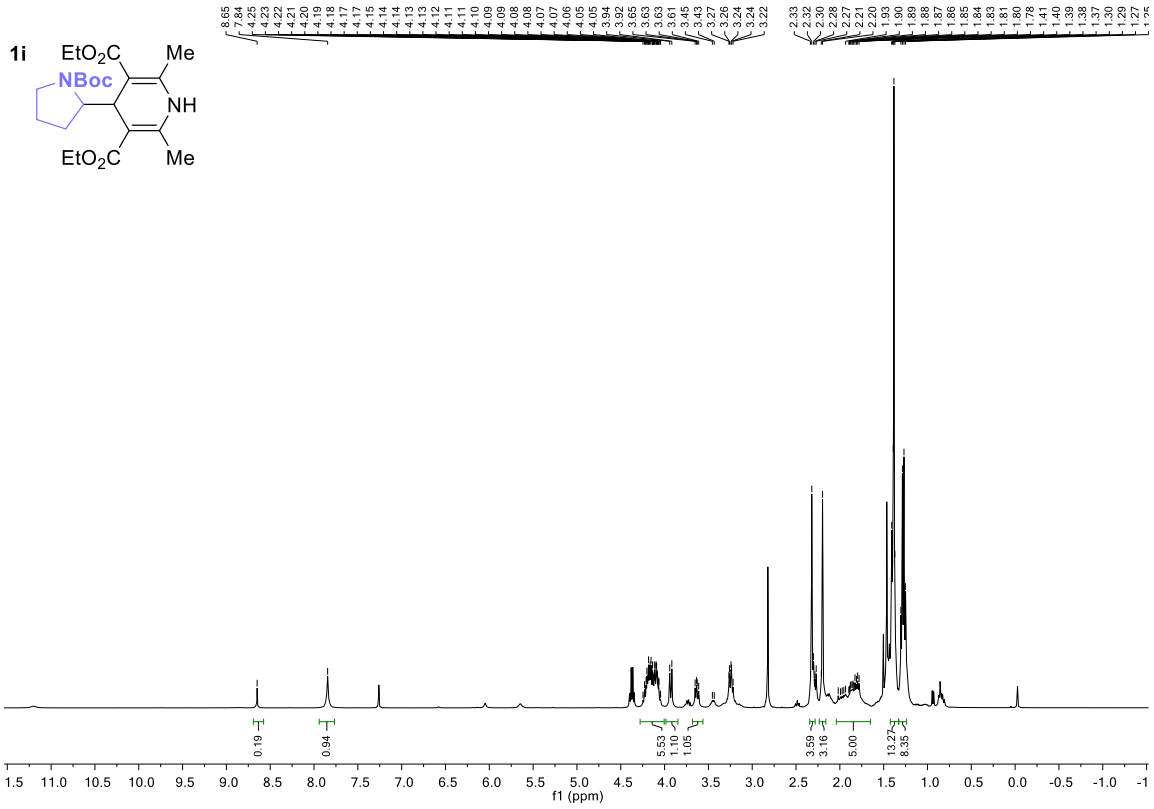

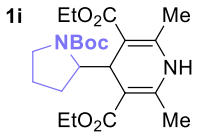

^{13}C NMR ($CDCl_3$, 101 MHz) of diethyl 4-(1-(*tert*-butoxycarbonyl)pyrrolidin-2-yl)-2,6-dimethyl-1,4-dihydropyridine-3,5-dicarboxylate (**6.1.9**)

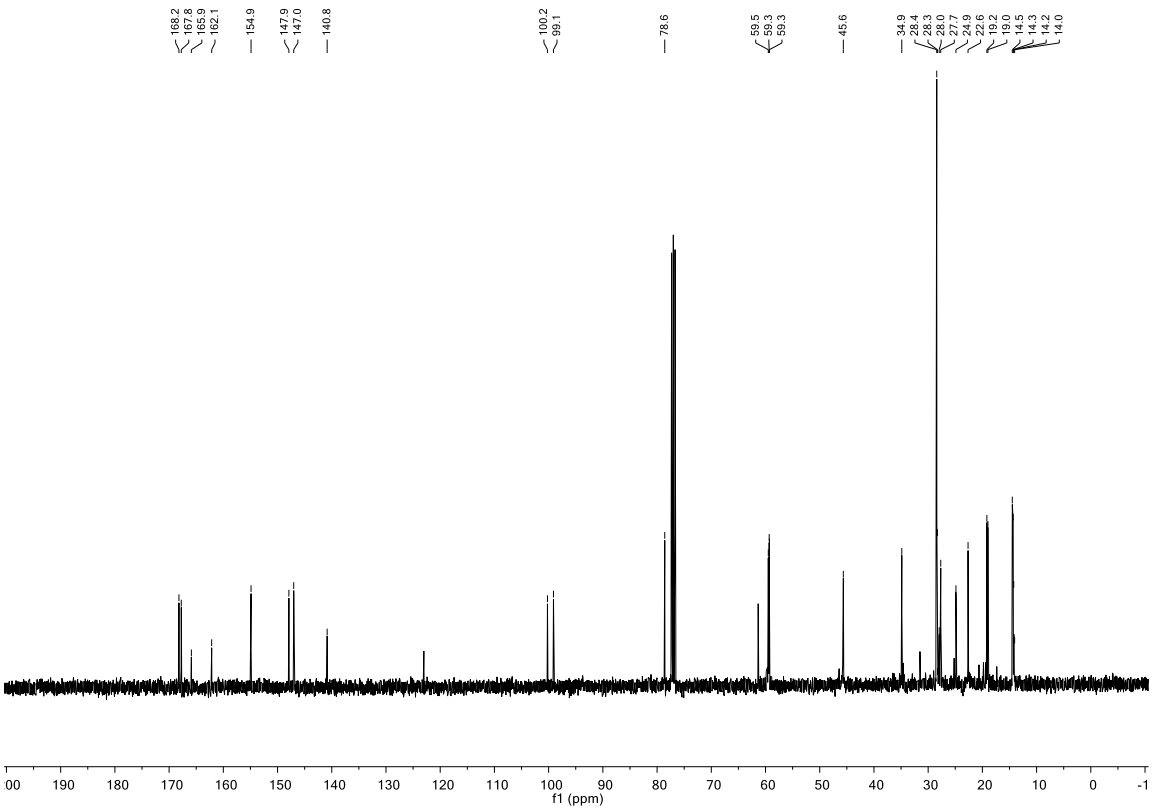

^{1}H NMR ($CDCl_3$, 500 MHz) of diethyl 4-(3-(*tert*-butoxycarbonyl)-2,2-dimethyloxazolidin-4-yl)-2,6-dimethyl-1,4-dihydropyridine-3,5-dicarboxylate (**6.1.10**)

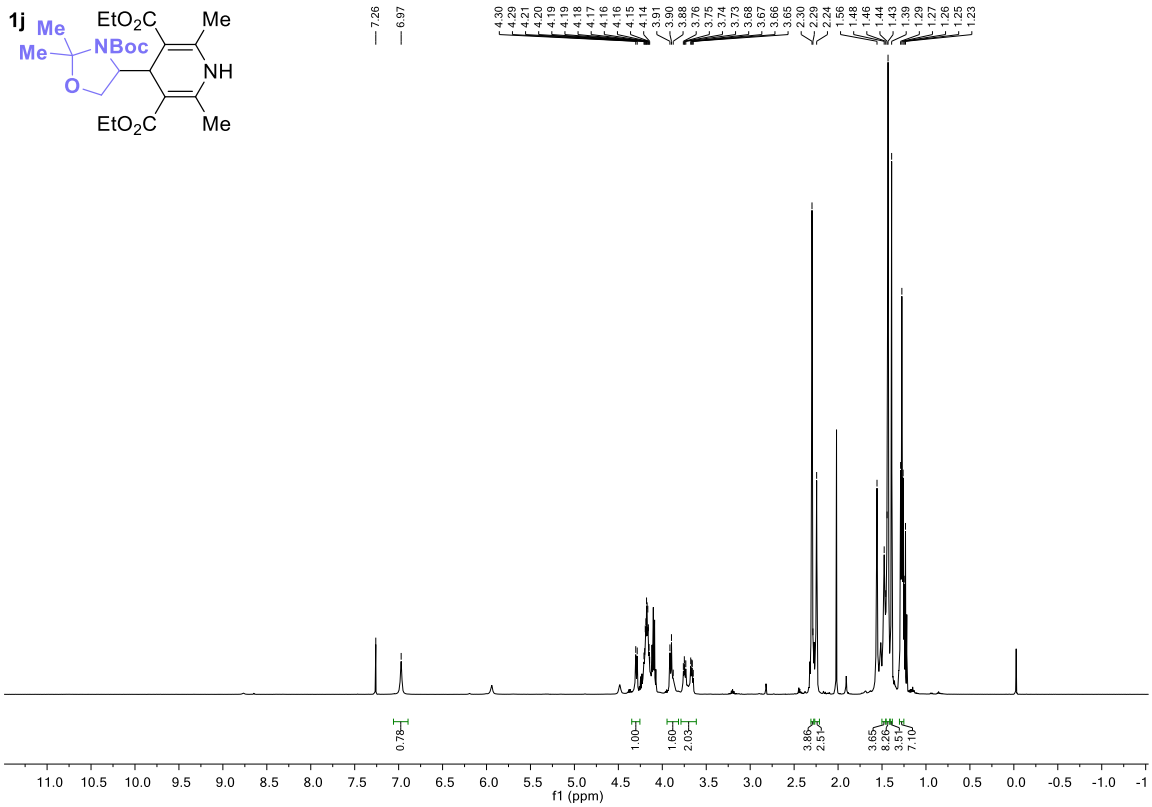

^{13}C NMR ($CDCl_3$, 126 MHz) of diethyl 4-(3-(*tert*-butoxycarbonyl)-2,2-dimethyloxazolidin-4-yl)-2,6-dimethyl-1,4-dihydropyridine-3,5-dicarboxylate (**6.1.10**)

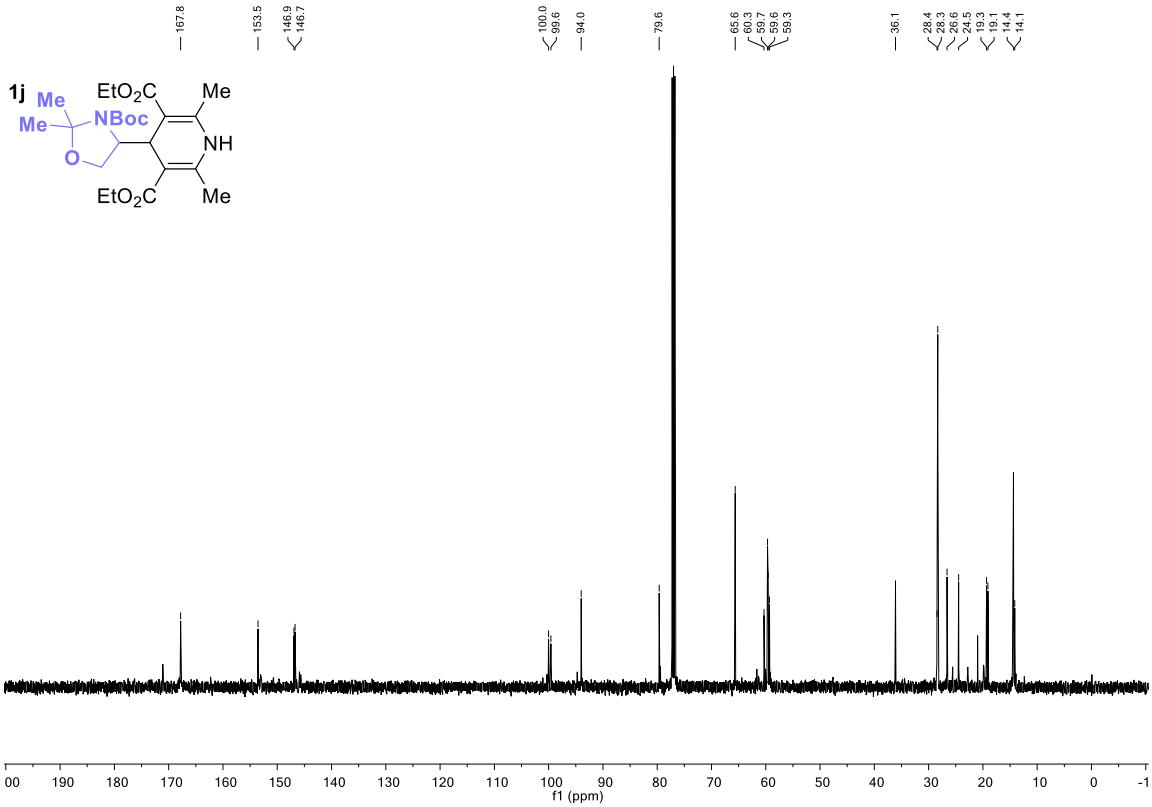

^{1}H NMR (DMSO-d_6, 400 MHz) of diethyl 4-(1-((*tert*-butoxycarbonyl)amino)-2-phenylethyl)-2,6-dimethyl-1,4-dihydropyridine-3,5-dicarboxylate (**6.1.11**)

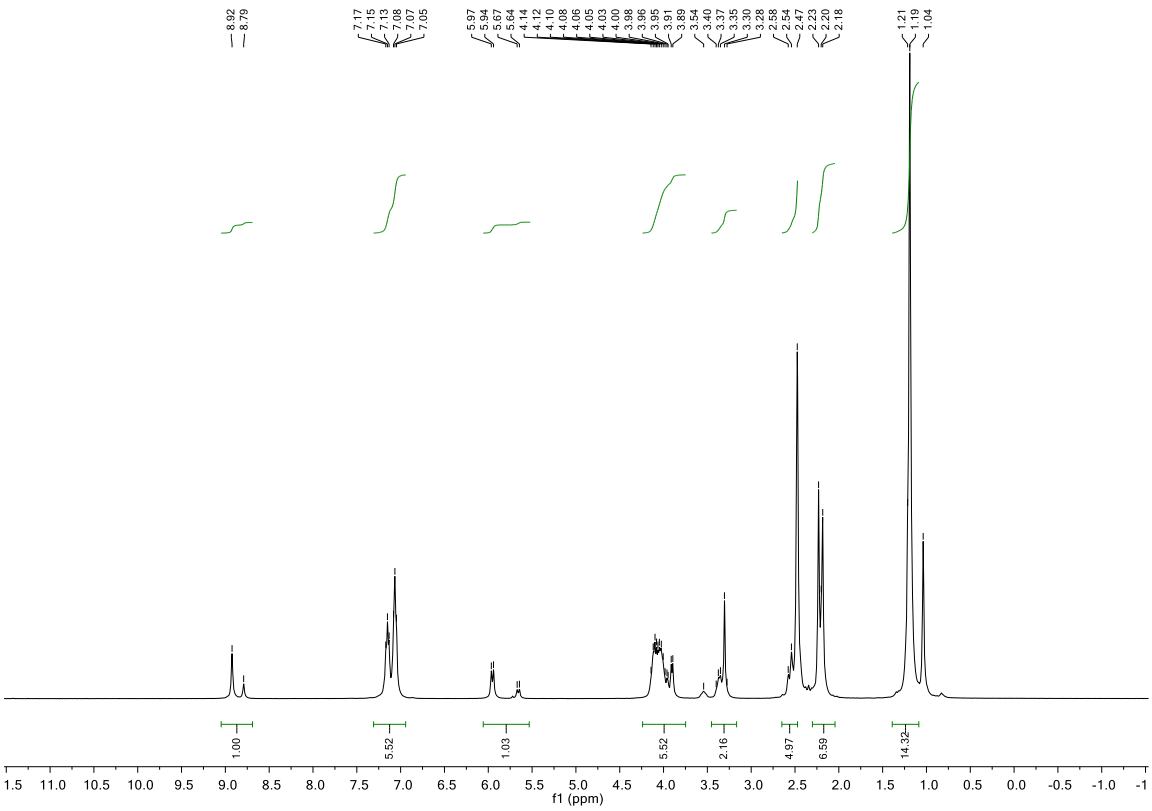

^{13}C NMR (DMSO-d_6, 101 MHz) of diethyl 4-(1-((*tert*-butoxycarbonyl)amino)-2-phenylethyl)-2,6-dimethyl-1,4-dihydropyridine-3,5-dicarboxylate (**6.1.11**)

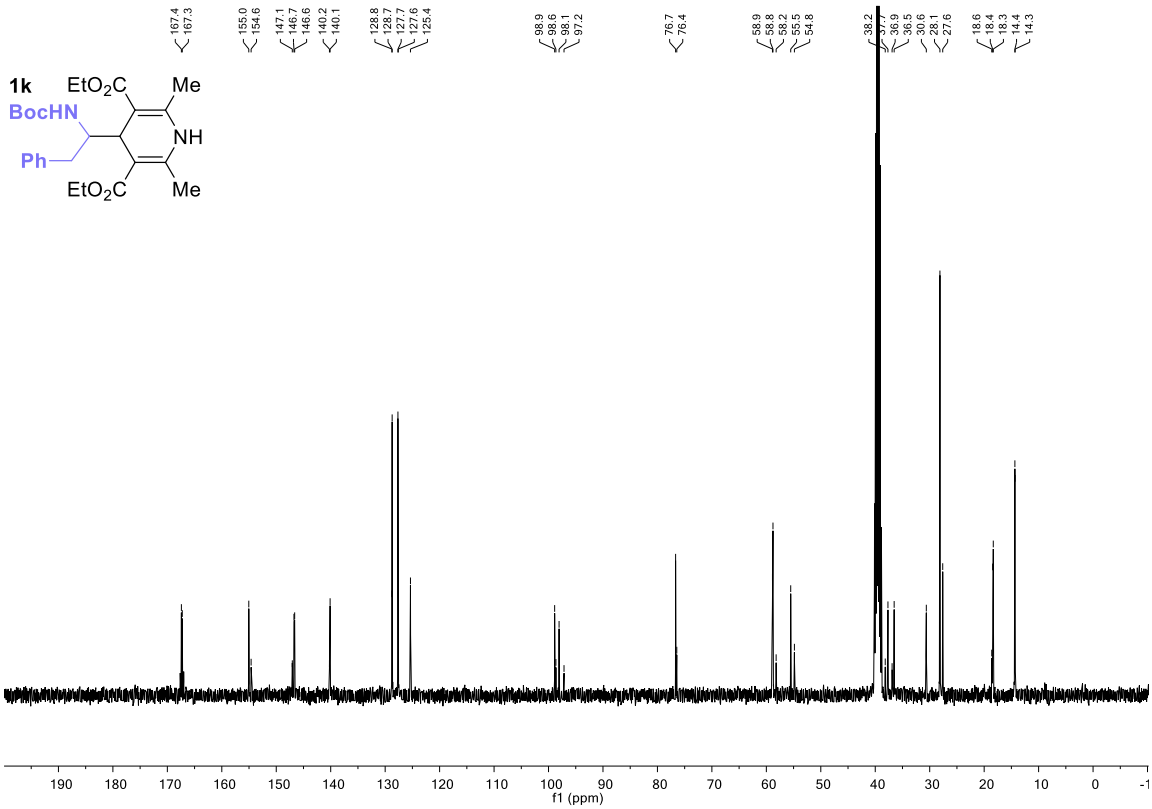

^{1}H NMR ($CDCl_3$, 500 MHz) of diethyl 2,6-dimethyl-4-((3a*R*,5*R*,5a*S*,8a*S*,8b*R*)-2,2,7,7-tetramethyltetrahydro-5H-bis([1,3]dioxolo)[4,5-b:4',5'-d]pyran-5-yl)-1,4-dihydropyridine-3,5-dicarboxylate (**6.1.12**)

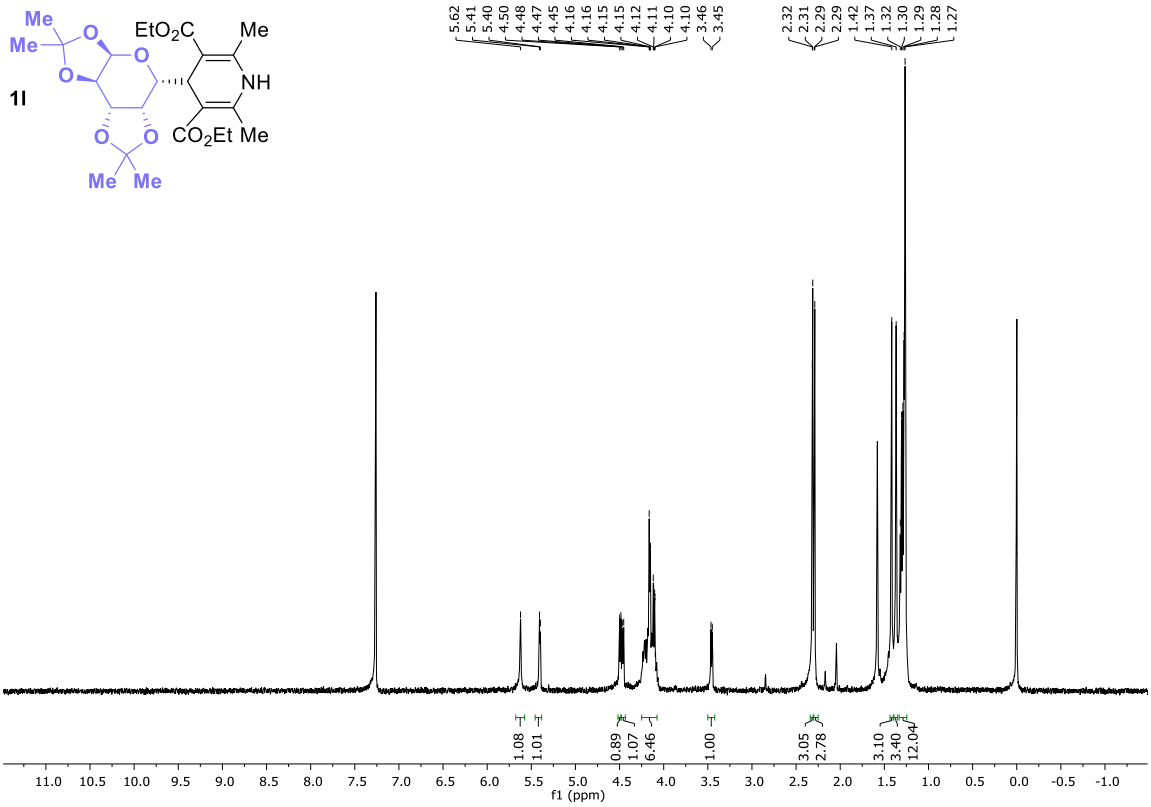

^{13}C NMR ($CDCl_3$, 126 MHz) of diethyl 2,6-dimethyl-4-((3a*R*,5*R*,5a*S*,8a*S*,8b*R*)-2,2,7,7-tetramethyltetrahydro-5H-bis([1,3]dioxolo)[4,5-b:4',5'-d]pyran-5-yl)-1,4-dihydropyridine-3,5-dicarboxylate (**6.1.12**)

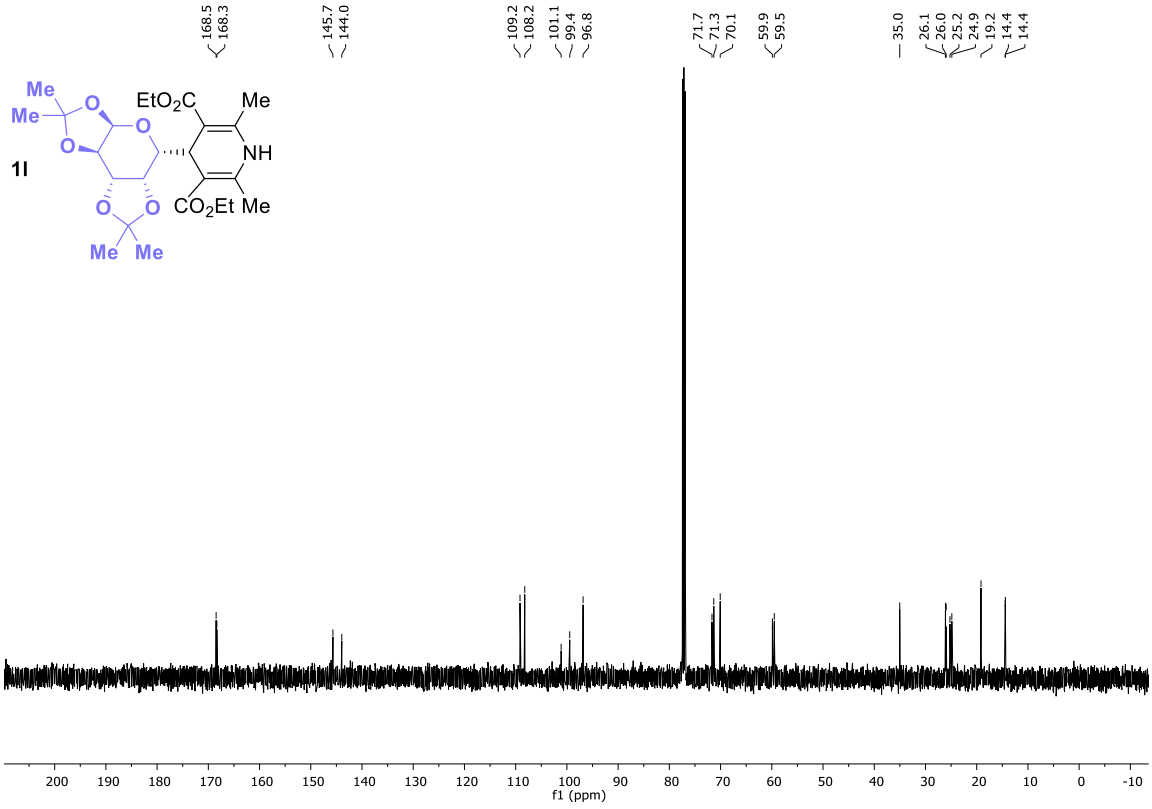

^{1}H NMR ($CDCl_3$, 500 MHz) of 4-isopropyl-2,6-dimethyl-1,4-dihydropyridine-3,5-dicarbonitrile (**6.3.1**)

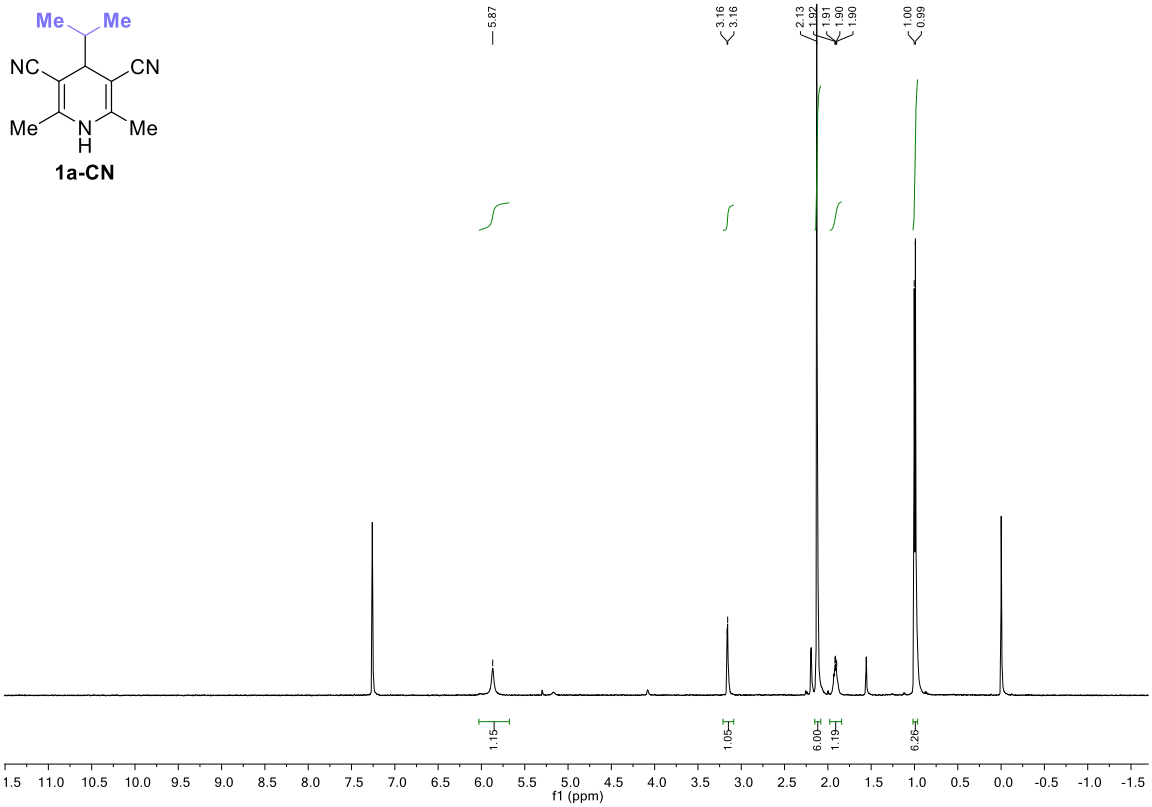

^{13}C NMR ($CDCl_3$, 126 MHz) of 4-isopropyl-2,6-dimethyl-1,4-dihydropyridine-3,5-dicarbonitrile (**6.3.2**)

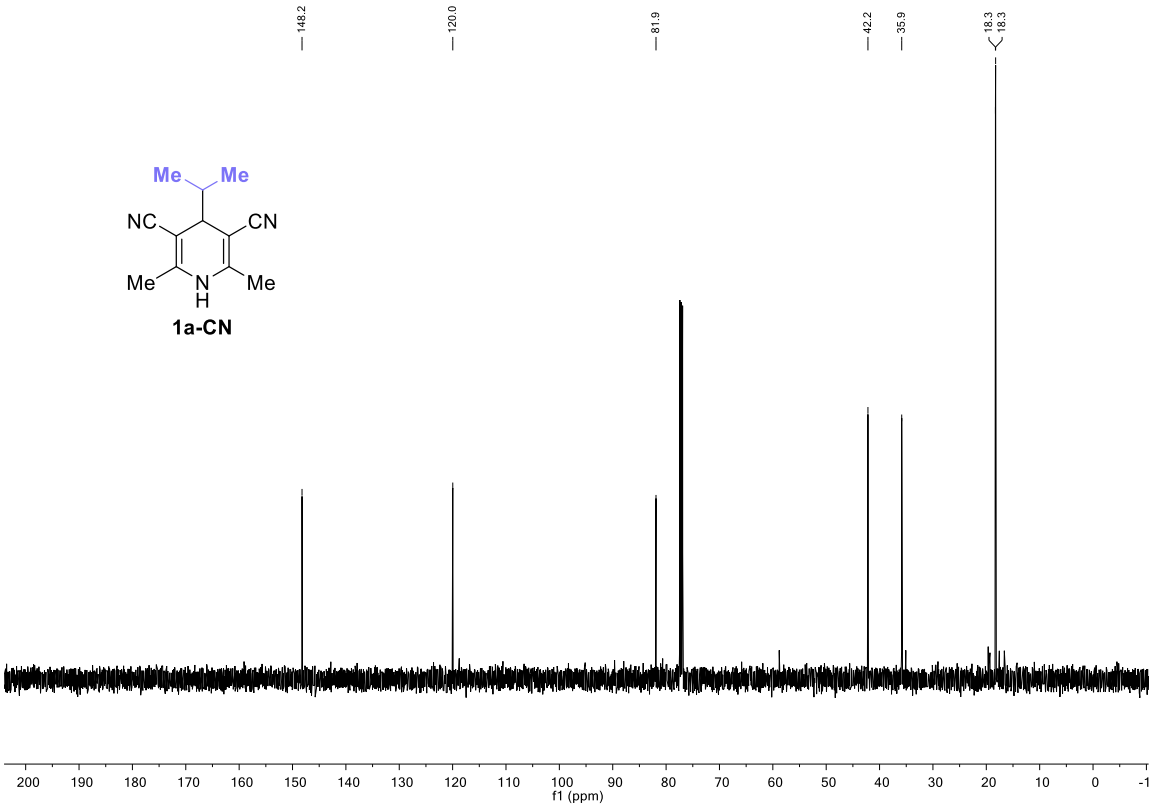

^{1}H NMR ($CDCl_3$, 500 MHz) of 4-isopropylbenzonitrile (**6.2.1**)

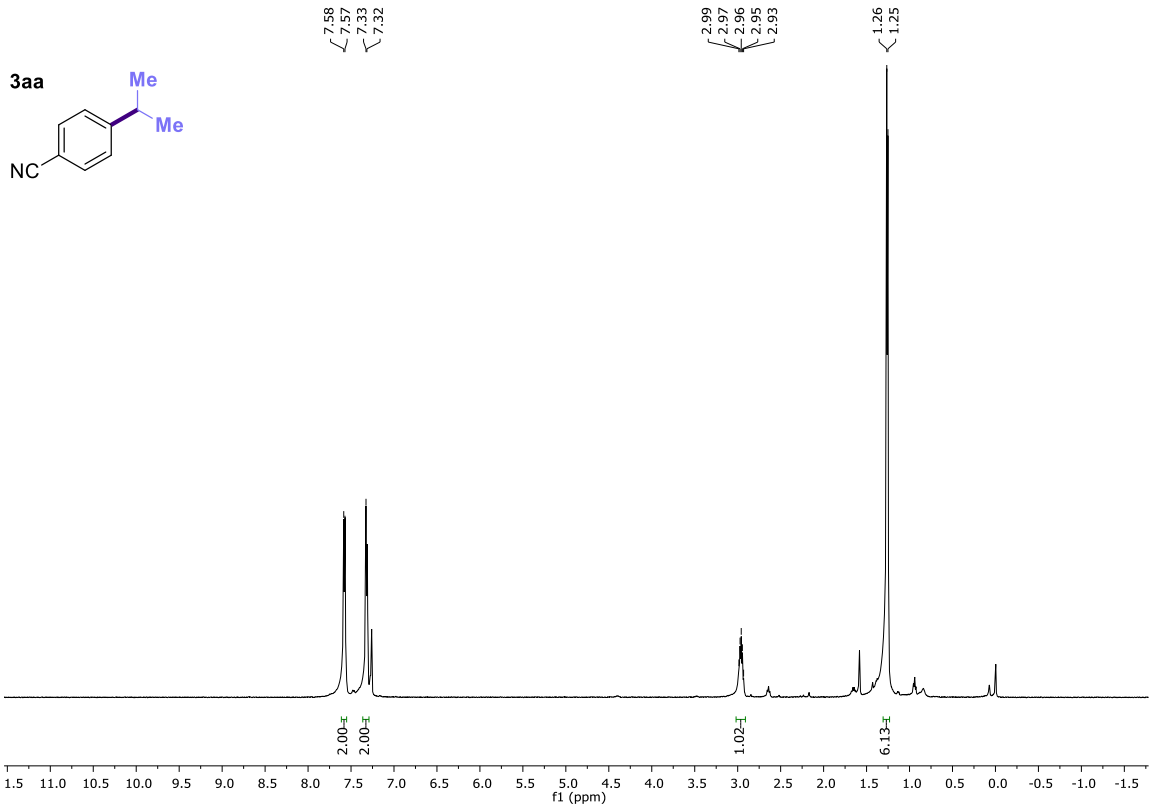

^{13}C NMR ($CDCl_3$, 126 MHz) of 4-isopropylbenzonitrile (**6.2.1**)

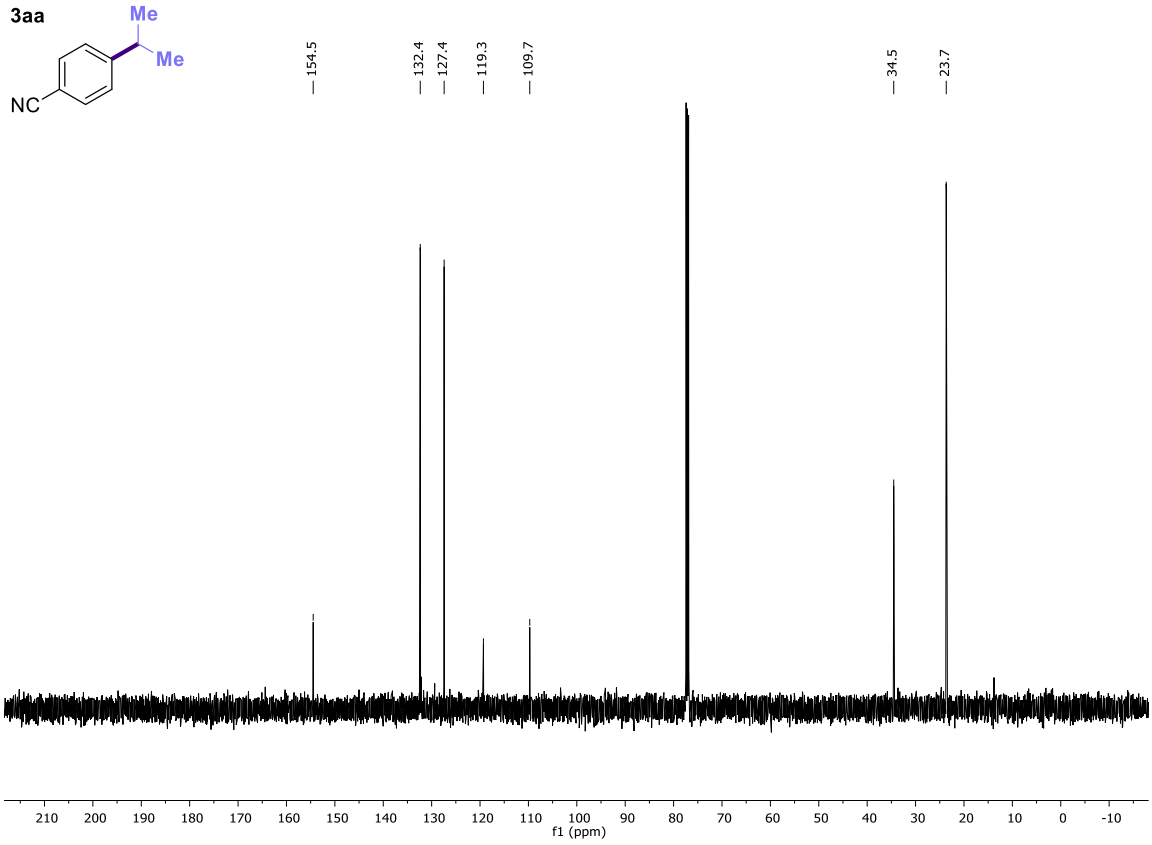

^{1}H NMR ($CDCl_3$, 500 MHz) of 2,2-dimethyl-4-(4-(trifluoromethyl)phenyl)-1,3-dioxolane (**6.3.1**)

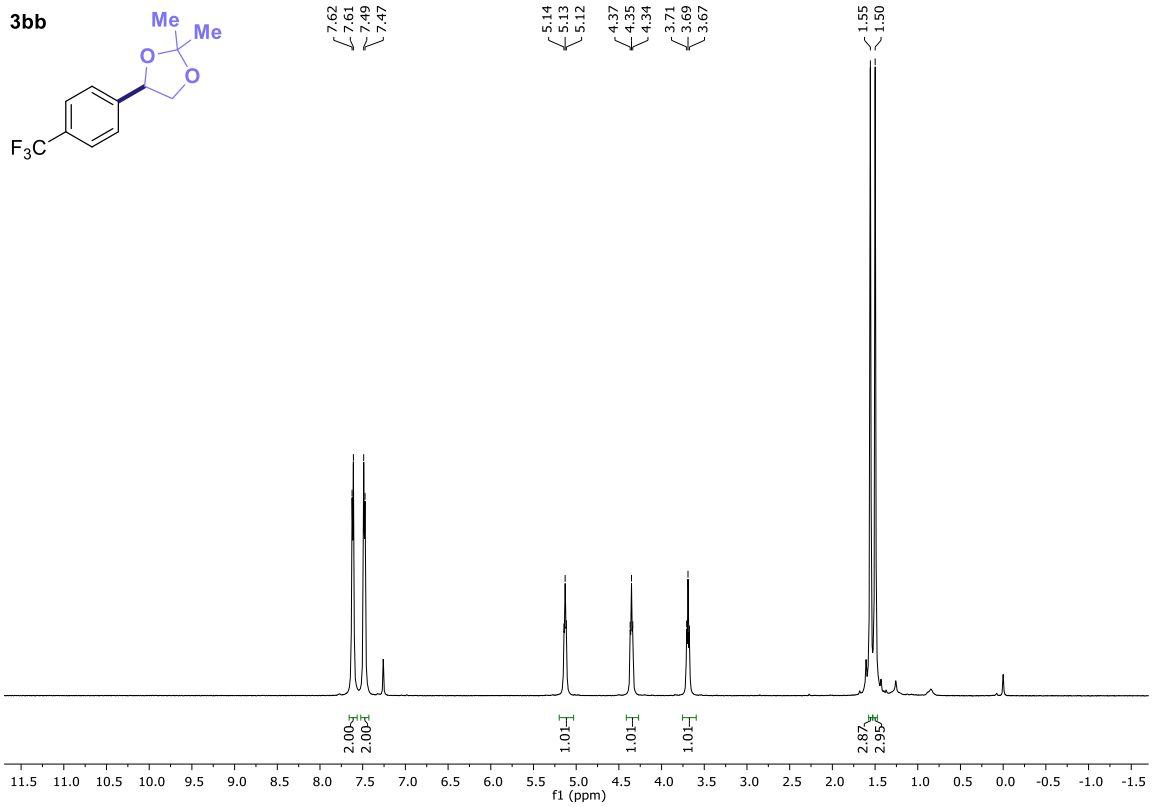

^{13}C NMR ($CDCl_3$, 126 MHz) of 2,2-dimethyl-4-(4-(trifluoromethyl)phenyl)-1,3-dioxolane (**6.3.1**)

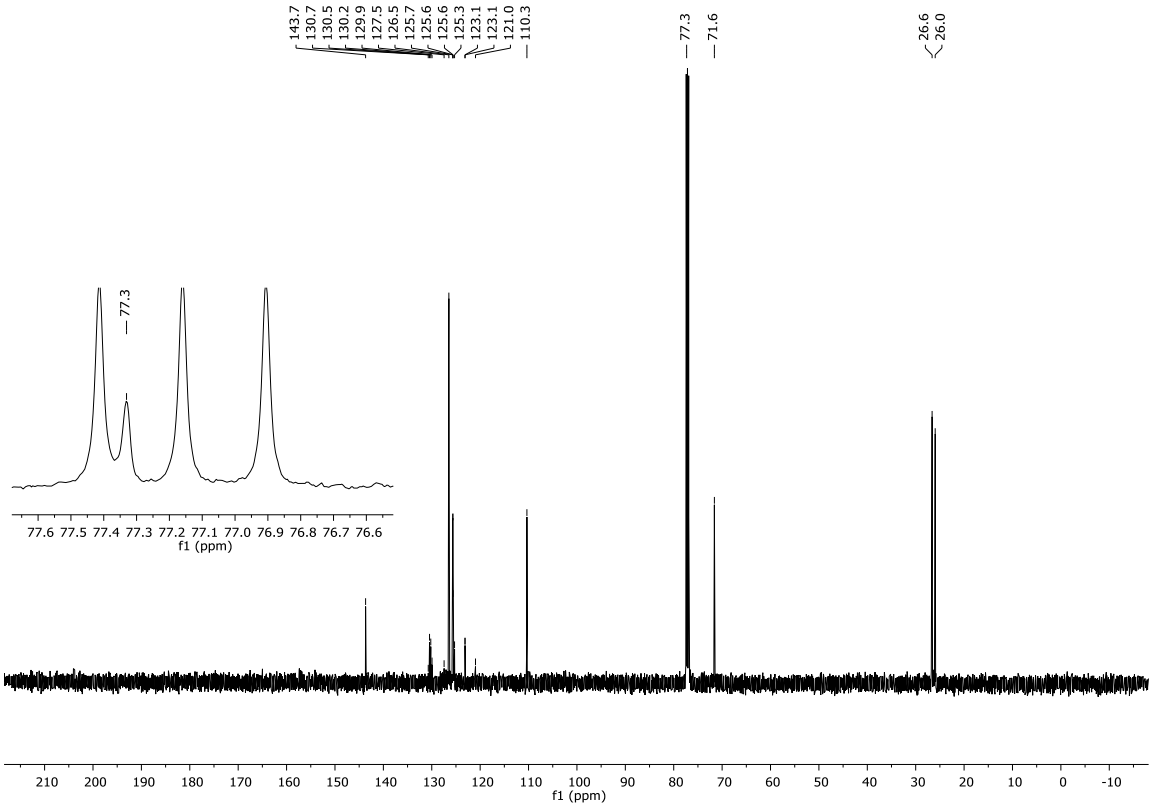

^{1}H NMR ($CDCl_3$, 500 MHz) of 2,2-dimethyl-4-(naphthalen-2-yl)-1,3-dioxolane (**6.3.1**)

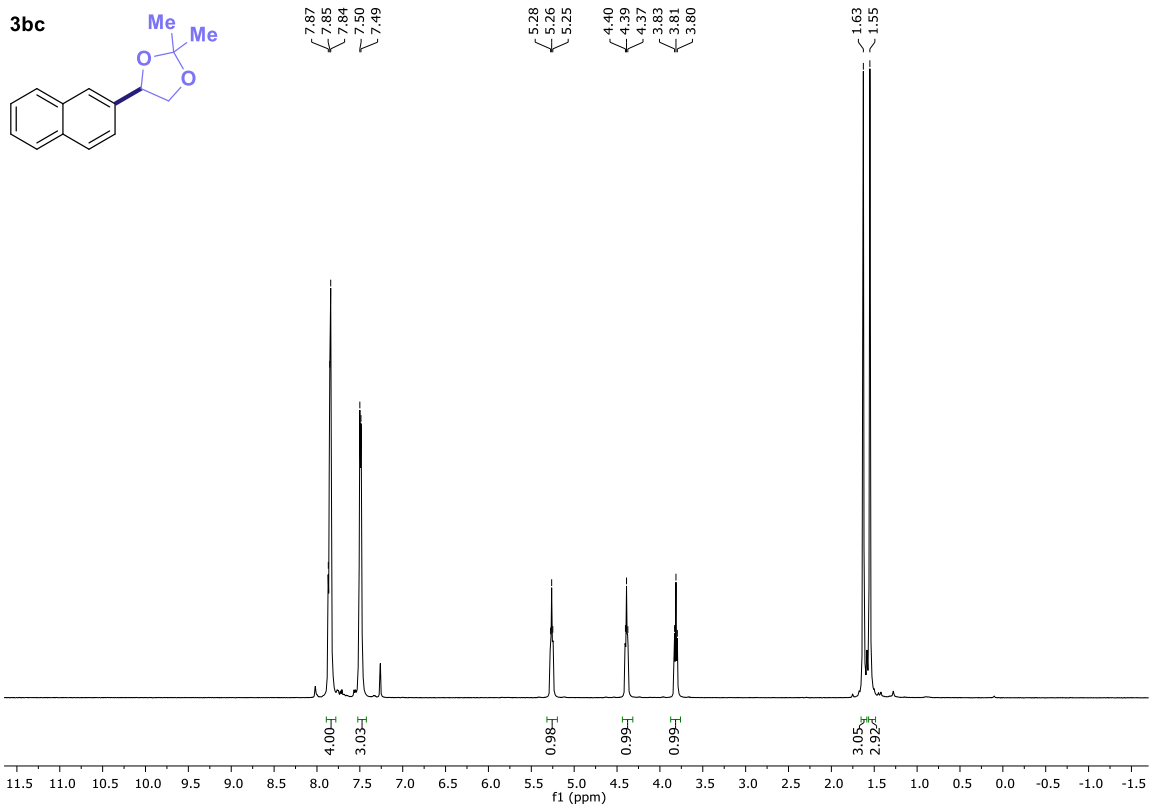

^{13}C NMR ($CDCl_3$, 126 MHz) of 2,2-dimethyl-4-(naphthalen-2-yl)-1,3-dioxolane (**6.3.2**)

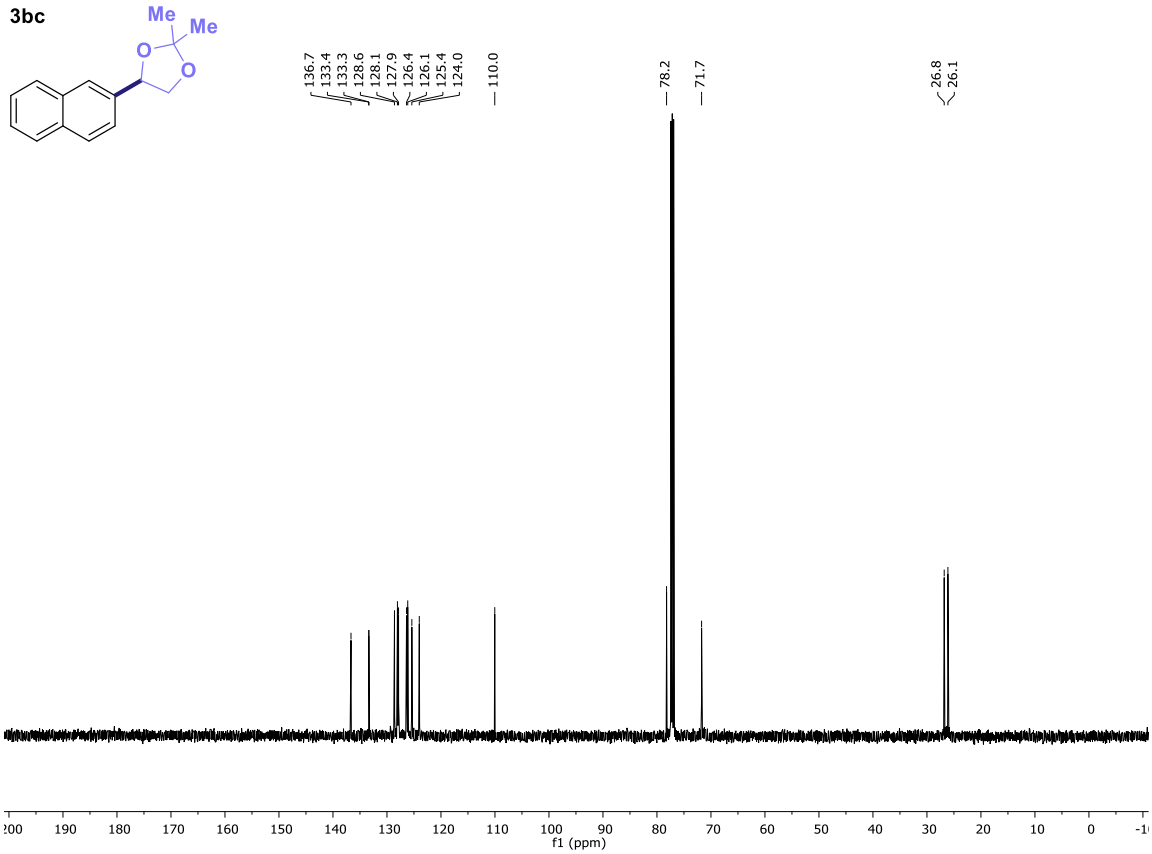

^{1}H NMR ($CDCl_3$, 500 MHz) of 2-(2,2-dimethyl-1,3-dioxolan-4-yl)-5-(trifluoromethyl)pyridine (**6.3.3**)

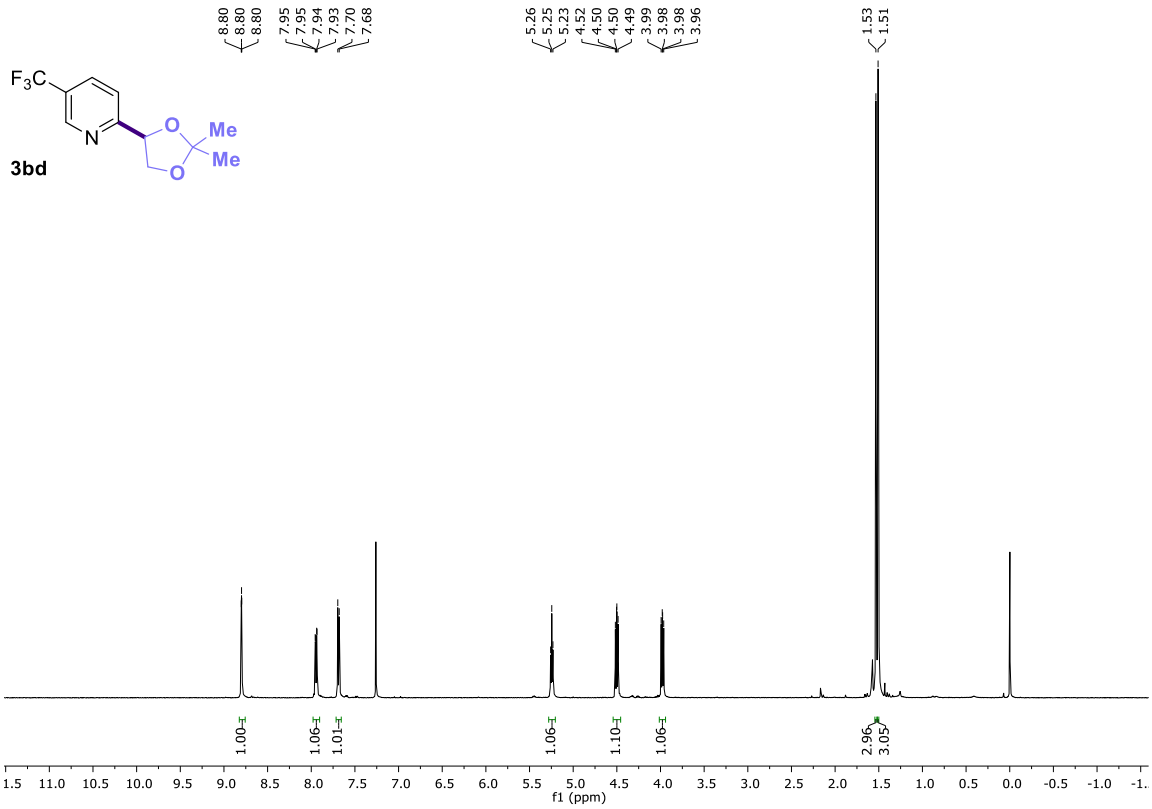

^{13}C NMR ($CDCl_3$, 126 MHz) of 2-(2,2-dimethyl-1,3-dioxolan-4-yl)-5-(trifluoromethyl)pyridine (**6.3.3**)

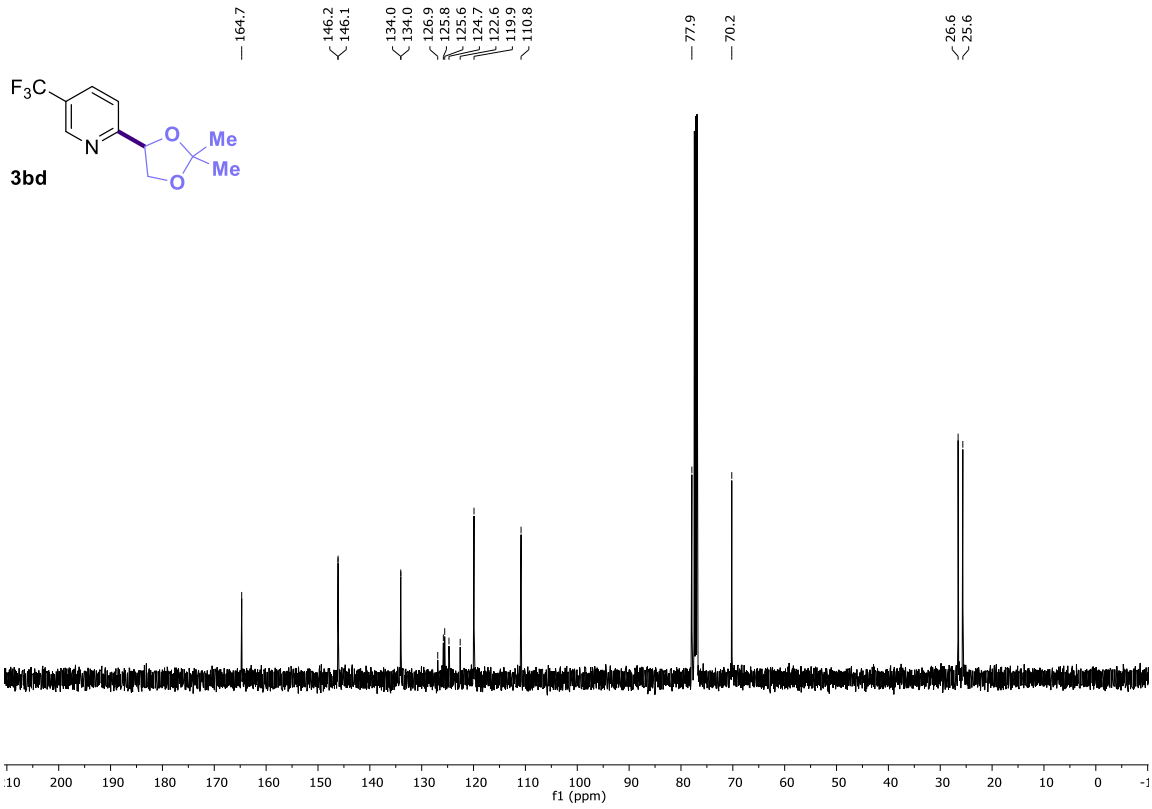

^{1}H NMR ($CDCl_3$, 500 MHz) of 2-(2,2-dimethyl-1,3-dioxolan-4-yl)thiazole (**6.3.4**)

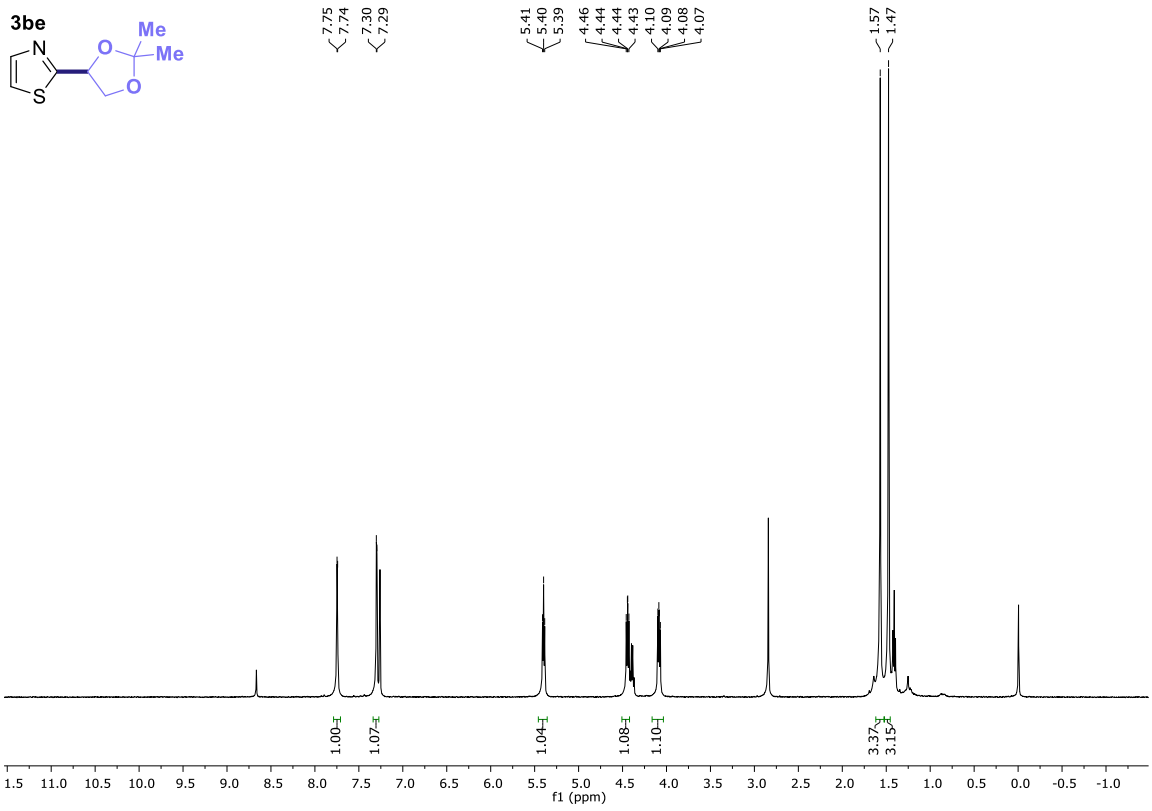

^{13}C NMR ($CDCl_3$, 126 MHz) of 2-(2,2-dimethyl-1,3-dioxolan-4-yl)thiazole (**6.3.4**)

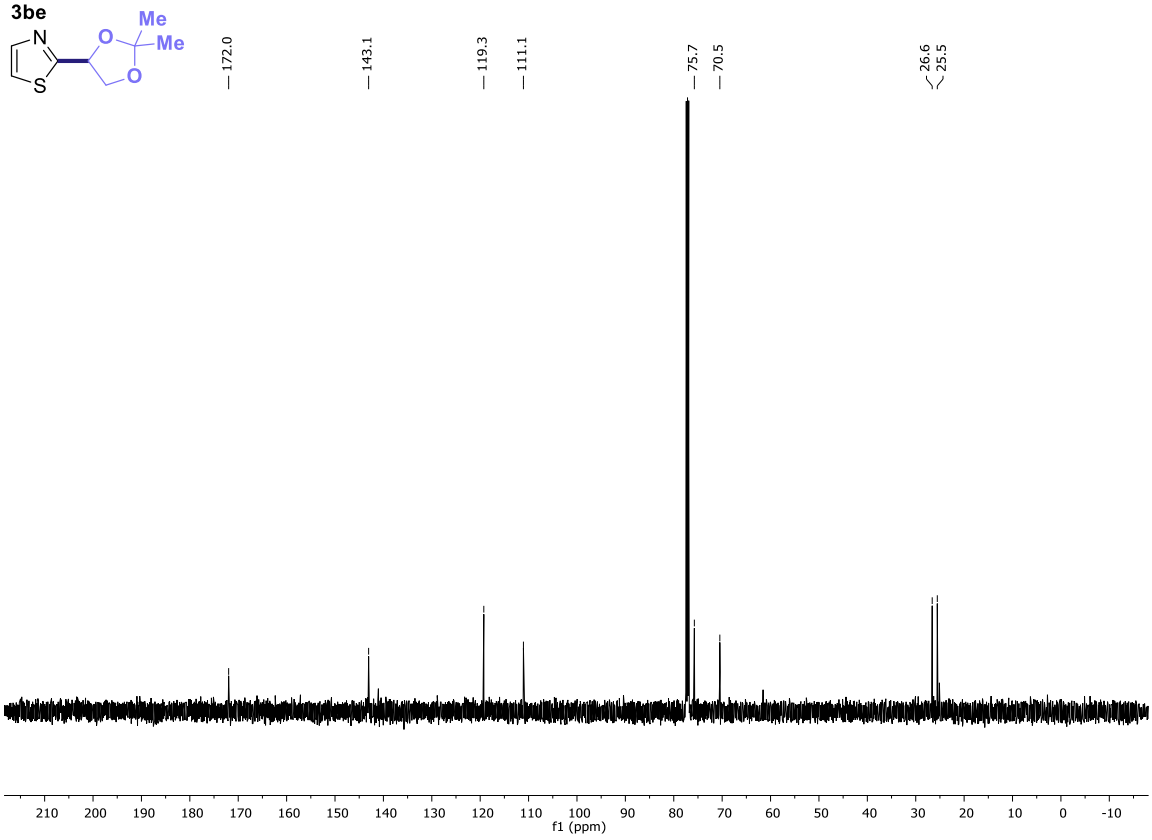

^{1}H NMR ($CDCl_3$, 500 MHz) of 4-(benzo[b]thiophen-2-yl)-2,2-dimethyl-1,3-dioxolane (**6.3.5**)

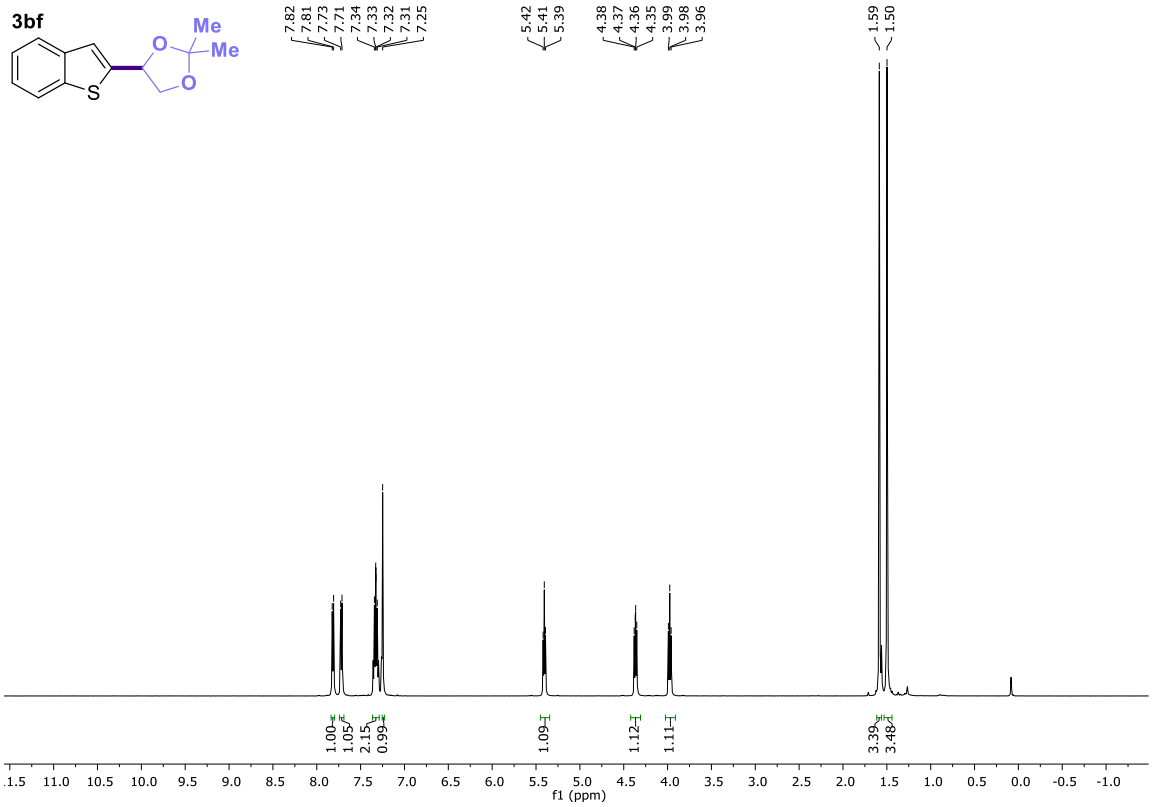

^{13}C NMR ($CDCl_3$, 126 MHz) of 4-(benzo[b]thiophen-2-yl)-2,2-dimethyl-1,3-dioxolane (**6.3.5**)

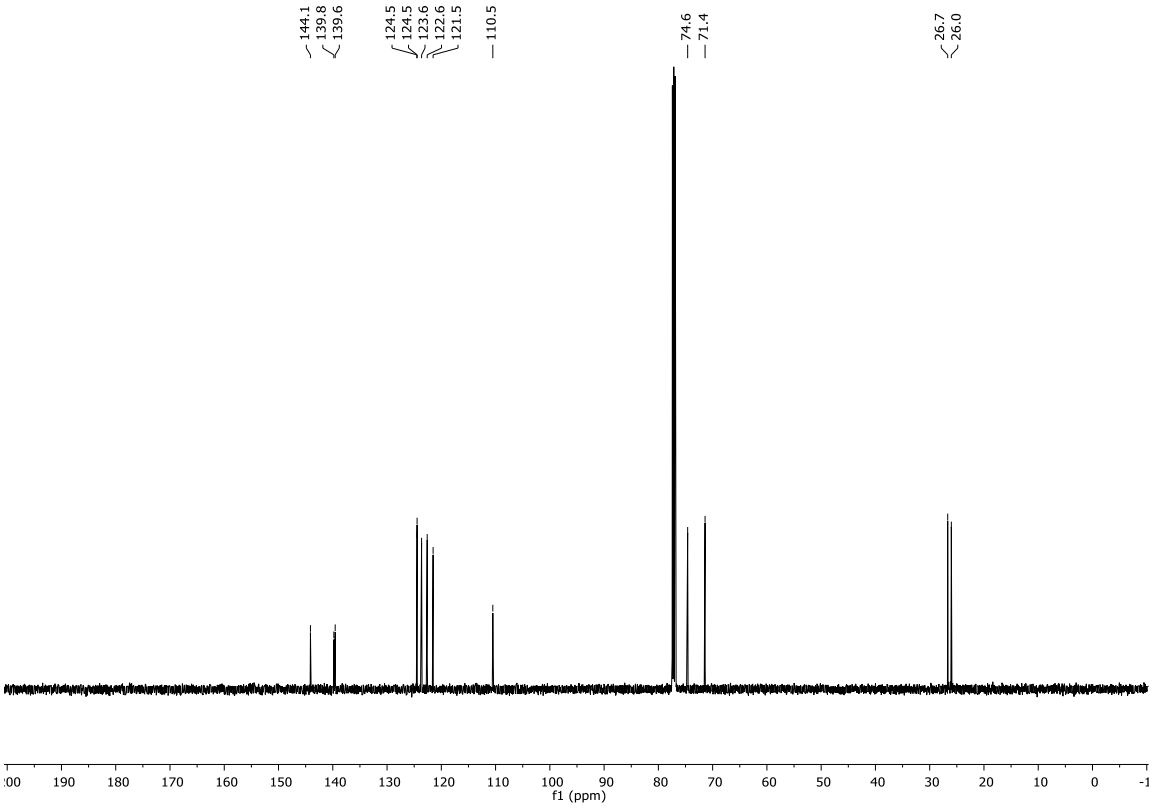

^{1}H NMR ($CDCl_3$, 500 MHz) of 5-(2,2-dimethyl-1,3-dioxolan-4-yl)thiophene-2-carbaldehyde (**6.3.6**)

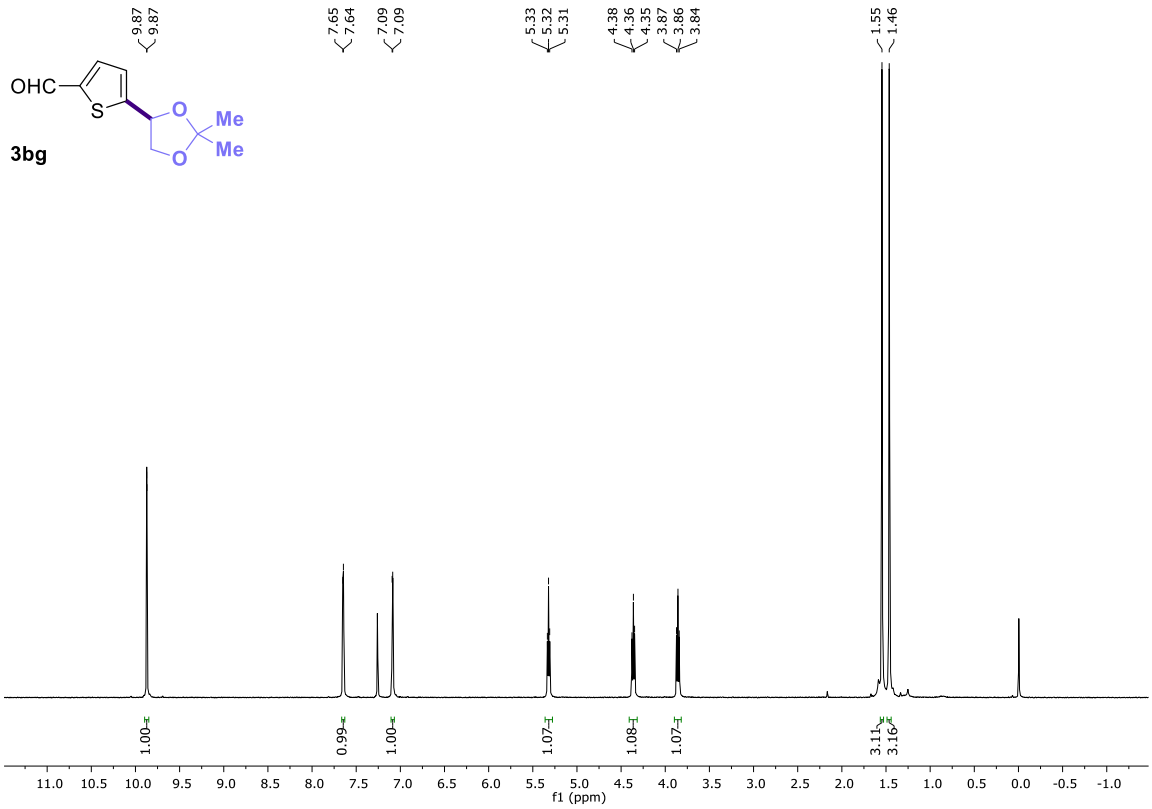

^{13}C NMR ($CDCl_3$, 126 MHz) of 5-(2,2-dimethyl-1,3-dioxolan-4-yl)thiophene-2-carbaldehyde (**6.3.6**)

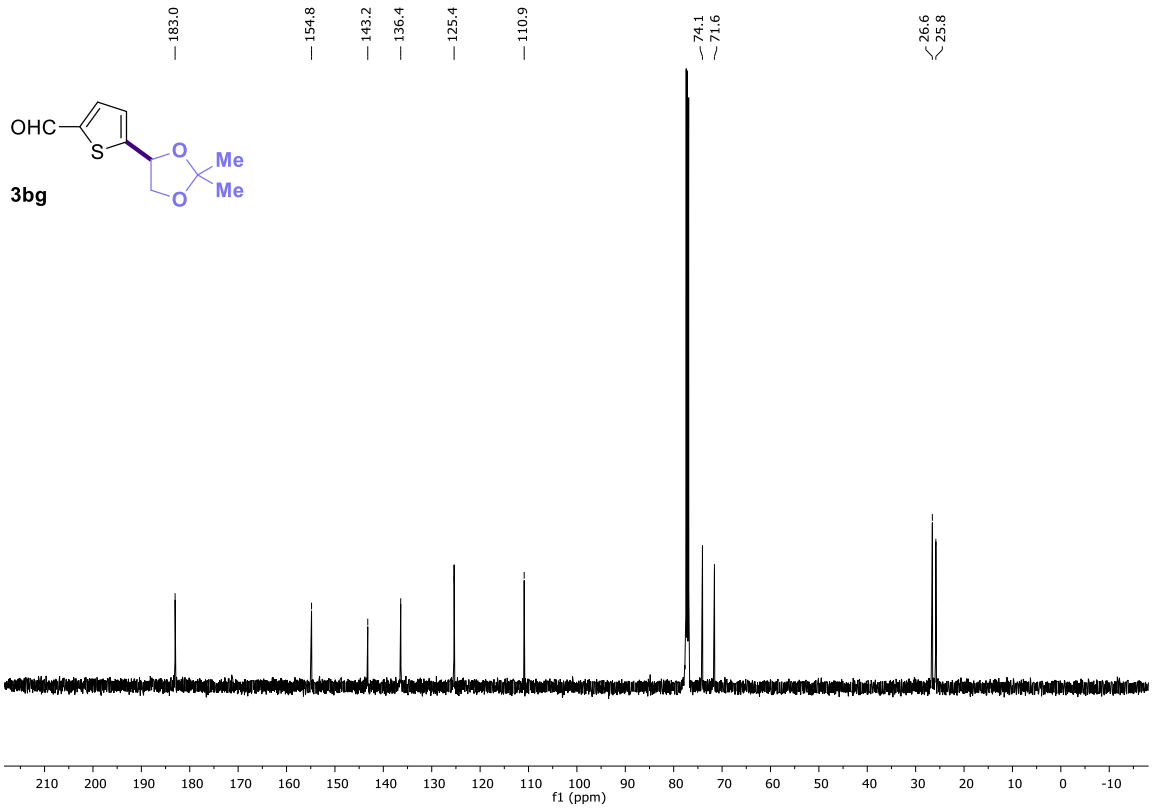

^{1}H NMR ($CDCl_3$, 500 MHz) of 1-(5-(2,2-dimethyl-1,3-dioxolan-4-yl)thiophen-2-yl)ethan-1-one (**6.3.7**)

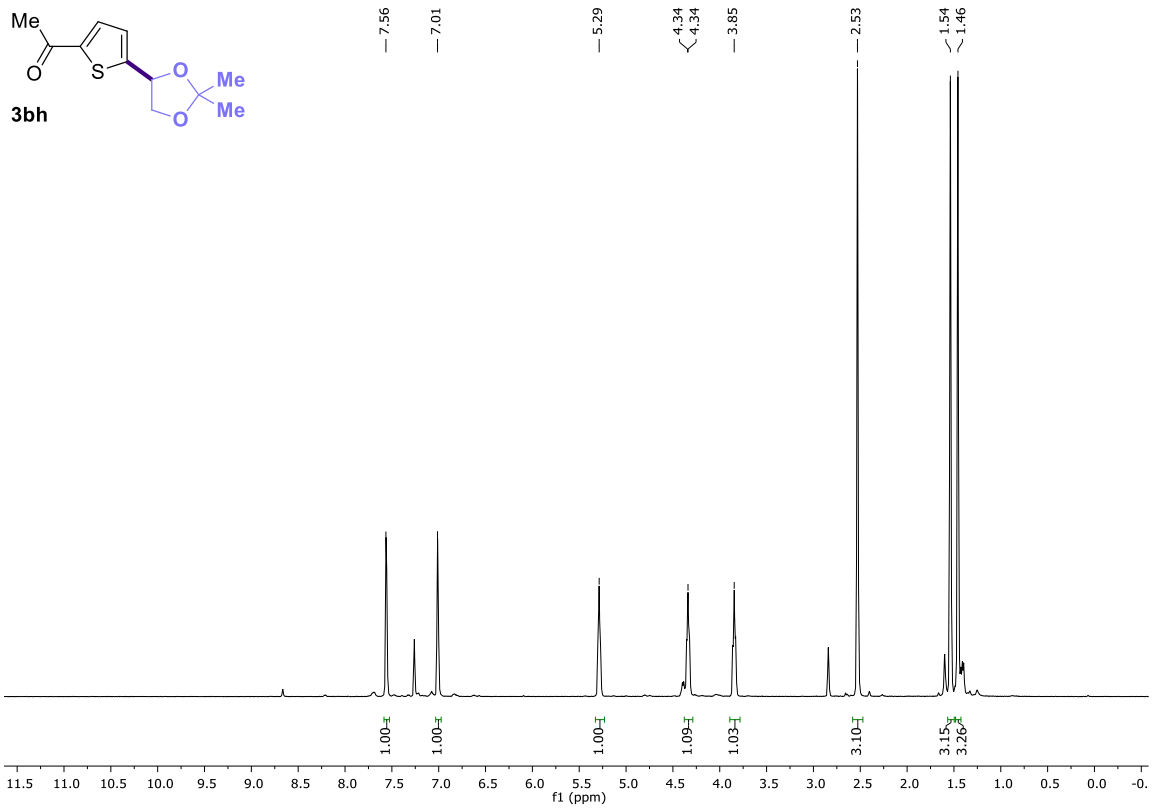

^{13}C NMR ($CDCl_3$, 126 MHz) of 1-(5-(2,2-dimethyl-1,3-dioxolan-4-yl)thiophen-2-yl)ethan-1-one (**6.3.7**)

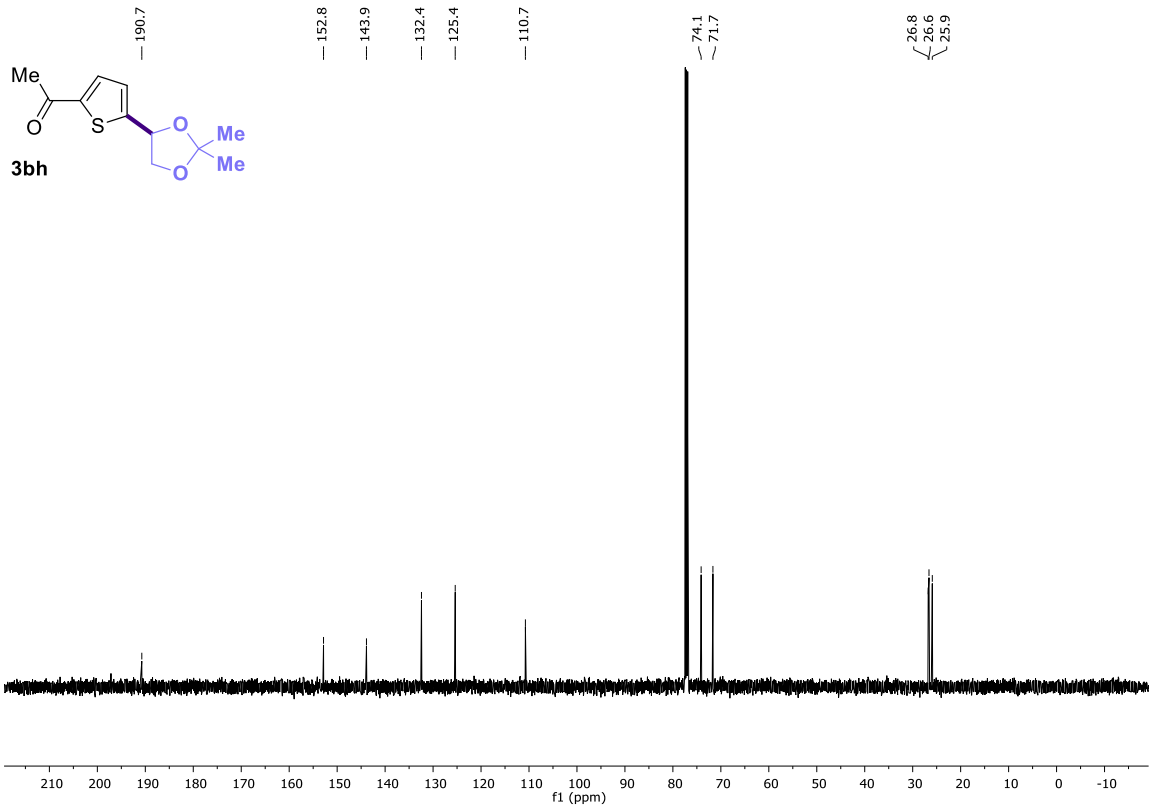

^{1}H and ^{13}C NMR Spectra: Scope of (Hetero)Aryl Bromides and Dihydropyridines

^{1}H NMR ($CDCl_3$, 500 MHz) of 2-isopropylbenzo[b]thiophene (**6.4.1**)

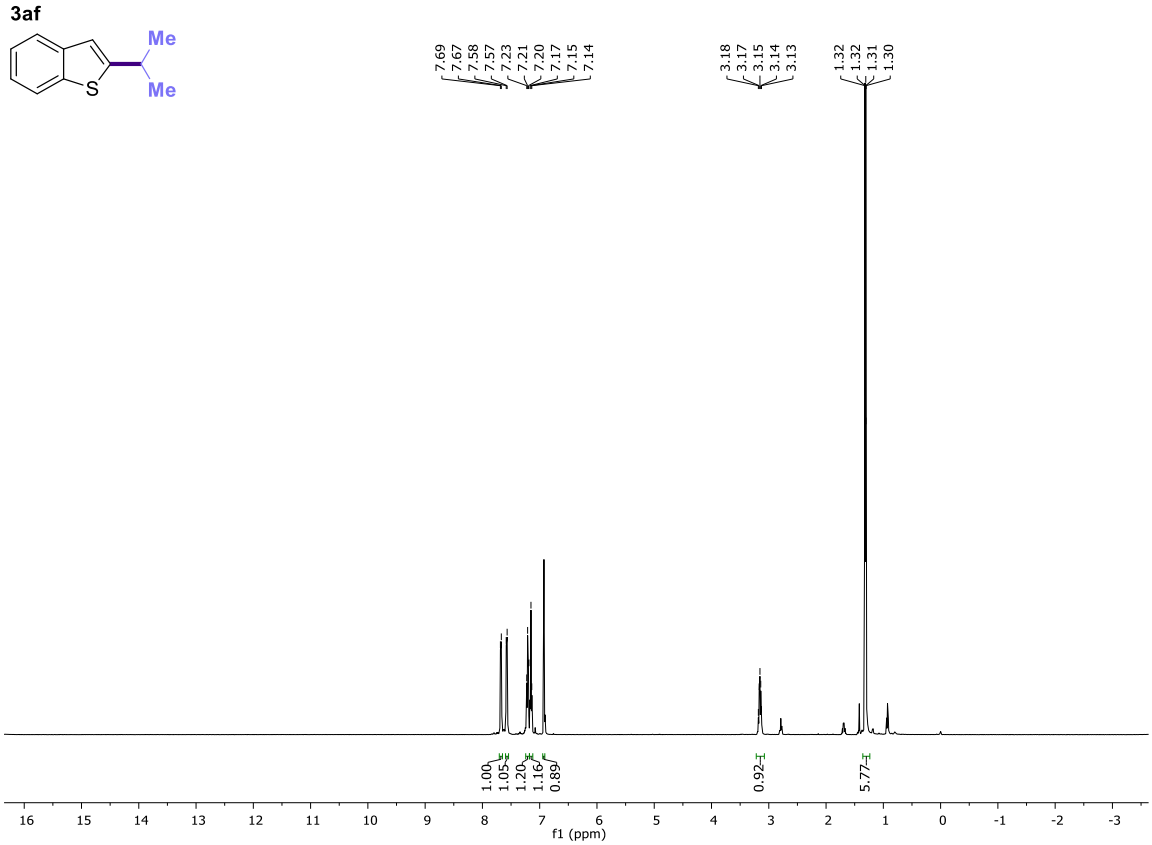

^{13}C NMR ($CDCl_3$, 126 MHz) of 2-isopropylbenzo[b]thiophene (**6.4.1**)

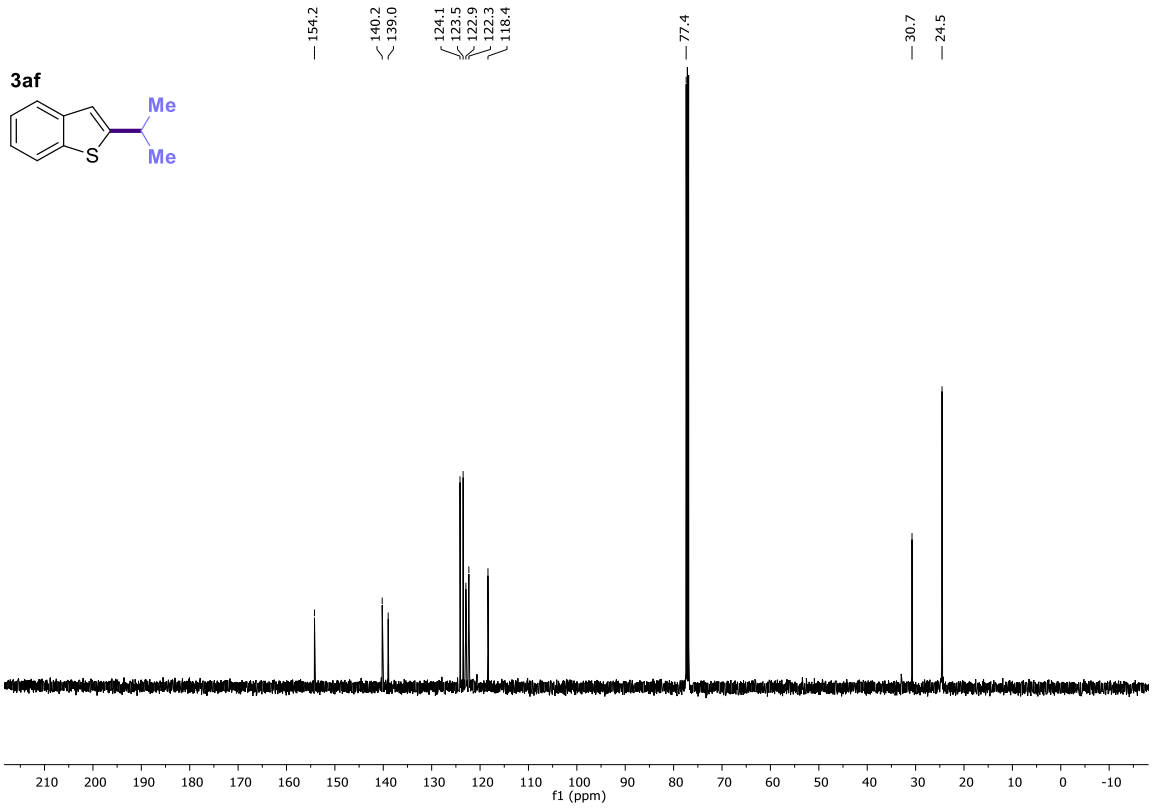

^{1}H NMR ($CDCl_3$, 500 MHz) of ethyl 5-cyclohexylfuran-2-carboxylate (**6.4.2**)

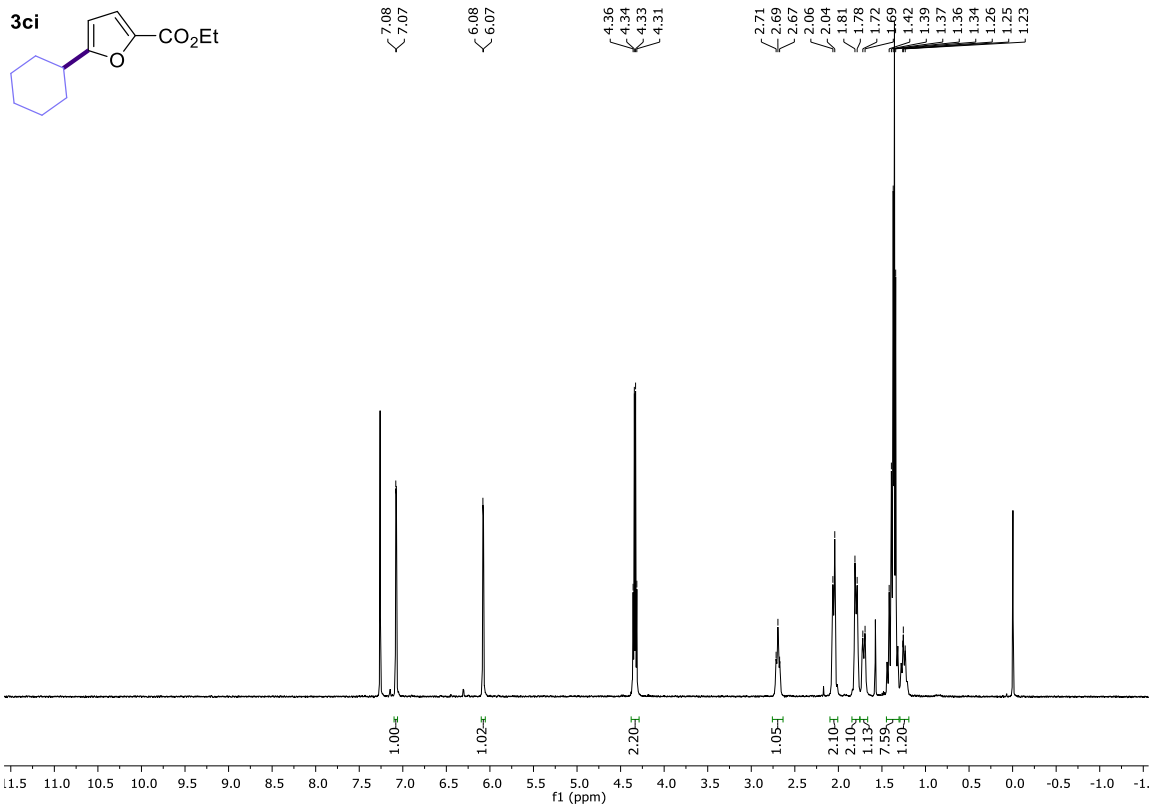

^{13}C NMR ($CDCl_3$, 126 MHz) of ethyl 5-cyclohexylfuran-2-carboxylate (**6.4.2**)

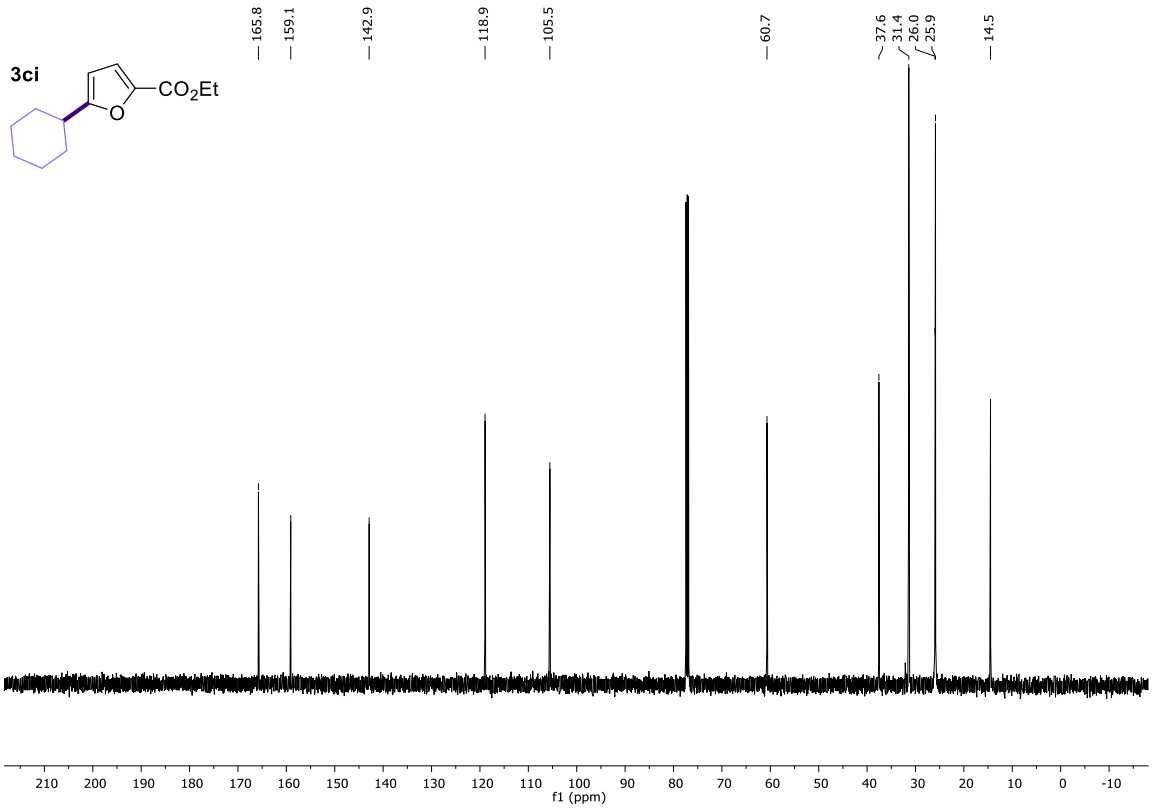

^{1}H NMR ($CDCl_3$, 500 MHz) of 1-(5-cyclohexylthiophen-2-yl)ethan-1-one (**6.4.3**)

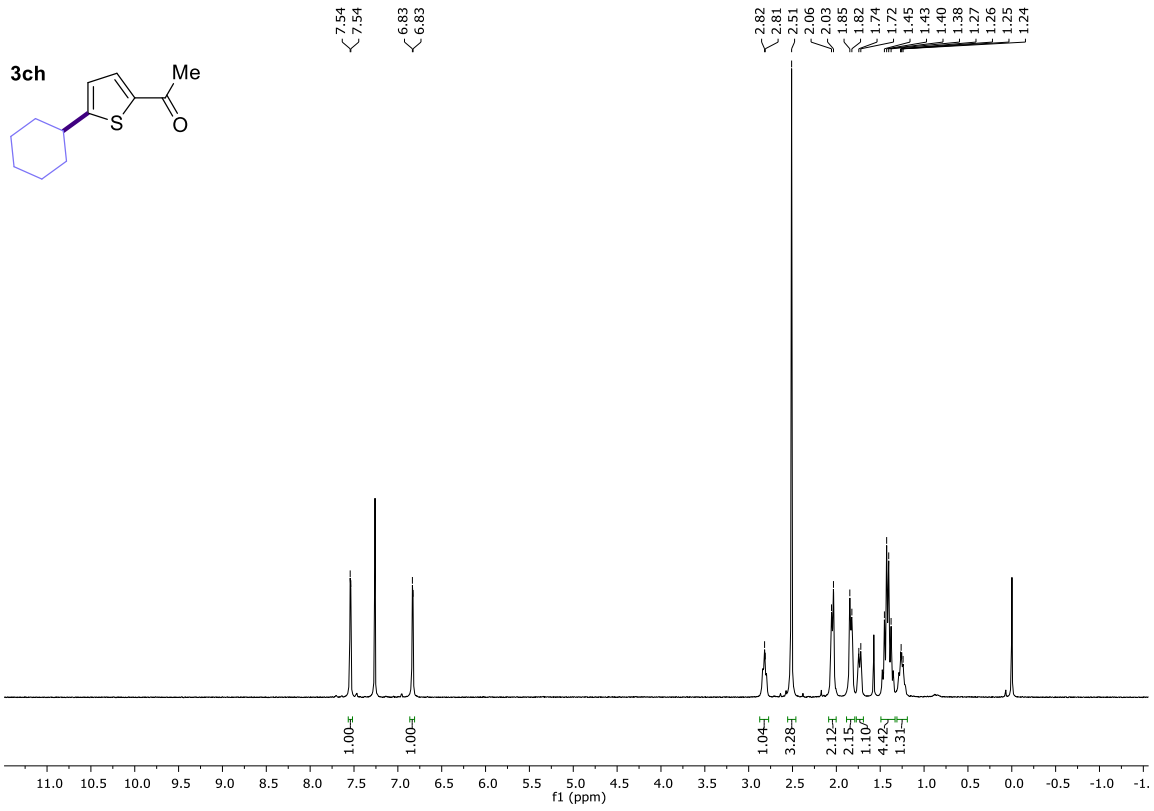

^{13}C NMR ($CDCl_3$, 126 MHz) of 1-(5-cyclohexylthiophen-2-yl)ethan-1-one (**6.4.3**)

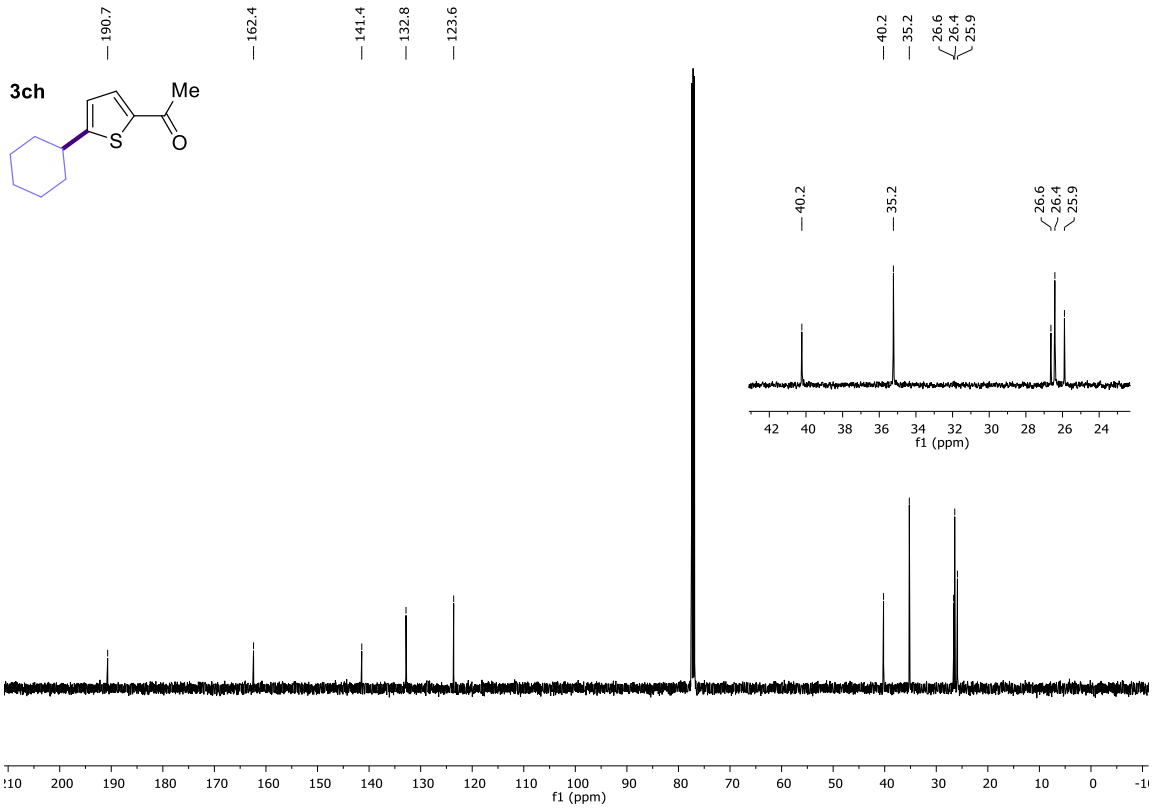

^{1}H NMR ($CDCl_3$, 500 MHz) of 5-cyclohexylthiophene-2-sulfonamide (**6.4.4**)

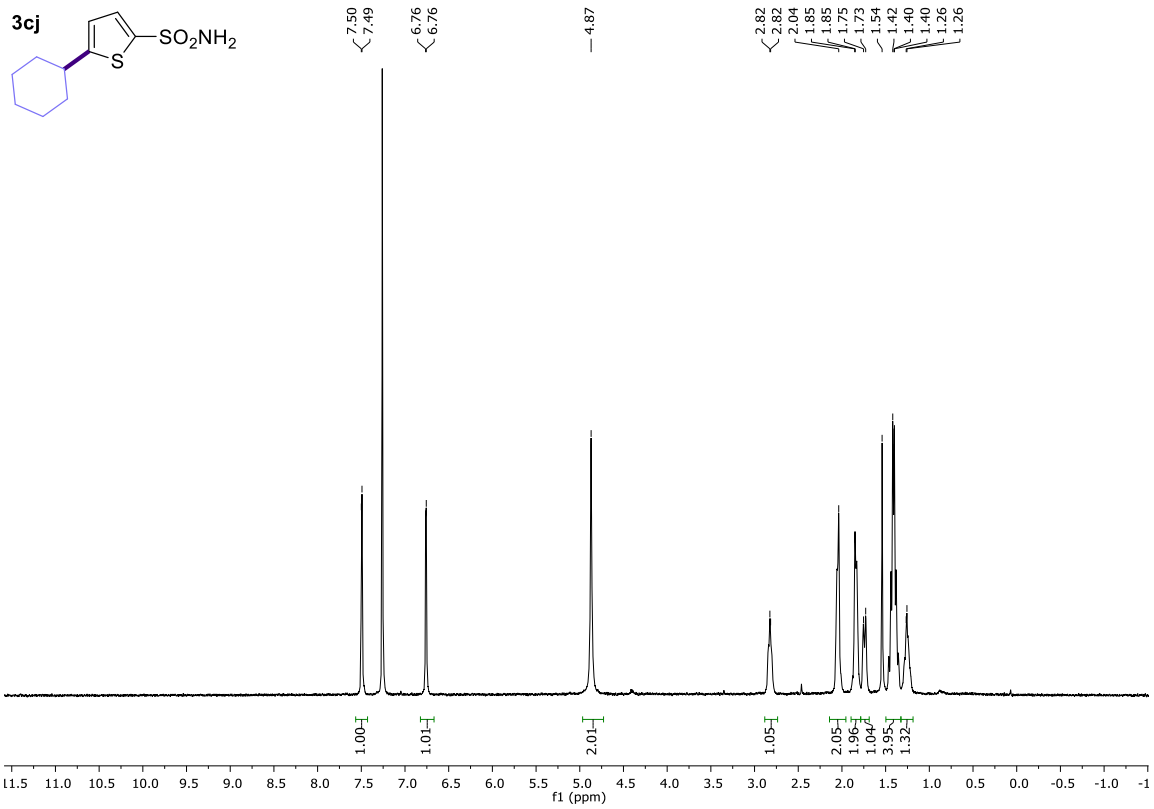

^{13}C NMR ($CDCl_3$, 126 MHz) of 5-cyclohexylthiophene-2-sulfonamide (**6.4.4**)

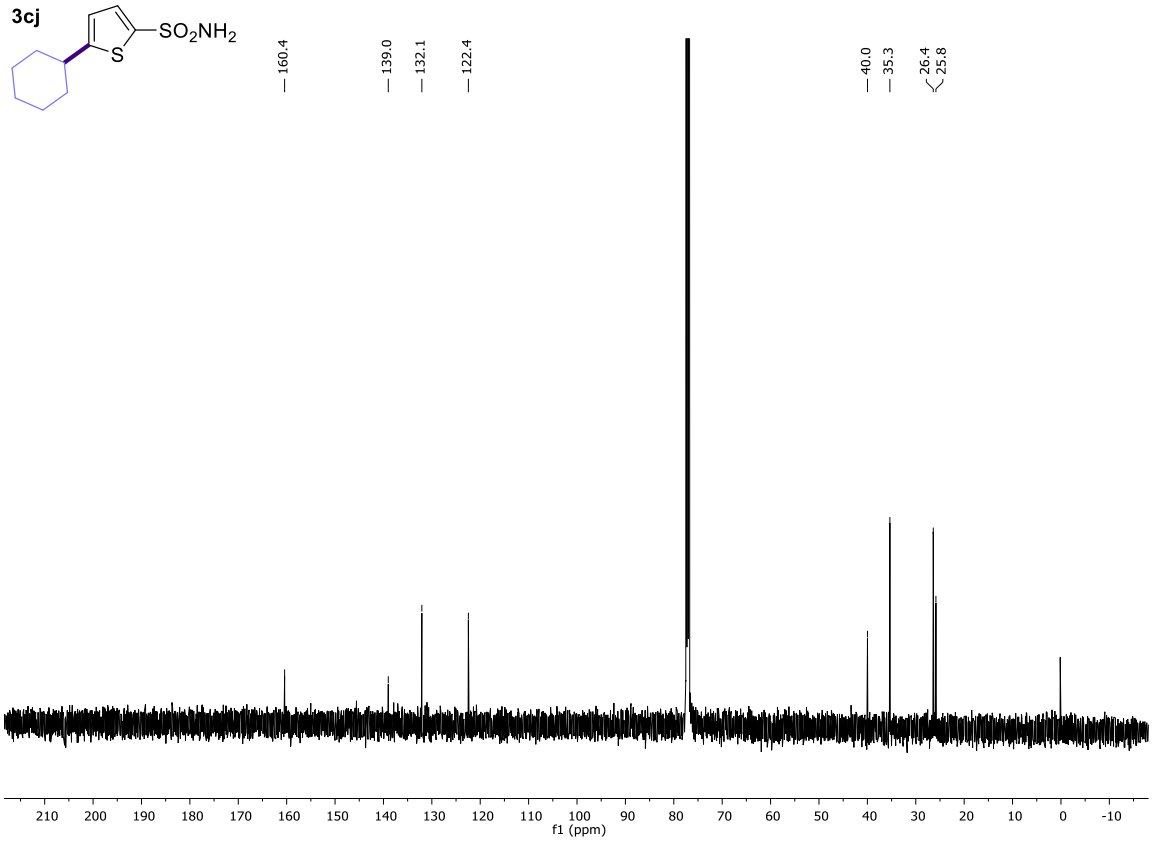

^{1}H NMR ($CDCl_3$, 500 MHz) of 1',2',3',6'-tetrahydro-[1,1'-biphenyl]-4-carbonitrile (**6.4.5**)

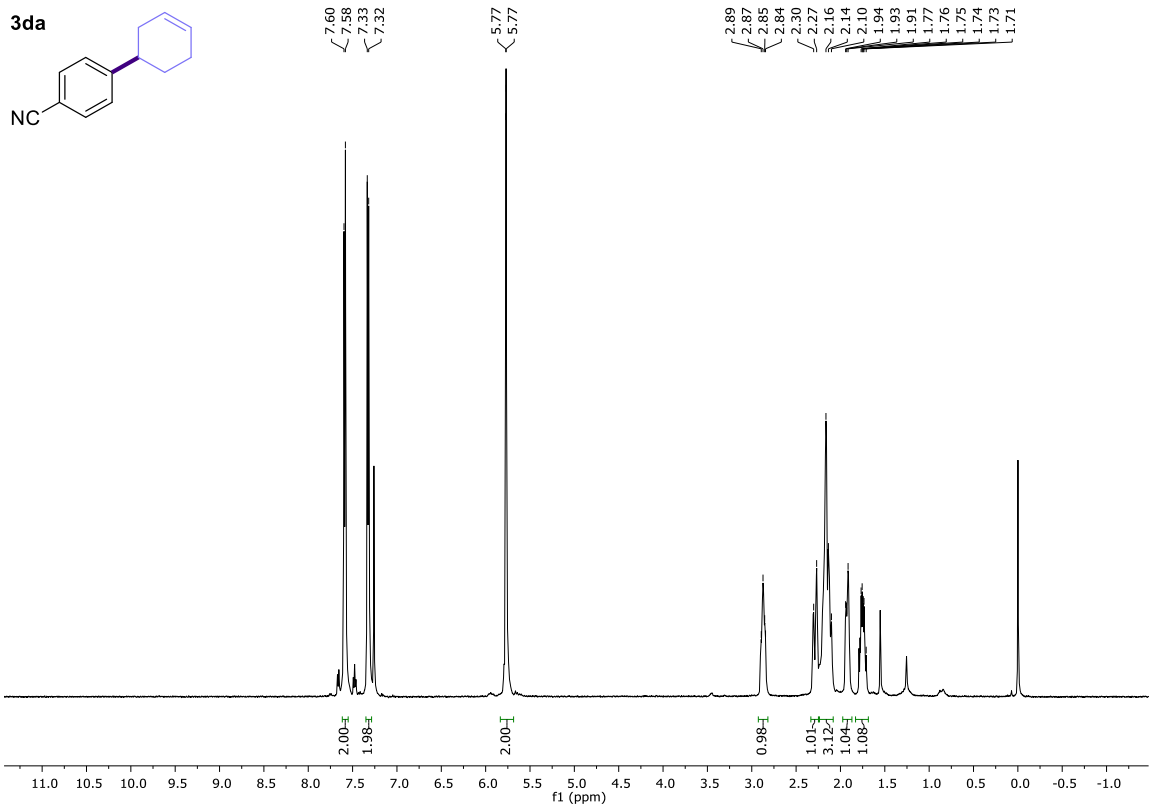

^{13}C NMR ($CDCl_3$, 126 MHz) of 1',2',3',6'-tetrahydro-[1,1'-biphenyl]-4-carbonitrile (**6.4.5**)

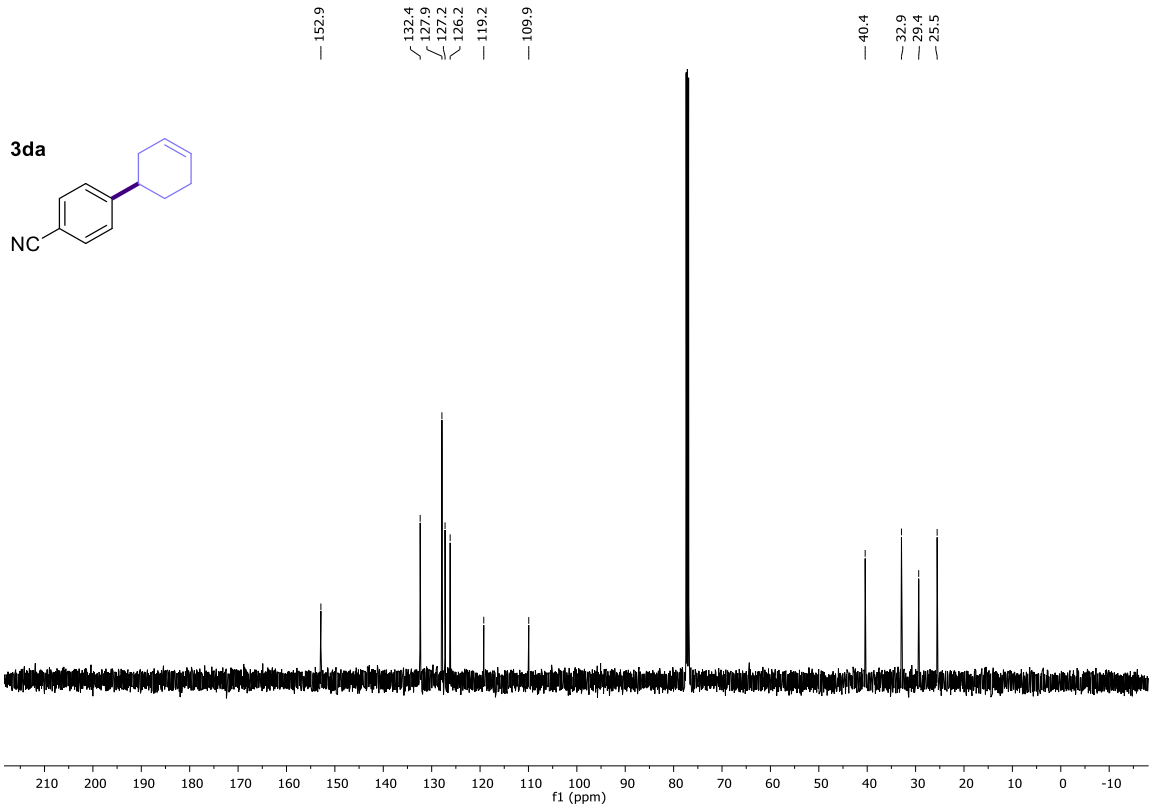

^{1}H NMR ($CDCl_3$, 500 MHz) of 2-(cyclohex-3-en-1-yl)benzo[b]thiophene (**6.4.6**)

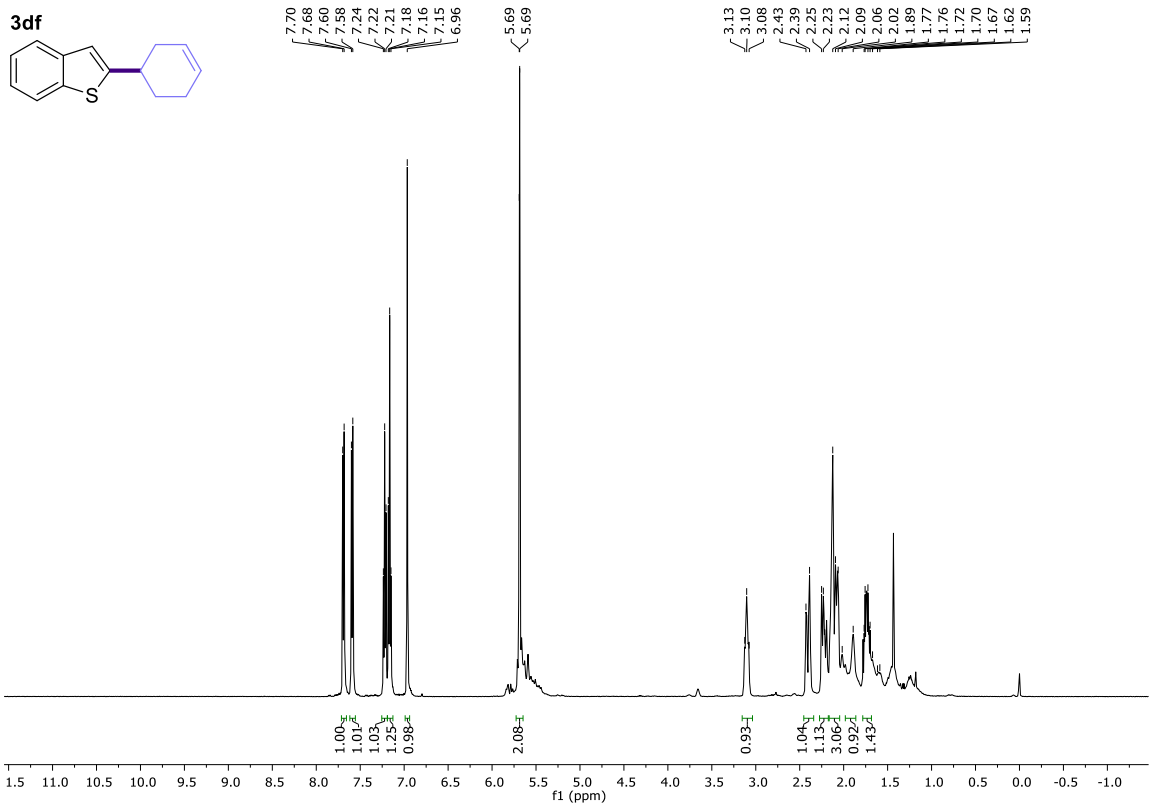

^{13}C NMR ($CDCl_3$, 126 MHz) of 2-(cyclohex-3-en-1-yl)benzo[b]thiophene (**6.4.6**)

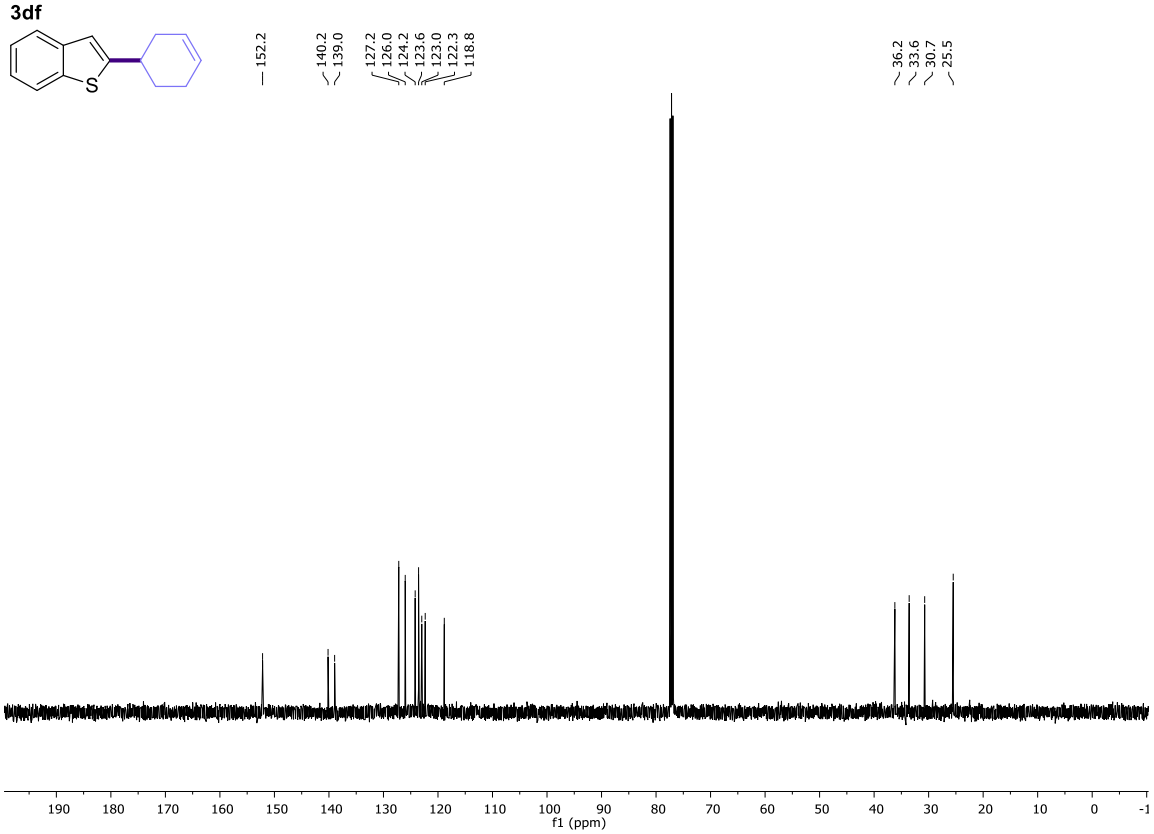

^{1}H NMR ($CDCl_3$, 500 MHz) of 1-(5-(cyclohex-3-en-1-yl)thiophen-2-yl)ethan-1-one (**6.4.7**)

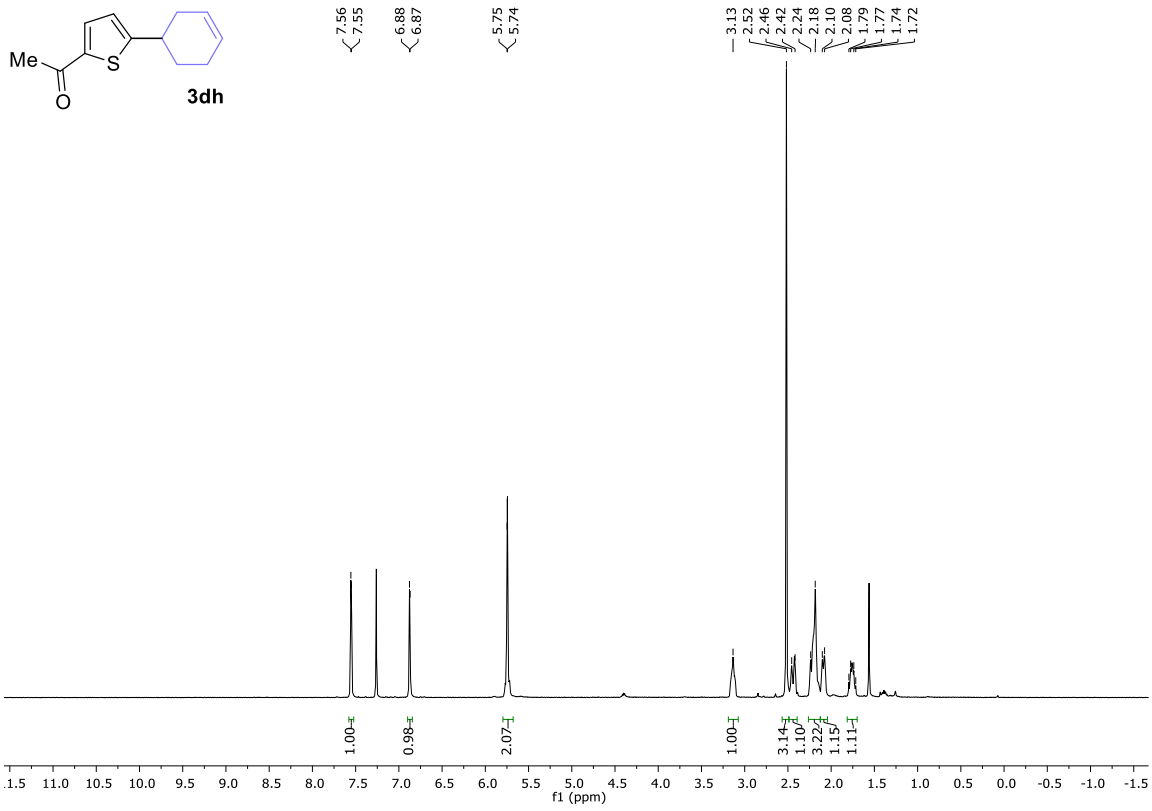

^{13}C NMR ($CDCl_3$, 126 MHz) of 1-(5-(cyclohex-3-en-1-yl)thiophen-2-yl)ethan-1-one (**6.4.7**)

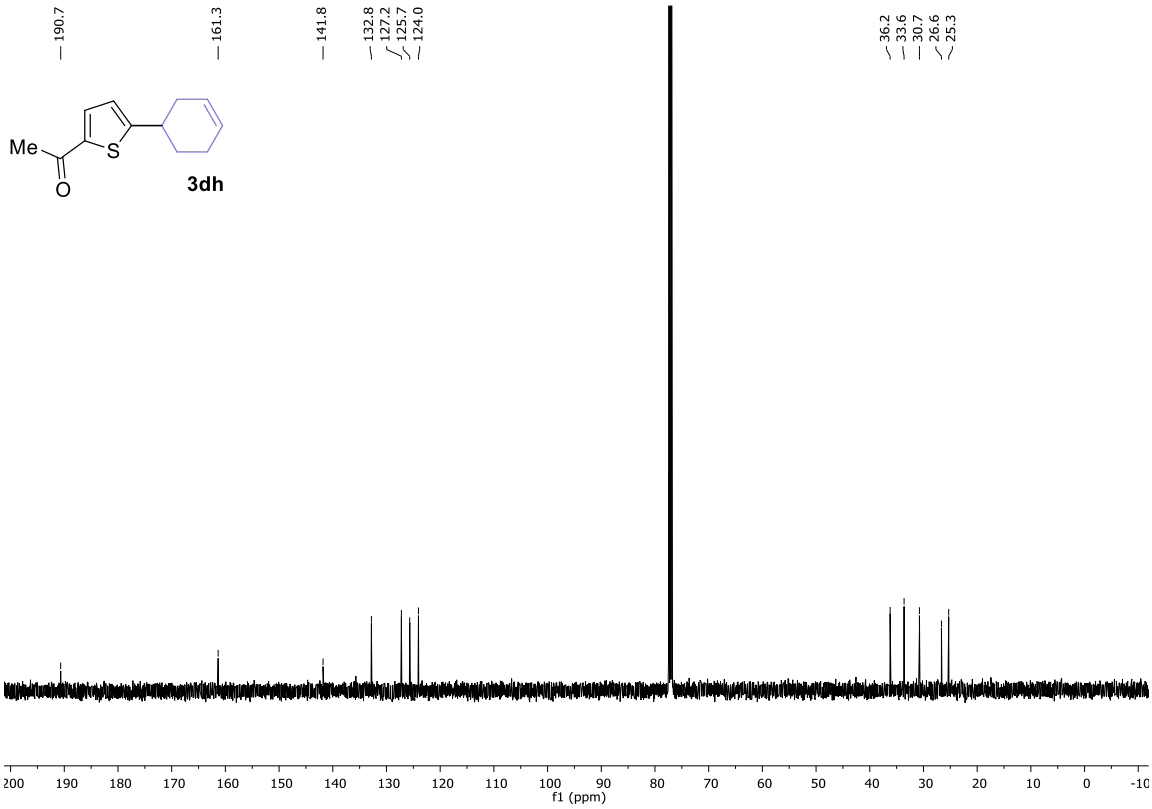

^{1}H NMR ($CDCl_3$, 500 MHz) of 4-(heptan-3-yl)benzonitrile (**6.4.8**)

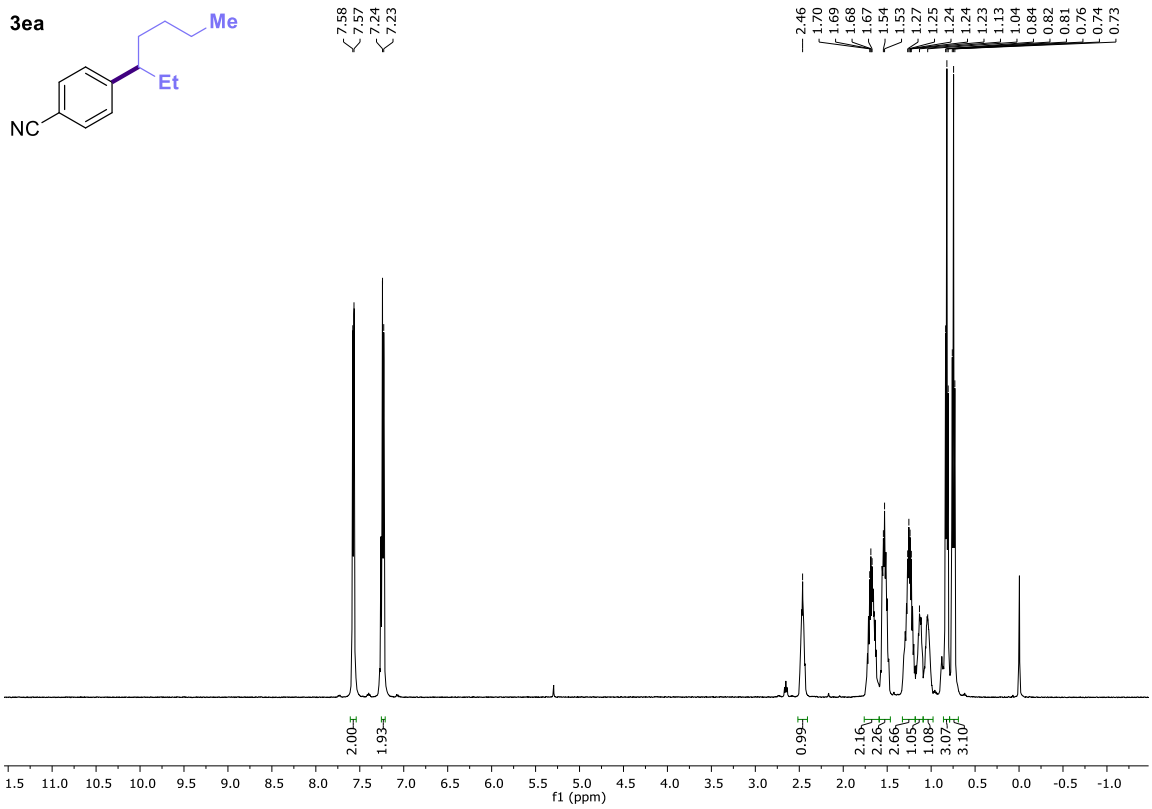

^{13}C NMR ($CDCl_3$, 126 MHz) of 4-(heptan-3-yl)benzonitrile (**6.4.8**)

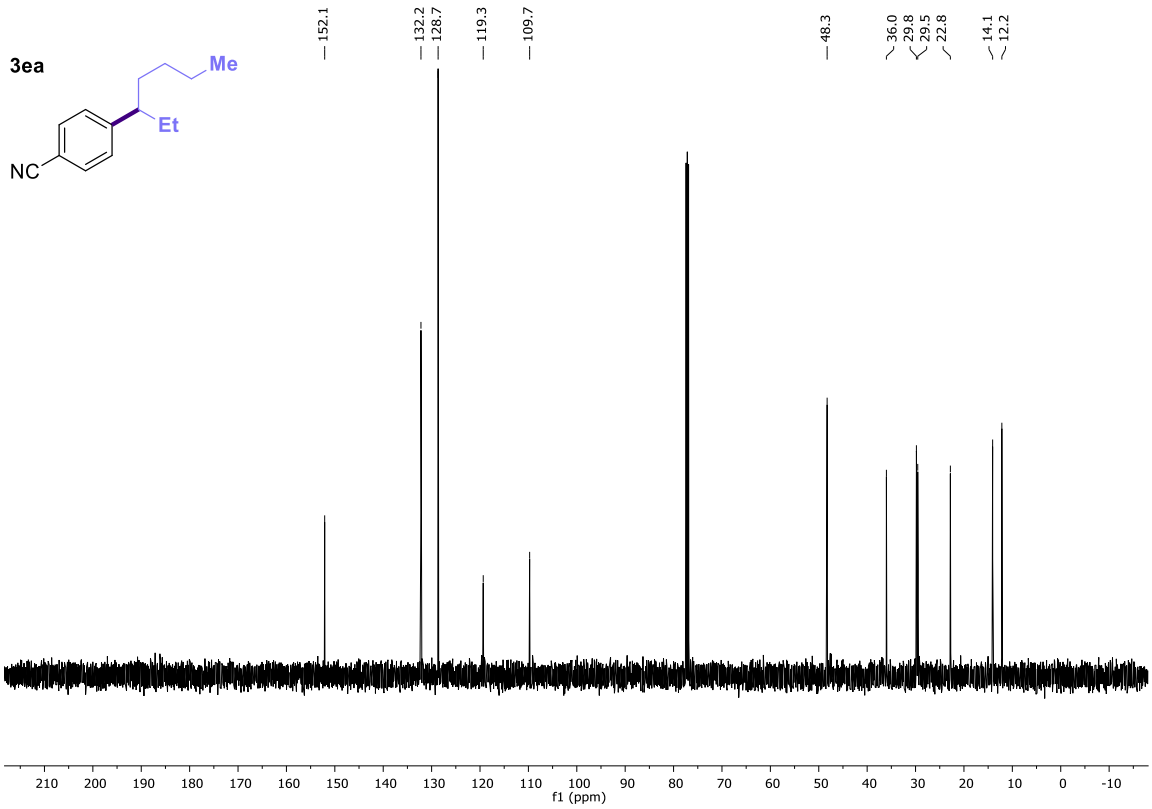

^{1}H NMR ($CDCl_3$, 500 MHz) of 1-(5-(heptan-3-yl)thiophen-2-yl)ethan-1-one (**6.4.9**)

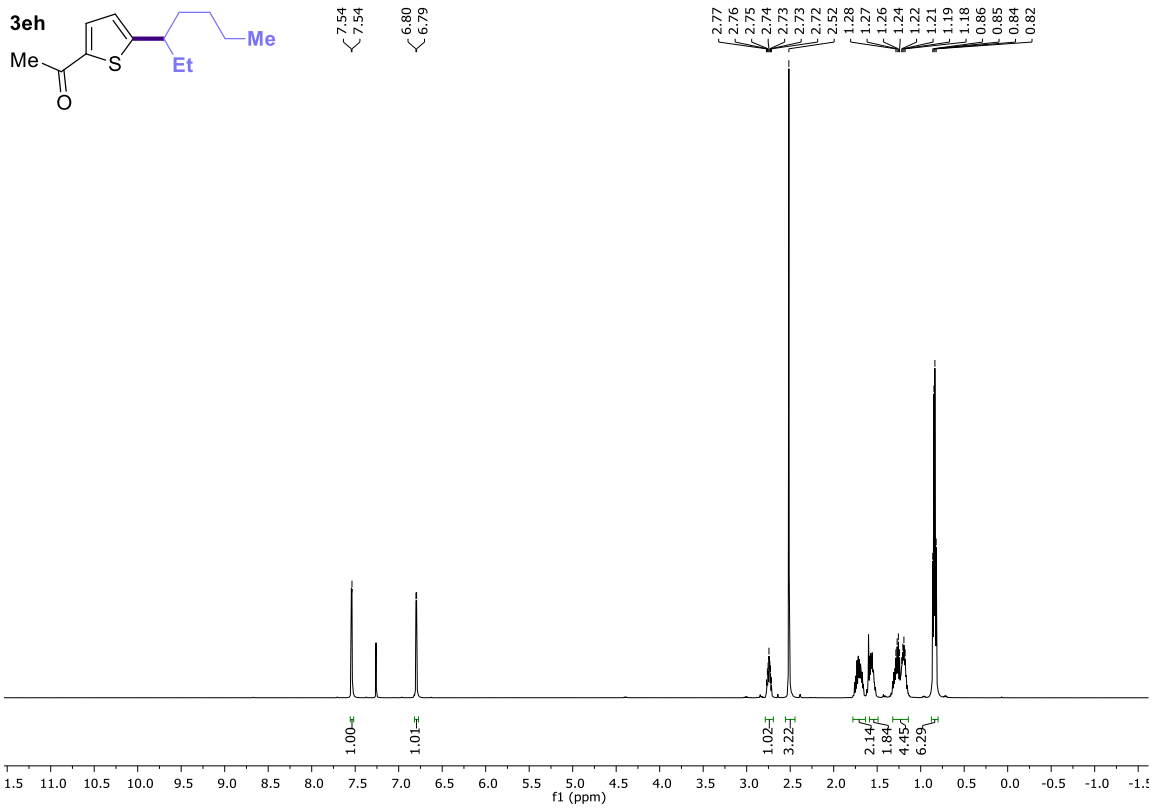

^{13}C NMR ($CDCl_3$, 126 MHz) of 1-(5-(heptan-3-yl)thiophen-2-yl)ethan-1-one (**6.4.9**)

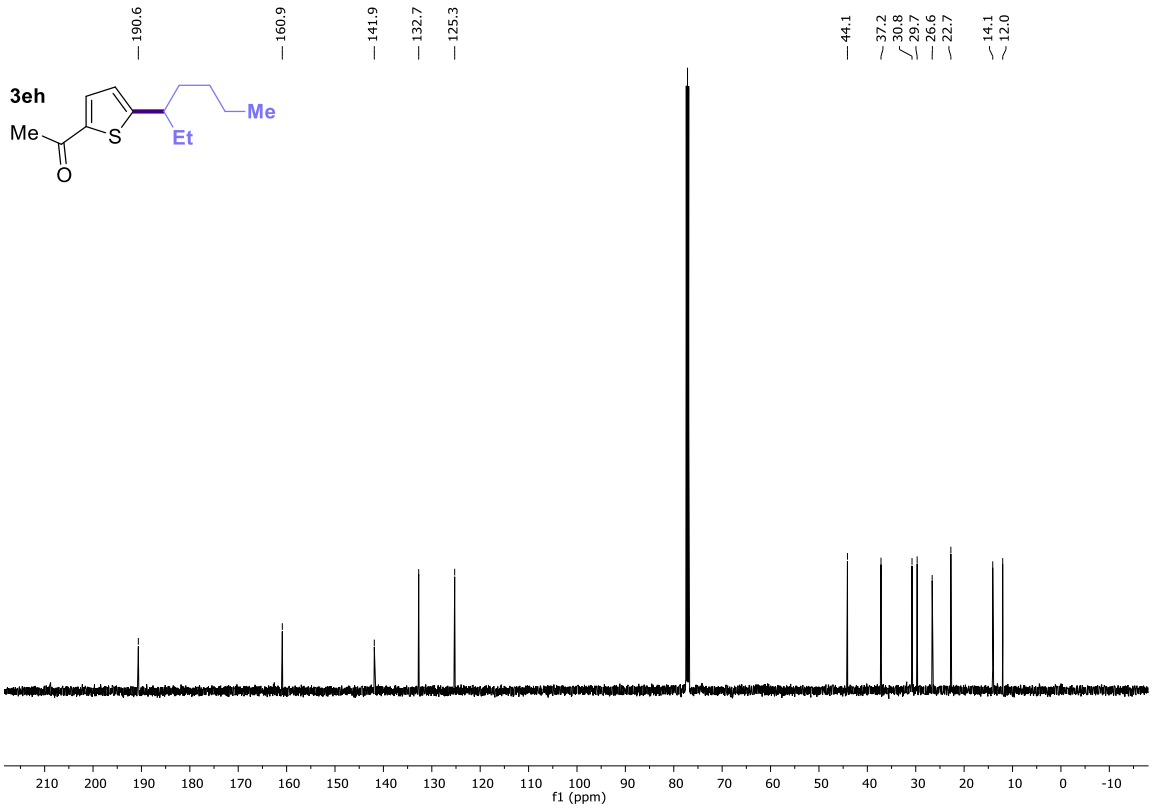

^{1}H NMR ($CDCl_3$, 500 MHz) of 1-(5-(6-methylhept-5-en-2-yl)thiophen-2-yl)ethan-1-one (**6.4.10**)

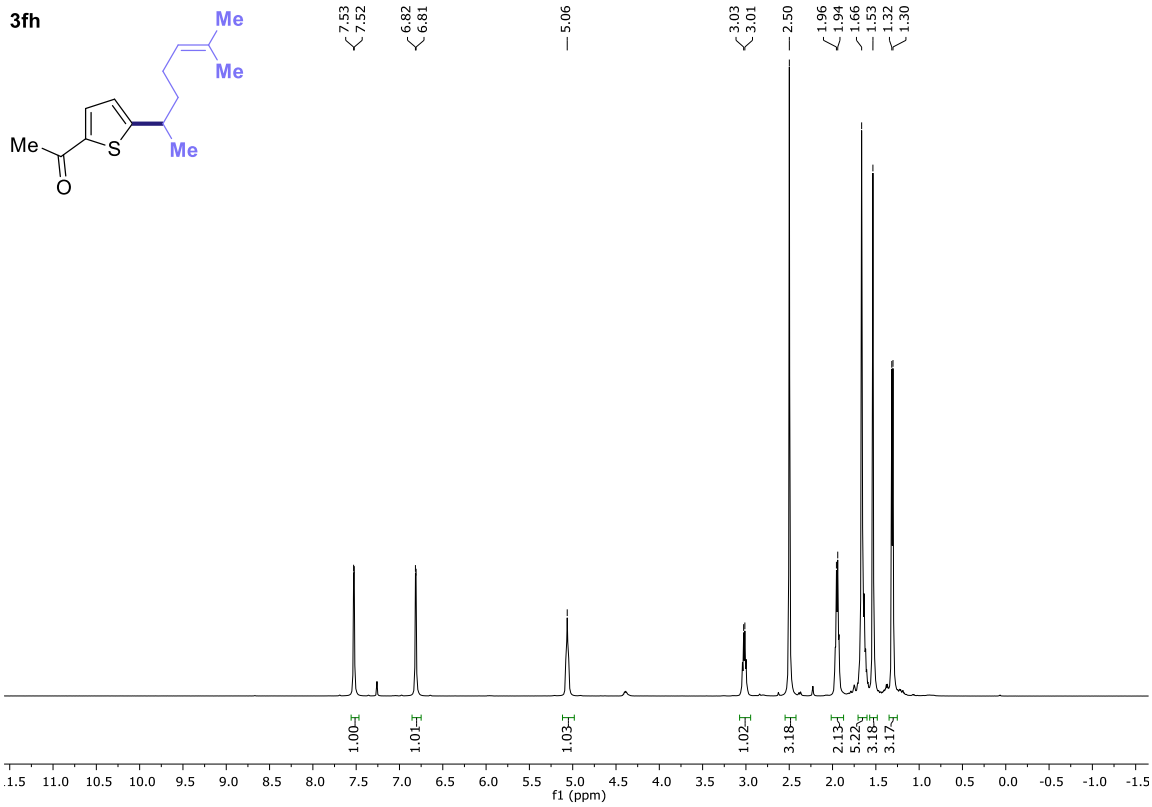

^{13}C NMR ($CDCl_3$, 126 MHz) of 1-(5-(6-methylhept-5-en-2-yl)thiophen-2-yl)ethan-1-one (**6.4.10**)

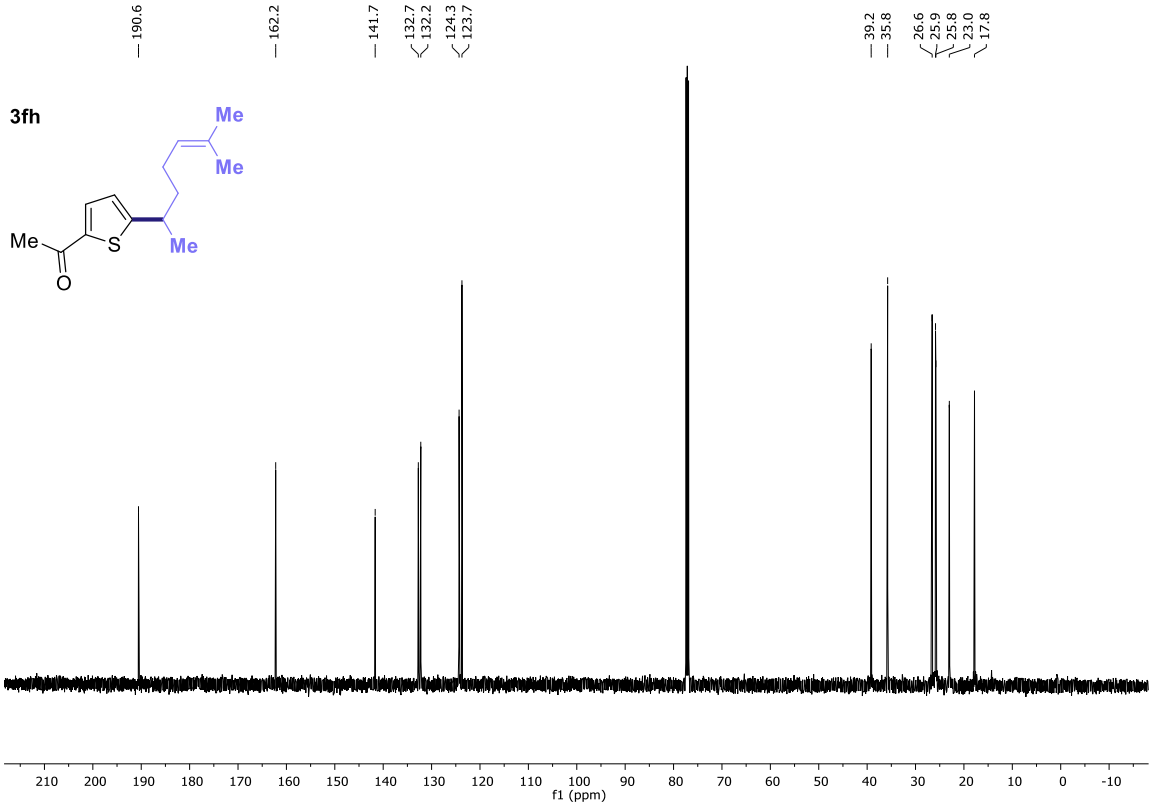

^{1}H NMR ($CDCl_3$, 500 MHz) of 1-(5-(tetrahydro-2H-pyran-4-yl)thiophen-2-yl)ethan-1-one (**6.4.11**)

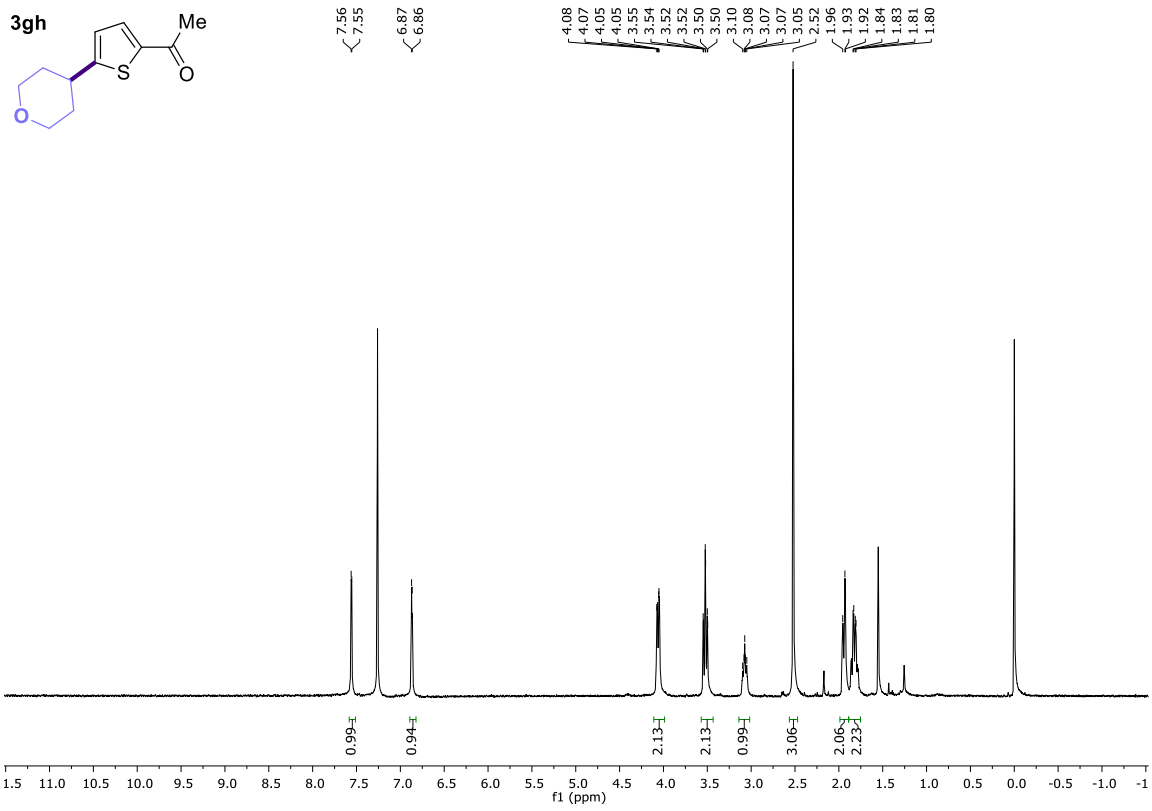

^{13}C NMR ($CDCl_3$, 126 MHz) of 1-(5-(tetrahydro-2H-pyran-4-yl)thiophen-2-yl)ethan-1-one (**6.4.11**)

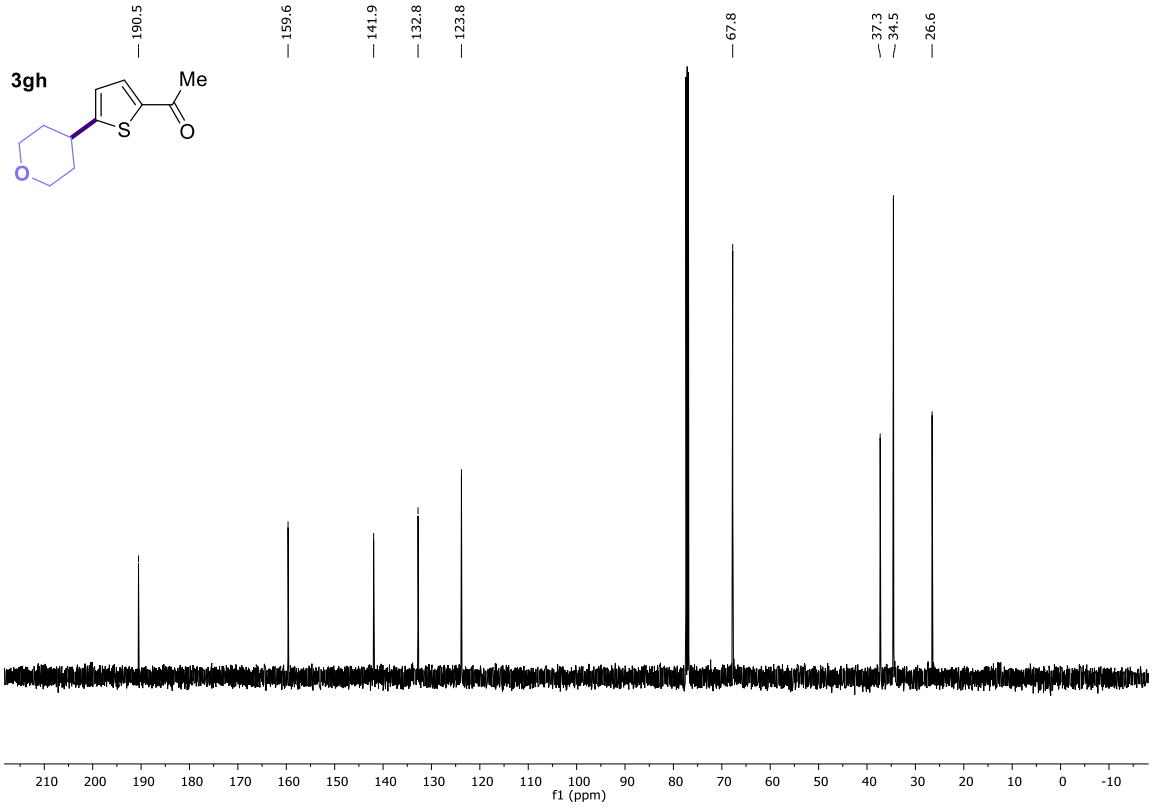

^{1}H NMR ($CDCl_3$, 500 MHz) of 3-benzyl-5-chloropyridine (**6.4.12**)

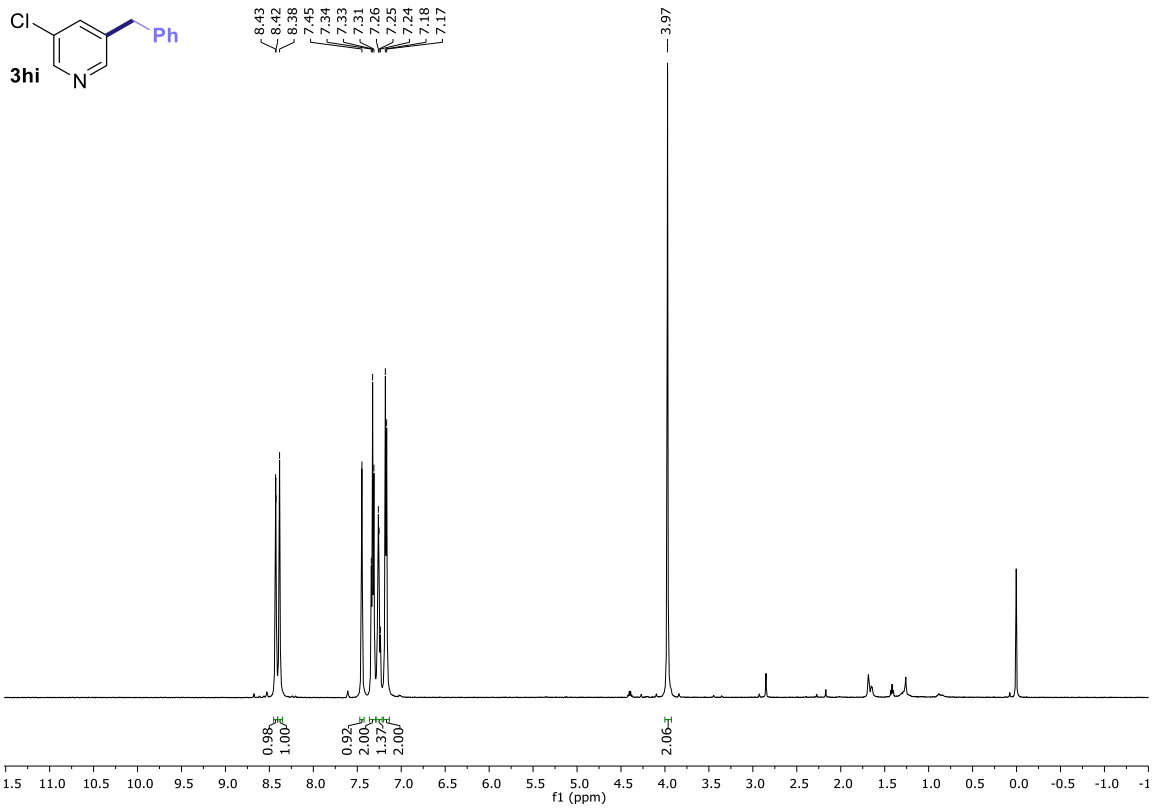

^{13}C NMR ($CDCl_3$, 126 MHz) of 3-benzyl-5-chloropyridine (**6.4.12**)

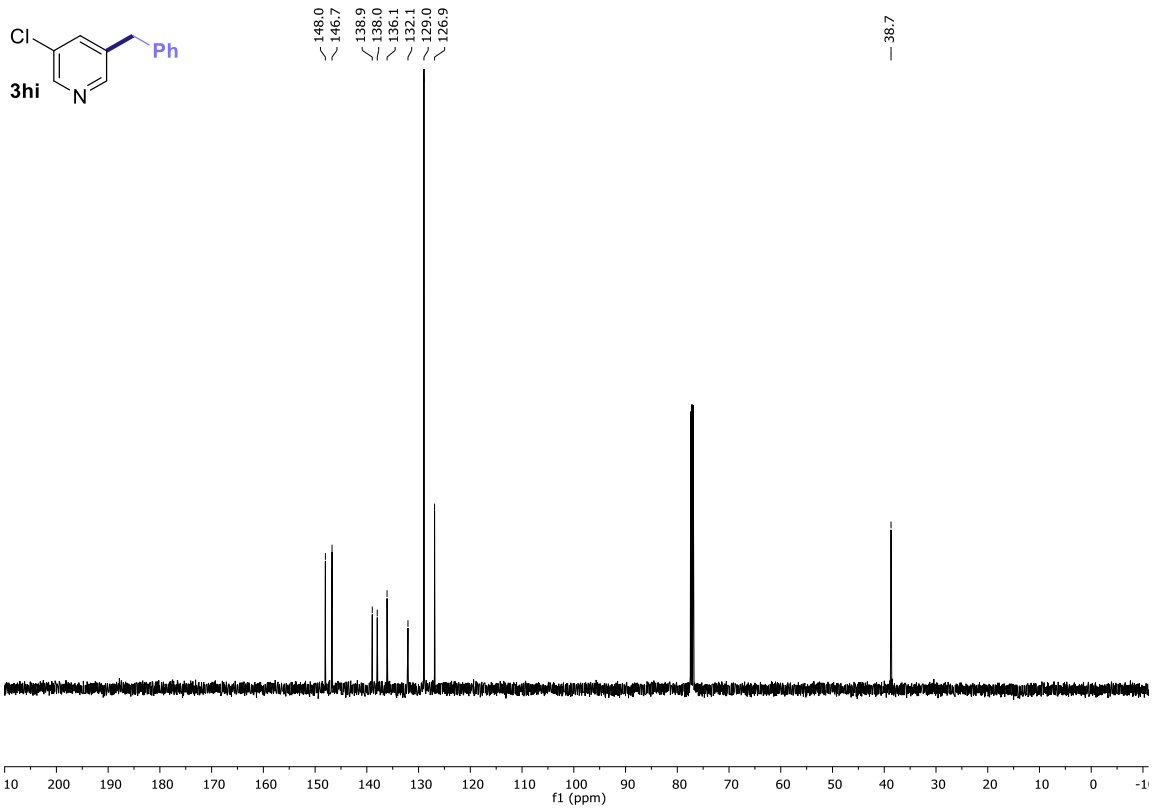

^{1}H NMR ($CDCl_3$, 500 MHz) of *tert*-butyl 2-(3-acetylphenyl)pyrrolidine-1-carboxylate (**6.4.13**)

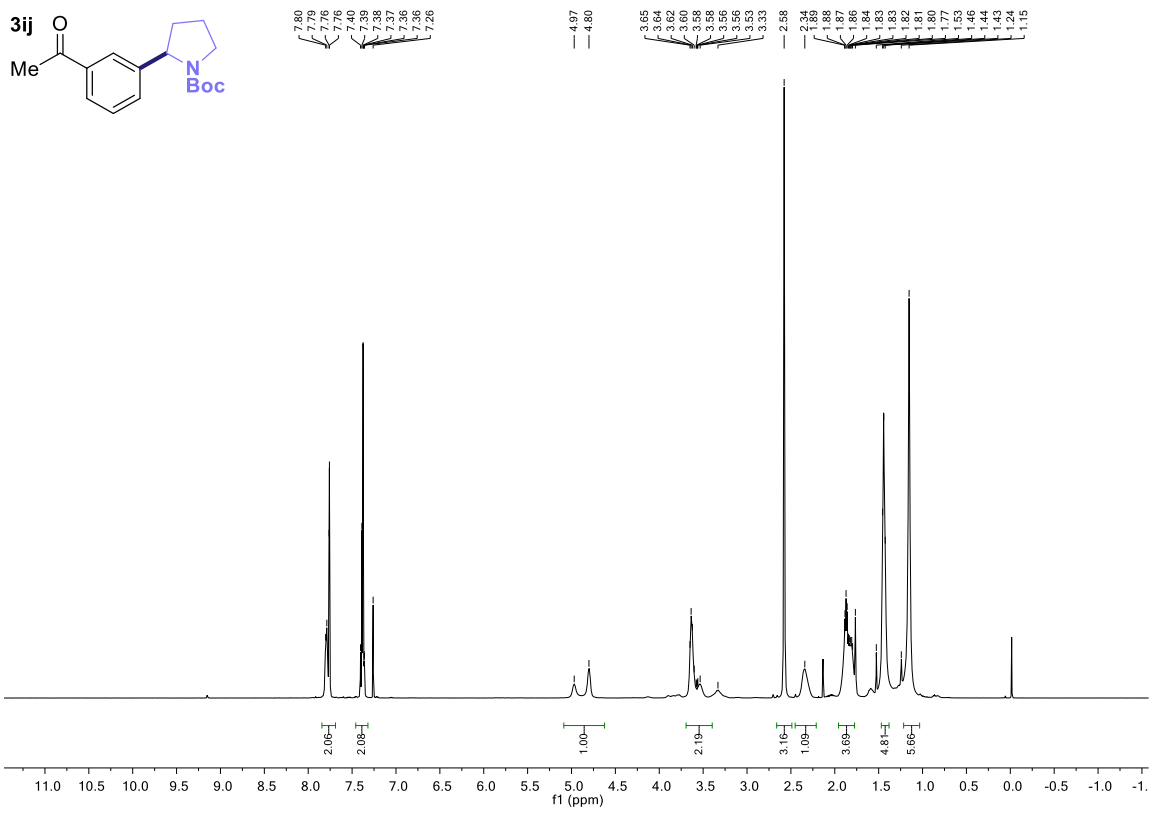

^{13}C NMR ($CDCl_3$, 126 MHz) of *tert*-butyl 2-(3-acetylphenyl)pyrrolidine-1-carboxylate (**6.4.13**)

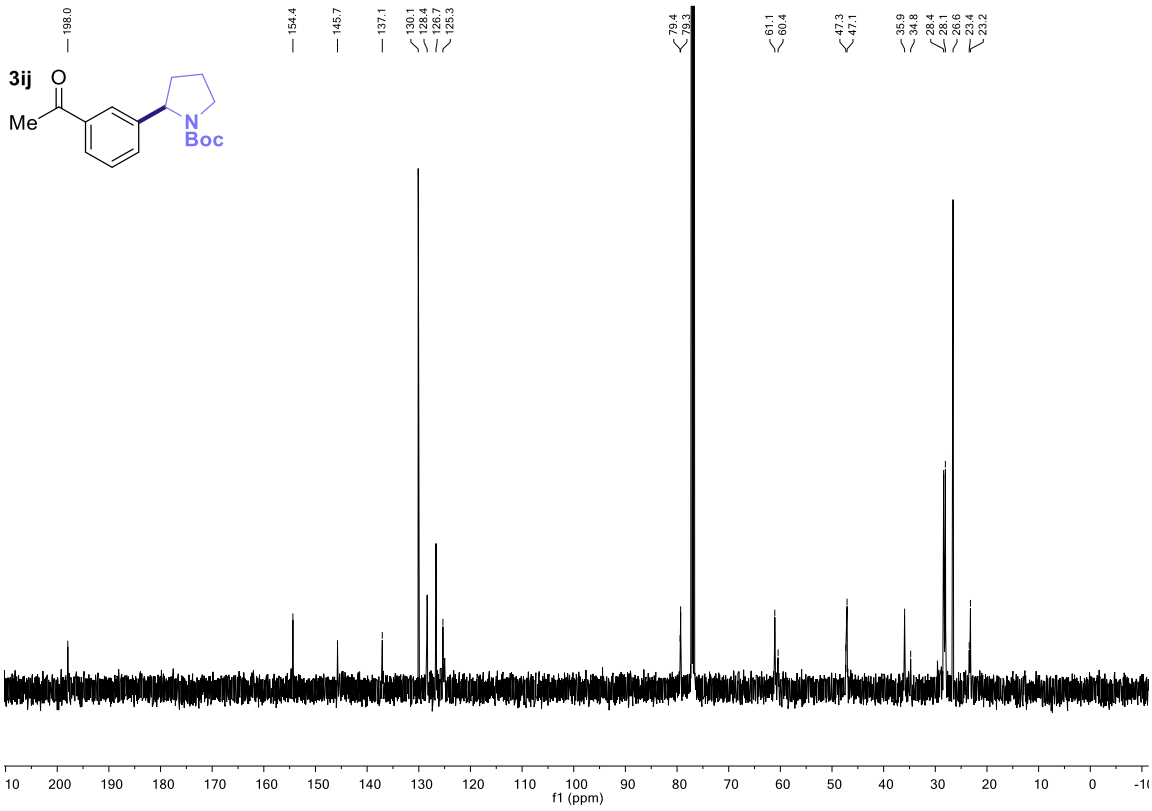

^{1}H NMR ($CDCl_3$, 500 MHz) of *tert*-butyl 4-(4-cyanophenyl)-2,2-dimethyloxazolidine-3-carboxylate (**6.4.14**)

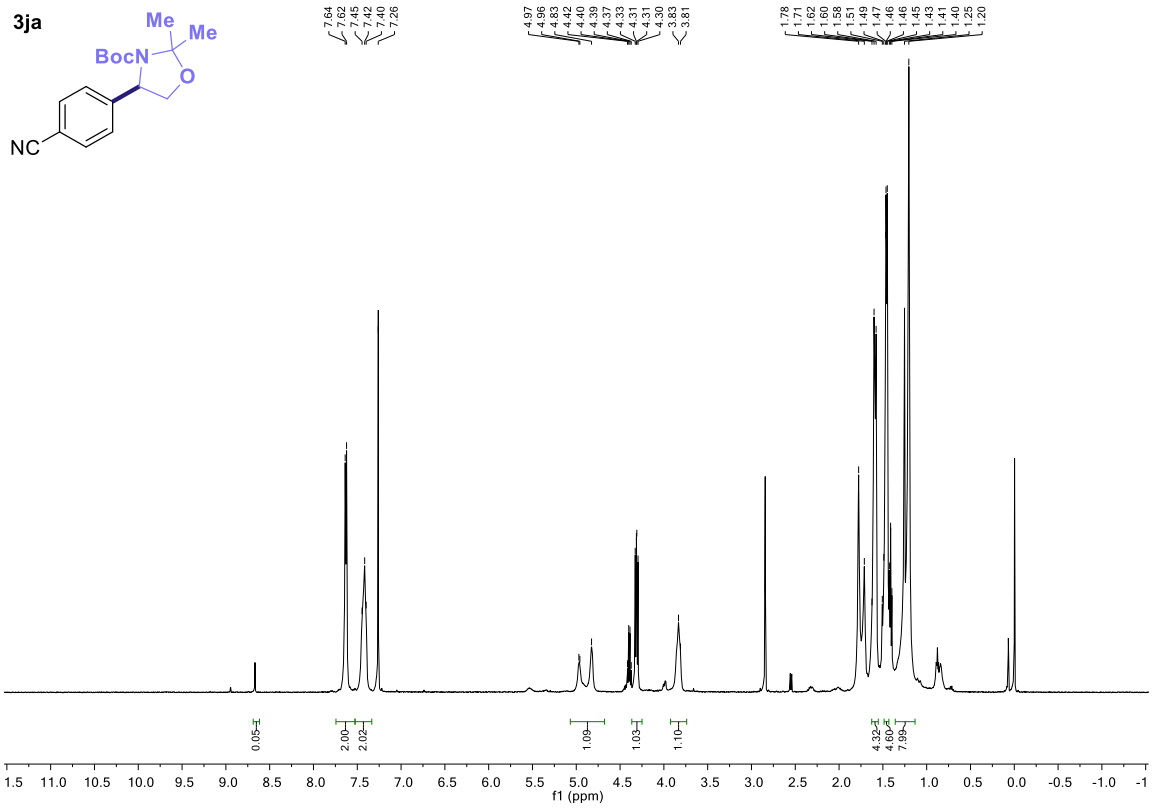

^{13}C NMR ($CDCl_3$, 126 MHz) of *tert*-butyl 4-(4-cyanophenyl)-2,2-dimethyloxazolidine-3-carboxylate (**6.4.14**)

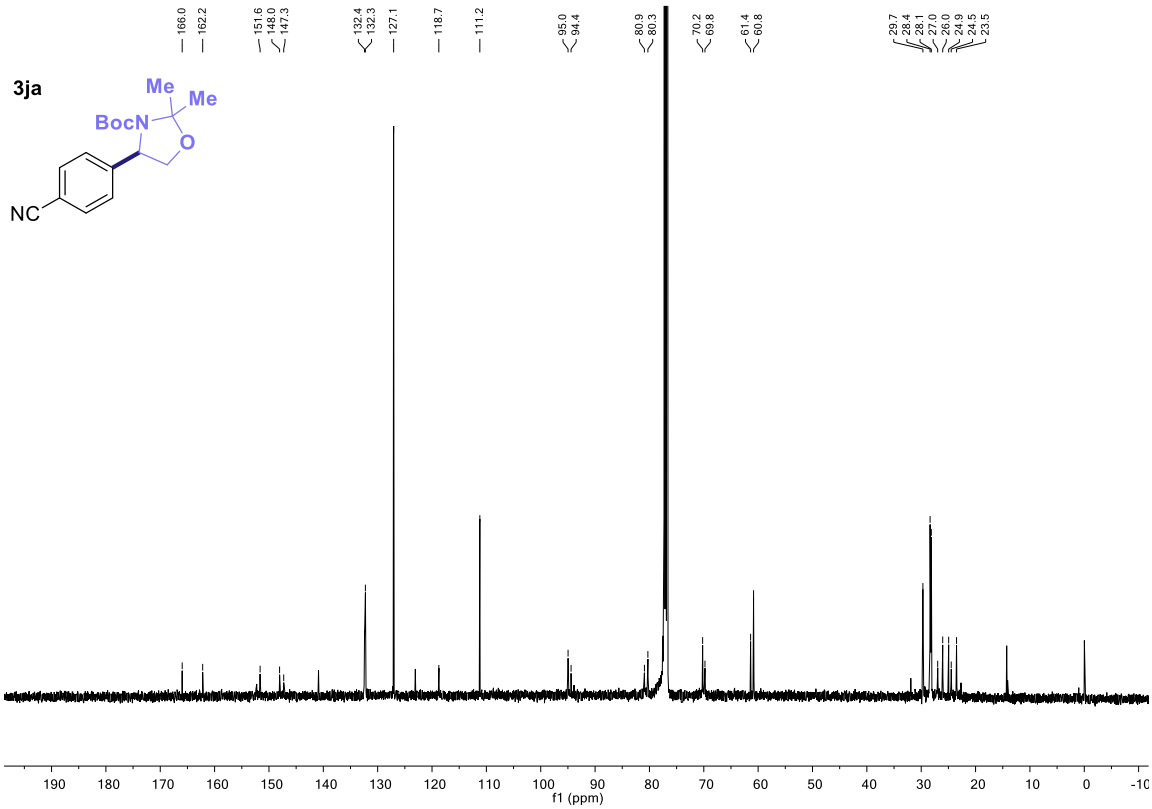

^{1}H NMR ($CDCl_3$, 500 MHz) of *tert*-butyl (1-(4-cyanophenyl)-2-phenylethyl)carbamate (**6.4.15**)

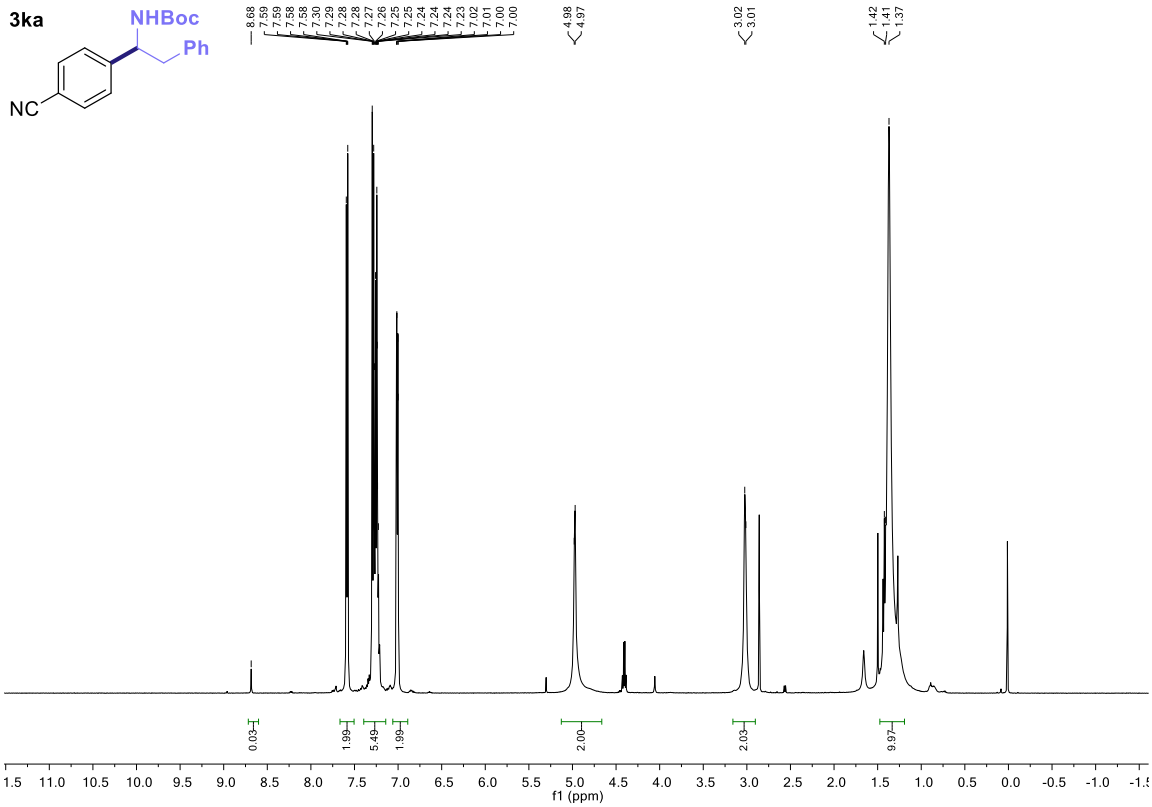

^{13}C NMR ($CDCl_3$, 126 MHz) of *tert*-butyl (1-(4-cyanophenyl)-2-phenylethyl)carbamate (**3ka**, **6.4.15**)

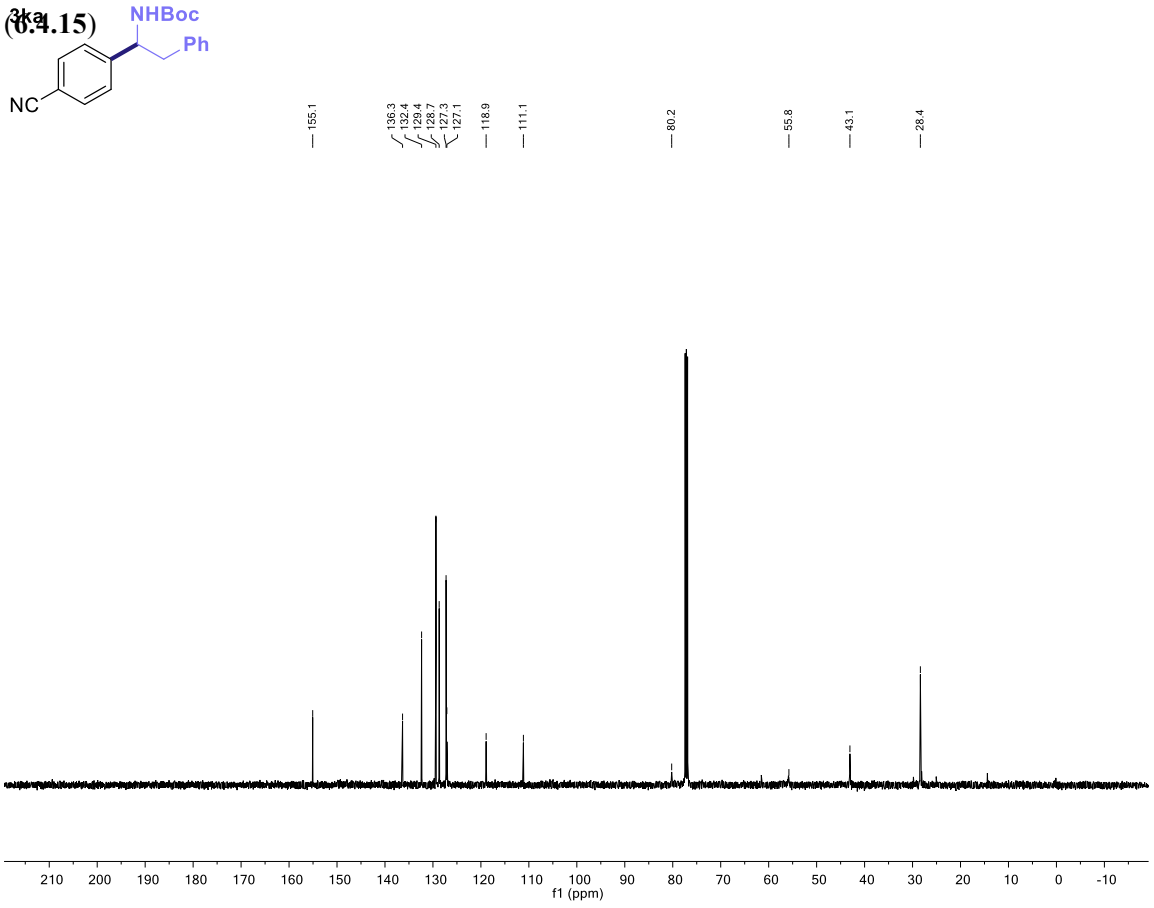

^{1}H and ^{13}C NMR Spectra: Synthesis of Aryl-Containing Saccharides

^{1}H NMR (DMSO-d_6, 500 MHz) of (3a*R*,5*S*,5a*R*,8a*S*,8b*R*)-5-(benzo[b]thiophen-2-yl)-2,2,7,7-tetramethyltetrahydro-5H-bis([1,3]dioxolo)[4,5-b:4',5'-d]pyran (**6.5.1**)

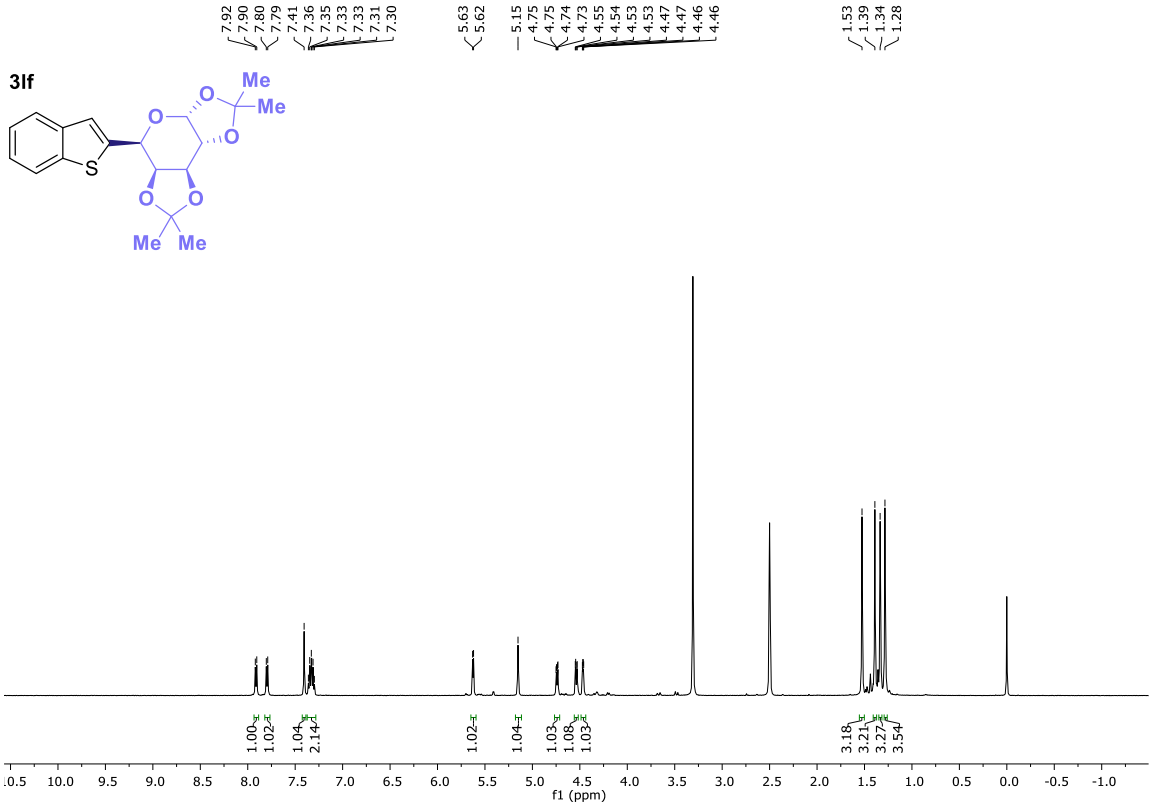

^{13}C NMR (DMSO-d_6, 126 MHz) of (3a*R*,5*S*,5a*R*,8a*S*,8b*R*)-5-(benzo[b]thiophen-2-yl)-2,2,7,7-tetramethyltetrahydro-5H-bis([1,3]dioxolo)[4,5-b:4',5'-d]pyran (**6.5.1**)

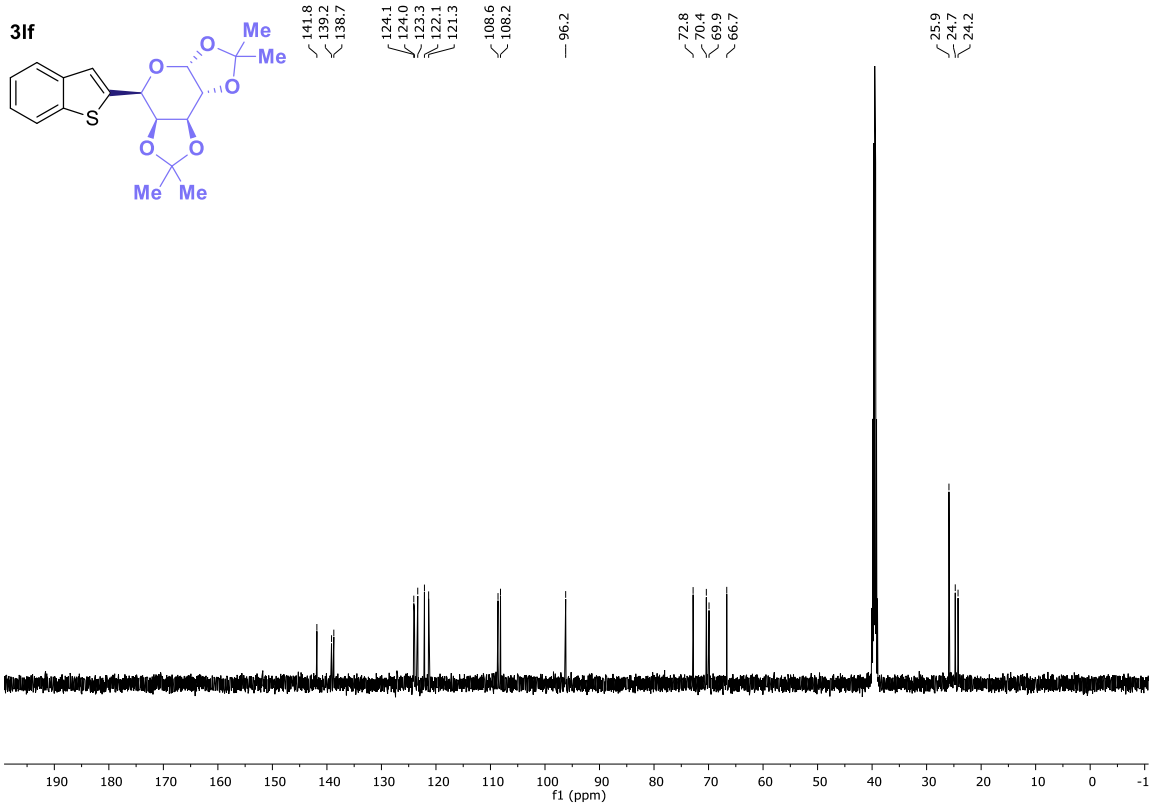

^{1}H NMR (DMSO-d_6, 500 MHz) of (2*R*,3*S*,4*S*,5*R*,6*S*)-2-(hydroxymethyl)-6-((6-(6-methylhept-5-en-2-yl)naphthalen-2-yl)oxy)tetrahydro-2H-pyran-3,4,5-triol (**6.5.2**)

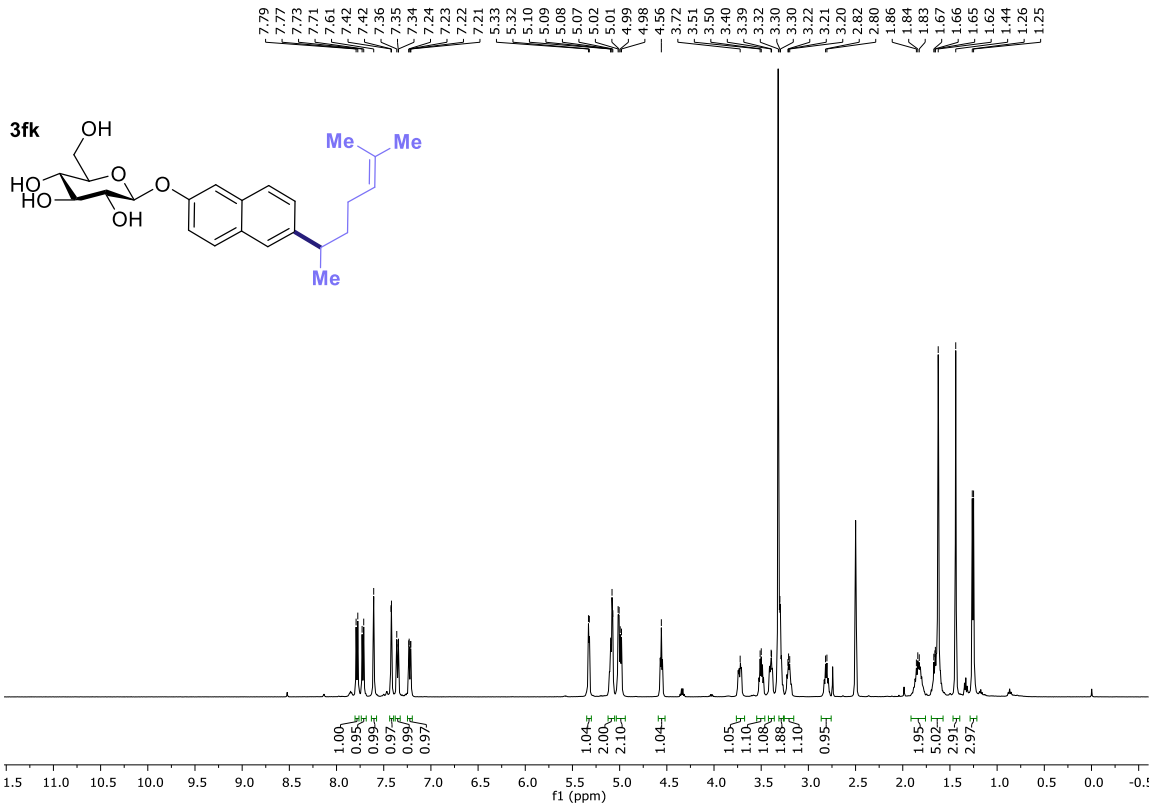

^{13}C NMR (DMSO-d_6, 126 MHz) of (2*R*,3*S*,4*S*,5*R*,6*S*)-2-(hydroxymethyl)-6-((6-(6-methylhept-5-en-2-yl)naphthalen-2-yl)oxy)tetrahydro-2H-pyran-3,4,5-triol (**6.5.2**)

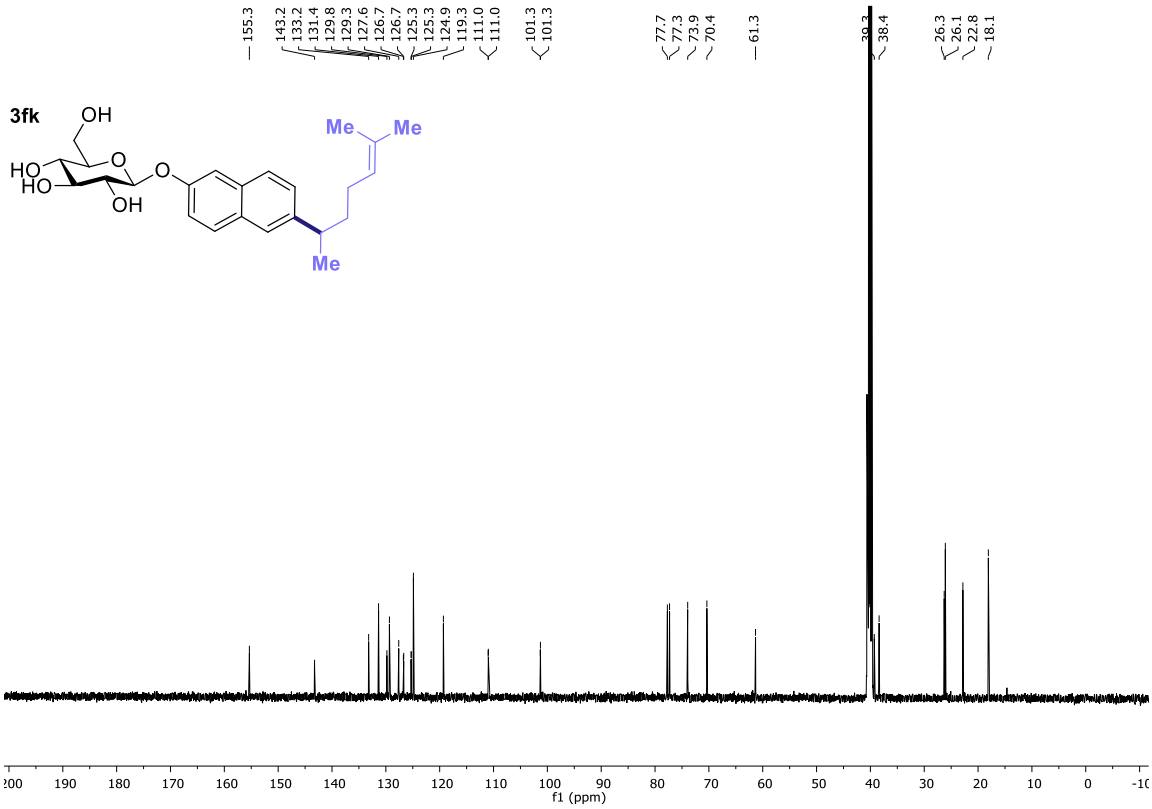

Chapter 7. Accessing Non-Classical Arylated Saccharides *via* Photoredox/Ni Dual Catalysis

7.1 Introduction

The incorporation of saccharide derivatives into lead compounds represents an attractive way to diversify drug candidate scaffolds by modulating crucial parameters related to the in vivo efficacy of a therapeutic drug (e.g., solubility, membrane transport, pharmacodynamics or pharmacokinetics).[1†] Notably, "reverse aryl C-glycosides"[2] comprise a class of saccharides that have proven to be efficient antibiotics,[3] antitumor agents[4] or inhibitors for diabetes.[2d,5] These glycosides have the particularity of bearing an aromatic moiety directly attached to the carbohydrate through a C-C bond, differentiating them from the usual O-glycosides, thus leading to better stability to both enzymatic and acidic hydrolysis, while preserving excellent biological efficacy.

Several routes toward anomeric, arylated saccharides have been reported,[2] such as Friedel-Crafts reactions or nucleophilic additions of organometallic reagents (e.g., organolithium or Grignard reagents) to suitable electrophiles. However, such methods suffer from serious drawbacks, including harsh acidic or basic conditions, low functional group tolerance, and undesired side-products arising from elimination or epimerization processes.

Recently, the transition metal-catalyzed cross-coupling of *in situ* generated glycosyl radicals[6] (from the corresponding glycosyl chloride or bromide) with organometallic reagents (aryl- or alkenylzinc and magnesium reagents) has emerged as one of the most efficient ways to access aryl C-saccharides (Figure 7.1). This transformation has been achieved in the presence of nickel,[7]

---

† Reproduced in part from Dumoulin, A.; Matsui, J. K.; Gutierrez-Bonet, A.; Molander, G. A. *Angew. Chem. Int. Ed.* **2018**, *57*, 6614.

cobalt[8] or iron[9] catalysts, affording the desired saccharide derivatives in moderate to good yields. Alternatively, pyranosylstannanes could be coupled with aryl halides in the presence of a palladium catalyst.[10] Despite these improvements, such reaction conditions remain limited in terms of functional group tolerance and operational simplicity as they involve highly reactive organometallic species that need to be freshly prepared and suffer from β-elimination.8a Furthermore, stoichiometric amounts of metal waste are generated. Finally, these processes rely on substitution reactions at the anomeric center, thus preventing the substrate from being further functionalized by traditional chemistry at the anomeric carbon.

In this context, the development of straightforward, modular, and operationally simple conditions to access C-arylated saccharides remains an unsolved challenge and, specifically, methods that would preserve the anomeric carbon to afford non-classical "reverse aryl C-glycosides" are particularly scarce. Indeed, despite their attractive biological properties,[11] few synthetic efforts have been carried out in this regard.[12]

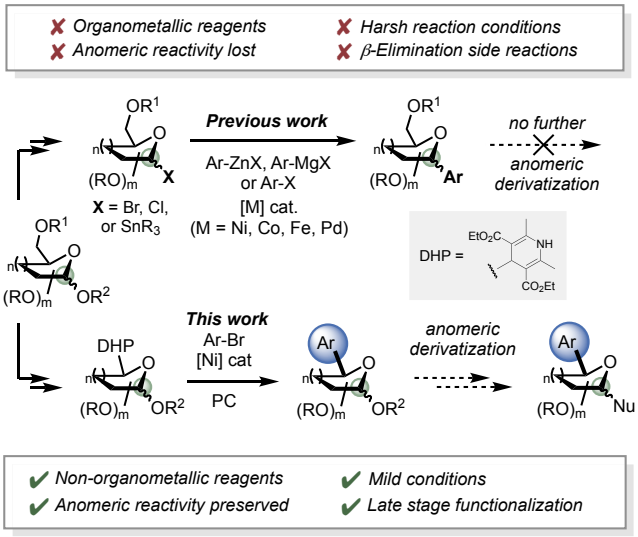

Figure 7.1. Previous routes accessing aryl monosaccharides.

Other approaches toward the synthesis of "reverse aryl C-glycosides" have been reported, such as the [4+2] cycloaddition between Danishefsky's dienes and aromatic aldehydes, yielding glycal derivatives,[13] or the addition of organozinc reagents to 4α-epoxypyranosides (Figure 7.2).[14]

However, these strategies are restricted to pyranoses, lack modularity, and require several extra steps to obtain the desired "reverse aryl C-glycoside."

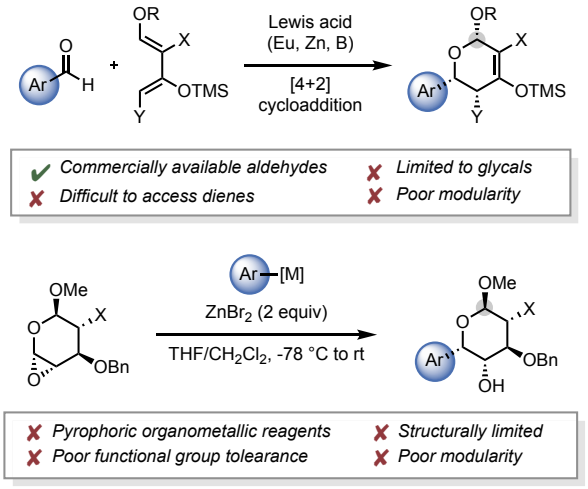

Figure 7.2. Cycloaddition and ring-opening approaches targeting reverse aryl C-glycosides.

In recent years, photoredox/nickel cross-coupling reactions have drawn extensive attention from the chemistry community.[15] Such processes allow the cross-coupling of Csp^3 nucleophiles under mild conditions by invoking a single-electron transmetalation pathway. Taking advantage of these modular and operationally simple conditions would allow access to virtually unexplored, non-classical, arylated saccharides. This approach would be a chemoselective strategy wherein arylation is directed to one of the two potential anomeric positions, one being masked by the DHP.[12]

7.2 Reaction Desigan and Results

With the goal of accessing glycosyl radicals that could be engaged in such dual catalytic processes, we turned our attention to 4-alkyl-1,4-dihydropyridine derivatives (DHPs).[16] These species have proven to afford Csp^3-centered alkyl radicals efficiently upon SET oxidation. In

addition to being bench stable and easy to handle, these compounds tolerate high functionalization levels owing to the mild reaction conditions required for their preparation from the corresponding aldehyde. A wide range of 4-glycosyl-1,4-DHPs was accessed from commercially available pentose and hexose derivatives via deprotection and oxidation chemistry to form the aldehyde. Using Tripathi and coworker's procedure, the monosaccharide DHPs were accessed via the reported acid-catalyzed condensation reaction.[17] It is worth mentioning that this synthetic pathway accommodated a broad range of carbohydrate derivatives (e.g., ribonucleoside, furanoses and pyranoses).

Next, the feasibility of the photoredox/nickel cross-coupling reaction between DHPs and 2-bromonaphthalene was studied by means of microscale high-throughput experimentation. Results from the screening revealed that the organic photocatalyst 4CzIPN (excited state E_{red} = +1.35 V vs SCE)[18] was extremely efficient in oxidatively cleaving the DHP [E_{red} = +1.20 V vs SCE], delivering the desired glycosyl radical (Figure 7.3). Among the advantages of 4CzIPN compared to traditional iridium-based photocatalyst are its lower cost ($4.7/mmol vs $140.0/mmol),[19] which provides significant benefit when it comes to industrial application. After further screening, the best yields were obtained in the presence of 2 mol % of 4-CzIPN photocatalyst, 5 mol % of $NiBr_2$•dme and 7 mol % of dMeObpy as a ligand in acetone at room temperature for 24 h. As expected, control experiments showed that all parameters were essential for the transformation to proceed.

Next, the generality of the reaction with respect to the DHP derivative was explored. As illustrated in Figure 7.3, the reaction was remarkably tolerant of substitution in the saccharide scaffold, providing the desired products in moderate to high yields. Notably, good to excellent diastereoselectivity was observed for certain furanosyl units (**7.3.1**, **7.3.4**, and **7.3.5**), likely because of steric interactions with the adjacent substituent, an effect observed by Nakamura and coworkers in their recent iron-catalyzed arylation of halosugars.[9] Excellent diastereoselectivity has also been

observed in the field of photoredox/Ni catalysis when 2-methylcyclopentyltrifluoroborate was coupled with aryl bromide, affording exclusively the trans product.[19]

The steric control on the L-arabinofuranose and D-xylofuranose derivatives was made evident when comparing the effect of the vicinal substituent, where small substituents (e.g., MeO and F, **7.3.2** and **7.3.3**, respectively) afforded poor drs, whereas sterically encumbered, TBS-protected moieties afforded excellent steric control (9:1 dr). D-Ribofuranosyl DHP afforded excellent dr. X-Ray crystallography confirmed the retention of configuration (**7.3.7**). Likewise, uridine-derived DHP afforded excellent diastereoselectivity, although in low yields; again, this highlights the prevalent role of steric interactions. Additionally, aryl pyranose **7.3.8** generated excellent dr with the aryl group cis to the dimethyl acetal protecting group (confirmed by X-ray crystallography). Not surprisingly, the more flexible radical leading to **7.3.9** afforded lower diastereoselectivity.[6,20,21] Finally, the TBS protecting group choice allowed the formation of unprotected derivative **7.3.5** upon TBAF addition to the crude reaction mixture of **7.3.4**.

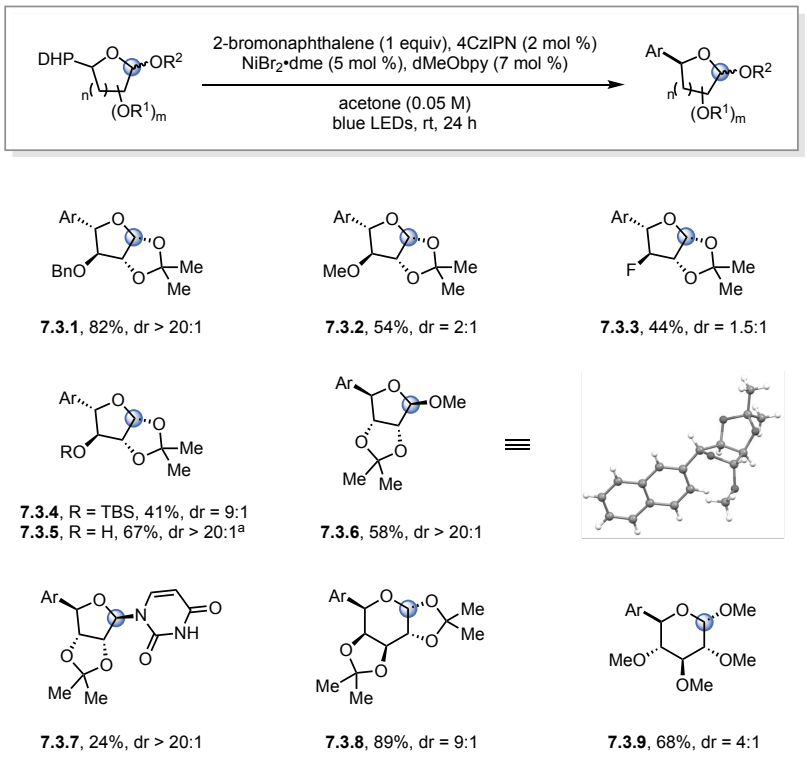

Figure 7.3. Modulating monosaccharide backbone.

The next step was to explore the limitations with respect to the (hetero)aryl bromide partner (Figure 7.4). Aryl bromides bearing electron-withdrawing groups exhibited excellent reactivity, affording the corresponding product in good yields and high diastereoselectivities (**7.3.1**–**7.3.2**, **7.3.4**–**7.3.7**). In addition, electron-neutral and electron-rich aryl bromides were tolerated (**7.3.8**–**7.3.11**). Notably, a pinacol boronic ester (**7.3.9**) was well accommodated, providing a group for further functionalization.[22] Although excellent functional group tolerance was observed, we hypothesize that the diminished yields with electron-neutral aryl bromides (**7.3.10** and **7.3.11**) result from a challenging oxidative addition. To access more complex structures, (hetero)aryl bromides, such as pyridine moieties (**7.3.12** and **7.3.13**), oxadiazoles (**7.3.14** and **7.3.16**) and thiophene derivatives (**7.3.15** and **7.3.17**), were successfully employed. Interestingly, carbonyl groups, which could react in the presence of organometallic reagents, pose no problem (**7.3.5**, **7.3.6** and **7.3.15**).

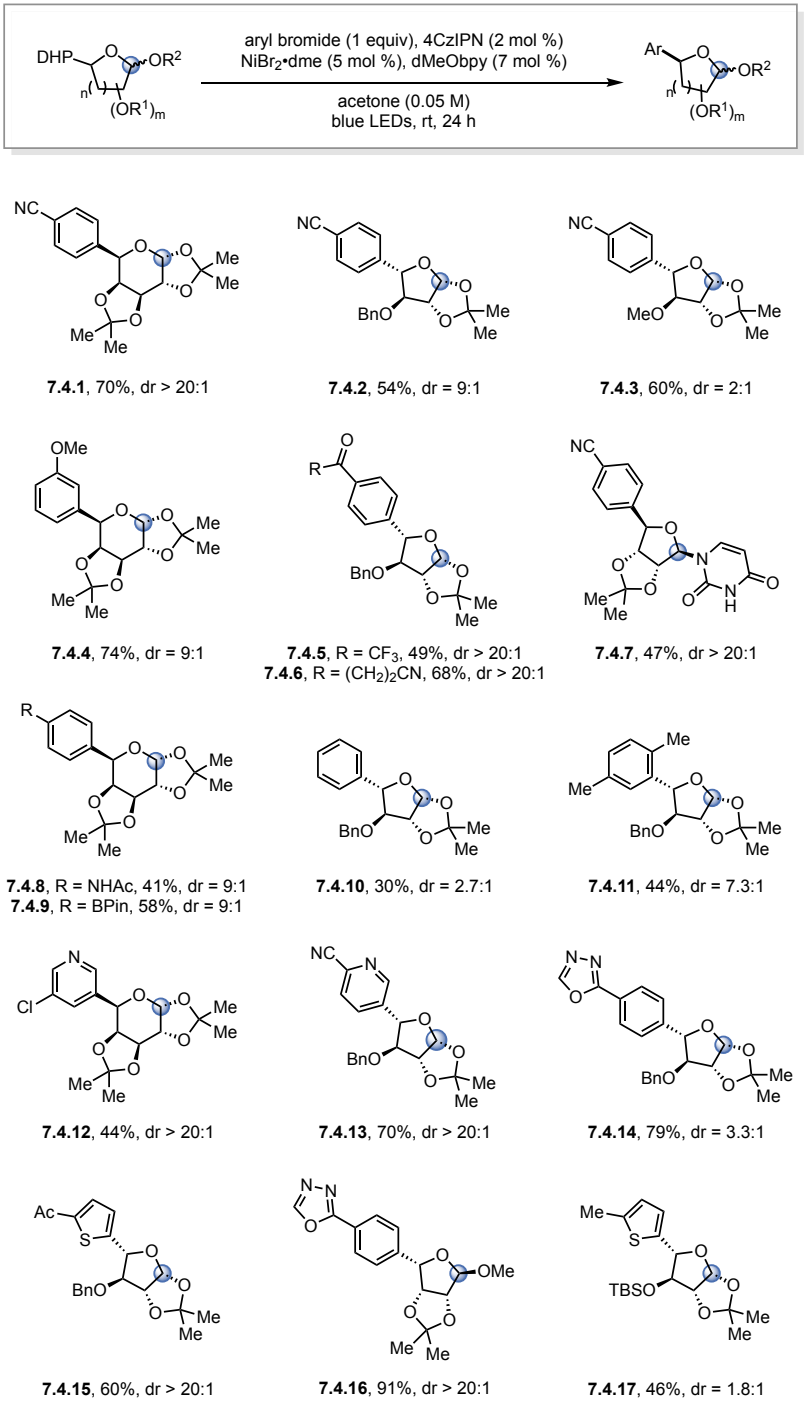

Figure 7.4. Demonstrating diversity with various aryl- and heteroaryl bromides.

To explore further the chemical diversity accessible through this method, several structurally complex molecules were engaged under the developed reaction conditions (Figure 7.5).

Coupling with a steroid derivative (**7.4.1**) proved successful, thus offering a privileged substructure of use in medicinal chemistry.[23] Recognizing the potential for late-stage functionalization, we introduced functional group-dense aryl bromides from Merck's chemistry informer library containing drug-like motifs.[24] A quinoxalinedione derivative, which is encountered in ionotropic glutamate receptor antagonists,[25] exhibited good reactivity under optimized conditions to furnish pyranose product **7.5.2** with excellent diastereocontrol. Even the more complex 3-bromothiophene derivative bearing a guanidine motif, belonging to the family of aspartic protease inhibitors,[26] afforded the desired products in high yield (**7.4.3**). In addition, a furanosyl residue could be introduced into the loratadine scaffold (**7.4.4**) under the standard reaction conditions.

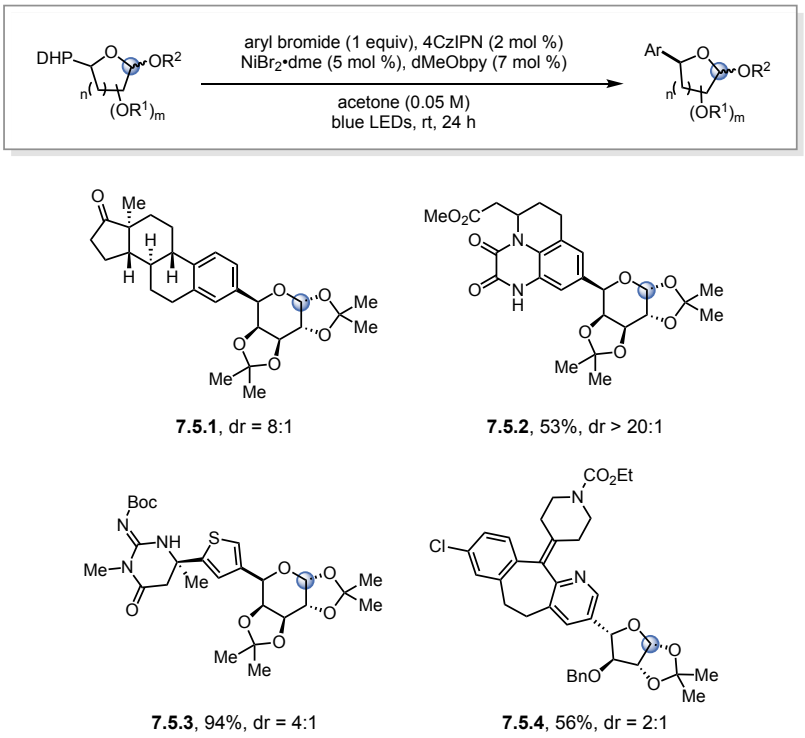

Figure 7.5. Late-stage functionalization.

Based on previous reports on the reactivity of DHPs under Ni/photoredox dual catalytic conditions,[16c,d] a plausible mechanism is outlined in Figure 7.6. This pathway involves the initial photoexcitation of the 4CzIPN photocatalyst (E_{red} = +1.35 V vs SCE), which undergoes reductive

quenching with the DHP derivative [E_{red} = + 1.20 V vs SCE]. The resulting radical cation A rapidly fragments to generate an aromatized pyridine derivative along with the corresponding saccharyl radical **B**. This latter species would first add to the active Ni(0) catalyst, thus producing a Ni(I)-saccharyl complex **C** that would undergo oxidative addition with the aryl bromide to afford the corresponding Ni(III) complex **D**.[27] Subsequent reductive elimination would take place to yield the cross-coupling product **2** and a Ni(I) species **E**. This latter complex would then be reduced to Ni(0) F with the reduced form of the 4CzIPN photocatalyst (E_{red} = + 1.21 V vs SCE), thus regenerating both active catalysts for subsequent catalytic cycles.

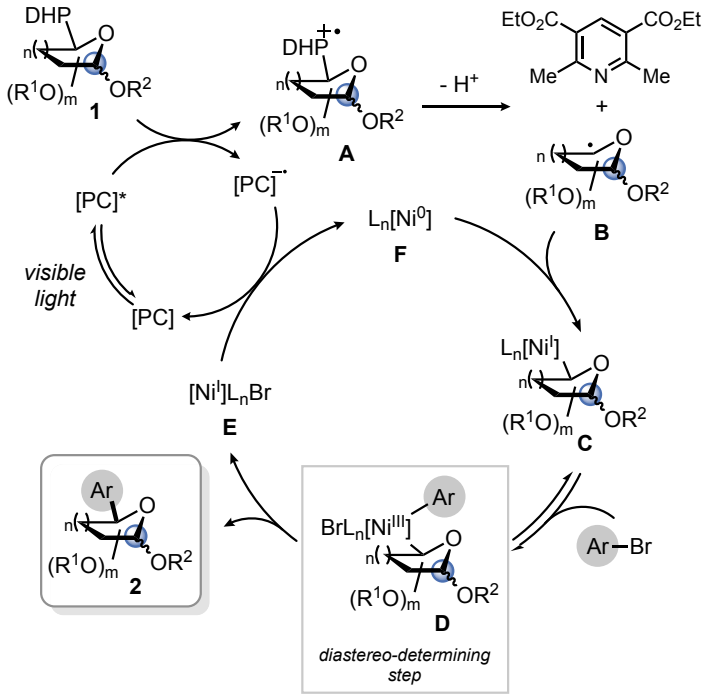

Figure 7.6. Proposed mechanism.

It is worth noting that although the saccharide backbone plays a key role in the observed diastereomeric ratios, leading in certain cases to substrate control products (e.g., **7.3.6**–**7.3.8**), it is evident when looking at other examples that the aryl bromide is playing a role as well (e.g., **7.4.2** and **7.4.10**), where different substitution patterns in the aromatic backbone lead to different

diastereoselectivity in the presence of the same saccharyl radical. Previous mechanistic studies suggest the high-valent Ni(III) species **D** ultimately dictates the observed diastereoselectivity after the irreversible reduction elimination;[28] therefore, we sought to improve the lower drs by identifying suitable ligands. Bidentate and tridentate ligands were screened with both Ni(0) and Ni(II) species. Modifying the bipyridine backbone by replacing electron-donating methoxy groups with bulkier, less electron-rich, *tert*-butyl substituents afforded excellent diastereoselectivities, improving from 3.3:1 dr to >20:1, for example (**7.7.2**). Alternatively, the use of phenanthroline resulted in a >20:1 dr for hexose 1,4-dihydropyridine (**7.7.3**), whereas the previously successful dtbbpy showed no improvement. Although the subtleties dictating the diastereoselectivity remain elusive, it is clear that diastereoselectivities can be improved on a case-by-case basis, if needed, through effective screening efforts. Further mechanistic studies are ongoing to shed light on these ligand effects.

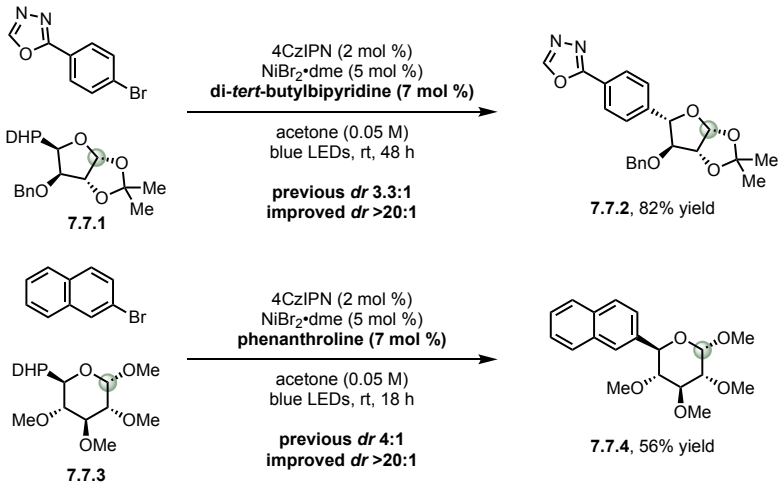

Figure 7.7. Modulating diastereoselectivity.

7.3 Conclusion

In summary, we disclosed the first general synthesis of non-classical, "reverse" aryl C-glycosides via Ni/photoredox dual catalysis using dihydropyridyl saccharide motifs as radical

precursors. The optimized conditions provide straightforward access to a wide variety of highly functionalized, arylated saccharides. Further studies were conducted to improve observed diastereoselectivities by targeting the diastereo-determining step, reductive elimination from the high-valent Ni(III) complex. This new strategy could find broad applications in the field of medicinal chemistry research, affording structurally novel materials that have been largely underexplored

7.4 References

[1] Gantt, R.W.; Peltier-Pain, P.; Thorson, J. S. *Nat. Prod. Rep.* **2011**, *28*, 1811.

[2] Selected books and reviews: a) Jaramillo, C.; Knapp, S. *Synthesis* **1994**, 1. b) Lee, D. He, M.. *Curr. Top. Med. Chem.* **2005**, *5*, 1333. c) Bililign, T.; Griffith, B. R.; Thorson, J. S. *Nat. Prod. Rep.* **2005**, *22*, 742. d) Bokor, E.; Kun, S.; Goyard, D.; Tth, M.; Praly, J.-P.; Vidal, S.; Somsk, L. *Chem. Rev.* **2017**, *117*, 1687.

[3] a) Hacksell, U.; Daves, G. D. *Progress in Medicinal Chemistry* Vol. 22, Elsevier, Amsterdam, **1985**, pp. 1. b) Buchanan, J. G. *Progress in the Chemistry of Organic Natural Products*, Vol. 44, Springer, New York, **1985**, p. 243.

[4] Selected examples: a) Hosoya, T.; Takashiro, E.; Matsumoto, T.; Suzuki, K. *J. Am. Chem. Soc.* **1994**, *116*, 1004. b) Parker, K. A.; Koh, Y. *J. Am. Chem. Soc.* **1994**, *116*, 11149. c) Cai, X.; Ng, K.; Panesar, H.; Moon, S.-J.; Paredes, M.; Ishida, K.; Hertweck, C.; Minehan, T. G. *Org. Lett.* **2014**, *16*, 2962.

[5] Selected reviews and articles: a) Fujita, Y.; Inagaki, N. J. *Diabetes Invest.* **2014**, *5*, 265. b) Zhang, Y.; Liu, Z.-P. *Curr. Med. Chem.* **2016**, *23*, 832. c) Goodwin, N. C.; Ding, Z.-M.; Harrison, B. A.; Strobel, E. D.; Harris, A. L.; Smith, M.; Thompson, A. Y.; Xiong, W.; Mseeh,

F.; Bruce, D. J.; Diaz, D.; Gopinathan, S.; Li, L.; ONeill, E.; Thiel, M.; Wilson, A. G. E.; Carson, K. G.; Powell, D. R.; Rawlins, D. B. *J. Med. Chem.* **2017**, *60*, 710.

[6] Togo, H.; He, W.; Waki, Y.; Yokoyama, M. *Synlett* **1998**, *7*, 700.

[7] Gong, H.; Gagn, M. R. *J. Am. Chem. Soc.* **2008**, *130*, 12177.

[8] a) Nicolas, L.; Angibaud, P.; Stansfield, I.; Bonnet, P.; Meerpoel, L.; Reymond, S.; Cossy, J. *Angew. Chem. Int. Ed.* **2012**, *51*, 1110. b) Nicolas, L.; Izquierdo, E.; Angibaud, P.; Stansfield, I.; Meerpoel, L.; Reymond, S.; Cossy, J. *J. Org. Chem.* **2013**, *78*, 11807.

[9] Adak, L.; Kawamura, S.; Toma, G.; Takenaka, T.; Isozaki, K.; Takaya, H.; Orita, A.; Li, H. C.; Shing, T. K. M., Nakamura, M. *J. Am. Chem. Soc.* **2017**, *139*, 10693.

[10] a) Zhu, F.; Rodriguez, J.; Yang, T.; Kevlishvili, I.; Miller, E.; Yi, D.; ONeill, S.; Rourke, M. J.; Liu, P.; Walczak, M. A. *J. Am. Chem. Soc.* **2017**, *139*, 17908. b) Zhu, F.; Rourke, M. J.; Yang, T.; Rodriguez, J.; Walczak, M. A. *J. Am. Chem. Soc.* **2016**, *138*, 12049.

[11] For selected examples: a) Goodwin, N. C.; Mabon, R.; Harrison, B. A.; Shadoan, M. K.; Almstead, Z. Y.; Xie, Y.; Healy, J.; Buhring, L. M.; DaCosta, C. M.; Bardenhagen, J.; Mseeh, F.; Liu, Q.; Nouraldeen, A.; Wilson, A. G. E.; Kimball, S. D.; Powell, D. R.; Rawlins, D. B. *J. Med. Chem.* **2009**, *52*, 6201. b) Zˇupancˇic´, N.; Ban, Zˇ.; Matic´, J.; Saftic´, D.; Glavasˇ-Obrovac, L.; Zˇinic´, B. *Croat. Chem. Acta* **2015**, *88*, 43.

[12] a) Hashmi, I. A.; Feist, H.; Michalik, M.; Reinke, H.; Peseke, K.; *J. Carbohydr. Chem.* **2006**, *25*, 19. b) Hashmi, I. A.; Ali, F. I.; Fiest, H.; Peseke, K. *Synth. Commun.* **2010**, *40*, 1243. c) Kaliappan, K. P.; Subrahmanyam, A. V. *Org. Lett.* **2007**, *9*, 1121. d) Chakraborty, S.; Das, G.; Ghosh, S.; Mal, D. *Org. Biomol. Chem.* **2016**, *14*, 10636.

[13] (a) Bednarski, M.; Danishefsky, S. *J. Am. Chem. Soc.* **1986**, *108*, 7060. (b) Berkowitz, D. B.; Danishefsky, S. J.; Schulte, G. K. *J. Am. Chem. Soc.* **1992**, *114*, 4518. (c) Helliwell, M.; Phillips, I. M.; Pritchard, R. G.; Stoodley, R. J. *Tetrahedron Lett.* **1999**, *40*, 8651.

[14] Cheng, G.; Fan, R.; Hernández-Torres, J. M.; Boulineau, F. P.; Wei, A. *Org. Lett.* **2007**, *9*, 4849.

[15] For selected reviews: (a) Prier, C. K.; Rankic, D. A.; MacMillan, D. W. C. *Chem. Rev.* **2013**, *113*, 5322. (b) Tellis, J. C.; Kelly, C. B.; Primer, D. N.; Jouffroy, M.; Patel, N. R.; Molander, G. A. *Acc. Chem. Res.* **2016**, *49*, 1429. (c) Cavalcanti, L. N.; Molander, G. A. *Top. Curr. Chem.* **2016**, *374*, 39.

[16]For selected examples: (a) Nakajima, K.; Nojima, S.; Sakata, K.; Nishibayashi, Y. *ChemCatChem* **2016**, *8*, 1028. (b) Chen, W.; Liu, Z.; Tian, J.; Li, J.; Ma, J.; Cheng, X.; Li, G. *J. Am. Chem. Soc.* **2016**, *138*, 12312. (c) Nakajima, K.; Nojima, S.; Nishibayashi, Y. *Angew. Chem. Int. Ed.* **2016**, *55*, 14106. (d) Gutiérrez-Bonet, Á; Tellis, J. C.; Matsui, J. K.; Vara, B. A.; Molander, G. A. *ACS Catal.* **2016**, *6*, 8004. (e) Gutiérrez-Bonet, Á; Remeur, C.; Matsui, J. K.; Molander, G. A. *J. Am. Chem. Soc.* **2017**, *139*, 12251. (f) Buzzetti, L.; Prieto, A.; Roy, S. R.; Melchiorre, P. *Angew. Chem., Int. Ed.* **2017**, *56*, 15039. (g) Verrier, C.; Alandini, N.; Pezzetta, C.; Moliterno, M.; Buzzetti, L.; Hepburn, H. B.; Vega-Penaloza, A.; Silvi, M.; Melchiorre, P. *ACS Catal.* **2018**, *8*, 1062.

[17] Tewari, N.; Dwivedi, N.; Tripathi, R. P. *Tetrahedron Lett.* **2004**, *45*, 9011.

[18] Luo, J.; Zhang, J. *ACS Catalysis* **2016**, *6*, 873.

[19] Primer, D. N.; Karakaya, I.; Molander, G. A. *J. Am. Chem. Soc.* **2015**, *137*, 2195.

[20] For selected reviews on the conformation of glycosyl radical species: (a) Dupuis, J.; Giese, B.; Rüegge, D.; Fischer, H.; Korth, H.-G.; Sustmann, R. *Angew. Chem. Int. Ed.* **1984**, *23*, 896. (b) Giese, B. *Angew. Chem. Int. Ed*. **1989**, *28*, 969. (c) Beckwith, A. L. J.; Duggan, P. J. *Tetrahedron* **1998**, *54*, 6919. (d) Rychnovsky, S. D.; Powers, J. P.; LePage, T. J. *J. Am. Chem. Soc*. **1992**, *114*, 8375.

[21] Absolute configurations were determined either by comparison with the literature data or by X-ray crystal structure analysis when possible (see the Experimental Section for further details).

[22] Yamashita, Y.; Tellis, J. C.; Molander, G. A. *Proc. Natl. Acad. Sci.* **2015**, *112*, 12026.

[23] Ono, M.; Takamura, C.; Sugita, F.; Masuoka, C.; Yoshimitsu, H.; Ikeda, T.; Nohara, T. *Chem. Pharm. Bull.* **2007**, *55*, 551.

[24] Kutchukian, P. S.; Dropinski, J. F.; Dykstra, K. D.; Li, B.; DiRocco, D. A.; Streckfuss, E. C.; Campeau, L.-C.; Cernak, T.; Vachal, P.; Davies, I. W.; Krska, S. W.; Dreher, S. D. *Chem. Sci.* **2016**, *7*, 2604.

[25] Turski, L.; Schneider, H. H.; Neuhaus, R.; McDonald, F.; Jones, G. H.; Löfberg, B.; Schweinfurth, H.; Huth, A.; Krüger, M.; Ottow, E. *Restor. Neurol. Neurosci.* **2000**, *17*, 45.

[26] Iserloh, U.; Gu, H.; Qian, G.; Tadesse, D.; Lai, G.; Duo, J. Heterocyclic aspartyl protease inhibitors. PCT Int. Appl. WO2008/103351 A2, 2008.

[27] a) Anderson, T. J.; Jones, G. D.; Vicic, D. A. *J. Am. Chem. Soc*. **2004**, *126*, 8100. (b) Jones, G. D.; McFarland, C.; Anderson, T. J.; Vicic, D. A. *Chem. Comm.* **2005**, *33*, 421.

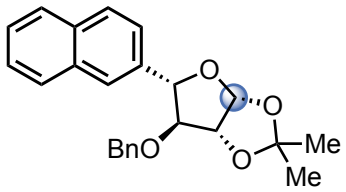

(3a*R*,5*S*,6*S*,6a*R*)-6-(Benzyloxy)-2,2-dimethyl-5-(naphthalen-2-yl)tetrahydrofuro[2,3-d][1,3]dioxole (7.3.1): Following General Procedure I using corresponding DHP (375.9 mg, 0.75 mmol, 1.5 equiv), 2-bromonaphthalene (103.0 mg, 0.5 mmol, 1.0 equiv), 4-CzIPN (7.8 mg, 0.01 mmol, 2 mol %), $NiBr_2$·dme (7.7 mg, 0.025 mmol, 5 mol %), and dMeObpy (7.5 mg, 0.035 mmol, 7 mol %) in anhydrous acetone (5.0 mL, 0.1 M). The product was purified by flash chromatography on silica gel (hexanes/EtOAc 0 to 10%, 10 to 30%) to afford a semi solid (154.2 mg, 82% yield). dr > 20:1 based on ^{1}H NMR of the crude reaction mixture.

^{1}H NMR (500 MHz, $CDCl_3$) δ 7.89 (s, 1H), 7.81 (d, *J* = 7.7 Hz, 3H), 7.48 (dd, *J* = 17.7, 7.8 Hz, 3H), 7.33 (d, *J* = 19.5 Hz, 5H), 6.06 (s, 1H), 5.19 (s, 1H), 4.84 – 4.68 (m, 2H), 4.61 (d, *J* = 11.7 Hz, 1H), 4.19 (s, 1H), 1.40 (s, 3H), 1.38 (s, 3H) ppm.

^{13}C NMR (126 MHz, $CDCl_3$) δ 137.4, 137.0, 133.2, 133.0, 128.7, 128.2, 128.2, 128.2, 128.0, 127.8, 126.3, 126.0, 124.8, 123.9, 114.0, 105.5, 88.3, 86.0, 84.8, 72.4, 27.3, 27.0 ppm.

IR (neat, cm^{-1}): 3060, 2936, 1455, 1382, 1074, 860.

HRMS (EI+) *calcd for* $C_{24}H_{24}O_4$ $[M]^+$ 376.1675, *found* 376.1670.

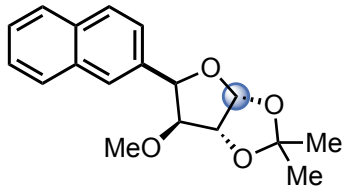

(3a*R*,5*R*,6*S*,6a*R*)-6-Methoxy-2,2-dimethyl-5-(naphthalen-2-yl)tetrahydrofuro[2,3-d][1,3]dioxole (7.3.2): Following General Procedure II using corresponding DHP (300.9 mg, 0.6 mmol, 2.0 equiv), 2-bromonaphthalene (62.1 mg, 0.3 mmol, 1.0 equiv), 4-CzIPN (4.7 mg, 0.006 mmol, 2 mol %), $NiBr_2$·dme (9.2 mg, 0.03 mmol, 10 mol %), and dMeObpy (9.1 mg, 0.042 mmol, 14 mol %) in anhydrous acetone (6.0 mL, 0.05 M). The product was purified by flash chromatography on silica gel (hexanes/EtOAc 0 to 15%) to afford a white solid (40.0 mg, 44% yield). dr = 2:1 based on ^{1}H NMR of the crude reaction mixture. mp = 68-70 °C. ^{1}H NMR (500 MHz, $CDCl_3$, major diastereomer) δ 7.95 (s, 1H), 7.87 – 7.81 (m, 3H), 7.59 – 7.44 (m, 3H), 6.04 (d, *J* = 4.0 Hz, 1H), 5.10 (d, *J* = 5.0 Hz, 1H), 4.71 (dd, *J* = 4.0, 1.5 Hz, 1H), 3.97 (dd, *J* = 4.5, 1.0 Hz, 1H), 3.50 (s, 3H), 1.43 (s, 3H), 1.39 (s, 3H) ppm. ^{1}H NMR (500 MHz, $CDCl_3$, minor diastereomer) δ 7.92 (s, 1H), 7.87 – 7.81 (m, 3H), 7.59 – 7.44 (m, 3H), 6.16 (d, *J* = 3.5 Hz, 1H), 5.44 (d, *J* = 3.0 Hz, 1H), 4.73 (d, *J* = 3.5 Hz, 1H), 3.91 (d, *J* = 3.0 Hz, 1H), 3.05 (s, 3H), 1.61 (s, 3H), 1.41 (s, 3H) ppm. ^{13}C NMR (126 MHz, $CDCl_3$, major diastereomer) δ 137.1, 133.3, 133.1, 128.2, 128.2, 127.8, 126.3, 126.0, 124.9, 123.9, 113.9, 105.4, 90.6, 85.5, 84.8, 58.1, 27.4, 27.0 ppm. ^{13}C NMR (126 MHz, $CDCl_3$, minor diastereomer) δ 137.1, 133.3, 133.2, 128.3, 128.2, 127.7, 126.1, 125.9, 125.1, 123.9, 111.8, 105.0, 86.3, 82.9, 81.9, 58.6, 27.0, 26.4 ppm. IR (neat, cm^{-1}): 2987, 2934, 1373, 1382, 1315, 1193, 958. HRMS (EI+) *calcd for* $C_{18}H_{20}O_4$ $[M]^+$ 300.1362, *found* 300.1350.

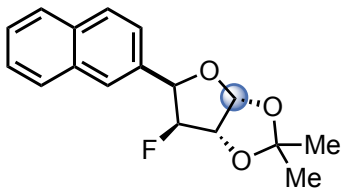

(3a*R*,6*S*,6a*S*)-6-Fluoro-2,2-dimethyl-5-(naphthalen-2-yl)tetrahydrofuro[2,3-*d*][1,3]dioxole (7.3.3): Following General Procedure II using corresponding DHP (248.1 mg, 0.6 mmol, 2.0

equiv), 2-bromonaphthalene (62.1 mg, 0.3 mmol, 1.0 equiv), 4-CzIPN (4.7 mg, 0.006 mmol, 2 mol %), $NiBr_2$·dme (9.3 mg, 0.03 mmol, 10 mol %), and dMeObpy (9.1 mg, 0.042 mmol, 14 mol %) in anhydrous acetone (6.0 mL, 0.05 M). The two diastereomers were independently isolated by flash chromatography on silica gel (hexanes/EtOAc 0 to 5%) as crystalline white solids (25.1 mg, 29% yield, dr = 6.7:1 for the major diastereomer, 12.9 mg, 15% yield, dr > 20:1 for the minor diastereomer. 44% combined yield). mp (minor) = 81-84 ºC, mp (major) = 90-94 ºC. dr = 1.5:1 based on ^{1}H NMR of the crude reaction mixture. ^{1}H NMR (500 MHz, $CDCl_3$, minor diastereomer) δ 7.97 (s, 1H), 7.90 – 7.80 (m, 3H), 7.54 (d, *J* = 8.5 Hz, 1H), 7.51 – 7.44 (m, 2H), 6.17 (d, *J* = 3.9 Hz, 1H), 5.49 (d, *J* = 24.1 Hz, 1H), 5.29 (d, *J* = 50.1 Hz, 1H), 4.87 (dd, *J* = 14.7, 4.0 Hz, 1H), 1.31 (s, 3H), 1.18 (s, 3H) ppm. ^{13}C NMR (126 MHz, $CDCl_3$, minor diastereomer) δ 133.1, 133.0, 128.3, 128.2, 127.8, 126.5, 126.2 (2C), 125.0, 123.7, 113.7, 106.0, 99.2 (d, *J* = 182.5 Hz), 86.1 (d, *J* = 26.8 Hz), 84.7 (d, *J* = 32.0 Hz), 26.5, 26.3 ppm. ^{1}H NMR (500 MHz, $CDCl_3$, major diastereomer) δ 7.92 (s, 1H), 7.89 – 7.81 (m, 3H), 7.57 – 7.44 (m, 3H), 6.23 (d, *J* = 3.7 Hz, 1H), 5.45 (d, *J* = 29.4 Hz, 1H), 5.06 (dd, *J* = 49.7, 1.8 Hz, 1H), 4.86 (dd, *J* = 10.1, 3.8 Hz, 1H), 1.61 (s, 3H), 1.41 (s, 3H) ppm. ^{13}C NMR (126 MHz, $CDCl_3$, major diastereomer) δ 133.4, 133.3, 131.3 (d, *J* = 3.7 Hz), 128.2, 128.0, 127.9, 126.5, 126.3, 126.3, 124.9, 112.4, 105.0, 95.2 (d, *J* = 187.2 Hz), 83.0 (d, *J* = 32.8 Hz), 81.6 (d, *J* = 19.2 Hz), 26.9, 26.4 ppm. ^{19}F NMR (471 MHz, $CDCl_3$) δ -183.14, -203.98 ppm. IR (neat, cm^{-1}): 2960, 2924, 2850, 1374, 1119, 1053, 1001 (minor diastereomer), 2992, 2938, 1386, 1374, 1217, 1163, 1079, 1020 (major diastereomer). HRMS (EI+) *calcd for* $C_{18}H_{20}O_4$ $[M]^+$ 288.1156, *found* 288.1177.

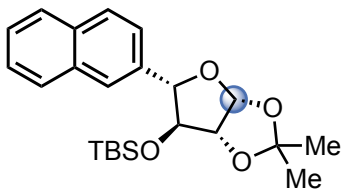

***tert*-Butyl(((3a*R*,6*S*,6a*R*)-2,2-dimethyl-5-(naphthalen-2-yl)tetrahydrofuro[2,3-*d*][1,3]dioxol-6-yl)oxy)dimethylsilane (7.3.4):** Following General Procedure I using corresponding DHP (262.9 mg, 0.5 mmol, 2.0 equiv), 2-bromonaphthalene (51.8 mg, 0.25 mmol, 1.0 equiv), 4-CzIPN (3.9 mg, 0.005 mmol, 2 mol %), $NiBr_2 \cdot$dme (3.9 mg, 0.00125 mmol, 5 mol %), and dMeObpy (3.8 mg, 0.0175 mmol, 7 mol %) in anhydrous acetone (5.0 mL, 0.05 M). The product was purified by flash chromatography on silica gel (hexanes/EtOAc 0 to 10%) to afford a yellow, viscous oil (40.9 mg, 41% yield). dr = 9:1 based on ^{1}H NMR of the crude reaction mixture. ^{1}H NMR (500 MHz, $CDCl_3$) δ 7.90 (s, 1H), 7.88 – 7.76 (m, 3H), 7.53 (d, J = 8.5 Hz, 1H), 7.49 – 7.42 (m, 2H), 6.02 (d, J = 4.0 Hz, 1H), 4.97 (d, J = 4.9 Hz, 1H), 4.58 (d, J = 4.0 Hz, 1H), 4.32 (d, J = 4.9 Hz, 1H), 1.43 (s, 3H), 1.37 (s, 3H), 0.90 (s, 9H), 0.05 (s, 3H), -0.03 (s, 3H) ppm. ^{13}C NMR (126 MHz, $CDCl_3$) δ 136.8, 133.2, 133.1, 128.2, 128.1, 127.8, 126.2, 125.9, 125.1, 124.0, 113.8, 105.1, 88.6, 87.1, 82.6, 27.5, 27.2, 25.8, 18.1, -4.6, -4.8 ppm. IR (neat, cm^{-1}): 2953, 2930, 2858, 1472, 1382, 1257, 1119, 1079, 1017. HRMS (EI+) *calcd for* $C_{23}H_{32}O_4Si$ $[M]^+$ 400.2070, *found* 400.2080.

For the conformation elucidation of product **2d**, a combination of DEPT 45, COSY, HMBC and HSQC experiments were taken to unequivocally assigned each proton and carbon signals. Next, coupled ^{13}C NMR experiment allowed us to detect a $^2J_{C3,H4}$ constant of 5.5 Hz. When compared this value with previous literature, a relative *trans configuration* between the OTBS and the naphthyl groups was established.[1]

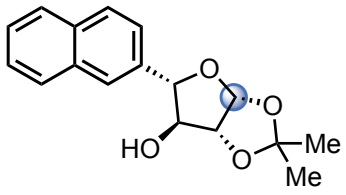

[1] Napolitano, J. G.; Gavín, J. A.; García, C.; Norte, M.; Fernández, J. J.; Hernández Daranas, A. *Chem. Eur. J.* **2011**, *17*, 6338.

(3a*R*,6*S*,6a*R*)-2,2-Dimethyl-5-(naphthalen-2-yl)tetrahydrofuro[2,3-d][1,3]dioxol-6-ol (7.3.5): Following General Procedure II using corresponding DHP (262.9 mg, 0.5 mmol, 2.0 equiv), 2-bromonaphthalene (51.8 mg, 0.25 mmol, 1.0 equiv), 4-CzIPN (3.9 mg, 0.005 mmol, 2 mol %), $NiBr_2$·dme (7.8 mg, 0.0025 mmol, 10 mol %), and dMeObpy (7.6 mg, 0.035 mmol, 14 mol %) in anhydrous acetone (4.0 mL, 0.05 M). After 24 h, a solution of TBAF (1.5 mL, 1.0 M in THF, 6.0 equiv) was added dropwise at 0 °C. The reaction was allowed to stir for 5 h at rt, then quenched by addition of a saturated aq solution of $NaHCO_3$ (15 mL). The aqueous layer was extracted with EtOAc (3 x 15 mL), the combined organic layers were dried ($MgSO_4$) and concentrated under reduced pressure. The crude was purified by flash chromatography on silica gel (hexanes/EtOAc 0 to 40%) to afford a crystalline solid (48.4 mg, 67% yield). dr > 20:1 based on ^{1}H NMR of the crude reaction mixture. mp = 105-107 °C. ^{1}H NMR (500 MHz, $CDCl_3$) δ 7.92 (s, 1H), 7.87 – 7.70 (m, 3H), 7.55 (dd, *J* = 8.6, 1.6 Hz, 1H), 7.50 – 7.36 (m, 2H), 6.04 (d, *J* = 4.1 Hz, 1H), 5.07 (d, *J* = 4.5 Hz, 1H), 4.66 (dd, *J* = 4.1, 1.5 Hz, 1H), 4.46 (s, 1H), 2.67 (d, *J* = 4.0 Hz, 1H), 1.34 (s, 6H) ppm. ^{13}C NMR (126 MHz, $CDCl_3$) δ 136.5, 133.2, 133.1, 128.3, 128.2, 127.8, 126.3, 126.1, 124.9, 123.9, 113.8, 105.3, 88.0, 87.0, 81.3, 27.0, 26.9 ppm. IR (neat, cm^{-1}): 3437, 2986, 2937, 1374, 1316, 1212, 1070, 1014. HRMS (EI+) *calcd for* $C_{17}H_{18}O_4$ $[M]^+$ 286.1205, *found* 286.1201.

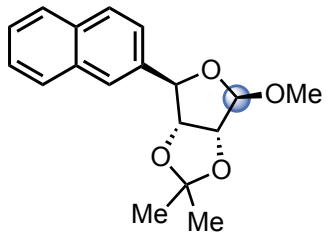

(3a*R*,4*R*,6*R*,6a*R*)-4-Methoxy-2,2-dimethyl-6-(naphthalen-2-yl)tetrahydrofuro[3,4-*d*][1,3]dioxole (7.3.6): Following General Procedure II using corresponding DHP (191.5 mg, 0.45 mmol, 1.5 equiv), 2-bromonaphthalene (62.1 mg, 0.3 mmol, 1.0 equiv), 4-CzIPN (4.7 mg, 0.006

mmol, 2 mol %), $NiBr_2$·dme (9.3 mg, 0.03 mmol, 10 mol %), and dMeObpy (9.1 mg, 0.042 mmol, 14 mol %) in anhydrous acetone (6.0 mL, 0.05 M). The product was purified by flash chromatography on silica gel (hexanes/EtOAc 0 to 10%) to afford a crystalline white solid (52.0 mg, 58% yield). mp = 104-106 ºC. dr > 20:1 based on ^{1}H NMR of the crude reaction mixture. ^{1}H NMR (500 MHz, $CDCl_3$) δ 7.87 – 7.80 (m, 4H), 7.53 (d, *J* = 8.9 Hz, 1H), 7.50 – 7.45 (m, 2H), 5.41 (s, 1H), 5.19 (s, 1H), 4.97 (dd, *J* = 5.9, 1.6 Hz, 1H), 4.72 (d, *J* = 6.0 Hz, 1H), 3.41 (s, 3H), 1.62 (s, 3H), 1.38 (s, 3H) ppm. ^{13}C NMR (126 MHz, $CDCl_3$) δ 138.0, 133.3, 133.0, 128.3, 128.2, 127.7, 126.3, 126.1, 125.3, 124.4, 113.1, 110.2, 89.4, 86.0, 85.9, 55.6, 27.0, 25.4 ppm. IR (neat, cm^{-1}): 2949, 2927, 2854, 1456, 1370, 1199, 1082, 825. HRMS (EI+) *calcd for* $C_{18}H_{20}O_4$ $[M]^+$ 300.1362, *found* 300.1369.

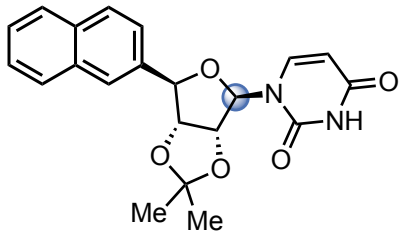

1-((3a*R*,6*R*,6a*R*)-2,2-Dimethyl-6-(naphthalen-2-yl)tetrahydrofuro[3,4-d][1,3]dioxol-4-yl) pyrimidine-2,4(1H,3H)-dione (7.3.7): Following General Procedure II using corresponding DHP (151.4 mg, 0.3 mmol, 1.0 equiv), 2-bromonaphthalene (124.2 mg, 0.6 mmol, 2.0 equiv), 4-CzIPN (4.7 mg, 0.006 mmol, 2 mol %), $NiBr_2$·dme (9.3 mg, 0.03 mmol, 10 mol %), and dMeObpy (9.1 mg, 0.042 mmol, 14 mol %) in anhydrous acetone (6.0 mL, 0.05 M). The product was purified by flash chromatography on silica gel (CH_2Cl_2/MeOH 0 to 10%) to afford a white solid (27,4 mg, 24% yield). mp = 137-139 ºC. dr > 20:1 based on ^{1}H NMR of the crude reaction mixture. ^{1}H NMR (500 MHz, $CDCl_3$) δ 9.13 (br s, 1H), 7.87 (d, *J* = 8.6 Hz, 1H), 7.85 – 7.80 (m, 3H), 7.52 (dd, *J* = 8.5, 1.5 Hz, 1H), 7.51 – 7.45 (m, 2H), 7.27 (d, *J* = 5.2 Hz, 1H), 5.86 (d, *J* = 2.2 Hz, 1H), 5.75 (d, *J* = 8.0

Hz, 1H), 5.18 (d, *J* = 5.3 Hz, 1H), 5.11 (dd, *J* = 6.5, 2.2 Hz, 1H), 4.98 (t, *J* = 5.0 Hz, 1H), 1.70 (s, 3H), 1.40 (s, 3H) ppm. ^{13}C NMR (126 MHz, $CDCl_3$) δ 163.4, 150.0, 142.3, 135.5, 133.4, 133.2, 128.9, 128.2, 127.9, 126.5, 126.4, 125.1, 123.5, 115.5, 102.9, 93.4, 87.6, 85.4, 84.4, 27.5, 25.6 ppm. IR (neat, cm^{-1}): 3214, 3085, 2981, 2919, 1697, 1387, 1293, 1072. HRMS (ES+) *calcd for* $C_{21}H_{21}N_2O_5$ $[M+H]^+$ 381.1450, *found* 381.1474.

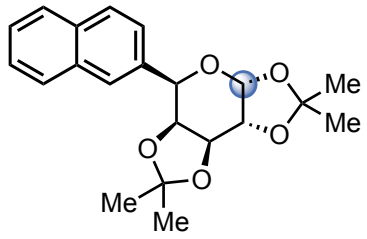

(3a*R*,5*R*,5a*S*,8a*S*,8b*R*)-2,2,7,7-Tetramethyl-5-(naphthalen-2-yl)tetrahydro-5H-bis([1,3]dioxolo)[4,5-b:4',5'-d]pyran (7.3.8): Following General Procedure I using corresponding DHP (216.7 mg, 0.45 mmol, 1.5 equiv), 2-bromonaphthalene (62.1 mg, 0.3 mmol, 1.0 equiv), 4-CzIPN (4.7 mg, 0.006 mmol, 2 mol %), $NiBr_2$·dme (4.6 mg, 0.015 mmol, 5 mol %), and dMeObpy (4.5 mg, 0.021 mmol, 7 mol %) in anhydrous acetone (6.0 mL, 0.05 M). The product was purified by flash chromatography on silica gel (hexanes/EtOAc 0 to 10%) to afford a white solid (95.1 mg, 89% yield). mp = 122-124 ºC. dr = 9:1 based on ^{1}H NMR of the crude reaction mixture. ^{1}H NMR (500 MHz, $CDCl_3$) δ 7.89 (s, 1H), 7.86 – 7.79 (m, 3H), 7.56 (d, *J* = 8.5 Hz, 1H), 7.49 – 7.42 (m, 2H), 5.80 (d, *J* = 5.0 Hz, 1H), 5.09 (s, 1H), 4.78 (dd, *J* = 7.8, 2.2 Hz, 1H), 4.57 (dd, *J* = 7.8, 1.9 Hz, 1H), 4.48 – 4.44 (m, 1H), 1.63 (s, 3H), 1.50 (s, 3H), 1.42 (s, 3H), 1.32 (s, 3H) ppm. ^{13}C NMR (126 MHz, $CDCl_3$) δ 135.3, 133.3, 133.1, 128.2, 127.8, 127.7, 126.0, 125.8 (2C), 125.0, 109.4, 108.8, 97.1, 74.0, 71.3, 70.9, 69.7, 26.4, 26.1, 25.1, 24.4 ppm. IR (neat, cm^{-1}): 2988, 1381, 1372, 1253, 1142, 1102, 963. HRMS (ES+) *calcd for* $C_{21}H_{24}O_5Na$ $[M+Na]^+$ 379.1516, *found* 379.1520.

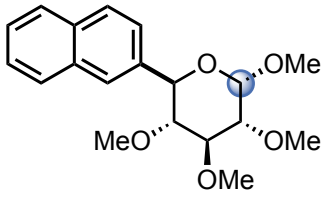

(2*S*,3*R*,4*S*,5*R*)-2,3,4,5-Tetramethoxy-6-(naphthalen-2-yl)tetrahydro-2H-pyran (7.3.9): Following General Procedure II using corresponding DHP (171.6 mg, 0.375 mmol, 1.5 equiv), 2-bromonaphthalene (51.8 mg, 0.25 mmol, 1.0 equiv), 4-CzIPN (3.9 mg, 0.005 mmol, 2 mol %), $NiBr_2$·dme (7.8 mg, 0.025 mmol, 10 mol %), dMeObpy (7.8 mg, 0.036 mmol, 14 mol %) in anhydrous acetone (5.0 mL, 0.05 M). The product was purified by flash chromatography on silica gel (hexanes/EtOAc 0 to 30%) to afford a colorless oil (56.8 mg, 68% yield). dr = 4:1 based on ^{1}H NMR of the crude reaction mixture. ^{1}H NMR (500 MHz, $CDCl_3$) δ 7.99 – 7.77 (m, 4H), 7.61 – 7.45 (m, 3H), 4.96 (d, *J* = 3.6 Hz, 1H), 4.62 (d, *J* = 9.7 Hz, 1H), 3.66 (s, 3H), 3.65 (s, 1H), 3.60 (s, 3H), 3.46 (s, 3H), 3.41 (dd, *J* = 9.6, 3.6 Hz, 1H), 3.20 (t, *J* = 9.3 Hz, 1H), 3.00 (s, 3H) ppm. ^{13}C NMR (126 MHz, $CDCl_3$) δ 136.4, 133.5, 133.3, 128.3, 128.2, 127.8, 127.2, 126.3, 126.2, 125.2, 98.1, 85.9, 83.4, 82.0, 73.1, 61.2, 60.6, 59.3, 55.5 ppm. (*Only the signals corresponding to the major stereoisomer are reported*). IR (neat, cm^{-1}): 2930, 2831, 1444, 1158, 1126, 1094, 1067, 1048, 1030. HRMS (ES+) *calcd for* $C_{19}H_{24}O_5Na$ $[M+Na]^+$ 355.1521, *found* 355.1526.

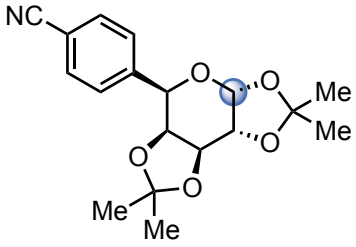

4-((3a*R*,5*R*,5a*S*,8a*S*,8b*R*)-2,2,7,7-Tetramethyltetrahydro-5H-bis([1,3]dioxolo)[4,5-b:4',5'-d] pyran-5-yl)benzonitrile (2j): Following General Procedure I using corresponding DHP (216.7 mg, 0.45 mmol, 1.5 equiv), 4-bromobenzonitrile (54.6 mg, 0.3 mmol, 1.0 equiv), 4-CzIPN (4.7 mg, 0.006 mmol, 2 mol %), $NiBr_2$·dme (4.6 mg, 0.015 mmol, 5 mol %), and dMeObpy (4.5 mg,

0.021 mmol, 7 mol %) in anhydrous acetone (6.0 mL, 0.05 M). The product was purified by flash chromatography on silica gel (hexanes/EtOAc 0 to 10%) to afford a white solid (69.6 mg, 70% yield). mp = 89-91 ºC. dr > 20:1 based on ^{1}H NMR of the crude reaction mixture. ^{1}H NMR (360 MHz, $CDCl_3$) δ 7.63 (d, *J* = 8.4 Hz, 2H), 7.49 (d, *J* = 8.1 Hz, 2H), 5.70 (d, *J* = 5.0 Hz, 1H), 4.92 (d, *J* = 1.3 Hz, 1H), 4.73 (dd, *J* = 7.8, 2.4 Hz, 1H), 4.45 – 4.40 (m, 2H), 1.56 (s, 3H), 1.42 (s, 3H), 1.37 (s, 3H), 1.28 (s, 3H) ppm. ^{13}C NMR (91 MHz, $CDCl_3$) δ 143.3, 131.9 (2C), 127.7 (2C), 119.0, 111.4 (2C), 109.7, 109.0, 96.9, 73.5, 71.1, 70.7, 69.1, 26.3, 26.0, 25.0, 24.3 ppm. IR (neat, cm^{-1}): 2988, 2227, 1382, 1254, 1142, 1042, 974. HRMS (EI+) *calcd for* $C_{17}H_{18}NO_5$ [M-CH_3] 316.1185, *found* 316.1195.

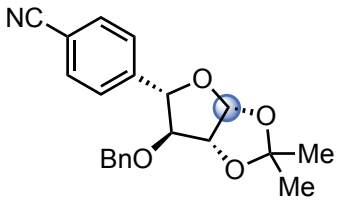

4-((3a*R*,5*R*,6*S*,6a*R*)-6-(Benzyloxy)-2,2-dimethyltetrahydrofuro[2,3-d][1,3]dioxol-5-yl) benzonitrile (2k): Following General Procedure I using corresponding DHP (225.7 mg, 0.45 mmol, 1.5 equiv), 4-bromobenzonitrile (54.6 mg, 0.3 mmol, 1.0 equiv), 4-CzIPN (4.7 mg, 0.006 mmol, 2 mol %), $NiBr_2$·dme (4.6 mg, 0.015 mmol, 5 mol %), and dMeObpy (4.5 mg, 0.021 mmol, 7 mol %) in anhydrous acetone (6.0 mL, 0.05 M). The product was purified by flash chromatography on silica gel (hexanes/EtOAc 0 to 10%) to afford a colorless oil (56.9 mg, 54% yield). dr = 9:1 based on ^{1}H NMR of the crude reaction mixture. ^{1}H NMR (360 MHz, $CDCl_3$) δ 7.61 (d, *J* = 8.3 Hz, 2H), 7.50 (d, *J* = 8.5 Hz, 2H), 7.43 – 7.28 (m, 5H), 6.03 (d, *J* = 4.1 Hz, 1H), 5.06 (d, *J* = 4.4 Hz, 1H), 4.75 (d, AB syst, *J* = 11.5 Hz, 1H), 4.74 (dd, *J* = 4.0, 0.7 Hz, 1H), 4.59 (d, AB syst, *J* = 11.8 Hz, 1H), 4.05 (d, *J* = 4.4 Hz, 1H), 1.35 (s, 3H), 1.31 (s, 3H) ppm. ^{13}C NMR (91 MHz, $CDCl_3$) δ 145.2, 137.0, 132.2 (2C), 128.7 (2C), 128.3, 128.0 (2C), 126.4 (2C), 118.9,

113.9, 111.5, 105.7, 88.0, 85.4, 84.0, 72.4, 27.1, 26.8 ppm. IR (neat, cm^{-1}): 2988, 2937, 2228, 1609, 1455, 1383, 1308, 888. HRMS (ES+) *calcd for* $C_{21}H_{21}NO_4Na$ $[M+Na]^+$ 374.1363, *found* 374.1385.

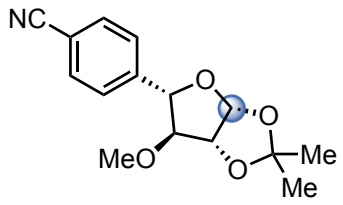

4-((3a*R*,5*R*,6*S*,6a*R*)-6-Methoxy-2,2-dimethyltetrahydrofuro[2,3-d][1,3]dioxol-5-yl) benzonitrile (2l): Following General Procedure I using corresponding DHP (191.5 mg, 0.45 mmol, 1.5 equiv), 4-bromobenzonitrile (54.6 mg, 0.3 mmol, 1.0 equiv), 4-CzIPN (4.7 mg, 0.006 mmol, 2 mol %), $NiBr_2 \cdot$dme (4.6 mg, 0.015 mmol, 5 mol %), and dMeObpy (4.5 mg, 0.021 mmol, 7 mol %) in anhydrous acetone (6.0 mL, 0.05 M). The product was purified by flash chromatography on silica gel (hexanes/EtOAc 0 to 15%) to afford a colorless oil (49.5 mg, 60% yield). dr = 2:1 based on ^{1}H NMR of the crude reaction mixture. ^{1}H NMR (360 MHz, $CDCl_3$, major diastereomer) δ 7.64 (d, *J* = 8.4 Hz, 2H), 7.58 (d, *J* = 8.2 Hz, 2H), 5.99 (d, *J* = 4.1 Hz, 1H), 4.97 (d, *J* = 4.4 Hz, 1H), 4.66 (dd, *J* = 4.1, 1.2 Hz, 1H), 3.85–3.82 (m, 1H), 3.48 (s, 3H), 1.35 (s, 3H), 1.32 (s, 3H) ppm. ^{1}H NMR (360 MHz, $CDCl_3$, minor diastereomer) δ 7.64 (d, *J* = 8.4 Hz, 2H), 7.49 (d, *J* = 8.1 Hz, 2H), 6.07 (d, *J* = 3.7 Hz, 1H), 5.28 (d, *J* = 3.1 Hz, 1H), 4.69 (d, *J* = 3.7 Hz, 1H), 3.84 (d, *J* = 3.2 Hz, 1H), 3.10 (s, 3H), 1.56 (s, 3H), 1.38 (s, 3H) ppm. ^{13}C NMR (91 MHz, $CDCl_3$, major diastereomer) δ 141.4, 131.8 (2C), 127.7 (2C), 118.9, 111.9, 111.5, 105.0, 85.9, 82.3, 81.0, 58.3, 26.8, 26.2 ppm. IR (neat, cm^{-1}): 2989, 2229, 1733, 1406, 1375, 1164 (major diastereomer), 2936, 2228, 1458, 1376, 1286, 1223. HRMS (EI+) *calcd for* $C_{14}H_{14}NO_4$ $[M-CH_3]^+$ 260.0923, *found* 260.0911.

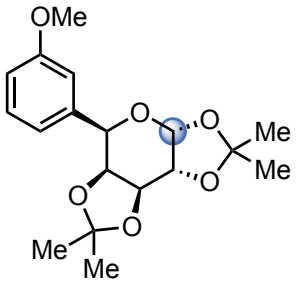

(3a*R*,5*R*,5a*S*,8a*S*,8b*R*)-5-(3-Methoxyphenyl)-2,2,7,7-tetramethyltetrahydro-5H-bis ([1,3]dioxolo) [4,5-b:4',5'-d]pyran (2m): Following General Procedure I using corresponding DHP (216.7 mg, 0.45 mmol, 1.5 equiv), 3-bromoanisole (44.3 mg, 0.3 mmol, 1.0 equiv), 4-CzIPN (4.7 mg, 0.006 mmol, 2 mol %), $NiBr_2 \cdot$dme (4.6 mg, 0.015 mmol, 5 mol %), and dMeObpy (4.5 mg, 0.021 mmol, 7 mol %) in anhydrous acetone (6.0 mL, 0.05 M). The product was purified by flash chromatography on silica gel (hexanes/EtOAc 0 to 20%) to afford a colorless oil (74.5 mg, 74% yield). dr = 9:1 based on ^{1}H NMR of the crude reaction mixture. ^{1}H NMR (360 MHz, $CDCl_3$) δ 7.25 (t, *J* = 7.9 Hz, 1H), 7.03 – 6.94 (m, 2H), 6.82 (dd, *J* = 8.0, 2.3 Hz, 1H), 5.71 (d, *J* = 5.0 Hz, 1H), 4.88 (d, *J* = 0.8 Hz, 1H), 4.72 (dd, *J* = 7.8, 2.3 Hz, 1H), 4.44 (dd, *J* = 7.8, 1.9 Hz, 1H), 4.40 (dd, *J* = 5.0, 2.3 Hz, 1H), 3.81 (s, 3H), 1.57 (s, 3H), 1.47 (s, 3H), 1.38 (s, 3H), 1.31 (s, 3H) ppm. ^{13}C NMR (91 MHz, $CDCl_3$) δ 159.5, 139.4, 129.1, 119.2, 113.3, 112.8, 109.4, 108.8, 97.1, 74.0, 71.3, 70.9, 69.4, 55.3, 26.3, 26.1, 25.1, 24.4 ppm. IR (neat, cm^{-1}): 2989, 1684, 1491, 1455, 1381, 1287, 1252, 1102. HRMS (ES+) *calcd for* $C_{18}H_{24}O_6Na$ $[M+Na]^+$ 359.1471, *found* 359.1476.

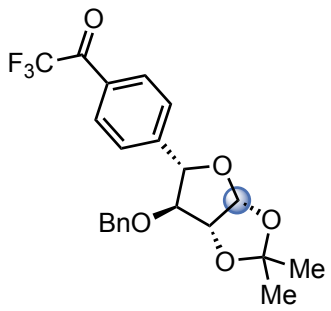

1-(4-((3a*R*,5*S*,6*S*,6a*R*)-6-(Benzyloxy)-2,2-dimethyltetrahydrofuro[2,3-d][1,3]dioxol-5-yl)phenyl)-2,2,2-trifluoroethan-1-one (2n): Following General Procedure I using corresponding DHP (375.9 mg, 0.75 mmol, 1.5 equiv), 1-bromo-2-(trifluoromethyl)benzene (112.0 mg, 0.5 mmol, 1.0 equiv), 4-CzIPN (7.8 mg, 0.01 mmol, 2 mol %), $NiBr_2$·dme (7.7 mg, 0.025 mmol, 5 mol %), and dMeObpy (7.5 mg, 0.035 mmol, 7 mol %) in anhydrous acetone (5.0 mL, 0.1 M). The product was purified by flash chromatography on silica gel (hexanes/EtOAc 0 to 10%, 10 to 25%) to afford a semi solid (100.5 mg, 49% yield). dr > 20:1 based on ^{1}H NMR of the crude reaction mixture. ^{1}H NMR (500 MHz, $CDCl_3$) δ 7.42 (d, *J* = 8.3 Hz, 2H), 7.40 – 7.29 (m, 5H), 7.17 (d, *J* = 8.2 Hz, 2H), 6.00 (d, *J* = 4.1 Hz, 1H), 5.00 (d, *J* = 4.8 Hz, 1H), 4.77 – 4.69 (m, 2H), 4.59 (d, *J* = 11.7 Hz, 1H), 4.06 (d, *J* = 4.8 Hz, 1H), 1.36 (s, 6H) ppm. ^{13}C NMR (126 MHz, $CDCl_3$) δ 148.7, 138.4, 137.2, 128.7, 128.2, 127.9, 127.4, 120.9, 114.0, 105.4, 100.1, 88.2, 85.8, 83.8, 72.3, 27.2, 27.0 ppm. IR (neat, cm^{-1}): 2990, 1939, 1725, 1260, 1222, 1164. HRMS (EI+) *calcd for* $C_{21}H_{21}F_3O_5$ $[M]^+$ 410.1341, *found* 410.1367.

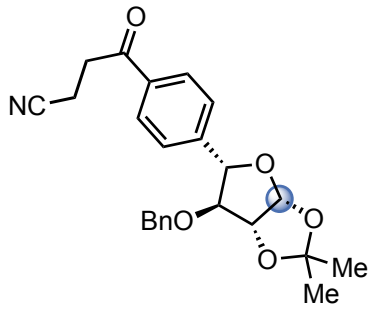

4-(4-((3a*R*,5*S*,6*S*,6a*R*)-6-(Benzyloxy)-2,2-dimethyltetrahydrofuro[2,3-d][1,3]dioxol-5-yl)phenyl)-4-oxobutanenitrile (2o): Following General Procedure I using corresponding DHP (225.6 mg, 0.45 mmol, 1.5 equiv), 2-bromo-1,4-dimethylbenzene (71.1 mg, 0.3 mmol, 1.0 equiv), 4-CzIPN (4.7 mg, 0.006 mmol, 2 mol %), $NiBr_2$·dme (4.6 mg, 0.015 mmol, 5 mol %), and dMeObpy (4.5 mg, 0.021 mmol, 7 mol %) in anhydrous acetone (6.0 mL, 0.05 M). The product

was purified by flash chromatography on silica gel (hexanes/EtOAc 0 to 20%) to afford a clear oil (83.0 mg, 68% yield). dr > 20:1 based on ^{1}H NMR of the crude reaction mixture. ^{1}H NMR (500 MHz, $CDCl_3$) δ 7.91 (d, *J* = 8.1 Hz, 2H), 7.52 (d, *J* = 8.1 Hz, 2H), 7.41 – 7.28 (m, 5H), 6.03 (s, 1H), 5.08 (s, 1H), 4.74 (d, *J* = 11.8 Hz, 2H), 4.60 (d, *J* = 11.7 Hz, 1H), 4.09 (d, *J* = 15.6 Hz, 1H), 3.36 (t, *J* = 7.3 Hz, 2H), 2.77 (t, *J* = 7.2 Hz, 2H), 1.35 (s, 3H), 1.33 (s, 3H) ppm. ^{13}C NMR (126 MHz, $CDCl_3$) δ 195.0, 146.1, 137.1, 134.9, 128.7, 128.3, 128.2, 128.0, 126.2, 119.3, 113.9, 105.7, 88.1, 85.5, 84.2, 72.3, 60.5, 53.9, 34.4, 29.4, 27.1, 26.8, 21.2, 14.3, 11.9 ppm. IR (neat, cm^{-1}): 2937, 1685, 1608, 1374, 1212, 1073. HRMS (EI+) *calcd for* $C_{24}H_{25}NO_5$ $[M]^+$ 407.1733, *found* 407.1714.

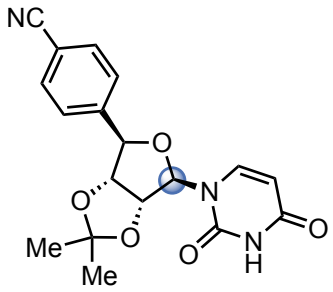

4-((3a*R*,4*R*,6*R*,6a*R*)-6-(2,4-Dioxo-3,4-dihydropyrimidin-1(2H)-yl)-2,2-dimethyltetrahydrofuro [3,4-d][1,3]dioxol-4-yl)benzonitrile (2p): Following General Procedure II using corresponding DHP (151.6 mg, 0.3 mmol, 1.0 equiv), 4-bromobenzonitrile (109.8 mg, 0.6 mmol, 2.0 equiv), 4-CzIPN (4.7 mg, 0.006 mmol, 2 mol %), $NiBr_2$·dme (9.3 mg, 0.03 mmol, 10 mol %), and dMeObpy (9.1 mg, 0.042 mmol, 14 mol %) in anhydrous acetone (6.0 mL, 0.05 M). The product was purified by flash chromatography on silica gel (CH_2Cl_2/EtOAc 0 to 30%) to afford a white solid (50.1 mg, 47% yield). mp = 131-133 ºC. dr > 20:1 based on ^{1}H NMR of the crude reaction mixture. ^{1}H NMR (360 MHz, $CDCl_3$) δ 9.54 (s, 1H), 7.63 (d, *J* = 8.3 Hz, 2H), 7.50 (d, *J* = 8.2 Hz, 2H), 7.24 (s, 1H), 5.77 (d, *J* = 6.8 Hz, 1H), 5.67 (d, *J* = 1.4 Hz, 1H), 5.16 (dd, *J* = 6.4, 1.4 Hz, 1H), 5.00 (d, *J* = 5.5 Hz, 1H), 4.89 (t, *J* = 5.9 Hz, 1H), 1.64 (s, 3H), 1.37 (s, 3H) ppm. ^{13}C NMR (126 MHz, $CDCl_3$) δ 163.5, 150.0, 143.9, 143.2, 132.5 (2C), 126.5 (2C), 118.8, 115.6, 112.1, 103.1, 95.0, 87.4, 85.7, 84.2, 27.5, 25.6 ppm. IR (neat, cm^{-}

[1]): 2989, 2228, 1632, 1612, 1421, 1156, 1018. HRMS (EI+) *calcd for* $C_{17}H_{14}N_3O_5$ $[M\text{-}CH_3]^+$ 340.0933, *found* 340.0936.

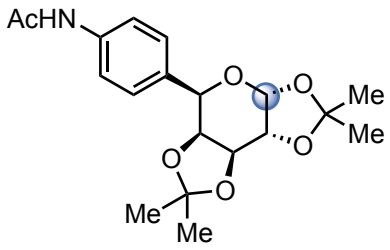

***N*-(4-((3a*R*,5*R*,5a*S*,8a*S*,8b*R*)-2,2,7,7-Tetramethyltetrahydro-5H-bis([1,3]dioxolo)[4,5-b:4',5'-d]pyran-5-yl)phenyl)acetamide (2q):** Following General Procedure I using corresponding DHP (216.7 mg, 0.45 mmol, 1.5 equiv), *N*-acetyl-4-bromoaniline **2c** (64.2 mg, 0.3 mmol, 1.0 equiv), 4-CzIPN (4.7 mg, 0.006 mmol, 2 mol %), $NiBr_2 \cdot$dme (4.6 mg, 0.015 mmol, 5 mol %), and dMeObpy (4.5 mg, 0.021 mmol, 7 mol %) in anhydrous acetone (6.0 mL, 0.05 M). The product was purified by flash chromatography on silica gel (hexanes/EtOAc 0 to 50%) to afford a white solid (44.6 mg, 41% yield). mp = 204-206 ºC. dr = 9:1 based on ^{1}H NMR of the crude reaction mixture. ^{1}H NMR (360 MHz, $CDCl_3$) δ 7.47 (d, *J* = 8.4 Hz, 2H), 7.41 (s, 1H), 7.34 (d, *J* = 8.4 Hz, 2H), 5.69 (d, *J* = 5.0 Hz, 1H), 4.85 (s, 1H), 4.70 (dd, *J* = 7.8, 2.2 Hz, 1H), 4.43–4.34 (m, 2H), 2.12 (s, 3H), 1.56 (s, 3H), 1.45 (s, 3H), 1.37 (s, 3H), 1.29 (s, 3H) ppm. ^{13}C NMR (91 MHz, $CDCl_3$) δ 168.4, 137.4, 133.7, 127.7 (2C), 119.6 (2C), 109.4, 108.7, 97.0, 73.9, 71.2, 70.8, 69.2, 26.3, 26.1, 25.1, 24.7, 24.3 ppm. IR (neat, cm^{-1}): 1667, 1604, 1535, 1411, 1381, 1142, 1040, 962. HRMS (ES+) *calcd for* $C_{19}H_{25}NO_6Na$ $[M+Na]^+$ 386.1580, *found* 386.1583.

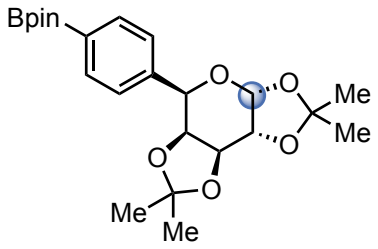

4,4,5,5-Tetramethyl-2-(4-((3a*R*,5*R*,5a*S*,8a*S*,8b*R*)-2,2,7,7-tetramethyltetrahydro-5H-bis([1,3]dioxolo)[4,5-b:4',5'-d]pyran-5-yl)phenyl)-1,3,2-dioxaborolane (2r): Following General Procedure I using corresponding DHP (288.9 mg, 0.6 mmol, 2.0 equiv), (4-bromophenyl)-pinacolborane (84.9 mg, 0.3 mmol, 1.0 equiv), 4-CzIPN (4.7 mg, 0.006 mmol, 2 mol %), $NiBr_2$·dme (4.6 mg, 0.015 mmol, 5 mol %), and dMeObpy (4.5 mg, 0.021 mmol, 7 mol %) in anhydrous acetone (6.0 mL, 0.05 M). The product was purified by flash chromatography on silica gel (hexanes/EtOAc 0 to 3%) to afford a white crystalline solid (75.4 mg, 58% yield). mp = 135-137 °C. dr = 9:1 based on ^{1}H NMR of the crude reaction mixture. ^{1}H NMR (500 MHz, $CDCl_3$) δ 7.79 (d, *J* = 7.8 Hz, 2H), 7.40 (d, *J* = 7.8 Hz, 2H), 5.72 (d, *J* = 4.9 Hz, 1H), 4.91 (s, 1H), 4.71 (dd, *J* = 7.7, 1.9 Hz, 1H), 4.44 (dd, *J* = 7.8, 1.4 Hz, 1H), 4.39 (d, *J* = 2.4 Hz, 1H), 1.56 (s, 3H), 1.44 (s, 3H), 1.37 (s, 3H), 1.33 (s, 12H), 1.27 (s, 3H) ppm. ^{13}C NMR (126 MHz, $CDCl_3$) δ 141.0, 134.6 (2C), 126.1 (2C), 111.2, 109.4, 108.7, 97.0, 83.8 (2C), 74.0, 71.2, 70.8, 69.6, 26.3, 26.0, 25.1, 25.0 (4C), 24.4 ppm. ^{11}B NMR (128.38 MHz, $CDCl_3$) δ 30.7 (br,s). IR (neat, cm^{-1}): 2980, 1399, 1358, 1210, 1165, 1142, 1088, 1066. HRMS (ES+) *calcd for* ($C_{23}H_{33}BO_7Na$, $[M+Na]^+$) 454.2253, *found* 454.2278.

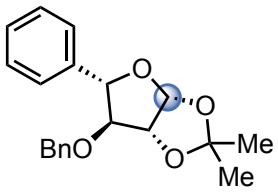

(3a*R*,6*S*,6a*R*)-6-(Benzyloxy)-2,2-dimethyl-5-phenyltetrahydrofuro[2,3-*d*][1,3]dioxole (2s): Following General Procedure II using corresponding DHP (225.7 mg, 0.45 mmol, 1.5 equiv), 2-bromobenzene (47.1 mg, 0.3 mmol, 1.0 equiv), 4-CzIPN (4.7 mg, 0.006 mmol, 2 mol %), $NiBr_2$·dme (4.6 mg, 0.015 mmol, 5 mol %), and dMeObpy (4.5 mg, 0.021 mmol, 7 mol %) in anhydrous acetone (6.0 mL, 0.05 M). The product was purified by flash chromatography on silica gel (hexanes/EtOAc 0 to 10%) to afford a colorless oil (29.7 mg, 30% yield). dr = 2.6:1 based on ^{1}H NMR of the crude reaction mixture. ^{1}H NMR (500 MHz, $CDCl_3$, major diastereomer) δ 7.42 (d, *J* = 7.5 Hz, 2H), 7.38 – 7.27 (m, 8H), 6.00 (d, *J* = 4.1 Hz, 1H), 5.02 (d, *J* = 4.9 Hz, 1H), 4.74 (d, *J* = 3.6 Hz, 1H), 4.70 (d, *J* = 11.6 Hz, 1H), 4.59 (d, *J* = 11.7 Hz, 1H), 4.10 (d, *J* = 4.7 Hz, 1H), 1.40 (s, 3H), 1.37 (s, 3H) ppm. ^{1}H NMR (500 MHz, $CDCl_3$, minor diastereoisomer) δ 7.44 – 7.31 (m, 6H), 7.23 – 7.20 (m, 2H), 6.94 – 6.87 (m, 2H), 6.12 (d, *J* = 3.9 Hz, 1H), 5.28 (d, *J* = 3.0 Hz, 1H), 4.71 (d, *J* = 3.7 Hz, 1H), 4.25 (d, *J* = 11.9 Hz, 1H), 4.08 (d, *J* = 12.0 Hz, 1H), 3.98 (d, *J* = 3.1 Hz, 1H), 1.56 (s, 3H), 1.37 (s, 3H) ppm. ^{13}C NMR (126 MHz, $CDCl_3$, major diastereomer) δ 139.6, 137.4, 128.6 (2C), 128.4 (2C), 128.1, 127.9 (2C), 127.7, 126.0 (2C), 113.9, 105.3, 88.4, 86.0, 84.4, 72.3, 27.3, 27.1 ppm. ^{13}C NMR (126 MHz, $CDCl_3$, minor diastereomer) δ 137.43, 135.75, 128.4 (2C), 128.1 (2C), 127.8, 127.8, 127.7 (2C), 127.3 (2C), 111.7, 105.1, 83.6 (2C), 81.9, 72.4, 27.0, 26.4 ppm. IR (neat, cm^{-1}): 2930, 1724, 1498, 1455, 1374, 1071, 1020 (major diastereomer), 2981, 2923, 2854, 1724, 1454, 1075 (minor diastereomer). HRMS (EI+) *calcd for* $C_{19}H_{19}O_4$ [M-CH_3] 311.1283, *found* 311.1305.

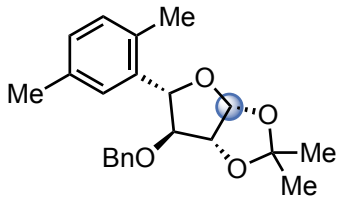

(3a*R*,5*S*,6*S*,6a*R*)-6-(Benzyloxy)-5-(2,5-dimethylphenyl)-2,2-dimethyltetrahydrofuro[2,3-d][1,3] dioxole (2t): Following General Procedure I using corresponding DHP (225.6 mg, 0.45

mmol, 1.5 equiv), 2-bromo-1,4-dimethylbenzene (54.6 mg, 0.3 mmol, 1.0 equiv), 4-CzIPN (4.7 mg, 0.006 mmol, 2 mol %), $NiBr_2$·dme (4.6 mg, 0.015 mmol, 5 mol %), and dMeObpy (4.5 mg, 0.021 mmol, 7 mol %) in anhydrous acetone (6.0 mL, 0.05 M). The product was purified by flash chromatography on silica gel (hexanes/EtOAc 0 to 20%) to afford a clear oil (46.8 mg, 44% yield). dr = 7.3:1 based on ^{1}H NMR of the crude reaction mixture. ^{1}H NMR (500 MHz, $CDCl_3$) δ 7.41 (s, 1H), 7.32 (dt, *J* = 14.2, 7.3 Hz, 5H), 7.01 (t, *J* = 8.3 Hz, 2H), 6.00 (d, *J* = 4.2 Hz, 1H), 5.20 (d, *J* = 4.9 Hz, 1H), 4.74 (d, *J* = 4.1 Hz, 1H), 4.68 (d, *J* = 11.6 Hz, 1H), 4.51 (d, *J* = 11.5 Hz, 1H), 4.08 (d, *J* = 4.9 Hz, 1H), 2.30 (s, 3H), 2.26 (s, 3H), 1.57 (s, 3H), 1.40 (s, 3H) ppm. ^{13}C NMR (126 MHz, $CDCl_3$) δ 137.4, 137.2, 135.4, 132.4, 130.4, 128.6, 128.4, 128.1, 127.9, 126.9, 113.9, 105.5, 88.2, 85.6, 83.4, 72.3, 27.3, 27.0, 21.3, 19.1 ppm. IR (neat, cm^{-1}): 3581, 2941, 1455, 1214, 1074, 864. HRMS (EI+) *calcd for* $C_{22}H_{26}O_4$ $[M]^+$ 354.1831, *found* 354.1856.

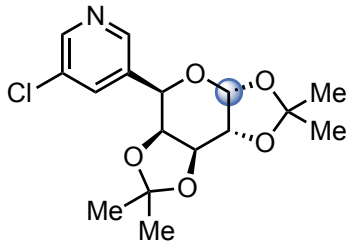

3-Chloro-5-((3a*R*,5*R*,5a*S*,8a*S*,8b*R*)-2,2,7,7-tetramethyltetrahydro-5H-bis([1,3]dioxolo)[4,5-b:4',5'-d]pyran-5-yl)pyridine (2u): Following General Procedure I using corresponding DHP (216.7 mg, 0.45 mmol, 1.5 equiv), 3-bromo-5-chloropyridine (57.7 mg, 0.3 mmol, 1.0 equiv), 4-CzIPN (4.7 mg, 0.006 mmol, 2 mol %), $NiBr_2$·dme (4.6 mg, 0.015 mmol, 5 mol %), and dMeObpy (4.5 mg, 0.021 mmol, 7 mol %) in anhydrous acetone (6.0 mL, 0.05 M). The product was purified by flash chromatography on silica gel (hexanes/EtOAc 0 to 30%) to afford a colorless foam (45.1 mg, 44% yield). dr > 20:1 based on ^{1}H NMR of the crude reaction mixture. ^{1}H NMR (360 MHz, $CDCl_3$) δ 8.47 (d, *J* = 7.0 Hz, 2H), 7.75 (t, *J* = 1.7 Hz, 1H), 5.68 (d, *J* = 5.0 Hz, 1H), 4.90 (d, *J* =

1.3 Hz, 1H), 4.73 (dd, *J* = 7.8, 2.4 Hz, 1H), 4.43–4.36 (m, 2H), 1.57 (s, 3H), 1.45 (s, 3H), 1.37 (s, 3H), 1.29 (s, 3H) ppm. ^{13}C NMR (91 MHz, $CDCl_3$) δ 147.9, 146.2, 135.1, 135.0, 129.8, 109.8, 109.1, 96.9, 73.3, 71.1, 70.7, 67.4, 26.3, 26.0, 25.0, 24.3 ppm. IR (neat, cm^{-1}): 2980, 2929, 1424, 1382, 1372, 1142, 1024, 1000. HRMS (ES+) *calcd for* $C_{16}H_{21}ClNO_5$ $[M+H]^+$ 342.1108, *found* 342.1093.

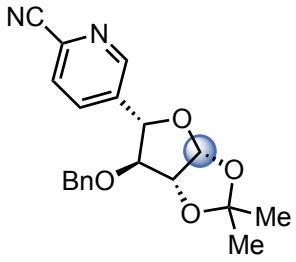

5-((3a*R*,5*S*,6*S*,6a*R*)-6-(Benzyloxy)-2,2-dimethyltetrahydrofuro[2,3-d][1,3]dioxol-5-yl) picolinonitrile (2v): Following General Procedure I using corresponding DHP (225.6 mg, 0.45 mmol, 1.5 equiv), 5-bromopicolinonitrile (54.6 mg, 0.3 mmol, 1.0 equiv), 4-CzIPN (4.7 mg, 0.006 mmol, 2 mol %), $NiBr_2$·dme (4.6 mg, 0.015 mmol, 5 mol %), and dMeObpy (4.5 mg, 0.021 mmol, 7 mol %) in anhydrous acetone (6.0 mL, 0.05 M). The product was purified by flash chromatography on silica gel (hexanes/EtOAc 0 to 20%) to afford a clear oil (73.9 mg, 70% yield). dr > 20:1 based on ^{1}H NMR of the crude reaction mixture. ^{1}H NMR (500 MHz, $CDCl_3$) δ 8.71 – 8.68 (m, 1H), 7.84 (ddd, J = 8.1, 2.2, 1.0 Hz, 1H), 7.66 – 7.60 (m, 1H), 7.36 (q, J = 7.3, 6.6 Hz, 5H), 6.04 (d, J = 4.1 Hz, 1H), 5.10 (d, J = 4.2 Hz, 1H), 4.78 – 4.74 (m, 2H), 4.59 (d, J = 11.8 Hz, 1H), 4.07 (dd, J = 4.3, 1.3 Hz, 1H), 1.34 (s, 3H), 1.27 (s, 3H). ^{13}C NMR (126 MHz, $CDCl_3$) δ 148.9, 139.5, 136.7, 134.3, 133.0, 128.9, 128.5, 128.1, 128.0, 117.3, 114.0, 106.6, 105.9, 87.5, 85.2, 82.3, 72.5, 61.6, 27.5, 27.0, 26.6, 25.0, 14.4 ppm. IR (neat, cm^{-1}): 2987, 2938, 1720, 1455, 1374, 1212, 1075. HRMS (EI+) *calcd for* $C_{20}H_{20}N_2O_4$ $[M]^+$ 352.1423, *found* 352.1450.

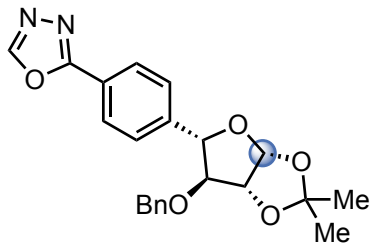

2-(4-((3aR,5S,6S,6aR)-6-(Benzyloxy)-2,2-dimethyltetrahydrofuro[2,3-d][1,3]dioxol-5-yl)phenyl) -1,3,4-oxadiazole (2w): Following General Procedure II using the corresponding DHP (225.7 mg, 0.45 mmol, 1.5 equiv), aryl bromide **2e** (66.9 mg, 0.3 mmol, 1.0 equiv), 4-CzIPN (4.7 mg, 0.006 mmol, 2 mol %), $NiBr_2$·dme (4.6 mg, 0.015 mmol, 5 mol %), and dMeObpy (4.5 mg, 0.021 mmol, 7 mol %) in anhydrous acetone (6.0 mL, 0.05 M). The product was purified by flash chromatography on silica gel (hexanes/EtOAc 0 to 10%) to afford a colorless oil (29.7 mg, 30% yield). dr = 2.6:1 based on ^{1}H NMR of the crude reaction mixture. ^{1}H NMR (500 MHz, $CDCl_3$, major diastereomer) δ 7.42 (d, *J* = 7.5 Hz, 2H), 7.38 – 7.27 (m, 8H), 6.00 (d, *J* = 4.1 Hz, 1H), 5.02 (d, *J* = 4.9 Hz, 1H), 4.74 (d, *J* = 3.6 Hz, 1H), 4.70 (d, *J* = 11.6 Hz, 1H), 4.59 (d, *J* = 11.7 Hz, 1H), 4.10 (d, *J* = 4.7 Hz, 1H), 1.40 (s, 3H), 1.37 (s, 3H) ppm. ^{1}H NMR (500 MHz, $CDCl_3$, minor diastereoisomer) δ 7.44 – 7.31 (m, 6H), 7.23 – 7.20 (m, 2H), 6.94 – 6.87 (m, 2H), 6.12 (d, *J* = 3.9 Hz, 1H), 5.28 (d, *J* = 3.0 Hz, 1H), 4.71 (d, *J* = 3.7 Hz, 1H), 4.25 (d, *J* = 11.9 Hz, 1H), 4.08 (d, *J* = 12.0 Hz, 1H), 3.98 (d, *J* = 3.1 Hz, 1H).

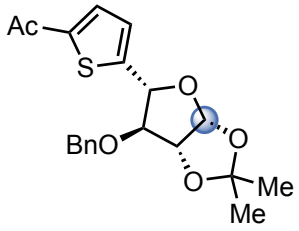

1-(5-((3a*R*,5*R*,6*R*,6a*R*)-6-(Benzyloxy)-2,2-dimethyltetrahydrofuro[2,3-d][1,3]dioxol-5-yl) thiophen-2-yl)ethan-1-one (2x): Following General Procedure I using corresponding DHP (225.6 mg, 0.45 mmol, 1.5 equiv), 1-(5-bromothiophen-2-yl)ethan-1-one (61.1 mg, 0.3 mmol, 1.0 equiv), 4-CzIPN (4.7 mg, 0.006 mmol, 2 mol %), $NiBr_2$·dme (4.6 mg, 0.015 mmol, 5 mol %), and dMeObpy (4.5 mg, 0.021 mmol, 7 mol %) in anhydrous acetone (6.0 mL, 0.05 M). The product was purified by flash chromatography on silica gel (hexanes/EtOAc 0 to 20%) to afford a yellow oil (87.5 mg, 78% yield). dr > 20:1 based on ^{1}H NMR of the crude reaction mixture. ^{1}H NMR (500 MHz, $CDCl_3$) δ 7.55 (d, *J* = 3.8 Hz, 1H), 7.34 (m, 5H), 7.03 (d, *J* = 3.8 Hz, 1H), 5.99 (d, *J* = 4.0 Hz, 1H), 5.19 (d, *J* = 4.1 Hz, 1H), 4.75 – 4.68 (m, 2H), 4.61 (d, *J* = 11.6 Hz, 1H), 4.18 (d, *J* = 4.1 Hz, 1H), 2.53 (s, 3H), 1.35 (s, 6H) ppm. ^{13}C NMR (126 MHz, $CDCl_3$) δ 190.8, 152.2, 143.6, 136.9, 132.4, 128.8, 128.3, 128.0, 125.6, 114.2, 106.6, 105.8, 88.2, 85.6, 81.5, 72.6, 29.9, 27.1, 26.9, 26.9 ppm. IR (neat, cm^{-1}): 2987, 2937, 1722, 1663, 1251, 1214, 1073, 855. HRMS (EI+) *calcd for* $C_{20}H_{22}O_5S$ $[M]^+$ 374.1188, *found* 374.1203.

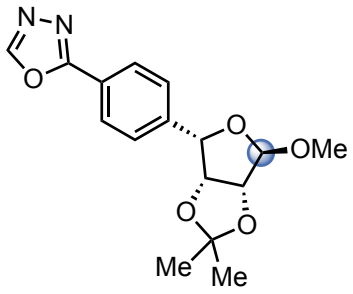

(3a*R*,5*S*,5a*R*,8a*S*,8b*R*)-5-(Benzo[b]thiophen-2-yl)-2,2,7,7-tetramethyltetrahydro-5H-bis ([1,3]dioxolo)[4,5-b:4',5'-d]pyran (2y): Following General Procedure II using corresponding DHP (216.7 mg, 0.45 mmol, 1.5 equiv), aryl bromide **2e** (66.9 mg, 0.3 mmol, 1.0 equiv), 4-CzIPN (4.7 mg, 0.006 mmol, 2 mol %), $NiBr_2$·dme (9.2 mg, 0.03 mmol, 10 mol %), and dMeObpy (9.1 mg, 0.042 mmol, 14 mol %) in anhydrous acetone (6.0 mL, 0.05 M). The product was purified by flash chromatography on silica gel (hexanes/EtOAc 0 to 20%) to afford a clear oil

(76.1 mg, 70% yield). dr > 20:1 based on ^{1}H NMR of the crude reaction mixture. ^{1}H NMR (500 MHz, $CDCl_3$) δ 8.46 (s, 1H), 8.15 – 8.02 (m, 2H), 7.57 (d, J = 8.3 Hz, 2H), 5.29 (d, *J* = 2.3 Hz, 1H), 5.16 (s, 1H), 4.87 (dd, *J* = 6.0, 2.2 Hz, 1H), 4.68 (d, *J* = 5.9 Hz, 1H), 3.40 (s, 3H), 1.59 (s, 3H), 1.37 (s, 3H). ^{13}C NMR (126 MHz, $CDCl_3$) δ 164.8, 152.8, 145.1, 127.4, 127.2, 123.0, 113.4, 110.4, 88.8, 86.0, 85.9, 55.9, 27.1, 25.5. IR (neat, cm^{-1}): 2988, 2937, 1719, 1617, 1558, 1516, 1498, 1458, 1374, 1211, 1104. HRMS (EI+) *calcd for* $C_{15}H_{15}N_2O_5$ $[M\text{-}CH_3]^+$ 303.0981, *found* 303.0957.

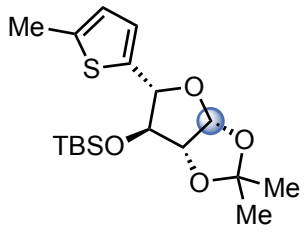

***tert*-Butyl(((3a*R*,5*R*,6*R*,6a*R*)-2,2-dimethyl-5-(5-methylthiophen-2-yl)tetrahydrofuro[2,3-d][1,3] dioxol-6-yl)oxy)dimethylsilane (2z):** Following General Procedure I using using corresponding DHP (262.9 mg, 0.5 mmol, 2.0 equiv), 2-bromo-5-methylthiophene (44.3 mg 0.25 mmol, 1.0 equiv), 4-CzIPN (3.9 mg, 0.005 mmol, 2 mol %), $NiBr_2$·dme (3.9 mg, 0.00125 mmol, 5 mol %), and dMeObpy (3.8 mg, 0.0175 mmol, 7 mol %) in anhydrous acetone (5.0 mL, 0.05 M). The product was purified by flash chromatography on silica gel (hexanes/EtOAc 0 to 10%) to afford a colorless foam (42.8 mg, 46% yield). dr = 1.8:1 based on ^{1}H NMR of the crude reaction mixture. ^{1}H NMR (500 MHz, $CDCl_3$) δ 6.80 (d, *J* = 3.3 Hz, 1H), 6.63 – 6.52 (m, 1H), 5.91 (d, *J* = 4.0 Hz, 1H), 4.91 (d, *J* = 4.4 Hz, 1H), 4.51 (dd, *J* = 4.1, 1.5 Hz, 1H), 4.34 (dd, *J* = 4.4, 1.4 Hz, 1H), 2.45 (s, 3H), 1.42 (s, 3H), 1.35 (s, 3H), 0.88 (s, 9H), 0.06 (s, 3H), 0.01 (s, 3H) ppm. ^{13}C NMR (126 MHz, $CDCl_3$) δ 140.1, 140.0, 125.3, 124.6, 113.8, 105.1, 88.4, 84.1, 82.5, 27.3, 27.2, 25.8 (3C), 18.1, 15.5, 0.1, -4.8 ppm. (*Only the signals corresponding to the major stereoisomer are reported*).

IR (neat, cm^{-1}): 2929, 2857, 1471, 1382, 1373, 1254, 1213, 1119, 1017, 837. HRMS (ES+) *calcd for* $C_{12}H_{16}O_4S$ $[M\text{-}TBS]^+$ 256.0769, *found* 256.0764.

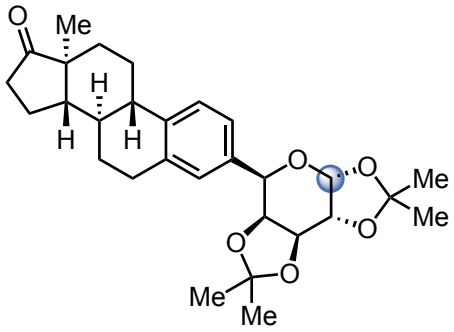

(8*R*,9*S*,13*S*,14*S*)-13-Methyl-3-((3a*R*,5*R*,5a*S*,8a*S*,8b*R*)-2,2,7,7-tetramethyltetrahydro-5H-bis([1,3]dioxolo)[4,5-b:4',5'-d]pyran-5-yl)-6,7,8,9,11,12,13,14,15,16-decahydro-17H-cyclopenta[a]phenanthren-17-one (3a): Following General Procedure II using corresponding DHP (216.7 mg, 0.45 mmol, 1.5 equiv), estrone derivative[2] (57.7 mg, 0.3 mmol, 1.0 equiv), 4-CzIPN (4.7 mg, 0.006 mmol, 2 mol %), $NiBr_2 \cdot dme$ (4.6 mg, 0.015 mmol, 5 mol %), and dMeObpy (4.5 mg, 0.021 mmol, 7 mol %) in anhydrous acetone (6.0 mL, 0.05 M). The product was purified by flash chromatography on silica gel (hexanes/EtOAc 0 to 20%) to afford a slightly yellow solid (60.8 mg, 42% yield). mp = 70-72 ºC. dr = 8:1 based on ^1H NMR of the crude reaction mixture. ^1H NMR (360 MHz, $CDCl_3$) δ 7.28 (d, *J* = 8.2 Hz, 1H), 7.20 (d, *J* = 8.2 Hz, 1H), 7.12 (s, 1H), 5.70 (d, *J* = 5.0 Hz, 1H), 4.84 (s, 1H), 4.71 (dd, *J* = 7.9, 2.3 Hz, 1H), 4.44 (dd, *J* = 7.9, 1.8 Hz, 1H), 4.39 (dd, *J* = 5.0, 2.3 Hz, 1H), 2.93 (dd, *J* = 8.7, 3.9 Hz, 2H), 2.56 – 2.37 (m, 2H), 2.34 – 2.24 (m, 1H), 2.19 – 1.92 (m, 4H), 1.68 – 1.58 (m, 2H), 1.57 – 1.41 (m, 10H), 1.37 (s, 3H), 1.31 (s, 3H), 0.90 (s, 3H) ppm. ^{13}C NMR (91 MHz, $CDCl_3$) δ 190.9, 139.0, 136.2, 135.3, 127.5, 125.2, 124.4, 109.4, 108.7, 97.1, 72.9, 71.3, 70.9, 69.3, 50.7, 48.1, 44.5, 38.2, 36.0, 31.8, 29.6, 26.7, 26.3, 26.1,

[2] Prepared following the littérature porcedure from the corresponding triflate: Pan, J.; Wang, X.; Zhang, Y.; Buchwald, S. L. *Org. Lett.* **2011**, *13*, 4974.

25.8, 25.1, 24.4, 21.7, 14.0 ppm. IR (neat, cm^{-1}): 2987, 2931, 1736, 1380, 1372, 1209, 1100, 1066, 997. HRMS (EI+) *calcd for* $C_{29}H_{38}O_6$ $[M]^+$ 482.2668, *found* 482.2667.

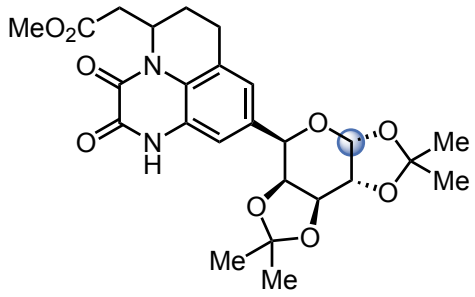

Methyl 2-(2,3-Dioxo-9-((3a*R*,5*R*,5a*S*,8a*S*,8b*R*)-2,2,7,7-tetramethyltetrahydro-5H-bis ([1,3] dioxolo)[4,5-b:4',5'-d]pyran-5-yl)-2,3,6,7-tetrahydro-1H,5H-pyrido[1,2,3-de]quinoxalin-5-yl) acetate (3b): Following General Procedure II using corresponding DHP (72.2 mg, 0.15 mmol, 1.5 equiv), the heteroaryl bromide (35.3 mg, 0.1 mmol, 1.0 equiv), 4-CzIPN (1.5 mg, 0.002 mmol, 2 mol %), $NiBr_2$·dme (3.1 mg, 0.01 mmol, 10 mol %), and dMeObpy (3.0 mg, 0.014 mmol, 14 mol %) in anhydrous acetone (2.0 mL, 0.05 M). The product was purified by flash chromatography on silica gel (hexane/EtOAc/MeOH 6/3/1) to afford a white solid (26.7 mg, 53% yield). mp = 93-95 ºC. dr = 9:1 based on ^{1}H NMR of the crude reaction mixture. ^{1}H NMR (360 MHz, $CDCl_3$) mixture of rotamers: δ 11.50 (br s, 1H), 7.18 – 7.07 (m, 2H), 5.69 (dd, *J* = 4.8, 3.3 Hz, 1H), 5.44 – 5.31 (m, 1H), 4.92 (s, 1H), 4.74 (td, *J* = 7.6, 2.2 Hz, 1H), 4.57 (dd, *J* = 7.9, 1.7 Hz, 0.5H, rot.1), 4.48 (dd, *J* = 7.9, 1.7 Hz, 0.5H, rot.2), 4.41 – 4.35 (m, 1H), 3.70 (br s, 3H), 3.06 – 2.90 (m, 1H), 2.89 – 2.69 (m, 2H), 2.58 – 2.47 (m, 1H), 2.28 (br s, 1H), 2.04 – 1.83 (m, 1H), 1.57 (s, 1.5H, rot.1), 1.56 (s, 1.5H, rot.2), 1.50 (s, 1.5H, rot.1), 1.46 (s, 1.5H, rot.2), 1.36 (s, 3H), 1.32 (s, 1.5H, rot.1), 1.29 (s, 1.5H, rot.2) ppm. ^{13}C NMR (91 MHz, $CDCl_3$) mixture of rotamers: δ 170.6, 155.5/155.0 (rot.1/rot.2), 154.2, 134.4, 124.6/124.5 (rot.1/rot.2), 124.4, 123.4/123.2 (rot.1/rot.2), 122.1/121.9 (rot.1/rot.2), 112.9/112.8 (rot.1/rot.2), 109.6/109.5 (rot.1/rot.2), 109.0, 96.9, 73.9, 71.1, 70.8, 68.6/68.5 (rot.1/rot.2), 52.1, 48.0/47.9 (rot.1/rot.2), 35.3, 26.4, 26.1, 25.0, 24.3, 23.3, 22.0/21.8

(rot.1/rot.2) ppm. IR (neat, cm^{-1}): 2980, 2901, 1696, 1674, 1326, 1256, 1165, 1101, 1064. HRMS (ES+) *calcd for* $C_{25}H_{31}N_2O_9$ $[M+H]^+$ 503.2030, *found* 503.2046.

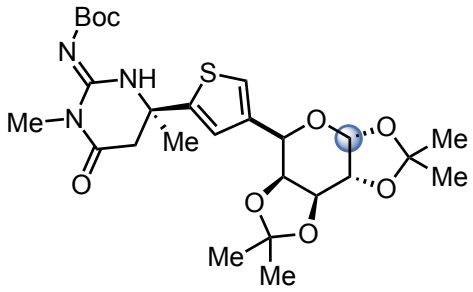

***tert*-Butyl ((*R*,*Z*)-1,4-Dimethyl-6-oxo-4-(4-((3a*R*,5*R*,5a*S*,8a*S*,8b*R*)-2,2,7,7-tetramethyl tetrahydro-5H-bis([1,3]dioxolo)[4,5-b:4',5'-d]pyran-5-yl)thiophen-2-yl) tetrahydro pyrimidin-2(1H)-ylidene)carbamate (3c):** Following General Procedure II using corresponding DHP (72.2 mg, 0.15 mmol, 1.5 equiv), the heteroaryl bromide (35.3 mg, 0.1 mmol, 1.0 equiv), 4-CzIPN (1.5 mg, 0.002 mmol, 2 mol %), $NiBr_2 \cdot$dme (3.1 mg, 0.01 mmol, 10 mol %), and dMeObpy (3.0 mg, 0.014 mmol, 14 mol %) in anhydrous acetone (2.0 mL, 0.05 M). The product was purified by flash chromatography on silica gel (hexane/EtOAc/acetone 85:10:5) to afford a yellow oil (51.8 mg, 94% yield). dr = 4:1 based on ^{1}H NMR of the crude reaction mixture. ^{1}H NMR (500 MHz, $CDCl_3$) δ 10.28 (br s, 1H), 7.20 (s, 1H), 6.97 (d, *J* = 1.2 Hz, 1H), 5.61 (d, *J* = 5.0 Hz, 1H), 4.82 (s, 1H), 4.66 (dd, *J* = 7.8, 2.3 Hz, 1H), 4.36 – 4.30 (m, 2H), 3.25 (s, 3H), 3.12 (d, *J* = 16.2 Hz, 1H), 2.88 (d, *J* = 16.2 Hz, 1H), 1.74 (s, 3H), 1.55 (s, 3H), 1.51 (s, 9H), 1.47 (s, 3H), 1.35 (s, 3H), 1.31 (s, 3H) ppm. ^{13}C NMR (126 MHz, $CDCl_3$) δ 167.5, 163.9, 157.6, 147.4, 138.6, 124.3, 122.7, 109.5, 108.8, 96.9, 80.0, 73.3, 71.1, 70.7, 66.7, 53.3, 45.9, 30.0, 28.6, 28.3 (3C), 26.4, 26.1, 25.0, 24.5 ppm. IR (neat, cm^{-1}): 2989, 1713, 1640, 1597, 1269, 1251, 1157, 1066, 997. HRMS (ES+) *calcd for* $C_{26}H_{38}N_3O_8S$ $[M+H]^+$ 552.2380, *found* 552.239

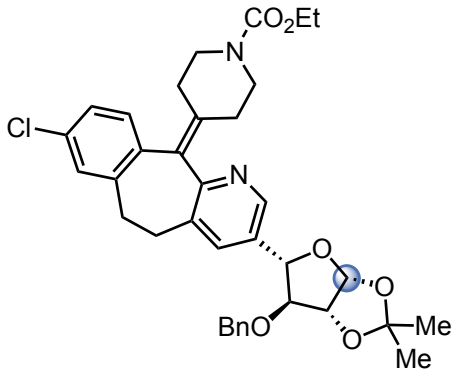

Ethyl 4-(3-((3a*R*,5*S*,6*S*,6a*R*)-6-(Benzyloxy)-2,2-dimethyltetrahydrofuro[2,3-d][1,3]dioxol-5-yl)-8-chloro-5,6-dihydro-11H-benzo[5,6]cyclohepta[1,2-b]pyridin-11-ylidene)piperidine-1-carboxylate (3d): Following General Procedure I using corresponding DHP (225.6 mg, 0.45 mmol, 3.0 equiv), ethyl 4-(3-bromo-8-chloro-5,6-dihydro-11*H*-benzo[5,6]cyclohepta[1,2-*b*]pyridin-11-ylidene)piperidine-1-carboxylate (69.0 mg, 0.15 mmol, 1.0 equiv), 4-CzIPN (2.3 mg, 0.006 mmol, 2 mol %), $NiBr_2$·dme (2.3 mg, 0.015 mmol, 5 mol %), and dMeObpy (2.3 mg, 0.021 mmol, 7 mol %) in anhydrous acetone (3.0 mL, 0.05 M). The product was purified by flash chromatography on silica gel (hexanes/EtOAc 0 to 60%) to afford a light yellow oil (78.5 mg, 83% yield). dr > 20:1 based on ^{1}H NMR of the crude reaction mixture. ^{1}H NMR (500 MHz, $CDCl_3$, major diastereomer) δ 8.42 (s, 1H), 7.52 – 7.41 (m, 1H), 7.32 – 7.27 (m, 5H), 7.19 – 7.10 (m, 3H), 5.98 (d, *J* = 4.1 Hz, 1H), 4.96 (dd, *J* = 9.4, 4.7 Hz, 1H), 4.75 – 4.67 (m, 2H), 4.58 – 4.53 (m, 1H), 4.14 (q, *J* = 7.2 Hz, 2H), 4.04 (dd, *J* = 17.3, 4.8 Hz, 1H), 3.79 (d, *J* = 14.9 Hz, 2H), 3.41 – 3.28 (m, 2H), 3.12 (ddt, *J* = 14.3, 10.0, 5.2 Hz, 2H), 2.79 (dddd, *J* = 15.1, 11.1, 8.2, 3.9 Hz, 2H), 2.48 (t, *J* = 13.1 Hz, 1H), 2.40 – 2.25 (m, 3H), 1.35 (s, 6H), 1.26 (d, *J* = 7.1 Hz, 3H) ppm. ^{13}C NMR (126 MHz, $CDCl_3$, mixture of rotamers) δ 155.6, 139.6, 138.9, 138.7, 137.8, 137.7, 137.0 (2C), 133.2, 130.7, 130.6, 129.1 (2C), 128.8 (2C), 128.7 (2C), 128.6 (2C), 128.4, (2C), 128.3 (2C), 128.2 (2C), 128.1, 128.1, 128.0, 127.7 (2C), 127.6, 126.4, 114.1, 114.0, 111.9, 105.5, 105.3, 87.7, 87.5, 85.7, 85.6, 82.4 (2C), 82.0 (2C), 75.7, 73.6, 72.9, 72.4 (2C), 72.2, 71.5, 61.6, 61.5, 44.9, 44.8, 31.7 (3C), 30.9, 30.7, 29.9, 27.3 (2C), 26.9, 26.5, 14.8, 14.4, 14.3, 0.2. IR (neat, cm^{-1}): 2931, 1696, 1445,

1383, 1229, 1074, 769, 699. HRMS (ES+) *calcd for* $C_{36}H_{40}ClN_2O_6$ $[M+H]^+$ 631.2575, *found* 631.2589.

^{1}H NMR ($CDCl_3$, 500 MHz) of (3a*R*,5*S*,6*S*,6a*R*)-6-(benzyloxy)-2,2-dimethyl-5-(naphthalen-2-yl)tetrahydrofuro[2,3-d] [1,3]dioxole (**7.3.1**)

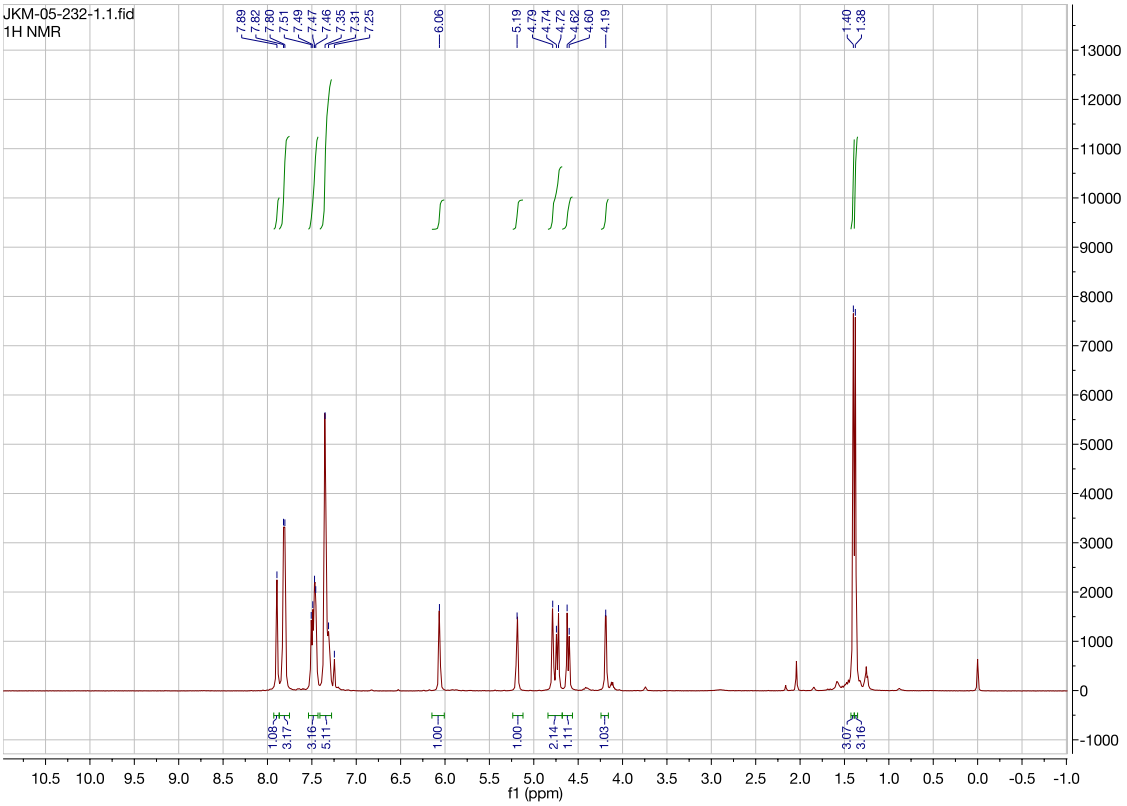

^{13}C NMR (126 MHz, $CDCl_3$) of (3a*R*,5*S*,6*S*,6a*R*)-6-(benzyloxy)-2,2-dimethyl-5-(naphthalen-2-yl)tetrahydrofuro[2,3-d] [1,3]dioxole (**7.3.1**)

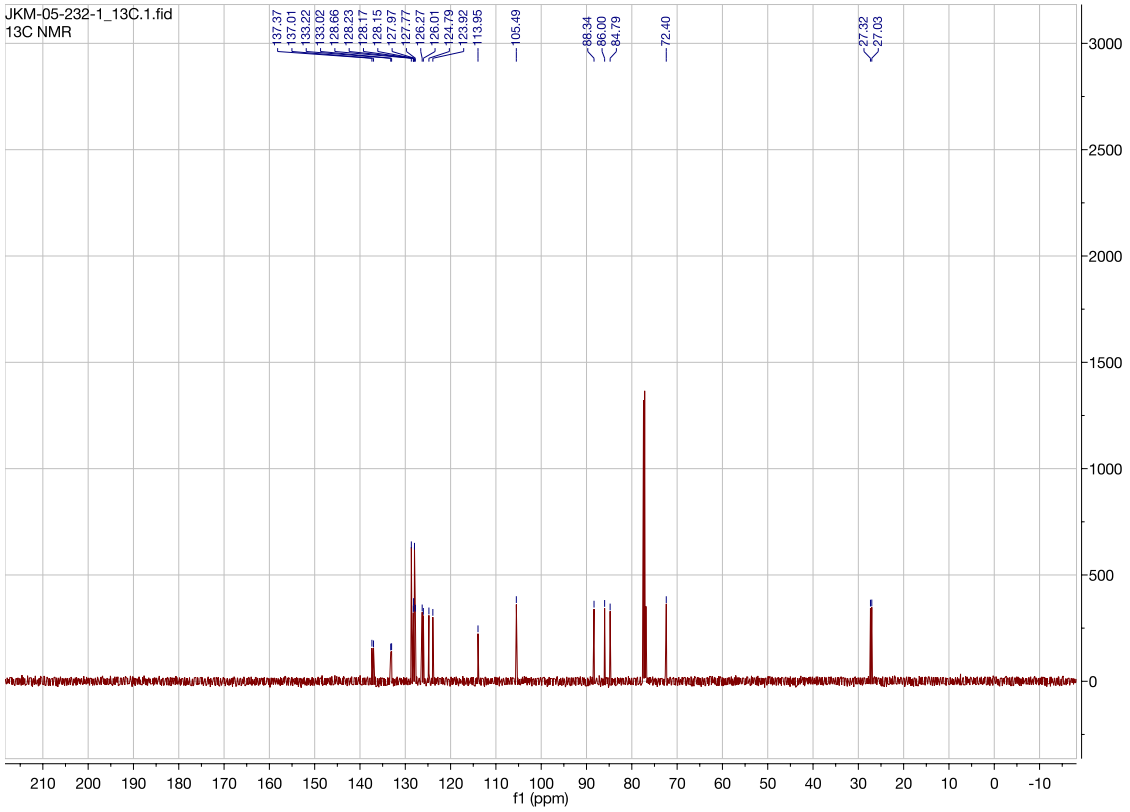

^{1}H NMR ($CDCl_3$, 500 MHz) of (3a*R*,5*R*,6*S*,6a*R*)-6-methoxy-2,2-dimethyl-5-(naphthalen-2-yl)tetrahydrofuro[2,3-d] [1,3]dioxole (**7.3.2**)

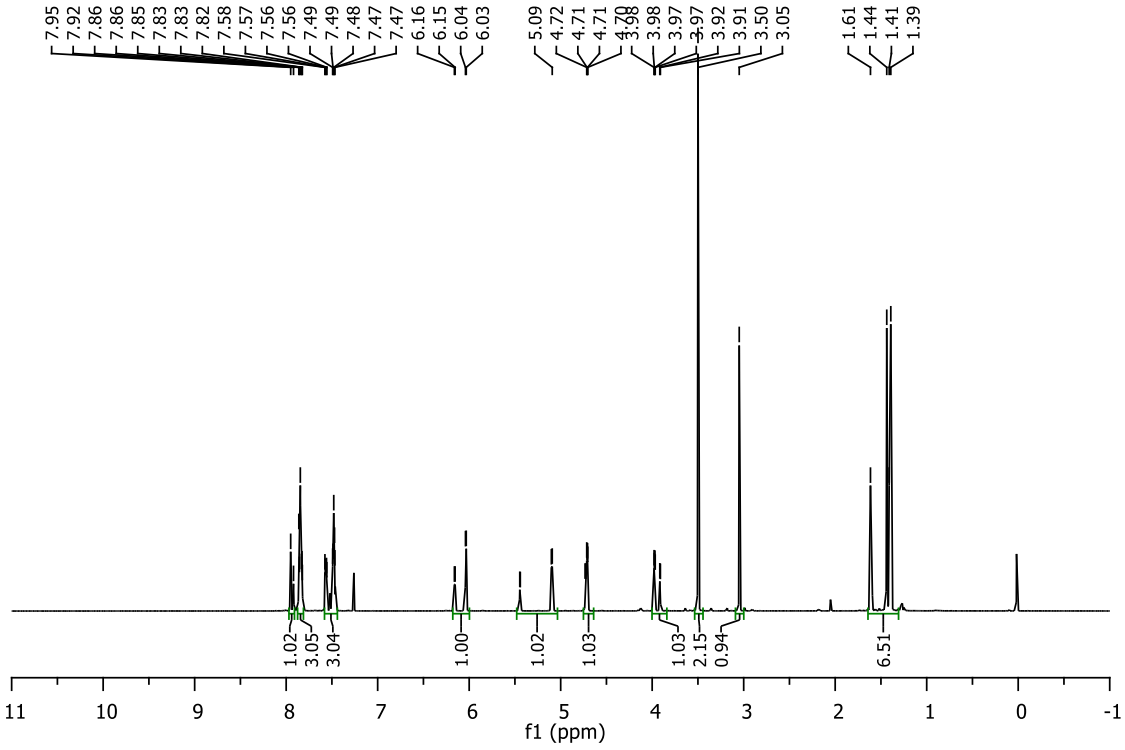

^{13}C NMR (126 MHz, $CDCl_3$) of (3a*R*,5*R*,6*S*,6a*R*)-6-methoxy-2,2-dimethyl-5-(naphthalen-2-yl)tetrahydrofuro[2,3-d] [1,3]dioxole (**7.3.3**)

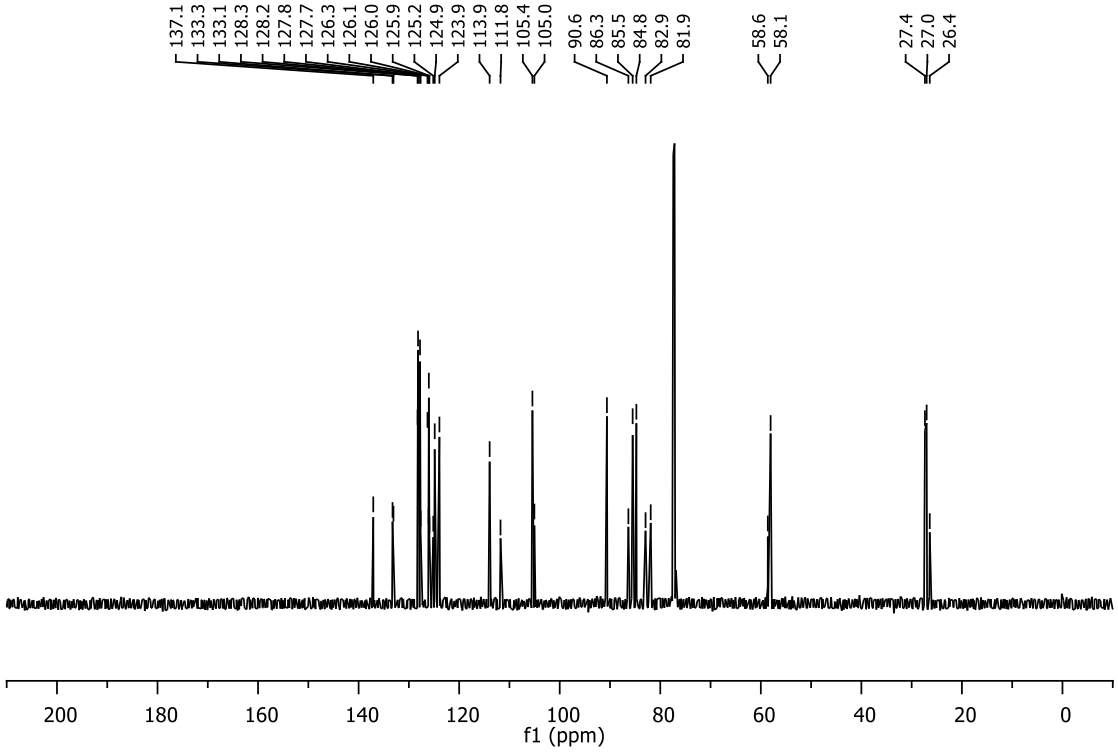

^{1}H NMR ($CDCl_3$, 500 MHz) of (3a*R*,6*S*,6a*S*)-6-Fluoro-2,2-dimethyl-5-(naphthalen-2-yl) tetrahydrofuro[2,3-*d*][1,3]dioxole (**7.3.3**)

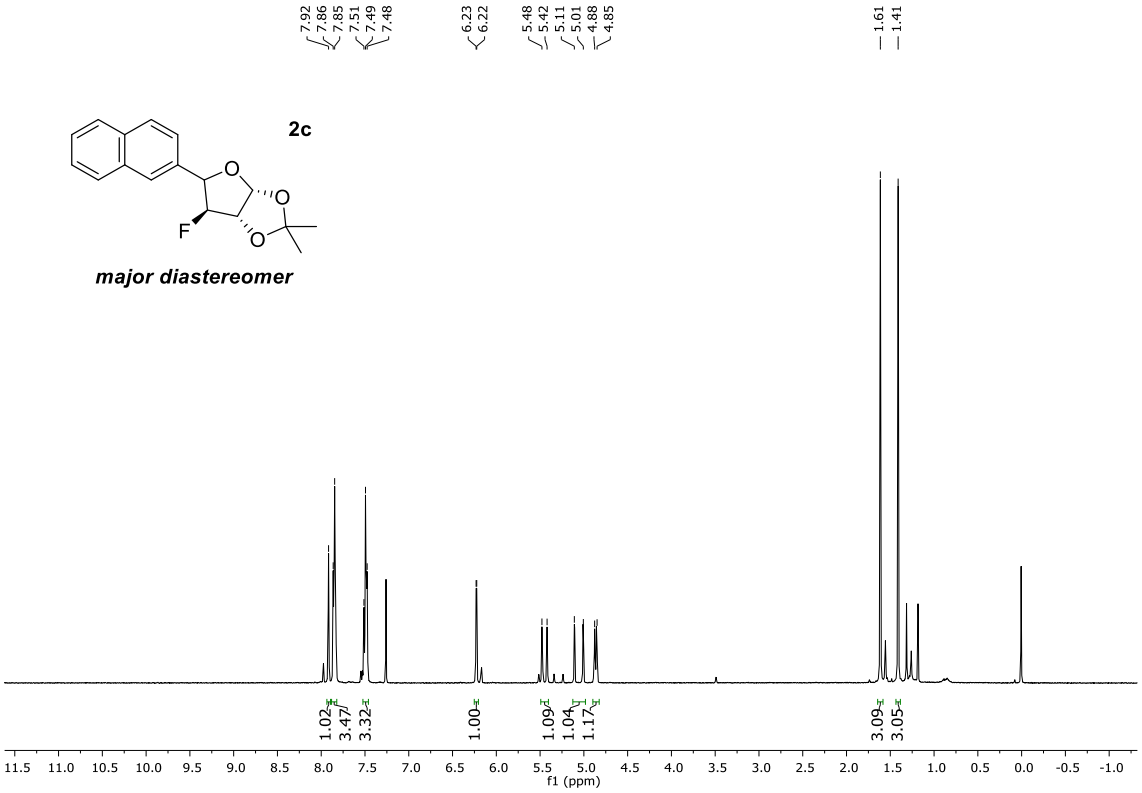

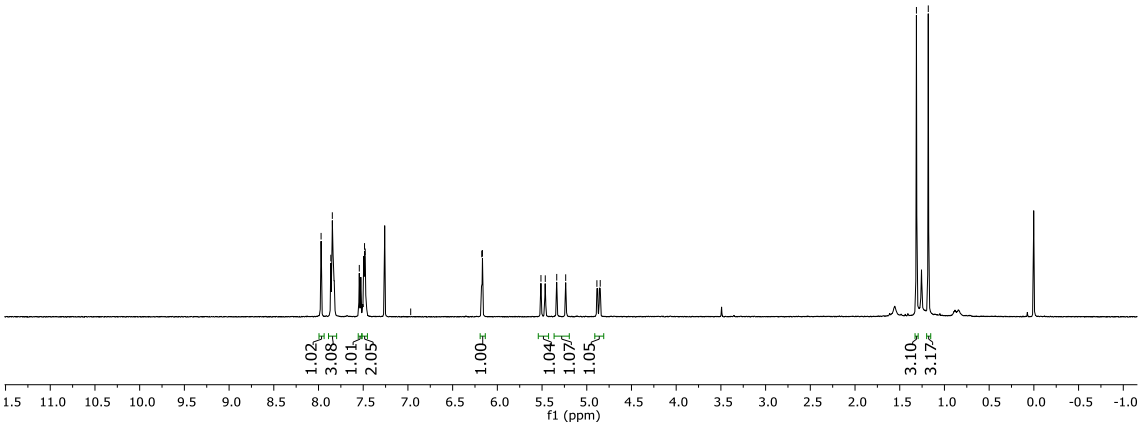

^{13}C NMR (126 MHz, $CDCl_3$) of (3a*R*,6*S*,6a*S*)-6-Fluoro-2,2-dimethyl-5-(naphthalen-2-yl) tetrahydrofuro[2,3-*d*][1,3]dioxole (**7.3.3**)

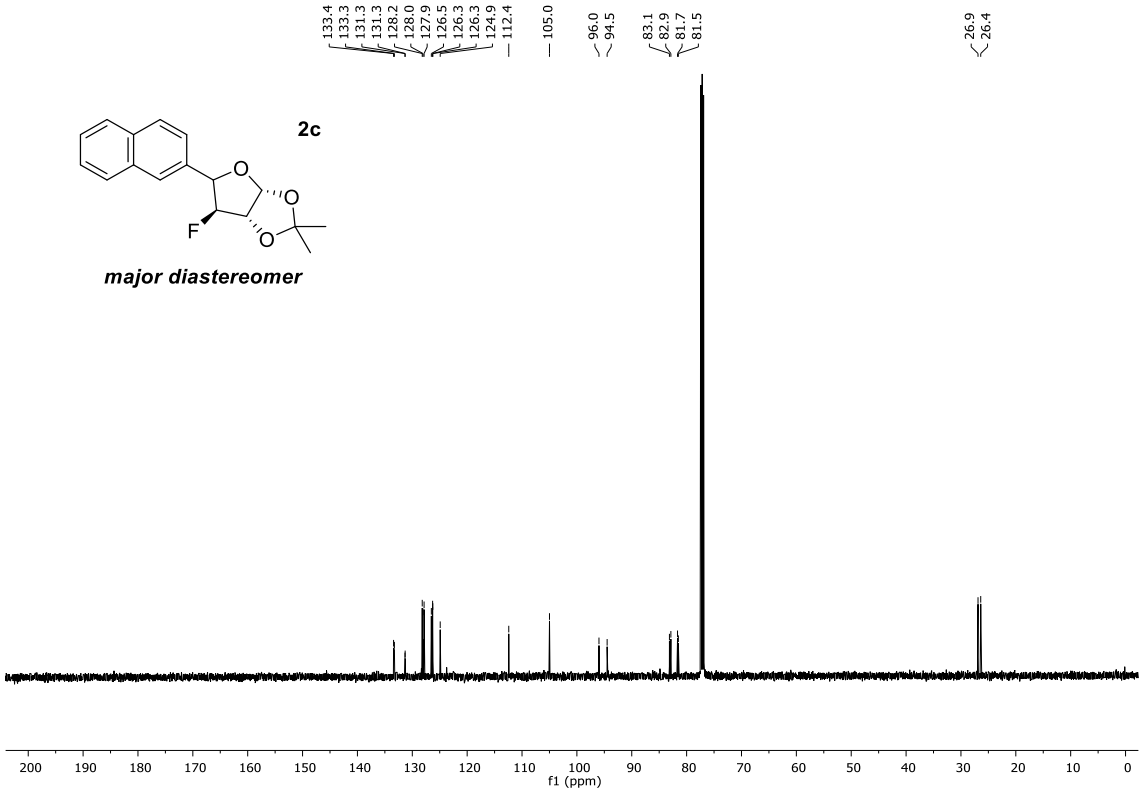

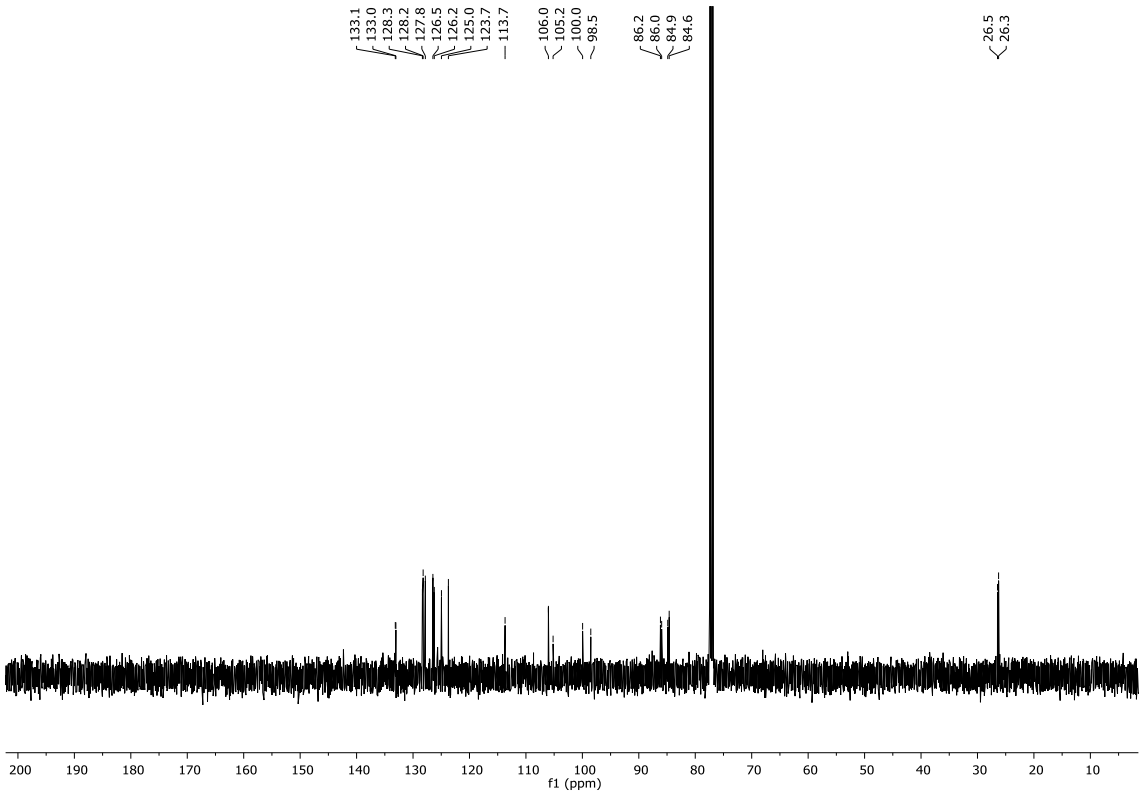

^{19}F NMR (471 MHz, $CDCl_3$) of (3a*R*,6*S*,6a*S*)-6-Fluoro-2,2-dimethyl-5-(naphthalen-2-yl) tetrahydrofuro[2,3-*d*][1,3]dioxole (**7.3.3**)

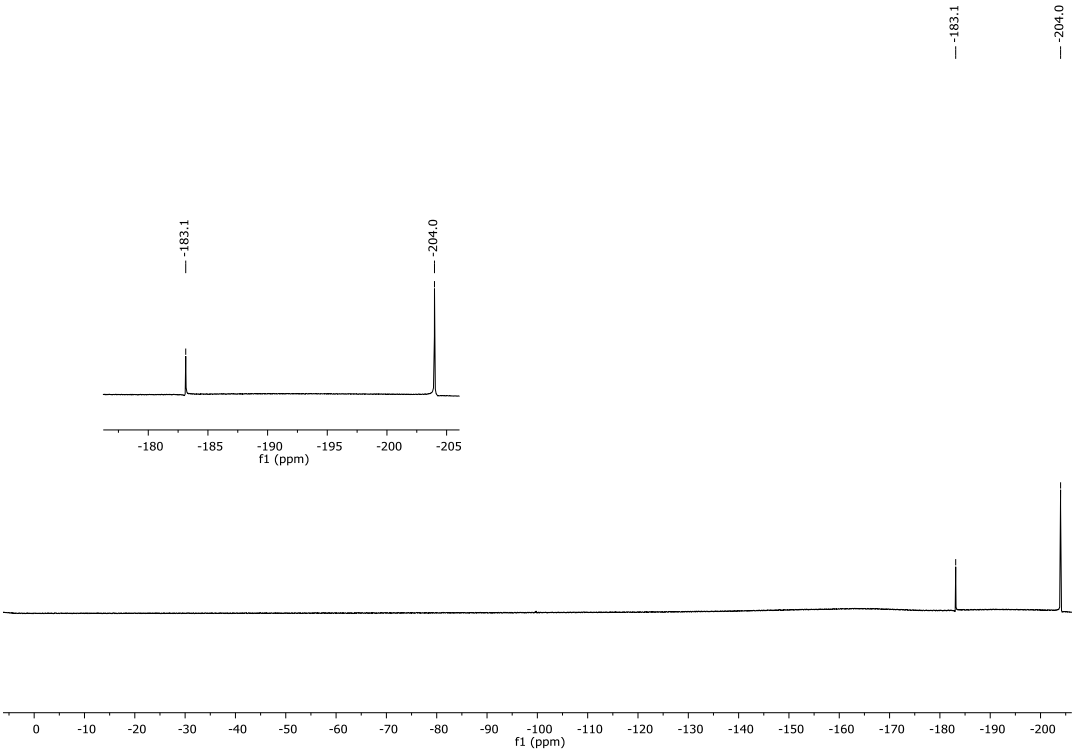

^{1}H NMR ($CDCl_3$, 500 MHz) of *tert*-Butyl(((3a*R*,6*S*,6a*R*)-2,2-dimethyl-5-(naphthalen-2-yl)tetrahydrofuro[2,3-*d*][1,3]dioxol-6-yl)oxy)dimethylsilane (**7.3.4**)

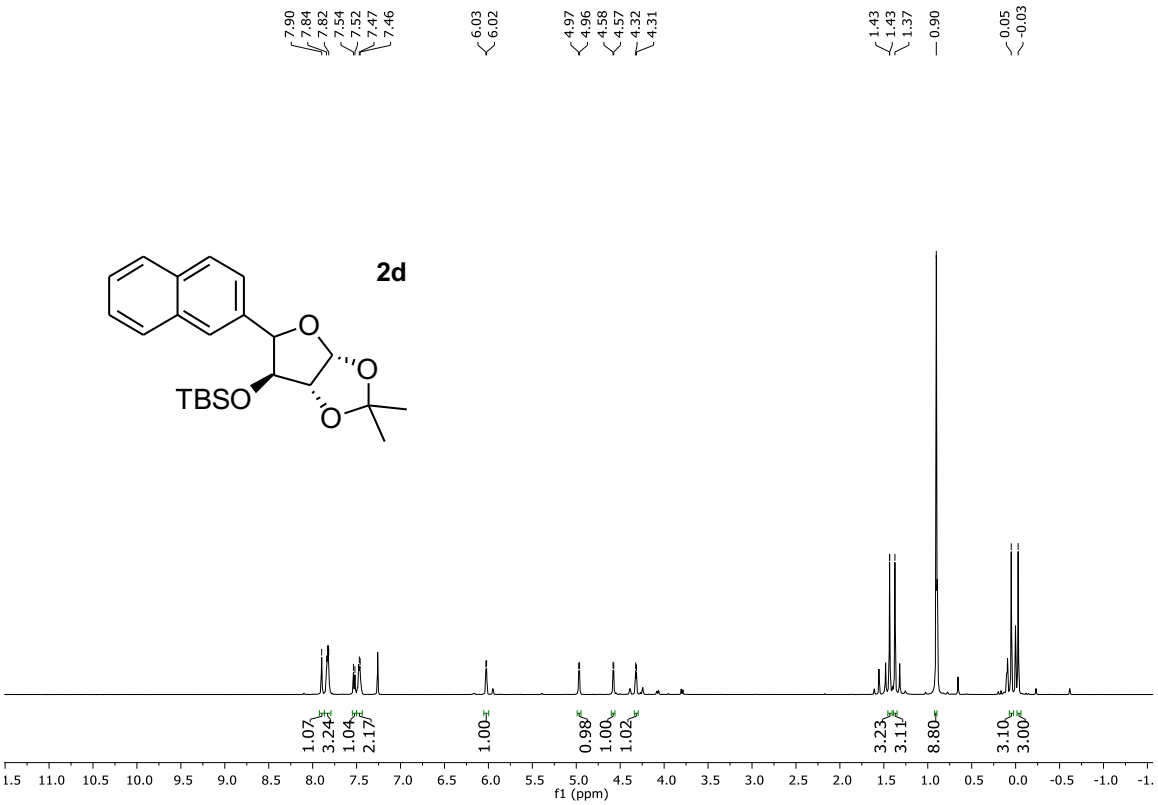

^{13}C NMR (126 MHz, $CDCl_3$) of *tert*-Butyl(((3a*R*,6*S*,6a*R*)-2,2-dimethyl-5-(naphthalen-2-yl)tetrahydrofuro[2,3-*d*][1,3]dioxol-6-yl)oxy)dimethylsilane (**7.3.4**)

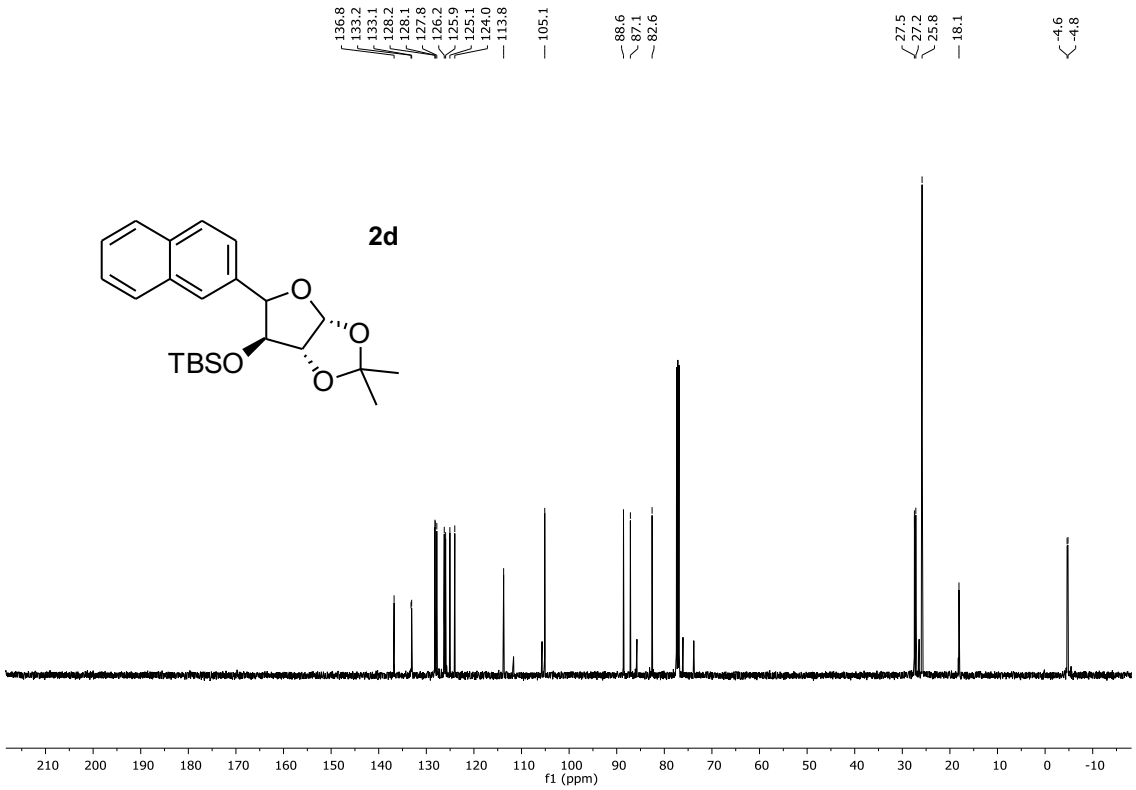

^{1}H NMR ($CDCl_3$, 500 MHz) of (3a*R*,6*S*,6a*R*)-2,2-dimethyl-5-(naphthalen-2-yl)tetrahydrofuro[2,3-d][1,3]dioxol-6-ol (**7.3.5**)

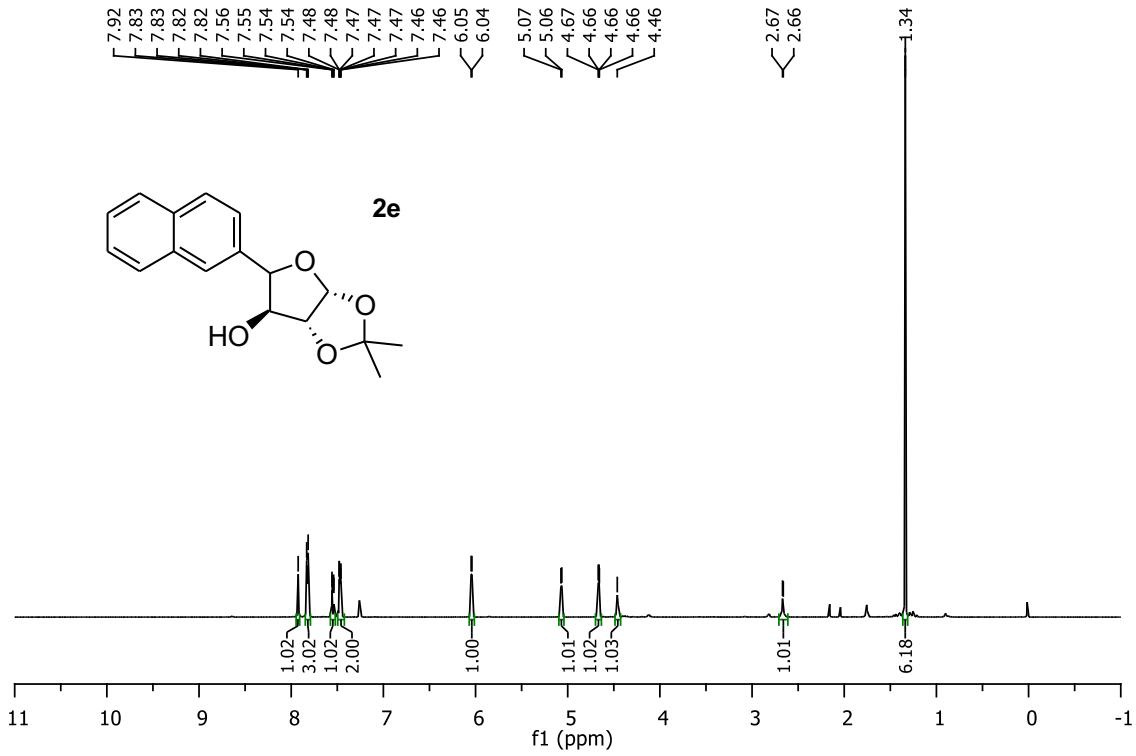

^{13}C NMR ($CDCl_3$, 126 MHz) of (3a*R*,6*S*,6a*R*)-2,2-dimethyl-5-(naphthalen-2-yl)tetrahydrofuro[2,3-d][1,3]dioxol-6-ol (**7.3.5**)

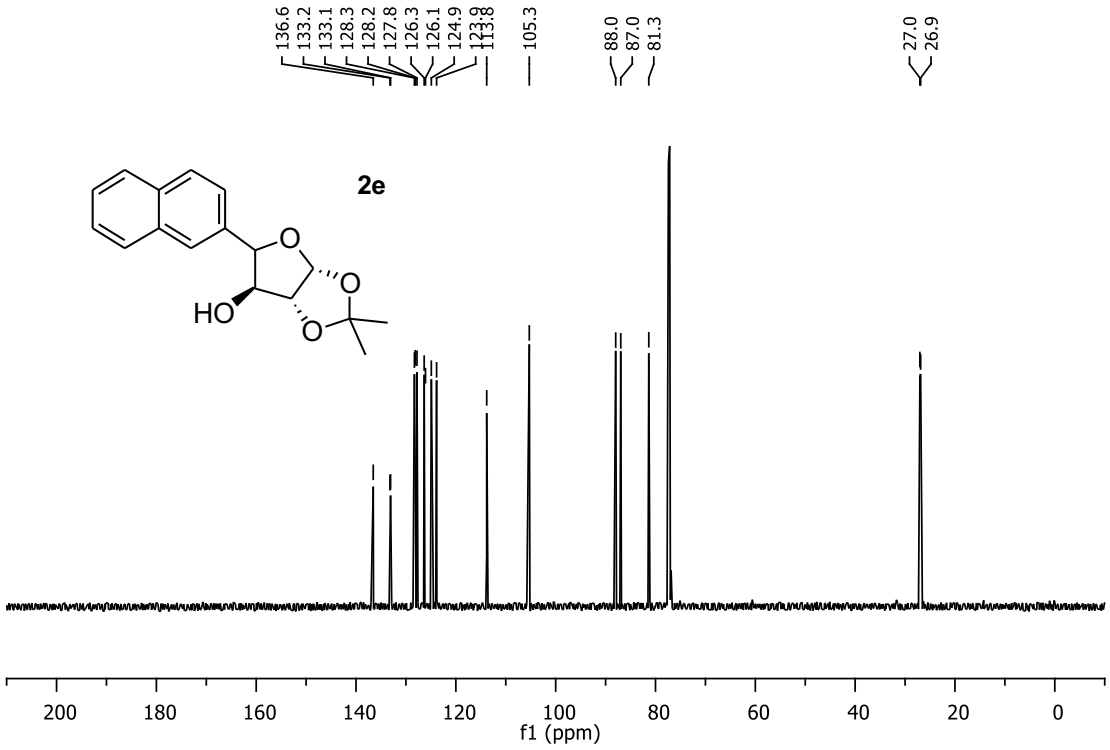

^{1}H NMR ($CDCl_3$, 500 MHz) of (3a*R*,4*R*,6*R*,6a*R*)-4-Methoxy-2,2-dimethyl-6-(naphthalen-2-yl)tetrahydrofuro[3,4-*d*][1,3]dioxole (**7.3.6**)

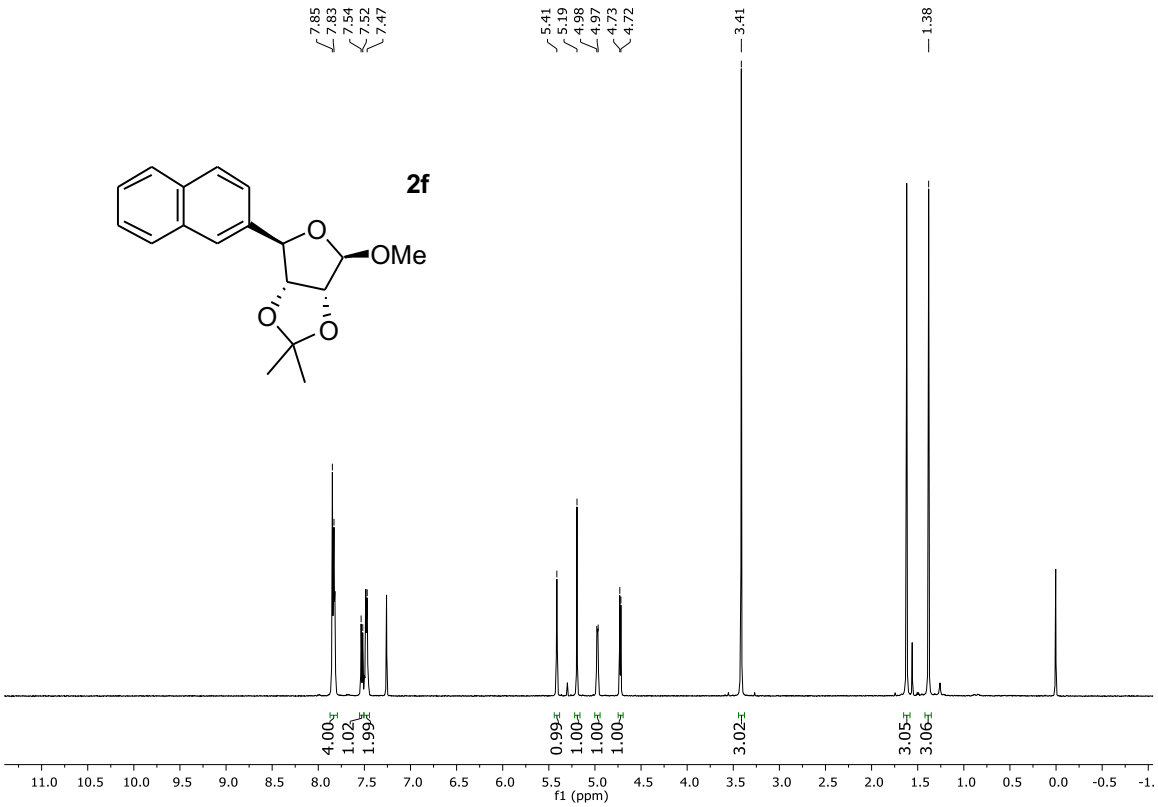

^{13}C NMR (126 MHz, $CDCl_3$) of (3a*R*,4*R*,6*R*,6a*R*)-4-Methoxy-2,2-dimethyl-6-(naphthalen-2-yl)tetrahydrofuro[3,4-*d*][1,3]dioxole (**7.3.6**)

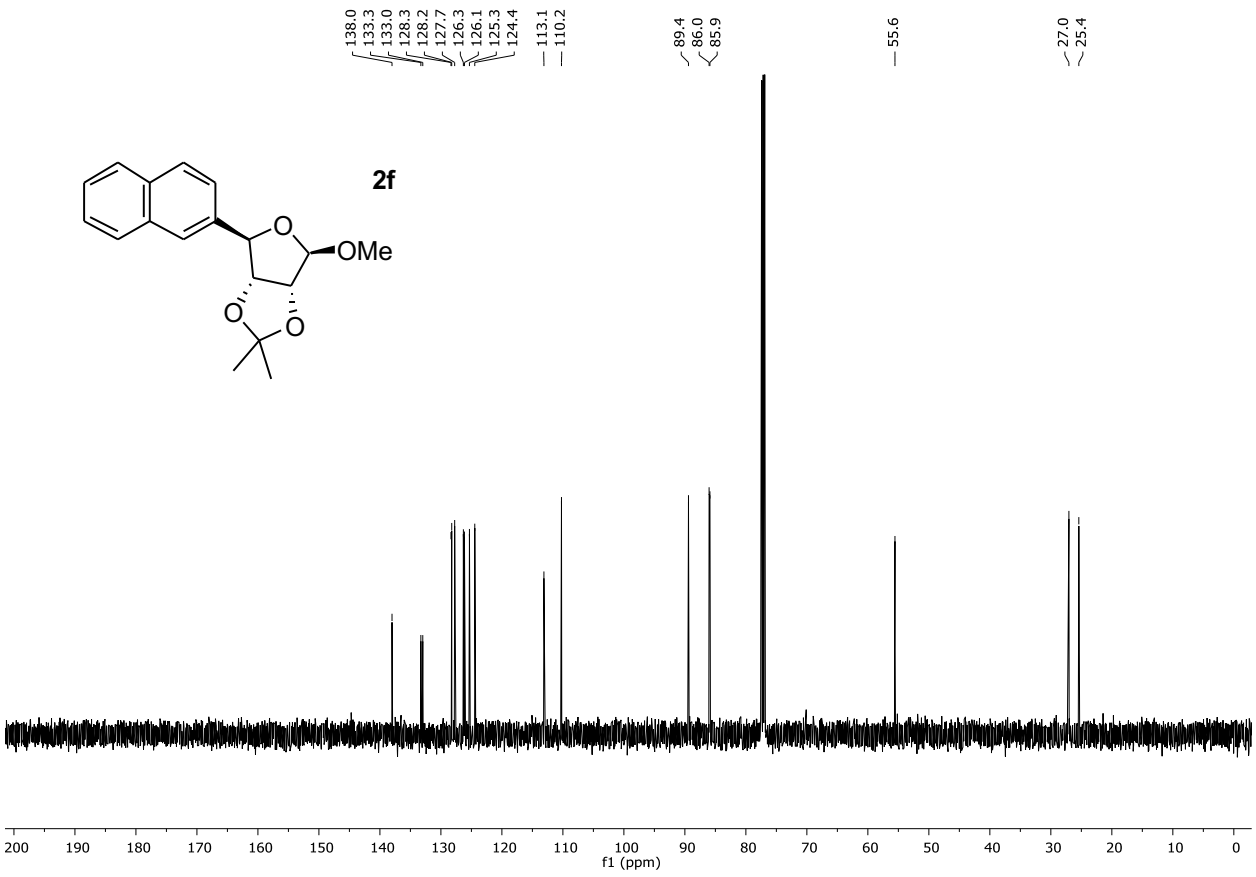

^{1}H NMR ($CDCl_3$, 500 MHz) of 1-((3a*R*,4*R*,6*R*,6a*R*)-2,2-dimethyl-6-(naphthalen-2-yl) tetrahydrofuro[3,4-d][1,3]dioxol-4-yl) pyrimidine-2,4(1H,3H)-dione (**7.3.7**)

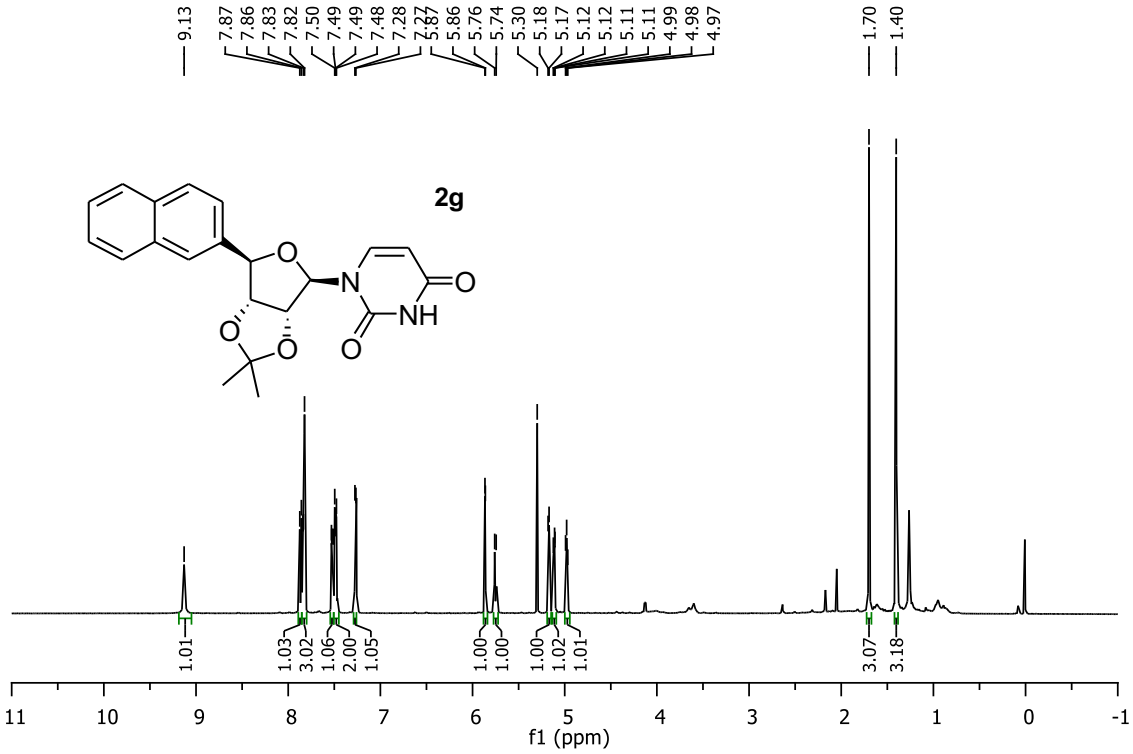

^{13}C NMR (126 MHz, $CDCl_3$) of 1-((3a*R*,4*R*,6*R*,6a*R*)-2,2-dimethyl-6-(naphthalen-2-yl) tetrahydrofuro[3,4-d][1,3]dioxol-4-yl) pyrimidine-2,4(1H,3H)-dione (**7.3.7**)

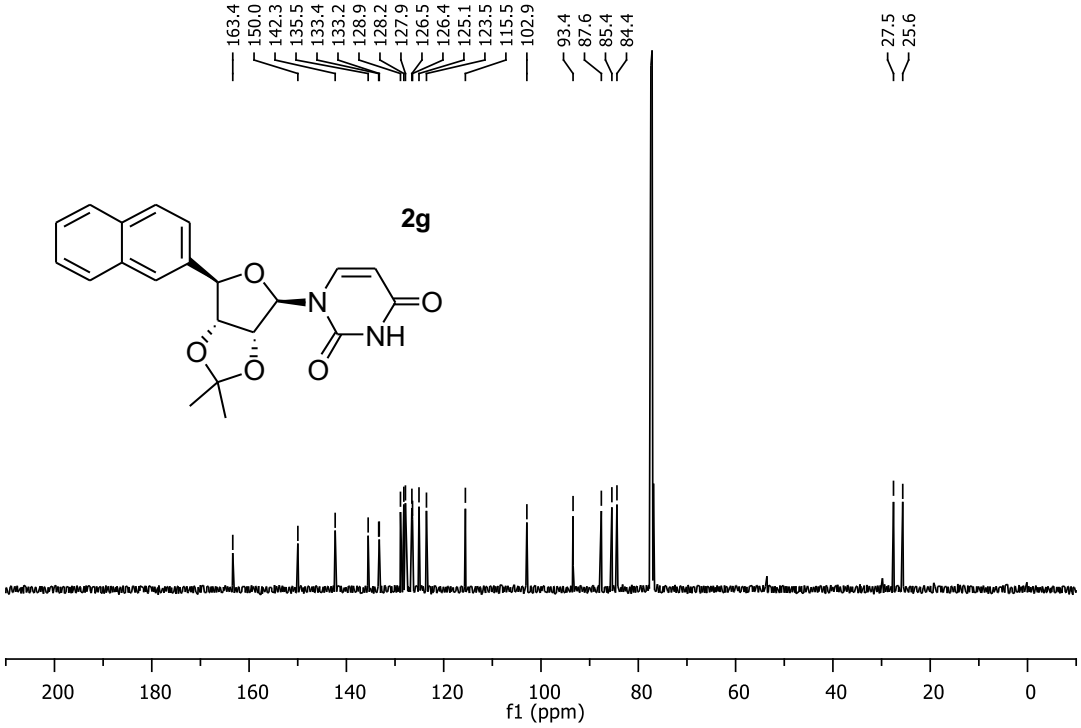

^{1}H NMR ($CDCl_3$, 500 MHz) of (3a*R*,5*R*,5a*S*,8a*S*,8b*R*)-2,2,7,7-tetramethyl-5-(naphthalen-2-yl)tetrahydro-5H-bis ([1,3]dioxolo)[4,5-b:4',5'-d]pyran (**7.3.8**)

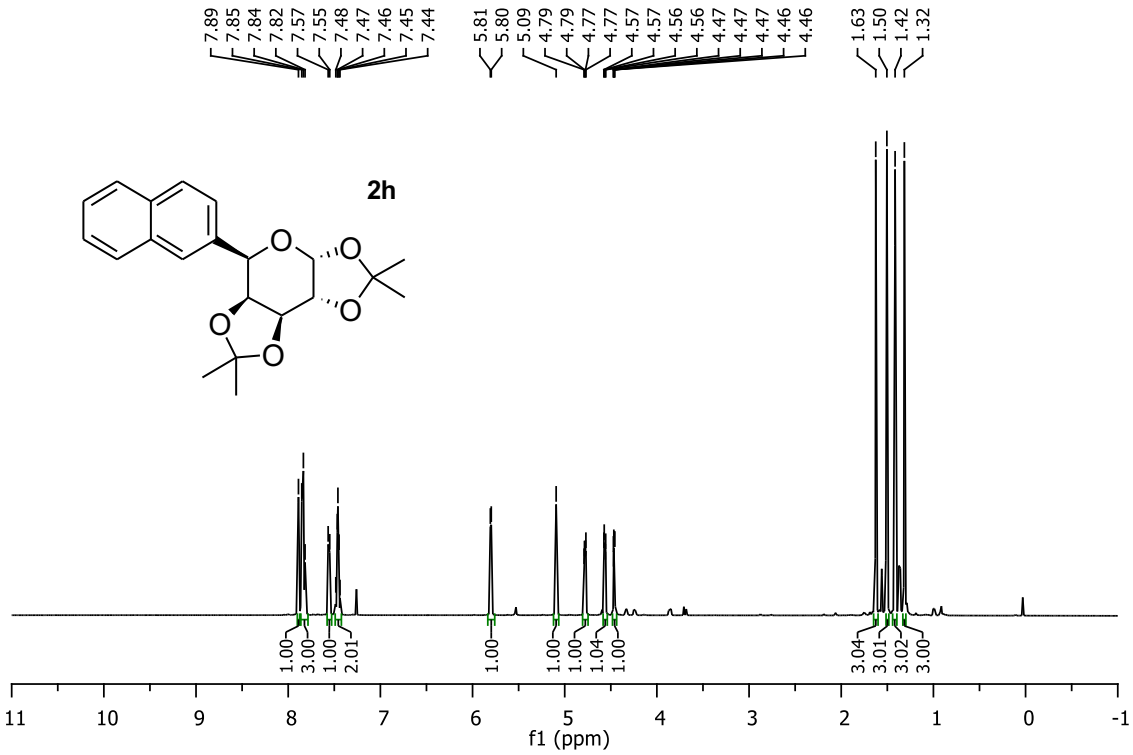

^{13}C NMR (126 MHz, $CDCl_3$) of (3a*R*,5*R*,5a*S*,8a*S*,8b*R*)-2,2,7,7-tetramethyl-5-(naphthalen-2-yl)tetrahydro-5H-bis ([1,3]dioxolo)[4,5-b:4',5'-d]pyran **(7.3.8)**

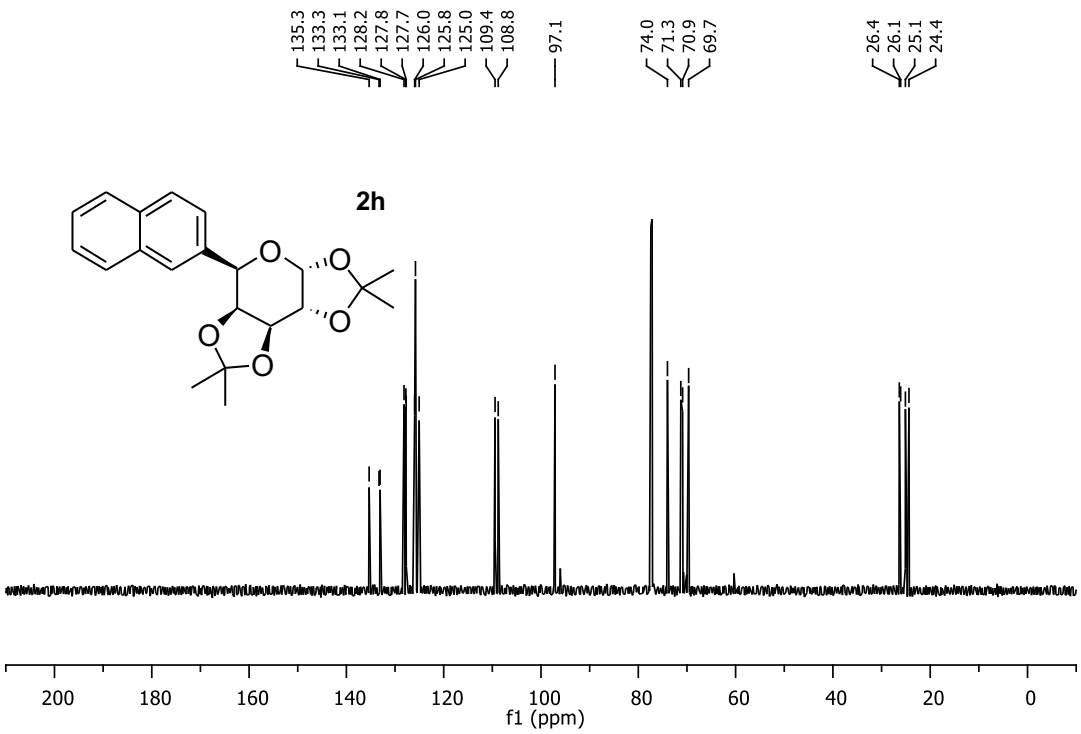

^{1}H NMR ($CDCl_3$, 500 MHz) of (2*S*,3*R*,4*S*,5*R*)-2,3,4,5-tetramethoxy-6-(naphthalen-2-yl)tetrahydro-2H-pyran (**7.3.9**)

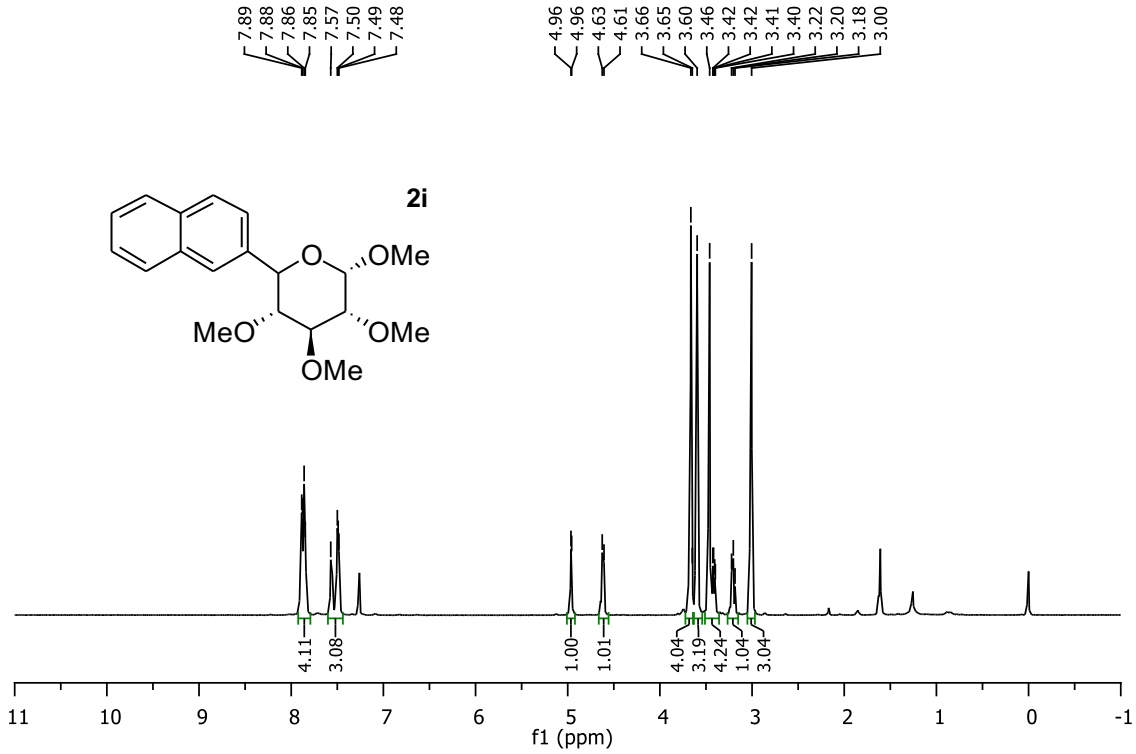

^{13}C NMR ($CDCl_3$, 126 MHz) of (2*S*,3*R*,4*S*,5*R*)-2,3,4,5-tetramethoxy-6-(naphthalen-2-yl)tetrahydro-2H-pyran (**7.3.9**)

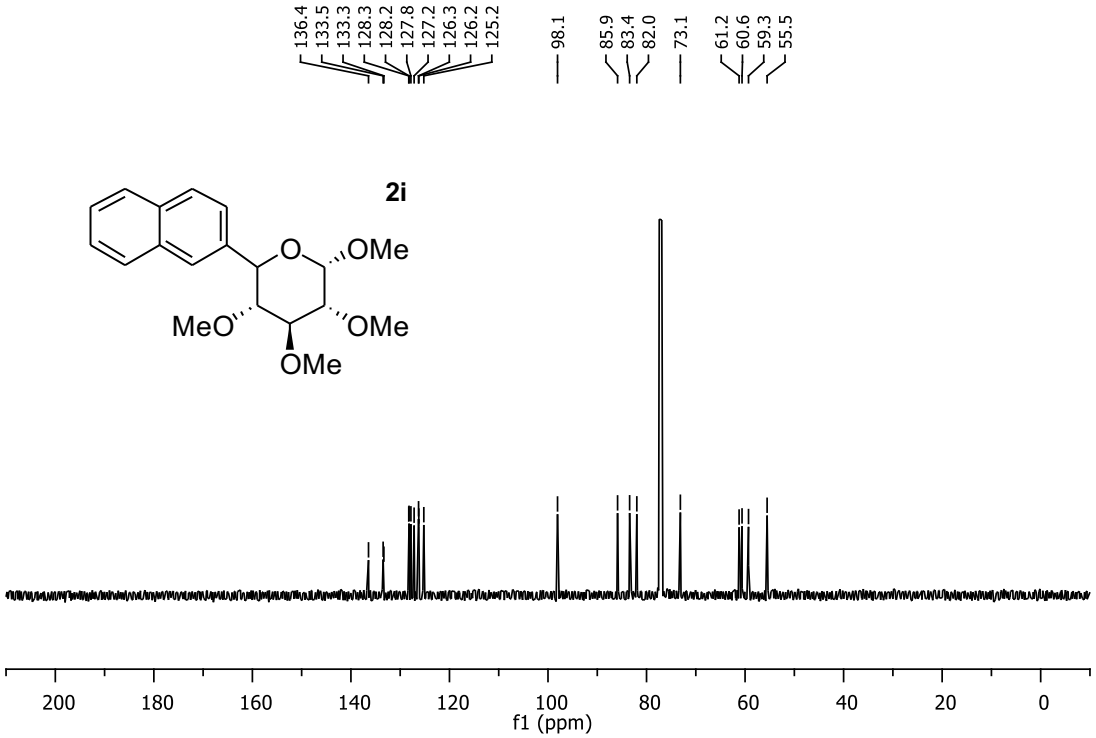

^{1}H NMR ($CDCl_3$, 360 MHz) of 4-((3a*R*,5*R*,5a*S*,8a*S*,8b*R*)-2,2,7,7-tetramethyltetrahydro-5H-bis([1,3]dioxolo)[4,5-b:4',5'-d] pyran-5-yl)benzonitrile (**7.4.1**)

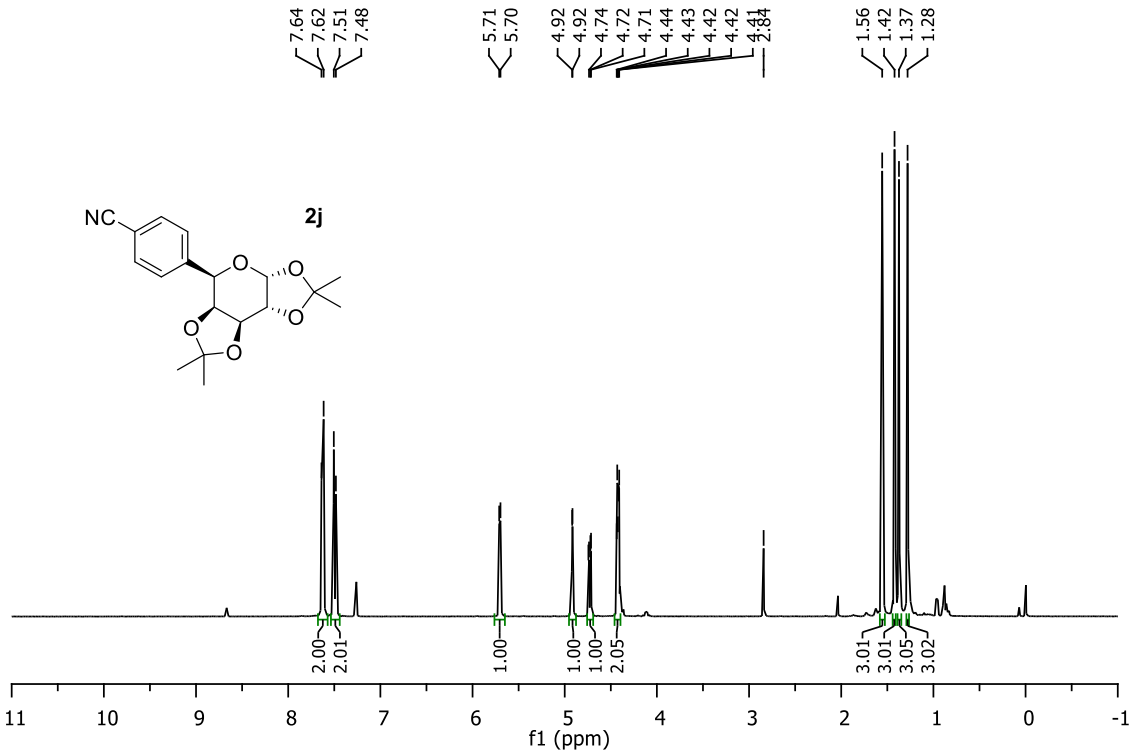

^{13}C NMR ($CDCl_3$, 91 MHz) of of 4-((3a*R*,5*R*,5a*S*,8a*S*,8b*R*)-2,2,7,7-tetramethyltetrahydro-5H-bis([1,3]dioxolo)[4,5-b:4',5'-d] pyran-5-yl)benzonitrile (**7.4.1**)

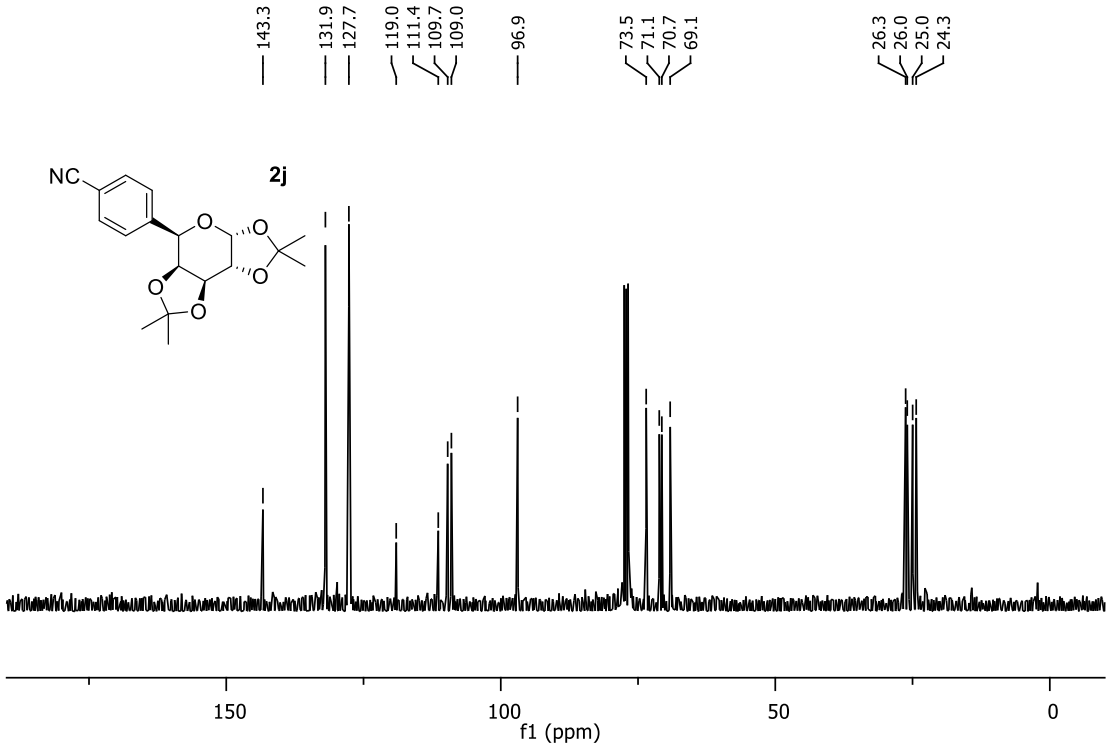

^{1}H NMR ($CDCl_3$, 360 MHz) of
4-((3a*R*,5*R*,6*S*,6a*R*)-6-(benzyloxy)-2,2-dimethyltetrahydrofuro [2,3-d] [1,3]dioxol-5-yl)benzonitrile (**7.4.2**)

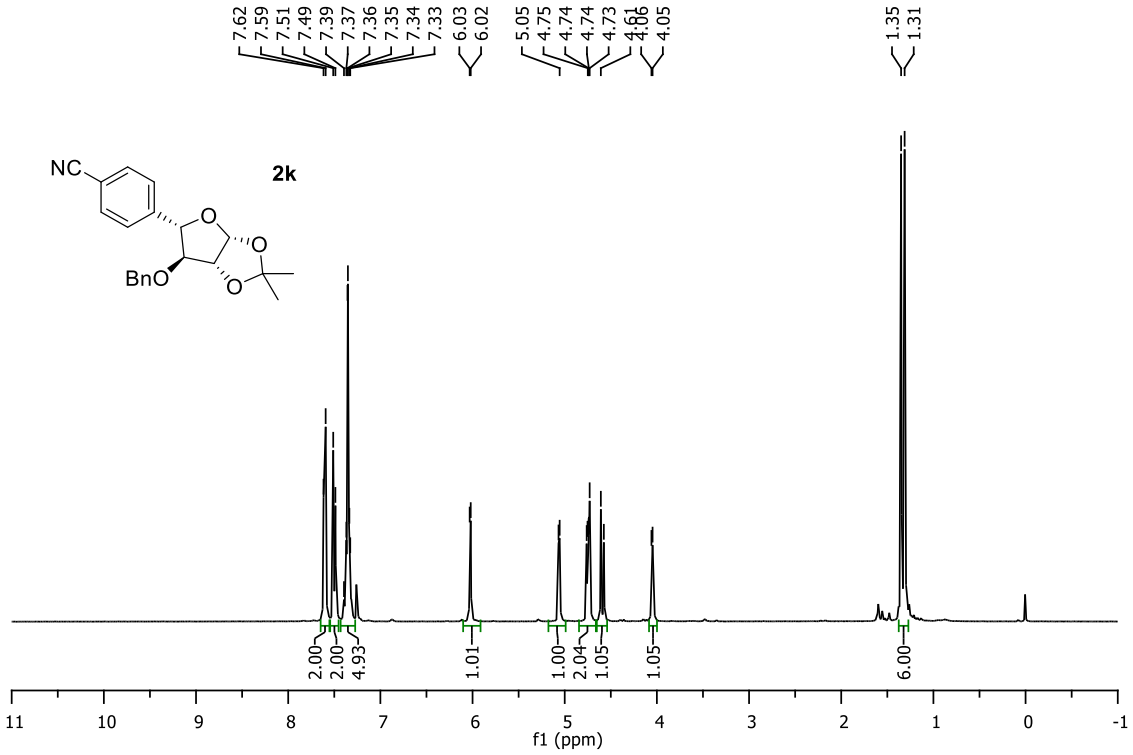

^{13}C NMR ($CDCl_3$, 91 MHz) of
4-((3a*R*,5*R*,6*S*,6a*R*)-6-(benzyloxy)-2,2-dimethyltetrahydrofuro [2,3-d] [1,3]dioxol-5-yl)benzonitrile (**7.4.2**)

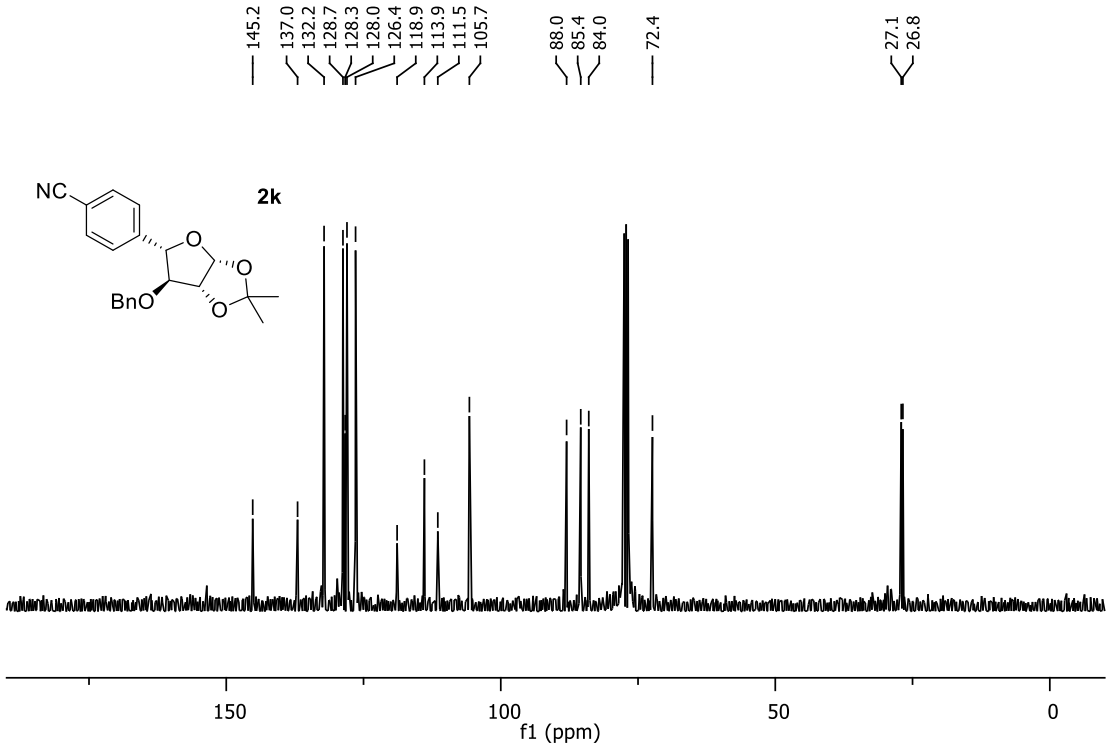

^{1}H NMR ($CDCl_3$, 360 MHz) of 4-((3a*R*,5*R*,6*S*,6a*R*)-6-methoxy-2,2-dimethyltetrahydrofuro[2,3-d][1,3]dioxol-5-yl) benzonitrile (**7.4.3**)

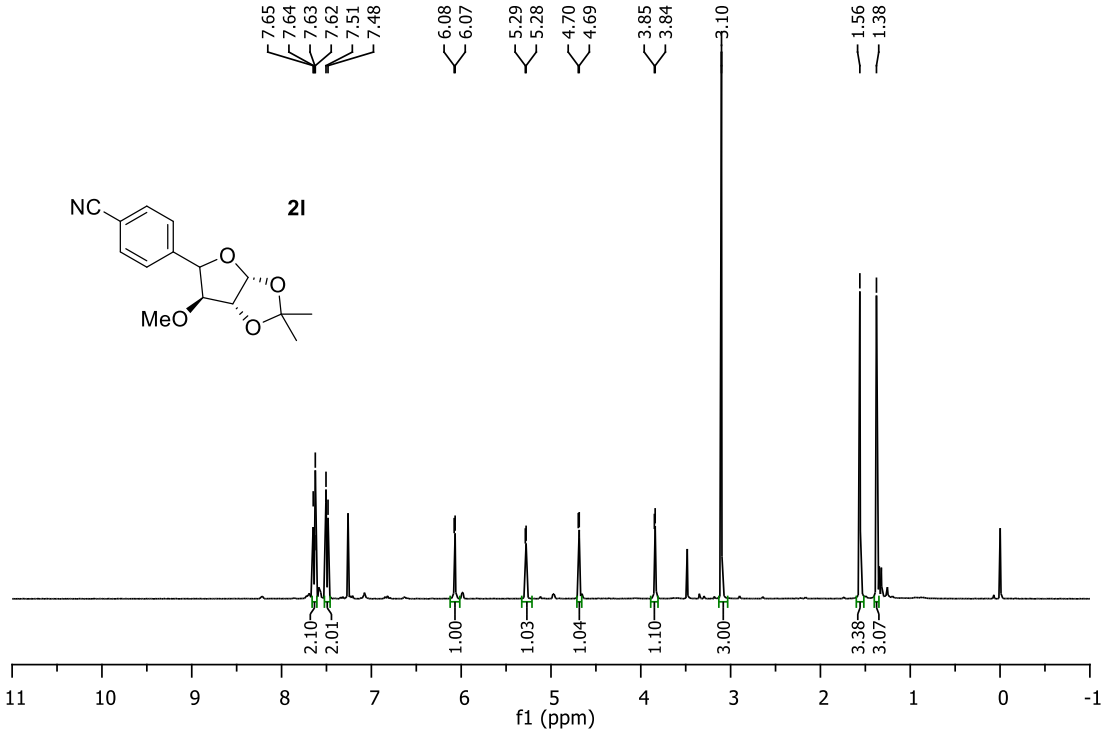

^{13}C NMR ($CDCl_3$, 91 MHz) of 4-((3a*R*,5*R*,6*S*,6a*R*)-6-methoxy-2,2-dimethyltetrahydrofuro[2,3-d][1,3]dioxol-5-yl) benzonitrile (**7.4.3**)

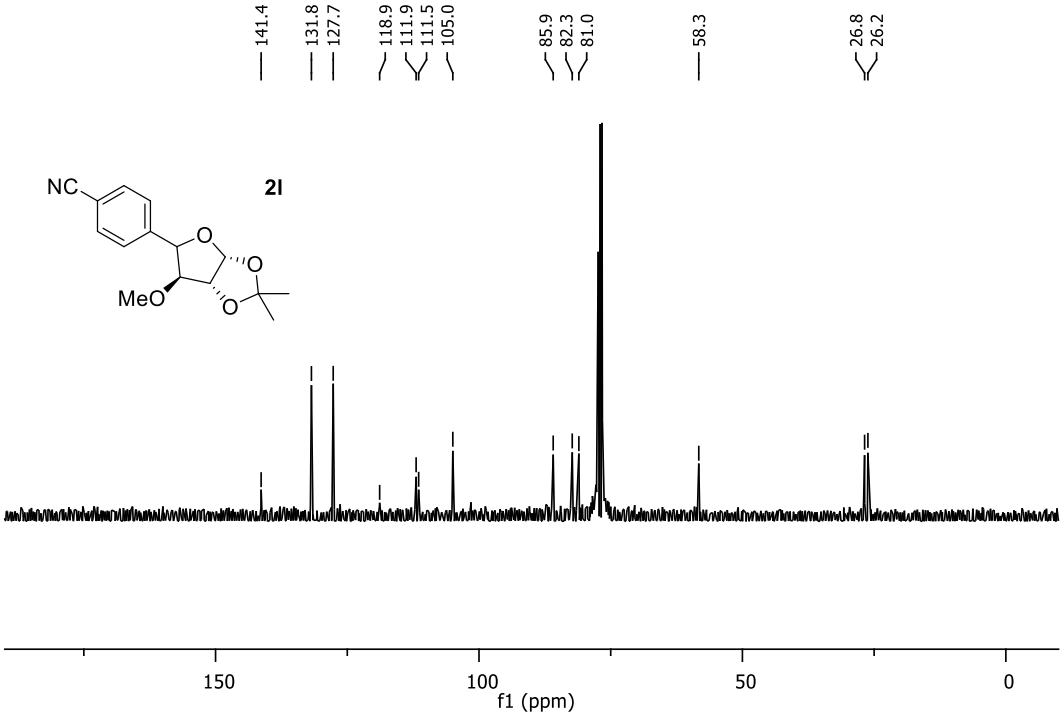

^{1}H NMR ($CDCl_3$, 360 MHz) of (3a*R*,5*R*,5a*S*,8a*S*,8b*R*)-5-(3-methoxyphenyl)-2,2,7,7-tetramethyltetrahydro-5H-bis([1,3]dioxolo)[4,5-b:4',5'-d]pyran (**7.4.4**)

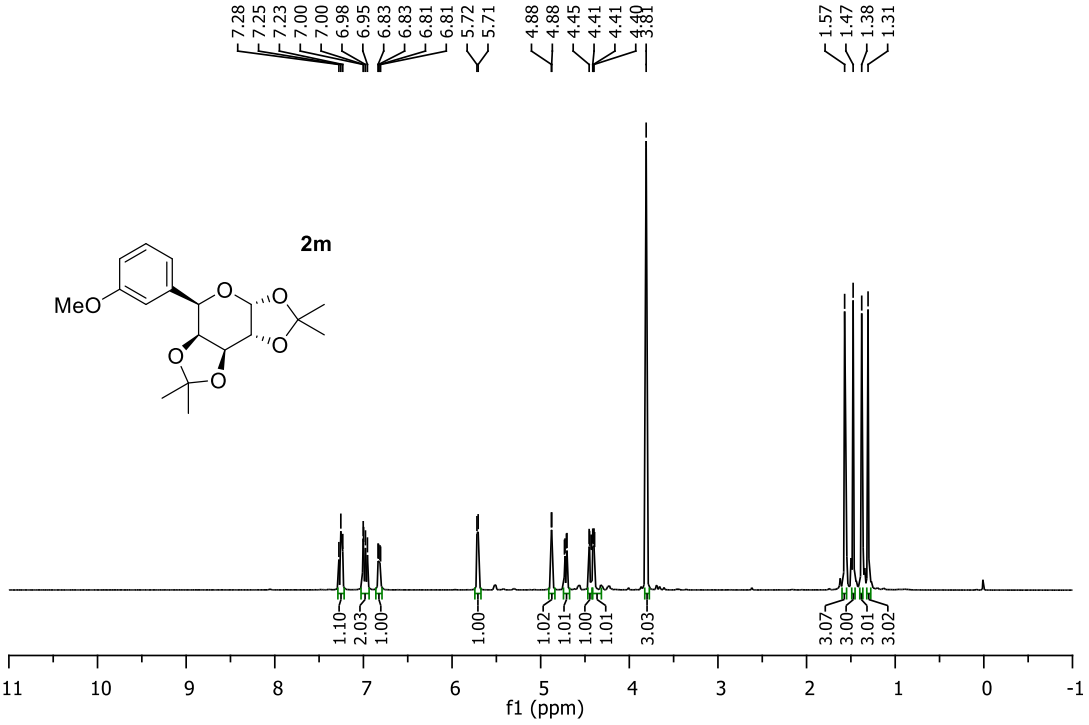

^{13}C NMR ($CDCl_3$, 91 MHz) of (3a*R*,5*R*,5a*S*,8a*S*,8b*R*)-5-(3-methoxyphenyl)-2,2,7,7-tetramethyltetrahydro-5H-bis([1,3]dioxolo)[4,5-b:4',5'-d]pyran (**7.4.4**)

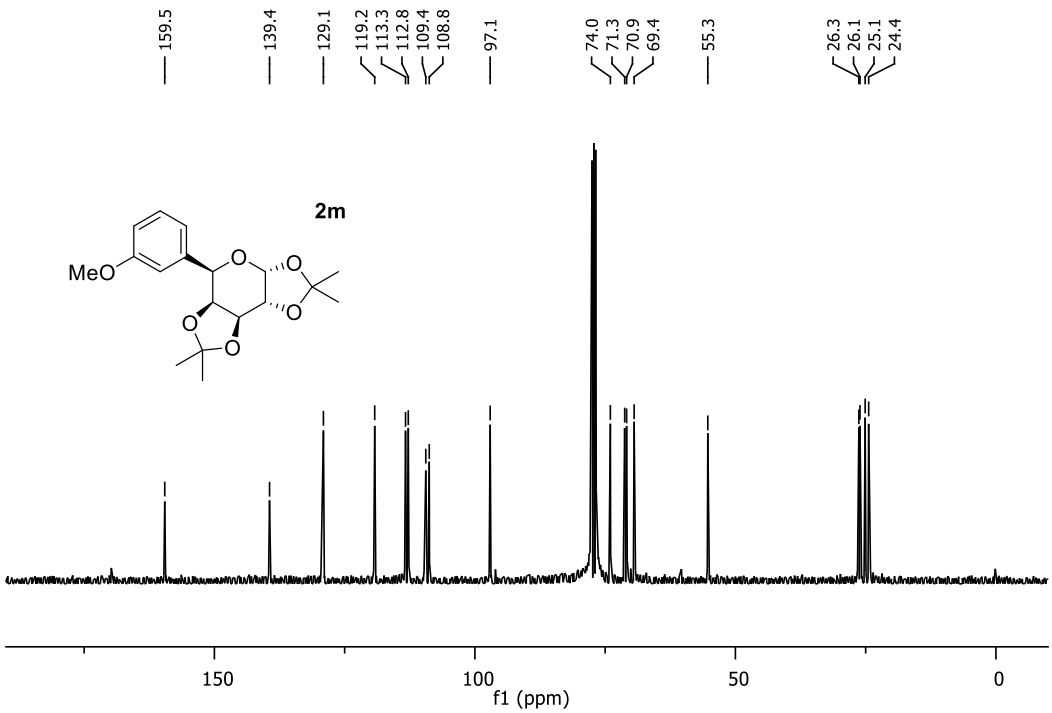

^{1}H NMR ($CDCl_3$, 500 MHz) of 1-(4-((3a*R*,5*S*,6*S*,6a*R*)-6-(benzyloxy)-2,2-dimethyltetrahydrofuro [2,3-d][1,3]dioxol-5-yl)phenyl)-2,2,2-trifluoroethan-1-one (**7.4.5**)

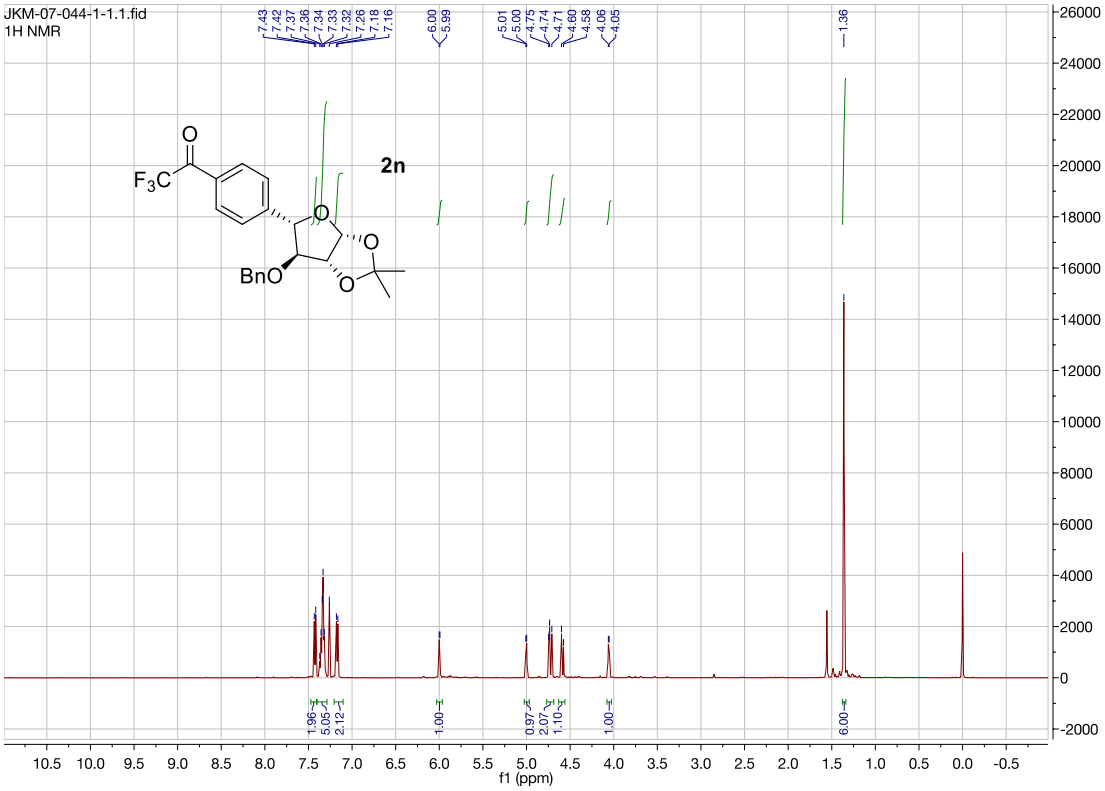

^{13}C NMR ($CDCl_3$, 126 MHz) of 1-(4-((3a*R*,5*S*,6*S*,6a*R*)-6-(benzyloxy)-2,2-dimethyltetrahydrofuro [2,3-d][1,3]dioxol-5-yl)phenyl)-2,2,2-trifluoroethan-1-one (**7.4.5**)

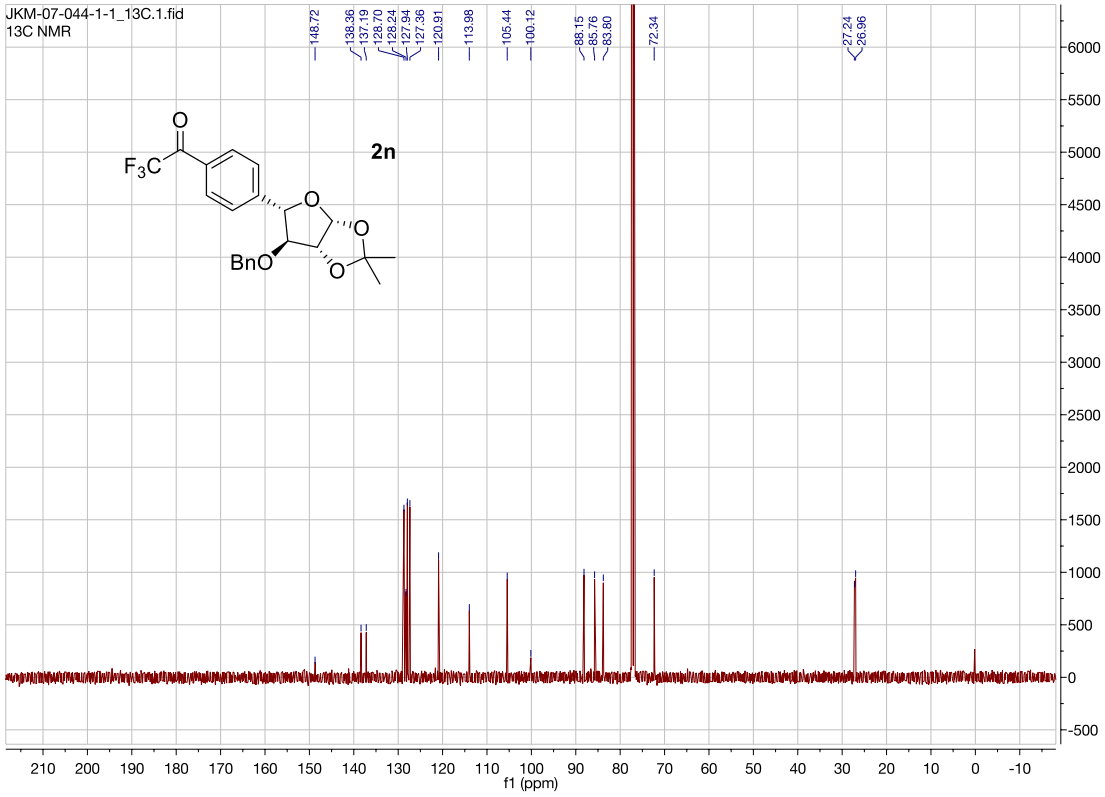

^{1}H NMR ($CDCl_3$, 500 MHz) of 4-(4-((3aR,5S,6S,6aR)-6-(benzyloxy)-2,2-dimethyltetrahydrofuro [2,3-d][1,3]dioxol-5-yl)phenyl)-4-oxobutanenitrile (**7.4.6**)

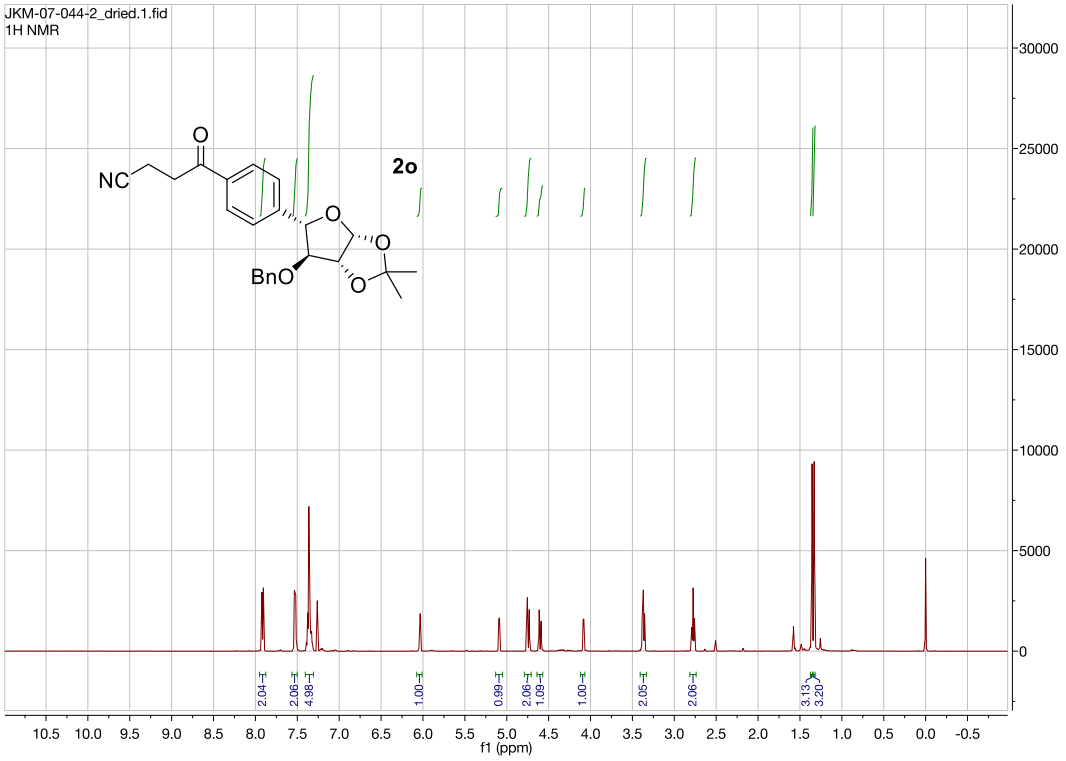

^{13}C NMR ($CDCl_3$, 126 MHz) of 4-(4-((3aR,5S,6S,6aR)-6-(benzyloxy)-2,2-dimethyltetrahydrofuro [2,3-d][1,3]dioxol-5-yl)phenyl)-4-oxobutanenitrile (**7.4.6**)

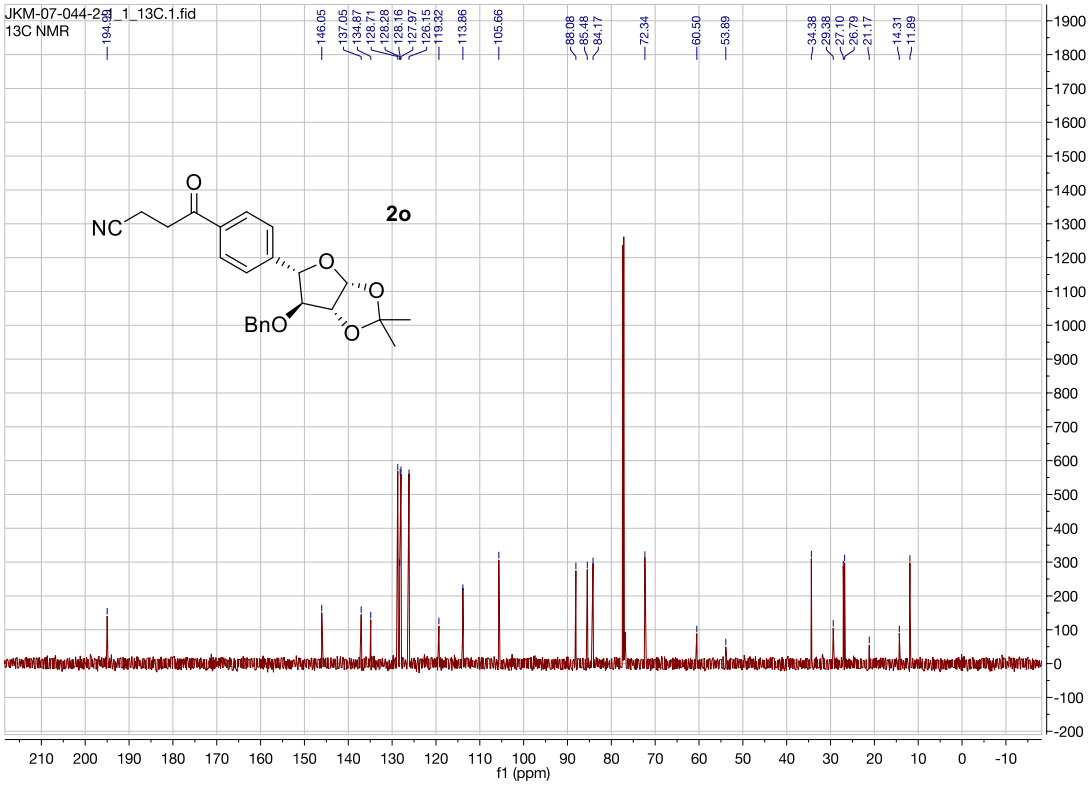

^{1}H NMR ($CDCl_3$, 360 MHz) of 4-((3a*R*,4*R*,6*R*,6a*R*)-6-(2,4-dioxo-3,4-dihydropyrimidin-1(2H)-yl)-2,2-dimethyltetrahydrofuro[3,4-d][1,3]dioxol-4-yl)benzonitrile (**7.4.7**)

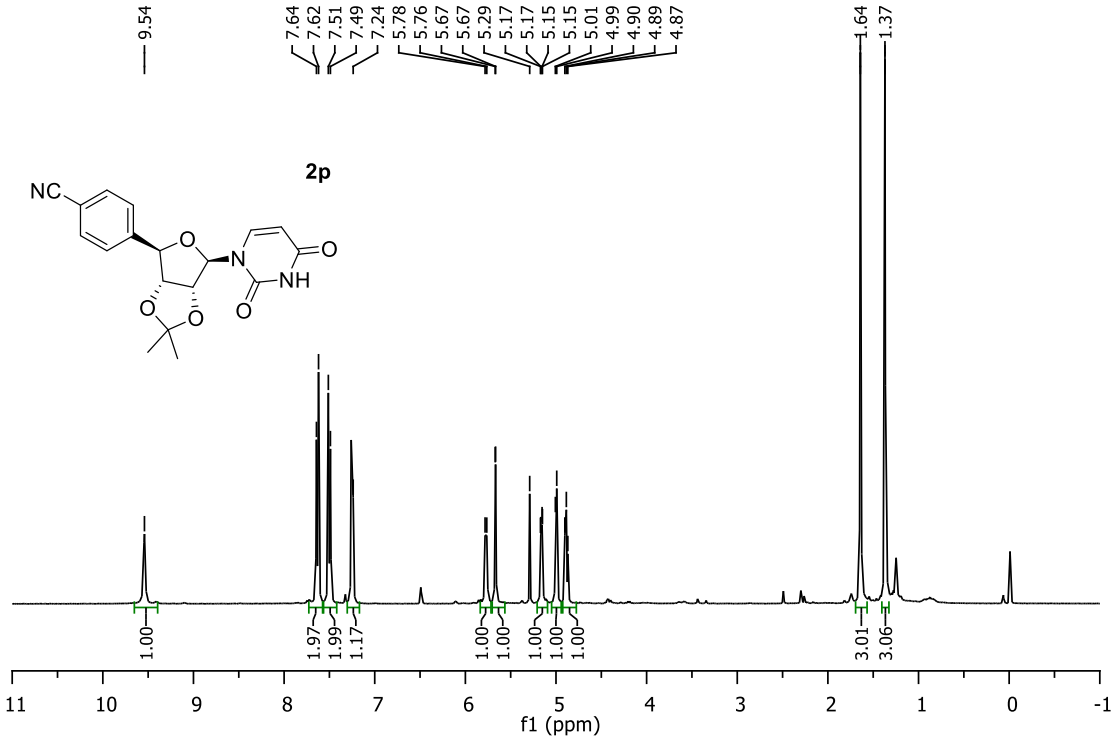

^{13}C NMR ($CDCl_3$, 126 MHz) of 4-((3a*R*,4*R*,6*R*,6a*R*)-6-(2,4-dioxo-3,4-dihydropyrimidin-1(2H)-yl)-2,2-dimethyltetrahydrofuro[3,4-d][1,3]dioxol-4-yl)benzonitrile (**7.4.7**)

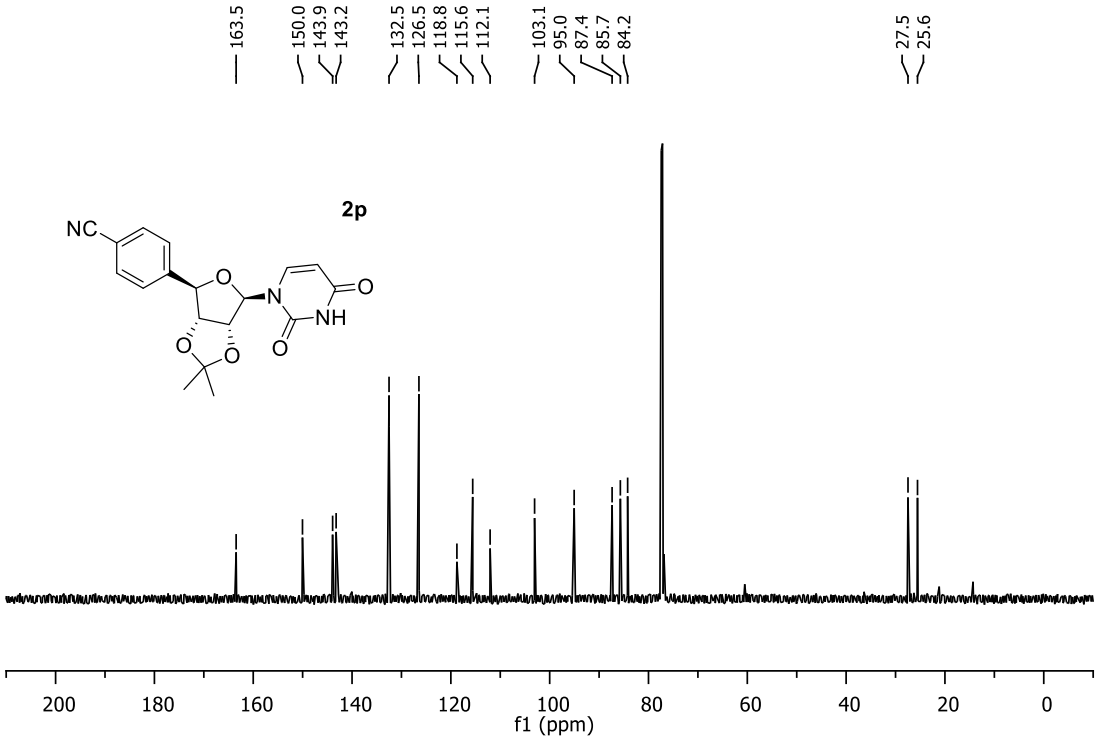

^{1}H NMR ($CDCl_3$, 360 MHz) of *N*-(4-((3a*R*,5*R*,5a*S*,8a*S*,8b*R*)-2,2,7,7-tetramethyltetrahydro-5H-bis([1,3]dioxolo)[4,5-b:4',5'-d]pyran-5-yl)phenyl)acetamide (**7.4.8**)

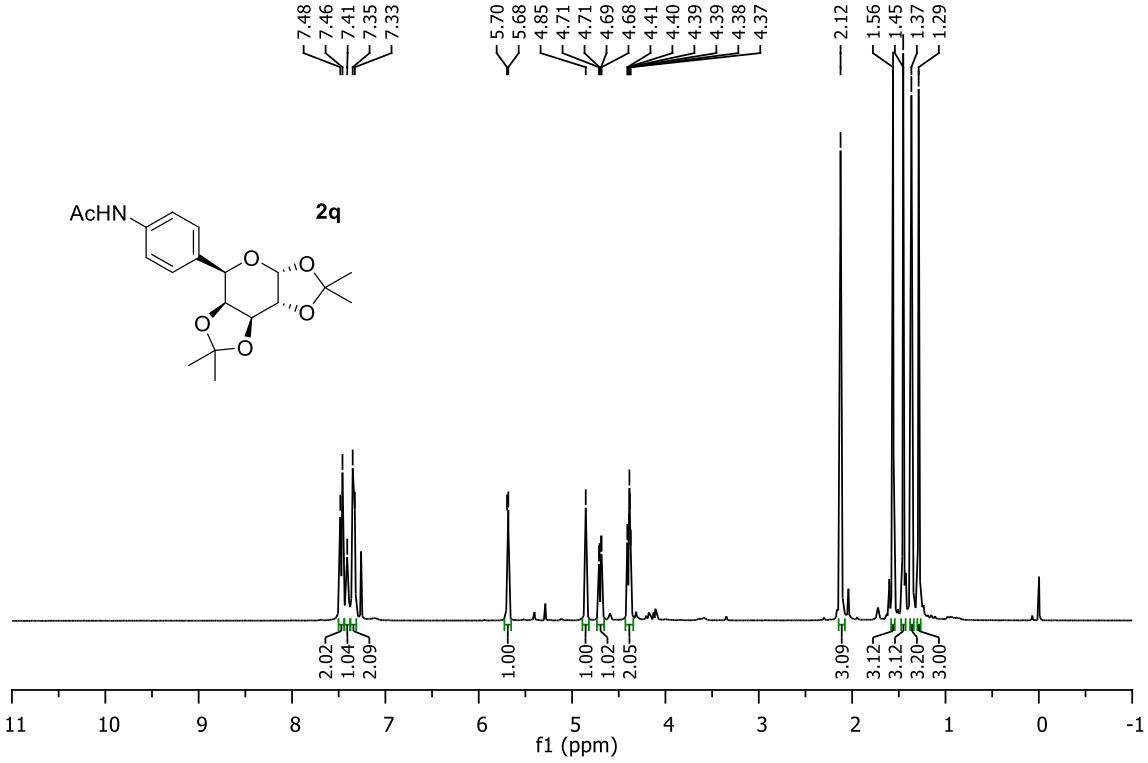

^{13}C NMR ($CDCl_3$, 91 MHz) of *N*-(4-((3a*R*,5*R*,5a*S*,8a*S*,8b*R*)-2,2,7,7-tetramethyltetrahydro-5H-bis([1,3]dioxolo)[4,5-b:4',5'-d]pyran-5-yl)phenyl)acetamide (**7.4.8**)

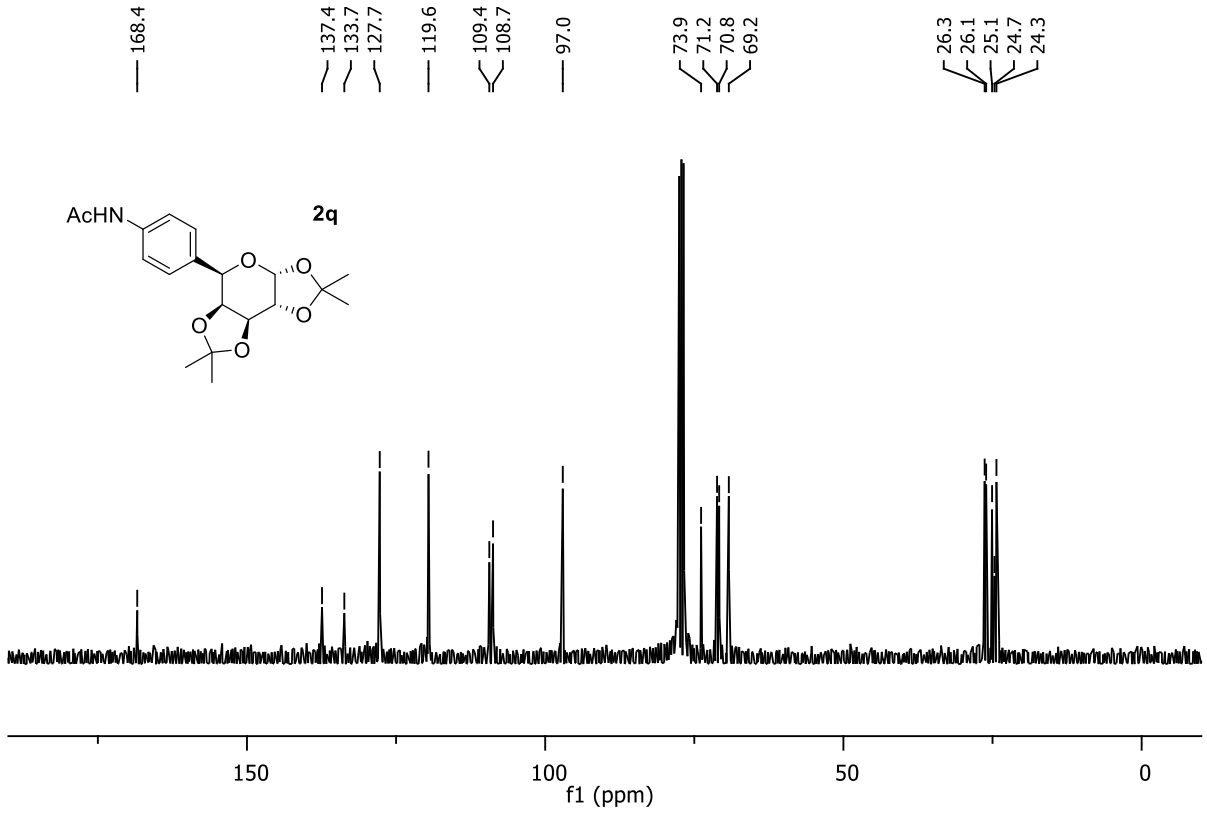

^{1}H NMR ($CDCl_3$, 360 MHz) of 4,4,5,5-tetramethyl-2-(4-((3a*R*,5*R*,5a*S*,8a*S*,8b*R*)-2,2,7,7-tetramethyltetrahydro-5H-bis ([1,3]dioxolo)[4,5-b:4',5'-d]pyran-5-yl)phenyl)-1,3,2-dioxaborolane (**7.4.9**)

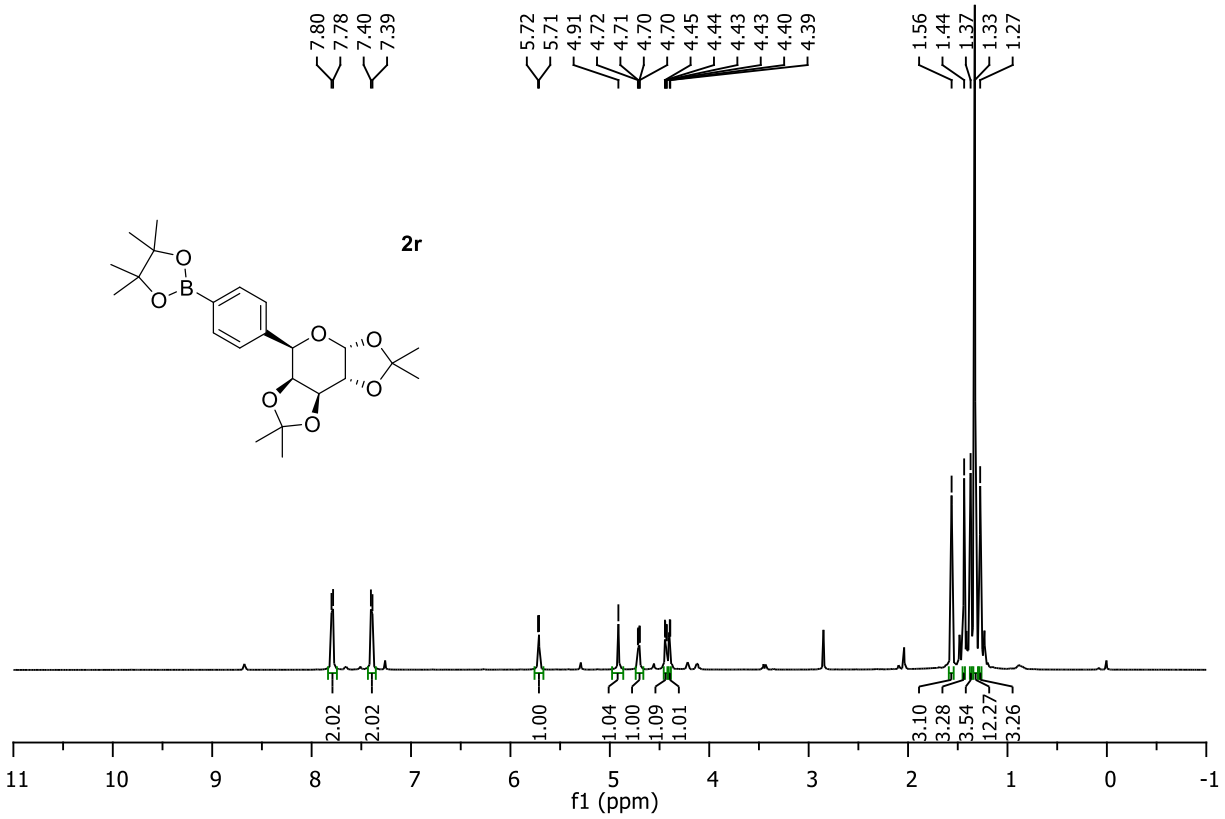

^{13}C NMR ($CDCl_3$, 91 MHz) of 4,4,5,5-tetramethyl-2-(4-((3a*R*,5*R*,5a*S*,8a*S*,8b*R*)-2,2,7,7-tetramethyltetrahydro-5H-bis ([1,3]dioxolo)[4,5-b:4',5'-d]pyran-5-yl)phenyl)-1,3,2-dioxaborolane (**7.4.9**)

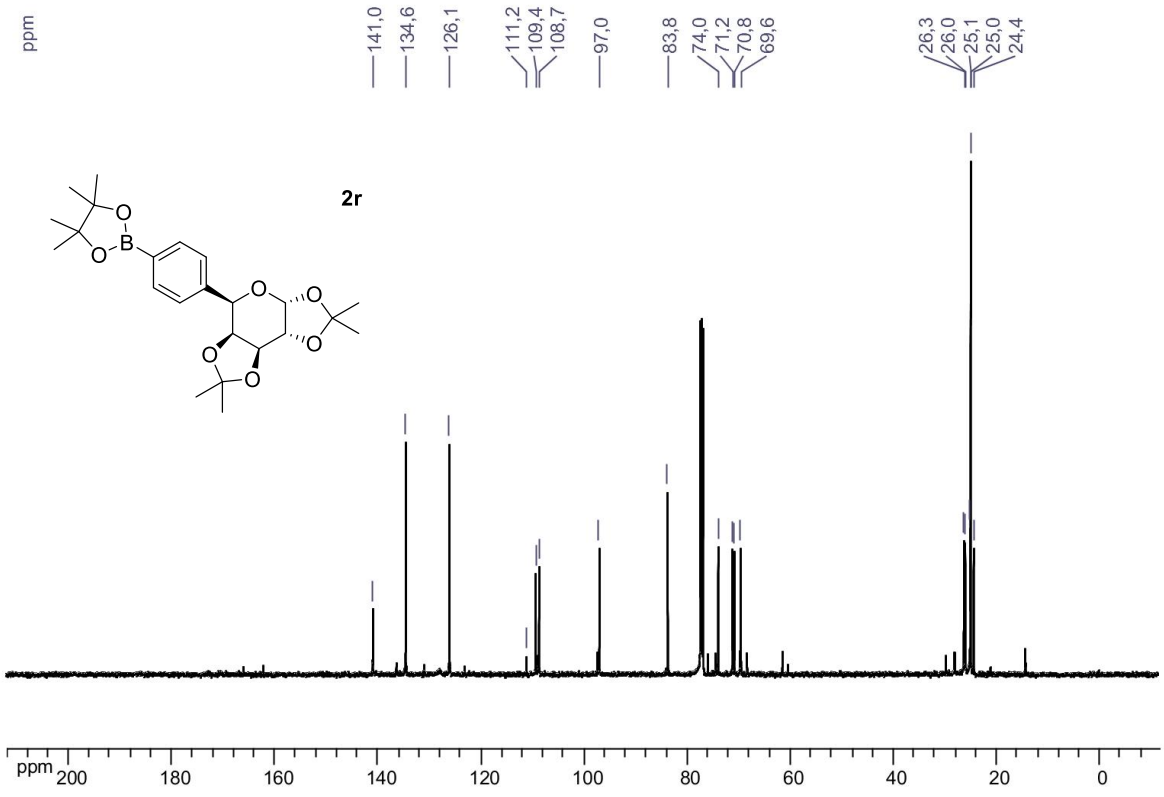

^{11}B NMR ($CDCl_3$, 128.38 MHz) of 4,4,5,5-tetramethyl-2-(4-((3a*R*,5*R*,5a*S*,8a*S*,8b*R*)-2,2,7,7-tetramethyltetrahydro-5H-bis ([1,3]dioxolo)[4,5-b:4',5'-d]pyran-5-yl)phenyl)-1,3,2-dioxaborolane (**7.4.9**)

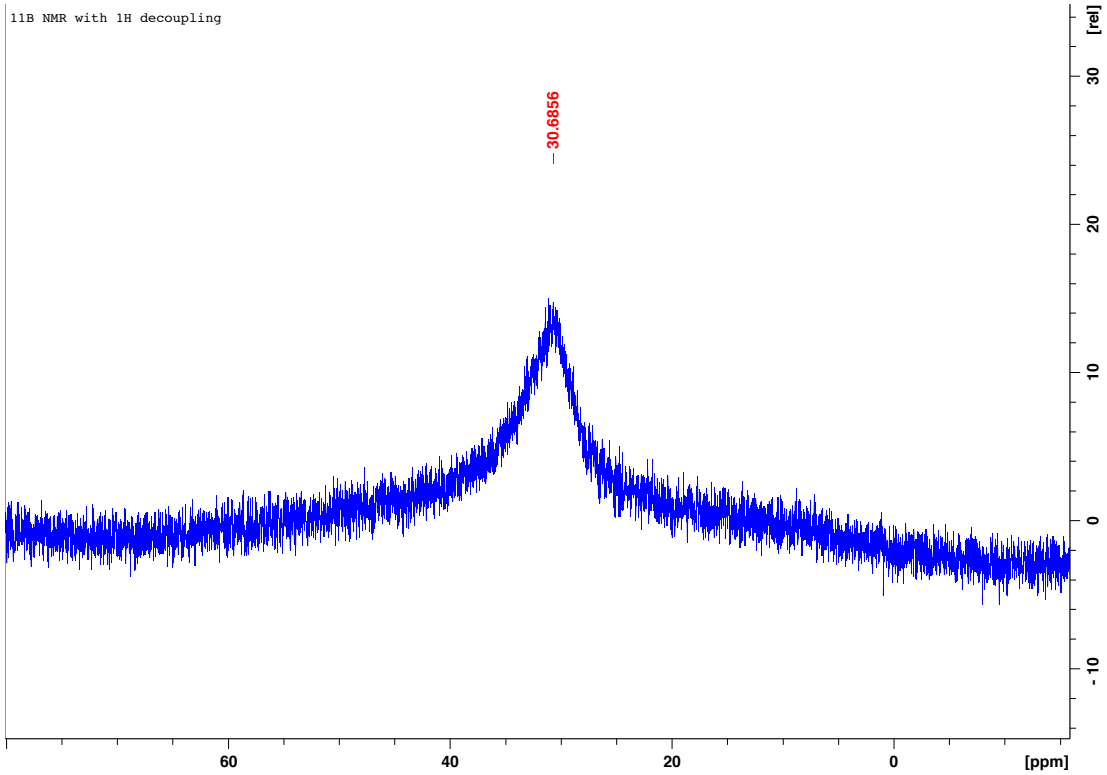

^{1}H NMR ($CDCl_3$, 500 MHz) of *tert*-b ^{1}H NMR ($CDCl_3$, 500 MHz) of (3a*R*,6*S*,6a*R*)-6-(Benzyloxy)-2,2-dimethyl-5-phenyltetrahydrofuro [2,3-*d*][1,3]dioxole (**7.4.10**)

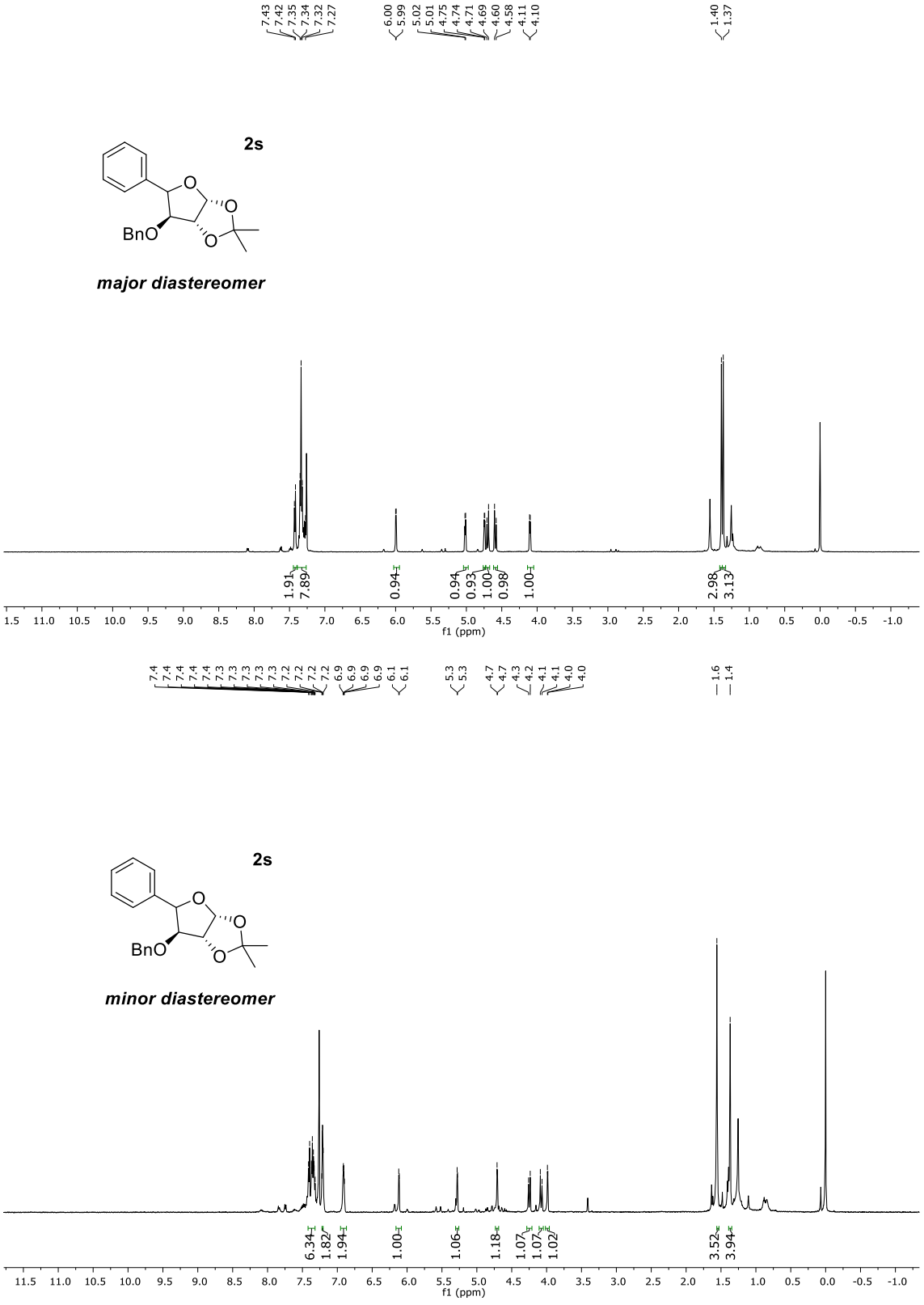

^{13}C NMR ($CDCl_3$, 126 MHz) of (3a*R*,6*S*,6a*R*)-6-(Benzyloxy)-2,2-dimethyl-5-phenyltetrahydrofuro [2,3-*d*][1,3]dioxole (**7.4.10**)

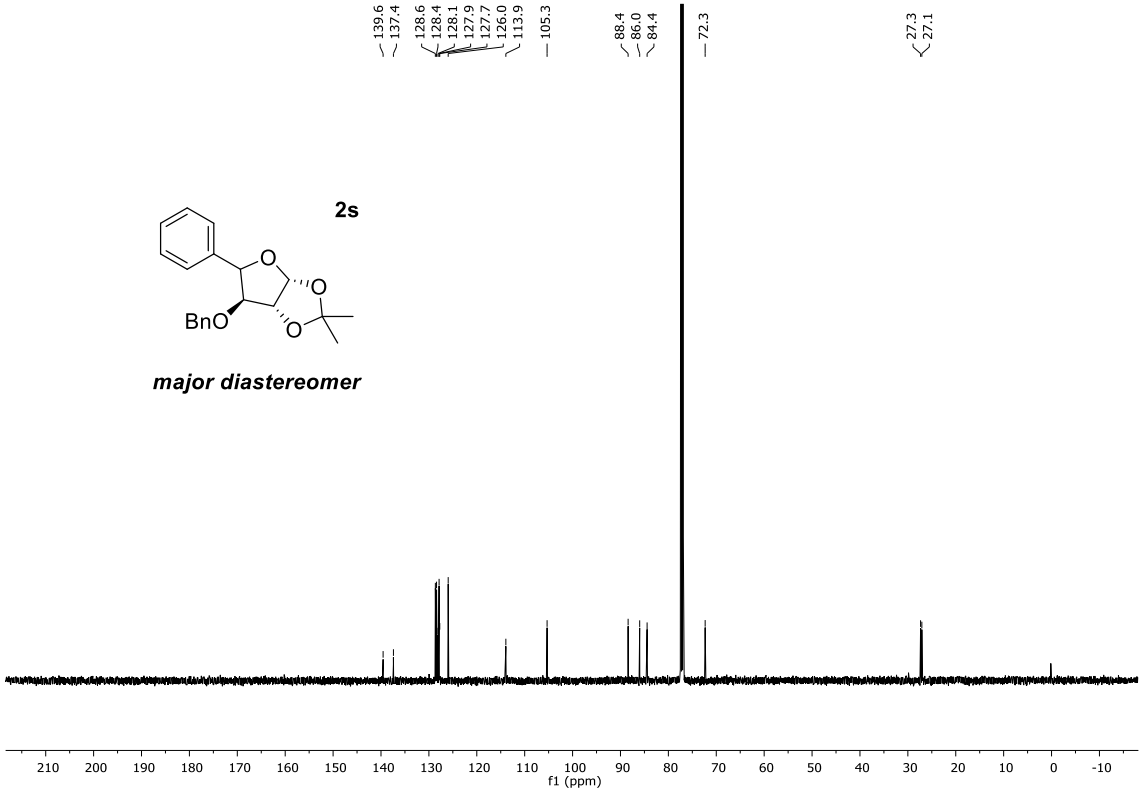

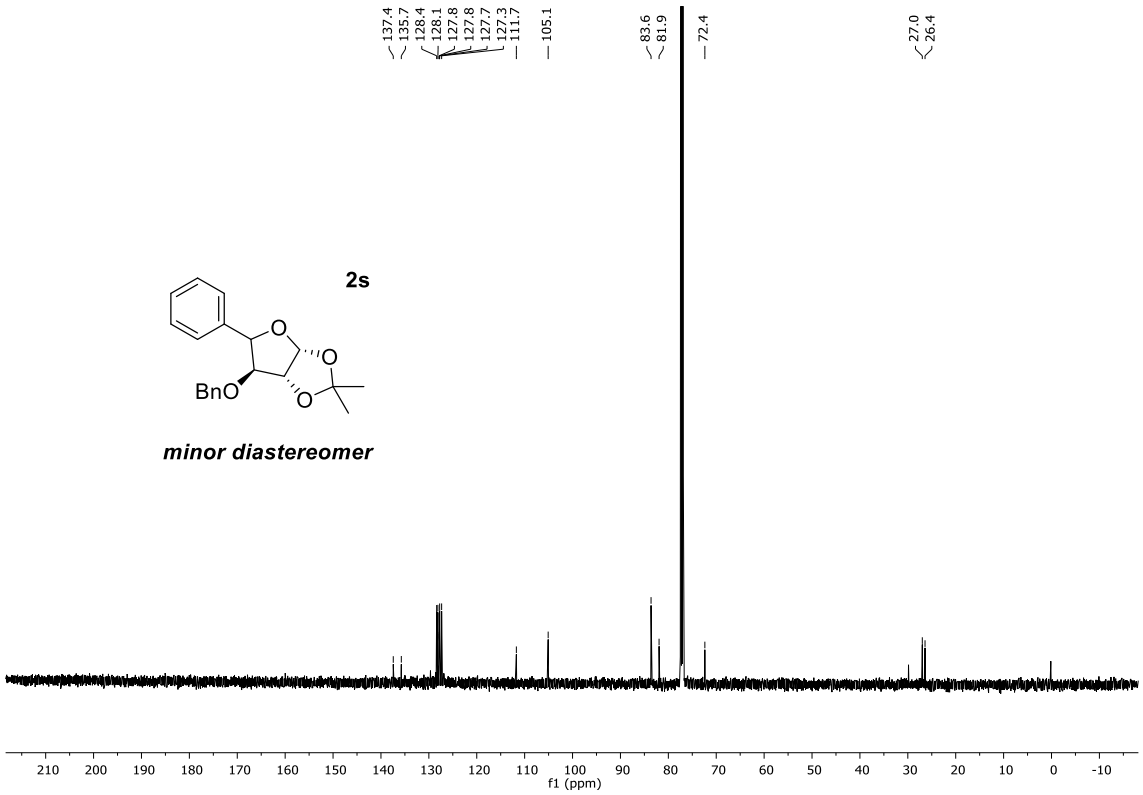

^{1}H NMR ($CDCl_3$, 500 MHz) of (3a*R*,5*S*,6*S*,6a*R*)-6-(benzyloxy)-5-(2,5-dimethylphenyl)-2,2-dimethyltetrahydrofuro[2,3-d][1,3]dioxole (**7.4.11**)

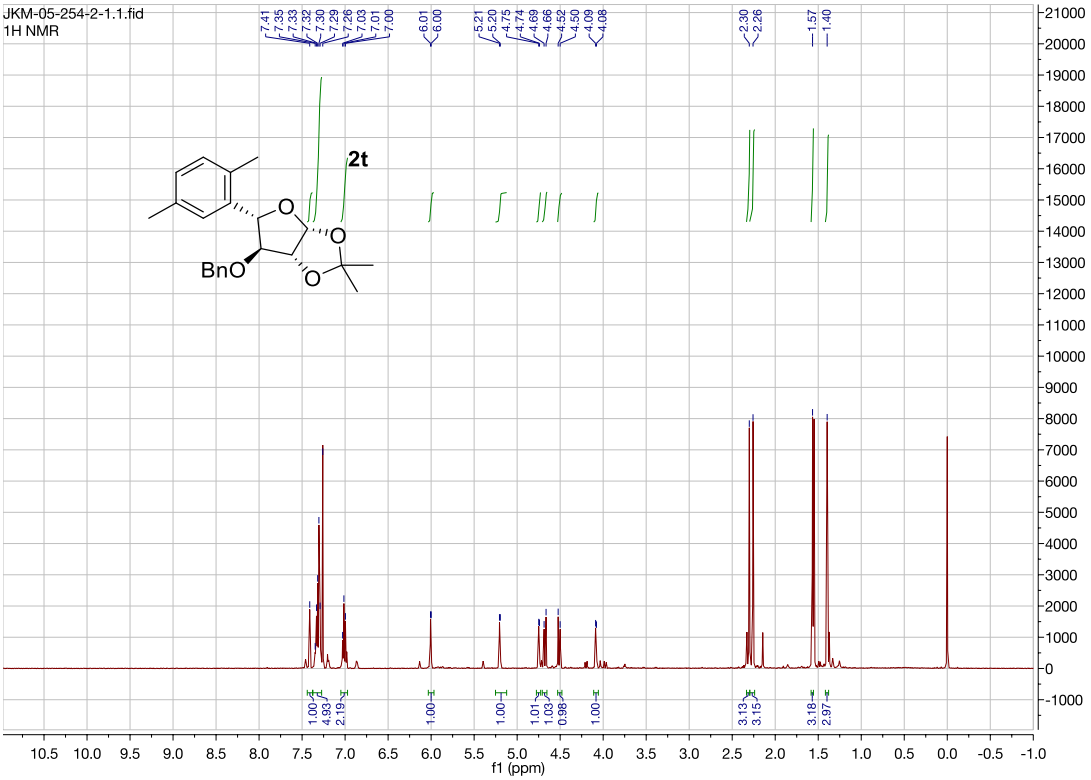

^{13}C NMR ($CDCl_3$, 126 MHz) of (3a*R*,5*S*,6*S*,6a*R*)-6-(benzyloxy)-5-(2,5-dimethylphenyl)-2,2-dimethyltetrahydrofuro[2,3-d][1,3]dioxole (**7.4.11**)

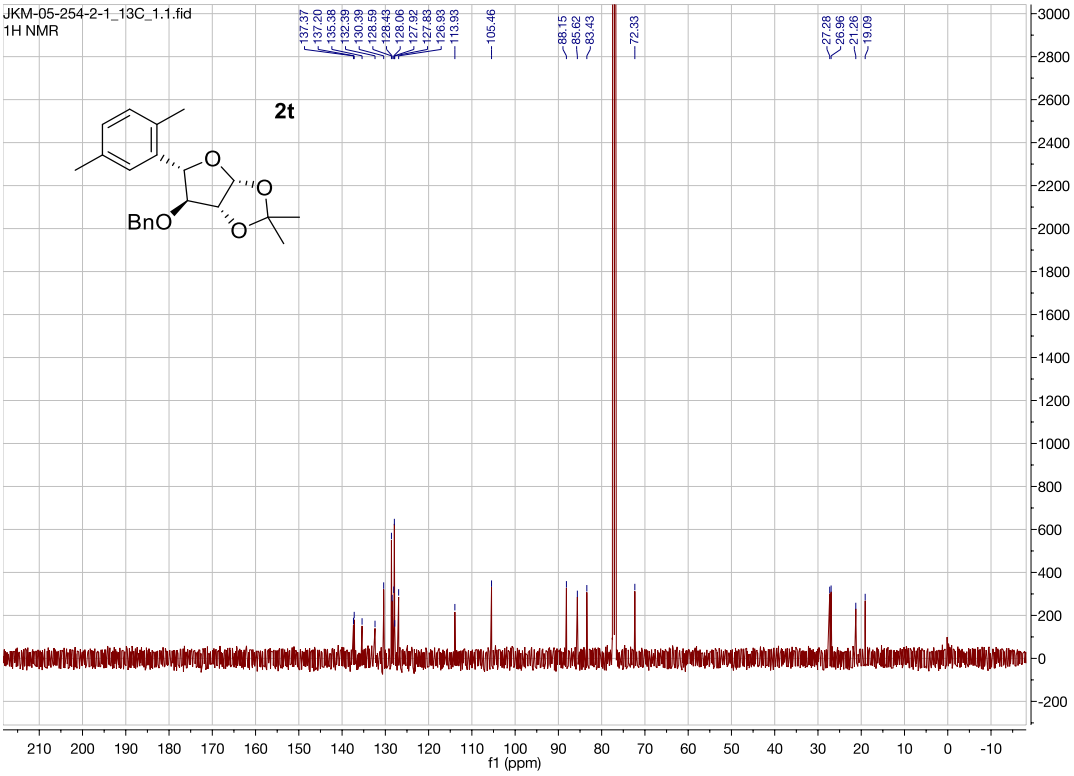

^{1}H NMR ($CDCl_3$, 360 MHz) of 3-chloro-5-((3a*R*,5*R*,5a*S*,8a*S*,8b*R*)-2,2,7,7-tetramethyltetrahydro-5H-bis([1,3]dioxolo)[4,5-b:4',5'-d]pyran-5-yl)pyridine (**7.4.12**)

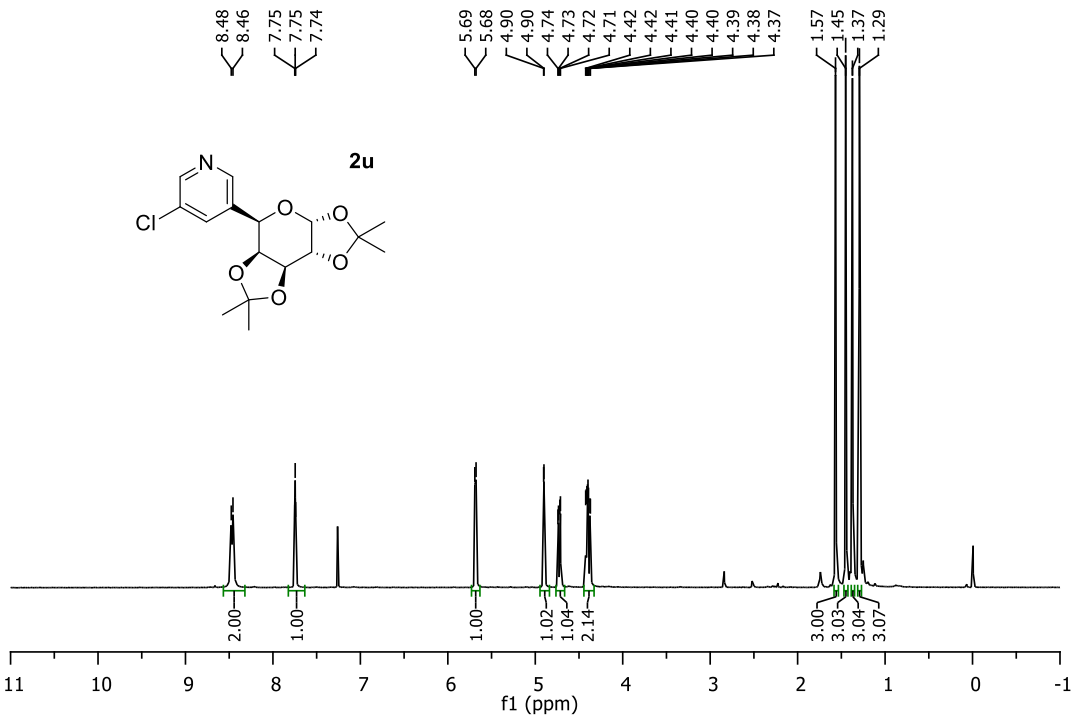

^{13}C NMR ($CDCl_3$, 91 MHz) of 3-chloro-5-((3a*R*,5*R*,5a*S*,8a*S*,8b*R*)-2,2,7,7-tetramethyltetrahydro-5H-bis([1,3]dioxolo)[4,5-b:4',5'-d]pyran-5-yl)pyridine (**7.4.12**)

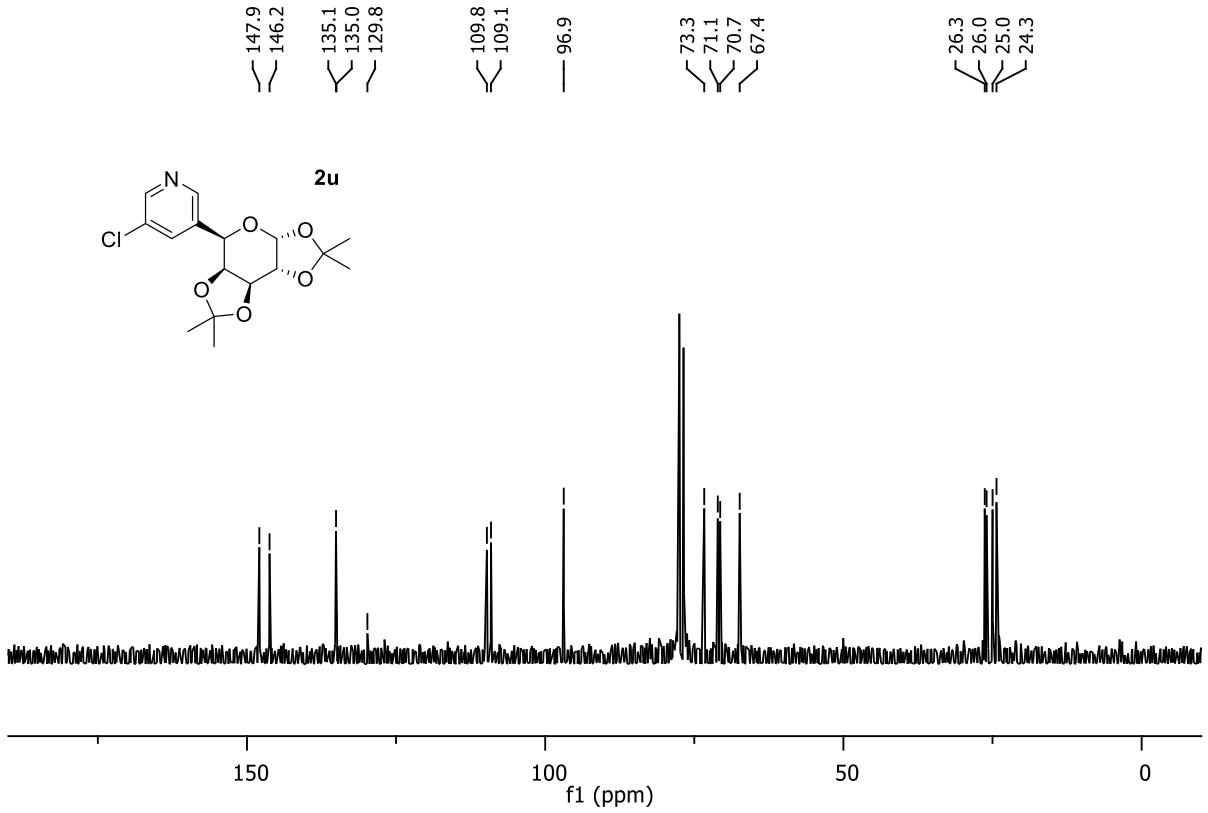

^{1}H NMR ($CDCl_3$, 500 MHz) of 5-((3a*R*,5*S*,6*S*,6a*R*)-6-(benzyloxy)-2,2-dimethyltetrahydrofuro[2,3-d][1,3]dioxol-5-yl) picolinonitrile (**7.4.13**)

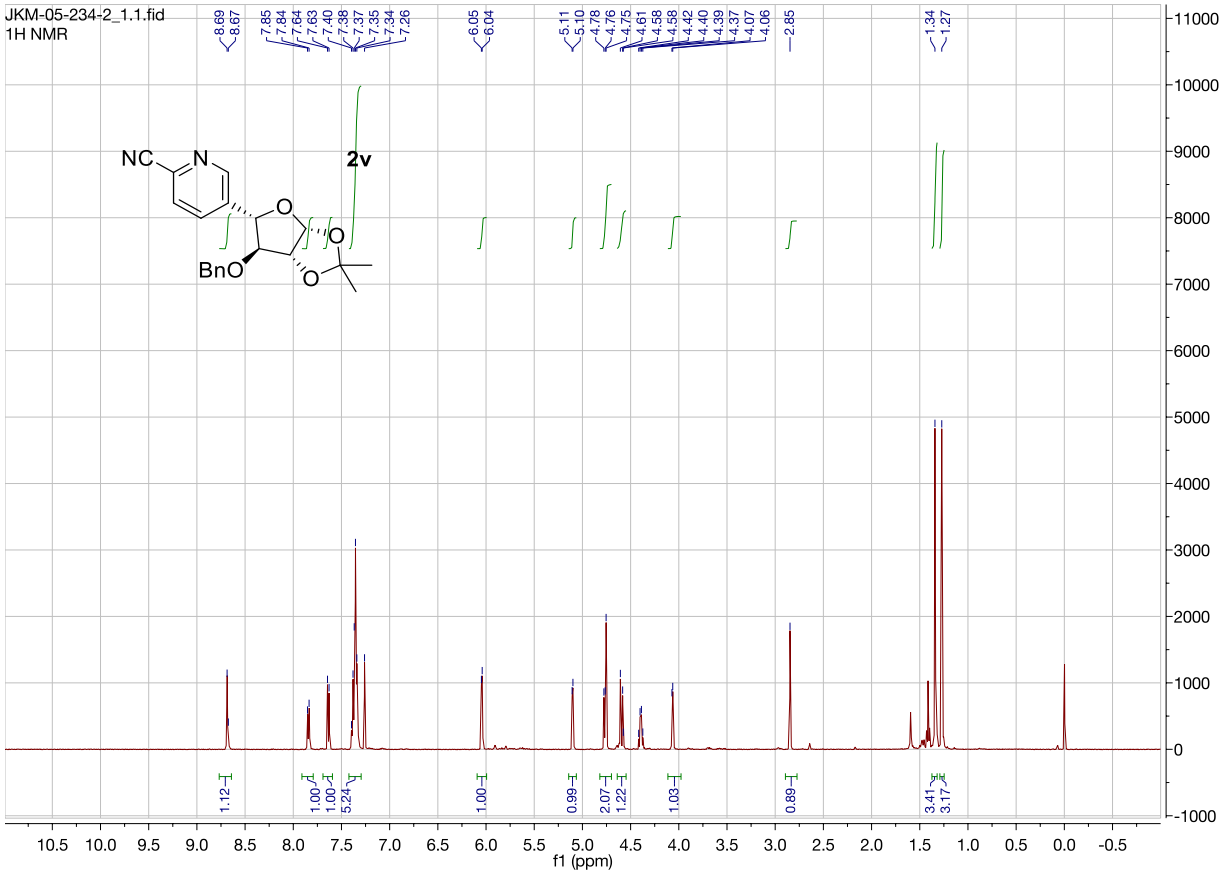

^{13}C NMR ($CDCl_3$, 126 MHz) of 5-((3a*R*,5*S*,6*S*,6a*R*)-6-(benzyloxy)-2,2-dimethyltetrahydrofuro[2,3-d][1,3]dioxol-5-yl) picolinonitrile (**7.4.13**)

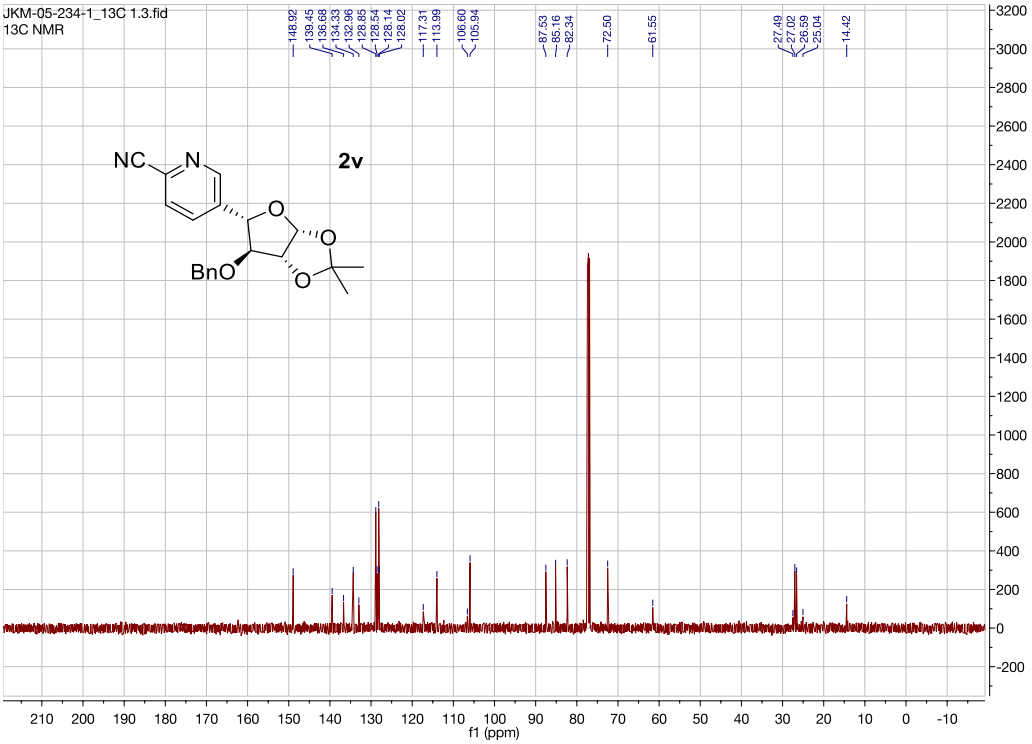

^{1}H NMR ($CDCl_3$, 500 MHz) of 2-(4-((3aR,5S,6S,6aR)-6-(benzyloxy)-2,2-dimethyltetrahydrofuro [2,3-d][1,3]dioxol-5-yl)phenyl) -1,3,4-oxadiazole (**7.4.14**)

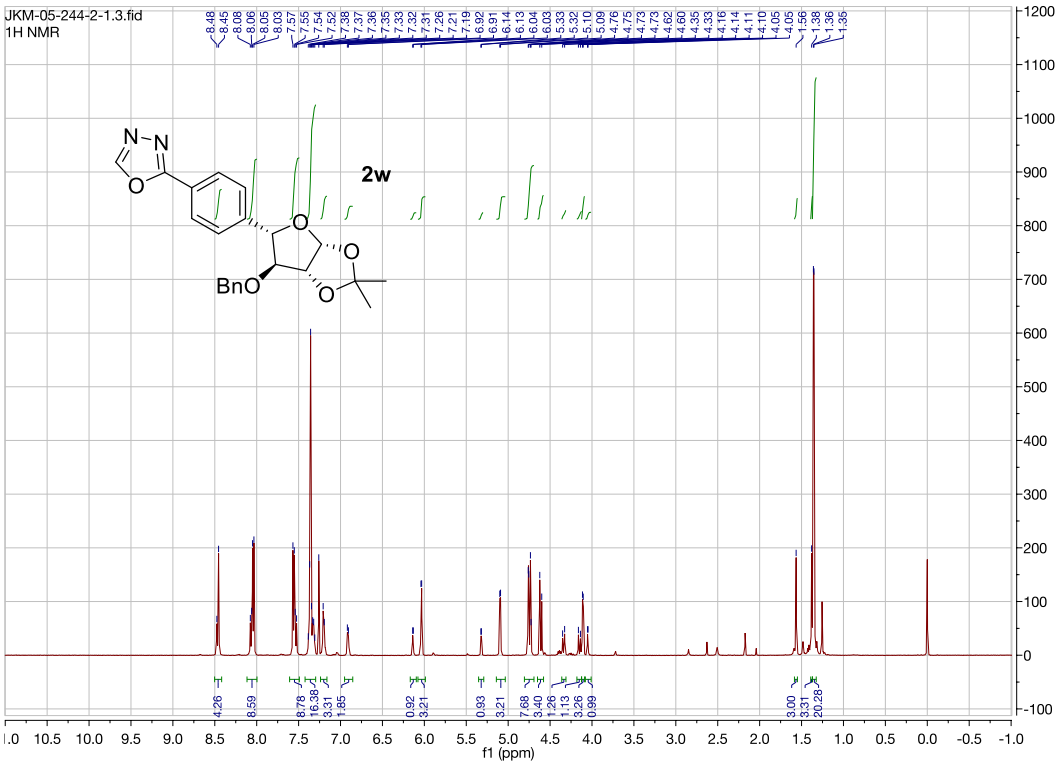

^{13}C NMR ($CDCl_3$, 126 MHz) of 2-(4-((3aR,5S,6S,6aR)-6-(benzyloxy)-2,2-dimethyltetrahydrofuro [2,3-d][1,3]dioxol-5-yl)phenyl) -1,3,4-oxadiazole (**7.4.14**)

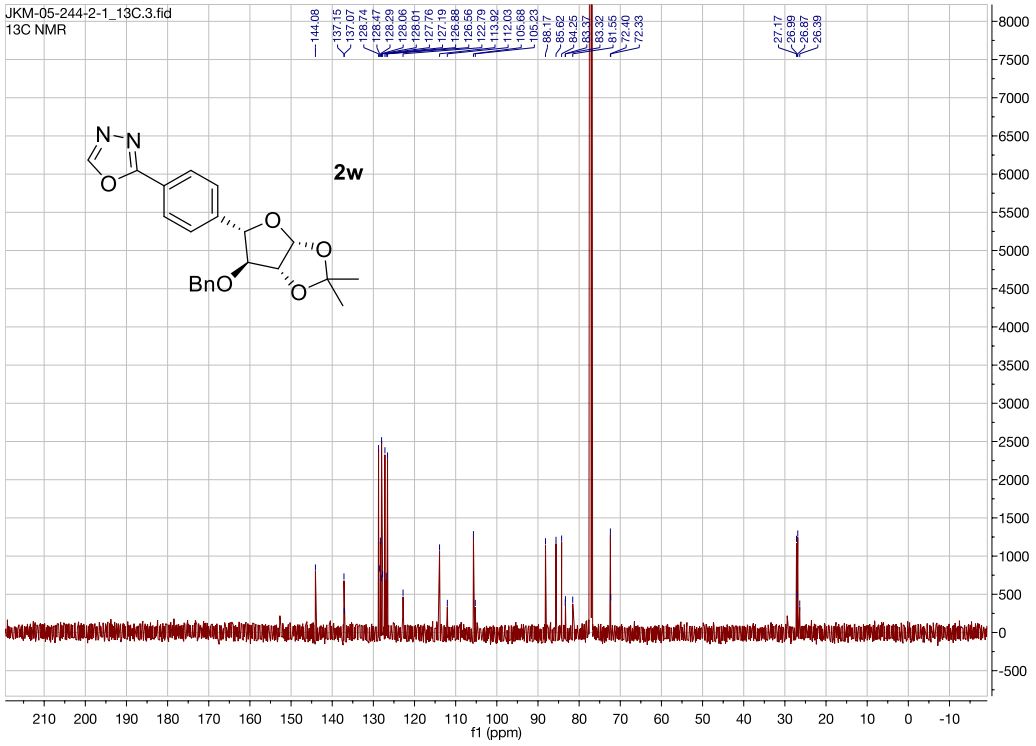

^{1}H NMR ($CDCl_3$, 500 MHz) of 1-(5-((3a*R*,5*R*,6*R*,6a*R*)-6-(benzyloxy)-2,2-dimethyltetrahydrofuro [2,3-d][1,3]dioxol-5-yl) thiophen-2-yl)ethan-1-one (**7.4.15**)

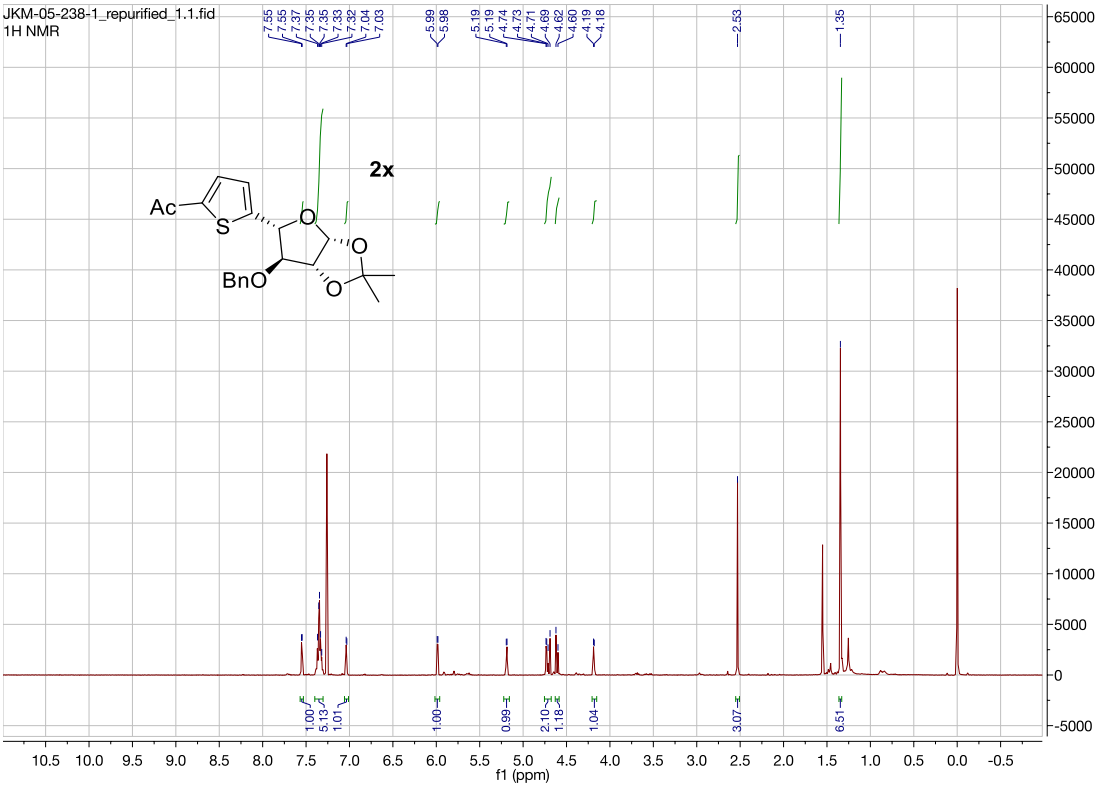

^{13}C NMR ($CDCl_3$, 126 MHz) of 1-(5-((3a*R*,5*R*,6*R*,6a*R*)-6-(benzyloxy)-2,2-dimethyltetrahydrofuro [2,3-d][1,3]dioxol-5-yl) thiophen-2-yl)ethan-1-one (**7.4.15**)

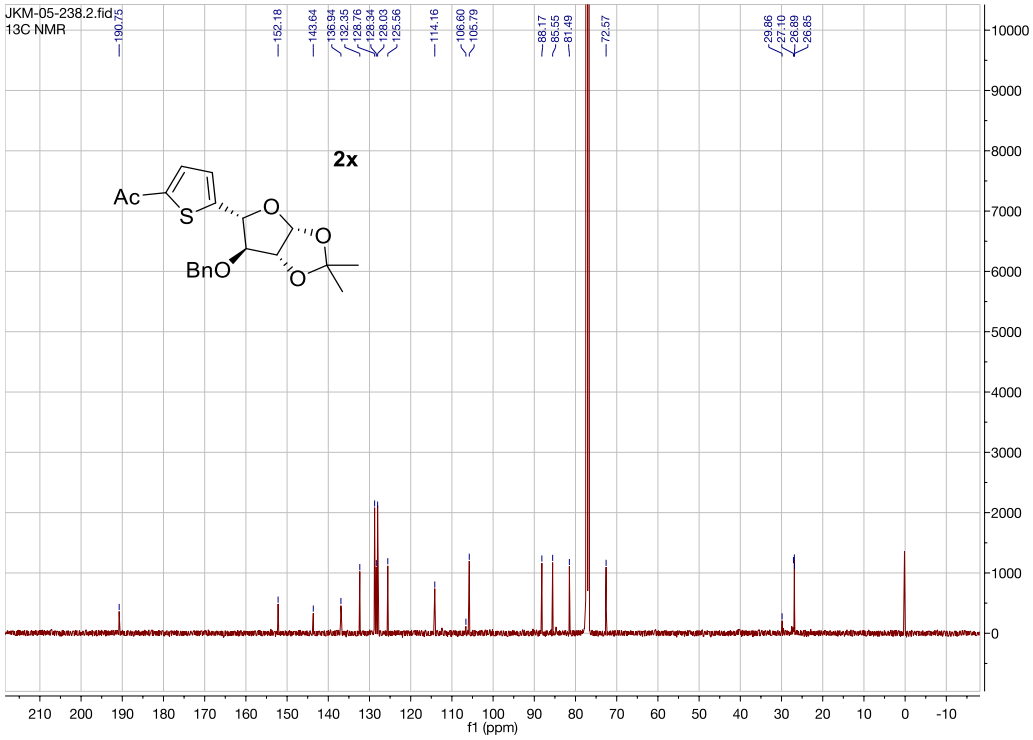

^{1}H NMR ($CDCl_3$, 500 MHz) of 2-(4-((3aR,4S,6R,6aR)-6-methoxy-2,2-dimethyltetrahydrofuro[3,4-d][1,3]dioxol-4-yl)phenyl)-1,3,4-oxadiazole (**7.4.16**)

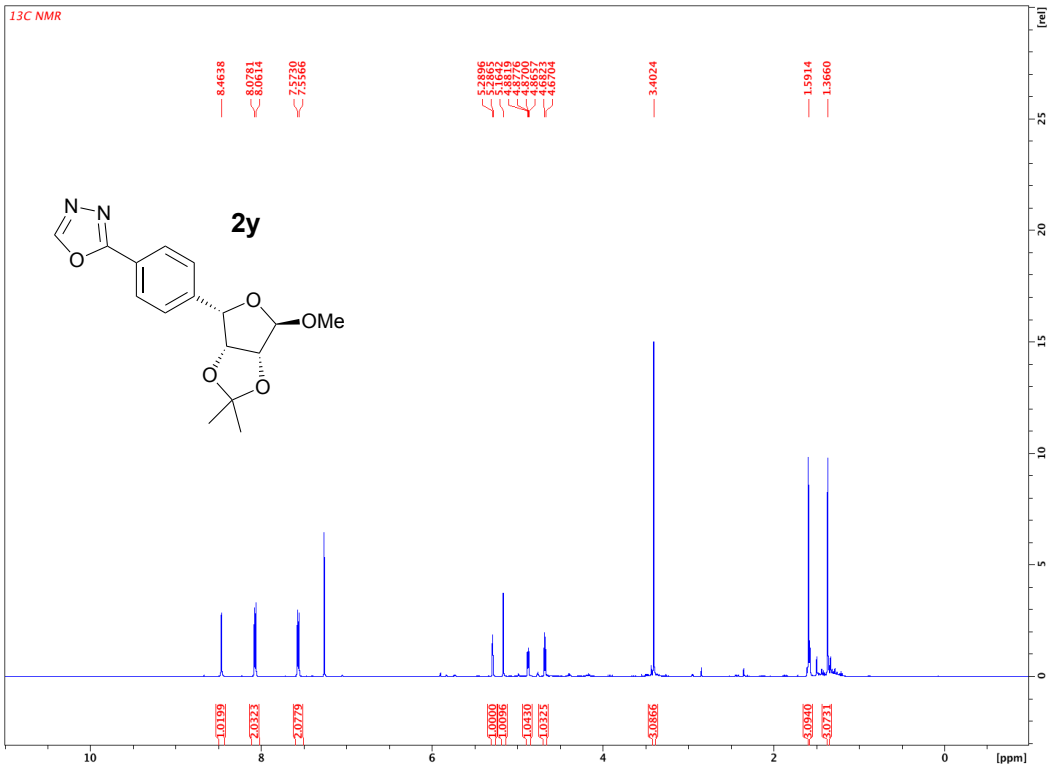

^{13}C NMR ($CDCl_3$, 126 MHz) of 2-(4-((3aR,4S,6R,6aR)-6-methoxy-2,2-dimethyltetrahydrofuro[3,4-d][1,3]dioxol-4-yl)phenyl)-1,3,4-oxadiazole (**7.4.16**)

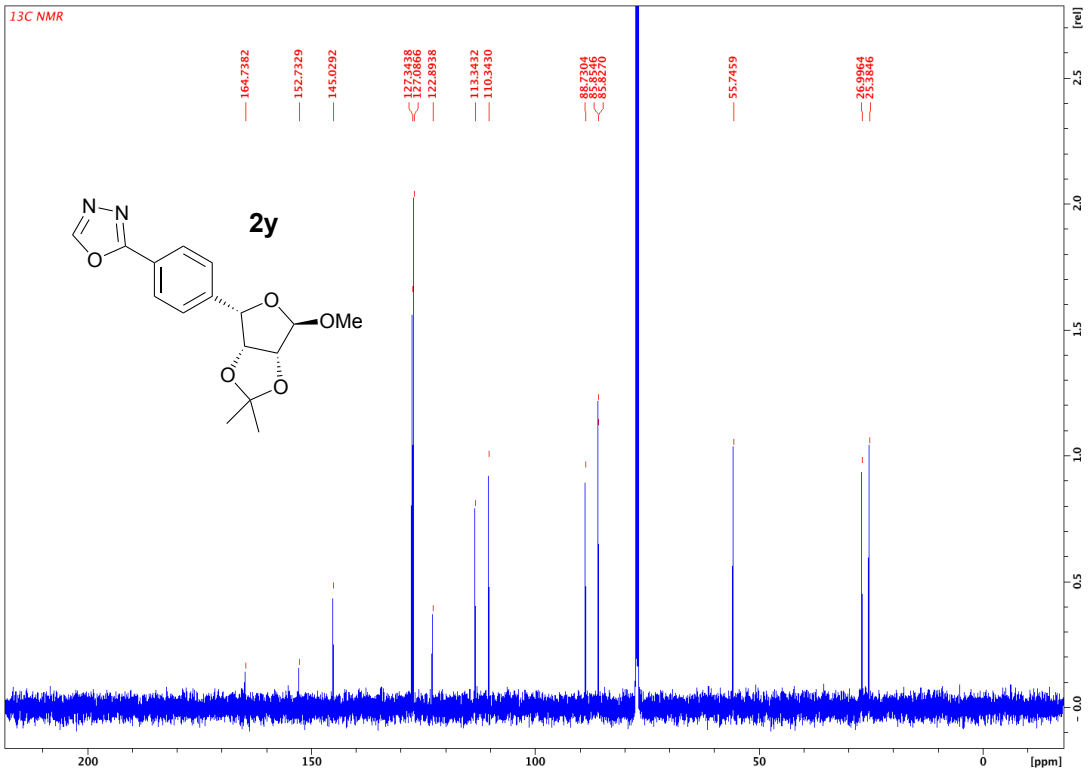

utyl(((3a*R*,5*R*,6*R*,6a*R*)-2,2-dimethyl-5-(5-methylthiophen-2-yl)tetrahydrofuro[2,3-d][1,3]dioxol-6-yl)oxy)dimethylsilane (**7.4.17**)

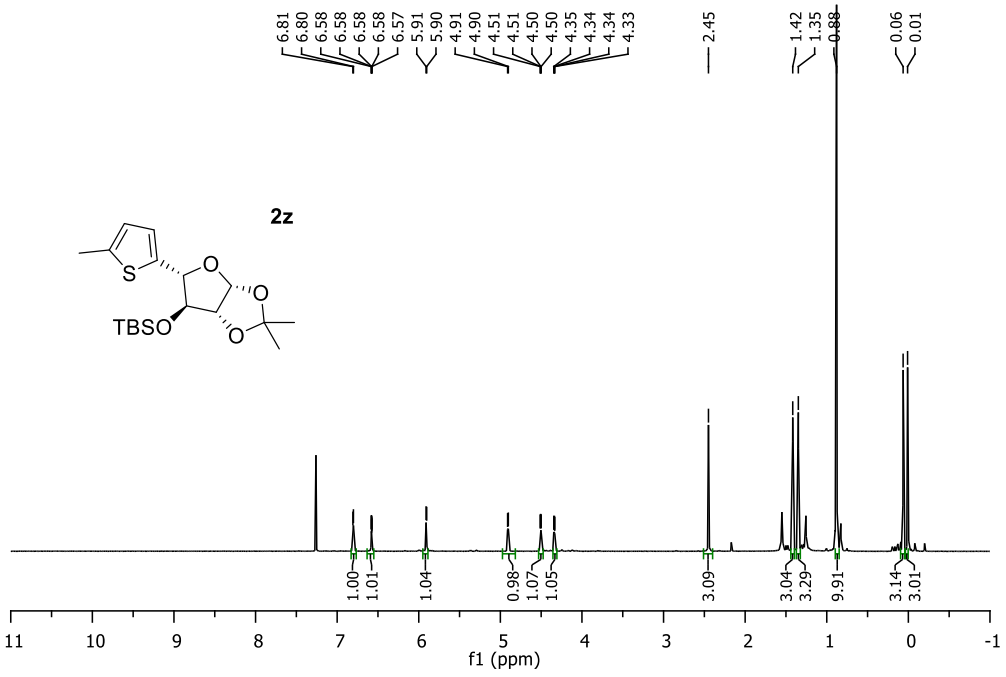

^{13}C NMR ($CDCl_3$, 126 MHz) of *tert*-butyl(((3a*R*,5*R*,6*R*,6a*R*)-2,2-dimethyl-5-(5-methylthiophen-2-yl)tetrahydrofuro[2,3-d][1,3] dioxol-6-yl)oxy)dimethylsilane (**7.4.17**)

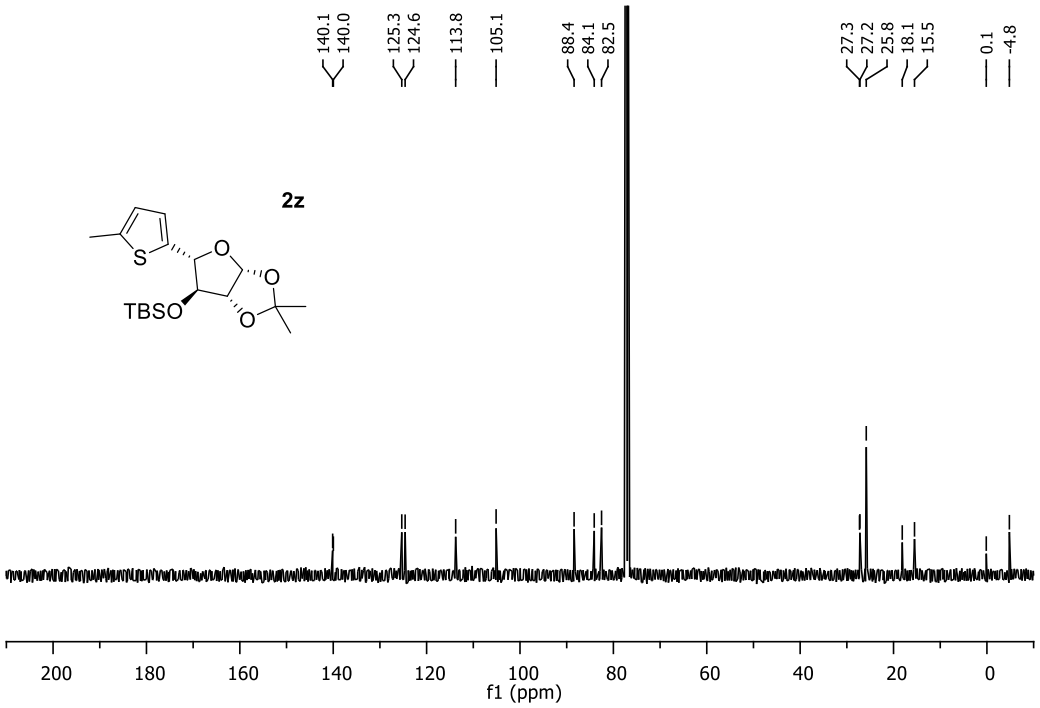

^{1}H NMR ($CDCl_3$, 360 MHz) of (8*R*,9*S*,13*S*,14*S*)-13-methyl-3-((3a*R*,5*R*,5a*S*,8a*S*,8b*R*)-2,2,7,7-tetramethyltetrahydro-5H-bis([1,3]dioxolo)[4,5-b:4',5'-d]pyran-5-yl)-6,7,8,9,11,12,13,14,15,16-decahydro-17H-cyclopenta[a]phenanthren-17-one (**7.5.1**)

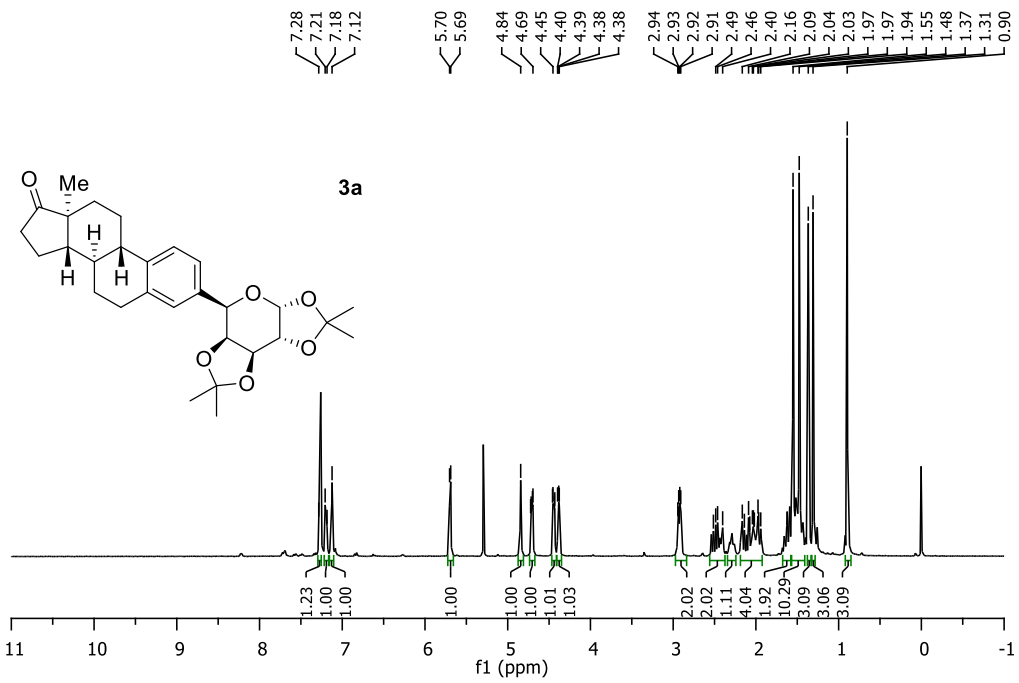

^{13}C NMR ($CDCl_3$, 91 MHz) of (8*R*,9*S*,13*S*,14*S*)-13-methyl-3-((3a*R*,5*R*,5a*S*,8a*S*,8b*R*)-2,2,7,7-tetramethyltetrahydro-5H-bis([1,3]dioxolo)[4,5-b:4',5'-d]pyran-5-yl)-6,7,8,9,11,12,13,14,15,16-decahydro-17H-cyclopenta[a]phenanthren-17-one (**7.5.1**)

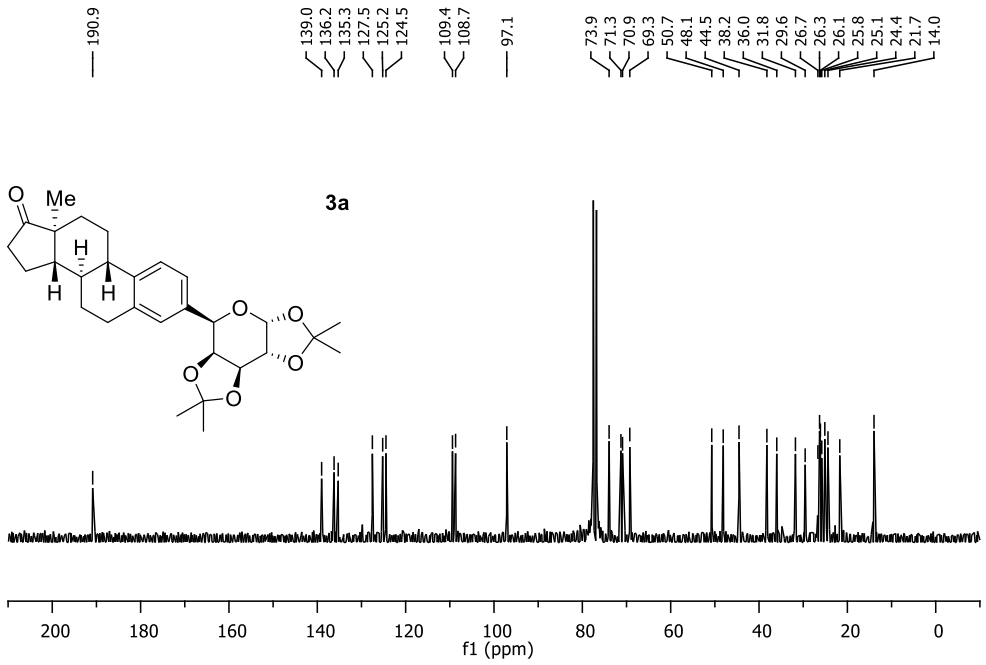

^{1}H NMR ($CDCl_3$, 360 MHz) of methyl 2-(2,3-dioxo-9-((3a*R*,5*R*,5a*S*,8a*S*,8b*R*)-2,2,7,7-tetramethyltetrahydro-5H-bis ([1,3] dioxolo)[4,5-b:4',5'-d]pyran-5-yl)-2,3,6,7-tetrahydro-1H,5H-pyrido[1,2,3-de]quinoxalin-5-yl) acetate (**7.5.2**)

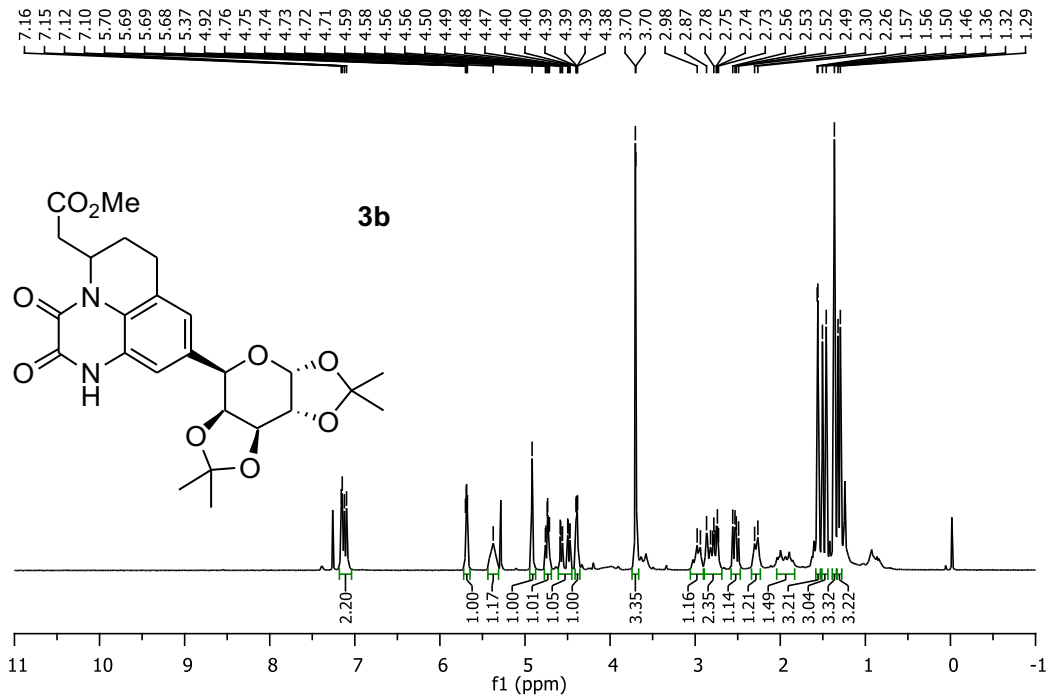

^{13}C NMR ($CDCl_3$, 91 MHz) of methyl 2-(2,3-dioxo-9-((3a*R*,5*R*,5a*S*,8a*S*,8b*R*)-2,2,7,7-tetramethyltetrahydro-5H-bis ([1,3] dioxolo)[4,5-b:4',5'-d]pyran-5-yl)-2,3,6,7-tetrahydro-1H,5H-pyrido[1,2,3-de]quinoxalin-5-yl) acetate (**7.5.2**)

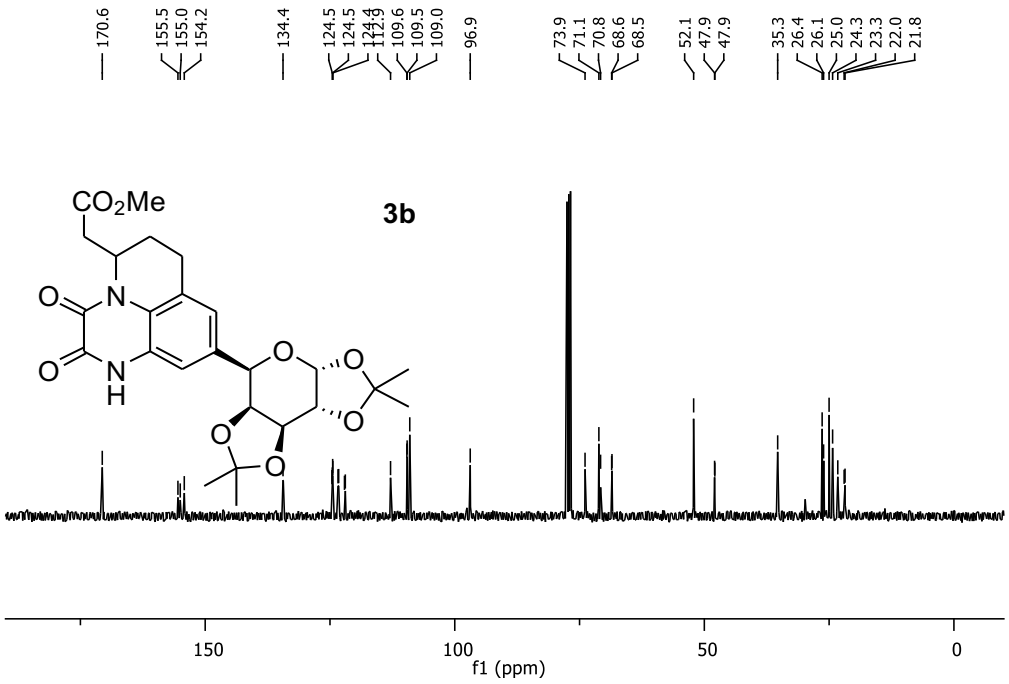

^{1}H NMR ($CDCl_3$, 500 MHz) of *tert*-butyl ((*R*,*Z*)-1,4-dimethyl-6-oxo-4-(4-((3a*R*,5*R*,5a*S*,8a*S*,8b*R*) -2,2,7,7-tetramethyl tetrahydro-5H-bis([1,3]dioxolo)[4,5-b:4',5'-d]pyran-5-yl)thiophen-2-yl) tetrahydro pyrimidin-2(1H)-ylidene)carbamate (**7.5.3**)

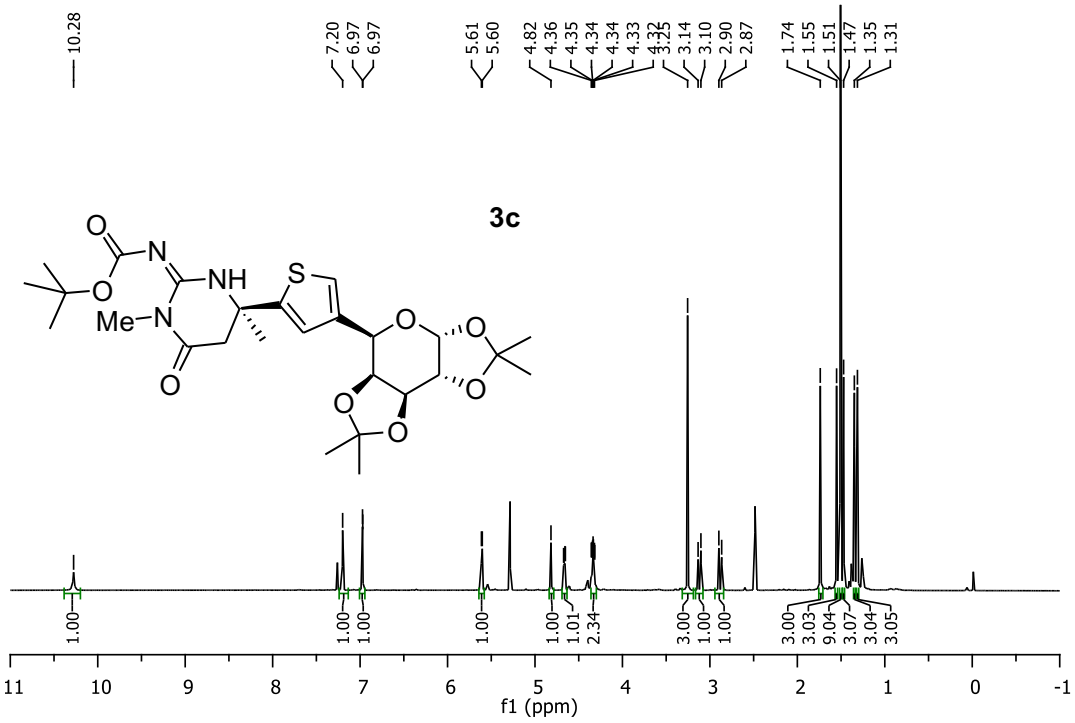

^{13}C NMR ($CDCl_3$, 126 MHz) of *tert*-butyl ((*R*,*Z*)-1,4-dimethyl-6-oxo-4-(4-((3a*R*,5*R*,5a*S*,8a*S*,8b*R*) -2,2,7,7-tetramethyl tetrahydro-5H-bis([1,3]dioxolo)[4,5-b:4',5'-d]pyran-5-yl)thiophen-2-yl) tetrahydro pyrimidin-2(1H)-ylidene)carbamate (**7.5.3**)

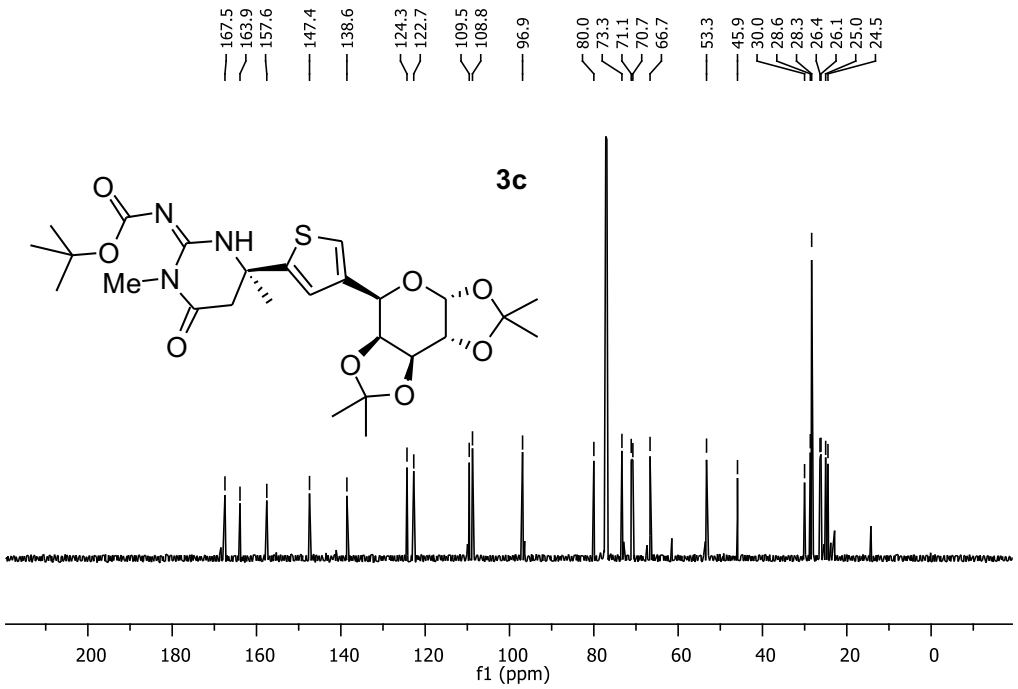

^{1}H NMR ($CDCl_3$, 500 MHz) of ethyl 4-(3-((3a*R*,5*S*,6*S*,6a*R*)-6-(benzyloxy)-2,2-dimethyltetrahydrofuro[2,3-d][1,3]dioxol-5-yl)-8-chloro-5,6-dihydro-11H-benzo[5,6]cyclohepta[1,2-b]pyridin-11-ylidene)piperidine-1-carboxylate (**7.5.4**)

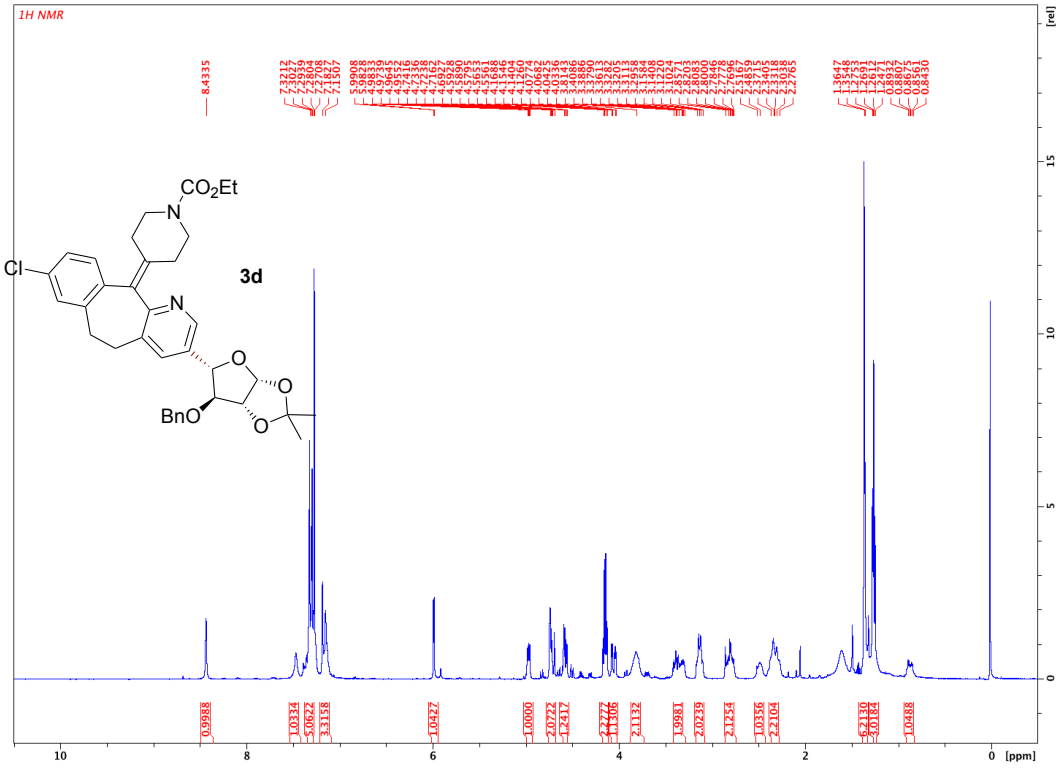

^{13}C NMR ($CDCl_3$, 126 MHz) of ethyl 4-(3-((3a*R*,5*S*,6*S*,6a*R*)-6-(benzyloxy)-2,2-dimethyltetrahydrofuro[2,3-d][1,3]dioxol-5-yl)-8-chloro-5,6-dihydro-11H-benzo[5,6]cyclohepta[1,2-b]pyridin-11-ylidene)piperidine-1-carboxylate (**7.5.4e**) (mixture of rotamers)